

Dissertation zur Erlangung des Doktorgrades
der Fakultät für Chemie und Pharmazie
der Ludwig-Maximilians-Universität München

Total Synthesis of Marine and Terrestrial
Natural Products

And

Development of Novel Photochromic Ligands
for Ion Channels, G-Protein Coupled Receptors
and Cytoskeletal Proteins

Nils Sebastian Winter
aus München, Deutschland

2018

Erklärung

Diese Dissertation wurde im Sinne von § 7 der Promotionsordnung vom 28. November 2011 von Herrn Prof. Dr. Dirk Trauner betreut.

Eidesstattliche Versicherung

Diese Dissertation wurde eigenständig und ohne unerlaubte Hilfe erarbeitet.

München, den 30.01.2018

Nils Sebastian Winter

Dissertation eingereicht am: 01.02.2018

1. Gutachter: Prof. Dr. Dirk Trauner

2. Gutachter: Prof. Dr. Oliver Trapp

Mündliche Prüfung am: 15.03.2018

Sarah und meiner Familie

Parts of this work have been published in peer-reviewed journals:

- “Optical Control of Dopamine Receptors Using a Photoswitchable Tethered Inverse Agonist” – Prashant C. Donthamsetti*, **Nils Winter***, Matthias Schönberger, Cherise Stanley, Jonathan A. Javitch, Ehud Y. Isacoff and Dirk Trauner, *J. Am. Chem. Soc.* **2017**, *139*, 18522–18535.

*equal contributions

- “Thiocarbonyl Ylide Chemistry Enables a Concise Synthesis of (±)-Hippolachnin A” – **Nils Winter** and Dirk Trauner, *J. Am. Chem. Soc.* **2017**, *139*, 11706–11709. Highlighted in Synfacts DOI: 10.1055/s-0036-1591428

Parts of this work have been presented on scientific conferences:

- “Total Synthesis of Hippolachnin A” – **Winter, N.**, Trauner, D. International Society of Heterocyclic Chemistry **2017**, Regensburg, Germany

Parts of this work are currently prepared for publication:

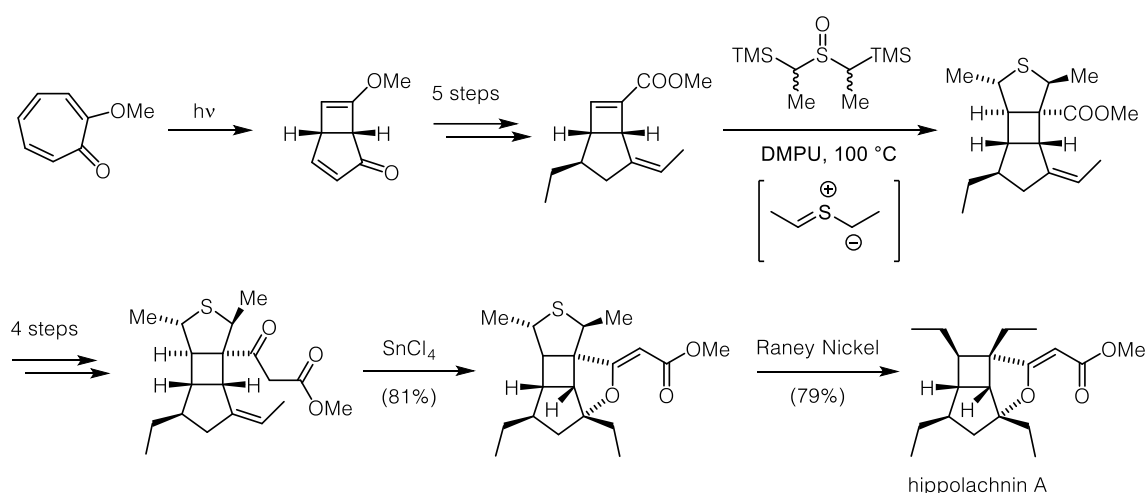
- “Novel Photochromic Channel Blockers for the Two-Pore Domain Potassium Channel TREK-1” – Philipp Leippe,[#] **Nils Winter**,[#] Martin P. Sumser Dirk Trauner*.

Abstract

Chapter I: Synthesis of the Marine Natural Product

Hippolachnin A

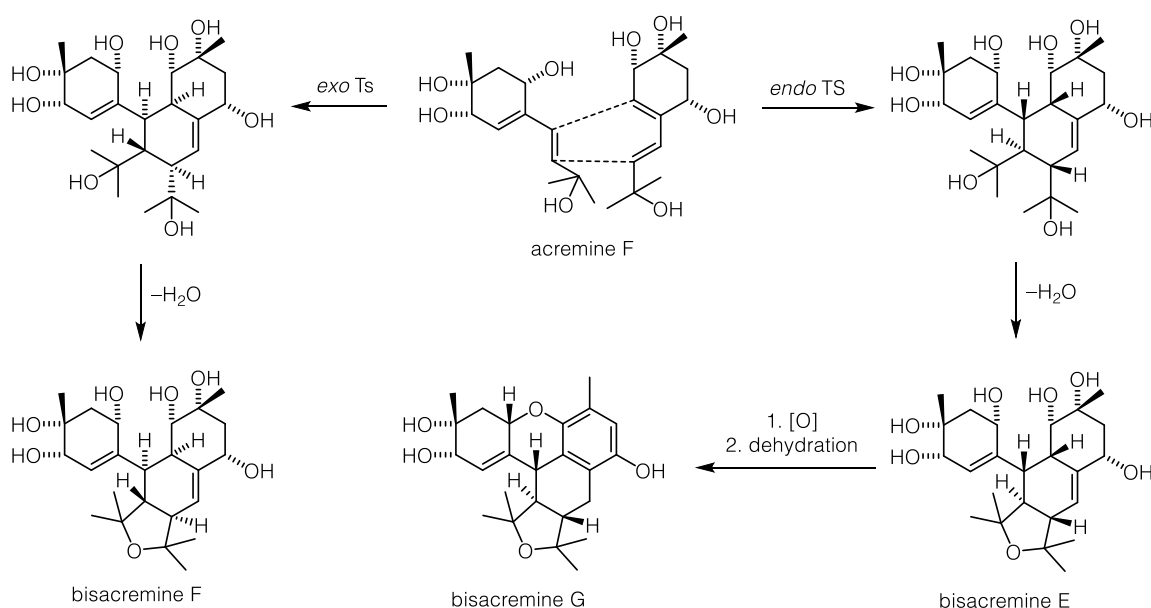
Marine organisms are a rich source of structurally diverse secondary metabolites.¹⁻³ In this regard, sponges have been intensively studied and have provided a large fraction of such natural products. In 2013, Lin and co-workers reported the isolation of the polyketide natural product hippolachnin A, together with its proposed biogenetic precursor, from the ethanolic extract of the South China Sea sponge *Hippospongia Lachne* collected from the waters at Xisha Islands.⁴ Hippolachnin A exhibited potent antifungal activity against the pathogenic fungi *Cryptococcus neoformans*, *Trichophyton rubrum*, and *Microsporium gypseum* with an MIC value of 0.41 μM for each fungus. The following work describes the total synthesis of hippolachnin A. The bicyclo[3.2.0]hepatadienenone core is installed *via* a disrotatory 4π -electrocyclization followed by excited state rearrangement of α -tropolone methyl ether. The synthetically challenging installation of the vicinal diethyl groups has been achieved by a [3+2] dipolar cycloaddition of a thiocarbonyl ylide to an electron-poor double bond. Chelation controlled trapping of an *in situ* generated carbocation by a tin enolate led to closure of the final tetrahydrofuran ring. The synthetic route provided over 100 mg of the natural product as well as access to derivatives thereof (Scheme A).



SCHEME A: Synthesis of hippolachnin A.

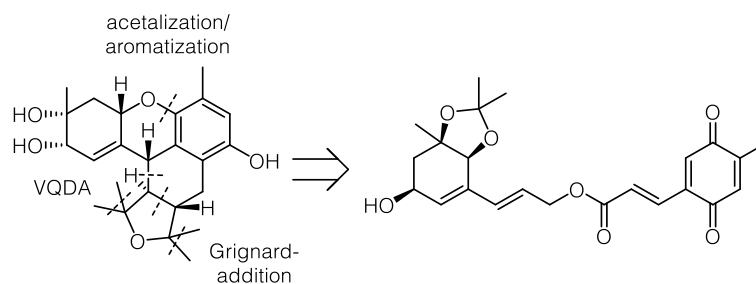
Chapter II: Synthetic Studies Towards the Meroterpenoids Bisacremin E, F and G.

Endophytic fungi grow within a plant host and usually live in a symbiotic relationship. Their growth involves continual metabolic interaction between fungus and host.⁵ Therefore endophytic fungi display a rich source of secondary metabolites often bearing interesting bioactivity.⁶ In 2015, Wei and co-workers discovered bisacremines E–G from a culture extract of the soil-derived strain *A. persicinum* SC0105.⁷ Bisacremin E and F are supposed to be derived from a formal [4+2] cycloaddition of two acremine F monomers, followed by dehydration to form the final tetrahydrofuran ring (scheme B). Though both the *endo* and the *exo* transition state would lead to a natural product, we assumed that this reaction would not require enzymatic catalysis but could proceed spontaneously in solution.



SCHEME B: Proposed biosynthesis of bisacremin E–G.⁷

This work describes the total synthesis of acremine F as well as studies towards its dimerization to form bisacremines E and F. Therefore, we investigated several mechanistic hypotheses for a biomimetic dimerization, including a cationic cascade, a radical cation Diels-Alder reaction and photochemical [2+2]-cycloaddition followed by formal Cope rearrangement to form the core of the natural products. Furthermore, studies towards the non-biomimetic synthesis of bisacremin G, involving a vinyl quinone Diels-Alder (VQDA) reaction, have been conducted (Scheme C).



SCHEME C: Retrosynthetic analysis of bisacremine G.

Chapter III: Exerting Photocontrol over G-Protein Coupled Receptors

Chapter three of this thesis describes the synthesis of light tunable modulators of G-protein coupled receptors (GPCRs). In detail, the synthesis of multiple tethered and non-tethered photoswitchable congeners derived from the known dopamine receptor (DAR) agonist PPHT are described as well as their ability to modulate DAR function *in cellulo*. Furthermore, the synthesis of light tunable derivatives of the known *m*AChR superagonist iperoxo is described as well as their effects when being applied to Langendorff preparations and cells transiently expressing *m*AChRs. The last part of this chapter describes the synthesis of photoswitchable derivatives of the TAS2R agonist denatonium (Figure A).

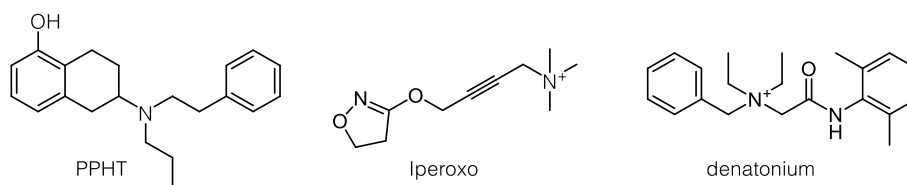


FIGURE A: Molecular structures of PPHT, iperoxo and denatonium

Chapter IV: Development of Photochromic Ion Channel Blockers

Chapter four of this thesis describes the synthesis of photoswitchable modulators of voltage gated ion channels and their evaluation in cellular systems. Therefore, we designed azobenzene containing derivatives of A-803467, a selective channel blocker of $\text{Na}_v1.8$, bupivacaine, a local anesthetic used in intensive medicine and raxatrigine, an anesthetic in clinical phase three. The ability of azo-bupivacain derivatives to photoblock voltage gated ion channels has been examined in HEK293T cells transiently overexpressing $\text{K}_v2.1$ and TREK channels as well as in mouse hippocampal neurons. The effect of azo-raxatrigine has been evaluated using high-throughput methods on cells stably expressing $\text{Na}_v1.5$, $\text{Na}_v1.7$ and $\text{K}_v1.3$ (Figure B).

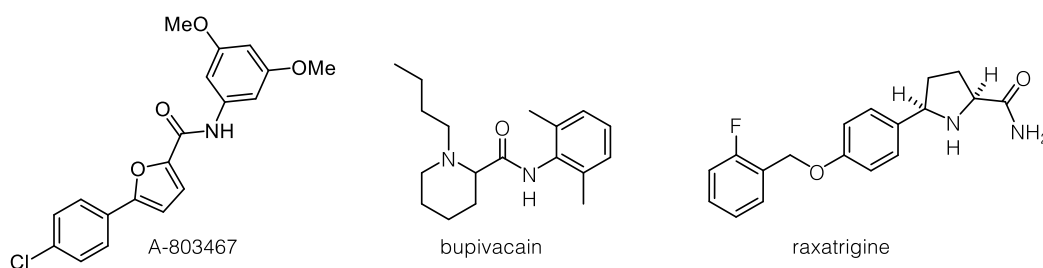


FIGURE B: Molecular structures of A-803467, bupivacaine and raxatrigine.

Chapter V: Studies Towards the Light-Dependent Regulation of Cytoskeletal Proteins

Chapter five of this thesis describes the development of photoswitchable modulators of the actin cytoskeleton network. In particular, a variety of light dependent inhibitors of Arp2/3 based on the selective inhibitors CK636 and CK666 have been synthesized and evaluated in *in vitro* assays confirming their ability to inhibit Arp2/3 dependent actin polymerization.

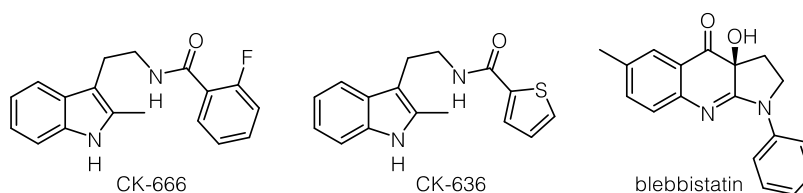


FIGURE C: Molecular structures of CK-666, CK-636 and blebbistatin.

Furthermore, we developed a robust route to azobenzene containing derivatives of the selective nonmuscular myosin II inhibitor blebbistatin which could be used for the investigation of myosin II dynamics in the actin network (Figure C).

Acknowledgements

First and foremost, I would like to thank my supervisor Prof. Dr. Dirk Trauner for giving me the opportunity to conduct my PhD in his group and for his support in the course of my PhD thesis. I am more than grateful for the challenging projects he provided and the freedom I was granted while working on them. His enthusiasm and patience for chemistry and for science in general are highly inspiring. Under his guidance I became a better a chemist and human.

Furthermore, I am very thankful to Prof. Dr. Oliver Trapp for agreeing to be the second reviewer of this thesis. I would also like to thank Prof. Dr. Anja Hoffmann-Röder, Prof. Dr. Konstantin Karaghiosoff, Prof. Dr. Ramus Linser and Dr. Dorian Didier for being on my defense committee.

I want to thank Dr. Julius Reyes, Dr. Nina Hartrampf, Felix Hartrampf, Dr. Martin Sumser, Daniel Terwilliger and Benjamin Williams who spend a considerable amount of time and effort on proofreading parts of this manuscript.

Further, I want to acknowledge my talented and very motivated students Dennis Rhein, Lina Judkele, Franziska Schüppel, Desirée Heerdegen, Alexander Kremsmair, Brigitta Bachmair, Elena Reinhardt, Henriette Lämmermann and Ebru Durak who did an amazing work and helped me a lot.

I am very thankful to all members of the Trauner and the Magauer group who made working during my PhD such a pleasant and inspiring experience. I especially want to thank Dr. Hongdong Hao and Dr. Julius Reyes for their advice and their great friendship in good and in hard times.

I would also like to thank the permanent staff of the Trauner group, Carrie Louis, Aleksandra Grilic, Luis de la Osa de la Rosa and Heike Traub for keeping the group running and always offering a helping hand.

Additionally, I would like to thank all the great people from different groups I was allowed to collaborate with, from whom I really learned a lot and who led me grow as a scientist: Dr. Andrea Brüggemann, Dr. Prashant Donthamsetti, Prof. Dr. Ehud Isacoff, Prof. Dr. Annette Nicke, Prof. Dr. Philipp Sasse, Dr. Maik Behrens, Prof. Dr. Erwin Sigel, Abou Ghali Majdouline, Dr. Julie Plastino and Prof. Dr. Marc Stadler.

I am also very grateful for the great work of the members of the analytical department: Dr. Werner Spahl, Sonja Kosak, Dr. David Stevenson, Claudia Dubler and Dr. Peter Mayer.

Most importantly, I want to thank my family for the great and sustained support they gave me and, especially Sarah for everything she has done. Without you all of this would not have been possible.

List of abbreviations

2,2-DMP	2,2-dimethoxypropane	DCC	dicyclohexylcarbodiimide
Å	Ångström	DCB	1,4-dicyanobenzene
ADP	adenosine diphosphate	DCE	1,2-dichloroethane
ADHD	attention deficient hyperactivity disorder	DDQ	2,3-dichloro-5,6-dicyano-1,4-benzoquinone
ADTN	2-amino-6,7-dihydroxy tetrahydronaphthalene	DIBAL-H	diisobutylaluminum hydride
Ac	acetyl	DIPA	diisopropylamine
ACh	acetylcholine	DIPEA	diisopropylethylamine
ATP	adenosine triphosphate	DMAP	4-(dimethylamino) pyridine
ATR	attenuated total reflection	DME	1,2-dimethoxyethane
AIDS	aaquired immune deficiency syndrome	DMF	dimethylforamide
Arp2/3	actin related protein complex	DMP	dess-martin periodinane
BHT	butylated hydroxytoluene	DMSO	dimethylsulfoxide
Boc	<i>t</i> -butyloxycarbonyl	DRG	dorsal root ganglion
° C	degree Celsius	<i>E</i>	opposite (trans)
cAMP	cyclic adenosine monophosphate	ECD	electron capture detector
CAN	ceric ammonium nitrate	<i>ee</i>	enantiomeric excess
CBS	Corey-Bakshi-Shibata	EI	electron impact ionization
CDI	1-1'-Carbonyldiimidazole	ESI	electrospray ionization
CNS	central nervous system	Et	ethyl
CoA	coenzyme A	EtOAc	ethyl acetate
CSA	camphersulfonic acid	FVP	flash vacuum pyrolysis
d	dublet (NMR)	G	gramm
δ	chemical shift (NMR)	GABA	γ-aminobutyric acid
DA	dopamine	GDP	guanosine diphosphate
DAG	diacylglycerol	GIRK	G-protein-coupled inwardly-rectifying potasium channel
DAR	dopamine receptor	GPCR	G-protein coupled receptor
DAMP	dimethyl diazomethyl phosphonate	GTP	guanosine triphosphate
		H	hour
		HEK	human embryonic kidney

HWE	Horner Wadsworth Emmons	Na _v	voltage gated sodium channel
IC ₅₀	half maximal inhibitory concentration	NBS	<i>N</i> -bromosuccinimide
IP3	inositol triphosphate	<i>n</i> -BuLi	<i>n</i> -butyllithium
IR	infrared	NEt ₃	triethylamine
<i>J</i>	coupling constant (NMR)	NHS	<i>N</i> -hydroxysuccinimide
kDa	kilodalton	Nm	nanometer
K _v	voltage gated potassium channel	NM II	nonmuscular myosin II
λ	wavelength	NMDA	<i>N</i> -methyl- <i>D</i> -aspartate
L	laevus (left)	NMR	nuclear magnetic resonance
LDA	lithium diisopropylamide	NPF	nucleation proliferation factor
LED	light-emitting diode	<i>o</i> DCB	1,2-dichlorobenzene
LiHMDS	lithium bis(trimethyl silyl)amide	PBS	phosphate-buffered saline
m	medium (IR)	PCC	pyridinium chlorochromate
m	meter	PDE	phosphodiesterase
m	multiplett (NMR)	PEG	polyethylene glycol
M2	myosin 2	Ph	phenyl
mAChR	muscarinic acetylcholine receptor	PhMe	toluene
μM	micromolar	PIFA	(bis(trifluoroacetoxy) iodo)benzene
Me	methyl	PIP2	phosphatidylinositol-4.5-bisphosphate
MeCN	acetonitrile	PLC	phospholipase C
Mes-Acr-Ph	9-mesityl-3,6-di- <i>tert</i> -butyl-10-phenylacridinium tetrafluoro borate	PMB	<i>para</i> -methoxybenzyl
MIC	minimal inhibitory concentration	PNS	peripheral nervous system
min	minutes	Ppm	parts per million
mmol	millimole	PPTS	pyridinium <i>p</i> -toluenesulfonate
MS	mass spectroscopy	PTSA	<i>p</i> -toluenesulfonic acid
MSN	spiny neuron	q	quartet (NMR)
nAChR	nicotinic acetylcholine receptor	R	undefined substituent
		R _f	retardation factor
		s	strong (IR)
		s	singulet (NMR)

t	time	TMS	trimethylsilyl
T	temperature	TIPS	triisopropylsilyl
TAS2R	taste receptor	TFA	trifluoroacetic acid
TBAF	tetrabutylammonium fluoride	TFE	trifluoroethanol
TBTA	tris[(1-benzyl-1 <i>H</i> -1,2,3-triazol-4-yl)methyl]amine	UV	ultra violet
TEMPO	2,2,6,6-tetramethyl piperinyloxy	VQDA	vinyl quinone diels alder
THF	tetrahydrofuran	w	weak (IR)
TMANO	trimethylamine N-oxide	wt%	weight percent
TBS	<i>tert</i> -butyldimethylsilyl	WASP	Wiskott-Aldrich syndrome family protein
TM	transmembrane domain	Z	together (cis)

Table of contents

Abstract.....	V
Acknowledgements.....	X
List of abbreviations.....	XII
Table of contents	XV
Chapter I	1
Synthesis of the Marine Natural Product Hippolachnin A	1
1.1 Introduction.....	2
1.1.1 Plakortin and Gracilioether natural products	2
1.1.2 Synthetic approaches towards the gracilioether family.....	3
1.1.3 Hippolachnin A – Isolation and Biosynthesis	9
1.1.4 Hippolachnin A as a target in total synthesis	10
1.2 Project outline.....	15
1.3 Results and Discussion.....	17
1.3.1 First generation approach – Retrosynthetic analysis.....	17
1.3.2 The [2+2]-Cycloaddition approach towards hippolachnin A	17
1.3.3 Second generation synthesis – The tropolone route to hippolachnin A ..	24
1.3.4 Synthesis of synthetic derivatives of hippolachnin A	29
1.4 Conclusion.....	30
Chapter II	31
Synthetic Studies Towards the Meroterpenoids Bisacremin E, F and G.....	31
2.2 Introduction.....	32
2.1.1 Acremine natural products – Isolation and biosynthesis.....	32
2.1.2 Synthetic approaches	35
2.1.3 Vinyl quinone Diels-Alder reactions in total synthesis.....	38
2.2 Project outline.....	42
2.3 Results and discussion	44
2.3.1 The cationic cascade	44
2.3.2 The radical cation Diels-Alder reaction approach	52
2.3.3 The divinylcyclobutane rearrangement	56
2.3.4 The classical Diels-Alder reaction route.....	58
2.3.5 Synthetic studies towards bisacremine G	67
2.4 Summary and outlook	73

Chapter III.....	75
Exerting Photocontrol over G-Protein Coupled Receptors.....	75
3.1 G-Protein coupled receptors (GPCRs).....	76
3.2 Dopamine receptors (DARs).....	78
3.2.1 Introduction.....	78
3.2.2 Project outline.....	81
3.2.3 Results and discussion.....	82
3.2.4 Summary and outlook.....	117
3.3 Muscarinic acetylcholine receptor (mAChR).....	118
3.3.1 Introduction.....	118
3.3.2 Project-outline.....	120
3.2.3 Results and discussion.....	121
3.3.4 Summary and outlook.....	125
3.4 TAS2R.....	126
3.4.1 Introduction.....	126
3.4.2 Project outline.....	127
3.4.3 Results and discussion.....	127
Chapter IV.....	131
Development of Photochromic Ion Channel Blockers.....	131
4.1 Introduction.....	132
4.2 Project outline.....	135
4.3 A-803467.....	136
4.4 Bupivacain.....	138
4.5 Raxatrigine.....	142
4.6 Conclusion.....	148
Chapter V.....	149
Studies Towards the Light-Dependent Regulation of Cytoskeletal Proteins.....	149
5.1 Development of Photoswitchable Arp2/3 Inhibitors.....	150
5.1.1 Introduction.....	150
5.1.2 Project Outline.....	154
5.1.3 Results and discussion.....	155
5.1.4 Conclusion.....	158
5.2 Development of Photoswitchable Inhibitors of Myosin II.....	159
5.2.1 Introduction.....	159
5.2.2 Project outline.....	161
5.2.3 Results and discussion.....	162

5.2.4	Conclusion	164
Chapter VI.....		165
Experimental Procedures		165
And Analytical Data		165
6.1	General experimental details	166
6.2	Experimental data for chapter I.....	168
6.3	Experimental data for chapter II.....	194
6.4	Experimental data for chapter III.....	237
6.4.1	Photoswitchable dopamine agonist.....	237
6.4.2	Photoswitchable mAChR agonists	266
6.4.3	Photoswitchable TAS2R agonists	275
6.5	Experimental data for chapter IV	278
6.5.1	Photoswitches based on A-803467.....	278
6.5.2	Photoswitches based on bupivacain	280
6.5.3	Photoswitches based on raxatrigine.....	288
6.6	Experimental data for chapter V	305
6.6.1	Photoswitches based on CK-636 and CK-666.....	305
6.6.1	Photoswitches based on blebbistatin	312
Chapter VII.....		325
Appendix		325
7.1	Crystallographic Data.....	326
7.2	¹ H and ¹³ C NMR spectra	334
7.2.1	¹ H and ¹³ C NMR spectra of Chapter I.....	335
7.2.2	¹ H and ¹³ C NMR spectra of Chapter II.....	428
7.2.3	¹ H and ¹³ C NMR spectra of Chapter III.....	366
7.2.4	¹ H and ¹³ C NMR spectra of Chapter IV	428
7.2.5	¹ H and ¹³ C NMR spectra of Chapter V	510
7.3	Literature	537

Chapter I

Synthesis of the Marine Natural Product Hippolachnin A

1.1 Introduction

1.1.1 Plakortin and Gracilioether natural products

Marine organisms are a rich source of structurally diverse secondary metabolites.¹⁻³ In this regard sponges have been largely studied and have provided a large fraction of such natural products. The plakortin family is a large class of polyketide natural products possessing high antimicrobial and antifungal activity derived from sponges of the genus *Plakortis* (Figure 1.1). Notably, many members of this family contain a cyclic peroxide.² Faulkner reported the first isolation of plakortin (**1.1**), a six-membered cycloperoxide, from *P. Halicondrioides* in 1978.⁸ However, it was not until 1999 that the absolute stereochemistry was assigned by Fattorusso.⁹ Subsequently, a series of related bioactive molecules have been isolated wherein the side chain at C6 differs by the length of the carbon chain demonstrating the diversity of building units that can be incorporated by the polyketide synthase.^{3, 10} While most of the isolated natural products offer some bioactivity, the plakortone-series proved to be highly potent activators of cardiac SR-Ca²⁺ ATPase.¹¹

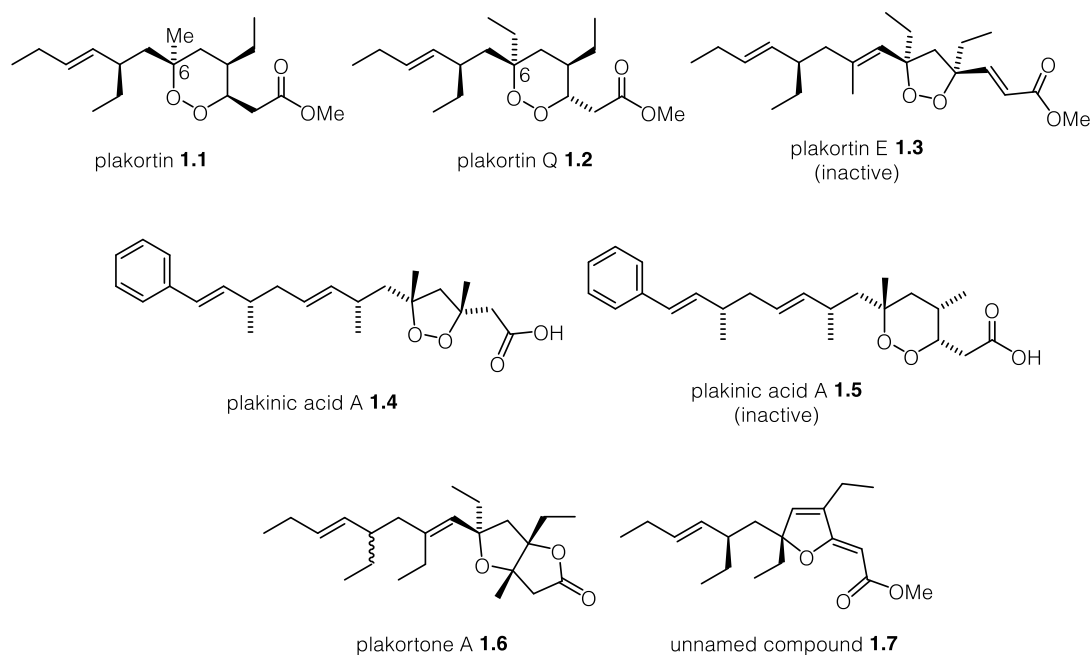


FIGURE 1.1: A selection of plakortin natural products.

In 2009, in hope of identifying potent leads from marine invertebrates against malaria infections, Fusetani and co-workers isolated the first members of the gracilioether family, a sub-class of the plakortin natural products, gracilioether A-C.¹² While all three isolated compounds showed antimalarial activity, only gracilioether A (**1.8**) featured a structurally interesting heterotricyclic ring system containing a six-membered endoperoxide (Figure

1.2). In 2012 the group of Zampella found further members of the gracilioethers, namely gracilioether E-J,¹³ and in 2013 the further oxidized natural product gracilioether K (**1.9**).¹⁴ While gracilioether E-G, I and J were almost completely inactive against all screened targets, gracilioether H (**1.10**) showed antimalarial activity against a chloroquine-resistant strain, proving the importance of the endoperoxide for bioactivity.¹³

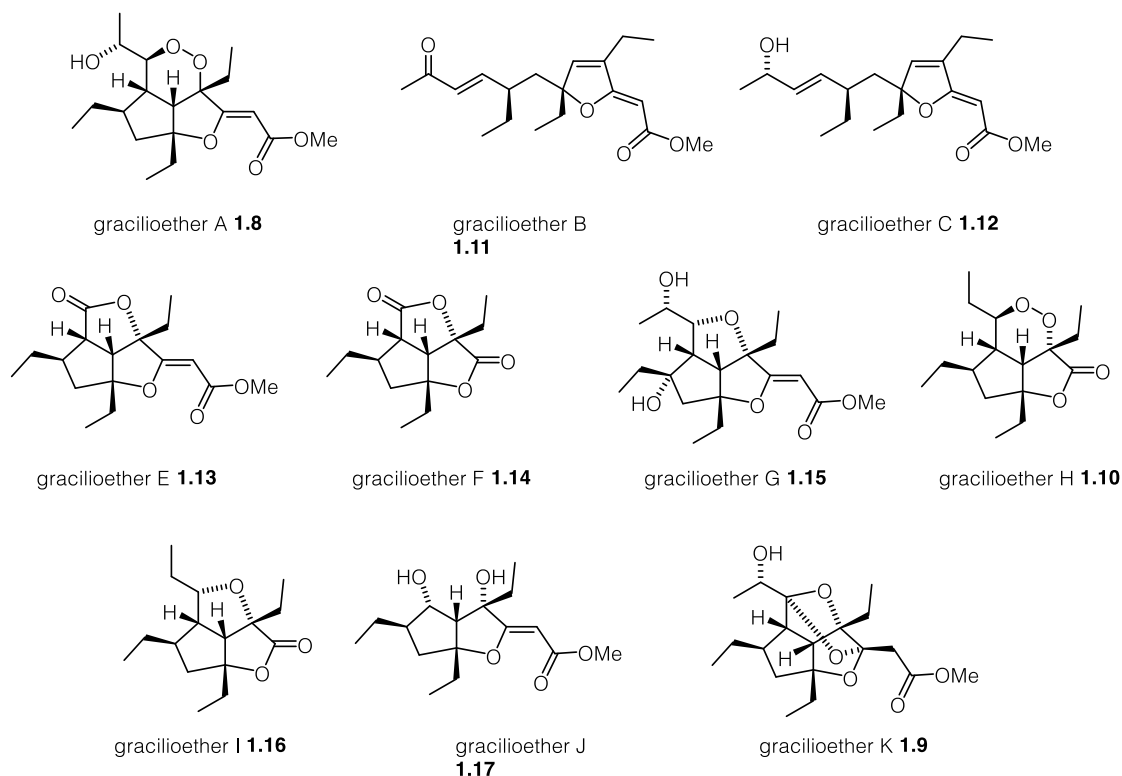
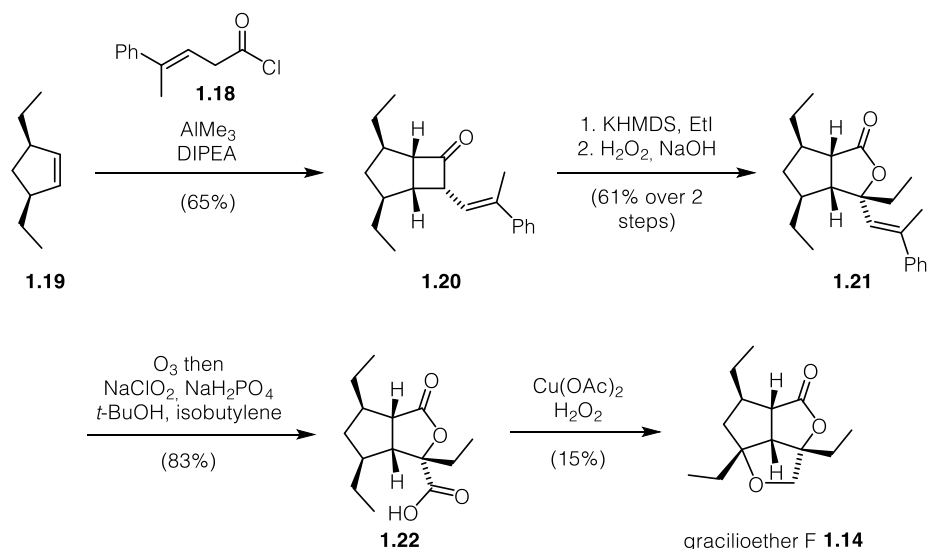


FIGURE 1.2: Members of the gracilioether family.

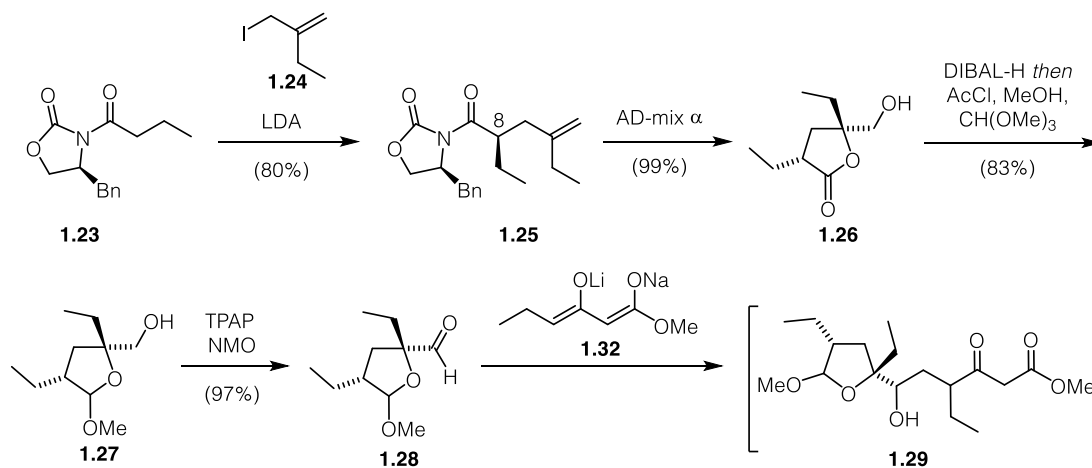
1.1.2 Synthetic approaches towards the gracilioether family

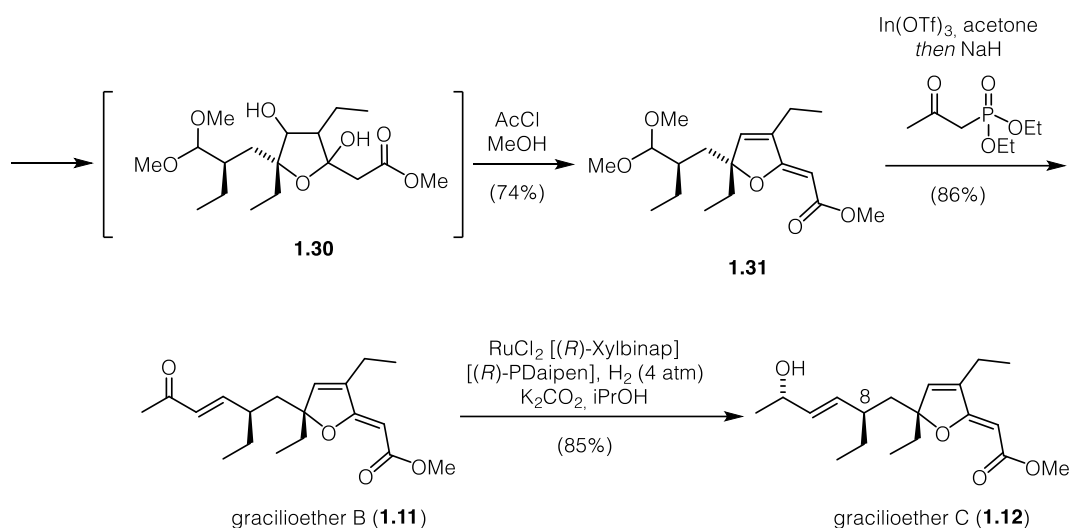
Due to their impressive structures and the diverse bioactivities, synthetic chemists immediately pursued *de novo* syntheses of members of this family. In 2014, Brown and co-workers reported the first synthesis of gracilioether F (**1.14**) (Scheme 1.1),¹⁵ relying on a late-stage C-H functionalization. Ketene formation from acid chloride **1.18** and subsequent [2+2]-cycloaddition with cyclopentene **1.19** furnished bicyclo[3.2.0]heptane **1.20**, which after alkylation and Baeyer-Villiger oxidation gave rise to bicyclic lactone **1.21**. After cleavage of the double bond and oxidative work-up, carboxylic acid **1.22** was obtained. C-H oxidation of the tertiary C-H bond then accessed gracilioether F (**1.14**).



SCHEME 1.1: Brown's synthesis of gracilioether F (1.14).¹⁵

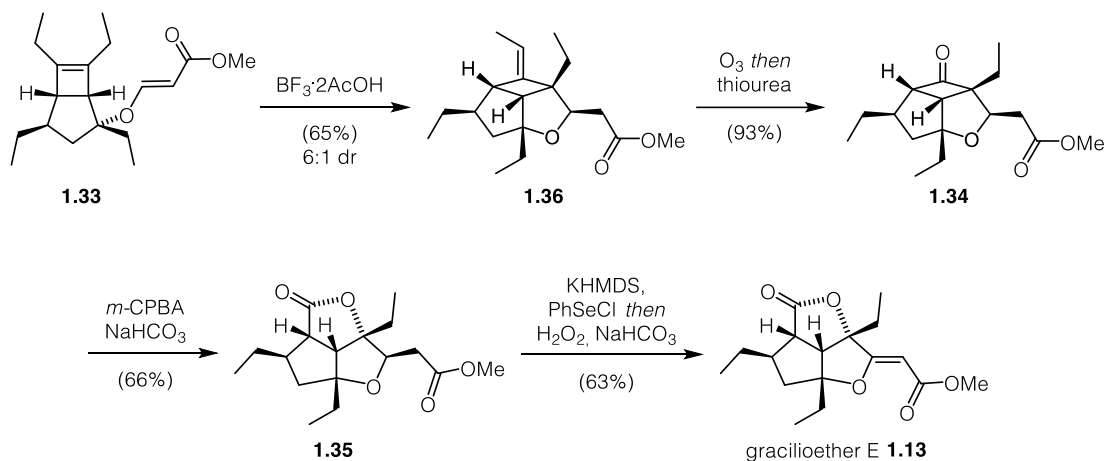
The first asymmetric total synthesis of gracilioether B (1.11) and C (1.12) was accomplished by Sorenson and co-workers in 2015 (Scheme 1.2).¹⁶ Alkylation of oxazolidinone 1.23 with allyl iodide 1.24 sets the C₈ stereocenter providing 1.25 in good yield. After dihydroxylation under Sharpless conditions and subsequent transesterification, lactone 1.26 was obtained, which could be converted into acetal 1.27 following reduction with DIBAL-H. Aldehyde 1.28 was then generated by Ley oxidation. Weiler alkylation then accessed β -ketoester 1.29, which directly underwent transacetalization to form hemiacetal 1.30 and dehydration in the same step to furnish furanylide 1.31. Transacetalization of 1.31 catalyzed by In(OTf)₃, followed by immediate Horner–Wadsworth–Emmons olefination with diethyl (2-oxopropyl)phosphonate afforded gracilioether B (1.11). Stereoselective reduction using Ru-catalysis then afforded gracilioether C (1.12) in good yield.





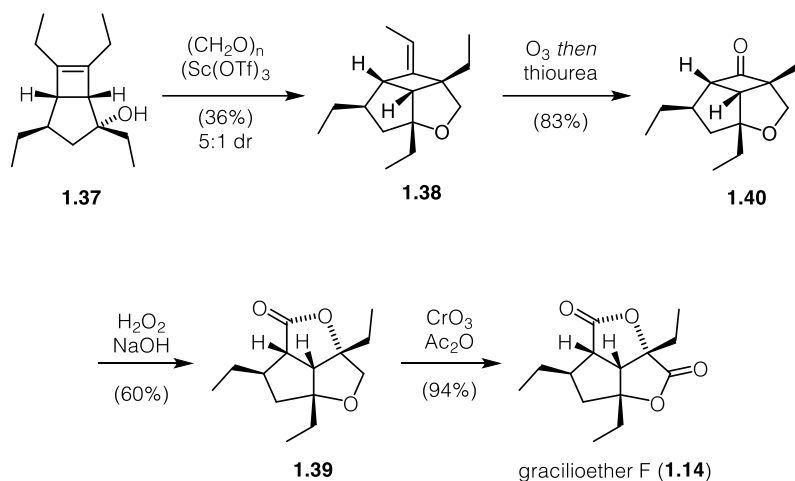
SCHEME 1.2: Sorenson's synthesis of gracilioether B (1.11) and C (1.12).¹⁶

Carreira and co-workers reported the first total synthesis of gracilioether E (1.13) in 2016.¹⁷ The tetrahydrofuran ring was obtained by a Lewis-acid catalyzed ene-cyclization of enone 1.33. Oxidative cleavage of the double bond then provided cyclobutanone 1.34, which was then subjected to Baeyer-Villiger oxidation to obtain the full heterocyclic core of 1.35. Installation of the (*Z*)-configured double bond by selenoxide elimination then furnished the natural product 1.13 (Scheme 1.3).



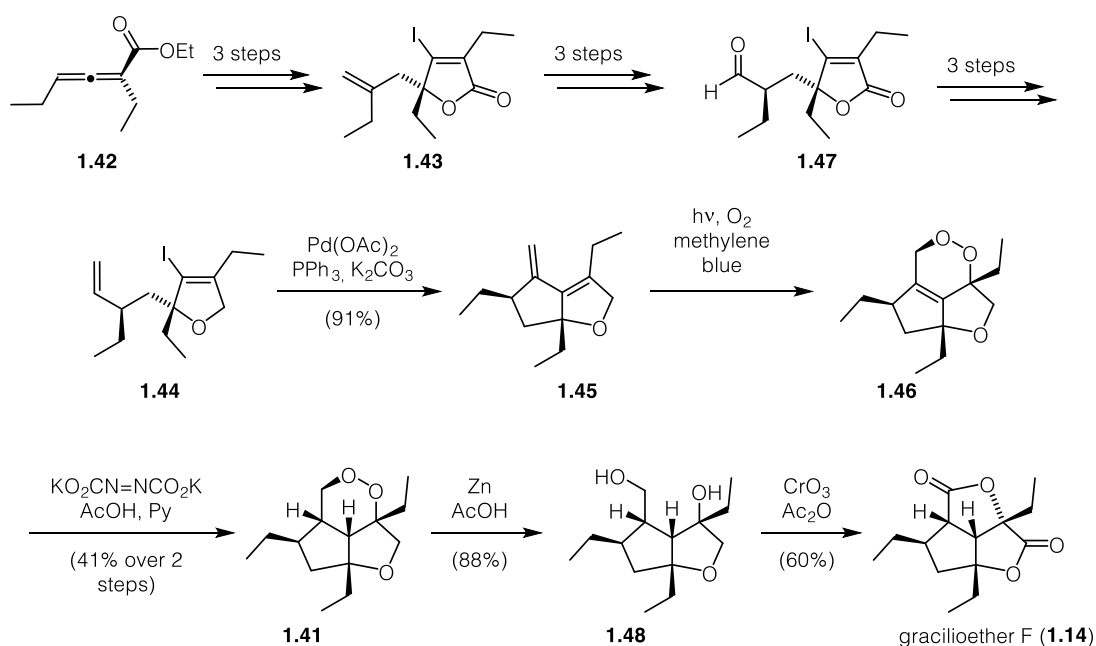
SCHEME 1.3: Carreira's synthesis of gracilioether E (1.13).¹⁷

Carreira applied a similar strategy to access gracilioether F (1.14), a congener lacking the vinylogous carbonate moiety. Prins-type cyclization of tertiary alcohol 1.37 with paraformaldehyde gave rise to tricycle 1.38 as a 5:1 mixture of diastereoisomers in moderate yield. Oxidative cleavage followed by Bayer-Villiger oxidation accessed the full core of 1.39. The natural product 1.14 was then obtained after oxidation of the most electron-rich C-H bond using CrO_3 (Scheme 1.4).



SCHEME 1.4: Carreira's synthesis of gracilioether F (1.14).¹⁷

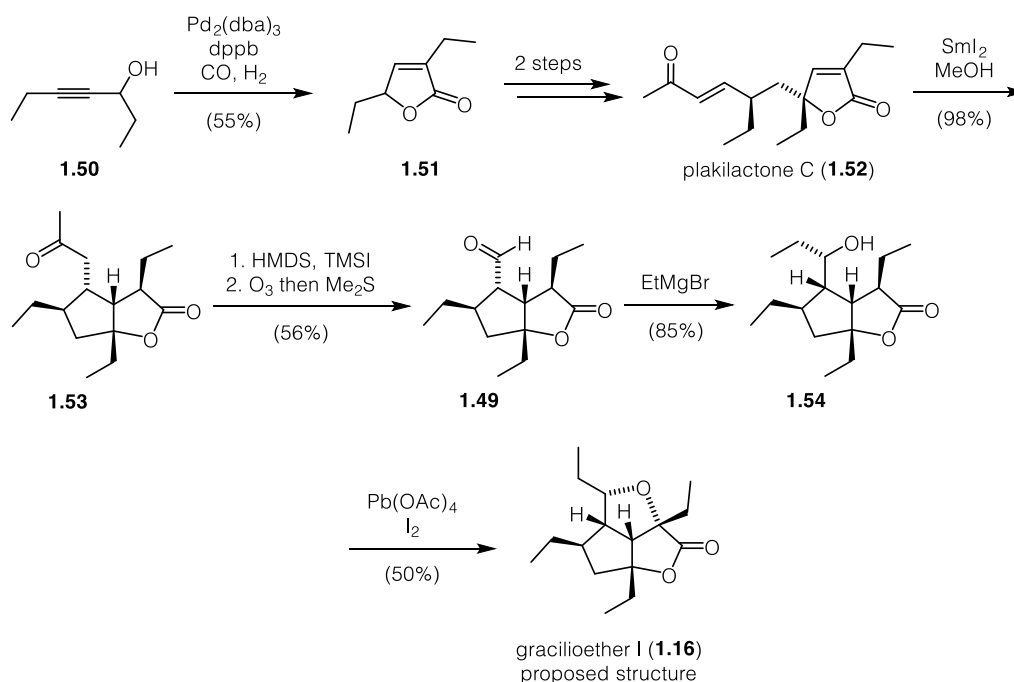
A biosynthetically-inspired total synthesis of gracilioether F (1.14) was reported by Wong and co-workers in 2016.¹⁸ Though the plakortin family of natural products contains many cyclic peroxides, he proposed that a 1,2-dioxane similar to 1.41 could serve as a common precursor to gracilioether members in a plausible biomimetic manner. Reductive cleavage of the O-O bond followed by oxidation could then for example access 1.14. The synthesis commences with allene 1.42 which was transformed into lactone 1.43 in three steps. Further manipulations then gave rise to vinyl iodide 1.44. Heck cyclization then provided diene 1.45 which underwent a Diels-Alder cycloaddition with singlet oxygen to obtain unstable 1,2-dihydrodioxine 1.46. 1.46 was immediately reduced to the stable 1,2-dioxane 1.41 utilizing diimide generated from dipotassium azodicarboxylate. Gracilioether F (1.14) was then furnished following



SCHEME 1.5: Wong's synthesis of gracilioether F (**1.14**).¹⁸

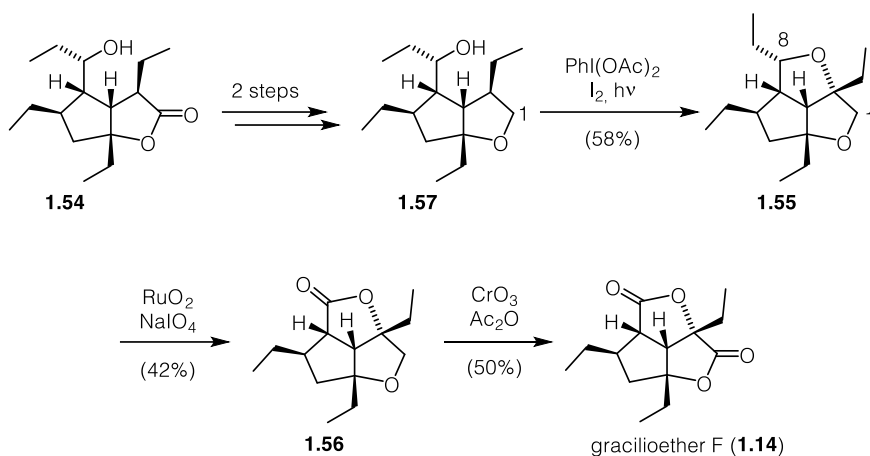
reductive cleavage of the O-O bond and twofold oxidation (Scheme 1.5).

In 2017, Wu and co-workers reported the syntheses of a variety of gracilioethers based on common precursor **1.49** (Scheme 1.6).¹⁹ Palladium-catalyzed hydrocarbonylation of alkyne **1.50** provided rapid access to lactone **1.51**. Further manipulations by alkylation, hydroboration and oxidation provided plakilactone C (**1.52**) which could then undergo a Sm(II)-mediated Michael-addition to yield ketone **1.53**. Silyl enol ether formation followed by oxidative cleavage furnished aldehyde **1.49** as a divergent precursor. Grignard addition and C-H oxidation accessed the proposed structure of gracilioether I (**1.16**). The C-H oxidation proved a challenging problem. All methods for this type of transformation failed, presumably due to the adjacent carbonyl group. Nevertheless, a mixture of Pb(OAc)₄ and iodine accomplished the transformation. Unexpectedly, the ¹H and ¹³C NMR data were not consistent with those reported by Zampella in 2012, suggesting that **1.16** had been incorrectly assigned.



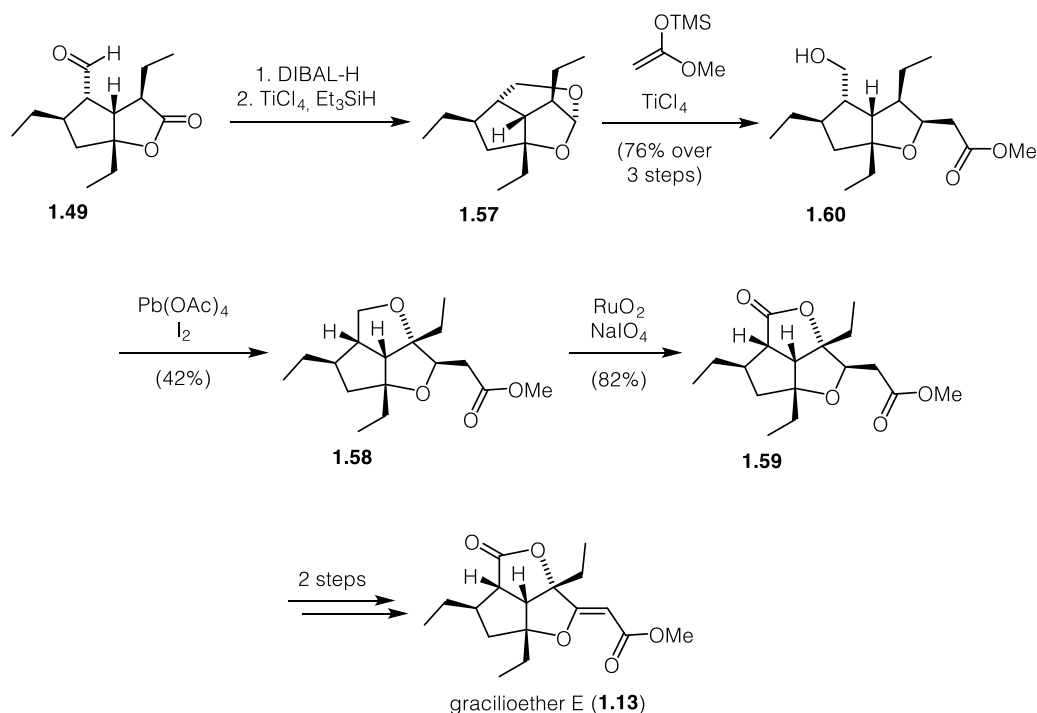
SCHEME 1.6: Wu's synthesis of the proposed structure of gracilioether I (**1.16**).¹⁹

Starting from alcohol **1.54**, Wu was also able to complete the formal synthesis of gracilioether F (**1.14**) (Scheme 1.7). Without the carbonyl group at C₁, the C-H oxidation proceeded well under standard conditions, giving cyclic ether **1.55**. Attempts to oxidize the C₁ position in order to obtain **1.16** resulted in oxidative cleavage of the C-C bond at position C₈, providing lactone **1.56**. The synthesis of **1.14** was then accomplished as previously described by Carreira and Wong.^{17-18, 20}



SCHEME 1.7: Wu's formal synthesis of gracilioether F (1.14).¹⁹

Wu's entry to gracilioether E (1.13) began with DIBAL-H reduction of aldehyde 1.49 followed by the addition of TiCl_4 and Et_3SiH to afford, unexpectedly, acetal 1.57. Mukaiyama aldol addition and C-H oxidation, as previously described, accessed 1.58. Oxidation of the most electron-rich C-H bond gave lactone 1.59, which could then be converted into gracilioether E (1.13) as described by Carreira¹⁷ (Scheme 1.8).



SCHEME 1.8: Wu's formal synthesis of gracilioether E (1.13).¹⁹

1.1.3 Hippolachnin A – Isolation and Biosynthesis

In 2013, Lin and co-workers reported the isolation of the polyketide natural product hippolachnin A (**1.61**), together with its proposed biogenetic precursor **1.62**, from the ethanolic extract of the South China Sea sponge *Hippospongia Lachne* collected from the Xisha Islands (Figure 1.3).⁴ While **1.62** was already disclosed as a PPAR γ antagonist,²¹ hippolachnin A (**1.61**) exhibited potent antifungal activity against the pathogenic fungi *Cryptococcus neoformans*, *Trichophyton rubrum*, and *Microsporum gypseum* with an MIC value of 0.41 μ M for each fungus. The structure **1.61** was elucidated based on NMR, IR and mass spectral data, comparison of the calculated and measured ECD spectra confirmed the absolute stereochemistry of the molecule. Hippolachnin A consists of a heterotricyclic core featuring six contiguous stereocenters and bears an unusual array of four ethyl groups on its convex face. It also contains a (*Z*)-configured vinylogous carbonate.

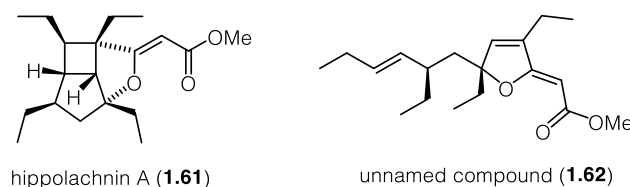
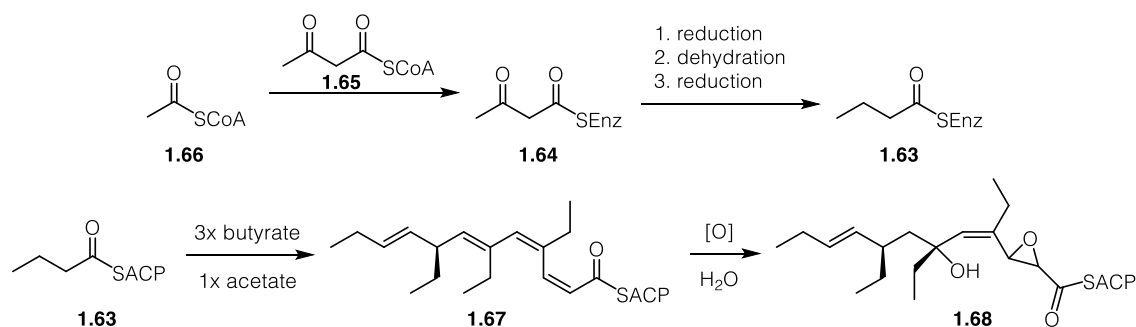
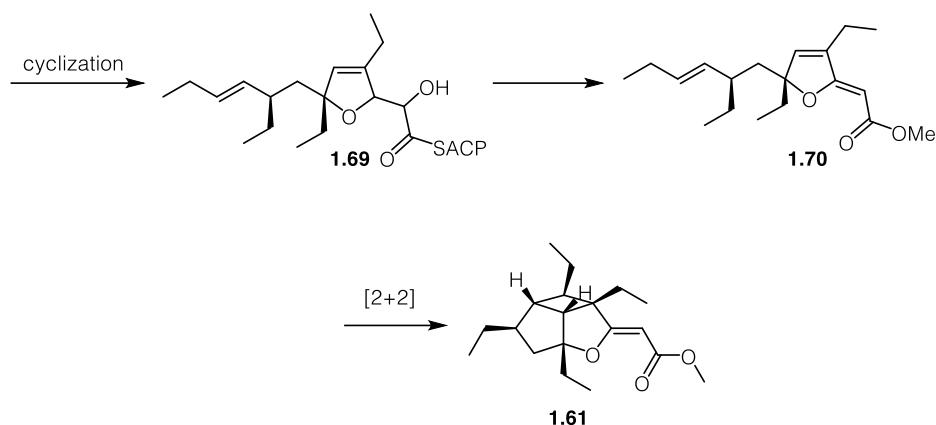


FIGURE 1.3: Hippolachnin A (**1.61**) and its proposed biogenetic precursor **1.62**.

Lin's biosynthetic proposal of hippolachnin A is shown in Scheme 1.9.⁴ The ethyl groups of the natural product are proposed to be derived from butyrate units (**1.63**). Kubanek and Anderson furthermore, proposed that the activated butyrate arises from a reduction-dehydration-reduction sequence of β -ketoester **1.64**.²² **1.64** itself is derived from the condensation of malonyl CoA (**1.65**) with acetyl CoA (**1.66**) followed by decarboxylation. Four butyrate and one acetate units are then assembled by a polyketide synthase to form tetraene **1.67**. Oxidation to epoxide **1.68** followed by cyclization then furnishes 2,3-dihydrofuran **1.69**, which upon elimination and transesterification gives cyclization precursor **1.70**. **1.70** subsequently undergoes a



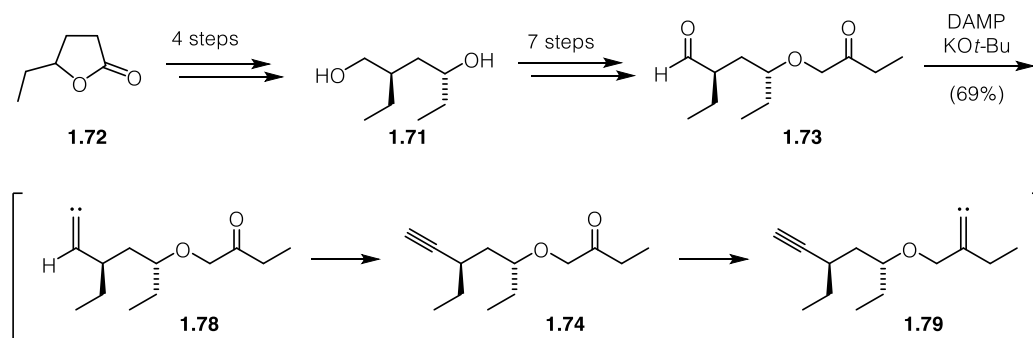


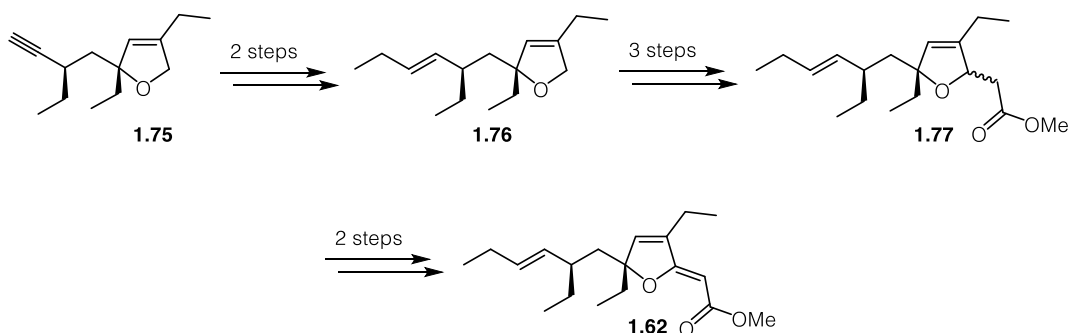
SCHEME 1.9: Proposed biosynthetic formation of hippolachnin A (**1.61**).⁴

[2+2]-cycloaddition to form the natural product.

1.1.4 Hippolachnin A as a target in total synthesis

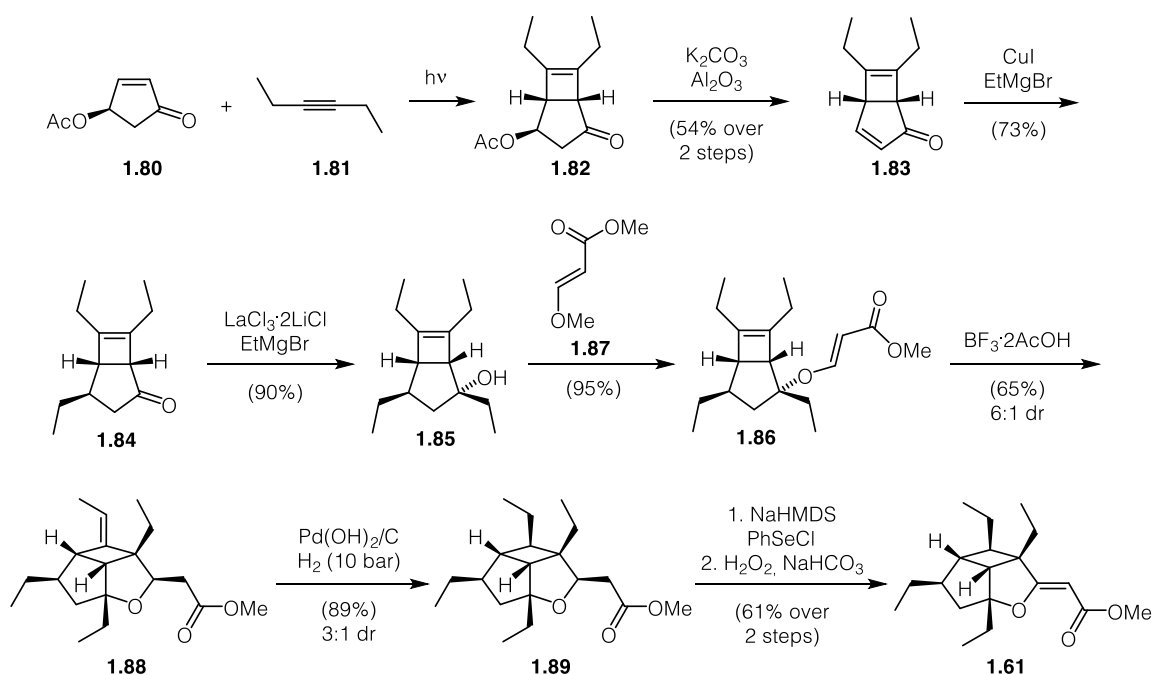
Although hippolachnin A is proposed to be derived from lactone **1.62**, the latter had already been isolated in 1980 from *Plakortis halichondrioides*.²³ In 2005, Ohira and co-workers reported the first total synthesis of **1.62**, relying on a late-stage C-H insertion.²⁴ Diol **1.71** was prepared from γ -caprolactone (**1.72**) by a four-step sequence. Further manipulations gave rise to the key intermediate **1.73**. Treatment of **1.73** with dimethyl diazomethylphosphonate (DAMP) first generated the vinylidene carbene from the aldehyde, which could undergo a 1,2-hydride shift to give alkyne **1.74**. A second equivalent of DAMP then generated the vinylidene carbene from the ketone that further underwent a 1,5 C-H insertion, forming dihydrofuran **1.75**. Alkene **1.76** was then obtained by a short alkylation and reduction sequence. Further manipulation accessed methyl ester **1.77** as an inconsequential mixture of diastereoisomers which could be transformed into the natural product **1.62** (Scheme 1.10).





SCHEME 1.10: Ohira's synthesis of lactone **1.62**.²⁴

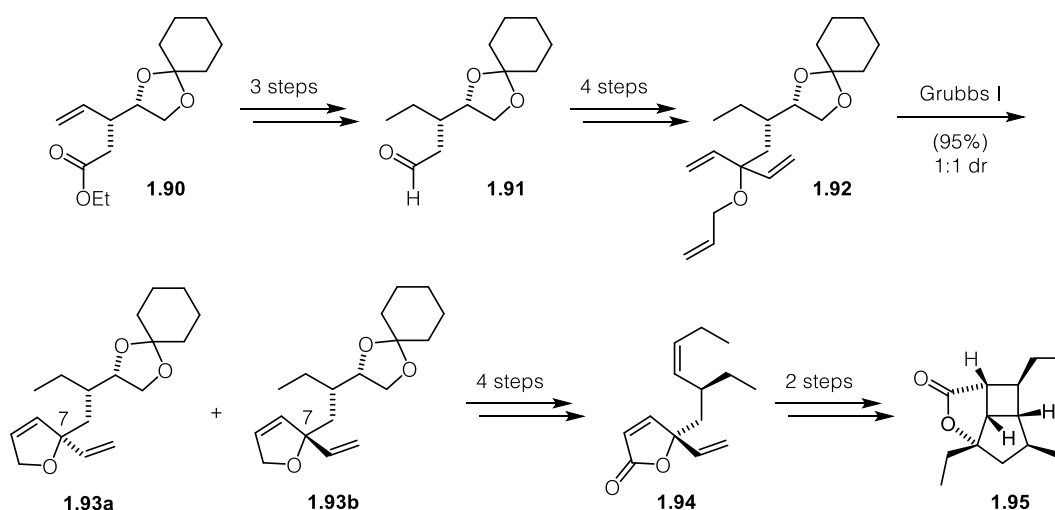
The first total synthesis of hippolachnin A (**1.61**) was reported in 2014 by Carreira and co-workers (Scheme 1.11).²⁰ His strategy relies on a [2+2]-cycloaddition to access the bicyclo[3.2.0]heptane core and a Lewis acid catalyzed ene-reaction to forge the tetrahydrofuran ring. The synthesis begins with a photochemical [2+2]-cycloaddition of cyclopentenone **1.80** with 3-hexyne (**1.81**), furnishing bicyclo[3.2.0]heptene **1.82**. Subsequent elimination under mildly basic conditions provided enone **1.83**. Stereoselective cuprate addition gave rise to ketone **1.84** that was then alkylated under Knochel's conditions to give tertiary alcohol **1.85**. While it proved difficult to alkylate **1.85**, vinylogous carbonate **1.86** was obtained when **1.85** was stirred neat in (*E*)-methyl-3-methoxyacrylate (**1.87**) in the presence of PPTS for prolonged reaction times. Lewis acid-catalyzed ene-cyclization accessed key cyclobutane **1.88** that could selectively be reduced under heterogeneous hydrogenation conditions to give the



SCHEME 1.11: Carreira's synthesis of hippolachnin A (**1.61**).²⁰

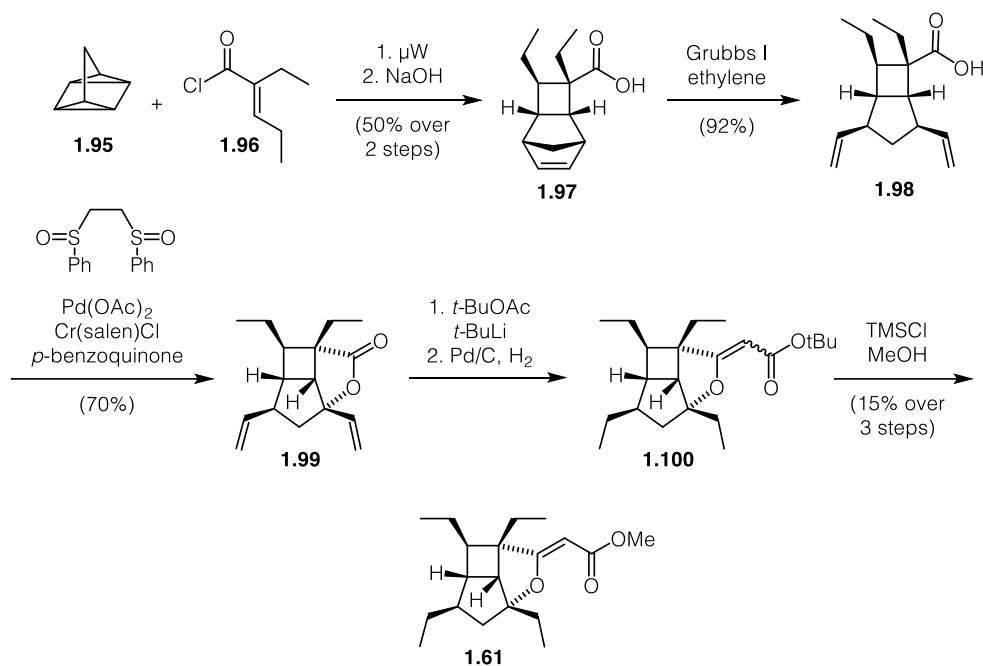
kinetic product **1.89**. Further α -phenylselenation followed by oxidation and elimination allowed for the clean formation of hippolachnin A (**1.61**).

Shortly after Carreira published his synthesis, Gosh reported his studies towards the asymmetric total synthesis of **1.61** employing a ring-closing metathesis and a photochemical [2+2]-cycloaddition (Scheme 1.12).²⁵ Ethyl ester **1.90** was derived from D-mannitol and could be transformed by a three-step procedure into aldehyde **1.91**. After further manipulations, key triene **1.92** was obtained. Ring-closing metathesis afforded 2,3-dihydrofuran **1.93a** and **1.93b** as a 1:1 mixture of diastereoisomers at C₇. **1.93b** was then transformed into the cycloaddition precursor **1.94** by a four-step protocol. Photochemical [2+2]-cycloaddition followed by hydrogenation of the vinyl group then provided lactone **1.95**, which is only lacking the vinylogous carbonate moiety and one ethyl group of the natural product. However, using D-mannitol as the starting material would lead to the unnatural enantiomer of hippolachnin A (**1.61**).



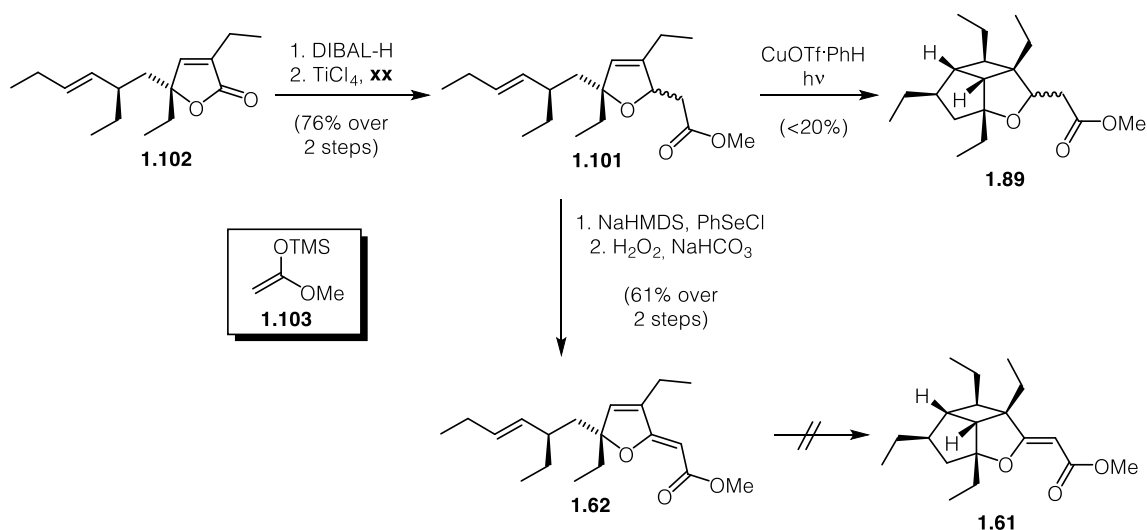
SCHEME 1.12: Gosh's synthetic studies towards hippolachnin A (**1.61**).²⁵

In 2016, Brown and Wood reported a collaborative synthesis of hippolachnin A (**1.61**),²⁶ the shortest up to date. The cyclobutane ring was formed through a [2+2+2]-cycloaddition of quadricyclane (**1.95**) to acid chloride **1.96** and the heterocycle by a late-stage allylic C–H oxidation (Scheme 1.13). Tricycle **1.97** underwent efficient ring-opening metathesis employing ethylene to form diene **1.98**. Allylic C–H oxidation using White's catalyst then provided lactone **1.99** in good yield. Aldol condensation followed by reduction of both double bonds furnished vinylogous carbonate **1.100** as a mixture of (*Z*)- and (*E*)- isomers. Finally, transesterification yielded the natural product **1.61**.



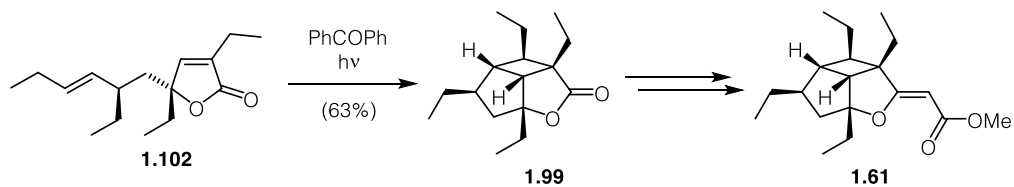
SCHEME 1.13: Wood and Brown's collaborative synthesis of hippolachnin A (**1.61**).²⁶

A biomimetic strategy towards **1.61** was reported in early 2017 by Wu (Scheme 1.14).¹⁹ **1.101** was obtained by employing conditions previously reported by Ohira with slight modifications. Even though hippolachnin A (**1.61**) is proposed to be derived from lactone **1.62**, irradiation of **1.62** with a mercury lamp did not trigger the desired [2+2]-cycloaddition but only led to isomerization of the double bond of the side chain. While the [2+2]-cycloaddition using the conjugate diene did not proceed, the Cu-catalyzed reaction of the isolated double bond gave access to Carreira's intermediate **1.89** in low yield.



SCHEME 1.14: Wu's attempted biomimetic synthesis of hippolachnin A (**1.61**).¹⁹

A more efficient reaction was found however, when lactone **1.102** was irradiated in the presence of benzophenone as a photosensitizer (Scheme 1.15). Resultant cyclobutane **1.99**, an advanced intermediate of Brown and Wood's synthesis was obtained in good yield, thus accomplishing a formal synthesis of hippolachnin A **1.61**.



SCHEME 1.15: Wu's formal synthesis of hippolachnin A (**1.61**).¹⁹

1.2 Project outline

Opportunistic infections by ubiquitous fungi represent a major challenge to the immunocompromised. The yeast *Cryptococcus neoformans*, for instance, can cause life-threatening meningitis and affect the lungs and skin of patients with advanced acquired immunodeficiency syndrome (AIDS).²⁷⁻³⁰ Hippolachnin A (**1.61**) was recently isolated from the South China Sea sponge *Hippospongia lachne* and proved to be highly potent against several pathogenic fungi, including *C. neoformans* (MIC = 0.41 μ M).⁴ Therefore, hippolachnin A (**1.61**) could provide an important lead in the search for novel drugs against these fungi.

Hippolachnin A (**1.61**) represents a unique synthetic challenge by virtue of bioactivity and molecular scaffold. At the beginning of the project, no complete synthesis of this natural product had been reported. Above all, the caged 4-5-5 heterotricyclic core featuring six contiguous stereocenters was expected to cause several difficulties in its preparation. Furthermore, the thermodynamically less favoured (*Z*)-double bond provides an additional distinct challenge. The goal of this project was to provide a scalable synthetic route also enabling the synthesis derivatives of the natural product and probe their bioactivity.

Therefore, we identified two possible retrosynthetic analyses of **1.61**. In the first retrosynthesis, we envisioned installation of the vinylogous carbonate late in the synthesis from lactone **1.99**. The cyclobutane and the tetrahydrofuran would simultaneously be formed by an intramolecular [2+2]-cycloaddition of a precursor containing a cyclopentene scaffold linked to an alkene (Figure 1.4).

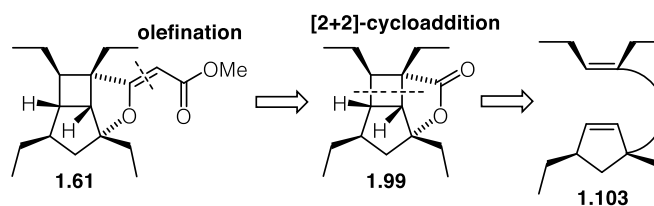


FIGURE 1.4: First retrosynthetic analysis of **1.61**.

Alternatively, the tetrahydrofuran ring of the natural product would be forged by a chelation-controlled trapping of a β -ketoester enolate by an *in situ* generated carbocation,³¹ forming the kinetic product (Figure 1.5). The vicinal diethyl groups would be accessed by a three-component coupling using α,β -unsaturated ester **1.104** and an ethyl nucleophile and ethyl electrophile. **1.104** should be accessible *via*

bicyclo[2.1.0]heptadienone **1.105** which would be formed from tropolone methyl ether **1.106** by disrotatory 4π -electrocyclization followed by excited state rearrangement.³²

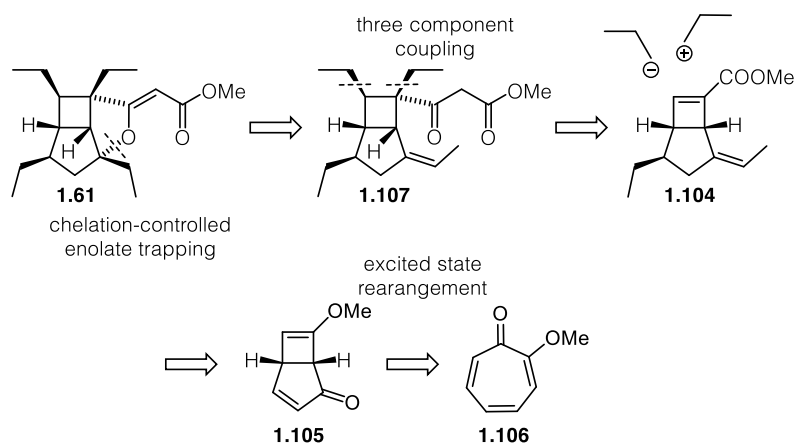
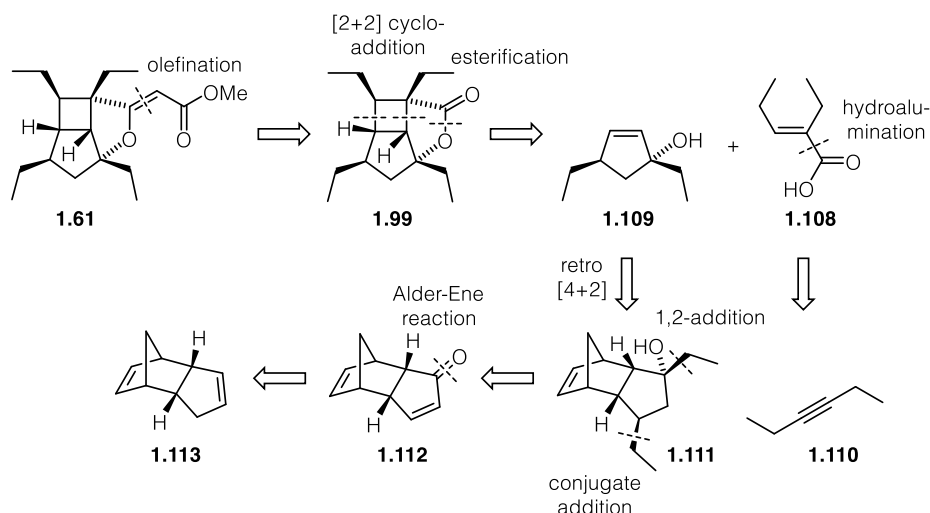


FIGURE 1.5: Second retrosynthetic analysis of **1.61**.

1.3 Results and Discussion

1.3.1 First generation approach – Retrosynthetic analysis

The first retrosynthetic analysis of hippolachnin A (**1.61**) is depicted in Scheme 1.16. It was envisioned to access **1.61** through Peterson olefination of lactone **1.99**, which would be derived by an intramolecular [2+2]-cycloaddition following esterification of acid **1.108** and tertiary alcohol **1.109**. **1.108** would be obtained by hydroalumination of 3-hexyne (**1.110**) followed by trapping with CO₂.³³ Tertiary alcohol **1.109** would be provided by retro-[4+2]-cycloaddition of bicycle **1.111**,³⁴ derived from enone **1.112** by conjugate addition³⁵ followed by 1,2-addition.³⁶ Additions to **1.112** should be governed by the shape of the bicycle and arrive from the convex side of the molecule. Schenk-ene reaction of dicyclopentadiene (**1.113**) with singlet oxygen would provide enone **1.112**.



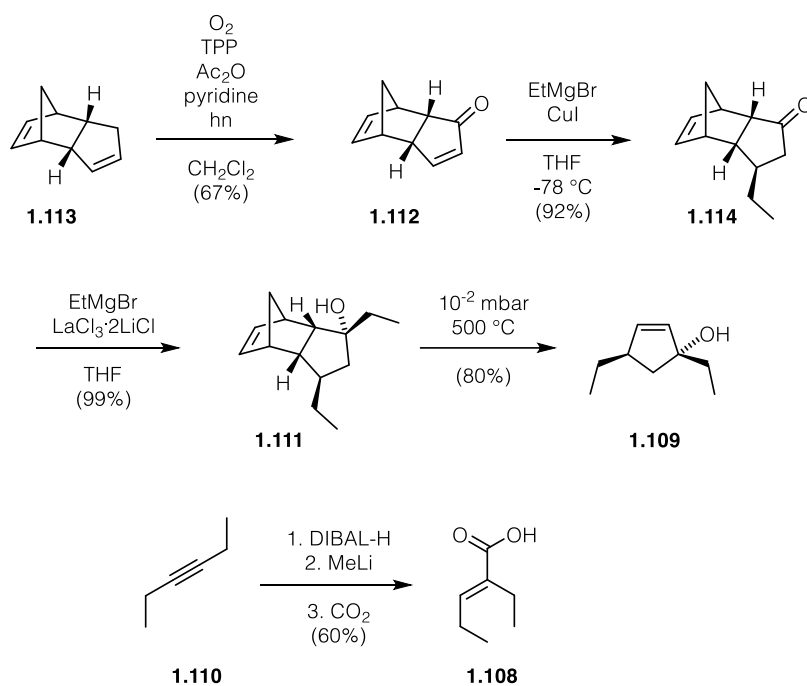
Scheme 1.16: Retrosynthetic analysis of hippolachnin A (**1.61**).

Even though the [2+2]-cycloaddition of an acyclic α,β -unsaturated ester was anticipated to provide a major challenge, we envisioned that, conducting the reaction in an intramolecular fashion, might allow efficient trapping of the initial diradical.

1.3.2 The [2+2]-Cycloaddition approach towards hippolachnin A

The synthesis commenced with the preparation of tertiary alcohol **1.109** from dicyclopentadiene (**1.113**) (Scheme 1.17). Conjugate addition from the convex side of enone **1.112** obtained from the Alder-ene reaction of **1.113** with singlet oxygen afforded ketone **1.114**. Subsequent 1,2-addition of EtMgBr mediated by LaCl₃·2LiCl yielded tertiary alcohol **1.111** as a single diastereoisomer. While initial attempts of activating the

bicycle by heat followed by *in situ*-trapping of the generated cyclopentadiene resulted only in recovered starting material or decomposition, flash vacuum pyrolysis (FVP) cleanly provided tertiary alcohol **1.109** in good yield. It is worth noting that a FVP-apparatus could be improvised, consisting of two vigreux columns connected to a cooled S-shaped tube.



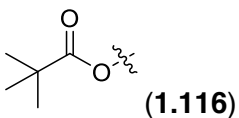
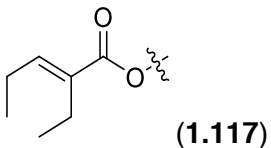
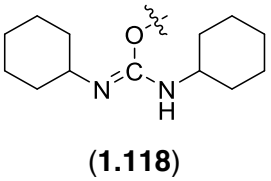
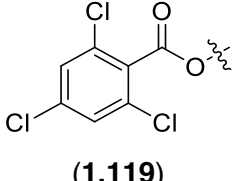
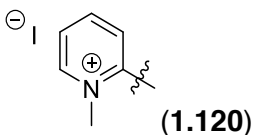
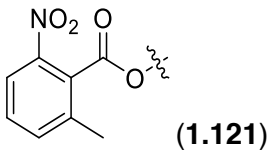
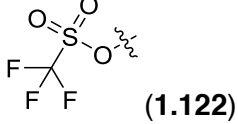
SCHEME 1.17: Synthesis of coupling partners **1.109** and **1.108**.

Hydroalumination of 3-hexyne (**1.110**) followed by aluminate formation allowed efficient trapping of carbon dioxide to carboxylic acid **1.108**.

With both building blocks in hand, several conditions for the esterification have been screened (Table 1.1).

TABLE 1.1: Conditions of the esterification of alcohol (**1.109**) and acid (**1.108**).

	R =	Base	Additive	Temp.	Observation
1	Cl (1.115)	pyridine	DMAP	0 °C - RT	starting material
2	Cl (1.115)	<i>i</i> -PrMgCl	none	0 °C	starting material

3	Cl (1.115)	<i>n</i> -BuLi	AgSbF ₆	-78 °C - 0 °C	decomposition
4	 (1.116)	<i>i</i> -PrMgCl	none	0 °C	starting material
5	 (1.117)	pyridine	DMAP	RT - 100 °C	starting material
6	 (1.118)	none	DMAP	RT	formation of 1.117
7	 (1.119)	NEt ₃	DMAP	40 °C	formation of 1.117
8	 (1.120)	NEt ₃	none	40 °C	formation of 1.117
9	 (1.121)	NEt ₃	DMAP	RT	formation of 1.117
10	 (1.122)	<i>n</i> -BuLi	none	-50 °C - RT	decomposition

Standard esterification conditions utilizing the acid chloride only resulted in isolation of the free acid after work up. Attempts to generate the naked acylium ion only led to decomposition of the starting materials. Using various mixed anhydrides as an electrophile provided anhydride **1.117** instead of the ester (Entry 6-9). **1.117** was found to be stable to column chromatography and proved to be inefficient in ester formation, even at elevated temperatures. While both the acid chloride and the mixed anhydride were able to react sufficiently with *t*-BuOK to form the *t*-butyl ester, acetylation of tertiary alcohol **1.109** with acetic anhydride and DMAP failed to show any traces of product even after prolonged reaction times.

As the steric hindrance of the tertiary alcohol could not be overcome, we decided to install the fourth ethyl group at a later state of the synthesis. The revised retrosynthesis is depicted in Scheme 1.18.

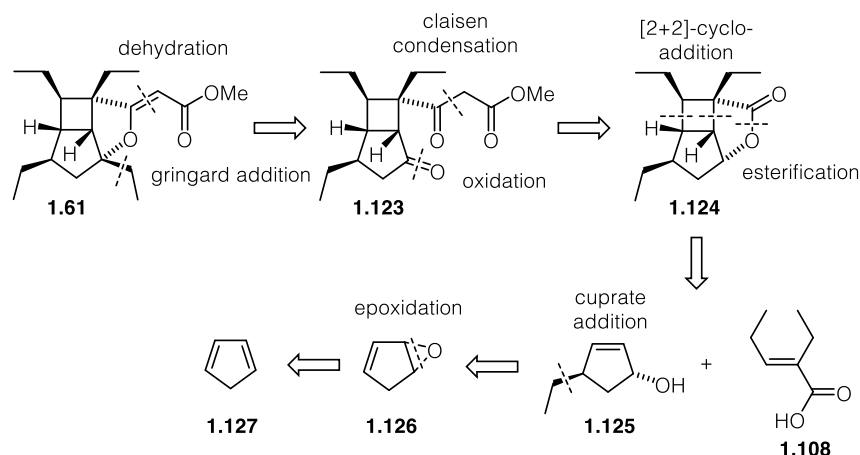
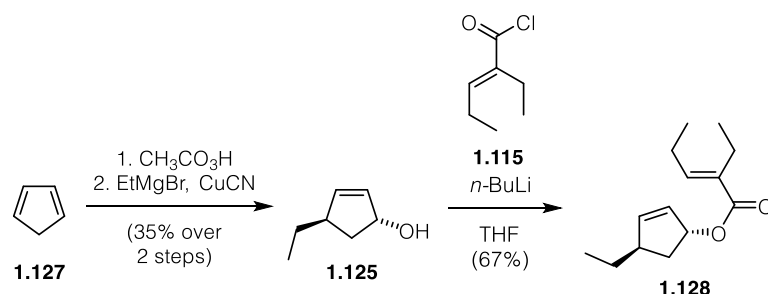


FIGURE 1.18: Revised retrosynthetic analysis of **1.61**.

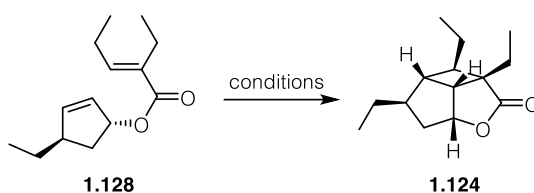
We envisioned closing the tetrahydrofuran ring by hemiketal-formation of a β -ketoester and a tertiary alcohol followed by dehydration. The tertiary alcohol would be generated by a Grignard addition to a ketone. The β -ketoester should be derived by Claisen condensation of methyl acetate and lactone **1.124**. Lactone **1.124** would be traced back to an intramolecular [2+2]-cycloaddition of an ester formed by alcohol **1.125** and acid **1.108**. Allylic alcohol **1.125** would again be derived from cyclopentadiene (**1.127**).

Epoxidation of cyclopentadiene (**1.127**) followed by S_N2' displacement with ethylcyanocuprate provided allylic alcohol **1.125** in moderate yield (Scheme 1.19). Quantitative formation of the lithium alkoxide and subsequent quenching with acid chloride **1.115** gave rise to allylic ester **1.128**.



SCHEME 1.19: Synthesis of allylic ester **1.128**.

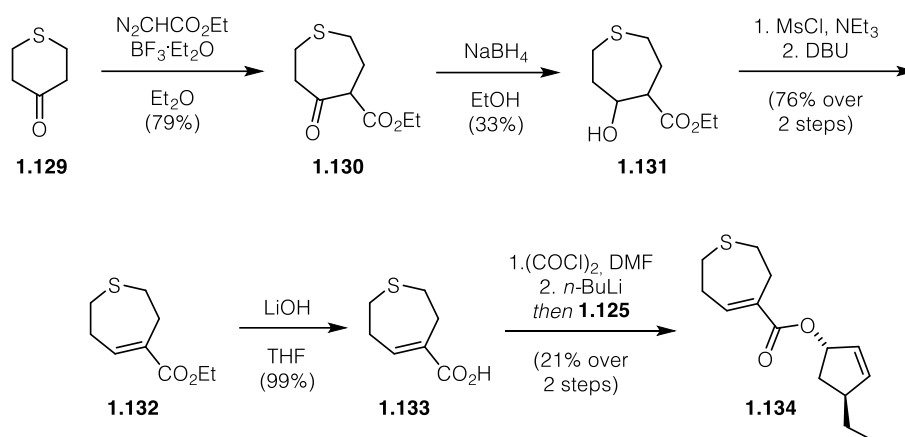
With the desired precursor in hand, we went on to screen the intramolecular [2+2]-cycloaddition of diene **1.128** (Table 1.2).

TABLE 1.2: Screening of the intramolecular [2+2]-cycloaddition of **1.128**.

Entry	Solution	Additive	Observation
1	acetone		starting material + (<i>E</i>) conformer
2	acetone / acetonitrile 1:1		starting material + (<i>E</i>) conformer
3	acetone / benzene 1:1		starting material + (<i>E</i>) conformer
4	acetone / CH ₂ Cl ₂ 1:1		starting material + (<i>E</i>) conformer
5	benzene	benzophenone	starting material + (<i>E</i>) conformer
6	methylene chloride	benzophenone	starting material + (<i>E</i>) conformer
7	acetonitrile	benzophenone	starting material + (<i>E</i>) conformer
8	acetone	benzophenone	starting material + (<i>E</i>) conformer
	CH ₂ Cl ₂	EtAlCl ₂	starting material
	CH ₂ Cl ₂	TiCl ₄	starting material
	CH ₂ Cl ₂	ZnBr ₂	starting material
	CH ₂ Cl ₂	Tf ₂ NH	starting material

All screening conditions were performed under high dilution conditions at 0.01 M, and irradiation was achieved using 310 nm LEDs in a Rayonet[®]-reactor. Unfortunately, no cycloaddition product could be observed, and only starting material commingled with its (*E*)-configured isomer was isolated. The addition of Lewis acids to these types of systems is known to activate the carbonyl group of the ester, which could lead to a Prins-type cyclization. Unfortunately, only starting material was observed.

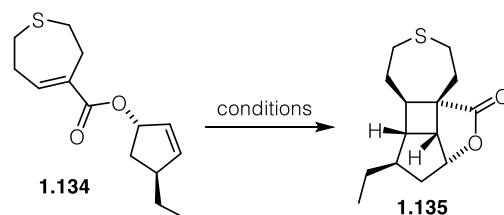
While excitation of the system proceeded smoothly as proved by the observation of the (*E*)-configured isomer, we wondered whether π -bond rotation was too fast to allow for capture of the diradical by the tethered olefin or whether the linker between the double bonds was too short, making it impossible for the double bonds to reach it other. In order to prevent isomerization, we wanted to incorporate the enone double bond into a ring system. This was achieved by stitching the ends of the ethyl groups together using a sulphur bridge. In order to increase the length between the two double bonds and allow the molecule to be more flexible, the ester moiety was elongated to a β -ketoester (Scheme 1.19).



SCHEME 1.19: Synthesis of cyclization precursor **1.134**.

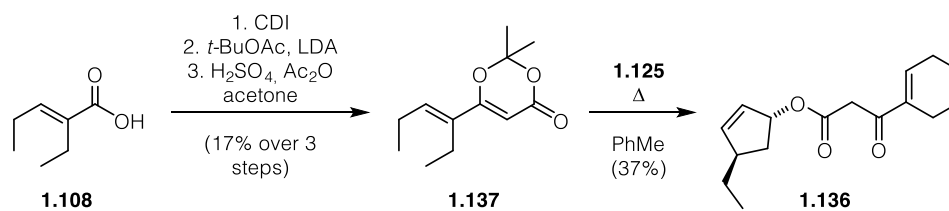
Ring expansion of tetrahydrothiopyranone **1.129** using ethyl diazoacetate gave rise to thiepanone **1.130** which, after reduction, mesylation and elimination provided ethyl ester **1.132**.³⁷ Saponification followed by activation of the carboxylic acid as the acid chloride and subsequent esterification accessed enoate **1.134** in moderate yields. With the cyclic cyclization precursor in hand, we investigated the [2+2]-cycloaddition (Table 1.3).

TABLE 1.3: Screening for the [2+2] cycloaddition under 310 nm irradiation.



Entry	Solvent	Observation
1	MeCN	decomposition
2	CH ₂ Cl ₂	decomposition
3	benzene	decomposition
4	acetone	decomposition

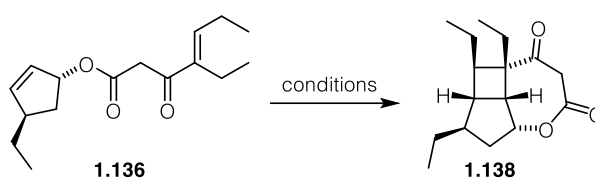
Unfortunately, illumination of **1.134** in different solvents showed no trace of product. After irradiation the clear solution became cloudy, and NMR analysis of the mixture indicated decomposition of the starting material. While excitation of the molecule was possible, no productive pathways could be observed, which might be due to a preferred conformation of the molecule where both olefins are pointing into opposite directions. In order to provide more flexibility to the molecule, β -ketoester **1.136** was prepared (Scheme 1.20).



SCHEME 1.20: Preparation of β -ketoester **1.136**.

Activation of acid **1.108** with CDI and subsequent Claisen condensation with *t*-BuOAc followed by ketalization gave dioxanone **1.137**. Retro-[4+2]-cycloaddition and trapping of the resulting ketene with alcohol **1.125** resulted in formation of β -ketoester **1.136**.

TABLE 1.4: Screening of the [2+2]-cycloaddition of **1.136** under 310 nm irradiation.



Entry	Solvent	Observation
1	MeCN	Complex mixture
2	CH ₂ Cl ₂	Complex mixture
3	benzene	Complex mixture
4	acetone	Complex mixture

Irradiation of **1.136** using 310 nm LEDs resulted in a complex mixture (Table 1.4) independent of the solvent used. As a result of the unsuccessful formation of the bicyclo[3.2.0]heptane core, we decided to modify the strategy as described in the next chapter.

1.3.3 Second generation synthesis – The tropolone route to hippolachnin A

Reproduced with permission from Nils Winter and Dirk Trauner, *J. Am. Chem. Soc.* **2017**, *139*, 11706–11709. Copyright 2017 American Chemical Society.³⁸

Thiocarbonyl Ylide Chemistry Enables a Concise Synthesis of (±)-Hippolachnin A

Nils Winter[†] and Dirk Trauner^{*,†,‡,§}

[†]Department of Chemistry, Ludwig-Maximilians-Universität München, Butenandtstraße 5-13, 81377 Munich, Germany

[‡]Department of Chemistry, New York University, Silver Center, 100 Washington Square East, Room 712, New York, 10003, United States

Supporting Information

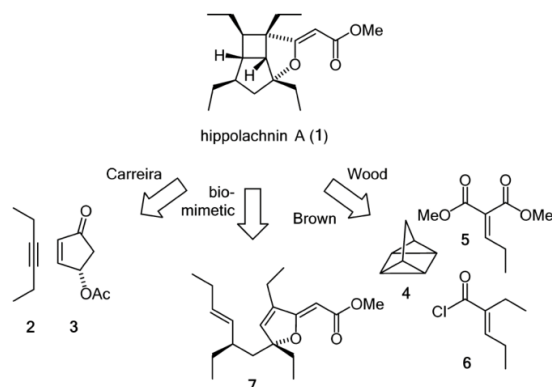
ABSTRACT: Hippolachnin A (**1**) is an antifungal polyketide that bristles with ethyl groups mounted onto a caged heterotricyclic core. It has shown potent activity against *Cryptococcus neoformans*, a yeast that can affect immunocompromised patients as an opportunistic pathogen. Herein we describe a concise, diversifiable, and scalable synthesis of (±)-hippolachnin A (**1**). It features a powerful photochemical opening step, a diastereoselective addition of an ethyl cuprate and an unusual strategy to install two additional ethyl groups that makes use of a thiocarbonyl ylide generated *in situ*.

Opportunistic infections with ubiquitous fungi represent a major challenge to the immunocompromised. The yeast *Cryptococcus neoformans*, for instance, can cause life-threatening meningitis and affect the lungs and skin of patients with advanced acquired immunodeficiency syndrome (AIDS).¹ Indeed, cryptococcosis is the second most common AIDS-related complication in sub-Saharan Africa. Although a combination of intravenously applied amphotericin and oral flucytosin provides an effective treatment, these drugs are associated with significant side effects, difficult administration regimes, high costs, and the emergence of resistance.² Therefore, the development of new drugs that target *C. neoformans* and related opportunistic fungal pathogens remains an important goal.

Hippolachnin A (**1**) could provide an important lead in this search. It was recently isolated from the South China Sea marine sponge *Hippospongia lachne*³ and proved to be highly potent against several pathogenic fungi, including *C. neoformans* (MIC = 0.41 μM). Biosynthetically, it was identified as a polyketide of the gracilioether family. Though it bears structural similarities to other members of this series, the 4–5–5 tricyclic core of hippolachnin A is unique.⁴ Presumed to be of photochemical origin, it features six contiguous stereocenters and bears an unusual array of four ethyl groups on its convex face.

Given its attractive molecular structure and potent bioactivity, it is no surprise that hippolachnin A has attracted the attention of several synthetic groups (Scheme 1). The first total synthesis was achieved by Carreira in 2015.⁵ In this case, the cyclobutane core was formed via photochemical [2+2] cycloaddition of 3-hexyne (**2**) to cyclopentenone **3** and the heterocycle was installed using an ene-type cyclization. In 2016,

Scheme 1. Synthetic Approaches to Hippolachnin A



Brown and Wood reported a collaborative synthesis in which the cyclobutane was formed through a [2+2+2] cycloaddition of quadricyclane (**4**) to either **5** or **6** and the heterocycle through a late-stage allylic C–H oxidation.⁶

The synthesis of a presumed biomimetic precursor, compound **7**, which was isolated together with **1**, was described by Ohira et al. in 2005⁷ and by Wu et al. in 2017.⁸ However, irradiation of **7** with UV light did not yield **1** but only resulted in isomerization of the vinylogous ester moiety.⁸ Possibly, the desired cyclization could be achieved using more biomimetic irradiation conditions, as has been recently demonstrated with other marine natural products.⁹

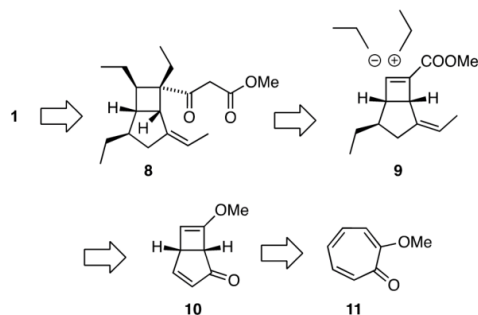
We now report a concise synthesis of hippolachnin A that is also based on a photochemical key step, albeit a decidedly nonbiomimetic one. Our retrosynthetic analysis is shown in Scheme 2. In a deviation from previous syntheses, we planned to close the heterocyclic ring in **1** by *O*-alkylation of an enolized β-keto ester **8**.¹⁰ The two vicinal ethyl groups would be installed by three-component coupling involving an ethyl nucleophile, an ethyl electrophile and the Michael acceptor **9**. This key intermediate, in turn, could be traced back to the known bicyclo[3.2.0]heptadiene derivative **10**, a photoisomer of the readily available tropolone ether **11**.

Accordingly, our synthesis opens with the photochemical conversion of **11** into methoxy bicyclo[3.2.0]heptadienone **10**

Received: June 30, 2017

Published: July 28, 2017

Scheme 2. Retrosynthetic Analysis of Hippolachnin A



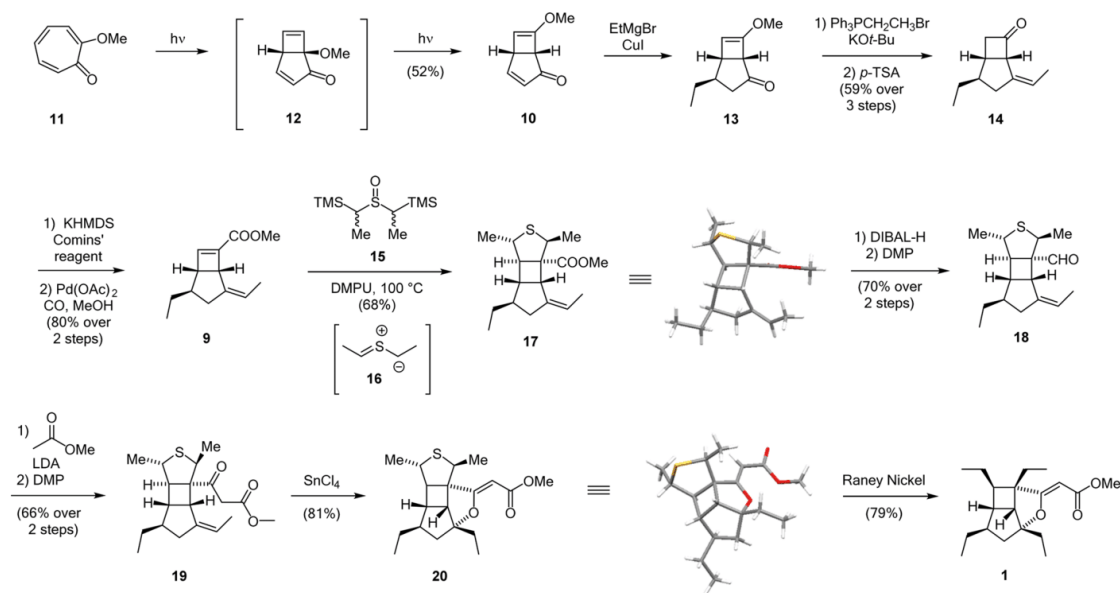
(Scheme 3). This unusual photochemical reaction has been studied in detail by Dauben et al. and proceeds via disrotatory 4π -electrocyclization of **11** to yield **12**, which then undergoes an excited state rearrangement to afford **10**.¹¹ Stereoselective conjugate addition of ethyl cuprate¹² from the convex side to **10**, followed by Wittig olefination¹³ and hydrolysis of the enol ether,¹⁴ gave rise to ketone **14** as a 10:1 mixture of *Z*- and *E*-isomers (major isomer shown). Homologation of ketone **14** was then achieved by formation of the vinyl triflate¹⁵ and subsequent carbomethoxylation.¹⁶

The stage was now set for the introduction of the two remaining ethyl groups. As outlined in our retrosynthesis (Scheme 1), we planned to achieve this by addition of an ethyl nucleophile, followed by alkylation with an ethyl electrophile. Ethyl cuprate addition to unsaturated ester **9** indeed occurred with complete regio- and stereoselectivity at C₁₀. However, the

subsequent deprotonation and alkylation with iodoethane only afforded a 1:2 mixture of diastereoisomers in favor of the desired isomer (see Supporting Information).¹⁷ Although the major isomer could be easily converted into an advanced intermediate of the Wood–Brown synthesis,⁶ we felt that such a low level of selectivity was not acceptable for an efficient synthesis of **1**.

To overcome this issue, we turned to a cycloaddition chemistry. We reasoned that the 1,3-dipolar addition of thiocarbonyl ylide **16** to the more reactive double bond of **9**, followed by reductive desulfurization of the resulting tetrahydrothiophene, would deliver both ethyl groups to the convex side.¹⁸ To this end, we synthesized the sulfoxide **15** as a precursor of the highly reactive **16**. Compound **15** is a homologue of the parent reagent introduced by Achiwa and was prepared in two steps from sodium sulfide and 1-chloroethyl trimethylsilane (see Supporting Information).¹⁹ Indeed, heating of **15** in the presence of **9** afforded tetrahydrothiophene **17** as a single diastereomer. Single crystal X-ray structure analysis showed that the methyl groups adopt a *trans*-configuration with respect to the tetrahydrothiophene ring, which can be explained by the stepwise nature of thiocarbonyl ylide cycloadditions.²⁰

The final phase of our synthesis required the elongation of the methyl ester into a β -keto ester and its closure to a tetrahydrofuran to obtain the full carbon skeleton of hippolachnin A. Unfortunately, all attempts at a crossed Claisen condensation or even hydrolysis of **17** failed, presumably due to steric hindrance.²¹ However, a reduction–oxidation sequence gave rise to aldehyde **18** in good yield. Aldol addition²² of methyl acetate then afforded the corresponding β -hydroxy ester, which could easily be oxidized to yield β -keto ester **19**.

Scheme 3. Total Synthesis of Hippolachnin A^a

^aKOt-Bu = potassium *tert*-butoxide, *p*-TSA = *para*-toluenesulfonic acid, KHMDS = potassium hexamethyldisilazide, DMF = dimethylformamide, DMPU = 1,3-dimethyl-3,4,5,6-tetrahydro-2(1*H*)-pyrimidinone, DIBAL-H = diisobutylaluminum hydride, DMP = Dess–Martin periodinane, LDA = lithium diisopropylamide, TBAB = tetrabutylammonium bromide, DCE = 1,2-dichloroethane.

Formation of the tin enolate followed by chelation-controlled trapping of the simultaneously generated tertiary carbocation¹⁰ gave rise to (*Z*)-configured vinylogous carbonate **20**.²³ Desulfurization with Raney nickel in THF²⁴ then provided hippolachnin A. Overall, the synthesis proceeds in 12 steps from the known bicyclo[3.2.0]heptane **10** and provides **1** on a 100 mg scale.

Our synthesis will serve as a platform for the development of more potent and more soluble antifungal agents as well as molecular probes with which to identify the biological target(s) of hippolachnin A. It relies on a photoisomerization of a tropolone to construct the bicyclic carbon core of the natural product. Asymmetric variants of this rearrangement have been described.²⁵ The distinctive four ethyl substituents of **1** are introduced by a cuprate conjugate addition, a Wittig olefination, followed by etherification, and a thiocarbonyl ylide cycloaddition, followed by eventual reductive desulfurization. The latter amounts to the addition of an alkane over an (electron poor) alkene. Despite its high strategic value, this sequence has been rarely used in synthesis.²⁶ This may be because, apart from the parent system, precursors of the requisite thiocarbonyl ylides have not been widely available. Future studies will expand on this chemistry and explore its usefulness in the synthesis of hippolachnin A derivatives as well as other complex natural products. Biological investigations of analogs of hippolachnin A, in particular compound **20** and its oxidation products, are currently ongoing and will be reported in due course.

■ ASSOCIATED CONTENT

5 Supporting Information

The Supporting Information is available free of charge on the ACS Publications website at DOI: 10.1021/jacs.7b06815.

Experimental procedures, spectroscopic data and copies of NMR-spectra (PDF)

CIF file for compound **17** (CCDC 1563493) and compound **20** (CCDC 1563492) (CIF files are also available free from charge on <https://www.ccdc.cam.ac.uk/structures/>) (CIF)

■ AUTHOR INFORMATION

Corresponding Author

*dirktrauner@nyu.edu

ORCID

Dirk Trauner: 0000-0002-6782-6056

Notes

The authors declare no competing financial interest.

■ ACKNOWLEDGMENTS

The authors thank Henriette Lämmermann for experimental assistance and Dr. Peter Mayer for X-ray structure analysis. Additionally, we acknowledge the Deutsche Forschungsgemeinschaft (SFB 749 and CIPSM) for generous funding. Dr. Julius R. Reyes is acknowledged for excellent support with the preparation of this manuscript.

■ REFERENCES

(1) (a) Kauffman, C. A. *Cryptococcosis*. In *Goldman-Cecil Medicine*, 25th ed.; Goldman, L., Schafer, A. I., Eds.; Elsevier Saunders, Philadelphia, PA, 2016; chap 336. (b) Govender, N. P.; Patel, J.; van Wyk, M.; Chiller, T. M.; Lockhart, S. R. *Antimicrob. Agents Chemother.* **2011**, *55*, 2606–2611. (c) Loyse, A.; Thangaraj, H.; Easterbrook, P.; Ford, N.; Roy, M.; Chiller, T.; Govender, N.

Harrison, T. S.; Bicanic, T. *Lancet Infect. Dis.* **2013**, *13*, 629–637. (d) Sabiiti, W.; Robertson, E.; Beale, M. A.; Johnston, S. A.; Brouwer, A. E.; Loyse, A.; Jarvis, J. N.; Gilbert, A. S.; Fisher, M. C.; Harrison, T. S.; May, R. C.; Bicanic, T. *J. Clin. Invest.* **2014**, *124*, 2000–2008. (e) Li, S. S.; Mody, C. H. *Proc. Am. Thorac. Soc.* **2010**, *7*, 186–196.

(2) Vermes, A.; Guchelaar, H. J.; Dankert, J. *J. Antimicrob. Chemother.* **2000**, *46*, 171–179.

(3) Piao, S. J.; Song, Y. L.; Jiao, W.-H.; Yang, F.; Liu, X. F.; Chen, W. S.; Han, B. N.; Lin, H. W. *Org. Lett.* **2013**, *15*, 3526–3529.

(4) (a) Festa, S.; De Marino, S.; D'Auria, M. V.; Deharo, E.; Gonzalez, G.; Deyssard, C.; Petek, S.; Bifulco, G.; Zampella, A. *Tetrahedron* **2012**, *68*, 10157–10163. (b) Festa, C.; D'Amore, C.; Renga, B.; Lauro, G.; De Marino, S.; D'Auria, M. V.; Bifulco, G.; Zampella, A.; Fiorucci, S. *Mar. Drugs* **2013**, *11*, 2314–2327.

(5) Ruider, S. A.; Sandmeier, T.; Carreira, E.-M. *Angew. Chem., Int. Ed.* **2015**, *54*, 2378–2382.

(6) McCallum, M. E.; Rasik, C. M.; Wood, J. L.; Brown, M.-K. *J. Am. Chem. Soc.* **2016**, *138*, 2437–2442.

(7) Akiyama, M.; Isoda, Y.; Nishimoto, M.; Kobayashi, A.; Togawa, D.; Hirao, N.; Kuboki, A.; Ohira, S. *Tetrahedron Lett.* **2005**, *46*, 7483–7485.

(8) Xu, Z. J.; Wu, Y. *Chem. - Eur. J.* **2017**, *23*, 2026–2030.

(9) (a) Matsuura, B. S.; Kölle, P.; de Vivie-Riedle, R.; Trauner, D.; Meier, R. *ACS Cent. Sci.* **2017**, *3*, 39–46. (b) Burckle, A. J.; Vasilev, V. H.; Burns, N. Z. *Angew. Chem., Int. Ed.* **2016**, *55*, 11476–11479. (c) Stichnoth, D.; Kölle, P.; Kimbrough, T.-J.; Riedle, E.; de Vivie-Riedle, R.; Trauner, D. *Nat. Commun.* **2014**, *5*, 5597.

(10) Reetz, M. T.; Chatziiosifidis, I.; Schweltnus, K. *Angew. Chem.* **1981**, *93*, 716–717.

(11) Dauben, W. G.; Koch, K.; Smith, S. L.; Chapman, O. L. *J. Am. Chem. Soc.* **1963**, *85*, 2616–2621.

(12) Demuyne, A. L. W.; Levecque, P.; Kidane, A.; Gammon, D. W.; Sickle, E.; Jacobs, P. A.; De Vos, D. E.; Sels, B. F. *Adv. Synth. Catal.* **2010**, *352*, 3419–3430.

(13) Barbasiewicz, M.; Michalak, M.; Grela, K. *Chem. - Eur. J.* **2012**, *18*, 14237–14241.

(14) Stille, J. R.; Santarsiero, B.D.; Grubbs, R. H. *J. Org. Chem.* **1990**, *55*, 843–862.

(15) Bonnaud, B.; Mariet, N.; Vacher, B. *Eur. J. Org. Chem.* **2006**, *2006*, 246–256. Molander, G. A.; Carey, J. S. *J. Org. Chem.* **1995**, *60*, 4845–4849.

(16) Magauer, T.; Mulzer, J.; Tiefenbacher, K. *Org. Lett.* **2009**, *11*, 5306–5309.

(17) Meier, R.; Trauner, D. *Angew. Chem., Int. Ed.* **2016**, *55*, 11251–11255.

(18) (a) Huisgen, R.; Mloston, G.; Polborn, K.; Sustmann, R. *Chem. - Eur. J.* **2003**, *9*, 2256–2263. (b) Huisgen, R.; Kalvinsch, I.; Li, X.; Mloston, G. *Eur. J. Org. Chem.* **2000**, *2000*, 1685–1694. (c) Kellogg, R. M. *Tetrahedron* **1976**, *32*, 2165–2184. (d) Hosomi, A.; Matsuyama, Y.; Sakurai, H. *J. Chem. Soc., Chem. Commun.* **1986**, 1073–1074. (e) Lan, Y.; Houk, K. N. *J. Am. Chem. Soc.* **2010**, *132*, 17921–17927.

(19) (a) Aono, M.; Hyodo, C.; Terao, Y.; Achiwa, K. *Tetrahedron Lett.* **1986**, *27*, 4039–4042. (b) Terao, Y.; Tanaka, M.; Imai, N.; Achiwa, K. *Tetrahedron Lett.* **1985**, *26*, 3011–3014. (c) Terao, Y.; Aono, M.; Imai, N.; Achiwa, K. *Chem. Pharm. Bull.* **1987**, *35*, 1734–1740. (d) Terao, Y.; Aono, I.; Takahashi, I.; Achiwa, K. *Chem. Lett.* **1986**, *15*, 2089–2092. (e) Ando, M.; Terao, Y.; Achiwa, K. *Heterocycles* **1995**, *40*, 249–260. (f) Cherney, R. J.; King, B. W.; Gilmore, J. L.; Liu, R.-Q.; Covington, M. B.; Duan, J. J.-W.; Decicco, C. P. *Bioorg. Med. Chem. Lett.* **2006**, *16*, 1028–1031.

(20) Terao, Y.; Aono, M.; Imai, N.; Achiwa, K. *Chem. Pharm. Bull.* **1987**, *35*, 1734–1740.

(21) McGarraugh, P. G.; Brenner, S. E. *Org. Lett.* **2009**, *11*, 5654–5657. (b) Lehmann, F.; Holm, M.; Laufer, S. *J. Comb. Chem.* **2008**, *10*, 364–367. (c) Nandurkar, N. S.; Bhanushali, M. J.; Patil, D. S.; Bhanage, B. M. *Synth. Commun.* **2007**, *37*, 4111–4115.

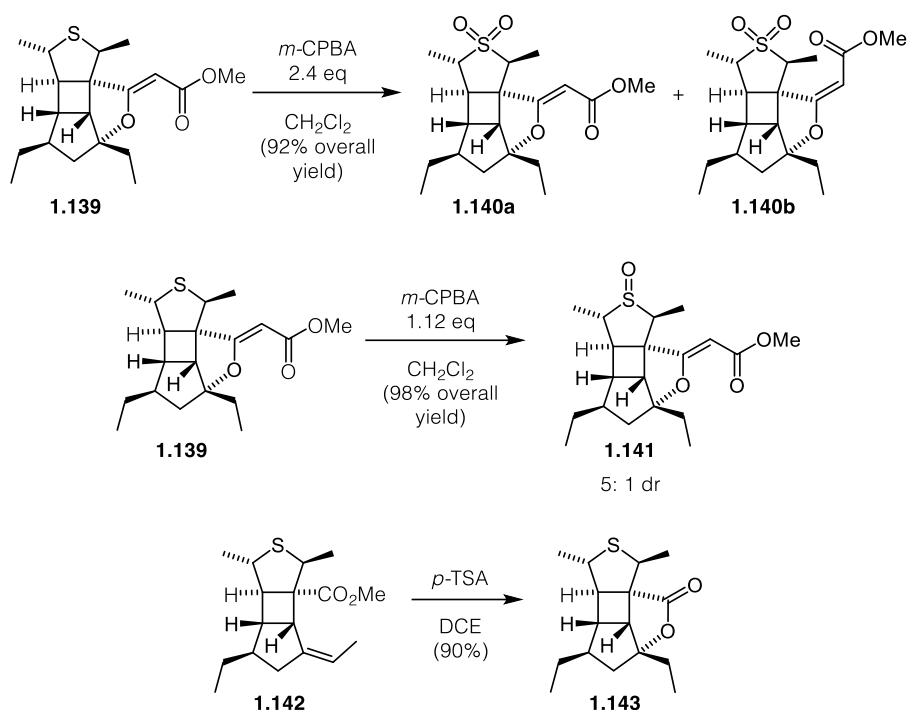
(22) Van der Veen, R.-H.; Geenevasen, J.-A.-J.; Cerfontain, H. *Can. J. Chem.* **1984**, *62*, 2202–2205.

- (23) Hanquet, G.; Salom-Roig, X. J.; Lemeitour, S.; Solladie, G. *Eur. J. Org. Chem.* **2002**, *2002*, 2112–2119.
- (24) (a) Lin, R.; Cao, L.; West, F. G. *Org. Lett.* **2017**, *19*, 552–555.
(b) Hauptmann, H.; Walter, W. F. *Chem. Rev.* **1962**, *62*, 347–404.
(c) Rentner, J.; Kljajic, M.; Offner, L.; Breinbauer, R. *Tetrahedron* **2014**, *70*, 8983–9027.
- (25) Tanaka, K.; Nagahiro, R.; Urbanczyk-Lipkowska, Z. *Org. Lett.* **2001**, *3*, 1567–1569.
- (26) (a) Speck, K.; Magauer, T. *Chem. - Eur. J.* **2017**, *23*, 1157–1165.
(b) Schröckeneder, A. Ph.D. Thesis, Universität München, 2012.
(c) Liang, B.; Carroll, P. J.; Joullie, M.-M. *Org. Lett.* **2000**, *2*, 4157–4160.

1.3.4 Synthesis of synthetic derivatives of hippolachnin A

Hippolachnin A was reported to offer interesting antifungal activity. In order to investigate structure-affinity relationships of hippolachnin A (**1.61**) and to improve the bioavailability of this barely water soluble molecule, we prepared several derivatives of the natural product.

To determine whether the (*Z*)-configured vinylogous carbonate was necessary for activity, derivatives lacking this group or having a different geometry were prepared. To improve the solubility in water, the thioether was oxidized to the sulfoxide and the sulfone. Scheme 1.21 shows the syntheses of the derivatives.



SCHEME 1.21: Syntheses of synthetic derivatives of **1.61**.

These compounds, together with intermediates **1.99**, **1.139** and the synthetic natural product were sent to Prof. Dr. Marc Stadler at the Helmholtz Centre for Infection Research in Braunschweig. Unfortunately, none of these compounds, including the natural product, showed any antifungal activity.

1.4 Conclusion

In conclusion, a concise, scalable and modular synthesis of the complex polyketidal natural product hippolachnin A was achieved, and several derivatives thereof have been prepared. These successful studies supported biological investigations of hippolachnin A.

Initial attempts to close the tetrahydrofuran ring as well as the cyclobutane ring in a single step by a non-biomimetic [2+2]-cycloaddition failed with multiple precursors. Revising the approach and constructing the bicyclo[3.2.0]heptanone core via a 4π -electrocyclization followed by excited state rearrangement provided rapid access to the core of hippolachnin A. While conventional methods to install the geminal diethyl groups suffered from low diastereoselectivity, the simultaneous installation of the two ethyl groups through 1,3-dipolar cycloaddition elegantly solved this problem. In order to close the eastern tetrahydrofuran ring, ester elongation was required. Attempted nucleophilic additions to the ester failed due to the remarkable steric congestion around this carbonyl group. This problem could be solved by converting the ester into the smaller and more reactive aldehyde. Chelation-controlled trapping of an *in situ* generated carbocation by a tin enolate of the β -ketoester constructed this last ring. Final reductive desulfurization yielded hippolachnin A in good yield. Notably, more than 100 mg of hippolachnin A was produced in a single pass of the entire synthetic route.

It was reported that hippolachnin A provides interesting antifungal activity and therefore derivatives of the natural product have been prepared in order to figure out structure-affinity relationships and to increase the bioavailability of the molecule. The thioether, installed in the carbonyl ylide cycloaddition, provided a functional handle for further transformations which would have been difficult otherwise, considering that the natural product is lacking functional groups. Unfortunately, hippolachnin A, as well as all the synthetic derivatives proved to be inactive against the proposed target.

Chapter II

Synthetic Studies Towards the Meroterpenoids Bisacremin E, F and G

2.2 Introduction

2.1.1 Acremine natural products – Isolation and biosynthesis

Endophytic fungi grow within a plant host and usually live in a symbiotic relationship. Their growth involves continuous metabolic interaction between fungus and host.⁵ Therefore endophytic fungi display a rich source of secondary metabolites often bearing interesting bioactivity.⁶ The genus *Acremonium* is part of this family and many bioactive natural products, including the β -lactam antibiotic cephalosporin, the immunosuppressants cyclosporins, the tremorgenic indole-diterpenoids lolitremes and some prenylated phenol inhibitors of *N*-SMase have been isolated from this genus.³⁹ In 2005, Torta and co-workers reported the isolation of six meroterpenoid natural products, acremine A-F (figure 2.1) from A20, a strain of *Acremonium bissoides*, isolated from grapevine leaves artificially inoculated with *Plasmopora viticola*.⁴⁰ The structure analysis was based on NMR and mass data. Furthermore, an X-ray crystal structure of acremine A confirmed the relative stereochemistry. The absolute stereochemistry was determined using Mosher's method. Acremines A-D showed moderate inhibition of *P. viticola* sporangia germination. All acremines possess either a cyclohexene or aromatic portion, which is likely derived *via* a polyketide pathway, and a prenyl unit. Further cyclization can then lead to either the benzofuran or the chromanone ring system.

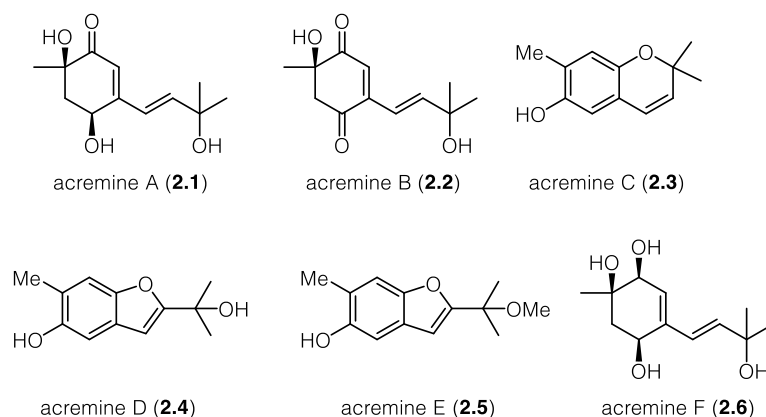
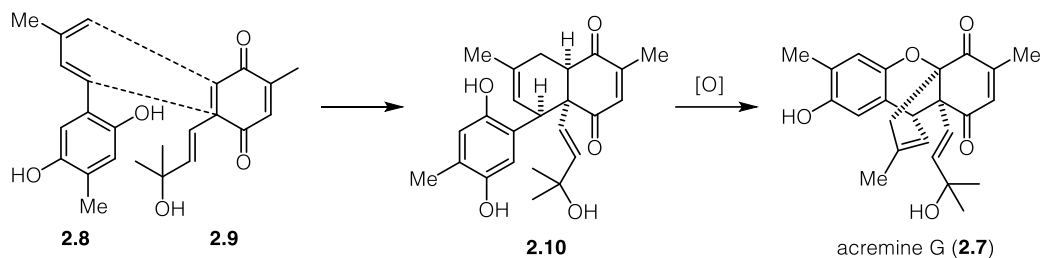


FIGURE 2.1: Molecular structures of acremine A-F.

In 2008, Malpezzi and co-workers reported the isolation and structural assignment of acremine G (**2.7**),⁶ the first dimeric member of the acremine family. It is believed that acremine G arises from a Diels-Alder reaction of prenyl benzoquinone **2.8**, possibly derived from acremine B (**2.2**), and aromatic diene **2.9**. Further oxidation could then furnish the natural product (scheme 2.1). Although this hypothesis makes sense from a

synthetic point of view, neither of the possible Diels-Alder partners have been isolated to date.



SCHEME 2.1: Possible biosynthesis of acremine G (2.7).⁶

Five further members, acremines H-N (figure 2.2), have been isolated from the same strain in 2008 by Nasini and co-workers.³⁹ Acremine H and I possess one and two oxirane rings respectively. Acremine L and M can be derived from these by epoxide opening and further reduction or cyclization.

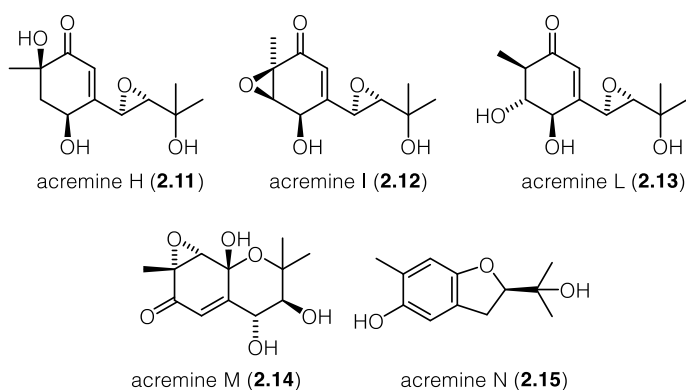


FIGURE 2.2: Molecular structures of acremine H-N.³⁹

In 2013, the acremine family became even more diverse due to the isolation of chlorinated derivatives 5-chloroacremine A (2.16) and 5-chloroacremine H (2.17) together with acremine O (2.18), P (2.19), Q (2.20) and R (2.21) by Garson and co-workers.⁴¹ In 2017, Garson revised the structure of acremine P (2.21).⁴² A further expansion of the acremine family was reported in 2014 when Afiyatulloev and co-workers reported the isolation of acremine S (2.22) from the marine-derived fungus *Isaria felina* KMM 4639⁴³ (Figure 2.3).

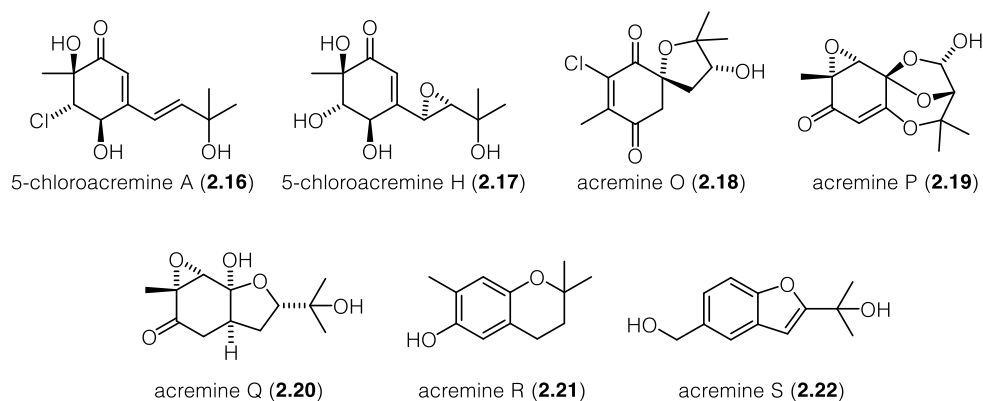
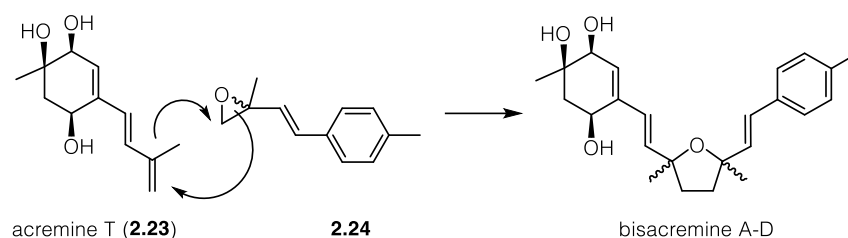


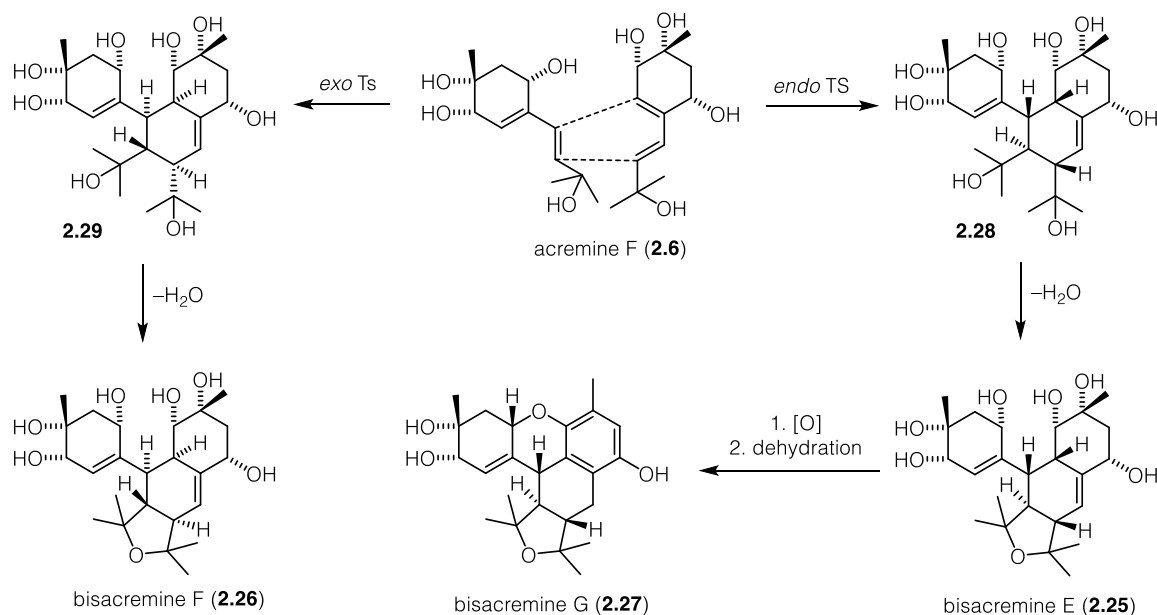
FIGURE 2.3: Molecular structure of 5-chloroacremine A and H and acremine O-R.^{39, 41-43}

Until 2015, acremine G remained the only dimeric acremine natural product. When Wei and co-workers were analyzing a culture extract of the soil-derived strain *A. persicinum* SC0105 that showed activity against *Staphylococcus aureus*, they discovered bisacremines A-D together with their possible biogenic precursor acremine T (**2.23**).⁴⁴ Bisacremines A-D are hypothesized to be derived from acremine T (**2.23**) and an oxirane precursor (**2.24**). **2.23** is assumed to nucleophilically open the epoxide of **2.24**, generating an allylic cation that can then be intercepted by the generated tertiary alcohol to form bisacremines A-D. This hypothesis seems to be substantial, considering that all possible stereoisomers are natural products (Scheme 2.2).



SCHEME 2.2: Proposed biosynthesis of bisacremines A-D.⁴⁴

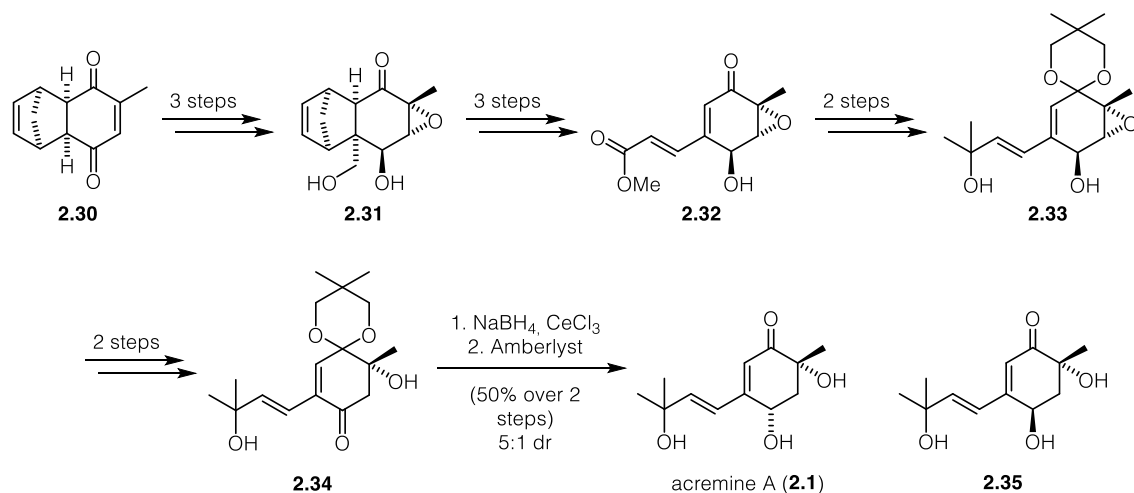
Later in 2015, Wei discovered three more bisacremines E-G from the same extract.⁷ Bisacremine E (**2.25**) and F (**2.26**) are supposed to be derived by a formal [4+2] cycloaddition of two acremine F monomers, followed by dehydration to form the final tetrahydrofuran ring (scheme 2.3). As both the endo- and the exo-transition state of the Diels-Alder reaction lead to different isolated natural products, it might be plausible that this reaction is not catalyzed by an enzyme. Oxidation and intramolecular acetalization of bisacremine F, followed by aromatizative dehydration would then



furnish bisacremine G (**2.27**). While bisacremine E-G were not cytotoxic against A549, MCF-7 and HepG2, bisacremine G showed dose-dependent effects in *in vitro* anti-inflammation assays.

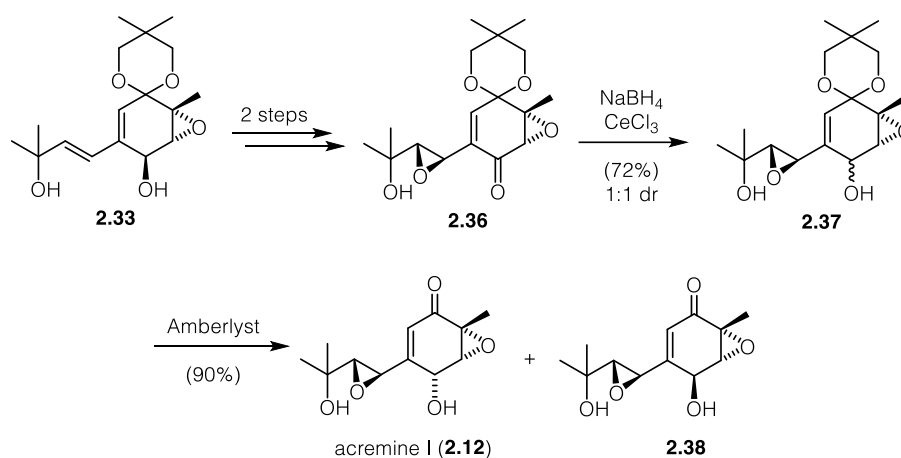
2.1.2 Synthetic approaches

The first total synthesis of acremine A (**2.1**) was reported in 2010 by Mehta⁴⁵ and marks the first total synthesis of an acremine natural product in general. The synthesis starts with bicycle **2.30**, which was converted into oxirane **2.31** through epoxidation followed by alkylation and reduction from the convex side of the system. Retro Diels-Alder reaction followed by oxidation and Wittig olefination gave rise to α,β -unsaturated



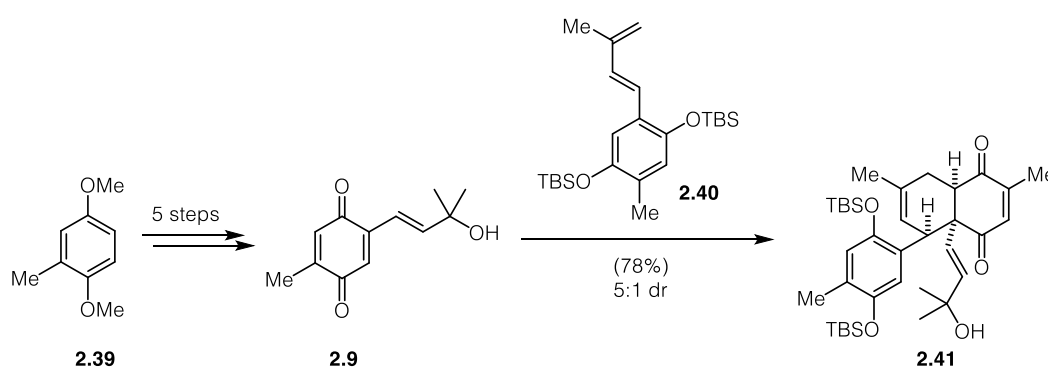
ester **2.32** in good yields. Diol **2.33** was then accessed by protection of the enone moiety and Grignard addition into the ester. Oxidation and reductive epoxide opening yielded ketone **2.34**. Reduction of **2.34** using Luche's conditions and further deprotection of the enone accessed acremine A (**2.1**) together with its epimer **2.35** in a 5:1 dr (Scheme 2.4).

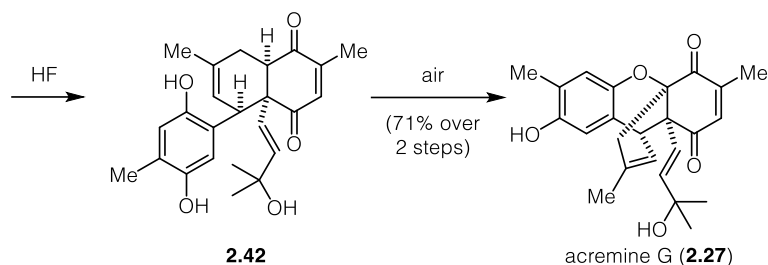
From intermediate **2.33** Mehta was also able to access acremine I (**2.12**). Directed epoxidation and oxidation of the secondary alcohol gave enone **2.36**. In this case, the Luche reduction had no preference for any side and provided secondary alcohol **2.37** as a 1:1 mixture of diastereoisomers. Hydrolysis of the ketal gave then rise to acremine I (**2.12**) and its stereoisomer **2.38** as a separable mixture (Scheme 2.5).



SCHEME 2.5: Mehta's synthesis of acremine I (**2.12**).⁴⁵

In 2009, Stratakis and co-workers reported the first biomimetic synthesis of acremine G (**2.27**),⁴⁶ in support of the proposed biosynthesis. Prenylated benzoquinone **2.9** was prepared from protected hydroquinone **2.39** in a five-step protocol and was able to undergo a Diels-Alder cycloaddition with unstable diene **2.40** yielding **2.41**. Double deprotection of the silyl ethers gave rise to hydroquinone **2.42** which upon standing on air formed acremine G (**2.27**), possibly by a radical pathway (Scheme 2.6). Mehta showed one year later that the reaction proceeds even at room temperature on silica

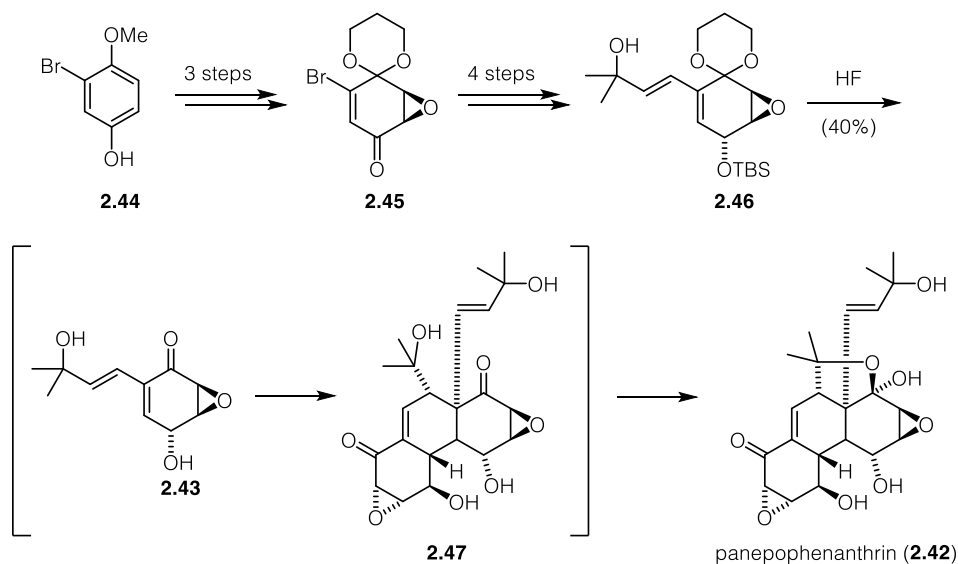




SCHEME 2.6: Stratakis' biomimetic synthesis of acremine G (**2.27**).⁴⁶

support.⁴⁷

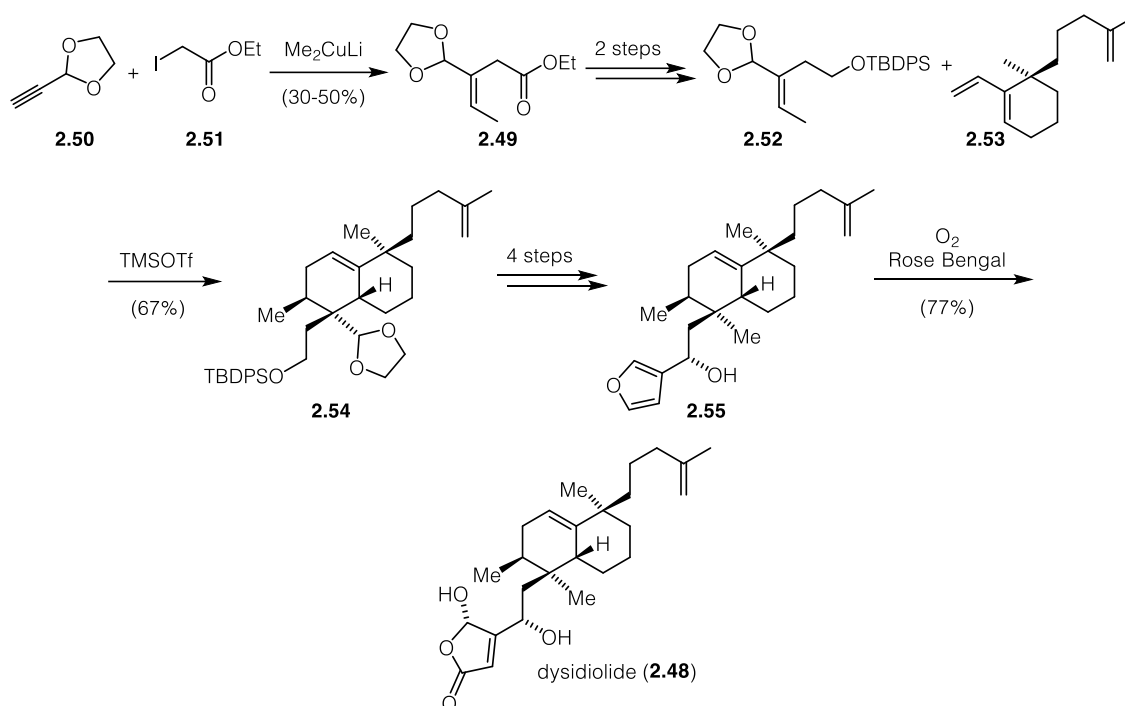
In 2003, Porco and co-workers described the biomimetic synthesis of the dimeric natural product panepophenanthrin (**2.42**), consisting of two units of enone **2.43**, which is structurally related to the acremine family (scheme 2.7).⁴⁸ Phenol **2.44** is converted into enone **2.45** by oxidation, transketalization and epoxidation. Further manipulations then elaborated tertiary alcohol **2.46** as a key intermediate. Global deprotection using aqueous HF uncaged enone **2.43** which spontaneously underwent a Diels-Alder cycloaddition to form pentacycle **2.47**, which could not be isolated. **2.47** underwent further intramolecular hemiketal formation and therefore stabilizes the otherwise thermodynamically less stable dimeric structure of panepophenanthrin (**2.42**).



SCHEME 2.7: Porco's biomimetic synthesis of panepophenanthrin (**2.42**).⁴⁸

Danishefsky reported a synthesis of dysidiolide (**2.48**) involving a Gassman Diels-Alder reaction to form the core of the natural product.⁴⁹ Dioxolane **2.49** was prepared by a three-component coupling employing alkyne **2.50**, dimethyl cuprate and iodide **2.51**. Reduction followed by protection of the primary alcohol gave dioxolane **2.52** as the key

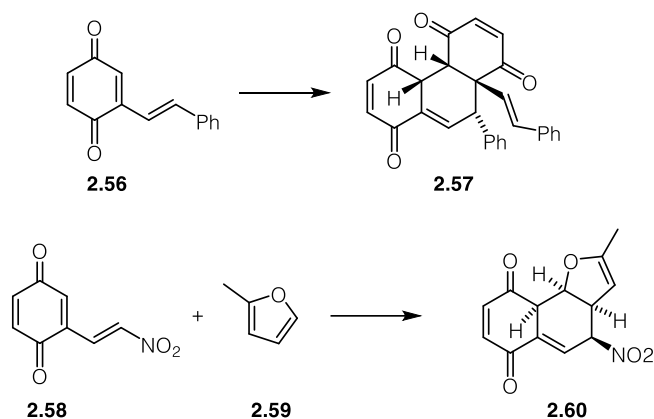
step precursor. **2.52** underwent a cationic Diels-Alder reaction with diene **2.53** to form the complete core of dysidiolide. Further manipulations installed the furan moiety that, upon oxidation using singlet oxygen, furnished **2.48** (Scheme 2.8).



SCHEME 2.8: Danishefsky's synthesis of dysidiolide (**2.48**).⁴⁹

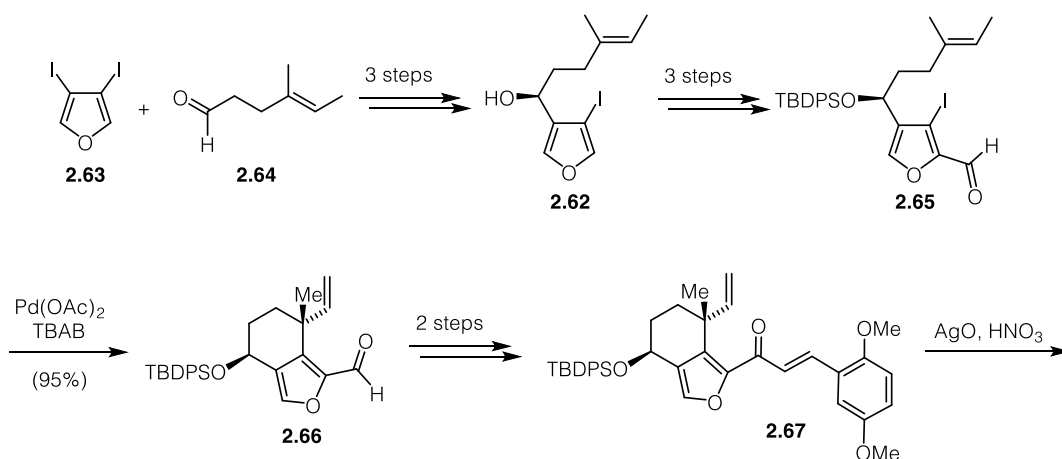
2.1.3 Vinyl quinone Diels-Alder reactions in total synthesis

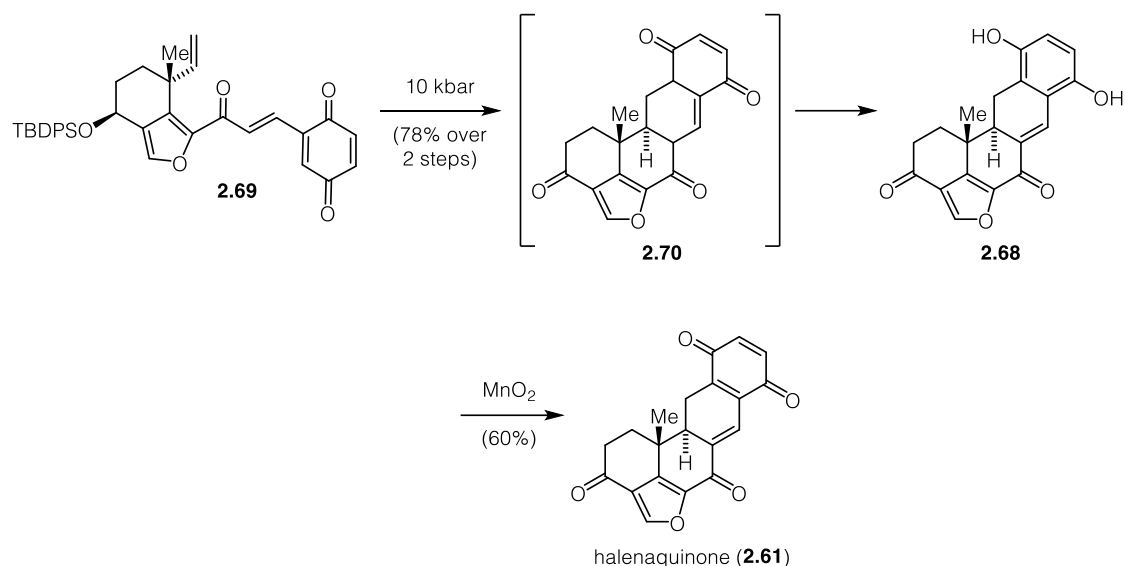
The first Diels-Alder reaction involving a vinyl quinone as a diene was reported in 1998 by Irgartinger⁵⁰ (scheme 2.9). When examining the chemistry of aryl-substituted vinylquinones, an unexpected dimerization was observed that proceeded *via* an inverse electron demanding Diels-Alder reaction. This methodology was extended in 1999 by Noland,⁵¹ when he showed that electron-deficient vinylquinones can undergo a Diels-Alder reaction with electron-rich alkenes. The resulting isoquinonemethide can be trapped with a nucleophile or, in many cases, tautomerize to the corresponding quinone.



SCHEME 2.9: Initial observations of VQDA reactions.⁵⁰⁻⁵¹

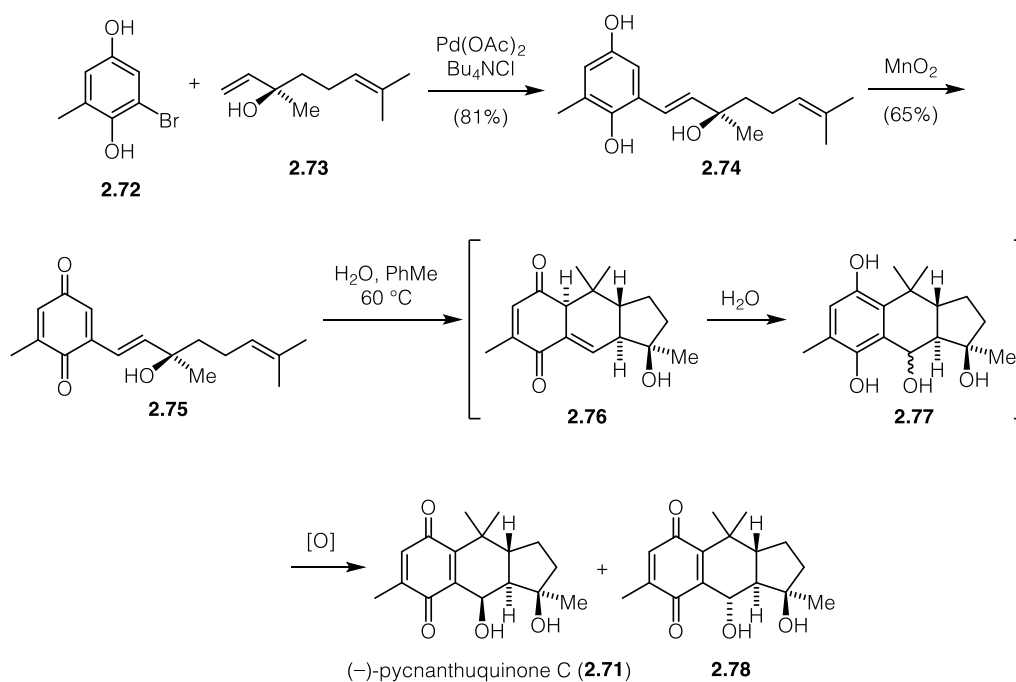
The first application of a VQDA reaction in total synthesis was reported by Trauner and co-workers in the synthesis of halenaquinone (**2.61**) in 2008.⁵² This report also marks the first example of an intramolecular VQDA reaction (scheme 2.10). **2.61** aroused much interest in the synthetic community due to its interesting polycyclic framework and versatile biological profile. Alcohol **2.62** was derived enantioselectively from 2,3-diiodofurane (**2.63**) and aldehyde **2.64** in a three-step protocol. Further manipulations yielded aldehyde **2.65** which could undergo an intramolecular Heck reaction to give alkene **2.66** as a single diastereoisomer. Nucleophilic addition followed by oxidation then gave rise to protected hydroquinone **2.67**. The key-step precursor was obtained by oxidation using AgO and HNO₃ and smoothly underwent the desired VQDA reaction under elevated pressure. Even though the reaction proceeded at room temperature, the yield could be significantly improved using high pressure conditions. The initial resulting isoquinonemethide could not be isolated but underwent fast tautomerization to the corresponding hydroquinone **2.68**. Halenaquinone (**2.61**) was obtained in good yields after further oxidation.





SCHEME 2.10: Trauner's synthesis of halenaquinone (**2.61**).⁵²

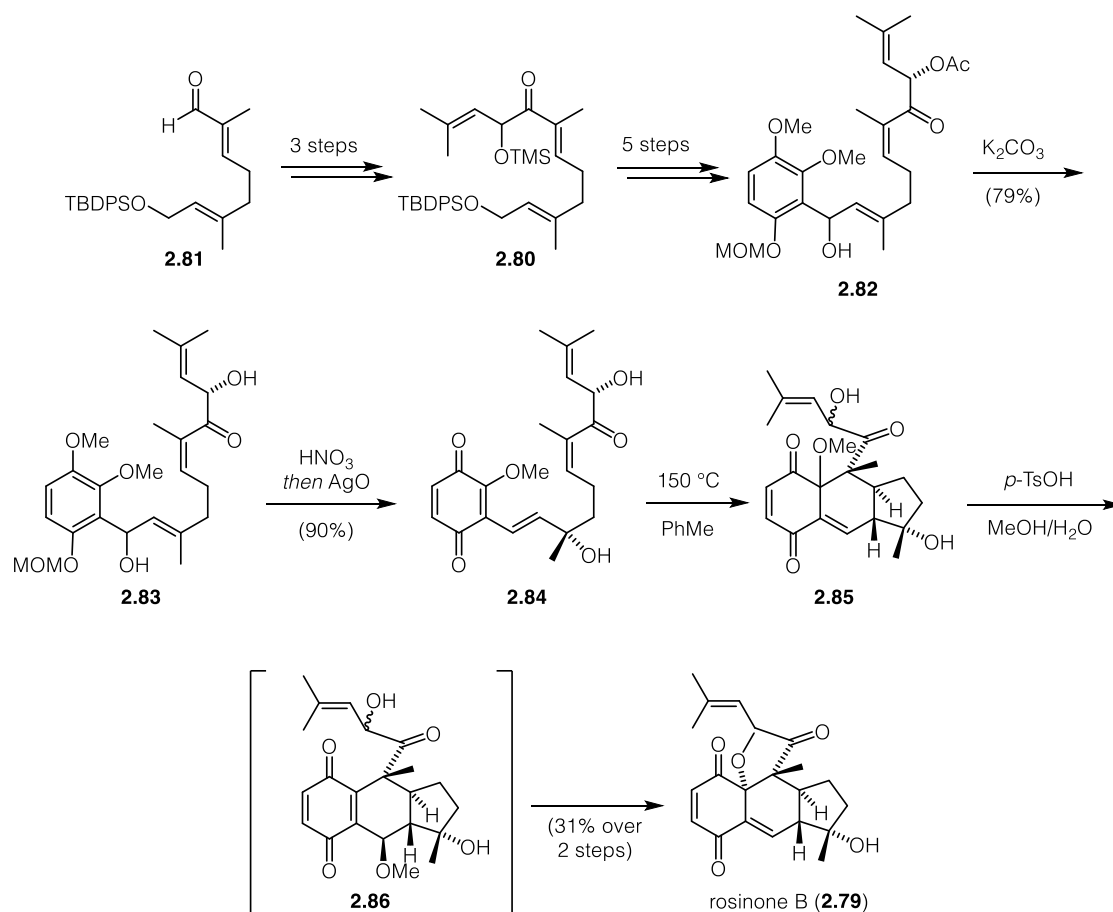
In 2009, Trauner expanded this methodology to the biomimetic total synthesis of (–)-pyncnanthuquinone C (**2.71**)⁵³ anticipating that this reaction plays a significant role in the biosynthesis of secondary metabolites. Heck coupling of hydroquinone **2.72** with (–)-linalool (**2.73**) yielded styrene **2.74** that could be further oxidized to the key vinyl quinone **2.75** using MnO_2 . When **2.75** was slightly heated in a mixture of PhMe and H_2O , the VQDA reaction proceeded smoothly to give isoquinonemethide **2.76** which was directly intercepted by water in a nonstereospecific manner. The resulting hydroquinone **2.77** could not be isolated as it was spontaneously oxidized upon



SCHEME 2.11: Trauner's synthesis of (–)-pyncnanthuquinone C (**2.71**).⁵³

exposure to air to give (–)-pcynanthuquinone C (**2.71**) and its epimer **2.78**, which Trauner predicted to be another natural product (Scheme 2.11).

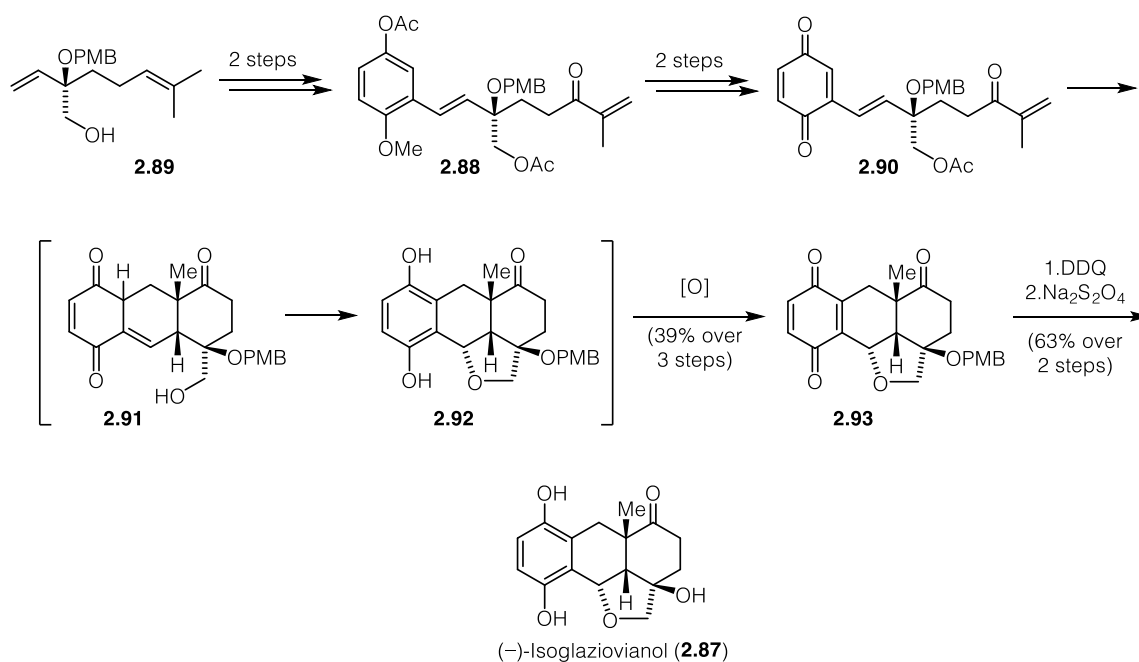
In the same publication, Trauner proposed that a VQDA reaction is a plausible pathway for the biosynthesis of rosinone B (**2.79**) as well, and in 2010, Zhang and co-workers reported the biomimetic synthesis of **2.79**.⁵⁴ Enone **2.80** was obtained by a three-step protocol from **2.81** and yielded acetate **2.82** after further manipulations. Hydrolysis of the acetate proceeded smoothly under basic conditions and gave protected hydroquinone **2.83** in good yields. 1,3-Allylic isomerization towards the thermodynamically more stable styrene followed by MOM deprotection and oxidation afforded vinyl quinone **2.84** in excellent yield. Heating a solution of **2.84** in PhMe gave rise to isoquinonemethide **2.85** which was directly treated with *p*-TsOH in a mixture of MeOH and H₂O. S_N2' displacement of methoxide afforded quinone **2.86**, that could undergo a second intramolecular S_N2' displacement to give rosinone B (**2.79**) (Scheme 2.12).



SCHEME 2.12: Zhang's synthesis of rosinone B (**2.79**).⁵⁴

In 2013, Trauner and co-workers reported the total synthesis of (–)-isoglazivianol (**2.87**),⁵⁵ marking the first example of trapping of the *in situ* generated isoquinonemethide

by an intramolecularly provided nucleophile (Scheme 1.13). Enone **2.88** is derived from primary alcohol **2.89** by a two-step protocol. Acetate cleavage and oxidation afforded vinylquinone **2.90** that spontaneously underwent the VQDA reaction at room temperature to form the isoquinonemethide **2.91**. Intramolecular attack of the primary hydroxyl group and tautomerization gave hydroquinone **2.92** that was oxidized upon work-up, affording quinone **2.93**. (–)-Isoglaziovianol (**2.87**) was obtained in good yield after removal of the PMB protecting group and reduction of the quinone moiety.



SCHEME 2.13: Trauner's synthesis of isoglaziovianol (**2.87**).⁵⁵

2.2 Project outline

Acremines are a rich class of meroterpenoid natural products mainly isolated from the *Acremonium* fungal species *A. byssoides* and *A. persicinum*.^{6-7, 39-44} They are mainly simple meroterpenoids comprising an isopentenyl unit linked to a C₇ tetraketide ring and can be defined as C₁₂ merohemiterpenoids. Acremines A–F and H–T are monomers containing a single C₁₂ unit, acremine G (**2.7**) was the first dimeric derivative consisting of two C₁₂ units. It is presumably generated from acremine A (**2.1**) and B (**2.2**) by a Diels-Alder reaction and subsequent oxidative coupling. Bisacremines E (**2.25**) and F (**2.26**) consist of an unusual tetracyclic core that is highly oxidized and features ten stereogenic centers. Bisacremine G (**2.27**), bearing six stereogenic centers, consists of a heteropentacyclic core and exhibits inhibitory effects on the production of TNF- α , IL-6, and nitric oxide in LPS-stimulated macrophages. **2.25** and **2.26** are supposed to be

biosynthetically derived from two acremine F (**2.6**) units which undergo a formal [4+2] cycloaddition to install the full carbon core and further condensation to complete the southern tetrahydrofuran ring. **2.27** is proposed to be derived from **2.25** through further oxidation and cyclization. Even though this biosynthesis seems to be appealing, it remained unclear how this [4+2] cycloaddition would occur in nature. As both the endo and the exo transition state would give natural products, we assumed that this reaction would not occur in an enzymatic pocket but could proceed spontaneously in solution. In order to prove these hypotheses, we wanted to synthesize **2.25** and **2.26** starting from **2.6** (Figure 2.4).

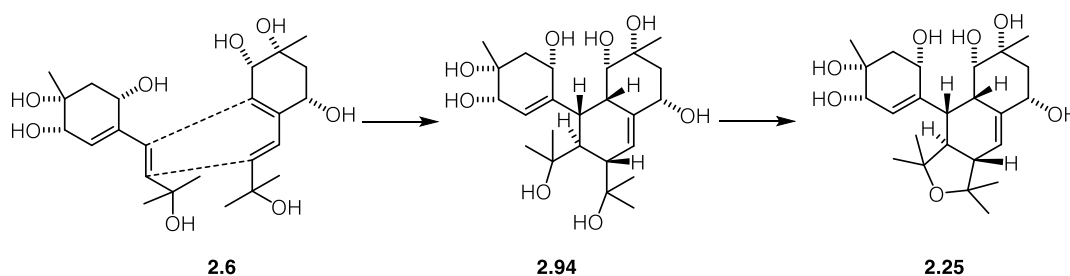


FIGURE 2.4: Proposed biosynthetic pathway of bisacremine E (**2.25**).

In addition, we thought we might as well be able to get access to the more bioactive natural product bisacremine G (**2.27**). We envisioned that a vinyl quinone Diels-Alder reaction could give fast access to the core of the natural product (Figure 2.5) and therefore expand the scope of this powerful methodology.

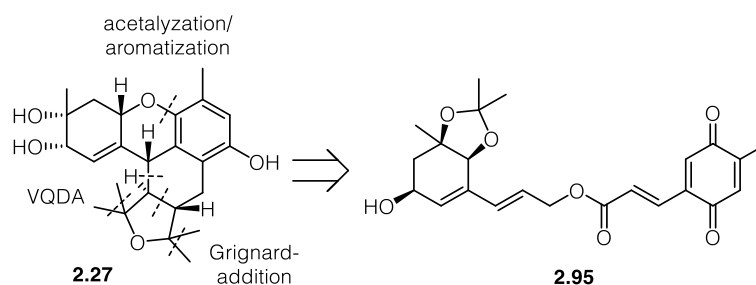
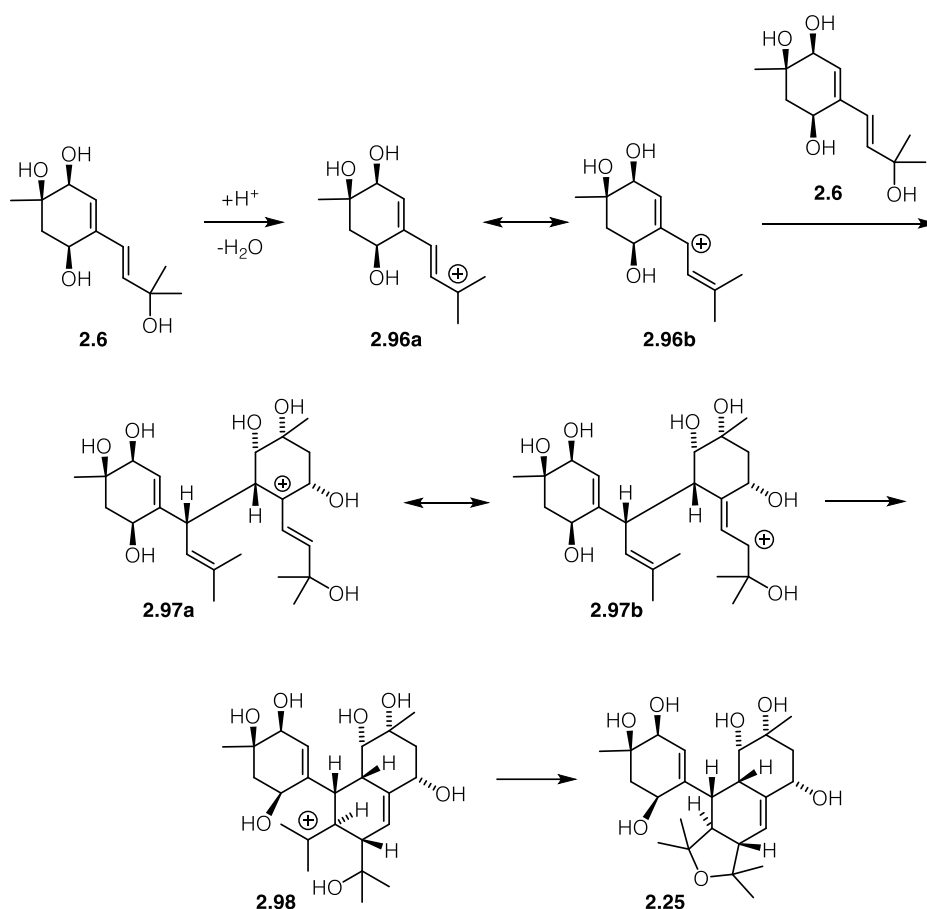


FIGURE 2.5: Retrosynthetic bond disconnections of bisacremine G (**2.27**).

2.3 Results and discussion

2.3.1 The cationic cascade

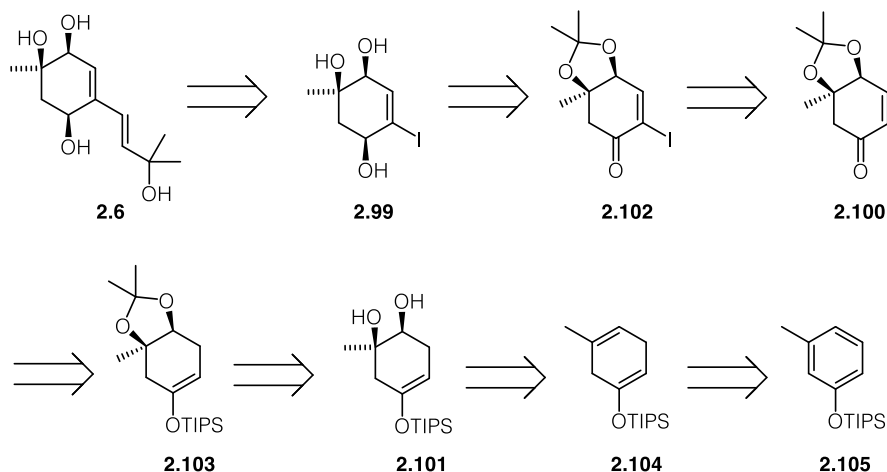
Bisacremine E (**2.25**) and its isomer bisacremine F (**2.26**) are supposed to be derived from acremine F (**2.6**) by a formal [4+2] cycloaddition followed by condensation to implement the final tetrahydrofuran ring.⁷ Though the electronic properties would not be matching for a classical Diels-Alder reaction involving an electron-poor dienophile and an electron-rich diene, we thought that this reaction might be ionic in nature. We envisioned to synthesize **2.25** through a cationic cascade, depicted in Scheme 2.14.



SCHEME 2.14: Proposed biomimetic cascade to form bisacremine E (**2.25**).

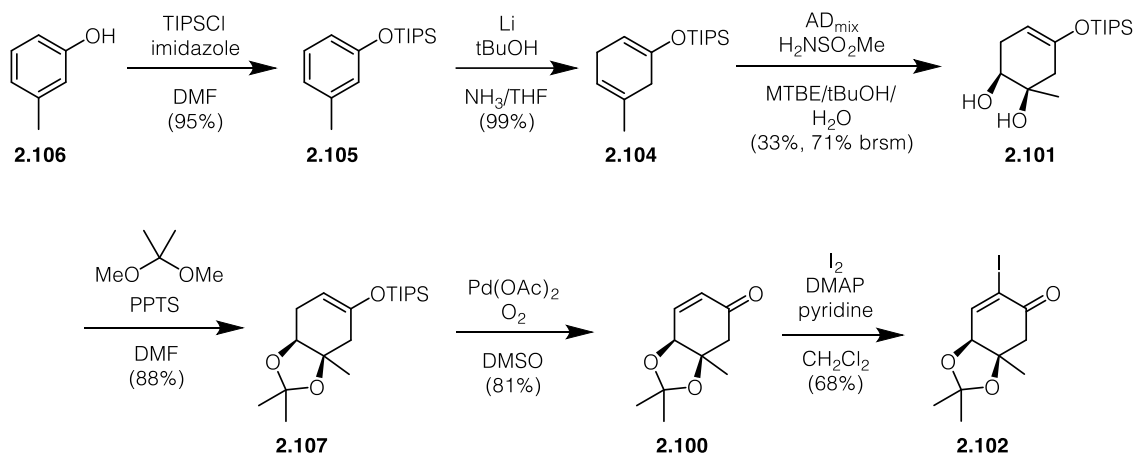
Upon treatment with acid the tertiary allylic alcohol **2.6** was supposed to expel water forming a stabilized allylic cation **2.96** which could be trapped by the trisubstituted double bond of a second molecule of **2.6**, again forming a stabilized cation **2.97**. **2.97** should then be intercepted by the neighbouring trisubstituted double bond, forming the six-membered ring of **2.98**. Trapping of the tertiary cation by the alcohol should then yield the natural product. Depending on whether the initial attack would come from the top or the bottom face, either **2.25** or **2.26** should be formed.

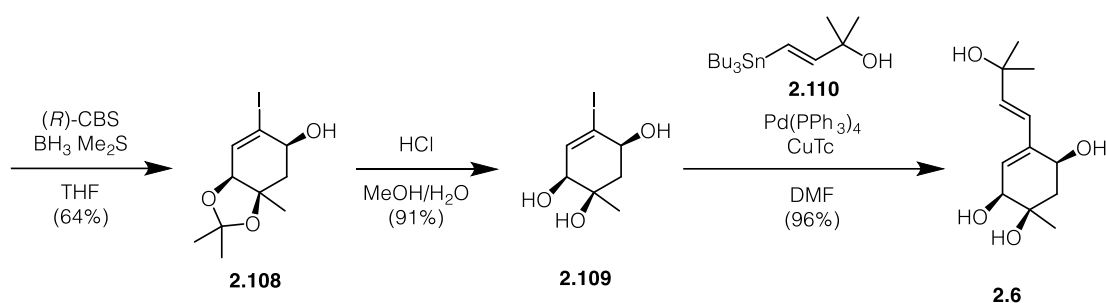
The prenyl side chain of **2.6** should be installed *via* Stille coupling of vinyl iodide **2.99**, which could be obtained after stereoselective reduction from enone **2.100**. **2.100** could be accessed from **2.101** after protection and Segusa oxidation. **2.101** could be traced back to protected *m*-cresol (**2.106**) by Birch reduction followed by asymmetric dihydroxylation⁵⁶ (scheme 2.15).



SCHEME 2.15: Retrosynthetic analysis of acremine F (**2.6**).

TIPS protection of **2.106** followed by Birch reduction gave rise to silyl enol ether **2.104** which could be dihydroxylated under Sharpless conditions to yield diol **2.101**. The diol was obtained in modest optical purity of 25% ee as determined at the stage of enone **2.100**. Unfortunately, all attempts to improve the enantioselectivity failed. Nevertheless, we kept this route because CBS reduction at a later state could improve the optical purity. Enone **2.100** as obtained from **2.101** after diol protection and Segusa oxidation of the



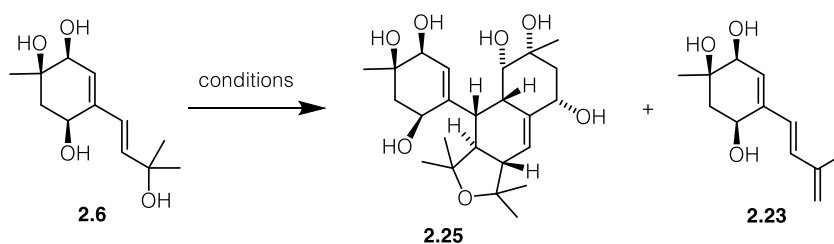


SCHEME 2.16: Synthesis of acremine F (**2.6**).

silyl enol ether. Alpha-iodination then accessed α -iodoenone **2.102** which could stereoselectively be reduced to allylic alcohol **2.108** that was obtained in 95% ee. Deprotection followed by Stille cross coupling with vinyl stannane accessed 300 mg quantities of **2.6** in a single pass (Scheme 2.16).

With this material in hand, we turned our focus onto the biomimetic cascade to form **2.25**. Table 2.1 shows the screening conditions.

TABLE 2.1: Screening for the biomimetic cascade



entry	solvent	additive	temperature	observation
1	H ₂ O	none	45 °C	starting material
2	H ₂ O	none	65 °C	starting material
3	H ₂ O	none	85 °C	2.23
4	H ₂ O	none	100 °C	decomposition
5	PBS	none	65 °C	starting material
6	PBS	none	85 °C	2.23
7	PhMe	none	110 °C	starting material
8	PhMe	none	110 °C to 150 °C	2.23
9	<i>o</i> -DCB	none	160 °C	decomposition
10	<i>o</i> -DCB	Hg(OAc) ₂	190 °C	decomposition
11	Et ₂ O	4 M LiClO ₄	RT	2.23
12	neat	none	45 °C	2.23

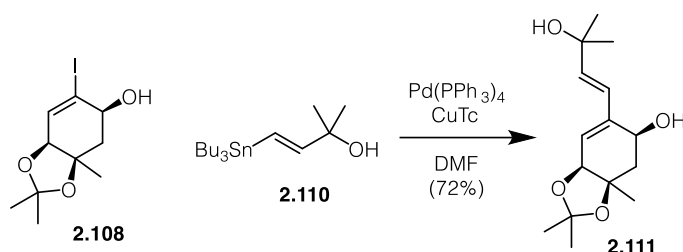
13	neat	none	50 °C to 100 °C	starting material
14	neat	none	110 °C	complex mixture
15	neat	none	130 °C	decomposition
16	MeCN	12 kbar	RT	starting material
17	CH ₂ Cl ₂	ZnBr ₂ , 14 kbar	RT	starting material
18	MeCN	AcOH, 7 kbar	RT	starting material
19	MeCN	HCOOH, 12 kbar	60 °C	decomposition
20	MeCN	AcOH, 12 kbar	60 °C	decomposition
21	MeCN	CSA	-40 °C to RT	2.23
22	neat	CSA	RT	decomposition
23	MeCN	AcOH	RT	starting material
24	MeCN	AcOH	45 °C	2.23
25	MeCN	AcOH	85 °C	elimination + acetate incorporation
26	MeCN/ H ₂ O	AcOH	85 °C	elimination + acetate incorporation
27	MeCN	HCOOH	90 °C	2.23
28	MeCN/PhMe	AcOH	90 °C	2.23
29	H ₂ O	H ₂ SO ₄	85 °C	decomposition
30	TFE	none	RT to 60 °C	TFE incorporation
31	neat	PPTS	40 °C to 60 °C	decomposition

Attempts to trigger the ionization of the tertiary allylic alcohol showed that the compound was stable until 65 °C in H₂O. **2.6** was originally obtained as a colourless oil, but when heated to 45 °C in H₂O the compound started to crystallize as colourless needles. Unfortunately, the crystals were not suitable for X-ray diffraction. At 85 °C the ionization took place but only elimination to triene **2.23** could be observed. Further heating to 100 °C resulted in rapid decomposition. The application of physiological salt concentrations had no beneficial effect. While **2.6** was only stable until 65 °C in H₂O it proved to be stable until 110 °C in toluene. At higher temperatures only decomposition of the starting material was observed. Using solvents with a high ionic strength led only to rapid elimination to the triene.

At this point, we realized that ionization of the tertiary allylic alcohol was feasible, but high temperatures seemed to favour elimination over dimerization. We thought that ionization under acidic conditions should be possible at lower temperatures and, in case

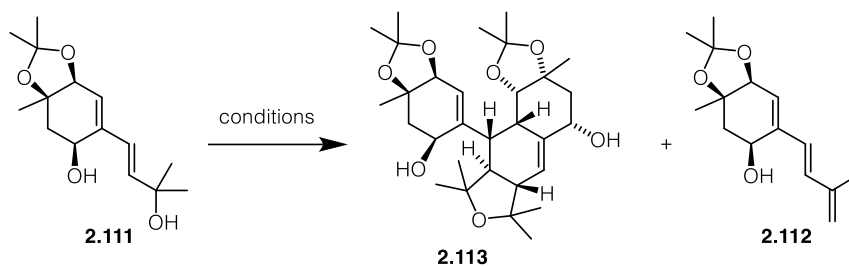
that elimination would occur, it might be reversible under these conditions. To our disappointment, strong acids led to elimination at low temperatures and to decomposition of the starting material at room temperature. **2.6** was stable towards weak acids at room temperature and showed elimination at 45 °C. When **2.6** was heated to 85 °C in the presence of acetic acid, acetate was incorporated into the molecule. Even though this showed that the allylic cation could be trapped by a nucleophile, the nucleophilic attack appeared selectively at the tertiary position of the molecule and not at the potentially less hindered secondary site. When **2.6** was stirred in TFE at 60 °C, TFE incorporation at the same site of the molecule could be observed. We thought that the application of high pressure might alter the selectivity. At room temperature under 14 kbar in the presence of either a nucleophilic or a non-nucleophilic acid did not lead to any conversion. At 60 °C only decomposition was observed.

We next wanted to see whether different protecting groups could have an influence on the stability and therefore allow higher reaction temperatures without decomposition. They might also help to improve the solubility in organic solvents and force the molecule to adapt the desired conformation. In order to see whether the *syn*-diol moiety was problematic, it was protected as an acetonide. Stille coupling of **2.108** with vinyl stannane **2.110** yielded diol **2.111** (scheme 2.17).



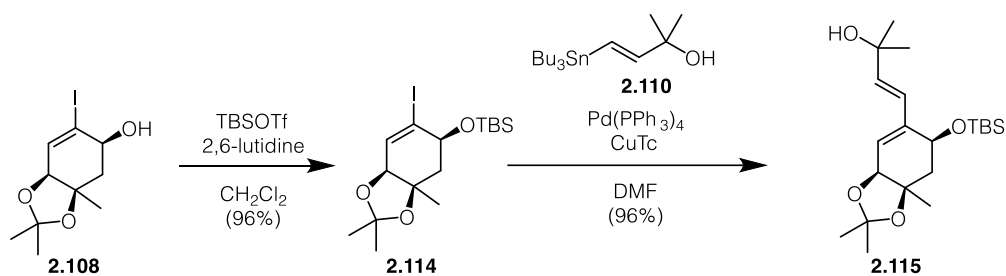
SCHEME 2.17: Synthesis of diol **2.111**.

2.111 was unstable in organic solvents at high temperatures and only triene **2.112** could be observed using normal glassware. While silica-based glassware can be slightly acidic we added an amine base which indeed could suppress elimination but unfortunately, no product could be observed under these conditions either. The same result was observed when **2.111** was heated without any solvent. The addition of Lewis acids was not well tolerated and mainly resulted in decomposition. When **2.111** was heated in either H₂O or a mixture of H₂O and MeOH deprotection of the acetonide was observed. This reaction had to be carefully monitored as rapid decomposition was observed after the starting material had been consumed (table 2.2).

TABLE 2.2: Screening for the dimerization of **2.111**.

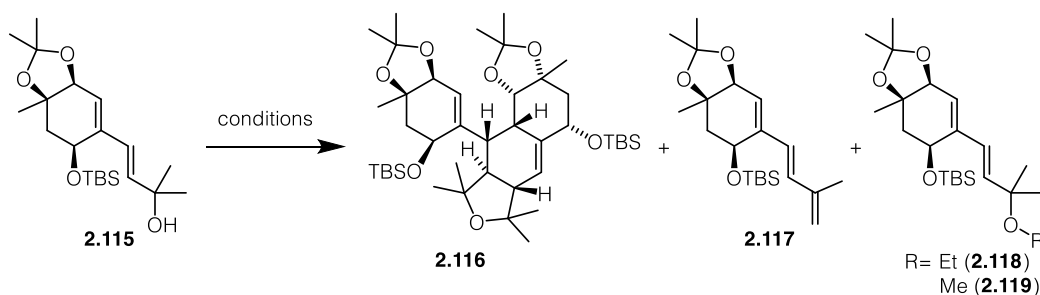
entry	solvent	additive	temperature	observation
1	PhMe	none	110 °C	2.112
2	PhMe	Net ₃	130 °C	starting material
3	DMF	CuTc/Pd(PPh ₃) ₄	150 °C	2.112
4	CH ₂ Cl ₂	EtAlCl ₂	-78 °C to RT	decomposition
5	neat	none	RT	starting material + elimination
6	neat	none	120 °C	2.112
7	neat	Net ₃	130 °C	starting material
8	neat	Er(fod) ₃	120 °C	decomposition
9	CH ₂ Cl ₂	15 kbar	RT	starting material
10	H ₂ O	none	65 °C	starting material
11	H ₂ O	none	100 °C	decomposition
12	H ₂ O/MeOH	none	65 °C	starting material
13	H ₂ O/MeOH	none	100 °C	acetal deprotection then decomposition
14	H ₂ O	H ₂ SO ₄	RT	decomposition

We therefore thought that the allylic alcohol might be unstable at temperatures needed to form the cation using Brønsted- or weak Lewis acid catalysis. We therefore protected the remaining secondary alcohol as a TBS-ether (scheme 2.18).

**SCHEME 2.18:** Synthesis of silyl ether **2.115**.

The addition of catalytic amounts of $\text{BF}_3\cdot\text{Et}_2\text{O}$ or SnCl_4 at cryogenic temperatures efficiently generated the allylic cation. When the reaction was quenched with EtOH stabilized CH_2Cl_2 , the cation was intercepted at the tertiary position and besides some elimination, the corresponding ethyl ether was obtained. The analogous result was observed when MeOH was used instead of EtOH. The allylic cation was stable at $-78\text{ }^\circ\text{C}$ but was not trapped by a second molecule of **2.115**. Warming of the reaction mixture showed that the cation was stable until $-30\text{ }^\circ\text{C}$ and decomposed upon warming to room temperature. While a dimerization was not possible, we wanted to know whether a smaller diene might be reactive enough to undergo a formal [4+2] reaction at all and therefore proving the general mechanism. The addition of 2,3-dimethyl-1,3-butadiene to the cation did not show any conversion at $-78\text{ }^\circ\text{C}$ and the reaction mixture decomposed upon slow warming to room temperature (table 2.3).

TABLE 2.3: Screening for the dimerization of **2.115**.

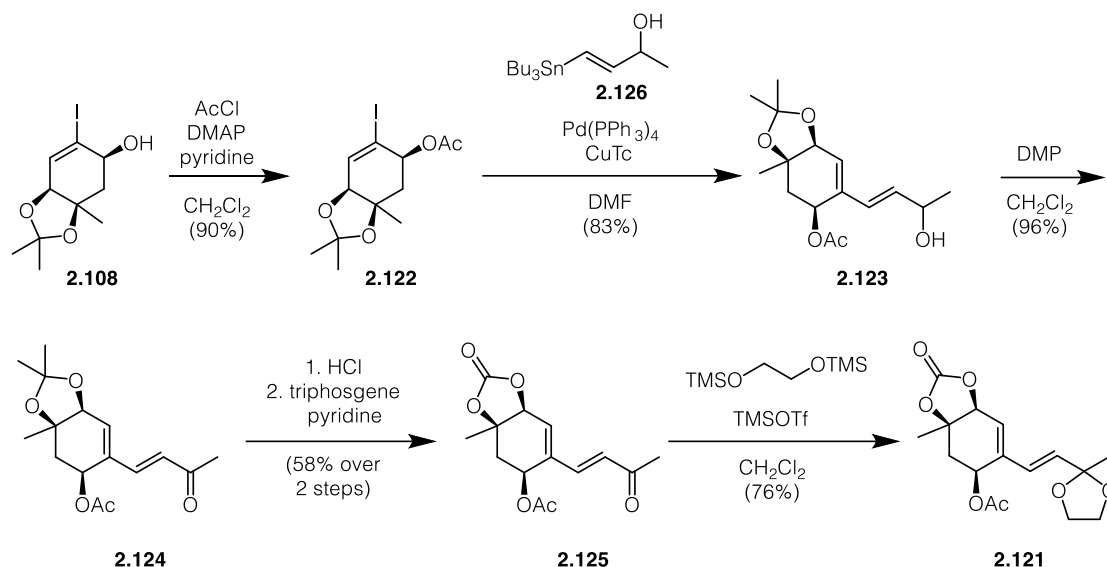


entry	solvent	additive	temperature	observation
1	CH_2Cl_2	$\text{BF}_3 \cdot \text{OEt}_2$ then ethanol	$-78\text{ }^\circ\text{C}$	2.118 + 2.117
2	CH_2Cl_2	$\text{BF}_3 \cdot \text{OEt}_2$ then methanol	$-78\text{ }^\circ\text{C}$	2.1189 + 2.117
3	CH_2Cl_2	SnCl_4 then ethanol	$-78\text{ }^\circ\text{C}$	2.118 + 2.117
4	CH_2Cl_2	$\text{BF}_3 \cdot \text{OEt}_2$ then methanol	$-78\text{ }^\circ\text{C}$ to $0\text{ }^\circ\text{C}$	decomposition
5	CH_2Cl_2	$\text{BF}_3 \cdot \text{OEt}_2$ then 2.120	$-78\text{ }^\circ\text{C}$	2.117
6	CH_2Cl_2	$\text{BF}_3 \cdot \text{OEt}_2$ then 2.120	$-78\text{ }^\circ\text{C}$ to RT	decomposition

2.120 = 2,3-dimethyl-1,3-butadiene

Even though we found conditions under which the allylic cation was stable, it was still too unreactive to dimerize. Gassman and co-workers did extensive work on ionic Diels-Alder reactions using allylic acetals and ketals as precursors.⁵⁷⁻⁵⁹ We hoped that this motif would prove to be more stable and yet reactive enough. We thus prepared dioxolane **2.121** as depicted in scheme 2.19. Acetylation of **2.108** under Steglich conditions gave rise to acetate **2.122** that could smoothly be transformed to allylic alcohol **2.123** by Stille coupling as a mixture of diastereoisomers. Enone **2.124** was obtained after Dess-Martin oxidation. Deprotection of the acetonide followed by reprotection as a carbonate

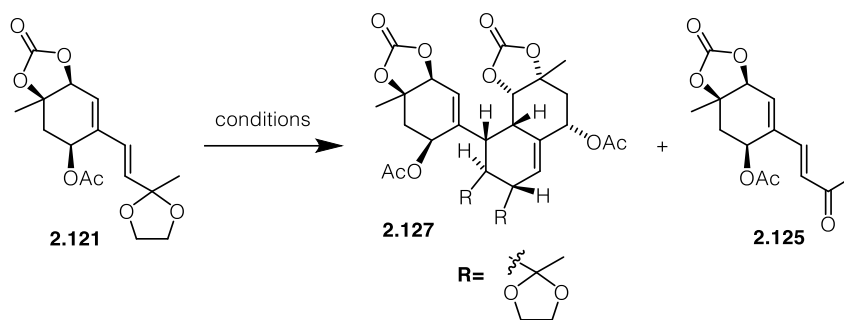
accessed **2.125**. The protecting group swap was necessary due to the instability of the acetonide group towards strong Lewis acids. Acetalization using Noyori's conditions resulted in dioxolane **2.121**.



SCHEME 2.19: Synthesis of dioxolane **2.121**.

Under Lewis acid catalysis the dioxolane was partially opened forming a carbocation as proven by the obtained deprotected ketone. The cation was stable to at least $-45\text{ }^{\circ}\text{C}$ and decomposed upon warming to room temperature. Unfortunately, no trace of the

TABLE 2.4: Screening for the ionic Diels-Alder reaction.



entry	solvent	additive	temperature	observation
1	Et ₂ O	4 M LiClO ₄ , CSA	RT	2.125
2	CH ₂ Cl ₂	Ti(O <i>i</i> Pr) ₄ , TiCl ₄	$-78\text{ }^{\circ}\text{C}$ to $-45\text{ }^{\circ}\text{C}$	2.125
3	CH ₂ Cl ₂	TMSOTf	$-78\text{ }^{\circ}\text{C}$	2.125
4	CH ₂ Cl ₂	BF ₃ OEt ₂	$-78\text{ }^{\circ}\text{C}$ to $-45\text{ }^{\circ}\text{C}$	2.125
5	CH ₂ Cl ₂	BF ₃ OEt ₂	$-78\text{ }^{\circ}\text{C}$ to RT	decomposition
6	CH ₂ Cl ₂	TMSOTf, 2.120	$-78\text{ }^{\circ}\text{C}$ to $0\text{ }^{\circ}\text{C}$	2.125

2.120 = 2,3-dimethyl-1,3-butadiene

desired dimerization product was observed. Addition of the smaller and more reactive 2,3-dimethyl-1,3-butadiene (**2.120**) showed that the cation is probably still not reactive enough (Table 2.4).

As we could not observe any trace of product until this point, we deemed unlikely to access **2.25** or **2.26** via a cationic Diels-Alder reaction.

2.3.2 The radical cation Diels-Alder reaction approach

While electron neutral Diels-Alder reactions are rarely described in the literature, the Diels-Alder reaction of radical cations are well known,⁶⁰⁻⁶³ although they have been hardly ever utilized in natural product synthesis.⁶⁴ Figure 2.6 shows the envisioned radical cascade Diels-Alder reaction. One electron oxidation of the diene moiety of **2.128** should lead to a radical cation, that should act as a dienophile in the Diels-Alder reaction with **2.128**. The newly formed radical should then result in **2.129** after electron transfer.

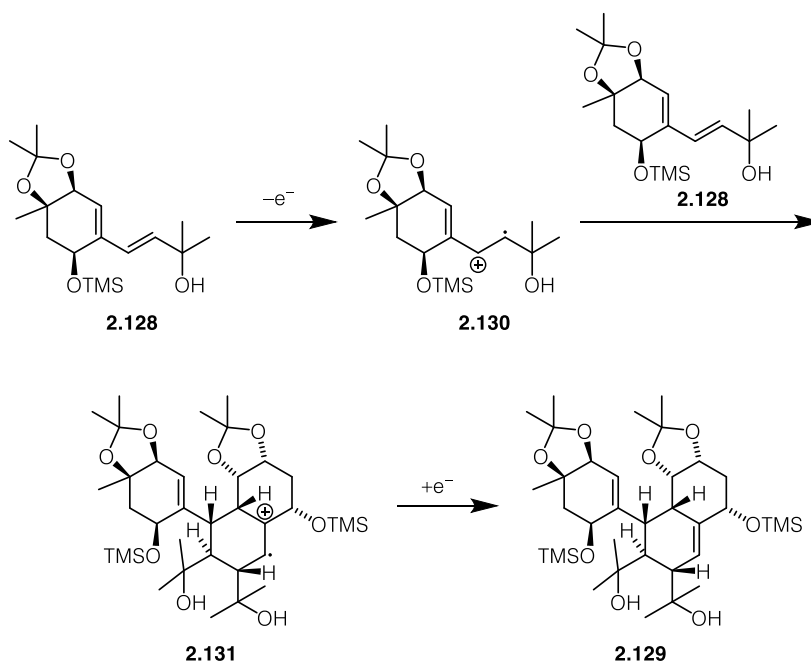
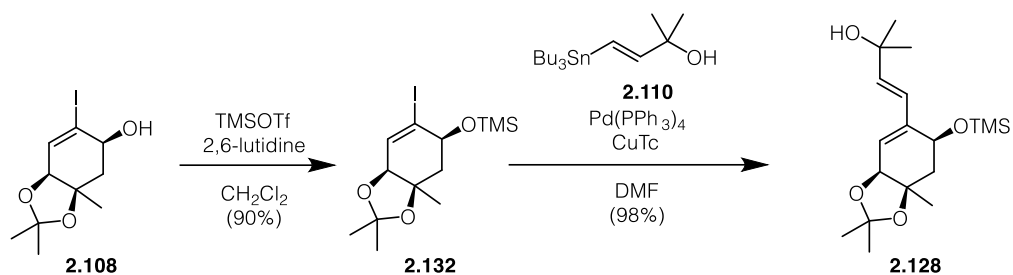


FIGURE 2.6: Proposed mechanism of the radical cation Diels-Alder reaction of **2.128**.

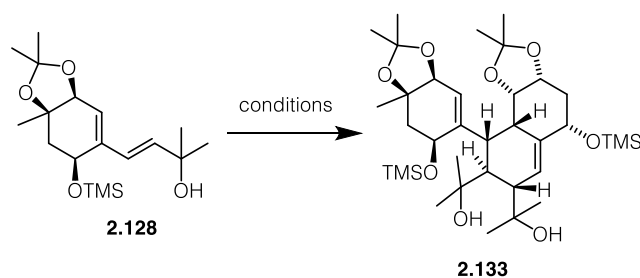
We chose allylic alcohol **2.128** as a reasonable substrate to explore the radical cation Diels-Alder reaction. TMS-protection of **2.108** followed by Stille-coupling yielded diene **2.128** in excellent yields (Scheme 2.20).



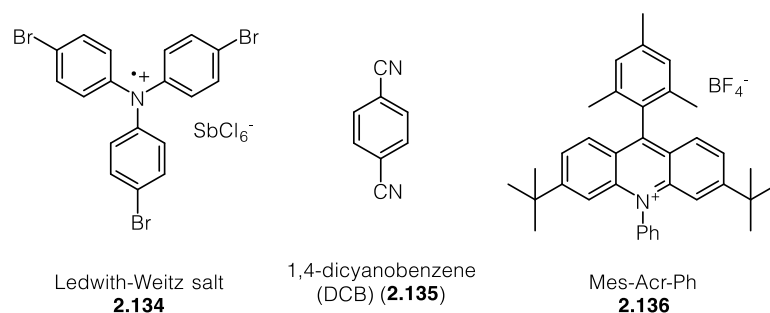
SCHEME 2.20: Synthesis of allylic alcohol **2.128**.

Attempts to generate a radical cation from the diene portion using Ledwith-Weitz salt resulted only in decomposition when the reaction was run at room temperature. In case the reaction was carried out at 0 °C, the only isolable product was triene **2.112**. Gassman and co-workers reported that in some cases reactions that were considered to run *via* a radical cation proceeded *via* a cation generated by acid residues in the Ledwith-Weitz salt. In order to see whether the elimination proceeded *via* a radical cation or was simply acid-catalyzed, we added 2,6-di-*tert*-butylpyridine to neutralize any residual acid. Under these conditions, no starting material was consumed, so we concluded that the redox potential of the Ledwith-Weitz salt was not sufficiently high to oxidize the diene. The use of TPPBF₄ resulted only in deprotection of the silyl ether, proving this catalyst is insufficient for the oxidation of the diene. When 1,4-dicyanobenzene (DCB) was used the starting material was decomposed (table 2.5).

TABLE 2.5: Screening for the radical cation Diels-Alder reaction.

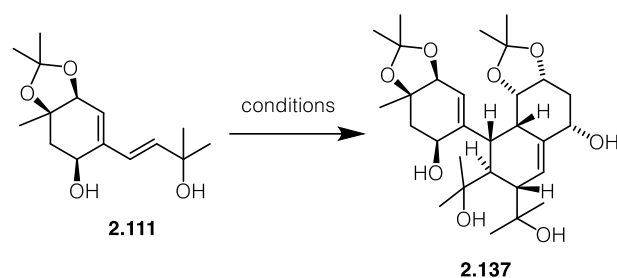


entry	solvent	additive	temperature	observation
1	CH ₂ Cl ₂	Ledwith-Weitz salt	RT	decomposition
2	CH ₂ Cl ₂	Ledwith-Weitz salt	0 °C	TMS deprotection and 2.112
3	CH ₂ Cl ₂	Ledwith-Weitz salt, 2,6-di- <i>tert</i> -butylpyridine	0 °C	starting material
4	MeCN	DCB, light	RT	decomposition
5	CH ₂ Cl ₂	TPPBF ₄ , light	0 °C	TMS deprotection



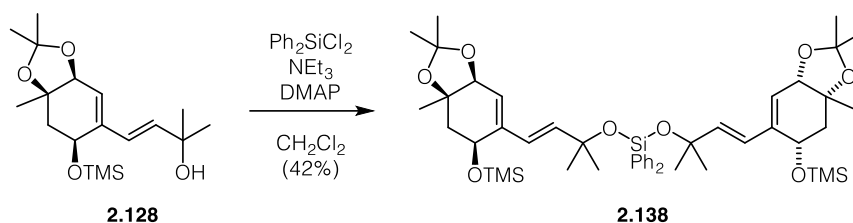
We next wanted to check whether the steric bulk of the TMS group was preventing any reaction. Using the strong photooxidation catalyst 9-mesityl-3,6-di-*tert*-butyl-10-phenylacridinium tetrafluoroborate (Mes-Acr-Ph) in combination with different additives on the free alcohol **2.111** only decomposition could be observed. The use of Ledwith-Weitz salt did not improve the reaction outcome (Table 2.6).

TABLE 2.6: Screening for the radical cation Diels-Alder reaction of **2.111**.



entry	solvent	catalyst	temperature	observation
1	CH_2Cl_2	Mes-Acr-Ph, DIPEA, PhSH, light	RT	starting material + partial decomposition
2	CH_2Cl_2	Mes-Acr-Ph, naphthalene, light	RT	decomposition
3	DCE	Mes-Acr-Ph, light	RT	decomposition
4	DCE	Mes-Acr-Ph, TEMPO, light	RT	decomposition
5	CH_2Cl_2	Ledwith-Weitz salt	RT	decomposition

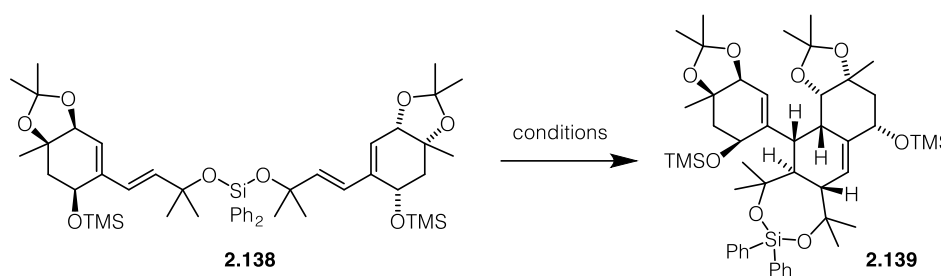
At this point we reasoned that decomposition pathways set in faster than dimerization of the potential radical cation might occur. We therefore prepared a tethered substrate where the second diene would be in close proximity to the presumably generated radical cation. Disiloxane **2.138** could be synthesized from tertiary alcohol **2.128** in moderate yields using dichlorodiphenylsilane and DMAP (Scheme 2.21).



SCHEME 2.21: Synthesis of disiloxane **2.138**.

Using Ledwith-Weitz salt as an oxidant, all silyl groups were removed from the molecule. This experimental result could be suppressed by the addition of base. When 2,6-di-*tert*-butylpyridine or NaHCO_3 were added to the reaction, no conversion was detected at all, again showing that the catalyst is insufficient for this oxidation. When a photocatalyst with a higher oxidation potential was applied, only decomposition could be observed (table 2.7). As the intramolecular radical cation Diels-Alder reaction was unable to produce any product, we were wondering whether the electron-neutral Diels-Alder reaction could be carried out on a tethered substrate. The application of 14 kbar did not give any conversion at all. Even though the substrate proved to be remarkably stable

TABLE 2.7: Screening for the intramolecular radical cation Diels-Alder reaction.



entry	solvent	additive	temperature	observation
1	CH_2Cl_2	Ledwith-Weitz salt	0 °C	complete silyl deprotection
2	CH_2Cl_2	Ledwith-Weitz salt, basic quench	0 °C	complete silyl deprotection
3	CH_2Cl_2	Ledwith-Weitz salt, 2,6-di- <i>tert</i> -butylpyridine	0 °C to RT	starting material
4	CH_2Cl_2	Ledwith-Weitz salt, NaHCO_3	0 °C to RT	starting material
5	MeCN	DCB, light	RT	decomposition
6	CH_2Cl_2	TPPBF ₄ , light	0 °C	decomposition
7	PhMe	none	200 °C	partial deprotection
8	CH_2Cl_2	14 kbar	RT	starting material

towards heat, no product was identified in the reaction mixture when **2.138** was heated to 200 °C.

At this point we were convinced that a radical cation Diels-Alder reaction would not be suitable to deliver the product and we revised our strategy.

2.3.3 The divinylcyclobutane rearrangement

Conjugated dienes are known to undergo an excited state [2+2]-cycloaddition when exposed to UV-light in the presence of a photosensitizer.⁶⁵⁻⁶⁷ The resulting divinylcyclobutane could then undergo a formal Cope rearrangement,⁶⁸⁻⁶⁹ leading to our desired product (Figure 2.7). While the stereochemistry next to the cyclohexane rings might be inconsequential for the cycloaddition step, we were optimistic that the tertiary alcohols would be on opposite faces due to steric repulsion.

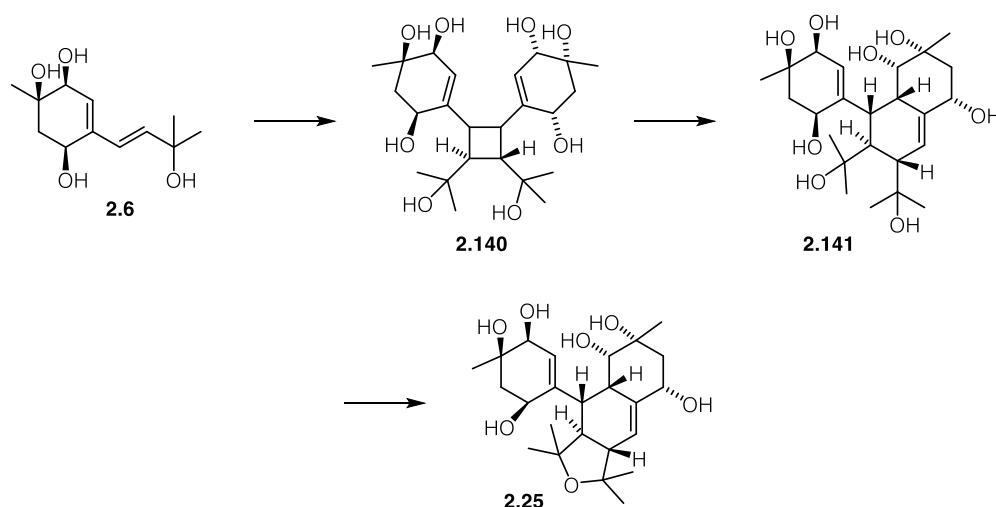
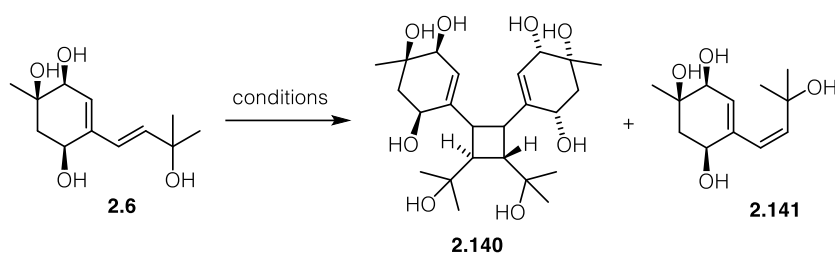


FIGURE 2.7: Predicted reaction pathway towards **2.25**.

When **2.6** was exposed to blue light in the presence of Fukuzumi's catalyst (Mes-Acr-Ph), only decomposition was observed (table 2.8). Metal-catalyzed reactions using Ni⁰ did not show any conversion at all. When **2.6** was irradiated with a mercury lamp in the presence of different photosensitizers and in various solvents, ¹H-NMR analysis only suggested isomerization of the disubstituted double bond. These experiments

TABLE 2.8: Screening for the [2+2]-cycloaddition.

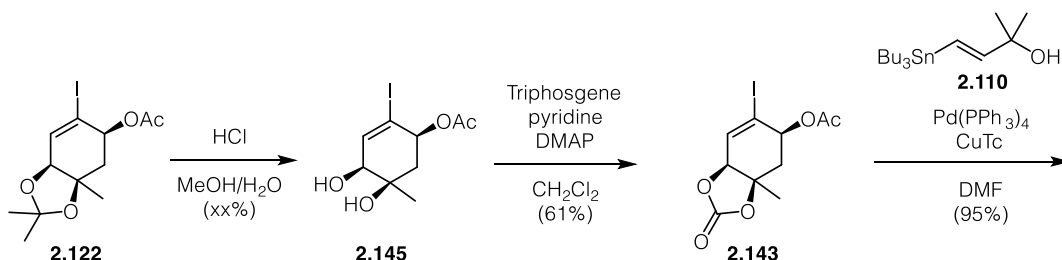


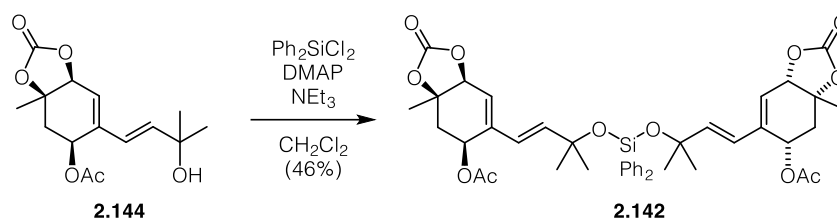
entry	solvent	additive	temperature	observation
1	DMF	Mes-Acr-Ph, light	RT	decomposition
2	PhMe	Ni(cod) ₂ , PPh ₃	80 °C	starting material
3	Benzene	Ni(cod) ₂ , PPh ₃	60 °C	starting material
4	DMF	DCB, light	RT	2.141
5	MeCN	DCB, light	RT	2.141
6	MeCN	Benzophenone, light	RT	2.141
7	Acetone	light	RT	2.141

Light source: medium pressure Hg lamp

showed it was indeed possible to excite the diene and form the diradical needed for the [2+2]-cycloaddition to proceed. Unfortunately, isomerization of the double bond was faster than any intermolecular reaction.

In order to see whether the dimerization would proceed in an intramolecular reaction we prepared the tethered substrate **2.142**.⁷⁰⁻⁷² As we were not sure whether the acetonide groups were sterically demanding we exchanged them by carbonates. Deprotection of **2.122** followed by reprotection delivered carbonate **2.143** that underwent a Stille-coupling with vinyl stannane **2.110** to give tertiary alcohol **2.144**. The disiloxane **2.142** could be obtained after reacting **2.144** with dichlorodiphenylsilane in the presence of DMAP (scheme 2.22).

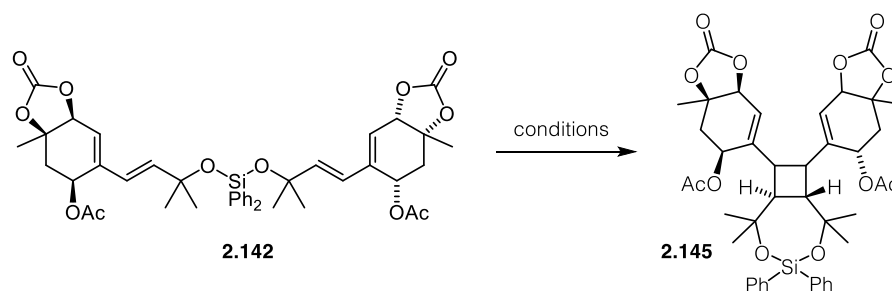




SCHEME 2.22: Synthesis of disiloxane **2.142**.

Unfortunately, when **2.142** was exposed to UV light in the presence of either benzophenone or acetone as a photosensitizer, the starting material decomposed completely within 1 h (table 2.9). As we knew from the previous experiments that the diene could be excited under these conditions, we concluded that the substrate was not suitable for the desired cycloaddition.

TABLE 2.9: Screening for the intramolecular [2+2]-cycloaddition.

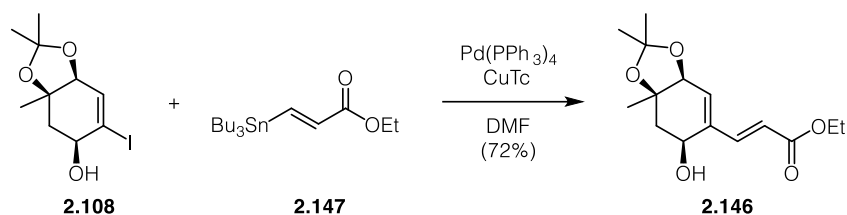


entry	solvent	additive	temperature	observation
1	MeCN	benzophenone, light	RT	decomposition
2	acetone	light	RT	decomposition

As we could not detect any trace of product, we decided to change our route as depicted in the next chapter.

2.3.4 The classical Diels-Alder reaction route

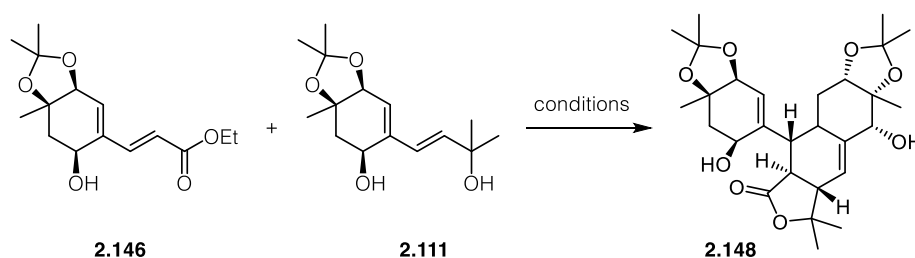
After all attempts to dimerize a monomeric building block in order to form a symmetrical or unsymmetrical dimer had failed, we considered a classical Diels-Alder reaction, utilizing an electron-rich diene and an electron-poor dienophile, suitable to form the natural product.⁷³ We first prepared ethyl ester **2.146** by Stille coupling of vinyl iodide **2.108** with vinyl stannane **2.147** (scheme 2.23).



SCHEME 2.23: Synthesis of ethyl ester **2.146**.

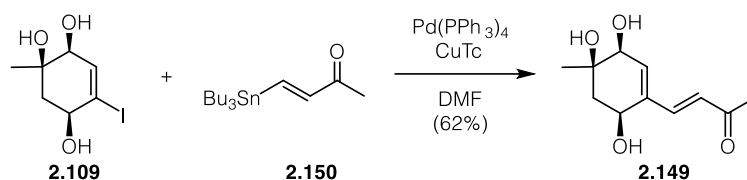
We attempted to react **2.146** with diene **2.111** to form the cyclohexene ring of **2.25**. We further expected the cycloaddition product to undergo spontaneous lactonization due to the close proximity of the tertiary alcohol and the ester group. The reactants were stable, yet unreactive in PhCF_3 up to 110 °C. At 130 °C, alcohol **2.111** underwent elimination to triene **2.112**. The elimination could be prevented by the addition of NEt_3 . Unfortunately, no reaction occurred under these conditions, either. When the reactants were heated without solvents, no cycloaddition occurred and only the eliminated product could be observed (table 2.10).

TABLE 2.10: Screening for the Diels-Alder reaction between **2.111** and **2.112**.



entry	solvent	additive	temperature	observation
1	PhCF_3	$\text{Eu}(\text{fod})_3$	110 °C	starting material
2	PhCF_3	$\text{Eu}(\text{fod})_3$	130 °C	2.112
3	PhMe	NEt_3	110 °C	starting material
4	neat	none	130 °C	2.112

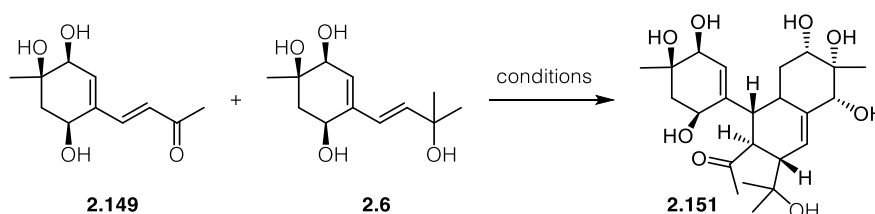
We wondered whether the α,β -unsaturated ester was not reactive enough and if the acetonide groups were creating too much steric hindrance. Therefore, we prepared enone **2.149** by Stille-coupling of vinyl iodide **2.109** with vinyl stannane **2.150** (Scheme 2.24).



SCHEME 2.24: Synthesis of enone **2.149**.

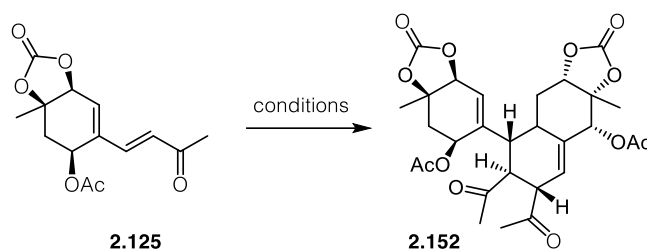
When 14 kbar in the presence of ZnBr_2 were applied to the reactants, the formation of a complex mixture was observed. The same was obtained when the reaction was carried out neat at 50 °C. Both reactants were stable in H_2O up to 50 °C and decomposed when heated to 100 °C. While the ketone was stable in PhMe at 110 °C, the alcohol decomposed without entering any productive reaction pathway (Table 2.11).

TABLE 2.11: Screening for the reaction of **2.149** with **2.6**.



entry	solvent	additive	temperature	observation
1	CH_2Cl_2	ZnBr_2 , 14 kbar	RT	complex mixture
2	neat	none	50 °C	complex mixture
3	H_2O	none	50 °C	starting material
4	H_2O	none	100 °C	decomposition
5	PhMe	none	110 °C	decomposition

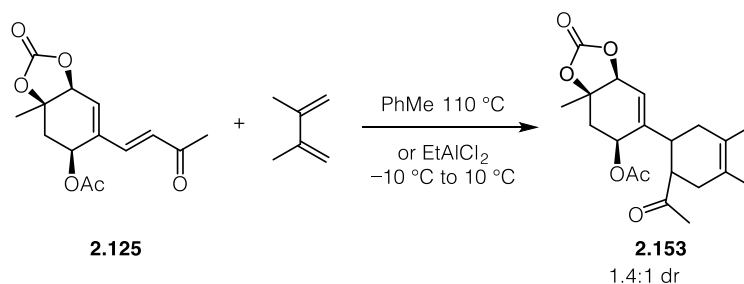
Sorbic acid is known to form dimers by a Diels-Alder reaction to give a mixture of regio- and stereoisomers. We were interested whether we could also dimerize enone **2.125** in a similar manner (Table 2.12).

TABLE 2.12: Screening for the dimerization of **2.125**.

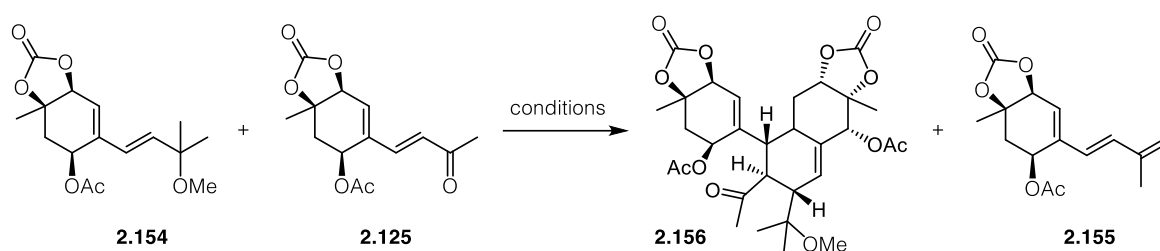
entry	solvent	additive	temperature	observation
1	<i>o</i> -DCB	none	180 °C	starting material
2	DCE	EtAlCl ₂	-30 °C to 80 °C	starting material
3	neat	none	180 °C	complex mixture

Even though sorbic acid dimerizes at 110 °C in the absence of any solvent, **2.125** was still unreactive at 180 °C in *o*-DCB. When heated neat, the starting material was directly converted into a complex mixture which did not show any characteristic signals in the ¹H-NMR spectrum. Lewis acid catalysis did also not prove to be successful and resulted in unreacted starting material.

At this point we investigated whether **2.125** was able to undergo a Diels-Alder reaction as a dienophile. To our delight, the reaction of **2.125** with 2,3-dimethyl-1,3-butadiene proceed smoothly under either thermal or Lewis acid-catalyzed conditions giving **2.153** as a 1.4:1 mixture of diastereoisomers (Scheme 2.25).

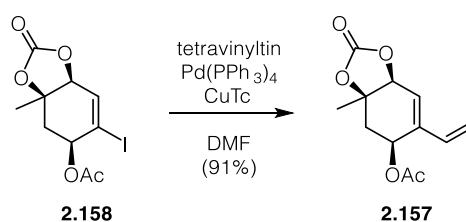
**SCHEME 2.25:** Diels-Alder reaction of **2.125** and 2,3-dimethyl-1,3-butadiene.

We hoped that protecting the tertiary alcohol as a methyl ether would prevent elimination and reduce the Lewis basicity of the alcohol. **2.154** did not react with **2.125** in the presence of EtAlCl₂ at low temperatures. When the reaction mixture was gradually heated, elimination to triene **2.155** could be observed at 80 °C. When both reactants were heated neat, no reaction occurred until both compounds decomposed at 200 °C (Table 2.13).

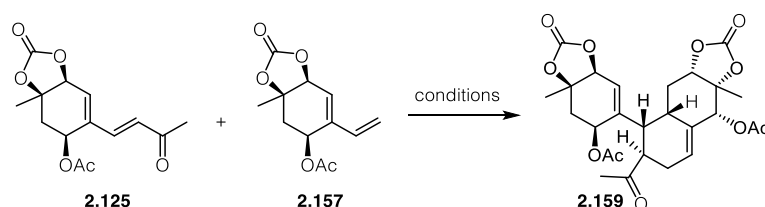
TABLE 2.13: Reaction of **2.125** with alcohol **2.154**.

entry	solvent	additive	temperature	observation
1	DCE	EtAlCl ₂	-30 °C to 80 °C	2.155
2	neat	none	60 °C to 100 °C	starting material
3	neat	none	100 °C to 200 °C	decomposition

Next, we wanted to figure out whether the tertiary alcohol would be too hindered for the reaction to proceed. We therefore prepared the shorter diene **2.157** by Stille coupling of vinyl iodide **2.158** and tetravinyltin (scheme 2.26).

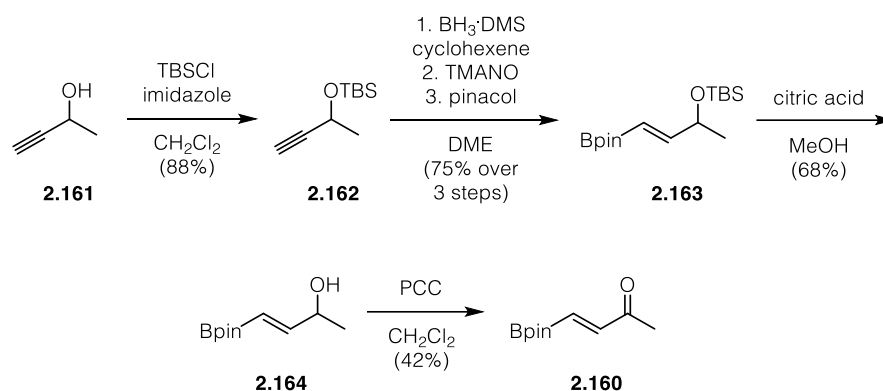
**SCHEME 2.26:** Synthesis of diene **2.157**.

Even though we were expecting high temperatures to be needed for the reaction to proceed, no conversion could be detected until 180 °C. The addition of EtAlCl₂ could not enforce the reaction at low temperatures and decomposition of the reactants was observed upon heating (scheme 2.27).

**SCHEME 2.27:** Attempted reaction of **2.125** with **2.157**.

These results showed that the low reactivity of the diene was not due to the steric hindrance of the tertiary alcohol, as initially expected. Although we could not see any desired reactivity of the diene portion by now, we wanted to investigate the reactivity of this part in a Diels-Alder reaction. Therefore, we synthesized the strong dienophile **2.160**

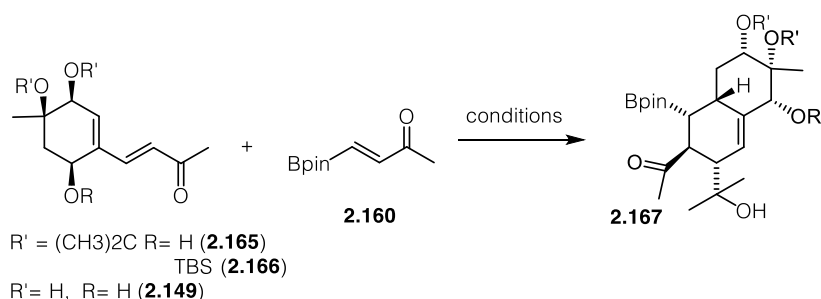
as depicted in Scheme 2.28. 3-butyn-2-ol (**2.161**) was TBS-protected under standard conditions and gave **2.162** in good yields. Further hydroboration using *in situ*-generated dicyclohexylborane followed by oxidation to the boronic acid and esterification with pinacol accessed boronic ester **2.163**. Enone **2.160** was obtained after TBS deprotection under mild conditions and further allylic oxidation.⁷⁴



SCHEME 2.28: Synthesis of boronic ester **2.160**.

With **2.160** in hand, we went on screening different protecting patterns on **2.6** in order to investigate the reactivity of the substrate (table **2.14**).

TABLE 2.14: Investigation of **2.160** as a dienophile.

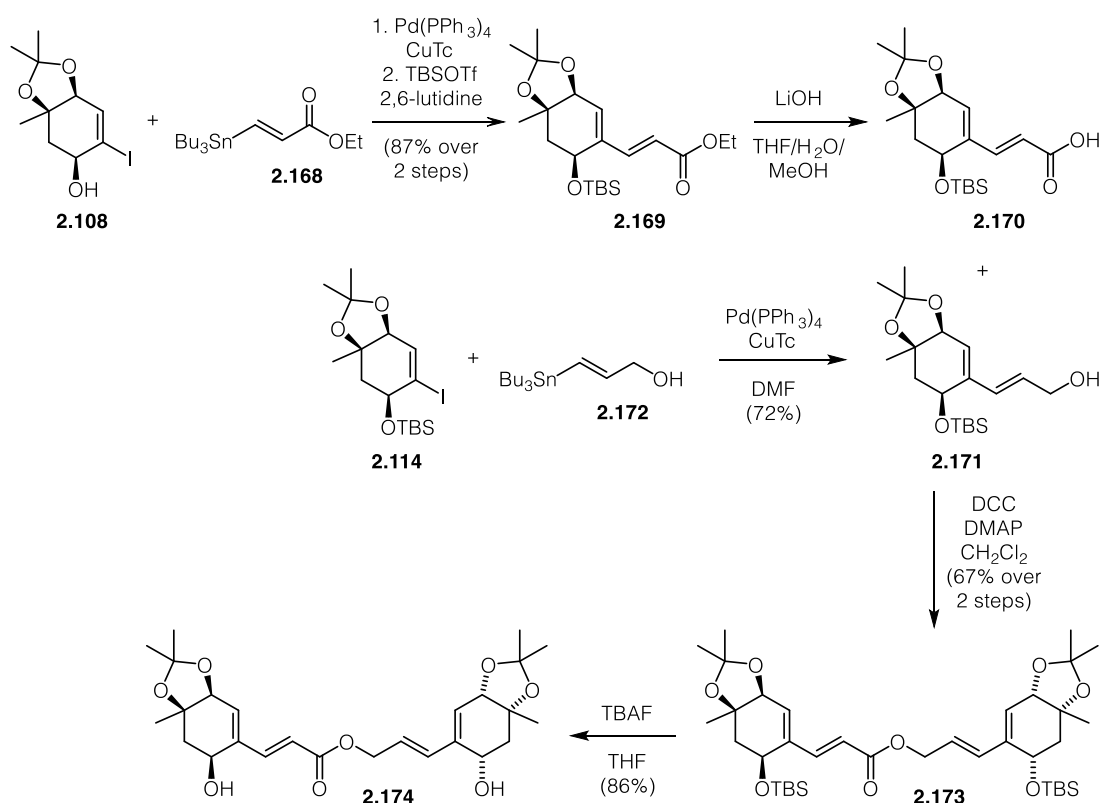


entry	R=	R' =	solvent	temperature	observation
1	(CH ₃) ₂ C	TBS	PhMe	110 °C	starting material
2	(CH ₃) ₂ C	H	PhMe	110 °C	starting material
3	H	H	PhMe	80 °C	product
4	H	H	PhMe	110 °C	product

Protection of the secondary allylic alcohol had no effect, at least in case that the *syn* diol moiety was still protected. As long as the acetonide was still part of the molecule, no reaction with **2.160** was observed using standard conditions. To our delight, unprotected diol **2.6** reacted already at 80 °C smoothly with **2.160**. The reaction required prolonged reaction times and was not significantly accelerated at 110 °C. Even though, NMR data

clearly suggested the formation of a Diels-Alder product as a single diastereoisomer, we were unable to completely purify the compound by column chromatography, probably due to the instability of the boronic ester towards silica. The regio selectivity may possibly be explained by coordination of the boronic ester to the free diol.

At this point we decided that either the sterical or electronical properties of the substrates were not sufficient for the reaction to proceed. Both characteristics should improve drastically, in case the reaction would be carried out in an intramolecular fashion. We therefore decided to link the two monomeric building blocks *via* an ester bond. While all attempts to form the ester from a tertiary alcohol failed, we utilized the primary alcohol and planned to install the dimethyl groups later in the synthesis. Stille coupling between vinyl iodide **2.108** and vinyl stannane **2.168** followed by TBS protection gave ethyl ester **2.169** that upon saponification gave acid **2.170**. **2.170** could be esterified with allylic alcohol **2.171**, which was obtained by Stille coupling between vinyl iodide **2.114** and vinyl stannane **2.172**. The silyl ethers of allylic ester **2.173** were then deprotected under standard conditions giving free diol **2.174** (Scheme 2.29).

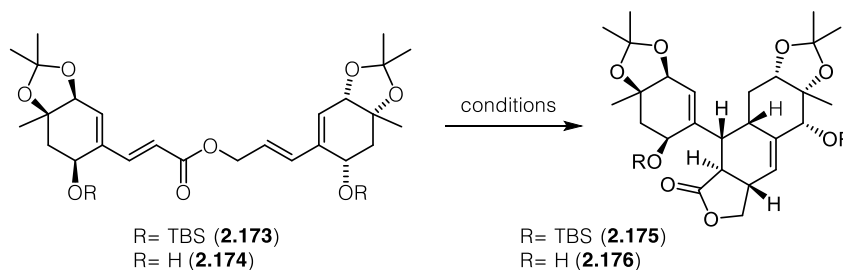


SCHEME 2.29: Synthesis of allylic ester **2.174**.

The protected alcohol **2.173** was first applied to the intramolecular Diels-Alder reaction (Table 2.15). No reaction proceeded by exposure of **2.173** to 14 kbar and resulted in recovered starting material. Heating a solution **2.173** in *o*-DCB to high temperatures

decomposed the compound. The free diol **2.174** was also not stable at high temperatures and decomposed at 180 °C. Addition of $\text{Sc}(\text{OTf})_3$ had no effect on the reaction. Upon exposure of **2.174** to EtAlCl_2 , no conversion was detected when the

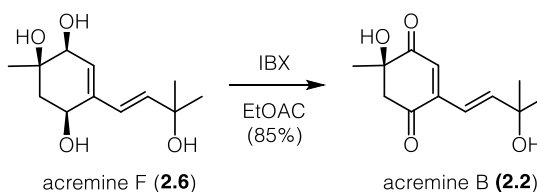
TABLE 2.15: Screening for the intramolecular cycloaddition.



entry	R=	solvent	additive	temperature	observation
1	TBS	CH_2Cl_2	14 kbar	RT	starting material
2	TBS	<i>o</i> -DCB	BHT	180 °C	decomposition
3	TBS	<i>o</i> -DCB	BHT	200 C	decomposition
4	H	<i>o</i> -DCB	BHT	180 °C	decomposition
5	H	CH_2Cl_2	$\text{Sc}(\text{OTf})_3$	-78 °C - RT	starting material
6	H	CH_2Cl_2	$\text{Sc}(\text{OTf})_3$	RT - 70 °C	starting material
7	H	CH_2Cl_2	EtAlCl_2	-78 °C - RT	starting material
8	H	PhMe	$\text{Sm}(\text{OTf})_3$	70 °C	starting material
9	H	PhMe	$\text{Sm}(\text{OTf})_3$	110 °C	decomposition

reaction was warmed from -78 °C to room temperature. When $\text{Sm}(\text{OTf})_3$ was used as a Lewis acid, the starting material was not consumed until 70 °C but decomposed upon heating to 110 °C. The instability of the substrate to heat is most likely to the labile allylic ester used to link the two fragments. Unfortunately, at this point we were running out of time to revise our retrosynthesis.

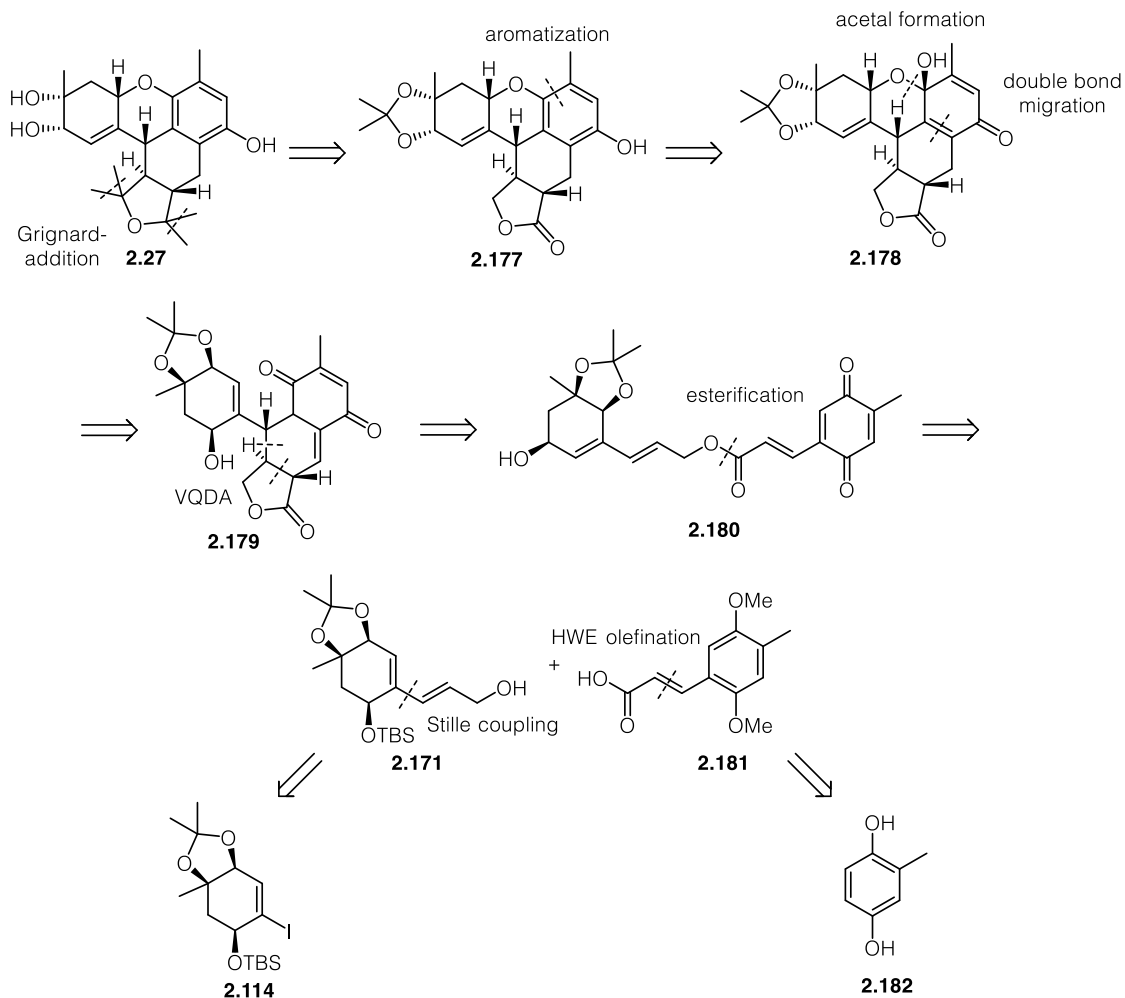
With acremine F (**2.6**) in hand we were wondering whether we could transform the compound into the related natural product acremine B (**2.2**). Treatment of **2.6** with excess IBX smoothly accessed acremine B (**2.2**) (Scheme 2.30).



SCHEME 2.30: Synthesis of acremine B (2.2).

2.3.5 Synthetic studies towards bisacremine G

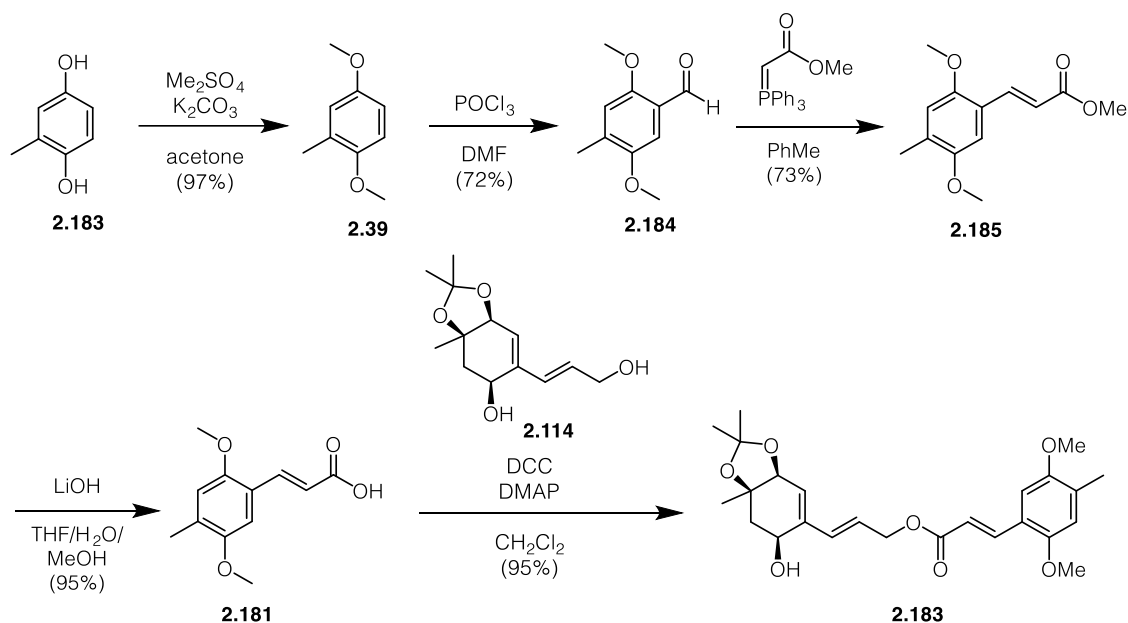
The retrosynthetic analysis of bisacremine G (**2.27**) is depicted in scheme 2.31. It was envisioned to install the four methyl groups through Grignard addition into ester **2.177** followed by oxidation of the resulting primary alcohol, a second Grignard attack and acid catalysed ring closure of the tetrahydrofuran ring. **2.177** would be derived from hemiketal **2.178** by reductive aromatization. Tetrahydropyran **2.178** would be formed from diketone **2.179** by acetal formation and migration of the double bond to the thermodynamically more stable position. An intramolecular vinyl quinone Diels-Alder reaction of allylic ester **2.180**, derived from acid **2.181** and allylic alcohol **2.171**, would give access to the tricyclic core of **2.27** and setting all remaining stereogenic centers. Allylic alcohol **2.171** would be obtained *via* Stille coupling of vinyl iodide **2.114** whereas carboxylic acid **2.181** would be derived from methylhydroquinone (**2.182**) by Vilsmeier-Haack formylation followed by HWE olefination.



SCHEME 2.31: Proposed cascade reaction leading to **2.27**.

The key cyclization precursor **2.180** could be generated from **2.183** via global deprotection and further oxidation of the hydroquinone moiety.

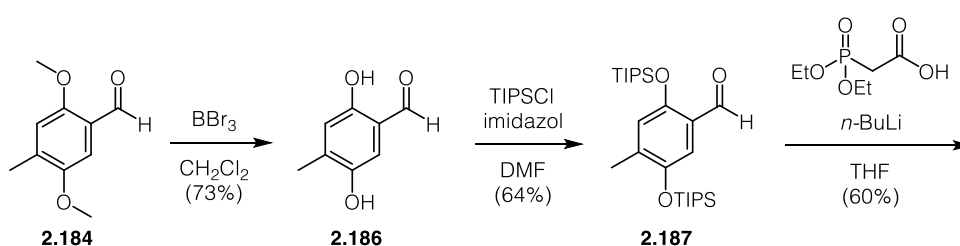
Methylation of methylhydroquinone **2.182** using dimethyl sulfate gave methyl ether **2.39** that could be formylated under Vilsmeier-Haack conditions to yield aldehyde **2.184**. Carboxylic acid **2.181** was obtained after Wittig-reaction followed by hydrolysis and was esterified with alcohol **2.114** to give allylic ester **2.183** (Scheme 2.32).

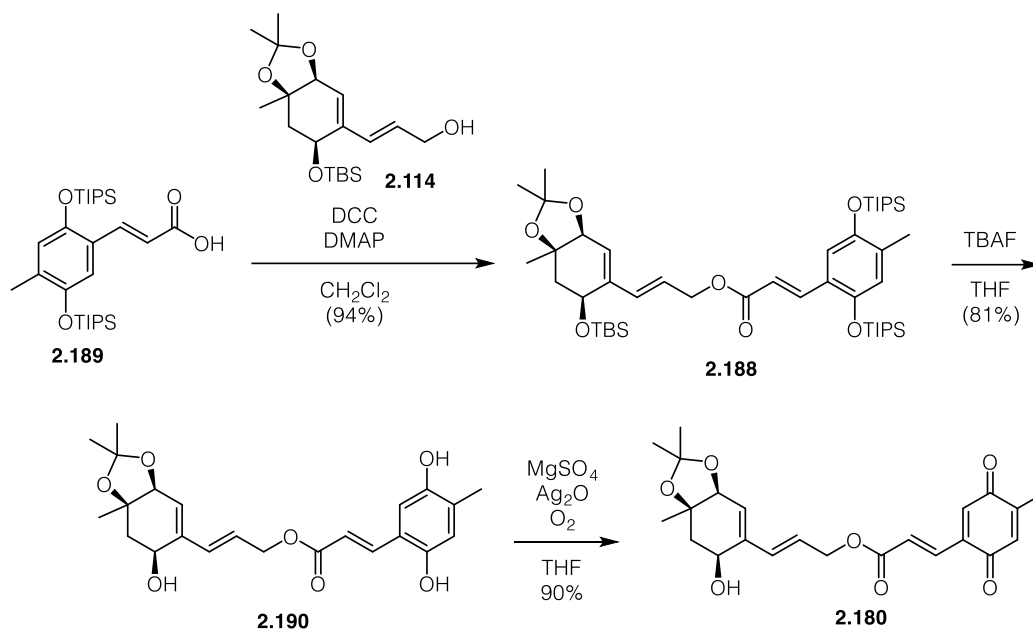


SCHEME 2.32: Synthesis of allylic ester **2.183**.

The next step of the synthesis would require the oxidation of the protected hydroquinone. Unfortunately, attempts to oxidize the dimethyl hydroquinone using CAN or 4-iodophenoxyacetic acid and oxone in various solvent mixtures resulted either in decomposition or recovered starting material. The same results were observed upon attempts to deprotect the methyl ethers without direct oxidation.

As this protecting group pattern proved to be unsuitable for our synthesis, we switched the protecting groups (Scheme 2.33). **2.184** was demethylated to hydroquinone **2.186** using BBr_3 and reprotected to give TIPS-ether **2.187**. Allylic ester **2.188** was obtained by a similar sequence as described above.

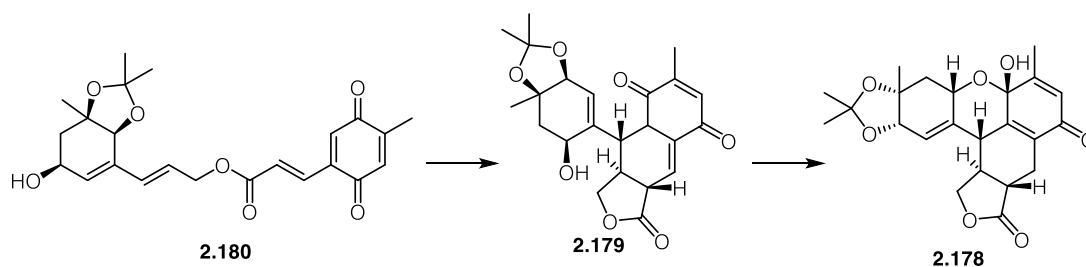




SCHEME 2.33: Synthesis of cyclization precursor **2.180**.

Vinylquinone **2.189** was obtained after removal of all three silyl ethers followed by oxidation using Ag_2O . As **2.189** turned out to be unstable towards column chromatography, the crude material was used to investigate the cyclization cascade (Table 2.16).

TABLE 2.16: Screening for the VQDA reaction

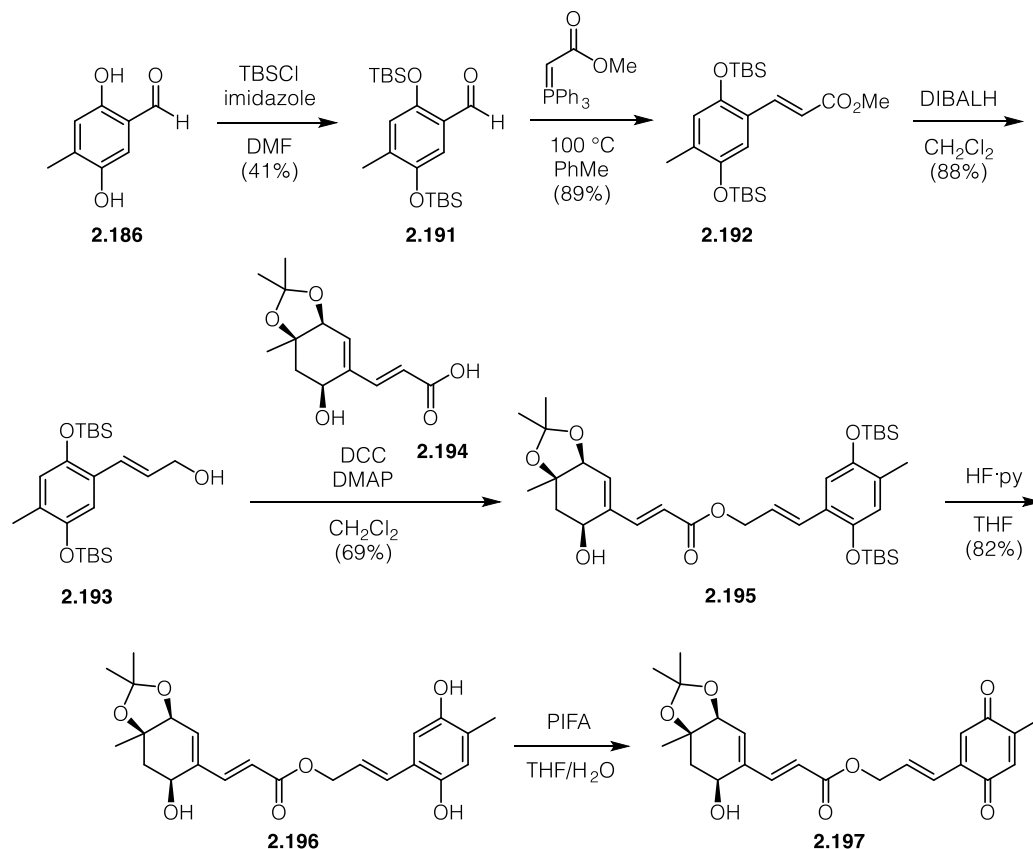


entry	solvent	additive	temperature	observation
1	PhMe	none	110 °C	2.190
2	H ₂ O/THF	none	60 °C	2.190
3	PhMe	BHT	150 °C	decomposition
4	<i>o</i> -DCB	BHT	200 °C	ester cleavage
5	CH ₂ Cl ₂	12 kbar	RT	decomposition
6	MeCN	Sc(OTf) ₃	RT	no reaction
7	Et ₂ O	LiClO ₄	RT	no reaction

Most literature known VQDA reactions proceed either at room temperature or in moderately heated solutions.^{52, 55} Heating a solution of **2.180** in PhMe, H₂O or THF gave,

besides decomposition, hydroquinone **2.190**. When a solution **2.180** in PhMe was heated to 150 °C in a sealed tube, only decomposition could be observed. Upon further heating of **2.180** in *o*-DCB to 180 °C, alcohol **2.114** could be isolated from the reaction mixture, suggesting that the allylic ester had been cleaved. We therefore assumed that vinyl quinone **2.180** was not stable enough at temperatures required for a Diels-Alder cycloaddition. Trauner reported that VQDA reaction can benefit from Lewis acid catalysis or high pressure. Unfortunately, when 12 kbar were applied to a solution of **2.180** in CH₂Cl₂, only decomposition was observed. The addition of Sc(OTf)₃ could also not accelerate the reaction. Diels-Alder reactions are known to be facilitated by the use of solvents containing a high ionic strength, such as 4 M LiClO₄ in Et₂O. Unfortunately, when these conditions were applied to **2.180** no conversion could be detected.

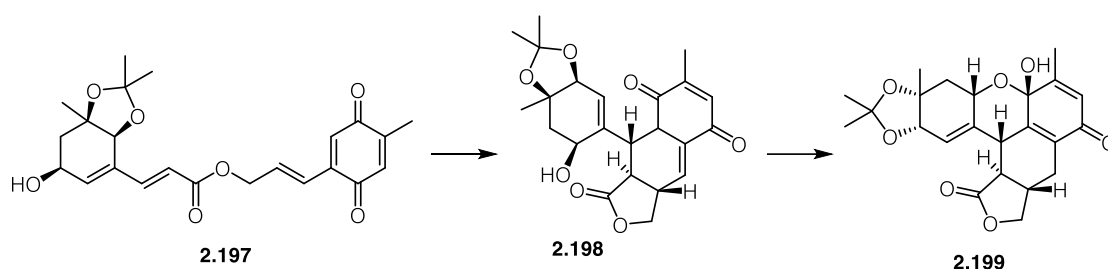
While the electronic character of the substrate seems to match the requirements of an inverse electron demanding Diels-Alder reaction, it is known that electron deficient vinyl quinones dimerize easily. Trauner and co-workers also showed that changing the electronic properties of the substrate may help the reaction to proceed.⁵⁵ We therefore redesigned our substrate by swapping the place of the carbonyl group in the allylic ester and therefore change the polarity of the substrate (Scheme 2.34).



SCHEME 2.34: Synthesis of allylic ester **2.197**.

TBS protection of hydroquinone **2.186** gave access to aldehyde **2.191** which could undergo a Wittig-reaction to yield methyl ester **2.192**. **2.192** could be reduced to allylic alcohol **2.193** using DIBAL-H which could then be esterified with acid **2.194** to obtain allylic ester **2.195**. While the deprotection of the silyl ethers under strongly basic conditions using TBAF resulted in hydrolysis of the ester, using HF-pyridine as a fluoride source smoothly yielded triol **2.196**. It turned out that the oxidation of the hydroquinone moiety could best be obtained by the use of PIFA as the oxidant, giving rise to vinyl quinone **2.197**. **2.197** was unstable towards chromatography and was therefore used crude in the following cyclization attempts (Table 2.17).

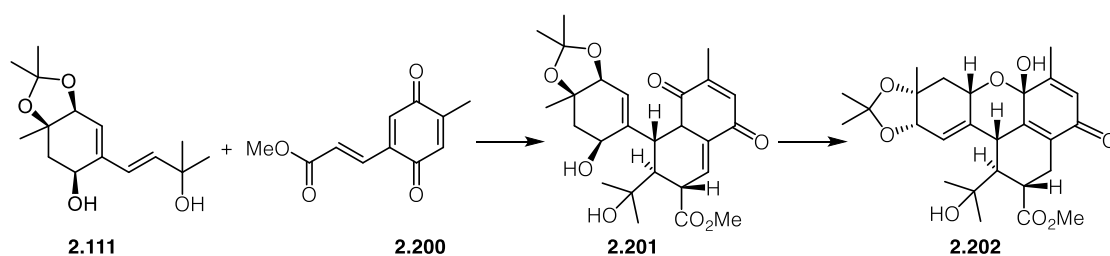
TABLE 2.17: Screening for the VQDA reaction of **2.197**.



entry	solvent	additive	temperature	observation
1	PhMe	none	60 °C	decomposition
2	<i>o</i> -DCB	none	180 °C	decomposition
3	CH ₂ Cl ₂	12 kbar	RT	complex mixture

Unfortunately, attempts to trigger a VQDA reaction thermally or under high pressure resulted in complete decomposition of the starting material. Therefore, we reasoned that vinyl quinone **2.197** is unstable under conditions required for a VQDA reaction.

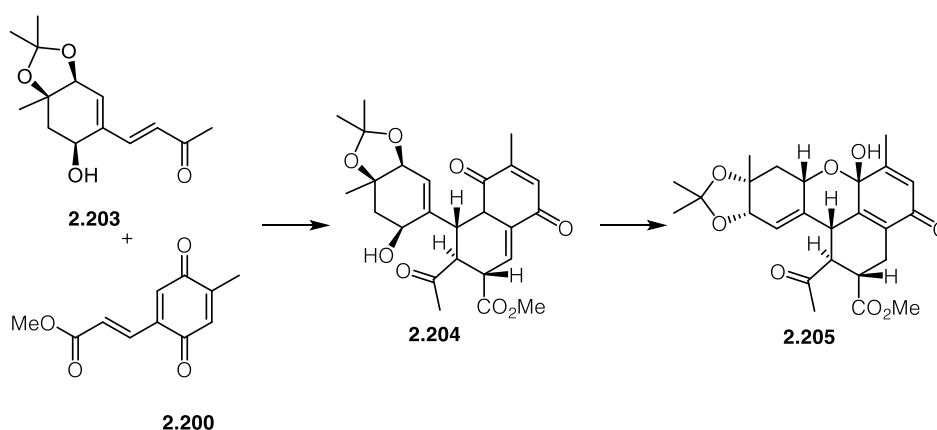
As we had only investigated intramolecular VQDAs we thought it might be worthwhile examining intermolecular reactions. We therefore wanted to see whether a VQDA reaction between vinyl quinone **2.200** and allylic alcohol **2.111** would be feasible (Table 2.18).

Table 2.18: Screening for the VQDA reaction of **2.111** and **2.200**.

entry	solvent	additive	temperature	observation
1	PhMe	none	60 °C	starting material
2	PhMe	none	110 °C	complex mixture
3	neat	Eu(fod) ₃	60 °C	complex mixture
4	CH ₂ Cl ₂	Sm(OTf) ₃	-78 °C - RT	starting material
5	CH ₂ Cl ₂	Sc(OTf) ₃ , MS 5 A	-78 °C - RT	decomposition of alcohol
6	H ₂ O/THF	none	60 °C	quinone dimerization

While a solution of **2.111** and **2.200** in PhMe showed no conversion until 60 °C, both compounds were converted to a complex mixture upon heating to 110 °C. The addition of Sm(OTf)₃ could not accelerate the reaction as well as Eu(fod)₃. The addition of Sc(OTf)₃ in combination with molecular sieves as a desiccant were supposed to accelerate the acetalization in order to facilitate the following VQDA reaction. Unfortunately, this combination led to decomposition of alcohol **2.111**. When **2.111** and **2.200** were heated in a mixture of H₂O and THF the ¹H-NMR data suggested the dimerization of the vinyl quinone.

These results suggested that the reaction is most likely to proceed when both partners are electron-deficient. In order to prove this hypothesis a reaction between enone **2.203** and vinyl quinone **2.200** could be carried out (scheme 2.35).

SCHEME 2.35: VQDA reaction between **2.203** and **2.200**.

2.4 Summary and outlook

In conclusion, we investigated the biomimetic dimerization of acremine F (**2.6**) to bisacremine E (**2.25**) and F (**2.26**). We proposed an ionic cascade that could lead to the natural product and therefore examined the reactivity of **2.6**. An allylic cation could be generated under various conditions and trapped with different nucleophiles. Nevertheless, the generated cation was trapped with the wrong regiochemistry making the proposed biosynthesis unlikely. We next investigated a radical cation Diels-Alder reaction as a possible mechanistic pathway. Our experiments on a variety of substrates showed that this pathway is unlikely or at least not feasible with the substrates examined. Furthermore, we examined a photochemical pathway in which **2.6** was supposed to dimerize in a [2+2]-cycloaddition forming a divinylcyclobutane that should then undergo a formal Cope rearrangement to form the core of the natural product. Intensive experiments showed the difficulties in forming the 4-membered ring necessary for the Cope rearrangement. We conducted further studies on the nonbiomimetic synthesis of **2.25** and **2.26** employing several monomeric and tethered substrates. Even though the biogenic synthesis remains unclear we gained insight into the reactivity of **2.6**. In addition, we were able to establish the first asymmetric total syntheses of acremine B (**2.2**) and F (**2.6**). The route proved to be robust and therefore provides access to the whole class of the acremine natural product family.

Furthermore, we conducted synthetic studies towards the asymmetric total synthesis of bisacremine G (**2.27**) employing a VQDA reaction. To this end, we prepared three highly sophisticated vinyl quinones as substrates for the cyclization cascade. Even though we were unable to induce the reaction, we gained insight into this largely unexplored methodology. While a VQDA reaction using an electron-rich partner did not lead to any product, it remains to be investigated whether the reaction proceeds with an electron-poor dienophile as indicated by the homodimerization of **2.200**. This reaction could provide a fast access to the core of bisacremine G and extend the scope of this powerful methodology.

Chapter III

Exerting Photocontrol over G-Protein Coupled Receptors

3.1 G-Protein coupled receptors (GPCRs)

Signal transduction presents one of the most important processes in all organisms and is required to ensure coordination of cellular activity and maintain cellular homeostasis.⁷⁵⁻⁷⁷ The transmission from the external to the internal environment is usually rendered by membrane proteins at the cell surface that sense signalling molecules such as hormones, neurotransmitters or paracrine factors. The probably largest and most diverse class of transmembrane proteins is the heterotrimeric guanine nucleotide binding protein (G-protein) coupled receptors (GPCRs).⁷⁸⁻⁷⁹ More than 1000 GPCRs are encoded in the mammalian genomes with most of them coding for sensory receptors like taste or olfactory receptors.⁷⁶ They are considered as major contributors to the information flow into the cells and, as such, are associated with a range of diseases.⁸⁰ Therefore, it is not surprising that GPCRs are one of major drug targets and account for more than 50% of human therapeutics currently on the market.⁷⁹ GPCRs can be divided into three main classes A, B and C based on protein sequence homologies.⁷⁸ Class A GPCRs comprise the largest group, accounting for almost 85% of all GPCR genes, whose archetype is rhodopsin.⁷⁵ Despite the lack of homology in between the classes, all GPCRs share a conserved transmembrane structure comprising seven α -helices between an extracellular *N*-terminus and an intracellular *C*-terminus.⁷⁷ GPCRs can detect a variety of extracellular signals including photons, ions, small organic molecules and entire proteins. Upon ligand binding, the receptor undergoes a conformational change leading to activation of the heterotrimeric G-protein.⁷⁶ It consists of α -subunit as well as a β -

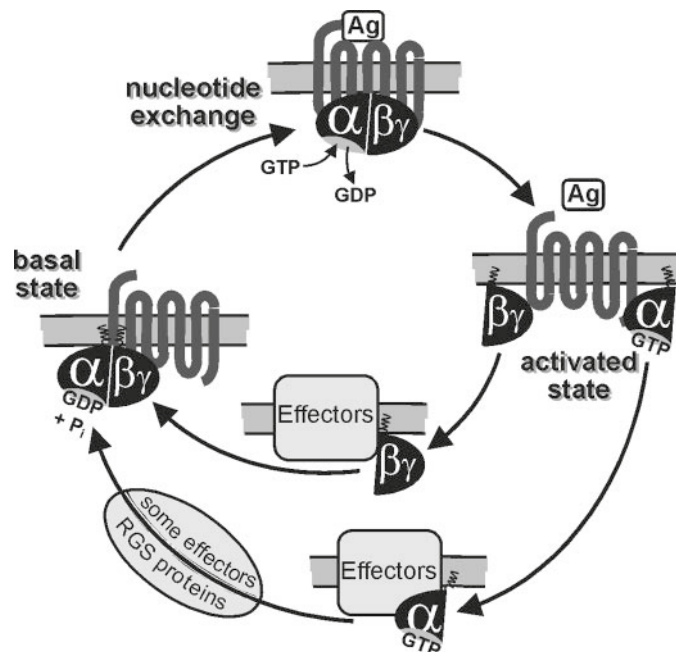


FIGURE 3.1: Functional cycle of G-protein activity.⁷⁶

and a γ -subunit which are forming an undissociable complex. In the resting state, the GDP-bound α -subunit and the $\beta\gamma$ -complex are associated. Binding of an effector to the GPCR promotes exchange of GDP for GTP on the α -subunit that triggers the dissociation from the $\beta\gamma$ -complex. Both subparts are then able to modulate effector functions. The inherent GTPase activity of the α -subunit then hydrolyses GTP to GDP leading to reassociation of the $\alpha\beta\gamma$ subunits (Figure 3.1). The basic properties of G-proteins are defined by the α -subunits which can be divided into four families: $G\alpha_s$, $G\alpha_i/G\alpha_o$, $G\alpha_q/G\alpha_{11}$ and $G\alpha_{12}/G\alpha_{13}$.⁷⁷

$G\alpha_s$ and $G\alpha_i/G\alpha_o$ both affect the adenylate cyclase and therefore the intracellular level of cAMP. While $G\alpha_s$ has an activating effect, $G\alpha_i/G\alpha_o$ shows inhibiting function the enzyme. $G\alpha_q/G\alpha_{11}$ activates phospholipase C which catalyses the cleavage of phosphatidylinositol-4,5-biphosphate (PIP2) into inositoltrisphosphate (IP3) and diacylglycerol (DAG).⁷⁶ IP3 leads to the release of Ca^{2+} from the ER and therefore increases the intracellular Ca^{2+} -level while DAG activates protein kinase C. $G\alpha_{12}/G\alpha_{13}$ has activating effects on RhoGEF. Although $G\beta\gamma$ had been considered to be passive for a long time, it can affect various ion channels such as the G-protein regulated inwardly rectifying potassium channel (GIRK), voltage gated Ca^{2+} -channels, isoforms of adenylyl cyclase phospholipase C as well as isoforms of phosphoinositide-3-kinase.⁷⁶ Most receptors can activate multiple G-protein subtypes and activation results therefore in activation of several signal transduction cascades.

3.2 Dopamine receptors (DARs)

3.2.1 Introduction

3.2.1.1 Dopamine receptors (DARs)

Dopamine (DA) is a fundamental neurotransmitter that is part of the catecholamine family and plays a major role in the mammalian brain.⁸¹ It controls a multiplicity of functions such as locomotor activity, cognition, emotion, positive reinforcement, food intake and endocrine regulation.⁸² DA is also abundant in the periphery where it acts as a modulator of cardiovascular function, catecholamine release, hormone secretion, vascular tone, renal function and gastrointestinal motility.⁸¹ Disorders in the dopamine homeostasis are related to several diseases, such as Parkinson's disease, schizophrenia and attention deficit hyperactivity disorder (ADHD).⁸³ Dopamine receptors (DARs) are part of the family A G protein coupled receptors (GPCRs) which makes up the majority of the GPCR superfamily (ca. 85%) and represent the target of 25–30% of all available medications.⁸⁴ DARs are divided into two subfamilies, the D1-like receptors and the D2-like receptors, based on sequence homology and function.⁸⁵ D1-like receptors (D1/D5) couple to $G_{s/olf}$ and therefore have a stimulating effect on the adenylyl cyclase which catalyses the synthesis of the secondary messenger cyclic AMP (cAMP).⁸¹ They are found exclusively postsynaptically on dopamine receptive cells, such as GABA-ergic medium spiny neurons (MSNs) in the striatum.⁸¹ D2-like receptors (D2/D3/D4) couple to $G_{i/o/z}$ resulting in an inhibitory effect on the enzyme. They are found postsynaptically on dopamine target cells as well as presynaptically on dopaminergic neurons. Changes in the cAMP level directly and indirectly modulate an array of downstream proteins, including kinases, ion channels and transcription factors.⁸² Despite from the cAMP pathway, DARs can directly control downstream proteins such as GIRK channels *via* the $G\beta\gamma$ subunits.⁸¹ DARs also recruit arrestins, which terminate G protein signalling and facilitate G protein-independent signalling and can therefore directly take control over downstream proteins. Although DARs within a given subfamily couple to similar downstream signalling transducers, they diverge functionally by interacting with unique accessory proteins *via* their intracellular loops and C-termini (e.g. D1R and D5R can interact directly with NMDA and GABA receptors, respectively) and have distinct cellular localization patterns.⁸²

The individual members of the subfamilies of the D1 and D2 class receptor share a high level of homology of their heptahelical transmembrane domains.⁸⁶ D1 and D5 are 80% homologous in this domain whereas D3 and D4 share 75% and 53% homology with the D2 receptor respectively.⁸¹ The number of amino acid residues in the N-terminal domain

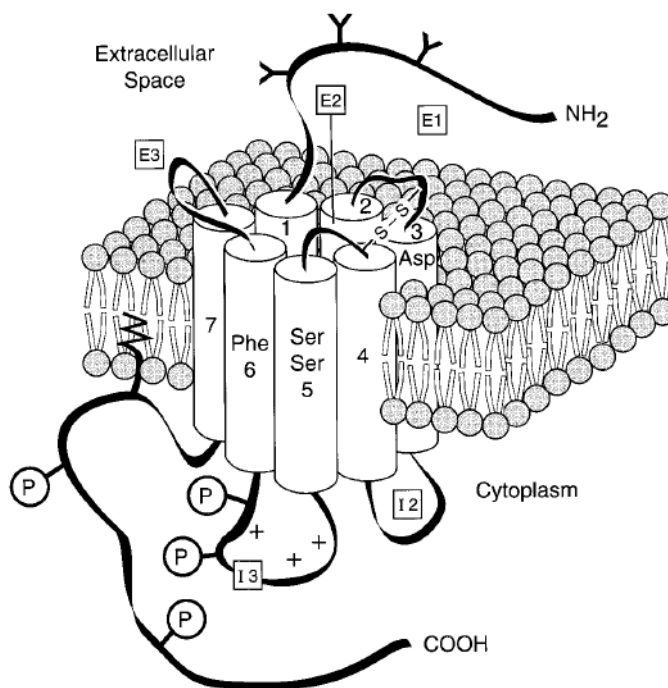


FIGURE 3.2: Structure of a D1-like receptor. E1-E3, extracellular loops; 1-7, transmembrane domains; I2-I3, intracellular loops.⁸²

is largely consistent all over DARs whereas the C-terminal domain of the D1 class is seven times longer than that of the D2 class. DARs possess two cysteine residues in the extracellular loops 2 and 3 that are supposed to form an intramolecular disulphide bridge stabilising the structure.⁸² D2 like receptors are characterized by a long third intracellular loop whereas the third loop in D1 like receptors is shortened (Figure 3.2). The core of the protein contains highly conserved residues defining a narrow binding pocket that corresponds to the agonist binding site. The binding of the amino group of the catecholamine is likely to happen *via* an aspartate residue in the transmembrane domain 3 (TM3). TM5 provides two serine residues which act as hydrogen bond donors to bind the hydroxyl groups of the catechol moiety. A phenylalanine residue in TM6 is highly conserved over all receptors and is supposed to form stabilizing orthogonal interactions with the aromatic core of the ligand. An allosteric interaction is suggested to be provided by an aspartate residue in TM2.⁸²

3.2.2.1 Structure-affinity relationship for 2-aminotetralines

The dopaminergic activity of 2-aminotetralins was identified in the late 1960s and led to active synthetic affords optimizing the structures over the following decades.⁸⁷⁻⁸⁹ The development of dopamine receptor agonists follows two main strategies: Rigidification of the dopamine (**3.1**) skeleton, arresting the α -conformation of the molecule and dissection of the semisynthetic agonist apomorphine (**3.2**). The design of aminotetralines presents a combination of both approaches.⁸⁹ The class of phenolic 2-aminotetralines has been studied intensively and showed comparatively high dopaminergic activity. Structure affinity relationships aimed on the determination of the positional effect of the hydroxyl moiety, the effect of substituents on the nitrogen atom and the absolute configuration.⁹⁰ The hydroxyl group on the aromatic ring turned out to be crucial most likely due to hydrogen bond donation to residues in the ligand binding site. Hydroxyl groups in position 5, 6 and 7 increased the potency and showed a maximum effect when the hydroxyl group was in position 5. Alkyl substituents at the nitrogen showed an increase in efficacy with an optimum for a propyl chain. While the first substituent should not exceed the length of a propyl group, variations on the second substituent are well tolerated. Lipophilic motives such as homobenzylic residues showed best results.⁹⁰ Figure 3.3 shows the natural DAR agonist dopamine (**3.1**), the semisynthetic agonist apomorphine (**3.2**) and the synthetic agonist PPHT (**3.3**).



FIGURE 3.3: DA receptor agonists.

3.2.2 Project outline

Dopamine receptors (DARs) provide a promising target for debilitating disorders such as Parkinson's disease, schizophrenia, addiction, ADHD, obsessive compulsive disorder and Tourette's syndrome.⁸⁴ Even though DARs have been intensively studied over the last decades, the role of individual DARs *in vivo* remains not fully understood. However, there are few ligands that selectively bind individual DARs due to the highly conserved orthosteric dopamine binding site. Additionally, diffusible ligands are not cell-type specific and therefore are unable to differentiate between DARs that have distinct and, in some cases, opposing roles in neighbouring neurons or brain regions. In order to obtain spatio-temporally precise activation of DARs, we sought to implement a photoswitchable moiety into the known DA receptor agonist PPHT (**3.3**). This should be achieved by extension of the homobenzylic residue to an azobenzene (Figure 3.4). Structure-affinity relationships suggested that large residues would be tolerated at that site without great loss of activity.⁸⁹ Upon irradiation with UV light the molecule should undergo a conformational change altering its shape and therefore its ability to activate the receptor. In order to obtain cell-type specificity, we wanted to install a molecular anchor at the end of the photoswitch which can react with a cysteine residue that is genetically engineered near to the binding site of a desired receptor. This strategy needs only a single point mutation and therefore maintains all features of a wild type receptor, including their endogenous DA binding site and receptor elements that control signaling, localization and trafficking. In a second approach, we sought to implement a SNAP-tag motif enabling the use a fully wild type receptor.

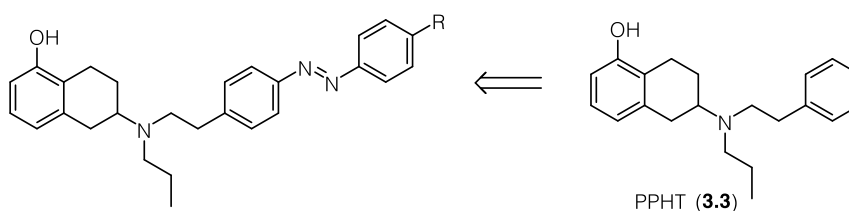


FIGURE 3.4: Azologization strategy for photoswitchable DAR agonists.

3.2.3 Results and discussion

3.2.3.1 Azobenzene-PPHT (AP) and Maleimide-Azobenzene-PPHT (MAD)

Reproduced with permission from Prashant Donthamsetti, Nils Winter, Matthias Schönberger, Joshua Levitz, Cherise Stanley, Jonathan A. Javitch, Ehud Y. Isacoff, and Dirk Trauner, *J. Am. Chem. Soc.* **2017**, *139*, 18522–18535. Copyright 2017 American Chemical Society.⁹¹

Optical Control of Dopamine Receptors Using a Photoswitchable Tethered Inverse Agonist

Prashant C. Donthamsetti,^{†,⊗} Nils Winter,^{‡,⊗} Matthias Schönberger,[‡] Joshua Levitz,[†] Cherise Stanley,[†] Jonathan A. Javitch,^{§,||} Ehud Y. Isacoff,^{*,†,⊥,#} and Dirk Trauner^{*,‡,∇,Ⓢ}

[†]Department of Molecular and Cell Biology, University of California, Berkeley, California 94720, United States

[‡]Department of Chemistry and Center for Integrated Protein Science, Ludwig-Maximilians-Universität, Butenandtstraße 5-13, Munich 81377, Germany


[§]Departments of Psychiatry and Pharmacology, Columbia University, New York, New York 10027, United States

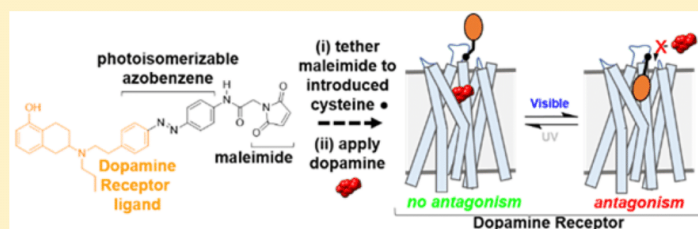
^{||}Division of Molecular Therapeutics, New York State Psychiatric Institute, New York, New York 10032, United States

[⊥]Helen Wills Neuroscience Institute, University of California, Berkeley, California 94720, United States

[#]Bioscience Division, Lawrence Berkeley National Laboratory, Berkeley, California 94720, United States

[∇]Department of Chemistry, New York University, New York, New York 10003, United States

 Supporting Information



ABSTRACT: Family A G protein-coupled receptors (GPCRs) control diverse biological processes and are of great clinical relevance. Their archetype rhodopsin becomes naturally light sensitive by binding covalently to the photoswitchable tethered ligand (PTL) retinal. Other GPCRs, however, neither bind covalently to ligands nor are light sensitive. We sought to impart the logic of rhodopsin to light-insensitive Family A GPCRs in order to enable their remote control in a receptor-specific, cell-type-specific, and spatiotemporally precise manner. Dopamine receptors (DARs) are of particular interest for their roles in motor coordination, appetitive, and aversive behavior, as well as neuropsychiatric disorders such as Parkinson's disease, schizophrenia, mood disorders, and addiction. Using an azobenzene derivative of the well-known DAR ligand 2-(*N*-phenethyl-*N*-propyl)amino-5-hydroxytetralin (PPHT), we were able to rapidly, reversibly, and selectively block dopamine D1 and D2 receptors (D1R and D2R) when the PTL was conjugated to an engineered cysteine near the dopamine binding site. Depending on the site of tethering, the ligand behaved as either a photoswitchable tethered neutral antagonist or inverse agonist. Our results indicate that DARs can be chemically engineered for selective remote control by light and provide a template for precision control of Family A GPCRs.

INTRODUCTION

Heptahelical G protein-coupled receptors (GPCRs) constitute the largest superfamily of membrane proteins.¹ GPCRs are activated by diverse stimuli (e.g., hormones, odorants, or neurotransmitters) and regulate a wide variety of biological processes via heterotrimeric G protein and arrestin signaling proteins. The Family A GPCRs make up the majority of the GPCR superfamily (~85%)¹ and represent targets of 25–30% of all available medications.² Recent genetic and structural advancements have substantially enhanced our understanding of this receptor family.³ However, because of the high degree of similarity between related Family A GPCRs as well as their heterogeneous expression across diverse cell types throughout the body, it has been difficult to selectively

target and thus uncover the roles of individual receptors *in vivo*.

A major challenge in neuroscience has been to elucidate the physiological and behavioral roles of neuromodulator-binding Family A GPCRs that regulate synaptic and circuit function in the central nervous system. Dopamine (DA) and its five receptors (DARs) are particularly notable, as they control critical functions such as locomotion, learning, and memory.⁴ DARs are divided into two subfamilies based on sequence homology and function. Whereas D1-like receptors (D1/D5) couple to G_{s/olf}, D2-like receptors (D2/D3/D4) couple to G_{i/o/z}.⁵ These G proteins have

Received: July 21, 2017

Published: November 22, 2017

opposing actions on adenylyl cyclases, which catalyze the synthesis of the secondary messenger cyclic AMP (cAMP). Changes in cAMP directly and indirectly modulate an array of downstream proteins, including kinases,⁶ ion channels,^{7–11} and transcription factors.¹² DARs can directly control downstream proteins such as G protein-coupled inwardly rectifying potassium channels (GIRKs) via *Gβγ* subunits.^{13,14} DARs also recruit arrestins,^{15,16} which terminate G protein signaling and facilitate G protein-independent signaling.¹⁷ Although DARs within a given subfamily couple to similar downstream signaling transducers, they diverge functionally by interacting with unique accessory proteins via their intracellular loops and C-termini (e.g., dopamine receptors 1 and 5, D1R and D5R, can interact directly with NMDA¹⁸ and GABA_A¹⁹ receptors, respectively) and have distinct cellular localization patterns.²⁰

Deciphering the roles of individual DARs *in vivo* has implications not only for understanding the synaptic and neural circuit actions of DA but also the mechanisms underlying debilitating disorders such as Parkinson's disease,²¹ schizophrenia,²² addiction,²³ ADHD,²⁴ obsessive compulsive disorder,²⁵ and Tourette's syndrome.²⁶ However, current tools that are used to target DARs suffer from substantial limitations. A rich pharmacological toolkit of DAR agonists (full, partial) and antagonists (neutral antagonists, inverse agonists) has been developed over more than half a century.^{27,28} Nevertheless, there are few ligands that selectively bind individual DARs due to the high degree of similarity in their orthosteric binding sites (OBSs) that bind DA.²⁹ Of note, there are no ligands that selectively bind D1R over D5R or D2R over D3R/D4R.²⁹ In any case, diffusible ligands are not cell-type-specific and thus cannot differentiate between a DAR that has distinct and, in some cases, opposing roles in neighboring neurons or brain regions.²⁰ Therefore, it is impossible to disambiguate the roles of individual DARs using a classical pharmacological approach.

Alternatively, genetic approaches, i.e., the overexpression, knockdown, or knockout of individual proteins, can be used to control individual DARs in specific cell types.³⁰ However, these modifications affect receptor function over long time scales, which limits our understanding of the temporal aspects of DAR activation and can result in confounding compensatory effects on neuronal physiology.

Optogenetic and pharmacogenetic tools, such as optoXRs^{31–33} and RASSLs³⁴/DREADDs,³⁵ respectively, have been developed to cell-type-specifically interrogate GPCR function *in vivo* with greater temporal control than traditional genetic approaches. For example, a chimeric receptor, consisting of a partial sequence of D1R as well as the naturally light-sensitive components of rhodopsin (opto-D1R), was used to remotely activate D1R-mediated signaling *in vivo*.³⁶ However, although such tools represent a powerful means to engage GPCR-dependent processes, they are non-native proteins that lack critical aspects of DARs, including their endogenous ligand binding site that binds DA, and/or receptor elements that control signaling, localization, and trafficking. Furthermore, they cannot be used to block DARs from being activated by DA, which is required for establishing which receptors are necessary for mediating specific DA-dependent processes. Thus, current opto- and pharmacogenetic tools may provide an incomplete, and possibly inaccurate, view of DAR function *in vivo*.

To address these limitations, we sought to engineer DARs that can be activated or blocked *in vivo* in a receptor-specific, cell-type-specific, and spatiotemporally precise manner. To develop such tools, we pursued a strategy implemented previously that

utilizes azobenzene-containing, photoswitchable tethered ligands (PTLs) to optically control various ion channels.^{37–42} For example, we developed ionotropic glutamate receptors (iGluRs) that can be controlled with light (LiGluRs) *in vitro*^{37,43,44} and *in vivo*.⁴⁵ At a cysteine introduced adjacent to the glutamate binding site, LiGluR reacts covalently with the maleimide of maleimide–azobenzene–glutamate (MAG). The azobenzene transitions from a *trans*-to-*cis* configuration and vice versa in response to UV and visible light, respectively, altering the position of glutamate with respect to its receptor binding site. The channel can be either activated or blocked depending on where MAG is tethered. Unlike the opto- and pharmacogenetic tools described above,^{31,35} these light-gated receptors are near-native proteins with only a single point mutation.^{46,47}

We recently extended this approach to metabotropic GluRs (LimGluRs),⁴⁸ which are Family C GPCRs. In contrast to iGluRs and mGluRs, which have large extracellular “venus flytrap” domains that bind glutamate, DARs bind DA within the upper third of the transmembrane bundle.⁴⁹ Whether light-insensitive Family A GPCRs, such as DARs, are amenable to optical control using azobenzene-containing PTLs was hitherto unknown, although previous studies indicate that synthetic, non-photoswitchable covalent ligands can bind and activate or block this class of receptors.^{50–53} Furthermore, we showed recently that untethered azobenzene-containing photochromic ligands (PCLs) can photoswitch Family A GPCRs including opioid⁵⁴ and muscarinic acetylcholine receptors.⁵⁵ Moreover, the archetypical Family A GPCR rhodopsin obtains its sensitivity to light by binding covalently to retinal, making retinal a natural PTL.⁵⁶

In this study, we used a tetherable azobenzene conjugated to the synthetic DAR agonist 2-(*N*-phenethyl-*N*-propyl)amino-5-hydroxytetralin (PPHT) to develop light-gated DARs (LiDARs; Figure 1) of D1R and D2R (LiD1R and LiD2R). These tools have the potential to enhance our understanding of DAR function *in vivo* and inform the development of therapeutics with enhanced efficacy and decreased side effects for DA-associated disorders.

RESULTS

Synthesis of a Photoswitchable Tethered Dopamine Receptor Ligand, MAP. To develop light-gated receptors, we first set out to conjugate a DAR ligand to the cysteine-conjugating photoswitch, maleimide–azobenzene. The catechol of DA (Figure S1) is sensitive to oxidation in aqueous solution⁵⁶ as well as metabolism *in vivo*,⁵⁷ making it undesirable as a parent compound for a DAR PTL. Instead, we used PPHT (Figure S1), a rigidified aminotetralin analogue of DA that contains only one hydroxyl as well as *N*-propyl and *N*-phenylethyl groups that enhance metabolic stability and affinity toward DARs.^{58–63} In addition, the *N*-phenylethyl group was previously chemically modified for the development of fluorescent tracers of DARs,⁶⁴ suggesting that PPHT may tolerate the incorporation of azobenzene at this position without impairing its activity at DARs. Thus, we synthesized maleimide–azobenzene–PPHT (MAP; Figure 1B) as well as its non-covalent analogue azobenzene–PPHT (AP).

The synthesis of MAP (**1**; Scheme 1) starts with permethylation of dihydroxy naphthalene (**3** to **4**) that was followed by birch reduction using sodium in ethanol. The resulting methyl enol ether (**5**) was cleaved during acidic workup and tautomerized to the corresponding tetralone. Reductive amination with propylamine gave rise to aminotetraline (**6**). Reductive amination using freshly prepared homobenzylic aldehyde (**7**) installed the

photoswitch into the molecule (8). For further functionalization, the nitro group was then reduced to the corresponding

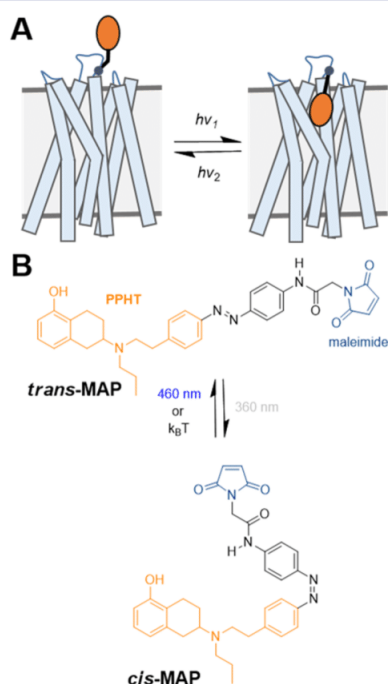
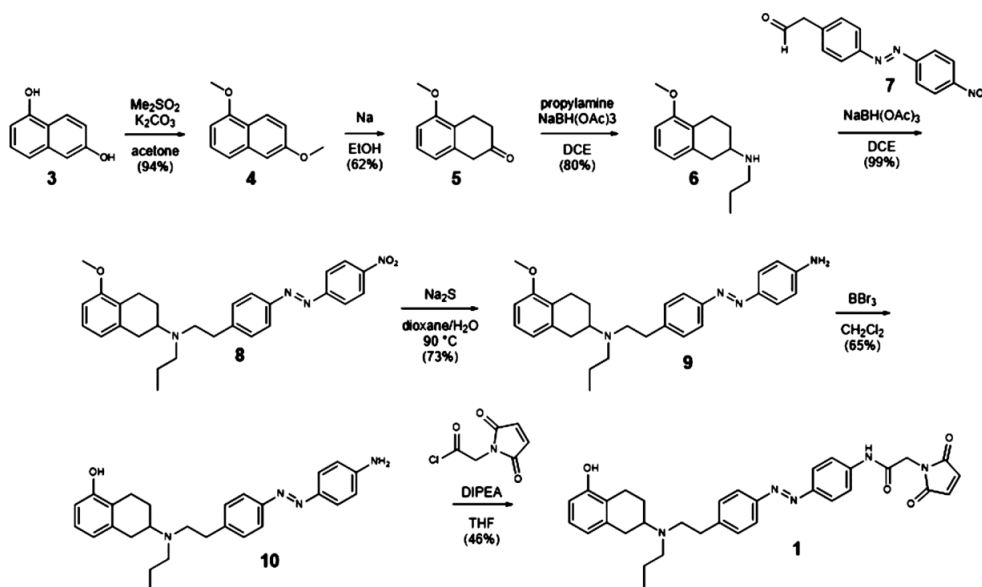


Figure 1. Design of a photoswitchable tethered ligand (PTL) to control DARS with light. (A) Schematic of a dopamine receptor (DAR) bound covalently to a PTL. (B) Azobenzene and maleimide (blue) incorporated into the DAR ligand PPHT (orange). Maleimide-azobenzene-PPHT (MAP) photoisomerizes from its *trans*-to-*cis* isomer and vice versa in response to UV and blue light, respectively.

Scheme 1. Synthesis of Maleimide-Azobenzene-PPHT (MAP)



aniline (9). Deprotection of the methyl ether (10) and amide bond formation accomplished the synthesis of MAP. AP (2) was synthesized (Supplementary Scheme 1) with good overall yield through two sequential reductive aminations using amine 11 and propionic aldehyde.

Structure-Activity Relationship Analysis of MAP at DARS. We evaluated the effects of azobenzene and maleimide-azobenzene addition (AP and MAP, respectively) to a close analogue of PPHT, 4-amino-PPHT⁶⁴ (Figure S1), at D1R and D2R using previously established bioluminescence resonance energy transfer (BRET)-based, DAR-mediated G protein activation assays. G_s -activation downstream of D1R was measured indirectly using the cAMP sensor YFP-Epac-Rluc (CAMYEL; Figure S2A).⁶⁵ In response to a G_s -mediated enhancement in cAMP, a conformational change in the cAMP-binding protein Epac results in a decrease in RET between *Renilla* luciferase (Rluc) and YFP. G_{i1} -activation downstream of D2R was measured directly by assessing agonist-induced conformational changes within the G protein (Figure S2B).⁶⁶ $G_{\alpha_{i1}}$ was fused with *Renilla* luciferase 8 at position 91 of the α -helical domain ($G_{\alpha_{i1}}$ -Rluc8) and $G\beta_1$ and $G\gamma_2$ were fused to a split mVenus (V1- $G\beta_1$ and V2- $G\gamma_2$) at their N-termini. Receptor activation induces a conformational change and/or the dissociation between $G_{\alpha_{i1}}$ and $G\beta_1\gamma_2$, resulting in decreased RET.

In these assays, 4-amino-PPHT was a potent and robust agonist of D1R and D2R relative to DA (Figure 2). We assessed the activity of *trans*-AP and *trans*-MAP using preparations of these compounds that were unexposed to light. Both compounds activated D1R and D2R with similar or slightly reduced efficacy compared to 4-amino-PPHT (Figure 2B,E). However, the azobenzene of AP significantly decreased its potency relative to 4-amino-PPHT (248- and 52-fold at D1R and D2R, respectively; Figure 2C,F). The potencies of AP and MAP were not significantly different, indicating that maleimide did not further decrease agonist activity (Figure 2C,F).

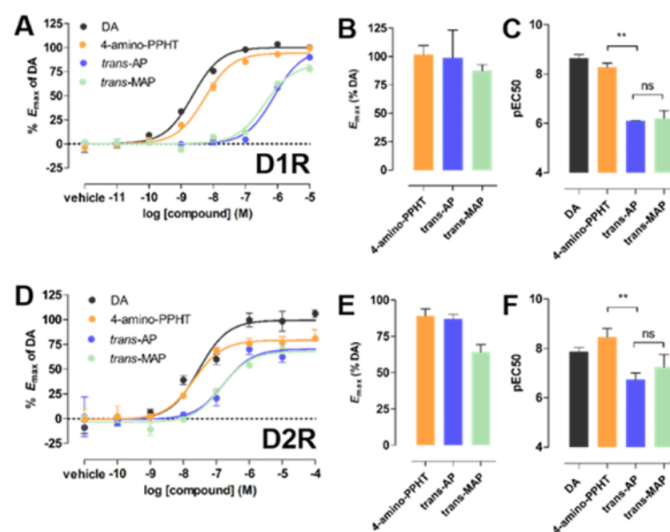


Figure 2. Incorporation of azobenzene but not maleimide into PPHT decreases agonist potency at D1R and D2R. Representative dose–response curves for dopamine (DA), 4-amino-PPHT, *trans*-AP, and *trans*-MAP in (A) a D1R-dependent cAMP accumulation assay and (D) a D2R-dependent G protein activation assay. Dose–response curves are representative of three independent experiments performed in triplicate. E_{\max} values for these compounds are summarized for D1R (B) and D2R (E). The potencies of these compounds (pEC₅₀s) are summarized for D1R (C) and D2R (F) (** $p < 0.001$, ns = not significant, one-way ANOVA, Tukey’s posthoc comparison test). Error bars indicate SEM.

Photochemical Properties of MAP. We characterized the photochemical properties of AP and MAP using UV/vis spectroscopy. Both compounds were efficiently converted from their *trans*- to *cis*-configuration by irradiation with 360 nm light and vice versa by 460 nm light (Figure S3A). Both compounds could efficiently be switched over several cycles without any loss of activity (Figure S3B). Furthermore, consistent with the photochemical properties of azobenzenes lacking any strong auxochromic groups, the *cis*-configuration of these compounds is sufficiently stable toward thermal relaxation ($T_{1/2} > 1$ h; Figures S3B), and thus the compounds are considered bistable.

Photoswitching Properties of an Untethered Analogue of MAP, AP. We next evaluated the light sensitivity of AP modulation of DARs. Untethered, azobenzene-containing PCLs have been used to rapidly and reversibly control a variety of biological molecules with light,^{67,68} albeit with off-target effects associated with untethered ligands and slower kinetics than their tethered counterparts. In iGluRs, the ability of PCLs to photoswitch their receptor targets was predictive of the success of tethered variants that were designed from them.⁶⁹ We compared G protein activation by AP that was not exposed to light and was therefore in the *trans* configuration (*trans*-AP) to G protein activation by AP that had been exposed to 360 nm light and was therefore largely in the *cis* configuration (*cis*-AP; Figure 3A). *cis*-AP was ~1.5- and ~3-fold more potent at D1R and D2R, respectively (two-tailed paired t test, $P = 0.005$ and 0.003 , respectively; Figure 3B,C). Similarly, *cis*-AP was ~4-fold more potent than *trans*-AP in a BRET-based, D2R-mediated arrestin recruitment assay⁶⁶ (Figure S2C; Figure 3D), which measures D2R-mediated translocation of arrestin3 to the plasma membrane. The enhancement of AP’s potency in these functional assays could result from increased affinity and/or efficacy. To address this, we evaluated AP binding to D2R in a homogeneous time-resolved fluorescence resonance energy transfer (HTRF) binding assay⁷⁰ and found that *cis*-AP

displayed ~3-fold higher affinity than *trans*-AP for D2R (two-tailed unpaired t test, $P = 0.017$; Figure 3E). Thus, the *cis*-isomer of AP is a higher affinity agonist than the *trans*-isomer.

MAP as a Photoswitchable Tethered Ligand of D1R. Based on the functionality and isomer dependence of action of AP, we pursued MAP as a PTL of D1R. We hypothesized that, while the untethered AP is an agonist, tethered MAP could behave as an agonist or antagonist, depending on where it was tethered and thus its orientation within the D1R orthosteric binding site (OBS). The OBS of D1R, like in all aminergic Family A GPCRs, is formed by TMs 3, 5, 6 and 7, and is “capped” by the second extracellular loop (EL2).⁷¹ DA binds to this site via an interaction between its catechol and a cluster of aromatic residues in TM6, as well as a salt bridge between its protonated amine and an aspartate in TM3 (D96^{3,32} according to Ballesteros–Weinstein numbering⁷²). In addition, the two hydroxyls of DA form hydrogen bonds with three TMS serines (S198^{5,42}, S199^{5,43}, and S202^{5,46}), interactions that promote receptor activation.⁷³ Based on this, an interaction between MAP and the aromatic cluster and/or D96^{3,32}, but not the TMS serines, would be expected to result in antagonism, whereas all three interactions are required for agonism.

Guided by a homology model of D1R based on a crystal structure of the Family A GPCR, β 2-adrenergic receptor (β 2AR),⁷⁴ we individually mutated to cysteine 15 residues in D1R, which cluster in TM2, EL1, EL2, or TM7. These sites were chosen because they are predicted to be accessible to solvent and encompass the majority of the surface area surrounding the entryway to the OBS. To evaluate photoswitching, we used D1R-mediated activation of the G protein activated inward rectifier potassium (GIRK) channel. D1R cysteine mutants were individually co-expressed with GIRK1 and GIRK2 subunits (to form the GIRK1/2 heterotetrameric channel) as well as with a chimeric G protein consisting of G_{α} , that contains the terminal 13 residues of G_{α_s} ($G_{\alpha_{s13}}$),⁷⁵ which

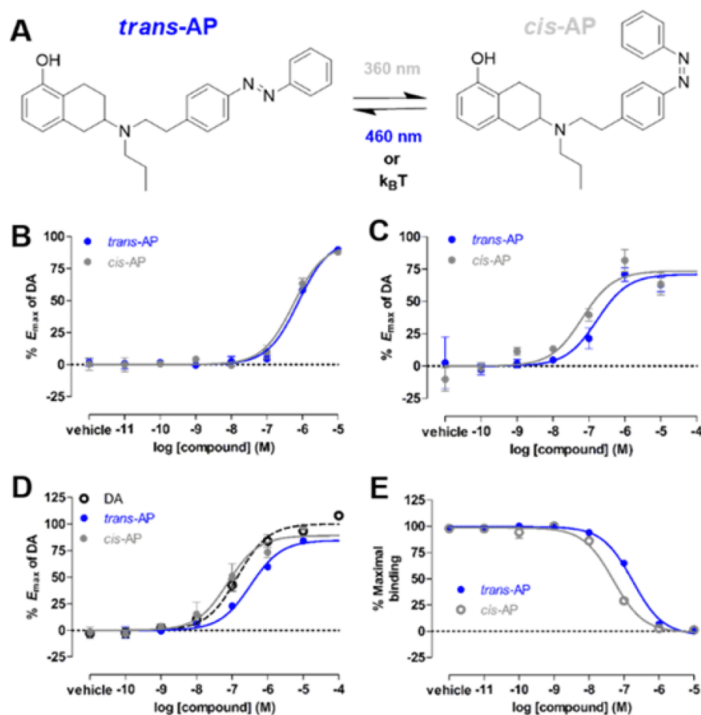


Figure 3. Characterization of the photochromic ligand (PCL) azobenzene-PPHT (AP) at D1R and D2R. (A) AP photoisomerizes from its *trans*- to *cis*-isomer and vice versa in response to UV and blue light, respectively. (B) In a D1R-dependent cAMP accumulation assay, AP exposed to UV light (*cis*-AP) was slightly more potent (~ 1.5 -fold) than when not exposed to light (*trans*-AP). Shown are representative dose–response curves for three independent experiments performed in triplicate. Error bars indicate SEM. (C) In a D2R-dependent G protein activation assay, *cis*-AP was ~ 3 -fold more potent than *trans*-AP. Shown are representative dose–response curves for three independent experiments performed in triplicate. Error bars indicate SEM. (D) In a D2R-mediated arrestin recruitment assay, *cis*-AP was ~ 4 -fold more potent than *trans*-AP. Shown are representative dose–response curves for three independent experiments performed in triplicate. Error bars indicate SEM. (E) In a D2R binding assay, *cis*-AP had ~ 3 -fold higher affinity for D2R than *trans*-AP. Representative binding curves for two independent experiments performed in duplicate. A decrease in the maximal binding indicates the displacement of the fluorescent D2R antagonist NAPS-DY-647 by AP. Error bars indicate SEM.

enables the G_s -coupled D1R to activate GIRK. Following incubation and washout of MAP, transfected cells were patch-clamped in whole-cell configuration and exposed to alternating 360 and 460 nm light, interconverting MAP between its *cis*- and *trans*-isomers, respectively. There was no effect on wildtype (WT) D1R, which does not contain an introduced cysteine anchoring site for MAP (Figure S4B), indicating that our washout conditions efficiently removed untethered MAP.

MAP most robustly photoswitched D1R(I183C), which contains a cysteine in EL2 (Figure 4A). This mutant localized to the plasma membrane like WT (Figure S5A) and was activated by DA with similar potency to WT D1R ($pEC_{50} = 6.2$ and 6.4 , D1R(I183C) and WT D1R, respectively; Figure S5B). In addition, the synthetic D1-like receptor partial agonist SKF38393⁷⁶ similarly activated WT D1R and D1R(I183C) (Figures S5C–E). Thus, the introduction of cysteine at position I183 did not substantially alter receptor function. Following incubation and washout of MAP ($30 \mu\text{M}$ for 60 min), transition from 360 to 460 nm light resulted in a reversible reduction (by $41 \pm 3\%$, $n = 9$) in inward-current evoked by a saturating concentration ($10 \mu\text{M}$) of DA (Figure 4B), indicating that *trans*-MAP is a D1R antagonist when tethered to I183C. The magnitude of photoblock at this mutant is comparable to that observed for a previously reported photoblocked

metabotropic glutamate receptor 2 (LimGluR2-block).⁴⁸ Voltage ramps showed that the MAP photoblocked current is inwardly rectifying, consistent with the antagonism of the D1R activation of GIRK channels (Figure 4C). The kinetics of onset and offset of MAP photoblock were similar ($\tau_{\text{onset}} = 6.0$ s, $\tau_{\text{offset}} = 5.7$ s; Figure 4D). Both the photoblock and its reversal persisted in the dark after the light flash, consistent with bistability of MAP (Figure 4E), as has been shown for azobenzene PTLs of glutamate receptors.^{42,48,77} The magnitude of photoblock decreased with increasing concentrations of DA, in accordance with a competitive interaction between DA and MAP (Figure 4F).

Although MAP photoblocked DA-induced activation of D1R(I183C), it had no effect on basal inward-current (Figure 4B). This was in striking contrast to the effects of MAP on D1R(G88C), which contains a cysteine in EL1 (Figure 5A). The transition from 360 to 460 nm light (*cis*- to *trans*-MAP) reduced the DA-evoked current, but also reduced the basal inward current ($35 \pm 4\%$ and $15 \pm 4\%$ of maximal DA-evoked current, respectively, $n = 5$; Figure 6B). The photoblock of basal inward current was repeatable (Figure 5C) and bistable (Figure 5D), consistent with the photochemical properties of MAP. The effect of MAP in its *trans*-configuration on both basal and agonist-induced current suggested that it may be an

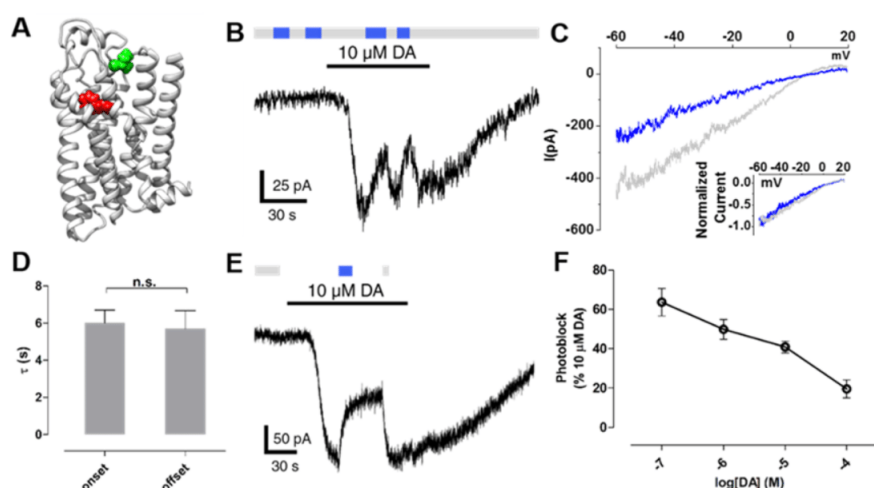


Figure 4. MAP is a neutral antagonist at D1R(I183C). (A) Ribbon representation of a D1R homology model bound to protonated DA (red). Amino acid I183 in EL2 is shown in green above the OBS that binds DA. (B) When MAP is attached to I183C, photoswitching between 360 nm (gray bars) and 460 nm light (blue bars) had no effect. However, current evoked by DA was photoblocked in response to 460 nm light. (C) Representative trace of currents induced by DA under 360 nm light (gray) or 460 nm light (blue). Ramp currents were subtracted from baseline ramps taken in the absence of DA under 360 nm light. Currents show inward rectification typical of GIRK current. Inset shows close overlap between the normalized traces. (D) The kinetics of the onset and offset of photoblock at D1R(I183C) by MAP were not significantly different (n.s. = not significant, two-tailed, unpaired *t* test). Error bars represent SEM. (E) Photoblock of D1R(I183C) by MAP is bistable. A brief flash of 460 nm light (blue bar) induced a decrease in dopamine-evoked current that was sustained in the dark for ~30 s until it was reversed by a brief flash of 360 nm light (gray bar). (F) The magnitude of photoblock of D1R(I183C) by MAP decreases with increasing concentrations of DA. Error bars represent SEM for $n = 3-9$ cells per concentration of DA.

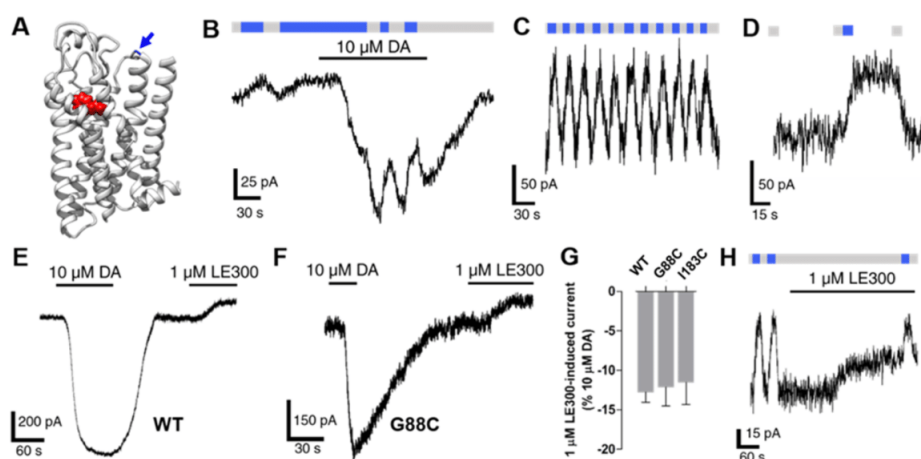


Figure 5. MAP is an inverse agonist at D1R(G88C). (A) Ribbon representation of a D1R homology model bound to protonated DA (red). Amino acid G88 in EL1 (shown in blue and highlighted by an arrow) is adjacent to the OBS that binds DA. (B) When MAP is attached to G88C, photoswitching from 360 and 460 nm light decreases both basal and DA-evoked inward current. (C) Photoswitching of the basal current is repeatable. (D) Photoswitching of the basal current is bistable. (E) Basal inward current is reduced in response to LE300 in cells expressing wildtype D1R. (F) Basal inward current is reduced in response to LE300 in cells expressing D1R(G88C). (G) Summary of the effects of LE300 on basal inward current in cells expressing WT D1R, G88C, and I183C. Error bars represent SEM for $n = 3-4$ cells per receptor (not significant, one-way ANOVA). (H) LE300 partially attenuated the ability of MAP to photoblock the basal inward current in cells expressing D1R(G88C).

inverse agonist that reduces constitutive receptor activity. To address this possibility, we tested whether WT D1R, D1R(I183C), and D1R(G88C) exhibit constitutive activity by measuring changes in basal inward current in response to a saturating concentration of the D1-like receptor inverse agonist LE300.⁷⁸ LE300 similarly reduced inward current

in cells expressing WT D1R, D1R(I183C), and D1R(G88C) (Figure 5E–G), indicating that they each have constitutive activity, consistent with basal current photoblock being of this constitutive activity. If this interpretation is correct and MAP is, indeed, an inverse agonist, its photoeffect on basal current would be reduced by LE300. This prediction was borne out

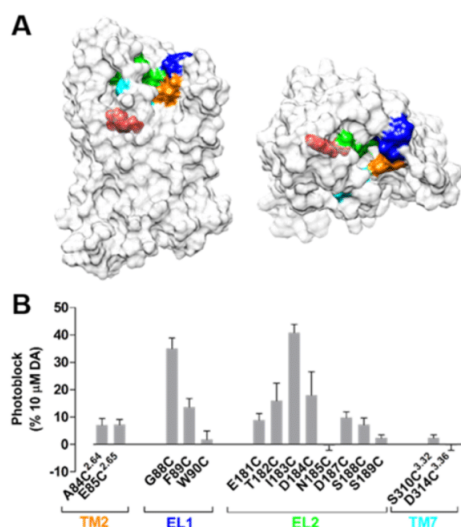


Figure 6. MAP photoblocks D1R. (A) A surface representation of a D1R homology model. Fifteen residues surrounding the DA binding site of D1R were individually mutated to cysteines. These sites were located on the extracellular face of TM2 (orange), EL1 (blue), EL2 (green), or extracellular face of TM7 (cyan). Protonated DA is shown bound to the OBS of D1R (red). (B) Summary of photoblock at cysteine mutants of D1R by MAP. Error bars represent SEM for $n = 3-9$ cells per cysteine mutant.

(Figure 5H). However, LE300 did not completely abolish the effect of MAP on basal current of D1R(G88C) (Figure 5H), suggesting that MAP is a more robust inverse agonist than LE300.

MAP photoswitched mutants of D1R with cysteines in EL1 or EL2, and to a lesser degree TM2 and TM7 (Figure 6). DA-mediated activation of all photoswitchable D1R mutants was blocked in response to 460 nm light, indicating that *trans*-MAP inhibits D1R when tethered to the receptor.

MAP as a Photoswitchable Tethered Ligand of D2R.

Although both D1R and D2R bind and are activated by DA, they are only ~40% homologous in their TM domains⁷⁹ and have no similarity in their ELs. This dissimilarity suggests that MAP could have distinct effects at these receptors. We first evaluated MAP at WT D2R, which unlike D1R contains a native cysteine deep within its OBS (C118^{3.36}). We previously found this cysteine to be sensitive to covalent modification by selected methyl thiosulfate (MTS) compounds based on their charge.⁸⁰ We determined the effects of MAP, MTSEA, and MTSES on WT D2R by measuring DA-induced G protein activation following incubation and washout. Consistent with our previous results, whereas negatively charged MTSES had no effect on D2R activation, positively charged MTSEA completely abolished receptor activity (Figure S6A). Notably, MAP had little effect, suggesting lack of accessibility of C118 to this relatively bulky reagent. Consistent with this, following incubation and washout of WT D2R in MAP, exposure to DA still activated GIRK channels (Figure S6B,C), and channel activity was not photoswitched by alternating exposure between 360 and 460 nm light (Figure S6C).

Fourteen D2R residues located near the OBS, based on a homology model that used the crystal structure of D3R⁴⁹ (Figure 7B) were mutated to cysteine to introduce the MAP

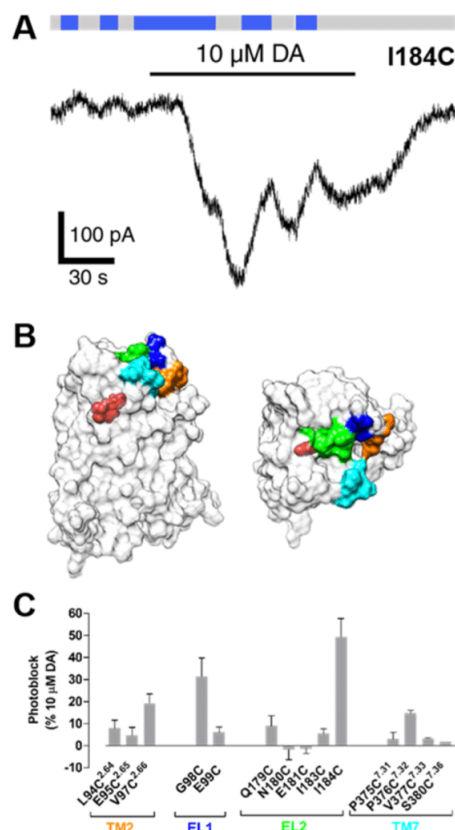


Figure 7. MAP photoblocks D2R. (A) When MAP is attached to I184C, photoswitching from 360 and 460 nm light decreases both basal and DA-evoked current. (B) A surface representation of a D2R homology model. Fourteen residues surrounding the dopamine binding site of D2R were individually mutated to cysteines. These sites were located on the extracellular face of TM2 (orange), EL1 (blue), EL2 (green), or extracellular face of TM7 (cyan). Protonated dopamine is shown bound to the orthosteric binding site (OBS) of D2R (red). (C) Summary of photoblock of cysteine mutants of D2R by MAP. Error bars represent SEM for $n = 3-7$ cells per cysteine mutant.

conjugation site. The largest photomodulation of D2R was seen when MAP was tethered to I184C in EL2. The transition from 360 to 460 nm light photoblocked (by $49 \pm 8\%$, $n = 6$) the GIRK current evoked by $10 \mu\text{M}$ DA (Figure 7A,C). Here too, as seen in D1R above, basal GIRK current was reduced by 460 nm light (Figure 7A), suggesting that *trans*-MAP is an inverse agonist. Consistent with this, spiperone, a robust inverse agonist of D2R,⁸¹ also reduced inward current both in cells expressing WT D2R or D2R(I184C) (Figures S8).

Aside from the ability to conjugate to MAP and endow the receptor with photocontrol, the I184-to-cysteine mutation did not alter the function of D2R: localization of D2R to the plasma membrane was normal (Figure S7A), and there was no change in sensitivity to DA ($\text{pEC}_{50} = 6.3$ and 6.0 for WT and mutant, respectively; Figure S7B) or activation by the synthetic D2-like agonist quinpirole (Figures S7C-E).

Interestingly, MAP operated as a *trans*-inverse photoagonist when attached to cysteines to either EL1 or EL2 of D2R (Figure 7A). This is in contrast to its effects at D1R, whereby

MAP was a neutral antagonist or inverse agonist when tethered to cysteines in EL1 or EL2, respectively (Figures 4 and 5).

DISCUSSION

In this study, we developed a DAR PCL (AP) and PTL (MAP) based on the synthetic agonist PPHT. MAP attached to an introduced cysteine near the OBS yielded photoblock of both D1R ("LiD1R") and D2R ("LiD2R"), providing what to our knowledge is the first means to remotely control full-length DARs in a receptor subtype-specific, cell-type-specific, and spatiotemporally precise manner. Because MAP can be directly anchored to a given DAR, off-target effects at other DARs and non-DAR proteins are avoided. Thus, MAP is a reversible and selective ligand of individual DARs. Moreover, because these tools are controlled with light, they can be used to rapidly regulate individual DARs on time scales that are relevant to native dopaminergic signaling in the brain.⁸²

A major goal of this study was to use MAP to selectively photoblock DARs. Photoblockade is a powerful means to determine whether a receptor of interest is necessary for specific physiological or behavioral processes *in vivo*. Photoactivation, on the other hand, can be used to determine whether it is sufficient. Like 4-amino-PPHT and AP, MAP activated D1R and D2R in its untethered form. In contrast, when tethered to a receptor, MAP either had no effect or photoblocked the receptor at the variety of cysteine attachment positions that we tested. This is not a surprise given that photoantagonism could arise from a variety of geometries that improperly position the ligand in the OBS, whereas photoagonism demands proper docking. Indeed, only one out of eight attachment sites for the mGluR2 photoswitch, MAG, produced photoactivation.⁴⁸

The distinction between photoagonism and photoantagonism could be due to subtle differences in the anchoring site of the PTL from one residue to its neighbor in three-dimensional space, as well as differences in the PTL's length and bond angles. A non-photoswitchable, covalent agonist of D2R was developed recently,⁵⁰ suggesting that it may be possible to achieve photoagonism at DARs. Toward this end, further chemical modifications of MAP may result in photoagonism, e.g., by adjusting the linker length between PPHT and azobenzene and/or azobenzene and the maleimide (Figure 1B), thus altering how MAP is positioned within the OBS. Alternatively, the position and number of hydroxyls in aminotetralins are known to dictate efficacy at DARs, and it is possible that MAP is limited as a photoagonist because it has only a single hydroxyl.^{61,62} Thus, an additional hydroxyl could enhance photoagonism, albeit at the cost of the metabolic stability of the compound.

Interestingly, we found MAP to be either a photoswitchable tethered neutral antagonist (PTNA) or photoswitchable tethered inverse agonist (PTIA) at D1R, depending on where it is tethered. GPCRs like DARs are dynamic ensembles of inactive and active conformations.⁸³ It has been proposed that neutral antagonists occlude the binding of agonists but do not shift the equilibrium between active and inactive states, whereas inverse agonists stabilize inactive states and reduce constitutive activity.⁸⁴ Crystallographic studies of Family A GPCRs suggest that chemically related neutral antagonists and inverse agonists bind similarly within the OBS and stabilize receptor states with only minor structural differences.⁵¹ Similarly, MAP may adopt subtly distinct binding poses within the OBS, depending on where it is tethered, allowing it to behave as a neutral antagonist or inverse agonist.

Remarkably, despite the low overall degree of homology between D1R and D2R, MAP most robustly photoblocked

these receptors when tethered to cysteines in EL2 (I183C and I184C, respectively), and to a lesser degree EL1. Although EL2 is highly divergent in sequence between D1R and D2R, it commonly serves as a "lid" over the OBS. This combined with the fact that EL2 is relatively conformationally dynamic⁸⁵ may allow MAP greater freedom to access the OBS than if tethered to the TM domain. EL2 acts as a lid over the OBS of a variety of Family A GPCRs,⁷¹ suggesting that it may represent a common target for controlling other receptors in this family using PTLs.

The ability to photoblock DARs is of great clinical interest. Notably, all antipsychotics are blockers of D2R-like receptors.^{86,87} However, because these medications are nonselective for D2R-like receptors and are diffusible, it has been challenging to identify which of these D2-like receptors (D2R, D3R, or D4R) is responsible or to determine which cells expressing the receptor(s) play a role in efficacy and side effects. LiD2R offers the possibility of blocking D2R in a cell-type-specific manner, allowing us to mimic selected effects of antipsychotic medications in isolation. Moreover, antipsychotics have varying degrees of inverse agonism at D2R, and it is unclear if and where in the brain this is relevant to clinical efficacy.⁸⁸ LiD2R variants that operate as inverse photoagonists may help to resolve this issue.

Several approaches have developed recently to interrogate GPCR function *in vivo*, including DREADDs³⁵ and opto-XRs.^{31–33} Opto-XRs are of particular interest because, like the light-gated receptors developed here, they can be precisely controlled with light. Although opto-XRs cannot be used to block receptors from being activated by their endogenous ligands, they can be targeted to specific cell types and activated in an inducible-manner. Interestingly, Siuda et al. developed biased mutants of opto- β 2AR that selectively activate only a subset of signaling proteins downstream of this receptor (i.e., G proteins versus arrestins).³³ Considerable effort has gone toward uncovering the roles of distinct signaling pathways downstream of DARs,⁵ and a number of biased DAR mutants have been developed.^{89,90} Given that mutations in these receptors are not involved in ligand binding, they can likely be integrated into LiDARs, which would enable signaling-pathway-specific and spatiotemporally precise control of near-native DARs.

CONCLUSION

Family A GPCRs are subdivided into groups of structurally related receptors, making it difficult in particular cases to target individual receptor subtypes. Considerable medicinal chemistry efforts have gone toward developing subtype-selective drugs, with varying degrees of success.²⁹ However, our understanding of the physiological and clinical roles of a given receptor will require not only receptor-specific but also cell-type-specific and spatiotemporally precise control over its function. The success of LiDARs indicates that Family A GPCRs are amenable to rapid, cell-type- and receptor-specific control using PTLs. Thus, we anticipate that our approach will also work for difficult-to-target Family A GPCRs, including but not limited to the neuromodulator-binding opioid, serotonin, and cannabinoid receptors.

EXPERIMENTAL SECTION

General Experimental Details. All reactions were carried out with magnetic stirring and, if moisture- or air-sensitive, under nitrogen or argon atmosphere using standard Schlenk techniques in oven-dried glassware (140 °C oven temperature). External bath temperatures were used to record all reaction temperatures. Low temperature

reactions were carried out in a Dewar vessel filled with acetone/dry ice ($-78\text{ }^{\circ}\text{C}$) or distilled water/ice ($0\text{ }^{\circ}\text{C}$). High temperature reactions were conducted using a heated silicon oil bath in reaction vessels equipped with a reflux condenser or in a sealed flask. Tetrahydrofuran (THF) was distilled over sodium and benzophenone prior to use. Dichloromethane (CH_2Cl_2), triethylamine (Et_3N), and diisopropylethylamine (DIPEA) were distilled over calcium hydride under a nitrogen atmosphere. All other solvents were purchased from Acros Organics as "extra dry" reagents. All other reagents with a purity $>95\%$ were obtained from commercial sources (Sigma-Aldrich, Acros, Alfa Aesar, and others) and used without further purification.

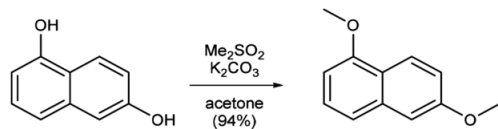
Flash column chromatography was carried out with Merck silica gel 60 (0.040–0.063 mm). Analytical thin layer chromatography (TLC) was carried out using Merck silica gel 60 F254 glass-backed plates and visualized under UV light at 254 nm. Staining was performed with ceric ammonium molybdate (CAM) or by oxidative staining with an aqueous basic potassium permanganate (KMnO_4) solution and subsequent heating.

NMR spectra (^1H NMR and ^{13}C NMR) were recorded in deuterated chloroform (CDCl_3) or deuterated methanol ($d_4\text{-MeOH}$) on a Bruker Avance III HD 400 MHz spectrometer equipped with a CryoProbe, a Varian VXR400 S spectrometer, a Bruker AMX600 spectrometer, or a Bruker Avance III HD 800 MHz spectrometer equipped with a CryoProbe and are reported as follows: chemical shift δ in ppm (multiplicity, coupling constant J in Hz, number of protons) for ^1H NMR spectra and chemical shift δ in ppm for ^{13}C NMR spectra. Multiplicities are abbreviated as follows: s = singlet, d = doublet, t = triplet, q = quartet, quint = quintet, br = broad, m = multiplet, or combinations thereof. Residual solvent peaks of CDCl_3 ($\delta\text{H} = 7.26$ ppm, $\delta\text{C} = 77.16$ ppm) and $d_4\text{-MeOH}$ ($\delta\text{H} = 3.31$ ppm, $\delta\text{C} = 49.00$ ppm) were used as an internal reference. NMR spectra were assigned using information ascertained from COSY, HMBC, and HSQC experiments.

High-resolution mass spectra (HRMS) were recorded on a Varian MAT CH7A, or a Varian MAT 711 MS instrument by electron impact (EI) or electrospray ionization (ESI) techniques at the Department of Chemistry, Ludwig-Maximilians-Universität Munich.

Infrared (IR) spectra were recorded from 4000 to 600 cm^{-1} on a Perkin Elmer Spectrum BX II instrument. For detection a Smiths Detection DuraSampIR II Diamond ATR sensor was used. Samples were prepared as a neat film or a thin powder layer. IR data in frequency of absorption (cm^{-1}) is reported as follows: w = weak, m = medium, s = strong, br = broad, or combinations thereof.

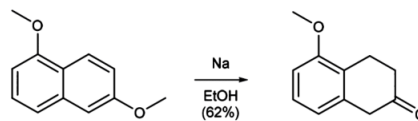
All yields are isolated, unless otherwise specified.



Dimethylsulfate (43.3 mL, 468 mmol) was added to a suspension of potassium carbonate (75.5 g, 548 mmol) and 1,6-dihydroxynaphthalene (25 g, 156 mmol) in acetone (250 mL). The mixture was heated at $70\text{ }^{\circ}\text{C}$ for 3.5 h, cooled to room temperature, and filtered. The solvent was evaporated under reduced pressure, and the resulting residue was redissolved in ethyl acetate. The solution was washed with a solution of sodium hydroxide (1 M) and brine and dried over magnesium sulfate. Evaporation of the solvent *in vacuo* and purification of the resulting residue by flash column chromatography (EtOAc: pentane = 0:100–20:80, $R_f = 0.7$ (EtOAc: pentane 20:80)) gave 1,6-dimethoxynaphthalene 4 (27.6 g, 147 mmol, 94%) as a colorless solid.

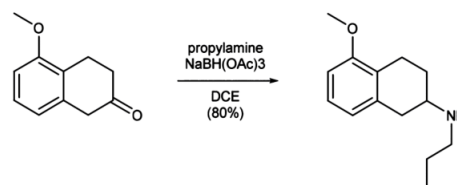
Data for 4: ^1H NMR (400 MHz, CDCl_3): δ (ppm) = 8.17 (dt, $J = 8.8, 0.8$ Hz, 1H), 7.38–7.31 (m, 2H), 7.15–7.10 (m, 2H), 6.70 (dd, $J = 6.9, 1.7$ Hz, 1H), 3.99 (s, 3H), 3.92 (s, 3H). ^{13}C NMR (100 MHz, CDCl_3): δ (ppm) = 158.2, 155.8, 136.0, 126.8, 123.8, 120.9, 119.4, 117.6, 105.8, 102.1, 55.6, 55.4. IR (ATR): ν_{max} (cm^{-1}) = 2997 (w), 2966 (w), 2836 (w), 1929 (w), 1625 (m), 1599 (m), 1581 (s), 1510 (w), 1468 (w), 1451 (s), 1430 (s), 1372 (s), 1386 (w), 1372 (s), 1254 (m), 1220 (vs), 1199 (m), 1165 (m), 1143 (m), 1098 (m), 1070 (m), 1026 (vs), 988 (m), 935 (m), 871 (m), 839 (m), 828 (s), 782 (vs),

748 (s), 727 (m), 695 (m). HRMS (EI): calcd for $\text{C}_{12}\text{H}_{12}\text{O}_2$ $[\text{M}]^+$ 188.0837, found 188.0819.



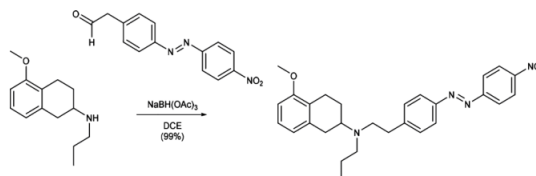
Sodium (33.69 g, 1.47 mol) was added portionwise to a solution of 1,6-dimethoxynaphthalene 4 (27.6 g, 147 mmol) in ethanol (400 mL) at $50\text{ }^{\circ}\text{C}$, and the mixture was then stirred at $80\text{ }^{\circ}\text{C}$ for 2.5 h. After cooling down to room temperature the mixture was acidified with concentrated hydrochloric acid to pH = 1, heated at $80\text{ }^{\circ}\text{C}$ for 30 min, and stirred at room temperature overnight. The solution was diluted with water (230 mL) and extracted with CH_2Cl_2 . The organic phase was washed with a solution of sodium chloride (10%) and brine and dried over magnesium sulfate. Evaporation of the solvent *in vacuo* and purification of the resulting residue by flash column chromatography (EtOAc: pentane = 0:100–10:90, $R_f = 0.5$ (EtOAc: pentane 10:90)) gave 3,4-dihydro-1,6-dimethoxynaphthalenone 5 (15.94 g, 90.47 mmol, 62%) as a yellow oil.

Data for 5: ^1H NMR (400 MHz, CDCl_3): δ (ppm) = 7.16 (t, $J = 7.9$ Hz, 1H), 6.76 (dd, $J = 8.2, 1.0$ Hz, 1H), 6.70 (dd, $J = 7.6, 1.0$ Hz, 1H), 3.83 (s, 3H), 3.52 (s, 2H), 3.06 (t, $J = 6.8$ Hz, 2H), 2.48 (dd, $J = 7.4, 6.2$ Hz, 2H). ^{13}C NMR (100 MHz, CDCl_3): δ (ppm) = 210.4, 156.2, 134.8, 127.3, 124.8, 120.2, 108.2, 55.2, 44.4, 44.4, 37.6, 37.6, 20.8. IR (ATR): ν_{max} (cm^{-1}) = 2957 (w), 2904 (w), 2838 (w), 1713 (vs), 1587 (s), 1471 (s), 1441 (m), 1403 (w), 1344 (w), 1299 (w), 1263 (vs), 1237 (m), 1197 (w), 1172 (w), 1087 (vs), 1076 (s), 1025 (w), 977 (w), 963 (m), 849 (m), 778 (s), 745 (m), 724 (m), 695 (m). MS (EI): calcd for $\text{C}_{11}\text{H}_{12}\text{O}_2$ $[\text{M}]^+$ 176.08, found 176.03.



Propylamine (2.1 mL, 25.54 mmol) and $\text{NaBH}(\text{OAc})_3$ (6.50 g, 30.66 mmol) were sequentially added to a solution of 3,4-dihydro-1,6-dimethoxynaphthalenone 5 (3.00 g, 17.02 mmol) in DCE (100 mL), and the reaction was stirred at room temperature overnight. The solvent was removed under reduced pressure, and the resulting residue was partitioned between EtOAc and aqueous NaHCO_3 solution. The organic phase was washed with brine, dried over magnesium sulfate, and concentrated under reduced pressure to yield secondary amine 6 (2.99 g, 13.62 mmol, 80%) as a colorless oil.

Data for 6: ^1H NMR (400 MHz, $d_4\text{-MeOH}$): δ (ppm) = 7.07 (t, $J = 7.9$ Hz, 1H), 6.69 (dd, $J = 13.6, 7.9$ Hz, 2H), 3.79 (s, 3H), 2.98 (dddd, $J = 27.8, 20.8, 17.7, 5.4, 2.6$ Hz, 3H), 2.81–2.69 (m, 2H), 2.57 (ddd, $J = 30.0, 16.8, 8.0$ Hz, 2H), 2.16 (ddt, $J = 11.9, 5.7, 2.9$ Hz, 1H), 1.69–1.48 (m, 3H), 0.99 (t, $J = 7.4$ Hz, 3H). ^{13}C NMR (100 MHz, $d_4\text{-MeOH}$): δ (ppm) = 158.6, 136.7, 127.6, 125.5, 122.4, 108.3, 55.6, 54.9, 49.4, 36.2, 29.1, 23.3, 23.2, 12.0. IR (ATR): ν_{max} (cm^{-1}) = 2936 (m), 2875 (w), 2835 (m), 2792 (m), 2734 (m), 2537 (w), 2445 (w), 1587 (s), 1468 (vs), 1438 (s), 1395 (w), 1382 (w), 1346 (w), 1312 (w), 1284 (w), 1258 (vs), 1094 (s), 1068 (m), 1036 (m), 987 (m), 954 (m), 914 (w), 892 (w), 876 (w), 832 (w), 765 (vs), 709 (m), 694 (m). HRMS (EI): calcd for $\text{C}_{14}\text{H}_{22}\text{NO}^+$ $[\text{M}+\text{H}]^+$ 220.1696, found 220.1696.

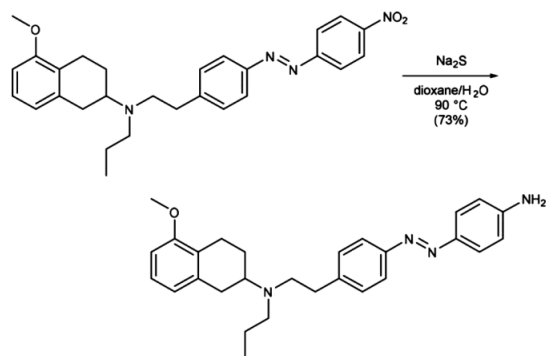


DMP (8.33 g, 21.06 mmol) was added to a solution of (*E*)-2-(4-((4-nitrophenyl)diazenyl)phenyl) ethan-1-ol (1.90 g, 7.02 mmol) in CH_2Cl_2 , and the reaction was stirred at room temperature for 3 h. The mixture was washed with aqueous $\text{Na}_2\text{S}_2\text{O}_3$ solution, water, and brine, dried over magnesium sulfate, and evaporated to dryness. The resulting residue was redissolved in DCE (100 mL), secondary amine **6** (700 mg, 3.19 mmol) and $\text{NaBH}(\text{OAc})_3$ (2.23 g, 10.53 mmol) were sequentially added, and the reaction mixture was stirred at room temperature overnight. The solvent was removed under reduced pressure, and the residue was portioned between EtOAc and aqueous NaHCO_3 solution. The organic phase was washed with brine, dried over magnesium sulfate, and concentrated under reduced pressure. Purification of the resultant residue by flash column chromatography ($\text{MeOH}:\text{CH}_2\text{Cl}_2 = 3:97$, $R_f = 0.3$) gave azobenzene **8** (1.49 g, 3.16 mmol, 99%) as a red solid.

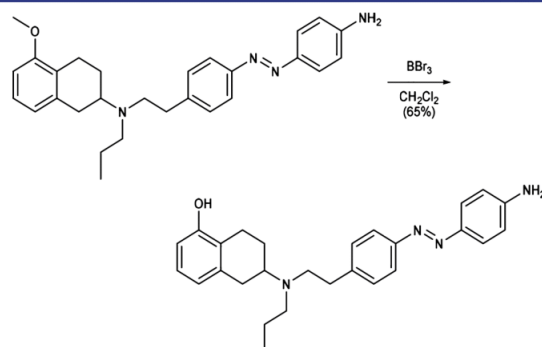
Data for **8**: ^1H NMR (400 MHz, CDCl_3): δ (ppm) = 8.42–8.38 (m, 2H), 8.06–8.02 (m, 2H), 7.94–7.90 (m, 2H), 7.43–7.38 (m, 2H), 7.11 (t, $J = 7.9$ Hz, 1H), 6.72 (dd, $J = 7.6, 1.0$ Hz, 1H), 6.67 (d, $J = 8.1$ Hz, 1H), 3.83 (s, 3H), 3.01 (dddd, $J = 10.8, 8.6, 5.5, 2.7$ Hz, 2H), 2.87 (s, 5H), 2.81–2.71 (m, 1H), 2.62–2.49 (m, 3H), 2.07 (ddd, $J = 14.5, 4.6, 2.0$ Hz, 1H), 1.63–1.48 (m, 3H), 0.92 (t, $J = 7.3$ Hz, 3H). ^{13}C NMR (100 MHz, CDCl_3): δ (ppm) = 157.4, 156.0, 151.0, 148.7, 146.6, 138.1, 130.0, 126.3, 125.4, 124.9, 123.6, 123.5, 121.8, 107.1, 56.7, 55.4, 52.8, 52.6, 36.3, 32.5, 25.9, 24.0, 22.4, 12.1. IR (ATR): ν_{max} (cm^{-1}) = 2931 (m), 2836 (w), 1738 (vw), 1602 (w), 1586 (m), 1521 (s), 1499 (w), 1468 (m), 1438 (w), 1416 (vw), 1360 (vs), 1259 (m), 1218 (w), 1143 (m), 1106 (m), 1093 (m), 1071 (m), 1008 (w), 963 (w), 908 (w), 858 (s), 766 (w), 754 (w), 729 (s), 710 (w), 688 (w). HRMS (EI): calcd for $\text{C}_{28}\text{H}_{33}\text{N}_4\text{O}_3^+$ $[\text{M}+\text{H}]^+$ 473.2547, found 473.2543.

A suspension of azobenzene **8** (500 mg, 1.06 mmol) and sodium sulfide (2.33 mg, 2.12 mmol) in 1,4-dioxane (50 mL) and water (50 mL) was stirred at 90 °C overnight. The reaction was cooled to room temperature, diluted with aqueous NaOH (1 M), and extracted with EtOAc. The organic phase was washed with water and brine, dried over magnesium sulfate, and concentrated under reduced pressure. Purification of the resultant residue by flash column chromatography ($\text{MeOH}:\text{CH}_2\text{Cl}_2 = 2:98$, $R_f = 0.2$) gave aniline **9** (341 mg, 0.770 mmol, 73%) as a red solid.

Data for **9**: ^1H NMR (400 MHz, CDCl_3): δ (ppm) 7.80 (t, $J = 8.3$ Hz, 4H), 7.32 (d, $J = 8.2$ Hz, 2H), 7.10 (t, $J = 7.8$ Hz, 1H), 6.73 (dd, $J = 8.3, 6.5$ Hz, 3H), 6.66 (d, $J = 8.1$ Hz, 1H), 4.03 (s, 2H), 3.81 (s, 3H), 3.12–2.94 (m, 2H), 2.94–2.71 (m, 6H), 2.68–2.44 (m, 3H), 2.08 (dt, $J = 13.7, 4.2$ Hz, 1H), 1.68–1.46 (m, 3H), 0.91 (t, $J = 7.3$ Hz, 3H). ^{13}C NMR (100 MHz, CDCl_3): δ (ppm) = 157.3, 151.4, 149.5,



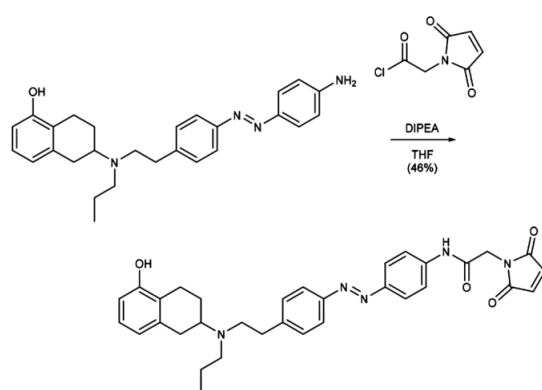
145.7, 143.2, 138.1, 129.5, 126.3, 125.3, 125.1, 122.4, 121.8, 114.8, 107.0, 67.2, 56.8, 55.3, 52.8, 35.9, 32.4, 25.9, 24.0, 22.3, 12.1. IR (ATR): ν_{max} (cm^{-1}) = 3336 (w), 2933 (m), 2837 (vw), 2508 (w), 2246 (vw), 2212 (vw), 1623 (w), 1586 (m), 1516 (m), 1468 (m), 1438 (w), 1378 (vw), 1346 (vw), 1260 (m), 1216 (vw), 1180 (vw), 1128 (vw), 1094 (m), 1071 (m), 96.2 (vw), 907 (s), 826 (m), 768 (m), 700 (vs). HRMS (EI): calcd for $\text{C}_{28}\text{H}_{35}\text{N}_4\text{O}^+$ $[\text{M}+\text{H}]^+$ 443.2805, found 443.2811.



BBr_3 (1 M in CH_2Cl_2 , 3.18 mL, 3.18 mmol) was added to a solution of aniline **9** (704 mg, 1.59 mmol) in CH_2Cl_2 (30 mL) at -78 °C, and the reaction was stirred 1 h at the same temperature and 1 h at room temperature. The reaction mixture was diluted with MeOH (5 mL) and aqueous NaHCO_3 solution and extracted with EtOAc. The organic phase was washed with brine, dried over magnesium sulfate, and concentrated under reduced pressure. Purification by flash column chromatography ($\text{MeOH}:\text{CH}_2\text{Cl}_2 = 2:98$ to $6:94$, $R_f = 0.6$ ($\text{MeOH}:\text{CH}_2\text{Cl}_2 = 6:94$)) gave phenol **10** (440 mg, 1.03 mmol, 65%) as a red solid.

Data for **10**: ^1H NMR (400 MHz, CDCl_3): δ (ppm) 7.81 (t, $J = 7.6$ Hz, 4H), 7.31 (d, $J = 8.0$ Hz, 2H), 6.99 (t, $J = 7.8$ Hz, 1H), 6.73 (d, $J = 8.3$ Hz, 2H), 6.68 (d, $J = 7.6$ Hz, 1H), 6.58 (d, $J = 7.9$ Hz, 1H), 4.04 (s, 2H), 3.09–2.73 (m, 8H), 2.59 (ddd, $J = 23.4, 10.2, 5.8$ Hz, 3H), 2.12 (dd, $J = 12.5, 5.5$ Hz, 1H), 1.70–1.47 (m, 3H), 0.92 (t, $J = 7.3$ Hz, 3H). ^{13}C NMR (100 MHz, CDCl_3): δ (ppm) = 153.7, 151.4, 149.5, 145.6, 143.0, 138.9, 129.5, 126.5, 125.1, 123.3, 122.5, 121.6, 114.8, 112.1, 56.8, 52.7, 52.6, 35.5, 32.2, 25.8, 23.8, 21.9, 12.1. IR (ATR): ν_{max} (cm^{-1}) = 3370 (w), 2313 (w), 3027 (w), 2930 (m), 2870 (w), 1907 (vw), 1726 (vw), 1619 (m), 1598 (vs), 1505 (m), 1463 (s), 1428 (m), 1404 (w), 1374 (w), 1341 (w), 1297 (m), 1275 (s), 1138 (vs), 1083 (m), 1065 (m), 1012 (m), 949 (w), 836 (s), 751 (vs), 711 (m), 666 (w). HRMS (EI): calcd for $\text{C}_{27}\text{H}_{33}\text{N}_4\text{O}^+$ $[\text{M}+\text{H}]^+$ 429.2649, found 429.2645.

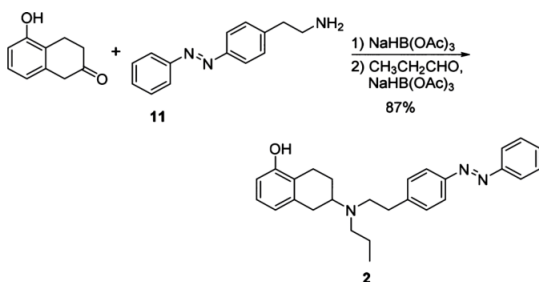
Oxalyl chloride (0.05 mL, 0.610 mmol) and DMF (1 drop) were added sequentially to a solution of 2-maleimidoacetic acid (73 mg, 0.469 mmol) in CH_2Cl_2 (5 mL), and the reaction mixture was stirred for 2 h at room temperature. The solvent was evaporated *in vacuo*, and the resulting residue was redissolved in THF (3 mL). The solution was



added dropwise to an ice-cooled solution of phenol **10** (67 mg, 0.156 mmol) and DIPEA (0.10 mL, 0.610 mmol) in THF (3 mL), and the reaction was stirred for 30 min at room temperature. The solvent was evaporated under reduced pressure, and the resulting residue was purified by flash column chromatography ($\text{MeOH}:\text{CH}_2\text{Cl}_2 = 3:97$,

$R_f = 0.25$) to give Mal-Azo-PPHT (41 mg, 0.072 mmol, 46%) as a red solid.

Data for 1: $^1\text{H NMR}$ (400 MHz, CDCl_3): δ (ppm) 8.00 (s, 1H), 7.86 (d, $J = 8.4$ Hz, 2H), 7.80 (d, $J = 8.0$ Hz, 2H), 7.62 (d, $J = 8.5$ Hz, 2H), 7.31 (d, $J = 8.0$ Hz, 2H), 6.98 (t, $J = 7.7$ Hz, 1H), 6.79 (s, 2H), 6.67 (d, $J = 7.6$ Hz, 1H), 6.58 (d, $J = 7.9$ Hz, 1H), 5.56 (s, 1H), 4.37 (s, 2H), 3.04–2.70 (m, 8H), 2.62–2.50 (m, 3H), 1.61 (tt, $J = 12.1$, 6.2 Hz, 1H), 1.50 (p, $J = 7.4$ Hz, 2H), 0.89 (t, $J = 7.3$ Hz, 3H). $^{13}\text{C NMR}$ (100 MHz, CDCl_3): δ (ppm) = 170.3, 164.5, 153.6, 151.1, 138.5, 134.7, 129.7, 126.5, 124.3, 124.0, 123.1, 122.9, 122.7, 121.8, 121.7, 120.1, 112.1, 56.7, 52.7, 52.6, 41.4, 35.9, 32.3, 25.8, 23.8, 22.2, 12.1. IR (ATR): ν_{max} (cm^{-1}) = 2933(m), 1741(s), 1595 (vs), 1560 (s), 1501 (m), 1464 (m), 1408 (s), 1301 (s), 1253 (s), 1156 (s), 1012 (w), 846 (s), 771 (m), 676 (w). HRMS (ESI): calcd for $\text{C}_{33}\text{H}_{36}\text{N}_3\text{O}_4^+$ $[\text{M}+\text{H}]^+$ 566.2762, found 566.2763.



$\text{NaHB}(\text{OAc})_3$ (103 mg, 0.46 mmol) was added to a solution of amine 11 (73 mg, 0.32 mmol) and 5-hydroxytetralone (50 mg, 0.31 mmol) in DCE (2 mL), and the resulting suspension was stirred at room temperature overnight. The reaction mixture was partitioned between EtOAc and aqueous NaHCO_3 solution, and the organic phase was further washed with aqueous NaHCO_3 solution, a solution of sodium chloride (10%), and brine. The solution was dried over Na_2SO_4 and concentrated under reduced pressure, yielding the crude alkylation product as an orange oil, which was immediately transferred to the next step.

The freshly prepared secondary amine (described above) was redissolved in DCE (1.5 mL) and treated with propionaldehyde (25 μL , 0.34 mmol) followed by $\text{NaHB}(\text{OAc})_3$ (103 mg, 0.46 mmol). After 5 h, the reaction was quenched and worked up as described above, yielding the crude product tertiary amine. Medium-pressure chromatography (Biotage, 25 g SiO_2 column, EtOAc:hexanes = 10:90–100:0, $R_f = 0.6$ EtOAc:hexanes = 1:1) afforded AP 2 as an orange oil (110 mg, 0.27 mmol, 87% over 2 steps).

Data for 2: $^1\text{H NMR}$ (600 MHz, CDCl_3): δ = 7.94–7.89 (m, 2H), 7.89–7.83 (m, 2H), 7.54–7.49 (m, 2H), 7.49–7.44 (m, 1H), 7.37–7.32 (m, 2H), 6.99 (t, $J = 7.8$, 1H), 6.68 (d, $J = 7.7$, 1H), 6.60 (d, $J = 7.9$, 1H), 5.40 (s, 1H), 3.06–2.87 (m, 3H), 2.85 (s, 4H), 2.82–2.66 (m, $J = 28.9$, 15.2, 9.4, 1H), 2.63–2.53 (m, 3H), 2.13–2.07 (m, 1H), 1.68–1.57 (m, 1H), 1.57–1.47 (m, 2H), 0.91 (t, $J = 7.3$, 3H). $^{13}\text{C NMR}$ (100 MHz, CDCl_3): (151 MHz, CDCl_3) δ = 153.46, 152.72, 151.07, 144.48, 138.37, 130.72, 129.52, 129.04, 126.40, 122.94, 122.83, 122.73, 121.68, 111.97, 56.58, 52.62, 52.54, 35.81, 32.24, 25.70, 23.60, 22.08, 11.93. IR (ATR): ν_{max} (cm^{-1}) = 3043 (w), 2931 (m), 1585 (s), 1499 (w), 1484 (w), 1464 (s), 1373 (m), 1340 (m), 1277 (s), 1221 (w), 1154 (m), 1104 (w), 1070 (w), 1012 (m), 919 (w), 836 (m), 808 (w), 766 (vs), 712 (w), 687 (vs). HRMS (ESI): calcd for $\text{C}_{27}\text{H}_{32}\text{N}_3\text{O}^+$ $[\text{M}+\text{H}]^+$ 414.2545, found 414.2537.

Homology Modeling and Docking. DAR homology models were generated using Bioluminate (Schrodinger, Inc.).⁹¹ Models of D1R and D2R were based on β_2 -adrenergic receptor ($\beta_2\text{AR}$) and D3R, respectively, because of the high relative degree of homology between these receptors. The amino acid sequence of D1R was first aligned to $\beta_2\text{AR}$ in BLAST,⁹² and the TM segments were then structurally aligned with the crystal structure of $\beta_2\text{AR}$ bound to the inverse agonist carazolol (PDB: 2RH1). The sequence of D2R was aligned to D3R as described previously,⁴⁹ and the homology model

was generated based on a crystal structure of D3R bound to the antagonist eticlopride (PDB: 3PBL). The three extracellular loops of either D1R or D2R were refined using extended sampling. For docking DA into either D1R or D2R, DA was first prepared using LigPrep (Schrodinger, Inc.) and docked with extra precision (XP) using Glide.⁹³ The hydroxyl groups of the three TMS serines (Ser^{5.42}, Ser^{5.43}, and Ser^{5.46}) in D1R or D2R that contribute to the OBS were allowed to rotate during the docking procedure. As expected, the protonated amine and hydroxyls of DA were oriented toward Asp^{3.32} in TM3 and the TMS serines, respectively. All molecular representations of D1R or D2R were prepared using Chimera, which was developed by the Resource for Biocomputing, Visualization, and Informatics at the University of California, San Francisco (supported by NIGMS P41-GM103311).

Molecular Biology and Heterologous Expression. For the BRET-based assays used in this study, HEK293T cells were seeded onto 10 cm plates and transfected with a 1:1 ratio of DNA:polyethylenimine (linear, MW 25 000; PolySciences, Inc.). Human D1R and the short isoform of human D2R were cloned into the expression vector pcDNA3.1 with a signal peptide to enhance receptor expression.⁹⁴ For the BRET-based D1R-mediated cAMP accumulation assay, we transfected pcDNA3.1 plasmids encoding D1R (5 μg) and CAMYEL⁶⁵ (6 μg ; ATCC). For the BRET-based D2R-mediated G protein activation assay, we transfected pcDNA3.1 plasmids encoding D2R (2 μg) and human $G\alpha_{i1}$ with *Renilla* luciferase 8 (Rluc8) inserted at position 91 ($G\alpha_{i1}$ -91-Rluc8; 0.2 μg)⁹⁵ and mVenus fragments V1 and V2 fused to human $G\beta_1$ and human $G\gamma_2$, respectively (V1- β_1 and V2- γ_2 ; 1 and 7 μg , respectively).⁹⁶ For the D2R-mediated arrestin recruitment assay, we transfected D2R (2 μg), Rluc8-arrestin3-Sp1 (0.25 μg), mem-linker-citrine-SH3 (5 μg), and GRK2 (5 μg).⁹⁷

For the HTRF-based D2R binding assay, D2R was cloned into pcDNAs/FRT/TO (Invitrogen) with a signal peptide and SNAP-tag added to its N-terminus.⁷⁰ HEK293 cells were stably transfected with this plasmid using the Flp-in T-Rex system (Invitrogen).

For electrophysiological studies, cysteine mutations were introduced into D1R or D2R using the QuickChange mutagenesis kit (Agilent). Human $G\alpha_{i1}$, human chimeric $G\alpha_{i13}$,⁷⁵ human GIRK1, human GIRK2, or tdTomato was cloned into pcDNA3.1. HEK293T cells, sparsely seeded onto 18 mm coverslips, were transiently transfected overnight with GIRK1, GIRK2, and tdTomato (as a marker of transfection) with Lipofectamine 2000 (Invitrogen) at a ratio of 7:7:1 (total DNA of 1.5 μg per coverslip). Each coverslip was also transfected with either 0.7 μg of D1R and 0.35 μg $G\alpha_{i13}$ or 0.1 μg D2R and 0.1 μg $G\alpha_{i1}$.

Resonance Energy Transfer (RET) Assays. All RET studies were performed in HEK293 or HEK293T cells that were maintained in DMEM (Invitrogen) with 10% fetal bovine serum at 37 °C under 5% CO_2 . For the BRET studies, HEK293T cells were transiently transfected with the plasmids described above. Cells used in the G protein activation and arrestin recruitment assays were prepared and assayed as described previously in detail.^{96,97} Briefly, cells were washed, harvested, and resuspended in PBS containing 5 mM glucose at room temperature. Cells (~40 μg of protein per well according to a BCA protein assay kit, ThermoScientific) were distributed into a 96-well microplate (Wallac, PerkinElmer Life, and Analytical Sciences). After incubation with coelenterazine H (5 μM) (Dalton Pharma Services) for 8 min, different ligands were injected and incubated for 2–10 min. Just prior its addition to cells, AP was switched to the *cis* configuration (*cis*-AP) by illumination with a hand-held UVGL-15 UV-lamp (power output: ~1 mW/mm²; irradiance: 365 nm; UVP, LLC) for 1 min. Using a Pherastar FS plate reader (BMG Labtech), BRET¹ signal was determined by quantifying and calculating the ratio of the light emitted by mVenus (510–540 nm) over that emitted by Rluc8 (485 nm).

For experiments used to determine whether MAP binds covalently to WT D2R, MTS reagents or MAP were incubated for 1 h at room temperature with transfected HEK293T cells expressing D2R, $G\alpha_{i1}$ -91-Rluc8, V1- β_1 , and V2- γ_2 . To avoid inactivation of the $G\alpha_{i1}$ by either the MTS reagents or MAP, residue C351 was mutated to an isoleucine.

The HTRF-based binding assay was described previously in detail.⁷⁰ Briefly, 10 000 cells per well were seeded into black 96-well plates

(Greiner) pretreated with 50 $\mu\text{g}/\text{mL}$ poly-D-lysine. Cells were induced with 1 $\mu\text{g}/\text{mL}$ tetracycline in growth medium 24 h after seeding. Forty-eight hours after seeding, cells were incubated with 100 nM Tag-Lite Lumi4 (CisBio) in growth medium for 1 h and washed three times with Tris-Krebs buffer (20 mM Tris, pH 7.4; 118 mM NaCl; 1.2 mM KH_2PO_4 ; 1.2 mM MgSO_4 ; 4.7 mM KCl; 1.8 mM CaCl_2). Twenty nanomoles of NAPS (*N*-azidophenethylspiperone)–DY-647 (Cisbio), along with various concentrations of test ligand in a total volume of 200 μL Tris-Krebs/0.1% bovine serum albumin buffer, were added to each well, and plates were incubated for 2 h at room temperature. *cis*-AP-containing wells were illuminated every 5 min for 30 s with a hand-held UVGL-15 UV-lamp (1 mW/mm^2 at 365 nm) to maintain the compound in the *cis* configuration. Following this incubation period, preparations were excited at 337 nm (excitation of Tag-Lite Lumi4), and emission was measured at 620 nm (emission for Tag-Lite Lumi4) and 665 nm (emission for DY-647) on a Pherastar FS plate reader. We measured 400 μs readings after a 50 μs delay to avoid short-life fluorescence background from the signal.

Electrophysiology. HEK293T cells were maintained in DMEM (Invitrogen) with 10% fetal bovine serum on poly-L-lysine-coated coverslips. Cells were patch-clamped in whole-cell configuration 16–24 h after transfection in high potassium solution containing 120 mM KCl, 25 mM NaCl, 10 mM HEPES, 2 mM CaCl_2 , and 1 mM MgCl_2 , pH 7.4. Glass pipettes with a resistance of 3–7 $\text{M}\Omega$ were filled with intracellular solution containing 140 mM KCl, 10 mM HEPES, 3 mM Na₂ATP, 0.2 mM Na₂GTP, 5 mM EGTA, and 3 mM MgCl_2 , pH 7.4. Cells were voltage clamped to –60 or –80 mV using an Axopatch 200A (Molecular Devices) amplifier.

All pharmacological compounds were applied using a gravity-driven perfusion system. Illumination was applied to the entire field of view using a Polychrome V monochromator (TILL Photonics) through a 20X objective (4 mW/mm^2 at 460 nm or 0.5 mW/mm^2 at 360 nm). pClamp software was used for both data acquisition and control of illumination. For bistable switching, the shutter was manually turned on or off at specific time points. To conjugate MAP to WT and cysteine mutants of D1R or D2R, cells were incubated with 30 μM MAP for 60 min in the dark at 23–27 $^\circ\text{C}$ in standard extracellular cell buffers. These conditions are comparable to those used to label other engineered light-gated receptors with maleimide-azobenzene photoswitches.^{48,77}

Statistics and Data Analysis. Data were analyzed using GraphPad Prism (GraphPad), Clampfit (Axon instruments), or Origin (OriginLab) software. For dose–response curves, data were normalized to vehicle (0%) and dopamine (100%), and nonlinear regression analysis was performed using the sigmoidal dose–response function in GraphPad Prism. To calculate the percentage photoblock of DA by MAP, the DA-induced current under 460 nm light (*trans*-MAP_{+DA}) was divided by DA-induced current under 360 nm light (*cis*-MAP_{+DA}), subtracted from one, and multiplied by 100. Basal current under 360 nm light (*cis*-MAP_{-DA}) was used as the baseline. This is described below as eq 1:

$$\% \text{ photoblock} = 1 - \frac{\text{trans-MAP}_{+DA}}{\text{cis-MAP}_{+DA}} \times 100 \quad (1)$$

To calculate inverse photoagonism as a percentage of maximal DA activation, the current under 460 nm light (*trans*-MAP_{-DA}) was subtracted from *cis*-MAP_{-DA}, divided by *cis*-MAP_{+DA}, and multiplied by 100. This is described below as eq 2:

$$\text{inverse agonism} = \frac{\text{cis-MAP}_{-DA} - \text{trans-MAP}_{-DA}}{\text{cis-MAP}_{+DA}} \times 100 \quad (2)$$

Statistical analyses were performed using Graphpad Prism. All values reported are mean \pm SEM.

■ ASSOCIATED CONTENT

Supporting Information

The Supporting Information is available free of charge on the ACS Publications website at DOI: 10.1021/jacs.7b07659.

Experimental procedures and characterization of compounds (PDF)

■ AUTHOR INFORMATION

Corresponding Authors

*ehud@berkeley.edu

*dirktrauner@nyu.edu

ORCID

Dirk Trauner: 0000-0002-6782-6056

Author Contributions

⊗P.C.D. and N.W. contributed equally.

Notes

The authors declare no competing financial interest.

■ ACKNOWLEDGMENTS

The work was supported by National Institutes of Health Nanomedicine Development Center for the Optical Control of Biological Function (2PN2EY018241), Instrumentation Awards S10RR028971, U01NS090527, U01MH109069, and R01MH54137, as well as by the Deutsche Forschungsgemeinschaft (SFB 749 and CIPSM). We thank C. Habrian and Y. Yu for helpful discussions.

■ REFERENCES

- (1) Lagerstrom, M. C.; Schiöth, H. B. *Nat. Rev. Drug Discovery* **2008**, *7*, 339.
- (2) Rask-Andersen, M.; Almen, M. S.; Schiöth, H. B. *Nat. Rev. Drug Discovery* **2011**, *10*, 579.
- (3) Kobilka, B. K. *Biochim. Biophys. Acta, Biomembr.* **2007**, *1768*, 794.
- (4) Beninger, R. J. *Brain Res. Rev.* **1983**, *6*, 173.
- (5) Beaulieu, J. M.; Gainetdinov, R. R. *Pharm. Rev.* **2011**, *63* (1), 182.
- (6) Greengard, P.; Allen, P. B.; Nairn, A. C. *Neuron* **1999**, *23*, 435.
- (7) Surmeier, D. J.; Eberwine, J.; Wilson, C. J.; Cao, Y.; Stefani, A.; Kitai, S. T. *Proc. Natl. Acad. Sci. U. S. A.* **1992**, *89*, 10178.
- (8) Surmeier, D. J.; Bargas, J.; Hemmings, H. C., Jr.; Nairn, A. C.; Greengard, P. *Neuron* **1995**, *14*, 385.
- (9) Cepeda, C.; Chandler, S. H.; Shumate, L. W.; Levine, M. S. *J. Neurophysiol.* **1995**, *74*, 1343.
- (10) Hernandez-Lopez, S.; Bargas, J.; Surmeier, D. J.; Reyes, A.; Galarraga, E. *J. Neurosci.* **1997**, *17*, 3334.
- (11) Schiffmann, S. N.; Lledo, P. M.; Vincent, J. D. *J. Physiol.* **1995**, *483*, 95.
- (12) Andersson, M.; Konradi, C.; Cenci, M. A. *J. Neurosci.* **2001**, *21*, 9930.
- (13) Pillai, G.; Brown, N. A.; McAllister, G.; Milligan, G.; Seabrook, G. R. *Neuropharmacology* **1998**, *37*, 983.
- (14) Kuzhikandathil, E. V.; Yu, W.; Oxford, G. S. *Mol. Cell. Neurosci.* **1998**, *12*, 390.
- (15) Conroy, J. L.; Free, R. B.; Sibley, D. R. *ACS Chem. Neurosci.* **2015**, *6*, 681.
- (16) Kim, K. M.; Valenzano, K. J.; Robinson, S. R.; Yao, W. D.; Barak, L. S.; Caron, M. G. *J. Biol. Chem.* **2001**, *276*, 37409.
- (17) DeWire, S. M.; Ahn, S.; Lefkowitz, R. J.; Shenoy, S. K. *Annu. Rev. Physiol.* **2007**, *69*, 483.
- (18) Lee, F. J.; Xue, S.; Pei, L.; Vukusic, B.; Chery, N.; Wang, Y.; Wang, Y. T.; Niznik, H. B.; Yu, X. M.; Liu, F. *Cell* **2002**, *111*, 219.
- (19) Liu, F.; Wan, Q.; Pristupa, Z. B.; Yu, X. M.; Wang, Y. T.; Niznik, H. B. *Nature* **2000**, *403*, 274.
- (20) Tritsch, N. X.; Sabatini, B. L. *Neuron* **2012**, *76*, 33.
- (21) Dauer, W.; Przedborski, S. *Neuron* **2003**, *39*, 889.
- (22) Howes, O. D.; Kapur, S. *Schizophr. Bull.* **2009**, *35*, 549.
- (23) Volkow, N. D.; Fowler, J. S.; Wang, G. J.; Swanson, J. M.; Telang, F. *Arch. Neurol.* **2007**, *64*, 1575.
- (24) DiMaio, S.; Grizenko, N.; Joober, R. J. *Psychiatry Neurosci.* **2003**, *28*, 27.

- (25) Denys, D.; Zohar, J.; Westenberg, H. G. J. *Clin. Psychiatry* **2004**, *65*, 11.
- (26) Buse, J.; Schoenefeld, K.; Munchau, A.; Roessner, V. *Neurosci. Biobehav. Rev.* **2013**, *37*, 1069.
- (27) Seeman, P. *Pharmacol. Rev.* **1980**, *32*, 229.
- (28) Mailman, R. B.; Huang, X. *Handbook of Clinical Neurology* **2007**, *83*, 77.
- (29) Michino, M.; Beuming, T.; Donthamsetti, P.; Newman, A. H.; Javitch, J. A.; Shi, L. *Pharmacol. Rev.* **2015**, *67*, 198.
- (30) Kreitzer, A. C. *Annu. Rev. Neurosci.* **2009**, *32*, 127.
- (31) Airan, R. D.; Thompson, K. R.; Fenno, L. E.; Bernstein, H.; Deisseroth, K. *Nature* **2009**, *458*, 1025.
- (32) Kim, J. M.; Hwa, J.; Garriga, P.; Reeves, P. J.; RajBhandary, U. L.; Khorana, H. G. *Biochemistry* **2005**, *44*, 2284.
- (33) Siuda, E. R.; McCall, J. G.; Al-Hasani, R.; Shin, G.; Il Park, S.; Schmidt, M. J.; Anderson, S. L.; Planer, W. J.; Rogers, J. A.; Bruchas, M. R. *Nat. Commun.* **2015**, *6*, 8480.
- (34) Conklin, B. R.; Hsiao, E. C.; Claeysen, S.; Dumuis, A.; Srinivasan, S.; Forsayeth, J. R.; Guettier, J. M.; Chang, W. C.; Pei, Y.; McCarthy, K. D.; Nissenson, R. A.; Wess, J.; Bockaert, J.; Roth, B. L. *Nat. Methods* **2008**, *5*, 673.
- (35) Urban, D. J.; Roth, B. L. *Annu. Rev. Pharmacol. Toxicol.* **2015**, *55*, 399.
- (36) Gunaydin, L. A.; Grosenick, L.; Finkelstein, J. C.; Kauvar, I. V.; Fenno, L. E.; Adhikari, A.; Lammel, S.; Mirzabekov, J. J.; Airan, R. D.; Zalocusky, K. A.; Tye, K. M.; Anikeeva, P.; Malenka, R. C.; Deisseroth, K. *Cell* **2014**, *157*, 1535.
- (37) Volgraf, M.; Gorostiza, P.; Numano, R.; Kramer, R. H.; Isacoff, E. Y.; Trauner, D. *Nat. Chem. Biol.* **2006**, *2*, 47.
- (38) Lin, W. C.; Tsai, M. C.; Davenport, C. M.; Smith, C. M.; Veit, J.; Wilson, N. M.; Adesnik, H.; Kramer, R. H. *Neuron* **2015**, *88*, 879.
- (39) Lin, W. C.; Davenport, C. M.; Mouro, A.; Vyta, D.; Smith, C. M.; Medeiros, K. A.; Chambers, J. J.; Kramer, R. H. *ACS Chem. Biol.* **2014**, *9*, 1414.
- (40) Sandoz, G.; Levitz, J.; Kramer, R. H.; Isacoff, E. Y. *Neuron* **2012**, *74*, 1005.
- (41) Chambers, J. J.; Banghart, M. R.; Trauner, D.; Kramer, R. H. *J. Neurophysiol.* **2006**, *96*, 2792.
- (42) Berlin, S.; Szobota, S.; Reiner, A.; Carroll, E. C.; Kienzler, M. A.; Guyon, A.; Xiao, T.; Trauner, D.; Isacoff, E. Y. *eLife* **2016**, *5*, 12040.
- (43) Szobota, S.; Gorostiza, P.; Del Bene, F.; Wyart, C.; Fortin, D. L.; Kolstad, K. D.; Tulyathan, O.; Volgraf, M.; Numano, R.; Aaron, H. L.; Scott, E. K.; Kramer, R. H.; Flannery, J.; Baier, H.; Trauner, D.; Isacoff, E. Y. *Neuron* **2007**, *54*, 535.
- (44) Janovjak, H.; Szobota, S.; Wyart, C.; Trauner, D.; Isacoff, E. Y. *Nat. Neurosci.* **2010**, *13*, 1027.
- (45) Gaub, B. M.; Berry, M. H.; Holt, A. E.; Reiner, A.; Kienzler, M. A.; Dolgova, N.; Nikonov, S.; Aguirre, G. D.; Beltran, W. A.; Flannery, J. G.; Isacoff, E. Y. *Proc. Natl. Acad. Sci. U. S. A.* **2014**, *111*, E5574.
- (46) Fehrentz, T.; Schönberger, M.; Trauner, D. *Angew. Chem., Int. Ed.* **2011**, *50*, 12156.
- (47) Broichhagen, J.; Frank, J. A.; Trauner, D. *Acc. Chem. Res.* **2015**, *48*, 1947.
- (48) Levitz, J.; Pantoja, C.; Gaub, B.; Janovjak, H.; Reiner, A.; Hoagland, A.; Schoppik, D.; Kane, B.; Stawski, P.; Schier, A. F.; Trauner, D.; Isacoff, E. Y. *Nat. Neurosci.* **2013**, *16*, 507.
- (49) Chien, E. Y.; Liu, W.; Zhao, Q.; Katritch, V.; Han, G. W.; Hanson, M. A.; Shi, L.; Newman, A. H.; Javitch, J. A.; Cherezov, V.; Stevens, R. C. *Science* **2010**, *330*, 1091.
- (50) Weichert, D.; Kruse, A. C.; Manglik, A.; Hiller, C.; Zhang, C.; Hubner, H.; Kobilka, B. K.; Gmeiner, P. *Proc. Natl. Acad. Sci. U. S. A.* **2014**, *111*, 10744.
- (51) Rosenbaum, D. M.; Rasmussen, S. G.; Kobilka, B. K. *Nature* **2009**, *459*, 356.
- (52) Portoghese, P. S.; Larson, D. L.; Sayre, L. M.; Fries, D. S.; Takemori, A. E. *J. Med. Chem.* **1980**, *23*, 233.
- (53) Takemori, A. E.; Portoghese, P. S. *Annu. Rev. Pharmacol. Toxicol.* **1985**, *25*, 193.
- (54) Schönberger, M.; Trauner, D. *Angew. Chem., Int. Ed.* **2014**, *53*, 3264.
- (55) Agnetta, L.; Kauk, M.; Canizal, M. C. A.; Messerer, R.; Holzgrabe, U.; Hoffmann, C.; Decker, M. *Angew. Chem., Int. Ed.* **2017**, *56*, 7282.
- (56) Richter, H. W.; Waddell, W. H. *J. Am. Chem. Soc.* **1983**, *105*, 5434.
- (57) Meiser, J.; Weindl, D.; Hiller, K. *Cell Commun. Signaling* **2013**, *11*, 34.
- (58) Van der Weide, J.; De Vries, J. B.; Tepper, P. G.; Horn, A. S. *Eur. J. Pharmacol.* **1986**, *125*, 273.
- (59) Horn, A. S.; Tepper, P.; Van der Weide, J.; Watanabe, M.; Grigoriadis, D.; Seeman, P. *Pharm. Weekbl.* **1985**, *7*, 208.
- (60) Horn, A. S.; Tepper, P.; Kebabian, J. W.; Beart, P. M. *Eur. J. Pharmacol.* **1984**, *99*, 125.
- (61) Seiler, M. P.; Markstein, R. *Mol. Pharmacol.* **1984**, *26*, 452.
- (62) Seiler, M. P.; Markstein, R. *Mol. Pharmacol.* **1982**, *22*, 281.
- (63) Summers, C.; Dijkstra, D.; de Vries, J. B.; Horn, A. S. *Naunyn-Schmiedeberg's Arch. Pharmacol.* **1981**, *316*, 304.
- (64) Madras, B. K.; Canfield, D. R.; Pfaelzer, C.; Vittimberga, F. J., Jr.; Difiglia, M.; Aronin, N.; Bakthavachalam, V.; Baidur, N.; Neumeier, J. L. *Mol. Pharmacol.* **1990**, *37*, 833.
- (65) Jiang, L. I.; Collins, J.; Davis, R.; Lin, K. M.; DeCamp, D.; Roach, T.; Hsueh, R.; Rebres, R. A.; Ross, E. M.; Taussig, R.; Fraser, I.; Sternweis, P. C. *J. Biol. Chem.* **2007**, *282*, 10576.
- (66) Clayton, C. C.; Donthamsetti, P.; Lambert, N. A.; Javitch, J. A.; Neve, K. A. *J. Biol. Chem.* **2014**, *289*, 33663.
- (67) McKenzie, C. K.; Sanchez-Romero, I.; Janovjak, H. *Adv. Exp. Med. Biol.* **2015**, *869*, 101.
- (68) Reiner, A.; Levitz, J.; Isacoff, E. Y. *Curr. Opin. Pharmacol.* **2015**, *20*, 135.
- (69) Volgraf, M.; Gorostiza, P.; Szobota, S.; Helix, M. R.; Isacoff, E. Y.; Trauner, D. *J. Am. Chem. Soc.* **2007**, *129*, 260.
- (70) Michino, M.; Donthamsetti, P.; Beuming, T.; Banala, A.; Duan, L.; Roux, T.; Han, Y.; Trinquet, E.; Newman, A. H.; Javitch, J. A.; Shi, L. *Mol. Pharmacol.* **2013**, *84*, 854.
- (71) Shi, L.; Javitch, J. A. *Annu. Rev. Pharmacol. Toxicol.* **2002**, *42*, 437.
- (72) Ballesteros, A.; Weinstein, H. *Methods Neurosci.* **1995**, *25*, 366.
- (73) Pollock, N. J.; Manelli, A. M.; Hutchins, C. W.; Steffey, M. E.; MacKenzie, R. G.; Frail, D. E. *J. Biol. Chem.* **1992**, *267*, 17780.
- (74) Cherezov, V.; Rosenbaum, D. M.; Hanson, M. A.; Rasmussen, S. G.; Thian, F. S.; Kobilka, T. S.; Choi, H. J.; Kuhn, P.; Weis, W. I.; Kobilka, B. K.; Stevens, R. C. *Science* **2007**, *318*, 1258.
- (75) Leaney, J. L.; Milligan, G.; Tinker, A. *J. Biol. Chem.* **2000**, *275*, 921.
- (76) Salmi, P.; Isacson, R.; Kull, B. *CNS Drug Rev.* **2004**, *10*, 230.
- (77) Gorostiza, P.; Volgraf, M.; Numano, R.; Szobota, S.; Trauner, D.; Isacoff, E. Y. *Proc. Natl. Acad. Sci. U. S. A.* **2007**, *104*, 10865.
- (78) Kassack, M. U.; Hofgen, B.; Decker, M.; Eckstein, N.; Lehmann, J. *Naunyn-Schmiedeberg's Arch. Pharmacol.* **2002**, *366*, 543.
- (79) Fredriksson, R.; Lagerstrom, M. C.; Lundin, L. G.; Schioth, H. B. *Mol. Pharmacol.* **2003**, *63*, 1256.
- (80) Javitch, J. A.; Li, X.; Kaback, J.; Karlin, A. *Proc. Natl. Acad. Sci. U. S. A.* **1994**, *91*, 10355.
- (81) Roberts, D. J.; Strange, P. G. *Br. J. Pharmacol.* **2005**, *145*, 34.
- (82) Schultz, W. *Annu. Rev. Neurosci.* **2007**, *30*, 259.
- (83) Nygaard, R.; Zou, Y.; Dror, R. O.; Mildorf, T. J.; Arlow, D. H.; Manglik, A.; Pan, A. C.; Liu, C. W.; Fung, J. J.; Bokoch, M. P.; Thian, F. S.; Kobilka, T. S.; Shaw, D. E.; Mueller, L.; Prosser, R. S.; Kobilka, B. K. *Cell* **2013**, *152*, 532.
- (84) Strange, P. G. *Trends Pharmacol. Sci.* **2002**, *23* (2), 89.
- (85) Kmiecik, S.; Jamroz, M.; Kolinski, M. *Biophys. J.* **2014**, *106*, 2408.
- (86) Creese, I.; Burt, D. R.; Snyder, S. H. *Science* **1976**, *192*, 481.
- (87) Seeman, P.; Lee, T.; Chau-Wong, M.; Wong, K. *Nature* **1976**, *261*, 717.
- (88) Strange, P. G. *Trends Pharmacol. Sci.* **2008**, *29*, 314.

- (89) Lan, H.; Liu, Y.; Bell, M. I.; Gurevich, V. V.; Neve, K. A. *Mol. Pharmacol.* **2009**, *75*, 113.
- (90) Peterson, S. M.; Pack, T. F.; Wilkins, A. D.; Urs, N. M.; Urban, D. J.; Bass, C. E.; Lichtarge, O.; Caron, M. G. *Proc. Natl. Acad. Sci. U. S. A.* **2015**, *112*, 7097.
- (91) Zhu, K.; Day, T.; Warshaviak, D.; Murrett, C.; Friesner, R.; Pearlman, D. *Proteins: Struct., Funct., Genet.* **2014**, *82*, 1646.
- (92) NCBI Ressource Coordinators. *Nucleic Acids Res.* **2017**, *45*, D12–D17.
- (93) Friesner, R. A.; Banks, J. L.; Murphy, R. B.; Halgren, T. A.; Klicic, J. J.; Mainz, D. T.; Repasky, M. P.; Knoll, E. H.; Shelley, M.; Perry, J. K.; Shaw, D. E.; Francis, P.; Shenkin, P. S. *J. Med. Chem.* **2004**, *47*, 1739.
- (94) Guo, W.; Shi, L.; Javitch, J. A. *J. Biol. Chem.* **2003**, *278*, 4385.
- (95) Sauliere, A.; Bellot, M.; Paris, H.; Denis, C.; Finana, F.; Hansen, J. T.; Altie, M. F.; Seguelas, M. H.; Pathak, A.; Hansen, J. L.; Senard, J. M.; Gales, C. *Nat. Chem. Biol.* **2012**, *8*, 622.
- (96) Newman, A. H.; Beuming, T.; Banala, A. K.; Donthamsetti, P.; Pongetti, K.; LaBounty, A.; Levy, B.; Cao, J.; Michino, M.; Luedtke, R. R.; Javitch, J. A.; Shi, L. *J. Med. Chem.* **2012**, *55*, 6689.
- (97) Donthamsetti, P.; Quejada, J. R.; Javitch, J. A.; Gurevich, V. V.; Lambert, N. A. *Curr. Protoc. Pharmacol.* **2015**, *70*, 2.14.1–2.14.14.

Supporting Information

for

Optical Control of Dopamine Receptors Using a Photoswitchable Tethered Inverse Agonist

Prashant C. Donthamsetti^{1,*}, Nils Winter^{2,*}, Matthias Schönberger², Joshua Levitz¹, Cherise Stanley¹,
Jonathan A. Javitch^{3,4}, Ehud Y. Isacoff^{5,6,#} and Dirk Trauner^{2,7,#}

¹ Department of Molecular and Cell Biology, University of California, Berkeley, California 94720, USA

² Department of Chemistry and Center for Integrated Protein Science, Ludwig-Maximilians-Universität,
Butenandtstraße 5-13, Munich 81377, Germany

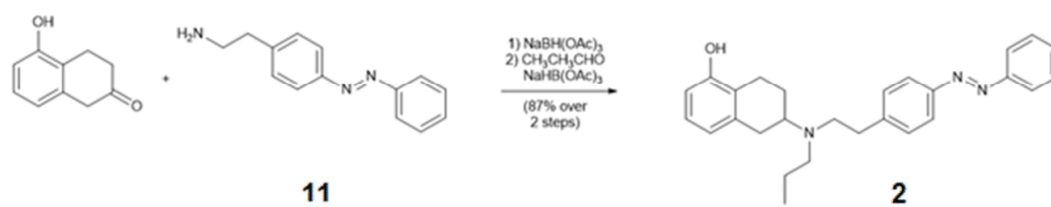
³ Departments of Psychiatry & Pharmacology, Columbia University, New York, New York 10027, USA

⁴ Division of Molecular Therapeutics, New York State Psychiatric Institute, New York, New York 10032,
United States

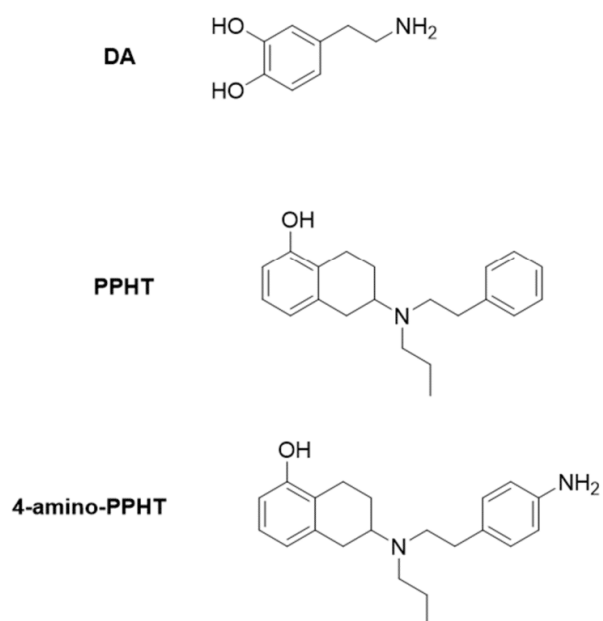
⁵ Helen Wills Neuroscience Institute, University of California, Berkeley, California, 94720

⁶ Bioscience Division, Lawrence Berkeley National Laboratory, Berkeley, California, 94720

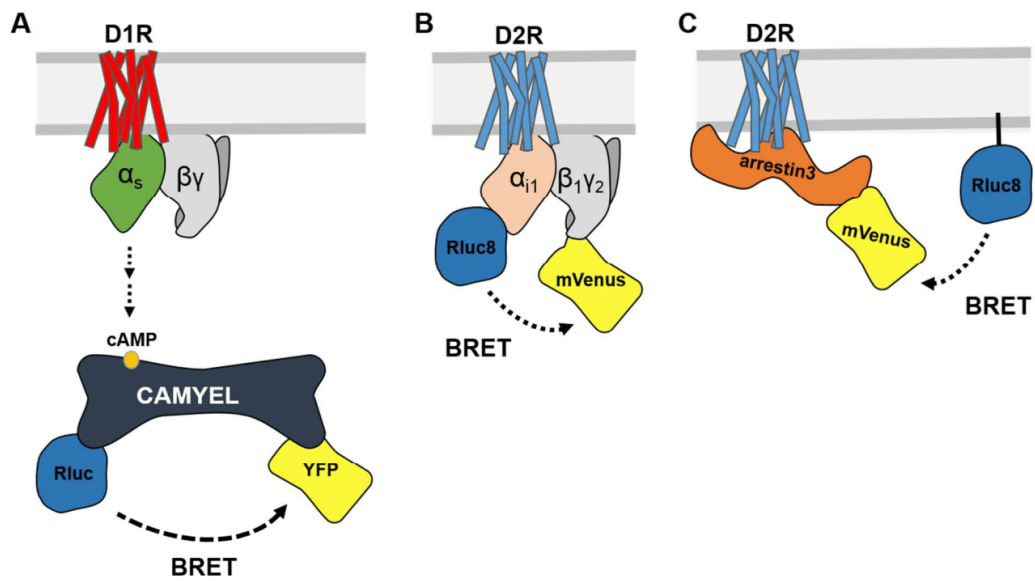
⁷ Department of Chemistry, New York University, New York City, New York, 10003



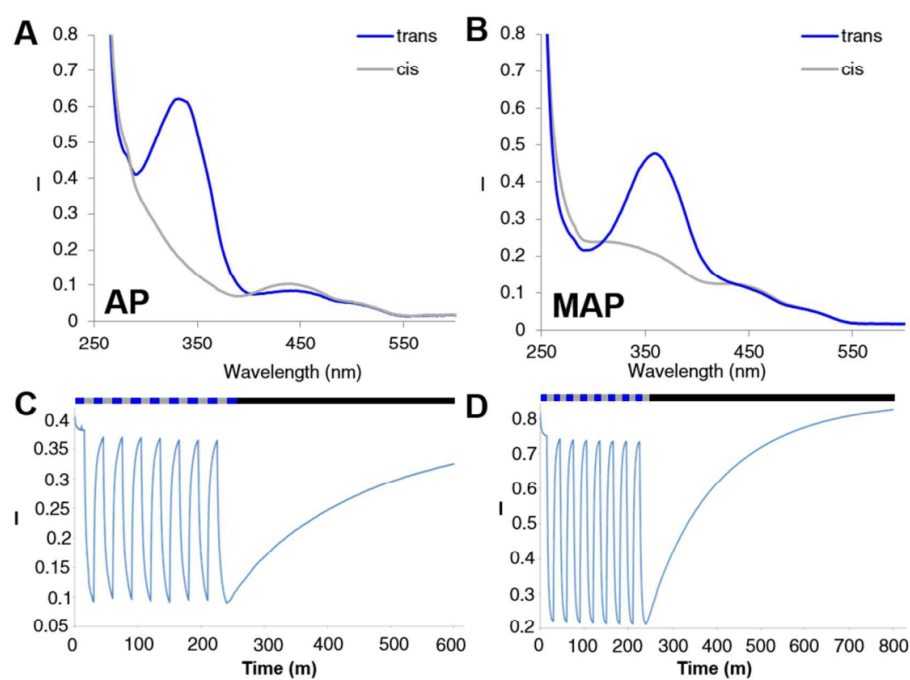
Supplementary Scheme 1. Synthesis of azobenzene-PPHT (AP).



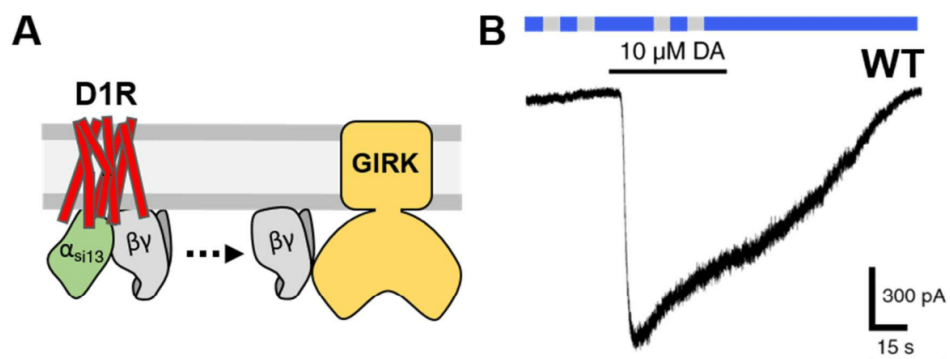
Supplementary Figure 1. Structures of dopamine (DA), PPHT and 4-amino-PPHT.



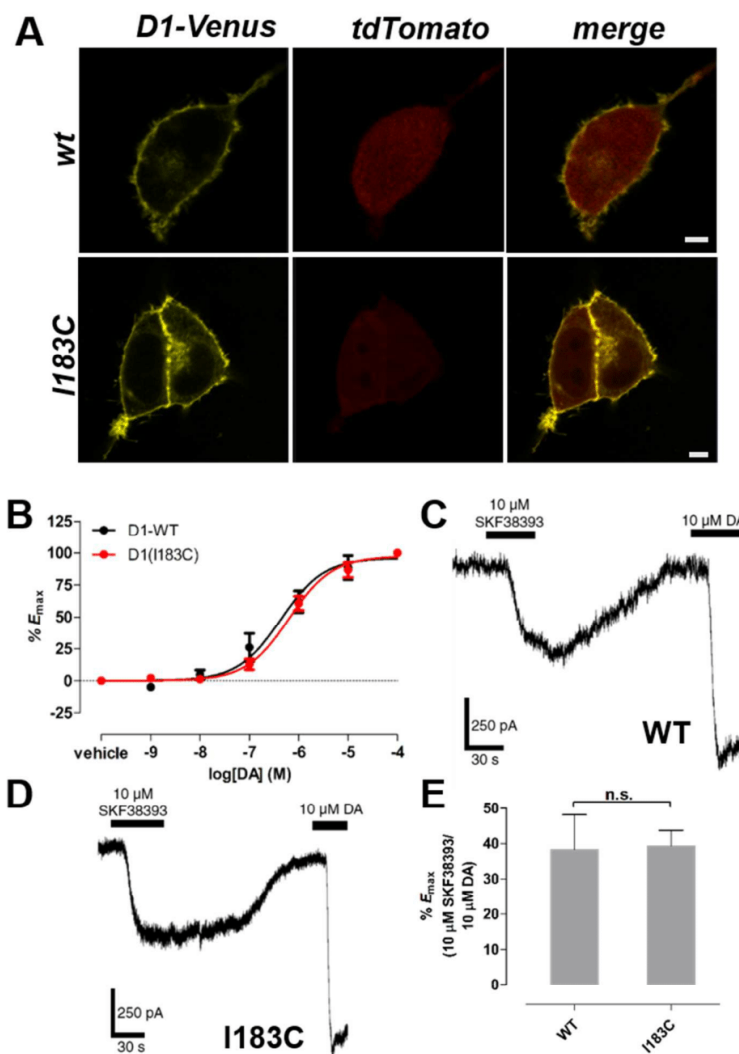
Supplementary Figure 2. Schematic representation of the bioluminescence resonance energy transfer (BRET)-based assays for measuring DAR function. (A) A D1R-mediated cAMP accumulation assay using the Epac-containing CAMYEL sensor. (B) A D2R-mediated G protein activation that measures conformational changes and/or the dissociation of G_{i1} in response to receptor activation. (C) A D2R-mediated arrestin recruitment that measures receptor-mediated arrestin3 translocation to the plasma membrane.



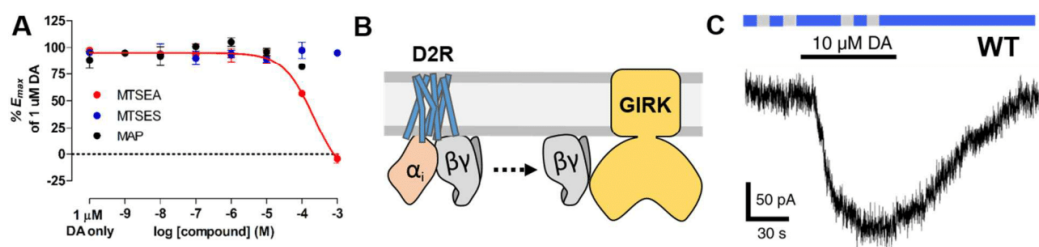
Supplementary Figure 3. Photochemical characterization of AP and MAP. (A) UV/Vis-spectra of the *cis*- and *trans*-isomers of AP (left) and MAP (right). (B) Switching of AP (left) and MAP (right) over several cycles of illumination with 360 and 460 nm light (grey and blue bars, respectively), as well the relaxation of their *cis*- to *trans*-isomers in the dark (black bars).



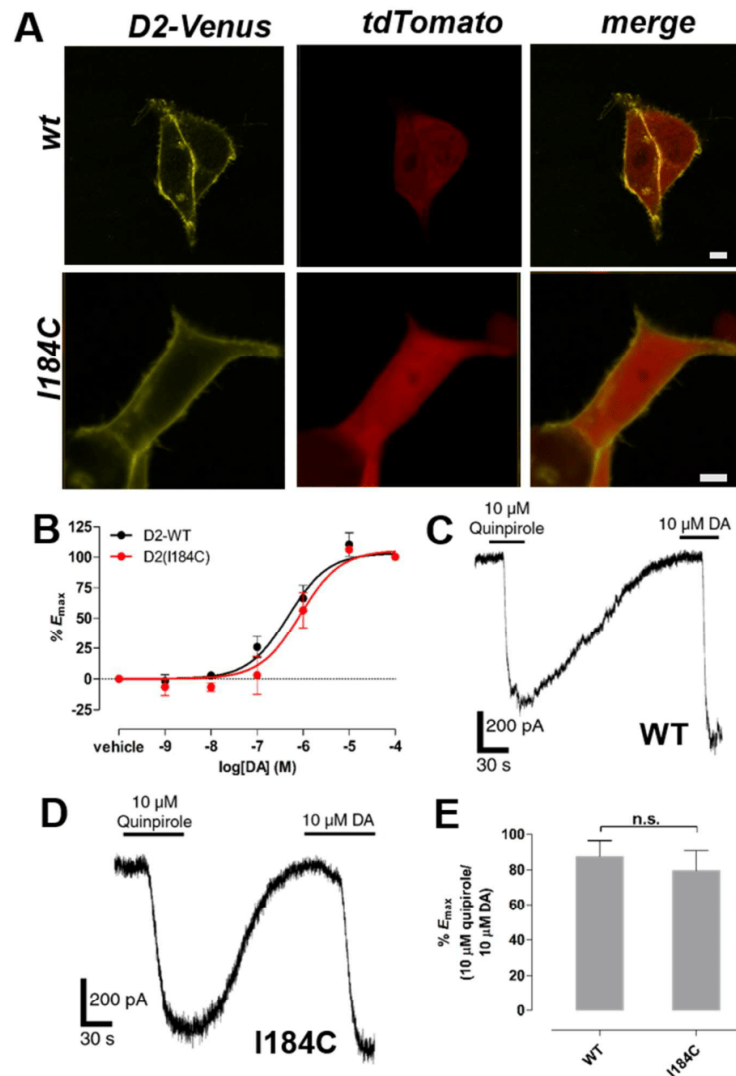
Supplementary Figure 4. MAP has no effect on wildtype D1R. (A) Schematic of the D1R-mediated GIRK activation assay. As a G_s -coupled receptor, D1R cannot activate GIRK channels. However, co-transfection of a chimeric G protein of $G\alpha_{i1}$ and $G\alpha_s$ ($G\alpha_{si13}$) allows D1R to activate GIRK. (B) After labeling and washout, MAP does not photoswitch wildtype D1R in response to 360 nm and 460 nm light in the D1R-mediated GIRK activation assay.



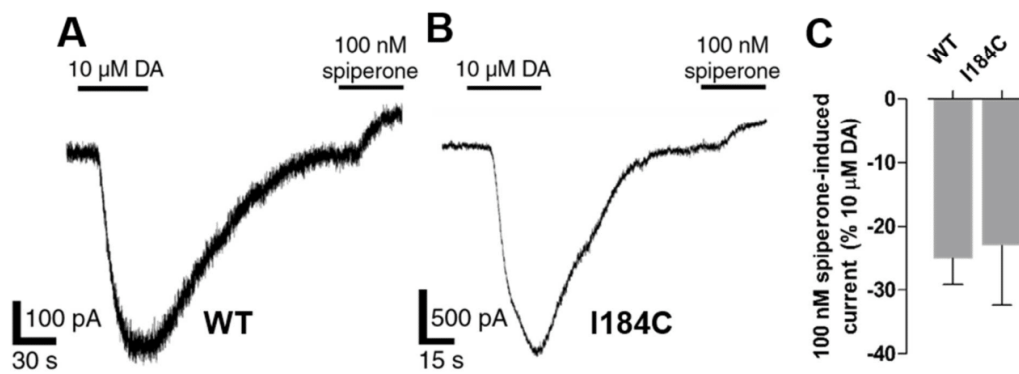
Supplementary Figure 5. Characterization of D1R(I183C). (A) D1R(I183C) expresses at the cell surface of HEK293T cells similar to wildtype D1R. D1Rs were tagged with mVenus at their C-termini. tdTomato was used as cytosolic marker. Bar= 5 μ m. (B) DA activates wildtype D1R and D1R(I183C) with similar potency. Error bars represent S.E.M for n=5-7 cells per concentration of DA. (C) The selective D1-like receptor agonist SKF38393 partially activates wildtype D1R in the GIRK activation assay. (D) SKF38393 partially activates D1R(I183C) in the GIRK activation assay. (E) 10 μ M SKF38393 similarly activates wildtype D1R and D1R(I183C) relative to 10 μ M DA (n.s.= not significant, two-tailed, unpaired t-test). Error bars represent S.E.M for n=3-6 cells per receptor.



Supplementary Figure 6. MAP has no effect on wildtype D2R. (A) MTSEA but not MTSES or MAP react covalently with C118 of D2R, impairing receptor activation by DA in the D2R-mediated G protein activation assay. Error bars represent S.E.M. (B) Schematic of the D2R-mediated GIRK activation assay. (C) After labeling and washout, MAP does not photoswitch wildtype D2R in response to 360 nm and 460 nm light in the D2R-mediated GIRK activation assay.



Supplementary Figure 7. Characterization of D2R(I184C). (A) D2R(I184C) expresses at the cell surface of HEK293T cells similar to wildtype D2R. D2Rs were tagged with mVenus at their C-termini. tdTomato was used as cytosolic marker. Bar= 5 μ m. (B) DA activates wildtype D2R and D2R(I184C) with similar potency. Error bars represent S.E.M for n=3-8 cells per concentration of DA. (C) The selective D2-like receptor agonist quinpirole activates wildtype D2R in the GIRK activation assay. (D) Quinpirole activates D2R(I184C) in the GIRK activation assay. (E) 10 μ M quinpirole similarly activates wildtype D2R and D2R(I184C) relative to 10 μ M DA (n.s.= not significant, two-tailed, unpaired t-test). Error bars represent S.E.M for n=3-5 cells per receptor.

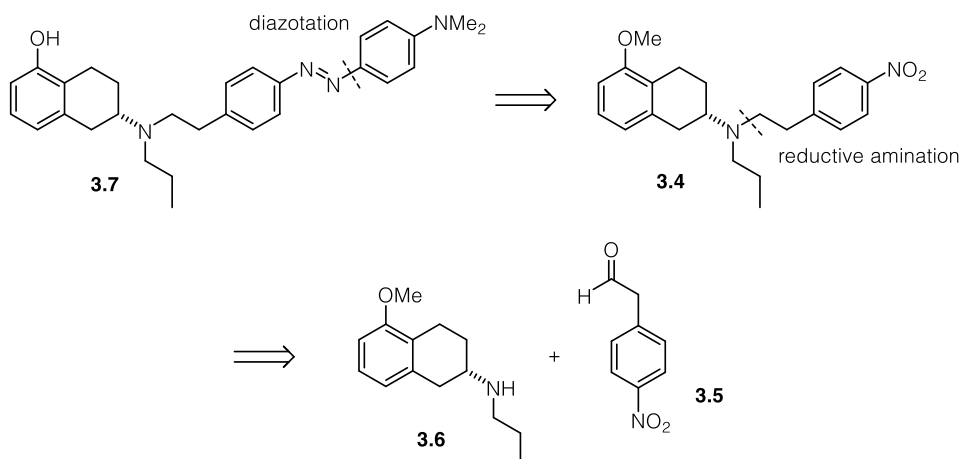


Supplementary Figure 8. D2R(I184C) is constitutively active in the GIRK-activation assay. (A) Basal inward current is reduced in response to spiperone in cells expressing wildtype D2R. (B) Basal inward current is reduced in response to spiperone in cells expressing D2R(I184C). (C) Summary of the effects of spiperone on basal inward current in cells expressing D2R wildtype and I184C. Error bars represent S.E.M for n=3-4 cells per receptor (not significant, one-way ANOVA).

3.2.3.2 Red-Shifted Azobenzene-PPHT (DMS-PPHT)

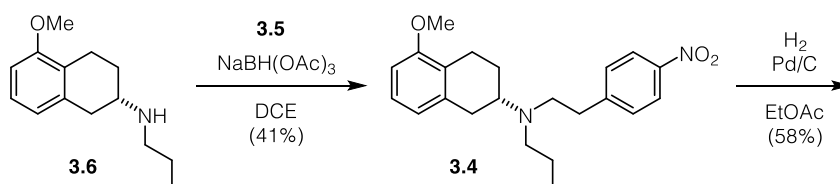
Using UV light to switch the ligand *in vivo* has several disadvantages such as tissue damaging caused by high energy photons and low penetration depth. To avoid these insufficiencies of a regular substituted azobenzene, we sought to increase the wavelength needed for photo-switching. The bathochromic shift can be achieved by the introduction of a dimethylamino group in the 4-position of the azobenzene.

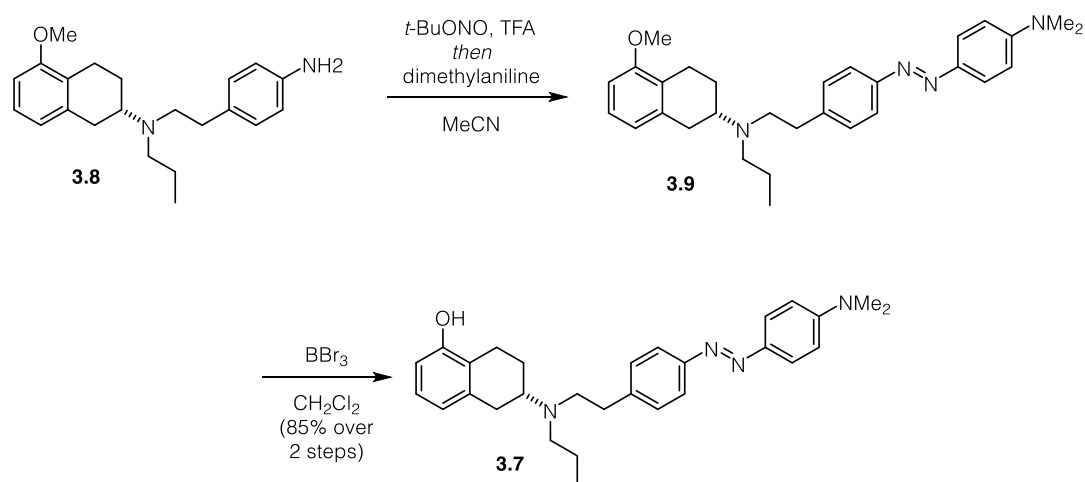
Our retrosynthetic analysis of DMS-PPHT is depicted in Scheme 3.1. The azobenzene should be introduced by diazonium ion formation and subsequent trapping with dimethylaniline. The aniline was supposed to be derived by reduction of nitrobenzene **3.4**. The ethylphenyl residue should be installed by reductive amination of aldehyde **3.5** and aminotetraline **3.6**.



SCHEME 3.1: Retrosynthetic analysis of **3.7**.

Following these considerations, reductive amination of aldehyde **3.5** with aminotetraline **3.6** gave nitro benzene **3.4** in moderate yields (Scheme 3.2). Further reduction of the nitro group under heterogeneous conditions gave access to aniline **3.8**. Diazonium ion generation and subsequent trapping with dimethylaniline furnished azobenzene **3.9**. Lewis acid-mediated deprotection of the methyl ether completed the synthesis of DMS-PPHT (**3.7**).





SCHEME 3.2: Synthesis of **3.7**.

With DMS-PPHT (**3.7**) in hand, we next investigated the photophysical properties of the molecule. Irradiation of **3.7** in DMSO with 420 nm sufficiently switched the compound from its *trans*- to its *cis*-conformation. When the *cis*-conformation was left in the dark, thermal relaxation restored the *trans*-configuration within 10 min. This process could be accelerated by illuminating the molecule with 600 nm light (Figure 3.5).

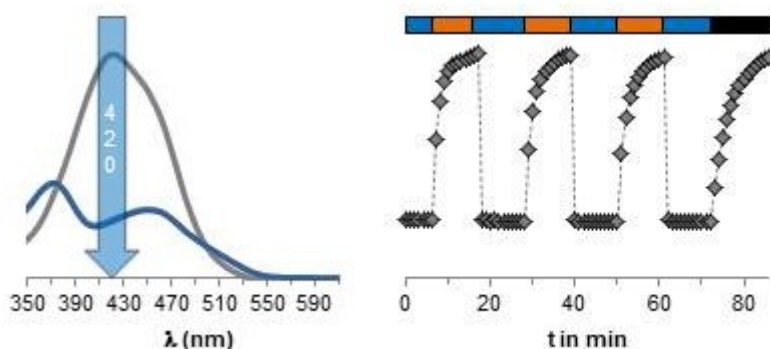


FIGURE 3.5: UV/Vis absorption spectra of *cis*- and *trans*-**3.7** (left), reversible photoswitching of **3.7** (right).

While DMSO would not necessarily be the solvent of choice for biological applications, we were interested in solvent dependencies on the photophysical properties. We therefore repeated the experiments in two protic and unprotic solvents with increasing polarity (Figure 3.6). The absorption maximum proved to be solvent dependent but was unfortunately lacking any trend. The switching kinetics as well as the photostationary states both provided a maximum in CHCl_3 and no switching was observed in MeOH. The switching properties in DMSO proved to be similar to those recorded in *i*-PrOH.

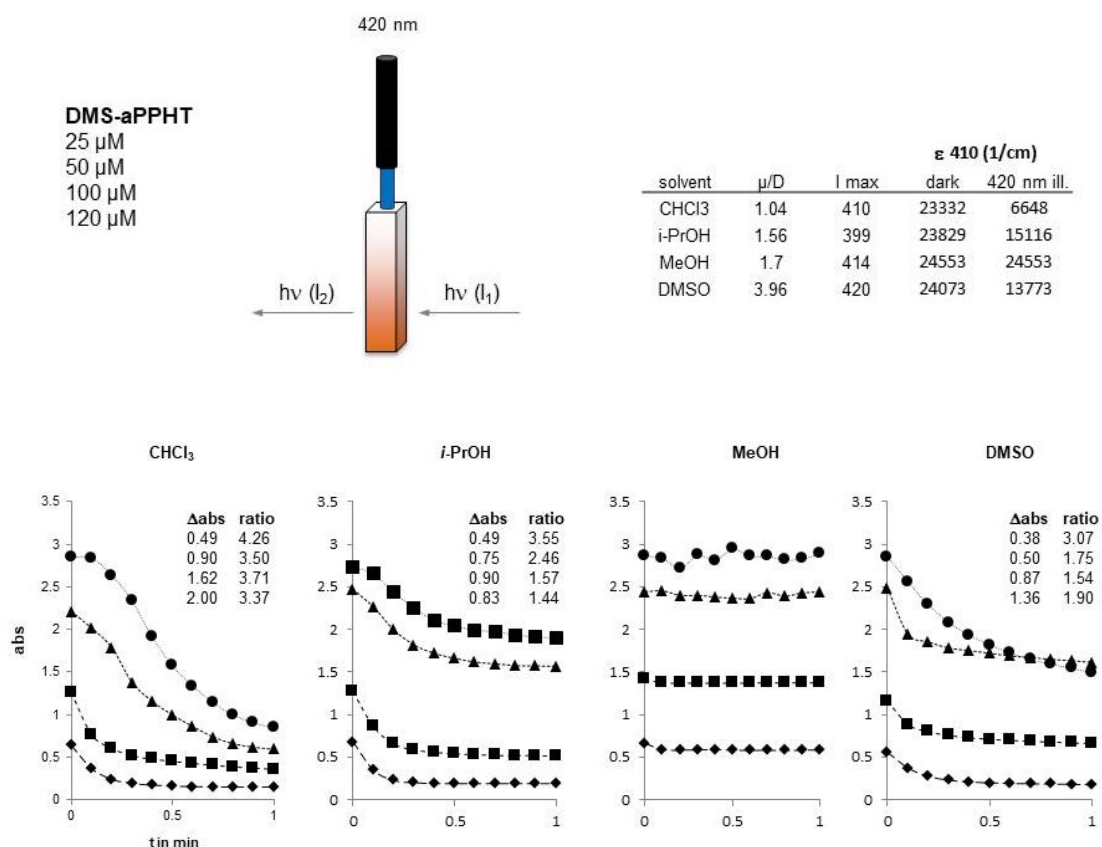


FIGURE 3.6: Solvent dependence on the absorption (up) switching kinetics (down) of **3.7**.

The effect of DMS-PPHT on HEK293T cells overexpressing DARs was then evaluated by Dr. Mathias Schönberger. Upon irradiation with 420 nm (purple bars), the molecule was converted into the active conformation and activated DARs. The molecule could then be truncated by illumination with 600 nm (yellow bars). This process could be repeated over several cycles without any loss of activity (Figure 3.7).

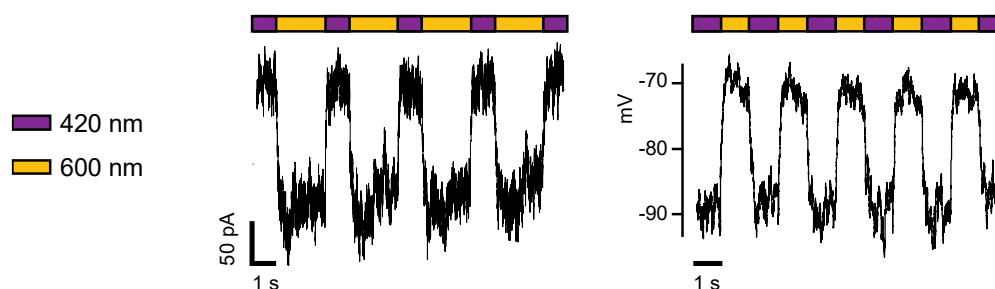
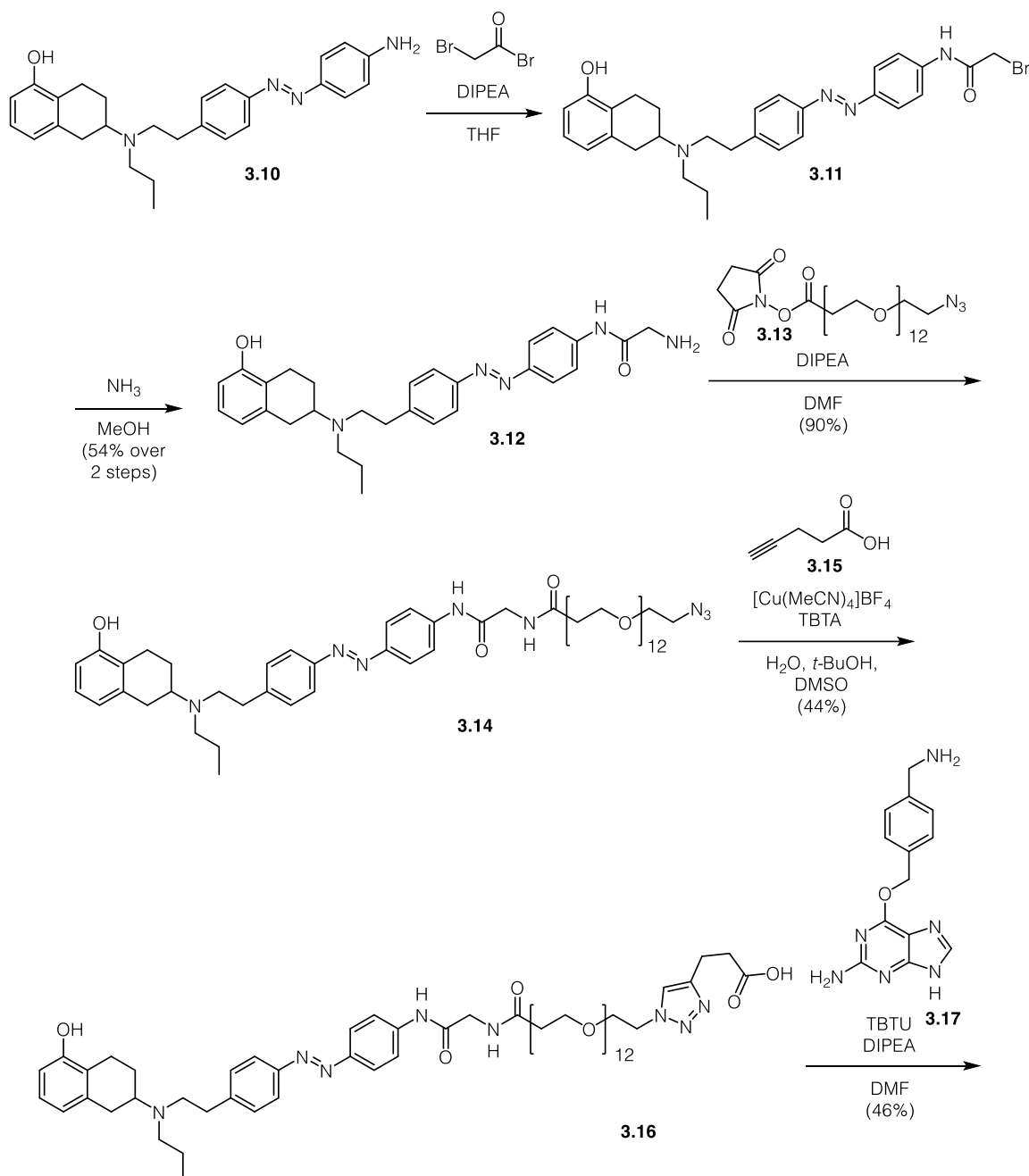
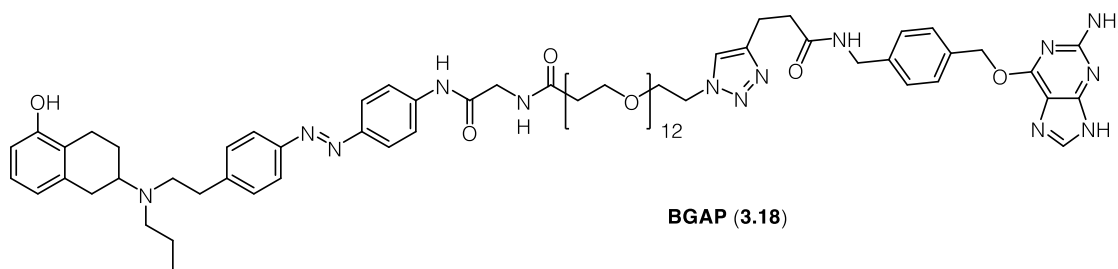


FIGURE 3.7: Current clamp (left) and voltage clamp (right) experiments on HEK293T cells overexpressing DARs.

3.2.3.3 Benzylguanine-Azobenzene-PPHT (BGAP)

The SNAP Tag tethering motif is becoming increasingly popular for the connection of a specific ligand to a protein of interest (POI). Therefore, an anchoring protein is genetically engineered to the POI which can react with a benzylguanine moiety attached to the ligand, forming a covalent bond. In this approach, it is possible to use a native, fully functional protein. Therefore, we decided to synthesize a photoswitchable PPHT





SCHEME 3.3: Synthesis of BGAP (3.18).

derivate providing a benzylguanidine attached *via* a polyethylene glycol (PEG) linker. The synthesis of benzylguanidine-azobenzene-PPHT (BGAP) is outlined in Scheme 3.3.

Acetylation of aniline **3.10** using bromoacetyl bromide gave bromoacetamide **3.11** which could undergo nucleophilic displacement by ammonia to yield glycine **3.12**. Previous attempts to install the glycine moiety by amide coupling with Fmoc-protected glycine resulted in cleavage of the amide bond under conditions needed for the following deprotection. The PEG linker was installed by amide coupling of **3.12** and PEGylated NHS ester **3.13**. Copper(I)-mediated click reaction⁹² of **3.14** with 4-pentynoic acid (**3.15**) accessed carboxylic acid **3.16**. BGAP (**3.18**) was obtained after TBTU mediated amide bond formation of **3.16** with benzylguanidine **3.17**.⁹³ Purification of **3.18** proved to be challenging due to cleavage of the benzylguanidine in several conditions used for chromatography.

We next evaluated the photophysical properties of the molecule. BGAP was efficiently converted from its *trans*- to *cis*-configuration by irradiation with 360 nm light and *vice versa* by 460 nm light. The compound could efficiently be switched over several cycles without any loss of activity (Figure 3.8). As BGAP lacks any strong auxochromic groups, the *cis*-configuration of the compound is sufficiently stable towards thermal relaxation

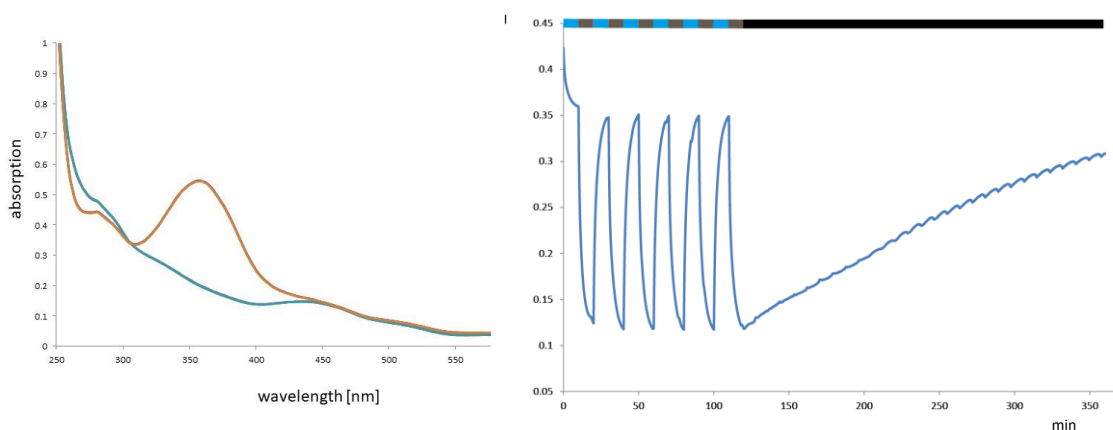


FIGURE 3.8: UV/Vis-spectra of *cis* and *trans* BGAP (left), switching BGAP over several cycles followed by thermal relaxation (right).

($T_{1/2} > 1$ h), and thus the compound is considered bistable.

The biological properties of BGAP were subsequently evaluated by Dr. Prashant Donthamsetti in the Isacoff lab at UC Berkeley. When the compound was attached to D1R, irradiation with 460 nm light evoked a photocurrent that disappeared upon illumination with 360 nm light. The effect was reversible and could be repeated over at least two cycles without any loss of function. The application of DA further increased the current showing that BGAP is a partial agonist in its *trans*-configuration on D1R (Figure 3.9). When BGAP was attached to D2R, the current evoked by DA was photoblocked in response to 460 nm light and returned to its former state in response to 360 nm light, showing that BGAP is an antagonist in its *trans*-configuration on D2R.

The UV/Vis-spectrum proposed that the compound can efficiently be switched to its *cis*-configuration with 360 nm light. Nevertheless, the broad absorption band of the π - π^* transition indicates that other wavelengths would be suitable as well, albeit with reduced efficiency. The wavelength screening on D1R revealed that switching is possible in a range from 320–390 nm with a maximum efficiency between 360 nm and 370 nm.

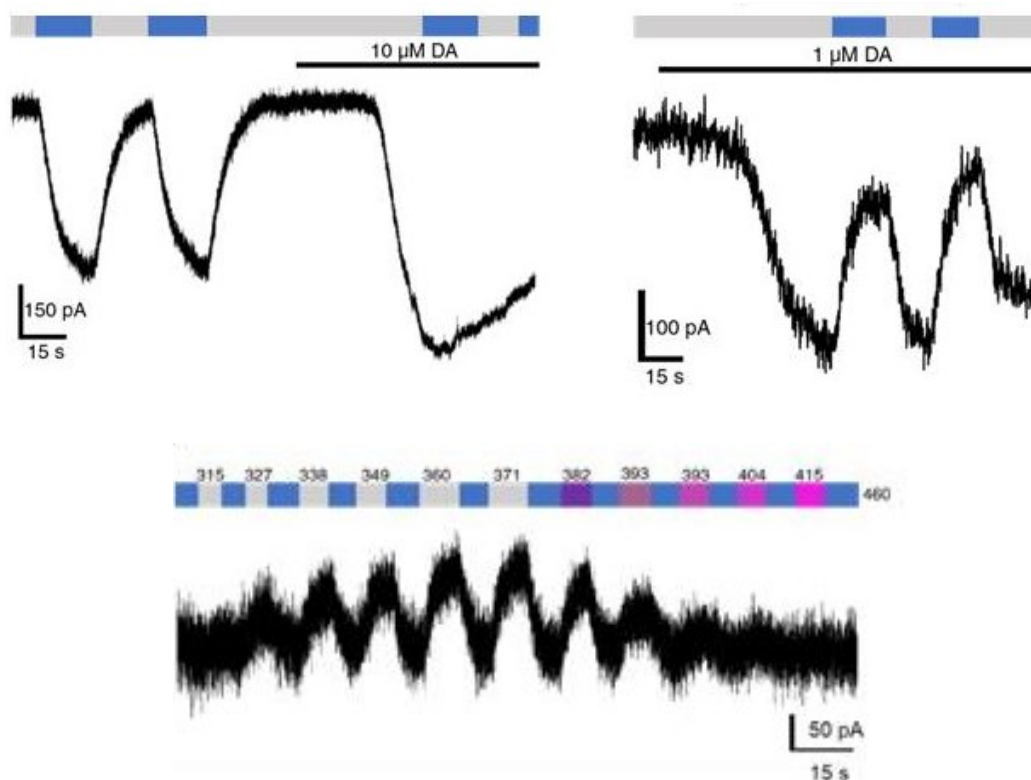
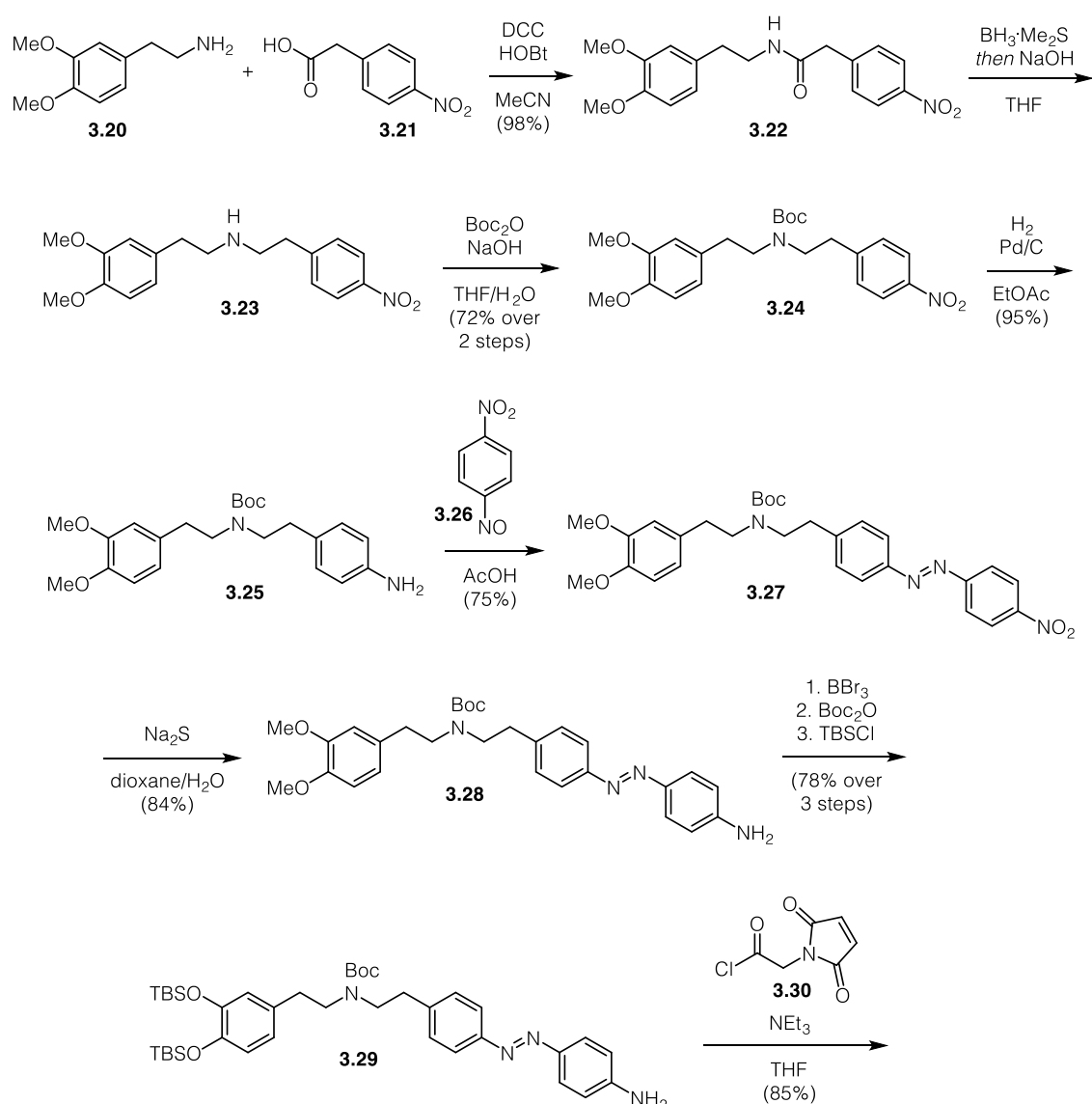
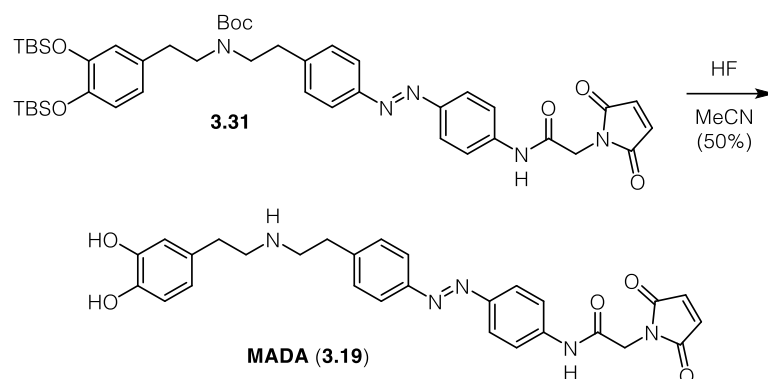


FIGURE 3.9: BGAP is a partial agonist on D1R (top left); BGAP is an antagonist on D2R (top right); wavelength dependence on the deactivation of BGAP (bottom).

3.2.3.4 Maleimide-Azobenzene-Dopamine (MADA)

Although PPHT is a DAR agonist, MAP behaved either as an inverse agonist or as an antagonist depending on the attachment site. In order to create a photoswitchable tethered DAR agonist we changed our initial strategy and attached the azobenzene to the natural ligand dopamine. We were confident that the substituent on the primary amine would be tolerated as many DAR agonists contain secondary amines. Even though we knew that catechols are prone to oxidation we sought agonism might benefit from this moiety.⁸⁹⁻⁹⁰ The synthesis of maleimide azobenzene dopamine (MADA, **3.19**) is depicted in Scheme 3.4.





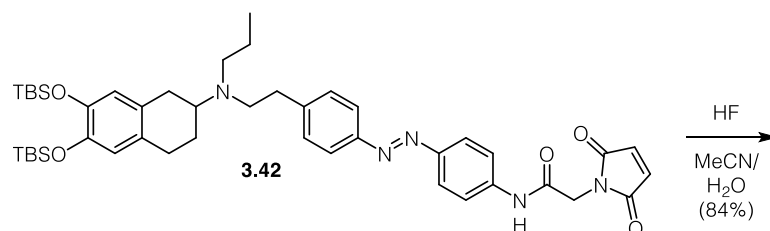
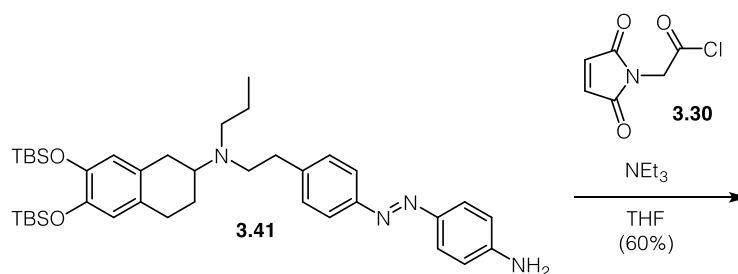
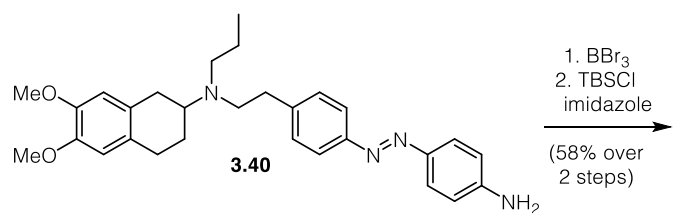
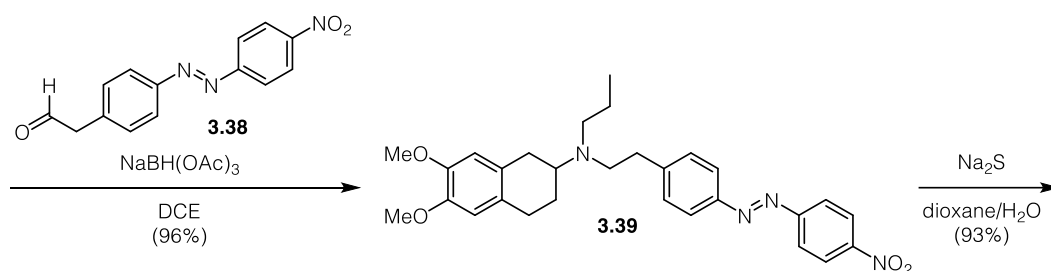
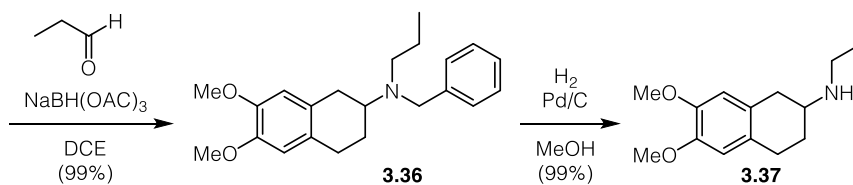
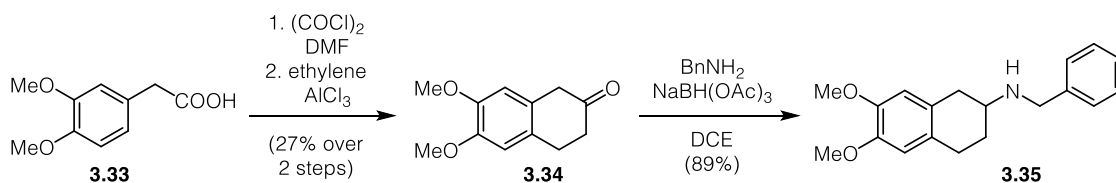
SCHEME 3.4: Synthesis of MADA (**3.19**).

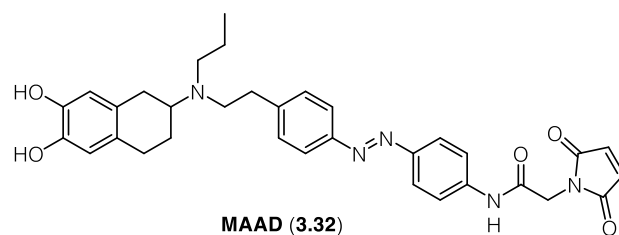
The synthesis commences with amide coupling of homoveratrylamine (**3.20**) and 4-nitrophenylacetic acid (**3.21**). Reduction of the amide using DMS borane and subsequent Boc-protection gave nitrobenzene **3.24** in good yields. Reduction of the aromatic nitro group under heterogenic hydrogenation conditions, followed by Baeyer-Mills coupling with 1-nitro-4-nitrosobenzene (**3.26**) yielded azobenzene **3.27**. The nitro group was then chemoselectively reduced utilizing Na_2S as reductant. The free catechol moiety, which was obtained upon demethylation using BBr_3 , turned out to be unstable under a variety of conditions. Boc-protection of the secondary amine followed by reprotection of the catechol as TBS-ethers afforded aniline **3.29**. Amide bond formation with acid chloride **3.30**⁹⁴ gave access to silyl ether **3.31**. Global deprotection using aqueous HF smoothly yielded **3.19**.

MADA was then sent to Dr. Prashant Donthamsetti from the Isacoff lab at UC Berkeley, where it is currently under investigation for its biological properties.

3.2.3.5 Maleimide-Azobenzene-ADTN (MAAD)

As MAP was not showing any agonistic effects, we were interested to see if we could design a photoswitchable tethered agonist based on the known DAR agonist ADTN.⁹⁵ The molecule shares similarities with MAP but contains the catechol moiety which we sought might be beneficial for agonism. The synthesis of maleimide-azobenzene-ADTN (MAAD **3.32**) is depicted in Scheme 3.5.





SCHEME 3.5: Synthesis of MAAD (**3.32**).

β -Tetralone **3.34** was obtained by acid chloride formation of 3,4-dimethoxyphenylacetic acid (**3.33**) and subsequent double Friedl-Crafts acylation of ethylene.⁹⁶ Reductive amination with benzylamine furnished secondary amine **3.35** which could then undergo a second reductive amination with propionaldehyde to yield tertiary amine **3.36**. Cleavage of the benzyl group furnished secondary amine **3.37** which could undergo a reductive amination with freshly prepared aldehyde **3.38** to give azobenzene **3.39** in good yield. Reduction of the aromatic nitro group under mild conditions accessed aniline **3.40** which, after protecting group swap, furnished silyl ether **3.41**. MAAD (**3.32**) was obtained after amide bond formation with acid chloride **3.30**⁹⁴ followed by global deprotection using aqueous HF. **3.32** proved to be air-sensitive in solution and was transformed into an unidentified oxidation product after being allowed to stand in MeOH for a few days. The biological properties of the compound are currently being investigated in the Isacoff lab at UC Berkeley by Dr. Prashant Donthamsetti.

3.2.4 Summary and outlook

In summary, we have synthesized and characterized the first photoswitchable ligand for a class A GPCR. To this end, we have developed four different photoswitchable DAR modulators based on the known DAR agonist PPHT. The synthesis is based on a three step sequence to install the amino tetralone core which can be employed into modular synthetic pathways to vary the substitution pattern on the azobenzene. The synthesis proved to be reliable and scalable and allows for the rapid installation of various tethering motifs at the eastern end of the molecule. DMS-PPHT could evoke currents in HEK293T cells overexpressing the DAR/GIRK system in response to blue light. While all diffusible molecules lacked selectivity, we could overcome this issue by the addition of a tethering unit. MAP can directly be attached to the binding site of the receptor, carrying only a single point mutation. Depending on the tethering site, the molecule can either act as neutral antagonist or an inverse agonist. BGAP can be attached *via* a SNAP-TAG to the native molecule. When attached to D1R the molecule behaves as a partial agonist and as an antagonist on D2R.

As the PPHT derived tethered ligand MAP showed antagonistic activity or behaved as inverse agonists we additionally developed a route of the photoswitchable DA derivative MADA. The 11-step synthesis proved to be scalable and diversifiable with regard to many sides of the molecule. However, the biological properties of the molecule remain to be evaluated.

Furthermore, we developed a scalable 11-step synthesis of a photoswitchable derivative of the DAR agonist ADTN. The key β -tetralone **3.34** is formed by a nowadays rarely used method employing ethylene as a nucleophile. Changes in the substitution pattern of the molecule can be introduced at various steps, underlying the modularity of the synthetic plan. In the future we will evaluate the biological properties of the molecule in terms of DAR activation in response to light.

3.3 Muscarinic acetylcholine receptor (mAChR)

3.3.1 Introduction

3.3.1.1 Muscarinic acetylcholine receptor (mAChR)

Acetylcholine (ACh) is one of the most abundant neurotransmitter in the central nervous system (CNS) as well as in the peripheral nervous system (PNS).⁹⁷⁻⁹⁸ The effects of ACh are mediated by two classes of receptors, namely the nicotinic acetylcholine receptor (nAChR) and the muscarinic acetylcholine receptor (mAChR).⁹⁸ The nAChR belongs to the superfamily of pentameric ion-channels and is besides ACh also responsive to nicotine.⁹⁹ The mAChRs are responding to ACh and muscarine and are part of the large class of G-protein coupled receptors.¹⁰⁰ They are widely expressed in both the CNS and in the periphery and mediate a variety of physiological functions ranging from nervous functions such as arousal, memory and alertness to vegetative processes such as regulation of heart rate and cardiac output, blood pressure and temperature regulation.¹⁰¹ mAChRs can be divided into two classes based on their coupling to different G-proteins. M₁, M₃ and M₅ activate G_{q/11} and therefore predominantly activate phospholipase C (PLC) *via* their α -subunit.¹⁰¹⁻¹⁰² Activation of PLC leads to cleavage of phosphatidyl-inositol-4,5-biphosphate (PIP₂) to diacylglycerol (DAG) and inositol triphosphate (IP₃).

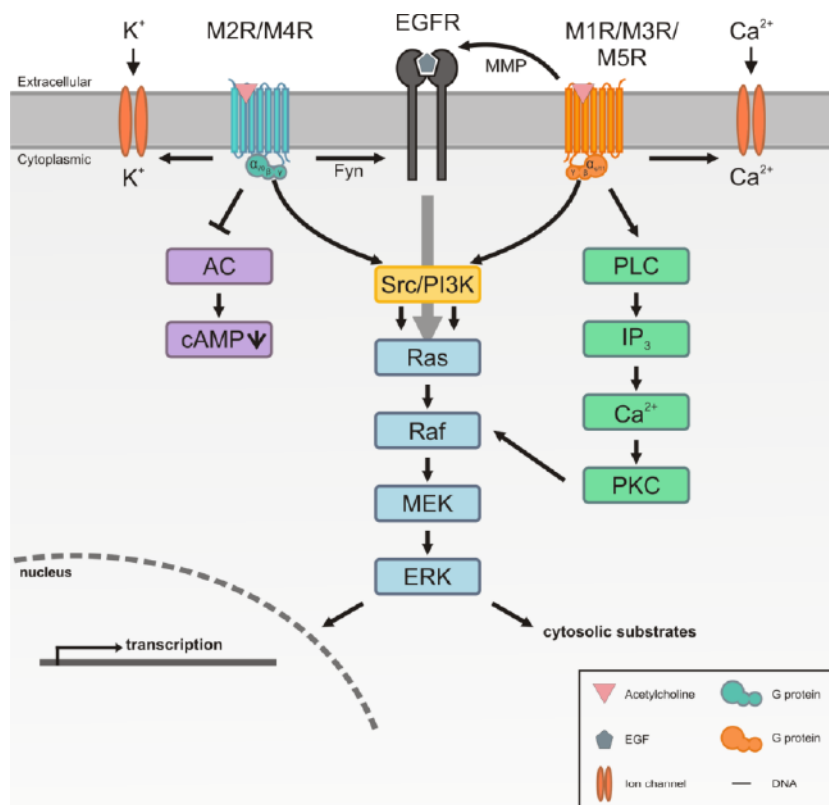


FIGURE 3.10: Canonical signalling pathways of mAChRs.

M₂ and M₄ preferentially couple to G_{i/o}, inhibit the adenylyl cyclase *via* the α -subunit and therefore reduce the intracellular level of cAMP. Furthermore, mAChRs can modulate the activity of either K⁺- or Ca²⁺-channels by means of the $\beta\gamma$ -subunit (Figure 3.10).¹⁰³⁻¹⁰⁵

M₁ and M₄ are predominantly expressed in the CNS while M₂ is mainly localized in the heart slowing the heart rate down to normal sinus rhythm.^{104, 106} M₃ was mostly found in the smooth muscle of blood vessels and in the lungs.¹⁰⁵

The genes encoding for mAChRs are highly compact and lack the abundance of introns.^{98, 107} The structure of the muscarinic receptor is highly conserved over the different subtypes. The high degree of sequence similarity in the transmembrane core of those receptors creates a significant challenge for the development of small molecule ligands which can discriminate between specific mAChRs.¹⁰⁴ Due to the close homology of the orthosteric binding site, most drugs target to non-classical (allosteric) binding sites of certain mAChR subtypes located in the less conserved extracellular loops of the receptor. The overall structure of all mAChRs is similar to that of other GPCRs revealing a network of hydrogen bonding interactions extending from the binding pocket to the cytoplasmic surface.¹⁰⁴ In mAChRs, this network is part of long aqueous channel leading into the membrane accommodating the ligand binding pocket.¹⁰⁴ The channel is extended beyond the binding pocket and separated from the cytoplasmic surface by a hydrophobic amino acid layer. Figure 3.11 shows the crystal structure of M2 bound to the orthosteric ligand QNB.

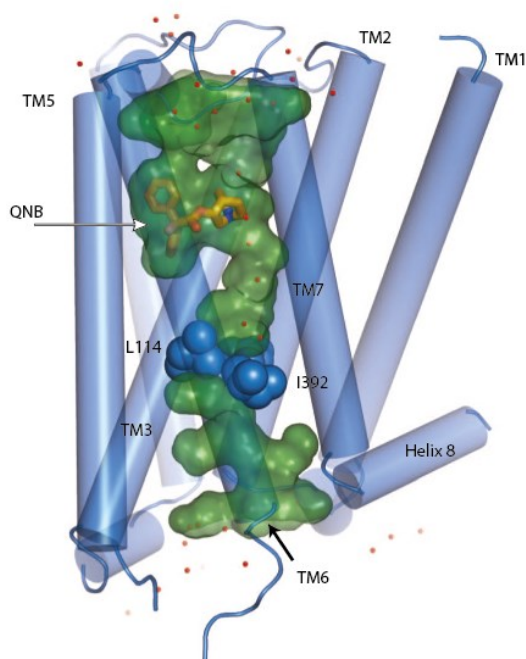


Figure 3.11: Crystal structure of M2 bound to QNB.¹⁰⁴

3.3.1.2 Iperoxo

In 1999, during the search for novel subtype-selective agonists of mAChRs Impicciatore and co-workers developed the muscarinic superagonist iperoxo (**3.42**)¹⁰⁸ (Figure 3.12). **3.42** provided an activity which is more than two orders of magnitude higher than the activity of the endogenous ligand acetylcholine even though it proved to be unable to differentiate between different receptor subtypes.¹⁰⁹ The molecular scaffold has later been incorporated into dualsteric hybrid agonist combining receptor subtype preference and signalling pathway selectivity.¹¹⁰⁻¹¹¹ Therefore, Mohr and co-workers showed that linkage of voluminous residues to the iperoxo skeleton does not severely compromise agonist efficacy.¹¹²

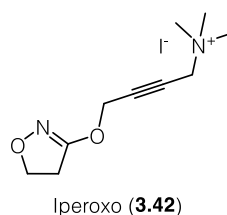


FIGURE 3.12: Molecular structure of iperoxo (**3.42**).

3.3.2 Project-outline

mAChRs are abundant in the CNS as well as in the PNS and therefore present an interesting target for the treatment of Alzheimer's disease and pain.⁹⁷ Furthermore, they are involved in controlling a variety of physiological functions.¹⁰⁰ While the structure of mAChRs was sufficiently determined by X-ray crystallography,¹⁰⁴⁻¹⁰⁶ the specific role of a receptor in an individual cell remains still not fully understood mainly due to the lack of subtype specific agonist. Spatio-temporally precision can be obtained by the use of a photoswitchable ligand which can undergo a configurational change upon light irradiation and therefore alter its ability to activate a certain receptor. In order to obtain such a light-dependent ligand we wanted to incorporate a photoswitchable azobenzene in the known mAChR superagonist iperoxo (**3.42**) (Figure 3.13).

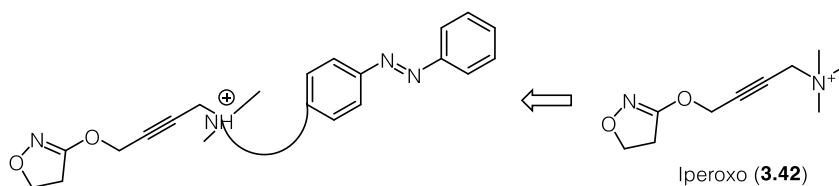


FIGURE 3.13: General design of photoswitchable mAChR agonist based on iperoxo (**3.42**).

The molecule can then be used as a tool to investigate mAChR signalling in a time resolved manner in a cell of interest. Furthermore, such a molecule could be of clinical interest in the development of artificial cardiac pacemaker.

3.2.3 Results and discussion

Iperoxo appeared to be a promising template for the design of a photoswitchable M2R agonist. From personal communications with Prof. Sasse we knew that the optimal length of a linker between the ammonium portion and the azobenzene should be around 6 to 8 methylene units. Based on this information, we decided to design our photoswitch as depicted in Figure 3.14. In order to get a more rapid access to the desired building blocks and facilitate the syntheses, we incorporated an additional oxygen atom next to the azobenzene.

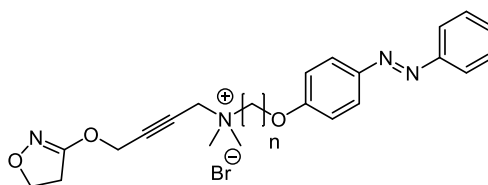
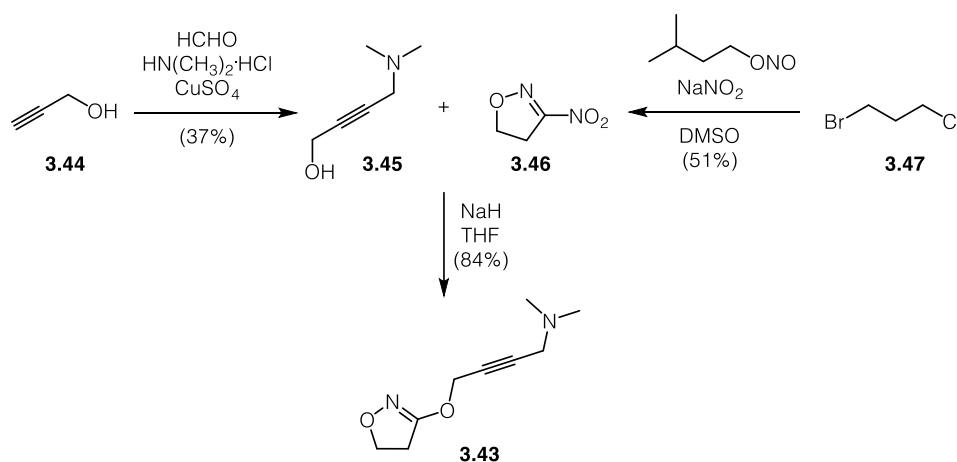


FIGURE 3.14: Generalized structure of azoiperoxo.

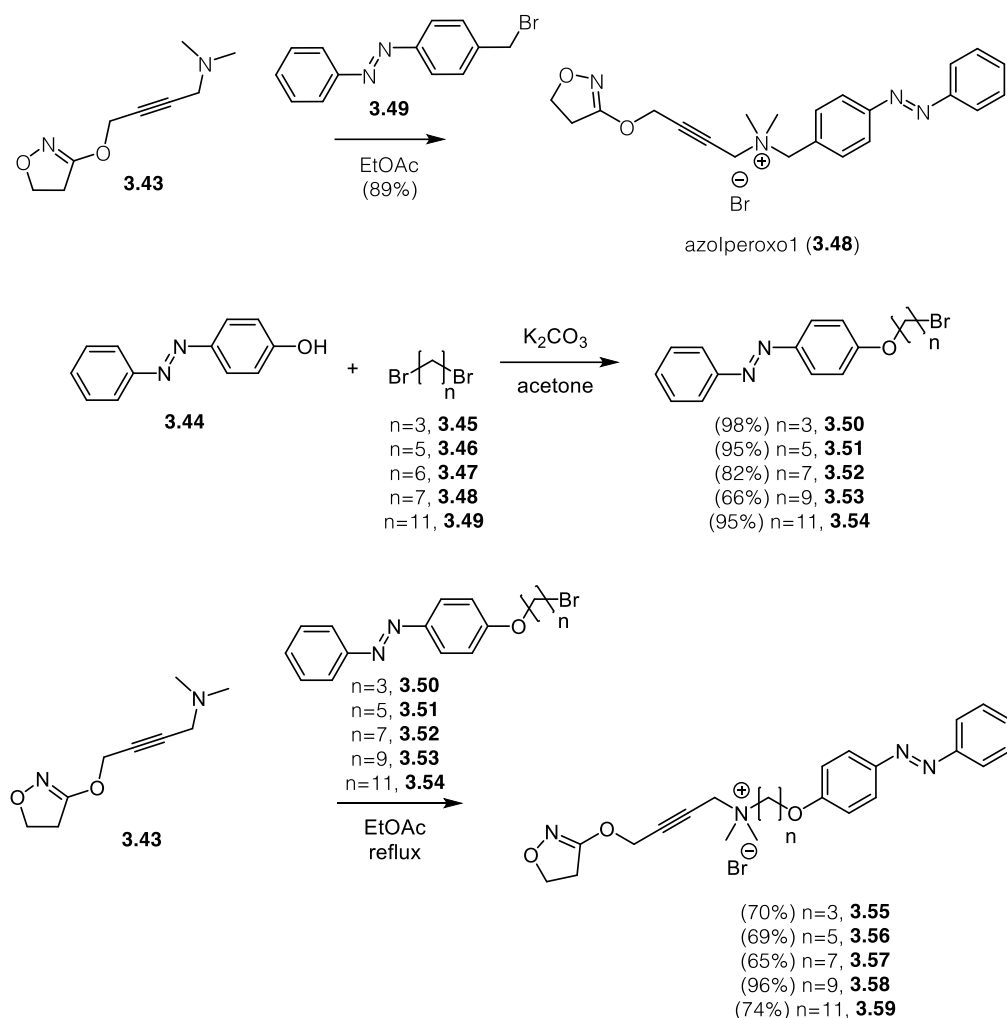
Scheme 3.6 shows the synthesis iperoxo base (**3.43**), the common synthetic precursor for all photoswitchable derivatives. Mannich reaction employing formaldehyde, dimethylamine and propargyl alcohol (**3.44**) accessed alcohol **3.45** in moderate yield. 2-isoxazoline **3.46** was accessed by reaction of 1-bromo-3-chloropropane (**3.47**) with isoamyl nitrite in the presence of NaNO_2 . Nucleophilic displacement then afforded



SCHEME 3.6: Synthesis of iperoxo base (**3.43**).

iperoxo base (**3.43**) in good yields.¹¹³

The first derivative, azoiperoxo1 (**3.48**) could be accessed by nucleophilic displacement of benzylic bromide **3.49** with **3.43**. Carbon linkers were attached to phenol **3.44** by reaction of the corresponding dibromides **3.45-3.49** and gave alkyl bromides **3.50-3.54** generally in good yields. Nucleophilic substitution of **3.50-3.54** with iperoxo base (**3.43**) gave access to azoiperoxos **3.55-3.59** (Scheme 3.7). This reaction proved to be satisfying to the operator as the product was the only insoluble part in this reaction and could easily be purified by washing the precipitate with EtOAc.



SCHEME 3.7: Synthesis of azoiperoxo1-11 (**3.55-3.59**).

3.55-3.59 showed similar UV/Vis-absorbance spectra and switching behaviour as expected for azobenzenes lacking auxochromic substituents. Exemplary spectra are depicted in Figure 3.15, illustrated on azoiperoxo7 (**3.57**) and azoiperoxo11 (**3.59**). All compounds could efficiently be converted from their *trans*- to their *cis*-conformer by irradiation with 370 nm and *vice versa* by 460 nm. Switching was independent on whether the experiment was performed in DMSO or aqueous buffer with the exception

of azoiperoxo11 (**3.59**). When the experiment was performed in aqueous buffer, precipitate formation was observed and the intensity of the absorption dropped significantly upon irradiation with 370 nm light. This result indicates a decreasing solubility of the *cis*-conformer in aqueous buffer. This effect should be general for all other compounds made as well, but exceeds the limit of solubility with the eleven membered carbon chain.

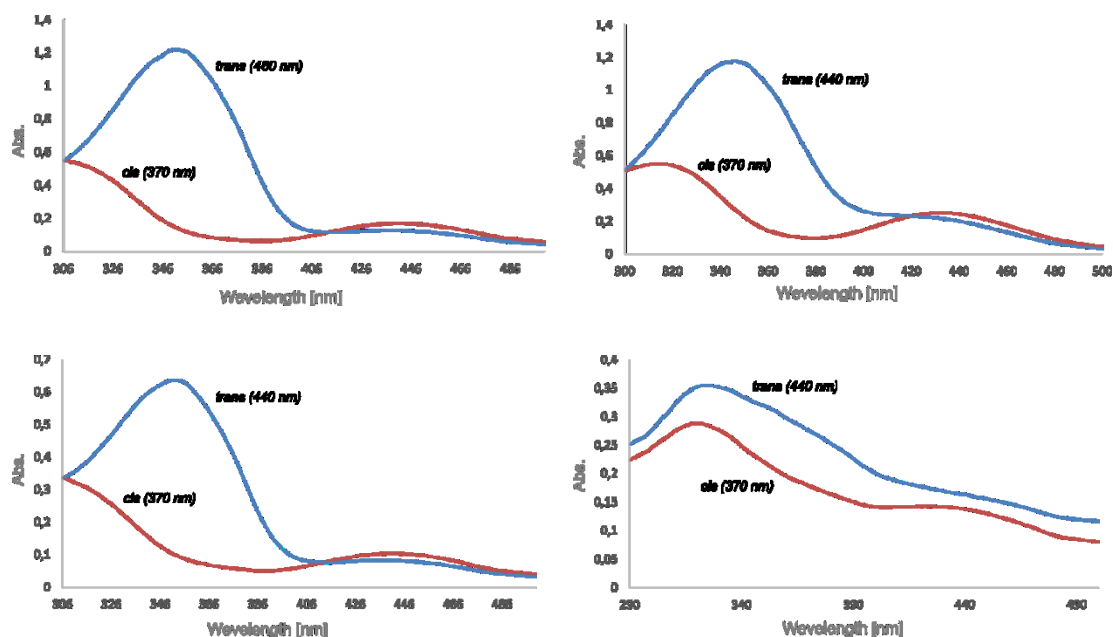


FIGURE 3.15: UV/Vis-spectra of azoiperoxo7 (**3.57**) in DMSO (top left) and buffer (top right) and azoiperoxo11 (**3.59**) in DMSO (bottom left) and aqueous buffer (bottom right).

In the next step, we were evaluating the ability of the compounds to activate M2Rs. These experiments were performed by Dr. Arunas Damijonaitis. To be able to observe GPCR activation with an electrophysiological readout, the experiments were conducted using HEK293T cells overexpressing M2 and GIRK. After activation of the trimeric G-protein, dissociation of the $\beta\gamma$ -unit leads to opening the ion-channel. When *cis*-azoiperoxo3 (**3.55**) was applied under constant illumination with 360 nm light, receptor activation could not be observed. Irradiation with 460 nm light evoked a current, indicating activation of M2 (Figure 3.16). The same observation was made, when azoiperoxo5 (**3.56**) was applied under the same experimental conditions, with the exception that the evoked photocurrent became larger and therefore showed that **3.56** is a more effective activator of M2. Both experiments were conducted using a concentration of 10 μ M of the photoswitchable agonist. The activation was even more sufficient when azoiperoxo7 (**3.57**) was applied to the same experimental conditions proving the influence of linker (data not shown).

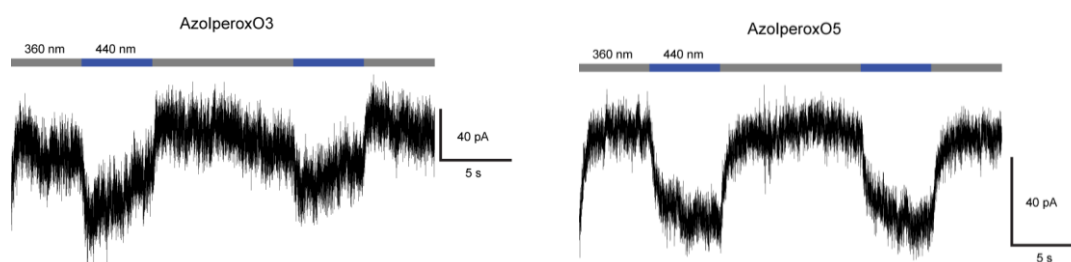


FIGURE 3.16: **3.55** (left) and **3.56** (right) act as a *trans*-agonist on M2Rs.

Like the parental molecule our compounds could activate M2 in the M2 GIRK assay. Nevertheless, the concentrations needed for the activation were significantly higher. We then sent azoiperoxo7 (**3.57**) to Prof. Philipp Sasse at the university of Bonn who performed *ex vivo* experiments in Langendorff preparations (Figure 3.17).

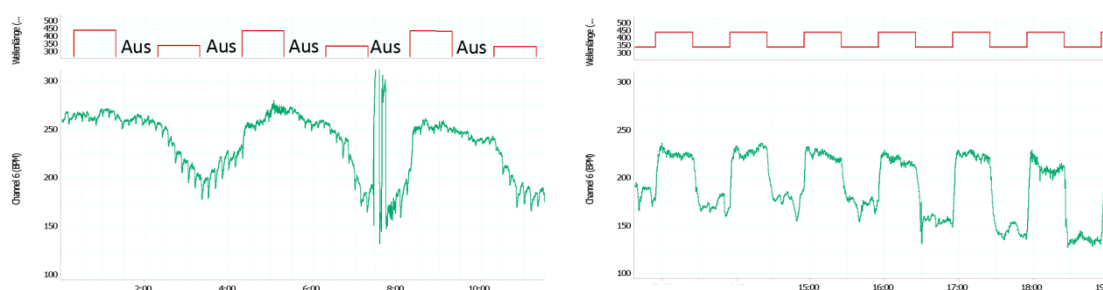


FIGURE 3.17: The application of **3.57** enables the light-dependent modulation of the heart rate in Langendorff preparations.

The application of **3.57** (50 nM) led to intense cardiac arrhythmia with av-blocks and a slow heart rate which was not photo-tunable by irradiation with either 360 nm or 440 nm light. Nevertheless, after washing for approximately 10 min, the sinus rhythm was restored and it became possible to modulate the heart rate by irradiation with light. Illumination with 360 nm light slowed down the heart beat while illumination with 440 nm restored the heart.

Although these results appeared promising, they raised several questions. Application of the compound led to a massive effect which was not photo-tunable and, after wash-out, the desired effect was observed. This observation might either propose that **3.57** is highly potent and the initially applied concentration was reduced to an optimal range after wash-out, or that the sample has been contaminated and this contamination causes serious side effects. In the initial patch-clamp experiments, concentrations in the μM range and illumination with 460 nm light were necessary to sufficiently activate the receptor, while nM concentrations were sufficient in Langendorff-preparations and activation occurred upon irradiation with 360 nm light. This contrast might hardly be

explained by the different assays used and the different origins of the receptors. Nevertheless, it might be plausible that **3.57** is less potent on M2 but more effective on an unknown receptor which is responsible for the change in heart rhythm observed in the Langendorff experiments.

3.3.4 Summary and outlook

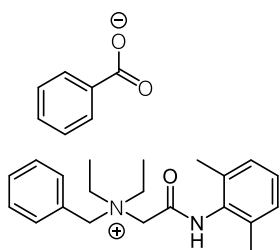
In conclusion, we have developed a photoswitchable M2R agonist based on the known M2R superagonist iperoxo and prepared six derivatives thereof. These derivatives differ in the carbon spacer length between the pharmacophore and the photoswitchable moiety. We could demonstrate that ligand efficiency depends on the length of the spacer. In addition, we evaluated the photophysical and biological properties of the synthesized molecules. Prof. Sasse showed that **3.57**, when being applied to Langendorff-preparations, has an effect on the heart rate, which can be modulated with 360 nm and 440 nm light. However, the exact origin of this effect still has to be investigated.

3.4 TAS2R

3.4.1 Introduction

The evaluation of nutritional value or potential toxicity of food prior to ingestion is essential for mammals.¹¹⁴ The detection of relevant food components is mediated by five basic taste qualities, sweet, sour, salty, umami and bitter.¹¹⁵ Although no clear correlation between bitterness and toxicity has yet been established, it is generally believed that bitter taste prevents mammals from poisoning.¹¹⁶ The gene family of human taste receptors (hTAS2Rs) consists of approximately 25 members belonging to the superfamily of G-protein coupled receptors (GPCRs).¹¹⁶⁻¹¹⁷ TAS2Rs are predominantly expressed in the oral cavity but can also be found in the urethra as this presents another potential entry for bacteria and harmful substances.¹¹⁸ TAS2Rs are activating gustducin, a G-protein found in taste receptor cells.¹¹⁷ Dissociation of the α -subunit leads to activation of a phosphodiesterase (PDE) and therefore to a decrease in cNMP (cyclic nucleotide) level. The $\beta\gamma$ -subunit mediates an increase in the levels of inositol triphosphate (IP₃) and diacylglycerol (DAG).¹¹⁷

Denatonium (**3.60**) is the most bitter chemical compound known and was discovered by J. R. Smith in 1958 during the search for local anesthetics (Figure 3.18). As the benzoate salt, it provides a bitterness threshold of 0.05 ppm. It is used to denature alcohol and harmful liquids.¹¹⁹



denatonium benzoate (**3.60**)

FIGURE 3.18: Structure of denatonium benzoate (**3.60**).

3.4.2 Project outline

One of the important questions in taste research remains how thousands of structurally diverse compounds are detected by only 25 receptors of the human TAS2R family.¹¹⁶⁻¹¹⁷ While some receptor subtypes recognise only a few agonists, other are more promiscuous.¹¹⁶ This contrariness proposes a complementary interaction of the receptors. We wanted to develop a photoswitchable TAS2R agonist in order to be able to study receptor activation in a spatio-temporal manner. Therefore, we wanted to incorporate an azobenzene moiety into the known TAS2R agonist denatonium (**3.60**).

3.4.3 Results and discussion

We chose denatonium as a template to develop a photoswitchable TAS2R agonist. The molecule contains two aromatic rings and therefore two possible sites for the extension to an azobenzene (Figure 3.19). Because we did not know at which side the azobenzene would be tolerated by the receptor, we decided to evaluate both possibilities.

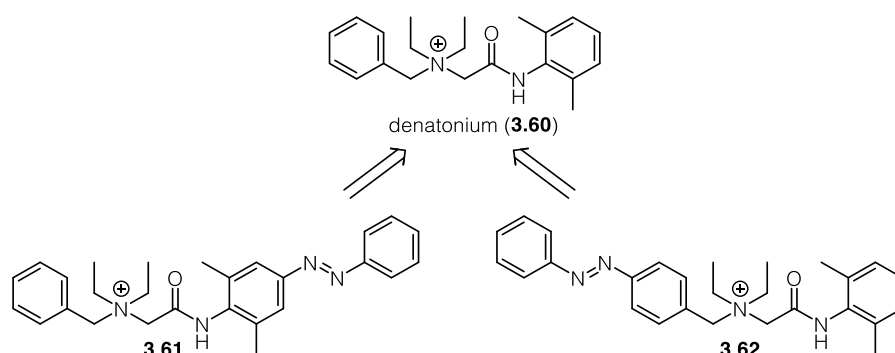
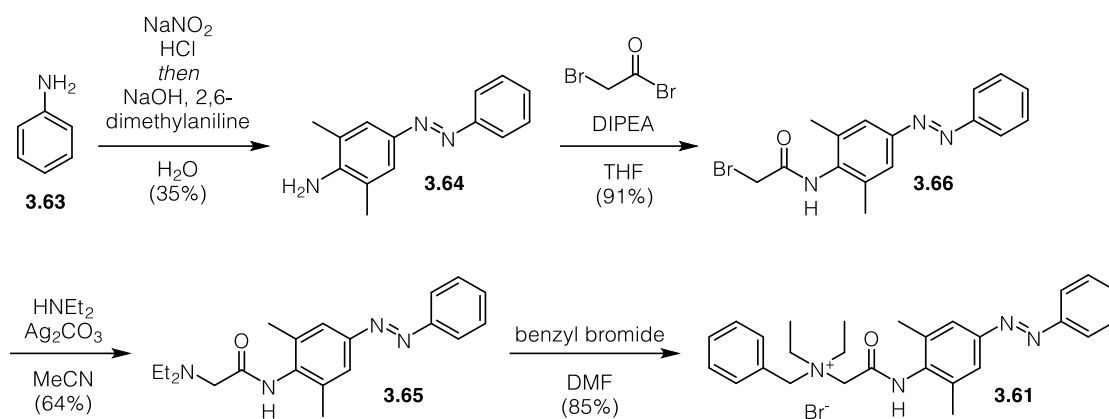


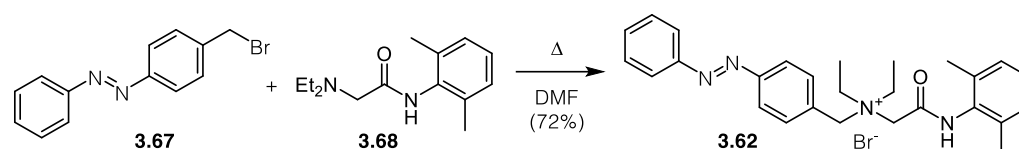
FIGURE 3.19: Azologization of denatonium (**3.60**).

The synthesis of **3.61** is depicted in Scheme 3.8. Diazonium ion formation of aniline (**3.63**) followed by subsequent trapping with 2,6-dimethylaniline furnished azobenzene **3.64** in moderate yield. Diethylamine **3.65** was obtained after acylation with bromoacetyl bromide followed by nucleophilic displacement with diethylamine. Formation of the quaternary ammonium ion using benzylbromide accessed the desired product in good yield.



SCHEME 3.8: Synthesis of **3.61**.

The synthesis of **3.62** could be accomplished by nucleophilic displacement of benzyl bromide **3.67** with lidocaine (**3.68**) (Scheme 3.9).



SCHEME 3.9: Synthesis of **3.62**.

With both compounds in hand, we went on to investigate the photophysical properties of the molecules. Both molecules had similar photophysical properties. The exemplary UV/Vis-spectra of **3.62** is shown in Figure 3.20. Upon irradiation with 360 nm light, **3.62** could efficiently be converted from its *trans*- to its *cis*-conformer and *vice versa* upon irradiation with 420 nm light. Additionally, the compound was sufficiently bistable in the dark as no change in the absorption spectrum could be observed after 30 min.

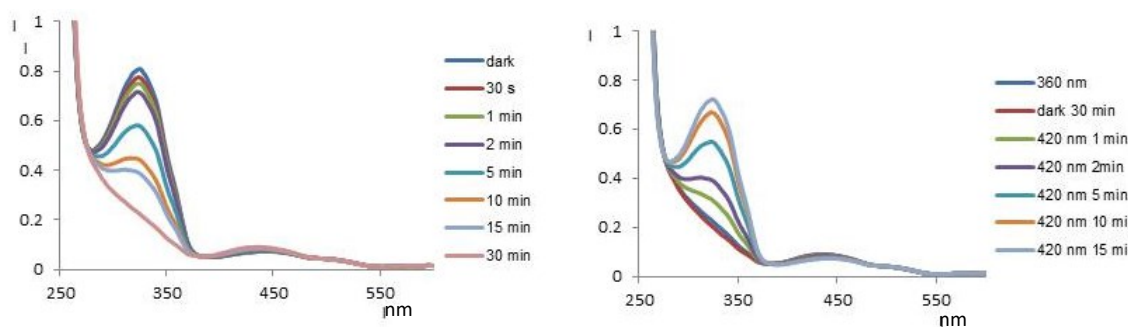


FIGURE 3.20: UV/Vis-spectra of **3.62** after irradiation with 360 nm light (left) and after subsequent irradiation with 420 nm light (right).

Both compounds were sent to Dr. Maik Behrens at the German Institute of Human Nutrition. Preliminary results (data not shown) indicate that both compounds are able to activate TAS2Rs and that the *cis*-isomer is less potent in activating the receptor.

3.4.4 Summary and outlook

In conclusion we have developed a photoswitchable TAS2R agonist based on the known TAS2R agonist denatonium. Two derivatives differing in the position of the attached azobenzene have been synthesized. Both compounds have been fully characterized regarding their photophysical properties. Preliminary data recorded by Dr. Maik Behrens indicate that both molecules possess agonistic behaviour on TAS2Rs and that the irradiated form exhibits less activity. Future experiments have to confirm these results and validate the data. These molecules could then be used as a tool to confirm the orientation of mobile groups inside the receptor.

Chapter IV

Development of Photochromic Ion Channel Blockers

4.1 Introduction

The detection and transmission of noxious stimuli from the periphery to the brain or within local circuits is essential for the protection from injuries.¹²⁰ Chemical, mechanical or thermal stimuli can activate specific receptors and ion channels in peripheral nerve endings resulting in the initiation of action potentials which propagate along axons of primary afferent pain fibres and trigger activation of second-order neurons by the release of neurotransmitters such as glutamate.¹²¹ Action potential initiation and propagation is mediated by voltage-gated ion channels (VGICs).¹²³⁻¹²⁴ Inflammation or nerve injury can cause maladaptive changes in the expression pattern of VGICs resulting in hyperexcitability of afferent pain-signaling neurons.¹²¹ Therefore VGICs present a promising target for the treatment of pathogenic pain.¹²² There are three main classes of VGICs, which can be grouped according to their specificity for a certain type of ion they conduct, e.g. Na⁺, K⁺ and Ca²⁺.¹²³⁻¹²⁴ Na_v channels are responsible for the initiation of the action potential whereas K_v channels are regulators of resting membrane potential and action potential repolarization. Ca_v-channels are important for the triggering of intracellular signalling pathways and heart contraction. The precisely timed opening and closing of Na_v- and K_v-channels is represented by the unique shape of action potentials. If the resting membrane potential, due to external stimuli, e.g. neurotransmitter release, reaches a certain threshold, Na_v-channels open followed by Na⁺ ion influx, which leads to the characteristic upstroke of the action potential. This is immediately followed by the opening of K_v-channels and a K⁺-ions efflux to repolarize the cell to the resting membrane potential levels.¹²³⁻¹²⁴

Na_v-channels (Figure 4.1) consist of an α -subunit of approximately 260 kDa associated with auxiliary β -subunits.¹²⁵ The α -subunit comprises four homologous domains (I-IV) each containing six transmembrane α -helices (S1-S6) and an additional pore loop located between the S5 and S6 segments. The S5 and S6 segments of four domains form the pore module whereas the voltage-sensing domains are constructed by the S1-S4 segments. The outer, narrow entry to the pore is sized by the pore loops forming the Na⁺-ion selectivity filter whereas the inner, wider exit of the pore is lined by the S5 and S6 segments. Channel activation in response to depolarization of the membrane is initiated by the positively charged amino acid residues (gating charges) in the S4 segments of each domain.¹²⁶

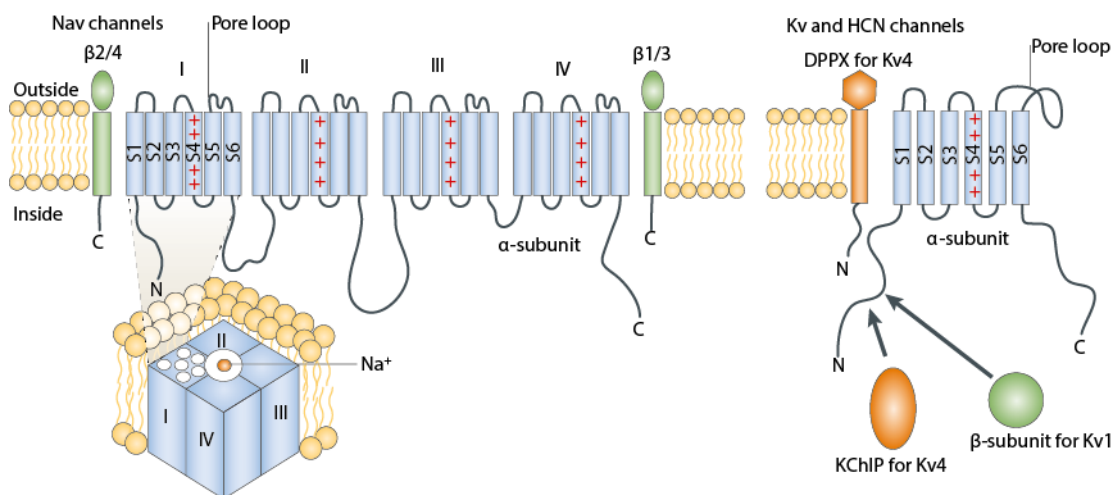


FIGURE 4.1: General structural topology of Na_V⁺- and K_V⁺- channels.¹²²

During sustained depolarization of the membrane, the intracellular loop between III and IV folds into the channel structure blocking the pore from the inside.¹²⁵ The kinetics and the voltage dependence of the channel gating are modified by the β -subunits. K_V- and Ca_V-channels, share common topology and function. Na_V-channels consist of a single α -subunit bearing four transmembrane domains which are expressed as a contiguous polypeptide. The family of mammalian Na_V-channels consist of the members Na_V1.1–Na_V1.9 and a designated Na_x encoded by ten different genes. In contrast, K_V-channels are encoded by approximately 70 genes grouped into 12 families, K_V1–K_V12 depending on their α -subunit.^{122, 125} K_V-channel diversity is further broadened by the assembly of different subunits into homo- or heterotetrameric structures.

Characterized by conduction behaviour at different voltage potentials, Na_v channels can exist either in open, resting or inactivated state.¹²¹ At resting membrane potential (approximately –70 mV), the channel is in a non-conducting closed state. When the cell becomes depolarized i.e. the membrane potential increases to reach a certain threshold, (approximately –40 mV), the pore is pulled open by an outward movement of the voltage sensing units (S1-S4). Subsequently, the channel is intrinsically converted into a non-conductive inactive state. To reactivate the channel, i.e. relieve the inactivation block, the membrane potential needs to return to resting levels.¹²⁶⁻¹²⁷

It is not surprising that Na_V-channels, as fundamental components of action potentials, are targets of various natural toxins derived from terrestrial and marine organisms such as spiders, scorpion or snakes.¹²⁸ These aim at paralysing their prey in an effective and fast way (Figure 4.2).

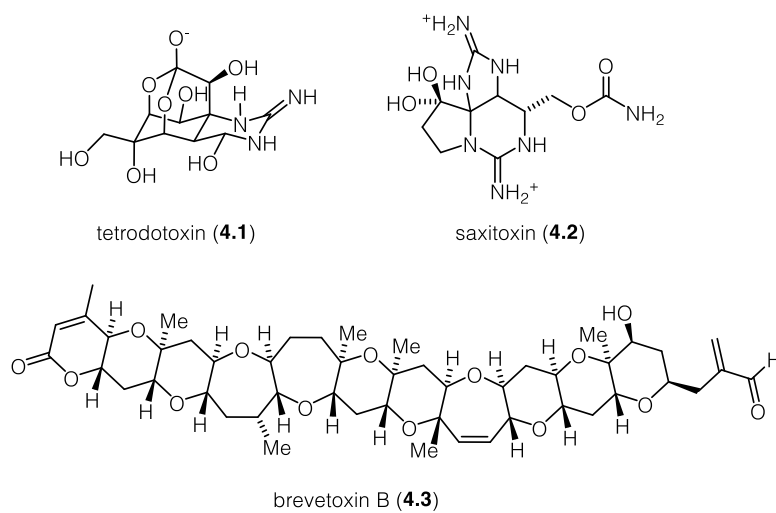


FIGURE 4.2: Selected toxins targeting Nav channels.

4.2 Project outline

Voltage-gated sodium channels are involved in action potential firing in excitable cells, displaying them as potential targets for the pharmacological treatment of pain.^{123, 128-129} Pain disorders are frequently associated with a malfunction in Na_v-channels resulting in a gain of function such as inherited erythromelalgia, paroxysmal extreme pain disorder or congenital insensitivity to pain.¹²⁰ Na_v1.7, Na_v1.8 and Na_v1.9 are of special interest as they are preferentially expressed in peripheral sensory neurons of the trigeminal and dorsal root ganglia (DRG), but are not essential for the function of CNS neurons or cardiac myocytes.¹³⁰ Therefore a photoswitchable channel blocker would enable the light-dependent control of ion-flux through Na_v-channels and undoubtedly become a valuable tool in order to study the role of Na_v-channels in pain sensation.

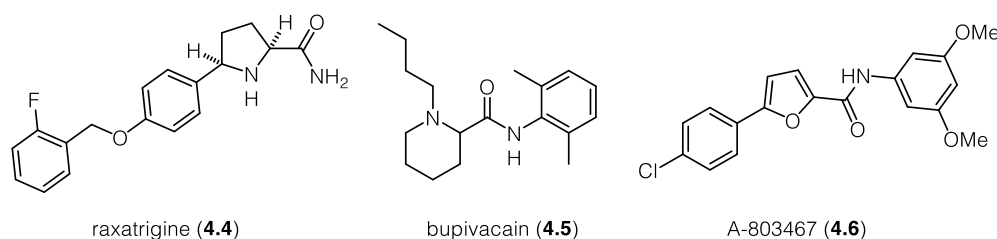


FIGURE 4.3: Structure of raxatrigine (4.4), bupivacaine (4.5) and A-803467 (4.6).

The aim of this project was to incorporate a light switchable azobenzene moiety into the known small molecule Na_v-channel blockers raxatrigine (4.4), bupivacaine (4.5) and A-803467 (4.6) (Figure 4.3) without disrupting the overall structure of the compound. These blockers have in common that they all are bearing azologable moieties, i.e. aryl amides which can be conservatively substituted with an azobenzene. These azologs can be switched between their *cis* and *trans* configuration using light. This structural change alters then the efficacy towards their target structure (Na_v-channels). Ultimately, we evaluated their ability to control ion-flux through Na_v- and K_v-channels in a light manner using cell cultures overexpressing these channels.

4.3 A-803467

The TTX-resistant Nav1.8 channel is the primary contributor of Na⁺-flux during the upstroke of the action potential in DRG neurons.¹³¹⁻¹³² Altered expression levels can lead to faster recovery from the inactivation state and a shift in the voltage dependence of activation to a more hyperpolarized potential, producing hyperexcitability of DRG neurons. Icagen and Abbott developed a small molecule inhibitor A-803467 (**4.6**) which showed selectivity for Nav1.8 over other Nav_v-channels.¹³³ The molecule comprises a largely expanded π -system containing a diaryl amide bond. This structural motif can be displaced by a diazene unit incorporating an azobenzene to make the molecule photoswitchable. Therefore, we chose **4.6** as a template for the development of a photoswitchable Nav1.8 inhibitor (**4.7**) (Figure 4.4).

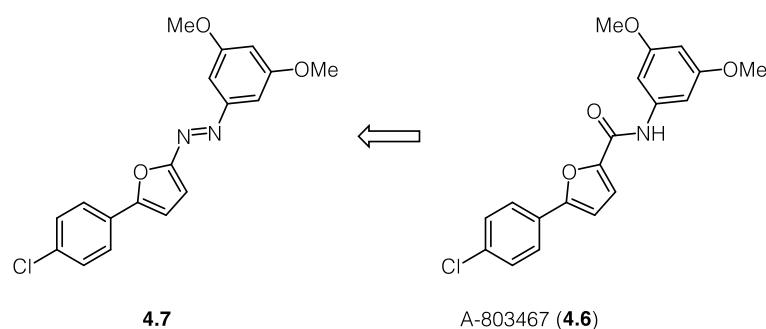
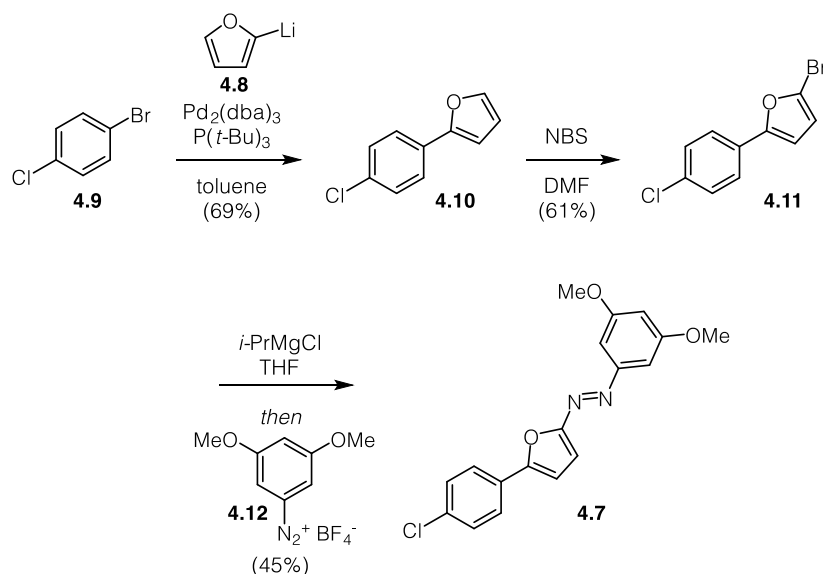


FIGURE 4.4: Azologization of A-803467 (**4.6**).

Pd-catalyzed cross coupling of lithiated furan (**4.8**) with 4-chlorobromobenzene (**4.9**) using Feringa's method¹³⁴ gave biaryl **4.10** which could further be brominated to yield



SCHEME 4.1: Synthesis of azo-A-803467 (**4.7**).

4.11. Azobenzene **4.7** was obtained after halogen magnesium exchange using *i*-PrMgCl·LiCl followed by trapping of diazonium salt **4.12** (Scheme 4.1).

The UV/Vis spectra of **4.7** revealed bathochromic shift of the absorption maximum, compared to an unsubstituted azobenzene, to approximately 415 nm. Irradiation with 420 nm light sufficiently converted *trans* **4.7** to its *cis*-conformer. In the dark, the compound underwent fast thermal relaxation within seconds (Figure 4.5).

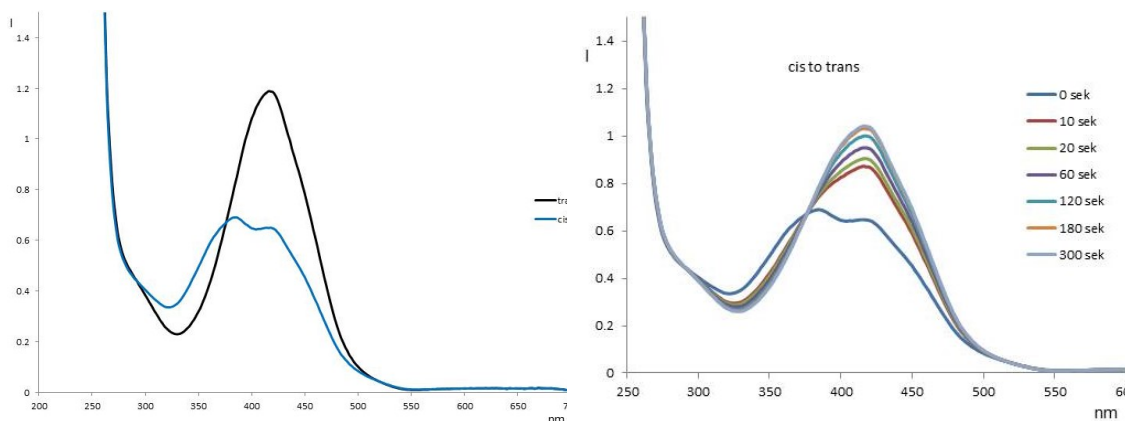


FIGURE 4.5: UV/Vis spectra of *trans* and *cis* **4.7** (left) and thermal relaxation of **4.7** (right).

Together with Dr. Andrea Brüggemann at Nanion we evaluated the biological properties of the compound on a SynchroPatch 768PE, which allows for the recording of electrical signal in theoretically 768 cells at a time. These experiments were conducted on cells stably expressing Nav1.8 channels. We could show that **4.7** was unable to reduce current flow after depolarization of the membrane with and without irradiation at 420 nm (data not shown).

4.4 Bupivacain

Bupivacain (**4.5**) is a local anaesthetic discovered in 1957 and is part of the world health organization's list of essential medicines.¹³⁵ **4.5** acts by blocking Na_V -channels but is also a potent inhibitor of K_V - and TREK-channels.¹³⁶⁻¹³⁹ Bupivacain contains an aryl amide linked to a piperidin ring. In order to render the molecule photoresponsive, we planned to extend the aromatic portion to an azobenzene (Figure 4.6).

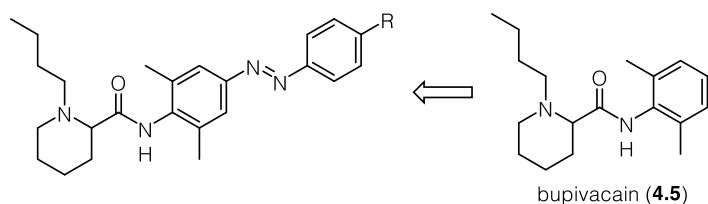
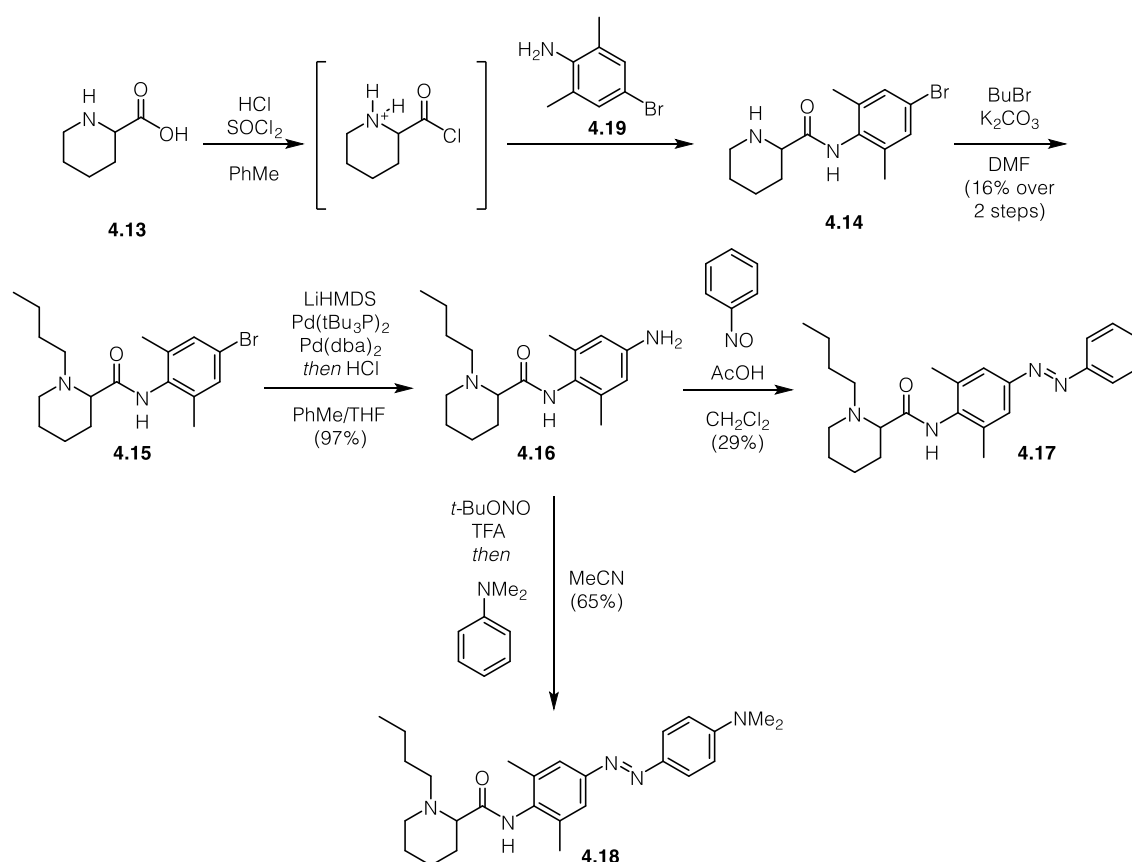


FIGURE 4.6: Azologization of bupivacain (**4.5**).

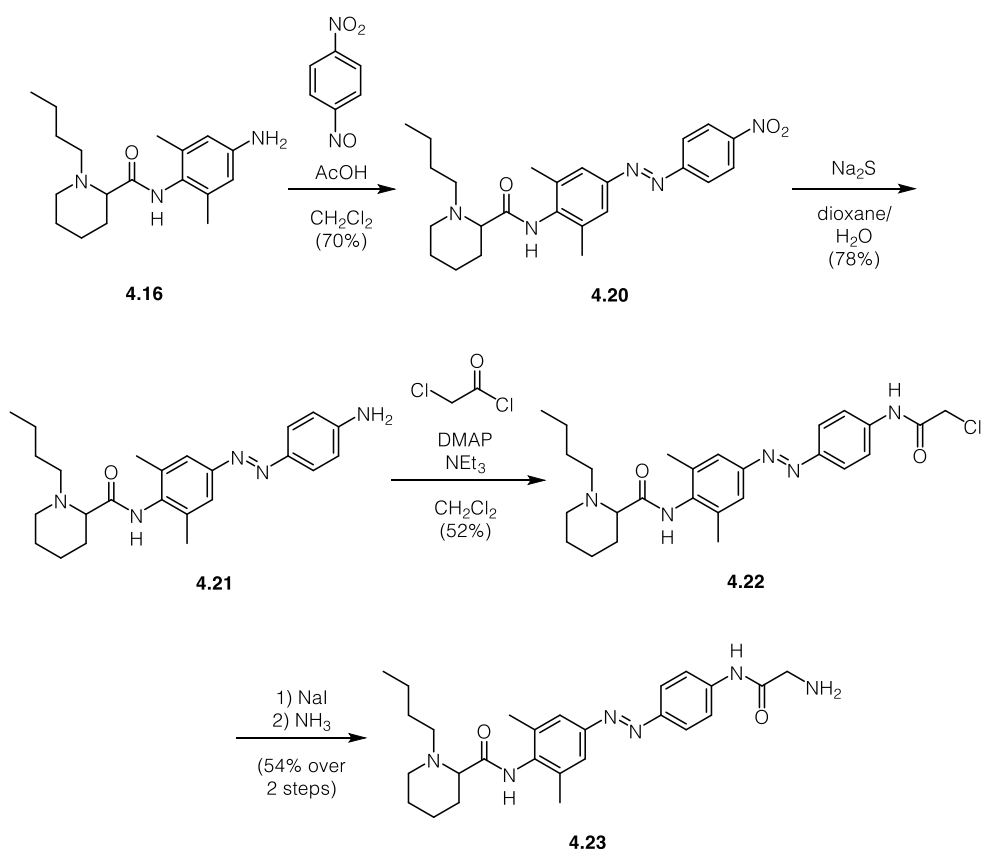
In situ protonation of homopropiline (**4.13**) followed by acid chloride formation and amide bond formation delivered amide **4.14** which was directly alkylated to give aryl bromide **4.15** in moderate yield. **4.15** then underwent Pd-catalyzed amination, using LiHMDS



SCHEME 4.2: Synthesis of **4.17** and **4.18**.

as a nucleophile, furnishing aniline **4.16** in good yields after deprotection of the disilazane. Azobenzene **4.17** was obtained from **4.16** by Baeyer-Mills coupling with nitrosobenzene in moderate yield. Aniline **4.16** could also be converted into dimethylaminoazobenzene **4.18** by azocoupling with dimethylaniline (Scheme 4.2).

Azobenzene **4.20** could be obtained from aniline **4.16** by Baeyer-Mills coupling with 4-nitrosobenzene. Reduction of the nitro group using sodium sulphide accessed aniline **4.21** in good yield which was then acetylated with chloroacetylchloride to furnish α -chloro amide **4.22**. Finkelstein reaction followed by nucleophilic displacement with ammonia accessed glycine derivative **4.23** (Scheme 4.3). Purification of **4.23** proved difficult as the molecule decomposed on silica but could be purified on C₁₈ silica.



SCHEME 4.3: Synthesis of **4.23**.

The UV/Vis-spectra of **4.17**, **4.18** and **4.23** show a gradual bathochromic shift of the $n \rightarrow \pi^*$ transition reflecting the increasing electron-donating character of the substituents in the 4-position of the azobenzene. Therefore, photoisomerization occurs at increasing wavelength and is in all cases fully reversibly. Half-lives of the thermal stability are decreasing and range from hours to seconds within this series (Figure 4.7).

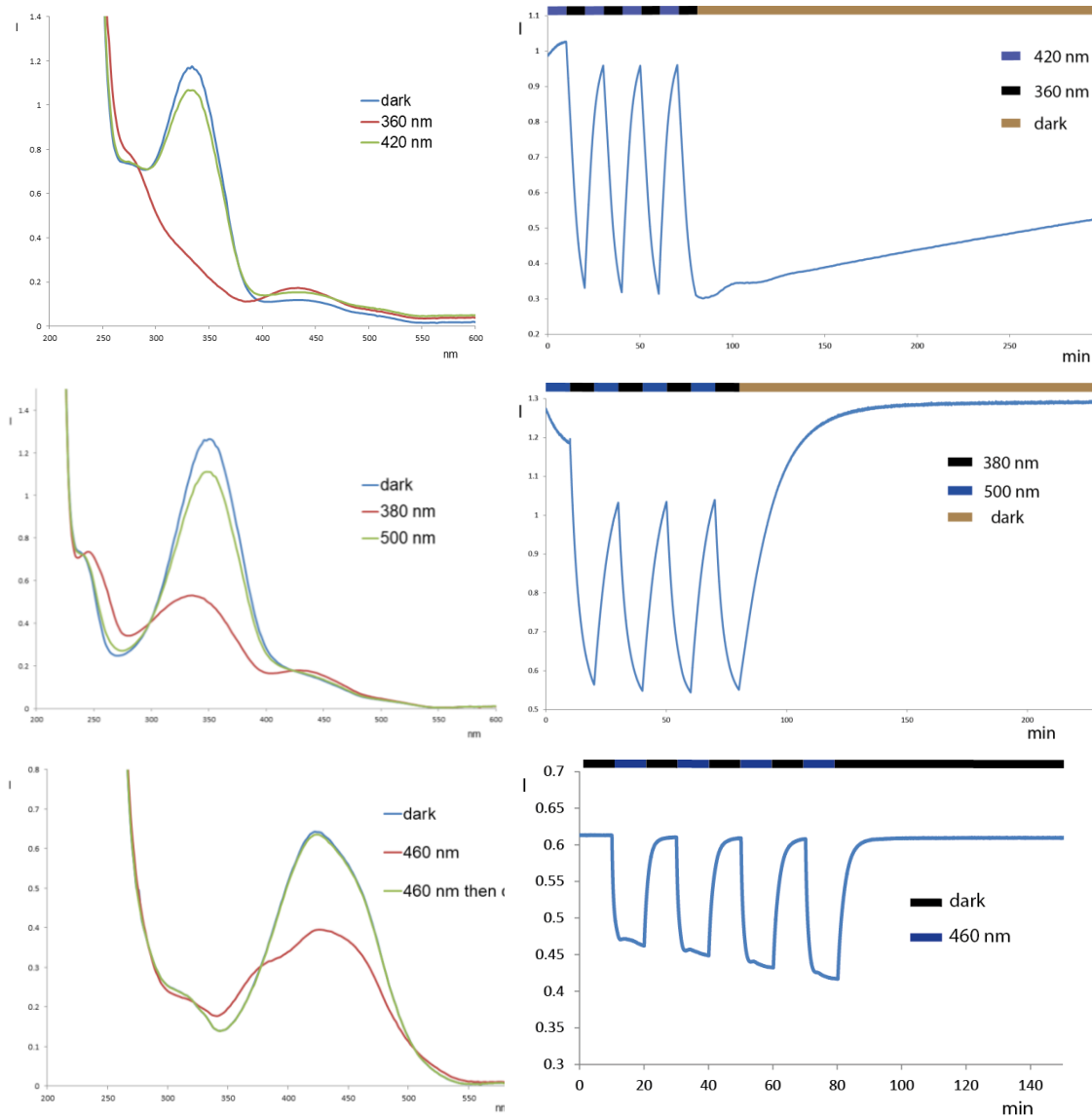


FIGURE 4.7: UV/Vis-spectra of **4.17** (top), **4.23** (middle) and **4.18** (bottom).

The effect of **4.17** on HEK293T cells overexpressing $K_v2.1$ and on mouse hippocampal CA1 neurons was then evaluated by Philipp Leippe and Dr. Martin Sumser. When **4.17** was applied under 360 nm illumination to HEK293T cells transiently overexpressing $K_v2.1$, potassium currents were slightly reduced, indicating that the *cis*-conformer has a small effect on these channels already. However, when applying irradiation with 420 nm light the K^+ -current was completely blocked and could be restored to previous levels using 360 nm. After washout of **4.17** currents returned to starting levels (Figure 4.8). In summary, we could effectively photosensitize K^+ -currents using **4.17**.

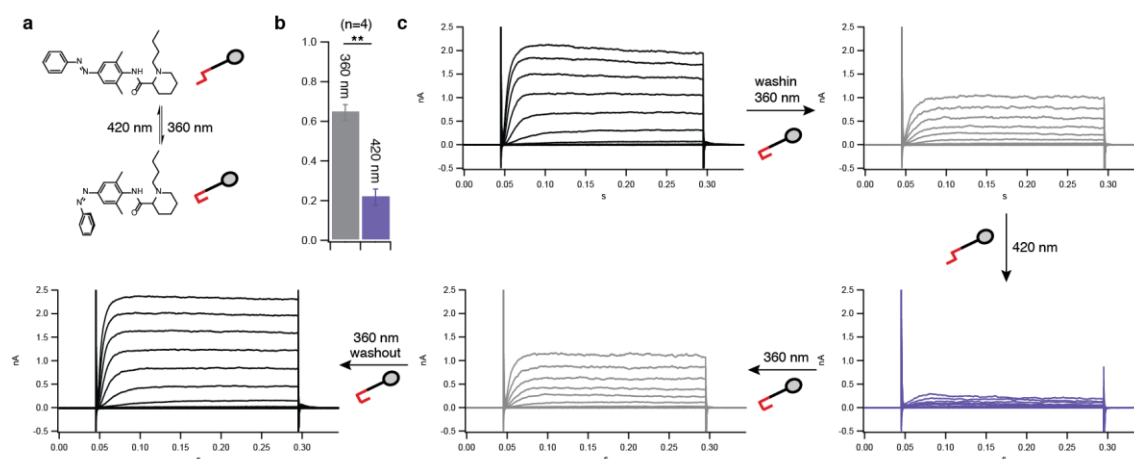


FIGURE 4.8: a) **4.17** reversibly isomerizes from *trans*- to *cis*- by illumination with UV-light and blue light respectively. b) $K_{v2.1}$ currents are blocked by **4.17** ($100 \mu\text{M}$) to $22\% \pm 4\%$ (blue light, *trans*) and $64\% \pm 4\%$ (UV light, *cis*) of initial current before application of the blocker. c) Currents are recorded before compound application followed by wash-in of **4.17** under UV-light irradiation. Irradiation with blue light leads to a channel block which is reversible under UV-light application. After wash-out the amplitude returns to its original value.

In hippocampal neurons action potentials, elicited through current injection, could be effectively blocked using **4.17** ($100 \mu\text{M}$) and 360 nm light illumination. Action potential firing could be restored upon irradiation with 420 nm (Figure 4.9). Noticeably, in this experimental setting the *cis*-conformer presents the active blocker. We then tested whether **4.17** shows the same logic when blocking intrinsic K_v^+ -channels in these neurons. We found that *cis* **4.17** is more potent in blocking K^+ -currents than *trans* **4.17** (Figure 4.9).

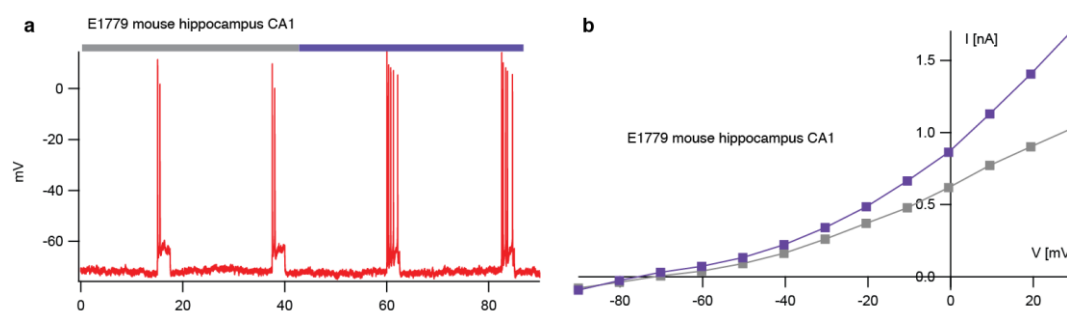


FIGURE 4.9: Effect of **4.17** ($100 \mu\text{M}$) on mouse hippocampal CA1 neurons. a) Action potentials are inhibited under UV-light illumination. b) Voltage-gate currents are blocked under UV-light irradiation.

4.5 Raxatrigine

CNV1014802 (raxatrigine **4.4**) is an oral state-dependent Nav^+ -channel blocker being developed by Convergence. **4.4** has completed Phase II trials for lumbosacral radiculopathy and entered Phase II trials for trigeminal neuralgia.¹⁴⁰⁻¹⁴³ It has been shown for $\text{Nav}1.7$ that **4.4** works in a state-dependent manner with a nine-fold shift between the resting state inhibition (IC_{50} 54 μM) and the open/inactive state inhibition (IC_{50} 6.3 μM) with a clear preference for the open/inactivated state.¹⁴⁰ Raxatrigine (**4.4**) consists of a disubstituted pyrrolidine and a methylene bridged diaryl ether. The latter motif offers an opportunity for the incorporation of an azobenzene into the molecule without any major changes in the overall shape of the molecule (Figure 4.10).

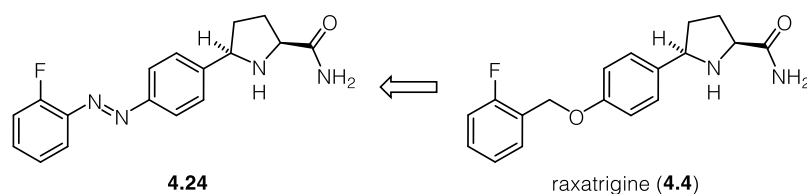
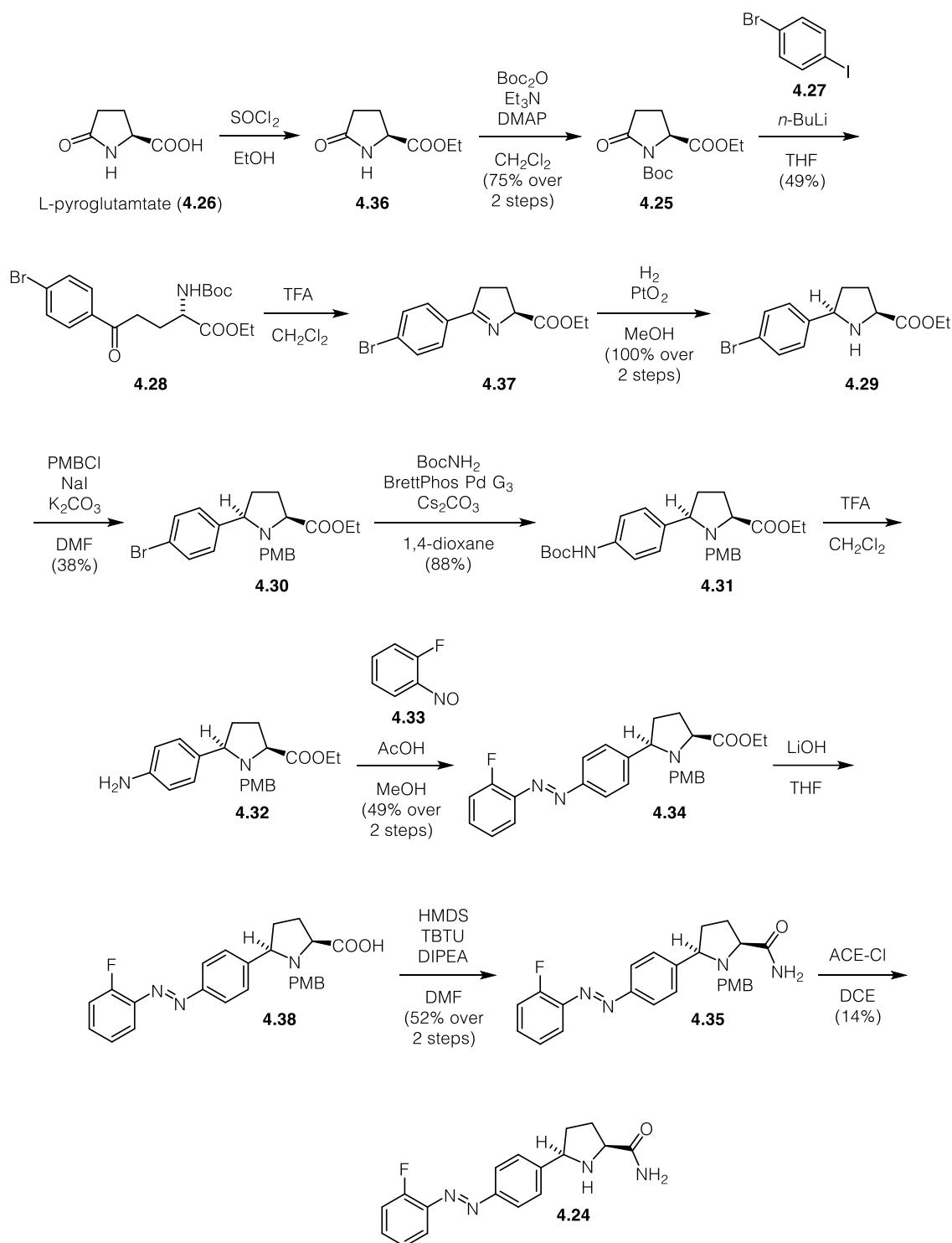


FIGURE 4.10: Azologization of raxatrigine (**4.24**).

The synthesis of a photoresponsive raxatrigine derivative is outlined in Scheme 4.4. Protection of the carboxylic acid as the ethyl ester followed by *N*-Boc protection of the amine allowed for the formation of lactam **4.25** from L-pyrroglutamate (**4.26**). Halogen metal exchange of 4-bromo-iodobenzene (**4.27**) with *n*-BuLi followed by reverse addition of **4.25** delivered ketone **4.28**. Boc-deprotection followed by intramolecular imide formation and stereoselective reduction using Adam's catalyst furnished pyrrolidine **4.29** as a single diastereoisomer. PMB protection of **4.29** under nucleophilic catalysis delivered aryl bromide **4.30** which then underwent Pd-catalyzed amidation under Buchwald's conditions to access carbamate **4.31** in good yield. Acid mediated deprotection of the Boc group liberated aniline **4.32** which was directly subjected to Baeyer-Mills coupling with nitrosobenzene **4.33** to furnish azobenzene **4.34**. Saponification of the ethyl ester followed by amide formation allowed for the formation of amide **4.35**. The final PMB-deprotection step proved rather difficult. Standard oxidative conditions resulted in low yields and the formation of several side products complicated the purification. Utilizing 1-chloroethyl chloroformate in the reaction could not significantly improve the yield but facilitated the removal of the generated side products.

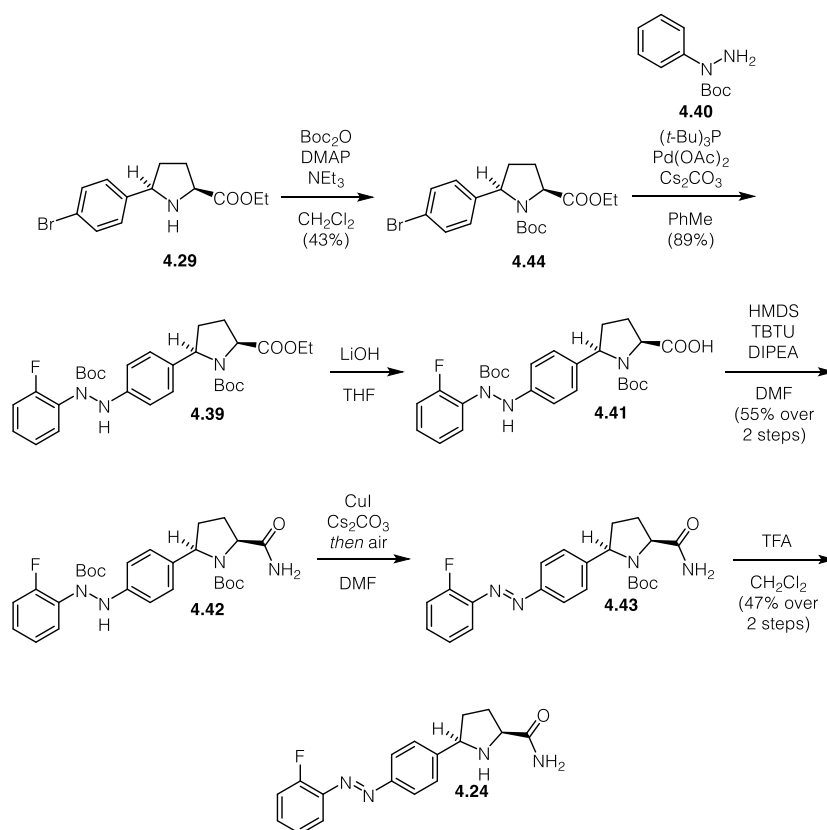


SCHEME 4.4: First generation synthesis of **4.24**.

The developed synthesis proved to be robust and scalable except for the final deprotection step. In order to get sufficient access to the desired molecule we decided to explore a second synthesis as depicted in Scheme 4.5.

Diphenylhydrazine **4.39** is derived from pyrrolidine **4.29** after Boc protection followed by Pd-catalyzed amination with phenylhydrazine **4.40**. Saponification of the ethyl ester

accessed carboxylic acid **4.41** which was directly converted into amide **4.42**. Regioselective deprotection of the Boc group followed by oxidation of the resulting phenylhydrazine allowed for the formation of azobenzene **4.43**. Further deprotection of the pyrrolidine under acidic conditions delivered **4.24**. The two-step deprotection sequence was necessary as the phenylhydrazine was not sufficiently freed under acidic conditions.



Furthermore, using a similar route, we synthesized the corresponding photoswitch containing the azobenzene in the 3-position (Figure 4.11).

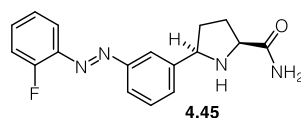


FIGURE 4.11: Structure of *meta*-substituted azobenzene **4.45**.

With the **4.24** in hand we examined the photophysical properties of the compound. **4.24** showed a maximum absorption for the $n \rightarrow \pi^*$ transition at 340 nm and was efficiently converted from its *trans*- to its *cis*-conformer by irradiation with 360 nm light and *vice versa* by 420 nm light. The compound could efficiently be switched over several cycles without any loss of activity (Figure 4.12). As **4.24** lacks any strong auxochromic groups,

the *cis*-configuration of the compound is sufficiently stable towards thermal relaxation ($T_{1/2} > 1$ h) and thus, the compound is considered bistable.

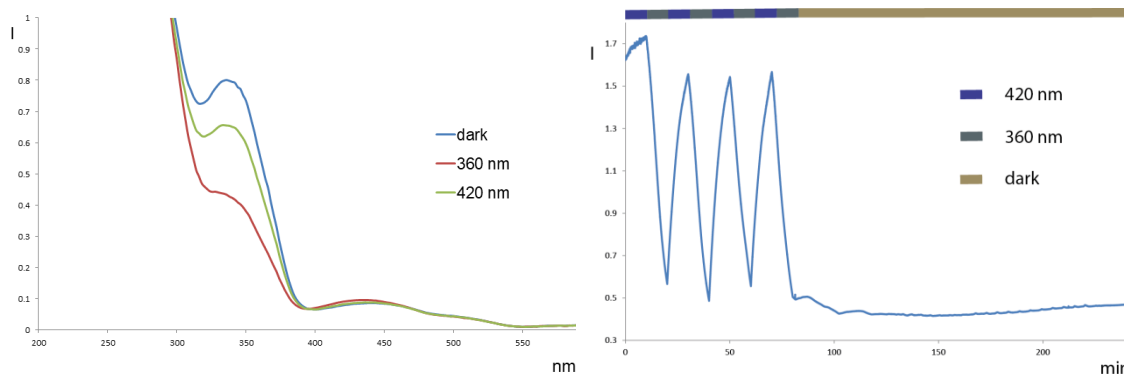


FIGURE 4.12: UV/Vis-spectra of **4.24** (left) and continuous switching (right).

The ability to block voltage gated ion channels was evaluated together with Dr. Andrea Brüggemann at Nanion Technologies on a SynchroPatch768PE. When **4.24** was applied to CHO cells stably overexpressing hNav1.7, Na⁺-currents evoked through membrane depolarization, were efficiently reduced (Figure 4.13 a and c). When **4.24** was preirradiated under 360 nm and then applied to the same experimental setup, **4.24** had only a small effect on Na⁺-currents (Figure 4.13 b and d), illustrating the difference in binding efficacy between the *trans* and the *cis* conformer.

We then tested whether **4.24** is also able to block K_v1.3-channels expressed in jurkat cells. *Trans* **4.24** showed as well higher potency to reduce K⁺-currents than its *cis* conformer (Figure 4.14 b and c). The IC₅₀ value was reduced to half its value upon irradiation with UV light. Furthermore, the IC₅₀ value of *trans* **4.24** increased approximately three times for K_v1.3 compared to Nav1.7. This observation indicates that **4.24** has a slightly higher ability to block Nav1.7 than K_v1.3 (Figure 4.14 a and b).

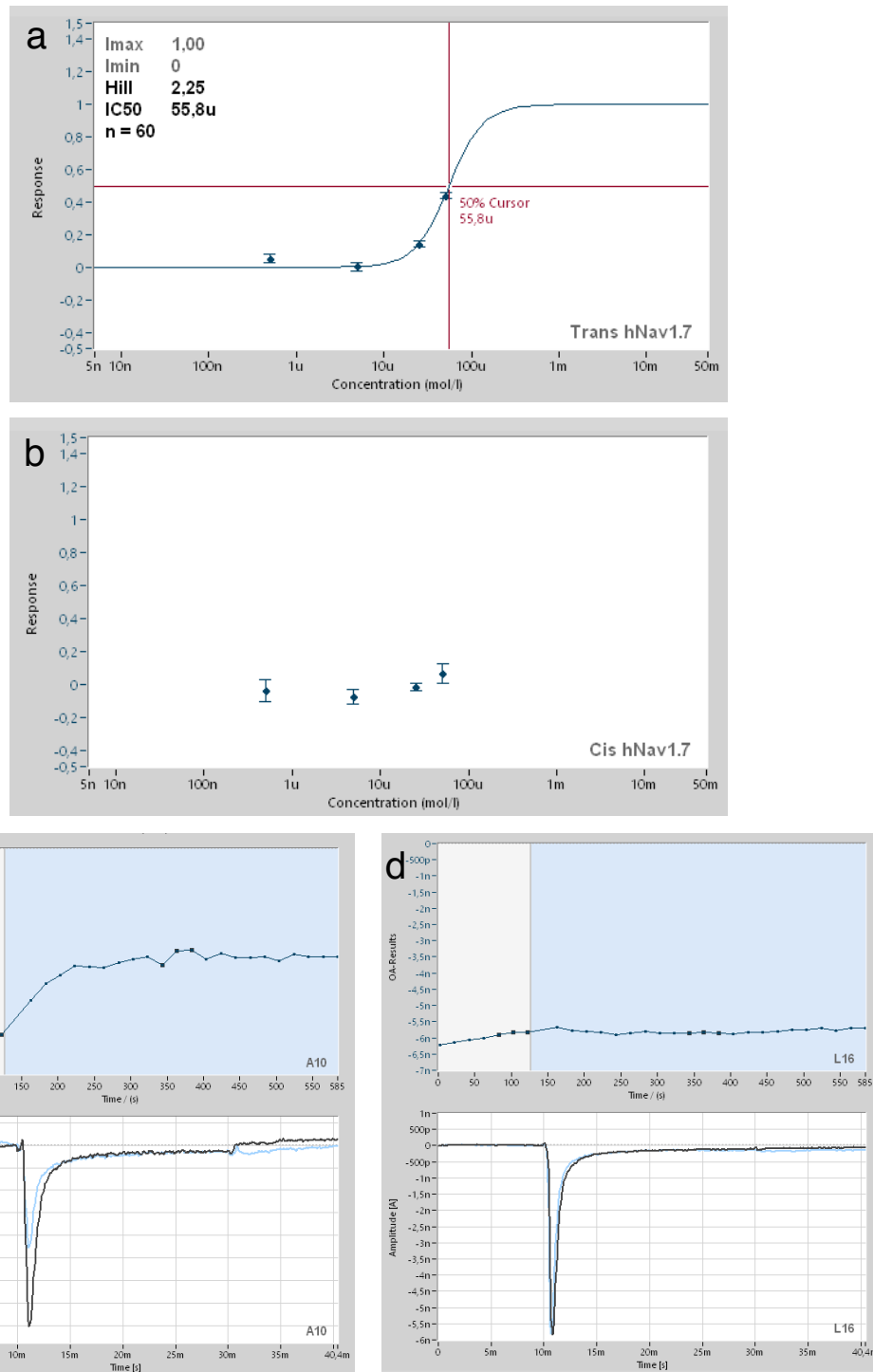


FIGURE 4.13: Effect of **4.24** on CHO cells overexpressing hNav_v1.7. a) Dose-response plot of *trans* **4.24** (dark adapted) and b) *cis* **4.24** (UV-pre-treated). c) and d) (top) Plot of Na⁺-current peak values before (white area) and after wash-in (blue area) of c) *trans* and d) *cis* **4.24**. (bottom) Example trace of depolarization evoked Na⁺-currents before (black trace) and after (blue trace) wash-in of c) *trans* and d) *cis* **4.24**.

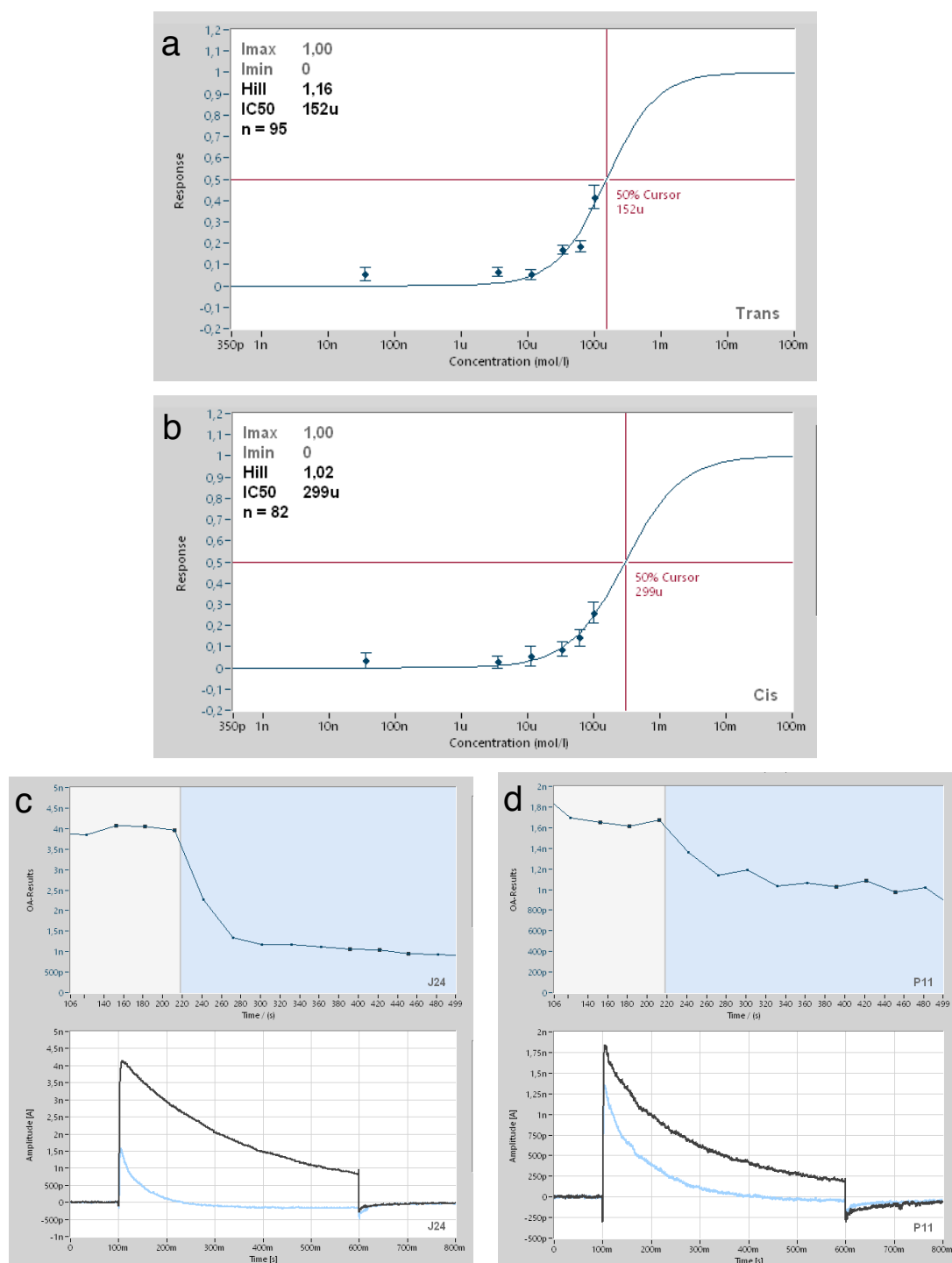


FIGURE 4.14: Effect of **4.24** on jurkat cells expressing hKv1.3. a) Dose-response plot of *trans* **4.24** (dark adapted) and b) *cis* **4.24** (UV-pre-treated). c) and d) (top) Plot of K⁺-current peak values before (white area) and after wash-in (blue area) of c) *trans* and d) *cis* **4.24**. (bottom) Example trace of depolarization evoked K⁺-currents before (black trace) and after (blue trace) wash-in of c) *trans* and d) *cis* **4.24**.

4.6 Conclusion

In conclusion, we have synthesized photoswitchable derivatives of three known blockers of voltage-gated ion channels. We developed synthetic routes, which proved to be sufficiently robust and scalable. Furthermore, all compounds have been fully characterized in terms of their photophysical properties and their ability to inhibit voltage-gated ion channels light-dependently.

4.7, a photoswitchable derivative of A-803467 has been synthesized by a three steps protocol employing the addition of an aryl magnesium species into a diazonium salt, a method that has been rarely investigated beforehand and optimized in our laboratory. Unfortunately, unlike its parental molecule, **4.7** showed no ability to block currents evoked upon depolarization of cells overexpressing Nav1.8.

A robust route to photoswitchable derivatives of bupivacaine has been developed, employing Hartwig's amination protocol utilizing LiHMDS simultaneously as a nucleophile and as a base. Further derivatization delivered three photoswitches differing in their switching behaviour. Compound **4.17** has been electrophysiologically characterized in cells overexpressing VGICs as well as in mouse hippocampal neurons. Compound **4.17** in its *trans* configuration showed a substantial block of K⁺-currents in cultured cells, with the *cis* conformer being less potent. Strikingly, the logic of this photoswitch is inverted when applied to hippocampal neurons, i.e. the *cis* conformer is the more potent configuration of **4.17**. Currently, we do not have an explanation for this sign inversion. Neurons express a large variety of VGICs as well as other types of ion channels and we do not know the exact target of **4.17**. But most likely **4.17** affects more than one specific type of channel.

Additionally, we developed and optimized an 11-step synthetic route to photoswitchable derivatives of the Phase II channel blocker raxatrigine. This route contains a stereoselective reduction of an imine as well as a Pd-catalyzed cross coupling to install the azobenzene moiety. The ability of **4.24** to block voltage-gated ion channels was evaluated by extensive electrophysiological investigations. **4.24** proved to be a sufficient blocker of Nav1.7 as well as Kv1.3. This ability was repealed when the compound was irradiated with UV-light.

Therefore, we have developed a new kit of pharmacological tools which can be used to investigate neuronal pathways.

Chapter V

Studies Towards the Light-Dependent Regulation of Cytoskeletal Proteins

5.1 Development of Photoswitchable Arp2/3 Inhibitors

5.1.1 Introduction

5.1.1.1 Actin

The cytoskeleton is responsible for the ability of eukaryotic cells to resist deformation, transport intracellular cargo and change shape during movement.¹⁴⁴ The machinery of these processes relies on the assembly of proteins where actin, a globular protein that forms filaments of different types of organization, is of significant relevance.¹⁴⁵ Actin is one of the most abundant proteins in eukaryotic cells reaching concentrations of 300 μM , and its structure is highly conserved across species. Monomeric actin (globular- or G-actin) assembles under physiological salt concentrations to form polymers (filamentous- or F-actin) which can be assembled into branched and cross-linked networks, parallel bundles, and anti-parallel contractile structures.¹⁴⁶ The cell cortex, a thin layer of actin, coats the plasma membrane at the back side of the cell and is important for maintenance and changes in the shape of the cell. The rest of the cell contains a three-dimensional network of cross-linked filaments blended with contractile bundles which are connected to the extracellular matrix by focal adhesion sites.¹⁴⁷ Actin monomers are proteins of 42 kDa usually loaded with MgATP. Polymerization of actin monomers at filament ends is followed by ATP hydrolysis and dissociation of the phosphate, leaving behind bound ADP.¹⁴⁶ Actin filaments assemble in a right-handed helix possessing two dynamically different ends, the barbed end and the pointed end. As the more dynamic end, the barbed end elongates 10 times faster than the pointed end at a rate of up to 3,000 subunits/s.

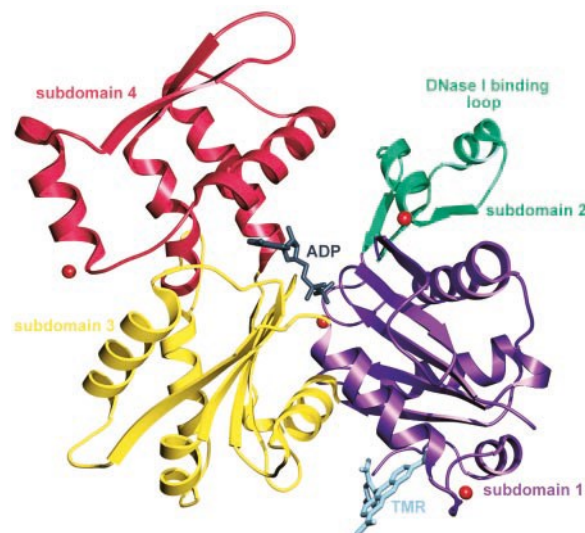


FIGURE 5.1: Structure of uncomplexed G-actin in the ADP bound state.¹⁴⁶

Actin filament assembly is limited by the nucleation step, consisting of the formation of dimers and trimers.¹⁴⁷ Once trimers are formed, the elongation proceeds rapidly as a function of the concentration of actin monomers. G-actin comprises four subdomains I-IV which are assembled around the ATP binding site. The exposed areas of I and III comprise the barbed end whereas II and IV refer to the pointed end (Figure 5.1).¹⁴⁶

5.1.1.2 The Arp 2/3 complex

The actin cytoskeleton plays important roles in cell processes, such as cell migration, endocytosis, vesicle trafficking and cytokinesis in eukaryotes.¹⁴⁸ To control these crucial functions, precise regulation of both the initiation of actin polymerization and organization of the resulting filaments is required. The dynamic assembly and disassembly of filaments as well as the formation of larger scale filament structures are crucial aspects of the actin network and therefore controlled by over one hundred actin-binding proteins.¹⁴⁹⁻¹⁵¹ They mediate structural changes such as nucleation, capping, bundling, crosslinking or depolymerisation. Polymerization appears mainly on the barbed ends of actin filaments which can be created from existing filaments by uncapping or severing or by *de novo* nucleation. Spontaneous nucleation of actin monomers is kinetically unfavored and therefore requires initiator proteins such as formins, spires or the actin-related-protein-2/3 (Arp2/3) complex.¹⁴⁸ The Arp2/3 complex comprises seven subunits ARPC1-5, Arp2 and Arp3, ranging in size from 16 to 50 kDa, with the latter two giving the complex its name. The complex weighs around 220 kDa and is highly conserved across species.¹⁵² ARPC2 and

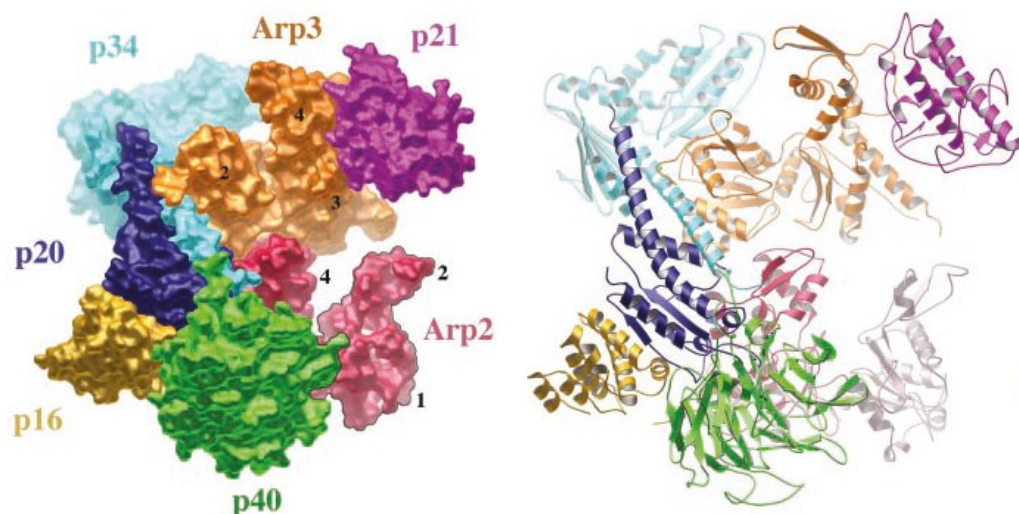


FIGURE 5.2: Crystal structure of bovine Arp2/3 complex.¹⁵²

ARPC4 form the structural core of the complex while the remaining subunits organize around them. Arp2 and Arp3 each contain a nucleotide binding cleft and share structural similarities to actin. The two are supposed to come together to form an actin-like dimer which serves as a template for filament formation (Figure 5.2).

The Arp2/3 complex on its own possesses little actin-nucleating activity and is activated by nucleation promoting factors (NPFs), such as ActA or Wiskott-Aldrich syndrome family protein (WASP).¹⁴⁹ WASP family proteins, the best characterized of the NPFs, bind the Arp2/3 complex and monomeric actin as well as upstream signalling molecules and therefore control where and when new actin filaments are created in the cell.¹⁵⁰ The activity of the so-formed complex is further stimulated by binding to the side of an existing actin filament. Upon binding to an existing mother filament, Arp2/3 initiates the formation of a Y-branched daughter filament in a characteristic angle of 70° .¹⁵² WASP activation is mediated by chemotactic signalling pathways that guide the direction of cellular movement (Figure 5.3).

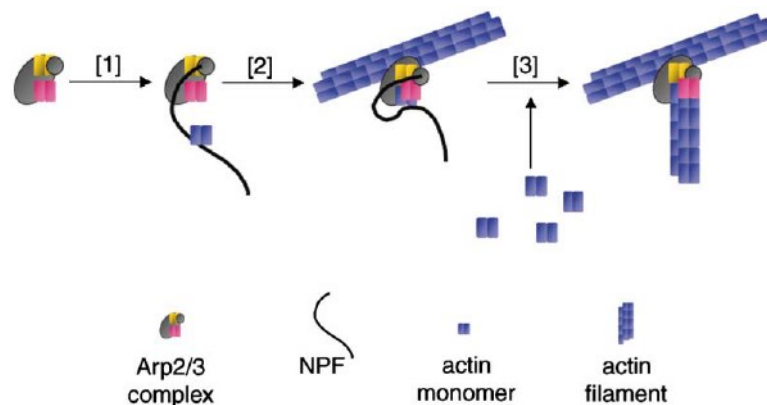


FIGURE 5.3: Actin filament nucleation and organization by Arp2/3 complex.¹⁴⁹

In the absence of NPFs, the two actin-related subunits Arp2 and Arp3 are splayed apart from each other. Upon activation, Arp2 moves approximately 25 \AA to form a dimer with Arp3 which mimics a short pitch actin-dimer within a filament and therefore provides a template for the nucleation of a new filament.¹⁴⁹

5.1.1.3 CK-636 and CK-666

CK-636 and CK-666 are small molecules which inhibit the ability of the Arp2/3 complex to nucleate actin filaments. CK-636 was discovered in 2009 by screening efforts involving over 400,000 small molecules for inhibition of actin polymerization stimulated by human (Hs) Arp2/3 and was able to inhibit bovine (Bt) Arp2/3 complex with an IC_{50} value of $32 \mu M$.¹⁵³

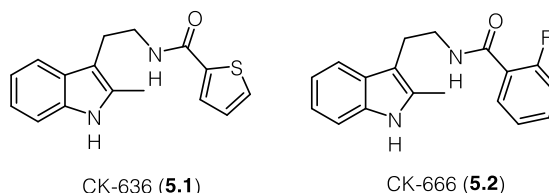


FIGURE 5.4: Molecular structures of CK-636 (5.1) and CK-666 (5.2).

In the same study, CK-666 was revealed as a more potent inhibitor by compound screening in a *Listeria* motility assay. CK-666 inhibited BtArp2/3 mediated actin polymerization with an IC_{50} value of $17 \mu M$ (Figure 5.4). Both compounds were shown to have no effect on actin or WASP directly as well as on Arp2/3 binding to WASP.¹⁵³ Furthermore, neither compound disrupted the microtubule network in THP.1 cells or showed irreversible off-target morphological effects, such as apoptosis, at concentrations up to $100 \mu M$. CK-636 and CK-666 function as allosteric effectors by stabilization of the inactive state of the complex.¹⁵⁴ Crystal structures of CK-636 and CK-666 bound to Arp2/3 indicate that stabilization is achieved by binding of the inhibitors to a pocket at the interface of Arp2 and Arp3 and therefore block the formation of the Arp2-Arp3 short pitch dimer (Figure 5.5).^{153, 155}

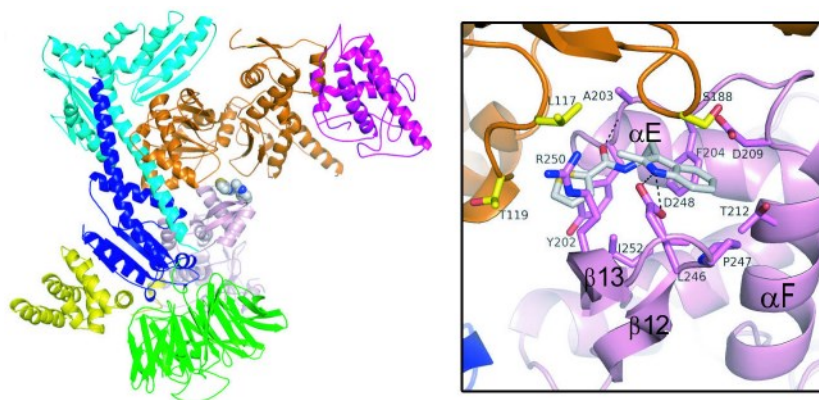


FIGURE 5.5: Crystal structure of BtArp2/3 complex with bound CK-636.¹⁵³

5.1.2 Project Outline

The actin-network is responsible for multiple cellular functions ranging from cell motility and the maintenance of cell shape and polarity to the regulation of transcription.¹⁴⁵ Furthermore, the interaction of myosin with filamentous actin constitutes the basic principle of muscle contraction. It is subject to complex dynamics which are resembled by a steady polymerization and depolymerization of filaments.¹⁴⁷ These dynamics are partially directed by polymerization of actin filaments directed by the Arp2/3 complex. The Arp2/3 complex comprises of seven subunits and catalyzes the kinetically unfavored process of actin filament nucleation, which allows the precise spatial and temporal control of the assembly of actin filament networks.¹⁵²

While many aspects of actin polymerization have been revealed over the last decades, the dynamics of the actin network still remain not fully understood. A photoswitchable inhibitor of the Arp2/3 complex could help to unravel several questions about its dynamics, as it would reversibly allow and preclude Arp2/3-mediated actin polymerization in real time. We chose CK-636 and CK-666 as a template for such an inhibitor as both compounds were shown to selectively target the Arp2/3 complex.¹⁵³⁻¹⁵⁵ Furthermore, crystal structures of both compounds bound to Arp2/3 are available suggesting which portions of the molecule are necessary for binding and which areas may be modified. Based on crystal structures, we sought to extend the eastern aryl amide of CK-636 and CK-666 to an azobenzene in order to obtain a photoswitchable inhibitor of Arp2/3 (Figure 5.6). This work was carried out in collaboration with Dr. Cenbin Lu.

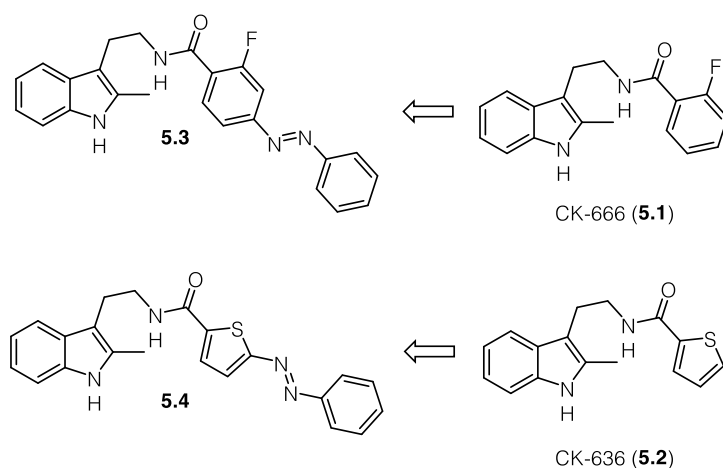
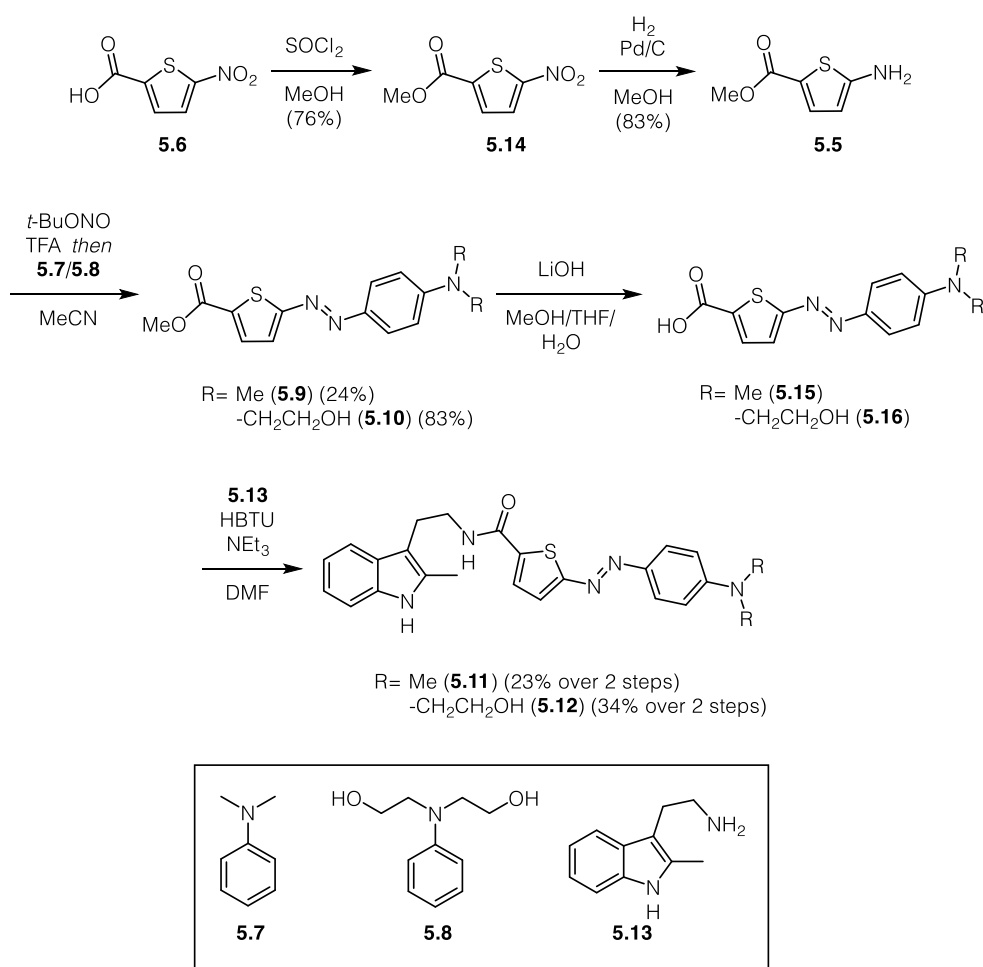


FIGURE 5.6: Design of photoswitchable inhibitors based on CK-636 (5.1) and CK-666 (5.2).

5.1.3 Results and discussion

The synthesis of photoswitchable Arp2/3 inhibitors based on CK-636 is depicted in Scheme 5.1. The thiophene moiety is pharmacologically considered to be equal to a benzene ring and the 2,5-substitution pattern resembles a 1,4-disubstituted benzene ring. Amine **5.5** is derived from thiophene **5.6** by methyl ester formation followed by reduction of the nitro group under heterogeneous conditions. Diazonium ion formation and subsequent trapping with either dimethylaniline (**5.7**) or *N*-phenyldiethanolamine (**5.8**) gave azobenzenes **5.9** and **5.10**. Amides **5.11** and **5.12** were obtained after hydrolysis of the methyl ester followed by amide bond formation with 2-methyltryptamine (**5.13**) in moderate yields.



SCHEME 5.1: Synthesis of azologues **5.11** and **5.12**.

To examine the ability to inhibit Arp2/3 dependent actin polymerization, we send compound **5.12**, together with azobenzenes **5.17**, **5.18**, **5.19** and **5.20** synthesized by Dr. Cenbin Lu, to Dr. Julie Plastino at the Institut Curie-Section de Recherche in Paris. To examine whether the compounds would prevent actin polymerization they were applied to 3 μm carboxylated polystyrene beads coated with GST-pVCA of WASP beads

which are placed in a motility mix (Arp2/3 complex, profilin, capping protein) with monomeric red actin (Alexa 594). The sample is then mounted and viewed by epifluorescence over approximately 15 minutes. Actin growth was then plotted over time (Figure 5.7).

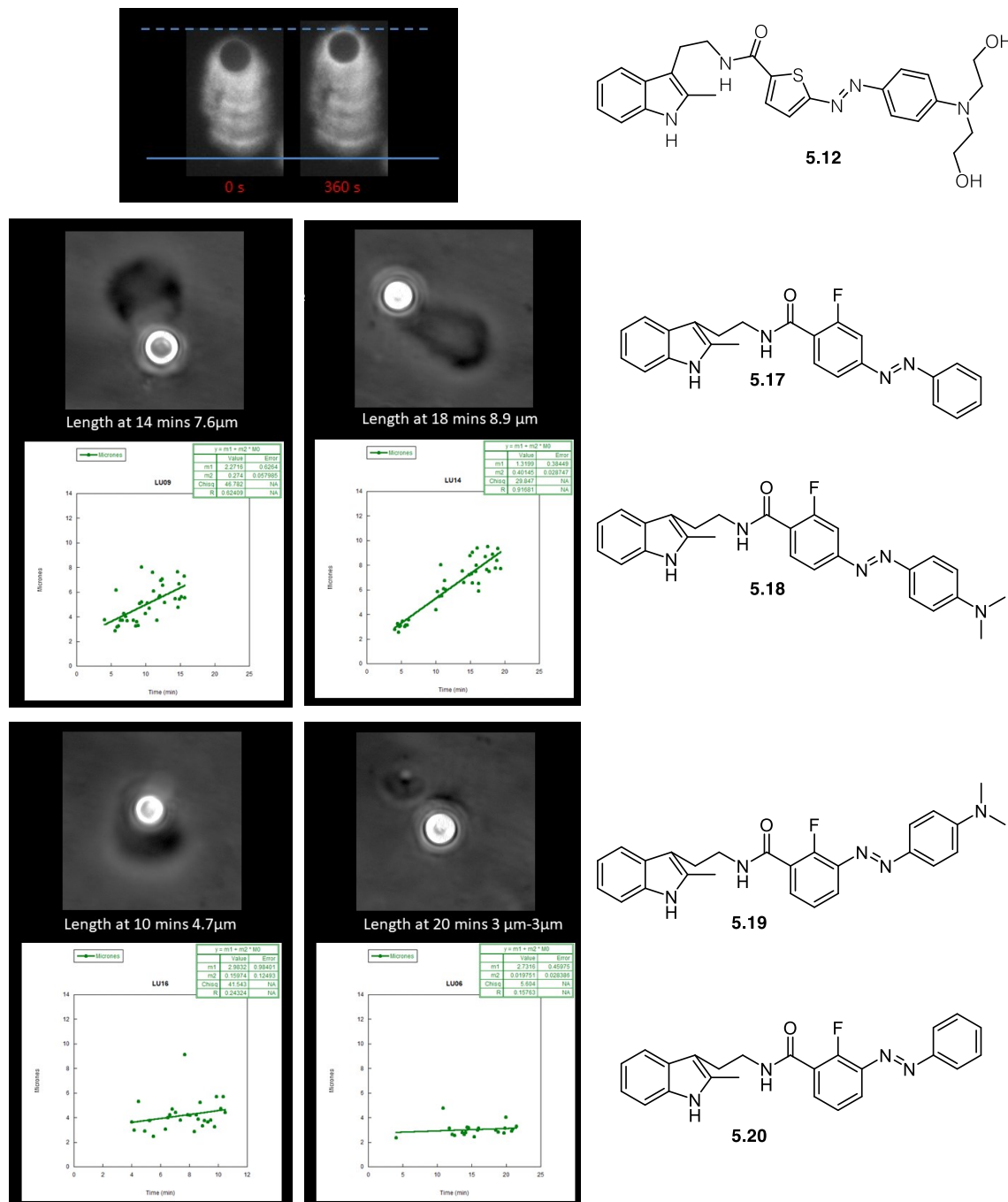
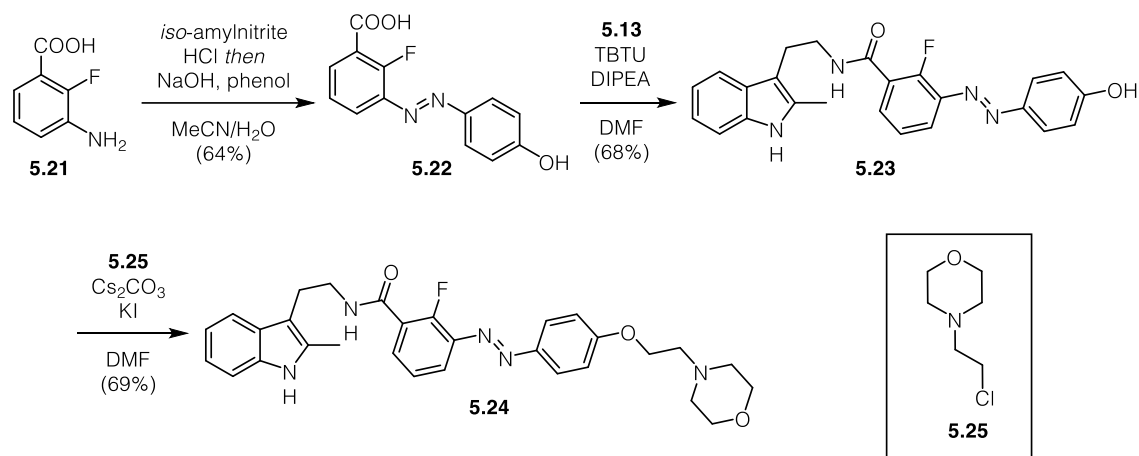


FIGURE 5.7: **5.12** (top), **5.17** (middle left) and **5.18** (middle right) do not inhibit actin polymerization; **5.19** (bottom left) and **5.20** (bottom left) inhibit actin polymerization.

Thiophene **5.12**, azobenzene **5.17** and dimethylaniline **5.18** showed no inhibition of Arp2/3 dependent actin polymerization while azobenzene **5.20** and dimethylaniline **5.19** sufficiently suppressed actin polymerization. We therefore reasoned that the *meta*-

substitution pattern is crucial for inhibition. This is consistent with the result for thiophene **5.12**, as its structure resembles that of a *para*-substituted azobenzene. Further studies indicated that **5.20** loses its ability to inhibit Arp2/3 upon illumination with 360 nm light (data not shown). Even though this result appeared to be quite promising, all compounds suffered from poor solubility in aqueous buffers.

To improve the solubility, we thought to install a morpholine unit as a solubility tag at the eastern end of the molecule, under the premise that substitutions would most likely be tolerated at that position. Azobenzene **5.21** was obtained after diazonium ion formation from aniline **5.22** followed by trapping with phenol. **5.21** was then subjected to amide bond formation with 2-methyltryptamine (**5.13**) to give amide **5.23** which was then transformed to morpholine **5.24** by nucleophilic displacement of chloride **5.25** (Scheme 5.2).



SCHEME 5.2: Synthesis of morpholine **5.24**.

The photophysical properties of **5.24** are consistent with those expected for azobenzenes bearing auxochromic groups which are not in direct conjugation. **5.24** was efficiently converted from its *trans*- to its *cis*-configuration by irradiation with 370 nm light and *vice versa* by 460 nm light. The compound could also efficiently be switched over

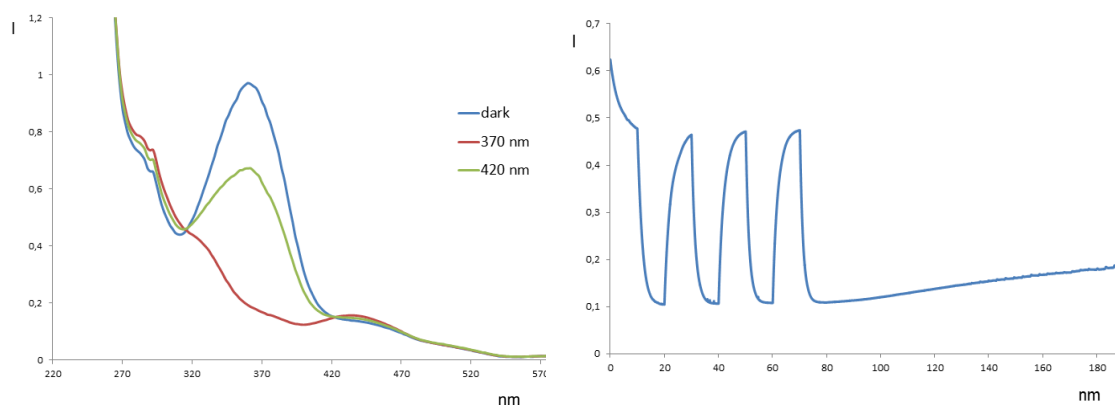


FIGURE 5.8: UV/Vis-spectra of **5.24** before and after irradiation with 370 and 420 nm light (left).

5.24 can be efficiently switched over several cycles (right).

several cycles without any loss and is sufficiently stable towards thermal relaxation ($T_{1/2} > 1$ h) and is thus considered bistable (Figure 5.8).

5.1.4 Conclusion

In conclusion we have developed a photoswitchable Arp2/3 inhibitor based on the known compound CK-666 and derivatives thereof. We showed that attachment of an azobenzene at the *meta* position of the benzene ring of CK-666 led to retention of its ability to inhibit Arp2/3-dependent actin polymerization while attachment of an azobenzene at the *para* position of CK-666 led to complete loss of activity. However, all prepared compounds suffered from poor solubility in aqueous buffers. We therefore currently pursue the synthesis of more water soluble derivatives which can be used to study actin network dynamics *in vivo*.

5.2 Development of Photoswitchable Inhibitors of Myosin II

5.2.1 Introduction

5.2.1.1 Myosin 2

Myosin is a molecular motor protein, identified over 100 years ago, which can generate pulling forces by mutual sliding of actin and myosin filaments.¹⁵⁶ The myosin superfamily consist of approximately 35 classes, found across all eukaryotic cells, that is responsible for diverse functions in the cell such as vesicle and organelle transport, muscle contraction, photo transduction, cell-cell adhesion, cell migration and cell division.¹⁵⁷ The most expressed subclass of the myosin superfamily is myosin II (M2). M2 is responsible for the production of muscle contractions in muscle cells, where it forms the thick filaments of the sarcomeres¹⁵⁸. Non-muscle M2 (NM II) plays an important role in cell motility, cytokinesis, cell shape determination and cell-cell junction formation.¹⁵⁹ The M2 subclass is the only member of the myosin superfamily which assembles into bipolar filaments and consists of a hexameric structure derived from two heavy chains, each with a weight of 230 kDa, and two pairs of tightly, but non-covalently, bound light chains.¹⁵⁶ The heavy chains contain the domains required for myosin function while the light chains are responsible for stabilization (essential light chain, 17 kDa) and regulation (regulatory light chain, 20 kDa) of the enzymatic activity. Three different isoforms of NM II are known which can be differentiated based on their three different heavy chains, NM II-A (Myh9), NM II-B (Myh10) and NM II-C (Myh4).¹⁶⁰ The *N*-terminal heavy chain is characterized by a globular shaped, conserved, catalytic head domain containing both an

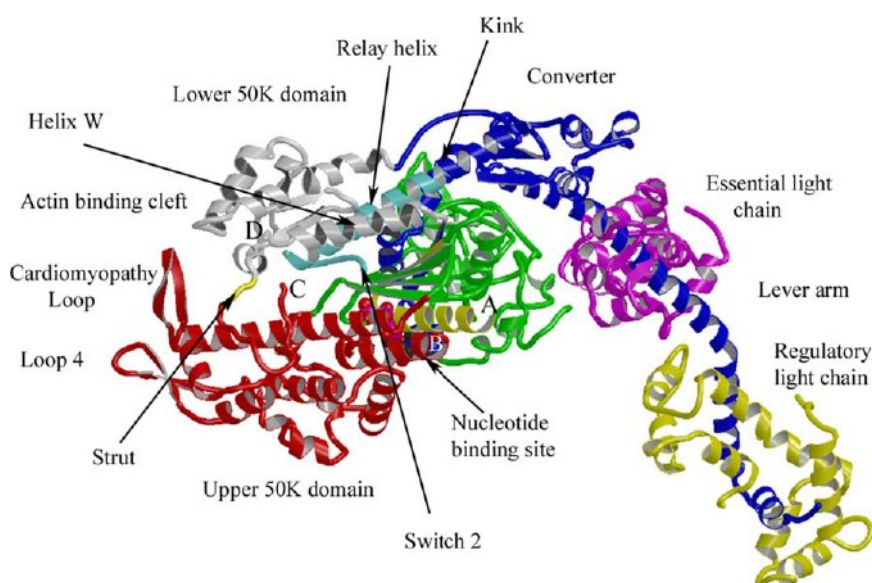
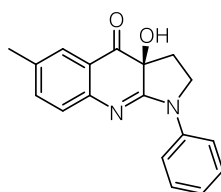


FIGURE 5.9: Structure of myosin II (M2).¹⁵⁸

MgATP binding domain and a nearby actin binding Domain (Figure 5.9). The C-terminal region comprises a double-stranded, α -helical coiled-coil rod which terminates in a non-helical tail region.^{157, 160} The ATPase activity is activated by actin and is crucial to slide actin-filaments past myosin and exert tension on actin-filaments. M2's affinity to bind actin is regulated by ATP hydrolysis whereby the ADP bound state provides a strong interaction between the myosin head and the actin filament.¹⁵⁸ Actin affinity drops significantly when ATP or ADP-P_i is bound to the catalytic domain. Furthermore, the enzymatic activity of M2 is regulated primarily by phosphorylation of the two conserved residues Ser19 and Thr18 in the regulatory light chain.¹⁵⁶ Malfunction in NM II activity has been associated with alterations in cell division and therefore with cancer.

5.2.1.2 Blebbistatin

Blebbistatin (**5.26**) was discovered by means of a high-throughput screening targeting non-muscle myosin II by Mitchison in 2003 (Figure 5.10). **5.26** showed inhibition of the adenosine triphosphatase (ATPase) and gliding motility activities of human platelet non-muscle myosin II without inhibiting myosin light chain kinase.¹⁶¹ While the (–)-enantiomer provided an IC₅₀ value of 2 μ M, the (+)-enantiomer was completely inactive. **5.26** inhibited NM II without showing any effects on the human myosin isoforms Ib, Va and X. The compound's name is derived from its ability to reversibly block cell blebbing.¹⁶² Blebbistatin was shown to block myosin II-dependent cell processes such as cell migration and cytokinesis.

**FIGURE 5.10:** Molecular structure of (–)-blebbistatin (**5.26**).

Blebbistatin acts as an uncompetitive inhibitor and binds to a hydrophobic pocket at the apex of the 50 kDa cleft, which is located close to the γ -phosphate binding pocket.¹⁶³⁻¹⁶⁴ **5.26** stabilizes a state where ADP and p_i are both bound to myosin and which precedes the force-generating step catalyzed by the release of phosphate when myosin rebinds to actin.¹⁶⁵ Binding of **5.26** is controlled by the hydrophobic effect, with the phenyl ring of blebbistatin being enclosed by Leu262, Phe466, Glu467 and Val630.¹⁶⁶ The

tetrahydropyrrolo ring mainly interacts with the residues of the side chains Ser456 and Ile471, while the methylquinolinone interacts with Tyr261, Thr474, Tyr634, Gln637 and Leu641.¹⁶⁷ Furthermore, the chiral hydroxyl group forms a hydrogen bond to the main chain carboxylate of Leu262 (Figure 5.11).

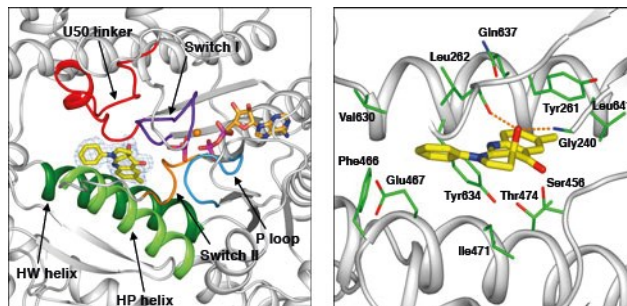


FIGURE 5.11: (-)-Blebbistatin (**5.26**) bound within the myosin cleft (left). Interaction of **5.26** with important amino acid residues (right).

It was shown, that blebbistatin undergoes photoconversion upon irradiation with blue light ($\lambda < 500$ nm), accompanied by the generation of reactive oxygen species responsible for its phototoxicity.¹⁶⁸ Additionally, **5.26** showed cytotoxic side effects even without irradiation.¹⁶⁹ Substitution of the C15 position by either a nitro or an amino group gave access to derivatives lacking the undesirable side effects while maintaining the level of myosin inhibition.^{162, 170} Furthermore, a photo-crosslinkable derivative of **5.26**, azidoblebbistatin, bearing an azide at the C15 position, has been developed.¹⁷¹

5.2.2 Project outline

Blebbistatin (**5.26**) is a cell-permeable, specific inhibitor of class II myosin. Myosin II is a group of actin-based ATP-driven motor proteins which are responsible for various biological processes such as muscle contraction, cell migration, differentiation and cytokinesis.¹⁶¹ **5.26** blocks myosin in a state of low actin-affinity and therefore prevents the formation of strongly-bound non-functional actomyosin complexes.^{163, 165-166} While blebbistatin showed side effects such as cellular phototoxicity and cytotoxicity in response to blue light,¹⁶⁸⁻¹⁶⁹ it has been shown that substitution at C15 by either a nitro or an amino group suppressed these undesirable effects while maintaining the ability to inhibit myosin II.^{162, 170}

A reversible, photoswitchable, small molecule myosin II inhibitor would provide a powerful tool to study dynamic processes within in the actomyosin network. We sought to develop such a molecule by incorporating an azobenzene photoswitch into the scaffold

of known myosin II inhibitor blebbistatin (**5.26**). While substitutions at the methylquinolinone reduced the affinity of the molecule to bind myosin, substitutions at C15 were well tolerated and removed the photolability of the molecule. Therefore, we planned to incorporate the existing phenyl ring of **5.26** into the photoswitchable moiety by extending it to an azobenzene (Figure 5.12).

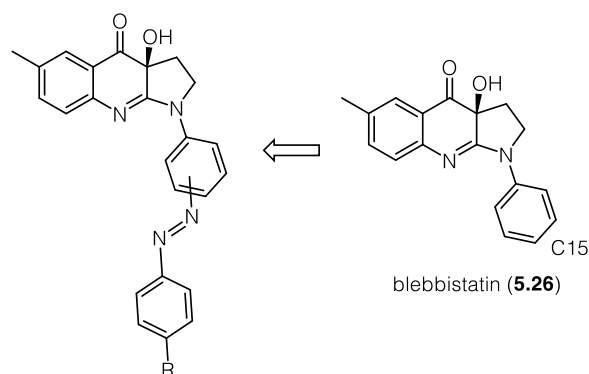
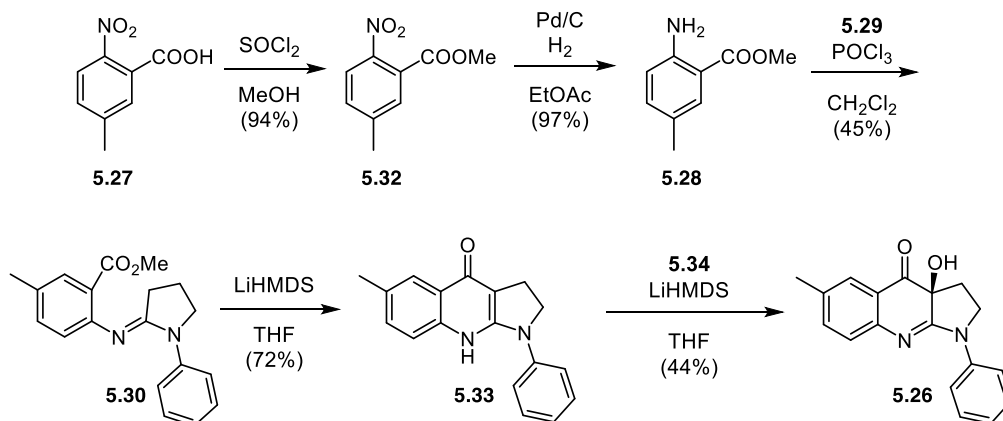
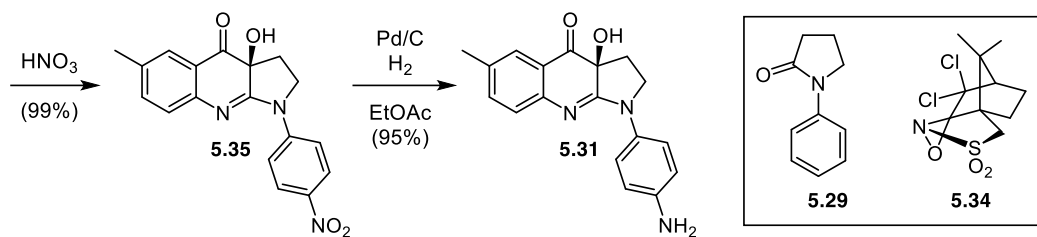


FIGURE 5.12: Design of photoswitchable inhibitors based on blebbistatin (**5.26**).

5.2.3 Results and discussion

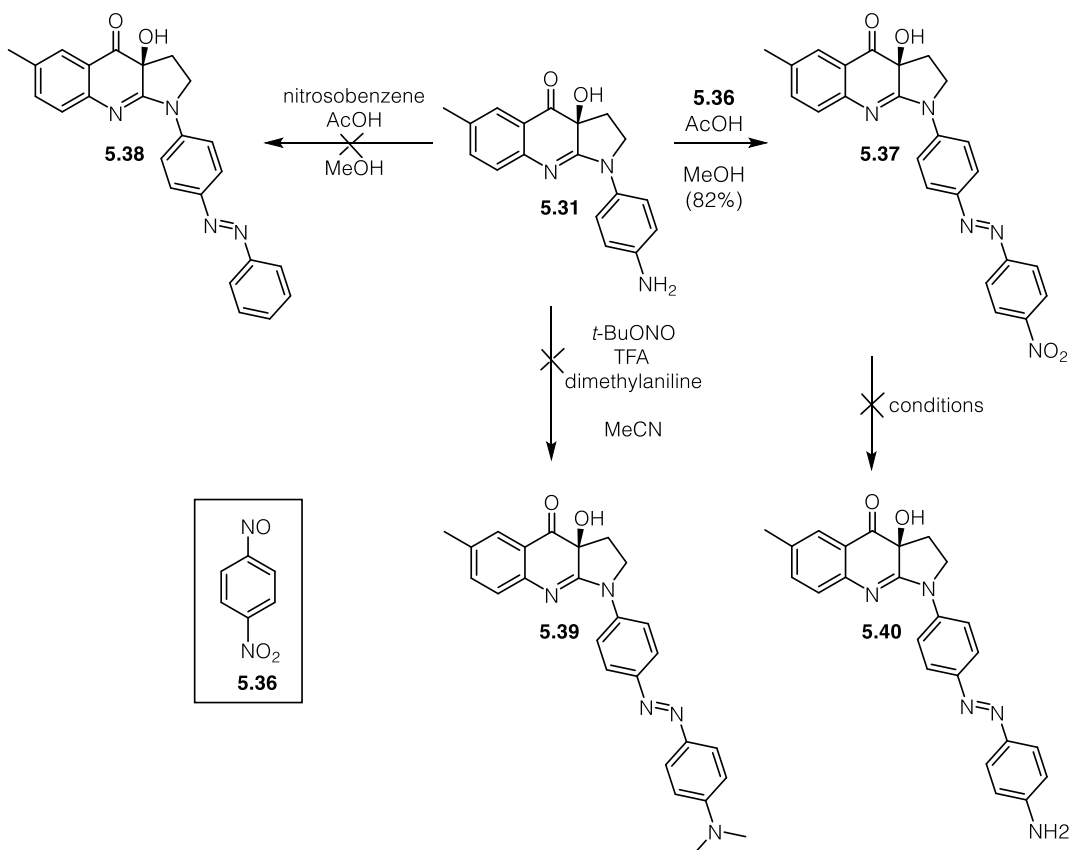
The synthesis starts with methyl ester formation of 5-methyl-2-nitrobenzoic acid (**5.27**) followed by reduction of the nitro group under heterogeneous conditions to form aniline **5.28**. Activation of 1-phenyl-2-pyrrolidinone (**5.29**) using phosphoryl chloride followed by subsequent trapping with **5.28** gave amidine **5.30** in good yield. Base mediated intramolecular ring closure and enantioselective α -oxygenation gave access to (–)-blebbistatin (**5.26**). Aniline **5.31** was obtained after nitration of **5.26** in HNO_3 and Pd-catalyzed reduction of the nitro group (Scheme 5.3).





SCHEME 5.3: Synthesis of (*S*)-aminoblebbistatin (**5.31**).

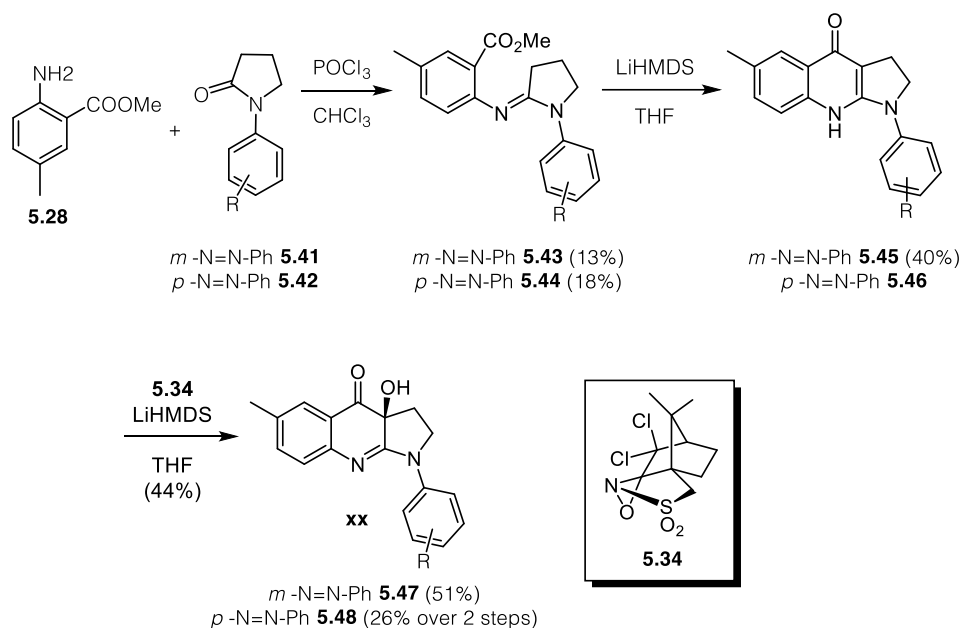
Diazoniumium formation followed by trapping with dimethylaniline resulted in a complex mixture and did not furnish the desired azobenzene. Attempts to install the azobenzene by Baeyer-Mills coupling were only successful using 4-nitro-nitrosobenzene (**5.36**) and resulted in decomposition when nitrosobenzene was employed in the reaction. Unfortunately, attempts to selectively reduce the nitro group of **5.37** resulted either in cleavage of the diazene unit, deoxygenation or decomposition (Scheme 5.4).



SCHEME 5.4: Attempted derivatization of **5.31**.

As the installation of the azobenzene late in the synthesis proved difficult, we wanted to start with an azobenzene as the starting material. Amidine formation using azobenzenes **5.41** and **5.42** gave amidines **5.43** and **5.44** in low yields but significantly lowered the step count compared to the previous synthesis. Base mediated ring closure accessed

5.45 and **5.46** which could sufficiently be oxidized using Davis' oxaziridine **5.34** (Scheme 5.5).



SCHEME 5.5: Synthesis of tertiary alcohols **5.47** and **5.48**.

5.2.4 Conclusion

In conclusion, we have synthesized four blebbistatin analogues containing a photoswitchable azobenzene moiety. The direct derivatization of blebbistatin itself proved difficult and was only possible for a narrow substrate scope. Furthermore, we could show that the reaction sequence could be carried out with substrates already containing the azobenzene and therefore giving a fast entry into this class of compounds.

It remains to be examined whether the azologue still contains the inhibitory properties of the parent compound and whether these can be altered by light application.

Chapter VI

Experimental Procedures

And Analytical Data

6.1 General experimental details

All reactions were carried out with magnetic stirring, and, if moisture- or air- sensitive, under nitrogen or argon atmosphere using standard Schlenk techniques in oven-dried glassware (140 °C oven temperature). External bath temperatures were used to record all reaction temperatures. Low temperature reactions were carried out in a Dewar vessel filled with acetone/dry ice (−78 °C) or distilled water/ice (0 °C). High temperature reactions were conducted using a heated silicon oil bath in reaction vessels equipped with a reflux condenser or in a sealed flask. Tetrahydrofuran (THF) and diethyl ether (Et₂O) were distilled over sodium and benzophenone prior to use. Dichloromethane (CH₂Cl₂), triethylamine (Et₃N), diisopropylethylamine (DIPEA) and diisopropylamine (DIPA) were distilled over calcium hydride under a nitrogen atmosphere. All other solvents were purchased from Acros Organics as 'extra dry' reagents. All other reagents with a purity > 95% were obtained from commercial sources (Sigma Aldrich, Acros, Alfa Aesar and others) and used without further purification.

Photochemical reactions were performed with a medium pressure mercury lamp (150 W) using a Heraeus power supply at room temperature.

Flash column chromatography was carried out with Merck silica gel 60 (0.040-0.063 mm). **Analytical thin layer chromatography (TLC)** was carried out using Merck silica gel 60 F254 glass-backed plates and visualized under UV light at 254 nm. Staining was performed with ceric ammonium molybdate (CAM) or by oxidative staining with an aqueous basic potassium permanganate (KMnO₄) solution and subsequent heating.

High performance liquid chromatography (HPLC). HPLC was performed with HPLC grade solvents and deionized H₂O that was purified on a TKA MicroPure H₂O purification system. All solvents were degassed with helium gas prior to use. Unless noticed otherwise, all experiments were carried out at room temperature.

Chiral HPLC spectra were recorded on a high performance liquid chromatography (HPLC) system from the Shimadzu 20A series (DGU-20A3R degasser, LC-20AD Binary Pump VL, SIL-20AHT autosampler, CTO-20A thermostated column compartment, SPD-M20A DAD diode array detector), which was computer controlled through Shimadzu LabSolutions Software (Version 5.42 SP5).

Optical rotation. Perkin-Elmer 241 or Krüss P8000-T polarimeter were used to measure optical rotation at the Sodium D-line (589 nm) at the given temperature (*T* in °C) and

concentrations (c in g/100 mL) using spectroscopic grade solvents. The measurements were carried out in a cell with a path length (d) of 0.5 dm.

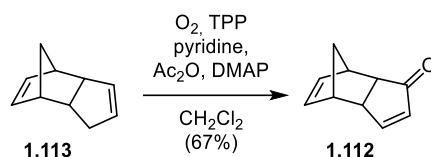
NMR spectra (^1H NMR and ^{13}C NMR) were recorded in deuterated chloroform (CDCl_3) on a Bruker Avance III HD 400 MHz spectrometer equipped with a CryoProbeTM, a Varian VXR400 S spectrometer, a Bruker AMX600 spectrometer or a Bruker Avance III HD 800 MHz spectrometer equipped with a CryoProbeTM and are reported as follows: chemical shift δ in ppm (multiplicity, coupling constant J in Hz, number of protons) for ^1H NMR spectra and chemical shift δ in ppm for ^{13}C NMR spectra. Multiplicities are abbreviated as follows: s = singlet, d = doublet, t = triplet, q = quartet, quint = quintet, br = broad, m = multiplet, or combinations thereof. Residual solvent peaks of CDCl_3 ($\delta\text{H} = 7.26$ ppm, $\delta\text{C} = 77.16$ ppm), C_6D_6 ($\delta\text{H} = 7.16$ ppm, $\delta\text{C} = 128.06$ ppm), d_6 -DMSO ($\delta\text{H} = 2.50$ ppm, $\delta\text{C} = 39.52$ ppm), d_6 -acetone ($\delta\text{H} = 2.05$ ppm, $\delta\text{C} = 29.84$ ppm, 206.26), and d_4 -MeOH ($\delta\text{H} = 3.31$ ppm, $\delta\text{C} = 49.00$ ppm) were used as an internal reference. NMR spectra were assigned using information ascertained from COSY, HMBC, HSQC and NOESY experiments.

High resolution mass spectra (HRMS) were recorded on a Varian MAT CH7A or a Varian MAT 711 MS instrument by electron impact (EI) or electrospray ionization (ESI) techniques at the Department of Chemistry, Ludwig-Maximilians-University Munich.

Infrared spectra (IR) were recorded from 4000 cm^{-1} to 600 cm^{-1} on a PERKIN ELMER Spectrum BX II, FT-IR instrument. For detection, a SMITHS DETECTION DuraSampl^{IR} II Diamond ATR sensor was used. Samples were prepared as a neat film or a thin powder layer. IR data in frequency of absorption (cm^{-1}) is reported as follows: w = weak, m = medium, s = strong, br = broad or combinations thereof.

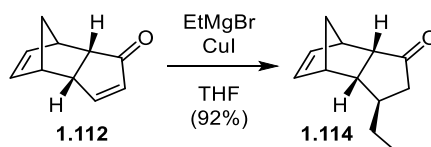
All yields are isolated unless otherwise specified.

6.2 Experimental data for chapter I



Enone 1.112: A solution of dicyclopentadiene (20.0 g, 151 mmol), Ac₂O (15.0 mL, 159 mmol), pyridine (6.20 mL, 76.8 mmol), TPP (100 mg, 0.160 mmol) and DMAP (400 mg, 3.27 mmol) in CH₂Cl₂ (50 mL) was stirred under an O₂-atmosphere at room temperature for 3 d while being irradiated with reptile lamp. The reaction was diluted with CH₂Cl₂ and washed with saturated aqueous NaHCO₃, aqueous HCl (1 M), saturated aqueous CuSO₄ and brine. The organic phase was dried over MgSO₄ and concentrated under reduced pressure. Purification by flash column chromatography (pentane:EtOAc 9:1, R_f = 0.2) gave enone **1.112** (14.7 g, 101 mmol, 67%) as a colorless oil.

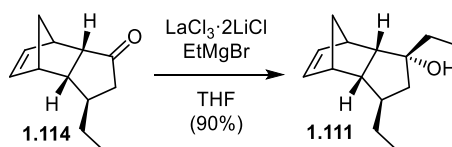
Data for 1.112: ¹H NMR (400 MHz, CDCl₃): δ (ppm) = 7.37 (dd, *J* = 5.7, 2.6 Hz, 1H, 6), 5.97 – 5.89 (m, 2H, 7 & 2), 5.76 (dd, *J* = 5.7, 3.0 Hz, 1H, 1), 3.46 – 3.36 (m, 1H, 8), 3.20 (s, 2H, 4), 2.95 (s, 2H, 9), 2.79 (t, *J* = 5.0 Hz, 1H, 5), 1.74 (d, *J* = 8.4 Hz, 1H, 3), 1.61 (d, *J* = 8.4 Hz, 1H, 3). ¹³C-NMR (101 MHz, CDCl₃): δ (ppm) = 210.9, 164.8, 137.0, 132.6, 132.5, 52.8, 50.3, 48.4, 45.1, 44.1. IR (ATR): ν_{max} (cm⁻¹) = 3060 (w), 2959 (m), 2930 (w), 2874 (w), 1727 (s), 1460 (w), 1402 (w), 1380 (w), 1340 (w), 1307 (w), 1231 (w), 1191 (m), 1158 (w), 1137 (w), 1089 (w), 1067 (w), 1022 (w), 957 (w), 909 (w), 860 (w), 779 (w), 730 (s). HRMS (EI): calc. for C₁₀H₁₀O [*M*]⁺: 146.0732, found: 146.0733.



Ketone 1.114:³⁵ CuI (426 mg, 2.24 mmol) was added to EtMgBr (0.9 M in THF, 73.8 mL, 66.4 mmol) at 0 °C and the mixture was stirred for 30 min at that temperature. The reaction was cooled to –78 °C and a solution of enone **1.112** (2.00 g, 13.7 mmol) in THF (60 mL) was added slowly. The reaction was stirred for 3 h at that temperature, quenched with saturated aqueous NH₄Cl and extracted with EtOAc. The combined organic phases were washed with brine, dried over MgSO₄ and concentrated under reduced pressure.

Purification of the resulting residue by flash column chromatography (pentane:EtOAc 95:5, $R_f = 0.2$) gave ketone **1.114** (2.22 g, 12.6 mmol, 92%) as a colorless oil.

Data for 1.114: $^1\text{H NMR}$ (400 MHz, CDCl_3): δ (ppm) = 6.15 (dd, $J = 5.8, 2.9$ Hz, 1H, 1), 6.11 (dd, $J = 5.8, 2.8$ Hz, 1H, 2), 3.15 (s, 1H, 4), 3.01 (s, 1H, 9), 2.91 (ddd, $J = 9.7, 4.8, 1.8$ Hz, 1H, 5), 2.61 (dt, $J = 9.4, 4.0$ Hz, 1H, 8), 2.19 (dd, $J = 18.6, 9.0$ Hz, 1H, 6), 1.92 (ddd, $J = 18.6, 6.7, 2.0$ Hz, 1H, 6), 1.66 – 1.56 (m, 1H, 7), 1.53 (d, $J = 8.2$ Hz, 1H, 3), 1.50 – 1.42 (m, 1H, 3), 1.41 – 1.32 (m, 2H, 10), 0.90 (t, $J = 7.3$ Hz, 3H, 11). $^{13}\text{C-NMR}$ (101 MHz, CDCl_3): δ (ppm) = 136.2, 135.4, 55.0, 52.4, 48.6, 48.1, 47.3, 46.3, 38.7, 30.7, 12.1. **IR (ATR):** ν_{max} (cm^{-1}) = 3062 (w), 2977 (w), 2872 (w), 1691 (s), 1580 (m), 1453 (w), 1348 (m), 1336 (m), 1297 (w), 1223 (m), 1195 (m), 1175 (m), 1125 (w), 1084 (w), 1052 (w), 1016 (m), 949 (w), 907 (m), 851 (m), 816 (w), 779 (s), 738 (m), 721 (s), 690 (w). **HRMS (EI):** calc. for $\text{C}_{12}\text{H}_{12}\text{O}$ $[M]^+$: 176.1201, found: 176.1204.

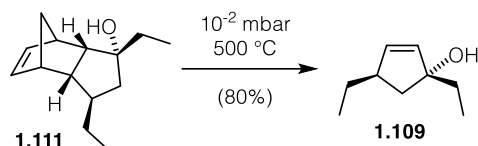


Tertiary alcohol 1.111: $\text{LaCl}_3 \cdot 2\text{LiCl}$ (0.6 M in THF, 21.0 mL, 12.60 mmol) was added to a solution of ketone **1.114** (2.22 g, 12.6 mmol) in THF (30 mL) and the solution was stirred for 1 h at room temperature. The solution was cooled to 0 °C, EtMgBr (0.60 M in THF, 28.0 mL, 25.2 mmol) was added slowly and the reaction was stirred for 1 h at 0 °C. The reaction was quenched by the addition of saturated aqueous NH_4Cl and extracted with Et_2O . The combined organic phases were washed with brine, dried over MgSO_4 and concentrated under reduced pressure to give tertiary alcohol **1.111** (2.33 g, 11.3 mmol, 90%) as a colorless oil.

Data for 1.111: $^1\text{H NMR}$ (400 MHz, CDCl_3): δ (ppm) = 6.42 (dd, $J = 5.8, 3.0$ Hz, 1H), 6.13 (dd, $J = 5.7, 3.2$ Hz, 1H), 2.77 (s, 2H, 4 & 9), 2.51 (dd, $J = 10.7, 3.8$ Hz, 1H, 5), 2.32 (td, $J = 10.5, 9.9, 4.1$ Hz, 1H, 8), 1.72 (dd, $J = 12.6, 5.7$ Hz, 1H, 6), 1.60 (d, $J = 7.9$ Hz, 1H, 3), 1.55 (q, $J = 7.4$ Hz, 2H, 12), 1.50 (s, 1H, OH), 1.45 (d, $J = 7.9$ Hz, 1H, 3), 1.39 – 1.25 (m, 3H, 10 & 6), 1.18 (ddt, $J = 12.6, 9.0, 6.2$ Hz, 1H, 7), 0.96 (t, $J = 7.4$ Hz, 3H, 13), 0.88 (t, $J = 7.4$ Hz, 3H, 11). $^{13}\text{C-NMR}$ (101 MHz, CDCl_3): δ (ppm) = 136.8, 135.4, 80.5, 57.9, 55.2, 54.9, 50.7, 45.4, 45.1, 41.9, 35.2, 28.3, 13.2, 9.0. **IR (ATR):** ν_{max} (cm^{-1}) = 3484 (w, b), 3057 (w), 2958 (s), 2920 (s), 2873 (m), 1459 (m), 1377 (m), 1345 (w), 1335

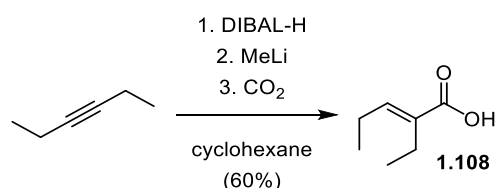
(w), 1304 (w), 1250 (w), 1229 (w), 1201 (w), 1147 (m), 1062 (w), 985 (m), 961 (m), 947 (m), 917 (w), 869 (w), 836 (w), 819 (w), 793 (w), 777 (w), 744 (s), 724 (w), 696 (w).

HRMS (EI): calc. for $C_{14}H_{22}O$ [M]⁺: 206.1665, found: 206.1622.



Cyclopentene 1.109: A solution of tertiary alcohol **1.111** (100 mg, 0.485 mmol) in Et₂O (2.0 mL) was subjected to flash vacuum pyrolysis. Purification of the resulting residue by flash column chromatography (pentane:Et₂O 3:1, R_f = 0.25) gave cyclopentene **1.109** (54 mg, 0.388 mmol, 80%) as a solution in pentane and ether.

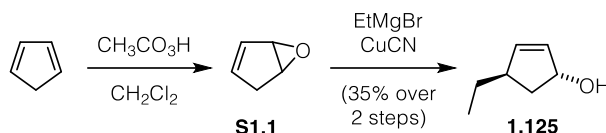
Data for 1.109: ¹H NMR (400 MHz, CDCl₃): δ (ppm) = 5.85 (dd, *J* = 5.6, 2.0 Hz, 1H), 5.68 (dd, *J* = 5.6, 2.4 Hz, 1H), 2.79 (dddt, *J* = 14.2, 8.1, 6.2, 2.2 Hz, 1H), 2.06 – 2.00 (m, 1H), 1.68 (qd, *J* = 7.5, 1.3 Hz, 2H), 1.54 – 1.49 (m, 1H), 1.43 (d, *J* = 2.7 Hz, 1H), 1.34 – 1.28 (m, 1H), 0.93 (dt, *J* = 9.7, 7.4 Hz, 6H). ¹³C-NMR (101 MHz, CDCl₃): δ (ppm) = 138.8, 135.4, 86.5, 46.0, 43.7, 33.8, 28.7, 12.5, 9.1. IR (ATR): ν_{max} (cm⁻¹) = 3374 (br), 2961 (vs), 2924 (s), 2875 (s), 2856 (m), 1730 (w), 1651 (w), 1461 (m), 1378 (m), 1326 (w), 1147 (w), 1030 (w), 996 (w), 834 (w), 757 (w). **MS (EI):** calc. for C₉H₁₅ [$M-OH$]⁺: 123.13, found: 123.12.



Carboxylic acid 1.108:³³ DIBAL-H (1 M, in PhMe, 25.0 mL, 25.0 mmol) was added slowly to a solution of 3-hexyne (2.84 mL, 25.0 mmol) in cyclohexane (12.5 mL) and the reaction was stirred at 60 °C for 2.5 h. The mixture was cooled to room temperature, MeLi (1.6 M in Et₂O, 15.6 mL, 25.0 mmol) was added and the solution was stirred for 15 min at room temperature. The reaction was cooled to -30 °C, purged with CO₂ and stirred for 3 h at that temperature. The mixture was poured into a mixture of aqueous conc. HCl and ice and extracted with Et₂O. The combined organic phases were dried over MgSO₄ and concentrated under reduced pressure. Purification of the resultant

residue by flash column chromatography (pentane:EtOAc 9:1, $R_f = 0.3$) gave carboxylic acid **1.108** (1.93 g, 15.0 mmol, 60%) as a colorless oil.

Data for 1.108: $^1\text{H NMR}$ (400 MHz, CDCl_3): δ (ppm) = 11.92 (s, 1H, OH), 6.87 (t, $J = 7.5$ Hz, 1H, 1), 2.31 (q, $J = 7.5$ Hz, 2H, 4), 2.23 (p, $J = 7.5$ Hz, 2H, 2), 1.06 (t, $J = 7.6$ Hz, 3H, 5), 1.02 (t, $J = 7.4$ Hz, 3H, 3). $^{13}\text{C-NMR}$ (101 MHz, CDCl_3): δ (ppm) = 173.8, 146.6, 132.9, 22.0, 19.8, 14.1, 13.4. **IR (ATR):** ν_{max} (cm^{-1}) = 2969 (m), 2937 (m), 2877 (m), 2654 (s), 2581 (s), 2539 (s), 1682 (h), 1638 (m), 1463 (s), 1418 (m), 1377 (s), 1304 (m), 1288 (m), 1166 (s), 1107 (s), 1072 (s), 1041 (s), 949 (s), 816 (s), 781 (s), 645 (s), 574 (s), 564 (s). **MS (EI):** calc. for $\text{C}_7\text{H}_{12}\text{O}_2$ [M] $^+$: 128.0832, found: 128.0849.

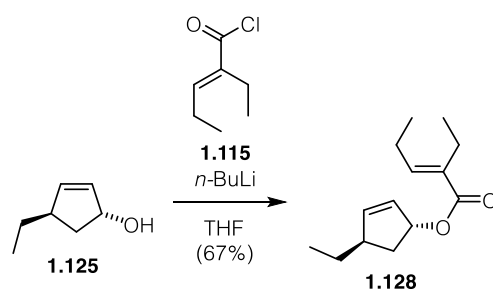


Allylic alcohol 1.125: Peracetic acid (40% in AcOH, 9.5 mL, 56.9 mmol) was added to a suspension of freshly distilled cyclopenta-1,3-diene (15.8 g, 238 mmol), Na_2CO_3 (30.8 g, 290 mmol) and NaOAc (390 mg, 4.76 mmol) in CH_2Cl_2 (150 mL) and the reaction was stirred for 1 h at room temperature. The CH_2Cl_2 was removed under reduced pressure and the resulting mixture was extracted with EtOAc. The combined organic phases were washed with brine, dried over MgSO_4 and concentrated under reduced pressure to give crude oxirane **S1.1** (3.19 g) as a colorless oil that was used in the next step without further purification.

EtMgBr (3.2 M in Et_2O , 15.8 mL, 50.6 mmol) was added slowly to a solution of CuCN (5.22 g, 58.3 mmol) in Et_2O (100 mL) at -40 °C and the mixture was stirred for 1 h at that temperature. A solution of crude oxirane **S1.1** (3.19 g) in Et_2O (10 mL) was added slowly and the reaction was allowed to warm to room temperature overnight. The mixture was extracted with Et_2O and the combined organic phases were washed with brine, dried over MgSO_4 and concentrated under reduced pressure. Purification of the resulting residue by flash column chromatography (pentane: Et_2O 3:1, $R_f = 0.2$) gave allylic alcohol **1.25** (2.21 g, 19.7 mmol, 35% over 2 steps) as a colorless oil.

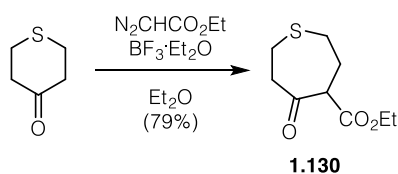
Data for 1.25: $^1\text{H NMR}$ (400 MHz, CDCl_3): δ (ppm) = 5.95 (ddd, $J = 5.6, 2.1, 0.8$ Hz, 1H), 5.82 (dt, $J = 5.6, 2.2$ Hz, 1H), 4.85 (dd, $J = 7.1, 2.4$ Hz, 1H), 2.80 (ddt, $J = 5.3, 4.4, 2.2$ Hz, 1H), 1.89 (dd, $J = 7.5, 2.7$ Hz, 1H), 1.79 (dd, $J = 7.0, 1.8$ Hz, 1H), 1.45 – 1.37 (m, 2H), 0.90 (t, $J = 7.4$ Hz, 3H). $^{13}\text{C-NMR}$ (101 MHz, CDCl_3): δ (ppm) = 140.1, 132.7, 77.4, 45.8, 40.3, 28.6, 12.2. **IR (ATR):** ν_{max} (cm^{-1}) = 3341 (m), 3055 (w), 2959 (vs), 2931 (s),

2874 (s), 2359 (w), 2341 (w), 2205 (w), 2167 (w), 2102 (w), 2049 (w), 2016 (w), 1981 (w), 1725 (m), 1616 (w), 1460 (s), 1408 (m), 1378 (s), 1325 (m), 1307 (m), 1264 (m), 1159 (m), 1112 (m), 1095 (m), 1069 (s), 1031 (vs), 1001 (vs), 948 (m), 907 (m), 867 (m), 832 (m), 795 (s), 777 (m), 750 (s), 726 (s), 709 (s), 668 (s), 645 (s), 622 (s), 615 (s), 607 (s), 597 (s), 580 (s), 572 (s), 564 (s), 556 (s). **MS (EI)**: calc. for C_7H_{11} $[M-OH]^+$: 95.08, found: 95.12.



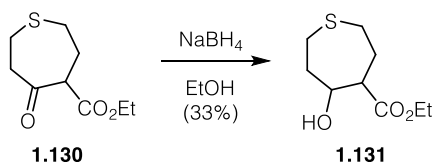
Allylic ester 1.128: *n*-BuLi (2.36 M in hexanes, 1.53 mL, 3.60 mmol) was added dropwise to an ice cooled solution of allylic alcohol **1.125** (337 mg, 3.00 mmol) in THF (17 mL) and the solution was stirred for 30 min at 0 °C. A solution of acid chloride **1.115** (540 mg, 3.68 mmol) in THF (5 mL) was added dropwise and the reaction was stirred for 2 h at 0 °C before the reaction was quenched with aqueous saturated NH_4Cl and extracted with Et_2O . The combined organic phases were washed with brine, dried over $MgSO_4$ and concentrated under reduced pressure. Purification of the resulting residue by flash column chromatography (hexanes: Et_2O 99:1, R_f = 0.2) gave allylic ester **1.128** (447 mg, 2.01 mmol, 67%) as a colorless oil.

Data for 1.128: 1H NMR (400 MHz, $CDCl_3$): δ (ppm) = 6.66 (t, J = 7.5 Hz, 1H), 6.05 (ddd, J = 5.6, 2.1, 0.8 Hz, 1H), 5.84 (dt, J = 5.6, 2.3 Hz, 1H), 5.74 (dq, J = 7.4, 2.8 Hz, 1H), 2.88 – 2.77 (m, 1H), 2.28 (q, J = 7.5 Hz, 2H), 2.17 (p, J = 7.5 Hz, 2H), 2.04 (ddd, J = 14.3, 7.7, 2.8 Hz, 1H), 1.85 (ddd, J = 14.4, 7.4, 5.1 Hz, 1H), 1.45 (ddd, J = 13.9, 7.6, 6.5 Hz, 1H), 1.38 – 1.30 (m, 1H), 1.04 (t, J = 7.6 Hz, 3H), 0.98 (t, J = 7.5 Hz, 3H), 0.92 (t, J = 7.4 Hz, 3H). ^{13}C -NMR (101 MHz, $CDCl_3$): δ (ppm) = 168.2, 143.4, 142.2, 133.9, 129.1, 80.3, 77.5, 76.8, 46.1, 36.9, 28.6, 21.8, 20.1, 14.2, 13.6, 12.23, 12.21.



Ethyl ester 1.130:³⁷ $\text{BF}_3 \cdot \text{OEt}_2$ (3.27 mL, 25.8 mmol) and ethyl diazoacetate (8.36 M in CH_2Cl_2 , 4.02 mL, 33.6 mmol) were sequentially added to a solution of tetrahydro-4*H*-thiopyran-4-one (3.00 g, 25.8 mmol) in Et_2O at $-30\text{ }^\circ\text{C}$ and the solution was stirred for 2 h at that temperature. The reaction was warmed to room temperature, quenched with aqueous K_2CO_3 (30%) and extracted with EtOAc. The combined organic phases were dried over Na_2SO_4 and concentrated under reduced pressure. Purification of the resultant residue by flash column chromatography (pentane:EtOAc 4:1, $R_f = 0.3$) gave ethyl ester **1.130** (4.14 g, 20.5 mmol, 79%) as a colorless oil.

Data for 1.130: $^1\text{H NMR}$ (400 MHz, CDCl_3): δ (ppm) = 12.84 (s, 1H), 4.18 (q, $J = 6.9$ Hz, 2H), 4.11 (q, $J = 7.1$ Hz, 2H), 3.74 (dd, $J = 10.5, 3.3$ Hz, 1H), 3.02 – 2.89 (m, 2H), 2.89 – 2.75 (m, 3H), 2.75 – 2.66 (m, 1H), 2.59 – 2.56 (m, 3H), 2.35 (m, 1H), 2.14 (m, 1H), 1.30 (t, $J = 7.1$ Hz, 3H), 1.25 (t, $J = 7.1$ Hz, 3H). $^{13}\text{C-NMR}$ (101 MHz, CDCl_3): δ (ppm) = 206.1, 169.7, 61.5, 60.9, 57.2, 47.1, 39.2, 32.8, 31.0, 29.1, 28.0, 26.9, 25.5, 14.4, 14.2. **IR (ATR):** ν_{max} (cm^{-1}) = 2980 (w), 2926 (w), 2363 (w), 1738 (vs), 1705 (vs), 1638 (w), 1465 (w), 1428 (m), 1368 (m), 1353 (m), 1325 (m), 1301 (s), 1268 (s), 1220 (vs), 1180 (vs), 1142 (vs), 1094 (s), 1055 (w), 1030 (s), 1005 (m), 963 (w), 932 (w), 852 (m), 838 (m), 818 (w), 728 (w), 650 (w), 607 (w), 591 (w), 575 (w), 567 (w), 560 (w). **HRMS (EI):** calc. for $\text{C}_9\text{H}_{14}\text{O}_3\text{S}$ [M]⁺: 202.0658, found: 202.0656.



Thiepane 1.131:³⁷ NaBH_4 (550 mg, 14.7 mmol) was added to a solution of ethyl ester **1.130** (2.38 g, 11.7 mmol) in EtOH (72 mL) at $-78\text{ }^\circ\text{C}$ and the mixture was stirred for 10 min at that temperature and for 2 h at room temperature. The reaction was quenched with saturated aqueous NaHCO_3 and the ethanol was removed under reduced pressure. The aqueous phase was extracted with EtOAc, the combined organic phases were washed with aqueous HCl (1 M), saturated aqueous NaHCO_3 and brine, dried over MgSO_4 and concentrated under reduced pressure. Purification of the resulting residue by flash column chromatography (pentane:EtOAc 5:1, $R_f = 0.35$) gave thiepane **1.131** (800 mg, 3.92 mmol, 33%) as a colorless oil.

Data for 1.131: $^1\text{H NMR}$ (400 MHz, CDCl_3): δ (ppm) = 4.36 (br, 1H, H-9), 4.17 (q, $J = 7.1$ Hz, 2H, H-2), 2.98 – 2.88 (m, 3H, H-4,6,10), 2.86 – 2.78 (m, 1H, H-7), 2.77 – 2.69 (m,

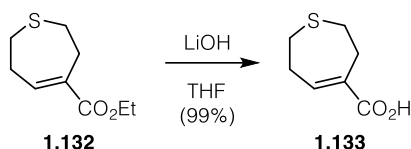
1H, H-6), 2.58 – 2.51 (m, 1H, H-7), 2.38 – 2.25 (m, 2H, H-5,8), 2.13 – 2.03 (m, 1H, H-5), 1.97 – 1.87 (m, 1H, H-8), 1.27 (t, $J = 7.1$ Hz, 2H, H-1). $^{13}\text{C-NMR}$ (101 MHz, CDCl_3): δ (ppm) = 176.4, 70.0, 61.0, 48.2, 38.1, 31.0, 27.2, 27.2, 14.3. **IR (ATR):** ν_{max} (cm^{-1}) = 3471 (m), 2923 (m), 1720 (vs), 1425 (m), 1368 (m), 1276 (m), 1207 (s), 1190 (s), 1156 (s), 1076 (m), 1031 (s), 931 (w), 908 (w), 858 (w), 628 (w), 601 (w), 581 (w), 567 (w). **HRMS (EI):** calc. for $\text{C}_9\text{H}_{16}\text{O}_3\text{S}$ [M] $^+$: 204.0815, found: 204.0816.



Alkene 1.132³⁷: NEt_3 (2.08 mL, 15.1 mmol) and MsCl (0.93 mL, 12.0 mmol) were sequentially added to an ice cooled solution of thiepane **1.131** (1.23 g, 6.02 mmol) in CH_2Cl_2 (40 mL) and the mixture was stirred for 4 h at that temperature before the reaction was quenched with saturated aqueous NaHCO_3 and extracted with CH_2Cl_2 . The combined organic phases were washed with brine, dried over MgSO_4 and concentrated under reduced pressure to give crude mesylate **S1.2** (1.74 g) that was used in the next step without further purification.

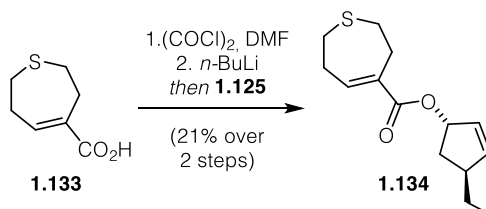
DBU (1.10 mL, 5.20 mmol) was added to a solution of crude mesylate **S1.2** (1.74 g) in THF (35 mL) and the reaction was stirred at room temperature for 2 h. The reaction mixture was diluted with EtOAc and washed with saturated aqueous NH_4Cl and brine. The organic phase was dried over MgSO_4 and concentrated under reduced pressure. Purification of the resulting residue by flash column chromatography (pentane: Et_2O 97:3, $R_f = 0.34$) gave alkene **1.132** (873 mg, 4.68 mmol, 76% over 2 steps) as a colorless oil.

Data for 1.132: $^1\text{H NMR}$ (400 MHz, CDCl_3): δ (ppm) = 7.17 (t, $J = 6.8$ Hz, 1H), 4.18 (q, $J = 7.1$ Hz), 3.03 – 2.99 (m, 2H), 2.80 – 2.74 (m, 2H), 2.67 – 2.62 (m, 4H), 1.29 (t, $J = 7.1$ Hz, 3H). $^{13}\text{C-NMR}$ (101 MHz, CDCl_3): δ (ppm) = 167.9, 142.5, 135.9, 61.0, 32.6, 31.1, 28.2, 27.1, 14.4. **IR (ATR):** ν_{max} (cm^{-1}) = 2979 (w), 2907 (w), 2359 (w), 1703 (vs), 1645 (w), 1442 (w), 1377 (w), 1283 (m), 1254 (s), 1205 (s), 1173 (w), 1154 (w), 1094 (w), 1057 (m), 1029 (w), 921 (w), 864 (w), 752 (w), 668 (w), 628 (w), 601 (w), 582 (w), 568 (w). **HRMS (EI):** calc. for $\text{C}_9\text{H}_{14}\text{O}_2\text{S}$ [M] $^+$: 186.0709, found: 186.0705.



Acid 1.133: An aqueous solution of LiOH (1 M, 40.3 mL, 40.3 mmol) was added to a solution of alkene **1.132** (150 mg, 0.805 mmol) in THF (53 mL) and the solution was stirred at room temperature for 17 h. The reaction acidified with aqueous HCl (1 M) and extracted with EtOAc. The combined organic phases were dried over Na₂SO₄ and concentrated under reduced pressure. Purification of the resulting residue by flash column chromatography (pentane:Et₂O 3:2, R_f = 0.3) gave acid **1.133** (127 mg, 0.799 mmol, 99%) as a colorless solid.

Data for 1.133: ¹H NMR (400 MHz, CDCl₃): δ (ppm) = 9.40 (br, 1H), 7.33 (t, *J* = 6.7 Hz, 1H), 3.04 – 2.99 (m, 2H), 2.86 – 2.77 (m, 2H), 2.71 – 2.64 (m, 4H). ¹³C-NMR (101 MHz, CDCl₃): δ (ppm) = 172.8, 145.7, 134.9, 32.8, 30.7, 28.2, 26.9. IR (ATR): ν_{max} (cm⁻¹) = 2359 (m), 1683 (m), 668 (m), 600 (m), 590 (m), 568 (vs). HRMS (EI): calc. for C₇H₁₀O₂S [M]⁺: 158.0396, found: 158.0399.

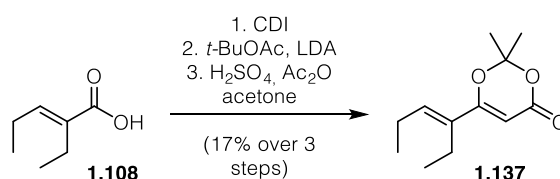


Allylic ester 1.134: DMF (1 drop) was added to an ice cooled solution of acid **1.133** (107 mg, 0.676 mmol) and oxalyl chloride (0.08 mL, 0.946 mmol) in CH₂Cl₂ (5.5 mL) and the reaction mixture was stirred for 15 min at that temperature and for 1 h at room temperature. Evaporation of the volatiles under reduced pressure gave crude acid chloride **S1.3** that was used in the next step without further purification.

n-BuLi (2.36 M in hexanes, 0.30 mL, 0.686 mmol) was added dropwise to an ice cooled solution of allylic alcohol **1.133** (63 mg, 0.563 mmol) in THF (3.5 mL) and the solution was stirred for 30 min at 0 °C. The mixture was added to an ice cooled solution of crude acid chloride **S1.3** in THF (5 mL) and the reaction was stirred at that temperature for 2 h. The reaction was quenched with MeOH (0.5 mL) and aqueous NaOH (1 M) and extracted with Et₂O. The combined organic phases were dried over MgSO₄ and concentrated under reduced pressure. Purification of the resulting residue by flash column chromatography

(pentane:Et₂O 95:5, R_f= 0.32) gave allylic ester **1.134** (36 mg, 0.143 mmol, 21% over 2 steps) as a colorless oil.

Data for 1.134: ¹H NMR (400 MHz, CDCl₃): δ (ppm) = 7.13 (t, *J* = 6.7 Hz, 1H), 6.07 (ddd, *J* = 5.6, 2.1, 0.8 Hz, 1H), 5.83 (dt, *J* = 5.7, 2.3 Hz, 1H), 5.71 (dtd, *J* = 7.3, 3.0, 2.2 Hz, 1H), 3.02 – 2.96 (m, 2H), 2.85 – 2.78 (m, 1H), 2.78 – 2.72 (m, 2H), 2.66 – 2.61 (m, 4H), 2.03 (ddd, *J* = 14.3, 7.6, 2.7 Hz, 1H), 1.85 (ddd, *J* = 14.4, 7.4, 5.2 Hz, 1H), 1.50 – 1.40 (m, 1H), 1.32 (dq, *J* = 13.6, 7.4 Hz, 1H), 0.92 (t, *J* = 7.4 Hz, 3H). ¹³C-NMR (101 MHz, CDCl₃): δ (ppm) = 168.0, 142.6, 136.1, 128.8, 80.9, 46.1, 36.8, 32.7, 31.2, 28.5, 28.3, 27.1, 12.2. IR (ATR): ν_{max} (cm⁻¹) = 3050 (w), 2958 (m), 2925 (m), 2873 (w), 2358 (w), 2333 (w), 2173 (w), 2148 (w), 2102 (w), 2048 (w), 2016 (w), 1968 (w), 1702 (vs), 1644 (w), 1460 (w), 1439 (w), 1420 (w), 1379 (w), 1367 (w), 1337 (w), 1296 (w), 1283 (m), 1252 (vs), 1204 (s), 1154 (m), 1093 (w), 1053 (m), 1021 (w), 968 (w), 943 (w), 911 (w), 887 (w), 831 (w), 800 (w), 752 (m), 667 (w), 646 (w), 632 (w), 623 (w), 614 (w), 607 (w), 597 (w), 580 (w), 570 (w), 556 (w). HRMS (EI): calc. for C₁₄H₂₀O₂S [*M*]⁺: 252.1179, found: 252.1177.



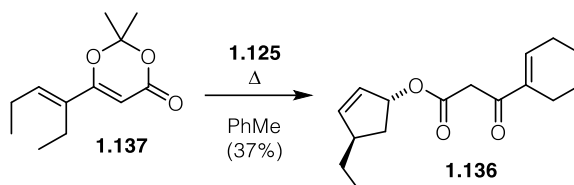
Dioxanone 1.137: CDI (151 mg, 0.936 mmol) was added to a solution of acid **1.108** (100 mg, 0.780 mmol) in THF (5 mL) and the reaction was stirred at room temperature for 17 h before it was diluted with saturated aqueous NaHCO₃ and extracted with Et₂O. The combined organic phases were dried over MgSO₄ and concentrated under reduced pressure to give crude amide **S1.4** that was used in the next step without further purification.

n-BuLi (2.36 M in hexanes, 0.37 mL, 0.87 mmol) was added dropwise to an ice cooled solution of DIPA (0.12 mL, 0.87 mmol) in THF (5 mL) and the solution was stirred for 30 min at 0 °C. The reaction mixture was cooled to –78 °C, *t*-BuOAc (0.12 mL, 0.87 mmol) was added dropwise and the resulting solution was stirred at –78 °C for 30 min. A solution of crude amide **S1.4** in THF (5 mL) was added and the reaction mixture was allowed to warm to room temperature overnight before the reaction was diluted with saturated aqueous NH₄Cl (5 mL) and aqueous HCl (1 M, 5 mL) and extracted with EtOAc. The combined organic phases were washed with brine, dried over MgSO₄ and

concentrated under reduced pressure. Purification of the resulting residue gave crude β -keto ester **S.1.5** (51 mg) that was used in the next step without further purification.

H_2SO_4 (conc. 20 μL , 0.448 mmol) was added to an ice cooled solution of crude β -keto ester **S.1.5** (51 mg) and Ac_2O (0.7 mL, 7.41 mmol) in acetone (0.7 mL) and the reaction mixture was slowed to warm to room temperature overnight. The reaction was diluted with aqueous K_2CO_3 and stirred for 30 min at room temperature before it was extracted with EtOAc. The combined organic phases were washed with brine, dried over MgSO_4 and concentrated under reduced pressure. Purification of the resulting residue by flash column chromatography (pentane: Et_2O 6:1, R_f = 0.3) gave dioxanone **1.137** (28 mg, 0.133 mmol, 59%) as a colorless oil.

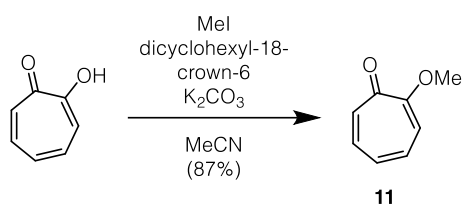
Data for 1.137: $^1\text{H NMR}$ (400 MHz, CDCl_3): δ (ppm) = 6.32 (t, J = 7.5 Hz, 1H), 5.45 (s, 1H), 2.24 (p, J = 7.5 Hz, 4H), 1.71 (s, 6H), 1.08 – 1.01 (m, 6H). $^{13}\text{C-NMR}$ (101 MHz, CDCl_3): δ (ppm) = 165.4, 162.8, 139.3, 133.3, 106.1, 91.3, 25.1, 21.8, 19.8, 14.0, 13.7. **IR (ATR):** ν_{max} (cm^{-1}) = 2970 (w), 2937 (w), 2876 (w), 2360 (w), 2340 (w), 1726 (vs), 1633 (m), 1593 (m), 1457 (w), 1392 (m), 1376 (m), 1339 (m), 1280 (m), 1254 (m), 1206 (m), 1147 (w), 1065 (w), 1039 (w), 1019 (w), 997 (w), 962 (w), 905 (w), 865 (w), 809 (w), 695 (w), 668 (w), 601 (w), 590 (w), 568 (w), 560 (w).



β -Keto ester 1.136: A solution of dioxanone **1.137** (90 mg, 0.427 mmol) and allylic alcohol **1.125** (47 mg, 0.427 mmol) in PhMe (10 mL) was stirred at 100 °C overnight. Evaporation of the volatiles under reduced pressure and purification of the resulting residue by flash column chromatography (pentane: Et_2O 99:1, R_f = 0.2) gave β -keto ester **1.136** (42 mg, 0.159 mmol, 37%) as a colorless oil. The product was obtained as mixture of tautomers.

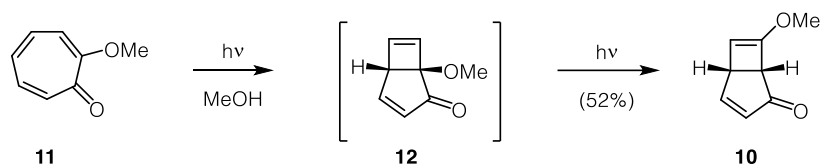
Data for 1.136: $^1\text{H NMR}$ (400 MHz, CDCl_3): δ (ppm) = 12.30 (s, 0H), 6.51 (d, J = 7.2 Hz, 1H), 6.45 (t, J = 7.4 Hz, 0H), 6.10 (dd, J = 5.6, 2.1 Hz, 0H), 5.84 (dt, J = 5.2, 2.3 Hz, 0H), 5.80 (dt, J = 5.2, 2.3 Hz, 1H), 5.73 (dt, J = 7.4, 2.4 Hz, 1H), 5.68 – 5.65 (m, 0H), 3.68 (s, 1H), 3.66 (s, 2H), 2.78 (dddd, J = 8.9, 6.6, 4.8, 2.8 Hz, 1H), 2.29 (qd, J = 7.5, 3.4 Hz, 5H), 2.20 (ddd, J = 15.0, 10.6, 7.2 Hz, 1H), 2.04 (ddd, J = 15.0, 7.6, 2.6 Hz, 1H), 1.81 (ddd, J = 14.5, 7.4, 5.3 Hz, 1H), 1.45 – 1.40 (m, 1H), 1.35 – 1.24 (m, 2H), 1.08 (t, J = 7.6

Hz, 4H), 1.03–0.98 (m, 1H), 0.92 (dt, $J = 11.5, 7.4$ Hz, 9H). **$^{13}\text{C-NMR}$ (101 MHz, CDCl_3):** δ (ppm) = 193.9, 168.3, 146.2, 143.0, 142.7, 128.3, 81.4, 46.0, 45.4, 36.6, 28.4, 22.3, 18.9, 13.9, 13.5, 12.2. **IR (ATR):** ν_{max} (cm^{-1}) = 2965 (m), 2934 (m), 2875 (m), 2360 (w), 2340 (w), 1735 (vs), 1671 (s), 1636 (m), 1461 (m), 1413 (m), 1366 (m), 1318 (m), 1298 (m), 1262 (m), 1237 (m), 1191 (m), 1150 (m), 1094 (m), 1068 (m), 1035 (m), 975 (m), 895 (w), 801 (m), 753 (w), 667 (w), 628 (w), 601 (w), 582 (w), 567 (w). **HRMS (EI):** calc. for $\text{C}_{16}\text{H}_{24}\text{O}_3$ [M] $^+$: 264.1720, found: 264.1719.



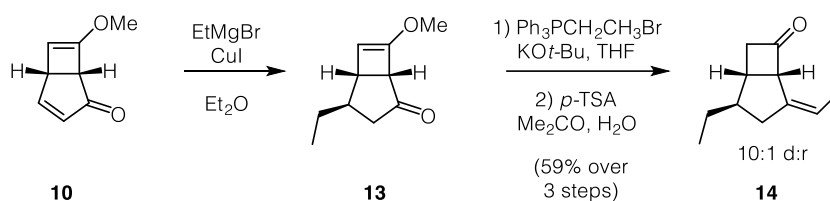
α -Tropolone methyl ester (11**)¹⁷²:** Methyl iodide (16.0 mL, 257 mmol) was added to a suspension of α -tropolone (6.43 g, 52.7 mmol), potassium carbonate (21.8 g, 158 mmol) and dicyclohexyl-18-crown-6 (2.00 g, 5.37 mmol) in acetonitrile (265 mL). The resulting mixture was stirred at 82 °C overnight, then cooled to room temperature, filtered and concentrated. The resulting residue was redissolved in methylene chloride and washed with saturated aqueous potassium carbonate. The organic phase was dried over magnesium sulfate and concentrated under reduced pressure. Purification by flash column chromatography (ethyl acetate) gave α -tropolone methyl ester **11** as a white solid (6.26 g, 46.0 mmol, 87%).

Data for 11: R_f : 0.2 (EtOAc); **$^1\text{H-NMR}$ (400 MHz, CDCl_3):** δ (ppm) = 7.26-7.23 (m, 2H), 7.09 (ddt, $J = 10.9, 9.9, 1.0$ Hz, 1H), 6.90-6.84 (m, 1H), 6.74 (dt, $J = 9.9, 0.7$ Hz, 1H), 3.96 (s, 3H). **$^{13}\text{C-NMR}$ (100 MHz, CDCl_3):** δ (ppm) = 180.7, 165.6, 137.1, 136.8, 132.8, 128.1, 112.5, 56.5. **IR (ATR):** ν_{max} (cm^{-1}) = 3476 (*br w*), 2942 (*w*), 1624 (*m*), 1590 (*s*), 1568 (*vs*), 1494 (*s*), 1470 (*s*), 1400 (*m*), 1278 (*s*), 1264 (*s*), 1231 (*m*), 1211 (*vs*), 1164 (*s*), 1078 (*s*), 986 (*m*), 948 (*m*), 906 (*m*), 870 (*m*), 851 (*w*), 769 (*s*), 706 (*s*), 665 (*m*). **HRMS (EI):** calc. for $\text{C}_8\text{H}_8\text{O}_2$ [M] $^+$: 136.0524, found: 136.0515.



Bicycle 10³²: A stirred solution of α -tropolone methyl ester **11** (2.00 g, 14.7 mmol) in MeOH (160 mL) was irradiated at room temperature for 13 h using a medium pressure mercury lamp (150 W) in an immersion well photoreactor containing a Pyrex[®] filter. After evaporation of the solvent, the crude product was purified by flash column chromatography (hexanes:EtOAc 5:1) to afford bicycle **10** (1.05 g, 7.71 mmol, 52%) as a colorless oil.

Data for 10: Rf: 0.4 (hexanes:EtOAc 5:1); **¹H-NMR (400 MHz, CDCl₃)**: δ (ppm) = 7.69 (dd, J = 5.8, 2.3 Hz, 1H), 5.98 (d, J = 5.7 Hz, 1H), 5.01 (s, 1H), 3.62 (d, J = 2.9 Hz, 1H), 3.60 (s, 3H), 3.58 (t, J = 2.6 Hz, 1H). **¹³C-NMR (100 MHz, CDCl₃)**: δ (ppm) = 204.9, 165.1, 155.6, 133.2, 100.9, 56.3, 54.5, 40.8. **IR (ATR)**: ν_{max} (cm⁻¹) = 2937 (*br w*), 1737 (*w*), 1693 (*vs*), 1628 (*vs*), 1573 (*w*), 1453 (*w*), 1435 (*w*), 1342 (*w*), 1296 (*s*), 1259 (*m*), 1208 (*m*), 1175 (*m*), 1150 (*w*), 1118 (*w*), 1078 (*m*), 1021 (*s*), 998 (*m*), 972 (*w*), 956 (*m*), 930 (*w*), 898 (*w*), 851 (*w*), 790 (*s*), 748 (*s*), 708 (*m*). **HRMS (EI)**: calc. for C₈H₈O₂ [*M*]⁺: 136.0524, found: 136.0520.



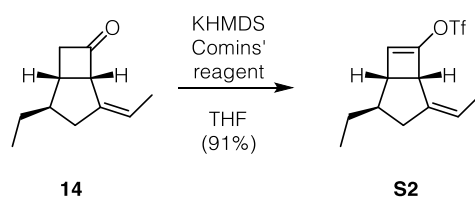
Ketone 13: EtMgBr (3.0 M in Et₂O, 15.31 mL, 45.92 mmol) was added dropwise to solution of CuI (4.37 g, 22.96 mmol) in Et₂O (190 mL) cooled to -5 °C and stirred for 30 min at that temperature. The solution was cooled to -78 °C and a solution of enone **10** (1.56 g, 11.48 mmol) in Et₂O (62 mL) was added dropwise. The reaction was stirred for 2 h at -78 °C before it was quenched with saturated aqueous NH₄Cl and extracted

with Et₂O. The combined organic phases were washed with brine, dried over MgSO₄ and concentrated under reduced pressure to give ketone **13**, which was used in the next step without further purification.

Enol ether S1: KO^tBu (3.86 g, 34.44 mmol) was added to an ice cooled suspension of ethyl triphenylphosphonium bromide (12.78 g, 34.44 mmol) in THF (67 mL) and stirred for 30 min at that temperature. A solution of crude ketone **13** in THF (38 mL) was added dropwise and the reaction was stirred for 2 h at room temperature before it was quenched with saturated aqueous NH₄Cl and extracted with Et₂O. The organic phase was dried over MgSO₄ and concentrated under reduced pressure to give crude enol **S1** ether which was used in the next step without further purification.

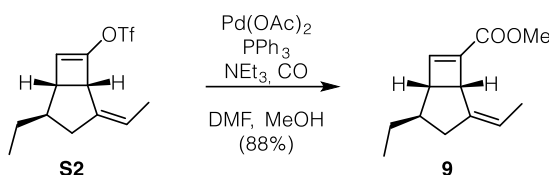
Ketone 14: A solution of *p*-TSA·H₂O (360 mg, 1.89 mmol) in water (80 mL) was added to a solution of crude enol ether **S1** in acetone (80 mL) and stirred for 2 h at room temperature. The reaction mixture was extracted with Et₂O. The combined organic phases were washed with saturated aqueous NaHCO₃ and brine and dried over MgSO₄. Evaporation of the solvent and purification by flash column chromatography (hexanes:Et₂O 94:6) afforded ketone **14** (1.12 g, 6.81 mmol, 59% over 3 steps, *Z*:*E* = 10:1 mixture of diastereomers at the double bond) as a colorless oil.

Data for 14: *Rf*: 0.4 (hexanes:Et₂O 94:6); ¹H-NMR (400 MHz, CDCl₃): δ (ppm) = 5.46 (qt, *J* = 7.0, 1.7 Hz, 1H), 4.17 – 4.05 (m, 1H), 3.15 (ddd, *J* = 18.1, 8.7, 4.9 Hz, 1H), 2.73 (ddd, *J* = 17.8, 5.6, 3.0 Hz, 1H), 2.69 – 2.60 (m, 2H), 2.20 (d, *J* = 15.7 Hz, 1H), 1.92 – 1.81 (m, 1H), 1.23 (dq, *J* = 17.1, 6.9 Hz, 2H), 0.89 (t, *J* = 7.4 Hz, 3H). ¹³C-NMR (100 MHz, CDCl₃): δ (ppm) = 207.6, 138.0, 120.0, 66.5, 51.2, 45.8, 37.7, 35.3, 27.8, 15.3, 12.2. IR (ATR): ν_{max} (cm⁻¹) = 2960 (*m*), 2918 (*m*), 1778 (*s*), 1724 (*w*), 1460 (*w*), 1381 (*w*), 1170 (*w*), 1079 (*m*), 816 (*w*), 777 (*w*). HRMS (EI): calc. for C₁₁H₁₅O [*M-H*]⁺: 163.1117, found: 163.1118.



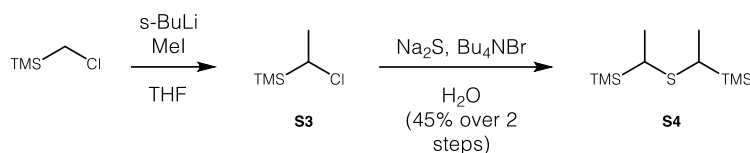
Vinyl triflate S2: KHMDS (0.5 M in toluene, 10.8 mL, 5.42 mmol) was added to a solution of ketone **14** in THF (36 mL) at $-78\text{ }^{\circ}\text{C}$ and stirred for 30 min at $0\text{ }^{\circ}\text{C}$ before a solution of Comins' reagent (2.13 g, 5.42 mmol) in THF (32 mL) was added slowly at $-78\text{ }^{\circ}\text{C}$. The solution was stirred for 2 h at $0\text{ }^{\circ}\text{C}$, quenched with saturated aqueous NaHCO_3 and extracted with Et_2O . The combined organic phases were washed with brine, dried over MgSO_4 and concentrated. Purification by flash column chromatography (hexanes: NEt_3 999:1) on silica gave vinyl triflate **S2** (1.21 g, 4.07 mmol, 91%, 10:1 mixture of diastereomers at the double bond) as a colorless liquid.

Data for S2: Rf: 0.4 (hexanes); $^1\text{H-NMR}$ (400 MHz, CDCl_3): δ (ppm) = 5.47 (d, $J = 10.3$ Hz, 2H), 4.02 – 3.97 (m, 1H), 2.81 (d, $J = 3.2$ Hz, 1H), 2.64 (ddd, $J = 16.7, 5.5, 2.4$ Hz, 1H), 2.04 (d, $J = 15.1$ Hz, 1H), 1.71 – 1.64 (m, 4H), 1.13 (pd, $J = 7.2, 2.2$ Hz, 2H), 0.87 (t, $J = 7.3$ Hz, 3H). $^{13}\text{C-NMR}$ (100 MHz, CDCl_3): δ (ppm) = 139.4, 135.1, 121.7, 119.0, 51.2, 45.9, 38.3, 35.3, 26.3, 14.7, 12.0. IR (ATR): ν_{max} (cm^{-1}) = 2962 (w), 2924 (w), 2860 (w), 1623 (m), 1424 (s), 1382 (w), 1277 (w), 1248 (m), 1205 (s), 1180 (m), 1138 (s), 1098 (w), 1076 (w), 1062 (w), 985 (w), 928 (s), 910 (m), 860 (s), 806 (m), 769 (w), 717 (m), 670 (w). HRMS (EI): calc. for $\text{C}_{12}\text{H}_{15}\text{F}_3\text{O}_3^{32}\text{S}$ [M] $^+$: 296.0694, found: 296.0701.



Methyl ester 9: Pd(OAc)_2 (36.6 mg, 0.163 mmol), PPh_3 (85.4 mg, 0.326 mmol) and NEt_3 (1.13 mL, 8.14 mmol) were sequentially added to a stirred solution of vinyl triflate **S2** (1.21 g, 4.07 mmol) in DMF (70 mL) and MeOH (70 mL). The solution was purged with CO gas and stirred for 1 h at $50\text{ }^{\circ}\text{C}$ under 1 atm CO pressure. The reaction mixture was cooled to room temperature and extracted with Et_2O . The combined organic phases were washed with brine, dried over MgSO_4 and concentrated. Purification by flash column chromatography (hexanes: Et_2O : NEt_3 969:30:1) gave methyl ester **9** (742 mg, 3.60 mmol, 88%) as a colorless liquid.

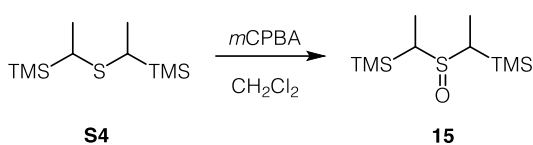
Data for 9: Rf: 0.3 (hexanes:Et₂O 95:5); **¹H-NMR (400 MHz, CDCl₃):** δ (ppm) = 6.81 (s, 1H), 5.43 – 5.35 (m, 1H), 3.89 – 3.84 (m, 1H), 3.70 (s, 3H), 2.95 (d, *J* = 3.2 Hz, 1H), 2.58 (ddd, *J* = 13.7, 5.7, 2.8 Hz, 1H), 1.98 (d, *J* = 15.0 Hz, 1H), 1.74 (dd, *J* = 6.8, 2.6 Hz, 3H), 1.72 – 1.64 (m, 1H), 1.12 (p, *J* = 7.4 Hz, 2H), 0.86 (t, *J* = 7.3 Hz, 3H). **¹³C-NMR (100 MHz, CDCl₃):** δ (ppm) = 162.5, 148.9, 139.0, 138.0, 119.7, 51.3, 50.9, 46.1, 38.3, 36.0, 26.2, 14.7, 12.0. **IR (ATR):** ν_{\max} (cm⁻¹) = 2955 (*m*), 2859 (*w*), 1725 (*s*), 1604 (*w*), 1459 (*w*), 1435 (*m*), 1380 (*w*), 1309 (*m*), 1276 (*m*), 1247 (*m*), 1213 (*w*), 1190 (*w*), 1164 (*m*), 1125 (*m*), 1105 (*m*), 988 (*w*), 838 (*s*), 753 (*m*). **HRMS (EI):** calc. for C₁₃H₁₈O₂ [*M*]⁺: 206.1307, found: 206.1291.



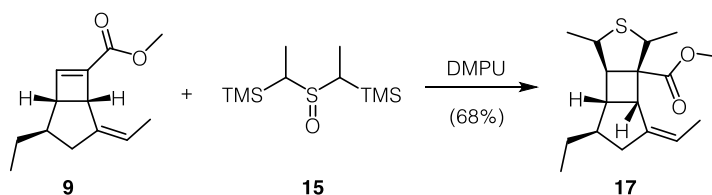
(1-chloroethyl)trimethylsilane (S3): *s*-BuLi (1.4 M in cyclohexane, 51.2 mL, 71.66 mmol) was added slowly to a solution of (chloromethyl)trimethylsilane (10 mL, 71.66 mmol) in THF (235 mL) at -78 °C and the reaction was stirred for 30 min before methyl iodide (4.4 mL, 71.66 mmol) was slowly added. The cloudy mixture was stirred for 20 min at that temperature and then warmed to room temperature. The reaction mixture was diluted with ether, washed five times with water and dried over MgSO₄. Most of the solvent was first removed at 300 mbar on a rotary evaporator (bath temperature 40 °C) and the residual solvent was distilled over a vigreux column to give (1-chloroethyl)trimethylsilane **S3** as a colorless liquid which was used in the next step without further purification.

Thioether S4: Tetrabutylammonium bromide (1.39 g, 4.30 mmol), water (15 mL) and sodium sulphide nonahydrate (8.61 g, 35.83 mmol) were added to (1-chloroethyl)-trimethylsilane **S3** and the resulting mixture was stirred at 100 °C overnight in a pressure tube. The mixture was cooled to room temperature and extracted with hexanes. The combined organic phases were washed with saturated aqueous NaHCO₃, dried over MgSO₄ and evaporated to dryness. Purification by flash column chromatography (hexanes) gave thioether **S4** (3.80 g, 16.19 mmol, 45% over 2 steps, 1:1 mixture of diastereomers) as a colorless liquid.

Data for S4: Rf: 0.3 (hexanes); **¹H-NMR (400 MHz, CDCl₃):** δ (ppm) = 2.06 (q, *J* = 7.2 Hz, 1H), 1.82 (q, *J* = 7.4 Hz, 1H), 1.34 (d, *J* = 7.5 Hz, 3H), 1.20 (d, *J* = 7.1 Hz, 3H), 0.06 (s, 9H), 0.06 (s, 9H). **¹³C-NMR (100 MHz, CDCl₃):** δ (ppm) = 29.0, 22.0, 18.5, 15.8, -2.8, -2.9. **IR (ATR):** ν_{max} (cm⁻¹) = 2954 (*m*), 2924 (*w*), 2898 (*w*), 2863 (*w*), 1446 (*w*), 1405 (*w*), 1372 (*w*), 1246 (*s*), 1147 (*w*), 1118 (*w*), 1052 (*w*), 1004 (*w*), 955 (*w*), 830 (*vs*), 751 (*s*), 716 (*m*), 688 (*m*). **HRMS (EI):** calc. for C₁₀H₂₆³²SSi₂ [*M*]⁺: 234.1294, found: 234.1287.

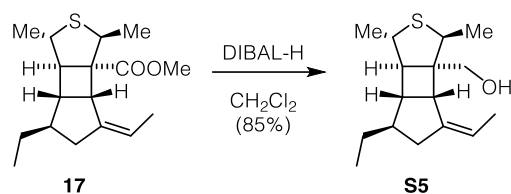


Sulfoxide 15: A solution of *m*CPBA (3.35 g, 19.47 mmol) in CH₂Cl₂ (42 mL) was added to a solution of thioether **S4** (4.15 g, 17.69 mmol) in CH₂Cl₂ (42 mL) at -78 °C. After stirring at -78 °C for 30 min, the reaction was warmed to 0 °C and stirred at 0 °C for 2 min. The reaction mixture was diluted with CH₂Cl₂, washed twice with saturated aqueous NaHCO₃ and dried over MgSO₄. Evaporation of the solvent under reduced pressure gave sulfoxide **15** as a colorless oil that was used without further purification.



Tricyclic 17: A mixture of crude sulfoxide **15** (4.42 g) and DMPU (1.8 mL) was added dropwise to a solution of methyl ester **9** (604 mg, 2.93 mmol) in DMPU (4.3 mL) at 100 °C. The reaction was stirred for further 10 min at 100 °C, cooled to room temperature, diluted with ether and washed with water and brine. The organic phase was dried over magnesium sulfate and evaporated to dryness. Flash column chromatography (hexanes:Et₂O 94:6 and hexanes:Et₂O 96:4) gave tricyclic **17** (589 mg, 2.00 mmol, 68%) as a colorless oil that crystallized upon standing at -20 °C.

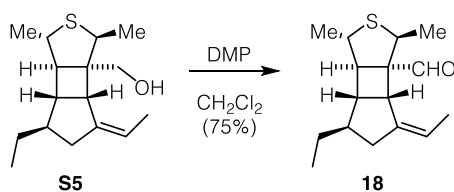
Data for 17: *Rf*: 0.3 (hexanes:Et₂O 94:6); ¹H-NMR (400 MHz, CDCl₃): δ (ppm) = 5.39 (q, *J* = 6.3 Hz, 1H), 3.71 (q, *J* = 6.5, 6.1 Hz, 1H), 3.59 (s, 3H), 3.28 (d, *J* = 7.2 Hz, 1H), 2.96 (q, *J* = 7.0 Hz, 1H), 2.90 (d, *J* = 5.0 Hz, 1H), 2.70 – 2.59 (m, 1H), 2.16 – 2.11 (m, 1H), 2.02 (d, *J* = 15.1 Hz, 1H), 1.66 (q, *J* = 7.2 Hz, 1H), 1.55 (d, *J* = 3.2 Hz, 3H), 1.53 (d, *J* = 3.4 Hz, 3H), 1.27 (d, *J* = 7.1 Hz, 3H), 1.03 (p, *J* = 7.3 Hz, 2H), 0.80 (t, *J* = 7.3 Hz, 3H). ¹³C-NMR (100 MHz, CDCl₃): δ (ppm) = 174.0, 142.5, 119.2, 61.2, 56.5, 51.6, 49.0, 46.4, 45.2, 45.0, 39.0, 37.1, 26.9, 23.1, 15.0, 14.2, 12.2. IR (ATR): ν_{max} (cm⁻¹) = 2961 (*m*), 2940 (*m*), 2914 (*m*), 2884 (*w*), 2850 (*w*), 1725 (*s*), 1682 (*w*), 1456 (*m*), 1432 (*m*), 1379 (*m*), 1328 (*w*), 1271 (*s*), 1226 (*s*), 1206 (*s*), 1191 (*m*), 1170 (*m*), 1150 (*w*), 1115 (*m*), 1067 (*s*), 1023 (*m*), 986 (*w*), 942 (*w*), 912 (*m*), 846 (*w*), 796 (*w*), 761 (*m*), 733 (*m*), 667 (*w*). HRMS (EI): calc. for C₁₇H₂₆O₂³²S [*M*]⁺: 294.1654, found: 294.1645.



Alcohol S5: DIBAL-H (1 M in PhMe, 3.76 mL, 3.76 mmol) was added dropwise to a stirred solution of tricyclic **17** (539 mg, 1.83 mmol) in CH₂Cl₂ (26 mL) at -78 °C and the

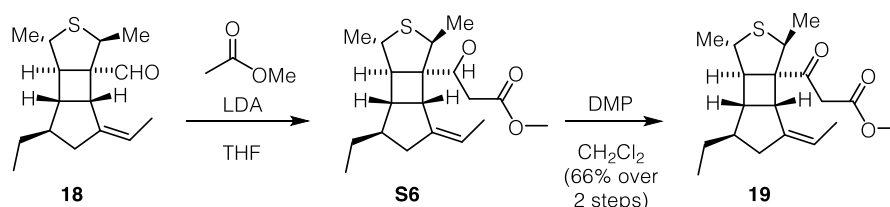
reaction was stirred for 1 h at $-78\text{ }^{\circ}\text{C}$ and 1 h at room temperature. The reaction was quenched by the addition of 1M HCl and stirred until a clear solution formed. The resulting mixture was extracted with CH_2Cl_2 and the combined organic phases were washed with brine, dried over MgSO_4 and evaporated to dryness. Purification by flash column chromatography (hexanes: Et_2O 75:25) gave alcohol **S5** (454 mg, 1.70 mmol, 93%) as a colorless oil that solidified upon standing at $-20\text{ }^{\circ}\text{C}$.

Data for S5: Rf: 0.3 (hexanes: Et_2O 75:25); $^1\text{H-NMR}$ (400 MHz, CDCl_3): δ (ppm) = 5.49 – 5.36 (m, 1H), 3.75 (q, J = 6.7 Hz, 1H), 3.62 – 3.45 (m, 2H), 3.06 (d, J = 7.0 Hz, 1H), 2.90 (q, J = 7.1 Hz, 1H), 2.72 – 2.59 (m, 1H), 2.17 – 2.07 (m, 3H), 1.64 (d, J = 7.1 Hz, 1H), 1.56 (dd, J = 6.8, 2.6 Hz, 3H), 1.48 (s, 1H), 1.40 (d, J = 6.7 Hz, 3H), 1.26 (d, J = 7.1 Hz, 3H), 1.06 (p, J = 7.3 Hz, 2H), 0.81 (t, J = 7.3 Hz, 3H). $^{13}\text{C-NMR}$ (100 MHz, CDCl_3): δ (ppm) = 143.8, 118.3, 65.1, 57.4, 56.1, 49.4, 46.9, 45.5, 45.1, 40.5, 35.7, 27.4, 23.8, 15.2, 13.8, 12.3. IR (ATR): ν_{max} (cm^{-1}) = 3411 (br), 2957 (s), 2919 (s), 2872 (m), 1447 (s), 1376 (s), 1328 (w), 1268 (w), 1251 (w), 1229 (w), 1210 (w), 1119 (w), 1096 (w), 1033 (s), 1009 (vs), 952 (w), 926 (w), 832 (m), 809 (w), 774 (m), 734 (m), 671 (m). HRMS (EI): calc. for $\text{C}_{16}\text{H}_{26}\text{O}_3\text{S}$ $[\text{M}]^+$: 266.1704, found: 266.1700.671 (m). HRMS (EI): calc. for $\text{C}_{16}\text{H}_{26}\text{O}^{32}\text{S}$ $[\text{M}]^+$: 266.1704, found: 266.1700.



Aldehyde 18: Dess-Martin periodinane (1.51 g, 3.56 mmol) was added to a stirred solution of alcohol **S5** (474 mg, 1.78 mmol) in CH_2Cl_2 (28 mL) and the resulting solution was stirred at room temperature for 2 h. Water (5 mL) and $\text{Na}_2\text{S}_2\text{O}_3$ (1 g) were added and the mixture was stirred until it became a clear solution. The reaction was diluted with CH_2Cl_2 and the phases were separated. The organic layer was dried over MgSO_4 and evaporated to dryness. Purification by flash column chromatography (hexanes: Et_2O 98:2) gave aldehyde **18** (353 mg, 1.33 mmol, 75%) as a colorless oil.

Data for 18: Rf: 0.2 (hexanes:Et₂O 98:2); ¹H-NMR (400 MHz, CDCl₃): δ (ppm) = 9.59 (s, 1H), 5.54 – 5.44 (m, 1H), 3.71 (q, *J* = 6.7 Hz, 1H), 3.36 (d, *J* = 7.3 Hz, 1H), 3.00 (q, *J* = 7.1 Hz, 1H), 2.67 (d, *J* = 4.8 Hz, 1H), 2.56 – 2.45 (m, 1H), 2.24 – 2.18 (m, 1H), 2.12 (d, *J* = 15.5 Hz, 1H), 1.69 (q, *J* = 7.3 Hz, 1H), 1.61 (dd, *J* = 6.8, 2.8 Hz, 3H), 1.50 (d, *J* = 6.7 Hz, 3H), 1.25 (d, *J* = 7.1 Hz, 3H), 1.06 (p, *J* = 7.3 Hz, 2H), 0.82 (t, *J* = 7.3 Hz, 3H). ¹³C-NMR (100 MHz, CDCl₃): δ (ppm) = 202.6, 140.7, 119.9, 63.6, 55.4, 49.7, 46.9, 45.1, 44.1, 38.9, 36.5, 27.2, 23.2, 15.2, 13.6, 12.1. IR (ATR): ν_{max} (cm⁻¹) = 2959 (*m*), 2924 (*m*), 2874 (*w*), 2718 (*w*), 1712 (*vs*), 1448 (*m*), 1377 (*m*), 1320 (*w*), 1251 (*w*), 1251(*w*), 1226 (*w*), 1125 (*w*) 1066 (*w*), 1031 (*w*), 987 (*w*), 835 (*w*), 775 (*w*), 667 (*w*) HRMS (EI): calc. for C₁₆H₂₄O³²S [*M*]⁺: 264.1548, found: 264.1544.

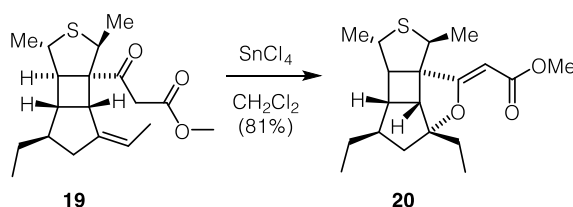


β-hydroxy ester S6: n-BuLi (2.21 M in hexanes, 0.89 mL, 1.96 mmol) was added an ice cooled solution of diisopropylamine (0.28 mL, 1.93 mmol) in THF (5.8 mL). The resulting solution was stirred at 0 °C for 30 min and then cooled to –78 °C. MeOAc (0.15 mL, 1.86 mmol) was added dropwise and the reaction was stirred at –78 °C for 30 min. A solution of aldehyde **18** (246 mg, 0.930 mmol) in THF (4.3 mL) was added dropwise and the solution was stirred for 2 h at the same temperature before it was quenched with saturated aqueous NH₄Cl and extracted with Et₂O. The combined organic phases were washed with brine, dried over MgSO₄ and evaporated to dryness to yield β-hydroxy ester **S6** that was used in the next step without further purification.

β-keto ester 19: Dess-Martin periodinane (791 mg, 1.86 mmol) was added to a stirred solution of β-hydroxyl ester **S6** in CH₂Cl₂ (17 mL) and the resulting solution was stirred at room temperature for 2 h. Water (5 mL) and Na₂S₂O₃ (1 g) was added and the mixture was stirred until it became a clear solution. The reaction was diluted with CH₂Cl₂ and the phases were separated. The organic layer was dried over MgSO₄ and evaporated to dryness. Purification by flash column chromatography (hexanes: Et₂O 92:8) gave β-keto

ester **19** (208 mg, 0.618 mmol, 66%, β -keto ester to enol ether = 1.4:1) as a colorless oil that solidifies upon standing at $-20\text{ }^{\circ}\text{C}$.

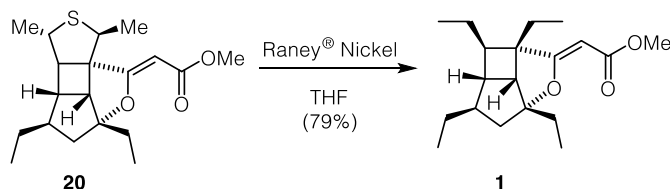
Data for 19: Rf: 0.2 (hexanes:Et₂O 98:2); ¹H-NMR (400 MHz, CDCl₃): δ (ppm) = 12.00 (s, 1H), 5.45 (d, J = 6.7 Hz, 1H), 5.37 (d, J = 6.5 Hz, 1H), 4.96 (s, 1H), 3.72 (d, J = 3.6 Hz, 7H), 3.66 (qd, J = 6.6, 3.7 Hz, 3H), 3.42 (s, 3H), 3.34 (d, J = 7.3 Hz, 1H), 3.26 (d, J = 7.3 Hz, 1H), 3.04 – 2.95 (m, 2H), 2.87 (d, J = 4.7 Hz, 1H), 2.58 (d, J = 4.5 Hz, 1H), 2.41 (s, 3H), 2.13 – 1.97 (m, 5H), 1.66 (dd, J = 6.8, 2.6 Hz, 4H), 1.63 (d, J = 7.1 Hz, 2H), 1.59 (dd, J = 6.8, 2.5 Hz, 4H), 1.57 – 1.46 (m, 9H), 1.32 (dd, J = 10.4, 7.1 Hz, 8H), 1.04 (ddt, J = 10.6, 7.4, 3.3 Hz, 5H), 0.81 (t, J = 7.3 Hz, 7H). ¹³C-NMR (100 MHz, CDCl₃): δ (ppm) = 203.1, 179.8, 173.3, 167.8, 142.2, 142.0, 120.3, 119.4, 87.4, 67.8, 59.7, 57.6, 52.5, 51.3, 49.6, 49.3, 48.1, 46.4, 46.1, 46.0, 45.3, 45.2, 45.2, 39.6, 39.2, 37.6, 37.5, 26.9, 26.8, 23.3, 23.3, 15.5, 15.3, 13.9, 13.7, 12.2, 12.1. IR (ATR): ν_{max} (cm⁻¹) = 2957 (m), 2927 (m), 2874 (w), 1750 (m), 1700 (m), 1615 (s), 1443 (s), 1396 (m), 1378 (m), 1312 (w), 1267 (m), 1226 (vs), 1196 (m), 1168 (m), 1133 (m), 1106 (w), 1058 (w), 1031 (m), 942 (w), 835 (m), 803 (m), 775 (w), 733 (w), 708 (w), 680 (w). HRMS (EI): calc. for C₁₉H₂₈O₃³²S [*M*]⁺: 336.1759, found: 336.1756.



Vinylogous carbonate 20: SnCl₄ (1 M in CH₂Cl₂, 0.12 mL, 0.120 mmol) was added dropwise to an ice-cooled solution of β keto ester **19** (200 mg, 0.594 mmol) in CH₂Cl₂ (12 mL) and the resulting solution was stirred for 2 h at room temperature. The reaction was diluted with CH₂Cl₂, washed with water and brine, dried over MgSO₄ and evaporated to dryness. Purification by flash column chromatography (hexanes: Et₂O 80:20) gave vinylogous carbonate **20** (162 mg, 0.481 mmol) as a colorless oil that solidified upon standing at $-20\text{ }^{\circ}\text{C}$.

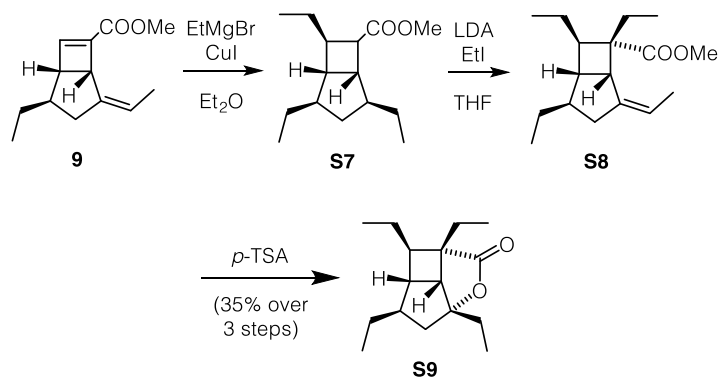
Data for 20: Rf: 0.3 (hexanes:Et₂O 4:1); ¹H-NMR (400 MHz, CDCl₃): δ (ppm) = 4.69 (s, 1H), 3.68 (s, 3H), 3.57 (q, J = 6.6 Hz, 1H), 3.08 (q, J = 7.2 Hz, 1H), 2.85 (d, J = 7.9 Hz,

1H), 2.46 (dd, $J = 14.1, 6.7$ Hz, 1H), 2.35 (d, $J = 2.7$ Hz, 1H), 2.09 (ddt, $J = 14.3, 11.6, 7.1$ Hz, 1H), 1.90 (ddd, $J = 7.7, 4.7, 2.8$ Hz, 1H), 1.77 – 1.68 (m, 2H), 1.45 (dd, $J = 14.1, 9.8$ Hz, 1H), 1.34 (dd, $J = 8.0, 3.0$ Hz, 5H), 1.17 (d, $J = 6.6$ Hz, 3H), 1.00 (t, $J = 7.4$ Hz, 3H), 0.86 (t, $J = 7.3$ Hz, 3H). **$^{13}\text{C-NMR}$ (100 MHz, CDCl_3):** δ (ppm) = 174.3, 166.8, 104.1, 84.9, 67.8, 65.7, 50.8, 48.6, 48.2, 45.8, 45.4, 45.0, 44.7, 31.6, 28.5, 24.9, 13.1, 12.6, 9.5. **IR (ATR):** ν_{max} (cm^{-1}) = 2960 (s), 2921 (s), 2874 (w), 1719 (vs), 1691 (s), 1637 (vs), 1459 (w), 1434 (w), 1364 (w), 1273 (m), 1243 (m), 1226 (m), 1210 (m), 1186 (m), 1162 (s), 1141 (s), 1101 (w), 1059 (m), 1036 (w), 1107 (w), 979 (m), 953 (w), 916 (w), 856 (vw), 799 (w), 696 (vw). **HRMS (EI):** calc. for $\text{C}_{19}\text{H}_{28}\text{O}_3^{32}\text{S}$ [M] $^+$: 336.1759, found: 336.1731.



Hippolachnin A (1): Raney[®] nickel (suspension in water 2800, Aldrich, 1 g) was added to a solution of vinylogous carbonate **20** (145 mg, 0.431 mmol) in THF (9 mL) and the resulting suspension was stirred at room temperature for 1 h. The mixture was filtered over celite and the resulting filtrate was washed with brine, dried over MgSO_4 and evaporated to dryness. Purification by flash column chromatography (hexanes: EtOAc 98:2 to 94:6) gave hippolachnin A **1** (104 mg, 0.339 mmol, 79%) as a colorless oil.

Data for 1: Rf: 0.3 (hexanes:Et₂O 4:1); **$^1\text{H-NMR}$ (400 MHz, CDCl_3):** δ (ppm) = 4.56 (s, 1H), 3.66 (s, 3H), 2.59 (d, $J = 8.0$ Hz, 1H), 2.43 (dd, $J = 13.8, 6.4$ Hz, 1H), 1.99 (ddd, $J = 9.9, 7.2, 5.0$ Hz, 1H), 1.79 (ddt, $J = 20.9, 18.5, 6.9$ Hz, 4H), 1.69 – 1.60 (m, 2H), 1.51 (dq, $J = 14.3, 7.3$ Hz, 1H), 1.43 – 1.37 (m, 1H), 1.37 – 1.27 (m, 3H), 1.02 (t, $J = 7.4$ Hz, 3H), 0.87 (t, $J = 7.3$ Hz, 6H), 0.79 (t, $J = 7.3$ Hz, 3H). **$^{13}\text{C-NMR}$ (100 MHz, CDCl_3):** δ (ppm) = 181.3, 167.4, 104.3, 83.6, 56.8, 53.0, 50.6, 49.5, 47.6, 46.4, 45.2, 30.9, 28.4, 24.7, 23.4, 13.2, 11.9, 9.8, 8.8. **IR (ATR):** ν_{max} (cm^{-1}) = 2961 (s), 2925 (m), 2876 (w), 1717 (s), 1688 (s), 1633 (vs), 1461 (m), 1433 (m), 1365 (m), 1335 (w), 1267 (m), 1214 (m), 1183 (m), 1151 (s), 1139 (s), 1083 (w), 1038 (m), 979 (m), 970 (m), 908 (w), 852 (w), 799 (m), 726 (w). **HRMS (EI):** calc. for $\text{C}_{19}\text{H}_{30}\text{O}_3$ [M] $^+$: 306.2195, found: 306.2189.



Ester S7: EtMgBr (3 M in Et_2O , 0.33 mL, 0.990 mmol) was added dropwise to a solution of CuI (93 mg, 0.488 mmol) in Et_2O (4 mL) cooled to $-5\text{ }^\circ\text{C}$ and stirred for 30 min at that temperature. The solution was cooled to $-78\text{ }^\circ\text{C}$ and a solution of methyl ester **9** (50 mg, 0.243 mmol) in dry Et_2O (1.3 mL) was added dropwise. The reaction mixture was stirred for 2 h at $-78\text{ }^\circ\text{C}$ before it was quenched with saturated aqueous NH_4Cl and extracted with Et_2O . The combined organic phases were washed with brine, dried over MgSO_4 and concentrated under reduced pressure to give ester **S7** which was used in the next step without further purification.

Alkene S8: $n\text{-BuLi}$ (2.36 M in hexanes, 0.23 mL, 0.548 mmol) was added to an ice cooled solution of diisopropylamine (75 μL , 0.532 mmol) in THF (1 mL). The resulting solution was stirred at $0\text{ }^\circ\text{C}$ for 30 min and then cooled to $-78\text{ }^\circ\text{C}$. A solution of freshly prepared **S7** in THF (4.3 mL) was added dropwise and the reaction was stirred for 45 min at $-78\text{ }^\circ\text{C}$. Ethyl iodide (37 μL , 0.462 mmol) was added and the reaction was stirred for 2 h at $-78\text{ }^\circ\text{C}$ before being quenched with saturated aqueous NH_4Cl and extracted with Et_2O . The combined organic phases were washed with brine, dried over MgSO_4 and concentrated under reduced pressure to give alkene **S8** which was used in the next step without further purification.

Lactone S9: A solution of crude alkene **S8** and $p\text{TSA}\cdot\text{H}_2\text{O}$ (46 mg, 0.243 mmol) in DCE (5.3 mL) was stirred at $84\text{ }^\circ\text{C}$ for 2 h. The solution was cooled to room temperature and extracted with Et_2O . The combined organic phases were washed with brine, dried over MgSO_4 and concentrated under reduced pressure. Purification by flash column chromatography (hexanes: Et_2O 9:1) gave lactone **S9** (21 mg, 0.085 mmol, 35% over 3 steps) as a colorless oil.

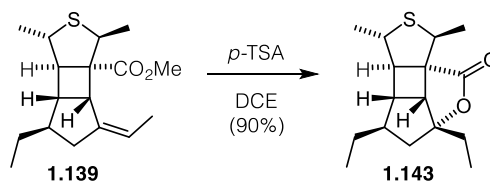
Data for S9: Rf: 0.4 (hexanes:Et₂O 9:1); **¹H-NMR (400 MHz, CDCl₃):** δ (ppm) = 2.71 (d, *J* = 8.2 Hz, 1H), 2.32 (dd, *J* = 13.7, 6.2 Hz, 1H), 2.05 – 1.95 (m, 1H), 1.93 – 1.84 (m, 2H), 1.83 – 1.73 (m, 2H), 1.67 – 1.57 (m, 3H), 1.42 – 1.29 (m, 4H), 1.00 (t, *J* = 7.5 Hz, 3H), 0.89 (t, *J* = 7.3 Hz, 6H), 0.82 (t, *J* = 7.2 Hz, 3H). **¹³C-NMR (100 MHz, CDCl₃):** δ (ppm) = 182.5, 96.2, 51.9, 49.6, 49.3, 47.6, 46.7, 45.0, 31.0, 28.3, 24.8, 21.7, 13.2, 11.6, 9.33, 9.31. **IR (ATR):** ν_{\max} (cm⁻¹) = 2962 (*m*), 2925 (*m*), 2876 (*w*), 2858 (*w*), 1753 (*s*), 1461 (*m*), 1380 (*w*), 1311 (*w*), 1214 (*m*), 1185 (*m*), 1145 (*w*), 1113 (*m*), 949 (*s*), 931 (*m*), 860 (*w*), 784 (*w*), 740 (*w*), 617 (*w*), 511 (*m*). **HRMS (EI):** calc. for C₁₆H₂₆O₂ [*M*]⁺: 250.1933, found: 250.1930.

¹H- and ¹³C-NMR chemical shifts in CDCl₃ of natural vs. synthetic hippolachnin A (1).

No.	¹ H-NMR	¹ H-NMR Synthetic	¹³ C-NMR	¹³ C-NMR
	Isolated 500 MHz, CDCl ₃ [ppm]	400 MHz, CDCl ₃ [ppm]	Isolated 125 MHz, CDCl ₃ [ppm]	Synthetic 100 MHz, CDCl ₃ [ppm]
1			167.3	167.4
2	4.56 (s, 1H)	4.56 (s, 1H)	83.5	83.6
3			181.1	181.3
4			56.6	56.8
5	2.59 (d, <i>J</i> = 8.0 Hz, 1H)	2.59 (d, <i>J</i> = 8.0 Hz, 1H)	49.4	49.5
6			104.2	104.3
7a	2.44 (q, <i>J</i> = 7.5 Hz, 1H)	2.43 (dd, <i>J</i> = 13.8 Hz, 6.4 Hz, 1H)	45.1	45.2
7b	1.40 (m, 1H) ^a	1.39 (m, 1H)		
8	1.98 (m, 1H)	1.99 (ddd, <i>J</i> = 9.9, 7.2, 5.0 Hz, 1H)	47.5	47.6
9	1.79 (m, 1H)	1.79 (m, 1H)	46.3	46.4
10	1.82 (m, 1H)	1.81 (m, 1H)	52.9	53.0
11a	1.64 (m, 1H)	1.64 (m, 1H)	24.6	24.7
11b	1.32 (m, 1H)	1.32 (m, 1H)		
12	0.88 (t, <i>J</i> = 7.5 Hz, 3H)	0.87 (t, <i>J</i> = 7.3 Hz, 3H)	11.8	11.9

13a	1.75 (m, 1H)	1.75 (m, 1H)	23.3	23.4
13b	1.52 (m, 1H)	1.51 (dq, $J = 14.3$, 7.3 Hz, 1H)		
14	0.80 (t, $J =$ 7.5 Hz, 3H)	0.79 (t, $J = 7.3$ Hz, 3H)	8.6	8.8
15a	1.82 (m, 1H)	1.82 (m, 1H)	30.8	30.9
15b	1.67 (m, 1H)	1.66 (m, 1H)		
16	1.02 (t, $J =$ 7.5 Hz, 3H)	1.02 (t, $J = 7.4$ Hz, 3H)	9.6	9.8
17a	1.30 (m, 1H)	1.32 (m, 1H)	28.3	28.4
17b	1.30 (m, 1H)	1.31 (m, 1H)		
18	0.88 (t, $J =$ 7.5 Hz, 3H)	0.87 (t, $J = 7.3$ Hz, 3H)	13.0	13.2
19	3.66 (s, 3H)	3.66 (s, 3H)	50.4	50.6

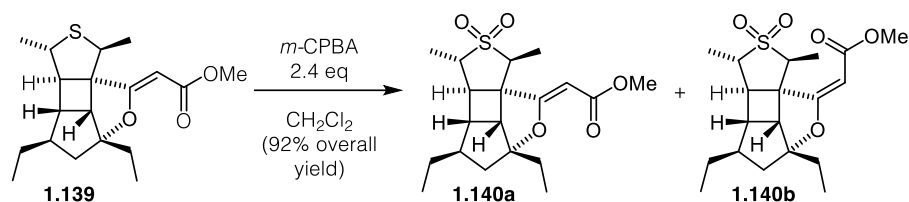
^aCarreira²⁰ et al. already reported a erroneously-reported H-7b proton shift of 1.32 ppm in the table of the isolation paper by S.-J. Piao et al.⁴ The shift of 1.40 ppm is taken directly from the reported spectrum



Lactone 1.143: A solution of tetrahydrothiophene **1.139** (10.0 mg, 0.034 mmol) and p TSA·H₂O (6.4 mg, 0.034 mmol) in DCE (0.74 mL) was stirred for 2 h at 84 °C. After cooling to room temperature the reaction mixture was diluted with H₂O and extracted with Et₂O, the combined organic phases were dried over MgSO₄ and concentrated under reduced pressure. Purification by flash column chromatography (hexanes:Et₂O 94:6-92:8) gave lactone **1.143** (8.6 mg, 0.307 mmol, 90%) as a colorless oil.

Data for 1.143: $R_f = 0.3$ (hexanes:Et₂O 92:8) ¹H NMR (400 MHz, CDCl₃): δ (ppm) 3.85 (q, $J = 6.6$ Hz, 1H), 3.14 (q, $J = 7.1$ Hz, 1H), 2.91 (d, $J = 7.3$ Hz, 1H), 2.53 (d, $J = 2.4$ Hz, 1H), 2.38 (dd, $J = 14.2, 6.3$ Hz, 1H), 2.10 – 2.05 (m, 2H), 1.72 (qd, $J = 7.4, 3.6$ Hz, 2H), 1.56 – 1.45 (m, 2H), 1.39 – 1.31 (m, 5H), 1.19 (d, $J = 6.7$ Hz, 3H), 0.98 (t, $J = 7.4$ Hz, 3H), 0.88 (t, $J = 7.4$ Hz, 3H). δ (ppm) = ¹³C-NMR (101 MHz, CDCl₃): δ (ppm) = 177.8,

97.3, 63.8, 62.1, 49.3, 48.1, 46.3, 44.9, 44.3, 43.7, 32.2, 28.4, 24.9, 13.0, 12.7, 9.1. **IR (ATR):** ν_{\max} (cm⁻¹) = 2960 (m), 2924 (m), 1755 (vs), 1458 (m), 1378 (w), 1318 (w), 1246 (m), 1152 (w), 1126 (w), 1102 (w), 974 (m), 935 (m). **HRMS (EI):** calc. for C₁₆H₂₄O₂S [M]⁺: 280.1492, found: 280.1493.

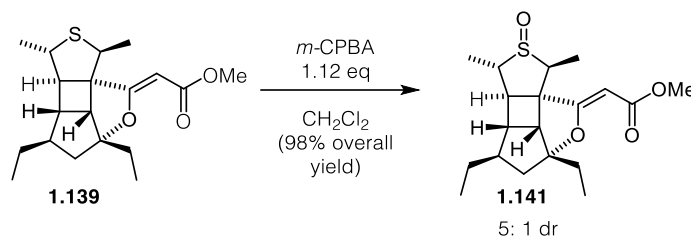


Sulfone 1.140a and 1.140b: A solution of *m*CPBA·H₂O (77%, 30 mg, 0.132 mmol) in CH₂Cl₂ (2.0 mL) was added to an ice cooled solution of vinyllogous carbonate **1.139** (20.0 mg, 0.059 mmol) in CH₂Cl₂ (1 mL) and the reaction was stirred at 0 °C for 30 min and at room temperature overnight. The mixture was diluted with CH₂Cl₂ and washed with aqueous Na₂S₂O₃, saturated aqueous NaHCO₃ and brine. The combined organic phases were dried over MgSO₄ and concentrated under reduced pressure. Purification of the resulting residue by flash column chromatography (hexanes:EtOAc 3:1) gave sulfone **1.140a** (10.9 mg, 0.030 mmol, 50%) and sulfone **1.140b** (9.1 mg, 0.025 mmol, 42%) as a colorless oils.

Data for 1.140a: R_f = 0.25 (hexanes:Et₂O 92:8) ¹H NMR (400 MHz, CDCl₃): δ (ppm) = 5.40 (s, 1H), 4.56 (q, *J* = 6.8 Hz, 1H), 3.63 (s, 3H), 3.41 (d, *J* = 8.2 Hz, 1H), 3.20 (qd, *J* = 7.6, 1.4 Hz, 1H), 2.22 (dd, *J* = 13.7, 6.0 Hz, 1H), 2.11 (ddd, *J* = 8.4, 6.7, 1.9 Hz, 1H), 2.05 – 1.93 (m, 1H), 1.72 (dq, *J* = 14.8, 7.4 Hz, 1H), 1.70 – 1.56 (m, 6H), 1.49 – 1.33 (m, 3H), 1.20 (d, *J* = 6.8 Hz, 3H), 0.97 (t, *J* = 7.5 Hz, 3H), 0.88 (t, *J* = 7.3 Hz, 3H). **¹³C-NMR (101 MHz, CDCl₃):** δ (ppm) = 177.6, 167.6, 101.2, 89.8, 63.0, 56.1, 54.2, 52.3, 51.2, 48.6, 48.2, 48.0, 45.4, 30.4, 27.8, 17.1, 13.2, 9.6, 5.7. **IR (ATR):** ν_{\max} (cm⁻¹) = 2958 (m), 1699 (m), 1623 (s), 1458 (w), 1363 (w), 1306 (m), 1240 (w), 1191 (w), 1166 (w), 1119 (vs), 1087 (w), 1064 (w), 951 (w), 829 (w), 758 (w). **HRMS (EI):** calc. for C₁₉H₂₈O₅S [M]⁺: 368.1652, found:368.1652.

Data for 1.140b: R_f = 0.6 (hexanes:Et₂O 92:8) ¹H NMR (400 MHz, CDCl₃): δ (ppm) = 4.68 (s, 1H), 3.68 (s, 3H), 3.24 (q, *J* = 6.8 Hz, 1H), 3.13 (qd, *J* = 7.3, 1.7 Hz, 2H), 2.51 (dd, *J* = 14.1, 6.6 Hz, 1H), 2.25 (dd, *J* = 3.2, 1.8 Hz, 1H), 2.19 (ddd, *J* = 11.5, 5.8, 2.8 Hz, 1H), 2.08 (ddd, *J* = 12.0, 9.3, 5.8 Hz, 1H), 1.73 (ddp, *J* = 21.7, 14.3, 7.4 Hz, 2H), 1.45 – 1.34 (m, 6H), 1.31 (d, *J* = 6.8 Hz, 3H), 0.99 (t, *J* = 7.4 Hz, 3H), 0.86 (t, *J* = 7.3 Hz, 3H).

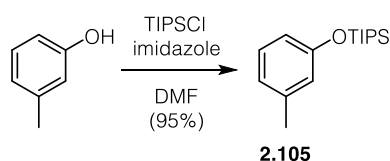
$^{13}\text{C-NMR}$ (101 MHz, CDCl_3): δ (ppm) = 173.7, 166.3, 104.9, 85.7, 60.6, 55.5, 55.4, 54.8, 51.0, 48.7, 46.3, 46.0, 45.0, 31.25, 28.3, 17.5, 13.1, 9.4, 5.9. **IR (ATR):** ν_{max} (cm^{-1}) = 2957 (m), 2877 (w), 1717 (s), 1638 (s), 1457 (m), 1436 (m), 1377 (w), 1310 (s), 1248 (w), 1232 (w), 1181 (m), 1168 (m), 1124 (s), 1107 (m), 1084 (w), 1053 (m), 1011 (w), 980 (w), 918 (w), 812 (w), 764 (w), 730 (w). **HRMS (EI):** calc. for $\text{C}_{19}\text{H}_{28}\text{O}_5\text{S}$ [M] $^+$: 368.1652, found:368.1649.



Sulfoxide 1.141: A solution of $m\text{CPBA} \cdot \text{H}_2\text{O}$ (77%, 14.8 mg, 0.066 mmol) in CH_2Cl_2 (2.0 mL) was added to a stirred solution of vinylogous carbonate **1.139** (20.0 mg, 0.059 mmol) in CH_2Cl_2 (1 mL) at -78°C and the reaction was stirred at that temperature for 45 min. The mixture was diluted with aqueous $\text{Na}_2\text{S}_2\text{O}_3$ and extracted with CH_2Cl_2 . The combined organic phases were washed with saturated aqueous NaHCO_3 and brine, dried over MgSO_4 and concentrated under reduced pressure. Purification of the resulting residue by flash column chromatography (hexanes:EtOAc 1:2) gave sulfoxide **1.141** (20.3 mg, 0.058 mmol, 98%) as a colorless oil. The product was obtained as a 5:1 mixture of diastereoisomers.

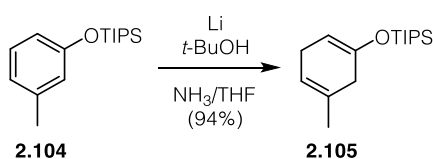
Data for 1.141: $R_f = 0.3$ (hexanes:Et₂O 92:8) $^1\text{H NMR}$ (400 MHz, CDCl_3): δ (ppm) = 4.77 (s, 1H), 4.63 (s, 0H), 3.68 (s, 0H), 3.67 (s, 3H), 3.39 (t, $J = 7.7$ Hz, 0H), 3.26 (qd, $J = 7.3$, 2.9 Hz, 1H), 3.13 (q, $J = 7.0$ Hz, 1H), 3.00 (q, $J = 6.9$ Hz, 0H), 2.72 (d, $J = 7.9$ Hz, 1H), 2.56 – 2.44 (m, 2H), 2.36 (ddd, $J = 8.2$, 5.1, 3.1 Hz, 0H), 2.05 (dddd, $J = 23.3$, 11.4, 9.6, 5.9 Hz, 1H), 1.91 (ddd, $J = 8.0$, 5.2, 2.8 Hz, 1H), 1.82 – 1.63 (m, 3H), 1.41 – 1.34 (m, 5H), 1.32 (d, $J = 7.3$ Hz, 4H), 0.98 (t, $J = 7.4$ Hz, 4H), 0.86 (t, $J = 7.4$ Hz, 4H). **$^{13}\text{C-NMR}$ (101 MHz, CDCl_3):** δ (ppm) = 173.9, 166.5, 104.5, 86.2, 60.2, 58.0, 57.8, 56.9, 50.9, 48.2, 46.8, 45.4, 45.3, 31.3, 28.2, 13.1, 11.1, 10.0, 9.5. **IR (ATR):** ν_{max} (cm^{-1}) = 3478 (br), 2962 (m), 2927 (m), 2875 (w), 1713 (s), 1687 (m), 1635 (s), 1458 (m), 1435 (m), 1373 (m), 1280 (m), 1224 (m), 1177 (s), 1159 (m), 1044 (vs), 1008 (m), 879 (m), 917 (m), 877 (w), 816 (w), 730 (m), 689 (w). **HRMS (EI):** calc. for $\text{C}_{19}\text{H}_{27}\text{O}_3\text{S}$ [M] $^+$: 352.1703, found: 352.1700.

6.3 Experimental data for chapter II



Silyl ether 2.105: TIPSCl (11 mL), 51.87 mmol) was added to a stirred solution of imidazole (7.10 g, 104 mmol) and *m*-cresol (6.25 mL, 59.70 mmol) in DMF (25 mL) and the reaction was stirred at room temperature for 20 h before it was poured into a mixture of Et₂O (50 mL), hexanes (50 mL) and 1M aqueous H₂SO₄ (75 mL). The organic layer was separated and washed three times with 1M aqueous NaOH and brine. Drying of the solvent over Na₂SO₄ and removal of the solvent under reduced pressure gave silyl ether **2.105** (13.1 g, 49.5 mmol, 95%) as a colorless oil.

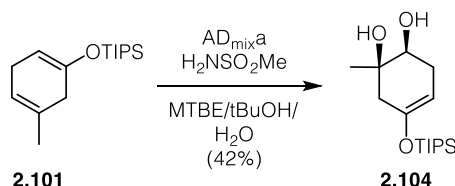
Data for 2.105: ¹H-NMR (400 MHz, CDCl₃): δ (ppm) = 7.09 (t, *J* = 7.7 Hz, 1H), 6.77 – 6.64 (m, 3H), 2.30 (s, 3H), 1.32 – 1.19 (m, 3H), 1.10 (d, *J* = 7.3 Hz, 18H). ¹³C-NMR (100 MHz, CDCl₃): δ (ppm) = 156.1, 139.4, 129.1, 121.9, 120.8, 116.9, 21.6, 18.1, 12.8. **IR (ATR):** ν_{max} (cm⁻¹) = 2944 (m), 2893 (w), 2867 (m), 1304 (m), 1586 (m), 1487 (s), 1463 (m), 1384 (w), 1368 (w), 1280 (vs), 1165 (s), 1158 (s), 1071 (w), 1006 (m), 996 (w), 956 (s), 920 (w), 882 (s), 859 (w), 813 (s), 776 (s), 734 (w), 688 (vs), 680 (s), 660 (m). **HRMS (EI):** calc. for C₁₆H₂₈OSi [*M*]⁺: 264.1909, found: 264.1906.



Silyl enol ether 2.104⁵⁶: Li (4.34 g, 6.21 mmol) was added to a solution of THF (285 mL), *t*-BuOH (64 mL) and NH₃ (500 mL) at –78 °C and the mixture was stirred until all metal was dissolved. Silyl ether **2.105** (27.4 g, 104 mmol) was added slowly and the reaction was stirred at –30 °C for 1 h. The solution was recooled to –78 °C and *t*-BuOH (30 mL) was added. After stirring for 30 min at –30 °C the solution was again cooled to –78 °C and NH₄Cl (32 g) was added portionwise until the blue colour disappeared. The mixture was slowly warmed to room temperature and the ammonia was evaporated under a slight stream of nitrogen. The reaction was diluted with H₂O and extracted with pentane. The organic phase was dried over Na₂SO₄ and the solvent was

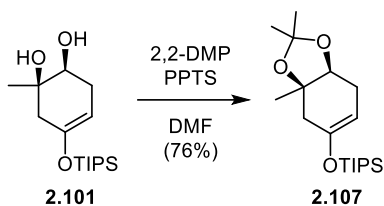
removed under reduced pressure to give silyl enol ether **2.104** (26 g, 97.6 mmol, 94%) as a colorless oil.

Data for 2.104: $^1\text{H-NMR}$ (400 MHz, CDCl_3): δ (ppm) = 5.36 (tp, J = 3.2, 1.6 Hz, 1H), 4.85 (tq, J = 3.6, 1.3 Hz, 1H), 2.72 (tdq, J = 6.3, 3.1, 1.7 Hz, 2H), 2.64 – 2.55 (m, 2H), 1.69 (s, 3H), 1.19 – 1.12 (m, 3H), 1.10 – 1.07 (m, 19H). $^{13}\text{C-NMR}$ (100 MHz, CDCl_3): δ (ppm) = 148.2, 131.1, 118.6, 100.1, 35.5, 27.4, 23.1, 18.2, 12.8. **IR (ATR):** ν_{max} (cm^{-1}) = 3040 (w), 2944 (w), 2891 (w), 2866 (m), 2822 (w), 1699 (w), 1667 (w), 1463 (w), 1384 (w), 1346 (w), 1240 (w), 1217 (s), 1137 (s), 1071 (w), 1014 (w), 996 (w), 960 (w), 936 (w), 927 (w), 882 (s), 822 (w), 776 (m), 682 (m). **HRMS (EI):** calc. for $\text{C}_{16}\text{H}_{30}\text{OSi}$ [M] $^+$: 266.2066, found: 266.2061.



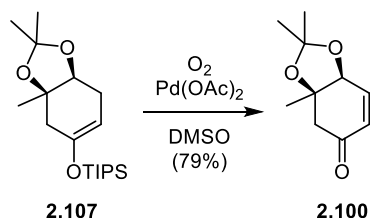
Diol 2.101⁵⁶: Methansulfonamide (2.36 g, 24.84 mmol) was added to a solution of $\text{AD}_{\text{mix}\alpha}$ (50.0 g) in t -BuOH (93 mL), MTBE (47 mL) and H_2O (142 mL) and the resulting solution was stirred for 15 min at room temperature before it was cooled to -8°C . Silyl enol ether **2.104** (9.37 g, 35.17 mmol) was added and the reaction was stirred at -8°C for 7 d, diluted with H_2O and extracted with EtOAc. The combined organic phases were sequentially washed with 10% aqueous $\text{Na}_2\text{S}_2\text{O}_3$, saturated NaHCO_3 and brine and dried over MgSO_4 . Removal of the solvent under reduced pressure and purification of the resultant residue by flash column chromatography (EtOAc:hexanes 1:1, R_f = 0.4) gave diol **2.101** (4.42 g, 14.71 mmol, 42%, 77% brsm, 25% ee) as a colourless oil.

Data for 2.101: $^1\text{H-NMR}$ (400 MHz, CDCl_3): δ (ppm) = 4.72 – 4.62 (m, 1H), 3.56 (t, J = 5.0 Hz, 1H), 2.39 – 2.12 (m, 6H), 1.22 (s, 3H), 1.16 – 1.09 (m, 3H), 1.08 – 1.01 (m, 18H). $^{13}\text{C-NMR}$ (100 MHz, CDCl_3): δ (ppm) = 148.2, 98.2, 72.4, 72.0, 41.7, 29.7, 25.0, 18.1, 12.7. **IR (ATR):** ν_{max} (cm^{-1}) = 3409 (m, br), 2946 (m), 2867 (m), 2361 (w), 1715 (m), 1659 (s), 1464 (w), 1377 (w), 1325 (w), 1257 (m), 1201 (m), 1165 (w), 1060 (m), 968 (w), 950 (w), 884 (m), 685 (w). **HRMS (EI):** calc. for $\text{C}_{16}\text{H}_{32}\text{O}_3\text{Si}$ [M] $^+$: 300.2121, found: 300.2119. $[\alpha]_D^{20} = +1.6$ (c = 0.06)



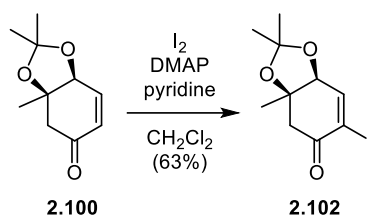
Acetonide 2.107⁵⁶: PPTS (307 mg, 1.21 mmol) was added to a stirred solution of diol **2.101** (7.30 g, 24.3 mmol) and 2,2-DMP (29.2 mL) in DMF (245 mL) and the solution was stirred for 2 h at room temperature before it was quenched with NEt₃ (18.2 mL). The reaction was diluted with aqueous NaHCO₃ and extracted with Et₂O. The combined organic phases were washed with brine and dried over Na₂SO₄. Removal of the solvent under reduced pressure and purification by flash column chromatography (EtOAc:hexanes 5:95, R_f = 0.4) gave acetonide **2.107** (6.28 g, 18.4 mmol, 76%) as a colourless oil.

Data for 2.107: ¹H-NMR (400 MHz, CDCl₃): δ (ppm) = 4.67 (dd, *J* = 2.2, 1.2 Hz, 1H), 3.93 (dt, *J* = 3.4, 1.6 Hz, 1H), 2.46 – 2.33 (m, 1H), 2.14 (dddd, *J* = 14.4, 5.4, 3.6, 1.6 Hz, 1H), 1.84 (ddd, *J* = 16.6, 6.0, 1.5 Hz, 1H), 1.79 – 1.67 (m, 1H), 1.37 (d, *J* = 3.5 Hz, 6H), 1.32 (s, 3H), 1.21 – 1.11 (m, 3H), 1.10 – 1.05 (m, 18H). ¹³C-NMR (100 MHz, CDCl₃): δ (ppm) = 151.2, 107.6, 107.2, 80.1, 77.3, 27.9, 27.7, 26.6, 24.4, 24.3, 18.2, 18.1, 12.7. IR (ATR): ν_{max} (cm⁻¹) = 2943 (m), 2893 (w), 2867 (m), 2361 (w), 1663 (m), 1464 (w), 1374 (w), 1326 (w), 1297 (w), 1239 (w), 1208 (s), 1191 (w), 1167 (w), 1132 (w), 1086 (s), 1066 (w), 1006 (m), 991 (m), 956 (w), 908 (w), 883 (s), 860 (w), 826 (w), 815 (w), 784 (w), 757 (w), 682 (m), 665 (w). HRMS (EI): calc. for C₁₆H₃₂O₃Si [*M*]⁺: 340.2434, found: 340.2424. [α]_D²⁰ = +24 ° (c = 0.01 g/mL).



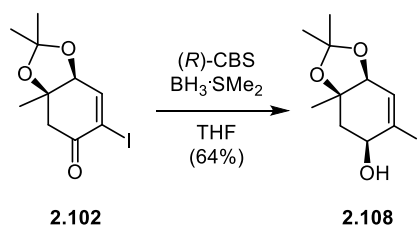
Ketone 2.100⁵⁶: Pd(OAc)₂ (4.14 g, 18.44 mmol) was added to a solution of acetonide **2.107** (6.28 g, 18.44 mmol) in DMSO (13.7 mL). The reaction was set under vacuum and backfilled with O₂ for three cycles and stirred at room temperature overnight before it was submitted to flash column chromatography (EtOAc:hexanes 15:85, R_f = 0.2) to give ketone **2.100** (2.67 g, 14.65 mmol, 79%) as a colorless oil.

Data for 2.100: $^1\text{H-NMR}$ (400 MHz, CDCl_3): δ (ppm) = 6.75 (dd, $J = 10.2, 3.7$ Hz, 1H), 6.08 (dd, $J = 10.2, 1.1$ Hz, 1H), 4.41 (dd, $J = 3.8, 1.1$ Hz, 1H), 2.84 (d, $J = 16.2$ Hz, 1H), 2.49 (d, $J = 16.3$ Hz, 1H), 1.42 (s, 3H), 1.38 (s, 3H), 1.35 (s, 3H). $^{13}\text{C-NMR}$ (100 MHz, CDCl_3): δ (ppm) = 197.1, 143.9, 130.7, 110.3, 80.7, 76.1, 47.5, 28.5, 28.4, 26.1. **IR (ATR):** ν_{max} (cm^{-1}) = 3362 (w, br), 2985 (w), 2936 (w), 1681 (s), 1459 (w), 1380 (m), 1312 (w), 1270 (w), 1233 (s), 1212 (m), 1180 (w), 1160 (w), 1144 (w), 1109 (w), 1082 (m), 1046 (s), 1020 (m), 988 (w), 956 (w), 944 (w), 894 (w), 866 (w), 830 (m), 807 (w), 772 (w), 705 (w), 668 (w). **HRMS (EI):** calc. for $\text{C}_{10}\text{H}_{14}\text{O}_3$ [M] $^+$: 182.0943, found: 182.0935. $[\alpha]_D^{20} = +12^\circ$ ($c = 0.01$ g/mL).



Vinyl iodide 2.102: A solution of iodine (11.18 g, 44.01 mmol) in CH_2Cl_2 (45 mL) and pyridine (11.83 mL) was added slowly to a solution of ketone **2.100** (2.67 g, 14.65 mmol) and DMAP (1.80 g, 14.65 mmol) in CH_2Cl_2 (100 mL) and the resulting solution was stirred for 36 h at room temperature in the dark before it was diluted with CH_2Cl_2 and washed with a 20% aqueous solution of $\text{Na}_2\text{S}_2\text{O}_3$, 1M aqueous HCl and brine. The organic phase was dried over Na_2SO_4 and the solvent was removed under reduced pressure. Purification of the resulting residue by flash column chromatography (EtOAc:hexanes 1:5, $R_f = 0.3$) gave vinyl iodide **2.102** (2.83 g, 9.18 mmol, 63%, 73% brsm) as a colorless oil).

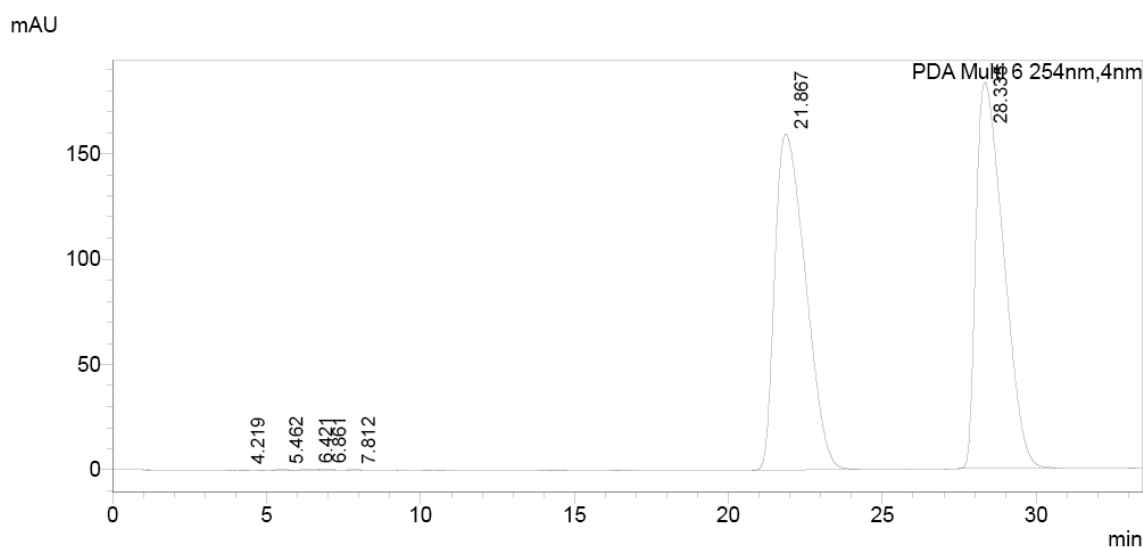
Data for 2.102: $^1\text{H-NMR}$ (400 MHz, CDCl_3): δ (ppm) = 7.51 (d, $J = 3.9$ Hz, 1H), 4.41 (d, $J = 3.8$ Hz, 1H), 3.12 (d, $J = 16.1$ Hz, 1H), 2.70 (d, $J = 16.1$ Hz, 1H), 1.46 (d, $J = 0.8$ Hz, 3H), 1.43 (s, 3H), 1.38 – 1.35 (m, 3H). $^{13}\text{C-NMR}$ (100 MHz, CDCl_3): δ (ppm) = 190.1, 152.9, 110.9, 106.5, 81.2, 78.6, 45.9, 28.7, 28.5, 26.1. **IR (ATR):** ν_{max} (cm^{-1}) = 2987 (w), 2935 (w), 1693 (s), 1599 (w), 1459 (w), 1377 (m), 1327 (w), 1296 (w), 1269 (w), 1235 (s), 1215 (s), 1181 (m), 1145 (w), 1113 (w), 1092 (m), 1053 (m), 1035 (m), 986 (w), 949 (w), 924 (w), 892 (w), 842 (w), 781 (w), 729 (w). **HRMS (EI):** calc. for $\text{C}_{10}\text{H}_{13}\text{IO}_3$ [M] $^+$: 307.9909, found: 307.9908. $[\alpha]_D^{20} = -17^\circ$ ($c = 0.05$ g/mL).



Allylic alcohol 2.108: $\text{BH}_3\cdot\text{SMe}_2$ (0.87 mL, 9.18 mmol) was added dropwise to an ice-cooled solution of (*R*)-CBS catalyst (1.27 g, 4.58 mmol) in THF (126 mL) and the solution was stirred for 15 min at that temperature before a solution of vinyl iodide **2.102** (2.83 g, 9.18 mmol) in THF (35 mL) was slowly added. The reaction was stirred at 0 °C for 2 h before it was quenched with MeOH and poured into brine and extracted with EtOAc. The combined organic layers were dried over Na_2SO_4 and the solvent was removed under reduced pressure. Purification of the resultant residue by flash column chromatography gave allylic alcohol **2.108** (1.81 g, 5.84 mmol, 64%, 95% ee) as a colorless oil.

Data for 2.108: $^1\text{H-NMR}$ (400 MHz, CDCl_3): δ (ppm) = 6.43 (d, $J = 3.6$ Hz, 1H), 4.17 (dd, $J = 3.6, 0.8$ Hz, 1H), 4.12 (dt, $J = 9.2, 4.3$ Hz, 1H), 3.32 (d, $J = 10.0$ Hz, 1H), 2.36 (dd, $J = 14.6, 3.8$ Hz, 1H), 2.10 (dd, $J = 14.6, 4.7$ Hz, 1H), 1.45 (s, 6H), 1.37 (s, 3H). $^{13}\text{C-NMR}$ (100 MHz, CDCl_3): δ (ppm) = 137.1, 110.7, 107.4, 79.4, 79.1, 72.7, 39.7, 29.2, 28.9, 26.3. IR (ATR): ν_{max} (cm^{-1}) = HRMS (EI): calc. for $\text{C}_{10}\text{H}_{15}\text{IO}_3$ [M] $^+$: 310.0066, found: 310.0056. $[\alpha]_D^{20} = -105.9$ ($c = 0.03$)

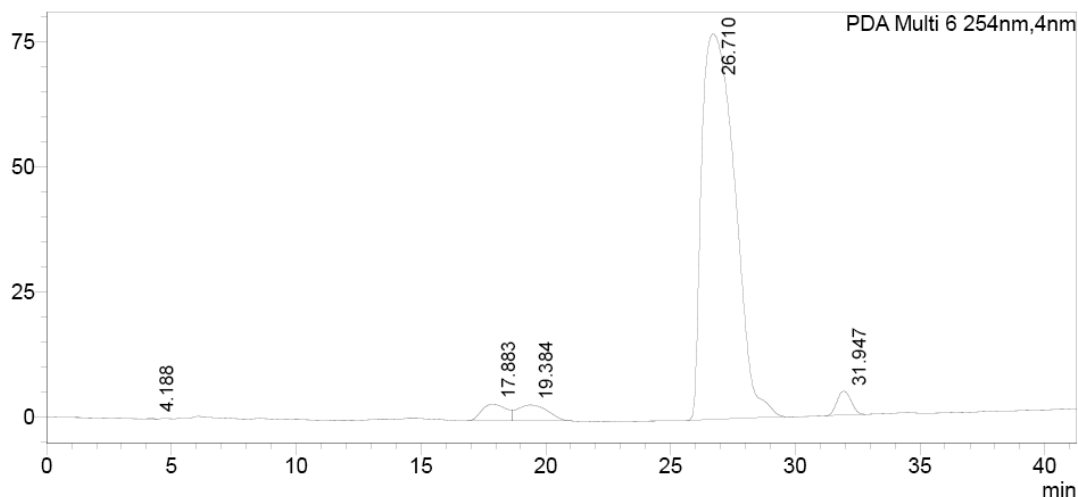
The enantiomeric excess was determined using chiral HPLC (chiralpak Od-h) *i*-PrOH:*n*-heptane 0.5:99.5-2:98 (over 30 min, 1 mL/min).



PDA Ch6 254nm

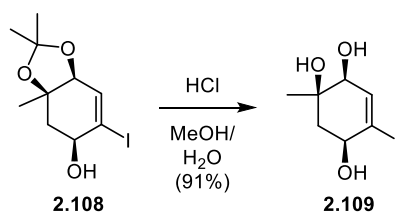
Peak#	Ret. Time	Area	Height	Conc.	Unit	Mark	Name
1	4.219	1224	124	0.000			
2	5.462	9684	475	0.000			
3	6.421	15975	607	0.000			
4	6.861	12144	628	0.000		V	
5	7.812	4480	302	0.000			
6	21.867	11051529	159434	0.000			
7	28.335	11362332	183375	0.000			
Total		22457368	344946				

mAU



PDA Ch6 254nm

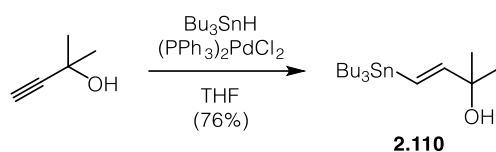
Peak#	Ret. Time	Area	Height	Conc.	Unit	Mark	Name
1	4.188	2991	254	0.000			
2	17.883	236756	3385	0.000			
3	19.384	278676	3243	0.000		V	
4	26.710	7118383	77141	0.000			
5	31.947	187958	4785	0.000			
Total		7824765	88808				



Triol 2.109: Aqueous 1M HCl (3.7 mL) was added to a stirred solution of vinyl iodide **2.108** (575 mg, 1.85 mmol) in MeOH (7.4 mL) and the solution was stirred overnight at room temperature in the dark. The reaction mixture was directly submitted to flash column chromatography (EtOAc) to give triol **2.109** (455 mg, 1.68 mmol, 91%) as a colorless oil.

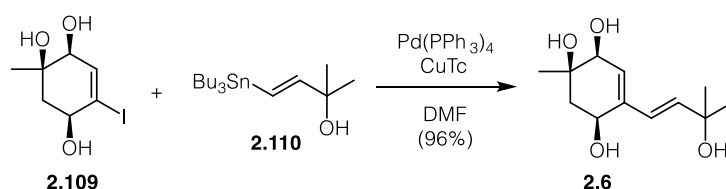
Data for 2.109: $^1\text{H-NMR}$ (400 MHz, d_4 -MeOH): δ (ppm) = 6.40 (dd, $J = 3.7, 0.8$ Hz, 1H), 4.04 (tt, $J = 5.4, 1.0$ Hz, 1H), 3.73 (dt, $J = 3.7, 0.9$ Hz, 1H), 2.05 (dd, $J = 13.6, 5.3$ Hz,

1H), 1.97 (ddd, $J = 13.6, 5.3, 0.7$ Hz, 1H), 1.20 (s, 3H). **$^{13}\text{C-NMR}$ (100 MHz, $\text{d}_4\text{-MeOH}$):** δ (ppm) = 141.5, 107.2, 74.8, 73.5, 70.9, 41.8, 25.5. **IR (ATR):** ν_{max} (cm^{-1}) = 3270 (s), 2971 (w), 2922 (w), 2863 (w), 1706 (w), 1625 (w), 12449 (w), 1431 (w), 1696 (w), 1374 (w), 1329 (w), 1284 (w), 1253 (m), 1142 (s), 1108 (m), 1066 (s), 1053 (vs), 1036 (s), 1000 (s), 934 (s), 908 (m), 869 (m), 833 (m), 742 (w). **HRMS (ESI):** calc. for $\text{C}_7\text{H}_{10}\text{IO}_3$ $[M-H]^-$: 268.9680, found: 298.9684. $[\alpha]_D^{20} = +14.0^\circ$ ($c = 0.0043$ g/mL).



Vinyl stannane 2.110: Bu_3SnH (1.58 mL, 5.96 mmol) was added dropwise to a suspension of 2-methyl-3-butyn-2-ol (0.58 mL, 5.94 mmol) and $(\text{PPh}_3)_2\text{PdCl}_2$ (83 mg, 0.119 mmol) in THF (17 mL) and the resultant solution was stirred for 1 h at room temperature before it was concentrated under reduced pressure. The resultant residue was purified by flash column chromatography (EtOAc:hexanes 8:92, $R_f = 0.3$) to yield vinyl stannane **2.110** (1.70 g, 4.53 mmol, 76%) as a colorless oil.

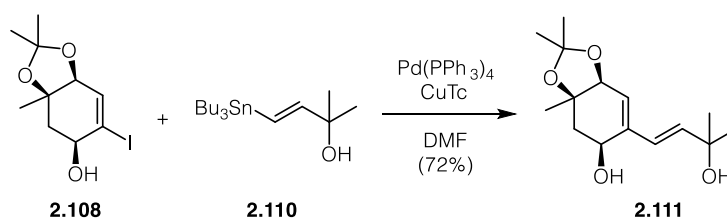
Data for 2.110: **$^1\text{H-NMR}$ (400 MHz, CDCl_3):** δ (ppm) = 6.19 – 5.97 (m, 2H), 1.71 (s, 1H), 1.54 – 1.41 (m, 6H), 1.33 – 1.23 (m, 5H), 0.86 (td, $J = 7.7, 1.6$ Hz, 15H). **$^{13}\text{C-NMR}$ (100 MHz, CDCl_3):** δ (ppm) = 155.7, 122.4, 72.5, 29.5, 29.2, 27.3, 13.8, 9.5. **IR (ATR):** ν_{max} (cm^{-1}) = 3357 (w, br), 2956 (s), 2923 (s), 2871 (w), 2853 (w), 1600 (w), 1521 (w), 1463 (w), 1417 (w), 1374 (m), 1292 (w), 1201 (w), 1147 (w), 1071 (w), 989 (m), 960 (w), 904 (w), 874 (w), 781 (w), 667 (m). **HRMS (EI):** calc. for $\text{C}_{17}\text{H}_{36}\text{OSn}$ $[M]^+$: 376.1788, found: 376.



Acremine F (2.6): A solution of triol **2.109** (430 mg, 1.59 mmol), vinyl stannane **2.110** (1.20 g, 3.19 mmol), $\text{Pd}(\text{PPh}_3)_4$ (177 mg, 0.153 mmol) and CuTc (381 mg, 2.00 mmol) in DMF (37 mL) was stirred at 65°C overnight in the dark. The reaction was cooled to room temperature, diluted with MeOH and filtered through a pad of celite. Evaporation of the

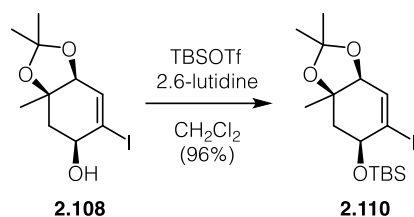
solvent under reduced pressure and purification of the resulting residue by flash column chromatography (EtOAc, $R_f = 0.25$) gave acremine F (**2.6**) (350 mg, 1.53 mmol, 96%) as a colorless oil.

Data for 2.6: $^1\text{H-NMR}$ (400 MHz, $\text{d}_4\text{-MeOH}$): δ (ppm) = 6.19 (d, $J = 16.1$ Hz, 1H), 6.08 (d, $J = 16.1$ Hz, 1H), 5.63 (d, $J = 2.8$ Hz, 1H), 4.35 (t, $J = 3.9$ Hz, 1H), 3.95 (d, $J = 2.8$ Hz, 1H), 2.09 (dd, $J = 14.3, 3.3$ Hz, 1H), 1.85 (dd, $J = 14.3, 4.5$ Hz, 1H), 1.33 (s, 3H), 1.32 (s, 3H), 1.27 (s, 3H). $^{13}\text{C-NMR}$ (100 MHz, $\text{d}_4\text{-MeOH}$): δ (ppm) = 139.4, 139.2, 130.8, 127.1, 73.8, 72.0, 71.4, 65.6, 42.0, 30.0, 29.9, 26.5. **IR (ATR):** ν_{max} (cm^{-1}) = 3372 (br), 2971 (s), 2927 (m), 2360 (m), 2168 (w), 2012 (w), 1622 (w), 1373 (m), 1264 (w), 1150 (s), 1072 (m), 1038 (s), 999 (m), 971 (m), 883 (w), 832 (w), 658 (w). **HRMS (EI):** calc for $[M-H]^-$: 227.1289, found: 227.1292 $[\alpha]_D^{20} = -46.6^\circ$ ($c = 0.009$ g/mL).



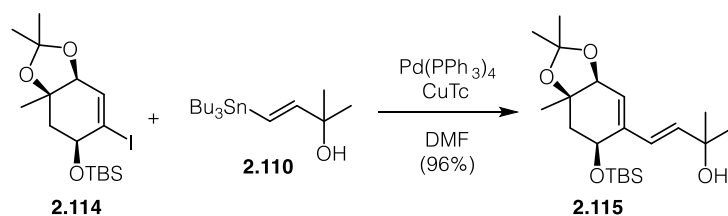
Diene 2.111: A mixture of alcohol **2.108** (100 mg, 0.322 mmol), vinyl stannane **2.110** (364 mg, 0.971 mmol), $\text{Pd}(\text{PPh}_3)_4$ (35 mg, 0.030 mmol), and CuTc (75 mg, 0.393 mmol) in DMF (10 mL) was stirred at 65°C overnight in the dark. The reaction was diluted with brine and extracted with EtOAc. The combined organic phases were dried over Na_2SO_4 and concentrated under reduced pressure. Purification of the resulting residue by flash column chromatography (EtOAc:hexanes 1:1, $R_f = 0.3$) gave diene **2.111** (62 mg, 0.231 mmol, 72%) as a colourless oil.

Data for 2.111: $^1\text{H-NMR}$ (400 MHz, CDCl_3): δ (ppm) = 6.12 (q, $J = 16.1$ Hz, 2H), 5.58 (d, $J = 3.5$ Hz, 1H), 4.33 (d, $J = 3.5$ Hz, 1H), 4.24 (ddd, $J = 10.6, 4.6, 2.7$ Hz, 1H), 3.44 (d, $J = 10.6$ Hz, 1H), 2.37 (dd, $J = 15.1, 2.7$ Hz, 1H), 1.84 (dd, $J = 15.0, 4.5$ Hz, 1H), 1.40 (s, 3H), 1.34 (s, 3H), 1.33 (s, 3H), 1.31 (s, 3H), 1.29 (s, 3H). $^{13}\text{C-NMR}$ (100 MHz, CDCl_3): δ (ppm) = 139.3, 139.0, 126.7, 126.3, 110.2, 80.2, 78.5, 71.1, 63.6, 39.6, 30.1, 29.6, 29.2, 26.9. **IR (ATR):** ν_{max} (cm^{-1}) = 3429 (m), 2974 (s), 2934 (m), 1458 (w), 1374 (s), 1314 (w), 1274 (w), 1238 (s), 1210 (m), 1164 (m), 1134 (w), 1085 (m), 1070 (m), 1027 (vs), 1004 (m), 971 (m), 914 (w), 887 (w), 860 (w), 828 (m), 800 (w). **HRMS (EI):** calc. for $[M-\text{CH}_3]^+$: 253.1434, found: 253.1425. $[\alpha]_D^{20} = -29.3^\circ$ ($c = 0.006$ g/mL).



Silyl ether 2.114: 2,6-lutidine (0.56 mL, 4.84 mmol) and TBSOTf (0.56 mL, 2.42 mmol) were sequentially added to an ice-cooled solution of vinyl iodide **2.108** (300 mg, 0.967 mmol) and the reaction was stirred at that temperature for 2 h before it was quenched with saturated aqueous NH_4Cl and extracted with CH_2Cl_2 . The combined organic layers were dried over Na_2SO_4 and concentrated under reduced pressure. Purification of the resulting residue by flash column chromatography (EtOAc:hexanes 2:98) gave silyl ether **2.114** (456 mg, 0.931 mmol, 96%) as a colourless oil.

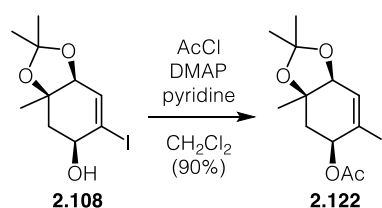
Data for 2.114: $^1\text{H-NMR}$ (400 MHz, CDCl_3): δ (ppm) = 6.57 (dd, $J = 4.9, 1.8$ Hz, 1H), 4.05 – 3.97 (m, 1H), 3.91 (dd, $J = 5.0, 1.2$ Hz, 1H), 1.98 (d, $J = 7.8$ Hz, 2H), 1.48 – 1.46 (m, 3H), 1.37 (d, $J = 0.7$ Hz, 3H), 1.32 (s, 3H), 0.94 (s, 9H), 0.20 (s, 3H), 0.12 (s, 3H). $^{13}\text{C-NMR}$ (100 MHz, CDCl_3): δ (ppm) = 133.7, 115.6, 110.0, 78.5, 71.2, 42.8, 28.7, 27.3, 26.0, 23.9, 18.3, $-4.0, -4.3$. **IR (ATR):** ν_{max} (cm^{-1}) = 2985 (w), 2952 (w), 2931 (m), 2886 (w), 2857 (w), 1625 (w), 1472 (w), 1461 (w), 1378 (w), 1369 (w), 1362 (w), 1352 (w), 1334 (w), 1295 (w), 1273 (w), 1250 (m), 1240 (m), 1219 (m), 1180 (m), 1119 (m), 1089 (s), 1070 (vs), 1031 (s), 1008 (w), 992 (m), 975 (w), 946 (m), 914 (w), 877 (s), 868 (s), 837 (s), 824 (m), 814 (m), 798 (m), 774 (s), 726 (w), 674 (w). **HRMS (EI):** calc. for $[\text{M}-\text{CH}_3]^+$: 409.0690; found: 409.0680. $[\alpha]_{\text{D}}^{20} = -7.4^\circ$ ($c = 0.023$ g/mL).



Diene 2.115: A mixture of silyl ether **2.114** (100 mg, 0.236 mmol), vinyl stannane **2.110** (177 mg, 0.472 mmol), $\text{Pd}(\text{PPh}_3)_4$ (26 mg, 0.022 mmol), and CuTc (55 mg, 0.288 mmol) in DMF (5.5 mL) was stirred at 65°C overnight in the dark. The reaction was diluted with brine and extracted with EtOAc. The combined organic phases were dried over MgSO_4 and concentrated under reduced pressure. Purification of the resulting residue by flash

column chromatography (EtOAc:hexanes 20:80, $R_f = 0.3$) gave diene **2.115** (87 mg, 0.227 mmol, 96%) as a colourless oil.

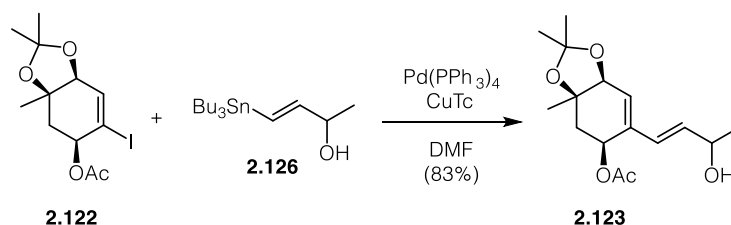
Data for 2.115: $^1\text{H-NMR}$ (400 MHz, CDCl_3): δ (ppm) = 6.30 (dd, $J = 16.0, 0.9$ Hz, 1H), 6.11 (d, $J = 16.0$ Hz, 1H), 5.87 (ddd, $J = 4.7, 1.7, 0.9$ Hz, 1H), 4.23 – 4.16 (m, 1H), 4.15 – 4.10 (m, 1H), 1.96 – 1.89 (m, 2H), 1.50 – 1.44 (m, 3H), 1.39 (s, 3H), 1.34 (s, 3H), 1.34 (s, 3H), 1.29 (s, 3H), 0.90 (s, 9H), 0.12 (s, 3H), 0.11 (s, 3H). $^{13}\text{C-NMR}$ (100 MHz, CDCl_3): δ (ppm) = 144.6, 139.2, 124.4, 118.3, 109.3, 78.4, 76.9, 71.1, 68.8, 42.6, 29.9, 29.7, 28.8, 27.3, 26.0, 23.9, 18.3, –3.9, –4.6. **IR (ATR):** ν_{max} (cm^{-1}) = 3450 (w), 2960 (m), 2931 (m), 2858 (m), 1473 (w), 1463 (w), 1369 (m), 1244 (m), 1212 (m), 1179 (m), 1118 (m), 1088 (s), 1073 (vs), 1032 (s), 991 (m), 973 (m), 915 (w), 879 (m), 859 (w), 837 (s), 774 (s), 728 (w), 672 (w). **HRMS (EI):** calc for $[M-H]^+$: 381.2456, found: 381.2447. $[\alpha]_D^{20} = -6.9^\circ$ ($c = 0.008$ g/mL).



Acetate 2.122: Pyridine (1.40 mL, 16.12 mmol) and AcCl (0.64 mL, 8.06 mmol) were sequentially added to an ice-cooled solution of vinyl iodide **2.108** (500 mg, 1.61 mmol) and DMAP (20 mg, 0.161 mmol) in CH_2Cl_2 (13 mL) and the reaction was stirred for 10 min at that temperature and for 3 h at room temperature before it was hydrolysed with H_2O . The solution was diluted with CH_2Cl_2 and washed with aqueous HCl (1 M), aqueous saturated NaHCO_3 and brine. The organic phase was dried over Na_2SO_4 and the solvent was removed under reduced pressure. Purification of the resulting residue by flash column chromatography (EtOAc:hexanes 10:90, $R_f = 0.25$) gave acetate **2.122** as a colorless oil.

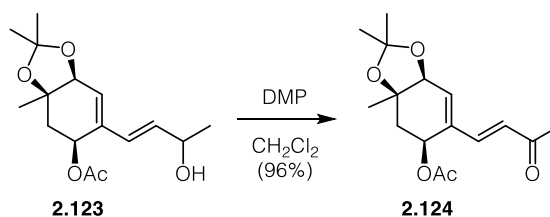
Data for 2.122: $^1\text{H-NMR}$ (400 MHz, CDCl_3): δ (ppm) = 6.66 (dd, $J = 4.8, 1.4$ Hz, 1H), 5.37 – 5.29 (m, 1H), 3.99 (d, $J = 4.7$ Hz, 1H), 2.14 (s, 3H), 2.06 (dd, $J = 7.4, 3.8$ Hz, 2H), 1.46 (s, 3H), 1.39 (s, 3H), 1.36 (s, 3H). $^{13}\text{C-NMR}$ (100 MHz, CDCl_3): δ (ppm) = 170.1, 137.2, 110.3, 105.3, 78.5, 77.8, 71.7, 38.5, 28.6, 27.66, 24.3, 21.4. **IR (ATR):** ν_{max} (cm^{-1}) = 2983 (w), 2934 (w), 2860 (w), 1741 (s), 1629 (w), 1456 (w), 1377 (m), 1367 (m), 1211 (vs), 1181 (s), 1116 (m), 1080 (m), 1065 (m), 1028 (s), 990 (m), 955 (m), 914 (m), 877

(m), 842 (w), 819 (w), 800 (w), 738 (w), 655 (w) **HRMS (EI)**: calc. for $C_{11}H_{14}O_4I$ [$M-CH_3$]⁺: 336.9931, found: 336.9937. $[\alpha]_D^{20} = -7.2^\circ$ (c = 0.009 g/mL).



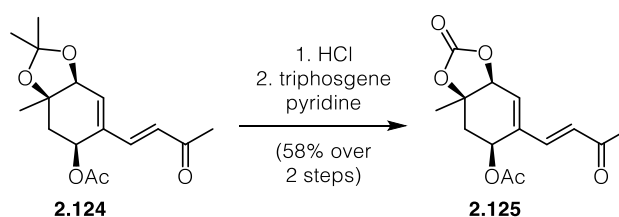
Allylic alcohol 2.123: A solution of acetate **2.122** (500 mg, 1.42 mmol), vinyl stannane **2.126** (769 mg, 2.13 mmol), Pd(PPh₃)₄ (160 mg, 0.138 mmol) and CuTc (340 mg, 1.78 mmol) in DMF (34 mL) was stirred at 65 °C overnight in the dark. After cooling to room temperature the mixture was diluted with EtOAc and filtered over a pad of celite. The filtrate was washed with brine, dried over MgSO₄ and concentrated under reduced pressure. Purification of the resulting residue by flash column chromatography (EtOAc:hexanes 1:2) gave allylic alcohol **2.123** (351 mg, 1.18 mmol, 83%) as mixture of diastereoisomers as a colourless oil.

Data for 2.123: ¹H-NMR (400 MHz, CDCl₃): δ (ppm) = 6.11 (dd, *J* = 16.0, 6.1 Hz, 1H), 5.92 (d, *J* = 4.3 Hz, 1H), 5.72 (dd, *J* = 16.0, 6.0 Hz, 1H), 5.51 (q, *J* = 5.6 Hz, 1H), 4.34 (h, *J* = 6.2 Hz, 1H), 4.25 (d, *J* = 4.4 Hz, 1H), 2.15 (dd, *J* = 13.8, 6.8 Hz, 1H), 2.04 (d, *J* = 1.4 Hz, 3H), 1.97 (dd, *J* = 13.8, 5.4 Hz, 1H), 1.42 (d, *J* = 2.8 Hz, 6H), 1.33 (s, 3H), 1.26 (d, *J* = 6.9 Hz, 3H). ¹³C-NMR (100 MHz, CDCl₃): δ (ppm) = 170.9, 170.9, 137.7, 137.6, 135.7, 135.6, 127.2, 127.2, 127.0, 126.9, 109.9, 77.8, 77.0, 68.7, 68.6, 66.7, 66.6, 37.7, 28.8, 28.3, 28.3, 25.5, 25.5, 23.5, 23.5, 21.4. **IR (ATR)**: ν_{max} (cm⁻¹) = 3373 (s), 2971 (m), 2928 (m), 2872 (w), 1717 (m), 1684 (m), 1636 (m), 1527 (w), 1457 (m), 1419 (s), 1373 (s), 1265 (s), 1150 (s), 1094 (m), 1072 (m), 1037 (s), 998 (m), 973 (m), 940 (m), 922 (m), 882 (m), 833 (m), 724 (m), 696 (m). **HRMS (EI)**: Mass peak could not be found. $[\alpha]_D^{20} = +0.85^\circ$ (c = 0.014 g/mL).



Enone 2.124: Dess-Martin periodinane (983 mg, 2.32 mmol) was added to a stirred solution of allylic alcohol **2.123** (351 mg, 1.18 mmol) in CH_2Cl_2 (10 mL) and the reaction was stirred at room temperature for 1 h. The mixture was diluted with H_2O and $\text{Na}_2\text{S}_2\text{O}_3$ (500 mg, 3.16 mmol) was added and the reaction was stirred until it became a clear solution. The solution was extracted with CH_2Cl_2 and the combined organic phases were washed with brine. Evaporation of the solvent under reduced pressure and purification of the resulting residue by flash column chromatography (EtOAc:hexanes 1:2) gave enone **2.124** (333 mg, 1.13 mmol, 96%) as a colourless oil.

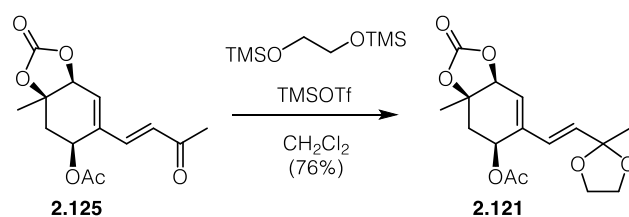
Data for 2.124: $^1\text{H-NMR}$ (400 MHz, CDCl_3): δ (ppm) = 7.05 (d, $J = 16.3$ Hz, 1H), 6.29 (d, $J = 4.1$ Hz, 1H), 6.14 (d, $J = 16.3$ Hz, 1H), 5.54 (t, $J = 5.5$ Hz, 1H), 4.33 (d, $J = 4.1$ Hz, 1H), 2.31 – 2.23 (m, 4H), 2.09 – 1.97 (m, 4H), 1.44 (s, 3H), 1.41 (s, 3H), 1.36 (s, 3H). $^{13}\text{C-NMR}$ (100 MHz, CDCl_3): δ (ppm) = 198.2, 170.8, 141.3, 136.3, 135.6, 128.5, 110.5, 77.7, 76.9, 65.5, 37.3, 28.8, 28.6, 28.1, 26.0, 21.3. **IR (ATR):** ν_{max} (cm^{-1}) 2934 (w), 1734 (s), 1673 (s), 1601 (w), 1426 (w), 1370 (m), 1242 (vs), 1174 (m), 1081 (w), 1033 (m), 991 (w), 923 (w), 864 (w). **HRMS (EI):** calc. for $\text{C}_{14}\text{H}_{16}\text{O}_6\text{S}$ [$M-\text{CH}_3$] $^+$: 279.1227, found: 279.1218. $[\alpha]_D^{20} = -10.0^\circ$ ($c = 0.015$ g/mL).



Carbonate 2.125: Aqueous 1 M HCl (4 mL) was added to a solution of enone **2.124** (333 mg, 1.13 mmol) in MeOH (2 mL) and THF (2 mL) and the solution was stirred at room temperature overnight. The solution was filtered over a pad of celite which was subsequently washed with EtOAc. The solvent was removed under reduced pressure and the resulting residue was redissolved in CH_2Cl_2 (11 mL) and pyridine (0.52 mL, 6.44 mmol). The solution was cooled to -78°C and treated with a solution of triphosgene (159 mg, 0.552 mmol) in CH_2Cl_2 (4.5 mL). The reaction was stirred for 30 min at that

temperature and at room temperature for 16 h. before it was quenched with an aqueous saturated solution of NH_4Cl and extracted with CH_2Cl_2 . The combined organic phases were washed with aqueous HCl (1 M), saturated aqueous NaHCO_3 and brine. The organic phase was dried over Na_2SO_4 and the solvent was removed under reduced pressure. Purification of the resulting residue by flash column chromatography (EtOAc:hexanes 2:1, $R_f = 0.4$) gave carbonate **2.125** (185 mg, 0.660 mmol, 58% over 2 steps) as a colourless solid.

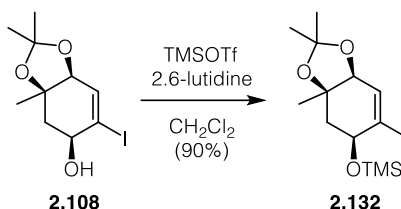
Data for 2.125: $^1\text{H-NMR}$ (400 MHz, CDCl_3): δ (ppm) = 7.08 (d, $J = 16.2$ Hz, 1H), 6.35 – 6.20 (m, 2H), 5.65 (t, $J = 3.5$ Hz, 1H), 4.89 (d, $J = 4.3$ Hz, 1H), 2.61 (dd, $J = 16.0, 2.9$ Hz, 1H), 2.31 (s, 3H), 2.08 (s, 3H), 1.92 (dd, $J = 16.0, 4.1$ Hz, 1H), 1.57 (s, 3H). $^{13}\text{C-NMR}$ (100 MHz, CDCl_3): δ (ppm) = 197.7, 170.7, 153.34, 139.9, 138.8, 131.1, 129.7, 79.4, 77.2, 76.6, 62.3, 35.6, 28.4, 26.9, 21.3. **IR (ATR):** ν_{max} (cm^{-1}) = 1797 (vs), 1735 (s), 1672 (m), 1602 (m), 1370 (m), 1229 (s), 1203 (m), 1187 (m), 1135 (w), 1075 (m), 1020 (s), 772 (w). **HRMS (EI):** calc. for $\text{C}_{12}\text{H}_{14}\text{O}_5$ [$M-\text{Ac}$] $^+$: 237.0757; found: 237.0769. $[\alpha]_D^{20} = -90.0^\circ$ ($c = 0.0064$ g/mL).



Dioxolane 2.121: 1,2-bis(trimethylsilyloxy)ethane (0.078 mL, 0.324 mmol) and TMSOTf (0.06 mL, 0.332 mmol) were sequentially added to a stirred solution of carbonate **2.125** (60 mg, 0.214 mmol) at -78°C and the reaction was stirred at that temperature for 8 h before it was quenched with NEt_3 (0.3 mL). The mixture was diluted with H_2O and extracted with EtOAc. The combined organic phases were washed with brine and dried over MgSO_4 . Evaporation of the solvent under reduced pressure and purification of the resulting residue by flash column chromatography (EtOAc:hexanes 1:1) gave dioxolane **2.121** (53 mg, 0.163 mmol, 76%) as a colourless solid.

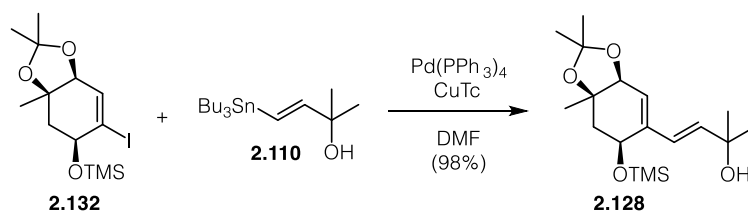
Data for 2.125: $^1\text{H-NMR}$ (400 MHz, CDCl_3): δ (ppm) = $^1\text{H NMR}$ (400 MHz, Chloroform- d) δ 6.32 (d, $J = 16.0$ Hz, 1H), 5.97 (d, $J = 4.4$ Hz, 1H), 5.76 (d, $J = 16.0$ Hz, 1H), 5.61 (t, $J = 3.6$ Hz, 1H), 4.84 (d, $J = 4.4$ Hz, 1H), 4.02 – 3.94 (m, 2H), 3.92 – 3.79 (m, 2H), 2.56 (dd, $J = 15.8, 3.1$ Hz, 1H), 2.07 (s, 3H), 1.89 (dd, $J = 15.9, 4.2$ Hz, 1H), 1.55 (s, 3H), 1.46 (s, 3H). $^{13}\text{C-NMR}$ (100 MHz, CDCl_3): δ (ppm) = 207.2, 170.9, 153.7, 139.5, 133.9, 127.6,

124.8, 107.2, 79.5, 77.2, 77.2, 64.9, 64.7, 62.9, 35.8, 31.1, 26.9, 25.1, 21.3. **IR (ATR):** ν_{\max} (cm⁻¹) = 2983 (w), 2935 (w), 1799 (vs), 1736 (s), 1676 (w), 1635 (w), 1426 (w), 1734 (w), 1388 (w), 1227 (s), 1202 (m), 1135 (w), 1101 (8w), 1075 (m), 1022 (s), 918 (w), 868 (w), 772 (w). **HRMS (EI):** Mass peak could not be found. $[\alpha]_D^{20} = -55.4^\circ$ (c = 0.019 g/mL).



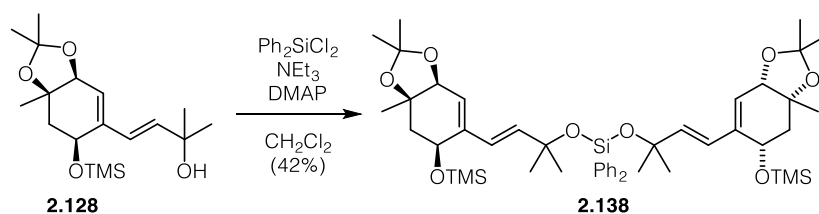
Silyl ether 2.132: 2,6-lutidine (0.20 mL, 1.72 mmol) and TMSOTf (0.16 mL, 0.861 mmol) were sequentially added to an ice-cooled solution of vinyl iodide **2.108** (107 mg, 0.345 mmol) and the reaction was stirred for 90 min at that temperature before it was quenched with saturated aqueous NH₄Cl and extracted with CH₂Cl₂. The combined organic layers were dried over Na₂SO₄ and concentrated under reduced pressure. Purification of the resulting residue by flash column chromatography (EtOAc:hexanes 4:96) gave silyl ether **2.132** (118 mg, 0.309 mmol, 90%) as a colourless oil.

Data for 2.132: ¹H-NMR (400 MHz, CDCl₃): δ (ppm) = 6.57 (dd, $J = 4.9, 1.8$ Hz, 1H), 4.04 – 3.97 (m, 1H), 3.90 (dt, $J = 4.9, 1.3$ Hz, 1H), 2.07 – 1.89 (m, 2H), 1.46 (d, $J = 0.7$ Hz, 3H), 1.37 (d, $J = 0.7$ Hz, 3H), 1.32 (d, $J = 0.8$ Hz, 3H), 0.21 (s, 9H). ¹³C-NMR (100 MHz, CDCl₃): δ (ppm) = 133.7, 115.6, 110.0, 78.5, 78.4, 71.2, 42.7, 28.7, 27.3, 23.8, 0.6. IR (ATR): 2963 (w), 2858 (w), 1627 (w), 1458 (w), 1378 (m), 1368 (m), 1251 (s), 1217 (s), 1183 (m), 1123 (m), 1094 (s), 1073 (s), 1032 (m), 992 (w), 949 (w), 916 (w), 887 (vs), 841 (vs), 803 (w), 749 (w). **IR (ATR)** ν_{\max} (cm⁻¹) = **HRMS (EI):** calc. for C₁₂H₂₀O₃ISi [M-CH₃]⁺: 367.0221, found: 367.0225. $[\alpha]_D^{20} = +109^\circ$ (c = 0.017 g/mL).



Diene 2.128: A mixture of silyl ether **2.132** (178 mg, 0.466 mmol), vinyl stannane **2.110** (349 mg, 0.931 mmol), $\text{Pd}(\text{PPh}_3)_4$ (51 mg, 0.044 mmol), and CuTc (108 mg, 0.566 mmol) in DMF (11 mL) was stirred at 65 °C overnight in the dark. The reaction was diluted with brine and extracted with EtOAc . The combined organic phases were dried over Na_2SO_4 and concentrated under reduced pressure. Purification of the resulting residue by flash column chromatography (EtOAc :hexanes 20:80, $R_f = 0.2$) gave diene **2.128** (156 mg, 0.458 mmol, 98%) as a colourless oil.

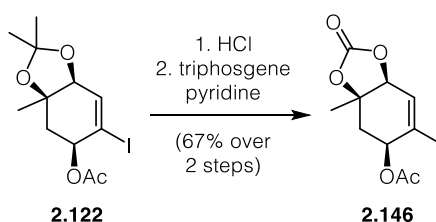
Data for 2.128: $^1\text{H-NMR}$ (400 MHz, CDCl_3): δ (ppm) = 6.29 – 6.09 (m, 2H), 5.86 (ddd, $J = 4.7, 1.6, 0.8$ Hz, 1H), 4.27 (ddt, $J = 10.7, 5.8, 1.5$ Hz, 1H), 4.12 (dd, $J = 4.8, 1.2$ Hz, 1H), 1.94 (dd, $J = 5.9, 1.0$ Hz, 1H), 1.65 – 1.61 (m, 1H), 1.48 – 1.44 (m, 3H), 1.39 – 1.38 (m, 3H), 1.35 (d, $J = 1.4$ Hz, 6H), 1.29 – 1.28 (m, 3H), 0.17 (s, 9H). $^{13}\text{C-NMR}$ (100 MHz, CDCl_3): δ (ppm) = 143.94, 139.8, 124.4, 119.9, 109.2, 78.3, 71.1, 68.6, 42.6, 29.9, 29.9, 28.8, 28.0, 27.3, 27.0, 23.7, 17.7, 13.8, 0.6. **IR (ATR):** ν_{max} (cm^{-1}) = 3433 (w), 2961 (m), 2932 (w), 2858 (w), 1458 (w), 1369 (m), 1249 (m), 1212 (m), 1179 (w), 1165 (w), 1119 (w), 1088 (m), 1073 (s), 1027 (s), 991 (w), 971 (m), 886 (s), 860 (s), 838 (vs), 749 (m), 725 (w), 683 (w). **HRMS (EI):** calc for $[M]^+$: 340.2064; found: 340.2081. $[\alpha]_D^{20} = -10.3^\circ$ ($c = 0.012$ g/mL).



Siloxane 2.138: Ph_2SiCl_2 (25 μL , 0.118 mmol) was added to an ice-cooled solution of diene **2.128** (80 mg, 0.235 mmol), DMAP (5 mg, 0.041 mmol) and NEt_3 (32 μL , 0.238 mmol) in CH_2Cl_2 (1 mL) and the reaction was stirred 10 min at that temperature and 1 h at room temperature before it was quenched with H_2O and extracted with CH_2Cl_2 . The combined organic layers were dried over Na_2SO_4 and concentrated under reduced pressure. Purification of the resulting residue by flash column chromatography

(EtOAc:hexanes 10:90) gave siloxane **2.138** (42 mg, 0.049 mmol, 42%) as a colourless oil.

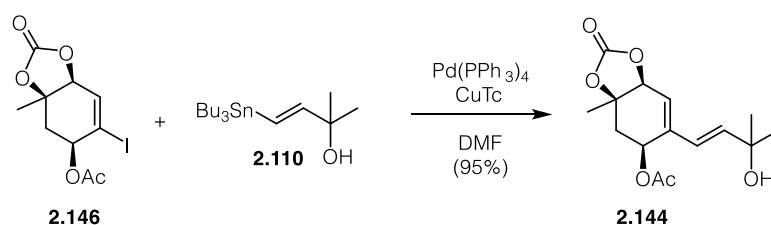
Data for 2.138: $^1\text{H-NMR}$ (400 MHz, CDCl_3): δ (ppm) = 7.73 – 7.59 (m, 4H), 7.35 (dddd, J = 15.2, 8.3, 5.9, 1.2 Hz, 6H), 6.28 – 6.06 (m, 2H), 5.73 (ddd, J = 4.8, 1.7, 0.8 Hz, 1H), 4.19 (dd, J = 10.2, 5.9 Hz, 1H), 4.08 (d, J = 4.7 Hz, 1H), 2.00 – 1.86 (m, 2H), 1.47 (s, 3H), 1.44 (s, 3H), 1.41 (s, 3H), 1.39 (s, 3H), 1.28 (s, 3H), 0.13 (s, 9H). $^{13}\text{C-NMR}$ (100 MHz, CDCl_3): δ (ppm) = 144.0, 140.2, 137.0, 135.4, 129.6, 127.5, 123.8, 119.2, 109.1, 78.3, 76.8, 75.3, 68.5, 42.6, 30.7, 30.5, 28.8, 27.3, 23.7, 0.6. **IR (ATR):** ν_{max} (cm^{-1}) = 2976 (w), 2932 (w), 2858 (w), 1594 (w), 1458 (w), 1430 (w), 1378 (m), 1368 (m), 1342 (w), 1304 (w), 1250 (m), 1240 (m), 1211 (m), 1179 (m), 1164 (m), 1114 (s), 1087 (m), 1072 (s), 1026 (vs), 997 (m), 969 (m), 894 (m), 839 (s), 804 (w), 743 (m), 719 (m), 701 (s). **HRMS (EI):** calc. for $[M]^+$: 860.4535, found: 860.4517. $[\alpha]_D^{20} = -16.8^\circ$ ($c = 0.008 \text{ g/mL}$).



Carbonate 2.146: A solution of acetate **2.122** (270 mg, 1.767 mmol) in MeOH (1 mL), THF (1 mL) and aqueous HCl (1 M, 2 mL) was stirred at room temperature overnight. The reaction mixture was directly submitted to flash column chromatography (hexanes:EtOAc 1:1) giving diol **2.145** (229 mg, 0.734 mmol) as a colorless oil.

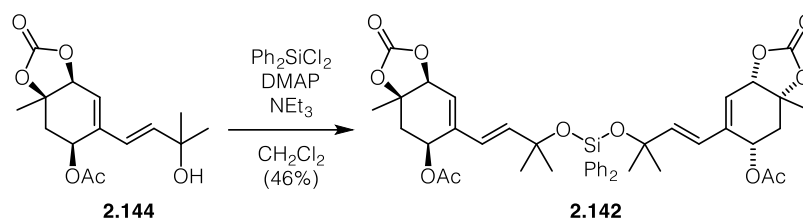
A solution of triphosgene (110 mg, 0.379 mmol) in CH_2Cl_2 (3 mL) was added dropwise to stirred solution of triol **2.145** (229 mg, 0.734 mmol) and pyridine (0.36 mL, 4.45 mmol) in CH_2Cl_2 (7.7 mL) at -78°C . The reaction was stirred for 30 min at -78°C and overnight at room temperature before it was quenched by the addition of aqueous saturated NH_4Cl (7 mL). The organic phase was separated and washed with aqueous HCl (1 M), aqueous saturated NH_4Cl and brine and dried over MgSO_4 . Evaporation of the solvent under reduced pressure and purification of the resulting residue by flash column chromatography (EtOAc:hexanes 3:7, $R_f = 0.3$) gave carbonate **2.146** (174 mg, 0.515 mmol, 67% over 2 steps) as a colorless oil.

Data for 2.146: $^1\text{H-NMR}$ (400 MHz, CDCl_3): δ (ppm) = 6.59 (d, J = 2.9 Hz, 1H), 5.44 (t, J = 4.6 Hz, 1H), 3.84 – 3.77 (m, 1H), 2.14 (d, J = 3.6 Hz, 4H), 2.08 (dd, J = 14.8, 5.3 Hz, 1H), 1.27 (s, 3H). $^{13}\text{C-NMR}$ (100 MHz, CDCl_3): δ (ppm) = 169.6, 144.1, 97.0, 73.8, 72.6, 68.8, 39.0, 25.1, 21.1. **IR (ATR):** ν_{max} (cm^{-1}) = 1789 (s), 1772 (s), 1752 (s), 1730 (s), 1623 (s), 1556 (s), 1461 (s), 1432 (s), 1340 (s), 1385 (s), 1372 (s), 1346 (s), 1306 (s), 1290 (m), 1242 (s), 1206 (vs), 1153 (w), 1110 (m), 1077 (w), 1057 (m), 1018 (vs), 996 (s), 970 (m), 959 (s), 940 (m), 899 (m), 860 (m), 814 (w), 778 (m), 760 (m), 715 (w). **HRMS (EI):** calc. for $[M+H]^+$: 338.9724, found: 338.9722. $[\alpha]_D^{20}$ = -72° (c = 0.0125 g/mL).



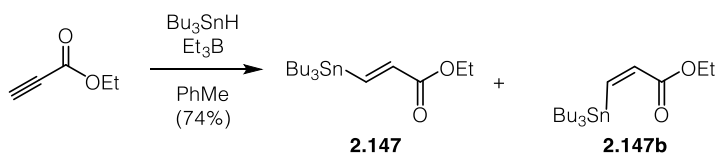
Allylic alcohol 2.144: A solution of carbonate **2.146** (50 mg, 0.148 mmol), vinyl stannane **2.110** (111 mg, 0.296 mmol), $\text{Pd}(\text{PPh}_3)_4$ (15 mg, 0.013 mmol) and CuTc (35 mg, 0.184 mmol) in DMF (4.5 mL) was stirred at 65°C overnight in the dark. The reaction was cooled to room temperature, diluted with EtOAc and filtered through a pad of celite. Evaporation of the solvent under reduced pressure and purification of the resulting residue by flash column chromatography (EtOAc :hexanes 2:1, R_f = 0.25) gave allylic alcohol **2.144** (41 mg, 0.140 mmol, 95%) as a colorless oil.

Data for 2.144: $^1\text{H-NMR}$ (400 MHz, CDCl_3): δ (ppm) = 6.25 (d, J = 16.1 Hz, 1H), 5.99 – 5.92 (m, 2H), 5.65 (s, 1H), 4.85 (d, J = 4.5 Hz, 1H), 2.58 – 2.51 (m, 1H), 2.07 (s, 3H), 1.89 (dd, J = 15.9, 4.1 Hz, 1H), 1.55 (s, 3H), 1.34 (s, 6H). $^{13}\text{C-NMR}$ (100 MHz, CDCl_3): δ (ppm) = 171.0, 153.8, 141.4, 140.0, 124.4, 123.6, 79.5, 77.4, 71.1, 62.9, 36.0, 29.9, 29.9, 27.0, 21.4. **IR (ATR):** ν_{max} (cm^{-1}) = 3482 (w), 2973 (w), 2932 (w), 1782 (s), 1732 (s), 1457 (w), 1426 (w), 1373 (m), 1338 (m), 1304 (w), 1224 (s), 1202 (s), 1187 (s), 1133 (m), 1075 (m), 1017 (vs), 996 (m), 971 (m), 912 (w), 847 (w), 816 (w), 752 (s). **HRMS (EI):** mass could not be found. $[\alpha]_D^{20}$ = -65.9° (c = 0.06 g/mL).



Siloxane 2.142: NEt₃ (18 μL, 0.129 mmol) and Ph₂SiCl₂ (12 μL, 0.057 mmol) were sequentially added to an ice-cooled solution of allylic alcohol **2.144** (40 mg, 0.135 mmol) in CH₂Cl₂ (1 mL) and the reaction was stirred for 10 min at that temperature and for 3 h at room temperature. The mixture was diluted with H₂O and extracted with CH₂Cl₂. The organic phase was washed with brine and dried over MgSO₄. Evaporation of the solvent and purification of the resulting residue by flash column chromatography (EtOAc:hexanes 2:2-1:1) gave siloxane **2.142** (24 mg, 0.031 mmol, 46%) as a colourless oil.

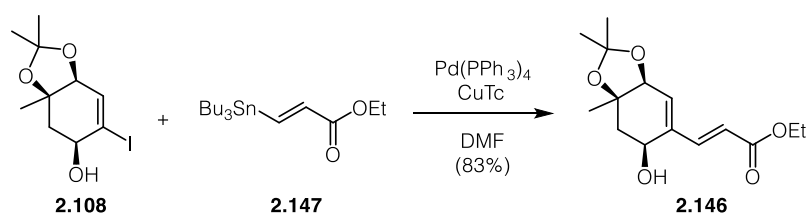
Data for 2.142: ¹H-NMR (400 MHz, CDCl₃): δ (ppm) = 7.59 (dt, *J* = 6.6, 1.5 Hz, 2H), 7.41 – 7.35 (m, 1H), 7.31 (dd, *J* = 7.8, 6.5 Hz, 2H), 6.14 (dd, *J* = 16.0, 13.2 Hz, 1H), 5.92 – 5.76 (m, 2H), 5.51 (t, *J* = 3.6 Hz, 1H), 4.83 (d, *J* = 4.3 Hz, 1H), 2.52 (dd, *J* = 15.9, 3.1 Hz, 1H), 1.98 (d, *J* = 3.0 Hz, 3H), 1.85 (dt, *J* = 15.9, 4.5 Hz, 1H), 1.54 (s, 3H), 1.34 (d, *J* = 2.4 Hz, 3H), 1.31 (s, 3H). ¹³C-NMR (100 MHz, CDCl₃): δ (ppm) = 170.8, 153.9, 141.6, 140.0, 136.2, 135.3, 130.0, 127.7, 124.3, 123.2, 79.6, 77.4, 77.2, 75.1, 62.9, 35.8, 30.4, 30.3, 26.9, 21.3. IR (ATR): ν_{max} (cm⁻¹) = 2974 (m), 2156 (w), 1802 (vs), 1737 (s), 1429 (m), 1382 (m), 1234 (s), 114 (m), 1076 (m), 1024 (s), 752 (m), 704 (m).) HRMS (EI): Mass could not be found. [α]_D²⁰ = –86.4 ° (c = 0.004 g/mL).



Vinyl stannanes 2.147 and 2.147b: Bu₃SnH (2.97 mL, 11.3 mmol) and Et₃B (1M in hexanes, 10.2 mL, 10.2 mmol) were sequentially added to a solution of ethyl propiolate (1.03 mL, 10.19 mmol) in PhMe (102 mL) at –78 °C. The solution was warmed to room temperature overnight and the solvent was removed under reduced pressure. Purification of the resulting residue by flash column chromatography (hexanes:CH₂Cl₂ 9:1 to 4:1) gave vinyl stannane as its (*Z*) – isomer **2.147b** (2.03 g, 5.22 mmol, 51%) and its (*E*) – isomer **2.147** (911 mg, 2.34 mmol, 23%) as a colorless oil.

Data for (Z) 2.147b: $^1\text{H-NMR}$ (400 MHz, CDCl_3): δ (ppm) = 7.15 (d, J = 12.9 Hz, 1H), 6.73 (d, J = 12.9 Hz, 1H), 4.21 (q, J = 7.1 Hz, 2H), 1.52 – 1.44 (m, 7H), 1.34 – 1.23 (m, 13H), 1.00 – 0.94 (m, 6H), 0.88 (t, J = 7.3 Hz, 13H). $^{13}\text{C-NMR}$ (100 MHz, CDCl_3): δ (ppm) = 167.8, 157.2, 135.5, 60.6, 29.3, 27.5, 14.5, 13.9, 11.2. **IR (ATR):** ν_{max} (cm^{-1}) = 2955 (m), 2920 (m), 2872 (w), 2853 (w), 1711 (s), 1464 (w), 1368 (w), 1334 (s), 1199 (vs), 1142 (w), 1072 (w), 1030 (m), 961 (w), 874 (w), 865 (w), 824 (m), 752(w), 723 (w), 668 (m). **HRMS (EI):** HRMS could not be found.

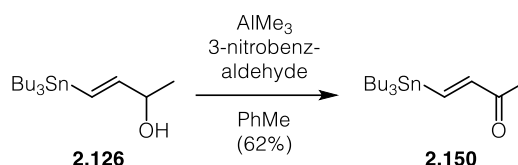
Data for (E) 2.147: $^1\text{H-NMR}$ (400 MHz, CDCl_3): δ (ppm) = 7.74 (d, J = 19.4 Hz, 1H), 6.30 (d, J = 19.4 Hz, 1H), 4.20 (q, J = 7.2 Hz, 2H), 1.61 – 1.39 (m, 7H), 1.36 – 1.25 (m, 10H), 1.00 – 0.94 (m, 5H), 0.89 (t, J = 7.3 Hz, 10H). $^{13}\text{C-NMR}$ (100 MHz, CDCl_3): δ (ppm) = 165.1, 152.6, 136.5, 60.5, 29.1, 27.4, 14.4, 13.8, 9.8. **IR (ATR):** ν_{max} (cm^{-1}) = 2955 (m), 2920 (m), 2871 (w), 2853 (w), 2360 (w), 1711 (m), 1583 (w), 1463 (w), 1419 (w), 1368 (w), 1334 (m), 1292 (w), 1199 (s), 1153 (w), 1096 (w), 1071 (w), 1030 (w), 960 (w), 939 (w), 923 (w), 874 (w), 823 (m), 751 (w), 723 (w), 667 (w) cm^{-1} . **HRMS (EI):** calc for $[M+H]^+$: 391.1654; found: 391.1666.



Ethyl ester 2.146: A solution of alcohol **2.108** (200 mg, 0.645 mmol), stannane **2.147** (502 mg, 1.29 mmol), $\text{Pd}(\text{PPh}_3)_4$ (65 mg, 0.056 mmol) and CuTc (153 mg, 0.802 mmol) in DMF (20 mL) was stirred at 65 °C overnight. After cooling to room temperature, the mixture was diluted with EtOAc , filtered over a pad of celite and concentrated. The resulting residue was purified by flash column chromatography (EtOAc :hexanes 1:4, R_f = 0.2) to give ethyl ester **2.146** (152 mg, 0.538 mmol, 83%) as a slightly yellowish oil.

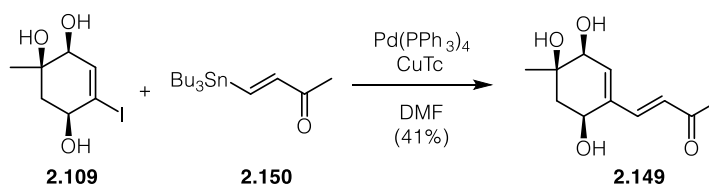
Data for 2.146: $^1\text{H-NMR}$ (400 MHz, CDCl_3): δ (ppm) = 7.28 (d, J = 15.7 Hz, 1H), 6.24 (d, J = 16.0 Hz, 1H), 5.99 (dt, J = 3.3, 0.7 Hz, 1H), 4.43 (d, J = 3.3 Hz, 1H), 4.31 (ddd, J = 10.8, 4.6, 2.4 Hz, 1H), 4.21 (qq, J = 7.2, 3.7 Hz, 2H), 3.56 (d, J = 10.9 Hz, 1H), 2.48 (dd, J = 15.2, 2.4 Hz, 1H), 1.93 (dd, J = 15.2, 4.5 Hz, 1H), 1.47 (d, J = 0.7 Hz, 3H), 1.42 (s, 3H), 1.37 – 1.35 (m, 3H), 1.29 (t, J = 7.1 Hz, 3H). $^{13}\text{C-NMR}$ (100 MHz, CDCl_3): δ (ppm) = 167.2, 144.0, 138.1, 134.1, 120.7, 110.6, 80.1, 78.0, 63.2, 60.6, 39.1, 29.5, 29.2, 26.9,

14.4. **IR (ATR):** ν_{\max} (cm^{-1}) = 3462 (w), 2956 (m), 2827 (m), 2871 (w), 2855 (w), 1628 (w), 1458 (w), 1412 (w), 1376 (s), 1330 (w), 1308 (w), 1271 (w), 1237 (s), 1219 (s), 1181 (m), 1162 (m), 1134 (w), 1106 (s), 1063 (s), 1049 (m), 1029 (vs), 1006 (m), 991 (m), 9401 (m), 915 (m), 890 (w), 874 (m), 846 (w), 825 (m), 799 (w), 774 (w), 747 (w), 723 (w), 694 (m). **HRMS (EI):** Mass peak could not be found. $[\alpha]_D^{20} = -70.0^\circ$ ($c = 0.049$ g/mL).



Enone 2.150: AlMe_3 (2M in hexanes, 0.083 mL, 0.166 mmol) was added to a solution of vinyl stannane **2.126** (600 mg, 1.66 mmol) in PhMe (7 mL) and the solution was stirred for 30 min at room temperature. 2-nitrobenzaldehyde (753 mg, 4.98 mmol) was added and the reaction was stirred 1 h at room temperature and concentrated under reduced pressure. Purification of the resulting residue by flash column chromatography (EtOAc:hexanes 4:96-6:94) gave enone **2.150** (369 mg, 1.03 mmol, 62%) as a colorless oil.

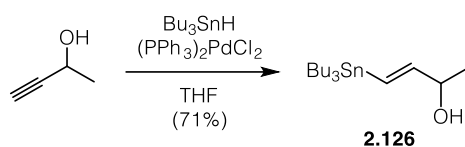
Data for 2.150: $^1\text{H-NMR}$ (400 MHz, CDCl_3): δ (ppm) = 7.55 (d, $J = 19.8$ Hz, 1H), 6.52 (d, $J = 19.8$ Hz, 1H), 2.27 (s, 3H), 1.59 – 1.39 (m, 7H), 1.31 (dq, $J = 14.5, 7.3$ Hz, 7H), 1.08 – 0.94 (m, 6H), 0.89 (t, $J = 7.3$ Hz, 10H). $^{13}\text{C-NMR}$ (100 MHz, CDCl_3): δ (ppm) = 197.8, 151.4, 146.6, 29.1, 27.4, 25.9, 13.8, 9.8. **IR (ATR):** ν_{\max} (cm^{-1}) = 2956 (m), 2822 (m), 2872 (m), 2852 (m), 1694 (w), 1676 (s), 1569 (w), 1464 (w), 1419 (w), 1377 (w), 1357 (m), 1282 (w), 1245 (vs), 1198 (m), 1169 (w), 1073 (w), 996 (s), 961 (w), 875 (w), 865 (w), 790 (w), 769 (w), 665 (s). **HRMS (EI):** mass could not be found.



Ketone 2.149: Triol **2.109** (50 mg, 0.185 mmol), enone **2.150** (133 mg, 0.370 mmol), $\text{Pd(PPh}_3)_4$ (21 mg, 0.018 mmol) and CuTc (44 mg, 0.231 mmol) in DMF (4 mL) was stirred at 65 °C overnight. The reaction mixture was cooled to room temperature, diluted

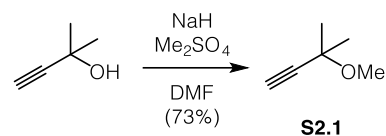
with EtOAc and filtered over a pad of celite. Evaporation of the solvent under reduced pressure and purification of the resulting residue by flash column chromatography (EtOAc, $R_f = 0.3$) gave ketone **2.149** (16 mg, 0.075 mmol, 41%) as a yellowish oil.

Data for 2.149: $^1\text{H-NMR}$ (400 MHz, $d_4\text{-MeOH}$): δ (ppm) = 7.22 (d, $J = 16.2$ Hz, 1H), 6.42 (d, $J = 16.2$ Hz, 1H), 6.11 (d, $J = 2.7$ Hz, 1H), 4.38 (t, $J = 3.7$ Hz, 1H), 4.00 (d, $J = 2.7$ Hz, 1H), 2.31 (s, 3H), 2.11 (dd, $J = 14.5, 3.0$ Hz, 1H), 1.88 (dd, $J = 14.5, 4.6$ Hz, 1H), 1.27 (s, 3H). $^{13}\text{C-NMR}$ (100 MHz, $d_4\text{-MeOH}$): δ (ppm) = 201.6, 145.5, 141.1, 138.8, 128.8, 73.9, 71.9, 64.9, 41.8, 27.3, 26.4. **IR (ATR):** ν_{max} (cm^{-1}) = 3374 (br), 2926 (m), 2511 (br), 1661 (s), 1638 (s), 1595 (s), 1423 (m), 1362 (m), 1260 (s), 1150 (s), 1097 (w), 1040 (s), 998 (w), 974 (s), 939 (m), 884 (w), 835 (m), 725 (w). **HRMS (EI/ESI):** mass peak could not be found. $[\alpha]_D^{20} = -68.9^\circ$ (MeOH, $c = 0.02$ g/mL).



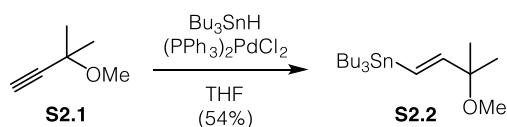
Vinyl stannane 2.126: Bu_3SnH (0.74 mL, 3.71 mmol) was added dropwise to a stirred solution of 3-butyn-2-ol (0.22 mL, 2.85 mmol) and $\text{Pd}(\text{PPh}_3)_2\text{Cl}_2$ (200 mg, 0.285 mmol) in THF (9 mL). The solution was stirred at -78°C for 3 h and then warmed to room temperature and concentrated under reduced pressure. Purification of the resulting residue by flash column chromatography (EtOAc:hexanes 4:96 to 6:94, $R_f = 0.25$) gave vinyl stannane **2.126** (728 mg, 2.02 mmol, 71%) as a colorless oil.

Data for 2.126: $^1\text{H-NMR}$ (400 MHz, CDCl_3): δ (ppm) = 6.33 – 5.79 (m, 2H), 4.26 (dtd, $J = 10.7, 6.5, 4.2$ Hz, 1H), 1.60 – 1.38 (m, 8H), 1.35 – 1.25 (m, 9H), 0.89 (t, $J = 7.3$ Hz, 14H). $^{13}\text{C-NMR}$ (100 MHz, CDCl_3): δ (ppm) = 152.2, 126.7, 71.5, 29.2, 27.4, 23.2, 13.9, 9.6. **IR (ATR):** ν_{max} (cm^{-1}) = 3324 (m), 2956 (s), 2924 (vs), 2872 (m), 2853 (m), 1603 (w), 1464 (m), 1457 (m), 1418 (w), 1376 (m), 1327 (w), 129 (w), 1250 (w), 1182 (w), 1121 (m), 1071 (w), 988 (w), 630 (w), 936 (m), 874 (m), 864 (m), 840 (w), 828 (w), 767 (w), 746 (w), 688 (s). **HRMS (EI):** calc. for $\text{C}_{16}\text{H}_{34}\text{OSn}$ [M] $^+$: 361.1548; found: 361.1567.



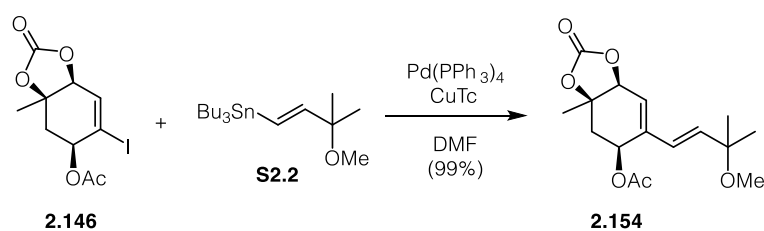
Methyl ether S2.1: NaH (60% in mineral oil, 3.05 g, 76.0 mmol) was added portionwise to a stirred solution of 2-methyl-3-butyn-2-ol (4.84 mL, 50.0 mmol) in DMF (50 mL) and the reaction was stirred for 30 min at that temperature. Dimethylsulfate (7.25 mL, 76.0 mmol) was added dropwise and the solution was stirred for 1 h at room temperature before it was quenched with AcOH (2.5 mL). The desired product was directly distilled out of the reaction mixture (b.p. 78-80 °C) to give methyl ether **S2.1** (3.61 g, 36.75 mmol, 73%) as a colorless liquid.

Data for S2.1: $^1\text{H-NMR}$ (400 MHz, CDCl_3): δ (ppm) = 3.37 (s, 3H), 2.42 (s, 1H), 1.46 (s, 6H). $^{13}\text{C-NMR}$ (100 MHz, CDCl_3): δ (ppm) = 85.8, 72.2, 70.4, 51.8, 28.3. **IR (ATR):** ν_{max} (cm^{-1}) = 3896 (w), 2987 (m), 2939 (w), 2828 (w), 1746 (w), 1683 (w), 1466 (w), 1380 (w), 1362 (w), 1237 (m), 1201 (w), 1174 (s), 1150 (s), 1074 (vs), 940 (w), 844 (s), 688 (m). **HRMS (EI):** calc for $[M-H]^+$: 97.0648; found: 97.0649.



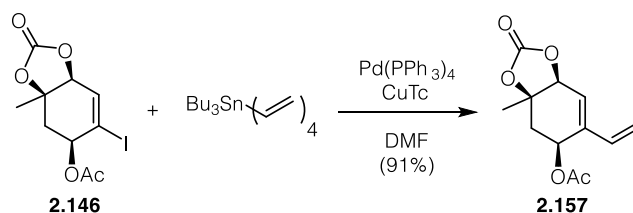
Vinyl stanine S2.2: Bu_3SnH (1.27 mL, 4.74 mmol) was added dropwise to a stirred solution of methyl ether **S2.1** (500 mg, 5.09 mmol) and $\text{Pd}(\text{PPh}_3)_2\text{Cl}_2$ (36 mg, 0.052 mmol) in THF (20 mL) and the reaction was stirred for 1 h at room temperature before it was concentrated under reduced pressure. Purification of the resulting residue by flash column chromatography (EtOAc:hexanes 4:96) gave vinyl stanine **S2.2** (1.07 g, 2.75 mmol, 54%) as a colorless oil.

Data for S2.2: $^1\text{H-NMR}$ (400 MHz, CDCl_3): δ (ppm) = 6.19 – 5.78 (m, 2H), 3.15 (s, 3H), 1.55 – 1.39 (m, 6H), 1.31 (dt, $J = 14.7, 7.3$ Hz, 6H), 1.25 (s, 6H), 0.89 (td, $J = 7.7, 7.3, 3.8$ Hz, 16H). $^{13}\text{C-NMR}$ (100 MHz, CDCl_3): δ (ppm) = 153.2, 126.9, 50.6, 29.2, 27.4, 25.5, 13.9, 9.6. **IR (ATR):** ν_{max} (cm^{-1}) = 2956 (s), 2825 (s), 2872(m), 2854 (m), 2822 (w), 1592 (w), 1524 (w), 1464 (m), 1418 (w), 1376 (m), 1360 (m), 1292 (w), 1246 (w), 1232 (w), 1166 (m), 1128 (w), 1076 (vs), 1000 (s), 960 (w), 874 (w), 852 (w), 778 (w), 749 (w), 664 (s). **HRMS (EI):** Mass peak could not be found.



Methyl ether 2.154: A solution of carbonate **2.146** (50 mg, 0.148 mmol), vinyl stannane **S2.2** (115 mg, 0.296 mmol), Pd(PPh₃)₄ (15 mg, 0.013 mmol) and CuTc (35 mg, 0.184 mmol) in DMF (4.5 mL) was stirred at 65 °C overnight in the dark. The reaction was cooled to room temperature, diluted with EtOAc and filtered through a pad of celite. Evaporation of the solvent under reduced pressure and purification of the resulting residue by flash column chromatography (EtOAc:hexanes 1:1, R_f = 0.25) gave methyl ether **2.154** (46 mg, 0.147 mmol, 99%) as a colorless oil.

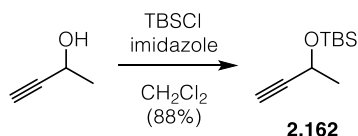
Data for 2.154: ¹H-NMR (400 MHz, CDCl₃): δ (ppm) = 6.11 (d, *J* = 16.4 Hz, 1H), 5.93 (d, *J* = 4.3 Hz, 1H), 5.81 (d, *J* = 16.4 Hz, 1H), 5.66 (t, *J* = 3.7 Hz, 1H), 4.85 (d, *J* = 4.3 Hz, 1H), 3.14 (s, 3H), 2.57 (dd, *J* = 15.9, 3.0 Hz, 1H), 1.91 (dd, *J* = 15.9, 4.2 Hz, 1H), 1.55 (s, 3H), 1.28 (s, 3H), 1.28 (s, 3H). ¹³C-NMR (100 MHz, CDCl₃): δ (ppm) = 170.9, 153.8, 139.9, 139.5, 126.8, 123.6, 79.6, 75.0, 62.8, 50.7, 35.8, 26.9, 26.1, 25.6, 21.3. IR (ATR): ν_{max} (cm⁻¹) = 2955 (w), 2925 (w), 2870 (w), 2855 (w), 1779 (s), 1728 (s), 1633 (w), 1587 (w), 1572 (w), 1528 (w), 1516 (w), 1464 (w), 1420 (w), 1371 (m), 1331 (m), 1304 (w), 1280 (w), 1235 (m), 1220 (m), 1200 (s), 1188 (s), 1132 (m), 1109 (m), 1074 (s), 1016 (s), 997 (m), 959 (m), 938 (w), 915 (w), 888 (w), 862 (w), 850 (w), 800 (w), 778 (w), 768 (m), 746 (w), 737 (w), 724 (w), 712 (w). HRMS (EI): Mass peak could not be found. [α]_D²⁰ = -71.1 ° (c = 0.013 g/mL).



Diene 2.157: A solution of carbonate **2.146** (50 mg, 0.148 mmol), tetravinyl stannane (87 μL, 0.296 mmol), Pd(PPh₃)₄ (15 mg, 0.013 mmol) and CuTc (35 mg, 0.184 mmol) in DMF (4.5 mL) was stirred at 65 °C overnight in the dark. The reaction was cooled to room temperature, diluted with EtOAc and filtered through a pad of celite. Evaporation of the

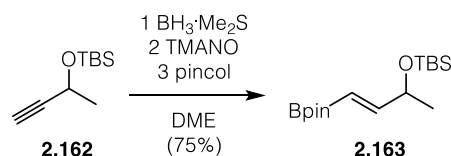
solvent under reduced pressure and purification of the resulting residue by flash column chromatography (EtOAc:hexanes 1:2, $R_f=0.25$) gave diene **2.157** (32 mg, 0.134 mmol, 91%) as a colorless oil.

Data for 2.157: $^1\text{H-NMR}$ (400 MHz, CDCl_3): δ (ppm) = 6.33 (dd, $J = 17.6, 11.0$ Hz, 1H), 5.95 (dd, $J = 4.5, 0.7$ Hz, 1H), 5.73 – 5.66 (m, 1H), 5.39 (d, $J = 17.6$ Hz, 1H), 5.30 (d, $J = 10.9$ Hz, 1H), 4.85 (d, $J = 4.4$ Hz, 1H), 2.57 (dd, $J = 15.9, 3.0$ Hz, 1H), 2.07 (s, 3H), 1.89 (dd, $J = 15.9, 4.2$ Hz, 1H), 1.55 (s, 3H). $^{13}\text{C-NMR}$ (100 MHz, CDCl_3): δ (ppm) = 170.9, 153.8, 140.4, 134.7, 124.2, 118.1, 79.6, 77.3, 62.1, 35.9, 27.0, 21.4. **IR (ATR):** ν_{max} (cm^{-1}) = 2959 (w), 1979 (vs), 1734 (s), 1609 (w), 1425 (w), 1374 (w), 1336 (w), 1301 (w), 1238 (s), 1202 (m), 1187 (m), 1136 (w), 1117 (w), 1073 (m), 1021 (s), 996 (m), 940 (w), 918 (w), 893 (w), 772 (w). **HRMS (EI):** calc. for $[M]^+$: 238.0836; found: 238.0853. $[\alpha]_D^{20} = -63.9^\circ$ ($c = 0.019$ g/mL).



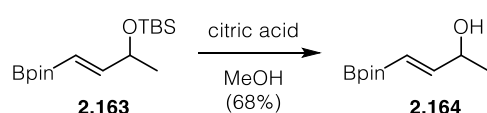
Silyl ether 2.162: Imidazole (1.50 g, 22 mmol) and TBSCl (3.0 g, 20 mmol) were sequentially added to an ice-cooled solution of 3-butyn-2-ol (1.56 mL, 20 mmol) and the reaction was stirred at room temperature overnight before it was diluted with H_2O (21 mL) and extracted with pentane. The combined organic layers were washed with brine, dried over MgSO_4 and concentrated under reduced pressure. Purification of the resulting residue by flash column chromatography (Et_2O :pentane 2:98) gave silyl ether **2.162** (3.25 g, 17.63 mmol, 88%) as a colorless oil.

Data for 2.162: $^1\text{H-NMR}$ (400 MHz, CDCl_3): δ (ppm) = δ 4.51 (qd, $J = 6.5, 2.1$ Hz, 1H), 2.37 (d, $J = 2.1$ Hz, 1H), 1.42 (d, $J = 6.5$ Hz, 3H), 0.90 (s, 10H), 0.12 (d, $J = 5.3$ Hz, 6H). $^{13}\text{C-NMR}$ (100 MHz, CDCl_3): δ (ppm) = 86.6, 71.3, 58.9, 25.9, 25.5, $-4.5, -4.9$. **IR (ATR):** ν_{max} (cm^{-1}) = 1716 (w), 1473 (w), 1362 (w), 1252 (m), 1121 (m), 1102 (s), 1058 (m), 1006 (w), 975 (s), 939 (w), 835 (vs), 804 (m), 776 (vs). **HRMS (EI):** calc. for $\text{C}_{10}\text{H}_{19}\text{OSi}^+$ [$M-H$] $^+$: 183.1200, found: 183.1197.



Vinyl boronate 2.163: Cyclohexane (0.55 mL, 5.42 mmol) was added to a stirred solution of $\text{BH}_3\cdot\text{Me}_2\text{S}$ (0.26 mL, 2.71 mmol) in DME (2.7 mL) and the reaction was stirred at room temperature for 1 h. Silyl ether **2.162** (500 mg, 2.71 mmol) was added and the solution was stirred at room temperature until it became clear. TMANO (407 mg, 5.42 mmol) was added and the solution was stirred at room temperature for 1 h before pinacol (0.33 mL, 2.71 mmol) was added and the solution was stirred at room temperature overnight and concentrated under reduced pressure. Purification by flash column chromatography (EtOAc:hexanes 5:95) gave vinyl boronate **2.163** (634 mg, 2.03 mmol, 75%) as a colorless oil.

Data for 2.163: $^1\text{H-NMR}$ (400 MHz, CDCl_3): δ (ppm) = 6.60 (dd, $J = 17.9, 4.0$ Hz, 1H), 5.61 (dd, $J = 17.9, 1.7$ Hz, 1H), 4.38 – 4.28 (m, 1H), 1.27 (s, 12H), 1.21 (d, $J = 6.5$ Hz, 3H), 0.89 (s, 10H). $^{13}\text{C-NMR}$ (100 MHz, CDCl_3): δ (ppm) = 157.2, 83.3, 69.9, 26.1, 25.0, 24.9, 23.8, 18.4, -4.6, -4.7. **IR (ATR):** ν_{max} (cm^{-1}) = 2978 (m), 2957 (m), 2930 (m), 2857 (m), 1642 (m), 1472 (s), 1390 (w), 1362 (s), 1336 (s), 1319 (s), 1256 (l), 1213 (w), 1144 (vs), 1094 (s), 1052 (m), 989 (m), 968 (m), 899 (m), 850 (m), 833 (vs), 806 (m), 774 (vs). **HRMS (EI):** calc. for $\text{C}_{15}\text{H}_{30}\text{O}_3\text{BSi}$ [$M-\text{CH}_3$] $^+$: 297.2052, found: 297.2052.

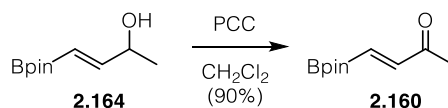


Allyl alcohol 2.164: Citric acid (425 mg, 2.02 mmol) was added to a stirred solution of vinyl boronate **2.163** (630 mg, 2.02 mmol) in MeOH (2 mL) at room temperature for 3 h. The reaction was diluted with EtOAc and washed with H_2O (2x) and brine. The organic phase was dried over MgSO_4 and the solvent was removed under reduced pressure. Purification by flash column chromatography (EtOAc:hexanes 1:4) gave allyl alcohol **2.164** (272 mg, 1.37 mmol, 68%) as a colorless oil.

Data for 2.164: $^1\text{H-NMR}$ (400 MHz, CDCl_3): δ (ppm) = 6.65 (dd, $J = 18.1, 4.9$ Hz, 1H), 5.62 (dd, $J = 18.1, 1.5$ Hz, 1H), 4.34 (dtd, $J = 6.5, 4.8, 1.7$ Hz, 1H), 1.54 (d, $J = 4.6$ Hz, 1H), 1.27 (s, 15H). $^{13}\text{C-NMR}$ (100 MHz, CDCl_3): δ (ppm) = 156.3, 83.5, 69.8, 25.0, 24.9, 22.8. **IR (ATR):** ν_{max} (cm^{-1}) = 3428 (br), 2978 (m), 2929 (w), 1643 (m), 1449 (w), 1358

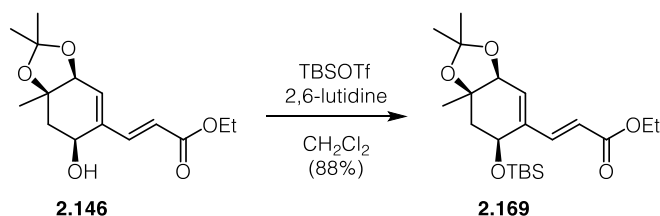
(s), 1323 (s), 1272 (w), 1213 (w), 1145 (s), 1058 (w), 997 (m), 970 (m), 898 (w), 850 (m).

HRMS (EI): calc. for $C_9H_{16}O_3B$ [$M-CH_3$] $^+$: 183.1187, found: 183.1184.



Enone 2.160: A solution of allyl alcohol **2.164** (100 mg, 0.505 mmol) in CH_2Cl_2 (0.5 mL) was added to a suspension of PCC (163 mg, 0.756 mmol) in CH_2Cl_2 (1 mL) and the reaction was stirred at room temperature for 2 h. The reaction mixture was diluted with Et_2O and filtered over a pad of silica to give enone **2.160** (89 mg, 0.455 mmol, 90%) as yellowish oil.

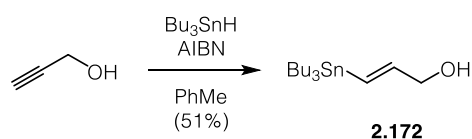
Data for 2.160: $^1\text{H-NMR}$ (400 MHz, CDCl_3): δ (ppm) = 6.80 (d, J = 18.6 Hz, 1H), 6.54 (d, J = 18.6 Hz, 1H), 2.29 (s, 3H), 1.29 (s, 12H). $^{13}\text{C-NMR}$ (100 MHz, CDCl_3): δ (ppm) = 199.3, 146.7, 84.3, 26.89, 24.9. **IR (ATR):** ν_{max} (cm^{-1}) = 2980 (w), 1683 (w), 1341 (s), 1247 (m), 1144 (m), 1002 (w), 848 (w). **HRMS (EI):** calc. for $C_9H_{14}O_3B$ [$M-CH_3$] $^+$: 1831.1031, found: 181.1029.



Silyl ether 2.167: 2,6-Lutidine (0.16 mL, 1.42 mmol) and TBSOTf (0.13 mL, 0.710 mmol) were sequentially added to an ice cooled solution of ethyl ester **2.146** (80 mg, 0.283 mmol) in CH_2Cl_2 (2 mL) and the reaction was stirred for 2 h at 0 °C and quenched with saturated aqueous ammonium chloride. The mixture was extracted with CH_2Cl_2 , the organic phase was dried over Na_2SO_4 and concentrated under reduced pressure. Purification of the resulting residue by flash column chromatography (EtOAc :hexanes 6:94) gave silyl ether **2.167** (99 mg, 0.250 mmol, 88%) as a colorless oil.

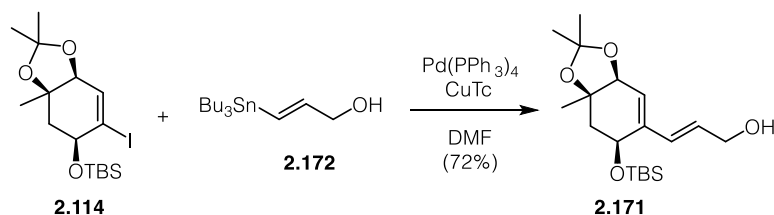
Data for 2.167: $^1\text{H-NMR}$ (400 MHz, CDCl_3): δ (ppm) = 7.37 (d, J = 16.0 Hz, 1H), 6.16 (d, J = 16.0 Hz, 1H), 6.13 – 6.10 (m, 1H), 4.32 – 4.25 (m, 1H), 4.21 (qt, J = 7.1, 3.7 Hz,

2H), 4.16 (d, $J = 4.4$ Hz, 1H), 2.00 – 1.88 (m, 2H), 1.47 (s, 3H), 1.40 (s, 3H), 1.31 – 1.26 (m, 6H), 0.90 (s, 9H), 0.14 (s, 3H), 0.11 (s, 3H). **$^{13}\text{C-NMR}$ (100 MHz, CDCl_3):** δ (ppm) = 166.7, 143.0, 142.5, 124.6, 120.9, 109.7, 78.3, 68.1, 60.5, 42.4, 28.8, 27.4, 25.9, 24.1, 18.2, 14.4, -3.7 , -4.7 . **IR (ATR):** ν_{max} (cm^{-1}) = 2958 (m), 2932 (m), 2858 (m), 1717 (s), 1640 (w), 1463 (w), 1369 (m), 1307 (m), 1252 (m), 1211 (m), 1174 (s), 1090 (s), 1075 (s), 1034 (s), 993 (w), 879 (m), 837 (s), 776 (m). **HRMS (EI):** calc. for $\text{C}_{20}\text{H}_{33}\text{O}_5\text{Si}$ [$M-\text{CH}_3$] $^+$: 381.2092, found: 381.2109. $[\alpha]_{\text{D}}^{20} = -0.65^\circ$ ($c = 0.925$ g/mL).



Vinyl stannane 2.172: Bu_3SnH (2.88 mL, 10.8 mmol, 1.2 eq) was added to a mixture of propargyl alcohol (0.52 mL, 9.0 mmol, 1.0 eq) and AIBN (22 mg, 0.13 mmol, 0.015 eq) in dry toluene (34 mL) and the reaction was stirred at 110°C for 2.5 h. Concentration under reduced pressure and purification by flash column chromatography (Et_2O :hexanes = 15:85, $R_f = 0.3$) gave vinyl stannane **2.172** (1.57 g, 4.51 mmol, 51%) as a colorless liquid.

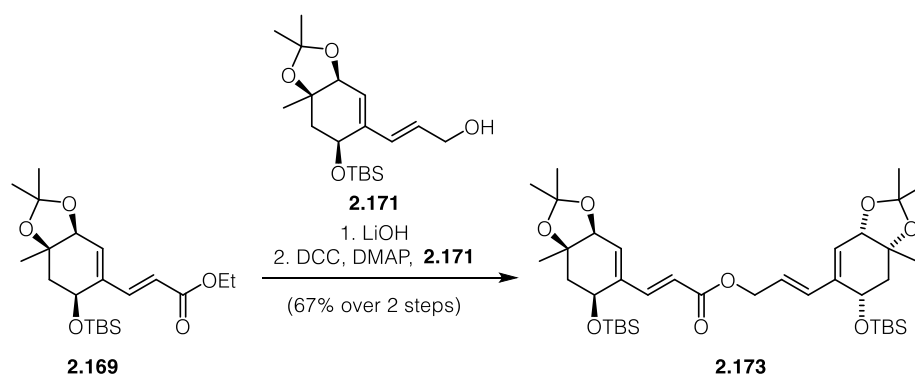
Data for 2.172: **$^1\text{H-NMR}$ (400 MHz, CDCl_3):** 6.35 – 6.01 (m, 2H), 4.23 – 4.12 (m, 2H), 1.58 (s, 1H), 1.52 – 1.40 (m, 6H), 1.35 – 1.26 (m, 6H), 0.89 (td, $J = 7.7, 7.3, 2.6$ Hz, 15H). **$^{13}\text{C-NMR}$ (100 MHz, CDCl_3):** δ (ppm) = 147.1, 128.5, 77.2, 66.6, 29.2, 27.4, 13.9, 9.6. **IR (ATR):** ν_{max} (cm^{-1}) = 3297 (w, br), 2955 (s), 2922 (s), 2871 (w), 2851 (w), 2361 (w), 1603 (w), 1463 (m), 1417 (w), 1376 (w), 1357 (w), 1340 (w), 1292 (w), 1248 (w), 1179 (w), 1071 (m), 990 (m), 960 (w), 873 (w), 725 (w), 689 (m), 664 (m) cm^{-1} . **HRMS (ESI):** calc for [$M-H$] $^-$: 347.1402; found: 347.1405.



Allylic alcohol 2.171: A solution of silyl ether **2.114** (200 mg, 0.471 mmol), vinyl stannane **2.172** (245 mg, 0.707 mmol), $\text{Pd(PPh}_3)_4$ (51 mg, 0.044 mmol) and CuTc

(110 mg, 0.324 mmol) in DMF (10 mL) was stirred at 65 °C overnight in the dark. After cooling to room temperature the mixture was diluted with EtOAc and washed with brine. The organic phase was dried over MgSO₄ and concentrated under reduced pressure. Purification of the resulting residue by flash column chromatography (EtOAc:hexanes 2:8) gave allylic alcohol **2.171** (120 mg, 0.338 mmol, 72%) as a colourless oil.

Data for 2.171: ¹H-NMR (400 MHz, CDCl₃): δ (ppm) = 6.35 – 6.27 (m, 1H), 6.10 (dt, *J* = 15.8, 5.6 Hz, 1H), 5.88 (dt, *J* = 4.8, 1.2 Hz, 1H), 4.26 – 4.18 (m, 3H), 4.13 (d, *J* = 4.6 Hz, 1H), 1.93 (d, *J* = 7.9 Hz, 2H), 1.39 (s, 3H), 1.28 (s, 3H), 0.90 (s, 9H), 0.11 (s, 3H), 0.10 (s, 3H). ¹³C-NMR (100 MHz, CDCl₃): δ (ppm) = 144.3, 130.6, 128.9, 128.5, 119.1, 109.3, 78.4, 68.6, 63.9, 42.5, 28.8, 27.4, 26.0, 23.9, 18.3, –3.7, –4.6. IR (ATR): ν_{max} (cm⁻¹) = 3427 (w), 2956 (m), 2930 (m), 2857 (m), 1613 (w), 1472 (w), 1463 (w), 1420 (w), 1369 (m), 1321 (w), 1276 (8w), 1244 (m), 1212 (m), 1178 (m), 1118 (m), 1089 (s), 1072 (vs), 1030 (s), 992 (w), 971 (w), 918 (w), 878 (s), 856 (m), 836 (s), 802 (m), 774 (s), 672 (w). HRMS (EI): Mass could not be found. [α]_D²⁰ = –6.1 ° (c = 0.001 g/mL).

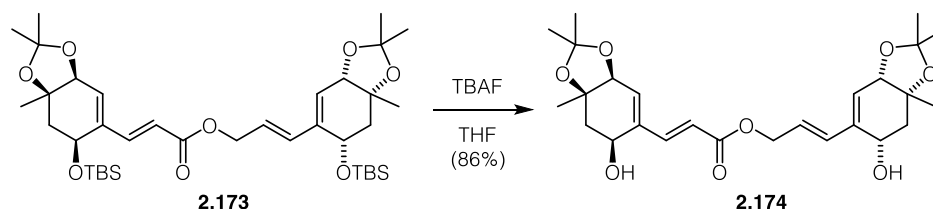


Allylic ester 2.173: LiOH·H₂O (36.5 mg, 0.870 mmol) was added to a solution of ethyl ester **2.169** (34 mg, 0.087 mmol) in THF (1 mL), MeOH (1 mL) and H₂O (1 mL) and the solution was stirred at 60 °C for 3 h. The reaction was acidified with aqueous HCl (1 M) and extracted with EtOAc. The combined organic phases were washed with brine, dried over MgSO₄ and concentrated under reduced pressure to give crude acid **2.170** that was used in the next step without further purification.

A solution of DCC (20 mg, 0.096 mmol) in CH₂Cl₂ (0.65 mL) was added dropwise to an ice-cooled solution of crude acid **2.170**, allylic alcohol **2.171** (31 mg, 0.087 mmol) and DMAP (5.5 mg, 0.045 mmol) in CH₂Cl₂ (0.65 mL) and the reaction was stirred for 30 min at that temperature and for 17 h at room temperature. The reaction mixture was filtered over a pad of celite and concentrated under reduced pressure. Purification of the

resulting residue by flash column chromatography (EtOAc:hexanes 1:9) gave allylic ester **2.173** (41 mg, 0.058 mmol, 67% over 2 steps) as a colorless solid.

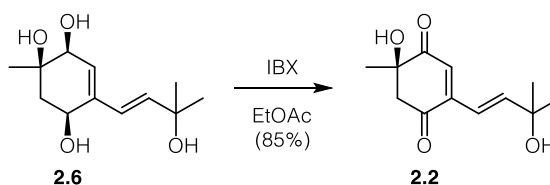
Data for 2.173: $^1\text{H-NMR}$ (400 MHz, CDCl_3): δ (ppm) = 6.16 (d, J = 16.0 Hz, 1H), 6.11 (dd, J = 4.4, 1.2 Hz, 1H), 4.68 (d, J = 6.0 Hz, 2H), 4.25 (dt, J = 26.2, 8.2 Hz, 2H), 4.14 (dd, J = 16.6, 4.6 Hz, 2H), 3.47 (q, J = 7.0 Hz, 3H), 1.97 – 1.89 (m, 4H), 1.46 (s, 6H), 1.39 (d, J = 4.6 Hz, 6H), 1.28 (d, J = 7.1 Hz, 6H), 1.20 (t, J = 7.0 Hz, 4H), 0.88 (s, 9H), 0.88 (s, 9H), 0.13 (s, 3H), 0.10 (s, 3H), 0.09 (s, 3H), 0.09 (s, 3H). $^{13}\text{C-NMR}$ (100 MHz, CDCl_3): δ (ppm) = 166.4, 144.1, 143.1, 142.9, 131.7, 125.6, 125.0, 120.5, 120.0, 109.7, 109.3, 78.4, 78.3, 76.8, 76.6, 68.5, 68.0, 66.0, 65.1, 42.5, 42.4, 28.8, 28.8, 27.4, 27.4, 26.0, 25.9, 24.1, 23.9, 18.3, 18.2, 15.4, -3.7, -3.8, -4.6, -4.6. **IR (ATR):** ν_{max} (cm^{-1}) = 2955 (w), 2931 (m), 2886 (w), 2857 (w), 1718 (m), 1637 (w), 1472 (w), 1463 (w), 1377 (m), 1369 (m), 1306 (w), 1274 (w), 1243 (m), 1211 (m), 1161 (s), 1118 (w), 1088 (s), 1072 (s), 1031 (s), 992 (m), 938 (w), 918 (w), 878 (m), 836 (s), 814 (w), 801 (w), 774 (s), 735 (w), 670 (w). **HRMS (ESI):** calc for $[M+\text{NH}_4]^+$: 722.4478; found: 722.4481. $[\alpha]_D^{20} = -6.7^\circ$ ($c = 0.0081$ g/mL).



Diol 2.174: TBAF (1 M in THF, 0.09 mL, 0.09 mmol) was added dropwise to an ice cooled solution of allylic ester **2.173** (20 mg, 0.028 mmol) in THF (3 mL) and the solution was stirred for 30 min at that temperature and for 3 h at room temperature. The reaction was quenched with a saturated aqueous solution of NH_4Cl and extracted with EtOAc. The combined organic phases were washed with brine, dried over Na_2SO_4 and concentrated under reduced pressure. Purification of the resulting residue by flash column chromatography (EtOAc:hexanes 1:1, R_f 0.3) gave diol **2.174** (11.3 mg, 0.024 mmol, 86%) as a colorless solid.

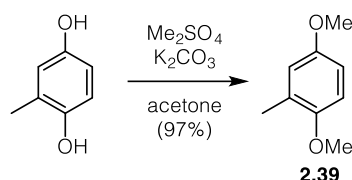
Data for 2.174: $^1\text{H-NMR}$ (400 MHz, CDCl_3): δ (ppm) = 7.29 (d, J = 15.9 Hz, 1H), 6.27 (dd, J = 15.9, 8.6 Hz, 2H), 6.09 (dt, J = 15.9, 6.0 Hz, 1H), 5.99 (d, J = 3.4 Hz, 1H), 5.67 (d, J = 3.5 Hz, 1H), 4.78 – 4.72 (m, 2H), 4.41 (dd, J = 12.8, 3.4 Hz, 2H), 4.30 (s, 2H), 3.55 (s, 2H), 2.45 (td, J = 15.0, 2.5 Hz, 2H), 1.91 (ddd, J = 15.1, 12.3, 4.5 Hz, 2H), 1.47

(s, 3H), 1.46 (s, 3H), 1.42 (s, 3H), 1.40 (s, 3H), 1.38 (s, 3H), 1.35 (s, 3H). **¹³C-NMR (100 MHz, CDCl₃):** δ (ppm) = 166.8, 144.5, 138.6, 138.1, 134.4, 133.3, 128.0, 125.4, 120.3, 110.6, 110.3, 80.2, 80.1, 78.3, 78.0, 64.9, 63.5, 63.2, 39.4, 39.10, 29.6, 29.5, 29.2, 29.2, 26.9, 26.8. **IR (ATR):** ν_{\max} (cm⁻¹) = 3528 (w), 2984 (w), 2931 (m), 1715 (s), 1638 (w), 1459 (w), 1374 (m), 1307 (w), 1280 (m), 1239 (s), 1207 (m), 1165 (s), 1135 (w), 1072 (m), 1056 (m), 1029 (s), 1006 (m), 919 (w), 863 (w), 827 (m). **HRMS (ESI):** calc for C₂₆H₄₀O₈N [M+NH₄]⁺: 494.2748, found: 494.2746. $[\alpha]_D^{20} = -14.7^\circ$ (c = 0.0039 g/mL).



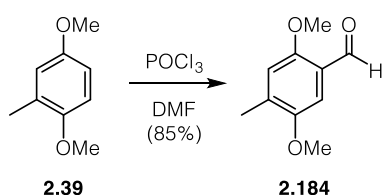
Acremine B (2.2): A suspension of acremine F (**2.6**) (30 mg, 0.131 mmol) and IBX (149 mg, 0.526 mmol) was vigorously stirred at 80 °C for 9 h. After cooling to room temperature, the solids were removed by filtration and the solvent was evaporated under reduced pressure. Purification by flash column chromatography (EtOAc:hexanes 1:1, R_f = 0.25) gave acremine B (**2.2**) (25 mg, 0.111 mmol, 85%) as a colourless solid.

Data for 2.2: **¹H-NMR (400 MHz, CDCl₃):** δ (ppm) = 6.80 (d, $J = 16.1$ Hz, 1H), 6.75 (s, 1H), 6.53 (dd, $J = 16.0, 0.7$ Hz, 1H), 3.67 (s, 1H), 3.19 – 2.99 (m, 2H), 1.66 (s, 1H), 1.43 (d, $J = 0.9$ Hz, 3H), 1.40 (s, 3H), 1.39 (s, 3H). **¹³C-NMR (100 MHz, CDCl₃):** δ (ppm) = 201.8, 195.6, 149.5, 147.9, 130.0, 118.5, 75.3, 71.6, 53.2, 29.7, 27.8. **IR (ATR):** ν_{\max} (cm⁻¹) = 3380 (br), 2975 (m), 2931 (w), 1681 (vs), 1634 (m), 159 (m), 1459 (w), 1373 (m), 1254 (m), 1129 (s), 1053 (w), 974 (m), 906 (w), 851 (w), 824 (w), 780 (w), 754 (w), 668 (w). **HRMS (EI):** calc for [M-CH₃]⁺: 209.0808, found: 209.0824. $[\alpha]_D^{20} = -64.9^\circ$ (c = 0.021 g/mL).



Methyl ether 2.39: Me₂SO₄ (23.0 mL, 242 mmol) was added to a suspension of K₂CO₃ (39.0 g, 282 mmol) and methyl hydroquinone (10.0 g, 80.55 mmol) in acetone (120 mL) and the reaction was stirred at 60 °C overnight. The solids were removed by filtration and the solvent was evaporated under reduced pressure. The resulting residue was redissolved in EtOAc and washed with aqueous 1M NaOH and brine. Drying of the organic phase over Mg₂SO₄, evaporation of the solvent under reduced pressure and purification of the resulting residue by flash column chromatography (EtOAc:hexanes 4:96) gave methyl ether **2.39** (11.9 g, 78.5 mmol, 97%) as a colorless solid.

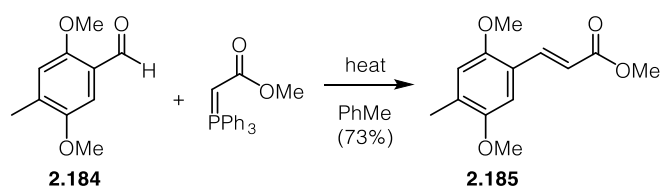
Data for 2.39: ¹H-NMR (400 MHz, CDCl₃): δ (ppm) = 6.79 – 6.73 (m, 2H), 6.69 (dd, *J* = 8.7, 3.1 Hz, 1H), 3.79 (s, 3H), 3.76 (s, 3H), 2.22 (s, 3H). ¹³C-NMR (100 MHz, CDCl₃): δ (ppm) = 153.5, 152.2, 128., 117.2, 111.0, 110.8, 56.0, 55.8, 16.6. IR (ATR): ν_{max} (cm⁻¹) = 2996 (w), 2984 (w), 2832 (w), 2361 (w), 2339 (w), 1968 (w), 1592 (w), 1502 (m), 1465 (w), 1442 (w), 1419 (w), 1378 (w), 1305 (w), 1280 (w), 1222 (s), 1180 (w), 1157 (w), 1130 (w), 1049 (w), 1032 (w), 923 (w), 866 (w), 797 (w), 752 (w), 711 (w), 699 (w), 668 (w) cm⁻¹. HRMS (EI): calc for C₉H₁₂O₂ [*M*]⁺: 152.0837; found: 152.0831.



Aldehyde 2.184: POCl₃ (14.6 mL, 160 mmol, 4.2 eq) was slowly added to a solution of methyl ether **2.39** (5.824 g, 38.45 mmol, 1.0 eq) in DMF (11.6 mL, 151 mmol, 3.9 eq) at 0 °C. The mixture was stirred at rt for 2.5 h, heated at 80 °C overnight, and poured into ice water after cooling down to rt. Extraction with Et₂O (3 × 15 mL), washing with H₂O (2 × 5 mL) and brine (5 mL), drying over Na₂SO₄ and the removal of the solvent under reduced pressure afforded aldehyde **2.184** (5.862 g, 32.53 mmol, 85%) as a yellow solid.

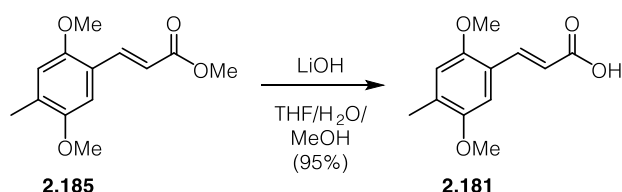
Data for 2.184: ¹H-NMR (400 MHz, CDCl₃): δ (ppm) = 10.40 (s, 1H, b), 7.25 (s, 1H, c), 6.81 (d, *J* = 0.9 Hz, 1H, a), 3.88 (s, 3H, e), 3.83 (s, 3H, f), 2.28 (d, *J* = 0.7 Hz, 3H, d) ¹³C-

NMR (100 MHz, CDCl₃): δ (ppm) = 189.4, 156.8, 152.1, 136.7, 123.0, 114.8, 107.8, 56.3, 55.9, 17.4. **IR (ATR):** ν_{\max} (cm⁻¹) = 3009 (w), 2943 (w), 2921 (w), 2858 (w), 2832 (w), 2780 (w), 2047 (w), 1738 (w), 1659 (s), 1611 (s), 1499 (s), 1484 (w), 1469 (m), 1404 (s), 1373 (w), 1329 (w), 1269 (m), 1252 (w), 1213 (s), 1170 (w), 1121 (w), 1043 (s), 1011 (w), 868 (w), 850 (w), 747 (w), 679 (w) cm⁻¹. **HRMS (EI):** calc C₁₀H₁₂O₃ for [M]⁺: 180.0786; found: 180.0792.



Methyl ester 2.185: A solution of aldehyde **2.184** (500 mg, 2.77 mmol) and methyl (triphenylphosphoranylidene) acetate (1.40 g, 4.16 mmol) in PhMe was stirred for 5 h at 100 °C, cooled to room temperature and concentrated under reduced pressure. Purification by flash column chromatography (EtOAc:hexanes 7:93) gave methyl ester **2.185** (480 mg, 2.03 mmol, 73%) as a colorless solid.

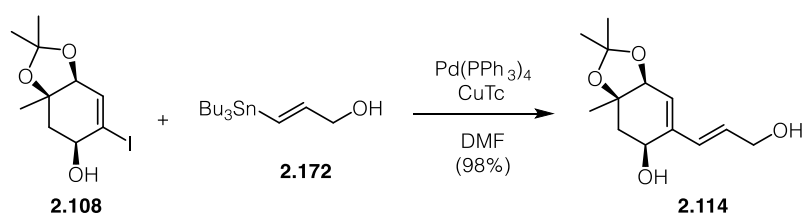
Data for 2.185: **¹H-NMR (400 MHz, CDCl₃):** δ (ppm) = 7.98 (d, J = 16.1 Hz, 1H), 6.93 (s, 1H), 6.73 (d, J = 0.8 Hz, 1H), 6.46 (d, J = 16.1 Hz, 1H), 3.83 (s, 3H), 3.80 (s, 3H), 3.80 (s, 3H), 2.24 (d, J = 0.7 Hz, 3H). **¹³C-NMR (100 MHz, CDCl₃):** δ (ppm) = 168.2, 152.7, 151.8, 140.4, 131.2, 121.0, 117.1, 114.6, 109.7, 56.2, 55.9, 51.7, 16.9. **IR (ATR):** ν_{\max} (cm⁻¹) = 1714 (m), 1697 (m), 1607 (w), 1505 (m), 1468 (m), 1437 (m), 1406 (m), 1376 (w), 1320 (w), 1251 (w), 1214 (s), 1195 (m), 1162 (m), 1044 (s), 999 (w), 899 (w), 872 (w), 856 (w), 833 (w), 668 (w). **HRMS (EI):** calc C₁₃H₁₆O₄ for [M-OMe]⁺: 205.0859; found: 205.0859.



Acid 2.181: A solution of methyl ester **2.185** (207 mg, 0.876 mmol) and LiOH hydrate (310 mg, 12.93 mmol) in THF (1 mL), MeOH (1 mL) and H₂O (1 mL) was stirred at 60 °C

overnight. After cooling to room temperature the reaction was acidified using aqueous 1M HCl and extracted with EtOAc. The organic phase was washed with brine and dried over MgSO₄. Evaporation of the solvent under reduced pressure gave acid **2.181** (184 mg, 0.828 mml, 95%) as a colourless solid.

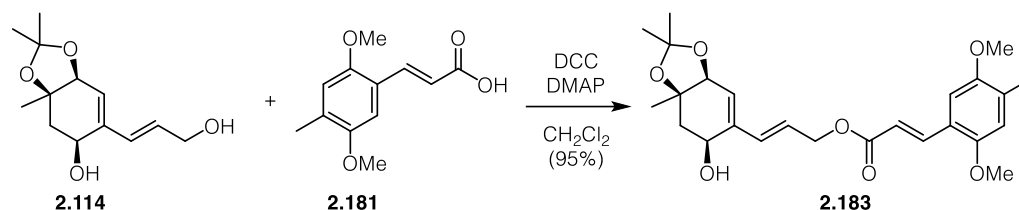
Data for 2.181: ¹H-NMR (400 MHz, CDCl₃): δ (ppm) = 11.89 (s, 1H), 8.09 (d, *J* = 16.1 Hz, 1H), 6.96 (s, 1H), 6.75 (s, 1H), 6.49 (d, *J* = 16.0 Hz, 1H), 3.85 (s, 3H), 3.82 (d, *J* = 2.2 Hz, 3H), 2.26 (s, 3H). ¹³C-NMR (100 MHz, CDCl₃): δ (ppm) = 172.9, 153.0, 151.9, 142.6, 131.9, 120.7, 116.4, 114.6, 109.8, 56.3, 56.0, 17.0. **IR (ATR):** ν_{max} (cm⁻¹) = 2954 (w), 2936 (w), 2830 (w), 2703 (w), 2585 (w), 1690 (s), 1617 (s), 1506 (m), 1463 (w)k 1452 (w), 1401 (m), 1366 (w), 1337 (m), 1294 (m), 1265 (m), 1205 (vs), 1191 (s), 1180 (m), 1121 (w), 1040 (s), 1103 (w), 892 (w), 944 (s), 851 (s), 754 (w), 705 (w), 662 (m). **HRMS (EI):** calc for C₁₂H₁₄O [M]⁺: 222.0887; found: 222.0887.



Allylic alcohol 2.114: A solution of alcohol **2.108** (316 mg, 1.02 mmol), stannane **2.172** (708 mg, 2.04 mmol), Pd(PPh₃)₄ (110 mg, 0.056 mmol) and CuTc (238 mg, 0.802 mmol) in DMF (20 mL) was stirred at 65 °C overnight. After cooling to room temperature, the mixture was diluted with EtOAc, filtered over a pad of celite and washed with brine. Concentration of the resulting residue and purification by flash column chromatography (EtOAc:hexanes 2:1, R_f = 0.3) to give allylic alcohol **2.114** (241 mg, 1.00 mmol, 98%) as a colourless oil.

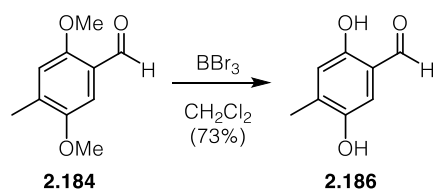
Data for 2.114: ¹H-NMR (400 MHz, CDCl₃): δ (ppm) = 6.26 (d, *J* = 16.0 Hz, 1H), 6.16 (dt, *J* = 15.9, 5.2 Hz, 1H), 5.66 (d, *J* = 3.5 Hz, 1H), 4.41 (d, *J* = 3.4 Hz, 1H), 4.36 – 4.30 (m, 1H), 4.27 (d, *J* = 5.2 Hz, 2H), 3.58 (d, *J* = 10.6 Hz, 1H), 2.45 (dd, *J* = 15.1, 2.6 Hz, 1H), 1.91 (dd, *J* = 15.2, 4.5 Hz, 1H), 1.58 (s, 1H), 1.48 – 1.46 (m, 3H), 1.41 (s, 3H), 1.40 – 1.38 (m, 3H). ¹³C-NMR (100 MHz, CDCl₃): δ (ppm) = 138.8, 130.6, 130.5, 127.1, 110.3, 80.2, 78.4, 77.2, 63.7, 63.5, 39.4, 29.6, 29.2, 26.9. **IR (ATR):** ν_{max} (cm⁻¹) = 3391 (m), 2984 (w), 2933 (m), 2868 (w), 1726 (w), 1460 (w), 1375 (m), 1314 (w), 1275 (w), 1239 (m), 1211 (m), 1163 (w), 1134 (w), 1070 (w), 1054 (w), 1027 (s), 1004 (m), 971 (m), 917

(w), 886 (w), 857 (w), 827 (m). **HRMS (EI)**: calc. for $[M+H]^+$: 241.1434, found: 241.1086. $[\alpha]_D^{20} = -32.0^\circ$ (c = 0.0043 g/mL).



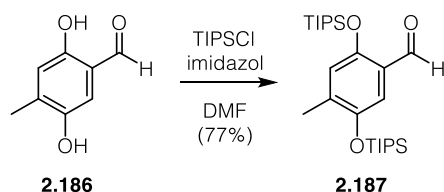
Allylic ester 2.183: A solution of DCC (95 mg, 0.460 mmol) in CH_2Cl_2 (3 mL) was added dropwise to an ice-cooled solution of allylic alcohol **2.114** (100 mg, 0.416 mmol) and acid **2.181** (93 mg, 0.416 mmol) in CH_2Cl_2 (3 mL) and the reaction was stirred 30 min at 0°C and at room temperature for 17 h. The resulting solids were removed by filtration and the solvent was evaporated under reduced pressure. Purification by flash column chromatography (EtOAc:hexanes 1:3 $R_f = 0.3$) gave allylic ester **2.183** (175 mg, 0.394 mmol, 95%) as a colorless solid.

Data for 2.183: $^1\text{H-NMR}$ (400 MHz, CDCl_3): δ (ppm) = 7.99 (d, $J = 16.1$ Hz, 1H), 6.93 (s, 1H), 6.73 (s, 1H), 6.49 (d, $J = 16.1$ Hz, 1H), 6.32 (d, $J = 15.9$ Hz, 1H), 6.15 (dt, $J = 15.9, 6.0$ Hz, 1H), 5.69 (d, $J = 3.4$ Hz, 1H), 4.80 (dt, $J = 6.2, 1.6$ Hz, 2H), 4.40 (d, $J = 3.4$ Hz, 1H), 4.34 (ddd, $J = 10.7, 4.5, 2.6$ Hz, 1H), 3.84 (s, 3H), 3.81 (s, 3H), 3.55 (d, $J = 10.7$ Hz, 1H), 2.45 (dd, $J = 15.1, 2.6$ Hz, 1H), 2.24 (s, 3H), 1.91 (dd, $J = 15.1, 4.5$ Hz, 1H), 1.47 (s, 3H), 1.41 (s, 3H), 1.40 (s, 3H). $^{13}\text{C-NMR}$ (100 MHz, CDCl_3): δ (ppm) = 167.4, 152.8, 151.9, 140.7, 138.7, 133.2, 131.3, 127.9, 125.7, 121.0, 117.2, 114.6, 110.3, 109.8, 78.3, 76.8, 64.8, 63.5, 56.3, 56.0, 39.4, 29.6, 29.3, 26.9, 16.9. **IR (ATR)**: ν_{max} (cm^{-1}) = 3520 (w), 2982 (w), 2934 (w), 1705 (s), 1626 (m), 1572 (w), 1507 (m), 1466 (m), 1403 (m), 1374 (m), 1333 (w), 1291 (w), 1256 (m), 1339 (m), 1212 (vs), 1156 (vs), 1070 (m), 1042 (s), 1027 (s), 1003 (m), 969 (m), 856 (m), 827 (m), 736 (w), 663 (w). **HRMS (ESI)**: calc. for $\text{C}_{25}\text{H}_{36}\text{O}_7\text{N}$ $[M+\text{NH}_4]^+$: 462.2486, found: 462.4286. $[\alpha]_D^{20} = -29.6^\circ$ (c = 0.0108 g/mL).



Diol 2.186: BBr₃ (6.5 mL, 68 mmol, 4.9 eq) was added dropwise to a -78 °C cold solution of aldehyde **2.184** (2.485 g, 13.79 mmol, 1.0 eq) in CH₂Cl₂ (85 mL). After stirring the mixture at -78 °C for 1 h and at rt for another 2 h, MeOH (30 mL) was added. The reaction was washed with H₂O and brine and dried over MgSO₄. Evaporation of the solvent under reduced pressure and column chromatography (EtOAc:hexanes 1:4, R_f = 0.2), gave diol **2.186** (1.535 g, 10.09 mmol, 73%) as a yellow solid.

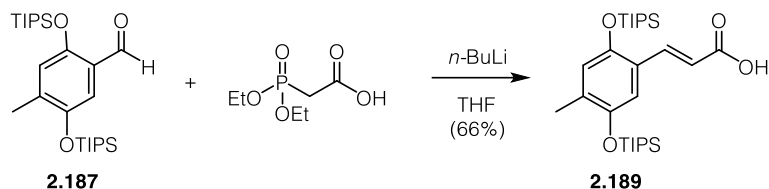
Data for 2.186: ¹H-NMR (400 MHz, CDCl₃): δ (ppm) = 10.64 (s, 1H), 9.76 (d, J = 0.6 Hz, 1H), 6.91 (s, 1H), 6.79 (s, 1H), 4.57 (s, 1H), 2.30 (s, 3H). ¹³C-NMR (100 MHz, CDCl₃): δ (ppm) = 195.4, 156.1, 147.1, 136.7, 119.7, 118.8, 117.3, 17.0. IR (ATR): ν_{max} (cm⁻¹) = 3386 (m, br), 2874 (w), 1645 (m), 1630 (s), 1567 (w), 1491 (s), 1469 (w), 1444 (w), 1450 (w), 1355 (w), 1289 (w), 1249 (s), 1200 (w), 1153 (m), 1036 (w), 1008 (w), 885 (w), 866 (w), 834 (w), 801 (w), 720 (w), 670 (w) cm⁻¹. HRMS (EI): calc for C₈H₈O₃ [M]⁺: 152.0473; found: 152.0461.



Silyl ether 2.187: TIPSCI (1.22 mL, 5.78 mmol) was added to a solution of diol **2.186** (350 mg, 2.30 mmol) and imidazole (547 mg, 8.03 mmol) in DMF (2 mL) and the solution was stirred at 80 °C overnight. After cooling to room temperature the solution was diluted with H₂O and extracted with Et₂O. The combined organic phases were washed with brine and dried over Na₂SO₄. Evaporation of the solvent under reduced pressure and purification of the resulting residue by flash column chromatography (Et₂O:hexanes 2:98) gave silyl ether **2.187** (820 mg, 1.76 mmol, 77%) as a colourless solid.

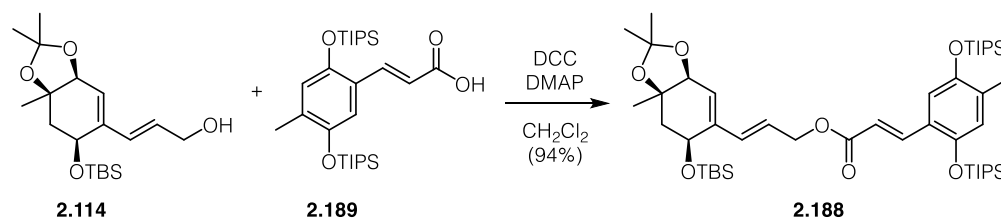
Data for 2.187: ¹H-NMR (400 MHz, CDCl₃): δ (ppm) = 7.16 (s, 1H), 6.66 (d, J = 0.8 Hz, 1H), 2.24 (s, 3H), 1.31 (dddd, J = 16.2, 8.3, 6.8, 1.2 Hz, 7H), 1.10 (dd, J = 7.4, 6.2 Hz, 36H). ¹³C-NMR (100 MHz, CDCl₃): δ (ppm) = 189.8, 153.7, 148.8, 138.6, 125.0, 122.1, 115.0, 18.2, 18.1, 13.1, 13.0. IR (ATR): ν_{max} (cm⁻¹) = 2956 (m), 2941 (s), 2888 (w), 2864

(s), 1677 (s), 1609 (m), 1487 (s), 1460 (m), 1405 (s), 1386 (m), 1367 (w), 1326 (w), 1271 (w), 1246 (m), 1209 (s), 1173 (m), 1130 (w), 1074 (w), 1061 (w), 1012 (m), 995 (m), 944 (s), 949 (m), 881 (vs), 854 (m), 800 (s), 688 (s). **HRMS (EI)**: calc. for $C_{26}H_{48}O_3Si_2$ [M]⁺: 464.3136; found: 464.3120.



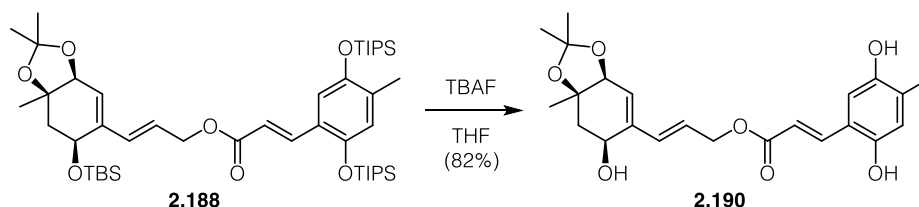
Acid 2.189: Diethylphosphonoacetic acid (35 μL , 0.215 mmol) was added dropwise to a solution of $n\text{-BuLi}$ (2.34M, 0.19 mL, 0.452 mmol) in THF (0.5 mL) at -60°C and the reaction was stirred for 30 min at that temperature before a solution of silyl ether **2.187** (100 mg, 0.215 mmol) in THF (0.5 mL) was added dropwise. The reaction was stirred at -60°C for 1 h and at room temperature overnight before it was diluted with H_2O and acidified with aqueous HCl (1 M). The mixture was extracted with EtOAc and the combined organic phases were washed with brine, dried over Na_2SO_4 and concentrated under reduced pressure. Purification of the resulting residue by flash column chromatography (EtOAc:hexanes 15:85) gave acid **2.189** (72 mg, 0.142 mmol, 66%) as a colourless solid.

Data for 2.189: $^1\text{H-NMR}$ (400 MHz, CDCl_3): 11.46 (s, 1H), 8.25 – 8.13 (m, 1H), 6.94 (s, 1H), 6.63 (s, 1H), 6.20 (d, $J = 16.1$ Hz, 1H), 2.21 (s, 3H), 1.28 (ddt, $J = 12.3, 7.0, 3.6$ Hz, 6H), 1.17 – 1.07 (m, 36H). $^{13}\text{C-NMR}$ (100 MHz, CDCl_3): δ (ppm) = 172.2, 149.4, 148.5, 142.7, 133.7, 122.6, 121.7, 115.4, 114.9, 18.0, 18.0, 17.6, 13.0, 12.9. **IR (ATR)**: ν_{max} (cm^{-1}) = 2945 (s), 2893 (m), 2868 (s), 1684 (vs), 1620 (m), 1492 (s), 1464 (m), 1408 (s), 1277 (m), 1246 (m), 1205 (vs), 1070 (w), 998(w), 932 (s), 882 (s), 809 (w), 724 (w), 683 (m). **HRMS (EI)**: calc. for $C_{28}H_{50}O_4Si_2$ [M]⁺: 506.3242, found: 506.3238.



Allylic ester 2.188: (A solution of DCC (11.2 mg, 0.545 mmol) in CH_2Cl_2 (5 mL) was added dropwise to an ice cooled solution of allylic alcohol **2.114** (173 mg, 0.489 mmol), acid **2.189** (248 mg, 0.489 mmol) and DMAP (41.3 mg, 0.338 mmol) in CH_2Cl_2 (5 mL) and the reaction was stirred for 30 min at that temperature and for 17 h at room temperature. The solids were removed by filtration and the solvent was evaporated under reduced pressure. Purification of the resulting residue by flash column chromatography (EtOAc:hexanes 4:96) gave allylic ester **2.188** (387 mg, 0.459 mmol, 94%) as a colorless solid.

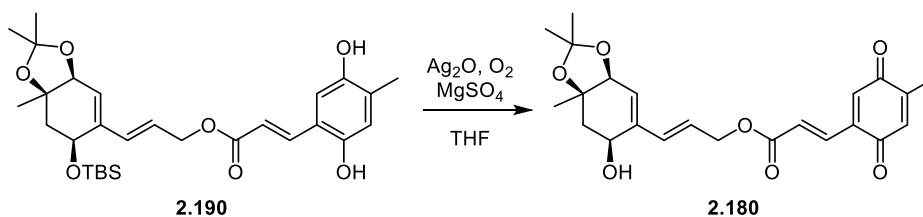
Data for 2.188: $^1\text{H-NMR}$ (400 MHz, CDCl_3): 8.12 (d, $J = 16.1$ Hz, 1H), 6.92 (s, 1H), 6.62 (s, 1H), 6.37 (d, $J = 15.8$ Hz, 1H), 6.19 (d, $J = 16.1$ Hz, 1H), 6.08 (dt, $J = 15.8, 6.2$ Hz, 1H), 4.81 – 4.65 (m, 2H), 4.23 (t, $J = 7.8$ Hz, 1H), 4.13 (d, $J = 4.6$ Hz, 1H), 2.20 (s, 3H), 1.93 (d, $J = 7.8$ Hz, 2H), 1.47 (s, 3H), 1.39 (s, 3H), 1.32 – 1.24 (m, 9H), 1.10 (d, $J = 7.3$ Hz, 37H), 0.88 (s, 9H), 0.10 (s, 3H), 0.09 (s, 3H). $^{13}\text{C-NMR}$ (100 MHz, CDCl_3): δ (ppm) = 167.1, 149.1, 148.4, 144.0, 140.7, 133.1, 131.3, 125.7, 122.9, 121.7, 119.7, 115.5, 115.1, 109.21, 78.3, 68.4, 64.8, 42.4, 28.7, 27.2, 25.8, 23.8, 18.1, 18.1, 18.0, 17.5, 13.0, 12.9, -3.9, -4.8. **IR (ATR):** ν_{max} (cm^{-1}) = 2944 (m), 2867 (m), 1711 (m), 1628 (s), 1491 (m), 1463 (s), 1406 (m), 1368 (s), 1294 (s), 1250 (m), 1207 (vs), 1155 (s), 1072 (m), 1031 (w), 990 (m), 935 (s), 880 (s), 836 (m), 812 (w), 755 (s). **HRMS (EI):** calc. for $\text{C}_{36}\text{H}_{82}\text{O}_7\text{Si}_3$ $[M+H]^+$: 842.5363, found: 842.5370. $[\alpha]_D^{20} = -4.34^\circ$ ($c = 0.044$ g/mL).



Triol 2.190: TBAF (1 M in THF, 0.30 mL, 0.30 mmol) was added to an ice cooled solution of allylic ester **2.188** (56 mg, 0.066 mmol) in THF (2 mL) and the solution was stirred at 0°C for 4 h before it was quenched with NH_4Cl and extracted with EtOAc. The combined organic phases were washed with brine, dried over MgSO_4 and concentrated under

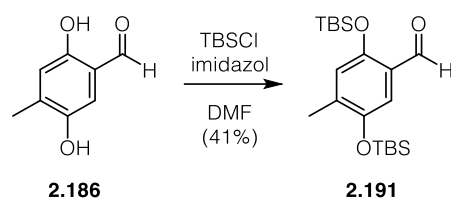
reduced pressure. Purification of the resulting residue by flash column chromatography (EtOAc:hexanes 1:1) gave triol **2.190** (22.5 mg, 0.054 mmol, 82%) as a colorless oil.

Data for 2.190: $^1\text{H-NMR}$ (400 MHz, CDCl_3): 7.88 (d, $J = 16.0$ Hz, 1H), 6.80 (s, 1H), 6.57 (s, 1H), 6.36 – 6.23 (m, 2H), 6.06 (dt, $J = 15.9, 6.1$ Hz, 1H), 5.69 (d, $J = 3.4$ Hz, 1H), 4.68 (t, $J = 5.7$ Hz, 2H), 4.39 (d, $J = 3.4$ Hz, 2H), 4.13 – 4.00 (m, 1H), 2.44 (dd, $J = 15.2, 2.6$ Hz, 1H), 2.15 (s, 3H), 1.91 (dd, $J = 15.1, 4.4$ Hz, 1H), 1.46 (s, 3H), 1.39 (s, 6H). $^{13}\text{C-NMR}$ (100 MHz, CDCl_3): δ (ppm) = 168.3, 149.6, 148.0, 141.1, 138.3, 132.9, 129.7, 128.1, 125.8, 119.7, 119.1, 116.4, 114.1, 110.4, 80.2, 78.2, 65.1, 63.6, 39.2, 29.5, 29.2, 26.7, 16.4. IR (ATR): ν_{max} (cm^{-1}) = 3334 (m), 2981 (w), 2932 (w), 1683 (m), 1618 (m), 1513 (w), 1421 (m), 1374 (m), 1286 (m), 1262 (m), 1237 (m), 1198 (s), 1160 (vs), 1068 (m), 1025 (m), 999 (m), 967 (m), 862 (m), 825 (m), 750 (w), 696 (w). HRMS (ESI): calc. for $\text{C}_{23}\text{H}_{32}\text{IO}_7\text{N}$ [$M+\text{NH}_4$] $^+$: 434.2173, found: 434.2171. $[\alpha]_D^{20} = -30.7^\circ$ ($c = 0.003$ g/mL).



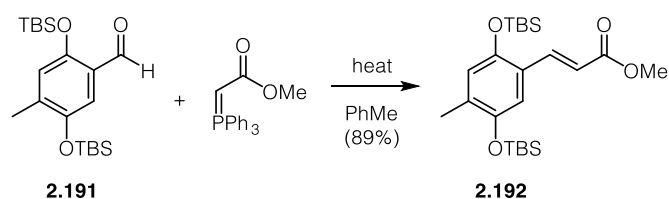
Vinyl quinone 2.180: A suspension of triol **2.190** (5.0 mg, 0.012 mmol), Ag_2O (28 mg, 0.120 mmol) and MgSO_4 (6 mg) in THF (1 mL) was stirred under an O_2 -atmosphere at room temperature for 45 min. The reaction mixture was filtered with the help of a syringe filter and concentrated under reduced pressure to give crude vinyl quinone **2.180** (4.5 mg). The product proved to be unstable on silica.

Data for 2.180: $^1\text{H-NMR}$ (400 MHz, CDCl_3): 7.51 (d, $J = 16.3, 0.9$ Hz, 1H), 6.87 – 6.81 (m, 2H), 6.66 (q, $J = 1.5$ Hz, 1H), 6.31 (d, $J = 15.9$ Hz, 1H), 6.11 (dt, $J = 15.8, 6.1$ Hz, 1H), 5.70 (d, $J = 3.5$ Hz, 1H), 4.80 (d, $J = 6.2$ Hz, 1H), 4.41 (d, $J = 3.6$ Hz, 1H), 4.33 (ddd, $J = 10.8, 4.6, 2.6$ Hz, 1H), 3.56 (d, $J = 10.7$ Hz, 1H), 2.45 (dd, $J = 15.1, 2.6$ Hz, 1H), 2.07 (d, $J = 1.6$ Hz, 3H), 1.95 – 1.87 (m, 2H), 1.46 (d, $J = 3.2$ Hz, 3H), 1.41 (d, $J = 2.2$ Hz, 3H), 1.39 (s, 3H).



Silyl ether 2.191: TBSCl (977 mg, 6.48 mmol) was added to an ice cooled solution of diol **2.186** (329 mg, 2.16 mmol) and imidazole (441 mg, 6.48 mmol) in DMF (5 mL) and the reaction was stirred at room temperature overnight. The mixture was portioned between Et₂O and H₂O and the organic phase was washed with brine and dried over Na₂SO₄. Evaporation of the solvent under reduced pressure and purification of the resulting residue by flash column chromatography (Et₂O:hexanes 3:97) gave silyl ether **2.191** (340 mg, 0.893 mmol, 41%) as a colorless solid.

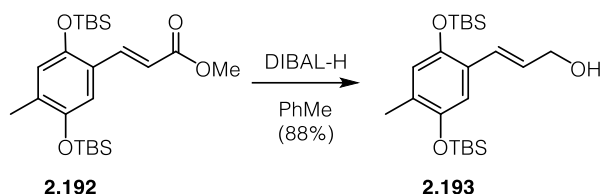
Data for 2.191: ¹H-NMR (400 MHz, CDCl₃): δ (ppm) = 10.32 (s, 1H), 7.14 (s, 1H), 6.66 (s, 1H), 2.21 (s, 3H), 1.00 (d, *J* = 1.9 Hz, 19H), 0.24 (s, 6H), 0.22 (s, 6H). ¹³C-NMR (100 MHz, CDCl₃): δ (ppm) = 189.7, 153.3, 148.6, 138.9, 125.5, 122.6, 115.6, 25.9, 25.8, 18.5, 18.4, 18.0, -4.2, -4.2. IR (ATR): ν_{max} (cm⁻¹) = 2955 (m), 2932 (m), 1292 (w), 2858 (m), 1682 (s), 1609 (w), 1485 (s), 1471 (m), 1404 (s), 1389 (w), 1322 (w), 1259 (s), 1244 (m), 1217 (vs), 1171 (w), 1121 (w), 1006 (w), 938 (vs), 882 (w), 833 (vs), 781 (s), 680 (m). HRMS (EI): calc. for C₁₉H₃₃O₃Si₂ [*M-CH₃*]⁺: 365.1963, found: 365.1981.



Methyl ester 2.192: A solution of aldehyde **2.191** (274 mg, 0.720 mmol) and methyl (triphenylphosphoranylidene) acetate (481 mg, 1.44 mmol) in PhMe (8 mL) was stirred for 5 h at 100 °C, cooled to room temperature and concentrated under reduced pressure. Purification by flash column chromatography (Et₂O:hexanes 4:96, R_f = 0.1) gave methyl ester **2.192** (280 mg, 0.641 mmol, 82%) as a colorless solid.

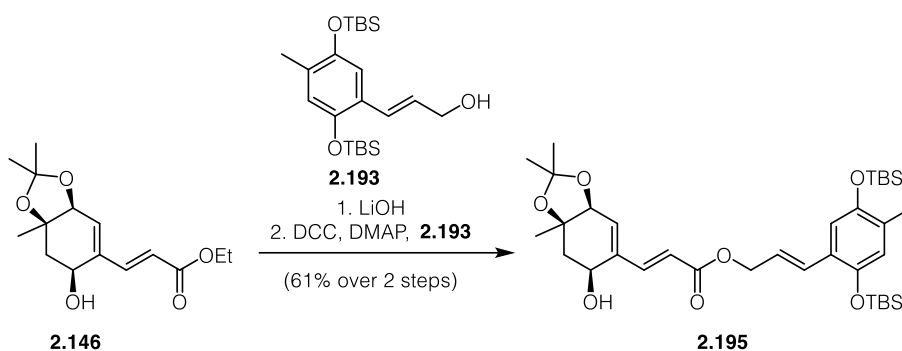
Data for 2.192: ¹H-NMR (400 MHz, CDCl₃): δ (ppm) = 7.99 (d, *J* = 16.2 Hz, 1H), 6.90 (s, 1H), 6.61 (d, *J* = 0.9 Hz, 1H), 6.24 (d, *J* = 16.1 Hz, 1H), 3.79 (s, 3H), 2.17 (d, *J* = 0.6 Hz, 3H), 1.03 (s, 9H), 1.01 (s, 9H), 0.20 (s, 6H), 0.19 (s, 6H). ¹³C-NMR (100 MHz, CDCl₃): δ (ppm) = 168.0, 148.9, 148.4, 140.6, 133.6, 123.6, 122.5, 116.0, 51.7, 25.9, 18.4, 18.4,

17.4, -4.1, -4.1. **IR (ATR):** ν_{\max} (cm⁻¹) = 2953 (w), 2930 (w), 2858 (w), 1720 (m), 1629 (w), 1492 (m), 1472 (w), 1434 (w), 1405 (m), 1294 (m), 1255 (m), 1204 (s), 1162 (s), 1043 (w), 1004 (w), 959 (w), 920 (s), 829 (vs), 778 (vs), 680 (w). **HRMS (EI):** calc. for C₂₃H₄₀O₄Si₂ [M]⁺: 436.2460, found: 436.2462.



Allylic alcohol 2.193: DIBAL-H (1.49M in PhMe, 0.86 mL, 1.28 mmol) was added dropwise to a stirred solution of methyl ester **2.192** (280 mg, 0.641 mmol) in CH₂Cl₂ (9 mL) at -78 °C and the solution was stirred at that temperature for 2 h and for 1 h at room temperature before an aqueous saturated solution of Rochelle's salt was added and the reaction was stirred for 1 h at room temperature. The mixture was extracted with CH₂Cl₂ and the organic phase was dried over MgSO₄. Evaporation of the solvent under reduced pressure and purification of the resulting residue by flash column chromatography (EtOAc:hexanes 1:9) gave allylic alcohol **2.193** (230 mg, 0.563 mmol, 88%) as a colourless solid.

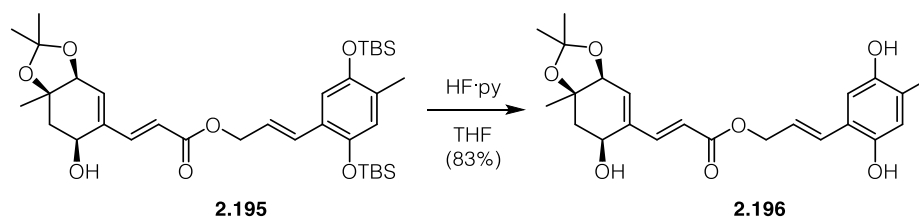
Data for 2.193: ¹H-NMR (400 MHz, CDCl₃): δ (ppm) = 6.88 – 6.79 (m, 2H), 6.56 (d, J = 0.9 Hz, 1H), 6.17 (dt, J = 16.0, 6.1 Hz, 1H), 4.29 (td, J = 6.0, 1.5 Hz, 2H), 2.14 (s, 3H), 1.35 (t, J = 6.0 Hz, 1H), 1.01 (d, J = 1.9 Hz, 18H), 0.20 (s, 6H), 0.17 (s, 6H). ¹³C-NMR (100 MHz, CDCl₃): δ (ppm) = 207.1, 148.1, 146.9, 129.6, 127.0, 126.9, 125.5, 121.9, 115.6, 64.4, 31.0, 25.9, 25.8, 18.3, 18.3, 17.0, -4.2, -4.2. **IR (ATR):** ν_{\max} (cm⁻¹) = 326 (w), 2955 (w), 2929 (m), 2886 (w), 2857 (w), 1492 (s), 1472 (m), 1463 (w), 1401 (s), 1374 (w), 1362 (w), 1288 (w), 1252 (m), 1198 (s), 1184 (m), 1094 (m), 1032 (w), 1003 (w), 966 (w), 924 (s), 882 (m), 830 (vs), 778 (vs), 726 (m), 684 (m). **HRMS (EI):** calc. for C₂₂H₄₀O₃Si₂ [M]⁺: 408.2510; found 408.2520.



Allylic ester 2.195: LiOH·H₂O (23.6 mg, 0.563 mmol) was added to a solution of ethyl ester **2.146** (22 mg, 0.079 mmol) in THF (1 mL), MeOH (1 mL) and H₂O (1 mL) and the solution was stirred at 60 °C for 3 h. The reaction was acidified with aqueous HCl (1 M) and extracted with EtOAc. The combined organic phases were washed with brine, dried over MgSO₄ and concentrated under reduced pressure to give crude acid **2.194** that was used in the next step without further purification.

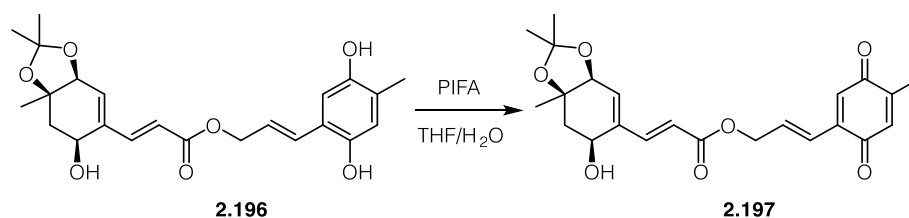
A solution of DCC (18 mg, 0.088 mmol) in CH₂Cl₂ (0.8 mL) was added dropwise to an ice cooled solution of acid **2.194**, allylic alcohol **2.193** (32 mg, 0.079 mmol) and DMAP (6.7 mg, 0.055 mmol) in CH₂Cl₂ (0.8 mL) and the reaction was stirred for 30 min at 0 °C and for 17 h at room temperature. The mixture was filtered through a pad of celite and concentrated under reduced pressure. Purification of the resulting residue by flash column chromatography (EtOAc:hexanes 1:9) gave allylic ester **2.195** (31 mg, 0.048 mmol, 61% over 2 steps) as a colourless oil.

Data for 2.195: ¹H-NMR (400 MHz, CDCl₃): δ (ppm) = 7.31 (d, *J* = 15.9 Hz, 1H), 6.89 (dt, *J* = 16.0, 1.4 Hz, 1H), 6.83 (s, 1H), 6.55 (d, *J* = 0.8 Hz, 1H), 6.28 (d, *J* = 15.9 Hz, 1H), 6.09 (dt, *J* = 16.0, 6.4 Hz, 1H), 6.00 (d, *J* = 3.4 Hz, 1H), 4.80 (dd, *J* = 6.4, 1.4 Hz, 2H), 4.43 (d, *J* = 3.3 Hz, 1H), 4.31 (ddd, *J* = 10.9, 4.6, 2.4 Hz, 1H), 3.55 (d, *J* = 10.8 Hz, 1H), 2.47 (dd, *J* = 15.2, 2.4 Hz, 1H), 2.13 (s, 3H), 1.93 (dd, *J* = 15.2, 4.5 Hz, 1H), 1.47 (s, 3H), 1.42 (s, 3H), 1.36 (s, 3H), 1.01 (s, 9H), 1.00 (s, 9H), 0.19 (s, 6H), 0.16 (s, 6H). ¹³C-NMR (100 MHz, CDCl₃): δ (ppm) = 166.9, 148.2, 147.1, 144.3, 138.1, 134.3, 130.1, 129.5, 125.4, 122.0, 121.8, 120.5, 115.7, 110.6, 80.1, 78.0, 65.8, 63.1, 39.1, 29.5, 29.2, 26.8, 26.0, 26.0, 18.4, 18.4, 17.1, -4.0, -4.1. IR (ATR): ν_{max} (cm⁻¹) = 2955 (w), 2930 (m), 2896 (w), 2858 (w), 1715 (m), 1639 (w), 1620 (w), 1494 (m), 1472 (w), 1463 (w), 1404 (m), 1374 (w), 1300 (w), 1279 (w), 1254 (m), 1238 (m), 1222 (m), 1204 (s), 1168 (s), 1159 (s), 1134 (w), 1088 (m), 1072 (m), 1056 (w), 1030 (m), 1004 (m), 972 (m), 930 (s), 880 (m), 863 (w), 828 (vs), 779 (vs), 733 (s), 681 (m). HRMS (EI): calc. for C₃₅H₅₆O₇Si₂ [*M*]⁺: 644.3565, found: 644.3564. [α]_D²⁰ = -9.2 ° (c = 0.009 g/mL).



Triol 2.196: HF-pyridine (70% HF in pyridine, 0.9 mL) was added to an ice cooled solution of allylic ester **2.195** (69 mg, 0.107 mmol) in THF (5.7 mL) and the reaction was stirred for 4 h at room temperature before it was diluted with aqueous saturated NH_4Cl . The mixture was extracted with EtOAc and the combined organic phases were washed with NaHCO_3 and brine. The organic phase was dried over MgSO_4 , concentrated under reduced pressure and purified by flash column chromatography (EtOAc:hexanes 1:1) to give triol **2.196** (37 mg, 0.089 mmol, 83%) as a colorless oil.

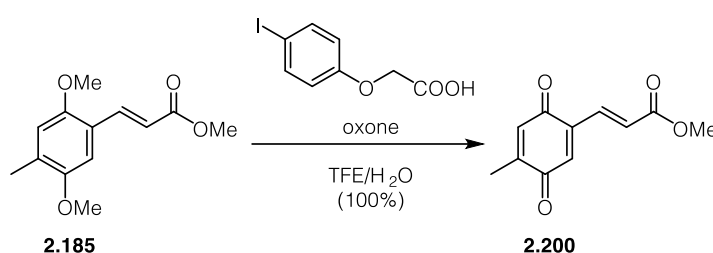
Data for 2.196: $^1\text{H-NMR}$ (400 MHz, CDCl_3): δ (ppm) = 7.29 (d, $J = 16.0$ Hz, 1H), 6.82 (d, $J = 16.0$ Hz, 1H), 6.76 (s, 1H), 6.55 (s, 1H), 6.24 (d, $J = 16.0$ Hz, 1H), 6.13 (dt, $J = 15.9, 6.6$ Hz, 1H), 6.00 (d, $J = 3.4$ Hz, 1H), 5.64 (s, 1H), 5.37 (s, 1H), 4.75 (ddd, $J = 6.6, 3.7, 1.4$ Hz, 2H), 4.43 (d, $J = 3.3$ Hz, 1H), 4.34 (ddd, $J = 10.7, 4.5, 2.5$ Hz, 1H), 3.83 (d, $J = 10.6$ Hz, 1H), 2.48 (dd, $J = 15.3, 2.5$ Hz, 1H), 2.16 (s, 3H), 1.93 (dd, $J = 15.2, 4.5$ Hz, 1H), 1.47 (s, 3H), 1.42 (s, 3H), 1.36 (s, 3H). $^{13}\text{C-NMR}$ (100 MHz, CDCl_3): δ (ppm) = 167.2, 147.9, 147.2, 144.3, 137.8, 134.6, 129.1, 126.0, 122.9, 121.8, 120.4, 118.7, 113.1, 110.7, 80.1, 77.9, 66.0, 63.2, 38.9, 31.1, 29.5, 29.1, 26.7, 16.1. IR (ATR): ν_{max} (cm^{-1}) = 3366 (m), 1984 (w), 2934 (w), 1695 (s), 1637 (w), 1621 (w), 1421 (m), 1375 (m), 1302 (m), 1280 (m), 1237 (m), 1172(vs), 1087 (m), 1069 (m), 1029 (m), 1002 (m), 972 (m), 944 (w), 909 (m), 864 (m), 826 (m), 729 (vs), 702 (w). HRMS (ESI): calc. for $\text{C}_{23}\text{H}_{32}\text{IO}_7\text{N}$ [$M+\text{NH}_4$] $^+$: 434.2173, found: 434.2176. $[\alpha]_D^{20} = -25.7^\circ$ ($c = 0.007$ g/mL).



Vinyl quinone 2.197: A solution of PIFA (9.7 mg, 12 μmol) in H_2O (0.10 mL) and THF (0.20 mL) was added to an ice cooled solution of triol **2.196** (5 mg, 12 μmol) in H_2O (0.25 mL) and THF (0.50 mL) and the solution was stirred at 0°C for 20 min. The reaction mixture was diluted with EtOAc, washed with saturated aqueous NaHCO_3 and brine,

dried over MgSO_4 and concentrated under reduced pressure to give vinyl quinone **2.197** as a yellow solid. The product proved to be unstable on silica.

Data for 2.197: $^1\text{H-NMR}$ (400 MHz, CDCl_3): δ (ppm) = 7.32 (d, J = 15.9 Hz, 1H), 6.72-6.67 (m, 1H), 6.64-6.56 (m, 2H), 6.28 (d, J = 15.9 Hz, 1H), 6.07-5.98 (m, 2H), 4.83 (dd, J = 5.4, 1.5 Hz, 1H), 4.44 (d, J = 3.4 Hz, 1H), 2.48 (dd, J = 15.2, 2.4 Hz, 1H), 2.05 (s, 3H), 1.94 (dd, J = 15.2, 4.6 Hz, 1H), 1.47 (s, 1H), 1.42 (s, 3H), 1.36 (s, 3H).

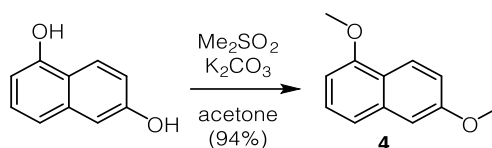


Vinyl quinone 2.200: Methyl ester **2.185** (200 mg, 0.846 mmol) and oxone[®] (2.14 g, 3.48 mmol) was added to a solution of 4-iodophenoxyacetic acid (11.6 mg, 42.5 μmol) in TFE (3 mL) and H₂O (6 mL) and the reaction was stirred at room temperature for 90 min. The reaction mixture was diluted with EtOAc, washed with H₂O, NaHCO₃ and brine, dried over MgSO_4 and concentrated under reduced pressure to give vinyl quinone **2.200** (174 mg, 0.844 mmol, 100%) as a yellow solid. The product proved unstable on silica.

Data for 2.200: $^1\text{H-NMR}$ (400 MHz, CDCl_3): δ (ppm) = 7.51 (dd, J = 16.2, 0.8 Hz, 1H), 6.86 (s, 1H), 6.82 (d, J = 16.2 Hz, 1H), 6.66 (q, J = 1.5 Hz, 1H), 3.81 (s, 3H), 2.08 (d, J = 1.6 Hz, 3H). $^{13}\text{C-NMR}$ (100 MHz, CDCl_3): δ (ppm) = 187.8, 186.1, 166.3, 146.4, 139.5, 135.8, 133.9, 133.5, 127.3, 52.3, 15.7.

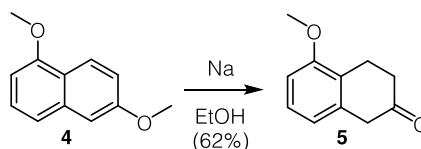
6.4 Experimental data for chapter III

6.4.1 Photoswitchable dopamine agonist



1,6-Dihydroxynaphthalene 4: Dimethylsulfate (43.3 mL, 468 mmol) was added to a suspension of potassium carbonate (75.5 g, 548 mmol) and 1,6-dihydroxynaphthalene (25 g, 156 mmol) in acetone (250 mL). The mixture was heated at 70 °C for 3.5 h, cooled to room temperature and filtered. The solvent was evaporated under reduced pressure and the resulting residue was redissolved in ethyl acetate. The solution was washed with a solution of sodium hydroxide (1 M) and brine and dried over MgSO₄. Evaporation of the solvent under reduced pressure and purification of the resulting residue by flash column chromatography (EtOAc:pentane 0:100–20:80, R_f = 0.7 (EtOAc:pentane 20:80)) gave 1,6-dihydroxynaphthalene **4** (27.6 g, 147 mmol, 94%) as a colorless solid.

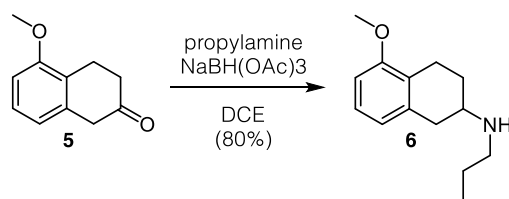
Data for 4: ¹H NMR (400 MHz, CDCl₃): δ (ppm) = 8.17 (dt, *J* = 8.8, 0.8 Hz, 1H), 7.38 – 7.31 (m, 2H), 7.15 – 7.10 (m, 2H), 6.70 (dd, *J* = 6.9, 1.7 Hz, 1H), 3.99 (s, 3H), 3.92 (s, 3H). ¹³C NMR (100 MHz, CDCl₃): δ (ppm) = 158.2, 155.8, 136.0, 126.8, 123.8, 120.9, 119.4, 117.6, 105.8, 102.1, 55.6, 55.4. **IR (ATR):** ν_{max} (cm⁻¹) = 2997 (w), 2966 (w), 2836 (w), 1929 (w), 1625(m), 1599 (m), 1581 (s), 1510 (w), 1468 (w), 1451 (s), 1430 (s), 1372 (s), 1386 (w), 1372 (s), 1254 (m), 1220 (vs), 1199 (m), 1165 (m), 1143 (m), 1098 (m), 1070 (m), 1026 (vs), 988 (m), 935 (m), 871 (m), 839 (m), 828 (s), 782 (vs), 748 (s), 727 (m), 695 (m). **HRMS (EI):** calc. for C₁₂H₁₂O₂ [*M*]⁺: 188.0837, found: 188.0819.



3,4-Dihydro-1,6-dimethoxynaphthalenone 5: Sodium (33.69 g, 1.47 mol) was added portionwise to a solution of 1,6-dimethoxynaphthalene **4** (27.6 g, 147 mmol) in ethanol (400 mL) at 50 °C and the mixture was then stirred at 80 °C for 2.5 h. After cooling down to room temperature the mixture was acidified with concentrated hydrochloric acid to pH = 1, heated at 80 °C for 30 min and stirred at room temperature overnight. The solution was

diluted with water (230 mL) and extracted with CH₂Cl₂. The organic phase was washed with a solution of sodium chloride (10%) and brine and dried over MgSO₄. Evaporation of the solvent under reduced pressure and purification of the resulting residue by flash column chromatography (EtOAc:pentane 0:100–10:90, R_f = 0.5 (EtOAc:pentane 10:90) gave 3,4-dihydronaphthalenone **5** (15.94 g, 90.47 mmol, 62%) as a yellow oil.

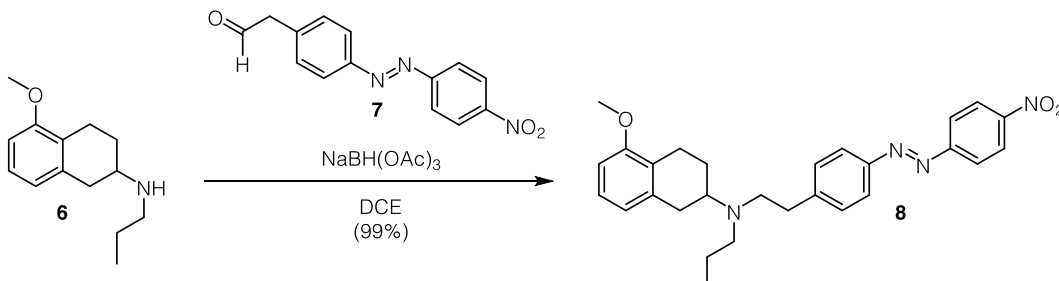
Data for 5: ¹H NMR (400 MHz, CDCl₃): δ (ppm) = 7.16 (t, *J* = 7.9 Hz, 1H), 6.76 (dd, *J* = 8.2, 1.0 Hz, 1H), 6.70 (dd, *J* = 7.6, 1.0 Hz, 1H), 3.83 (s, 3H), 3.52 (s, 2H), 3.06 (t, *J* = 6.8 Hz, 2H), 2.48 (dd, *J* = 7.4, 6.2 Hz, 2H). ¹³C NMR (100 MHz, CDCl₃): δ (ppm) = 210.4, 156.2, 134.8, 127.3, 124.8, 120.2, 108.2, 55.2, 44.4, 44.4, 37.6, 37.6, 20.8. IR (ATR): ν_{max} (cm⁻¹) = 2957 (w), 2904 (w), 2838 (w), 1713 (vs), 1587 (s), 1471 (s), 1441 (m), 1403 (w), 1344(w), 1299 (w), 1263 (vs), 1237 (m), 1197 (w), 1172 (w), 1087 (vs), 1076 (s), 1025 (w), 977 (w), 963 (m), 849 (m), 778 (s), 745 (m), 724 (m), 695 (m). MS (EI): calc. for C₁₁H₁₂O₂ [M]⁺: 176.08, found: 176.03.



Secondary amine 6: Propylamine (2.1 mL, 25.54 mmol) and NaBH(OAc)₃ (6.50 g, 30.66 mmol) were sequentially added to a solution of 3,4-dihydronaphthalenone **5** (3.00 g, 17.02 mmol) in DCE (100 mL) and the reaction was stirred at room temperature overnight. The solvent was removed under reduced pressure and the resulting residue was portioned between EtOAc and aqueous NaHCO₃ solution. The organic phase was washed with brine, dried over MgSO₄ and concentrated under reduced pressure to yield secondary amine **6** (2.99 g, 13.62 mmol, 80%) as a colorless oil.

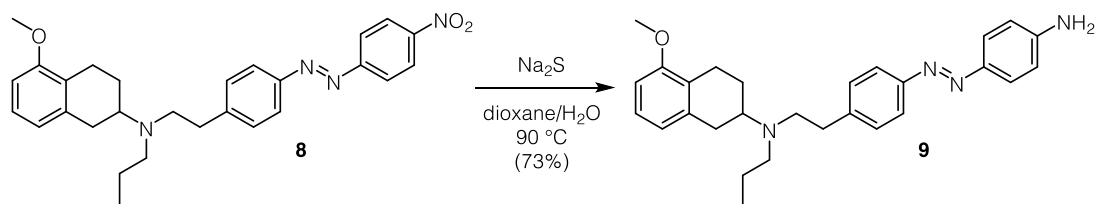
Data for 6: ¹H NMR (400 MHz, d₄-MeOH): δ (ppm) = 7.07 (t, *J* = 7.9 Hz, 1H), 6.69 (dd, *J* = 13.6, 7.9 Hz, 2H), 3.79 (s, 3H), 2.98 (dddd, *J* = 27.8, 20.8, 17.7, 5.4, 2.6 Hz, 3H), 2.81 – 2.69 (m, 2H), 2.57 (ddd, *J* = 30.0, 16.8, 8.0 Hz, 2H), 2.16 (ddt, *J* = 11.9, 5.7, 2.9 Hz, 1H), 1.69 – 1.48 (m, 3H), 0.99 (t, *J* = 7.4 Hz, 3H). ¹³C NMR (100 MHz, d₄-MeOH): δ (ppm) = 158.6, 136.7, 127.6, 125.5, 122.4, 108.3, 55.6, 54.9, 49.4, 36.2, 29.1, 23.3, 23.2, 12.0. IR (ATR): ν_{max} (cm⁻¹) = 2936 (m), 2875 (w), 2835 (m), 2792 (m), 2734 (m), 2537 (w), 2445 (w), 1587 (s), 1468 (vs), 1438 (s), 1395 (w), 1382 (w), 1346 (w), 1312 (w), 1284 (w), 1258 (vs), 1094 (s), 1068 (m), 1036 (m), 987 (m), 954 (m), 914 (w), 892 (w),

876 (w), 832 (w), 765 (vs), 709 (m), 694 (m). **HRMS (EI):** calc. for $C_{14}H_{22}NO^+$ [$M+H$] $^+$: 220.1696, found: 220.1696.



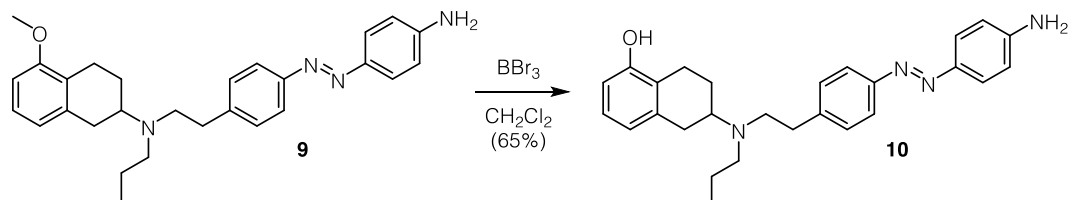
Azobenzene 8: DMP (8.33 g, 21.06 mmol) was added to a solution of (*E*)-2-(4-((4-nitrophenyl)diazenyl)phenyl)ethan-1-ol (1.90 g, 7.02 mmol) in CH_2Cl_2 and the reaction was stirred at room temperature for 3 h. The mixture was washed with aqueous $Na_2S_2O_3$ solution, water and brine, dried over magnesium sulfate and evaporated to dryness. The resulting residue was redissolved in DCE (100 mL), secondary amine **6** (700 mg, 3.19 mmol) and $NaBH(OAc)_3$ (2.23 g, 10.53 mmol) were sequentially added and the reaction mixture was stirred at room temperature overnight. The solvent was removed under reduced pressure and the residue was portioned between EtOAc and aqueous $NaHCO_3$ solution. The organic phase was washed with brine, dried over $MgSO_4$ and concentrated under reduced pressure. Purification of the resultant residue by flash column chromatography (MeOH: CH_2Cl_2 3:97, R_f = 0.3) gave azobenzene **8** (1.49 g, 3.16 mmol, 99%) as a red solid.

Data for 8: 1H NMR (400 MHz, $CDCl_3$): δ (ppm) = 8.42 – 8.38 (m, 2H), 8.06 – 8.02 (m, 2H), 7.94 – 7.90 (m, 2H), 7.43 – 7.38 (m, 2H), 7.11 (t, J = 7.9 Hz, 1H), 6.72 (dd, J = 7.6, 1.0 Hz, 1H), 6.67 (d, J = 8.1 Hz, 1H), 3.83 (s, 3H), 3.01 (dddd, J = 10.8, 8.6, 5.5, 2.7 Hz, 2H), 2.87 (s, 5H), 2.81 – 2.71 (m, 1H), 2.62 – 2.49 (m, 3H), 2.07 (ddd, J = 14.5, 4.6, 2.0 Hz, 1H), 1.63 – 1.48 (m, 3H), 0.92 (t, J = 7.3 Hz, 3H). ^{13}C NMR (100 MHz, $CDCl_3$): δ (ppm) = 157.4, 156.0, 151.0, 148.7, 146.6, 138.1, 130.0, 126.3, 125.4, 124.9, 123.6, 123.5, 121.8, 107.1, 56.7, 55.4, 52.8, 52.6, 36.3, 32.5, 25.9, 24.0, 22.4, 12.1. **IR (ATR):** ν_{max} (cm^{-1}) = 2931 (m), 2836 (w), 1738 (vw), 1602 (w), 1586 (m), 1521 (s), 1499 (w), 1468 (m), 1438 (w), 1416 (vw), 1360 (vs), 1259 (m), 1218 (w), 1143 (m), 1106 (m), 1093 (m), 1071 (m), 1008 (w), 963 (w), 908 (w), 858 (s), 766 (w), 754 (w), 729 (s), 710 (w), 688 (w). **HRMS (EI):** calc. for $C_{28}H_{33}N_4O_3^+$ [$M+H$] $^+$: 473.2547, found: 473.2543.



Aniline 9: A suspension of azobenzene **8** (500 mg, 1.06 mmol) and sodium sulfide (2.33 mg, 2.12 mmol) in 1,4-dioxane (50 mL) and water (50 mL) was stirred at 90 °C overnight. The reaction was cooled to room temperature, diluted with aqueous NaOH (1 M) and extracted with EtOAc. The organic phase was washed with water and brine, dried over MgSO₄ and concentrated under reduced pressure. Purification of the resultant residue by flash column chromatography (MeOH:CH₂Cl₂ 2:98, R_f=0.2) gave aniline **9** (341 mg, 0.770 mmol, 73%) as a red solid.

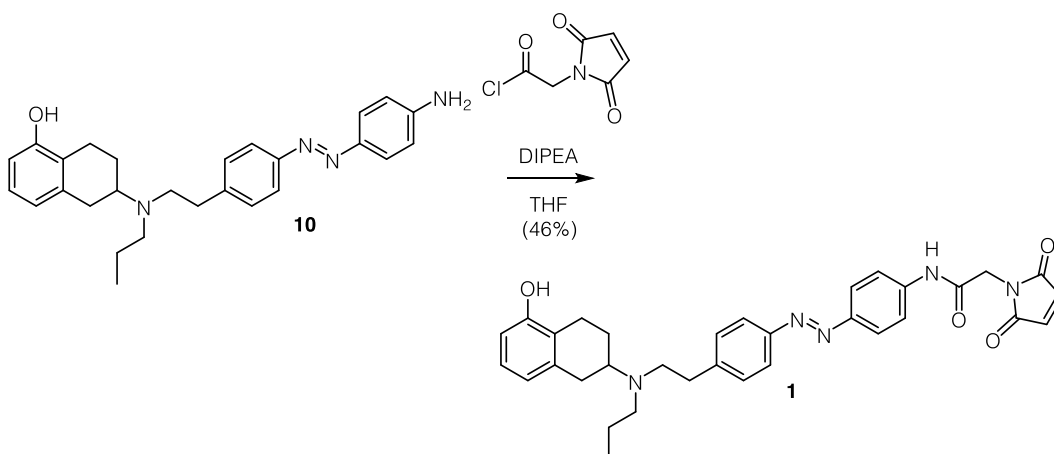
Data for 9: ¹H NMR (400 MHz, CDCl₃): δ (ppm) 7.80 (t, J = 8.3 Hz, 4H), 7.32 (d, J = 8.2 Hz, 2H), 7.10 (t, J = 7.8 Hz, 1H), 6.73 (dd, J = 8.3, 6.5 Hz, 3H), 6.66 (d, J = 8.1 Hz, 1H), 4.03 (s, 2H), 3.81 (s, 3H), 3.12 – 2.94 (m, 2H), 2.94 – 2.71 (m, 6H), 2.68 – 2.44 (m, 3H), 2.08 (dt, J = 13.7, 4.2 Hz, 1H), 1.68 – 1.46 (m, 3H), 0.91 (t, J = 7.3 Hz, 3H). ¹³C NMR (100 MHz, CDCl₃): δ (ppm) = 157.3, 151.4, 149.5, 145.7, 143.2, 138.1, 129.5, 126.3, 125.3, 125.1, 122.4, 121.8, 114.8, 107.0, 67.2, 56.8, 55.3, 52.8, 35.9, 32.4, 25.9, 24.0, 22.3, 12.1. IR (ATR): ν_{max} (cm⁻¹) = 3336 (w), 2933 (m), 2837 (vw), 2508 (w), 2246 (vw), 2212 (vw), 1623 (w), 1586 (m), 1516 (m), 1468 (m), 1438 (w), 1378 (vw), 1346 (vw), 1260 (m), 1216 (vw), 1180 (vw), 1128 (vw), 1094 (m), 1071 (m), 96.2 (vw), 907 (s), 826 (m), 768 (m), 700 (vs). HRMS (EI): calc. for C₂₈H₃₅N₄O⁺ [M+H]⁺: 443.2805, found: 443.2811.



Phenol 10: BBr₃ (1M in CH₂Cl₂, 3.18 mL, 3.18 mmol) was added to a solution of aniline **9** (704 mg, 1.59 mmol) in CH₂Cl₂ (30 mL) at –78 °C and the reaction was stirred 1 h at the same temperature and 1 h at room temperature. The reaction mixture was diluted with MeOH (5 mL) and aqueous NaHCO₃ solution and extracted with EtOAc. The organic phase was washed with brine, dried over MgSO₄ and concentrated under reduced

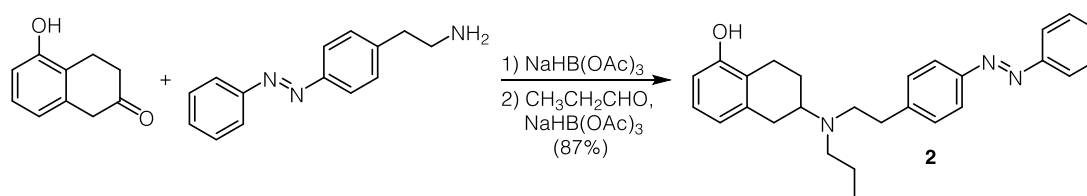
pressure. Purification by flash column chromatography (MeOH:CH₂Cl₂ = 2:98 to 6:94, R_f = 0.6 (MeOH:CH₂Cl₂ 6:94)) gave phenol **10** (440 mg, 1.03 mmol, 65%) as a red solid.

Data for 10: ¹H NMR (400 MHz, CDCl₃): δ (ppm) 7.81 (t, *J* = 7.6 Hz, 4H), 7.31 (d, *J* = 8.0 Hz, 2H), 6.99 (t, *J* = 7.8 Hz, 1H), 6.73 (d, *J* = 8.3 Hz, 2H), 6.68 (d, *J* = 7.6 Hz, 1H), 6.58 (d, *J* = 7.9 Hz, 1H), 4.04 (s, 2H), 3.09 – 2.73 (m, 8H), 2.59 (ddd, *J* = 23.4, 10.2, 5.8 Hz, 3H), 2.12 (dd, *J* = 12.5, 5.5 Hz, 1H), 1.70 – 1.47 (m, 3H), 0.92 (t, *J* = 7.3 Hz, 3H). ¹³C NMR (100 MHz, CDCl₃): δ (ppm) = 153.7, 151.4, 149.5, 145.6, 143.0, 138.9, 129.5, 126.5, 125.1, 123.3, 122.5, 121.6, 114.8, 112.1, 56.8, 52.7, 52.6, 35.5, 32.2, 25.8, 23.8, 21.9, 12.1. IR (ATR): ν_{max} (cm⁻¹) = 3370 (w), 2313 (w), 3027 (w), 2930 (m), 2870 (w), 1907 (vw), 1726 (vw), 1619 (m), 1598 (vs), 1505 (m), 1463 (s), 1428 (m), 1404 (w), 1374 (w), 1341 (w), 1297 (m), 1275 (s), 1138 (vs), 1083 (m), 1065 (m), 1012 (m), 949 (w), 836 (s), 751 (vs), 711 (m), 666(w). HRMS (EI): calc. for C₂₇H₃₃N₄O⁺ [*M+H*]⁺: 429.2649, found: 429.2645.



MalAzoPPHT (1): Oxalylchloride (0.05 mL, 0.610 mmol) and DMF (1 drop) were added sequentially to a solution of 2-maleimidoacetic acid (73 mg, 0.469 mmol) in CH₂Cl₂ (5 mL) and the reaction mixture was stirred for 2 h at room temperature. The solvent was evaporated *in vacuo* and the resulting residue was redissolved in THF (3 mL). The solution was added dropwise to an ice cooled solution of phenol **10** (67 mg, 0.156 mmol) and DIPEA (0.10 mL, 0.610 mmol) in THF (3 mL) and the reaction was stirred for 30 min at room temperature. The solvent was evaporated under reduced pressure and the resulting residue was purified by flash column chromatography (MeOH:CH₂Cl₂ 3:97, R_f = 0.25) to give MalAzoPPHT (**1**) (41 mg, 0.072 mmol, 46%) as a red solid.

Data for 1: $^1\text{H NMR}$ (400 MHz, CDCl_3): δ (ppm) 8.00 (s, 1H), 7.86 (d, $J = 8.4$ Hz, 2H), 7.80 (d, $J = 8.0$ Hz, 2H), 7.62 (d, $J = 8.5$ Hz, 2H), 7.31 (d, $J = 8.0$ Hz, 2H), 6.98 (t, $J = 7.7$ Hz, 1H), 6.79 (s, 2H), 6.67 (d, $J = 7.6$ Hz, 1H), 6.58 (d, $J = 7.9$ Hz, 1H), 5.56 (s, 1H), 4.37 (s, 2H), 3.04 – 2.70 (m, 8H), 2.62 – 2.50 (m, 3H), 1.61 (tt, $J = 12.1, 6.2$ Hz, 1H), 1.50 (p, $J = 7.4$ Hz, 2H), 0.89 (t, $J = 7.3$ Hz, 3H). $^{13}\text{C NMR}$ (100 MHz, CDCl_3): δ (ppm) = 170.3, 164.5, 153.6, 151.1, 138.5, 134.7, 129.7, 126.5, 124.3, 124.0, 123.1, 122.9, 122.7, 121.8, 121.7, 120.1, 112.1, 56.7, 52.7, 52.6, 41.4, 35.9, 32.3, 25.8, 23.8, 22.2, 12.1. **IR (ATR):** ν_{max} (cm^{-1}) = 2933(m), 1741(s), 1595(vs), 1560(s), 1501(m), 1464(m), 1408(s), 1301(s), 1253(s), 1156(s), 1012(w), 846(s), 771(m), 676(w). **HRMS (ESI):** calc. for $\text{C}_{33}\text{H}_{36}\text{N}_5\text{O}_4^+$ [$M+H$] $^+$: 566.2762, found: 566.2763.

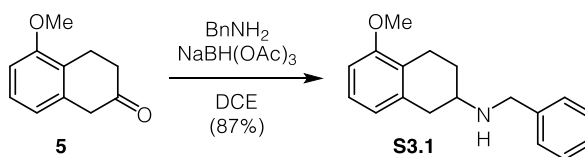


AP 2 (2): $\text{NaHB}(\text{OAc})_3$ (103 mg, 0.46 mmol) was added to a solution of amine 11 (73 mg, 0.32 mmol) and 5-hydroxytetralone (50 mg, 0.31 mmol) in DCE (2 mL) and the resulting suspension was stirred at room temperature overnight. The reaction mixture was portioned between EtOAc and aqueous. NaHCO_3 solution and the organic phase was further washed with aqueous. NaHCO_3 solution. a solution of sodium chloride (10%) and brine. The solution was dried over Na_2SO_4 and concentrated under reduced pressure yielding the crude alkylation product as an orange oil, which was immediately transferred to the next step.

The freshly prepared secondary amine (described above) was redissolved in DCE (1.5 mL) and treated with propionaldehyde (25 μL , 0.34 mmol) followed by $\text{NaHB}(\text{OAc})_3$ (103 mg, 0.46 mmol). After 5 h, the reaction was quenched and worked up as described above yielding the crude product tertiary amine. Medium pressure chromatography (Biotage, 25 g SiO_2 column, EtOAc:hexanes 10:90–100:0, $R_f = 0.6$ EtOAc:hexanes 1:1) afforded AP 2 (2) as an orange oil (110 mg, 0.27 mmol, 87% over 2 steps).

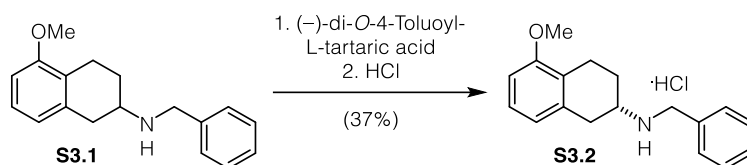
Data for 2: $^1\text{H NMR}$ (600 MHz, CDCl_3): δ (ppm) = 7.94 – 7.89 (m, 2H), 7.89 – 7.83 (m, 2H), 7.54 – 7.49 (m, 2H), 7.49 – 7.44 (m, 1H), 7.37 – 7.32 (m, 2H), 6.99 (t, $J = 7.8$, 1H), 6.68 (d, $J = 7.7$, 1H), 6.60 (d, $J = 7.9$, 1H), 5.40 (s, 1H), 3.06 – 2.87 (m, 3H), 2.85 (s, 4H), 2.82 – 2.66 (m, $J = 28.9, 15.2, 9.4$, 1H), 2.63 – 2.53 (m, 3H), 2.13 – 2.07 (m, 1H), 1.68 – 1.57 (m, 1H), 1.57 – 1.47 (m, 2H), 0.91 (t, $J = 7.3$, 3H). $^{13}\text{C NMR}$ (100 MHz, CDCl_3): δ

(ppm) = 153.46, 152.72, 151.07, 144.48, 138.37, 130.72, 129.52, 129.04, 126.40, 122.94, 122.83, 122.73, 121.68, 111.97, 56.58, 52.62, 52.54, 35.81, 32.24, 25.70, 23.60, 22.08, 11.93. **IR (ATR):** ν_{\max} (cm⁻¹) = 3043 (w), 2931 (m), 1585 (s), 1499 (w), 1484 (w), 1464 (s), 1373 (m), 1340 (m), 1277 (s), 1221 (w), 1154 (m), 1104 (w), 1070 (w), 1012 (m), 919 (w), 836 (m), 808 (w), 766 (vs), 712 (w), 687 (vs). **HRMS (ESI):** calc. for C₂₇H₃₂N₃O⁺ [*M+H*]⁺: 414.2545, found: 414.2537.



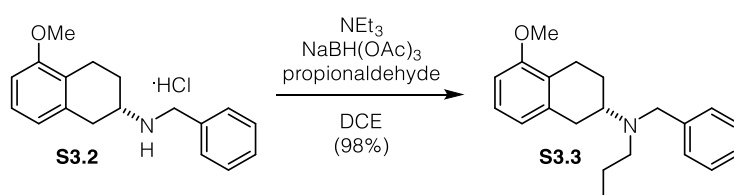
Benzylamine S3.1: To a solution of tetralone **5** (6.13 g, 34.81 mmol, 1.0 eq) in DCE (90 mL) was added benzyl amine (4.95 mL, 4.85 g, 45.3 mmol, 1.3 eq) followed by NaBH(OAc)₃ (13.3 g, 62.7 mmol, 1.8 eq). The reaction mixture was stirred over night at room temperature and then partitioned between saturated NaHCO_{3(aq)} (90 mL) and EtOAc (90 mL). The layers were separated and the aqueous layer was extracted with EtOAc (4 x 90 mL). The combined organic layers were washed with brine, dried over MgSO₄ and concentrated under reduced pressure. The resulting crude material was purified by flash chromatography (SiO₂, gradient 0 to 10 % MeOH in DCM + 1% NEt₃). Benzylamine **S3.1** was obtained as a brown oil (8.1 g, 30.2 mmol, 87 %).

Data for S3.1: R_f: 0.7 (MeOH:CH₂Cl₂:NEt₃ 4:95:1), **¹H NMR (400 MHz, dmsO-d₆):** δ (ppm) = 7.34 (dd, *J*=3.2, 5.2, 2H), 7.30 – 7.24 (m, 2H), 7.21 – 7.15 (m, 1H), 7.02 (t, *J*=7.9, 1H), 6.68 (d, *J*=8.0, 1H), 6.62 (d, *J*=7.6, 1H), 3.77 (s, 2H), 3.71 (s, 3H), 2.91 (dd, *J*=4.2, 16.0, 1H), 2.79 – 2.69 (m, 2H), 2.52 – 2.34 (m, 2H), 2.03 – 1.92 (m, 1H), 1.44 (dtd, *J*=5.8, 10.2, 12.7, 1H). **¹³C NMR (101 MHz, dmsO-d₆):** δ (ppm) = 157.10, 141.70, 137.02, 128.48, 128.37, 126.84, 126.52, 124.77, 121.66, 107.59, 55.49, 52.12, 50.53, 36.52, 28.83, 22.12. **HRMS (EI):** calc. for C₁₈H₂₁NO [*M*]⁻: 267.1623; found: 267.1625.



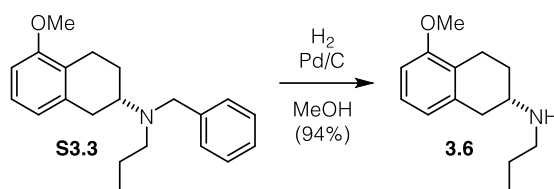
Secondary amine S3.2: The partially enriched aminotetraline from the resolution above was free based and treated with 1 eq (-)-di-*O*-4-toluoyl-L-tartaric acid. The precipitated tartrate salt was recrystallized until optical rotation was constant.

$[\alpha]_D^{20}$ (HCl salt) = - 58.4 ° (c = 2, MeOH).



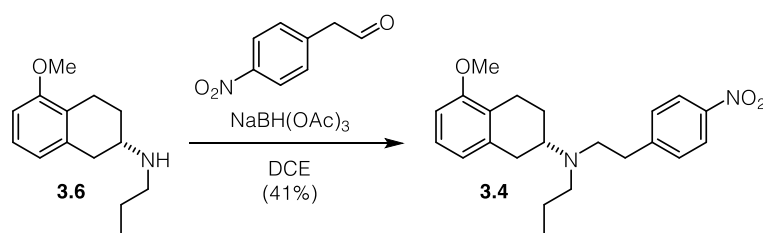
Tertiary amine S3.3: Propionaldehyde (0.28 mL, 3.96 mmol) and sodium triacetoxyborohydride (1.05 g, 4.96 mmol) were added to a solution of secondary amine **S3.2** (1.0 g, 3.29 mmol) and triethylamine (0.9 mL, 65.8 mmol) in dichloroethane (35 mL). The solution was stirred at room temperature overnight before the solvent was evaporated in vacuum. The resulting residue was portioned between a saturated solution of ammonium chloride and ethyl acetate. The organic phase was washed with a saturated solution of sodium bicarbonate and brine and dried over MgSO₄. Evaporation of the solvent under reduced pressure gave tertiary amine **S3.3** (995 mg, 3.22 mmol, 98%) as a colorless oil.

Data for S3.3: ¹H-NMR (400 MHz, CDCl₃, 23 °C): δ (ppm) = 7.31 (m, 4H), 7.24 (m, 1H), 7.09 (t, J = 7.9 Hz, 1H), 6.69 (m, 2H), 3.91 (s, 2H), 3.81 (s, 3H), 2.97 (m, 3H), 2.61 (m, 2H), 2.10 (m, 1H), 1.63 (m, 1H), ¹³C-NMR (400 MHz, CDCl₃, 23 °C): δ (ppm) = 157.4, 140.9, 136.9, 128.7, 128.4, 127.1, 126.4, 125.3, 121.8, 76.9, 55.4, 52.6, 51.4, 37.0, 29.3, 22.3. **HRMS (ESI):** calc. for C₂₁H₂₈NO [M+H]⁺: 310.2165, found: 310.2164.



Propylamine 3.6: Palladium on charcoal (10%, 170 mg) was added to a solution of tertiary amine **S3.3** (509 mg, 1.64 mmol) in methanol (7 mL). The flask was flushed three times with hydrogen and the reaction was stirred under a hydrogen atmosphere at room temperature overnight. Filtration over celite and subsequent removal of the solvent under reduced pressure gave propylamine **3.6** (337 mg, 1.54 mmol, 94%) as a colorless oil.

Data for 3.6: $^1\text{H-NMR}$ (400 MHz, CDCl_3 , 23 °C): δ (ppm) = 7.07 (t, J = 7.9 Hz, 1H), 6.69 (dd, J = 13.6, 7.9 Hz, 2H), 3.79 s, 3H), 3.10-2.87 (m, 3H), 2.80-2.70 (m, 2H), 2.68-2.48 (m, 2H), 2.17 (dt, J = 9.4, 3.1 Hz, 1H), 1.68-1.48 (m, 3H), 0.99 (t, J = 7.4 Hz, 3H). $^{13}\text{C-NMR}$ (400 MHz, CDCl_3 , 23 °C): δ (ppm) = 158.6, 136.7, 127.6, 125.5, 122.4, 108.3, 55.6, 54.9, 49.4, 36.2, 29.1, 23.3, 23.2, 12.0. **IR (ATR):** ν_{max} (cm^{-1}) = 2936 (m), 2875 (w), 2835 (m), 2792 (m), 2734 (m), 2537 (w), 2445 (w), 1587 (s), 1468 (vs), 1438 (s), 1395 (w), 1382 (w), 1346 (w), 1312 (w), 1284 (w), 1258 (vs), 1094 (s), 1068 (m), 1036 (m), 987 (m), 954 (m), 914 (w), 892 (w), 876 (w), 832 (w), 765 (vs), 709 (m), 694 (m). **HRMS (ESI):** calc. for $\text{C}_{14}\text{H}_{22}\text{NO}$ [$M+H$] $^+$: 220.1696, found: 220.1696.

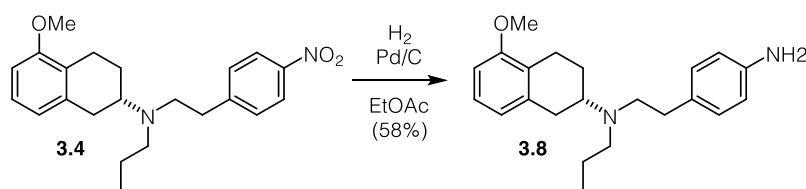


Nitrobenzene 3.4: DMP (3.50 g, 8.22 mmol) was added to a solution of 2-(4-nitrophenyl)ethan-1-ol (457 g, 2.74 mmol) in CH_2Cl_2 and the reaction was stirred at room temperature for 3 h. The mixture was washed with aqueous $\text{Na}_2\text{S}_2\text{O}_3$ solution, water and brine, dried over MgSO_4 and evaporated to dryness.

The resulting residue was redissolved in DCE (150 mL). 5-methoxy-N-propyl-1,2,3,4-tetrahydronaphthalen-2-amine (250 mg, 1.14 mmol) and $\text{NaBH}(\text{OAc})_3$ (300 g, 1.56 mmol) were sequentially added and the reaction mixture was stirred at room temperature overnight. The solvent was removed in vacuum and the residue was

portioned between EtOAc and aqueous NaHCO₃ solution. The organic phase was washed with brine, dried over MgSO₄ and concentrated under reduced pressure to yield nitrobenzene **3.4** (172 mg, 0.46 mmol, 41%) as a yellow solid.

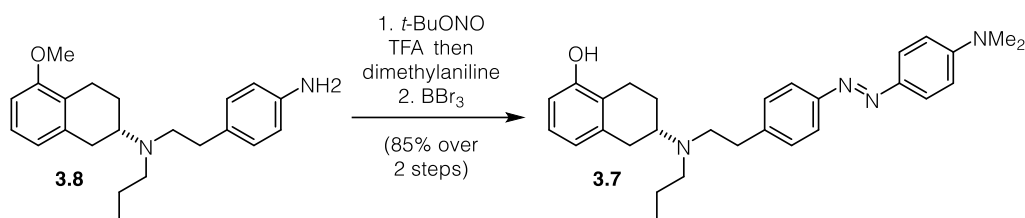
Data for **3.4**: **¹H-NMR (400 MHz, CDCl₃, 23 °C)**: δ = 8.19 – 8.10 (m, 2H), 7.41 – 7.32 (m, 2H), 7.09 (t, J = 7.9 Hz, 1H), 6.67 (dd, J = 14.0, 7.9 Hz, 2H), 3.81 (s, 3H), 2.96 (dddd, J = 13.9, 11.5, 5.2, 2.4 Hz, 2H), 2.90 – 2.76 (m, 5H), 2.70 (dd, J = 16.1, 11.2 Hz, 1H), 2.51 (ddd, J = 21.4, 10.3, 6.2 Hz, 3H), 1.99 (ddt, J = 12.7, 4.8, 2.4 Hz, 1H), 1.55 (tt, J = 12.1, 6.1 Hz, 1H), 1.49 – 1.38 (m, 2H), 0.87 (t, J = 7.3 Hz, 3H). **¹³C-NMR (400 MHz, CDCl₃, 23 °C)**: δ = 157.3, 149.2, 146.5, 137.9, 129.8, 126.3, 125.3, 123.6, 121.7, 107.1, 76.8, 56.5, 55.4, 52.6, 52.2, 36.0, 32.3, 25.7, 23.9, 22.2, 12.0. **IR (ATR)**: ν_{max} (cm⁻¹) = 2932 (w), 2838 (m), 2361 (w), 1734 (w), 1670 (w), 1654 (w), 1600 (m), 1586 (m), 1517 (s), 1469 (m), 1438 (m), 1344 (vs), 1260 (s), 1217 (w), 1167 (w), 1095 (m), 1072 (w), 1015 (vw), 964 (vw), 856 (m), 767 (m), 748 (vw), 711 (vw), 698 (w), 668 (vw). **HRMS (ESI)**: calc. for C₂₂H₂₉N₂O [M+H]⁺: 369.2173, found: 369.2178. [α]_D²⁰ = -27.5 ° (c=0.4, MeOH)



Aniline 3.8: A suspension of Pd/C (30 mg) and nitrobenzene **3.4** (150 mg, 0.41 mmol) in ethyl acetate (30 mL) was stirred under a hydrogen atmosphere at room temperature overnight. The reaction was filtered over celite and the resulting filtrate was concentrated under reduced pressure to yield aniline **3.8** (80 mg, 0.24 mmol, 58%) as a yellow oil.

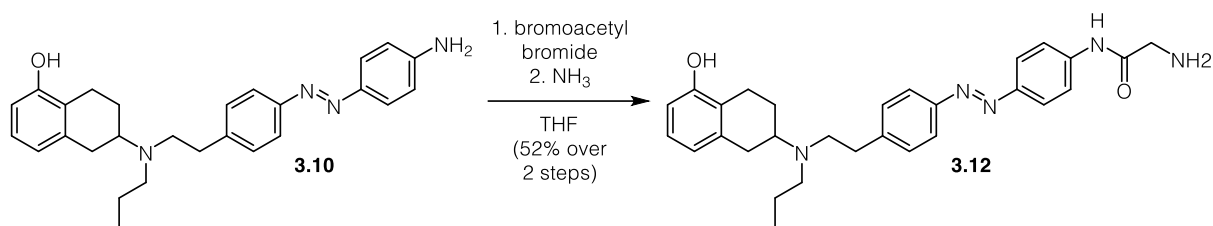
Data for **3.8**: **¹H-NMR (400 MHz, CDCl₃, 23 °C)**: δ (ppm) = 7.09 (t, J=7.9 Hz, 1H), 6.98 (d, J=7.9 Hz, 2H), 6.68 (dd, J=22.0, 7.9 Hz, 2H), 6.60 (d, J=7.9 Hz, 2H), 3.79 (s, 3H), 3.65 (s, 2H), 3.17 (s, 1H), 3.09-2.96 (m, 2H), 2.95-2.66 (m, 7H), 2.55 (td, J=12.0, 6.0 Hz, 1H), 2.31-2.14 (m, 1H), 1.77-1.57 (m, 3H), 0.94 (t, J=7.3 Hz, 3H). **¹³C-NMR (400 MHz, CDCl₃, 23 °C)**: δ (ppm) = 170.9, 157.0, 144.9, 129.3, 126.3, 124.5, 121.4, 115.1, 107.0, 60.2, 57.5, 55.0, 52.8, 52.3, 31.3, 24.9, 23.4, 20.8, 14.0, 11.6. **IR (ATR)**: ν_{max} (cm⁻¹) = 3336 (w), 2933 (m), 2508 (w), 2246 (vw), 1623 (m), 1586 (m), 1516 (s), 1486 (s), 1438 (m), 1378 (w), 1346 (w), 1260 (s), 1216 (m), 1180 (m), 1128 (m), 1094 (s), 1071 (m), 926

(w), 907 (vs), 826 (m), 768 (s). **HRMS (ESI):** calc. for $C_{22}H_{31}N_2O_3$ $[M+H]^+$: 339.2431, found: 339.2436. $[\alpha]_D^{20} = -26.8^\circ$ (c=0.3, MeOH)



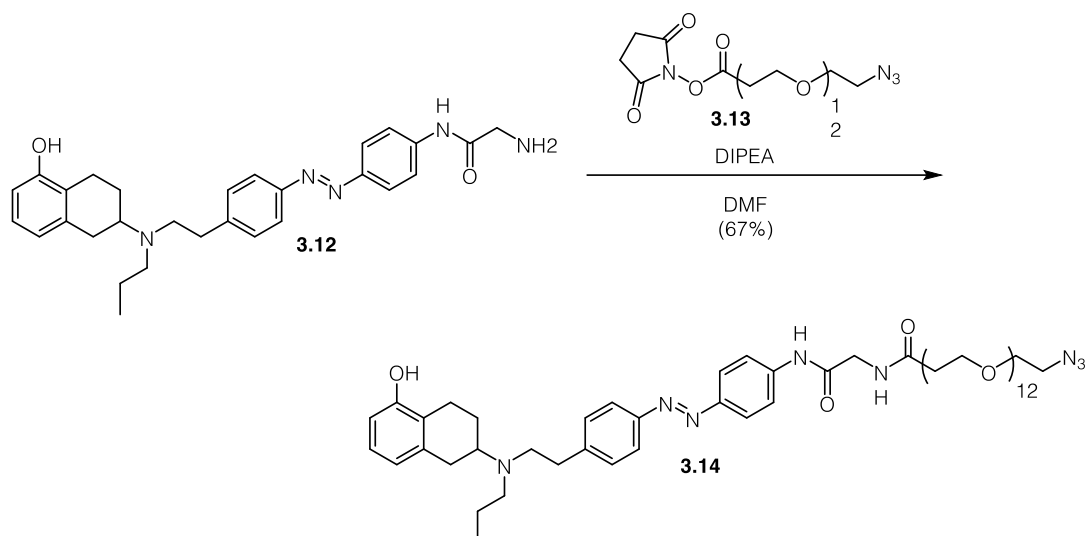
Dimethylaniline 3.7: TFA (0.06 mL, 0.75 mmol) and *t*BuNO₂ (0.04 mL, 0.50 mmol) were sequentially added to an ice cooled solution of aniline **3.8** (80 mg, 0.24 mmol) in MeCN (25 mL) and the reaction was stirred for 1 h at 0 °C. *N,N*-dimethylaniline (0.63 mL, 4.94 mmol) was added to the solution and the reaction was stirred at 0 °C for 1 h. The mixture was extracted with EtOAc and the organic phase was washed with aqueous NaOH (1 M), aqueous HCl (1 M) and brine, dried over MgSO₄ and concentrated under reduced pressure. The resulting residue was redissolved in CH₂Cl₂ (40 mL) and cooled to -78 °C. BBr₃ (1 M in CH₂Cl₂, 1 mL, 1 mmol) was added and the reaction was stirred 90 min at -78 °C and 1 h at room temperature. The mixture was quenched with MeOH (10 mL) and the reaction was extracted with CH₂Cl₂. The organic phase was dried over MgSO₄ and concentrated under reduced pressure. Purification of the resulting residue by flash column chromatography (MeOH:CH₂Cl₂ 2:98, R_f = 0.2) gave dimethylaniline **3.7** (90 mg, 0.20 mmol, 85% over 2 steps) as a red solid.

Data for 3.7: **¹H-NMR (400 MHz, CDCl₃ 23 °C):** δ (ppm) = 7.88 (d, J = 9.0 Hz, 2H), 7.78 (d, J = 8.3 Hz, 2H), 7.30 (d, J = 8.4 Hz, 2H), 6.99 (t, J = 7.8 Hz, 1H), 6.76 (d, J = 9.1 Hz, 2H), 6.69 (d, J = 7.6 Hz, 1H), 6.58 (d, J = 7.9 Hz, 1H), 3.08 (s, 6H), 3.05 – 2.95 (m, 2H), 2.94 – 2.89 (m, 1H), 2.84 (s, 4H), 2.77 (dd, J = 16.1, 11.4 Hz, 1H), 2.58 (ddd, J = 17.6, 10.6, 6.1 Hz, 3H), 2.19 – 2.04 (m, 1H), 1.59 (ddt, J = 41.0, 15.0, 6.9 Hz, 3H), 0.91 (t, J = 7.3 Hz, 3H). **¹³C-NMR (400 MHz, CDCl₃ 23 °C):** δ (ppm) = 153.6, 152.4, 151.7, 143.8, 142.6, 138.5, 129.5, 126.5, 124.9, 123.1, 122.3, 121.8, 112.1, 111.6, 76.84, 56.8, 52.8, 40.5, 35.8, 32.3, 25.8, 23.8, 22.1, 12.1. **IR (ATR):** ν_{max} (cm⁻¹) = 3028 (w), 2930 (m), 2870 (m), 2245 (w), 1904 (vw), 1586 (m), 1660 (w), 1598 (vs), 1516 (s), 1463 (m), 1444 (m), 1426 (m), 1402 (m), 1361 (s), 1312 (m), 1275 (s), 1248 (m), 1229 (m), 1138 (8vs), 1083 (m), 1063 (s), 1012 (m), 944 (m), 906 (s), 821 (s), 768 (s). **MS (ESI):** calc. for C₂₉H₃₇N₄O $[M+H]^+$: 457.2962, found: 457.2968. $[\alpha]_D^{20} = -26^\circ$ (c=0.1, MeOH)



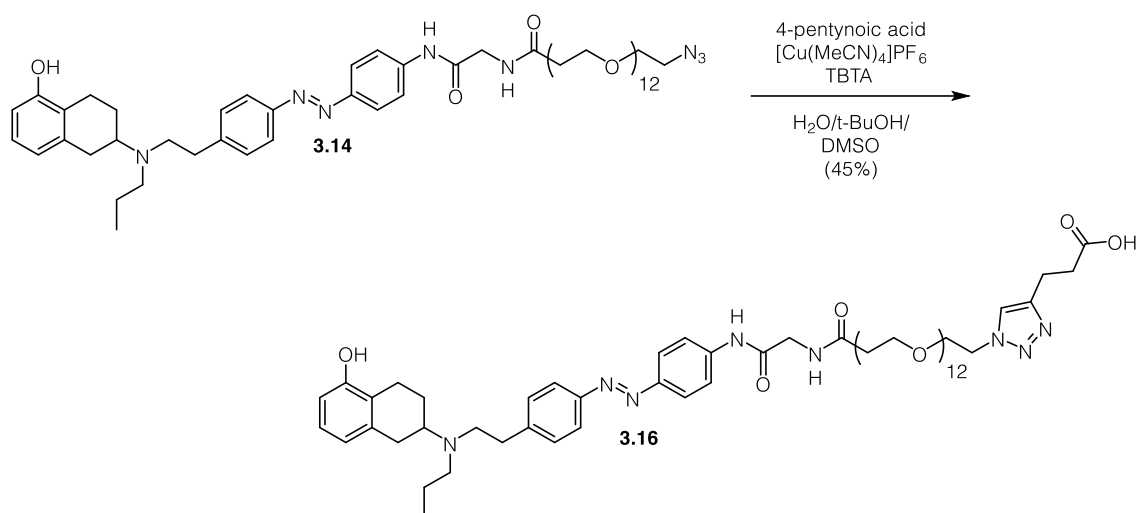
Amine 3.12: Bromoacetyl bromide (0.06 mL, 0.699 mmol) was added dropwise to an ice cooled solution of phenol **3.10** (214 mg, 0.499 mmol) and DIPEA (0.12 mL, 0.699 mmol) in THF (8 mL) and the resulting solution was stirred for 10 min at that temperature and for 8 h at room temperature. The reaction was diluted with EtOAc and washed with a saturated aqueous solution of NaHCO₃ and brine. The organic phase was dried over MgSO₄ and concentrated under reduced pressure. The resulting residue was redissolved in THF (11 mL) and cooled to 0 °C. Ammonia (7 M in MeOH, 4.00 mL, 28.0 mmol) was added and the mixture was stirred at room temperature overnight. The reaction was diluted with H₂O and extracted with EtOAc. The combined organic phases were washed with brine, dried over MgSO₄ and concentrated under reduced pressure. Purification of the resulting residue by flash column chromatography (MeOH:CH₂Cl₂:NH₃ (aq.) 4:96:1-7:93:1, R_f (MeOH:CH₂Cl₂:NH₃ (aq.) 8:92:1) = 0.6) gave amine **3.12** (125 mg, 0.257 mmol, 52%) as an orange solid).

Data for 3.12: ¹H NMR (600 MHz, *d*₄-MeOH): δ (ppm) = 7.87 (d, *J* = 8.6 Hz, 2H), 7.78 (dd, *J* = 10.5, 8.4 Hz, 4H), 7.35 (d, *J* = 8.1 Hz, 2H), 6.88 (t, *J* = 7.8 Hz, 1H), 6.55 (dd, *J* = 7.8, 3.5 Hz, 2H), 3.44 (s, 2H), 2.95 (dtd, *J* = 13.7, 7.3, 6.2, 3.5 Hz, 2H), 2.82 (s, 5H), 2.69 (dd, *J* = 15.7, 11.4 Hz, 1H), 2.63 – 2.55 (m, 2H), 2.49 (ddd, *J* = 17.6, 12.7, 6.2 Hz, 1H), 2.14 – 2.02 (m, 1H), 1.57 – 1.44 (m, 3H), 0.91 (t, *J* = 7.3 Hz, 3H). ¹³C NMR (100 MHz, *d*₄-MeOH): δ (ppm) = 173.7, 155.9, 152.4, 150.1, 145.5, 142.4, 138.6, 130.7, 127.2, 124.7, 124.3, 123.8, 121.6, 120.9, 112.6, 58.24, 53.7, 53.6, 45.7, 35.9, 33.3, 26.9, 24.8, 22.7, 12.3. IR (ATR): ν_{max} (cm⁻¹) = 3224 (w), 2918 (w), 1666 (s), 1584 (s), 1524 (vs), 1463 (s), 1404 (m), 1301 (m), 1278 (s), 1153 (m), 1083 (m), 1018 (w), 846 (s), 818 (m), 769 (s). HRMS (ESI): calc. for C₂₉H₃₆N₅O₂⁺ [*M*+*H*]⁺: 486.2864, found: 486.2861.



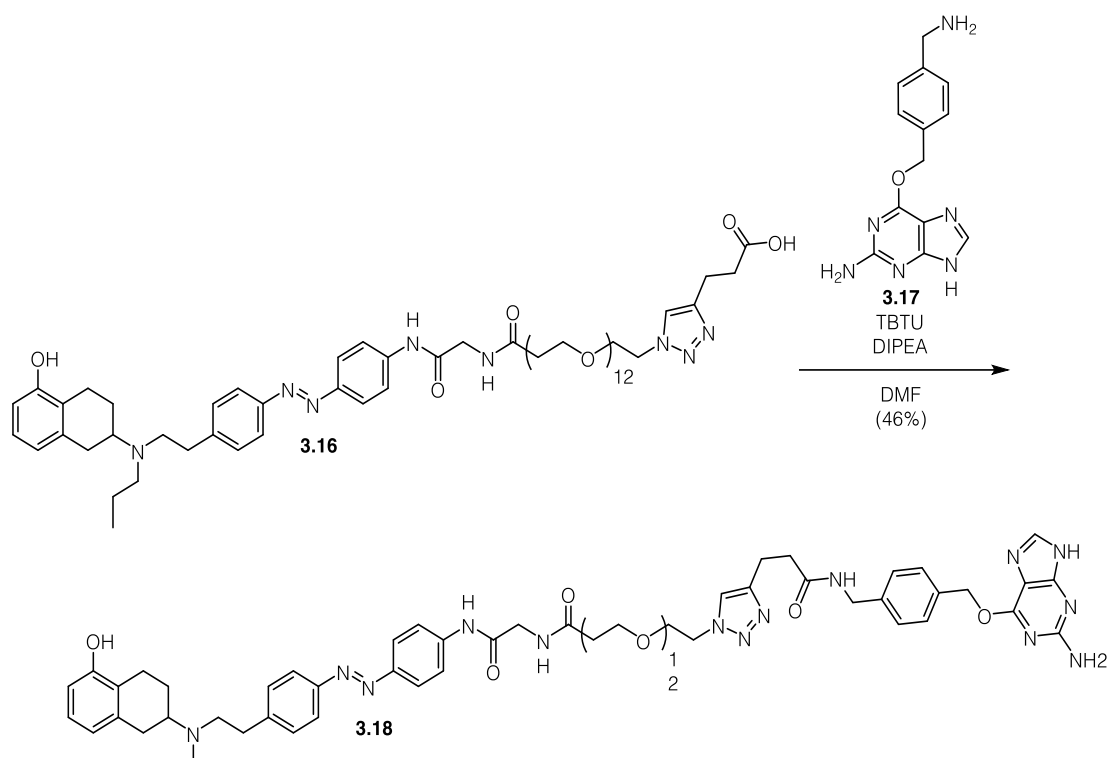
Azide 3.14: DIPEA (0.03 mL, 0.16 mmol) was added to a stirred solution of amine **3.12** (39.0 mg, 0.08 mmol) and Azido-(PEG)₁₂-NHS-ester (60.0 mg, 0.08 mmol) in DMF (0.5 mL) and the resulting solution was stirred at room temperature overnight. The reaction was diluted with EtOAc and washed with brine. The organic phase was dried over MgSO₄ and concentrated under reduced pressure. Purification of the resulting residue by reverse phase column chromatography (MeCN:HCl (aq. 0.1%))0:100-40:60) gave azide **3.14** (60 mg, 0.054 mmol, 67%) as an orange solid.

Data for 3.14: ¹H NMR (600 MHz, *d*_r-MeOH): δ (ppm) = 7.90 (td, *J* = 5.7, 3.0 Hz, 4H), 7.84 – 7.74 (m, 2H), 7.54 (d, *J* = 7.9 Hz, 2H), 6.98 (t, *J* = 7.8 Hz, 1H), 6.67 (dd, *J* = 8.0, 2.1 Hz, 1H), 6.62 (d, *J* = 7.9 Hz, 1H), 4.09 (s, 2H), 3.81 (t, *J* = 5.8 Hz, 3H), 3.76 – 3.49 (m, 48H), 3.48 – 3.32 (m, 4H), 3.31 – 3.05 (m, 8H), 2.75 – 2.51 (m, 3H), 2.40 (d, *J* = 11.8 Hz, 1H), 2.02 – 1.80 (m, 3H), 1.09 (t, *J* = 7.1 Hz, 3H). ¹³C NMR (100 MHz, *d*_r-MeOH): δ (ppm) = 174.81, 169.83, 156.08, 153.09, 149.95, 142.64, 140.87, 134.77, 131.03, 127.99, 124.83, 124.24, 123.01, 121.28, 121.09, 113.40, 71.53, 71.48, 71.45, 71.43, 71.38, 71.31, 71.26, 71.10, 68.22, 68.05, 67.60, 61.98, 61.93, 54.10, 53.86, 53.31, 53.02, 51.76, 44.33, 41.89, 37.25, 35.67, 32.20, 32.05, 30.88, 30.76, 25.00, 24.84, 23.76, 20.05, 19.87, 11.53. IR (ATR): *v*_{max} (cm⁻¹) = 3186 (w), 2972 (w), 2944 (w), 2878 (m), 2819 (m), 2533 (w), 2101 (m), 1946 (w), 1732 (s), 1662 (m), 1593 (m), 1541 (m), 1502 (m), 1464 (m), 1407 (w), 1347 (m), 1301 (m), 1284 (m), 1264 (w), 1247 (m), 1217 (m), 1192 (m), 1086 (s), 1030 (m), 991 (8w), 946 (m), 849 (m), 810 (w), 774 (m), 734 (w). HRMS (ESI): calc. for C₅₆H₈₇N₈O₁₅⁺ [*M*+*H*]⁺: 1111.6285, found: 1111.6261.



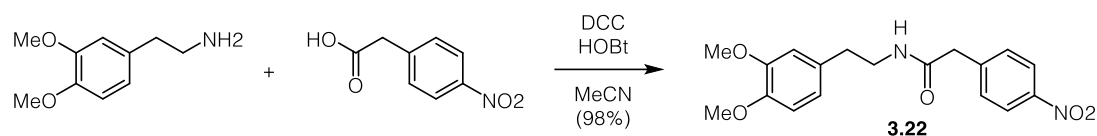
Acid 3.16: A solution of [Cu(MeCN)₄]PF₆ (12.4 mg, 0.033 mmol) in degassed *t*-BuOH/H₂O (2:1 3 mL) was added slowly to a solution of azide **3.14** (35 mg, 0.031 mmol), 4-pentynoic acid (6.2 mg, 0.063 mmol) and TBTA (17.7 mg, 0.033 mmol) in degassed *t*-BuOH (H₂O (2:2, 3 mL) and degassed DMSO (1 mL) at 0 °C and the mixture was stirred at room temperature for 24 h. The reaction was diluted with EtOAc and washed with brine. The organic phase was dried over MgSO₄ and concentrated under reduced pressure. Purification of the resulting residue by reverse phase column chromatography (MeCN:HCl (aq. 0.1%)) 0:100-40:60) gave acid **3.16** (17 mg, 0.014 mmol, 45%) as an orange solid.

Data for 3.16: ¹H NMR (600 MHz, *d*₄-MeOH): δ (ppm) = 8.50 (s, 1H), 7.91 (td, *J* = 6.7, 3.5 Hz, 4H), 7.84 – 7.76 (m, 2H), 7.59 – 7.54 (m, 2H), 7.00 (t, *J* = 7.8 Hz, 1H), 6.68 (dt, *J* = 7.6, 1.7 Hz, 1H), 6.64 (d, *J* = 7.9 Hz, 1H), 4.83 – 4.73 (m, 2H), 4.11 (s, 2H), 3.98 (dd, *J* = 5.5, 4.2 Hz, 2H), 3.82 (t, *J* = 5.9 Hz, 3H), 3.78 – 3.34 (m, 46H), 3.27 (dt, *J* = 12.5, 4.5 Hz, 3H), 3.23 – 3.06 (m, 5H), 2.82 (t, *J* = 6.9 Hz, 2H), 2.76 – 2.64 (m, 1H), 2.61 (t, *J* = 5.9 Hz, 2H), 2.42 (t, *J* = 8.0 Hz, 1H), 2.01 – 1.87 (m, 3H), 1.13 – 1.07 (m, 3H). ¹³C NMR (100 MHz, *d*₄-MeOH): δ (ppm) = 174.8, 173.8, 169.9, 156.2, 153.2, 150.0, 142.7, 140.9, 140.9, 134.8, 130.9, 128.4, 128.0, 124.8, 124.2, 123.0, 121.3, 121.1, 113.4, 71.5, 71.5, 71.4, 71.4, 71.3, 69.4, 68.2, 62.0, 62.0, 54.1, 54.0, 53.7, 53.2, 52.9, 44.3, 37.3, 32.9, 32.1, 32.0, 30.8, 30.7, 25.0, 24.8, 23.7, 20.2, 20.0, 19.8, 11.4, 11.4. IR (ATR): ν_{max} (cm⁻¹) = 3230 (br), 2878 (m), 1733 (m), 1669 (m), 1599 (m), 1543 (m), 1503 (m), 1465 (m), 1349 (m), 1300 (m), 1281 (m), 1251 (m), 1090 (vs), 950 (w), 852 (m), 780 (w). HRMS (ESI): calc. for C₆₁H₉₄N₈O₁₇⁺ [*M*+*H*]²⁺: 605.3363, found: 605.3363.



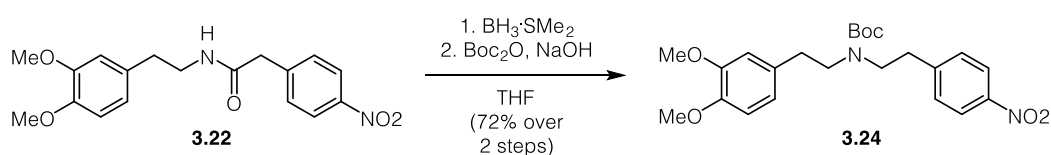
BGAP (3.18): DIPEA (0.02 mL, 115 μmol) was added to a solution of acid **3.16** (9.0 mg, 7.40 μmol), amine **3.17**⁹³ (4.0 mg, 14.9 μmol) and TBTU (5.2 mg, 16.0 μmol) in DMF (0.7 mL) and the resulting solution was stirred at room temperature overnight. Purification by reverse phase HPLC (MeCN:H₂O:HCOOH 10:90:0.1-100:0:0.1) gave BGAP (**3.18**) (5.0 mg, 3.40 μmol , 46%) as an orange solid.

Data for 3.18: ¹H NMR (600 MHz, *d*₄-MeOH): δ (ppm) = 8.50 (s, 2H), 7.88 (ddt, *J* = 9.1, 6.8, 2.5 Hz, 5H), 7.83 – 7.75 (m, 2H), 7.69 (s, 1H), 7.52 – 7.44 (m, 4H), 7.23 – 7.16 (m, 2H), 6.96 (t, *J* = 7.8 Hz, 1H), 6.66 – 6.59 (m, 2H), 5.53 (s, 2H), 4.44 (dd, *J* = 5.5, 4.5 Hz, 2H), 4.33 (s, 2H), 4.08 (s, 2H), 3.81 – 3.74 (m, 4H), 3.67 – 3.50 (m, 48H), 3.43 (dd, *J* = 10.3, 6.5 Hz, 2H), 3.13 (dddd, *J* = 24.0, 16.8, 9.8, 4.5 Hz, 6H), 3.00 (t, *J* = 7.3 Hz, 2H), 2.59 (td, *J* = 6.6, 5.9, 4.2 Hz, 4H), 2.38 – 2.28 (m, 1H), 1.86 – 1.79 (m, 2H), 1.05 (t, *J* = 7.3 Hz, 3H). ¹³C NMR (100 MHz, *d*₄-MeOH): δ (ppm) = 174.8, 174.3, 170.1, 170.0, 169.9, 161.7, 161.4, 156.1, 153.1, 150.1, 147.4, 142.7, 141.6, 140.1, 137.0, 135.4, 130.8, 129.7, 128.7, 127.9, 124.8, 124.4, 124.2, 123.3, 121.3, 121.2, 113.3, 71.4, 71.4, 71.3, 70.3, 68.5, 68.2, 61.3, 53.8, 53.1, 51.3, 44.3, 43.8, 37.4, 36.4, 32.8, 31.2, 25.2, 23.9, 22.6, 20.4, 11.5. IR (ATR): ν_{max} (cm⁻¹) = 2870 (s), 2361 (m), 1586 (vs), 1506 (w), 1465 (s), 1350 (m), 1280 (w), 1106 (s), 949 (w), 851 (w), 668 (w). HRMS (ESI): calc. for C₇₄H₁₀₆N₁₄O₁₇⁺ [*M*+2*H*]²⁺: 731.3916, found: 731.3925.



Amide 3.22: DCC (8.00 g, 38.62 mmol) was added portionwise to an ice cooled solution of 3,4-dimethoxyphenylamine (7.00 g, 38.62 mmol), 4-nitrophenylacetic acid (7.00 g, 38.62 mmol) and HOBT (7.58 g, 50.20 mmol) in MeCN (355 mL) and the reaction was stirred at room temperature for 20 h. The resulting precipitate was removed by filtration and the solvent was removed under reduced pressure. Purification of the resulting residue by flash column chromatography (MeOH : CH₂Cl₂ 4:96, R_f = 0.3) gave amide **3.22** (13.07 g, 37.95 mmol, 98%) as a white solid.

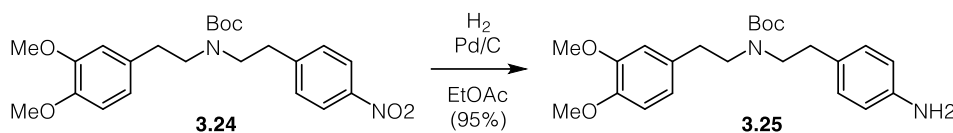
Data for 3.22: ¹H NMR (400 MHz, CDCl₃): δ (ppm) = 8.23 – 8.13 (m, 2H), 7.43 – 7.34 (m, 2H), 6.75 (d, *J* = 8.1 Hz, 1H), 6.66 (d, *J* = 2.0 Hz, 1H), 6.60 (dd, *J* = 8.1, 2.0 Hz, 1H), 5.47 (s, 1H), 3.87 (s, 3H), 3.85 (s, 3H), 3.61 (s, 2H), 3.52 (td, *J* = 6.9, 5.7 Hz, 2H), 2.75 (t, *J* = 6.9 Hz, 2H). ¹³C NMR (100 MHz, CDCl₃): δ (ppm) = 169.1, 149.2, 147.9, 147.3, 142.4, 130.9, 130.3, 124.1, 120.7, 111.8, 111.2, 56.0, 56.0, 43.5, 40.9, 35.1. IR (ATR): ν_{max} (cm⁻¹) = 3298 (m), 1655 (m), 1644 (m), 1611 (m), 1537 (vs), 1516 (s), 1464 (m), 1438 (w), 1418 (m), 1350 (vs), 1263 (s), 1231 (s), 1191 (m), 1155 (m), 1140 (s), 1107 (m), 1028 (s), 1013 (m), 945 (w), 872 (w), 858 (s), 848 (m), 807 (m), 765 (m), 708 (s). HRMS (ESI): calc. for C₁₈H₂₀N₂O₅⁺ [*M*]⁺: 344.1367, found: 344.1367.



Carbamate 3.24: BH₃·Me₂S (0.83 mL, 8.71 mmol) was added dropwise to an ice cooled solution of amide **3.22** (3.00 g, 8.71 mmol) in THF (380 mL) and the reaction was stirred at 65 °C for 3 h. The mixture was cooled to 0 °C and MeOH (25 mL) and an aqueous solution of NaOH (1M, 50 mL) were sequentially added. The reaction was stirred for 2 h at 65 °C and concentrated under reduced pressure. The resulting residue was portioned between EtOAc and H₂O and the organic phase was dried over MgSO₄ and concentrated under reduced pressure to give crude secondary amine **3.23** which was used in the next step without further purification.

Boc₂O (2.03 g, 9.28 mmol) was added to an ice cooled solution of crude amine **3.23** in THF (70 mL) and aqueous NaOH (1M, 22 mL) and the reaction was stirred at room temperature for 3.5 h. The mixture was extracted with EtOAc, the organic phase was washed with brine and dried over MgSO₄. Evaporation of the solvent under reduced pressure and purification of the resulting residue by flash column chromatography (EtOAc:hexanes 1:3, R_f = 0.3) gave carbamate **3.24** (2.65 g, 6.16 mmol, 72% over 2 steps) as a colourless solid. The product was received as mixture of rotamers.

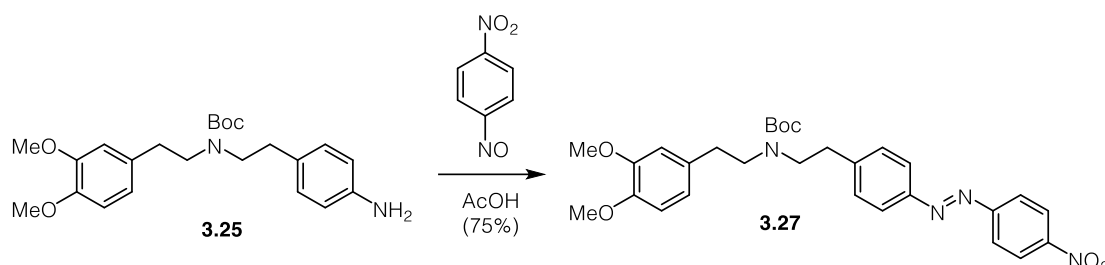
Data for 3.24: ¹H NMR (400 MHz, CDCl₃): δ (ppm) = 8.13 (d, *J* = 8.3 Hz, 2H), 7.37 – 7.25 (m, 2H), 6.75 – 6.61 (m, 2H), 3.85 (s, 3H), 3.84 (s, 3H), 3.31 (ddt, *J* = 29.7, 14.5, 7.3 Hz, 4H), 2.93 – 2.67 (m, 4H), 1.41 (s, 9H). ¹³C NMR (100 MHz, CDCl₃): δ (ppm) = 155.2, 155.1, 148.9, 147.6, 147.6, 147.2, 147.1, 146.6, 131.6, 129.7, 123.7, 120.69, 112.0, 111.9, 111.3, 79.7, 55.9, 55.8, 50.1, 49.6, 49.2, 48.9, 35.2, 34.9, 34.6, 34.1, 28.4. **IR (ATR):** ν_{max} (cm⁻¹) = 2973 (w), 2936 (w), 2835 (w), 1685 (s), 1599 (m), 1514 (vs), 1465 (m), 1452 (m), 1414 (s), 1365 (m), 1344 (vs), 1260 (s), 1235 (s), 1155 (vs), 1109 (m), 1028 (s), 940 (w), 894 (w), 855 (m), 806 (m), 764 (m), 748 (w), 699 (w). **HRMS (ESI):** calc. for C₁₈H₂₃N₂O₄⁺ [*M*-Boc+H]⁺: 331.1652, found: 331.1651.



Aniline 3.25: A suspension of carbamate **3.24** (2.44 g, 5.67 mmol) and Pd/C (250 mg, 10w%) in EtOAc (80 mL) was stirred under a H₂-atmosphere at room temperature overnight. Filtration of the reaction mixture over a pad of celite and evaporation of the solvent under reduced pressure gave aniline **3.25** (2.16 g, 5.39 mmol, 95%) as a slightly yellowish oil. The product was received as mixture of rotamers.

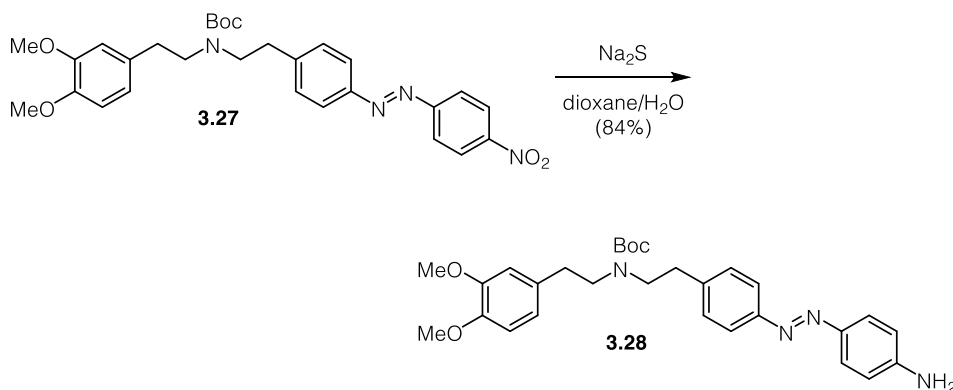
Data for 3.25: ¹H NMR (400 MHz, CDCl₃): δ (ppm) = 6.98 (d, *J* = 8.4 Hz, 1H), 6.94 – 6.87 (m, 1H), 6.78 (d, *J* = 8.1 Hz, 1H), 6.75 – 6.64 (m, 2H), 6.64 – 6.60 (m, 2H), 3.86 (s, 3H), 3.85 (s, 3H), 3.37 – 3.21 (m, 4H), 2.80 – 2.61 (m, 4H), 1.45 (s, 9H). ¹³C NMR (100 MHz, CDCl₃): δ (ppm) = 155.5, 148.9, 147.6, 147.5, 144.7, 144.6, 132.06, 129.8, 129.5, 129.4, 120.8, 115.4, 112.1, 111.3, 79.4, 56.0, 55.9, 50.2, 50.1, 49.9, 49.7, 35.0, 34.6, 34.3, 34.0, 28.6. **IR (ATR):** ν_{max} (cm⁻¹) = 3460 (w), 3368 (w), 2971 (w), 1684 (vs), 1625 (w), 1589 (w), 1516 (s), 1470 (m), 1460 (w), 1445 (w), 1365 (m), 1310 (w), 1286 (w), 1259 (s), 1232(s), 1164 (s), 1154 (s), 1138 (s), 1106 (w), 1024 (s), 969 (w), 939 (w), 917 (w),

879 (w), 856 (w), 817 (m), 778 (w), 763 (w). **HRMS (ESI)**: calc. for $C_{18}H_{25}N_2O_2^+$ [$M-Boc+H$] $^+$: 309.1911, found: 301.1910.



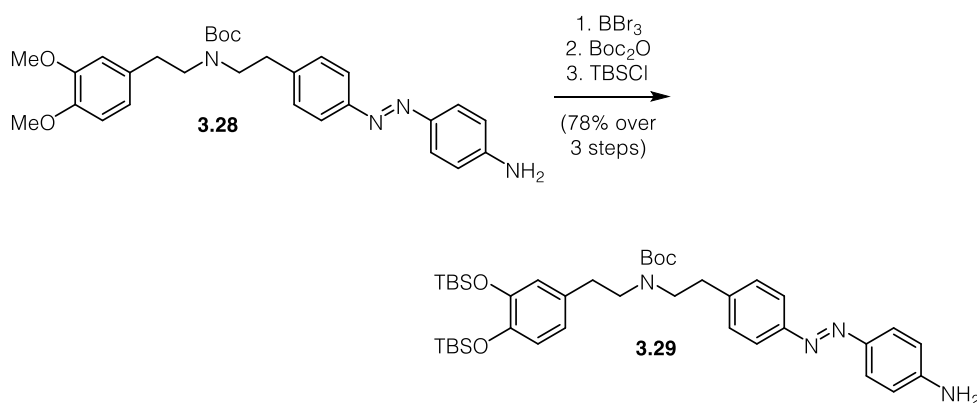
Azobenzene 3.27: A solution of aniline **3.25** (2.50 g, 6.24 mmol), 4-nitro(nitrosobenzene) (1.90 g, 12.48 mmol) and AcOH (20 mL) in CH_2Cl_2 (20 mL) and MeOH (30 mL) has been stirred at room temperature overnight and concentrated. The resulting residue was portioned between EtOAc and aqueous saturated $NaHCO_3$ and the organic phase was washed with brine and dried over $MgSO_4$. Evaporation of the solvent and purification by flash column chromatography (EtOAc:hexanes 20:80-30:70, $R_f = 0.3$) gave azobenzene **3.27** (2.50 g, 4.68 mmol, 75%) as a red solid. The product was received as mixture of rotamers.

Data for 3.27: 1H NMR (400 MHz, $CDCl_3$): δ (ppm) = 8.40 – 8.35 (m, 2H), 8.04 – 7.99 (m, 2H), 7.93 – 7.87 (m, 2H), 7.41 – 7.28 (m, 2H), 6.79 (d, $J = 8.0$ Hz, 1H), 6.75 – 6.62 (m, 2H), 3.86 (d, $J = 1.5$ Hz, 3H), 3.85 (s, 3H), 3.36 (s, 4H), 2.97 – 2.66 (m, 5H), 1.45 (s, 10H). ^{13}C NMR (100 MHz, $CDCl_3$): δ (ppm) = 155.9, 155.4, 151.2, 149.0, 148.7, 147.6, 144.8, 144.6, 131.9, 130.0, 124.9, 123.8, 123.5, 120.8, 112.1, 111.4, 79.7, 56.1, 56.0, 50.3, 50.3, 49.6, 49.4, 35.5, 35.0, 34.9, 34.3, 28.6. **IR (ATR)**: ν_{max} (cm^{-1}) = 3006 (w), 28975 (w), 2934 (w), 1682 (s), 1590 (m), 1514 (s), 1456 (m), 1445 (s), 1413 (s), 1363 (m), 1343 (s), 1308 (m), 1260 (m), 1236 (vs), 1199 (w), 1152 (vs), 1143 (s), 111 (s) 1027 (s), 934 (m), 878 (w), 857 (m), 851 (m), 823 (w), 798 (m), 755 (s), 728 (w), 686 (m). **HRMS (ESI)**: calc. for $C_{29}H_{33}N_4O_6^-$ [$M-H$] $^-$: 533.2406, found: 533.2418.



Amine 3.28: $\text{Na}_2\text{S}\cdot x\text{H}_2\text{O}$ (812 mg, 8.45 mmol) was added to a suspension of azobenzene **3.27** (2.26 g, 4.23 mmol) in dioxane (30 mL) and H_2O (30 mL) and the reaction was stirred at 100 °C for 4 h. After cooling to room temperature, the reaction was extracted with EtOAc and the combined organic layers were washed with aqueous NaOH (1M), aqueous $\text{Na}_2\text{S}_2\text{O}_3$ (20%) and brine and dried over MgSO_4 . Evaporation of the solvent under reduced pressure and purification of the resulting residue by flash column chromatography (MeOH: CH_2Cl_2 0:100-2:98) gave amine **3.28** (1.80 g, 3.57 mmol, 84%) as a red solid. The product was received as mixture of rotamers.

Data for 3.28: $^1\text{H NMR}$ (400 MHz, CDCl_3): δ (ppm) = 7.87 – 7.70 (m, 4H), 7.30 (d, J = 8.3 Hz, 3H), 6.83 – 6.56 (m, 5H), 4.05 (s, 2H), 3.91 – 3.82 (m, 6H), 3.47 – 3.14 (m, 4H), 2.97 – 2.58 (m, 4H), 1.46 (s, 9H). $^{13}\text{C NMR}$ (100 MHz, CDCl_3): δ (ppm) = 155.3, 151.6, 149.5, 148.8, 147.5, 145.5, 141.6, 141.4, 131.8, 129.5, 125.0, 122.5, 120.7, 114.6, 112.0, 111.2, 79.5, 77.4, 77.0, 76.7, 55.9, 55.8, 50.2, 49.7, 49.7, 49.5, 35.3, 34.6, 34.6, 34.2, 28.5. **IR (ATR):** ν_{max} (cm^{-1}) = 3448 (w), 3358 (w), 3236 (w), 2970 (w), 2934 (w), 1674 (s), 1629 (m), 1599 (vs), 1507 (s), 1464 (m), 1415 (s), 1365 (m), 1297 (m), 1260 (m), 1234 (s), 1154 (s), 1137 (vs), 1096 (m), 1026 (s), 940 (w), 892 (w), 838 (m), 807 (w), 764 (m). **HRMS (ESI):** calc. for $\text{C}_{29}\text{H}_{37}\text{N}_4\text{O}_4^+$ [$M+H$] $^+$: 505.2809, found: 505.2804.



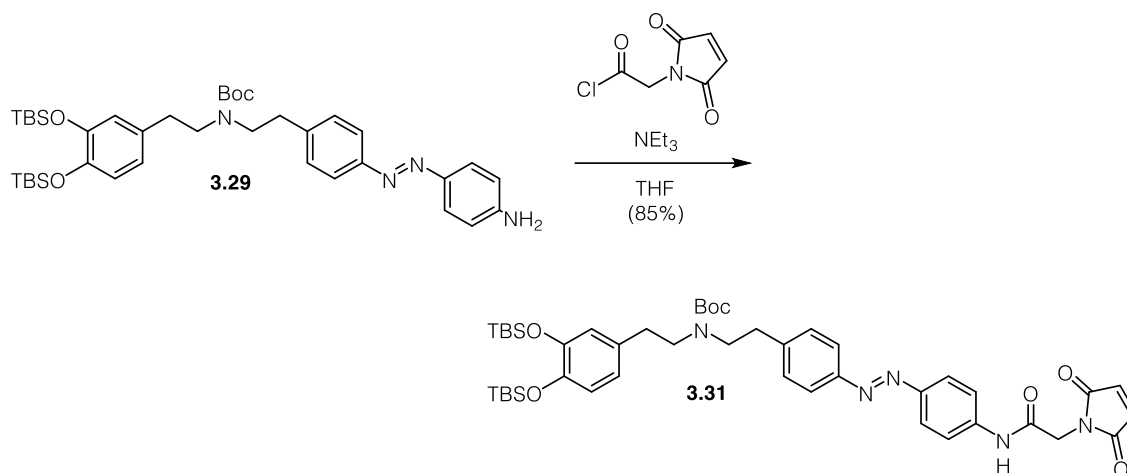
Silyl ether 3.29: BBr_3 (1 M in CH_2Cl_2 , 15.2 mL, 15.2 mmol) was added to a solution of amine **3.28** (1.53 g, 3.03 mmol) in CH_2Cl_2 (30 mL) at -78°C and the reaction was stirred for 1 h at that temperature and for 2 h at room temperature. The reaction was quenched by the slow addition of MeOH (3 mL) and concentrated under reduced pressure.

The resulting residue was redissolved THF (20 mL) and aqueous saturated NaHCO_3 (10 mL) and Boc_2O (728 mg, 3.34 mmol) was added. The reaction was stirred for 2 h at room temperature and extracted with EtOAc. The combined organic layers were washed with brine, dried over MgSO_4 and concentrated under reduced pressure.

The resulting residue was redissolved in MeCN (30 mL) and imidazole (727 mg, 10.79 mmol) and TBSCl (1.45 g, 10.0 mmol) were added sequentially. The reaction was stirred for 5 h at room temperature and diluted with aqueous saturated NH_4Cl (30 mL). The mixture was extracted with EtOAc and the combined organic layers were washed with brine, dried over MgSO_4 and concentrated under reduced pressure. Purification of the resulting residue by flash column chromatography (EtOAc:hexanes 1:4) gave silyl ether **3.29** (1.66 g, 2.35 mmol, 78%) as a red solid. The product was received as mixture of rotamers.

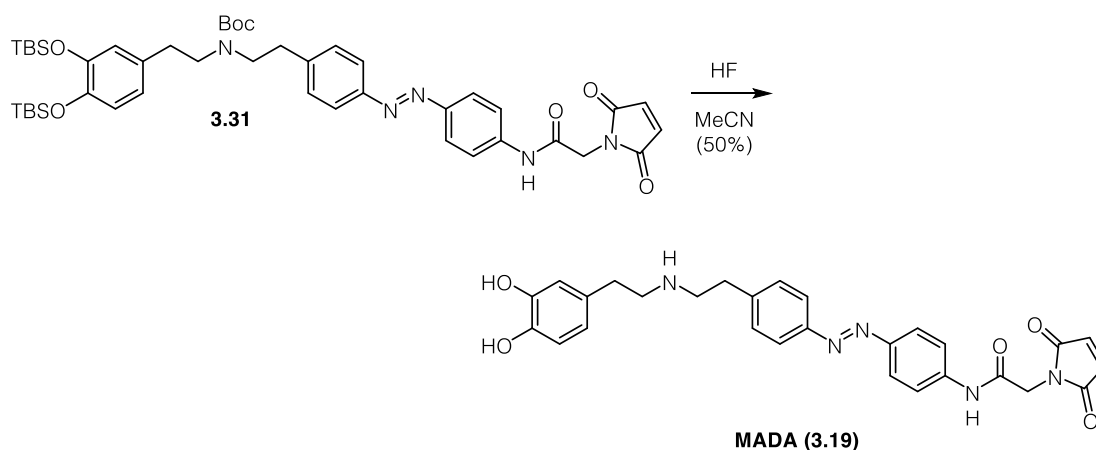
Data for 3.29: $^1\text{H NMR}$ (400 MHz, CDCl_3): δ (ppm) = 7.83 – 7.72 (m, 4H), 7.28 (d, J = 7.8 Hz, 1H), 7.21 (d, J = 7.6 Hz, 1H), 6.77 – 6.70 (m, 3H), 6.65 – 6.55 (m, 2H), 4.04 (s, 2H), 3.28 (dd, J = 47.0, 8.6 Hz, 4H), 2.89 – 2.59 (m, 4H), 1.50 – 1.45 (m, 9H), 0.98 (s, 9H), 0.96 (s, 9H), 0.17 (s, 6H), 0.16 (s, 6H). $^{13}\text{C NMR}$ (100 MHz, CDCl_3): δ (ppm) = 155.4, 151.6, 149.5, 146.7, 145.7, 145.4, 141.7, 132.8, 132.4, 129.6, 125.1, 122.6, 121.9, 121.8, 121.1, 114.8, 79.5, 77.2, 50.5, 50.1, 49.8, 49.8, 35.3, 34.8, 34.7, 34.1, 28.6, 28.5, 26.1, 26.0, 18.6, 18.6, -3.9 , -4.0 . **IR (ATR):** ν_{max} (cm^{-1}) = 3358 (w), 2956 (w), 2929 (w), 2858 (w), 1678 (m), 1622 (w), 1600 (s), 1578 (w), 1507 (s), 1472 (m), 1418 (m), 1391 (w), 1365 (m), 1296 (s), 1252 (s), 1156 (s), 1140 (s), 1096 (w), 1013 (w), 979 (w), 906

(m), 836 (vs), 780 (s), 733 (m). **HRMS (ESI)**: calc. for $C_{39}H_{61}NO_4Si_2^+$ $[M+H]^+$: 705.4226, found: 705.4222.



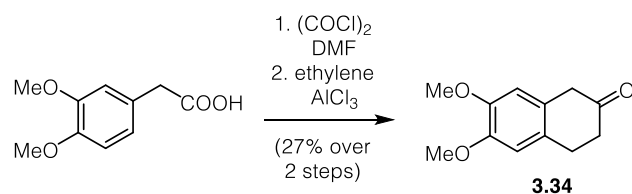
Amide 3.31: A solution of acid chloride **3.30**⁹⁴ (172 mg, 0.992 mmol) in THF (2 mL) was added dropwise to an ice cooled solution of silyl ether **3.29** (350 mg, 0.496 mmol) and NEt_3 (0.14 mL, 0.992 mmol) in THF (7 mL) and the reaction was stirred for 10 min at 0 °C and for 2 h at room temperature. H_2O (10 mL) was added and the reaction was extracted with EtOAc. The combined organic layers were washed with brine, dried over $MgSO_4$ and concentrated under reduced pressure. Purification of the resulting residue by flash column chromatography (EtOAc:hexanes 1:2, $R_f=0.2$) gave amide **3.31** (353 mg, 0.419 mmol, 85%) as a red solid. The product was received as mixture of rotamers.

Data for 3.31: 1H NMR (400 MHz, $CDCl_3$): δ (ppm) = 8.28 – 7.97 (m, 1H), 7.82 – 7.54 (m, 4H), 7.48 (d, $J = 8.4$ Hz, 2H), 7.10 (dd, $J = 21.4, 8.0$ Hz, 2H), 6.64 (s, 2H), 6.57 (d, $J = 8.1$ Hz, 1H), 6.50 – 6.38 (m, 2H), 4.22 (s, 2H), 3.32 – 2.99 (m, 4H), 2.80 – 2.36 (m, 4H), 1.31 (d, $J = 11.3$ Hz, 9H), 0.81 (s, 9H), 0.80 (s, 9H). ^{13}C NMR (100 MHz, $CDCl_3$): δ (ppm) = 170.3, 164.5, 155.5, 151.3, 149.4, 146.8, 145.5, 142.7, 139.7, 134.7, 134.6, 132.7, 132.3, 129.7, 124.0, 123.1, 121.9, 121.8, 121.1, 120.1, 79.7, 77.5, 77.2, 76.8, 50.4, 49.9, 49.7, 49.5, 41.3, 35.2, 34.8, 34.7, 34.1, 28.6, 26.1, 18.6, 18.5, –3.9, –4.0. **IR (ATR)**: ν_{max} (cm^{-1}) = 2956 (w), 2929 (w), 2858 (w), 1704 (s), 1601 (m), 1538 (m), 1510 (s), 1472 (m), 1417 (s), 1390 (w), 1364 (s), 1299 (s), 1250 (s), 1154 (s), 1126 (w), 1110 (w), 1096 (w), 1011 (w), 980 (w), 901 (m), 833 (vs), 779 (s), 696 (s). **HRMS (ESI)**: calc. for $C_{45}H_{64}N_5O_7Si_2^+$ $[M+H]^+$: 842.4339, found: 842.4331.



MADA (3.19): HF (60% in H₂O, 0.15 mL) was added to an ice cooled solution of amide **3.31** (140 mg, 0.166 mmol) in MeCN (1 mL) and the reaction was stirred for 6 h at room temperature. The resulting precipitate was collected and washed with MeCN to give **MADA (3.19)** as a red solid (43 mg, 0.083 mmol, 50%).

Data for 3.19: ¹H NMR (400 MHz, d₄-MeOH): δ (ppm) = 10.66 (s, 1H), 8.49 (s, 2H), 7.91 – 7.83 (m, 4H), 7.81 – 7.73 (m, 2H), 7.48 (d, *J* = 8.5 Hz, 2H), 7.16 (s, 2H), 6.68 (d, *J* = 7.9 Hz, 1H), 6.63 (d, *J* = 2.1 Hz, 1H), 6.50 (dd, *J* = 8.0, 2.1 Hz, 1H), 4.33 (s, 2H), 3.25 (dd, *J* = 9.7, 5.4 Hz, 2H), 3.17 – 3.08 (m, 2H), 3.01 (dd, *J* = 9.5, 6.5 Hz, 2H), 2.74 (dd, *J* = 9.5, 6.7 Hz, 2H). ¹³C NMR (100 MHz, d₄-MeOH): δ (ppm) = 170.7, 165.5, 151.0, 147.8, 145.4, 144.2, 141.5, 140.5, 135.1, 129.9, 127.6, 123.8, 122.7, 119.5, 119.4, 116.1, 115.7, 79.2, 48.3, 47.5, 40.5, 31.5, 31.2. IR (ATR): ν_{max} (cm⁻¹) = 3162 (br), 2361 (w), 1705 (s), 1602 (m), 1547 (m), 1434 (m), 1366 (w), 1322 (w), 1302 (w), 1260 (w), 1200 (w), 1156 (w), 1119 (w), 906 (w), 846 (m), 710 (s), 694 (s). HRMS (ESI): calc. for C₂₈H₂₈N₅O₅⁺ [*M+H*]⁺: 514.2085, found: 514.2079.

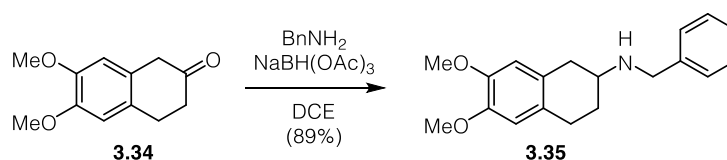


Tetralone 3.34: Oxalylchloride (2 M in CH₂Cl₂, 30.6 mL, 61.2 mmol) and DMF (0.2 mL) were added to an ice cooled solution of 3,4-dimethoxyphenylacetic acid (10.0 g, 50.97 mmol) in CH₂Cl₂ (150 mL) and the reaction was stirred for 10 min at that temperature and for 3 h at room temperature. Removal of the solvent under reduced

pressure gave crude acid chloride which was used in the next step without further purification.

A solution of crude acid chloride in CH_2Cl_2 (50 mL) was added slowly to an ice cooled suspension of AlCl_3 (27.2 g, 200 mmol) in CH_2Cl_2 (600 mL) and the reaction was purged with ethylene. The mixture was stirred for 4 h under an ethylene atmosphere at 0°C before it was diluted with H_2O (160 mL) and extracted with CH_2Cl_2 . The combined organic layers were washed with aqueous 1M HCl, aqueous saturated NaHCO_3 and brine and dried over MgSO_4 . Evaporation of the solvent under reduced pressure and purification of the resulting residue by flash column chromatography (EtOAc:hexanes 3:7) gave tetralone **3.34** (2.87 g, 13.92 mmol, 27% over 2 steps) as a brownish solid.

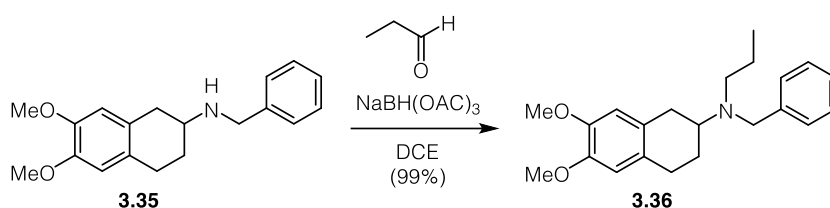
Data for 3.34: R_f : 0.1 (hexanes:EtOAc 7:3). $^1\text{H NMR}$ (400 MHz, CDCl_3): δ (ppm) = 6.74 (s, 1H), 6.62 (s, 1H), 3.88 (s, 3H), 3.86 (s, 3H), 3.51 (s, 2H), 3.00 (t, $J = 6.7$ Hz, 2H), 2.55 (dd, $J = 7.2, 6.2$ Hz, 2H). $^{13}\text{C NMR}$ (100 MHz, CDCl_3): δ (ppm) = 211.0, 148.0, 147.8, 128.6, 125.1, 111.4, 111.1, 56.12, 56.1, 44.4, 38.7, 28.3. **IR (ATR):** ν_{max} (cm^{-1}) = 1712 (s), 1610 (w), 1514 (vs), 1465 (m), 1416 (w), 1338 (m), 1291 (w), 1270 (m), 1247 (s), 1218 (m), 1193 (m), 1110 (s), 1027 (w), 1005 (w), 966 (w), 882 (w), 844 (w), 755 (w). **HRMS (EI):** calc. for $\text{C}_{12}\text{H}_{14}\text{O}_3^+$ [M] $^+$: 206.0937, found: 206.0934.



Secondary amine 3.35: $\text{NaBH}(\text{OAc})_3$ (5.19 g, 24.4 mmol) was added portionwise to a solution of tetralone **3.34** (2.80 g, 13.58 mmol) and benzylamine (1.92 mL, 17.7 mmol) in DCE (45 mL) and the reaction was stirred for 4 h at room temperature and concentrated. The resulting residue was portioned between aqueous saturated NaHCO_3 and EtOAc. The organic layer was washed with brine, dried over MgSO_4 and concentrated under reduced pressure. Purification of the resulting residue by flash column chromatography (MeOH: CH_2Cl_2 3:97) gave secondary amine **3.35** (3.60 g, 12.1 mmol, 89%) as a brownish wax.

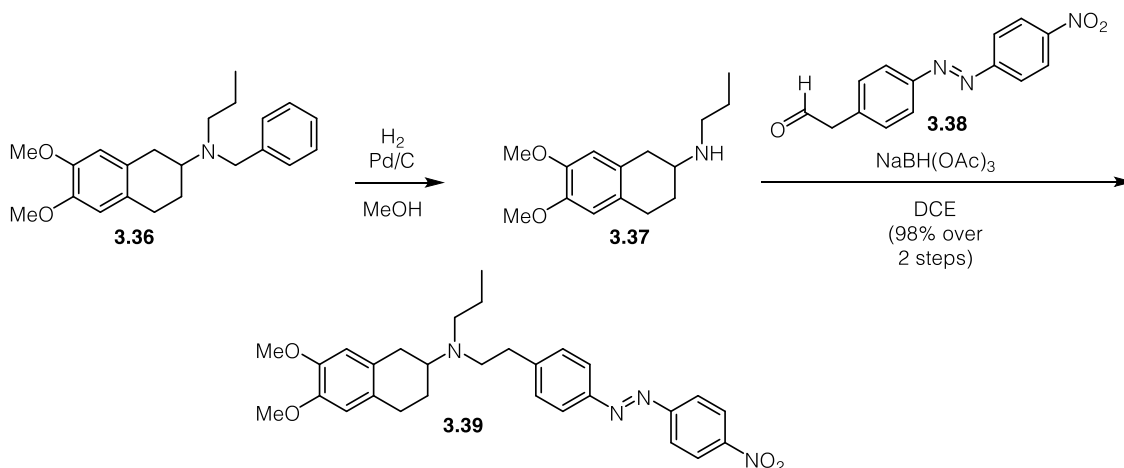
Data for 3.35: $^1\text{H NMR}$ (400 MHz, CDCl_3): δ (ppm) = 7.37 – 7.31 (m, 4H), 7.26 (s, 1H), 6.58 (s, 1H), 6.57 (s, 1H), 3.91 (s, 2H), 3.84 (s, 3H), 3.84 (s, 3H), 3.03 – 2.92 (m, 2H), 2.78 (pd, $J = 11.2, 4.8$ Hz, 2H), 2.66 – 2.54 (m, 1H), 2.12 – 2.02 (m, 1H), 1.65 (dtd, $J =$

12.7, 10.0, 6.0 Hz, 2H). **¹³C NMR (100 MHz, CDCl₃):** δ (ppm) = 147.2, 147.2, 140.7, 128.6, 128.3, 128.1, 127.1, 127.0, 112.1, 111.5, 56.0, 56.0, 53.0, 51.3, 36.4, 29.7, 27.7. **IR (ATR):** ν_{max} (cm⁻¹) = 29.15 (m), 2833 (w), 1609 (w), 1516 (vs), 1464 (m), 1452 (m), 1409 (w), 1353 (w), 1327 (w), 1289 (w), 1265 (m), 1248 (s), 1223 (s), 1113 (s), 1018 (w), 971 (w), 907 (w), 849 (w), 737 (m), 699 (m). **HRMS (ESI):** calc. for C₁₉H₂₄NO₂⁺ [*M+H*]⁺: 298.1802, found: 298.1800.



Tertiary amine 3.36: NaBH(OAc)₃ (4.51 g, 21.3 mmol) was added portionwise to a solution of secondary amine **3.35** (3.52 g, 11.8 mmol) and propionaldehyde (1.11 mL, 15.4 mmol) in DCE (70 mL) and the reaction was stirred at room temperature overnight and concentrated under reduced pressure. The organic layer was washed with brine, dried over MgSO₄ and concentrated under reduced pressure. Purification of the resulting residue by flash column chromatography (MeOH:CH₂Cl₂ 2:98) gave tertiary amine **3.36** (3.98 g, 11.7 mmol, 99%) as a brownish wax.

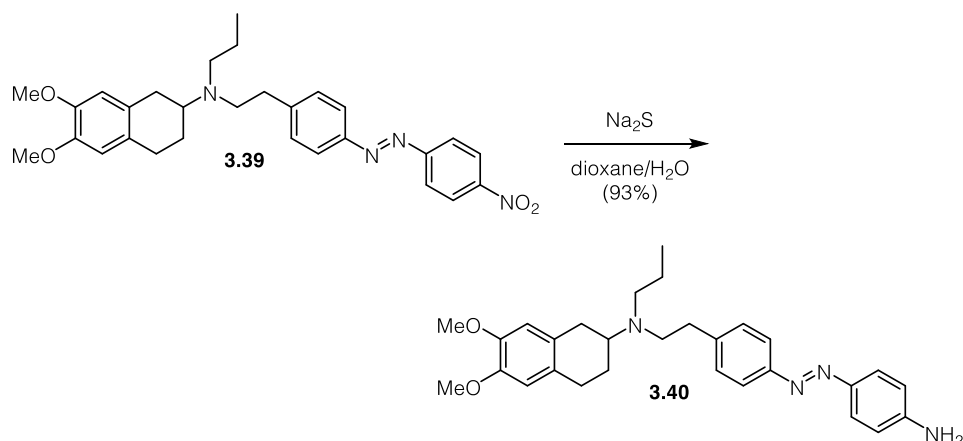
Data for 3.36: **¹H NMR (400 MHz, CDCl₃):** δ (ppm) = 7.39 (d, *J* = 7.5 Hz, 2H), 7.30 (t, *J* = 7.4 Hz, 2H), 7.21 (t, *J* = 7.2 Hz, 1H), 6.58 (s, 1H), 6.55 (s, 1H), 3.84 (s, 3H), 3.83 (s, 3H), 3.72 (q, *J* = 9.9, 8.7 Hz, 2H), 2.96 (dd, *J* = 14.2, 5.7 Hz, 1H), 2.87 – 2.70 (m, 4H), 2.52 (t, *J* = 7.2 Hz, 2H), 2.09 – 2.03 (m, 1H), 1.64 (tt, *J* = 12.0, 6.1 Hz, 1H), 1.46 (h, *J* = 7.3 Hz, 2H), 0.87 (t, *J* = 7.3 Hz, 3H). **¹³C NMR (100 MHz, CDCl₃):** δ (ppm) = 147.1, 141.6, 128.5, 128.4, 128.2, 126.6, 112.2, 111.4, 56.1, 56.0, 56.0, 54.6, 52.1, 43.6, 31.7, 29.8, 25.6, 21.8, 12.0. **IR (ATR):** ν_{max} (cm⁻¹) = 2931 (m), 2832 (w), 1609 (w), 1515 (vs), 1494 (w), 1463 (m), 1452 (m), 1408 (w), 1355 (w), 1333 (w), 1264 (s), 1245 (s), 1226 (s), 1209 (s), 1114 (s), 1070 (w), 1018 (m), 972 (w), 936 (w), 906 (w), 847 (m), 824 (w), 735 (m), 697 (m). **HRMS (ESI):** calc. for C₂₂H₃₀NO₂⁺ [*M+H*]⁺: 340.2271, found: 230.2270.



Azobenzene 3.39: Pd/C (340 mg) was added to a solution of tertiary amine (3.40 g, 10.0 mmol) in MeOH (30 mL) and the reaction was purged with H₂. The mixture was stirred at room temperature under H₂ overnight, filtered over a pad of celite and concentrated under reduced pressure to give crude secondary amine **3.37** that was used in the next step without further purification.

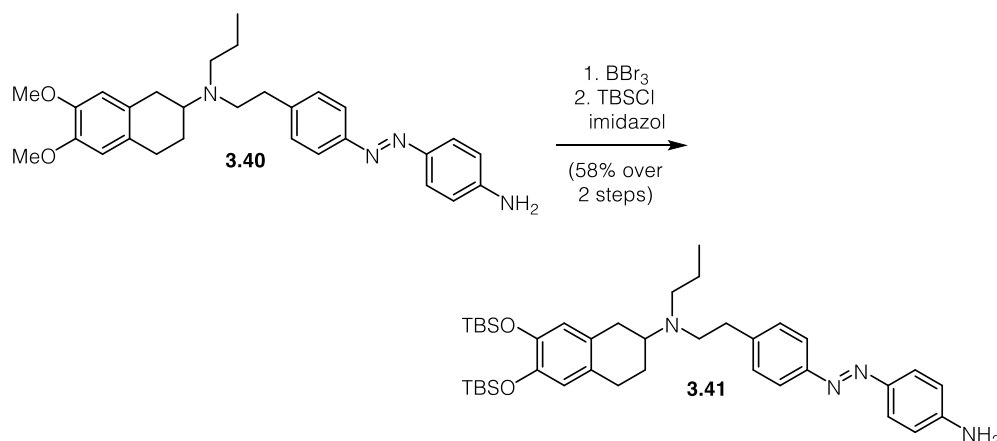
NaBH(OAc)₃ (3.98 g, 18.8 mmol) was added portionwise to a stirred solution of secondary amine **3.37** and freshly prepared homobenzylidene aldehyde **3.38** (2.56 g, 9.50 mmol) in DCE (150 mL) and the reaction was stirred at room temperature overnight and concentrated under reduced pressure. The organic layer was washed with brine, dried over MgSO₄ and concentrated under reduced pressure. Purification of the resulting residue by flash column chromatography (MeOH:CH₂Cl₂ 2:98) gave azobenzene **3.39** (4.94 g, 9.82 mmol, 98% over 2 steps) as a brownish wax.

Data for 3.39: ¹H NMR (400 MHz, CDCl₃): δ (ppm) = 8.38 – 8.31 (m, 2H), 7.99 (d, *J* = 8.8 Hz, 2H), 7.90 (d, *J* = 8.1 Hz, 2H), 7.39 (d, *J* = 8.1 Hz, 2H), 6.57 (d, *J* = 1.6 Hz, 2H), 3.83 (d, *J* = 1.5 Hz, 6H), 3.00 (td, *J* = 11.6, 5.1, 2.5 Hz, 1H), 2.89 – 2.64 (m, 8H), 2.57 (dd, *J* = 8.5, 6.3 Hz, 2H), 1.99 (dq, *J* = 13.7, 3.4, 3.0 Hz, 1H), 1.48 (p, *J* = 7.4 Hz, 3H), 0.90 (t, *J* = 7.3 Hz, 3H). ¹³C NMR (100 MHz, CDCl₃): δ (ppm) = 155.8, 150.9, 148.5, 147.1, 147.1, 146.5, 129.9, 128.2, 128.1, 124.7, 123.5, 123.3, 112.1, 111.4, 77.4, 57.1, 55.9, 52.7, 52.5, 36.2, 31.7, 29.6, 26.3, 22.3, 12.0. **HRMS (ESI):** calc. for C₂₉H₃₅N₄O₄⁺ [*M+H*]⁺: 503.2653. found: 503.2657.



Aniline 3.40: $\text{Na}_2\text{S}\cdot x\text{H}_2\text{O}$ (1.28 g, 13.3 mmol) was added to a suspension of azobenzene **3.39** (3.35 g, 6.67 mmol) in dioxane (47 mL) and H_2O (47 mL) and the reaction was stirred at 100 °C for 4 h. After cooling to room temperature, the reaction was extracted with EtOAc and the combined organic layers were washed with aqueous NaOH (1 M), aqueous $\text{Na}_2\text{S}_2\text{O}_3$ (20%) and brine and dried over MgSO_4 . Evaporation of the solvent under reduced pressure and purification of the resulting residue by flash column chromatography (MeOH: CH_2Cl_2 0:100-3:97) gave aniline **3.40** (2.94 g, 6.22 mmol, 93%) as a red solid.

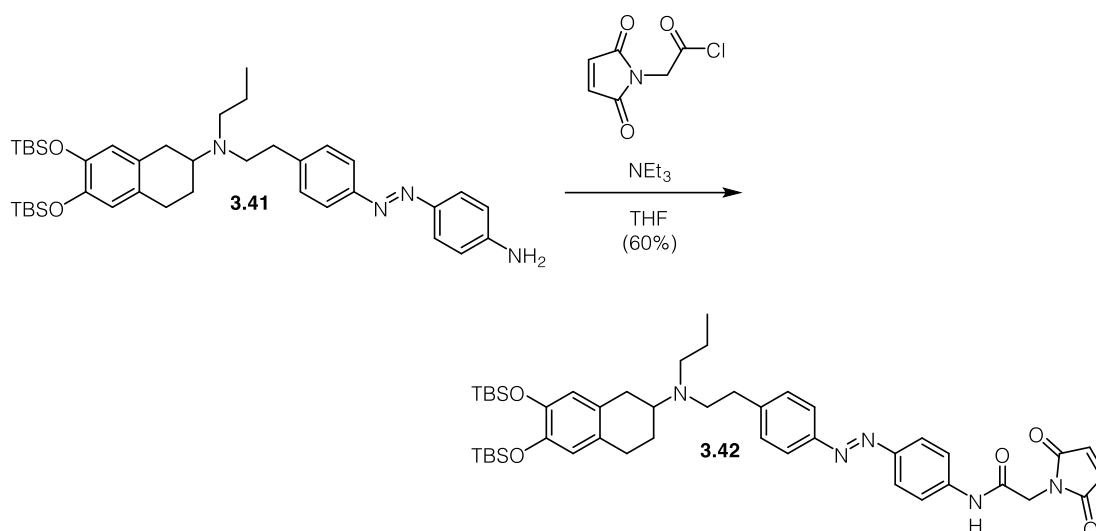
Data for 3.40: $^1\text{H NMR}$ (400 MHz, CDCl_3): δ (ppm) = 7.84 – 7.72 (m, 4H), 7.36 – 7.28 (m, 2H), 6.77 – 6.70 (m, 2H), 6.57 (s, 2H), 4.04 (s, 2H), 3.83 (s, 6H), 3.06 – 2.96 (m, 1H), 2.85 – 2.64 (m, 8H), 2.57 (dd, $J = 8.5, 6.6$ Hz, 2H), 2.06 – 1.96 (m, 1H), 1.56 (dq, $J = 40.3, 7.1$ Hz, 3H), 0.90 (t, $J = 7.3$ Hz, 3H). $^{13}\text{C NMR}$ (100 MHz, CDCl_3): δ (ppm) = 151.4, 149.5, 147.1, 145.7, 143.3, 129.5, 128.2, 125.1, 122.4, 114.8, 112.2, 111.4, 67.2, 57.2, 56.0, 52.8, 36.0, 31.8, 31.1, 29.7, 26.3, 22.3, 12.1. **IR (ATR):** ν_{max} (cm^{-1}) = 3370 (m), 2933 (m), 2834 (w), 1621 (m), 1599 (vs), 1515 (s), 1506 (s), 1463 (m), 1429 (w), 1406 (w), 1297 (w), 1264 (m), 1244 (m), 1227 (s), 1153 (m), 1139 (s), 1113 (s), 1076 (w), 1015 (w), 972 (w), 909 (m), 838 (s), 729 (s). **HRMS (ESI):** calc. for $\text{C}_{29}\text{H}_{37}\text{N}_4\text{O}_2^+$ [$M+H$] $^+$: 473.2911, found: 473.2907.



Silyl ether 3.41: BBr_3 (1 M in CH_2Cl_2 , 5.30 mL, 5.30 mmol) was added slowly to a stirred solution of aniline **3.40** (500 mg, 1.058 mmol) in CH_2Cl_2 (30 mL) at $-78\text{ }^\circ\text{C}$ and the resulting solution was stirred for 1 h at that temperature and for 4 h at room temperature. The reaction was quenched with MeOH (5 mL), diluted with EtOAc and washed with aqueous saturated NaHCO_3 and brine. The organic phase was dried over Na_2SO_4 and concentrated under reduced pressure to give crude catechol which was used in the next step without further purification.

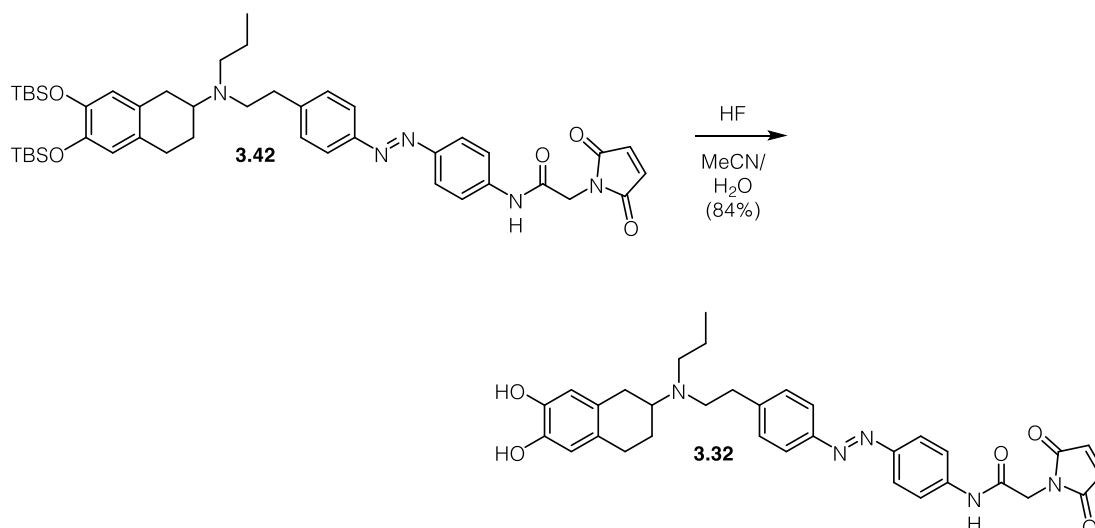
TBSCl (1.59 g, 10.6 mmol) was added to an ice cooled solution of crude catechol and imidazole (1.20 g, 17.7 mmol) in DMF (20 mL) and the reaction was stirred at room temperature overnight. The reaction was hydrolysed with H_2O (30 mL) and extracted with EtOAc. The combined organic phases were washed with brine, dried over MgSO_4 and concentrated under reduced pressure. Purification of the resulting residue by flash column chromatography (EtOAc:hexanes 1:3) gave silyl ether **3.41** (823 mg, 1.22 mmol, 58% over 2 steps) as a red solid.

Data for 3.41: $^1\text{H NMR}$ (400 MHz, CDCl_3): δ (ppm) = 7.79 (t, J = 8.8 Hz, 4H), 7.31 (d, J = 8.0 Hz, 2H), 6.74 (d, J = 8.4 Hz, 2H), 6.51 (d, J = 2.6 Hz, 2H), 4.03 (s, 2H), 2.83 – 2.53 (m, 10H), 1.95 (d, J = 7.7 Hz, 1H), 1.63 – 1.45 (m, 6H), 0.98 (s, 18H), 0.90 (t, J = 7.2 Hz, 3H), 0.18 (s, 9H). $^{13}\text{C NMR}$ (100 MHz, CDCl_3): δ (ppm) = 151.5, 149.5, 145.7, 144.7, 143.3, 129.7, 129.6, 129.1, 125.1, 124.6, 122.5, 121.5, 120.7, 114.8, 57.4, 52.9, 36.2, 31.5, 29.4, 26.4, 26.1, 22.4, 18.6, 12.1, -3.9 , -3.97 , -3.98 . **IR (ATR):** ν_{max} (cm^{-1}) = 2929 (m), 2858 (m), 2360 (w), 1621 (w), 1600 (s), 1509 (s), 1472 (w), 1411 (w), 1313 (w), 1254 (m), 1140 (m), 930 (m), 838 (s), 782 (m). **HRMS (ESI):** calc. for $\text{C}_{39}\text{H}_{61}\text{N}_4\text{O}_2\text{Si}_2^+$ [$M+H$] $^+$: 673.4328, found: 673.4323.



Maleimide 3.42: A solution of acid chloride **3.30**⁹⁴ (77.4 mg, 0.446 mmol) in THF (2 mL) was added slowly to an ice cooled solution of silyl ether **3.41** (200 mg, 0.297 mmol) and NEt₃ (52.0 μ L, 0.370 mmol) in THF (3 mL) and the reaction was stirred at room temperature for 2 h before it was hydrolysed with H₂O (4 mL) and extracted with EtOAc. The combined organic phases were washed with brine, dried over MgSO₄ and concentrated under reduced pressure. Purification of the resulting residue by flash column chromatography (MeOH:CH₂Cl₂ 3:97) gave maleimide **3.42** (145 mg, 0.179 mmol, 60%) as a red solid.

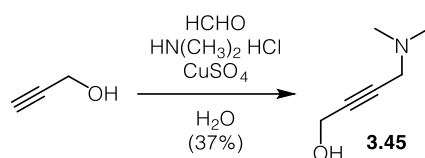
Data for 3.42: ¹H NMR (400 MHz, CDCl₃): δ (ppm) = 7.83 (dd, J = 21.8, 8.3 Hz, 4H), 7.64 (d, J = 8.5 Hz, 2H), 7.32 (d, J = 8.1 Hz, 2H), 6.77 (s, 2H), 6.52 (d, J = 2.1 Hz, 2H), 4.37 (s, 2H), 2.99 (p, J = 7.4, 5.6 Hz, 1H), 2.82 (s, 4H), 2.75 – 2.62 (m, 4H), 2.56 (dd, J = 8.8, 6.2 Hz, 2H), 1.97 (d, J = 12.3 Hz, 1H), 1.65 – 1.44 (m, 3H), 0.98 (s, 19H), 0.89 (t, J = 7.3 Hz, 3H), 0.18 (s, 12H). ¹³C NMR (100 MHz, CDCl₃): δ (ppm) = 172.8, 172.4, 163.8, 151.2, 149.2, 144.9, 140.3, 137.3, 130.5, 129.6, 128.8, 124.0, 123.0, 121.4, 120.7, 120.1, 117.9, 57.7, 54.7, 52.74, 52.65, 42.2, 36.9, 31.1, 29.8, 29.2, 26.1, 21.9, 18.6, 12.0, –3.95, –3.98. IR (ATR): ν_{\max} (cm⁻¹) = 2955 (w), 2929 (m), 2857 (w), 1716 (s), 1598 (m), 1551 (w), 1512 (m), 1472 (w), 1463 (w), 1414 (m), 1362 (w), 1317 (m), 1253 (s), 1228 (m), 1201 (w), 1170 (m), 1114 (w), 1083 (w), 1048 (w), 1011 (w), 926 (m), 909 (s), 837 (vs), 780 (s), 732 (s), 697 (w), 661 (w). HRMS (ESI): calc. for C₄₅H₆₂N₅O₂Si₂⁻ [$M-H$]⁻: 808.4295; found: 808.4310.



Catechol 3.32: HF (48% in H₂O, 1 mL) was added slowly to an ice cooled solution of maleimide **3.42** (100 mg, 0.123 mmol) in MeCN (1 mL) and the reaction was stirred for 30 min at that temperature and for 3 h at room temperature. The reaction was cooled to 0 °C, diluted with EtOAc and carefully washed with NaHCO₃. The organic phase was dried over Na₂SO₄ and concentrated under reduced pressure to give catechol **3.32** (60 mg, 0.103 mmol, 84%) as a red solid.

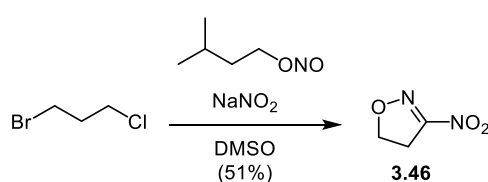
Data for 3.32: ¹H NMR (400 MHz, d₄-MeOH): δ (ppm) = 7.77 – 7.68 (m, 4H), 7.60 (d, *J* = 8.5 Hz, 2H), 7.37 (d, *J* = 8.0 Hz, 2H), 6.79 (s, 2H), 6.46 (d, *J* = 3.6 Hz, 1H), 6.41 (s, 1H), 4.27 (s, 2H), 3.63 (dt, *J* = 13.6, 6.5 Hz, 1H), 3.37 (ddq, *J* = 39.0, 12.8, 6.0, 5.5 Hz, 2H), 3.26 – 2.98 (m, 5H), 2.96 – 2.77 (m, 2H), 2.69 (dq, *J* = 8.5, 4.6 Hz, 2H), 2.22 – 2.07 (m, 1H), 1.73 (ttt, *J* = 19.6, 13.2, 12.6, 7.7 Hz, 3H), 0.95 (t, *J* = 7.3 Hz, 3H). ¹³C NMR (100 MHz, d₄-MeOH): δ (ppm) = 171.9, 167.4, 153.0, 150.0, 145.3, 144.9, 142.2, 140.6, 135.7, 130.8, 127.0, 124.8, 124.2, 124.1, 121.0, 116.6, 115.8, 62.3, 54.1, 53.2, 41.3, 32.1, 29.8, 28.6, 25.3, 19.8, 11.3. IR (ATR): ν_{max} (cm⁻¹) = 3346 (br), 1709 (vs), 1596 (s), 1527 (s), 1502 (m), 1431 (s), 1303 (m), 1255 (m), 1190 (w), 1152 (s), 1051 (s), 904 (w), 847 (s), 828 (s), 729 (m), 696 (s). HRMS (ESI): calc. for C₃₃H₃₆N₅O₅⁺ [*M+H*]⁺: 582.2711, found: 582.2707.

6.4.2 Photoswitchable mAChR agonists



Alcohol 3.45¹¹³: Dimethylamine hydrochloride (8.72 g, 0.107) was dissolved in H₂O (15 mL) and the pH was adjusted to 9 using NaOH (1 M). Formaline (37%, 11.2 mL, 0.15 mmol), propargyl alcohol (5.15 mL, 89.19 mmol) and a solution of copper sulfate pentahydrate (690 mg, 2.76 mmol) in H₂O (4.46 mL) were sequentially added, the pH was adjusted to 8 with NaOH (1 M) and the solution was stirred at 80 °C for 1 h. The solution was cooled to room temperature, poured into aqueous ammonia (25%, 30 mL) and extracted with Et₂O. The combined organic phases were dried over MgSO₄ and evaporated to dryness to give alcohol **3.45** (3.78 g, 33.4 mmol, 37%) as a yellow oil.

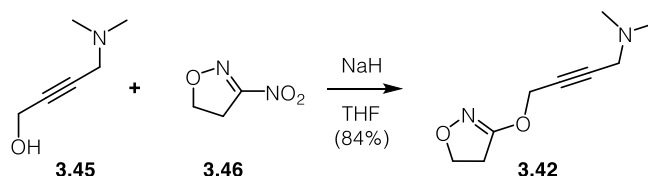
Data for 3.45: ¹H-NMR (400 MHz, CDCl₃): δ (ppm) = 4.28 (t, *J* = 1.9 Hz, 2H), 3.26 (t, *J* = 2.0 Hz, 2H), 2.29 (s, 6H). ¹³C-NMR (100 MHz, CDCl₃): δ (ppm) = 83.9, 80.6, 51.0, 48.2, 44.3. IR (ATR): ν_{max} (cm⁻¹) = 3175 (m), 2947 (w), 2861 (m), 2828 (m), 2782 (m), 1661 (w), 1628 (w), 1460 (m), 1356 (m), 1332 (m), 1258 (w), 1232 (w), 1177 (w), 1156 (w), 1135 (m), 1101 (s), 1109 (vs), 975 (m), 953 (w), 860 (s), 810 (s). HRMS (ESI): calc. for C₆H₁₂NO [*M+H*]⁺: 114.0913, found: 114.0914.



Dihydroisoxazol 3.46¹¹³: 1-bromo-3-chloropropane (4.1 mL, 50.81 mmol) was added dropwise to a solution of NaNO₂ (7.17 g, 50.0 mmol) and isopentyl nitrite (7.0 mL, 52.0 mmol) in DMSO (50 mL) and the reaction was stirred at room temperature for 24 h. The reaction mixture was poured into ice water and extracted with CH₂Cl₂. The combined organic phases were dried over MgSO₄ and evaporated to dryness to give dihydroisoxazol **3.46** (3.00 g, 25.84 mmol, 51%) as a yellow oil.

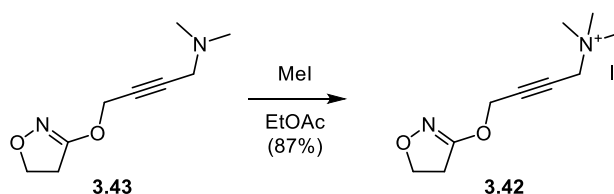
Data for 3.46: ¹H-NMR (400 MHz, CDCl₃): δ (ppm) = 4.90 (t, *J* = 10.9 Hz, 2H), 3.51 (t, *J* = 10.9 Hz, 2H). ¹³C-NMR (100 MHz, CDCl₃): δ (ppm) = 164.2, 75.7, 30.8. IR (ATR): ν_{max}

(cm^{-1}) = 1607 (m), 1529 (vs), 1471 (w), 1437 (m), 1364 (s), 1293 (s), 1221 (w), 1169 (w), 999 (w), 961 (s), 932 (m), 848 (s), 805 (vs), 725 (m). **HRMS (EI)**: calc. for $\text{C}_3\text{H}_{12}\text{NO}$ [M] $^+$: 116.0216, found: 116.0218.



Dimethylamine 3.43¹¹³: Sodium hydride (60% suspension in paraffin, 525 mg, 13.5 mmol) was added to a solution of alcohol **3.45** (1.50 g, 13.26 mmol) in THF (20 mL) and the resulting solution was stirred for 1 h at room temperature. A solution of isoxazol **3.46** (1.53 g, 13.18 mmol) in THF (10 mL) was added and the reaction was stirred at 60 °C for 3 h before it was poured onto ice and extracted with CHCl_3 . The combined organic phases were dried over MgSO_4 and evaporated to dryness. Purification by flash column chromatography (CH_2Cl_2 :MeOH 9:1, R_f =0.5) gave dimethylamine **3.43** (2.02 g, 11.09 mmol, 84%) as an orange oil.

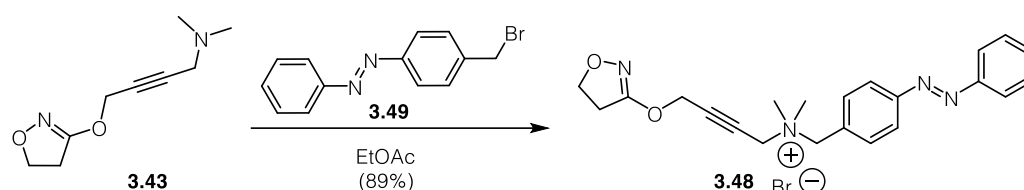
Data for 3.43: **$^1\text{H-NMR}$ (400 MHz, CDCl_3)**: δ (ppm) = 4.77 (t, J = 1.9 Hz, 1H), 4.38 (t, J = 9.6 Hz, 1H), 3.27 (t, J = 2.0 Hz, 1H), 2.96 (t, J = 9.6 Hz, 1H), 2.26 (s, 3H). **$^{13}\text{C-NMR}$ (100 MHz, CDCl_3)**: δ (ppm) = 167.0, 83.4, 78.7, 69.9, 58.2, 48.0, 44.3, 33.2. **IR (ATR)**: ν_{max} (cm^{-1}) = 2941 (m), 2878 (w), 2824 (w), 2777 (w), 1625 (s), 1454 (w), 1438 (m), 1402 (s), 1340 (vs), 1259 (m), 1178 (w), 1155 (w), 1123 (w), 1099 (w), 1033 (m), 1001 (m), 963 (s), 929 (s), 863 (m), 841 (m), 816 (w). **HRMS (ESI)**: calc. for $\text{C}_9\text{H}_{15}\text{N}_2\text{O}_2$ [$M+\text{H}$] $^+$: 183.1128, found: 183.1128.



lperoxo (3.42)¹¹³: Iodomethane (0.17 mL, 2.74 mmol) was added to a solution of dimethylamine **3.43** (200 mg, 1.10 mmol) in EtOAc (3.5 mL) and the reaction was stirred at room temperature for 24 h. The resulting precipitate was collected and dried and high vacuum to give lperoxo (**3.42**) (310 mg, 0.956 mmol, 87%) as a white solid.

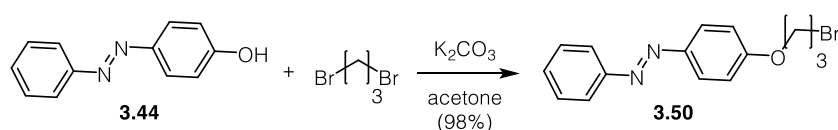
Data for 3.42: $^1\text{H-NMR}$ (400 MHz, $d_6\text{-DMSO}$): δ (ppm) = 4.94 (t, J = 1.8 Hz, 2H), 4.45 (t, J = 1.9 Hz, 2H), 4.32 (t, J = 9.6 Hz, 2H), 3.12 (s, 9H), 3.02 (t, J = 9.6 Hz, 2H).

$^{13}\text{C-NMR}$ (100 MHz, $d_6\text{-DMSO}$): δ (ppm) = 166.8, 86.0, 76.3, 69.7, 57.3, 55.1, 52.0, 32.3. **IR (ATR):** ν_{max} (cm^{-1}) = 3418 (m), 2922 (s), 2852 (m), 1625 (s), 1604 (m), 1584 (m), 1504 (m), 1472 (m), 1465 (m), 1437 (w), 1411 (m), 1346 (vs), 1255 (vs), 1144 (s), 1106 (w), 1069 (w), 1037 (w), 1014 (m), 1000 (m), 974 (m), 961 (s), 927 (s), 899 (m), 876 (w), 861 (m), 842 (s), 818 (w), 790 (w), 782 (m), 723 (m), 693 (s). **HRMS (ESI):** calc. for $\text{C}_{10}\text{H}_{17}\text{N}_2\text{O}_2$ $[\text{M}]^+$: 197.1285, found: 197.1284.



Azoiperoxo 1 (3.48): A solution of dimethylamine **3.43** (23 mg, 0.127 mmol) and azobenzene benzylbromide **3.49** (100 mg, 0.363 mmol) in EtOAc (5 mL) was stirred at room temperature for 24 h. The resulting precipitate was collected and dried under high vacuum to give azoiperoxo 1 (**3.48**) (50 mg, 0.109 mmol, 86%) as an orange solid.

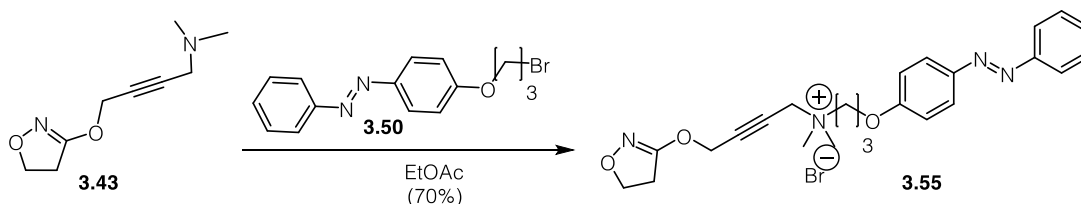
Data for azoiperoxo 1 (3.48): $^1\text{H-NMR}$ (400 MHz, $d_4\text{-MeOH}$): δ (ppm) = 8.11 – 8.04 (m, 2H), 8.01 – 7.92 (m, 2H), 7.85 – 7.79 (m, 2H), 7.63 – 7.54 (m, 3H), 4.99 (t, J = 1.7 Hz, 2H), 4.73 (s, 2H), 4.41 (t, J = 9.6 Hz, 2H), 4.35 (t, J = 1.8 Hz, 2H), 3.21 (s, 6H), 3.07 (t, J = 9.6 Hz, 2H). $^{13}\text{C-NMR}$ (100 MHz, $d_4\text{-MeOH}$): δ (ppm) = 168.8, 155.2, 153.9, 135.2, 133.1, 131.0, 130.4, 124.5, 124.1, 88.7, 76.9, 71.2, 67.5, 58.3, 54.9, 50.9, 33.7. **IR (ATR):** ν_{max} (cm^{-1}) = 2913 (w), 1626 (s), 1474 (w), 1444 (w), 1414 (m), 1350 (s), 1302 (w), 1268 (w), 1216 (w), 1166 (w), 1021 (w), 1000 (m), 977 (m), 961 (m), 930 (m), 885 (w), 860 (s), 824 (w), 770 (s), 721 (m), 686 (vs), 658 (w). **HRMS (ESI):** calc. for $\text{C}_{22}\text{H}_{25}\text{N}_4\text{O}_2$ $[\text{M}]^+$: 377.1972, found: 377.1973.



Alkyl bromide 3.50: 1,3-dibromopropane (0.41 mL, 4.05 mmol) was added to a suspension of 4-hydroxyazobenzene (200 mg, 1.01 mmol) and K_2CO_3 (699 mg,

5.06 mmol) in acetone (5 mL) and the reaction was stirred at 60 °C overnight. The resulting precipitate was removed by filtration and the solvent was removed under reduced pressure. Purification of the resulting residue by flash column chromatography (Et₂O:hexanes 3:97, R_f = 0.3) gave alkyl bromide **3.50** (317 mg, 0.993 mmol, 98%) as an orange solid.

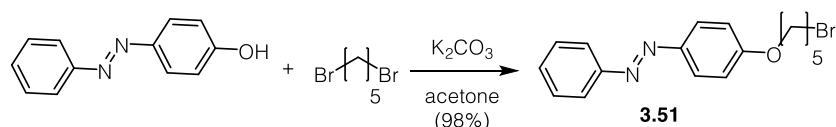
Data for 3.50: ¹H-NMR (400 MHz, CDCl₃): δ (ppm) = 7.96 – 7.90 (m, 2H), 7.90 – 7.85 (m, 2H), 7.55 – 7.47 (m, 2H), 7.47 – 7.40 (m, 1H), 7.06 – 6.98 (m, 2H), 4.20 (t, *J* = 5.8 Hz, 2H), 3.64 (t, *J* = 6.4 Hz, 2H), 2.37 (p, *J* = 6.1 Hz, 2H). ¹³C-NMR (100 MHz, CDCl₃): δ (ppm) = 161.3, 152.9, 147.3, 130.6, 129.2, 124.9, 122.7, 114.9, 65.7, 32.4, 30.0. IR (ATR): ν_{max} (cm⁻¹) = 2924 (m), 2853 (m), 1626 (w), 1602 (m), 1581 (m), 1498 (m), 1464 (m), 1440 (m), 1412 (w), 1383 (w), 1348 (m), 1326 (w), 1296 (w), 1245 (s), 1210 (m), 1140 (m), 1107 (w), 1055 (w), 1025 (m), 1016 (w), 921 (m), 835 (s), 818 (m), 794 (w), 765 (s), 718 (m), 684 (vs), 666 (w). HRMS (EI): calc. for C₁₅H₁₅N₂OBr [M]⁺: 318.0368, found: 318.0362.



Azoiperoxo 3 (3.55): A solution of dimethylamine **3.43** (57 mg, 0.313 mmol) and alkyl bromide **3.50** (100 mg, 0.313 mmol) in EtOAc (5 mL) was stirred at 70 °C overnight. The resulting precipitate was collected and dried under high vacuum to give azoiperoxo 3 (**3.55**) (45 mg, 0.090 mmol, 70%) as an orange solid. The resulting product is in a light driven equilibrium with its double bond isomer. The major trans isomer is described.

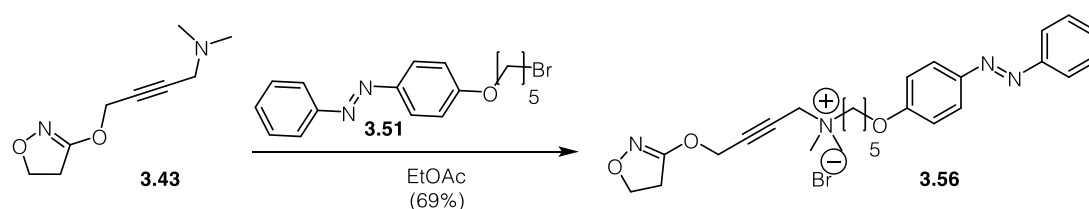
Data for azoiperoxo 3 (3.55): ¹H-NMR (400 MHz, d₄-MeOH): δ (ppm) = 7.95 – 7.90 (m, 2H), 7.89 – 7.83 (m, 2H), 7.60 – 7.43 (m, 3H), 7.18 – 7.09 (m, 2H), 6.94 – 6.81 (m, 1H), 4.92 (t, *J* = 1.7 Hz, 2H), 4.50 (t, *J* = 1.8 Hz, 2H), 4.34 (dt, *J* = 12.5, 9.5 Hz, 2H), 4.25 (t, *J* = 5.7 Hz, 2H), 3.79 – 3.70 (m, 2H), 3.68 (s, 0H), 3.27 (s, 6H), 3.04 – 2.97 (m, 2H), 2.35 (dq, *J* = 11.5, 5.6 Hz, 2H). ¹³C-NMR (100 MHz, d₄-MeOH): δ (ppm) = 168.7, 162.4, 154.0, 148.6, 131.8, 130.2, 125.8, 123.5, 116.0, 88.0, 76.5, 71.2, 66.0, 63.0, 58.2, 55.3, 51.3, 33.7, 24.0. IR (ATR): ν_{max} (cm⁻¹) = 3384 (m), 2966 (w), 2928 (w), 2884 (w), 1624 (m), 1597 (s), 1501 (m), 1472 (m), 1441 (w), 1400 (m), 1341 (s), 1302 (w), 1246 (vs), 1150 (m), 1139 (s), 1108 (w), 1056 (m), 1001 (w), 965 (m), 929 (w), 917 (m), 884 (w), 864 (w),

838 (s), 772 (s), 721 (w), 689 (s). **HRMS (ESI)**: calc. for $C_{24}H_{29}N_4O_3$ $[M]^+$: 421.2234, found: 421.2236.



Alkyl bromide 3.51: 1,5-dibromopentane (0.83 mL, 6.08 mmol) was added to a suspension of 4-hydroxyazobenzene (300 mg, 1.51 mmol) and K_2CO_3 (1.05 g, 7.59 mmol) in acetone (7 mL) and the reaction was stirred at 60 °C overnight. The resulting precipitate was removed by filtration and the solvent was removed under reduced pressure. Purification of the resulting residue by flash column chromatography (Et₂O:hexanes 6:97, R_f = 0.3) gave alkyl bromide **3.51** (484 mg, 1.39 mmol, 92%) as an orange solid.

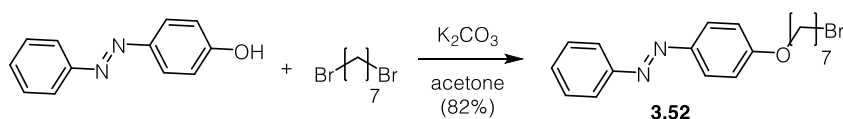
Data for 3.51: **¹H-NMR (400 MHz, CDCl₃)**: δ (ppm) = 7.96 – 7.85 (m, 4H), 7.55 – 7.47 (m, 2H), 7.47 – 7.40 (m, 1H), 7.04 – 6.97 (m, 2H), 4.06 (t, J = 6.3 Hz, 2H), 3.46 (t, J = 6.7 Hz, 2H), 1.96 (dt, J = 14.9, 6.8 Hz, 2H), 1.86 (dq, J = 8.3, 6.2 Hz, 2H), 1.73 – 1.61 (m, 2H). **¹³C-NMR (100 MHz, CDCl₃)**: δ (ppm) = 161.6, 152.9, 147.0, 130.5, 129.2, 124.9, 122.7, 114.8, 68.0, 33.7, 32.6, 28.5, 24.9. **IR (ATR)**: ν_{max} (cm⁻¹) = 2946 (w), 2863 (w), 1602 (m), 1580 (m), 1501 (m), 1471 (w), 1489 (m), 1435 (w), 1412 (m), 1329 (w), 1322 (w), 1306 (w), 1298 (w), 1257 (s), 1200 (m), 1137 (m), 1068 (w), 1036 (w), 1017 (m), 998 (w), 927 (w), 837 (s), 805 (m), 763 (s), 730 (m), 720 (m), 688 (vs). **HRMS (EI)**: calc. for $C_{17}H_{19}N_2OBr$ $[M]^+$: 346.0681, found: 346.0676.



Azoiperoxo 5 (3.56): A solution of dimethylamine **3.43** (105 mg, 0.576 mmol) and alkyl bromide **3.51** (200 mg, 0.576 mmol) in EtOAc (5 mL) was stirred at 70 °C for 5 d. The

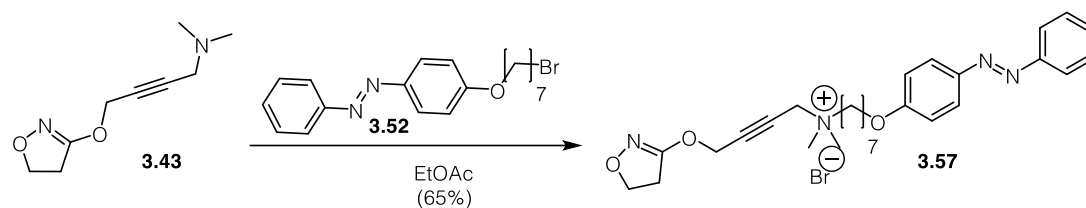
resulting precipitate was collected and dried under high vacuum to give azoiperoxo 5 (**3.56**) (211 mg, 0.399 mmol, 69%) as an orange solid.

Data for azoiperoxo 5 (3.56): $^1\text{H-NMR}$ (400 MHz, *d4*-MeOH): δ (ppm) = 8.08 – 7.72 (m, 4H), 7.67 – 7.40 (m, 3H), 7.09 (dd, J = 9.3, 2.4 Hz, 2H), 4.91 (d, J = 1.9 Hz, 2H), 4.48 – 4.33 (m, 4H), 4.15 (t, J = 6.1 Hz, 2H), 3.19 (d, J = 3.0 Hz, 6H), 3.02 (t, J = 9.6 Hz, 2H), 2.04 – 1.80 (m, 4H), 1.63 (p, J = 7.6 Hz, 2H). $^{13}\text{C-NMR}$ (100 MHz, *d4*-MeOH): δ (ppm) = 168.7, 163.1, 154.1, 148.2, 131.7, 125.8, 123.5, 115.9, 87.8, 76.6, 68.9, 65.3, 58.2, 55.1, 51.2, 49.3, 33.7, 29.7, 24.0, 23.4. **IR (ATR):** ν_{max} (cm^{-1}) = 1628 (m), 1607 (m), 1587 (w), 1501 (w), 1478 (m), 1460 (w), 1439 (w), 1416 (m), 1385 (w), 1351 (s), 1307 (w), 1251 (vs), 1188 (w), 1162 (m), 1147 (m), 1106 (w), 1048 (w), 1010 (m), 974 (m), 931 (s), 897 (w), 864 (w), 828 (vs), 783 (s), 738 (w), 720 (w), 694 (s). **HRMS (ESI):** calc. for $\text{C}_{26}\text{H}_{33}\text{N}_4\text{O}_3$ [M] $^+$: 449.2547, found: 449.2548.



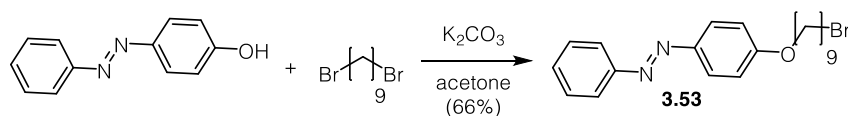
Alkyl bromide 3.52: 1,7-dibromoheptane (1.04 mL, 6.08 mmol) was added to a suspension of 4-hydroxyazobenzene (300 mg, 1.51 mmol) and K_2CO_3 (1.05 g, 7.59 mmol) in acetone (7 mL) and the reaction was stirred at 60 °C overnight. The resulting precipitate was removed by filtration and the solvent was removed under reduced pressure. Purification of the resulting residue by flash column chromatography (Et_2O :hexanes 2:98, R_f = 0.2) gave alkyl bromide **3.52** (467 mg, 1.24 mmol, 82%) as an orange solid.

Data for 3.52: $^1\text{H-NMR}$ (400 MHz, CDCl_3): δ (ppm) = 7.96 – 7.85 (m, 4H), 7.55 – 7.47 (m, 2H), 7.47 – 7.41 (m, 1H), 7.04 – 6.95 (m, 2H), 4.04 (t, J = 6.5 Hz, 2H), 3.43 (t, J = 6.8 Hz, 2H), 1.85 (ddt, J = 22.8, 8.2, 6.3 Hz, 4H), 1.56 – 1.38 (m, 6H). $^{13}\text{C-NMR}$ (100 MHz, CDCl_3): δ (ppm) = 161.7, 152.9, 147.0, 130.4, 129.2, 124.9, 122.7, 114.8, 68.3, 34.1, 32.8, 29.2, 28.7, 28.2, 26.0. **IR (ATR):** ν_{max} (cm^{-1}) = 2939 (m), 2852 (w), 1601 (m), 1581 (m), 1501 (m), 1463 (m), 1442 (w), 1433 (w), 1412 (w), 1389 (w), 1323 (w), 1296 (w), 1254 (s), 1233 (m), 1195 (m), 1141 (s), 1107 (m), 1070 (w), 1057 (w), 1021 (m), 989 (w), 923 (w), 835 (s), 810 (m), 790 (w), 769 (s), 720 (m), 686 (vs), 656 (w). **HRMS (EI):** calc. for $\text{C}_{19}\text{H}_{23}\text{N}_2\text{OBr}$ [M] $^+$: 374.0994, found: 374.0988.



Azoiperoxo 7 (3.57): A solution of dimethylamine **3.43** (97 mg, 0.533 mmol) and alkyl bromide **3.52** (200 mg, 0.533 mmol) in EtOAc (5 mL) was stirred at 70 °C for 5 d. The resulting precipitate was collected and dried under high vacuum to give azoiperoxo 7 (**3.57**) (193 mg, 0.346 mmol, 65%) as an orange solid. The resulting product is in a light driven equilibrium with its double bond isomer. The major trans isomer is described.

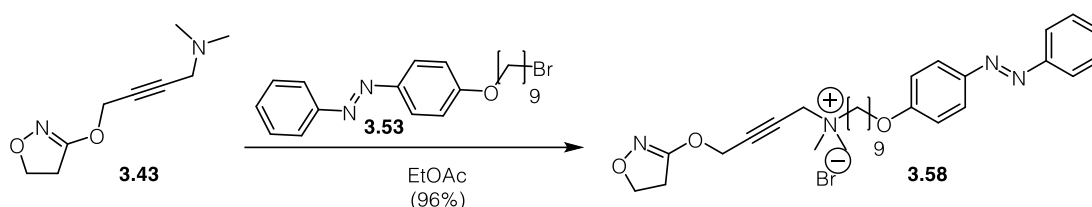
Data for azoiperoxo 7 (3.57): $^1\text{H-NMR}$ (400 MHz, *d4*-MeOH): δ (ppm) = 7.95 – 7.90 (m, 2H), 7.90 – 7.84 (m, 2H), 7.59 – 7.44 (m, 3H), 7.14 – 7.04 (m, 2H), 4.92 (t, J = 1.8 Hz, 2H), 4.45 – 4.35 (m, 5H), 4.13 (t, J = 6.3 Hz, 2H), 3.54 – 3.41 (m, 2H), 3.18 (d, J = 3.9 Hz, 7H), 3.04 (t, J = 9.6 Hz, 2H), 1.91 – 1.80 (m, 4H), 1.61 – 1.44 (m, 6H). $^{13}\text{C-NMR}$ (100 MHz, *d4*-MeOH): δ (ppm) = 168.7, 163.3, 154.1, 148.1, 130.2, 125.8, 123.5, 115.8, 87.7, 76.6, 71.2, 69.3, 65.4, 58.2, 55.0, 51.1, 33.7, 30.1, 29.8, 27.2, 26.9, 23.6. **IR (ATR):** ν_{max} (cm^{-1}) = 2940 (w), 1911 (w), 1624 (s), 1604 (s), 1580 (m), 1499 (w), 1472 (m), 1462 (w), 1414 (m), 1346 (s), 1313 (w), 1300 (m), 1255 (s), 1162 (w), 1148 (s), 1106 (w), 1070 (w), 1032 (m), 1011 (w), 991 (w), 969 (s), 928 (s), 894 (m), 878 (m), 840 (m), 832 (vs), 787 (s), 723 (m), 697 (s). **HRMS (ESI):** calc. for $\text{C}_{28}\text{H}_{37}\text{N}_4\text{O}_3$ [M] $^+$: 477.2860, found: 477.2856.



Alkyl bromide 3.53: 1,9-dibromononane (1.24 mL, 6.08 mmol) was added to a suspension of 4-hydroxyazobenzene (300 mg, 1.51 mmol) and K_2CO_3 (1.05 g, 7.59 mmol) in acetone (7 mL) and the reaction was stirred at 60 °C overnight. The resulting precipitate was removed by filtration and the solvent was removed under reduced pressure. Purification of the resulting residue by flash column chromatography (Et_2O :hexanes 4:96, R_f = 0.2) gave alkyl bromide **3.53** (400 mg, 0.992 mmol, 66%) as an orange solid.

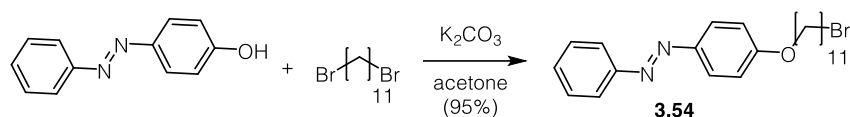
Data for 3.53: $^1\text{H-NMR}$ (400 MHz, CDCl_3): δ (ppm) = 7.96 – 7.83 (m, 4H), 7.54 – 7.47 (m, 2H), 7.47 – 7.41 (m, 1H), 7.04 – 6.96 (m, 2H), 4.04 (t, J = 6.5 Hz, 2H), 3.41 (td, J =

6.9, 2.6 Hz, 4H), 1.93 – 1.77 (m, 6H), 1.53 – 1.29 (m, 15H). **¹³C-NMR (100 MHz, CDCl₃):** δ (ppm) = 161.8, 152.9, 147.0, 130.4, 129.2, 124.9, 122.7, 114.8, 68.4, 34.2, 34.2, 32.9, 32.9, 29.5, 29.4, 29.4, 29.3, 28.8, 28.8, 28.3, 28.2, 26.1. **IR (ATR):** ν_{\max} (cm⁻¹) = 2936 (m), 1822 (m), 2851 (w), 1612 (m), 1581 (m), 1502 (m), 1490 (m), 1464 (m), 1443 (w), 1414 (w), 1425 (w), 1388 (w), 1327 (w), 1296 (m), 1253 (s), 1233 (s), 1152 (w), 1340 (m), 1107 (w), 1069 (w), 1059 (w), 1016 (w), 842 (s), 810 (s), 788 (w), 770 (s), 754 (w), 721 (m), 686 (vs), 656 (m). **HRMS (EI):** calc. for C₂₁H₂₇N₂OBr [M]⁺: 402.1307, found: 402.1300.



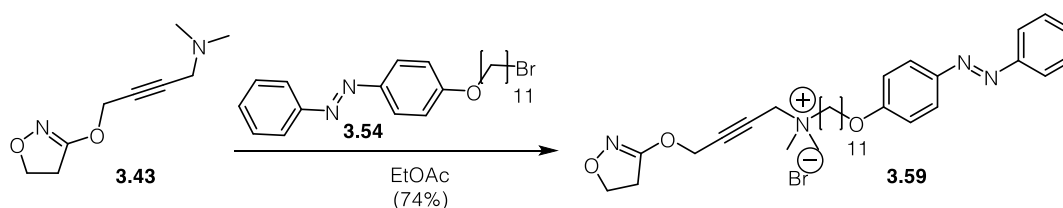
Azoiperoxo 9 (3.58): A solution of dimethylamine **3.43** (136 mg, 0.744 mmol) and alkyl bromide **3.53** (200 mg, 0.496 mmol) in EtOAc (5 mL) was stirred at 70 °C for 3 d. The resulting precipitate was collected and dried under high vacuum to give azoiperoxo 9 (**3.58**) (280 mg, 0.478 mmol, 96%) as an orange solid.

Data for azoiperoxo 9 (3.58): **¹H-NMR (400 MHz, CDCl₃):** δ (ppm) = 7.93 – 7.83 (m, 4H), 7.54 – 7.45 (m, 2H), 7.45 – 7.39 (m, 1H), 7.03 – 6.96 (m, 2H), 4.95 (d, J = 1.8 Hz, 2H), 4.84 – 4.80 (m, 3H), 4.45 – 4.39 (m, 3H), 4.03 (t, J = 6.5 Hz, 2H), 3.66 – 3.59 (m, 2H), 3.43 (d, J = 5.8 Hz, 7H), 3.01 (td, J = 9.7, 3.6 Hz, 3H), 1.99 – 1.70 (m, 8H), 1.50 – 1.31 (m, 13H). **¹³C-NMR (100 MHz, CDCl₃):** δ (ppm) = 166.8, 161.8, 152.8, 146.9, 130.5, 129.2, 124.9, 122.6, 114.8, 86.7, 77.5, 77.2, 76.8, 76.1, 70.2, 68.4, 64.3, 57.3, 55.0, 50.7, 50.6, 33.1, 29.4, 29.3, 29.2, 26.3, 26.1, 23.0. **IR (ATR):** ν_{\max} (cm⁻¹) = 3403 (m), 2937 (m), 2925 (m), 2858 (w), 1627 (s), 1607 (m), 1581 (m), 1504 (w), 1476 (m), 1461 (m), 1439 (w), 1414 (s), 1347 (vs), 1307 (w), 1263 (vs), 1162 (m), 1148 (s), 1105 (w), 1070 (w), 1018 (s), 1002 (m), 972 (s), 829 (s), 900 (m), 882 (m), 863 (m), 836 (m), 826 (s), 785 (s), 851 (w), 722 (m), 696 (s). **HRMS (ESI):** calc. for C₃₀H₄₁N₄O₃ [M]⁺: 505.3173, found: 505.3173



Alkyl bromide 3.54: 1,11-dibromoundecane (0.75 mL, 3.18 mmol) was added to a suspension of 4-hydroxyazobenzene (157 mg, 0.790 mmol) and K_2CO_3 (549 mg, 0.790 mmol) in acetone (5 mL) and the reaction was stirred at 60 °C overnight. The resulting precipitate was removed by filtration and the solvent was removed under reduced pressure. Purification of the resulting residue by flash column chromatography (Et_2O :hexanes 4:96, $R_f = 0.2$) gave alkyl bromide **3.54** (324 mg, 0.751 mmol, 95%) as an orange solid.

Data for 3.54: $^1\text{H-NMR}$ (400 MHz, CDCl_3): δ (ppm) = 7.98 – 7.84 (m, 4H), 7.57 – 7.40 (m, 3H), 7.07 – 6.97 (m, 2H), 4.04 (t, $J = 6.5$ Hz, 2H), 3.41 (t, $J = 6.8$ Hz, 4H), 1.93 – 1.79 (m, 6H), 1.54 – 1.25 (m, 22H). $^{13}\text{C-NMR}$ (100 MHz, CDCl_3): δ (ppm) = 161.9, 152.9, 147.0, 130.5, 129.2, 124.9, 122.7, 114.83, 8.16, 68.5, 34.3, 33.0, 31.1, 29.7, 29.6, 29.6, 29.5, 29.5, 29.3, 28.9, 28.3, 26.2. **IR (ATR):** ν_{max} (cm^{-1}) = 3919 (s), 2850 (m), 1603 (m), 1583 (m), 1502 (m), 1466 (s), 1441 (w), 1414 (w), 1389 (w), 1322 (w), 1298 (m), 1271 (w), 1249 (s), 1240 (w), 1212 (m), 1190 (w), 1142 (s), 1106 (m), 1070 (w), 1054 (w), 1027 (m), 1017 (m), 1007 (m), 976 (w), 982 (w), 921 (w), 842 (vs), 818 (m), 790 (m), 769 (vs), 721 (s), 685 (vs). **HRMS (EI):** calc. for $\text{C}_{23}\text{H}_{31}\text{N}_2\text{OBr}$ $[\text{M}]^+$: 430.1620, found: 430.1631.

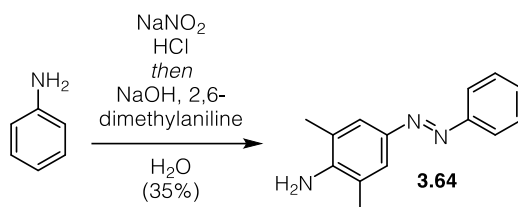


Azoiperoxo 11 (3.59): A solution of dimethylamine **3.43** (200 mg, 655 mmol) and alkyl bromide **3.54** (200 mg, 0.496 mmol) in EtOAc (5 mL) was stirred at 70 °C for 3 d. The resulting precipitate was collected and dried under high vacuum to give azoiperoxo 11 (**3.59**) (210 mg, 0.342 mmol, 74%) as an orange solid.

Data for azoiperoxo 11 (3.59): $^1\text{H-NMR}$ (400 MHz, $d_4\text{-MeOH}$): δ (ppm) = 7.96 – 7.85 (m, 4H), 7.59 – 7.45 (m, 3H), 7.12 – 7.06 (m, 2H), 4.46 – 4.37 (m, 10H), 4.16 – 4.07 (m, 3H), 3.52 – 3.40 (m, 5H), 3.19 (d, $J = 6.2$ Hz, 15H), 3.05 (td, $J = 9.6, 5.3$ Hz, 6H), 1.91 –

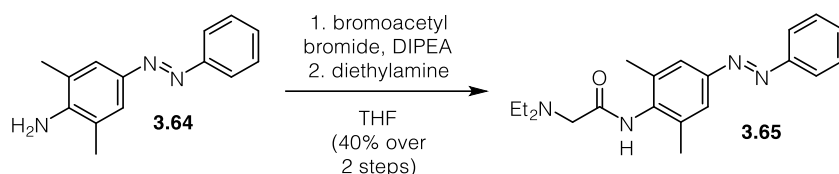
1.75 (m, 7H), 1.50 – 1.34 (m, 25H). **¹³C-NMR (100 MHz, *d*4-MeOH):** δ (ppm) = 167.3, 162.0, 152.7, 146.7, 130.2, 128.8, 124.4, 122.1, 114.4, 86.2, 75.2, 69.8, 68.0, 64.0, 60.1, 56.8, 53.6, 49.7, 32.3, 29.2, 29.1, 29.0, 28.9, 28.8, 28.8, 25.9, 25.7, 22.3. **IR (ATR):** ν_{\max} (cm⁻¹) = 3418 (w), 2923 (m), 2853 (w), 1625 (s), 1604 (m), 1585 (w), 1504 (w), 1465 (m), 1472 (m), 1437 (w), 1411 (m), 1345 (vs), 1311 (w), 1299 (w), 1256 (vs), 1155 (m), 1144 (m), 1106 (w), 1068 (w), 1036 (w), 1014 (m), 1000 (w), 974 (s), 961 (s), 926 (s), 898 (m), 876 (m), 862 (m), 842 (s), 818 (w), 790 (w), 782 (m), 736 (w), 723 (m), 693 (m). **HRMS (ESI):** calc. for C₃₂H₄₄N₄O₃ [M]⁺: 533.3486, found: 533.3484.

6.4.3 Photoswitchable TAS2R agonists



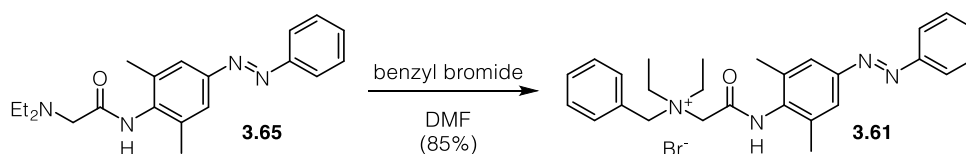
Aniline 3.64: A solution of NaNO₂ (8.86 g, 128 mmol) in H₂O (5 mL) was added dropwise to an ice cooled solution of aniline (9.80 mL, 107 mmol) and aqueous HCl (conc. 27 mL, 321 mmol) in H₂O (20 mL) and the reaction was stirred at 0 °C for 1 h. The mixture was added slowly to an ice cooled solution of 2,6-dimethylaniline and (13.0 g, 107 mmol) and NaOH (7.70 g, 193 mmol) in H₂O (100 mL) and the reaction mixture was stirred at 0 °C for 1 h. The resulting precipitate was collected and purified by flash column chromatography (hexanes:EtOAc 5:1, R_f = 0.2) to give aniline **3.64** (8.35 g, 37.1 mmol, 35%) as a red solid.

Data for 3.64: **¹H-NMR (400 MHz, CDCl₃):** δ (ppm) = 7.88 – 7.81 (m, 2H), 7.64 (s, 2H), 7.48 (dd, *J* = 8.5, 6.9 Hz, 2H), 7.42 – 7.37 (m, 1H), 4.05 (s, 2H), 2.27 (s, 6H). **¹³C-NMR (100 MHz, CDCl₃):** δ (ppm) = 153.2, 146.5, 144.9, 129.7, 129.1, 124.0, 122.4, 121.5, 17.8. **IR (ATR):** ν_{\max} (cm⁻¹) = 3397 (w), 2916 (w), 1619 (s), 1590 (m), 1479 (s), 1442 (m), 1412 (m), 1379 (w), 1298 (s), 1273 (m), 1120 (s), 1090 (m), 1029 (w), 894 (m), 759 (s), 734 (s), 690 (s). **HRMS (EI):** calc. for C₁₄H₁₅N₃ [M]⁺: 225.1260, found: 225.1259.



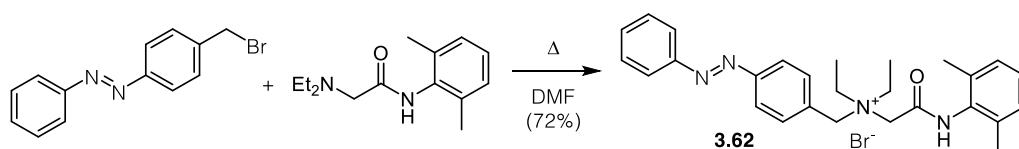
Diethylamine 3.65: Bromoacetyl bromide (0,19 mL, 2.22 mmol) was added dropwise to an ice cooled solution of aniline **3.64** (500 mg, 2.22 mmol) and DIPEA (0.45 mL, 2.66 mmol) in THF (10 mL) and the reaction was stirred at room temperature for 30 min. Diethylamine (2.32 mL, 22.2 mmol) and PhMe (20 mL) were added and the reaction was stirred at 100 °C for 2 h. The reaction was cooled to room temperature, the resulting precipitate was removed by filtration and the filtrate was extracted with aqueous HCl (3 M). The aqueous phase was basified with aqueous NaOH (4 M) and extracted with EtOAc. The combined organic phases were dried over MgSO₄ and concentrated under reduced pressure. Purification of the resulting residue by flash column chromatography (CH₂Cl₂:MeOH 96:4, R_f= 0.2) gave diethylamine **3.65** (300 mg, 0.886 mmol, 40%) as an orange solid,

Data for 3.65: ¹H-NMR (400 MHz, CDCl₃): δ (ppm) = δ 9.06 (s, 1H), 7.94 – 7.86 (m, 2H), 7.68 (s, 2H), 7.54 – 7.44 (m, 3H), 3.25 (s, 2H), 2.72 (q, *J* = 7.1 Hz, 4H), 2.34 (s, 6H), 1.16 (t, *J* = 7.1 Hz, 7H). ¹³C-NMR (100 MHz, CDCl₃): δ (ppm) = 170.4, 152.8, 151.0, 136.8, 136.0, 131.0, 129.2, 122.9, 122.8, 57.6, 49.1, 19.0, 12.8. IR (ATR): ν_{max} (cm⁻¹) = 3394 (br), 1976 (m), 1744 (m), 1684 (m), 1630 (s), 1531 (w), 1476 (s), 1454 (s), 1381 (m), 1208 (s), 1149 (w), 1119 (w), 1088 (w), 1069 (w), 1032 (m), 980 (w), 923 (w), 894 (w), 773 (s), 690 (s). HRMS (ESI): calc. for C₂₀H₂₇N₄O [M+H]⁺: 339.2179, found: 339.2178.



Arylamide 3.61: Benzyl bromide (0.08 mL, 0.680 mmol) was added to a solution of diethylamine **3.65** (230 mg, 0.680 mmol) in DMF (7 mL) and the solution was stirred at 80 °C overnight. Evaporation and purification of the resulting residue by reverse phase column chromatography (MeCN:H₂O (containing 0.1 M HCl) 0:100-40:60) gave arylamide **3.61** (248 mg, 0.578 mmol, 85%) as an orange solid.

Data for 3.61: $^1\text{H-NMR}$ (400 MHz, $d_4\text{-MeOH}$): δ (ppm) = $^1\text{H NMR}$ (400 MHz, Methanol- d_4) δ 7.92 (d, $J = 7.3$ Hz, 2H), 7.72 (s, 2H), 7.58 (dq, $J = 21.3, 7.9, 7.5$ Hz, 8H), 4.20 (s, 2H), 3.72 – 3.60 (m, 4H), 2.39 (s, 6H), 1.54 (t, $J = 6.4$ Hz, 6H). $^{13}\text{C-NMR}$ (100 MHz, $d_4\text{-MeOH}$): δ (ppm) = 164.0, 153.9, 152.8, 137.9, 136.7, 134.0, 132.4, 132.2, 130.7, 130.3, 128.6, 123.8, 123.5, 63.5, 56.8, 55.8, 18.9, 8.5. **IR (ATR):** ν_{max} (cm^{-1}) = 3377 (br), 2978 (m), 1682 (s), 1603 (w), 1533 (s), 1474 (s), 1456 (s), 1395 (m), 1292 (m), 1241 (m), 1150 (w), 1118 (w), 1071 (w), 1029 (w), 1002 (w), 967 (w), 868 (w), 767 (m), 150 (m), 724 (m), 703 (s), 689 (s). **HRMS (ESI):** calc. for $\text{C}_{27}\text{H}_{33}\text{N}_4\text{O}$ $[\text{M}]^+$: 429.2649, found: 429.2649.

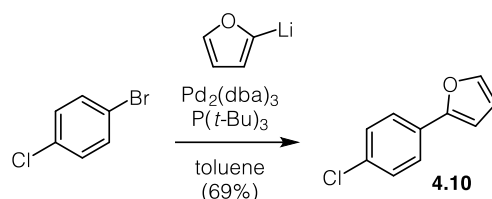


Arylamide 3.62: A solution of azobenzene benzylbromide (117 mg, 0.427 mmol) and lidocaine (100 mg, 0.427 mmol) in DMF (3 mL) was stirred at 80 °C overnight. Evaporation and purification of the resulting residue by reverse phase column chromatography (MeCN:H₂O (containing 0.1 M HCl) 0:100-40:60) gave arylamide **3.62** (143 mg, 0.308 mmol, 72%) as an orange solid.

Data for 3.62: $^1\text{H-NMR}$ (400 MHz, $d_4\text{-MeOH}$): δ (ppm) = 11.50 (s, 1H), 8.82 (d, $J = 8.1$ Hz, 2H), 8.78 – 8.70 (m, 2H), 8.66 (d, $J = 8.2$ Hz, 2H), 8.45 (h, $J = 3.8$ Hz, 3H), 7.93 (s, 3H), 5.75 (s, 2H), 5.15 (s, 2H), 4.37 (dt, $J = 9.5, 6.5$ Hz, 4H), 3.03 (s, 6H), 2.27 (t, $J = 7.1$ Hz, 6H). $^{13}\text{C-NMR}$ (100 MHz, $d_4\text{-MeOH}$): δ (ppm) = 171.8, 162.2, 161.4, 144.5, 143.8, 143.1, 141.7, 140.2, 139.1, 137.4, 136.6, 132.4, 132.3, 70.5, 65.2, 64.0, 27.8, 17.5. **IR (ATR):** ν_{max} (cm^{-1}) = 3364 (br), 2978 (w), 1679 (s), 1536 (m), 1469 (s), 1444 (m), 1279 (w), 1236 (w), 1156 (w), 1094 (w), 1070 (w), 1018 (w), 871 (w), 853 (w), 769 (s), 720 (m), 688 (s). **HRMS (ESI):** calc. for $\text{C}_{27}\text{H}_{33}\text{N}_4\text{O}$ $[\text{M}]^+$: 429.2649, found: 429.2652.

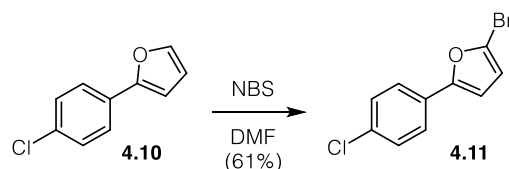
6.5 Experimental data for chapter IV

6.5.1 Photoswitches based on A-803467



Chloride 4.10¹³⁴: *n*-BuLi (2.39 M in hexanes, 1.64 mL, 3.92 mmol) was added dropwise to an ice cooled solution of furan (0.34 mL, 4.70 mmol) in THF (6.0 mL) and the reaction was stirred at 0 °C for 30 min. The resulting solution was added *via* a syringe pump to a solution of 1-bromo-4-chlorobenzene (500 mg, 2.61 mmol), Pd₂(dba)₃ (60 mg, 0.066 mmol) and P(*t*-Bu)₃ (1 M in PhMe, 0.198 mL, 0.198 mmol) in PhMe (5 mL) over the course of 1 h at room temperature. After the addition was completed, the reaction was diluted with saturated aqueous NH₄Cl and extracted with Et₂O. The combined organic phases were dried over MgSO₄ and concentrated under reduced pressure. Purification of the resulting residue by flash column chromatography (pentane R_f= 0.5) gave chloride **4.10** (319 mg, 1.79 mmol, 69%) as a colorless solid.

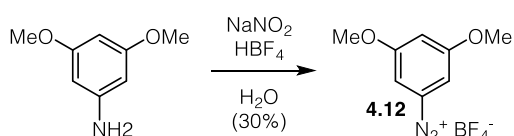
Data for 4.10: ¹H-NMR (400 MHz, CDCl₃): δ (ppm) = 7.60 (dd, *J* = 8.3, 1.2 Hz, 2H), 7.47 (d, *J* = 1.8 Hz, 1H), 7.35 (dd, *J* = 8.4, 1.2 Hz, 2H), 6.64 (d, *J* = 3.2 Hz, 1H), 6.48 (dt, *J* = 3.1, 1.4 Hz, 1H). ¹³C-NMR (100 MHz, CDCl₃): δ (ppm) = 153.0, 142.5, 133.1, 129.5, 129.0, 125.1, 111.9, 105.6. IR (ATR): ν_{max} (cm⁻¹) = 1682 (s), 1589 (s), 1571 (w), 1482 (s), 1410 (m), 1361 (w), 1282 (w), 1215 (m), 1758 (m), 1129 (w), 1094 (vs), 1012 (s), 814 (s), 790 (m), 761 (m), 733 (w), 682 (w). HRMS (EI): calc. for C₁₀H₇OCl [M]⁺: 178.0180, found: 178.0186.



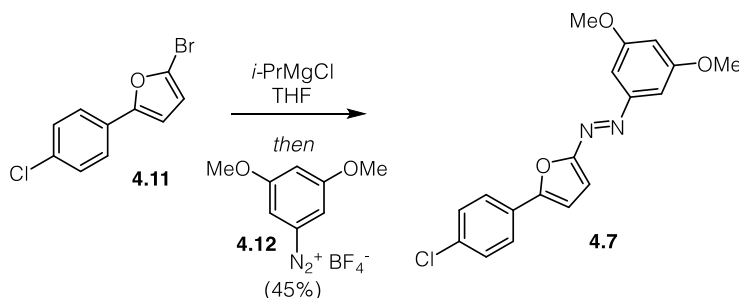
Aryl bromide 4.11: NBS (219 mg, 1.23 mmol) was added portionwise to a stirred solution of chloride **4.10** (200 mg, 1.12 mmol) in DMF (3 mL) and the solution was stirred at room temperature for 72 h. The reaction mixture was poured into cold water and

extracted with Et₂O. The combined organic phases were dried over MgSO₄ and concentrated under reduced pressure to give aryl bromide **4.11** (176 mg, 0.683 mmol, 61%) as a colorless solid.

Data for 4.11: ¹H-NMR (400 MHz, CDCl₃): δ (ppm) = 7.54 (dd, *J* = 8.5, 1.4 Hz, 2H), 7.38 – 7.31 (m, 2H), 6.58 (dd, *J* = 3.5, 1.2 Hz, 1H), 6.39 (dd, *J* = 3.5, 1.2 Hz, 1H). ¹³C-NMR (100 MHz, CDCl₃): δ (ppm) = 154.9, 133.5, 129.1, 128.5, 124.8, 122.0, 113.6, 107.9. IR (ATR): ν_{max} (cm⁻¹) = 1674 (s), 1586 (s), 1570 (m), 1489 (w), 1466 (w), 1401 (m), 1296 (w), 1282 (w), 1270 (w), 1210 (w), 1191 (w), 1175 (w), 1090 (s), 1009 (m), 972 (m), 917 (w), 882 (w), 841 (m), 820 (m), 761 (m) 729 (w). HRMS (EI): calc. for C₁₀H₆OBrCl [M]⁺: 255.9285, found: 255.9231.



Diazonium salt 4.12: A solution of NaNO₂ (451 mg, 6.53 mmol) in H₂O (1 mL) was added dropwise to an ice cooled solution of 3,5-dimethoxyaniline (1.00 g, 6.53 mmol) and aqueous HBF₄ (50%, 2.2 mL) in H₂O (3 mL) and the reaction was stirred for 30 min at 0 °C. The resulting precipitate was collected, washed with cold H₂O and redissolved in acetone (3 mL). Et₂O was added to the solution until no further precipitation could be observed, the resultant residue was collected, washed with Et₂O and dried under reduced pressure to give diazonium salt **4.12** (490 mg, 1.94 mmol, 30%) as a red solid.

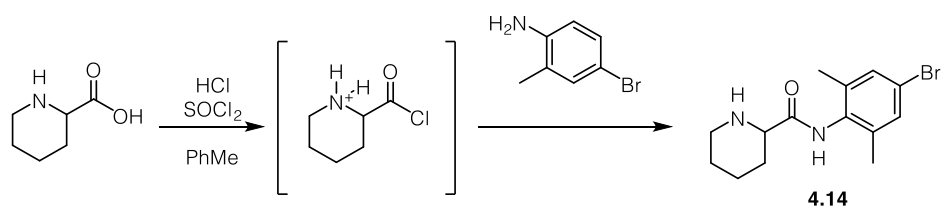


Azobenzene 4.7: *i*-PrMgCl·LiCl (1.3 M in THF, 0.15 mL, 0.15 mmol) was added to a solution of aryl bromide **4.11** (50 mg, 0.194 mmol) in THF (5 mL) at –15 °C and the

solution was stirred for 1 h at that temperature and for 1 h at room temperature. The reaction was cooled to $-78\text{ }^{\circ}\text{C}$ and a suspension of diazonium salt **4.12** (49 mg, 0.194 mmol) in THF (1 mL) was added. The mixture was stirred at $-78\text{ }^{\circ}\text{C}$ for 1 h and warmed to room temperature. The reaction was quenched with saturated aqueous NH_4Cl and extracted with EtOAc. The combined organic phases were washed with H_2O and brine, dried over MgSO_4 and concentrate under reduced pressure. Purification of the resulting residue by flash column chromatography (hexanes:EtOAc 9:1, $R_f = 0.3$) gave azobenzene **4.7** (20 mg, 0.064 mmol, 33%) as an orange solid.

Data for 4.7: $^1\text{H-NMR}$ (400 MHz, CDCl_3): δ (ppm) = 7.82 – 7.72 (m, 2H), 7.45 – 7.38 (m, 2H), 7.17 (d, $J = 3.7$ Hz, 1H), 7.11 (t, $J = 1.5$ Hz, 2H), 6.92 (d, $J = 3.7$ Hz, 1H), 6.57 (q, $J = 2.0$ Hz, 1H), 3.88 (s, 6H). $^{13}\text{C-NMR}$ (100 MHz, CDCl_3): δ (ppm) = 161.2, 160.0, 155.2, 154.2, 135.1, 129.3, 128.0, 126.3, 115.2, 109.9, 104.1, 100.8, 55.7. **IR (ATR):** ν_{max} (cm^{-1}) = 1601 (s), 1590 (s), 1562 (w), 1512 (w), 1468 (s), 1440 (w), 1425 (w), 1394 (s), 1361 (m), 1340 (w), 1310 (m), 1301 (m), 1264 (w), 1239 (w), 1200 (s), 1150 (s), 1116 (m), 1089 (m), 1054 (m), 1042 (s), 1010 (m), 971 (m), 939 (w), 913 (w), 884 (w), 870 (w), 828 (m), 818 (m), 801 (vs), 732 (w), 682 (w), 666 (s). **HRMS (EI):** calc. for $\text{C}_{10}\text{H}_7\text{OCl}$ [M] $^+$: 342.0766, found: 342.0763.

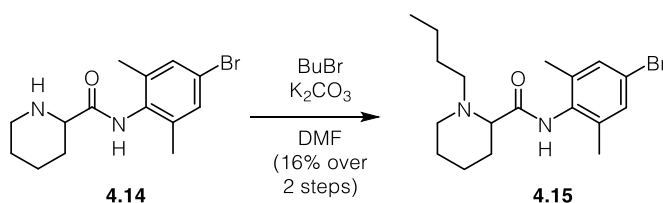
6.5.2 Photoswitches based on bupivacain



Pipecolic amide 4.14: HCl (4.00 M in dioxane, 10.3 mL, 41.3 mmol) was added dropwise to a stirred suspension of pipecolic acid (4.84 g, 37.5 mmol) in PhMe (75 mL). The mixture was heated to $55\text{ }^{\circ}\text{C}$, SOCl_2 (2.72 mL, 37.5 mmol) and DMF (0.04 mL, 0.509 mmol) were sequentially added and the reaction mixture was stirred at that temperature for 3 h. A solution of 2-bromo-4,6-dimethylaniline (15.0 g, 75.0 mmol) in toluene (15 mL) was slowly added and the reaction was stirred at $55\text{ }^{\circ}\text{C}$ overnight. The mixture was cooled to room temperature and the precipitate was collected, washed with PhMe and redissolved in water. The pH was adjusted to 5 utilizing aqueous NaOH (1 M) and the solution was washed with PhMe. The aqueous phase was basified to pH 14 with aqueous NaOH (4 M) and extracted with EtOAc. The combined organic phases were

washed with brine, dried over MgSO_4 and concentrated to give crude pipercolic amide **4.14** (2.44 g) as a white solid which was used in the next step without further purification. An analytical sample was purified by flash column chromatography (EtOAc:NEt₃ 98:2, R_f=0.2).

Data for 4.14: R_f: 0.2 (EtOAc:NEt₃ 98:2) **¹H-NMR (400 MHz, CDCl₃):** δ (ppm) = 7.27 (s, 2H), 3.45 (dd, J = 10.5, 3.2 Hz, 1H), 3.18 – 3.08 (m, 1H), 2.69 (ddd, J = 12.7, 11.3, 2.8 Hz, 1H), 2.19 (s, 5H), 2.04 (d, J = 8.8 Hz, 1H), 1.92 (ddd, J = 7.6, 4.3, 1.7 Hz, 1H), 1.68 – 1.55 (m, 2H), 1.55 – 1.42 (m, 1H). **¹³C-NMR (100 MHz, CDCl₃):** δ (ppm) = 172.6, 137.4, 133.0, 131.0, 120.5, 76.8, 60.6, 45.9, 30.4, 23.0, 24.1, 18.5. **IR (ATR):** ν_{max} (cm⁻¹) = 2919 (m), 1637 (vs), 1574 (m), 1468 (m), 1438 (m), 1391 (s), 1366 (m), 1258 (m), 1199 (s), 1108 (m), 1092 (s), 1065 (m), 1031 (w), 990 (w), 945 (w), 896 (w), 854 (s), 770 (m), 740 (m), 732 (w), 695 (w). **HRMS (ESI):** calc. for C₁₄H₁₈ON₂Br [*M-H*]⁻: 309.0608, found: 309.0611.

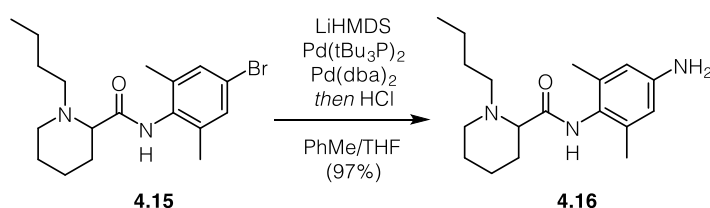


Tertiary amine 4.15: *n*-Butylbromide (1.30 mL, 10.5 mmol) was added to a suspension of pipercolic amide **4.14** (2.44 g used crude from the previous step) and potassium carbonate (1.74 g, 12.6 mmol) in DMF (23 mL) and the reaction mixture was stirred at 80 °C for 90 min. The suspension was cooled to room temperature, filtered and concentrated. The resulting residue was purified by flash column chromatography (hexanes:EtOAc 2:1 to 1:1, R_f = 0.3 (hexanes:EtOAc 1:1) to yield tertiary amine **4.15** (2.15 g, 5.85 mmol, 16% over 2 steps) as a yellow oil.

Data for 4.15: R_f: 0.3 (hexanes:EtOAc 1:1) **¹H-NMR (400 MHz, CDCl₃):** δ (ppm) = 8.12 (s, 1H), 3.27 – 3.13 (m, 1H), 2.87 (dd, J = 10.3, 3.7 Hz, 1H), 2.78 (ddd, J = 12.5, 10.6, 5.9 Hz, 1H), 2.30 – 2.23 (m, 1H), 2.21 (s, 5H), 2.11 – 2.01 (m, 2H), 1.79 – 1.63 (m, 3H), 1.53 – 1.40 (m, 1H), 1.38 – 1.25 (m, 2H), 0.92 (t, J = 7.3 Hz, 3H). **¹³C-NMR (100 MHz, CDCl₃):** δ (ppm) = 173.3, 137.6, 133.0, 131.2, 120.5, 68.6, 57.7, 51.7, 30.8, 29.9, 25.0, 23.6, 20.8, 18.7, 14.3. **IR (ATR):** ν_{max} (cm⁻¹) = 3167 (w), 2933 (m), 2860 (w), 1803 (w),

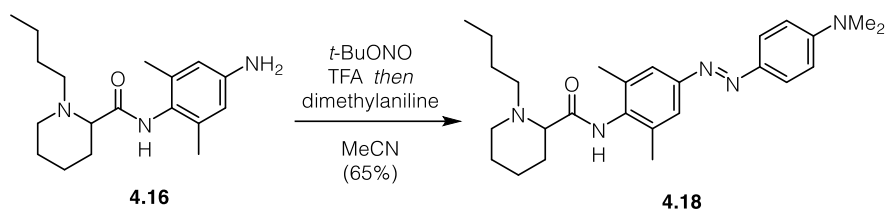
1652 (vs), 1594 (w), 1577 (w), 1526 (m), 1470 (s), 1434 (m), 1404 (w), 1374 (w), 1314 (w), 1287 (w), 1254 (w), 1230 (s), 1126 (w), 1092 (w), 1042 (w), 1012 (w), 998 (w), 967 (w), 945 (w), 879 (w), 864 (s), 853 (s), 808 (m), 774 (m), 731 (m), 716 (w), 702 (w).

HRMS (ESI): calc. for $C_{18}H_{28}ON_2Br$ $[M+H]^+$: 367.1380, found: 367.1357.



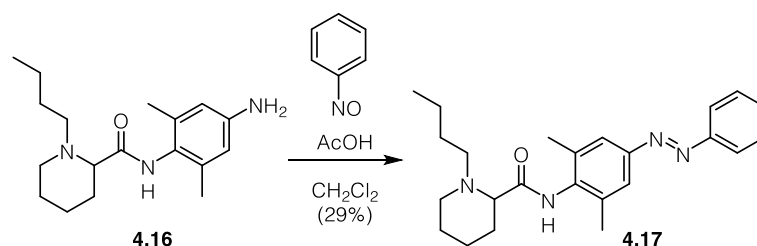
Aniline 4.16: LiHMDS (1.00 M in THF, 12.9 mL, 12.9 mmol) was added to a solution of tertiary amine **4.15** (2.15 g, 5.85 mmol), Pd(*dba*)₂ (168 mg, 0.293 mmol) and Pd(*t*-Bu₃P)₂ (151 mg, 0.293 mmol) in PhMe (14.6 mL) and the reaction was stirred at 60 °C for 20 h. The solution was cooled to room temperature, aqueous HCl (1.00 M, 10.0 mL) was added and the reaction mixture was stirred for 30 min at room temperature. The reaction was diluted with EtOAc, washed with aqueous NaOH (1 M) and brine and dried over MgSO₄. Evaporation of the solvent under reduced pressure and purification of the resulting residue by flash column chromatography (EtOAc:pentane:NEt₃ 100:100:5, R_f=0.2) gave aniline **4.16** (1.72 g, 5.67 mmol, 97%) as a white solid.

Data for 4.16: R_f: 0.2 (pentane:EtOAc:NEt₃ 100:100:5) **¹H-NMR (400 MHz, CDCl₃):** δ (ppm) = 7.97 (s, 1H), 6.39 (s, 2H), 3.37 (s, 0H), 3.23 – 3.14 (m, 1H), 2.89 – 2.74 (m, 2H), 2.27 – 2.17 (m, 1H), 2.13 (s, 6H), 2.08 – 1.96 (m, 2H), 1.78 – 1.57 (m, 2H), 1.53 – 1.39 (m, 1H), 1.36 – 1.26 (m, 1H), 0.90 (t, J = 7.3 Hz, 3H). **¹³C-NMR (100 MHz, CDCl₃):** δ (ppm) = 173.6, 145.4, 136.6, 124.7, 114.9, 68.9, 57.67, 51.9, 31.1, 29.8, 25.1, 23.7, 20.8, 18.9, 14.3. **IR (ATR):** ν_{max} (cm⁻¹) = 3430 (w), 3346 (m), 2952 (m), 2932 (m), 2858 (w), 2812(w), 2784 (w), 1738 (w), 1669 (vs), 1630 (m), 1601 (s), 1496 (s), 1468(m), 1444 (m), 1374 (m), 1344 (m), 1327 (m), 1303 8w), 1271 (w), 1258 (m), 1233 (m), 1219 (m), 1184 8w), 1161 (w), 1136 (w), 1096 (m), 1050 (m), 1030 (m), 990 (w), 960 (w), 941 (w), 885 (w), 865 (w), 542 (m), 786 (w), 733 (w), 670 (w), 678 (w). **HRMS (ESI):** calc. for $C_{18}H_{30}ON_3$ $[M+H]^+$: 304.2383, found: 304.2383.



Dimethylaniline 4.18: TFA (40.0 μL , 0.495 mmol) and *t*-BuONO (240. μl , 0.084 mmol) were sequentially added to an ice cooled solution of aniline **4.16** (50.0 mg, 0.165 mmol) in acetonitrile (5 mL) and the reaction was stirred for 1 h at 0 °C. Dimethylaniline (0.210 mL, 1.65 mmol) was added and the mixture was stirred at room temperature for 1 h. The reaction was diluted with water and extracted with EtOAc. The organic phase was washed with aqueous HCl (1 M), water and brine, dried over MgSO_4 and concentrated under reduced pressure. Purification of the resulting residue by flash column chromatography (pentane:EtOAc 2:1, $R_f=0.3$) gave dimethylaniline **4.18** (47.0 mg, 0.108 mmol, 65%) as a red solid.

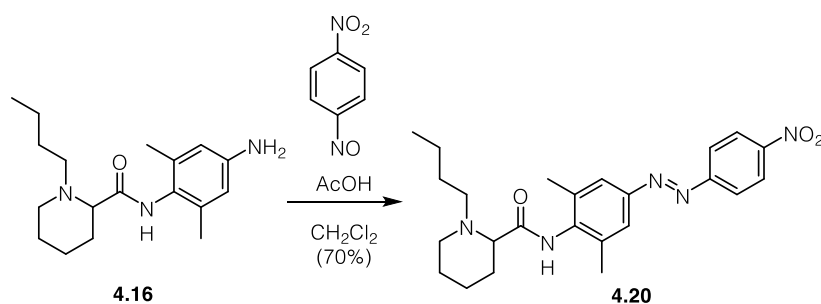
Data for 4.18: R_f : 0.3 (pentane:EtOAc 2:1) **$^1\text{H-NMR}$ (400 MHz, CDCl_3):** δ (ppm) = 8.25 (s, 1H), 7.86 (d, $J = 9.1$ Hz, 2H), 7.58 (s, 2H), 6.75 (d, $J = 9.1$ Hz, 2H), 3.28 – 3.19 (m, 1H), 3.08 (s, 6H), 2.96 – 2.79 (m, 2H), 2.32 (s, 7H), 2.19 – 2.00 (m, 2H), 1.82 – 1.46 (m, 7H), 1.33 (tdd, $J = 24.6, 13.9, 4.7$ Hz, 4H), 0.93 (t, $J = 7.3$ Hz, 3H). **$^{13}\text{C-NMR}$ (100 MHz, CDCl_3):** δ (ppm) = 173.2, 152.5, 151.6, 143.8, 136.0, 135.0, 125.0, 122.2, 111.6, 68.7, 57.7, 51.8, 40.5, 30.8, 23.9, 25.0 23.7, 20.8, 19.1, 18.9, 14.3. **IR (ATR):** ν_{max} (cm^{-1}) = 3260 (w), 2929 (m), 2857 (w), 2811 (w), 1668 (m), 1599 (vs), 1564 (w), 1515 (s), 1485 (s), 1444 (s), 1402 (m), 1360 (s), 1309 (w), 1264 (w), 1149 (vs), 1111 (m), 1054 (w), 1026 (w), 944 (m), 875 (w), 820 (s), 732 (s), 639 (w), 612 (w). **HRMS (ESI):** calc. for $\text{C}_{26}\text{H}_{37}\text{ON}_5$ [$M+H$] $^+$: 436.3072, found: 436.3071.



Azobenzene 4.17: AcOH (0.30 mL) was added to a solution of aniline **4.16** (20.0 mg, 0.066 mmol) and nitrosobenzene (14.0 mg, 0.131 mmol) in CH_2Cl_2 (4 mL) and the

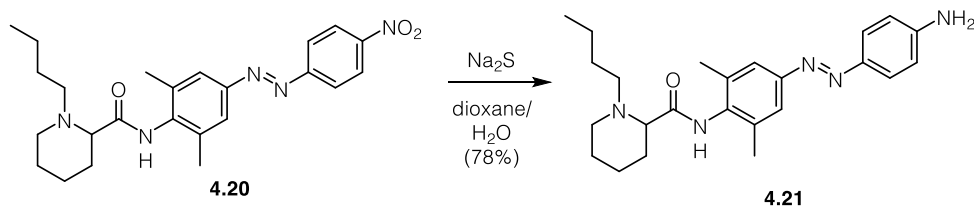
solution was stirred at room temperature for 24 h. The reaction was diluted with EtOAc, washed with NaHCO₃ and brine and dried over MgSO₄. Removal of the solvent under reduced pressure followed by purification of the resultant residue by flash column chromatography (hexanes:EtOAc 1:1, R_f=0.2) gave azobenzene **4.17** (7.4 mg, 0.019 mmol, 29%) as an orange solid.

Data for 4.17: R_f: 0.2 (hexanes :EtOAc 1:1) **¹H-NMR (400 MHz, CDCl₃):** δ (ppm) = 8.31 (s, 1H), 7.94 – 7.85 (m, 2H), 7.67 (s, 2H), 7.50 (dt, J = 13.6, 7.0 Hz, 3H), 3.22 (d, J = 11.8 Hz, 1H), 2.91 (dd, J = 10.2, 3.6 Hz, 1H), 2.83 (td, J = 11.6, 5.8 Hz, 1H), 2.35 (s, 6H), 2.31 – 2.24 (m, 1H), 2.16 – 2.06 (m, 2H), 1.82 – 1.70 (m, 3H), 1.65 (tq, J = 8.9, 5.1, 4.5 Hz, 1H), 1.51 (ddd, J = 12.1, 8.9, 3.7 Hz, 2H), 1.42 – 1.28 (m, 3H), 0.94 (t, J = 7.3 Hz, 3H). **¹³C-NMR (100 MHz, CDCl₃):** δ (ppm) = 173.2, 152.8, 151.0, 136.5, 136.2, 131.0, 129.2, 122.9, 122.9, 68.6, 57.7, 51.7, 30.7, 23.9, 25.0, 23.6, 20.9, 19.2. **IR (ATR):** ν_{max} (cm⁻¹) = 2244 (m), 2932 (s), 2858 (w), 2812 (w), 1666 (s), 1301 (w), 1482 (vs), 1416 (w), 1376 (w), 1311 (w), 1291 (w), 1258 (w), 1236 (w), 1185 (w), 1149 (w), 118 (w), 1097 (w), 1054 (w), 1041 (w), 1021 (w), 922 (w), 877 (m), 826 (w), 768 (s), 711 (w), 689 (w). **HRMS (ESI):** calc. for C₂₄H₃₂ON₄ [M+H]⁺: 393.2650, found: 393.2649.



Nitrobenzene **4.20**: A solution of aniline **4.16** (1.20 g, 3.95 mmol) and *p*-nitro-nitrosobenzene (901 mg, 5.93 mmol) in CH₂Cl₂ (70 mL) and AcOH (3.7 mL) was stirred at room temperature for 24 h before it was quenched with NaHCO₃. The mixture was extracted with CH₂Cl₂, the organic phase was dried over MgSO₄ and concentrated under reduced pressure. Purification of the resultant residue by flash column chromatography (CH₂Cl₂:MeOH 99:1 to 98:2, R_f=0.3) gave nitrobenzene **4.20** (1.21 g, 2.77 mmol, 70%) as a red solid.

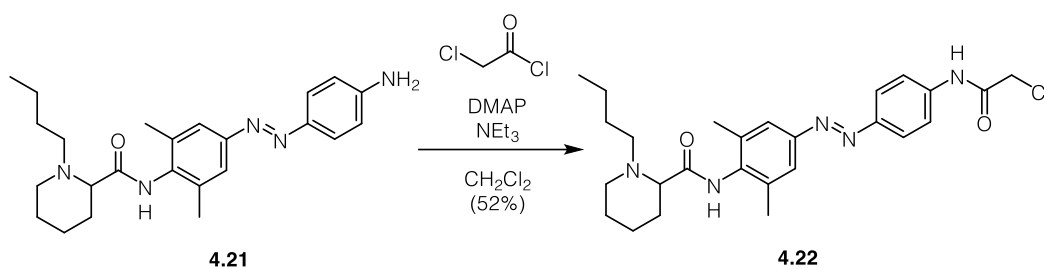
Data for 4.20: R_f : 0.3 (CH₂Cl₂:MeOH 98:2) **¹H-NMR (400 MHz, CDCl₃):** δ (ppm) = 8.42 – 8.30 (m, 3H), 7.99 (d, J = 8.7 Hz, 2H), 7.69 (s, 2H), 3.21 (dt, J = 12.1, 3.8 Hz, 1H), 2.92 (dd, J = 10.0, 3.6 Hz, 1H), 2.81 (ddd, J = 12.5, 10.7, 5.8 Hz, 1H), 2.35 (s, 7H), 2.09 (td, J = 11.4, 2.8 Hz, 2H), 1.83 – 1.69 (m, 3H), 1.64 (tt, J = 10.5, 5.6 Hz, 1H), 1.58 – 1.45 (m, 2H), 1.43 – 1.28 (m, 3H), 0.93 (t, J = 7.3 Hz, 3H). **¹³C-NMR (100 MHz, CDCl₃):** δ (ppm) = 173.07, 155.81, 150.66, 148.61, 138.00, 136.35, 124.79, 123.45, 123.44, 68.44, 57.66, 51.61, 30.52, 29.86, 24.84, 23.52, 20.82, 19.13, 14.28. **IR (ATR):** ν_{max} (cm⁻¹) = 3250 (w), 2934 (m), 2860 (w), 2814 (w), 1670 (m), 1607 (w), 1590 (w), 1523 (s), 1482 (m), 1457 (m), 1418 (w), 1378 (w), 1343 (vs), 1296 (w), 1235 (w), 1184 (w), 1122 (w), 1107 (w), 1054 (w), 1008 (w), 963 (w), 878 (w), 861 (w), 826 (w), 156 (w), 732 (w), 690 (w), 713 (w), 666 (w). **HRMS (ESI):** calc. for C₂₄H₃₂O₃N₅ [$M+H$]⁺: 438.2500, found: 483.2499.



Aniline 4.21: A solution of azobenzene **4.20** (1.21 g, 2.77 mmol) and Na₂Sx9H₂O (531 mg, 5.55 mmol) in 1,4-dioxane (19.5 mL) and H₂O (19.5 mL) was stirred at 90 °C for 2 h. After cooling to room temperature, the reaction was extracted with EtOAc and the organic phase was washed with aqueous NaOH (1 M) and brine and dried over MgSO₄. Removal of the solvent under reduced pressure and purification of the resultant residue by flash column chromatography (CH₂Cl₂:MeOH 98:2 to 97:3, R_f =0.3) gave aniline **4.21** (886 mg, 2.17 mmol, 78%) as a red solid.

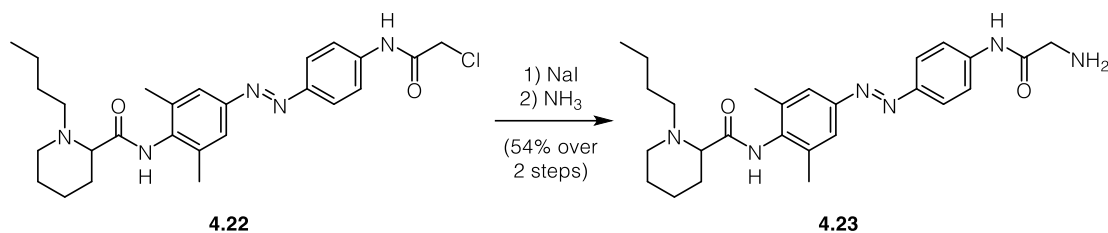
Data for 4.21: R_f : 0.3 (CH₂Cl₂:MeOH 97:3) **¹H-NMR (400 MHz, CDCl₃):** δ (ppm) = 7.80 (d, J = 8.4 Hz, 2H), 7.60 (s, 2H), 6.73 (d, J = 8.6 Hz, 2H), 4.10 (s, 2H), 3.24 (dt, J = 11.9, 3.7 Hz, 1H), 2.97 – 2.80 (m, 2H), 2.35 (s, 7H), 2.17 – 2.04 (m, 2H), 1.83 – 1.71 (m, 3H), 1.70 – 1.61 (m, 1H), 1.59 – 1.47 (m, 2H), 1.42 – 1.29 (m, 3H), 0.95 (t, J = 7.3 Hz, 3H). **¹³C-NMR (100 MHz, CDCl₃):** δ (ppm) = 173.20, 151.34, 149.71, 145.58, 136.05, 135.31, 125.13, 122.31, 114.70, 68.66, 57.72, 51.72, 30.76, 29.89, 24.97, 23.62, 20.82, 19.11, 14.31. **IR (ATR):** ν_{max} (cm⁻¹) = 3340 (m), 3223 (w), 2933 (m), 2858 (w), 2814 (w), 1668

(m), 1624 (m), 1599 (vs), 1505 (s), 1489 (s), 1460 (m), 1428 (m), 1378 (w), 1300 (m), 1212 (m), 1184 (w), 1145 (s), 1115 (m), 1097 (m), 1053 (w), 1027 (w), 960 (w), 876 (w), 836 (m), 735 (w), 701 (w). **HRMS (ESI):** calc. for $C_{24}H_{34}ON_5$ $[M+H]^+$: 408.2758, found: 408.2759.



Chloride 4.22: NEt_3 (0.49 mL, 3.58 mmol) and chloroacetyl chloride (0.122 mL, 1.55 mmol) were sequentially added to an ice cooled solution of aniline **4.21** (486 mg, 1.19 mmol) and DMAP (10 mg, 0.082 mmol) in CH_2Cl_2 and the solution was stirred for 10 min at 0 °C and for 3 h at room temperature. The mixture was diluted with EtOAc and washed with $NaHCO_3$ and brine, dried over $MgSO_4$ and concentrated under reduced pressure. Purification of the resultant residue by flash column chromatography (CH_2Cl_2 :MeOH 96:4, R_f = 0.3) gave chloride **4.22** (300 mg, 0.620 mmol, 52%) as a red solid.

Data for 4.22: R_f : 0.3 (CH_2Cl_2 :MeOH 96:4) **1H -NMR (400 MHz, $CDCl_3$):** δ (ppm) = 8.78 (s, 1H), 8.44 (s, 1H), 7.80 (d, J = 8.7 Hz, 2H), 7.63 – 7.51 (m, 4H), 4.20 (s, 2H), 3.23 (dt, J = 12.1, 3.9 Hz, 1H), 2.95 (dd, J = 10.0, 3.7 Hz, 1H), 2.91 – 2.79 (m, 1H), 2.33 (s, 7H), 2.15 – 2.07 (m, 2H), 1.84 – 1.70 (m, 3H), 1.70 – 1.60 (m, 1H), 1.51 (td, J = 10.5, 9.4, 5.4 Hz, 2H), 1.36 (tdd, J = 16.6, 11.1, 8.1 Hz, 3H), 0.94 (t, J = 7.3 Hz, 3H). **^{13}C -NMR (100 MHz, $CDCl_3$):** δ (ppm) = 173.6, 164.4, 151.2, 149.4, 139.6, 136.3, 136.1, 124.0, 122.8, 120.1, 68.5, 57.7, 51.7, 43.2, 30.5, 29.9, 24.8, 23.6, 20.8, 19.1, 14.3. **IR (ATR):** ν_{max} (cm^{-1}) = 3269 (w), 3199(w), 3030 (w), 3070 (w), 2934 (w), 2860 (w), 2815 (w), 1659 (s), 1596 (s), 1545 (s), 1501 (s), 1408 (m), 1377 (w), 1330 (m), 1296 (w), 1272 (w), 1250 (m), 1186 (w), 1151 (m), 1109 (w), 1097 (w), 1054 (w), 1029 (w), 1013 (w), 963 (w), 907 (m), 878 (w), 846 (M), 778 (w), 728 (vs), 686 (w). **HRMS (ESI):** calc. for $C_{26}H_{35}O_2N_5Cl$ $[M+H]^+$: 484.2479, found: 484.2474.

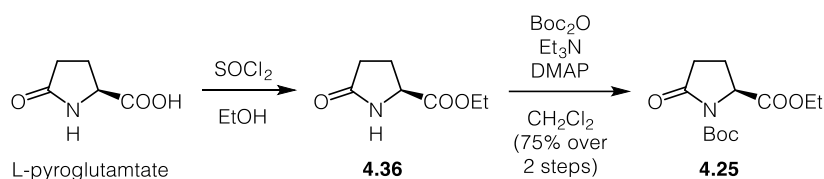


Amine 4.23: A suspension of chloride **4.22** (296 mg, 0.612 mmol) and NaI (137 mg, 0.917 mmol) in acetone (16 mL) was stirred for at room temperature in the dark overnight. The reaction mixture was washed with H₂O, dried over MgSO₄ and concentrated under reduced pressure to give iodide **S4.1** which was used in the next step without further purification.

NH₃ (7 M in MeOH, 1.4 mL, 9.80 mmol) was slowly added to an ice cooled solution of iodide **S4.1** in THF (4.3 mL) and the resulting solution was stirred for 15 min at 0 °C and for 4 h at room temperature. The reaction was diluted with EtOAc, washed with H₂O and brine, dried over MgSO₄ and concentrated under reduced pressure. Purification of the resultant residue by reverse phase column chromatography (MeCN:aqHCl (0.1 M) gave amine **4.23** (153 mg, 0.329 mmol, 77%) as a red solid.

Data for 4.23: ¹H-NMR (400 MHz, *d*₄-MeOH): δ (ppm) = 7.92 (d, *J* = 8.7 Hz, 2H), 7.82 (d, *J* = 8.6 Hz, 2H), 7.67 (s, 2H), 4.35 – 4.25 (m, 1H), 3.94 (s, 2H), 3.70 (d, *J* = 12.4 Hz, 1H), 3.21 (dd, *J* = 14.8, 9.1 Hz, 2H), 2.46 (d, *J* = 12.7 Hz, 1H), 2.34 (s, 6H), 2.15 (s, 1H), 2.04 – 1.72 (m, 7H), 1.42 (q, *J* = 7.4 Hz, 2H), 1.29 (s, 2H), 1.00 (t, *J* = 7.3 Hz, 3H). **¹³C-NMR (100 MHz, *d*₄-MeOH):** δ (ppm) = 168.4, 165.8, 152.8, 150.3, 142.2, 137.7, 136.54, 124.9, 123.4, 121.0, 67.3, 57.4, 53.3, 42.4, 30.6, 26.8, 23.8, 22.6, 21.0, 18.9, 13.9. **IR (ATR):** ν_{max} (cm⁻¹) = 2956(s), 2872 (m), 1685 (s), 1596 (s), 1547 (vs), 1501 (s), 1475 (m), 1410 (m), 1303 (s), 1255 (s), 1208 (m), 1151 (s), 1026 (m), 936 (m), 899 (m), 846 (s), 707 (m). **HRMS (ESI):** calc. for C₂₆H₃₇O₂N₆ [*M+H*]⁺: 465.2973, found: 465.7979.

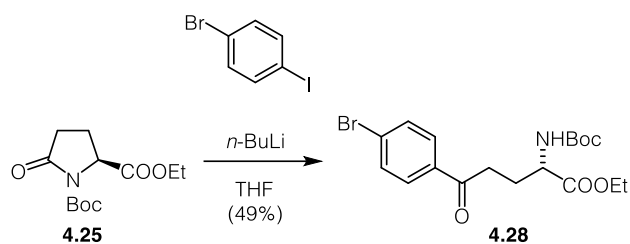
6.5.3 Photoswitches based on raxatrigine



Pyroglutamate 4.25: SOCl_2 (55.6 mL, 775 mmol) was added slowly to an ice cooled solution of L-pyroglutamate (25.0 g, 194 mmol) in EtOH (360 mL) and the reaction was stirred at room temperature for 3 h. The reaction mixture was slowly quenched with saturated aqueous NaHCO_3 and extracted with CH_2Cl_2 . The combined organic phases were dried over MgSO_4 and concentrated under reduced pressure to give crude ethyl ester **4.36** (27.2 g) which was used in the next step without further purification.

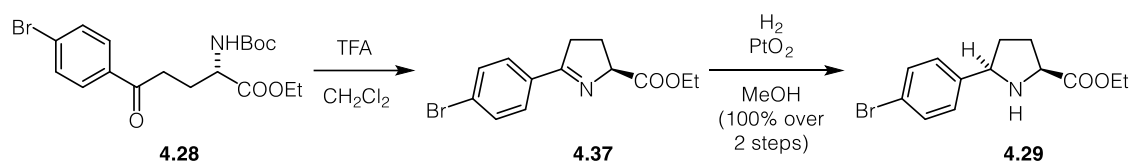
A solution of crude ethyl ester **4.36** (27.2 g), DMAP (21.1 g, 173 mmol), NEt_3 (24.0 mL, 173 mmol) and di-*tert*-butyldicarbonate (75.5 g, 346 mmol) in CH_2Cl_2 (370 mL) was stirred at room temperature overnight. The reaction mixture was washed with aqueous citric acid (10%) and brine, dried over MgSO_4 and concentrated under reduced pressure. Purification of the resulting residue by flash column chromatography (hexanes:EtOAc 3:2, $R_f = 0.4$) gave pyroglutamate **4.25** (37.5 g, 146 mmol, 75% over 2 steps) as colorless oil.

Data for 4.25: $^1\text{H-NMR}$ (400 MHz, CDCl_3): δ (ppm) = 4.55 (dd, $J = 9.5, 2.9$ Hz, 1H), 4.19 (q, $J = 7.1$ Hz, 2H), 2.58 (ddd, $J = 17.5, 10.2, 9.6$ Hz, 1H), 2.44 (ddd, $J = 17.4, 9.4, 3.5$ Hz, 1H), 2.28 (ddt, $J = 13.4, 10.3, 9.4$ Hz, 1H), 2.02 – 1.94 (m, 1H), 1.44 (s, 9H), 1.25 (t, $J = 7.1$ Hz, 3H). $^{13}\text{C-NMR}$ (100 MHz, CDCl_3): δ (ppm) = 173.7, 171.7, 149.6, 83.8, 62.0, 59.3, 3.5, 28.2, 21.9, 14.5. **IR (ATR):** ν_{max} (cm^{-1}) = 2981 (W), 1791 (S), 1742 (S), 1715 (S), 1477 (W), 1460 (W), 1394 (W), 1369 (M), 1359 (W), 1307 (S), 1285 (S), 1255 (S), 1189 (S), 1144 (VS), 1097 (W), 1043 (M), 1019 (S), 960 (W), 913 (W), 880 (W), 843 (M), 820 (W), 777 (M), 747 (M), 720 (W). **HRMS (ESI):** calc. for $\text{C}_{12}\text{H}_{20}\text{NO}_5$ $[M+H]^+$: 258.1336, found: 258.1331. $[\alpha]_D^{25} = -41.2$ (CHCl_3).



Ketone 4.28: *n*-BuLi (2.30 M in hexanes, 3.36 mL, 7.77 mmol) was added to a solution of 1-bromo-4-iodobenzene (2.74 g, 7.77 mmol) in THF (20 mL) at $-78\text{ }^{\circ}\text{C}$ and the reaction was stirred at that temperature for 1 h. The resulting solution was slowly added to a solution of pyroglutamate **4.25** (2.00 g, 7.77 mmol) in THF (20 mL) at $-78\text{ }^{\circ}\text{C}$ and the reaction was stirred at that temperature for 3 h. The reaction mixture was quenched with saturate aqueous NH_4Cl , diluted with H_2O and extracted with EtOAc. The combined organic phases were dried over MgSO_4 and concentrated under reduced pressure. Purification of the resulting residue by flash column chromatography (hexanes:EtOAc 5:1, $R_f = 0.3$) gave ketone **4.28** (1.59 g, 3.85 mmol, 50%) as a colorless solid.

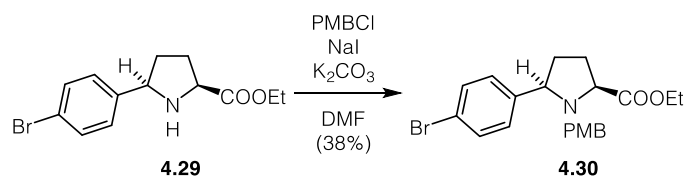
Data for 4.28: $^1\text{H-NMR}$ (400 MHz, CDCl_3): δ (ppm) = 7.81 (d, $J = 8.6$ Hz, 2H), 7.60 (d, $J = 8.4$ Hz, 2H), 5.15 (d, $J = 8.4$ Hz, 1H), 4.40 – 4.28 (m, 1H), 4.20 (q, $J = 7.1$ Hz, 2H), 3.14 – 2.95 (m, 2H), 2.35 – 2.26 (m, 1H), 2.05 (dtd, 14.3, 8.5, 5.9 Hz, 1H), 1.41 (s, 10H), 1.26 (t, $J = 7.2$ Hz, 3H). $^{13}\text{C-NMR}$ (100 MHz, CDCl_3): δ (ppm) = 198.3, 172.8, 155.9, 135.8, 132.4, 130.0, 126.6, 80.5, 62.0, 53.5, 35.0, 28.7, 27.5, 14.6. **IR (ATR):** ν_{max} (cm^{-1}) = 3365 (VW), 2979 (W), 2934 (W), 1709 (S), 1687 (S), 1586 (M), 1569 (W), 1504 (M), 1448 (M), 1393 (M), 1366 (S), 1348 (M), 1300 (M), 1249 (M), 1205 (S), 1161 (VS), 1114 (W), 1095 (M), 1070 (S), 1049 (M), 1026 (S), 1009 (S), 988 (M), 859 (W), 815 (M), 779 (M), 735 (S), 702 (M), 658 (W). **HRMS (ESI):** calc. for $\text{C}_{18}\text{H}_{25}\text{BrNO}_5$ [$M+H$] $^+$: 414.0911, found: 414.0916. $[\alpha]_D^{25} = +4.2$ (CHCl_3).



Pyrrolidine 4.29: TFA (4.07 mL, 53.2 mmol) was added dropwise to an ice cooled solution ketone **4.28** (1.46 g, 3.54 mmol) in CH_2Cl_2 (30 mL) and the reaction was allowed to warm to room temperature over 90 min. Evaporation of the volatiles under reduced pressure gave crude imine **4.37** as yellow oil which was used in the next step without further purification.

A suspension of crude imine **4.37** and PtO₂ (17 mg, 1.16w%) in MeOH was stirred under H₂-atmosphere overnight, filtered over a pad of celite and concentrated under reduced pressure. Purification of the resulting residue by flash column chromatography (hexanes:EtOAc 1:2-1.4) gave pyrrolidine **4.29** (1.07 g, 3.60 mmol, 100%) as a colorless solid.

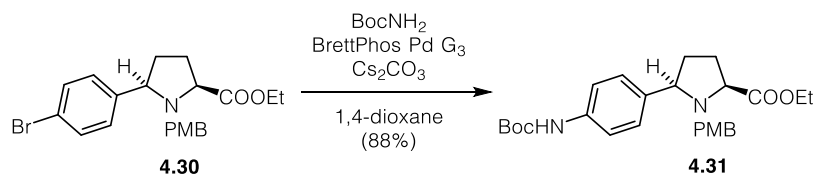
Data for 4.29: R_f: 0.5 (hexanes:EtOAc 1:2) **¹H-NMR (400 MHz, CDCl₃):** δ (ppm) = 9.73 (s, 2H), 7.55 (d, *J* = 8.1 Hz, 2H), 7.36 (d, *J* = 8.2 Hz, 2H), 4.84 – 4.78 (m, 1H), 4.62 – 4.56 (m, 1H), 4.29 (q, *J* = 7.2 Hz, 2H), 2.58 (s, 1H), 2.44 – 2.39 (m, 2H), 2.13 (dt, *J* = 12.3, 6.0 Hz, 1H), 1.33 (t, *J* = 7.2 Hz, 3H). **¹³C-NMR (100 MHz, CDCl₃):** δ (ppm) = 170.2, 132.8, 132.3, 129.2, 123.8, 63.5, 63.0, 59.0, 30.4, 28.9, 13.7. **IR (ATR):** ν_{max} (cm⁻¹) = 2968 (W), 1746 (M), 1718 (W), 1655 (S), 1637 (M), 1577 (W), 1559 (W), 1490 (W), 1466 (W), 1457 (W), 1433 (M), 1381 (W), 1305 (W), 1297 (W), 1235 (W), 1196 (S), 1170 (S), 1135 (VS), 1096 (M), 1084 (M), 1073 (M), 1061 (M), 1024 (W), 1012 (M), 988 (W), 853 (W), 835 (M), 816 (M), 796 (S), 720 (S), 698 (W), 686 (W). **HRMS (EI):** calc. for C₁₃H₁₆BrNO₂ [*M*]⁺: 297.0359, found: 297.0360. [α]_D²⁵ = -12.6 (CHCl₃).



Benzylamide 4.30: PMB-Cl (0.60 mL, 4.47 mmol) was added dropwise to a suspension of pyrrolidine **4.29** (1.02 g, 3.44 mmol), K₂CO₃ (713 mg, 5.16 mmol) and NaI (155 mg, 1.03 mmol) in DMF (20 mL) and the reaction was stirred at room temperature overnight. The resulting solution was diluted with H₂O and extracted with EtOAc. The combined organic phases were washed with brine, dried over MgSO₄ and concentrated under reduced pressure. Purification of the resulting residue by flash column chromatography (hexanes:EtOAc 10:1, R_f = 0.4) gave benzylamide **4.30** (547 mg, 1.31 mmol, 38%) as a colorless oil.

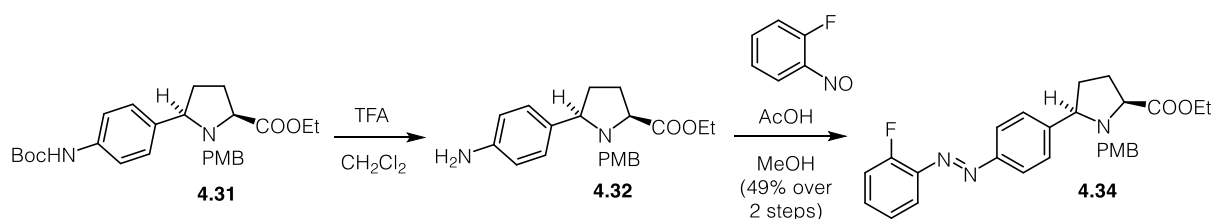
Data for 4.30: **¹H-NMR (400 MHz, CDCl₃):** δ (ppm) = 7.48 – 7.42 (m, 4H), 7.08 (d, *J* = 8.5 Hz, 2H), 6.78 (d, *J* = 8.9 Hz, 2H), 3.97 (qd, *J* = 7.1, 1.2 Hz, 2H), 3.81 (d, *J* = 5.7 Hz, 1H), 3.77 (s, 3H), 3.72 (dd, *J* = 9.5, 5.8 Hz, 1H), 3.46 – 3.41 (m, 2H), 2.12 – 1.91 (m, 3H), 1.87 – 1.75 (m, 1H), 1.17 (t, *J* = 7.2 Hz, 3H). **¹³C-NMR (100 MHz, CDCl₃):** δ (ppm) = 174.7, 160.7, 142.6, 131.3, 130.5, 129.4, 129.2, 120.5, 113.1, 67.9,

64.2, 60.2, 55.4, 55.0, 35.2, 28.8, 14.0. **IR (ATR):** ν_{\max} (cm⁻¹) = 2956 (W), 2835 (W), 1725 (S), 1611 (M), 1586 (W), 1511 (VS), 1486 (M), 1464 (M), 1442 (M), 1408 (W), 1370 (W), 1353 (W), 1301 (M), 1246 (VS), 1216 (M), 1170 (VS), 1106 (M), 1096 (M), 1069 (M), 1033 (S), 1010 (S), 819 (VS), 757 (M), 716 (W), 703 (W). **HRMS (EI):** calc. for C₂₁H₂₄BrNO₃ [M]⁺: 417.0934, found: 417.0946. $[\alpha]_D^{25} = +24.8$ (CHCl₃).



Carbamate 4.31: BrettPhos Pd G3 (15.7 mg, 0.02 mmol), BrettPhos (14.7 mg, 0.02), *t*-butylcarbamate, Cs₂CO₃ and benzylamide **4.30** (360 mg, 0.86 mmol) were suspended in degassed 1,4-dioxane and submitted to three additional freeze-pump-thaw cycles. The reaction was stirred at 100 °C overnight, filtered over a pad of celite and concentrated under reduced pressure. Purification of the resulting residue by flash column chromatography (hexanes:EtOAc 6:1, R_f = 0.3) gave carbamate **4.31** (344 mg, 0.76 mmol, 88%) as a yellowish oil.

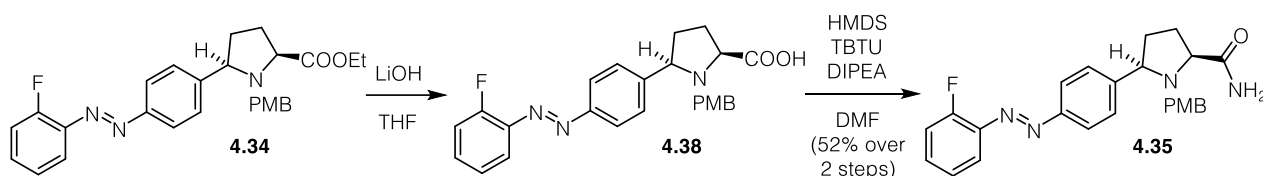
Data for 4.31: ¹H-NMR (400 MHz, CDCl₃): δ (ppm) = 7.48 (d, *J* = 8.1 Hz, 2H), 7.34 (d, *J* = 8.1 Hz, 2H), 7.08 (d, *J* = 8.2 Hz, 2H), 6.79 – 6.74 (m, 2H), 3.94 (q, *J* = 6.9 Hz, 2H), 3.83 – 3.78 (m, 1H), 3.77 (s, 3H), 3.68 (dd, *J* = 9.5, 5.5 Hz, 1H), 3.42 – 3.34 (m, 2H), 2.11 – 1.99 (m, 2H), 1.99 – 1.89 (m, 1H), 1.88 – 1.72 (m, 1H), 1.52 (s, 9H), 1.16 (t, *J* = 7.1 Hz, 3H). ¹³C-NMR (100 MHz, CDCl₃): δ (ppm) = 175.5, 159.0, 153.3, 138.6, 137.7, 131.2, 130.2, 128.7, 119.2, 113.7, 80.9, 77.7, 68.6, 64.8, 60.8, 55.7, 35.7, 29.4, 28.8, 14.6. **IR (ATR):** ν_{\max} (cm⁻¹) = 3343 (VW), 2977 (W), 1708 (S), 1612 (M), 1597 (W), 1558 (VW), 1525 (M), 1511 (S), 1464 (W), 1457 (W), 1444 (W), 1414 (M), 1392 (W), 1366 (M), 1312 (M), 1233 (S), 1156 (VS), 1110 (M), 1104 (M), 1050 (M), 1028 (M), 1017 (M), 902 (W), 836 (M), 822 (M), 766 (W). **HRMS (EI):** calc. for C₂₆H₃₄N₂O₅ [M]⁺: 454.2462, found: 454.2475. $[\alpha]_D^{25} = +18.7$ (CHCl₃).



Azobenzene 4.34: TFA (4.07 mL, 53.2 mmol) was added dropwise to an ice cooled solution of carbamate **4.31** (290 mg, 0.64 mmol) and anisole (2.08 mL, 19.2 mmol) in CH_2Cl_2 (30 mL) and the reaction was allowed to warm to room temperature over 2.5 h. The volatiles were removed under reduced pressure and the resulting residue was purified by flash column chromatography (CH_2Cl_2 :MeOH 96:4-94:6) gave crude aniline **4.32** (310 mg) that was used in the next step without further purification.

AcOH (0.3 mL) was added to a solution of crude aniline **4.32** (310 mg) and 1-fluoro-2-nitrosobenzene (130 mg, 1.05 mmol) in MeOH (10 mL) and the reaction was stirred at room temperature overnight. The volatiles were removed under reduced pressure, the resulting residue was redissolved in EtOAc and washed with saturated aqueous NaHCO_3 and brine. The organic phase was dried over MgSO_4 and concentrated under reduced pressure. Purification of the resulting residue by flash column chromatography (hexanes:EtOAc 8:1, $R_f = 0.3$) gave azobenzene **4.34** (144 mg, 0.31 mmol, 49%) as an orange oil. The resulting product is in a light driven equilibrium with its double bond isomer.

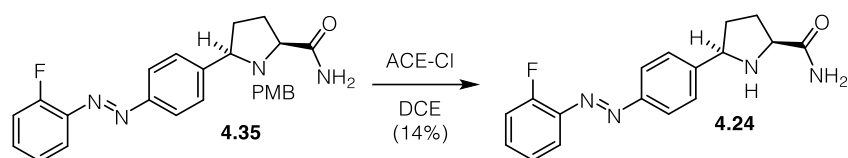
Data for 4.34: $^1\text{H-NMR}$ (400 MHz, CDCl_3): δ (ppm) = 7.94 (dd, $J = 8.7, 2.1$ Hz, 2H), 7.81 – 7.75 (m, 1H), 7.73 (d, $J = 8.4$ Hz, 2H), 7.26 – 7.19 (m, 1H), 7.12 (d, $J = 8.6$ Hz, 2H), 7.05 – 6.98 (m, 1H), 6.94 – 6.89 (m, 1H), 6.79 (d, $J = 8.6$ Hz, 2H), 3.99 (q, $J = 7.1$ Hz, 2H), 3.87 – 3.84 (m, 1H), 3.77 (s, 3H), 3.74 – 3.67 (m, 1H), 3.52 – 3.45 (m, 2H), 2.21 – 1.73 (m, 4H), 1.19 (t, $J = 7.1$ Hz, 3H). $^{13}\text{C-NMR}$ (100 MHz, CDCl_3): δ (ppm) = 175.3, 161.7, 159.2, 159.1, 152.7, 148.2, 141.2, 132.7, 132.6, 131.1, 128.7, 124.7, 123.7, 120.9, 118.2, 117.56, 117.4, 113.78, 68.9, 65.0, 60.9, 56.2, 55.7, 35.8, 29.5, 14.6. **IR (ATR):** ν_{max} (cm^{-1}) = 2953 (W), 2835 (W), 2361 (VW), 1727 (M), 1701 (W), 1684 (VW), 1654 (VW), 1604 (M), 1587 (W), 1559 (VW), 1540 (VW), 1511 (S), 1496 (M), 1483 (M), 1464 (M), 1458 (M), 1441 (M), 1419 (W), 1394 (VW), 1370 (W), 1349 (W), 1301 (M), 1266 (M), 1246 (S), 1227 (S), 1174 (S), 1149 (S), 1128 (S), 1102 (S), 1069 (W), 1032 (S), 1012 (M), 947 (W), 912 (VW), 892 (VW), 845 (S), 820 (M), 757 (VS), 722 (W), 659 (VW). **HRMS (EI):** calc. for $\text{C}_{27}\text{H}_{27}\text{FN}_3\text{O}_3$ [M] $^+$: 461.2109, found: 461.2117. $[\alpha]_D^{25} = +11.9$ (CHCl_3).



Amide 4.35: A solution of azobenzene **4.34** (111 mg, 0.24 mmol) and LiOH·H₂O (200 mg, 4.80 mmol) in THF (1.5 mL), H₂O (0.7 mL) and MeOH (0.7 mL) was stirred at room temperature for 2.5 h. The reaction was acidified with aqueous HCl (1 M) and extracted with EtOAc. The combined organic phases were dried over MgSO₄ and concentrated under reduced pressure to give crude acid **4.38** (103 mg) which was used in the next step without further purification.

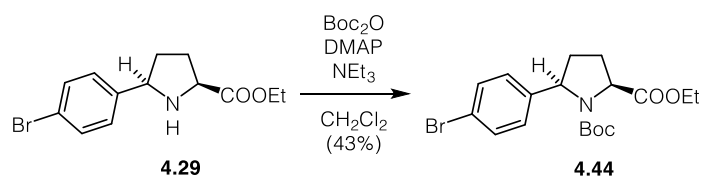
DIPEA (0.08 mL, 0.36 mmol) was added to a stirred solution of crude acid **4.38** (103 mg) and TBTU (84.0 mg, 0.26 mmol) in DMF (3 mL) and the reaction was stirred for 30 min at room temperature. HMDS (0.07 mL, 0.360 mmol) was added to the solution and the reaction was stirred 2 h at room temperature before saturated aqueous NaHCO₃ (3 mL) was added and the reaction was stirred at room temperature for 30 min. The resulting solution was diluted with H₂O and extracted with EtOAc. The combined organic phases were washed with brine, dried over MgSO₄ and concentrated under reduced pressure. Purification of the resulting residue by flash column chromatography (hexanes:EtOAc 1:6, R_f = 0.2) gave amide **4.35** (54 mg, 0.13 mmol, 52%) as an orange oil. The resulting product is in a light driven equilibrium with its double bond isomer.

Data for 4.35: ¹H-NMR (400 MHz, CDCl₃): δ (ppm) = 7.97 (d, *J* = 8.4 Hz, 2H), 7.78 (td, *J* = 7.8, 1.8 Hz, 1H), 7.56 (d, *J* = 8.4 Hz, 2H), 7.50 – 7.43 (m, 1H), 7.03 (d, *J* = 8.4 Hz, 2H), 6.96 – 6.88 (m, 1H), 6.80 (d, *J* = 8.4 Hz, 2H), 6.78 – 6.73 (m, 1H), 5.16 (s, 1H), 3.88 (dd, *J* = 10.4, 5.6 Hz, 1H), 3.77 (s, 3H), 3.76 – 3.63 (m, 1H), 3.53 – 3.46 (m, 2H), 2.35 – 2.23 (m, 1H), 2.22 – 1.96 (m, 2H), 1.85 – 1.69 (m, 1H). ¹³C-NMR (100 MHz, CDCl₃): δ (ppm) = IR (ATR): ν_{max} (cm⁻¹) = 3517 (W), 3398 (W), 3074 (VW), 3035 (W), 3014 (VW), 2961 (W), 2945 (W), 2923 (W), 2878 (W), 2870 (W), 2840 (W), 1685 (VS), 1654 (W), 1647 (W), 1637 (W), 1611 (M), 1602 (M), 1585 (M), 1550 (M), 1513 (S), 1499 (W), 1482 (S), 1464 (M), 1457 (M), 1449 (M), 1440 (M), 1419 (W), 1371 (M), 1320 (W), 1302 (W), 1278 (W), 1266 (M), 1249 (VS), 1214 (S), 1178 (M), 1150 (M), 1133 (M), 1122 (M), 1109 (M), 1102 (M), 1067 (W), 1031 (S), 1010 (M), 990 (W), 957 (W), 942 (W), 922 (W), 859 (M), 845 (S), 820 (S), 788 (W), 768 (VS), 740 (M), 719 (W). HRMS (EI): calc. for C₂₅H₂₅FN₄O₂ [M]⁺: 258.1336, found: 432.1958. [α]_D²⁵ = +44.3 (CHCl₃).



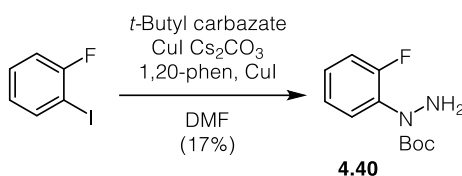
Azoraxatrigine 4.24: *o*-Chloroethylchloroformate (0,13 mL, 1.16 mmol) was added dropwise to a stirred solution of amide **4.35** (50 mg, 0.12 mmol) and the resulting solution was stirred at 80 °C for 6 h. The volatiles were removed under reduced pressure and the resulting residue was portioned between EtOAc and brine. Concentration of the organic phase under reduced pressure and purification of the resulting residue by flash column chromatography (CH₂Cl₂:MeOH 98:2-92:8) gave azoraxatrigine **4.24** (5.0 mg, 0.02 mmol, 14%) as an orange solid. The resulting product is in a light driven equilibrium with its double bond isomer. The major trans isomer is described.

Data for 4.24: ¹H-NMR (400 MHz, CDCl₃): δ (ppm) = 7.93 (d, *J* = 8.0 Hz, 2H), 7.76 (td, *J* = 7.8, 1.8 Hz, 1H), 7.54 (d, *J* = 8.0 Hz, 2H), 7.49 – 7.40 (m, 1H), 7.28 (d, *J* = 9.0 Hz, 1H), 6.89 (d, *J* = 9.0 Hz, 1H), 5.52 (d, *J* = 19.5 Hz, 1H), 4.44 (dd, *J* = 9.9, 5.8 Hz, 1H), 3.94 (dd, *J* = 10.0, 3.8 Hz, 1H), 2.40 – 2.27 (m, 1H), 2.27 – 2.08 (m, 2H), 1.75 – 1.66 (m, 1H). **IR (ATR):** ν_{\max} (cm⁻¹) = 3426 (W), 3322 (W), 3196 (W), 3064 (W), 2955 (M), 2924 (S), 2853 (M), 1737 (W), 1676 (VS), 1604 (M), 1589 (M), 1511 (W), 1500 (W), 1483 (M), 1464 (W), 1442 (W), 1413 (W), 1377 (W), 1366 (W), 1303 (W), 1267 (M), 1226 (M), 1151 (W), 1102 (M), 1029 (VW), 1013 (VW), 845 (W), 831 (W), 760 (M). **HRMS (ESI):** calc. for C₁₇H₁₇FN₄O [*M+H*]⁺: 313.1459, found: 313.1460



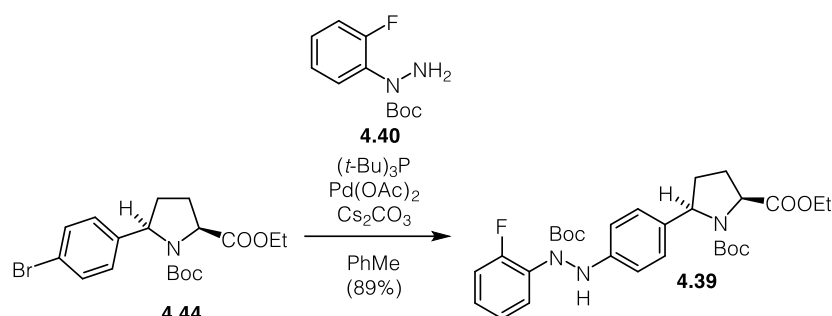
Carbamate 3.44: NEt₃ (5.04 mL, 36.2 mmol) was added to a solution of pyrrolidine **4.29** (5.60 g, 17.8 mmol), di-*tert*-butyldicarbonate (15.9 g, 72.2 mmol) and DMAP (4.40 g, 36.2 mmol) in CH₂Cl₂ (300 mL) and the reaction was stirred at room temperature overnight. The reaction mixture was washed with aqueous citric acid (10%) and brine, dried over MgSO₄ and concentrated under reduced pressure. Purification of the resulting residue by flash column chromatography (pentane:EtOAc 5:1, R_f = 0.3) gave carbamate **4.44** (3.00 g, 7.53 mmol, 43%) as a yellowish oil. The product was obtained as a mixture of Boc rotamers.

Data for 4.44: $^1\text{H-NMR}$ (400 MHz, CDCl_3): δ (ppm) = 7.45 (d, J = 4.4 Hz, 4H), 4.95 – 4.67 (m, 1H), 4.49 – 4.31 (m, 1H), 4.26 (q, J = 7.2 Hz, 2H), 2.31 (dq, J = 13.7, 7.2 Hz, 1H), 2.23 – 2.14 (m, 1H), 2.06 – 1.96 (m, 1H), 1.87 (dd, J = 12.3, 6.3 Hz, 1H), 1.40 (t, 9H), 1.16 (d, 3H). $^{13}\text{C-NMR}$ (100 MHz, CDCl_3): δ (ppm) = 173.0, 154.23, 143.3, 131.4, 131.1, 128.1, 127.9, 120.3, 80.5, 80.3, 62.4, 61.8, 61.2, 61.1, 60.8, 60.4, 35.5, 34.4, 29.0, 28.7, 28.2, 28.0, 14.3, 14.2. **IR (ATR):** ν_{max} (cm^{-1}) = 2978 (W), 1744 (M), 1694 (VS), 1489 (M), 1478 (W), 1454 (W), 1389 (S), 1291 (M), 1257 (W), 1189 (S), 1153 (VS), 1119 (M), 1102 (M), 1073 (M), 1032 (M), 1010 (M), 933 (W), 893 (VW), 858 (W), 821 (M), 752 (M), 716 (W), 701 (W), 665 (W). **HRMS (EI):** calc. for $\text{C}_{18}\text{H}_{24}\text{BrNO}_4$ $[M]^+$: 397-0889, found: 397.0891. $[\alpha]_D^{25} = +22\text{-}3$ (CHCl_3).



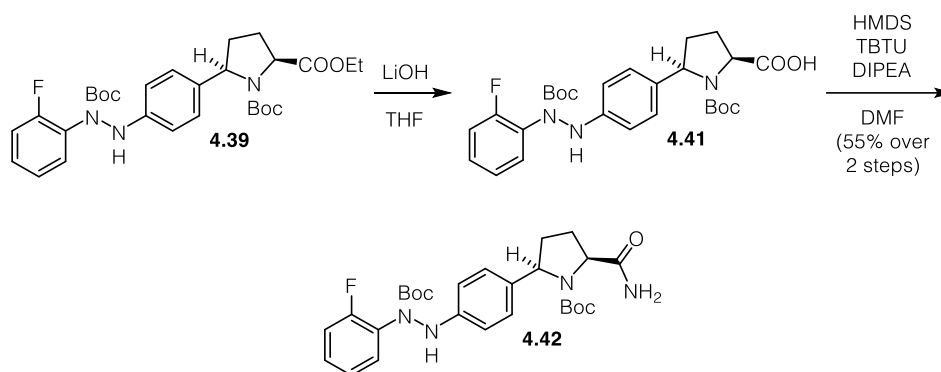
Phenylhydrazine 4.40: A solution of 1-fluoro-2-iodobenzene (2.62 mL, 22.5 mmol), *t*-butylcarbazate (4.18 g, 31.5 mmol), Cs_2CO_3 (20.3 g, 62.0 mmol), 1.10-phen (815 mg, 4.45 mmol) and CuI (95.0 mg, 0.450 mmol) in DMF (45 mL) was stirred at 80°C overnight. The reaction mixture was diluted with H_2O and extracted with EtOAc. The combined organic phases were washed with brine, dried over MgSO_4 and concentrated under reduced pressure. Purification of the resulting residue by flash column chromatography (hexanes:EtOAc 4:1, R_f = 0.4) gave phenylhydrazine **4.40** (856 mg, 3.77 mmol, 17%) as a red solid.

Data for 4.40: $^1\text{H-NMR}$ (400 MHz, CDCl_3): δ (ppm) = 7.31 (td, J = 7.8, 1.6 Hz, 1H), 7.24 – 7.16 (m, 1H), 7.15 – 7.02 (m, 2H), 4.88 – 4.14 (m, 2H), 1.43 (s, 9H). $^{13}\text{C-NMR}$ (100 MHz, CDCl_3): δ (ppm) = 158.4, 155.9, 155.8, 131.3, 131.2, 128.2, 128.1, 124.0, 124.0, 116.1, 115.9, 81.7, 28.1. **IR (ATR):** ν_{max} (cm^{-1}) = 3341 (W), 2979 (W), 2933 (W), 1697 (VS), 1630 (W), 1592 (W), 1501 (S), 1479 (W), 1456 (W), 1392 (M), 1367 (S), 1344 (S), 1291 (M), 1263 (M), 1222 (M), 1189 (S), 1178 (S), 1148 (VS), 1106 (M), 1053 (M), 1025 (M), 933 (W), 863 (W), 836 (M), 795 (W), 753 (S), 657 (M). **MS (EI):** calc. for $\text{C}_{11}\text{H}_{15}\text{FN}_2\text{O}_2$ $[M]^+$: 227.11, found: 227.09.



Diphenylhydrazine 4.39: A mixture of phenylhydrazine **4.40** (80 mg, 0.35 mmol), carbamate **4.44** (20.0 mg, 0.300 mmol), $\text{Pd}(\text{OAc})_2$ (13.0 mg, 0.060 mmol), $(t\text{-Bu})_3\text{P}$ (1 M, PhMe , 0.060 mL, 0.060 mmol) and Cs_2CO_3 (187 mg, 0.390 mmol) in PhMe (24 mL) was stirred at room temperature for 30 min and at 110 °C for 2.5 h. The resulting suspension was cooled to room temperature, diluted with EtOAc and filtered over a pad of celite. Removal of the solvent under reduced pressure and purification of the resulting residue by flash column chromatography (hexanes: EtOAc 4:1, $R_f = 0.3$) gave diphenylhydrazine **4.39** (166 mg, 0.310 mmol, 89%) as a brown solid. The product was obtained as a mixture of Boc rotamers.

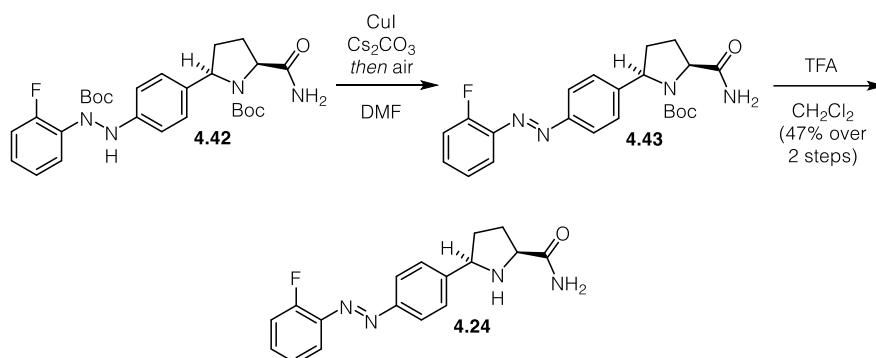
Data for 4.39: $^1\text{H-NMR}$ (400 MHz, CDCl_3): δ (ppm) = 7.44 (s, 2H), 7.22 – 7.12 (m, 2H), 7.09 (d, $J = 7.7$ Hz, 2H), 6.86 (d, $J = 7.2$ Hz, 2H), 6.46 (s, 1H), 4.72 – 4.40 (m, 1H), 4.34 – 4.18 (m, 3H), 2.21 (ddd, $J = 25.1, 12.4, 6.2$ Hz, 2H), 2.14 – 1.83 (m, 1H), 1.39 (s, 18H), 1.14 (s, 3H). $^{13}\text{C-NMR}$ (100 MHz, CDCl_3): δ (ppm) = 173.4, 173.3, 154.6, 154.6, 153.9, 146.6, 146.5, 137.0, 135.9, 127.4, 127.2, 124.3, 113.1, 82.4, 82.3, 80.2, 80.00, 62.7, 61.9, 61.2, 61.0, 60.5, 35.7, 34.6, 29.1, 28.8, 28.4, 28.2, 28.1, 14.4, 14.3. **IR (ATR):** ν_{max} (cm^{-1}) = 3312 (W), 2979 (W), 2189 (VW), 2103 (VW), 1691 (M), 1701 (W), 1615 (W), 1515 (W), 1498 (M), 1478 (W), 1456 (W), 1392 (M), 1366 (M), 1336 (M), 1301 (M), 1285 (W), 1246 (W), 1152 (S), 1128 (S), 1108 (M), 1074 (W), 1017 (M), 934 (W), 912 (VW), 832 (W), 845 (S), 799 (W), 754 (M). **HRMS (ESI):** calc. for $\text{C}_{29}\text{H}_{42}\text{F}_4\text{O}_6$ [$M+H$] $^+$: 561.3083, found: 561.3084. $[\alpha]_D^{25} = +66.0$ (CHCl_3).



Amide 4.42: A solution of LiOH·H₂O (100 mg, 2.44 mmol) in H₂O (2.5 mL) was added to a solution of diphenylhydrazine **4.39** (435 mg, 0.080 mmol) in THF (5.0 mL) and MeOH (2.5 mL) and the solution was stirred at room temperature overnight. The reaction was acidified with aqueous HCl (1 M) and extracted with EtOAc. The combined organic phases were washed with brine, dried over MgSO₄ and concentrated under reduced pressure to give crude acid **4.41** that was used in the next step without further purification.

DIPEA (22.5 μL, 1.35 mmol) was added to a solution of crude acid **4.41** and HATU (281 mg, 1.02 mmol) in DMF and the solution was stirred at room temperature for 30 min. HMDS (197 μL, 1.02 mmol) was added and the reaction was stirred at room temperature for 1.5 h, diluted with NaHCO₃ and H₂O and extracted with EtOAc. The combined organic phases were dried over MgSO₄ and concentrated under reduced pressure. Purification of the resulting residue by flash column chromatography (hexanes:EtOAc 1:2, R_f = 0.4) gave amide **4.42** (177 mg, 0.34 mmol, 55% over 2 steps) as an orange solid. The product was obtained as a mixture of Boc rotamers.

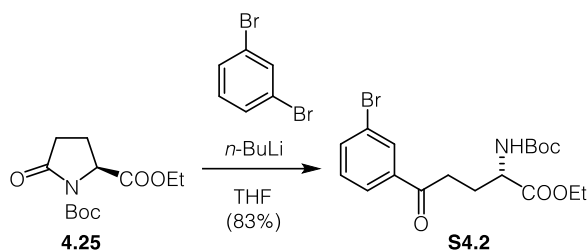
Data for 4.42: ¹H-NMR (400 MHz, CDCl₃): δ (ppm) = 7.45 – 7.39 (m, 1H), 7.25 – 7.16 (m, 1H), 7.17 – 7.08 (m, 4H), 6.87 – 6.82 (m, 2H), 6.52 (s, 1H), 5.50 (s, 1H), 4.62 (s, 1H), 4.45 (s, 1H), 2.49 (s, 1H), 2.31 – 2.20 (m, 1H), 1.97 (q, *J* = 9.7, 8.3 Hz, 2H), 1.63 (d, *J* = 4.7 Hz, 1H), 1.39 (s, 9H), 1.20 (s, 9H). ¹³C-NMR (100 MHz, CDCl₃): δ (ppm) = 174.5, 158.1, 155.6, 154.4, 146.7, 136.23, 130.7, 130.6, 128.2, 128.2, 127.5, 127.2, 124.1, 116.2, 116.0, 113.1, 82.2, 80.8, 63.2, 61.2, 28.0, 27.9. IR (ATR): ν_{max} (cm⁻¹) = 2974 (W), 2410 (W), 1667 (M), 1614 (W), 1514 (W), 1499 (W), 1480 (W), 1455 (W), 1392 (M), 1366 (M), 1338 (M), 1283 (W), 1263 (M), 1218 (W), 1151 (S), 1106 (M), 1102 (M), 1015 (W), 943 (W), 922 (W), 840 (M), 801 (W), 753 (S), 665 (M). HRMS (ESI): calc. for C₂₇H₃₉FN₅O₅ [M+NH₄]⁺: 532.2930, found: 532.2935. [α]_D²⁵ = +4.8 (CHCl₃).



Azoraxatrigine 4.24: A solution of amide **4.42** (581 mg, 1.13 mmol), Cs₂CO₃ (1.53 g, 4.69 mmol) and CuI (900 mg, 4.69 mmol) in DMF (16 mL) was stirred at 140 °C for 24 h. After cooling to room temperature, the reaction mixture was diluted with EtOAc and filtered over a pad of silica. Removal of the solvent under reduced pressure and purification of the resulting residue by flash column chromatography (CH₂Cl₂:MeOH 98:2-97:3, R_f = 0.4) gave crude azobenzene **4.43** which was used in the next step without further purification.

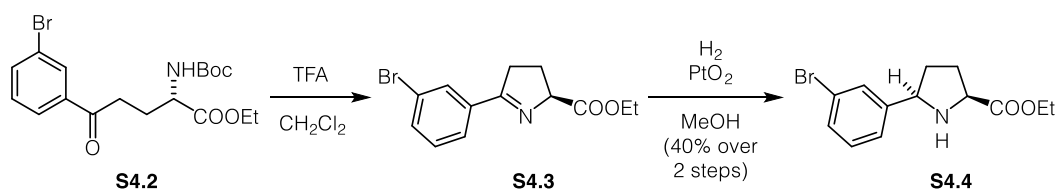
TFA (15 mL) was added to an ice cooled solution of crude azobenzene **4.43** in CH₂Cl₂ (29 mL) and the reaction was stirred at 0 °C for 30 min and at room temperature for 3 h. The mixture was diluted with saturated aqueous NaHCO₃ and extracted with CH₂Cl₂. The combined organic phases were washed with brine, dried over MgSO₄ and concentrated under reduced pressure. Purification of the resulting residue by flash column chromatography (CH₂Cl₂:MeOH 96:4, R_f = 0.4) gave azoraxatrigine **4.24** (166 mg, 0.53 mmol, 47%) as an orange solid. The resulting product is in a light driven equilibrium with its double bond isomer. The major trans isomer is described.

Data for 4.24: ¹H-NMR (400 MHz, *d*₂-MeOH): δ (ppm) = 7.95 – 7.89 (m, 2H), 7.77 (td, *J* = 7.8, 1.7 Hz, 1H), 7.68 – 7.63 (m, 2H), 7.53 (dddd, *J* = 8.6, 6.9, 5.0, 1.8 Hz, 1H), 7.37 – 7.25 (m, 2H), 4.37 (dd, *J* = 9.7, 6.0 Hz, 1H), 3.83 (dd, *J* = 9.6, 4.5 Hz, 1H), 2.33 (dtd, *J* = 12.4, 9.9, 7.4 Hz, 1H), 2.23 (dddd, *J* = 12.1, 7.3, 6.0, 2.9 Hz, 1H), 2.07 (dddd, *J* = 12.3, 7.5, 4.5, 2.9 Hz, 1H), 1.67 (dtd, *J* = 12.1, 9.9, 8.0 Hz, 1H). ¹³C-NMR (100 MHz, *d*₂-MeOH): δ (ppm) = 181.1, 162.7, 160.2, 153.3, 149.4, 133.9, 128.6, 125.6, 124.2, 118.6, 118.2, 118.0, 64.1, 61.4, 35.2, 32.1. IR (ATR): ν_{max} (cm⁻¹) = 3406 (W), 3190 (W), 3067 (W), 2929 (W), 2870 (W), 1687(M), 1654 (S), 1602 (M), 1588 (M), 1498 (M), 1480 (M), 1439 (M), 1400 (W), 1385 (M), 1350 (M), 1325 (M), 1299 (M), 1264 (M), 1243 (M), 1217 (M), 1181 (M), 1099 (M), 1029 (W), 1012 (W), 947 (W), 906 (W), 839 (M), 785 (M), 756 (VS), 728 (S), 717 (S), 661 (W). HRMS (ESI): calc. for C₁₇H₁₈FN₄ O [*M*+*H*]⁺: 313.1459, found: 313.1459. [α]_D²⁵ = +84.0 (CHCl₃).



Ketone S4.2: *n*-BuLi (2.21 M in hexanes, 9.30 mL, 19.4 mmol) was added to a solution of 1,3-dibromobenzene (4.85 g, 19.4 mmol) in THF (60 mL) at $-78\text{ }^{\circ}\text{C}$ and the reaction was stirred at that temperature for 30 min. The resulting solution was slowly added to a solution of pyroglutamate **4.25** (5.00 g, 19.4 mmol) in THF (60 mL) at $-78\text{ }^{\circ}\text{C}$ and the reaction was stirred at that temperature for 1.5 h. The reaction mixture was quenched with saturate aqueous NHCl_4 , diluted with H_2O and extracted with EtOAc. The combined organic phases were dried over MgSO_4 and concentrated under reduced pressure. Purification of the resulting residue by flash column chromatography (hexanes:EtOAc 4:1, $R_f = 0.3$) gave ketone **S4.2** (6.61 g, 16.04 mmol, 83%) as a yellowish oil.

Data for S4.2: $^1\text{H-NMR}$ (400 MHz, CDCl_3): δ (ppm) = 8.07 (t, $J = 1.8$ Hz, 1H), 7.87 (ddd, $J = 7.8, 1.7, 1.0$ Hz, 1H), 7.69 (ddd, $J = 8.0, 2.0, 1.1$ Hz, 1H), 7.34 (t, $J = 7.9$ Hz, 1H), 5.14 (d, $J = 8.3$ Hz, 1H), 4.36 (q, $J = 7.7, 5.6$ Hz, 1H), 4.22 – 4.13 (m, 2H), 3.17 – 2.94 (m, 2H), 2.31 (ddt, $J = 11.7, 8.4, 6.2$ Hz, 1H), 1.42 (s, 9H), 1.28 – 1.25 (m, 3H). $^{13}\text{C-NMR}$ (400 MHz, CDCl_3): δ (ppm): = 197.5, 172.3, 155.5, 138.4, 136.0, 131.5, 131.1, 130.2, 126.5, 123.0, 80.0, 61.6, 53.0, 34.6, 28.3, 27.0, 14.2. **IR (ATR):** ν_{max} (cm^{-1}) = 3376 (w), 2980 (w), 2940 (w), 2894 (w), 1744 (m), 1686 (vs), 1569 (w), 1511 (s), 1476 (w), 1446 (m), 1423 (m), 1409 (w), 1300 (m), 1251 (s), 1216 (s), 1166 (s), 1110 (m), 1082 (m), 1067 (m), 1050 (s), 1029 (s), 1018 (s), 996 (s), 959 (m), 901 (m), 871 (m), 860 (m), 827 (m), 802 (w), 785 (m), 770 (s), 757 (s), 678 (vs). **HRMS (EI):** calc. for $\text{C}_{18}\text{H}_{24}\text{BrNO}_5$ [M] $^+$: 413.0832, found: mass could not be found. $[\alpha]_D^{25} = +1.4$ (CHCl_3).

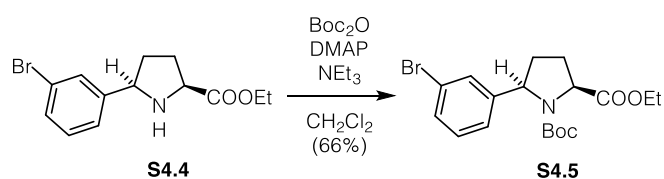


Pyrrolidine S4.4: TFA (11.5 mL, 146 mmol) was added dropwise to an ice cooled solution ketone **S4.2** (4.00 g, 9.70 mmol) in CH_2Cl_2 (50 mL) and the reaction was allowed to warm to room temperature over 90 min. Evaporation of the volatiles under reduced

pressure gave crude imine **S4.3** as yellow oil which was used in the next step without further purification.

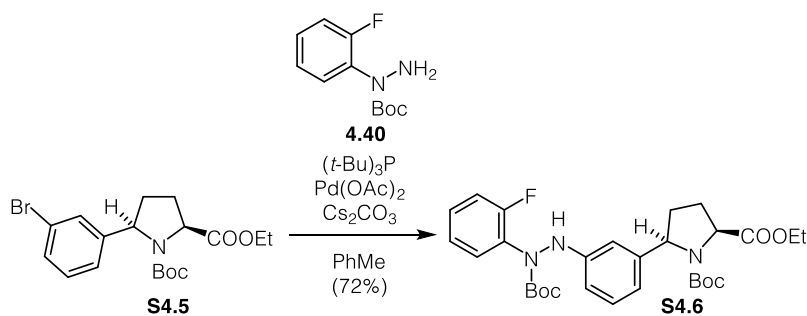
A suspension of crude imine **S4.3** and PtO₂ (106 mg, 4.64w%) in MeOH (38 mL) was stirred under H₂-atmosphere overnight, filtered over a pad of celite and concentrated under reduced pressure. Purification of the resulting residue by flash column chromatography (hexanes:EtOAc 1:2-1.4) gave pyrrolidine **S4.4** (1.15 g, 3.86 mmol, 40%) as a brownish solid.

Data for S4.4: R_f: 0.4 (hexanes:EtOAc 1:4) ¹H-NMR (400 MHz, CDCl₃): δ (ppm) = 8.07 (t, *J* = 1.8 Hz, 1H), 7.87 (ddd, *J* = 7.8, 1.7, 1.0 Hz, 1H), 7.69 (ddd, *J* = 8.0, 2.0, 1.1 Hz, 1H), 7.34 (t, *J* = 7.9 Hz, 1H), 5.14 (d, *J* = 8.3 Hz, 1H), 4.36 (q, *J* = 7.7, 5.6 Hz, 1H), 4.22 – 4.13 (m, 2H), 3.17 – 2.94 (m, 2H), 2.31 (ddt, *J* = 11.7, 8.4, 6.2 Hz, 1H), 1.42 (s, 9H), 1.28 – 1.25 (m, 3H). ¹³C-NMR (100 MHz, CDCl₃): δ (ppm) = 175.1, 146.3, 130.3, 130.1, 130.0, 125.5, 122.7, 63.0, 61.2, 60.20, 34.4, 30.5, 14.4. IR (ATR): ν_{max} (cm⁻¹) = 3451 (w), 3365 (w), 3059 (w), 3038 (w), 2977 (m), 2947 (w), 2919 (w), 2877 (w), 2828 (w), 1887 (w), 1733(vs), 1692 (m), 1590 (m), 1453 (m), 1567 (m), 1465 (m), 1453 (m), 1420 (m), 1356 (w), 1342 (w), 1309 (w), 1270 (w), 1242 (w), 1206 (s), 1192 (vs), 1177 (vs), 1138 (vs), 1114 (s), 1065 (m), 1048 (s), 1030 (m), 944 (m), 977(m), 950 (w), 936 (w), 901 (m), 880 (w), 854 (m), 822 (s), 780 (vs), 742 (m), 701 (s), 686 (s). HRMS (ESI): calc. for C₁₃H₁₇BrNO₂ [*M+H*]⁺: 298.0437, found: 298.0438. [α]_D²⁵ = -4.0 (CHCl₃).



Carbamate S4.5: NEt₃ (0.90 mL, 6.46 mmol) was added to a solution of pyrrolidine **S4.4** (1.00 g, 3.35 mmol), di-*tert*-butyldicarbonate (2.84 g, 12.9 mmol) and DMAP (790 mg, 6.46 mmol) in CH₂Cl₂ (57 mL) and the reaction was stirred at room temperature overnight. The reaction mixture was washed with aqueous citric acid (10%) and brine, dried over MgSO₄ and concentrated under reduced pressure. Purification of the resulting residue by flash column chromatography (pentane:EtOAc 5:1, R_f = 0.3) gave carbamate **S4.5** (877 mg, 2.20 mmol, 66%) as a yellowish oil. The product was obtained as a mixture of Boc rotamers.

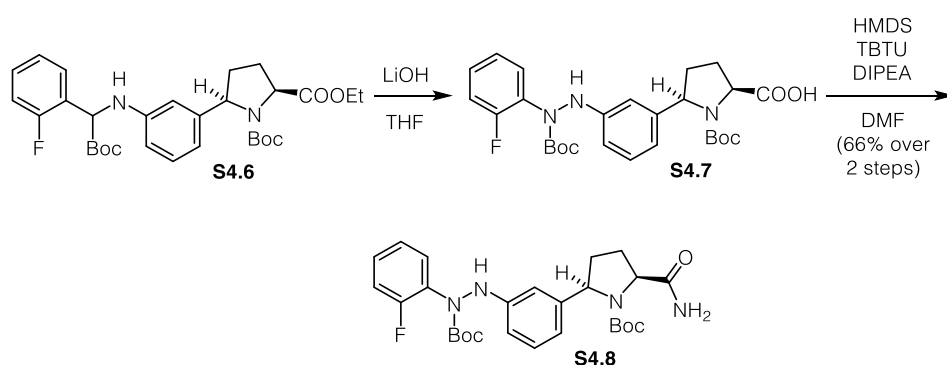
Data for S4.5: $^1\text{H-NMR}$ (400 MHz, CDCl_3): δ (ppm) = 7.71 (dt, J = 5.9, 1.8 Hz, 1H), 7.50 (dd, J = 14.7, 7.8 Hz, 1H), 7.39 – 7.31 (m, 1H), 7.22 – 7.15 (m, 1H), 4.73 – 4.39 (m, 1H), 4.27 (tt, J = 6.8, 4.2 Hz, 2H), 2.37 – 2.27 (m, 1H), 2.27 – 2.16 (m, 1H), 2.06 (qd, J = 11.4, 8.6, 3.9 Hz, 1H), 1.92 (tdt, J = 16.0, 6.6, 4.1 Hz, 1H), 1.49 – 1.18 (m, 9H), 1.16 (s, 6H). $^{13}\text{C-NMR}$ (100 MHz, CDCl_3): δ (ppm) = 172.8, 154.0, 153.6, 146.4, 145.4, 129.6, 129.3, 128.9, 124.8, 124.5, 122.4, 121.9, 80.4, 80.1, 61.0, 60.2, 28.7, 28.0, 14.2. **IR (ATR):** ν_{max} (cm^{-1}) = 3058 (w); 2978 (w), 2935 (w) 1742 (m), 1694 (vs), 1596 (w), 1571 (w), 1476 (w), 1448 (w), 1431 (w), 1387 (vs), 1366 (s), 1340 (m), 1288 (m), 1256 (w), 1188 (s), 1153 (vs), 1118 (m), 1092 (m), 1072 (m), 1032 (m), 1021 (m), 996(w), 933 (w), 912 (w), 875 (w), 858 (w), 823 (w), 781(m), 756 (m), 696 (w), 665 (w). **HRMS (ESI):** calc. for $\text{C}_{18}\text{H}_{24}\text{BrNO}_4$ [$M+H$] $^+$: 397.0889, found: 397.0894. $[\alpha]_D^{25} = +24.3$ (CHCl_3).



Diphenylhydrazine S4.6: A mixture of phenylhydrazine **4.40** (530 mg, 2.34 mmol), carbamate **S4.6** (943 mg, 2.13 mmol), Pd(OAc)_2 (96.2 mg, 0.430 mmol), $(t\text{-Bu})_3\text{P}$ (3 M, PhMe, 0.16 mL, 0.430 mmol) and Cs_2CO_3 (943 mg, 2.88 mmol) in PhMe (177 mL) was stirred at room temperature for 30 min and at 110 °C for 2.5 h. The resulting suspension was cooled to room temperature, diluted with EtOAc and filtered over a pad of celite. Removal of the solvent under reduced pressure and purification of the resulting residue by flash column chromatography (hexanes:EtOAc 4:1, R_f = 0.3) gave diphenylhydrazine **S4.6** (840 mg, 1.54 mmol, 72%) as a brown solid. The product was obtained as a mixture of Boc rotamers.

Data for S4.6: $^1\text{H-NMR}$ (400 MHz, CDCl_3): δ (ppm) = 7.53 (dt, J = 14.6, 7.0 Hz, 1H), 1.16 – 1.15 (m, 1H), 1.15 – 1.14 (m, 1H), 7.34 (td, J = 7.8, 1.8 Hz, 1H), 7.23 (ddt, J = 10.2, 5.5, 3.3 Hz, 3H), 7.13 – 7.10 (m, 1H), 6.81 (ddd, J = 8.0, 2.1, 1.0 Hz, 1H), 6.51 (d, J = 3.1 Hz, 1H), 4.71 (t, J = 6.9 Hz, 1H), 4.55 (s, 2H), 2.31 – 2.16 (m, 2H), 2.12 – 1.99 (m, 2H), 1.92 (dt, J = 10.9, 5.1 Hz, 1H), 1.50 – 1.35 (m, 18H), 1.34 – 1.28 (m, 3H). $^{13}\text{C-NMR}$ (100 MHz, CDCl_3): δ (ppm) = 173.0, 172.8, 158.3, 158.2, 155.9, 155.7, 154.5,

153.8, 147.8, 147.6, 145.3, 144.4, 131.3, 131.2, 130.9, 130.7, 129.1, 128.8, 128.4, 128.1, 128.0, 127.8, 124.1, 124.0, 123.9, 119.1, 118.9, 116.1, 115.9, 111.3, 111.2, 111.1, 110.9, 82.0, 81.6, 80.1, 79.9, 63.0, 62.1, 60.9, 35.4, 34.3, 30.8, 29.7, 28.9, 28.6, 28.2, 28.1, 28.0, 24.9, 14.2. **IR (ATR):** ν_{\max} (cm⁻¹) = 3336 (w), 2978 (w), 2933 (w), 1692 (s), 1609 (w), 1596 (w), 1499 (m), 1478 (w), 1455 (w), 1391 (m), 1366 (s), 1336 (s), 1290 (m), 1256 (m), 1221 (m), 1150 (s), 1128 (s), 1107 (m), 1073 (w), 1046 (w), 1018 (m), 937 (w), 859 (w), 838 (w), 782 (m), 754 (vs), 701 (m), 655 (w). **HRMS (ESI):** calc. for C₂₉H₄₂FN₄O₆ [M+NH₄]⁺: 561.3083, found: 561.3083. $[\alpha]_D^{25} = +48.1$ (CHCl₃).

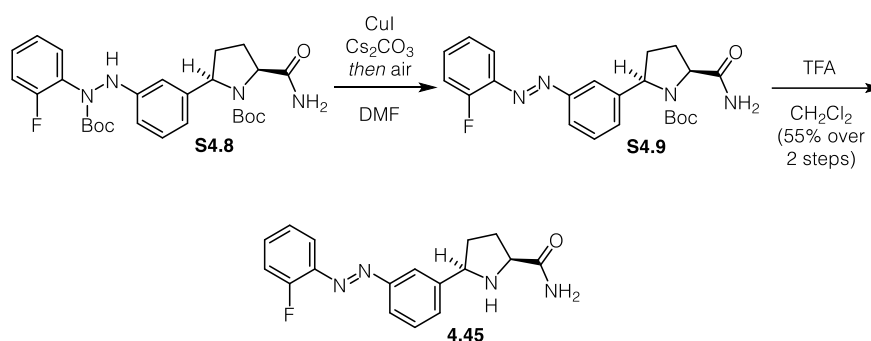


Amide S4.8: A solution of LiOH·H₂O (172 mg, 4.14 mmol) in H₂O (5.0 mL) was added to a solution of diphenylhydrazine **S4.6** (740 mg, 1.36 mmol) in THF (9.5 mL) and MeOH (5.0 mL) and the solution was stirred at room temperature overnight. The reaction was acidified with aqueous HCl (1 M) and extracted with EtOAc. The combined organic phases were washed with brine, dried over MgSO₄ and concentrated under reduced pressure to give crude acid **S4.7** that was used in the next step without further purification.

DIPEA (460 μL, 2.72 mmol) was added to a solution of crude acid **S4.7** and HATU (327 mg, 0.860 mmol) in DMF (5.6 mL) and the solution was stirred at room temperature for 30 min. HMDS (400 μL, 2.11 mmol) was added and the reaction was stirred at room temperature for 1.5 h, diluted with NaHCO₃ and H₂O and extracted with EtOAc. The combined organic phases were dried over MgSO₄ and concentrated under reduced pressure. Purification of the resulting residue by flash column chromatography (hexanes:EtOAc 1:2, R_f = 0.4) gave amide **S4.8** (461 mg, 0.900 mmol, 66% over 2 steps) as an orange solid. The product was obtained as a mixture of Boc rotamers.

Data for S4.8: ¹H-NMR (400 MHz, CDCl₃): δ (ppm) = 7.45 – 7.41 (m, 1H), 7.23 – 7.04 (m, 5H), 6.80 (d, *J* = 13.6 Hz, 2H), 5.31 (s, 1H), 4.62 (s, 1H), 4.45 (s, 1H), 2.52 – 2.19

(m, 2H), 1.92 (s, 3H), 1.54 (s, 9H), 1.37 (s, 9H). $^{13}\text{C-NMR}$ (100 MHz, CDCl_3): δ (ppm) = 154.4, 147.9, 129.1, 128.3, 128.2, 127.6, 124.2, 124.1, 119.0, 116.2, 116.0, 111.9, 110.5, 82.3, 80.9, 28.0, 27.9. **IR (ATR):** ν_{max} (cm^{-1}) = 3308 (w), 2976 (w), 2932 (w), 1675 (s), 1608 (m), 1498 (m), 1478 (w), 1455 (w), 1392 (m), 1366 (s), 1339 (s), 1256 (m), 1220 (m), 1157 (s), 1066 (w), 1045 (w), 1017 (m), 939 (w), 842 (w), 754 (s), 702 (m), 655 (w). **HRMS (ESI):** calc. for $\text{C}_{27}\text{H}_{39}\text{FN}_5\text{O}_5$ [$M+\text{NH}_4$] $^+$: 532.2930, found: 532.2928. $[\alpha]_{\text{D}}^{25} = +12.6$ (CHCl_3).



***m*-Azoraxatrigine 4.45:** A solution of amide **S4.8** (138 mg, 0.330 mmol), Cs_2CO_3 (503 mg, 1.54 mmol) and CuI (299 mg, 1.54 mmol) in DMF (6 mL) was stirred at 140°C for 24 h. After cooling to room temperature, the reaction mixture was diluted with EtOAc and filtered over a pad of silica. Removal of the solvent under reduced pressure and purification of the resulting residue by flash column chromatography (CH_2Cl_2 : MeOH 98:2-97:3, $R_f = 0.3$) gave crude azobenzene **S4.9** which was used in the next step without further purification.

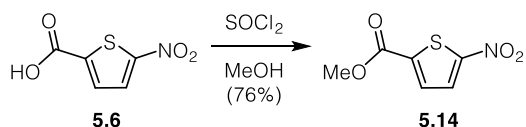
TFA (7 mL) was added to an ice cooled solution of crude azobenzene **S4.9** in CH_2Cl_2 (20 mL) and the reaction was stirred at 0°C for 30 min and at room temperature for 3 h. The mixture was diluted with saturated aqueous NaHCO_3 and extracted with CH_2Cl_2 . The combined organic phases were washed with brine, dried over MgSO_4 and concentrated under reduced pressure. Purification of the resulting residue by flash column chromatography (CH_2Cl_2 : MeOH 100:0-92:8, $R_f = 0.4$) gave *m*-azoraxatrigine **4.45** (56.0 mg, 0.180 mmol, 55%) as an orange solid. The resulting product is in a light driven equilibrium with its double bond isomer. The major trans isomer is described.

Data for 4.45: $^1\text{H-NMR}$ (400 MHz, d_4 - MeOH): δ (ppm) = 8.16 (t, $J = 1.9$ Hz, 1H), 8.02 (dt, $J = 7.9, 1.4$ Hz, 1H), 7.79 (td, $J = 7.3, 6.8, 5.6$ Hz, 2H), 7.69 (t, $J = 7.8$ Hz, 1H), 7.63 – 7.53 (m, 1H), 7.39 – 7.29 (m, 2H), 7.23 – 7.13 (m, 1H), 7.04 – 6.94 (m, 1H), 4.50 (dd, $J = 9.3, 3.4$ Hz, 1H), 2.61 (td, $J = 14.3, 11.2, 6.1$ Hz, 1H), 2.53 (dd, $J = 13.3, 6.9$ Hz, 1H),

2.48 – 2.39 (m, 1H), 2.29 (qd, $J = 12.8, 12.1, 7.4$ Hz, 2H). **$^{13}\text{C-NMR}$ (100 MHz, d_4 -MeOH):** δ (ppm) = 171.1, 161.5, 159.0, 153.1, 140.3, 135.9, 127.3, 123.6, 120.3, 117.2, 115.9, 63.7, 30.2. **IR (ATR):** ν_{max} (cm^{-1}) = 3665 (w), 3200 (w), 2752 (w), 2366 (w), 1663 (vs), 1485 (w), 1453 (w), 1386 (w), 1336 (w), 1269 (w), 1191 (vs), 1133 (vs), 1019 (w), 950 (w), 899 (w), 846 (m), 799 (s), 761 (m), 723 (m), 691 (m). **HRMS (ESI):** calc. for $\text{C}_{17}\text{H}_{18}\text{FN}_4\text{O}$ $[M+H]^+$: 313.1459, found: 313.1458. $[\alpha]_D^{25} = +11.2$ (CHCl_3).

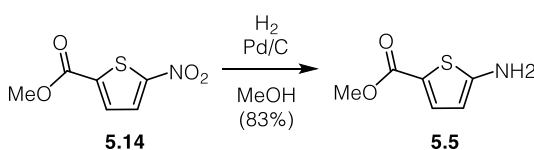
6.6 Experimental data for chapter V

6.6.1 Photoswitches based on CK-636 and CK-666



Methyl ester 5.14: SOCl₂ (8.90 mL, 116 mmol) was slowly added to an ice cooled solution of thiophene **5.6** (2.00 g, 11.6 mmol) in MeOH (20 mL) and the solution was stirred at 60 C overnight. The reaction was cooled to room temperature, carefully quenched with aqueous NaHCO₃ and extracted with CH₂Cl₂. The combined organic phases were dried over MgSO₄ and concentrated under reduced pressure to yield methyl ester **5.14** (1.63 g, 8.73 mmol, 76%) as a pale yellow solid.

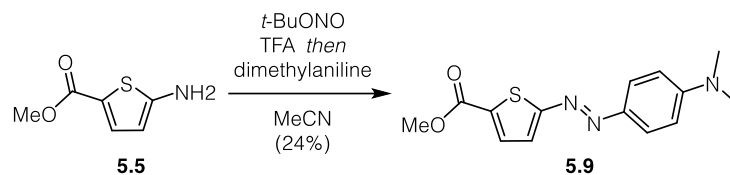
Data for 5.14: ¹H-NMR (400 MHz, CDCl₃): δ (ppm) = 7.87 (d, *J* = 4.3 Hz, 1H), 7.70 (d, *J* = 4.3 Hz, 1H), 3.95 (s, 3H). ¹³C-NMR (100 MHz, CDCl₃): δ (ppm) = 161.2, 138.5, 131.9, 128.1, 53.3. IR (ATR): ν_{max} (cm⁻¹) = 3115 (w), 3099 (w), 1727 (s), 1704 (s), 1535 (m), 1504 (s), 1445 (m), 1423 (m), 1355 (m), 1339 (m), 1280 (s), 1247 (s), 1216 (m), 1189 (m), 1121 (m), 1082 (m), 1034 (m), 945 (w), 924 (m), 841 (m), 816 (m), 794 (w), 746 (s), 731 (s), 680 (w), 671 (w). HRMS (EI): calc. for C₆H₅NO₄³²S [M]⁺: 186.9934, found: 186.9944.



Amine 5.5: A suspension of methyl ester **5.14** (1.50 g, 8.01 mmol) and Pd/C (300 mg) in MeOH (100 mL) was stirred under a H₂-atmosphere at room temperature for 3 d. The reaction was filtered over celite and the solvent was removed under reduced pressure. Purification of the resultant residue by flash column chromatography (hexanes:EtOAc 2:1, R_f = 0.3) gave amine **5.5** (1.05 g, 6.68 mmol, 83%) as a pale yellow solid.

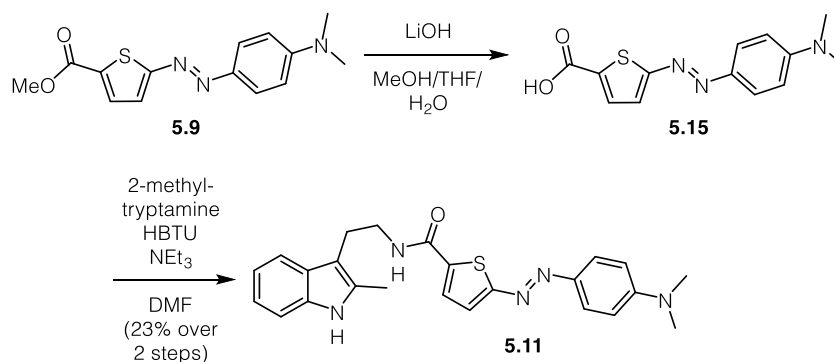
Data for 5.5: R_f: 0.3 (hexanes:EtOAc 2:1); ¹H-NMR (400 MHz, CDCl₃): δ (ppm) = 7.45 (d, *J* = 4.0 Hz, 1H), 6.09 (d, *J* = 4.0 Hz, 1H), 4.31 (s, 2H), 3.81 (s, 3H). ¹³C-NMR (100 MHz, CDCl₃): δ (ppm) = 163.3, 159.4, 135.2, 117.0, 107.8, 51.8. IR (ATR): ν_{max} (cm⁻¹) = 3336 (w), 1674 (s), 1619 (m), 1454 (s), 1433 (s), 1383 (m), 1278 (s), 1222 (m), 1187 (m),

1092 (s), 1032 (w), 976 (w), 958 (w), 924 (w), 784 (m), 745 (w), 689 (w). **HRMS (EI)**: calc. for $C_6H_7NO_2^{32}S$ [M]⁺: 157.0192, found: 157.0195.



Dimethylaniline 5.9: TFA (290 μL , 3.82 mmol) and *t*-BuONO (180 μL , 1.52 mmol) were sequentially added to an ice cooled solution of amine **5.5** (200 mg, 1.27 mmol) in MeCN (5 mL) and the solution was stirred 0 °C for 2 h. Dimethylaniline (1.60 mL, 12.7 mmol) was added and the reaction was warmed to room temperature overnight. The mixture was acidified with aqueous HCl (1 M) and extracted with EtOAc. The combined organic phases were washed with saturated aqueous NaHCO_3 and brine, dried over MgSO_4 and concentrated under reduced pressure. Purification of the resultant residue by flash column chromatography (hexanes:EtOAc 9:1, R_f = 0.3) gave dimethylaniline **5.9** (90 mg, 0.311 mmol, 24%) as a deep red solid.

Data for 5.9: R_f : 0.3 (hexanes:EtOAc 9:1); $^1\text{H-NMR}$ (400 MHz, CDCl_3): δ (ppm) = 7.86 – 7.80 (m, 2H), 7.78 (d, J = 4.1 Hz, 1H), 7.52 (d, J = 4.1 Hz, 1H), 6.79 – 6.70 (m, 2H), 3.90 (s, 3H), 3.12 (s, 6H). $^{13}\text{C-NMR}$ (100 MHz, CDCl_3): δ (ppm) = 165.9, 163.3, 152.9, 143.0, 133.4, 131.4, 127.2, 125.9, 111.9, 77.3, 52.4, 40.5. **IR (ATR)**: ν_{max} (cm^{-1}) = 1714 (s), 1607 (m), 1522 (w), 1453 (w), 1381 (w), 1357 (w), 1338 (m), 1313 (w), 1247 (s), 1192 (w), 1156 (m), 1094 (m), 949 (w), 823 (m), 809 (s), 742 (s). **HRMS (EI)**: calc. for $C_{14}H_{15}N_3O_2^{32}S$ [M]⁺: 289.0879, found: 289.0872.

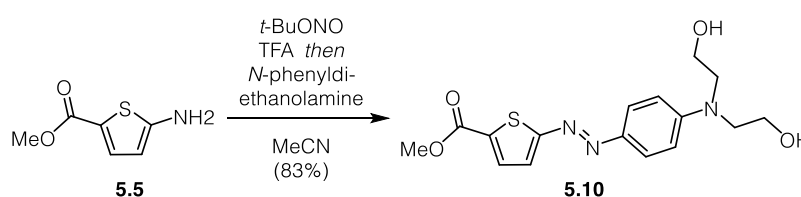


Thiophene 5.11: A solution of dimethylaniline **5.9** (21.1 mg, 0.073 mmol) and $\text{LiOH}\cdot\text{H}_2\text{O}$ (30.6 mg, 0.730 mmol) in MeOH (1 mL), THF (1 mL) and H_2O (1 mL) was stirred at 60 °C

overnight. The reaction mixture was cooled to room temperature, acidified with aqueous HCl (1 M) and extracted with EtOAc. The combined organic phases were dried over MgSO₄ and concentrated under reduced pressure to give crude acid **5.15** which was used in the next step without further purification.

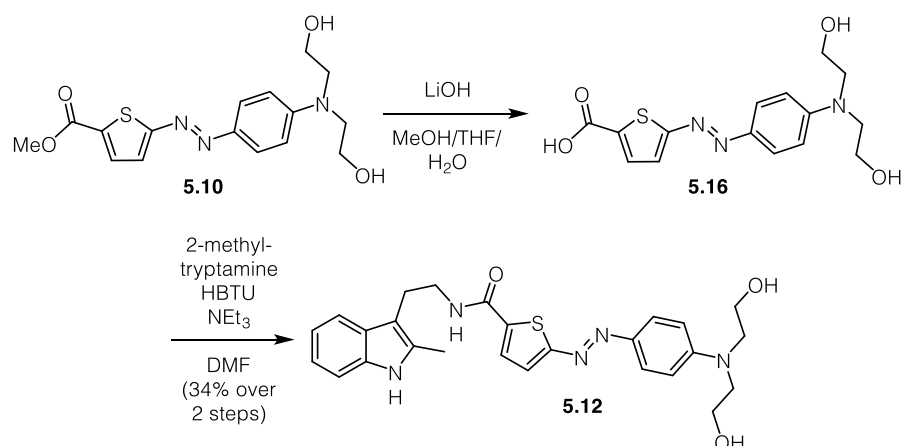
NEt₃ (30.0 μL, 0.218 mmol) was added to a solution of crude acid **5.15**, 2-methyltryptamine (13.0 mg, 0,073 mmol) and HBTU (83.0 mg, 0.218 mmol) in DMF (2 mL) and the solution was stirred at room temperature overnight. Removal of the solvent under reduced pressure and purification of the resulting residue by reverse phase HPLC (MeCN:H₂O (0.1% formic acid) 0:100 to 100:0) gave thiophene **5.11** (7.2 mg, 0.017 mmol, 23%) as a red solid.

Data for 5.11: ¹H-NMR (400 MHz, CDCl₃): δ (ppm) = 7.80 (s, 1H), 7.77 – 7.69 (m, 2H), 7.48 (dd, *J* = 7.4, 1.3 Hz, 1H), 7.36 (dd, *J* = 29.1, 4.0 Hz, 2H), 7.24 (dt, *J* = 8.2, 0.9 Hz, 1H), 7.12 – 7.00 (m, 2H), 6.70 – 6.61 (m, 2H), 5.96 (t, *J* = 5.9 Hz, 1H), 3.62 (q, *J* = 6.4 Hz, 2H), 3.04 (s, 6H), 2.96 (t, *J* = 6.6 Hz, 2H), 2.32 (s, 3H). ¹³C-NMR (100 MHz, CDCl₃): δ (ppm) = 163.6, 162.3, 152.9, 142.9, 136.6, 135.5, 132.3, 128.7, 128.6, 127.4, 125.7, 121.5, 119.7, 118.0, 111.7, 110.5, 108.5, 40.6, 40.5, 24.2, 11.9. IR (ATR): ν_{max} (cm⁻¹) = 1627 (w), 1596 (s), 1511 (m), 1460 (m), 1438 (w), 1351 (m), 1329 (w), 1308 (m), 1281 (m), 1211 (w), 1145 (vs), 1033 (w), 943 (w), 848 (m), 822 (s), 807 (m), 750 (m). HRMS (ESI): calc. for C₁₃H₁₄N₄O³²S [*M+H*]⁺: 431.1774, found: 274.0883.



Diethanolamine 5.10: TFA (290 μL, 3.82 mmol) and *t*-BuONO (180 μL, 1.52 mL) were sequentially added to an ice cooled solution of amine **5.5** (200 mg, 1.27 mmol) in MeCN (5 mL) and the solution was stirred 0 °C for 2 h. *N*-Phenyldiethanolamine (2.31 g, 12.7 mmol) was added and the reaction was warmed to room temperature overnight. The mixture was acidified with aqueous HCl (1 M) and extracted with EtOAc. The combined organic phases were washed with saturated aqueous NaHCO₃ and brine, dried over MgSO₄ and concentrated under reduced pressure. Purification of the resultant residue by flash column chromatography (hexanes:EtOAc 1:3, R_f = 0.3) gave diethanolamine **5.10** (370 mg, 1.06 mmol, 83%) as a deep red solid.

Data for 5.10: R_f : 0.3 (hexanes:EtOAc 1:3); $^1\text{H-NMR}$ (400 MHz, CDCl_3): δ (ppm) = 7.85 – 7.76 (m, 3H), 7.55 (d, J = 4.1 Hz, 1H), 6.78 – 6.73 (m, 2H), 3.96 (t, J = 4.9 Hz, 4H), 3.90 (s, 3H), 3.73 (t, J = 4.9 Hz, 4H), 2.93 (s, 2H). $^{13}\text{C-NMR}$ (100 MHz, CDCl_3): δ (ppm) = 165.7, 163.3, 151.1, 143.4, 133.4, 131.8, 127.7, 125.9, 112.4, 60.9, 55.3, 52.5. **HRMS (ESI):** calc. for $\text{C}_{16}\text{H}_{20}\text{N}_3\text{O}_4^{32}\text{S}$ [$M+H$] $^+$: 350.1169, found:3501173.

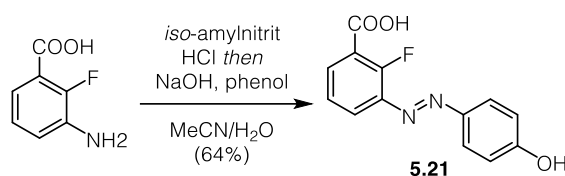


Thiophene 5.12: A solution of diethanolamine **5.10** (25.7 mg, 0.078 mmol) and LiOH·H₂O (32.7 mg, 0.780 mmol) in MeOH (1 mL), THF (1 mL) and H₂O (1 mL) was stirred at 60 °C overnight. The reaction mixture was cooled to room temperature, acidified with aqueous HCl (1 M) and extracted with EtOAc. The combined organic phases were dried over MgSO₄ and concentrated under reduced pressure to give crude acid **5.16** which was used in the next step without further purification.

NEt₃ (30.0 μL , 0.218 mmol) was added to a solution of crude acid **5.16**, 2-methyltryptamine (14.0 mg, 0,078 mmol) and HBTU (83.0 mg, 0.218 mmol) in DMF (2 mL) and the solution was stirred at room temperature overnight. Removal of the solvent under reduced pressure and purification of the resulting residue by reverse phase HPLC (MeCN:H₂O (0.1% formic acid) 0:100 to 100:0) gave thiophene **5.12** (7.2 mg, 0.017 mmol, 23%) as a red solid.

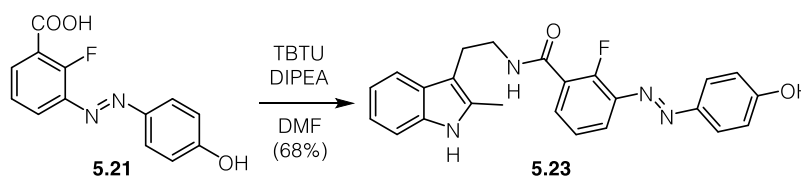
Data for 5.12: $^1\text{H-NMR}$ (400 MHz, $d_4\text{-MeOH}$): δ (ppm) = 7.80 – 7.72 (m, 2H), 7.57 (d, J = 4.1 Hz, 1H), 7.52 – 7.47 (m, 2H), 7.23 (dt, J = 8.0, 1.0 Hz, 1H), 7.04 – 6.92 (m, 2H), 6.91 – 6.85 (m, 2H), 3.79 (t, J = 5.8 Hz, 4H), 3.69 (t, J = 5.9 Hz, 4H), 3.54 (dd, J = 7.8, 6.7 Hz, 2H), 3.01 (t, J = 7.3 Hz, 2H), 2.37 (s, 3H). $^{13}\text{C-NMR}$ (100 MHz, $d_4\text{-MeOH}$): δ (ppm) = 165.3, 164.6, 152.8, 144.0, 138.8, 137.2, 133.3, 123.0, 129.4, 128.4, 126.6, 121.4, 119.5, 118.4, 113.0, 111.3, 108.8, 60.3, 55.0, 42.0, 25.2, 11.4. **IR (ATR):** ν_{max} (cm⁻¹) = 3283 (br), 2919 (w), 1594 (s), 1541 (m), 1511 (m), 1461 (w), 1400 (w), 1350

(m), 1304 (m), 1146 (vs), 1043 (m), 1001 (m), 822 (m), 741 (m). **HRMS (ESI)**: calc. for $C_{26}H_{30}N_5O_3^{32}S$ $[M+H]^+$: 492.2064, found: 492.2063.



Carboxylic acid 5.21: Aqueous conc. HCl (0.95 mL) was added to an ice cooled solution of 3-amino-2-fluorobenzoic acid (550 mg, 3.55 mmol) in MeCN (7 mL) and the solution was stirred for 5 min at that temperature. Isoamyl nitrite (0.48 mL, 3.55 mmol) was added and the reaction was stirred for 1 h at 0 °C. The resulting suspension was added dropwise to an ice cooled solution of phenol (334 mg, 3.55 mmol) in aqueous NaOH (2 M, 6.6 mL) and H₂O (0.4 mL) and the reaction was stirred for 1 h at 0 °C. The mixture was acidified with aqueous HCl (1 M) and extracted with EtOAc. The combined organic phases were washed with brine, dried over MgSO₄ and concentrated under reduced pressure. Purification of the resultant residue by flash column chromatography (CH₂Cl₂:MeOH:AcOH 96:4:0.1 to 94:6:0.1) gave carboxylic acid **5.21** (588 mg, 2.26 mmol, 64%) as a red solid.

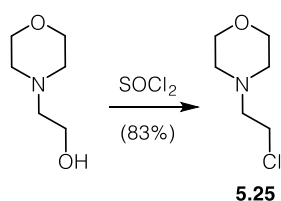
Data for 5.21: ¹H-NMR (400 MHz, *d*₄-MeOH): δ (ppm) = 8.02 – 7.94 (m, 1H), 7.90 – 7.81 (m, 3H), 7.29 (td, *J* = 7.9, 1.0 Hz, 1H), 6.96 – 6.88 (m, 2H). ¹³C-NMR (100 MHz, *d*₄-MeOH): δ (ppm) = 167.0, 167.0, 162.9, 161.5, 158.8, 147.7, 143.0, 142.9, 134.5, 126.6, 125.0, 124.9, 122.7, 122.1, 122.0, 116.8. **IR (ATR)**: ν_{max} (cm⁻¹) = 3079 (br), 1688 (vs), 1599 (s), 1590 (s), 1526 (w), 1502 (m), 1482 (m), 1460 (m), 1420 (w), 1358 (w), 1286 (m), 1243 (s), 1215 (m), 1163 (w), 1143 (s), 1102 (w), 841 (m), 764 (m), 667 (w). **HRMS (ESI)**: calc. for C₁₃H₈N₂O₃F $[M-H]^-$: 259.0524, found: 259.0526.



Amide 5.23: DIPEA (180 μL, 1.03 mmol) was added to a solution of carboxylic acid **5.21** (60.0 mg, 0.342 mmol), 2-methyltryptamine (89.0 mg, 0.342 mmol) and TBTU (165 mg, 0.517 mmol) in DMF (3.5 mL) and the solution was stirred at room temperature overnight.

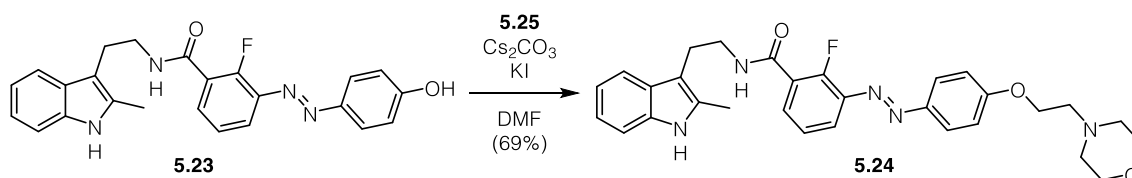
The reaction was diluted with EtOAc and washed with aqueous HCl (1 M) and brine. The organic phase was dried over MgSO₄ and concentrated under reduced pressure. Purification of the resultant residue by flash column chromatography (CH₂Cl₂:acetone 93:7 and CH₂Cl₂:MeOH 98:2) gave amide **5.23** (97 mg, 0.233 mmol, 68%) as an orange solid.

Data for 5.23: *R_f*: 0.2 (CH₂Cl₂:acetone 93:7); **¹H-NMR (400 MHz, CDCl₃):** δ (ppm) = 8.11 – 8.00 (m, 2H), 7.94 (s, 1H), 7.89 – 7.83 (m, 2H), 7.80 (td, *J* = 7.7, 1.9 Hz, 1H), 7.54 (dd, *J* = 7.5, 1.3 Hz, 1H), 7.26 (s, 2H), 7.09 (dtd, *J* = 16.2, 7.1, 1.3 Hz, 2H), 7.03 – 6.95 (m, 3H), 3.85 – 3.77 (m, 2H), 3.08 (t, *J* = 6.8 Hz, 2H), 2.37 (s, 3H). **¹³C-NMR (100 MHz, CDCl₃):** δ (ppm) = 207.6, 163.5, 160.2, 158.9, 156.4, 147.1, 141.2, 141.1, 135.5, 133.4, 132.4, 128.4, 125.7, 124.7, 124.6, 121.4, 121.1, 119.5, 118.0, 116.2, 110.5, 108.3, 40.8, 24.2, 11.8. **IR (ATR):** *v*_{max} (cm⁻¹) = 3260 (br), 1641 (m), 1586 (s), 1532 (m), 1504 (m), 1460 (m), 1428 (m), 1365 (w), 1274 (m), 1233 (m), 1206 (s), 1140 (vs), 1099 (w), 1010 (w), 843 (m), 822 (w), 743 (s), 668 (w). **HRMS (ESI):** calc. for C₂₄H₂₂N₄O₂F [M+H]⁺:417.1721, found:417.1718.



Chloride 5.25: 4-(2-Hydroxyethyl)morpholine (5.00 g, 38.1 mmol) was added dropwise to ice cooled SOCl₂ (50 mL, 689 mmol) and the reaction was stirred at 60 °C overnight. The volatiles were removed under reduced pressure and the resultant residue was portioned between CH₂Cl₂ and aqueous Na₂CO₃. The organic phase was washed with H₂O and brine, dried over MgSO₄ and concentrated under reduced pressure to give chloride **5.25** (4.71 g, 31.5 mmol, 83%) as a grey solid.

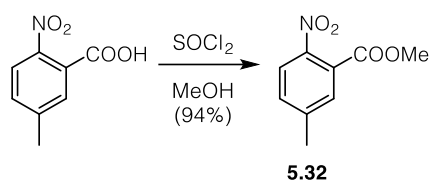
Data for 5.25: **¹H-NMR (400 MHz, *d*₆-DMSO):** δ (ppm) = 4.05 (t, *J* = 6.8 Hz, 2H), 3.93 (s, 2H), 3.80 (dd, *J* = 19.9, 8.6 Hz, 2H), 3.49 (t, *J* = 6.8 Hz, 2H), 3.43 (s, 2H), 3.21 – 3.04 (m, 2H). **¹³C-NMR (100 MHz, *d*₆-DMSO):** δ (ppm) = 63.1, 56.2, 51.2, 37.0. **IR (ATR):** *v*_{max} (cm⁻¹) = 2961 (w), 1855 (w), 2809 (w), 1450 (m), 1304 (m), 1271 (w), 1114 (vs), 1070 (m), 1006 (s), 913 (m), 866 (s), 806 (w), 732 (m), 666 (m). **HRMS (ESI):** calc. for C₆H₁₃NOCl [M+H]⁺:150.0680, found:150.0680.



Morpholine 5.24: A solution of amide **5.23** (45.0 mg, 0.108 mmol), Cs_2CO_3 (106 mg, 0.324 mmol) and KI (10 mg, 60.0 μM) in DMF (3 mL) was stirred at room temperature for 10 min. Chloride **5.25** (32 mg, 0.216 mmol) was added and the solution was stirred at 80 °C overnight. After cooling to room temperature the reaction was diluted with EtOAc and washed with H_2O and brine. The organic phase was dried over MgSO_4 and concentrated under reduced pressure. Purification of the resultant residue by flash column chromatography ($\text{CH}_2\text{Cl}_2:\text{MeOH}$ 98:2) gave morpholine **5.24** (39 mg, 0.074 mmol, 69%) as an orange solid. The product was obtained as a mixture of *cis* and *trans* conformers.

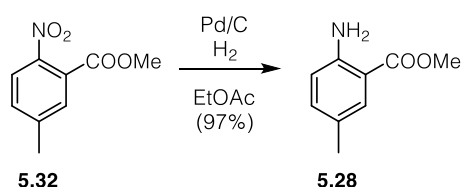
Data for 5.24: R_f : 0.4 ($\text{CH}_2\text{Cl}_2:\text{MeOH}$ 96:4); $^1\text{H-NMR}$ (400 MHz, CDCl_3): δ (ppm) = 8.19 – 8.12 (m, 1H), 7.98 – 7.88 (m, 3H), 7.82 (td, J = 7.6, 1.9 Hz, 1H), 7.59 – 7.54 (m, 1H), 7.33 – 7.26 (m, 2H), 7.15 – 7.06 (m, 2H), 7.04 – 7.00 (m, 2H), 6.93 – 6.85 (m, 1H), 4.21 (t, J = 5.7 Hz, 2H), 3.82 – 3.74 (m, 6H), 3.08 (t, J = 6.8 Hz, 2H), 2.86 (t, J = 5.7 Hz, 2H), 2.62 (t, J = 4.7 Hz, 4H), 2.41 (s, 3H). $^{13}\text{C-NMR}$ (100 MHz, CDCl_3): δ (ppm) = 163.1, 161.9, 159.0, 156.4, 147.3, 141.1, 141.0, 135.5, 133.7, 132.3, 128.5, 125.4, 124.6, 124.6, 123.3, 123.0, 122.9, 121.3, 120.9, 119.5, 118.0, 115.0, 110.4, 108.4, 67.0, 66.3, 57.6, 54.2, 40.7, 24.3, 11.8. **IR (ATR):** ν_{max} (cm^{-1}) = 3301 (br), 2919 (w), 2853 (w), 1648 (s), 1598 (s), 1582 (w), 1527 (m), 1500 (s), 1462 (m), 1452 (m), 1358 (w), 1298 (m), 1250 (vs), 1142 (8vs), 1114 (s), 1068 (w), 1036 (w), 1010 (w), 954 (w), 915 (w), 838 (m), 741 (s), 679 (w). **HRMS (ESI):** calc. for $\text{C}_{30}\text{H}_{33}\text{N}_5\text{O}_3\text{F}$ [$M+H$] $^+$: 530.2562, found: 530.2557.

6.6.1 Photoswitches based on blebbistatin



Methyl ester 5.32: Thionylchloride (27 mL, 372 mmol) was added to an ice cooled solution of 5-methyl-2-nitro-benzoate (7.46 g, 41.18 mmol) in methanol (100 mL). The solution was heated at 60 °C for 20 h, quenched with saturated aqueous NaHCO₃ and extracted with CH₂Cl₂. The organic phase was washed with brine, dried MgSO₄ and concentrated under reduced pressure to give methyl ester **5.32** (7.58 g, 38.85 mmol, 94%) as a colorless solid.

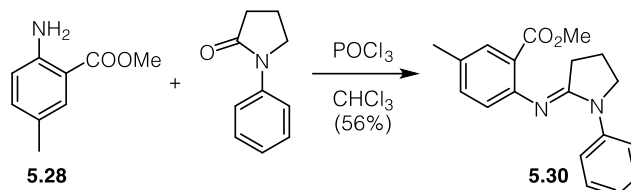
Data for 5.32: ¹H-NMR (400 MHz, CDCl₃): δ (ppm) = 7.83 (d, J = 8.3 Hz, 1H), 7.45 (m, 1H), 7.37 (m, 1H), 3.89 (s, 3H), 2.44 (s, 3H). ¹³C-NMR (100 MHz, CDCl₃): δ (ppm) = 166.6, 145.8, 1444.8, 132.1, 130.2, 128.3, 124.3, 53.4, 21.6. IR (ATR): ν_{max} (cm⁻¹) = 1722 (vs), 1590 (w), 1535 (s), 1492 (w), 1440 (s), 1378 (m), 1291 (vs), 1207 (s), 1137 (m), 1067 (m), 971 (s), 902 (w), 838 (vs), 783 (s), 741 (m), 705 (m), 670 (m), 618 (s). HRMS (EI): calc. for C₉H₉NO₄ [M]⁺: 195.0526, found: 195.0529.



Aniline 5.28: A suspension of methyl ester **5.32** (1.29 g, 6.61 mmol) and Pd/C (400 mg) in EtOAc (20 mL) was purged with H₂ and stirred under a H₂-atmosphere at room temperature overnight. The reaction mixture was filtered over a pad of celite and concentrated under reduced pressure to give aniline **5.28** (1.06 g, 6.39 mmol, 97%) as colorless solid.

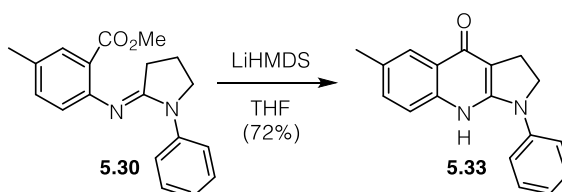
Data for 5.28: ¹H-NMR (400 MHz, CDCl₃): δ (ppm) = 7.64 (m, 1H), 7.07 (m, 1H), 6.57 (d, J = 8.3 Hz, 1H), 5.52 (bs, 1H), 3.84 (s, 3H), 2.21 (s, 3H). ¹³C-NMR (100 MHz, CDCl₃): δ (ppm) = 168.6, 148.3, 135.2, 130.8, 125.4, 51.5, 20.3. IR (ATR): ν_{max} (cm⁻¹) = 3472 (m), 3365 (m), 2946 (w), 2915 (vw), 2856 (vw), 1681 (s), 1625 (m), 1577 (m), 1559 (s), 1500 (m), 1455 (w), 1438 (s), 1380 (w), 1348 (w), 1293 (s), 1237 (s), 1201 (vs), 1186

(s), 1162 (s), 1087 (s), 1005 (m), 968 (m), 897 (m), 825 (s), 791 (s), 766 (m), 704 (m), 678 (m). **HRMS (EI)**: calc. for $C_9H_{11}NO_2$ $[M]^+$: 165.0784, found: 165.0790.



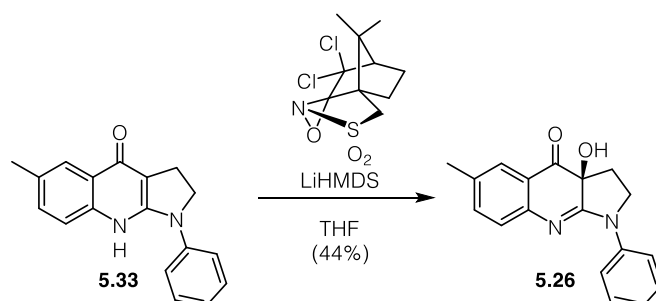
Amidine 5.30¹⁶⁷: $POCl_3$ (0.69 mL, 7.44 mmol) was added to a solution of 1-phenyl-2-pyrrolidinone (1.00 g, 6.20 mmol) in $CHCl_3$ (10 ml) and the reaction was stirred at room temperature for 3 h. A solution of aniline **5.28** (1.02 g, 6.20 mmol) in $CHCl_3$ (10 mL) was added and the reaction was stirred at 60 °C overnight. Evaporation of the volatiles under reduced pressure and purification of the resulting residue by flash column chromatography (CH_2Cl_2 :MeOH 96:4) gave amidine **5.30** (1.07 g, 3.48 mmol, 56%) as a colorless solid. Note: Prolonged exposure to silica led to hydrolysis of the product.

Data for 5.30: 1H -NMR (400 MHz, $CDCl_3$): δ (ppm) = 7.81 (d, J = 7.9 Hz, 2H), 7.66 (d, J = 2.1 Hz, 1H), 7.40 – 7.30 (m, 2H), 7.18 (ddd, J = 8.1, 2.2, 0.7 Hz, 1H), 7.10 – 6.99 (m, 1H), 6.72 (d, J = 8.1 Hz, 1H), 3.87 (t, J = 6.9 Hz, 2H), 3.82 (s, 3H), 2.46 (t, J = 7.8 Hz, 2H), 2.32 (s, 3H), 2.10 – 1.98 (m, 2H). ^{13}C -NMR (100 MHz, $CDCl_3$): δ (ppm) = 168.0, 159.9, 150.7, 141.6, 133.6, 131.2, 128.7, 123.2, 123.1, 122.1, 120.4, 51.9, 50.8, 29.3, 20.7, 19.9. **HRMS (EI)**: calc. for $C_{19}H_{20}N_2O_2$ $[M]^+$: 308.1519, found: 308.1481.



Enone 5.33¹⁶⁷: LiHMDS (1 M in THF, 4.77 mL, 4.77 mmol) was added dropwise to a solution of amidine **5.30** (680 mg, 2.21 mmol) in THF (30 mL) at -78 °C. The solution was allowed to warm to 0 °C over 5 h before it was quenched with saturated aqueous NH_4Cl (8 mL) and extracted with CH_2Cl_2 . The combined organic phases were washed with brine, dried over magnesium sulfate and concentrated under reduced pressure. Purification of the resulting residue by flash column chromatography (acetone R_f = 0.3) enone **5.33** (316 mg, 1.14 mmol, 72%) as a yellow solid.

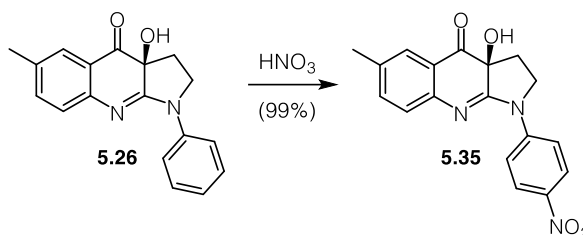
Data for 5.33: $^1\text{H-NMR}$ (400 MHz, $d_4\text{-MeOH}$): δ (ppm) = 7.94 (m, 1H), 7.51 (m, 2H), 7.43 (m, 2H), 7.34 (m, 3H), 4.12 (dd, $J = 9.1, 8.1$ Hz, 2H), 3.14 (dd, 9.2, 8.0, 2H). $^{13}\text{C-NMR}$ (100 MHz, $d_4\text{-MeOH}$): δ (ppm) = 171.3, 156.2, 141.2, 137.8, 134.4, 132.8, 131.3, 127.8, 124.8, 124.7, 124.7, 118.8, 105.5, 55.2, 24.3, 21.3. **IR (ATR):** ν_{max} (cm^{-1}) = 2900 (vw), 2852 (vw), 1626 (w), 1611 (w), 1598 (w), 1569 (s), 1546 (m), 1520 (m), 1494 (s), 1467 (m), 1451 (s), 1410 (m), 1375 (s), 1341 (m), 1307 (vs), 1292 (s), 1235 (m), 1181 (m), 1154 (m), 1127 (m), 1112 (m), 1058 (m), 989 (w), 955 (m), 912 (w), 878 (w), 857 (w), 817 (m), 784 (w), 775 (w), 751 (vs), 730 (m), 687 (vs), 668 (m). **HRMS (EI):** calc. for $\text{C}_{18}\text{H}_{16}\text{N}_2\text{O}$ [M] $^+$: 276.1257, found: 276.1204.



(S)-Blebbistatin (5.26)¹⁶⁷: LiHMDS (1.0 M in THF, 2.28 mL, 2.28 mmol) was added dropwise to a solution of enone **5.33** (316 mg, 1.14 mmol) in THF (5.0 mL) at -78 °C. The reaction was stirred at that temperature for 30 min, a solution of (–)-(8,8-Dichlorocamphorylsulfonyl) oxaziridine (817 mg, 2.74 mmol) in THF (10 mL) was added and the mixture was stirred at -10 °C for 16 h. The reaction was diluted with saturated aqueous NH_4Cl and ether, warmed to room temperature, diluted with aqueous NaS_2O_3 and extracted with EtOAc. The combined organic phases were dried over MgSO_4 and concentrated under reduced pressure. The resulting residue was portioned between CH_2Cl_2 and aqueous HCl (0.3 M). The aqueous phase was basified with aqueous NaOH (4 M) and extracted with EtOAc. The organic phase was dried over MgSO_4 and concentrated under reduced pressure. Purification of the resulting residue by recrystallization from MeCN gave (S)-blebbistatin (**5.26**) (147 mg, 0.502 mmol, 44%) as a bright yellow solid.

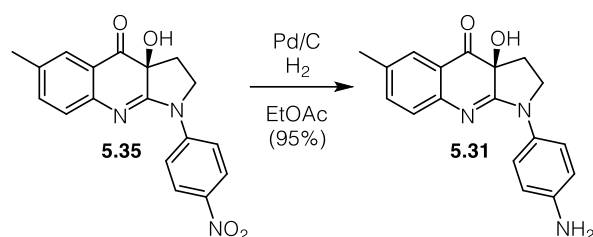
Data for 5.26: $^1\text{H-NMR}$ (400 MHz, CDCl_3): δ (ppm) = 7.85 (m, 2H), 7.61 (m, 1H), 7.41 (m, 2H), 7.15 (m, 2H), 6.98 (d, $J = 8.1$ Hz, 1H), 4.03 (bs, 1H), 3.80 (m, 2H), 2.38 (m, 1H), 2.30 (s, 3H), 2.19 (m, 1H). $^{13}\text{C-NMR}$ (100 MHz, CDCl_3): δ (ppm) = 194.5, 164.8, 148.7, 140.1, 137.5, 133.7, 129.0, 127.4, 126.3, 124.8, 120.5, 120.3, 73.9, 48.3, 29.2, 20.9. **IR (ATR):** ν_{max} (cm^{-1}) = 3060 (br), 1691 (s), 1592 (s), 1579 (s), 1481 (s), 1452 (w), 1433

(m), 1317 (m), 1297 (s), 1263 (m), 1223 (w), 1206 (m), 1192 (w), 1158 (m), 1108 (m), 1085 (w), 1060 (w), 979 (w), 939 (w), 904 (w), 844 (m), 800 (m), 758 (s), 734 (m), 706 (m), 692 (vs), 658 (m). **HRMS (ESI):** calc. for $C_{18}H_{17}N_2O_2$ $[M+H]^+$: 293.1285, found: 293.1281.



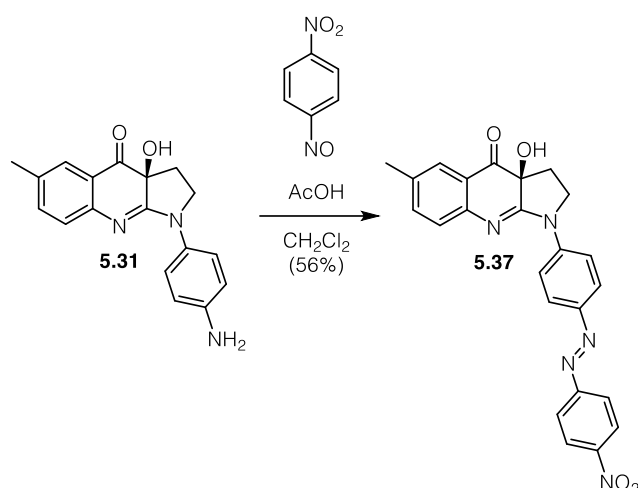
Nitrobenzene 5.35: A solution of (*S*)-blebbistatin (**5.26**) (142 mg, 0.486 mmol) in HNO_3 (65%, 5 mL) was stirred for 20 h at 50 °C, cooled to room temperature and poured onto ice. The resulting mixture was carefully basified with aqueous NaOH (1 M) and extracted with EtOAc. The combined organic phases were washed with brine, dried over MgSO_4 and concentrated under reduced pressure. Purification of the resulting residue by flash column chromatography (pentane:EtOAc 1:3, $R_f = 0.25$) gave nitrobenzene **5.35** (162 mg, 0.481 mmol, 99%) as a red solid.

Data for 5.35: $^1\text{H-NMR}$ (400 MHz, d_6 -DMSO): δ (ppm) = 8.07 – 7.99 (m, 2H), 7.84 (dd, $J = 2.0, 0.8$ Hz, 1H), 7.77 (dd, $J = 2.1, 0.8$ Hz, 1H), 7.47 – 7.37 (m, 2H), 7.23 – 7.14 (m, 1H), 7.09 (s, 1H), 4.13 (td, $J = 9.9, 5.9$ Hz, 1H), 4.04 (dd, $J = 10.1, 8.8$ Hz, 1H), 2.42 (dd, $J = 13.5, 9.2$ Hz, 1H), 2.36 (s, 3H), 2.26 (dd, $J = 13.3, 5.7$ Hz, 1H). **$^{13}\text{C-NMR}$ (100 MHz, d_6 -DMSO):** δ (ppm) = 192.3, 166.5, 145.3, 141.7, 139.8, 132.1, 130.0, 129.2, 128.7, 124.4, 122.8, 119.9, 73.4, 48.0, 27.9, 19.9. **HRMS (ESI):** calc. for $C_{18}H_{16}N_3O_4$ $[M+H]^+$: 338.1135, found: 338.1138.



Aniline 5.31: A suspension of nitrobenzene **5.35** (200 mg, 0.659 mmol) and Pd/C (20 mg) in EtOAc (20 mL) was purged with H₂ and stirred under a H₂-atmosphere at room temperature for 2 h. The reaction mixture was filtered over a pad of celite and concentrated under reduced pressure to give aniline **5.31** (192 mg, 0.623 mmol, 95%) as a red solid.

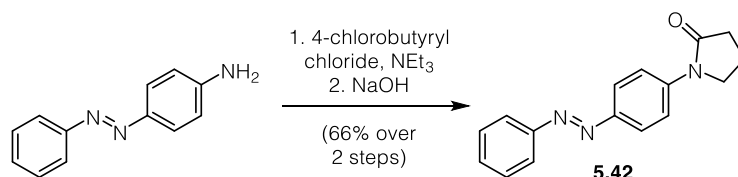
Data for 5.31: ¹H-NMR (400 MHz, CDCl₃): δ (ppm) = 7.95 – 7.83 (m, 2H), 7.46 – 7.35 (m, 2H), 7.19 – 7.12 (m, 1H), 7.12 – 7.08 (m, 1H), 6.77 (d, *J* = 1.9 Hz, 1H), 4.21 (td, *J* = 9.8, 5.9 Hz, 1H), 3.95 (t, *J* = 9.1 Hz, 1H), 2.46 (dd, *J* = 13.9, 5.8 Hz, 1H), 2.30 (ddd, *J* = 13.9, 9.9, 8.5 Hz, 1H), 2.24 (s, 3H). ¹³C-NMR (100 MHz, CDCl₃): δ (ppm) = 195.1, 162.7, 141.5, 140.5, 135.6, 134.1, 129.0, 124.3, 122.7, 120.3, 120.0, 117.3, 73.8, 48.1, 28.9, 21.1. IR (ATR): ν_{max} (cm⁻¹) = 3317 (br), 2918 (br), 1675 (m), 1623 (s), 1590 (s), 1491 (m), 1473 (m), 1441 (w), 1417 (m), 1342 (w), 1301 (vs), 1267 (m), 1230 (w), 1211 (m), 1188 (w), 1156 (w), 1102 (w), 1043 (w), 985 (w), 946 (w), 846 (w), 793 (m), 751 (s), 716 (s). HRMS (ESI): calc. for C₁₈H₁₈N₃O₂ [*M*+*H*]⁺: 308.1394, found: 308.1391.



Azobenzene 5.37: A solution of aniline **5.31** (20 mg, 0.065 mmol) and 4-nitroso-1-nitrobenzene (20 mg, 0.130 mmol) in CH₂Cl₂ (2 mL) and AcOH (1 mL) was stirred at room temperature overnight. The reaction mixture was diluted with saturated aqueous NaHCO₃ and extracted with EtOAc. The combined organic layers were washed with

brine, dried over MgSO_4 and concentrated under reduced pressure. Purification of the resulting residue by flash column chromatography (pentane:EtOAc 3:1, $R_f = 0.35$) gave azobenzene **5.37** (16 mg, 0.036 mmol, 56%) as a red solid.

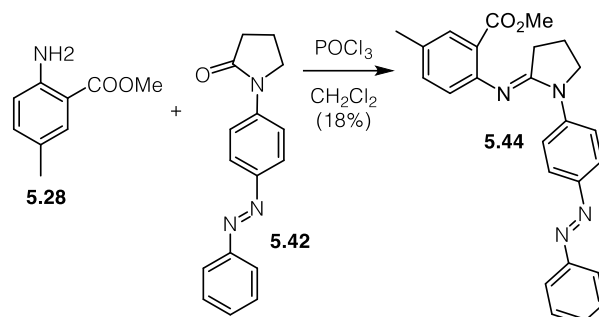
Data for 5.37: $^1\text{H-NMR}$ (400 MHz, $d_6\text{-DMSO}$): δ (ppm) = 8.57 – 8.52 (m, 2H), 8.36 – 8.31 (m, 2H), 8.20 – 8.14 (m, 2H), 7.82 (d, $J = 2.2$ Hz, 1H), 7.71 – 7.67 (m, 1H), 7.53 – 7.45 (m, 2H), 7.20 (t, $J = 7.4$ Hz, 1H), 7.06 (s, 1H), 4.10 (q, $J = 9.5, 8.1$ Hz, 2H), 2.39 (s, 3H), 2.36 – 2.28 (m, 2H). $^{13}\text{C-NMR}$ (100 MHz, $d_6\text{-DMSO}$): δ (ppm) = 193.6, 165.3, 155.7, 148.4, 147.1, 145.3, 140.4, 132.3, 131.4, 128.7, 125.3, 124.0, 123.3, 123.1, 122.5, 119.5, 73.0, 47.4, 28.1, 20.3. **IR (ATR):** ν_{max} (cm^{-1}) = 2918 (w), 2364 (m), 2168 (m), 1669 (m), 1618 (w), 1522 (w), 1494 (w), 1465 (w), 1419 (w), 1340 (s), 1260 (m), 1102 (s), 1023 (s), 858 (w), 802 (s), 754 (m). **HRMS (ESI):** calc. for $\text{C}_{24}\text{H}_{20}\text{N}_5\text{O}_4$ [$M+H$] $^+$: 442.1510, found: 442.1507.



Pyrrolidinone 5.42: NEt_3 (0.78 mL, 5.57 mmol) and 4-chlorobutyryl chloride (0.60 mL, 5.36 mmol) were sequentially added to an ice cooled solution of 4-aminoazobenzene (1.00 g, 5.07 mmol) in EtOAc (15 mL) and the reaction was stirred at room temperature for 4 h. The reaction mixture was washed with H_2O and brine, dried over MgSO_4 and concentrated under reduced pressure. The resulting residue was redissolved in *i*-PrOH (10 mL) and aqueous NaOH (6 M, 10 mL) and stirred at room temperature for 5 h. The reaction mixture was extracted with EtOAc and the combined organic phases were washed with aqueous citric acid (5%) and brine, dried over MgSO_4 and concentrated under reduced pressure. Purification of the resulting residue by flash column chromatography (pentane:EtOAc 1:1, $R_f = 0.35$) gave pyrrolidinone **5.42** (891 mg, 3.36 mmol, 66% over 2 steps) as an orange solid.

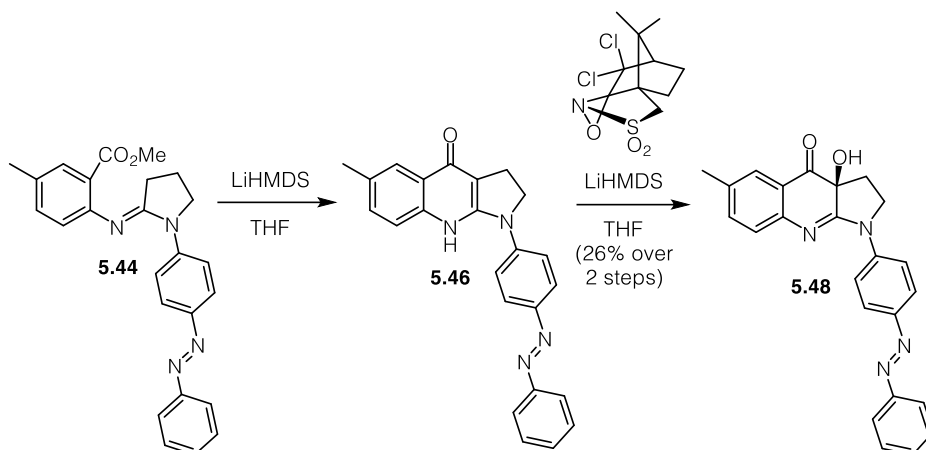
Data for 5.42: $^1\text{H-NMR}$ (400 MHz, CDCl_3): δ (ppm) = 7.99 – 7.94 (m, 2H), 7.93 – 7.88 (m, 2H), 7.84 – 7.79 (m, 2H), 7.55 – 7.43 (m, 3H), 3.92 (t, $J = 7.0$ Hz, 2H), 2.65 (t, $J = 8.1$ Hz, 2H), 2.25 – 2.13 (m, 2H). $^{13}\text{C-NMR}$ (100 MHz, CDCl_3): δ (ppm) = 174.7, 152.8, 148.9, 142.0, 130.9, 129.2, 123.8, 122.9, 119.7, 48.8, 33.0, 18.0. **IR (ATR):** ν_{max} (cm^{-1}) = 1682 (s), 1598 (m), 1500 (m), 1480 (w), 1462 (m), 1442 (w), 1417 (w), 1389 (m), 1325 (m), 1301 (m), 1223 (m), 1176 (w), 1154 (m), 1141 (m), 1120 (w), 1073 (w), 1026 (w),

1018 (w), 929 (w), 837 (s), 765 (s), 722 (m). **HRMS (EI)**: calc. for $C_{16}H_{15}N_3O$ [M]⁺: 265.1210, found: 265.1207.



Amidine 5.44: $POCl_3$ (0.26 mL, 2.83 mmol) was added to a solution of pyrrolidinone **5.42** (500 mg, 1.88 mmol) in CH_2Cl_2 (20 ml) and the reaction was stirred at room temperature for 3 h. A solution of aniline **5.28** (467 mg, 2.83 mmol) in CH_2Cl_2 (10 mL) was added and the reaction was stirred at 45 °C overnight. The reaction was diluted with CH_2Cl_2 , washed with saturated aqueous $NaHCO_3$, dried over $MgSO_4$ and concentrated under reduced pressure. Purification of the resulting residue by reverse phase column chromatography (MeCN:H₂O 0:100-100:0) gave amidine **5.44** (140 mg, 0.334 mmol, 18%) as an orange solid.

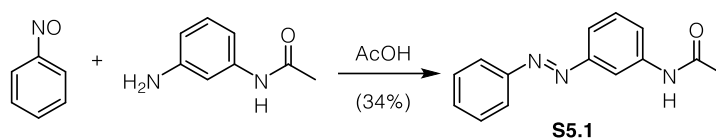
Data for 5.44: **¹H-NMR (400 MHz, CDCl₃)**: δ (ppm) = 8.07 – 8.01 (m, 2H), 7.99 – 7.92 (m, 2H), 7.92 – 7.87 (m, 2H), 7.69 (d, J = 2.1 Hz, 1H), 7.50 (dd, J = 8.4, 6.6 Hz, 2H), 7.47 – 7.42 (m, 1H), 7.22 (dd, J = 8.1, 2.2 Hz, 1H), 6.74 (d, J = 8.1 Hz, 1H), 3.95 (t, J = 6.8 Hz, 2H), 3.83 (s, 3H), 2.51 (t, J = 7.8 Hz, 2H), 2.34 (s, 3H), 2.09 (p, J = 7.4 Hz, 2H). **¹³C-NMR (100 MHz, CDCl₃)**: δ (ppm) = 167.8, 160.0, 153.0, 150.2, 147.9, 144.3, 133.8, 131.6, 131.3, 130.5, 129.2, 123.8, 122.8, 121.8, 119.9, 52.0, 50.7, 29.4, 20.8, 19.8. **HRMS (EI)**: calc. for $C_{25}H_{25}N_4O_2$ [$M+H$]⁺: 413.1972, found: 413.1972.



Tertiary alcohol 5.48: LiHMDS (1 M, in THF, 0.58 mL, 0.582 mmol) was added dropwise to a solution of amidine **5.44** (80 mg, 0.194 mmol) in THF (15 mL) at $-78\text{ }^{\circ}\text{C}$ and the reaction was allowed to warm to $0\text{ }^{\circ}\text{C}$ over 3 h before it was quenched with saturated aqueous NH_4Cl . The mixture was extracted with EtOAc and the combined organic phases were washed with H_2O and brine, dried over MgSO_4 and concentrated under reduced pressure to give crude enone **5.46** that was used in the next step without further purification.

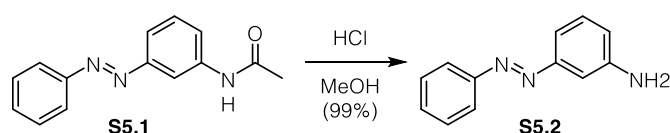
LiHMDS (1 M, in THF, 0.44 mL, 0.44 mmol) was added dropwise to a solution of crude enone **5.46** in THF (10 mL) at $-78\text{ }^{\circ}\text{C}$ and the solution was stirred at that temperature for 30 min. A solution of (-)-(8,8-Dichlorocamphorylsulfonyl) oxaziridine (160 mg, 0.535 mmol) in THF (5 mL) was added and the mixture was stirred at $-10\text{ }^{\circ}\text{C}$ overnight. After warming to room temperature, the reaction was quenched with aqueous NaS_2O_3 and extracted with Et_2O . The combined organic phases were dried over MgSO_4 and concentrated under reduced pressure. Purification of the resulting residue by recrystallization from MeCN gave tertiary alcohol **5.48** (20 mg, 0.050 mmol, 26% over 2 steps) as an orange solid.

Data for 5.48: $^1\text{H-NMR}$ (400 MHz, d_6 -DMSO): δ (ppm) = 8.40 – 8.33 (m, 2H), 8.03 – 7.97 (m, 2H), 7.89 (dd, $J = 7.2, 1.8$ Hz, 2H), 7.64 – 7.53 (m, 4H), 7.43 (dd, $J = 8.2, 2.1$ Hz, 1H), 7.22 (d, $J = 8.0$ Hz, 1H), 6.98 – 6.91 (m, 1H), 4.10 (ddt, $J = 15.7, 11.7, 5.9$ Hz, 2H), 2.36 – 2.27 (m, 5H). $^{13}\text{C-NMR}$ (100 MHz, d_6 -DMSO): δ (ppm) = 194.4, 165.4, 152.1, 148.4, 147.3, 143.4, 136.6, 133.2, 131.2, 129.5, 126.5, 126.3, 123.5, 122.5, 121.2, 119.7, 72.8, 47.6, 28.2, 20.3. **IR (ATR):** ν_{max} (cm^{-1}) = 1692 (m), 1618 (w), 1595 (m), 1575 (w), 1506 (w), 1482 (m), 1455 (w), 1426 (w), 1298 (m), 1234 (s), 1194 (m), 1158 (m), 1108 (s), 982 (s), 841 (m), 804 (m), 764 (m), 723 (w), 707 (w), 682 (m). **HRMS (EI):** calc. for $\text{C}_{24}\text{H}_{21}\text{N}_4\text{O}_2$ [$M+H$] $^+$: 397.1659, found: 397.1664.



Acetamide S5.1: A solution of nitrosobenzene (7.01 g, 46.7 mmol) and 3-aminoacetanilide (5.00 g, 46.7 mmol) in AcOH (50 mL) was stirred at 40 °C for 24 h and concentrated under reduced pressure. The resulting residue was portioned between saturated aqueous NaHCO₃ and EtOAc. The organic phase was washed with saturated aqueous NaHCO₃, aqueous HCl (1 M), aqueous NaOH (1 M), H₂O and brine, dried over MgSO₄ and concentrated under reduced pressure. Purification of the resulting residue by flash column chromatography (CH₂Cl₂:MeOH 96:4m R_f = 0.1) gave acetamide **S5.1** (3.77 g, 15.8 mmol, 34%) as a red solid.

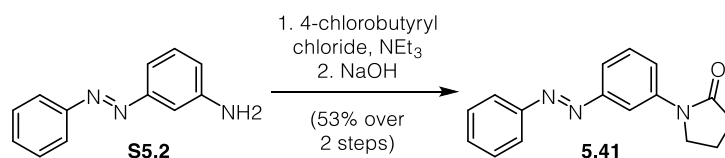
Data for S5.1: ¹H-NMR (400 MHz, CDCl₃): δ (ppm) = 8.02 (s, 1H), 7.92 (s, 1H), 7.90 – 7.83 (m, 2H), 7.72 (dt, *J* = 8.0, 1.4 Hz, 1H), 7.67 (dd, *J* = 7.8, 1.7 Hz, 1H), 7.53 – 7.42 (m, 4H), 2.20 (s, 3H). ¹³C-NMR (100 MHz, CDCl₃): δ (ppm) = 169.0, 153.2, 152.5, 138.9, 131.3, 129.7, 129.2, 123.0, 122.5, 119.7, 113.5, 24.7. IR (ATR): ν_{max} (cm⁻¹) = 3300 (w), 3066 (w), 1666 (s), 1596 (s), 1547 (s), 1490 (m), 1479 (m), 1414 (m), 1370 (m), 1322 (m), 1300 (m), 1286 (m), 1265 (m), 1150 (w), 1070 (w), 1020 (w), 1000 (w), 907 (w), 889 (w), 791 (m), 765 (m), 731 (m), 690 (s). HRMS (EI): calc. for C₁₄H₁₃N₃O [*M*]⁺: 239.1053, found: 239.1050.



Aniline S5.2: A solution of acetamide **S5.1** (3.77 g, 15.76 mmol) in MeOH (20 mL) and aqueous HCl (6 M, 20 mL) was stirred at 100 °C for 3 h. After cooling to room temperature, the reaction was extracted with EtOAc. The combined organic phases were washed with saturated aqueous NaHCO₃, H₂O and brine, dried over MgSO₄ and concentrated under reduced pressure to give aniline **S5.2** (3.09 g, 15.7 mmol, 99%) as a red solid.

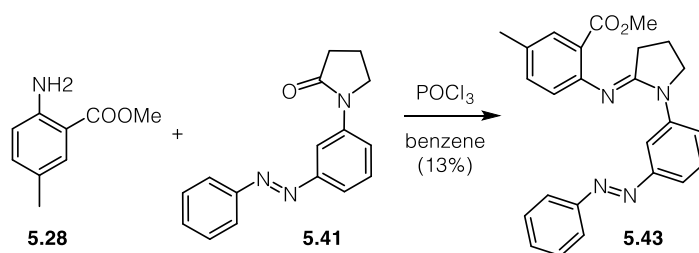
Data for S5.2: ¹H-NMR (400 MHz, CDCl₃): δ (ppm) = 7.94 – 7.86 (m, 2H), 7.56 – 7.45 (m, 3H), 7.37 (dt, *J* = 7.9, 1.4 Hz, 1H), 7.31 (t, *J* = 7.8 Hz, 1H), 7.23 (t, *J* = 2.1 Hz, 1H), 6.81 (ddd, *J* = 7.8, 2.4, 1.1 Hz, 1H), 3.83 (s, 2H). ¹³C-NMR (100 MHz, CDCl₃): δ (ppm) = 153.9, 152.8, 147.3, 131.0, 130.0, 129.2, 122.9, 118.0, 115.2, 107.5. IR (ATR): ν_{max}

(cm^{-1}) = 3399 (w), 333 (w), 1621 (s), 1606 (s), 1495 (w), 1480 (m), 1324 (w), 1308 (m), 1273 (s), 1149 (w), 1073 (w), 1023 (w), 993 (w), 955 (w), 920 (w), 864 (m), 756 (s), 767 (s). **HRMS (EI)**: calc. for $\text{C}_{14}\text{H}_{13}\text{N}_3\text{O}$ [M] $^+$: 239.1053, found: 239.1050.



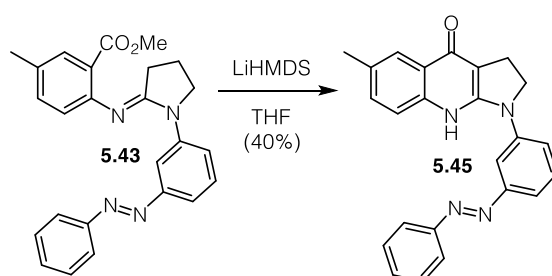
Pyrrolidinone 5.41: NEt_3 (0.78 mL, 5.57 mmol) and 4-chlorobutyryl chloride (0.60 mL, 5.36 mmol) were sequentially added to an ice cooled solution of 3-aminoazobenzene **S5.2** (1.00 g, 5.07 mmol) in EtOAc (15 mL) and the reaction was stirred at room temperature for 4 h. The reaction mixture was washed with H_2O and brine, dried over MgSO_4 and concentrated under reduced pressure. The resulting residue was redissolved in *i*-PrOH (10 mL) and aqueous NaOH (6 M, 10 mL) and stirred at room temperature for 5 h. The reaction mixture was extracted with EtOAc and the combined organic phases were washed with aqueous citric acid (5%) and brine, dried over MgSO_4 and concentrated under reduced pressure. Purification of the resulting residue by flash column chromatography (CH_2Cl_2 98:2, R_f = 0.5) gave pyrrolidinone **5.41** (713 mg, 2.69 mmol, 66% over 2 steps) as an orange solid.

Data for 5.41: $^1\text{H-NMR}$ (400 MHz, CDCl_3): δ (ppm) = 8.01 (t, J = 2.1 Hz, 1H), 7.97 (ddd, J = 8.2, 2.3, 1.0 Hz, 1H), 7.95 – 7.90 (m, 2H), 7.72 (ddd, J = 7.9, 1.8, 1.0 Hz, 1H), 7.55 – 7.47 (m, 4H), 3.97 (t, J = 7.0 Hz, 2H), 2.66 (t, J = 8.1 Hz, 2H), 2.24 – 2.17 (m, 2H). $^{13}\text{C-NMR}$ (100 MHz, CDCl_3): δ (ppm) = 174.6, 153.1, 152.7, 140.4, 131.3, 129.6, 129.2, 123.1, 122.6, 119.3, 113.5, 48.9, 33.0, 18.1. **IR (ATR)**: ν_{max} (cm^{-1}) = 1682 (vs), 1594 (m), 1480 (s), 1447 (w), 1397 (s), 1332 (m), 1317 (m), 1301 (w), 1280 (w), 1226 (s), 1169 (w), 1100 (w), 1022 (w), 32 (w), 898 (w), 883 (w), 790 (s), 767 (s), 729 (w). **HRMS (ESI)**: calc. for $\text{C}_{16}\text{H}_{16}\text{N}_3\text{O}$ [$M+H$] $^+$: 266,1288, found: 266,1287.



Amidine 5.43: POCl₃ (0.32 mL, 3.39 mmol) was added to a solution of pyrrolidinone **5.41** (600 mg, 2.26 mmol) in benzene (30 ml) and the reaction was stirred at room temperature for 3 h. A solution of aniline **5.28** (560 mg, 3.39 mmol) in benzene (20 mL) was added and the reaction was stirred at 80 °C overnight. The reaction was diluted with EtOAc, washed with saturated aqueous NaHCO₃ and brine, dried over MgSO₄ and concentrated under reduced pressure. Purification of the resulting residue by reverse phase column chromatography (MeCN:H₂O 0:100-100:0) gave amidine **5.43** (118 mg, 0.286 mmol, 13%) as an orange solid.

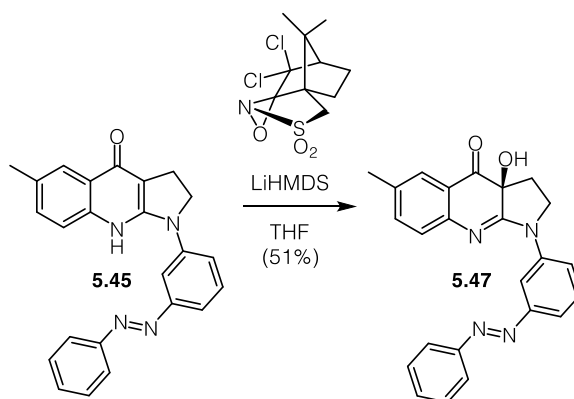
Data for 5.43: ¹H-NMR (400 MHz, CDCl₃): δ (ppm) = 8.26 (d, *J* = 8.2 Hz, 1H), 8.18 (s, 1H), 7.96 – 7.90 (m, 2H), 7.71 – 7.67 (m, 1H), 7.64 (d, *J* = 7.9 Hz, 1H), 7.49 (dt, *J* = 14.2, 6.8 Hz, 4H), 7.20 (dd, *J* = 8.3, 2.2 Hz, 1H), 6.75 (d, *J* = 8.1 Hz, 1H), 3.95 (t, *J* = 6.8 Hz, 2H), 3.84 (s, 3H), 2.50 (t, *J* = 7.8 Hz, 2H), 2.33 (s, 3H), 2.07 (q, *J* = 7.3 Hz, 2H). ¹³C-NMR (100 MHz, CDCl₃): δ (ppm) = 167.9, 160.0, 153.0, 152.7, 142.3, 133.7, 131.2, 131.0, 129.3, 129.1, 123.4, 123.0, 122.9, 122.0, 117.6, 114.1, 51.9, 50.8, 29.3, 20.7, 19.8. **HRMS (EI):** calc. for C₂₅H₂₅N₄O₂ [*M*+*H*]⁺: 413.1974, found: 413.1972.



Enone 5.45: LiHMDS (1 M, in THF, 0.86 mL, 0.86 mmol) was added dropwise to a solution of amidine **5.43** (118 mg, 0.286 mmol) in THF (10 mL) at –78 °C and the reaction was allowed to warm to room temperature and was stirred at that temperature for 7 h before it was quenched with saturated aqueous NH₄Cl. The mixture was extracted with EtOAc and the combined organic phases were washed with H₂O and brine, dried over MgSO₄ and concentrated under reduced pressure. Purification of the resulting residue

by flash column chromatography (pentane:EtOAc 2:1, $R_f = 0.3$) gave crude enone **5.45** (43 mg, 0.113 mmol, 40%) as an orange solid.

Data for 5.45: $^1\text{H-NMR}$ (400 MHz, CDCl_3): δ (ppm) = 7.87 (d, $J = 1.9$ Hz, 1H), 7.77 (dd, $J = 7.3, 2.4$ Hz, 2H), 7.72 (s, 1H), 7.48 – 7.35 (m, 6H), 7.26 – 7.13 (m, 3H), 3.85 (t, $J = 8.4$ Hz, 2H), 3.02 (t, $J = 8.4$ Hz, 2H), 2.29 (s, 3H). $^{13}\text{C-NMR}$ (100 MHz, CDCl_3): δ (ppm) = 171.3, 153.8, 153.3, 152.3, 141.4, 132.4, 131.4, 131.2, 129.9, 129.1, 128.8, 127.5, 123.7, 123.2, 123.0, 120.4, 119.2, 114.1, 104.4, 60.5, 23.3, 21.2. **HRMS (EI):** calc. for $\text{C}_{24}\text{H}_{27}\text{N}_4\text{O}$ [$M+H$] $^+$: 381.1710, found: 381.1713.



Tertiary alcohol 5.47: LiHMDS (1 M, in THF, 0.22 mL, 0.22 mmol) was added dropwise to a solution of enone **5.45** (43 mg, 0.113 mmol) in THF (10 mL) at -78 °C and the solution was stirred at that temperature for 30 min. A solution of (–)-(8,8-Dichlorocamphorylsulfonyl) oxaziridine (81 mg, 0.271 mmol) in THF (5 mL) was added and the mixture was stirred at -10 °C overnight. After warming to room temperature, the reaction was quenched with aqueous NaS_2O_3 and extracted with Et_2O . The combined organic phases were dried over MgSO_4 and concentrated under reduced pressure. Purification of the resulting residue by recrystallization from MeCN gave tertiary alcohol **5.47** (23 mg, 0.058 mmol, 51%) as an orange solid.

Data for 5.47: $^1\text{H-NMR}$ (400 MHz, $d_4\text{-MeOH}$): δ (ppm) = 8.55 (t, $J = 2.1$ Hz, 1H), 8.17 (dd, $J = 8.2, 2.0$ Hz, 1H), 7.95 (d, $J = 7.4$ Hz, 2H), 7.75 (d, $J = 7.9$ Hz, 1H), 7.66 – 7.53 (m, 5H), 7.42 – 7.37 (m, 1H), 7.20 (d, $J = 8.1$ Hz, 1H), 4.23 (td, $J = 9.8, 6.1$ Hz, 1H), 4.11 (t, $J = 8.8$ Hz, 1H), 2.42 (dt, $J = 16.1, 7.8$ Hz, 2H), 2.35 (s, 3H). $^{13}\text{C-NMR}$ (100 MHz, $d_4\text{-MeOH}$): δ (ppm) = 195.2, 165.7, 153.1, 152.5, 149.0, 141.4, 136.6, 133.2, 131.1, 129.2, 128.9, 126.5, 125.7, 123.1, 122.5, 121.0, 118.5, 114.7, 73.2, 28.6, 19.3. **IR (ATR):** ν_{max} (cm^{-1}) = 1683 (m), 1622 (s), 1590 (s), 1475 (s), 1452 (s), 1406 (m), 1325 (m), 1298 (s), 1266 (m), 1194 (w), 1142 (w), 1110 (w), 1069 (w), 1015 (w), 927 (w), 868 (w), 833 (w),

789 (m), 764 (m), 734 (w), 690 (s). **HRMS (EI)**: calc. for $C_{24}H_{21}N_4O_2$ $[M+H]^+$: 397.1659, found: 397.1659.

Chapter VII

Appendix

7.1 Crystallographic Data

- Tetrahydrothiophene 17 (CCDC 1563493)

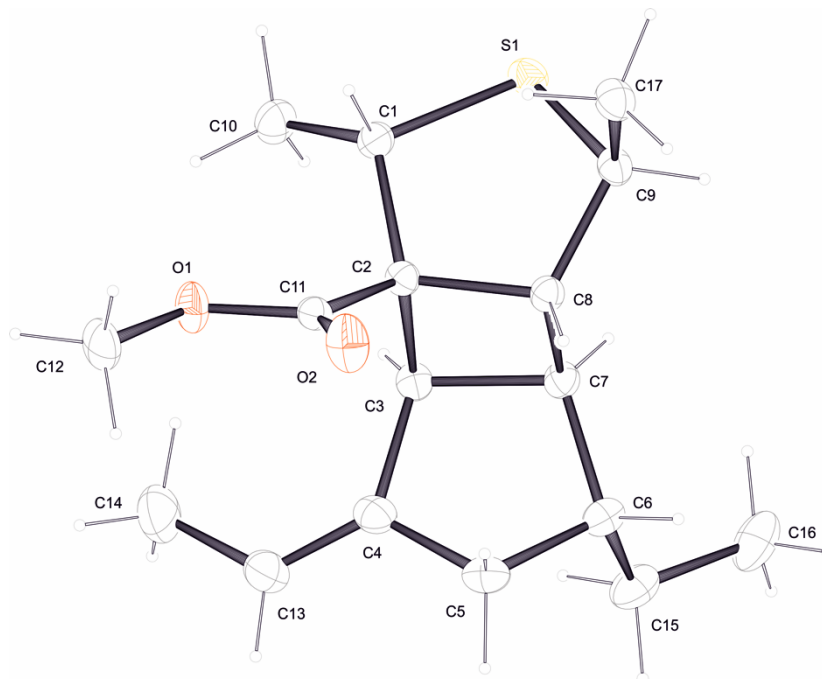


Figure 7.1. ORTEP of the molecular structure of tetrahydrothiophene **17**.

Table 7.1. Crystallographic data for tetrahydrothiophene 17.

net formula	C ₁₇ H ₂₆ O ₂ S
<i>M_r</i> /g mol ⁻¹	294.44
crystal size/mm	0.100 × 0.080 × 0.030
<i>T</i> /K	100.(2)
radiation	MoKα
diffractometer	'Bruker D8 Venture TXS'
crystal system	monoclinic
space group	'P 1 21/n 1'
<i>a</i> /Å	13.4104(4)
<i>b</i> /Å	9.3905(3)
<i>c</i> /Å	13.4470(3)
<i>α</i> /°	90
<i>β</i> /°	105.0380(10)
<i>γ</i> /°	90
<i>V</i> /Å ³	1635.39(8)
<i>Z</i>	4
calc. density/g cm ⁻³	1.196
μ/mm ⁻¹	0.198
absorption correction	Multi-Scan
transmission factor range	0.9076–0.9705
refls. measured	20641
<i>R</i> _{int}	0.0399
mean σ(<i>I</i>)/ <i>I</i>	0.0305

θ range	3.137–27.484
observed refls.	3149
x, y (weighting scheme)	0.0404, 0.8932
hydrogen refinement	constr
refls in refinement	3742
parameters	186
restraints	0
$R(F_{\text{obs}})$	0.0359
$R_w(F^2)$	0.0948
S	1.038
shift/error _{max}	0.002
max electron density/e \AA^{-3}	0.354
min electron density/e \AA^{-3}	-0.258

- Vinylogous carbonate **20** (CCDC 1563492)

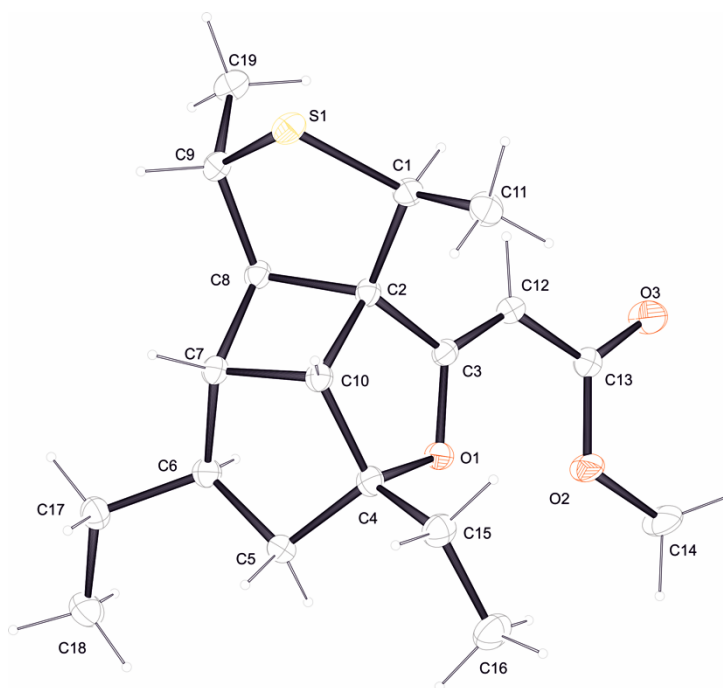


Figure 7.2. ORTEP of the molecular structure of tricycle **20**.

Table 7.2. Crystallographic data for tricycle 20.

net formula	$\text{C}_{19}\text{H}_{28}\text{O}_3\text{S}$
$M_r/\text{g mol}^{-1}$	336.47
crystal size/mm	$0.100 \times 0.090 \times 0.070$
T/K	100.(2)
radiation	MoK α
diffractometer	'Bruker D8 Venture TXS'
crystal system	triclinic
space group	'P -1'
$a/\text{\AA}$	9.6756(5)

$b/\text{\AA}$	9.9965(5)
$c/\text{\AA}$	10.5598(6)
$\alpha/^\circ$	73.852(2)
$\beta/^\circ$	71.287(2)
$\gamma/^\circ$	71.142(2)
$V/\text{\AA}^3$	897.95(8)
Z	2
calc. density/ g cm^{-3}	1.244
μ/mm^{-1}	0.193
absorption correction	Multi-Scan
transmission factor range	0.9062–0.9705
refls. measured	10749
R_{int}	0.0311
mean $\sigma(I)/I$	0.0350
θ range	3.303–26.342
observed refls.	3111
x, y (weighting scheme)	0.0396, 0.5084
hydrogen refinement	constr
refls in refinement	3637
parameters	213
restraints	0
$R(F_{\text{obs}})$	0.0356
$R_w(F^2)$	0.0954
S	1.062
shift/error $_{\text{max}}$	0.001
max electron density/ e \AA^{-3}	0.337
min electron density/ e \AA^{-3}	-0.257

- Enone 2.100

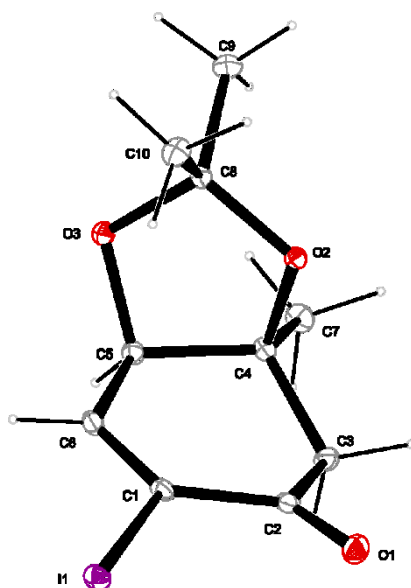


Figure 7.3. ORTEP of the molecular structure of enone 2.100.

Table 7.3. Crystallographic data for enone 2.100.

net formula	$C_{10}H_{13}IO_3$
$M_r/g\ mol^{-1}$	308.10
crystal size/mm	0.100 × 0.080 × 0.050
T/K	100.(2)
radiation	MoK α
diffractometer	'Bruker D8 Venture TXS'
crystal system	monoclinic
space group	'P 1 21/c 1'
$a/\text{\AA}$	5.5298(4)
$b/\text{\AA}$	12.2048(10)
$c/\text{\AA}$	16.1544(12)
$\alpha/^\circ$	90
$\beta/^\circ$	94.678(2)
$\gamma/^\circ$	90
$V/\text{\AA}^3$	1086.63(14)
Z	4
calc. density/ $g\ cm^{-3}$	1.883
μ/mm^{-1}	2.927
absorption correction	Multi-Scan
transmission factor range	0.5958–0.6367
refls. measured	20258
R_{int}	0.0530
mean $\sigma(I)/I$	0.0329
θ range	3.338–30.501
observed refls.	3010
x, y (weighting scheme)	0.0244, 0.5259
hydrogen refinement	constr
refls in refinement	3298
parameters	130
restraints	0
$R(F_{obs})$	0.0212
$R_w(F^2)$	0.0561
S	1.043
shift/error _{max}	0.001
max electron density/ $e\ \text{\AA}^{-3}$	0.902
min electron density/ $e\ \text{\AA}^{-3}$	–0.570

• Allylic alcohol 2.108

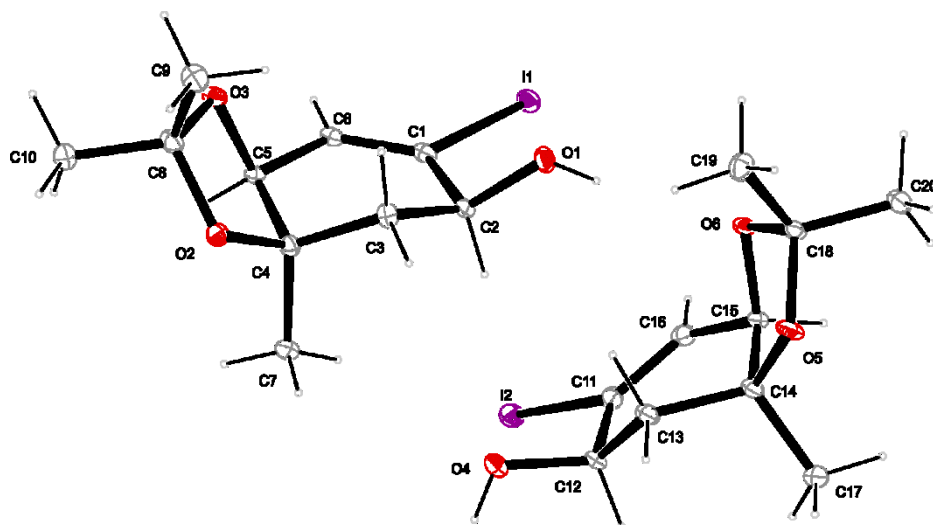


Figure 7.4. ORTEP of the molecular structure of allylic alcohol 2.108.

Table 7.4. Crystallographic data for allylic alcohol 2.108.

net formula	C ₁₀ H ₁₅ O ₃
<i>M</i> _r /g mol ⁻¹	310.12
crystal size/mm	0.100 × 0.080 × 0.020
<i>T</i> /K	100.(2)
radiation	MoKα
diffractometer	'Bruker D8 Venture TXS'
crystal system	triclinic
space group	'P -1'
<i>a</i> /Å	8.0873(5)
<i>b</i> /Å	12.0960(9)
<i>c</i> /Å	12.4087(9)
α/°	104.002(2)
β/°	103.200(2)
γ/°	92.314(2)
<i>V</i> /Å ³	1140.79(14)
<i>Z</i>	4
calc. density/g cm ⁻³	1.806
μ/mm ⁻¹	2.788
absorption correction	Multi-Scan
transmission factor range	0.5733–0.7454
refls. measured	19827
<i>R</i> _{int}	0.0403
mean σ(<i>I</i>)/ <i>I</i>	0.0341
θ range	3.158–26.372
observed refls.	4077
<i>x</i> , <i>y</i> (weighting scheme)	0.0417, 0.8914
hydrogen refinement	constr
refls in refinement	4630
parameters	261
restraints	0
<i>R</i> (<i>F</i> _{obs})	0.0286
<i>R</i> _w (<i>F</i> ²)	0.0756

<i>S</i>	1.063
shift/error _{max}	0.001
max electron density/e Å ⁻³	1.314
min electron density/e Å ⁻³	-1.036

• Allylic ester 2.146

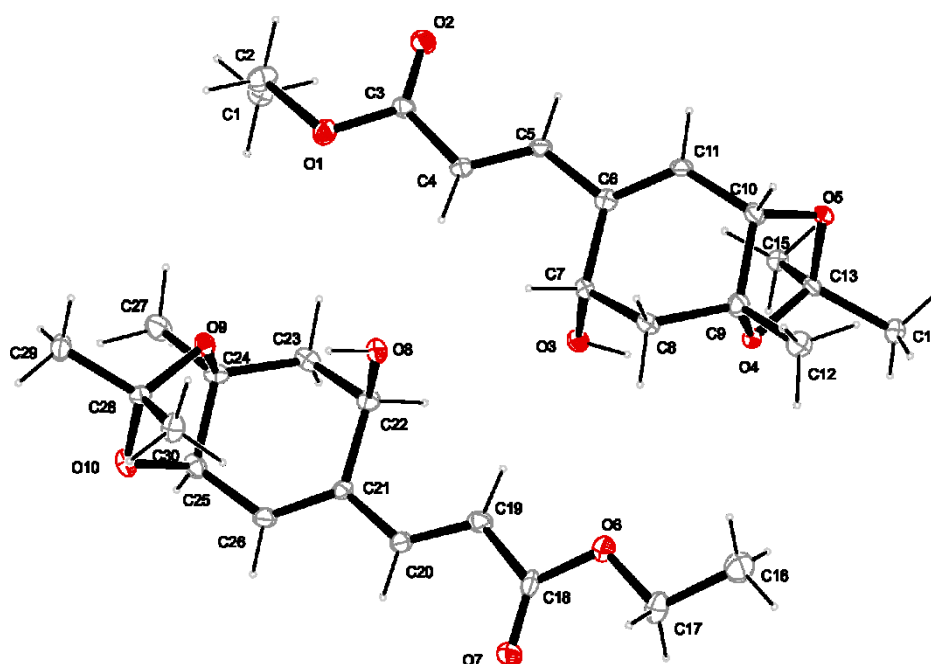


Figure 7.5. ORTEP of the molecular structure of allylic alcohol 2.146.

Table 7.5. Crystallographic data for allylic ester 2.146.

net formula	C ₁₅ H ₂₂ O ₅
<i>M_r</i> /g mol ⁻¹	282.32
crystal size/mm	0.100 × 0.100 × 0.020
<i>T</i> /K	100.(2)
radiation	MoKα
diffractometer	'Bruker D8 Venture TXS'
crystal system	monoclinic
space group	'P 1 21 1'
<i>a</i> /Å	14.0914(7)
<i>b</i> /Å	7.2146(3)
<i>c</i> /Å	15.0038(8)
<i>α</i> /°	90
<i>β</i> /°	105.2139(18)
<i>γ</i> /°	90
<i>V</i> /Å ³	1471.88(12)
<i>Z</i>	4
calc. density/g cm ⁻³	1.274
μ/mm ⁻¹	0.095
absorption correction	Multi-Scan
transmission factor range	0.8883–0.9593

refls. measured	18843
R_{int}	0.0477
mean $\sigma(I)/I$	0.0506
θ range	3.155–26.370
observed refls.	4963
x, y (weighting scheme)	0.0318, 2.7949
hydrogen refinement	mixed
Flack parameter	0.5
refls in refinement	5822
parameters	375
restraints	2
$R(F_{\text{obs}})$	0.0707
$R_w(F^2)$	0.1579
S	1.154
shift/error _{max}	0.001
max electron density/ $e \text{ \AA}^{-3}$	0.529
min electron density/ $e \text{ \AA}^{-3}$	-0.287

C-H: constr, O-H: refxyz, $U(\text{H})=1.5U(\text{O})$, one O-H distance fixed with DFIX. Refined as racemic twin.

• Tertiary alcohol 5.48

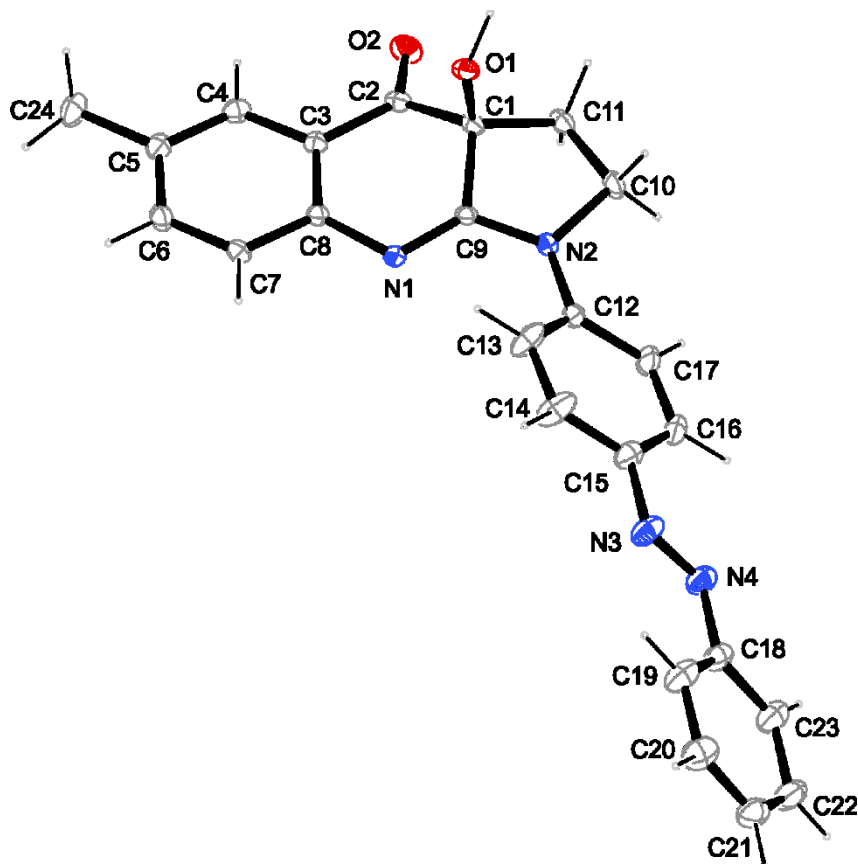


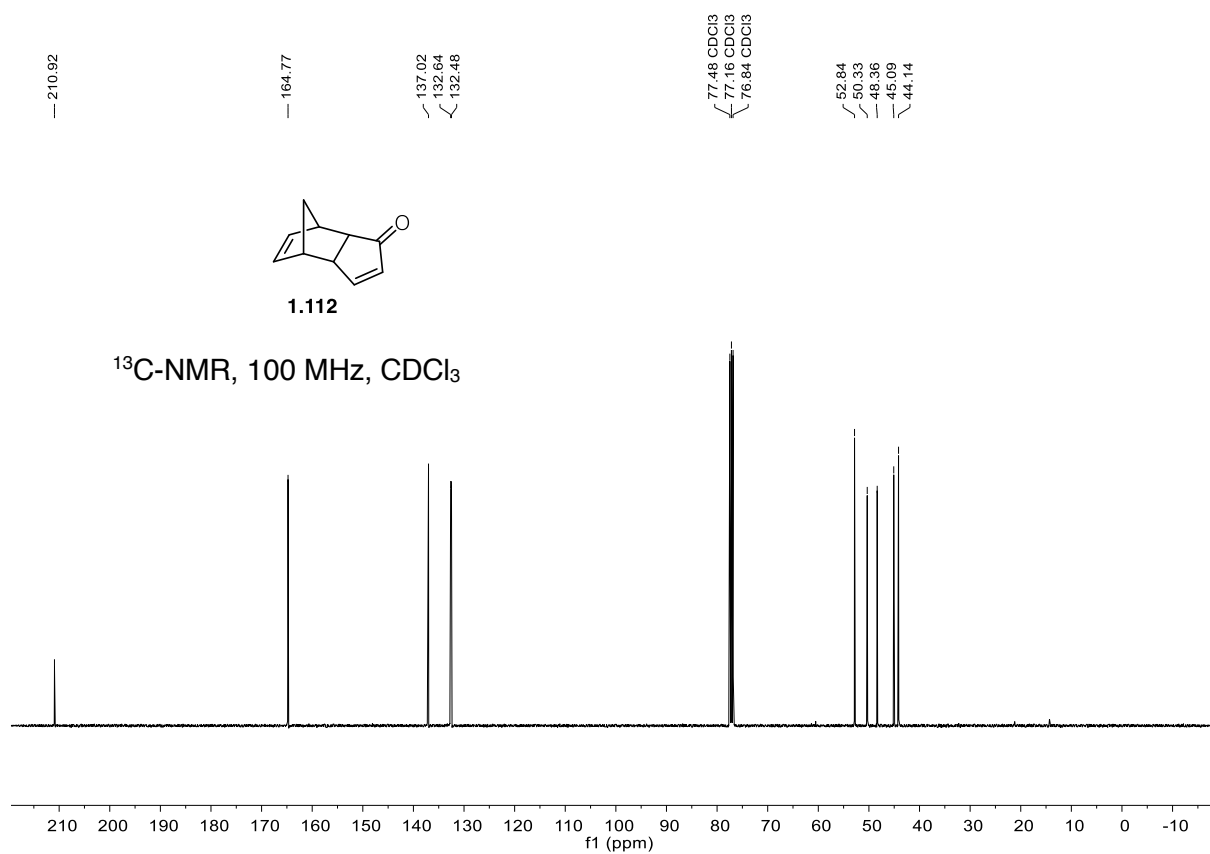
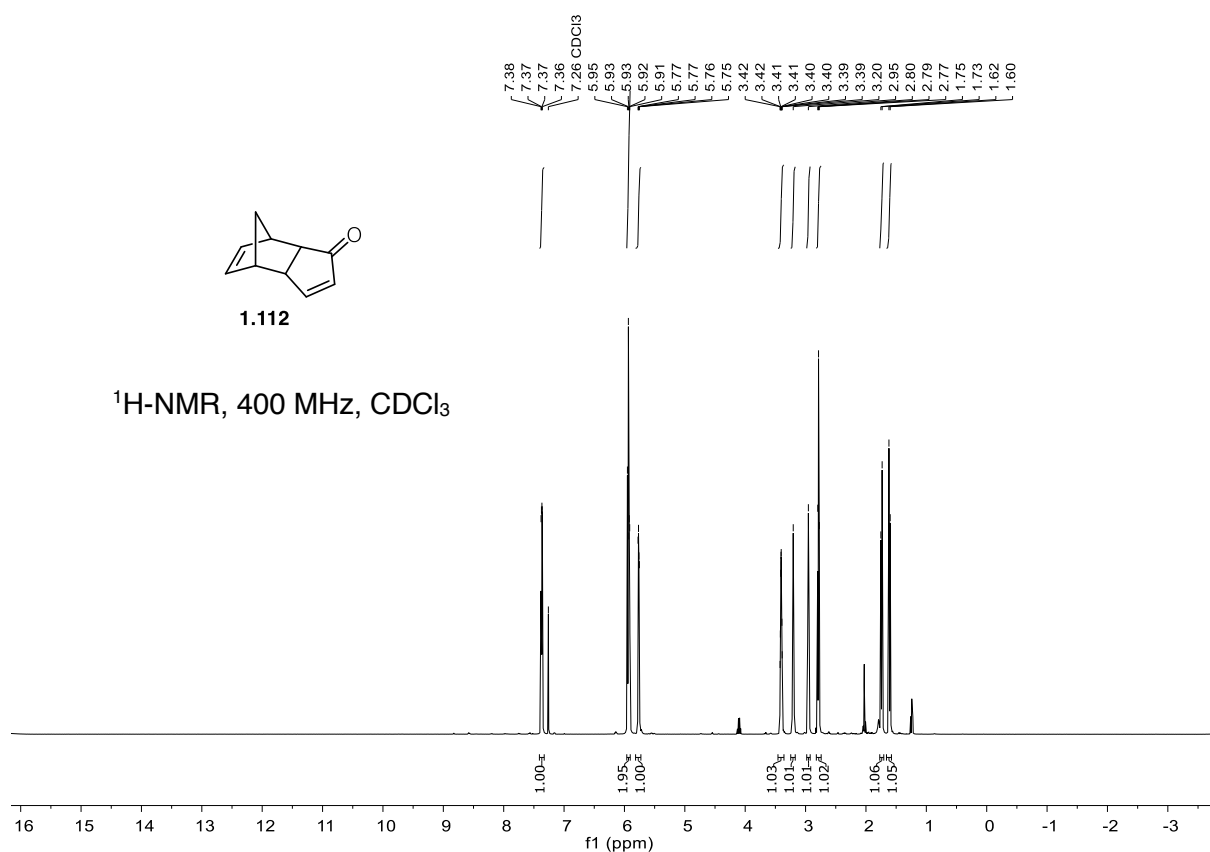
Figure 7.6. ORTEP of the molecular structure of allylic alcohol 5.48.

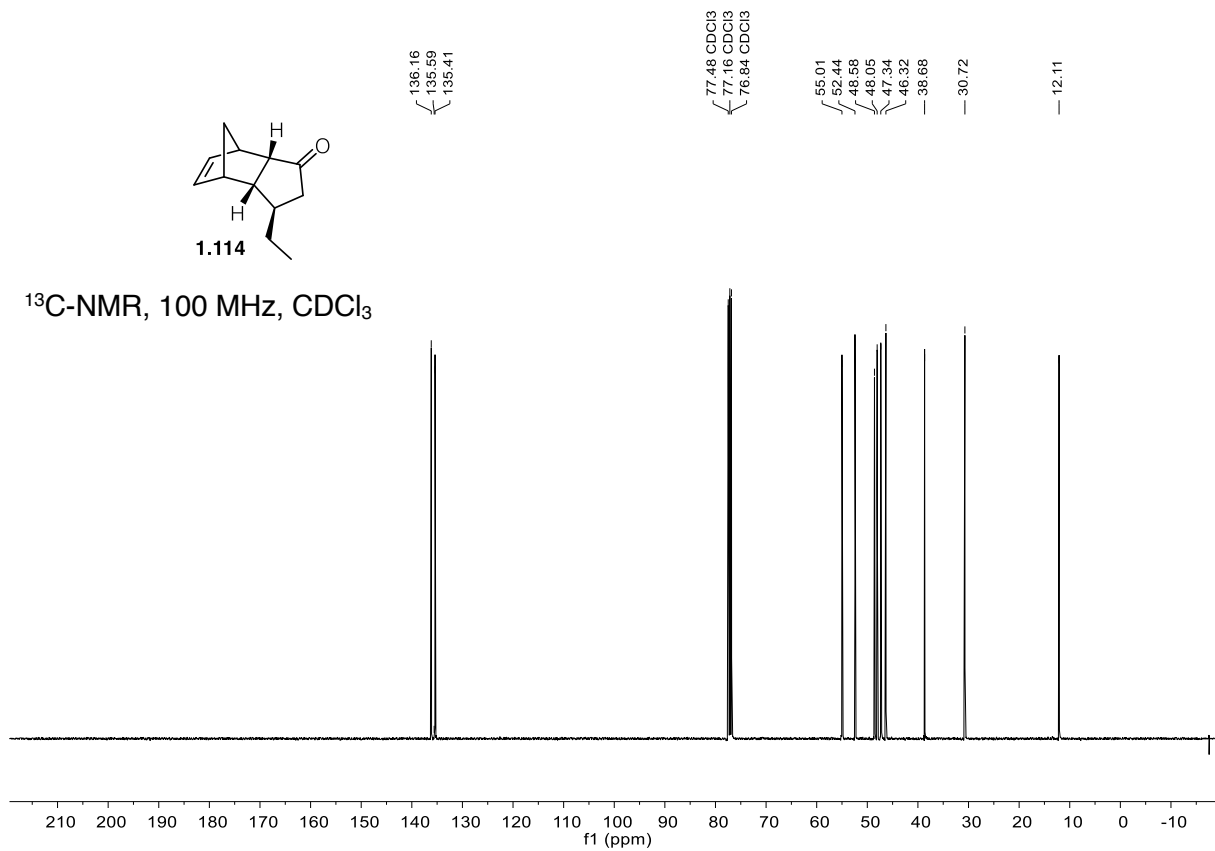
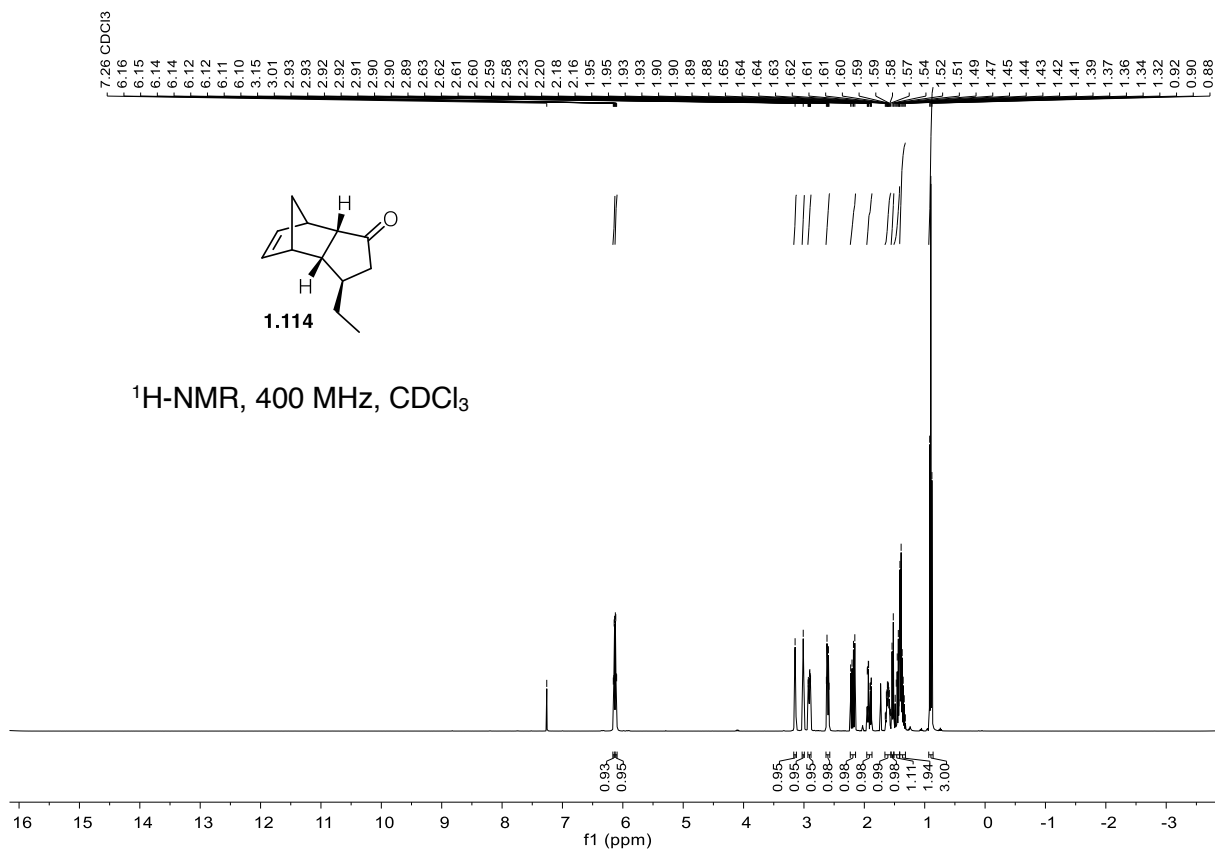
Table 7.6. Crystallographic data for tertiary alcohol 5.48.

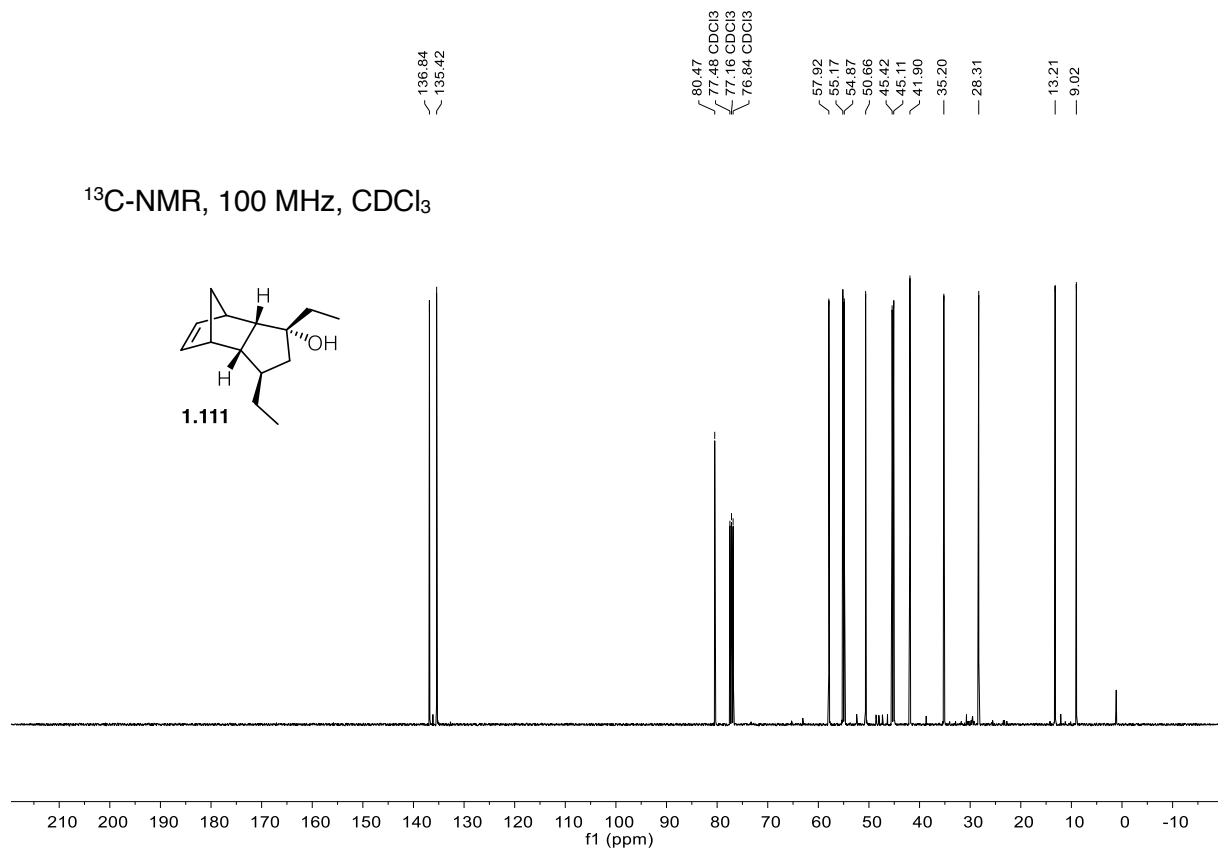
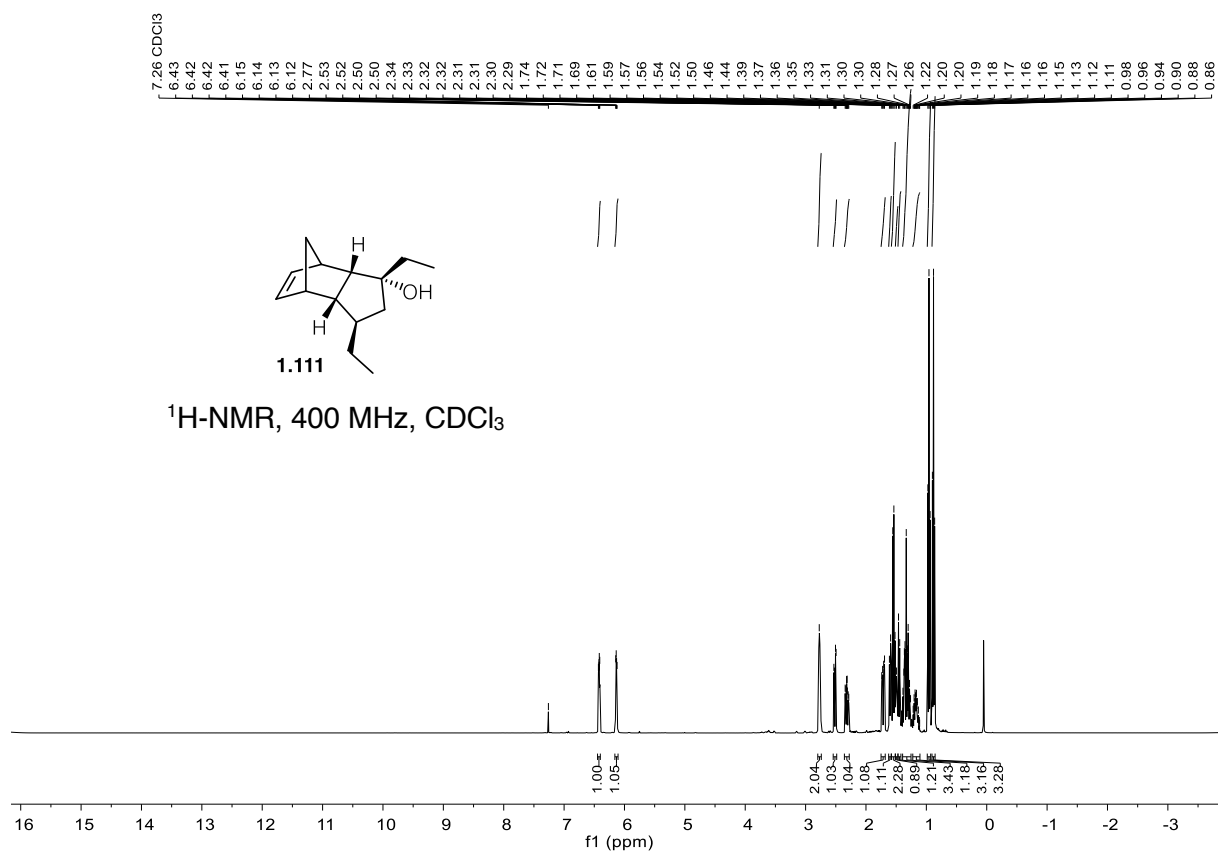
net formula	$C_{24}H_{20}N_4O_2$
$M_r/g\ mol^{-1}$	396.441
crystal size/mm	$0.180 \times 0.120 \times 0.020$
T/K	173(2)
radiation	'Mo $K\alpha$
diffractometer	'Bruker D8Quest'
crystal system	monoclinic
space group	$P2_1$
$a/\text{\AA}$	5.8301(3)
$b/\text{\AA}$	27.1534(14)
$c/\text{\AA}$	6.1864(3)
$\alpha/^\circ$	90
$\beta/^\circ$	92.7670(15)
$\gamma/^\circ$	90
$V/\text{\AA}^3$	978.21(9)
Z	2
calc. density/ $g\ cm^{-3}$	1.34596(12)
μ/mm^{-1}	0.088
absorption correction	multi-scan
transmission factor range	0.9081–0.9579
refls. measured	16076
R_{int}	0.0392
mean $\sigma(I)/I$	0.0298
θ range	3.00–25.07
observed refls.	3101
x, y (weighting scheme)	0.0391, 0.1704
hydrogen refinement	mixed
Flack parameter	–0.3(11)
refls in refinement	3441
parameters	276
restraints	1
$R(F_{obs})$	0.0343
$R_w(F^2)$	0.0779
S	1.058
shift/error _{max}	0.001
max electron density/ $e\ \text{\AA}^{-3}$	0.171
min electron density/ $e\ \text{\AA}^{-3}$	–0.180

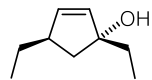
C-H: constr, O-H: refall.

7.2 ^1H and ^{13}C NMR spectra

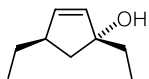
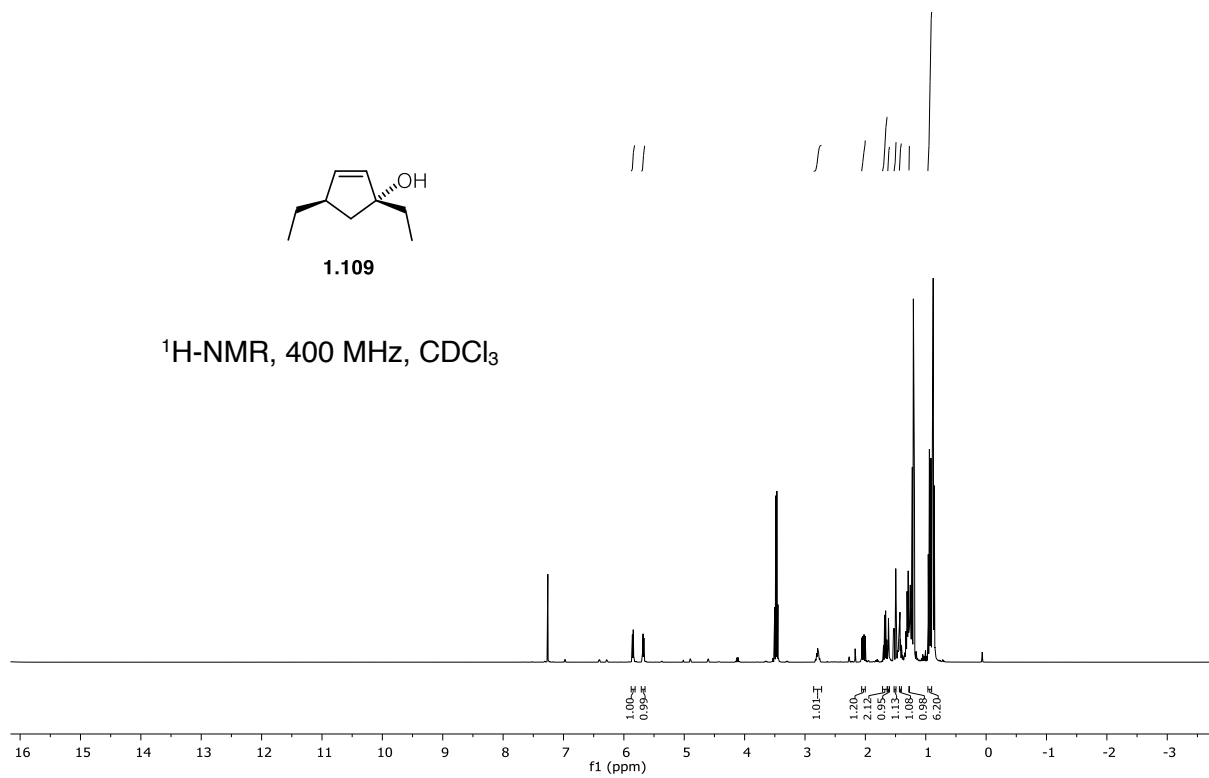
7.2.1 ^1H and ^{13}C NMR spectra of Chapter I



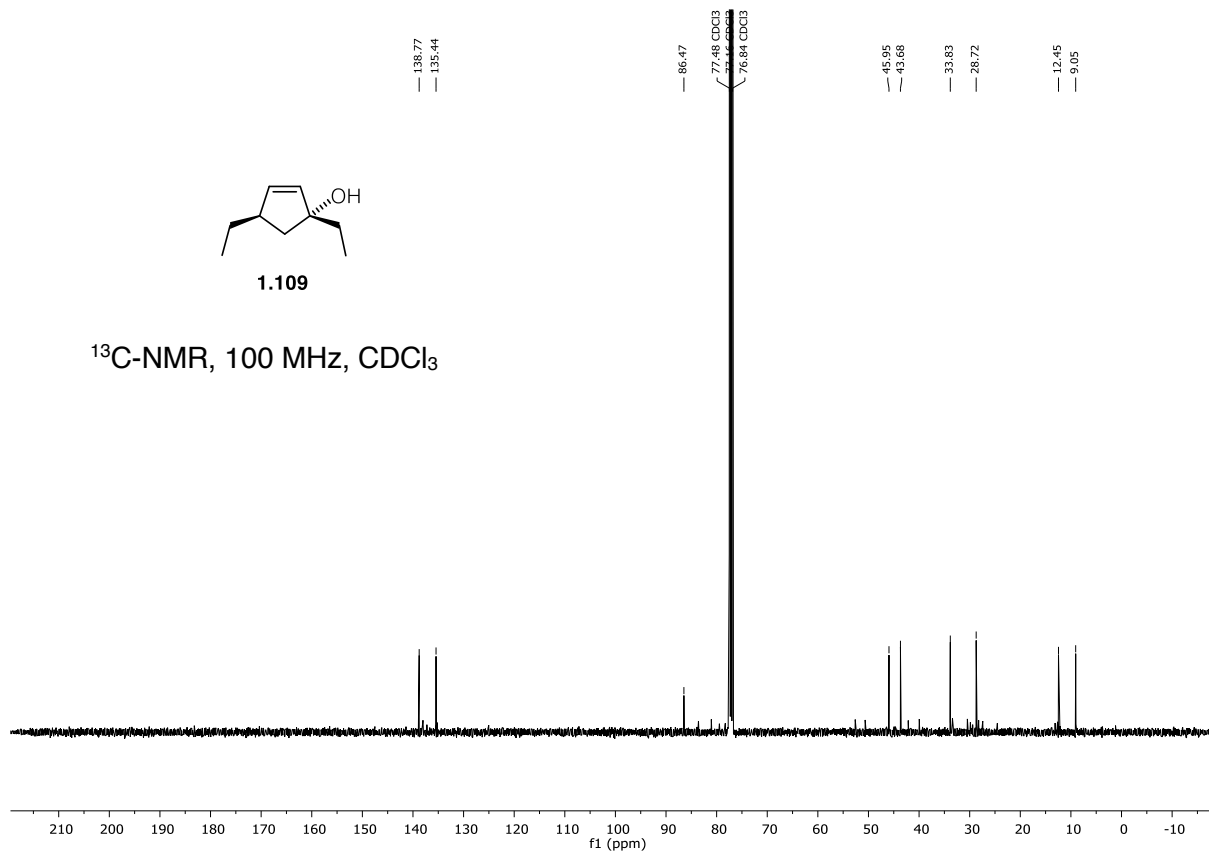


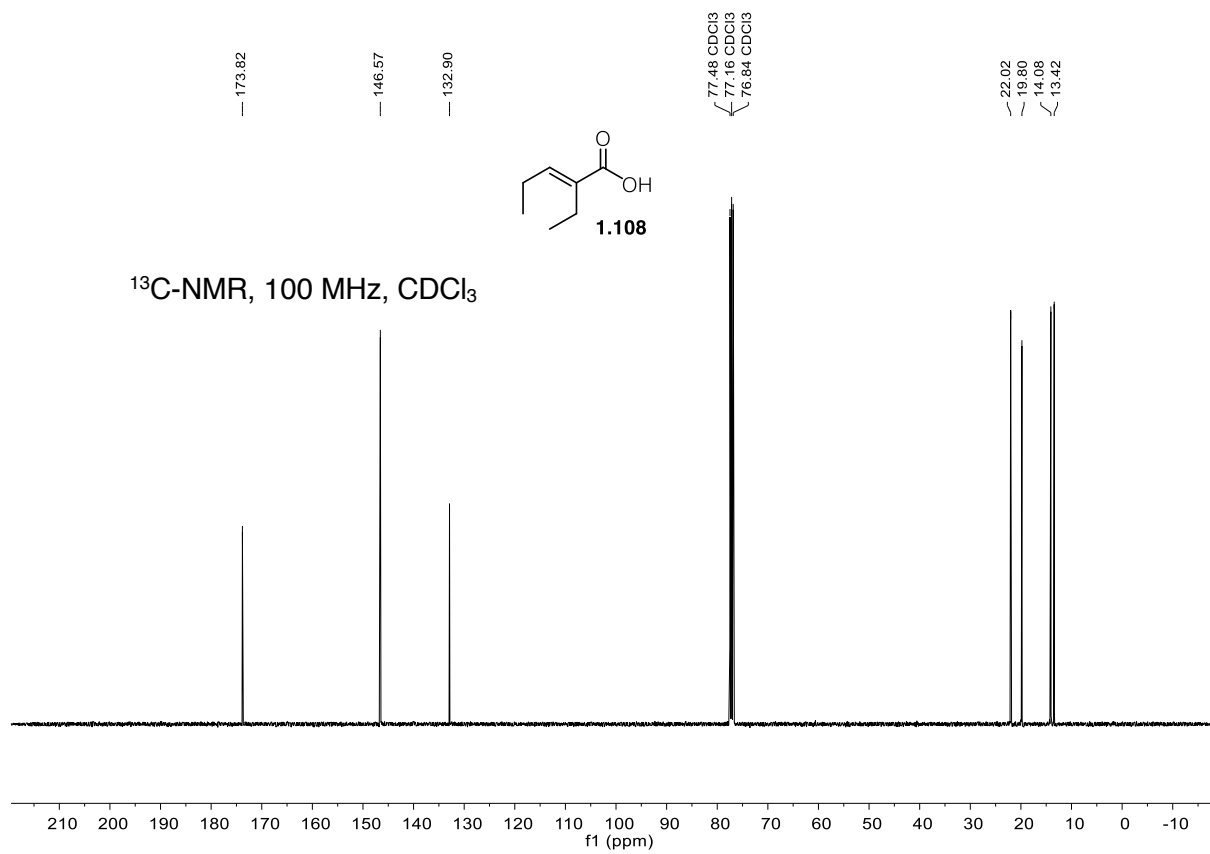
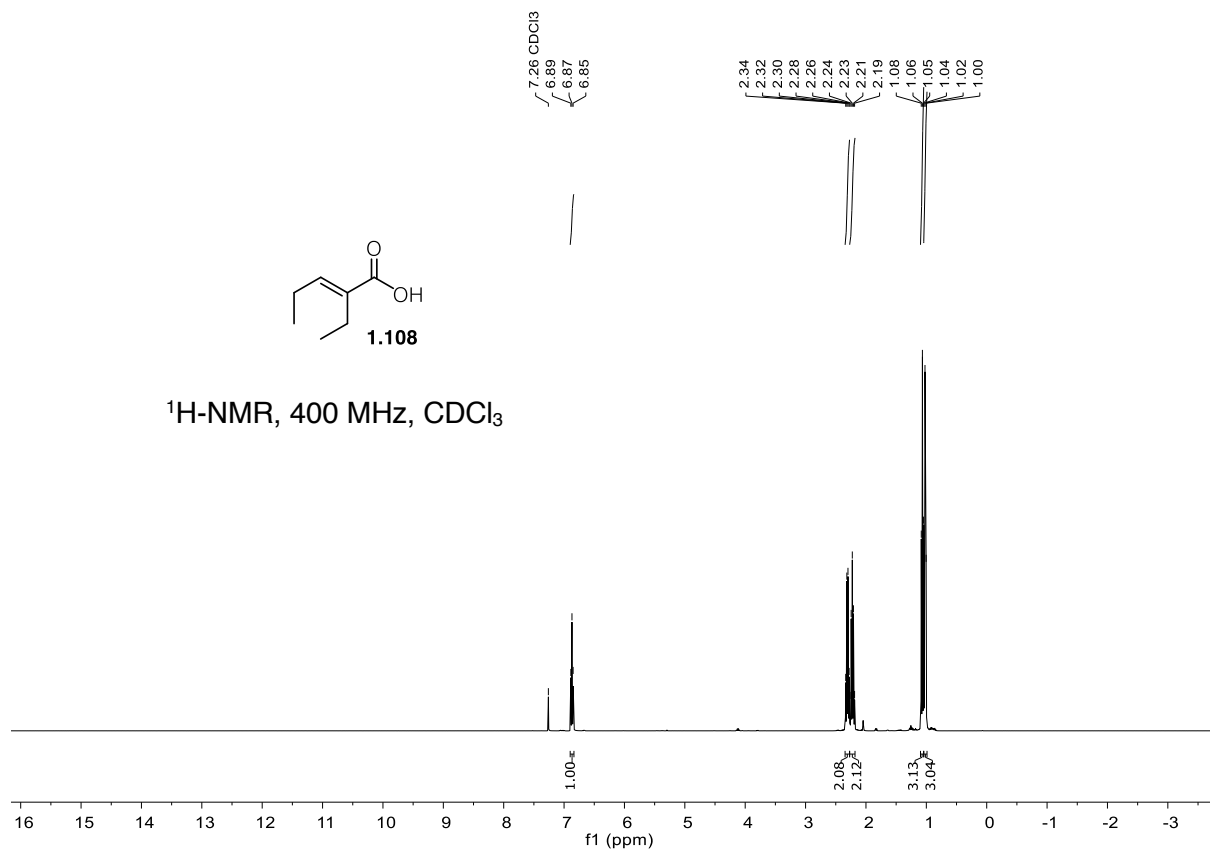


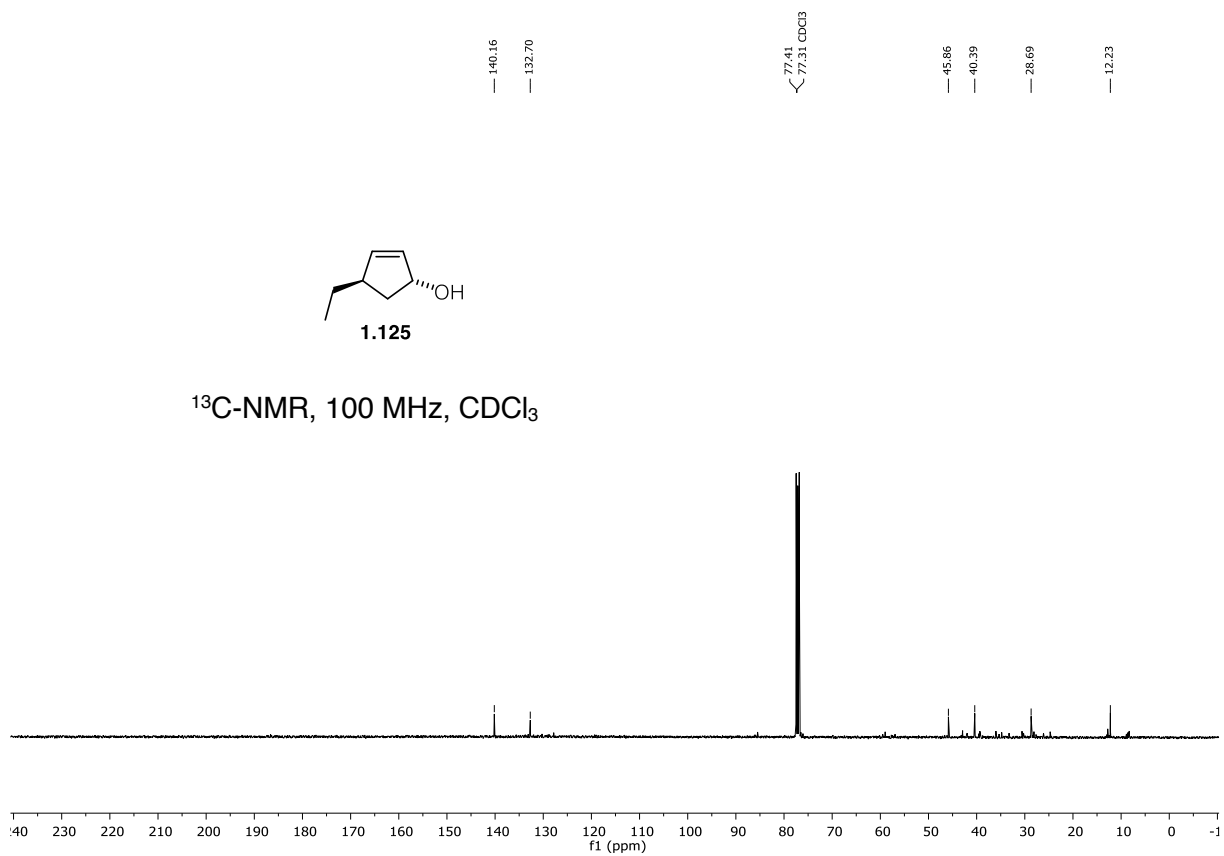
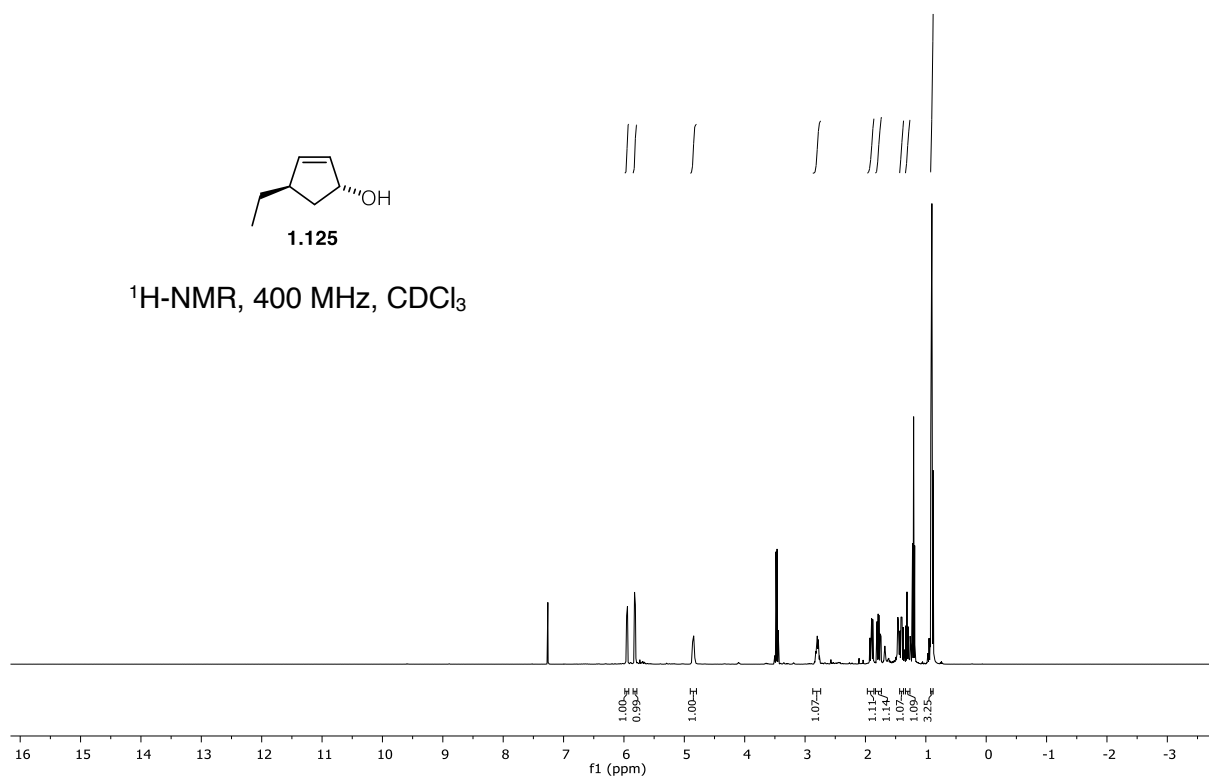
1.109

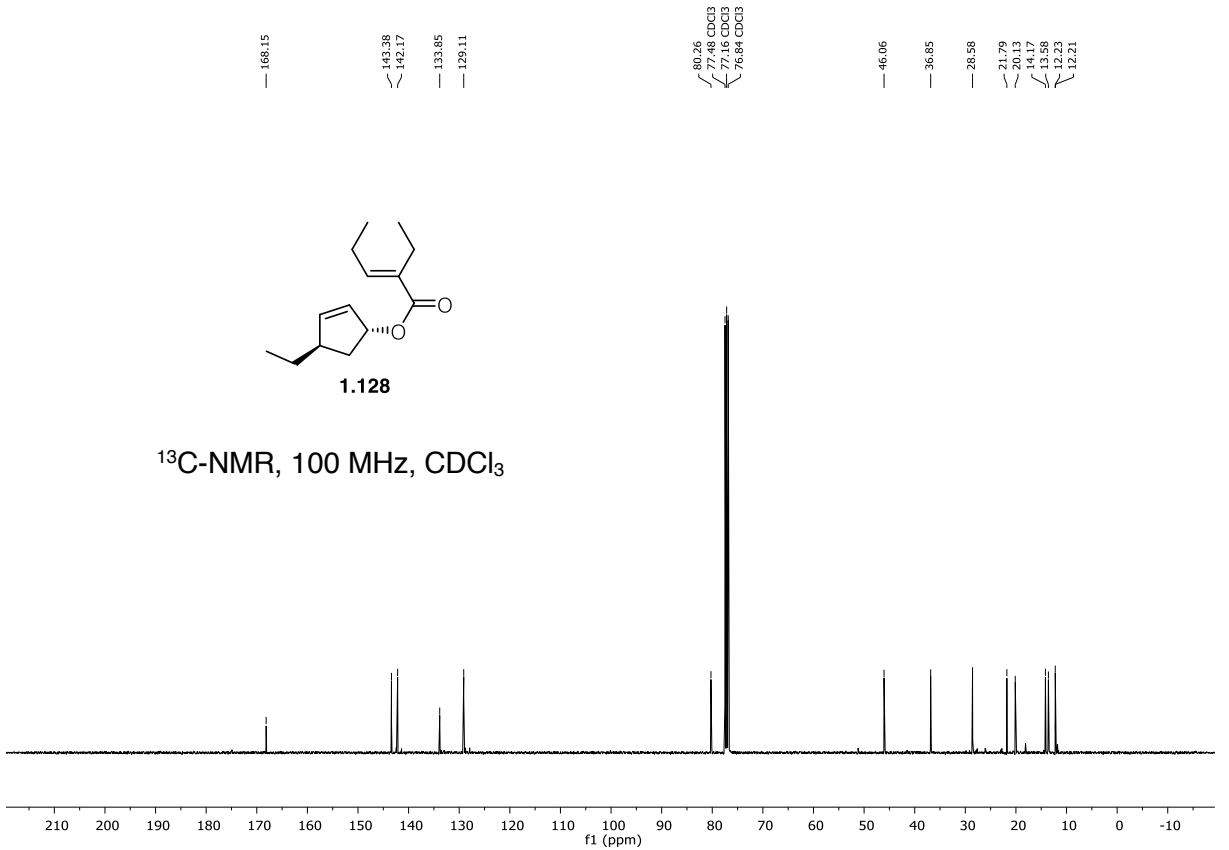
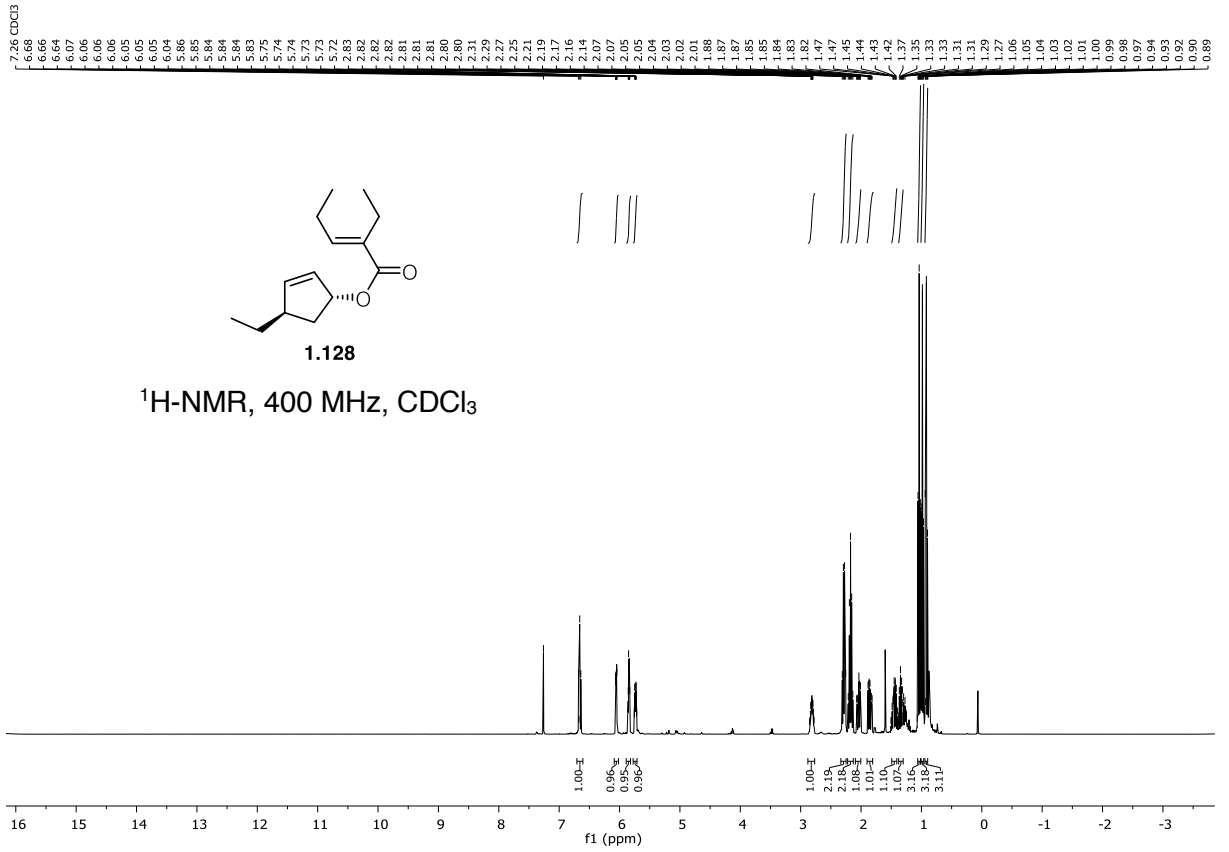
 $^1\text{H-NMR}$, 400 MHz, CDCl_3 

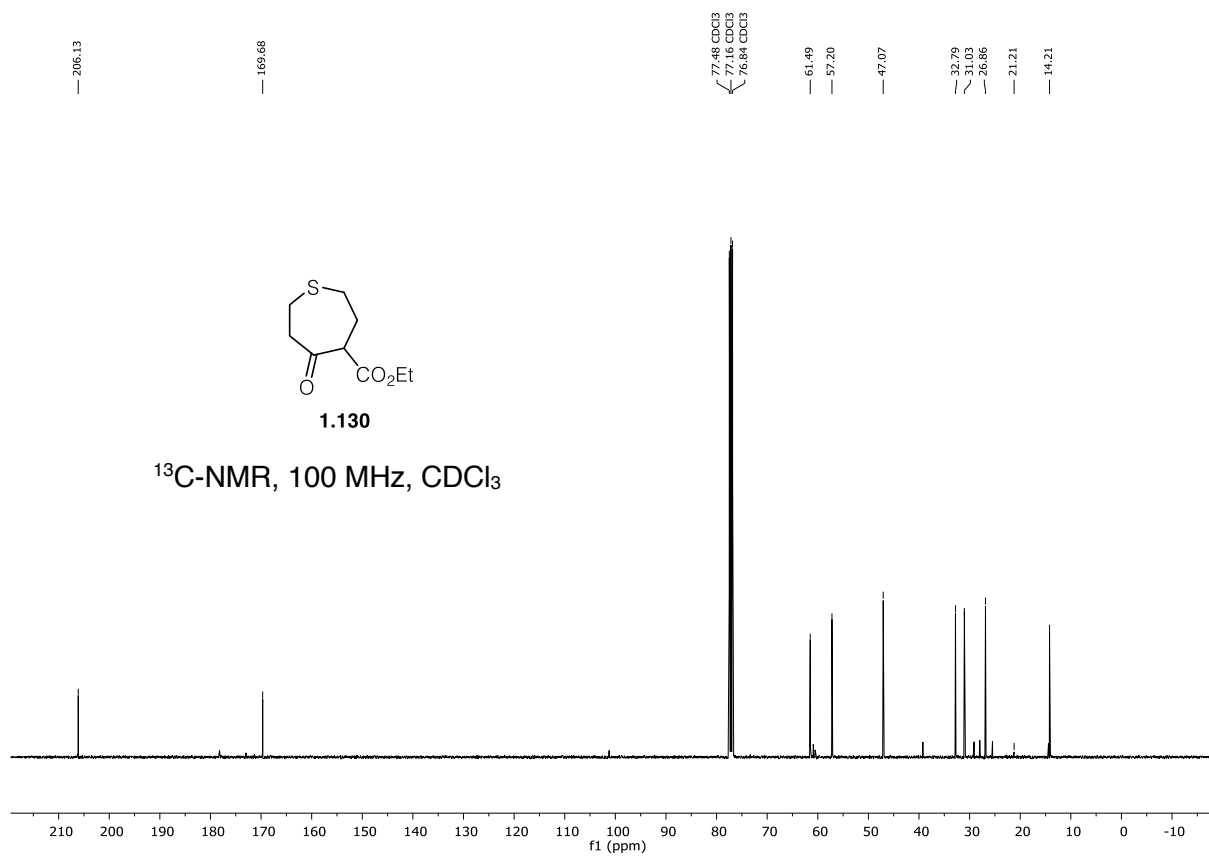
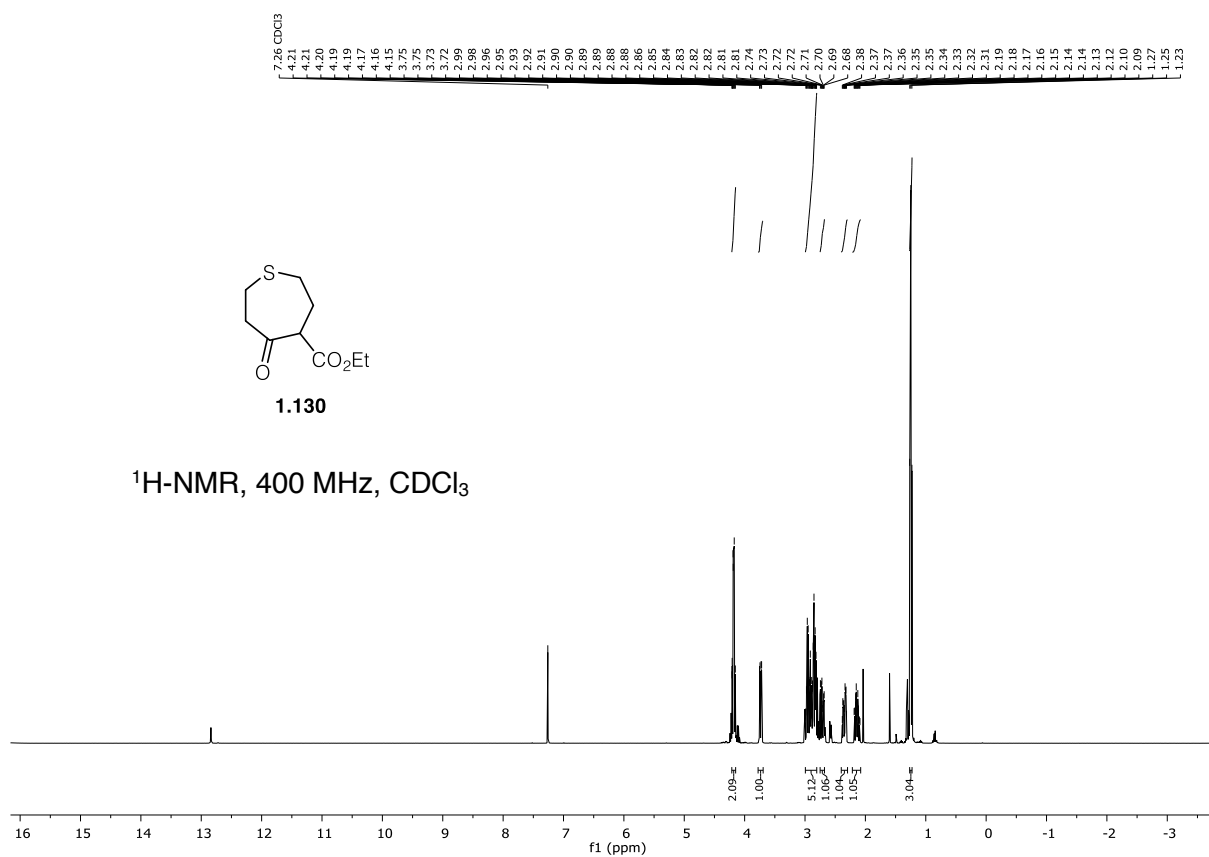
1.109

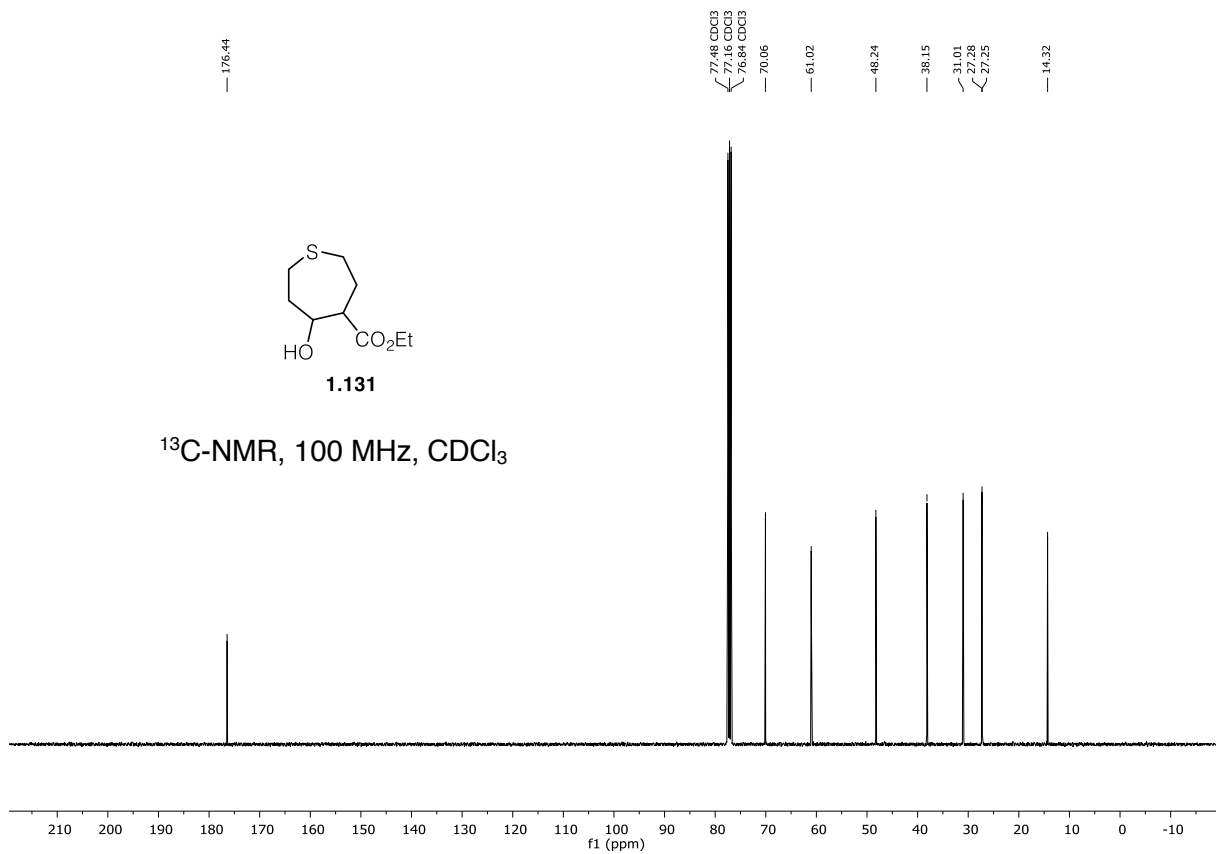
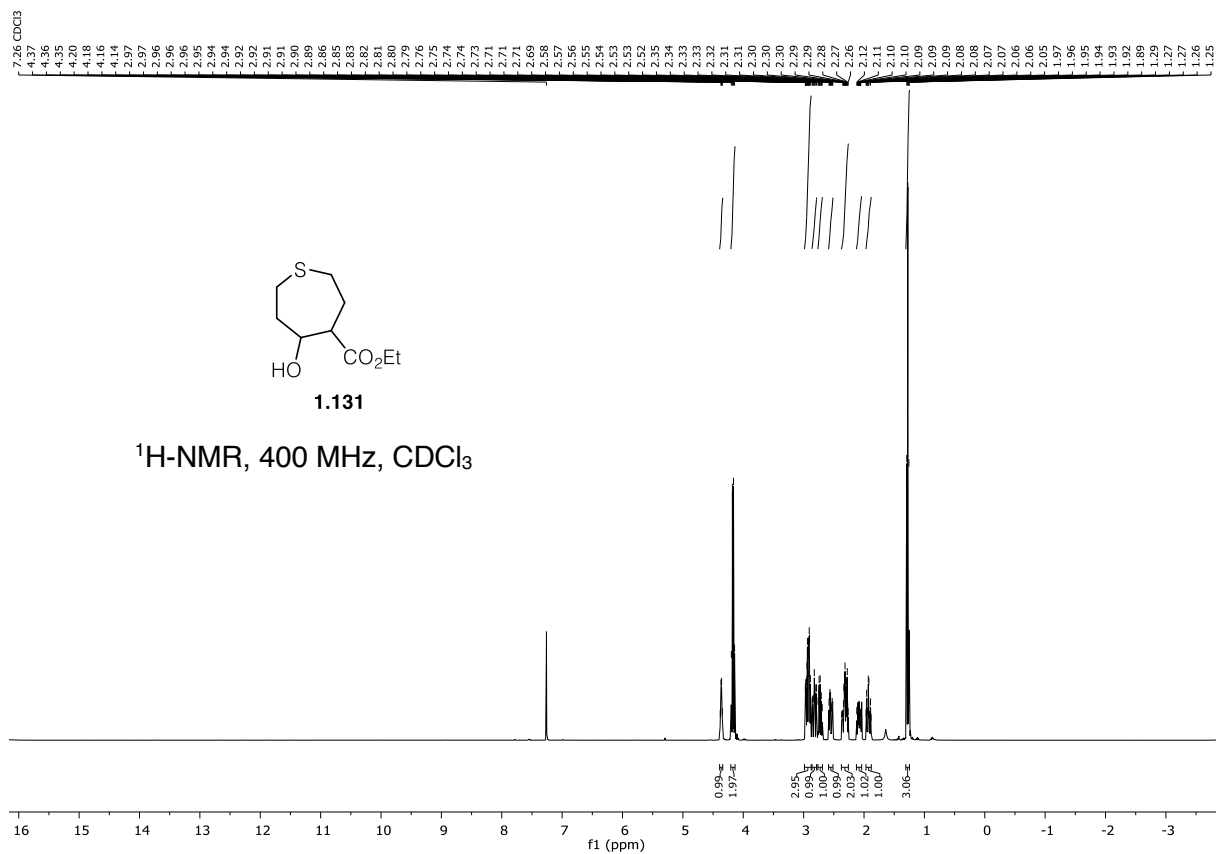
 $^{13}\text{C-NMR}$, 100 MHz, CDCl_3 

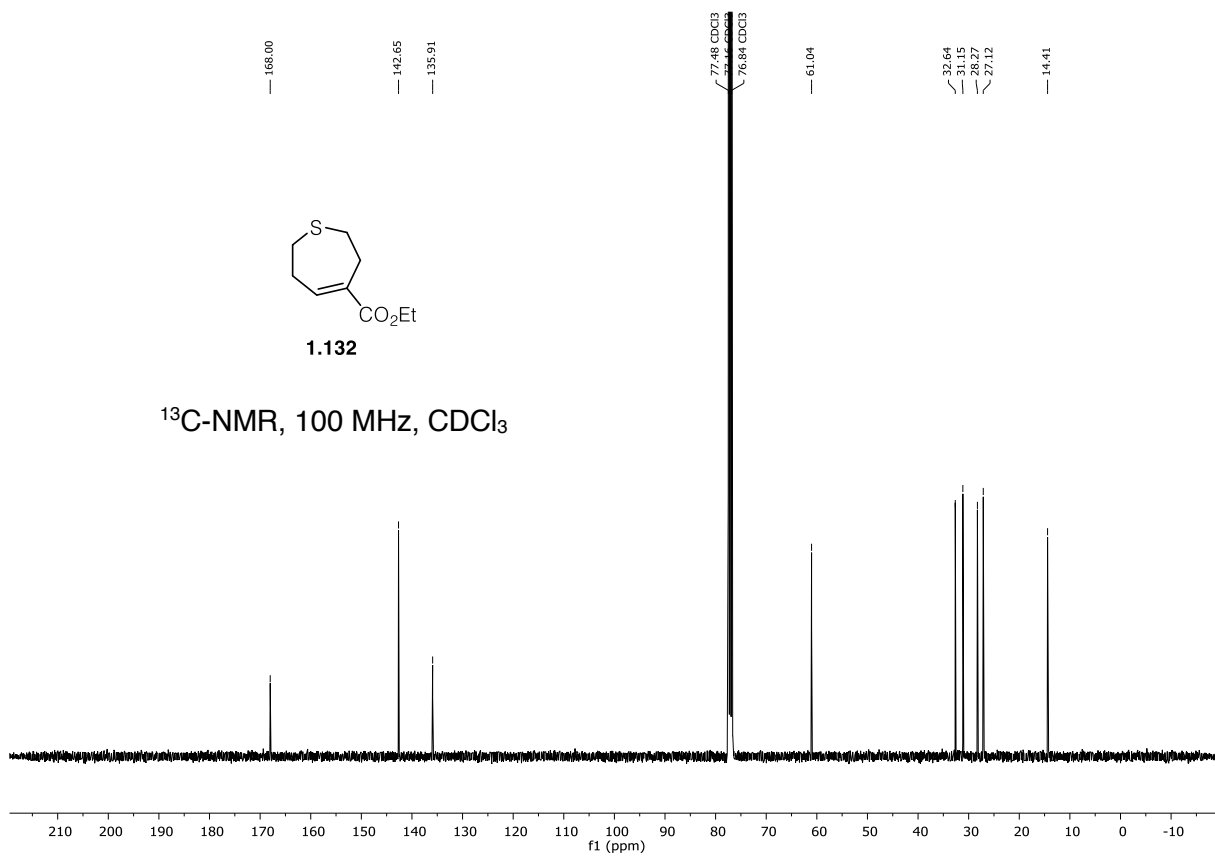
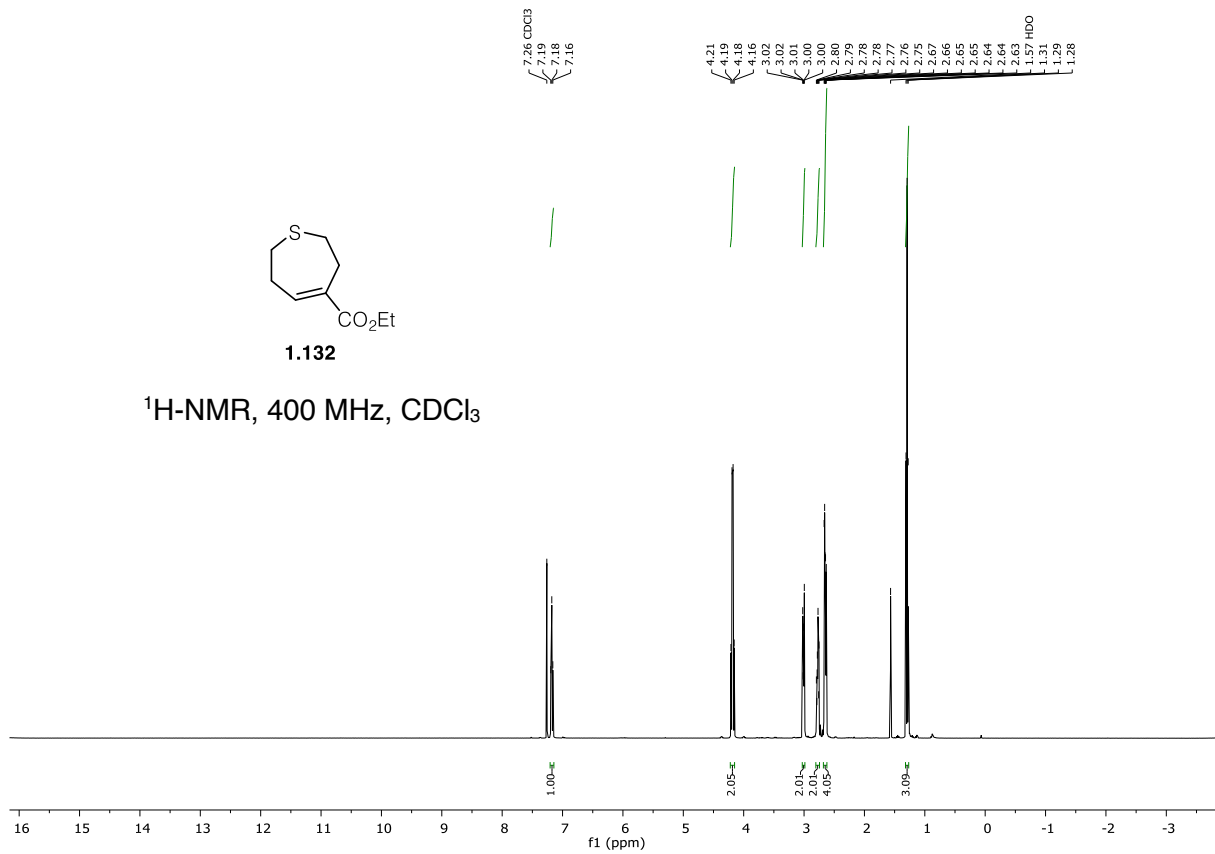


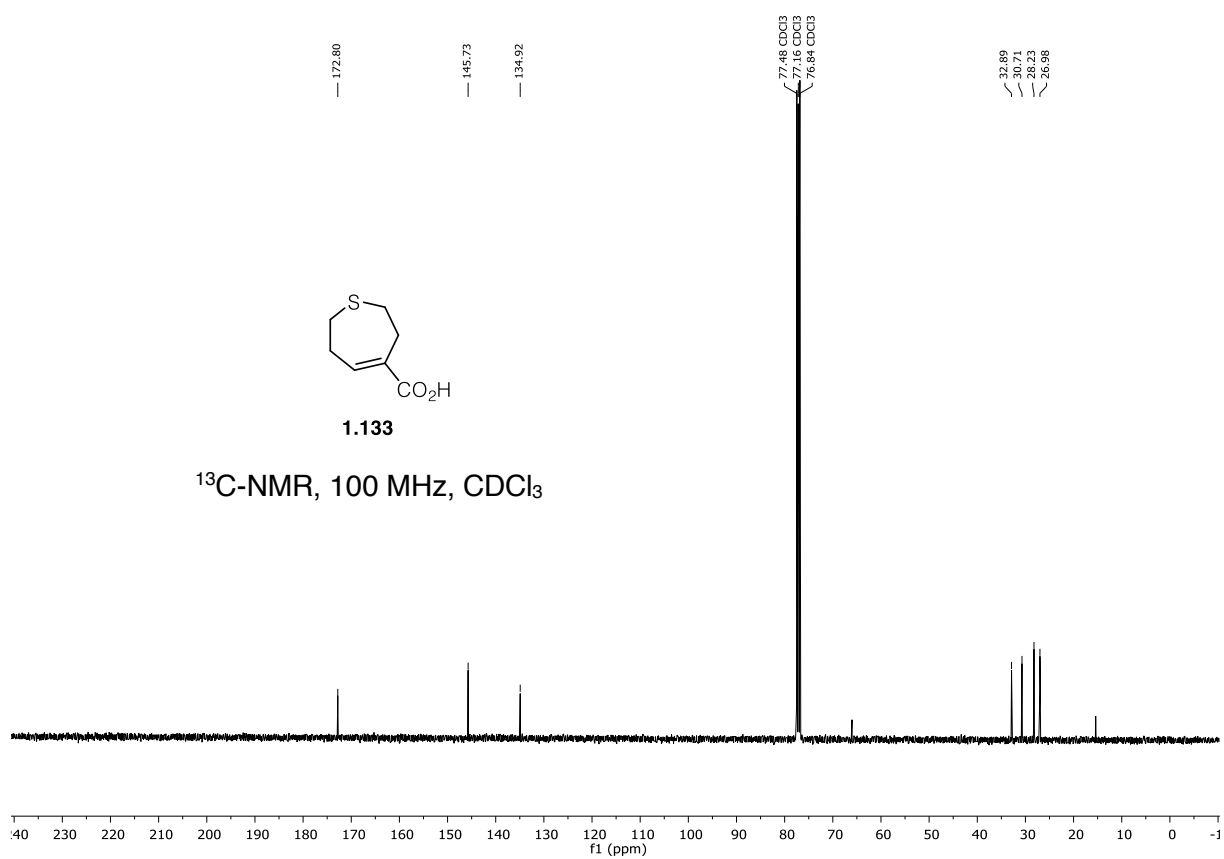
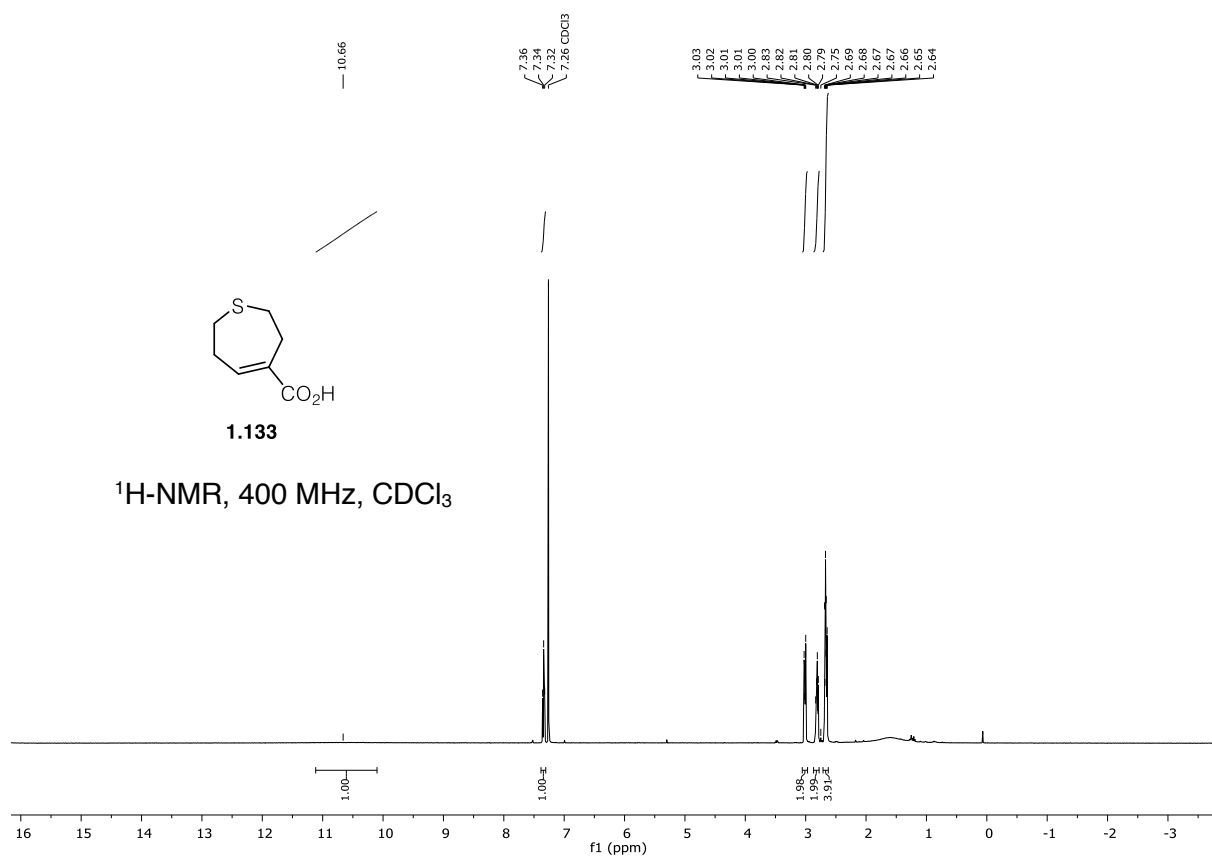


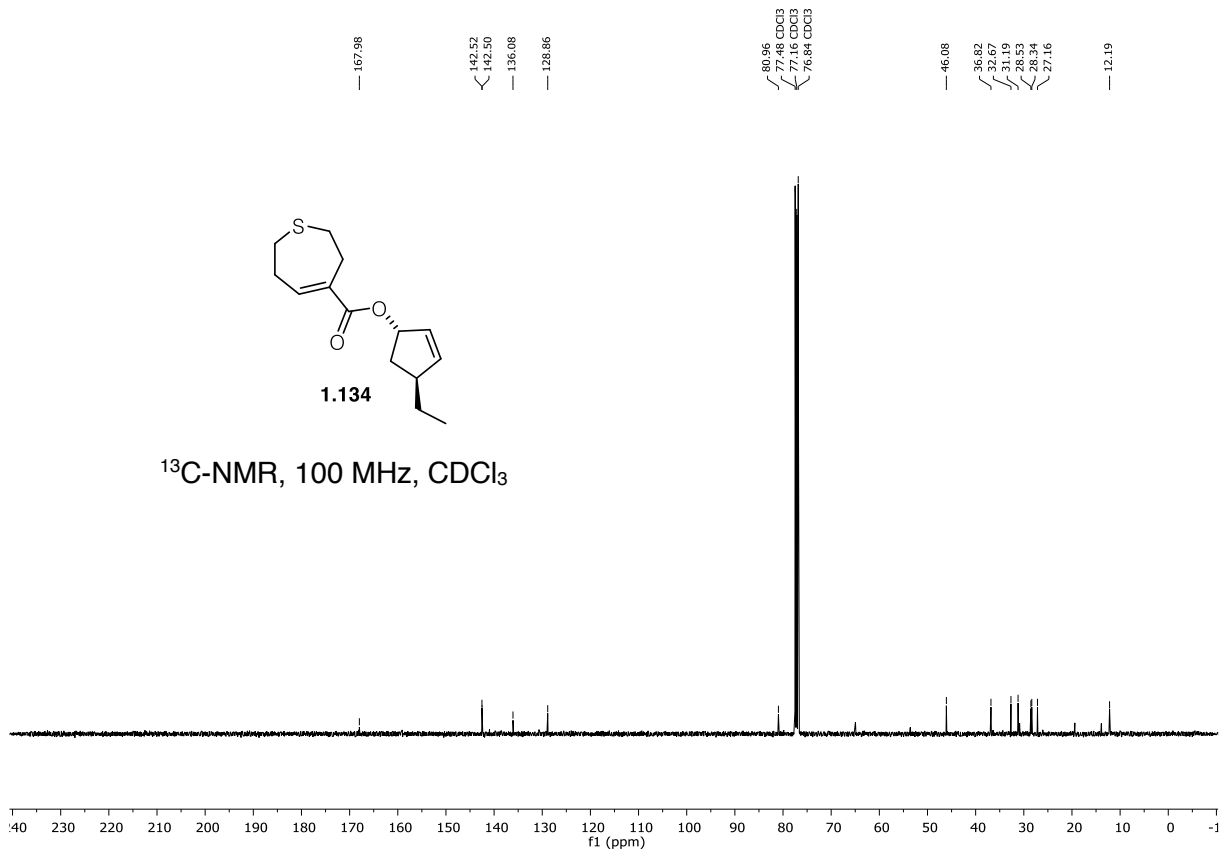
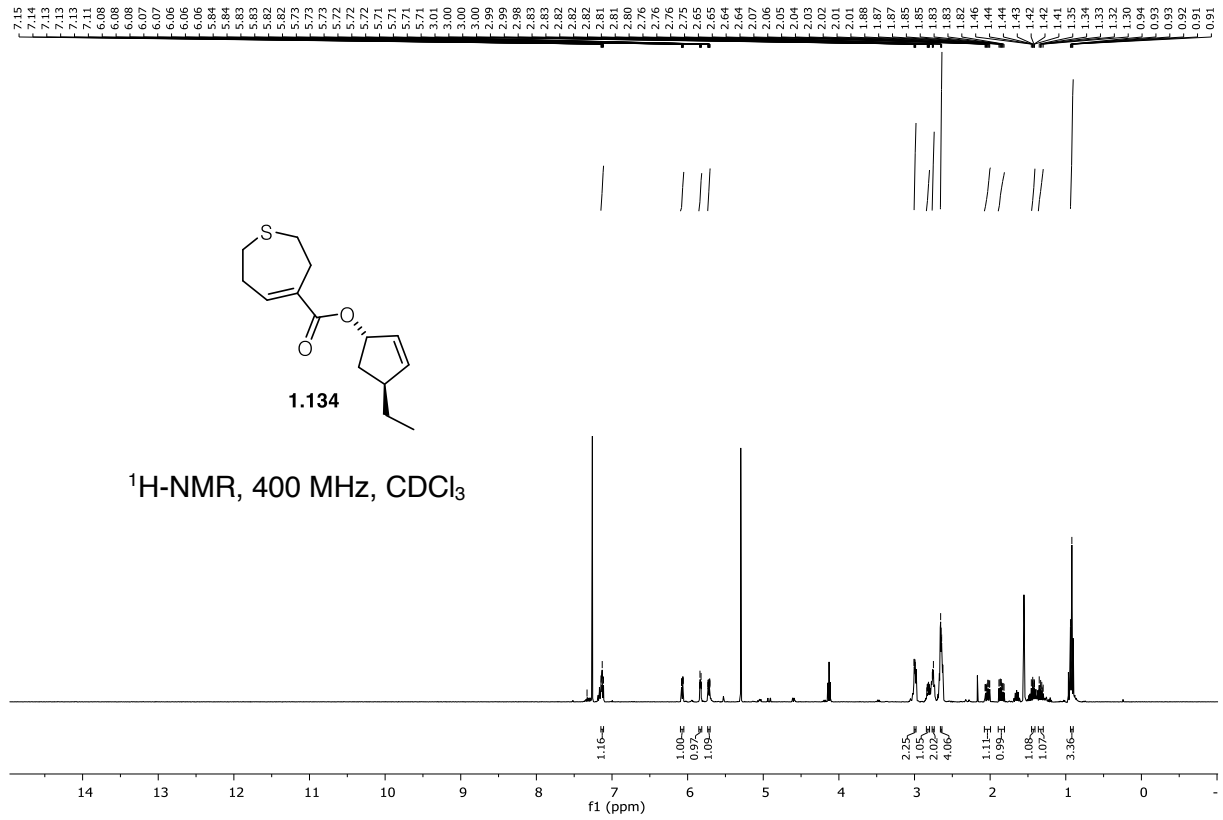


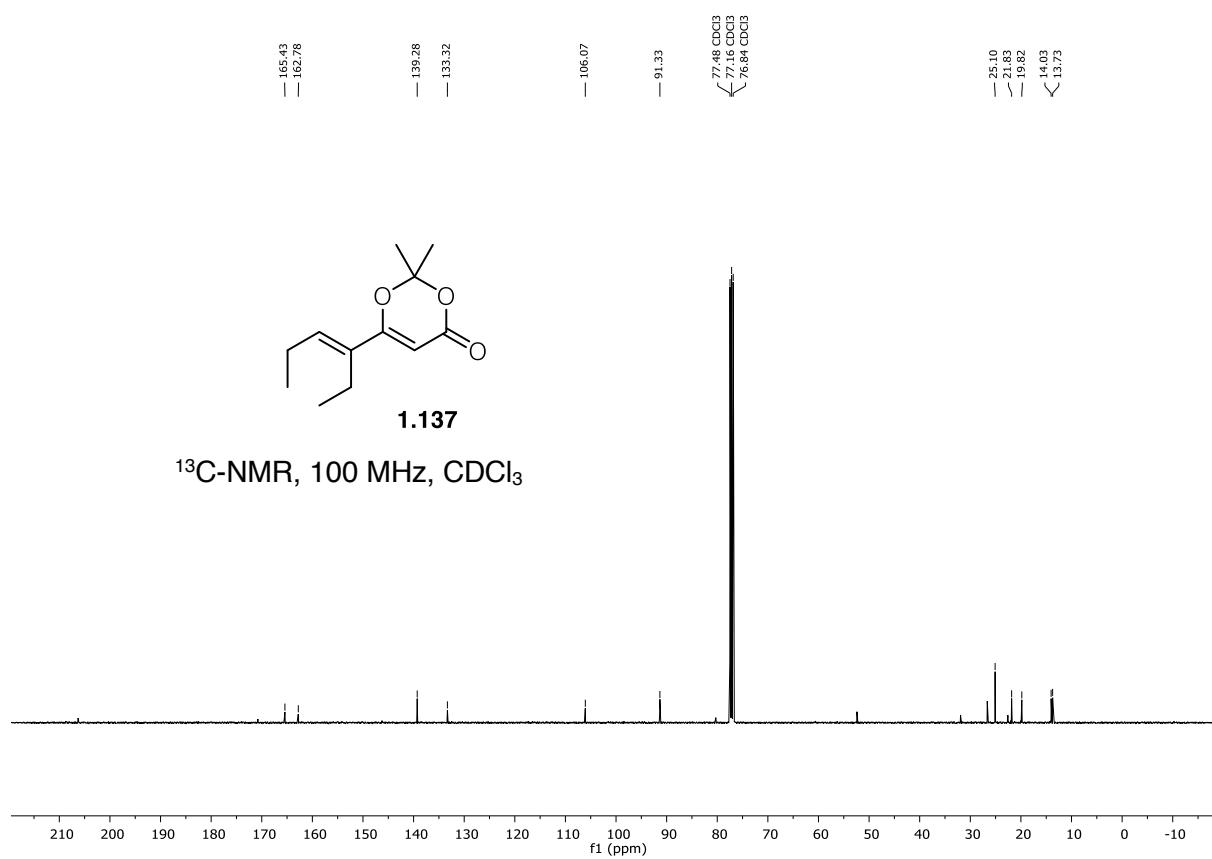
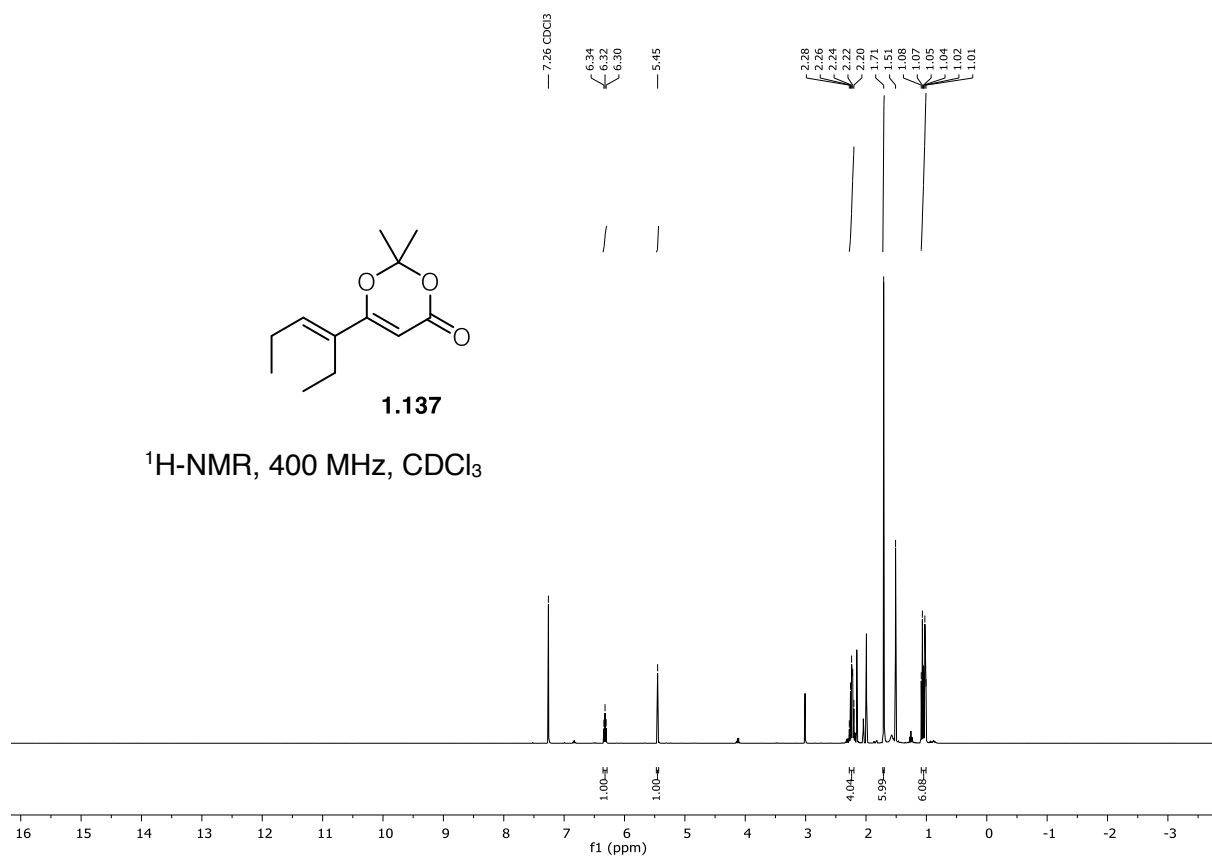


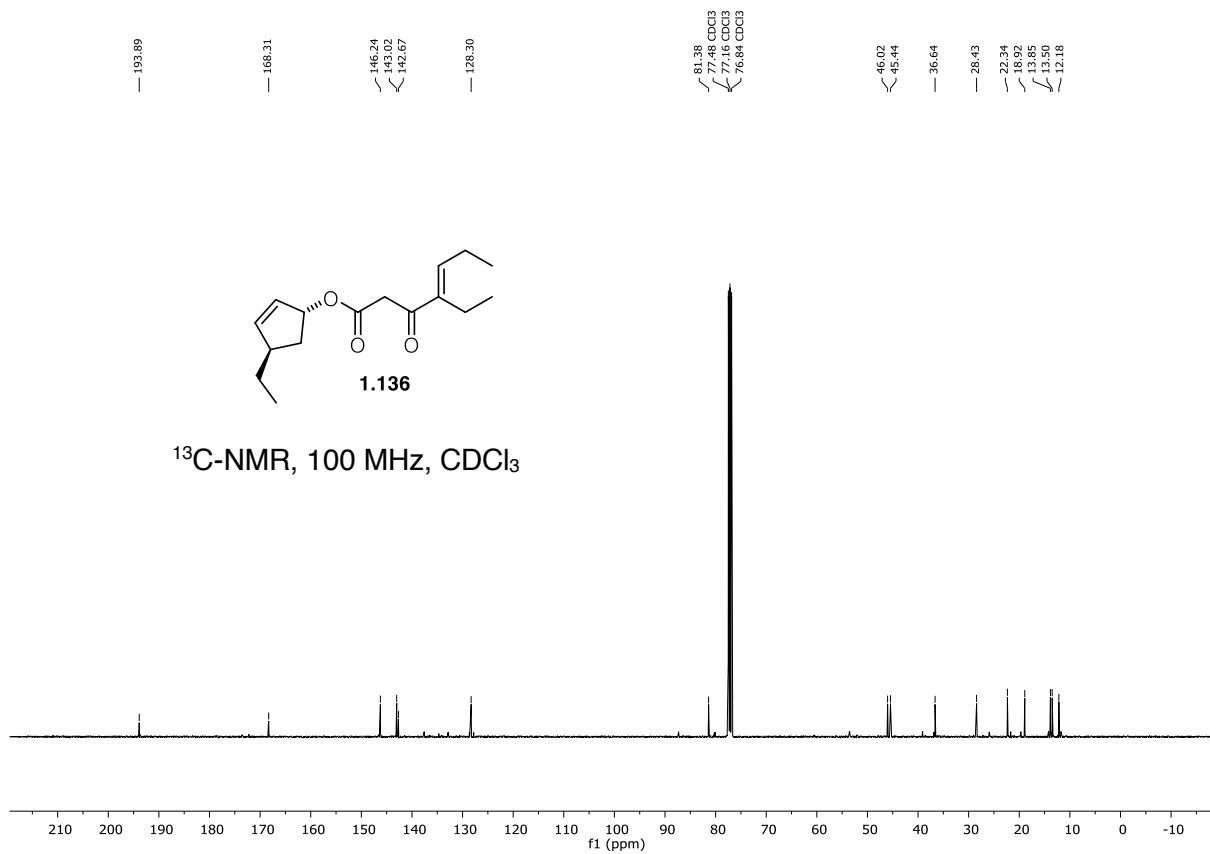
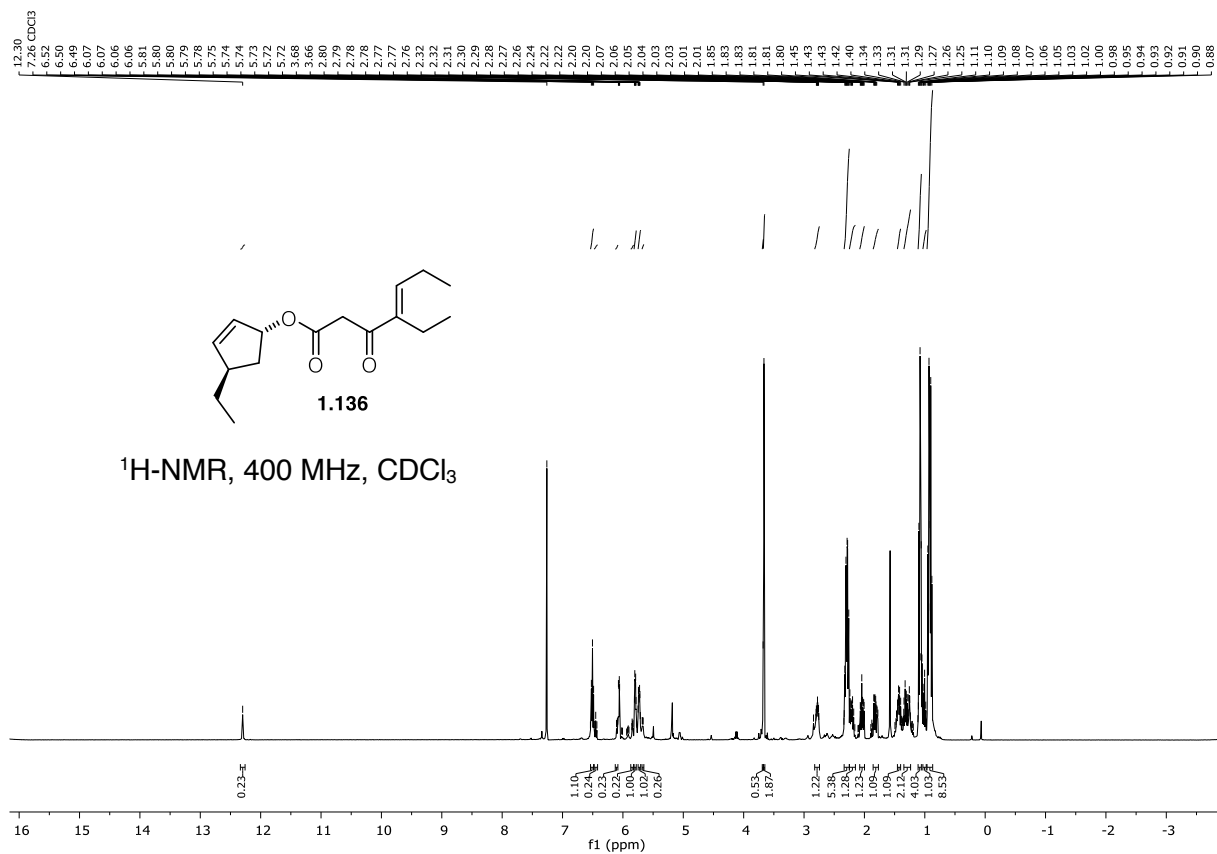


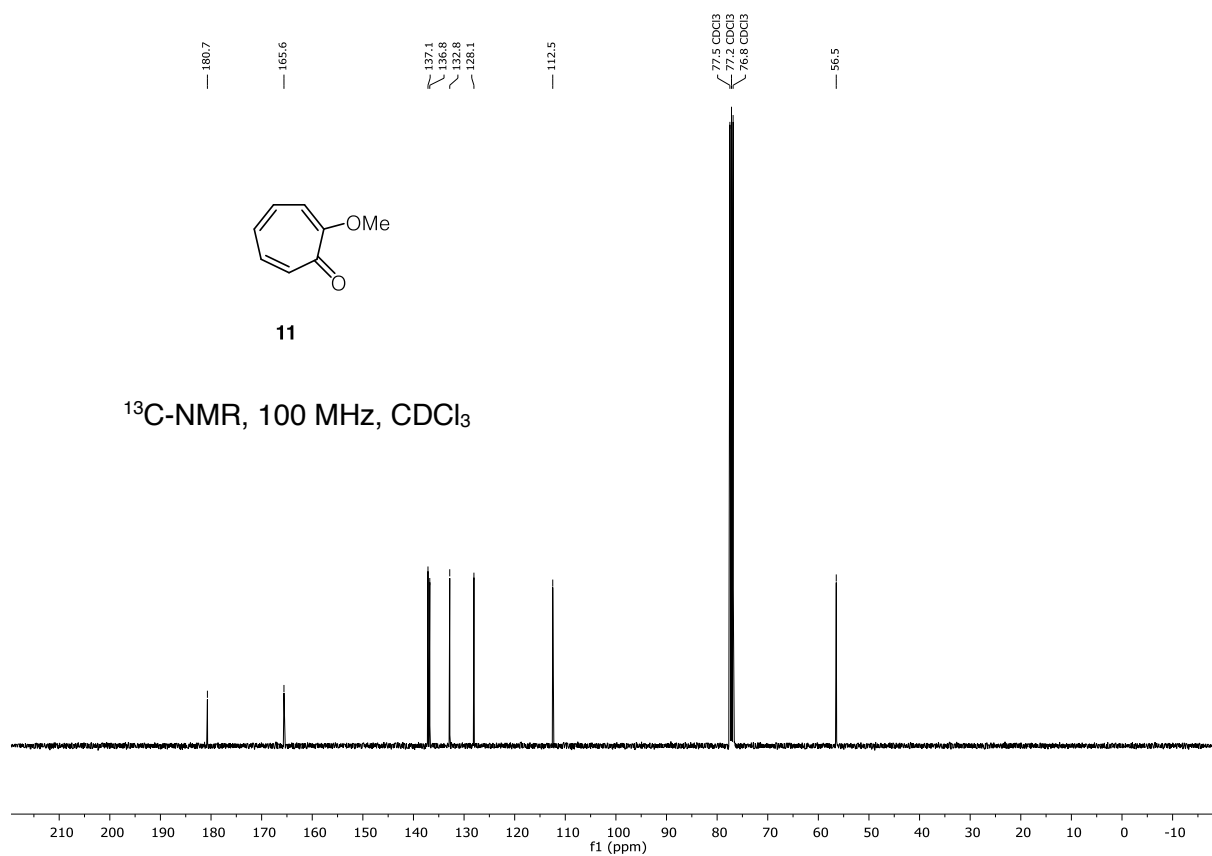
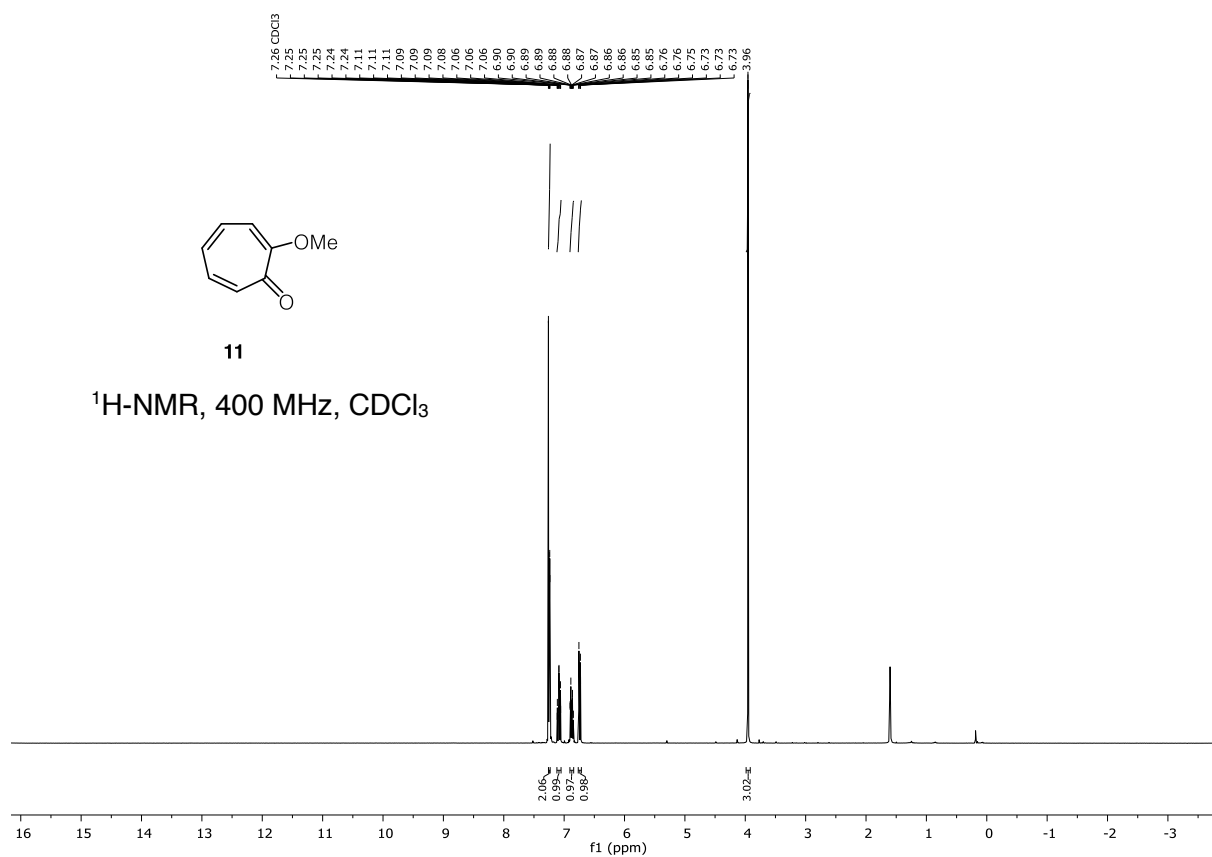


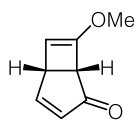
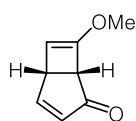
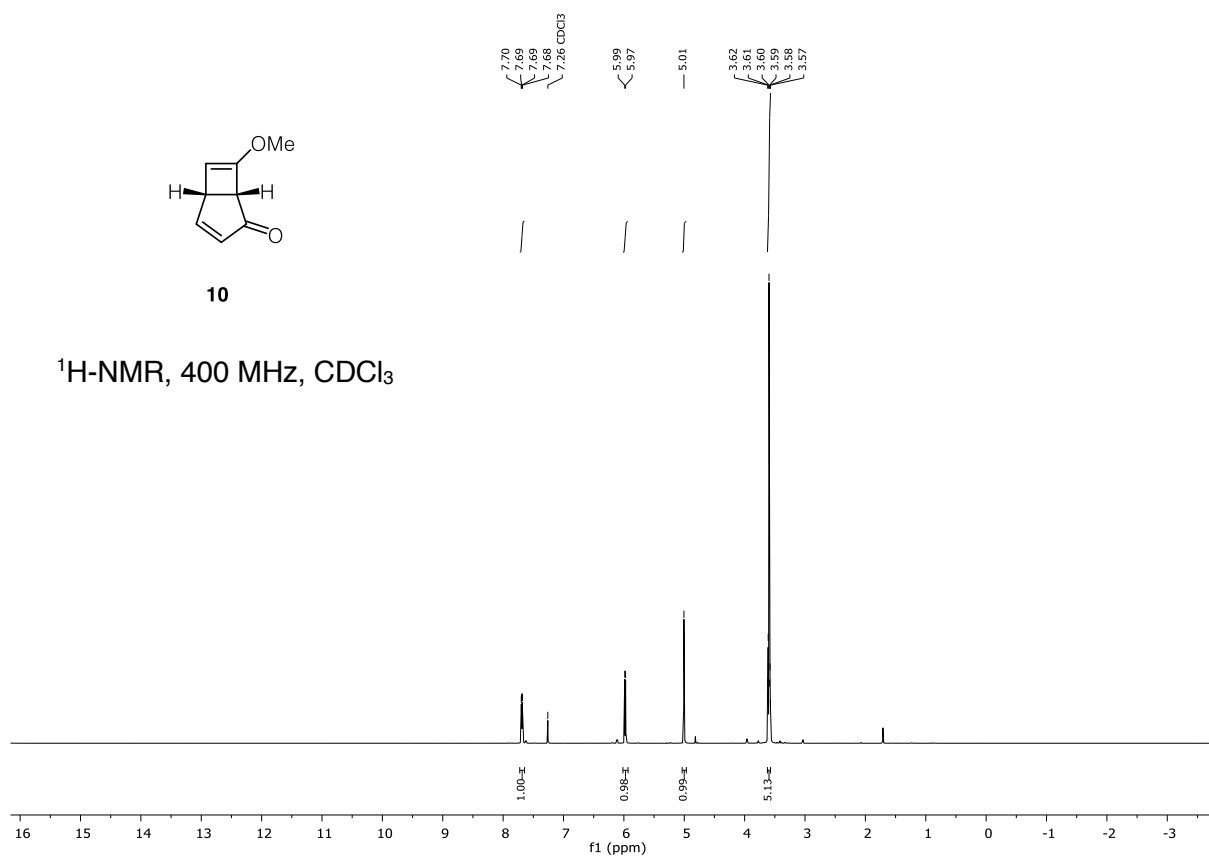
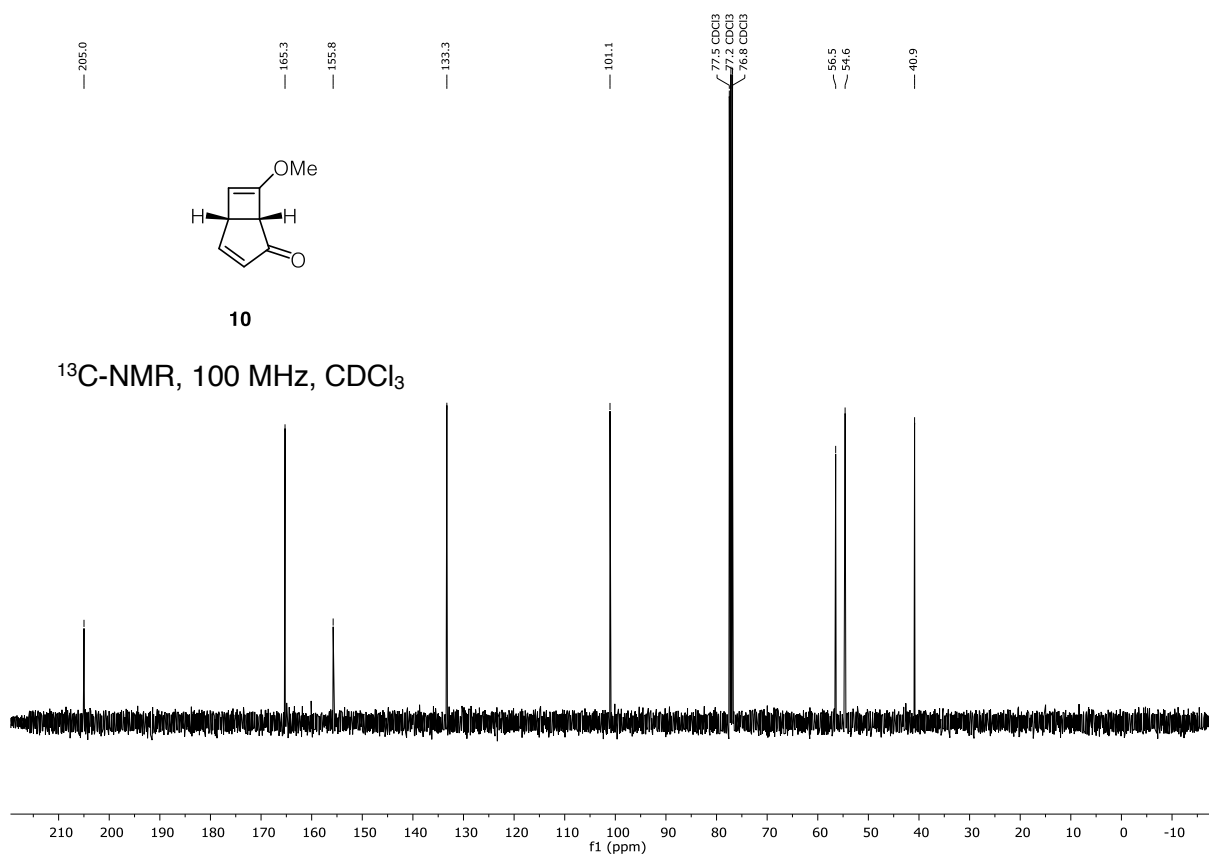


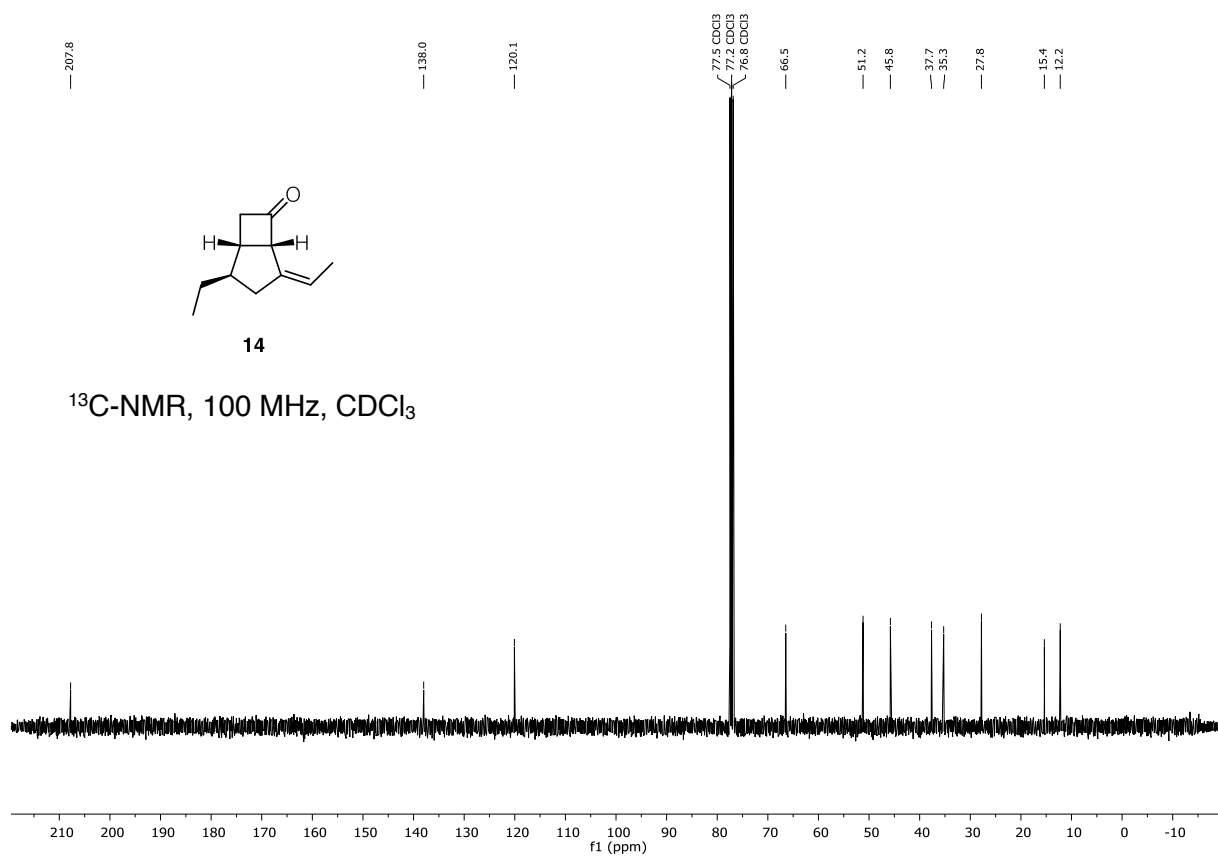
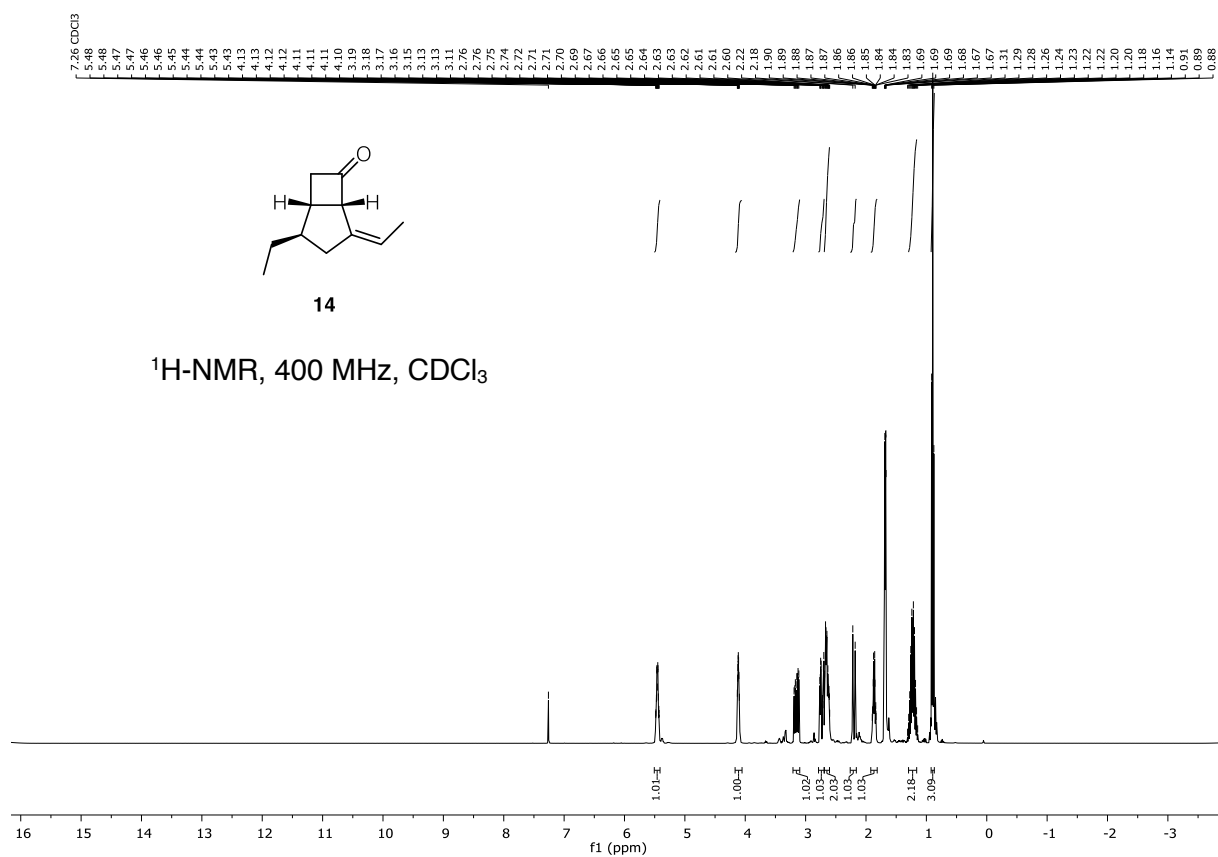


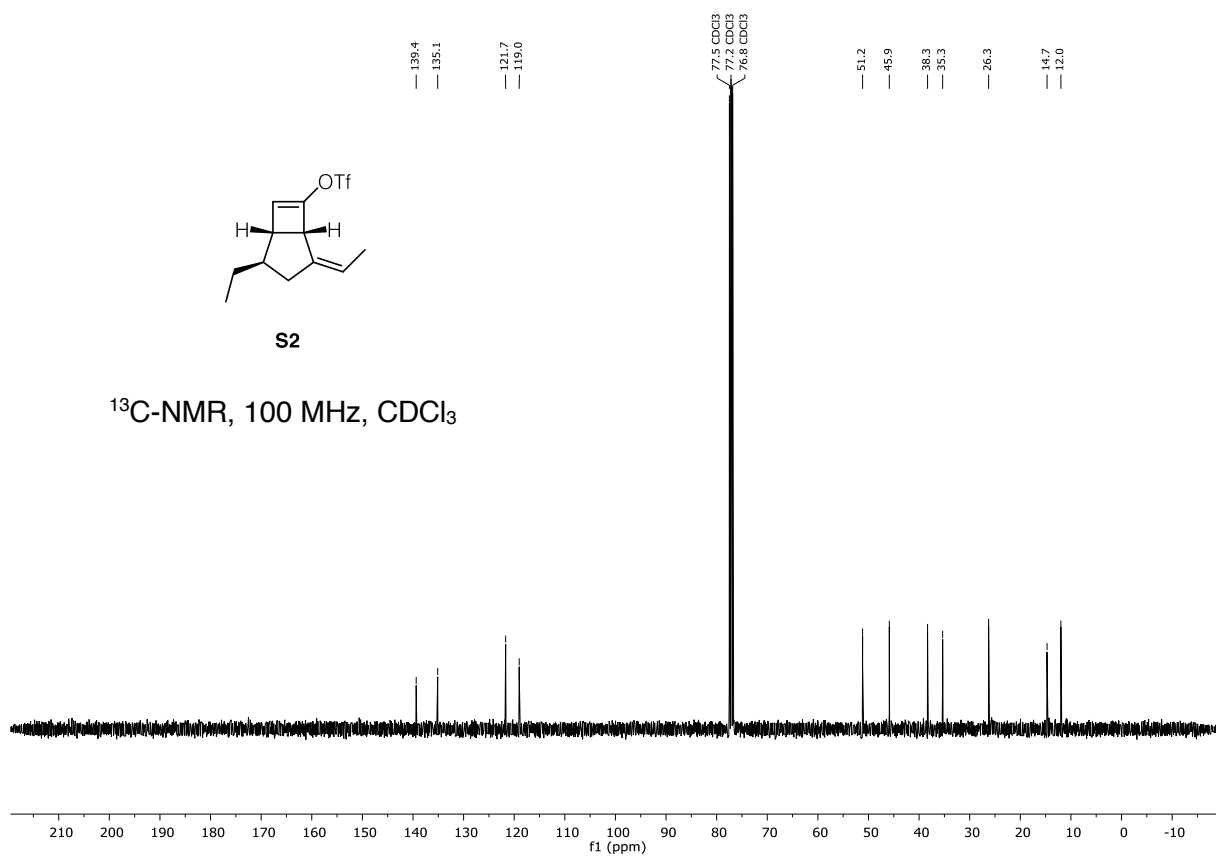
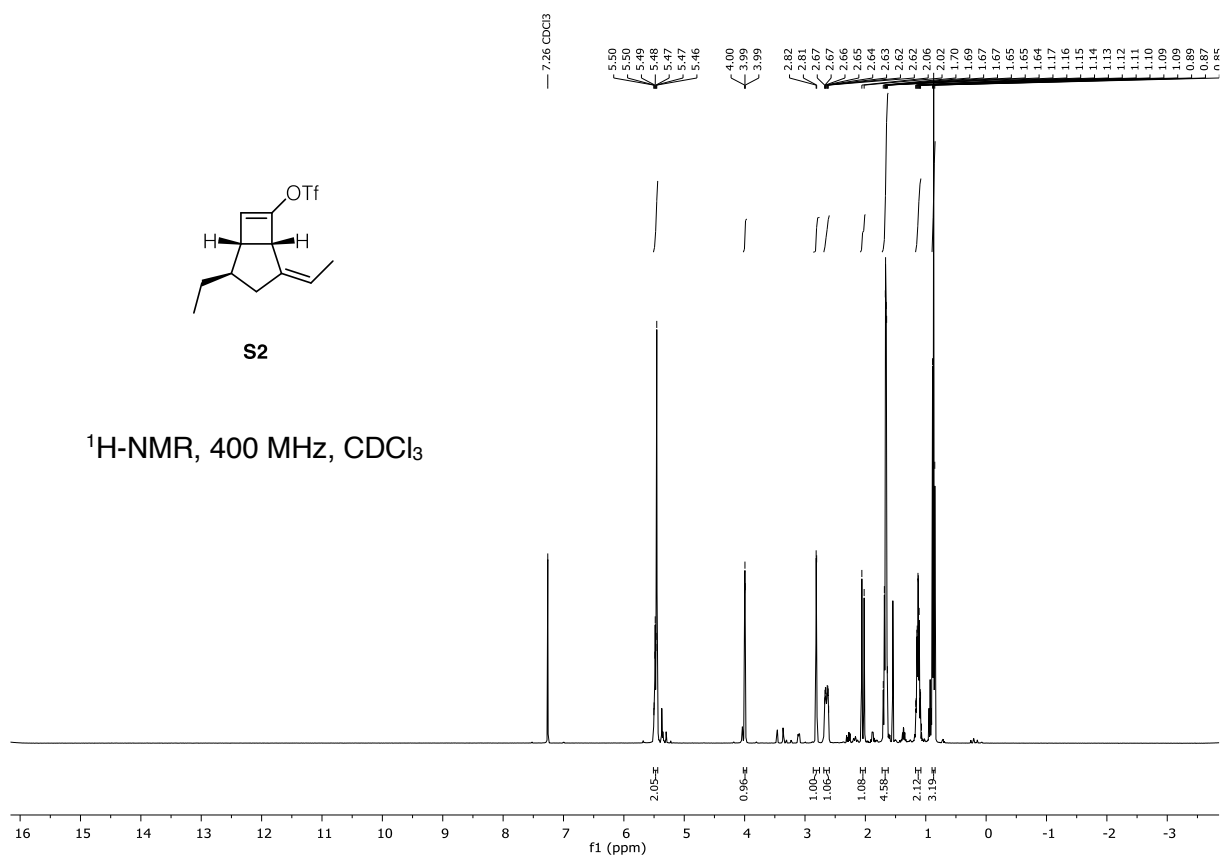


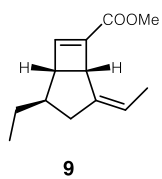




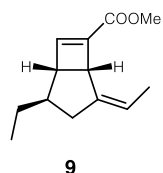
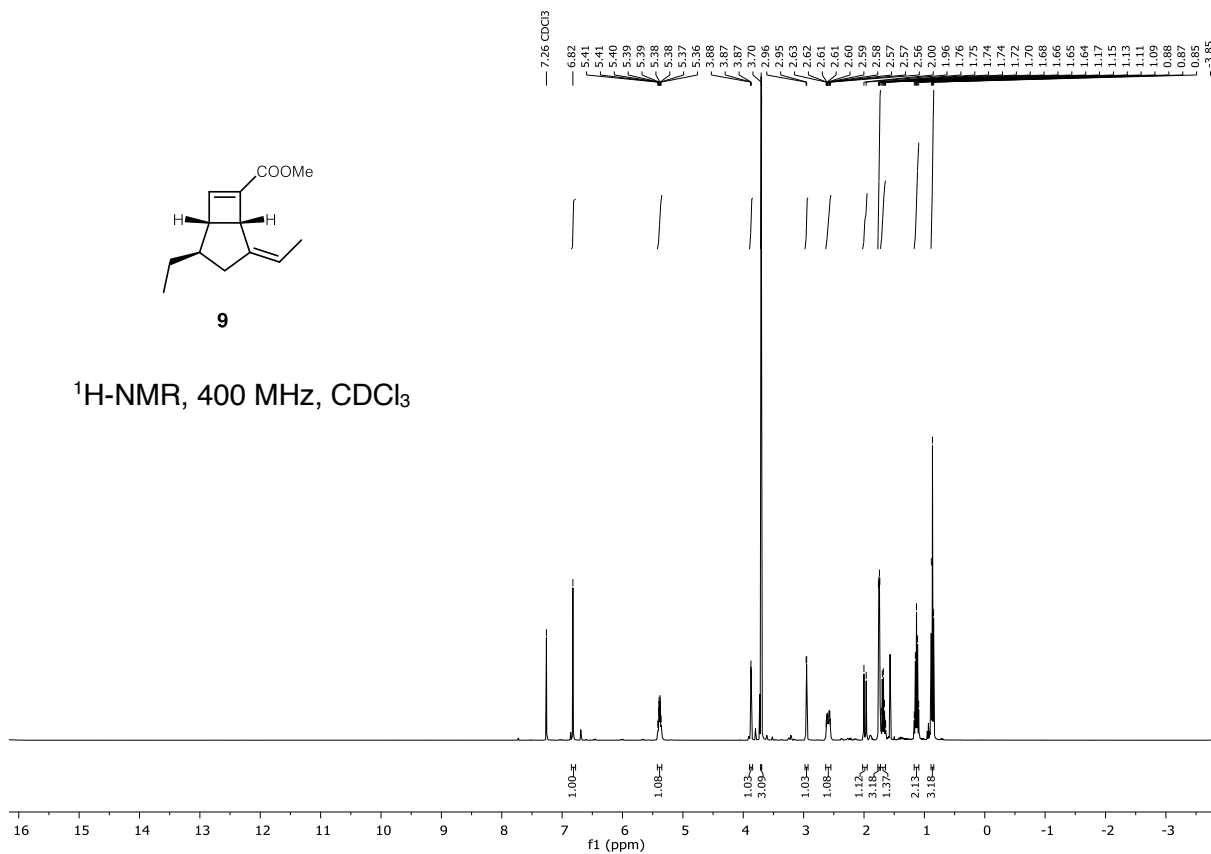
**10**¹H-NMR, 400 MHz, CDCl₃**10**¹³C-NMR, 100 MHz, CDCl₃



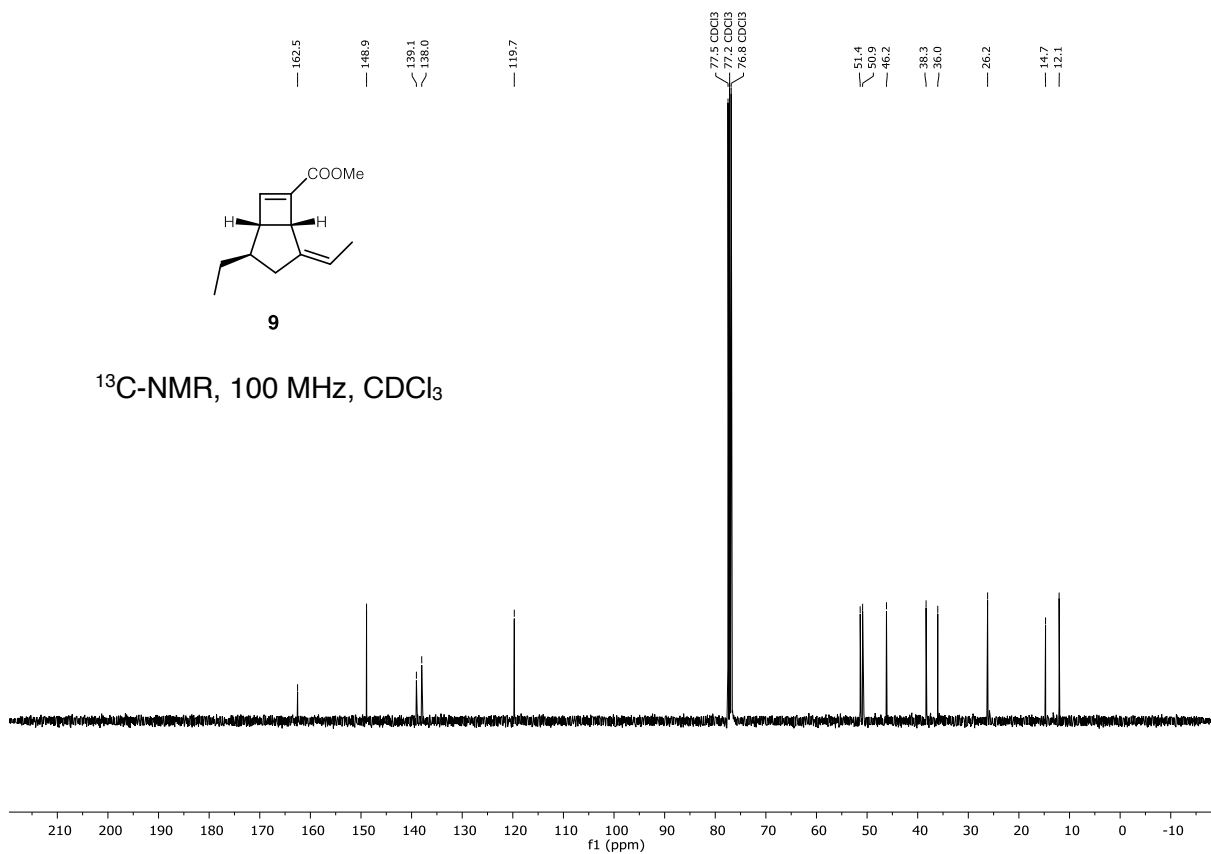


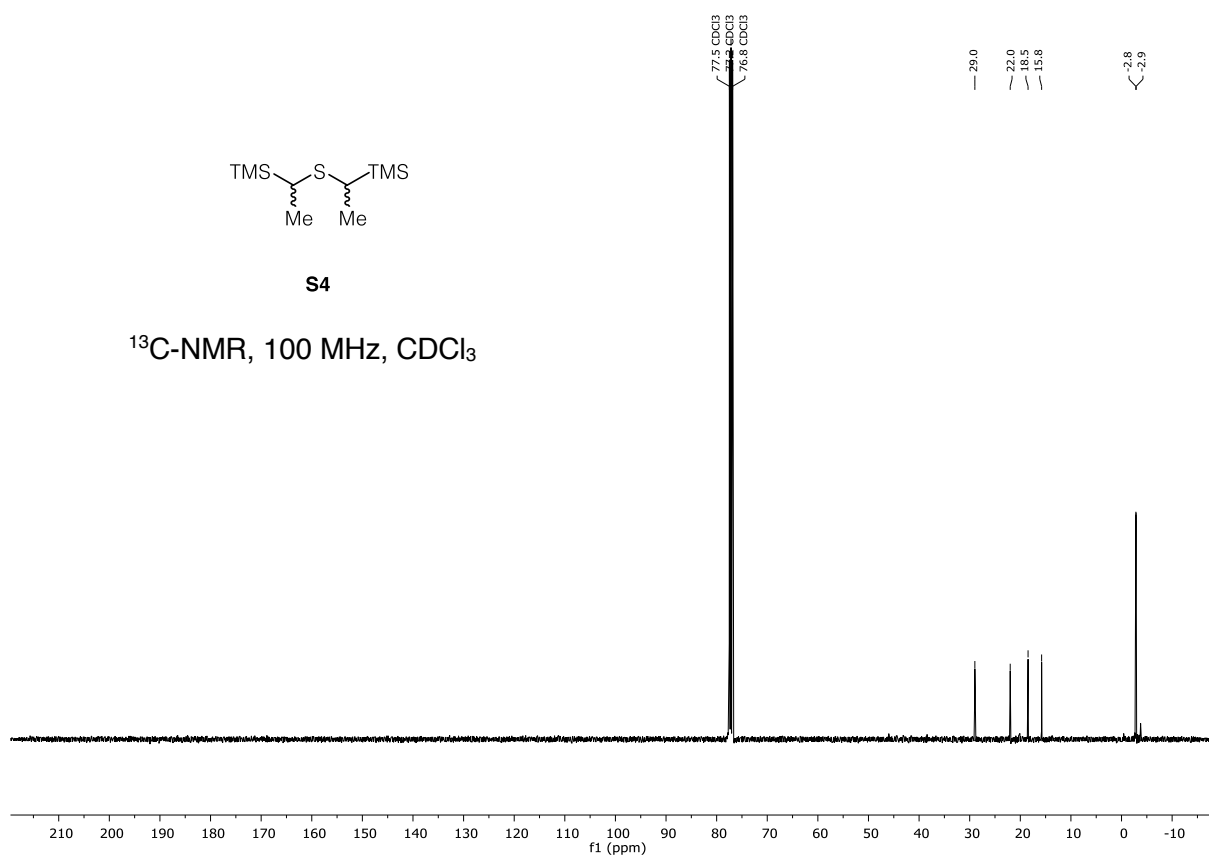
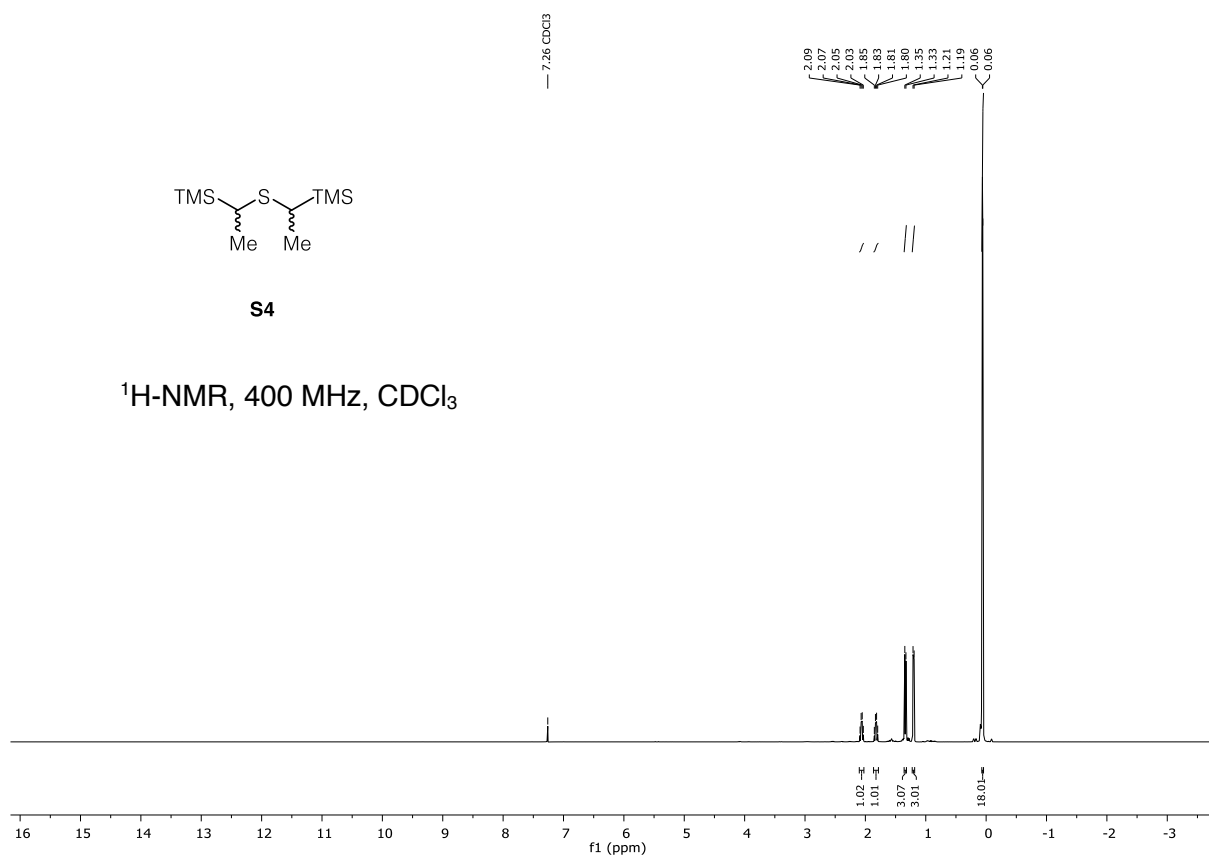


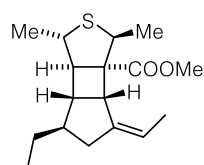
$^1\text{H-NMR}$, 400 MHz, CDCl_3



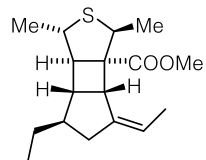
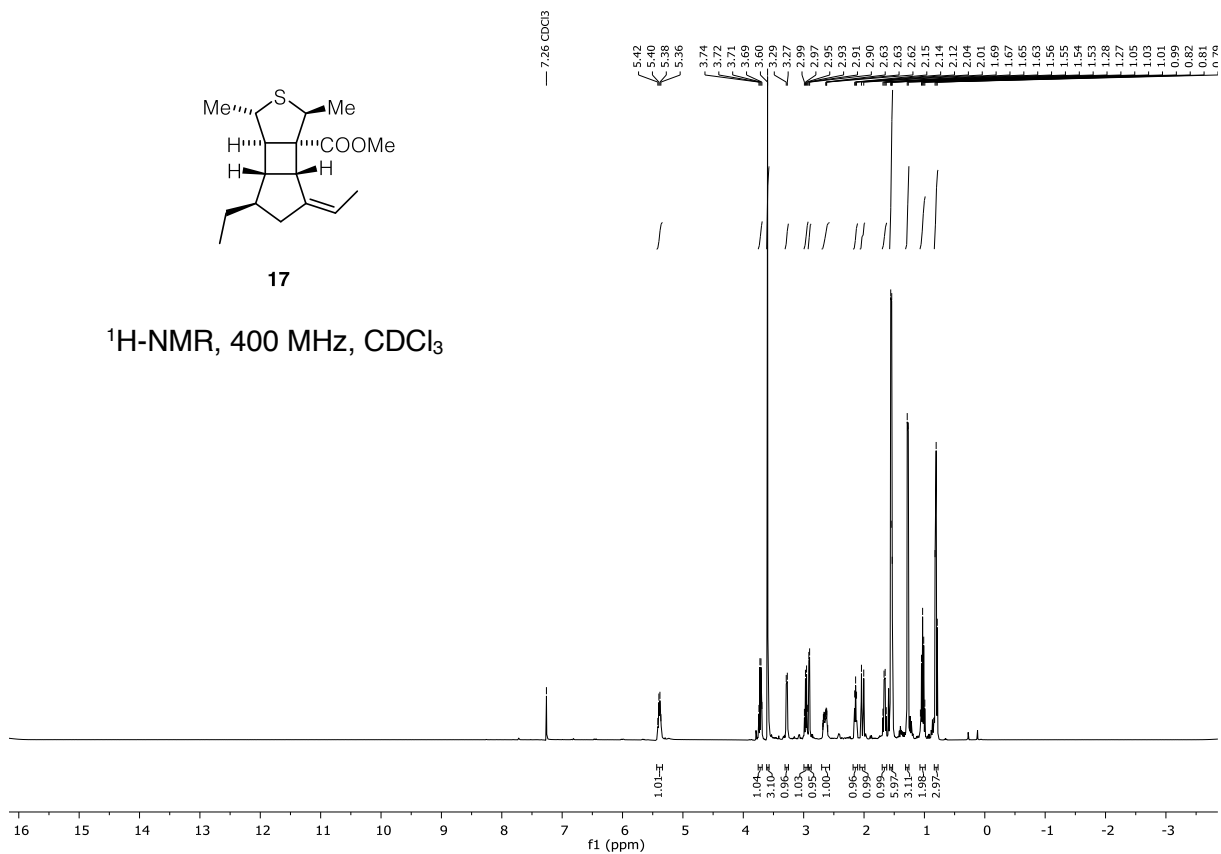
$^{13}\text{C-NMR}$, 100 MHz, CDCl_3



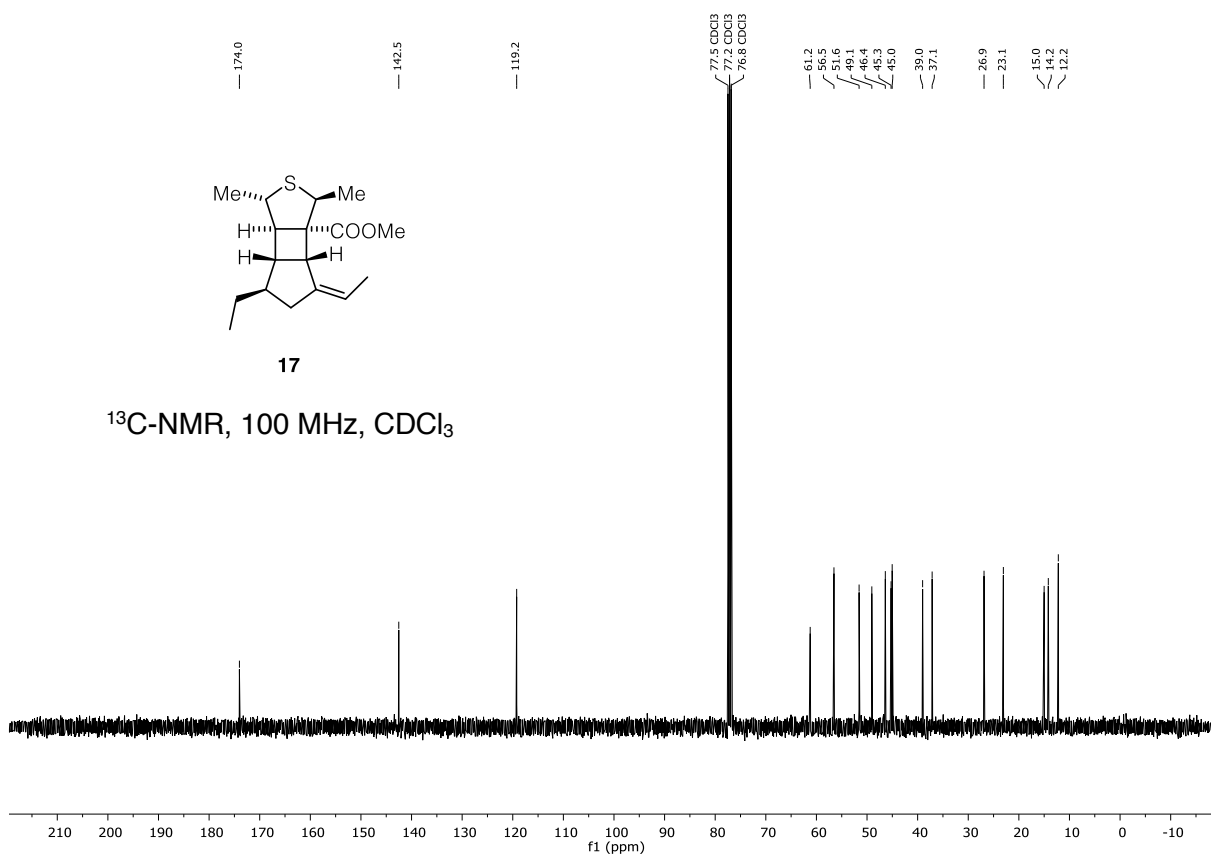


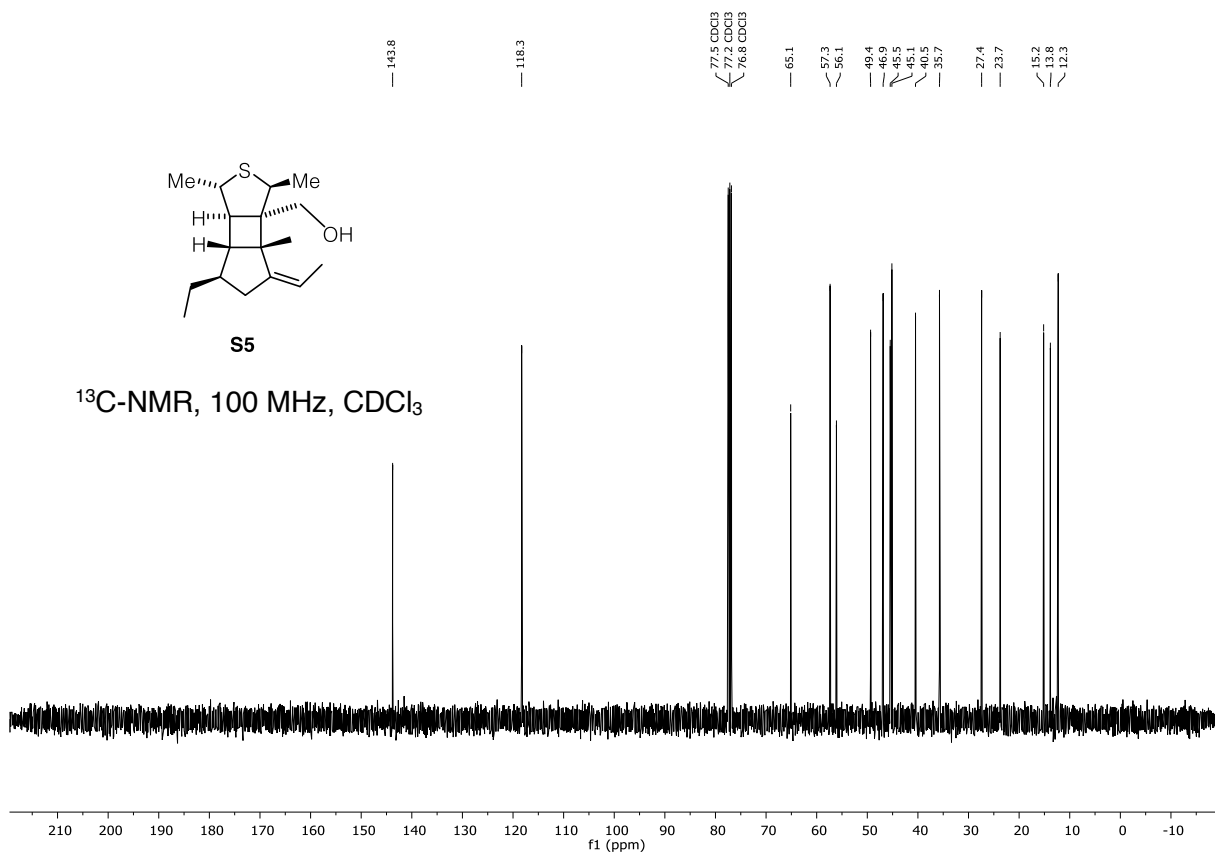
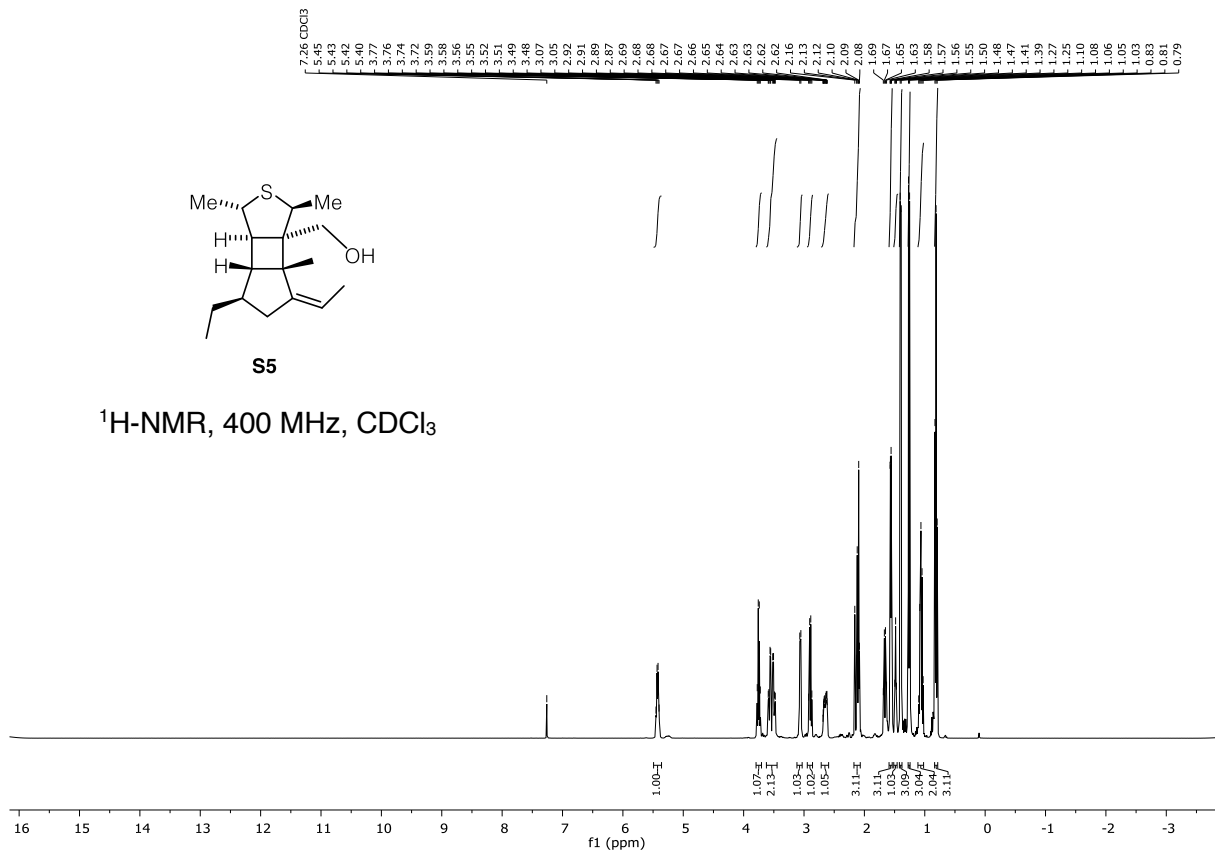


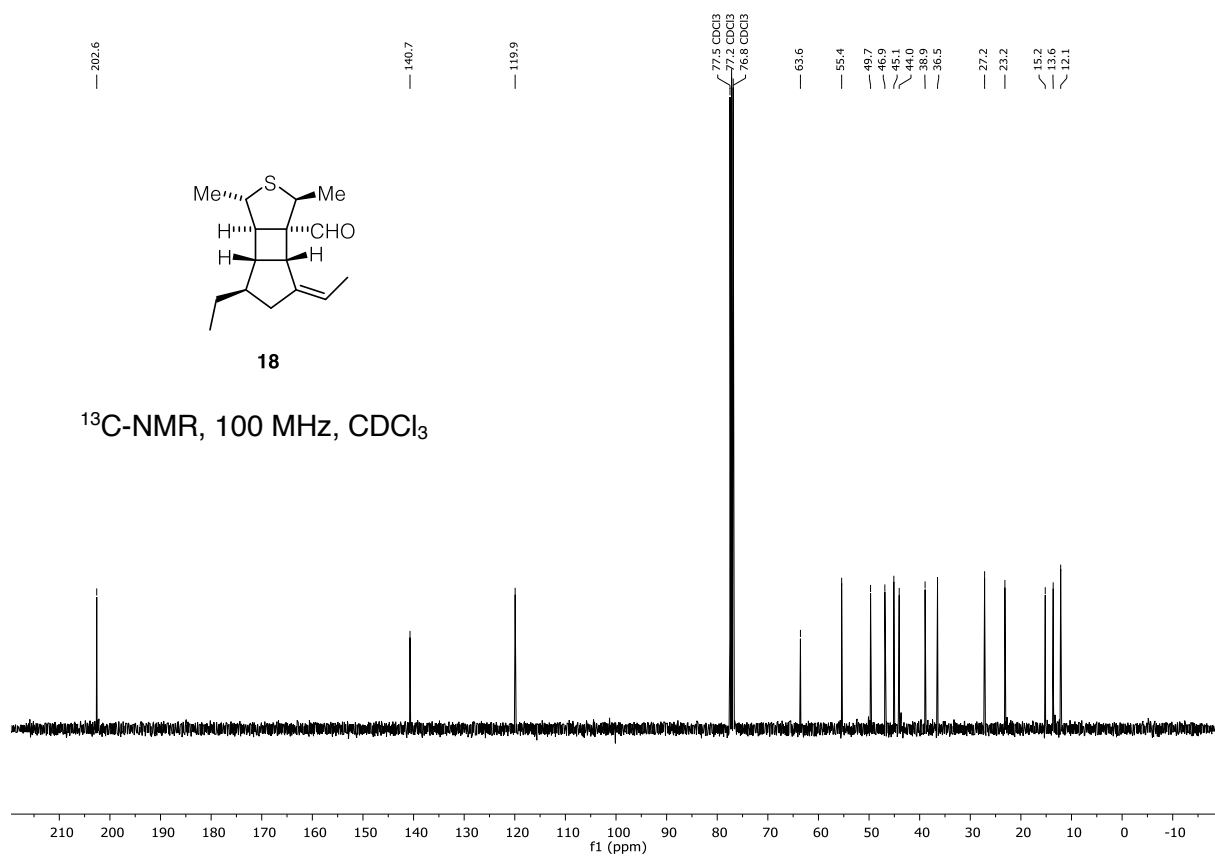
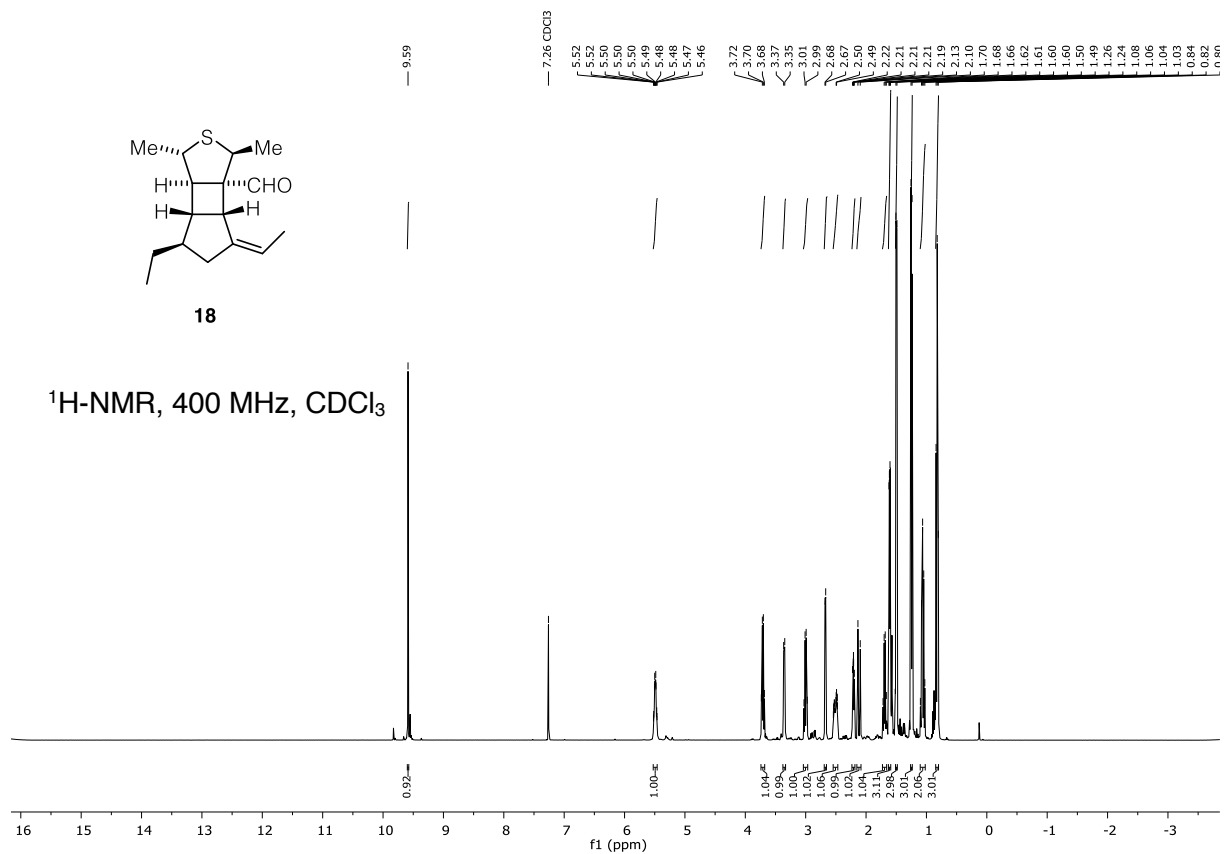
17

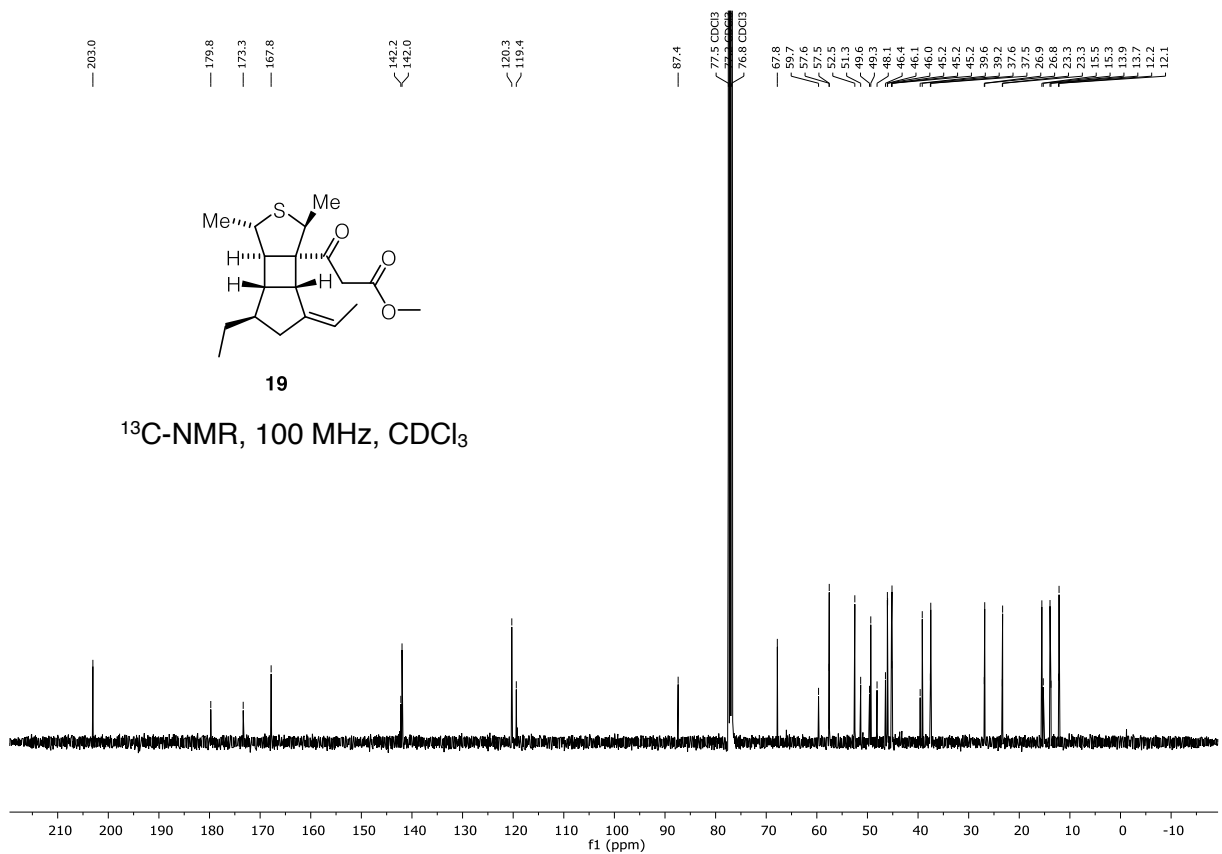
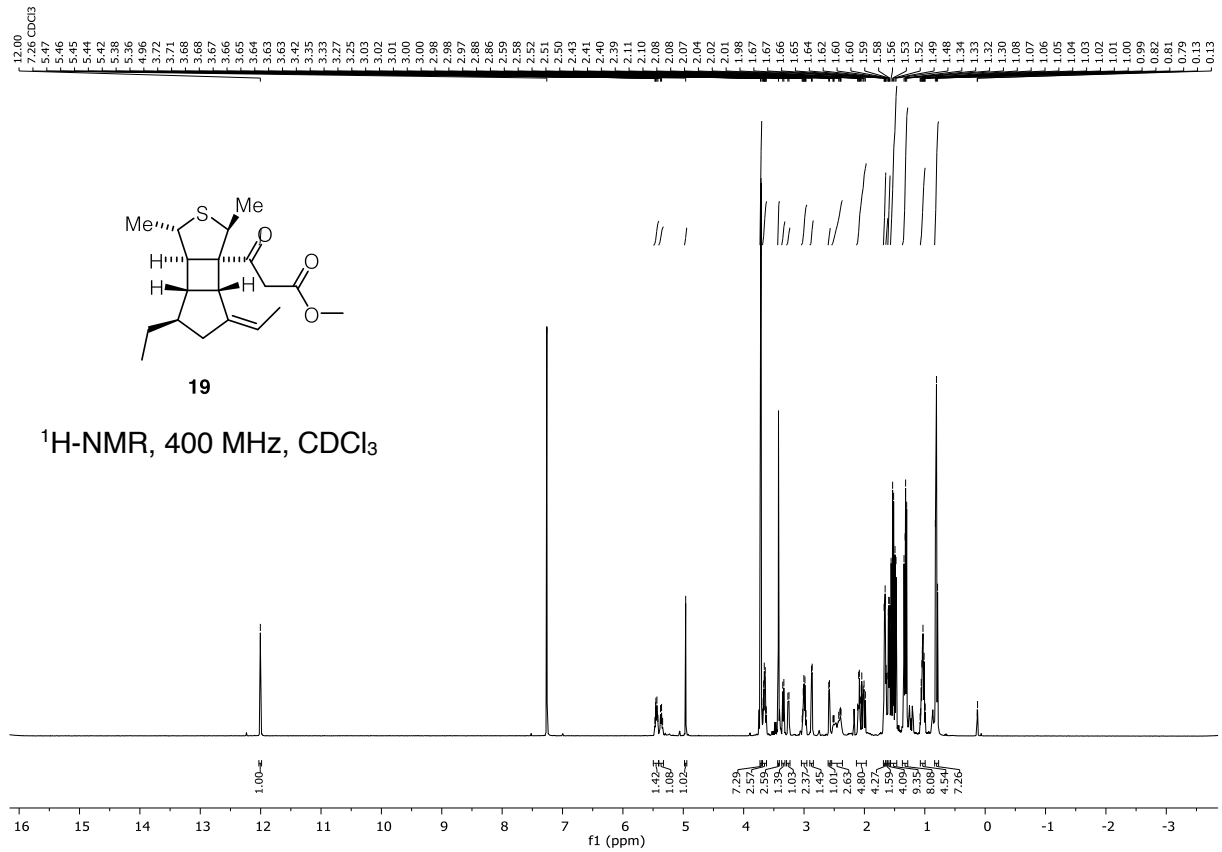
 $^1\text{H-NMR}$, 400 MHz, CDCl_3 

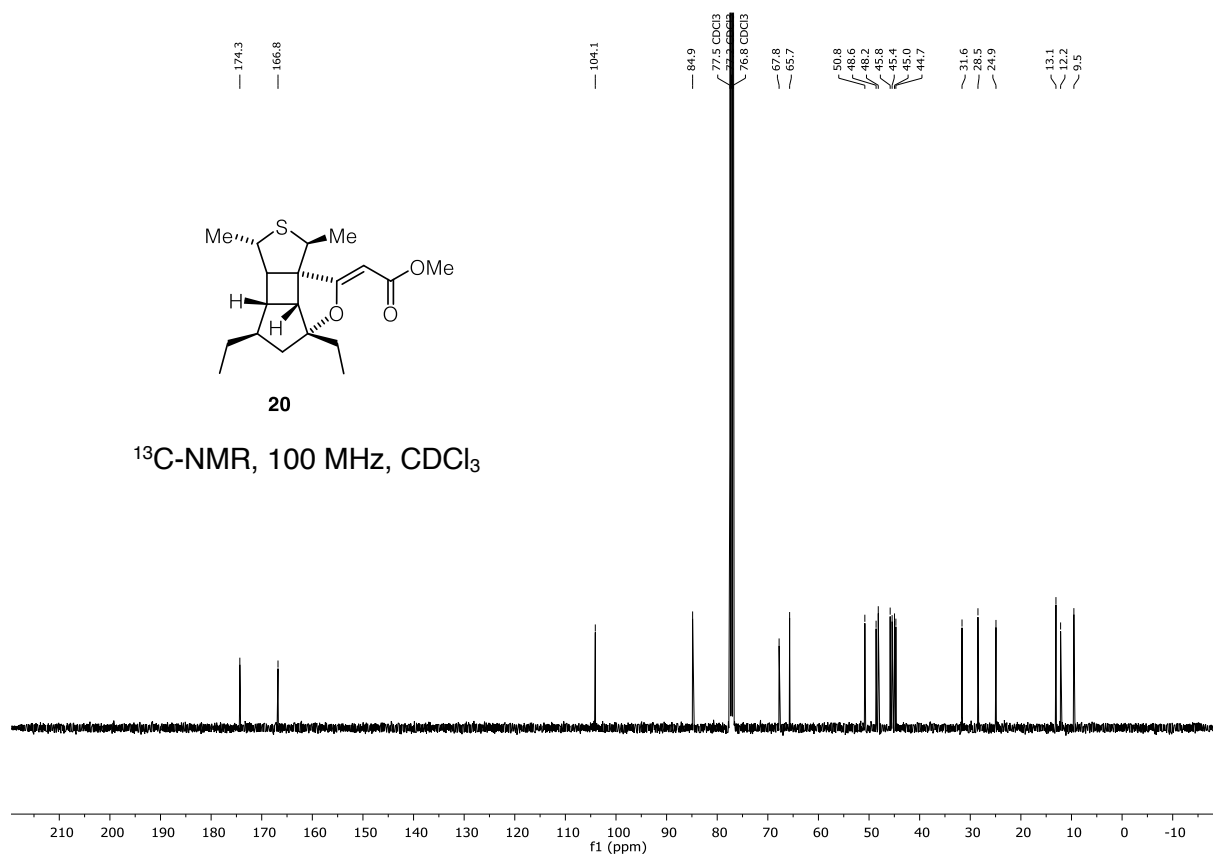
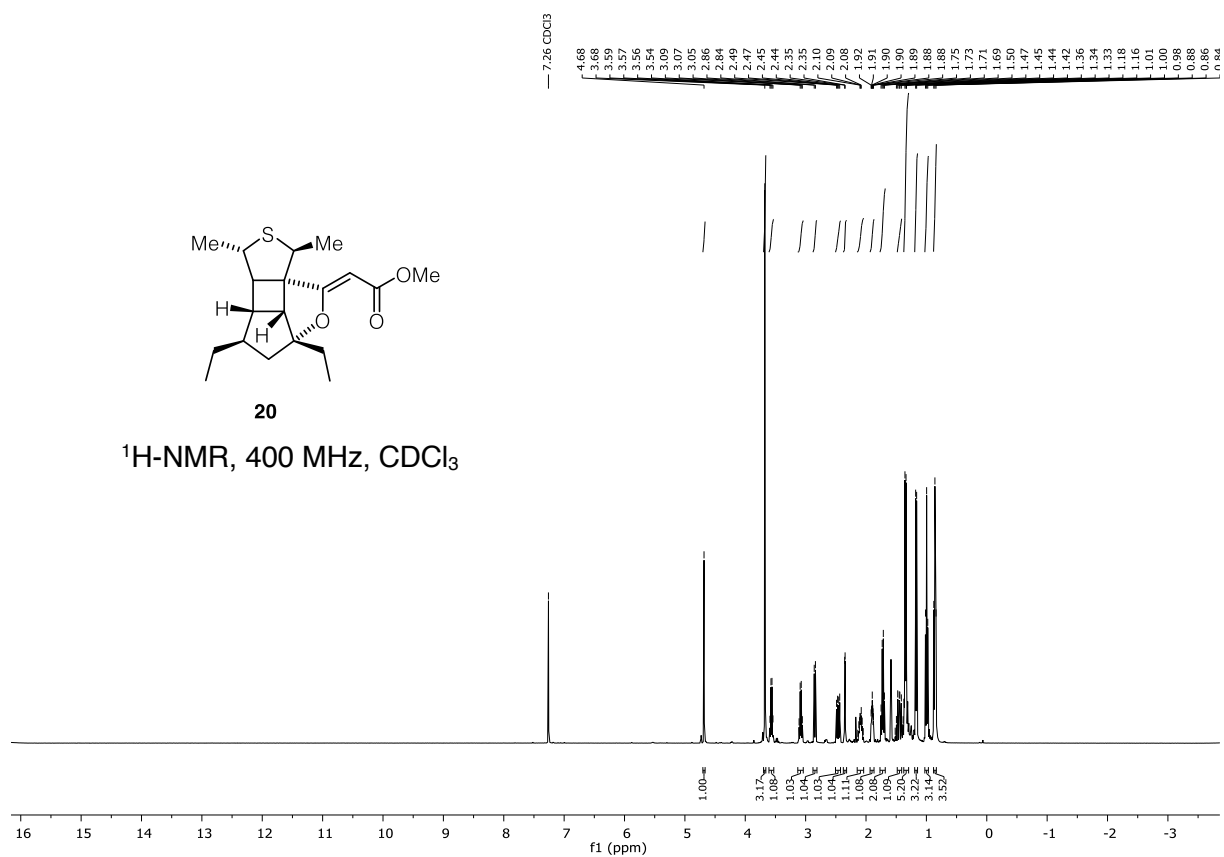
17

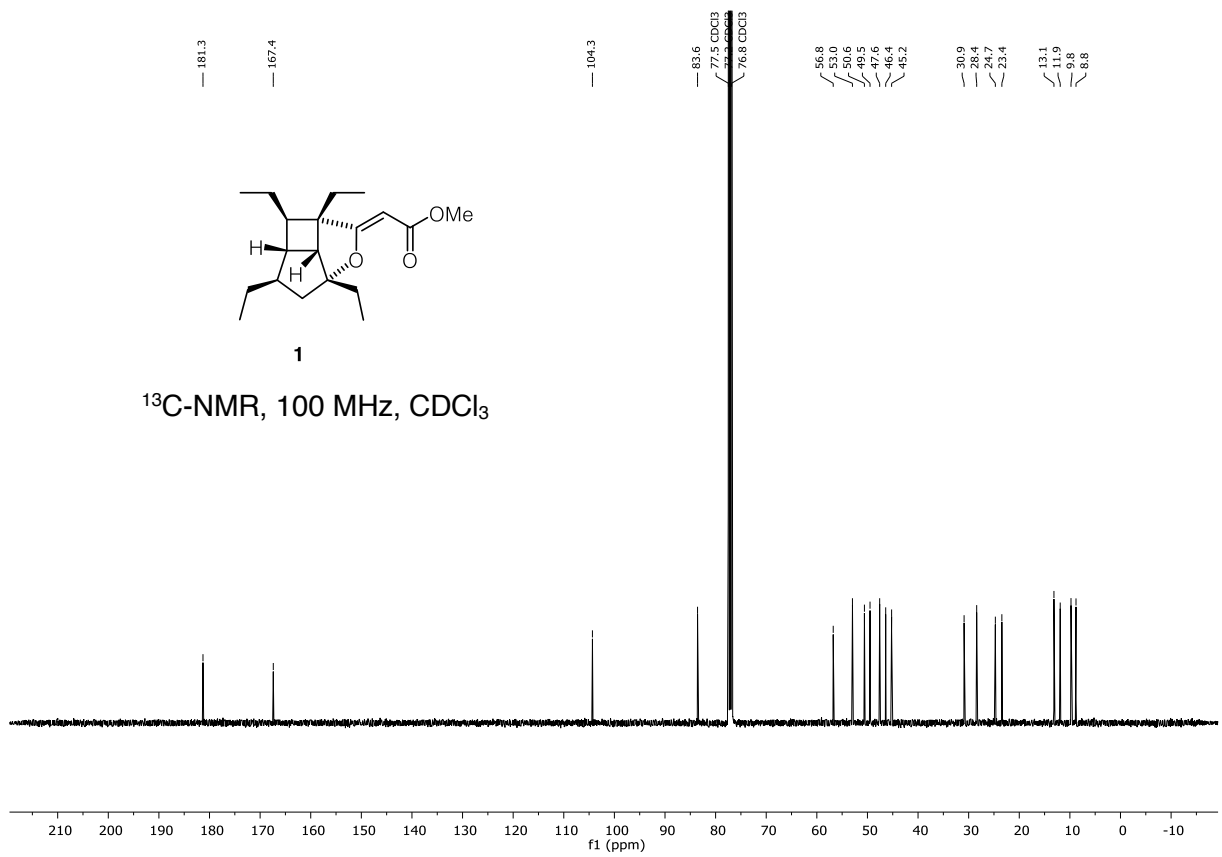
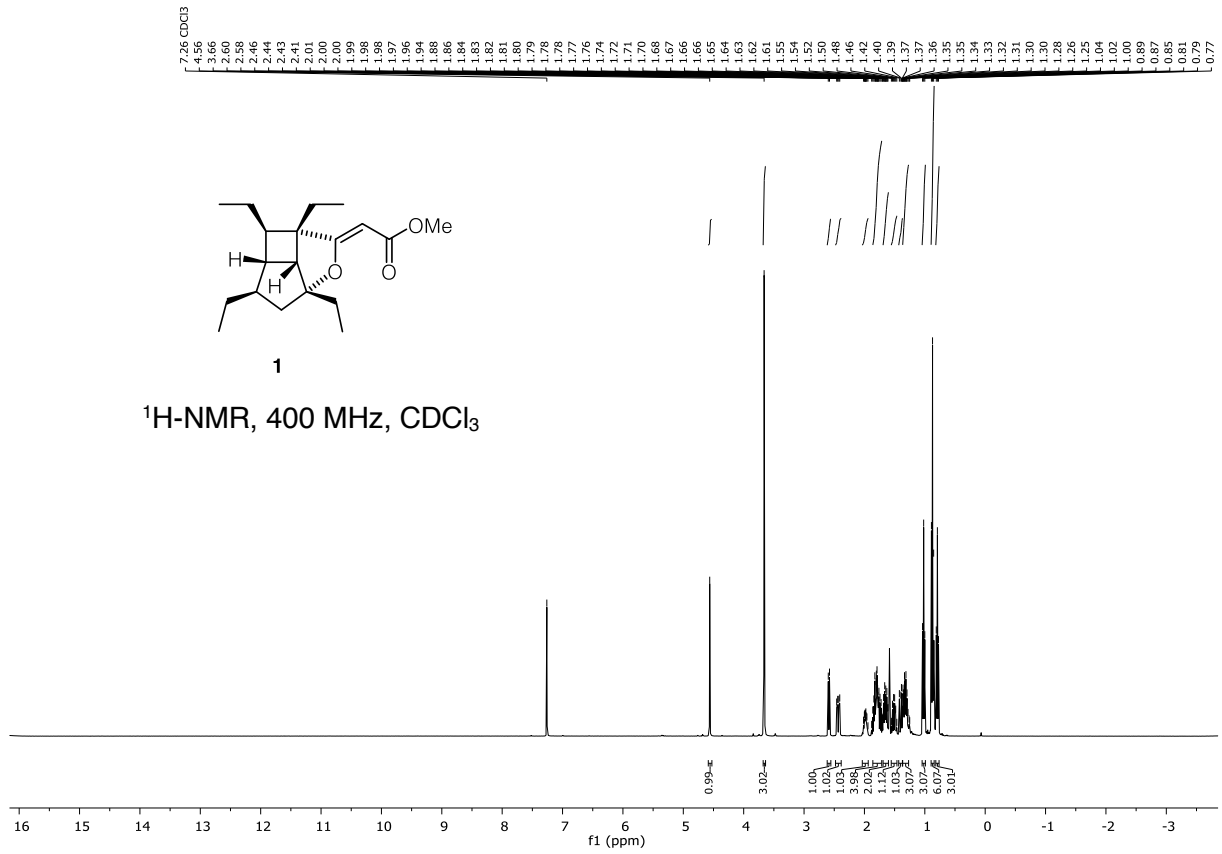
 $^{13}\text{C-NMR}$, 100 MHz, CDCl_3 

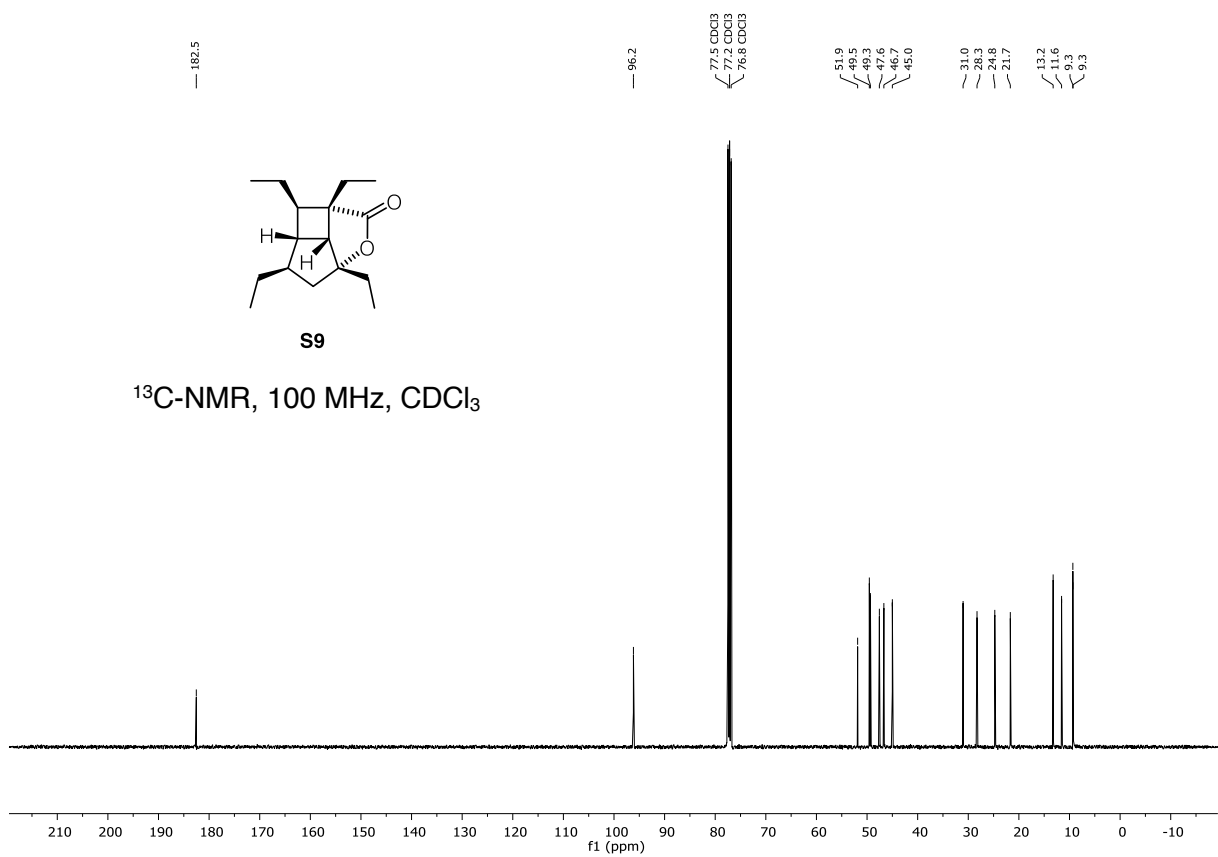
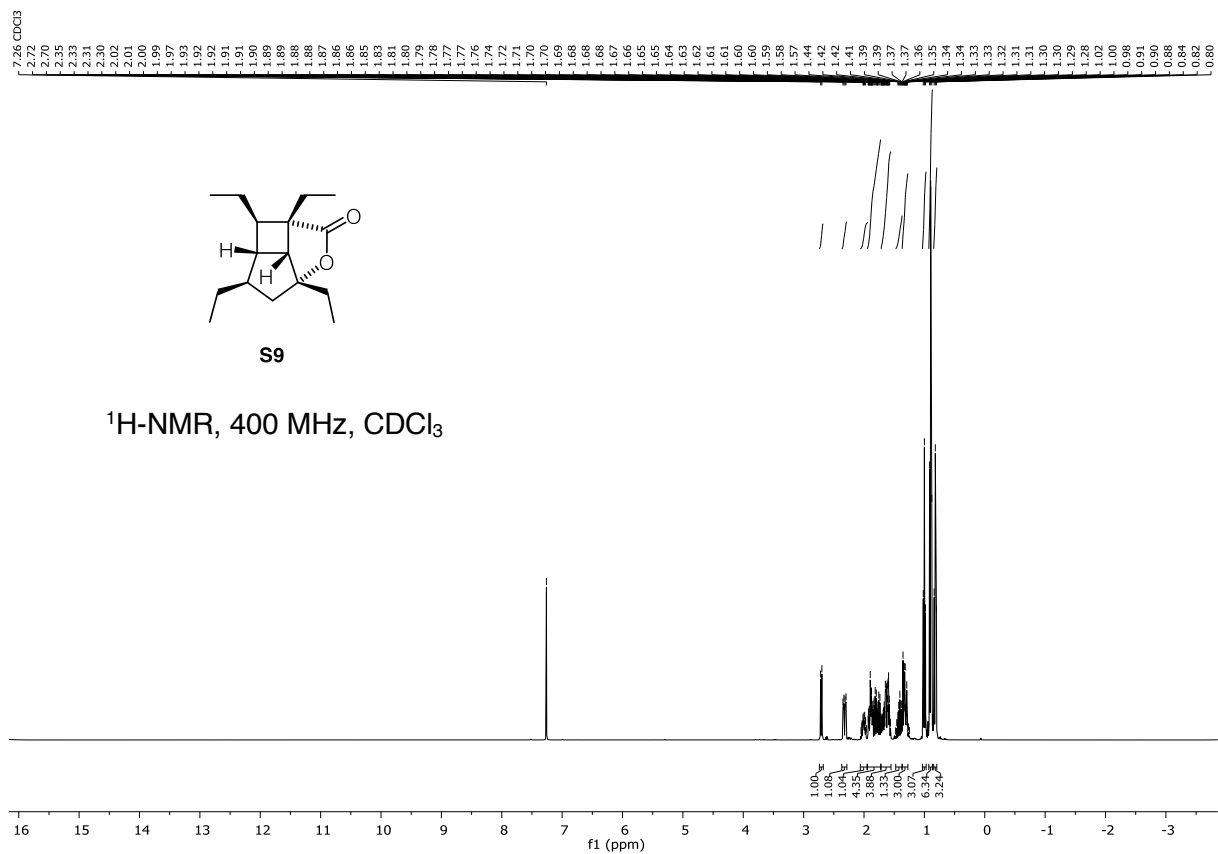


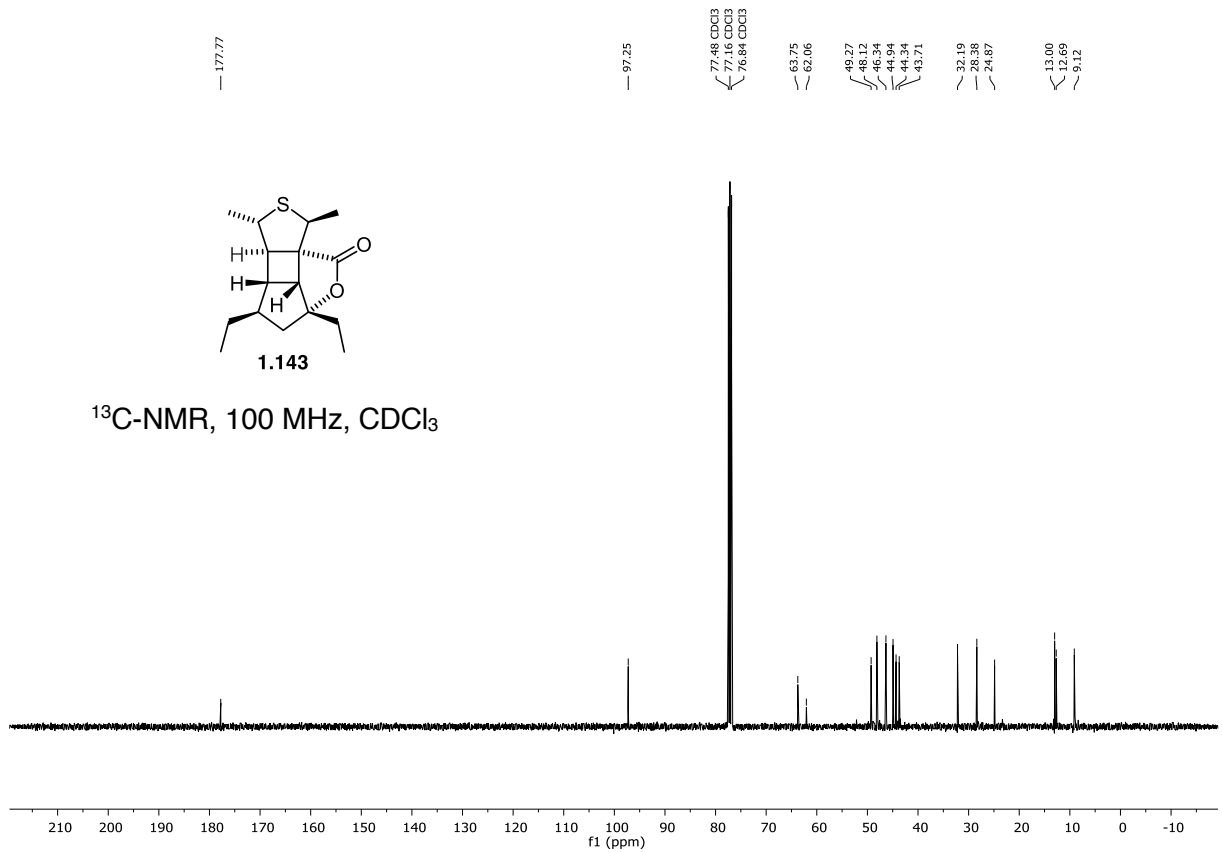
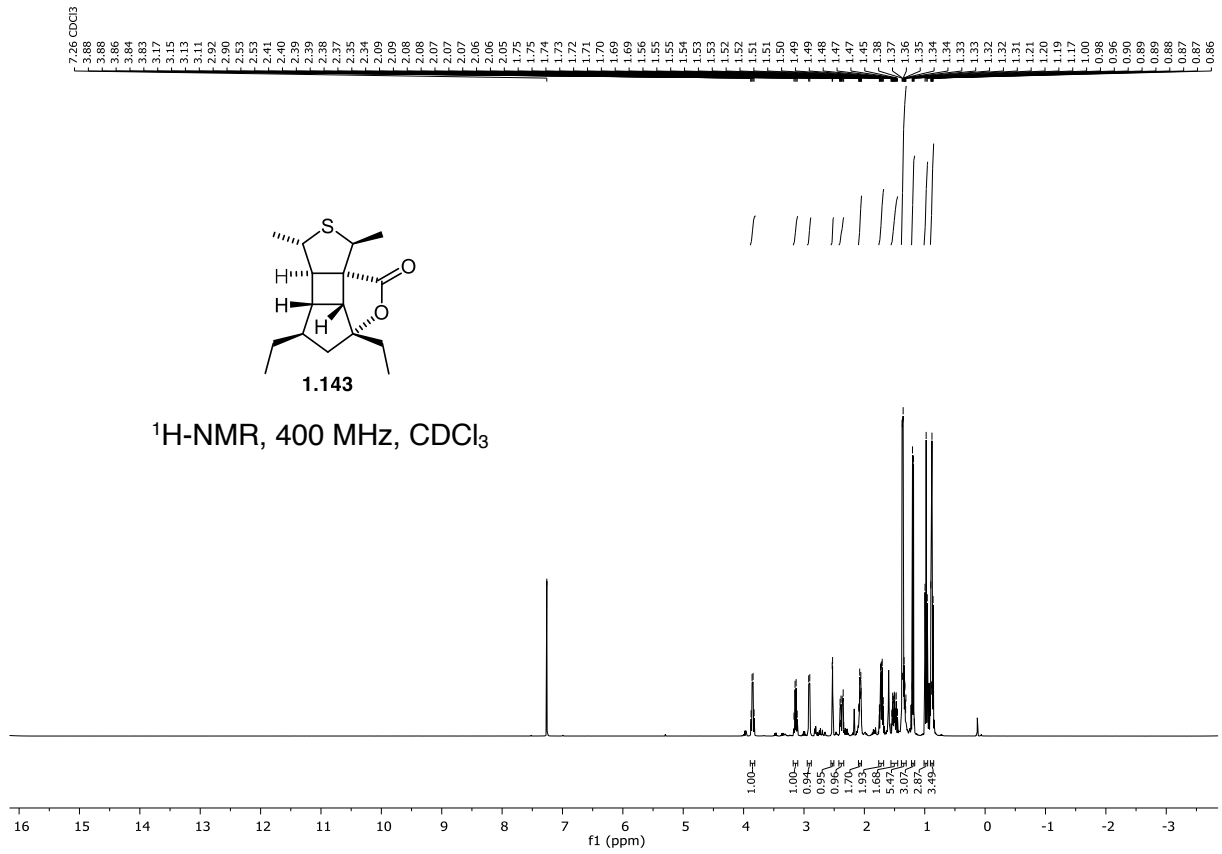


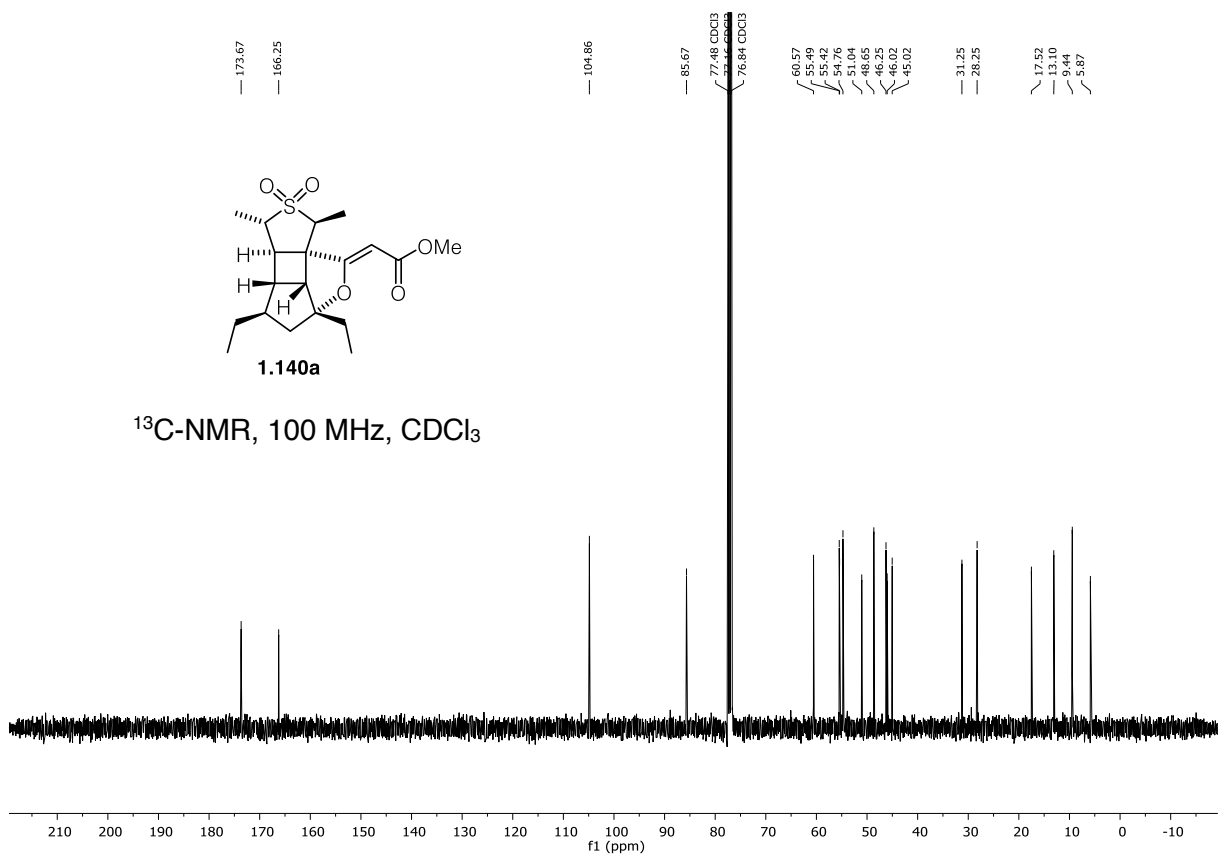
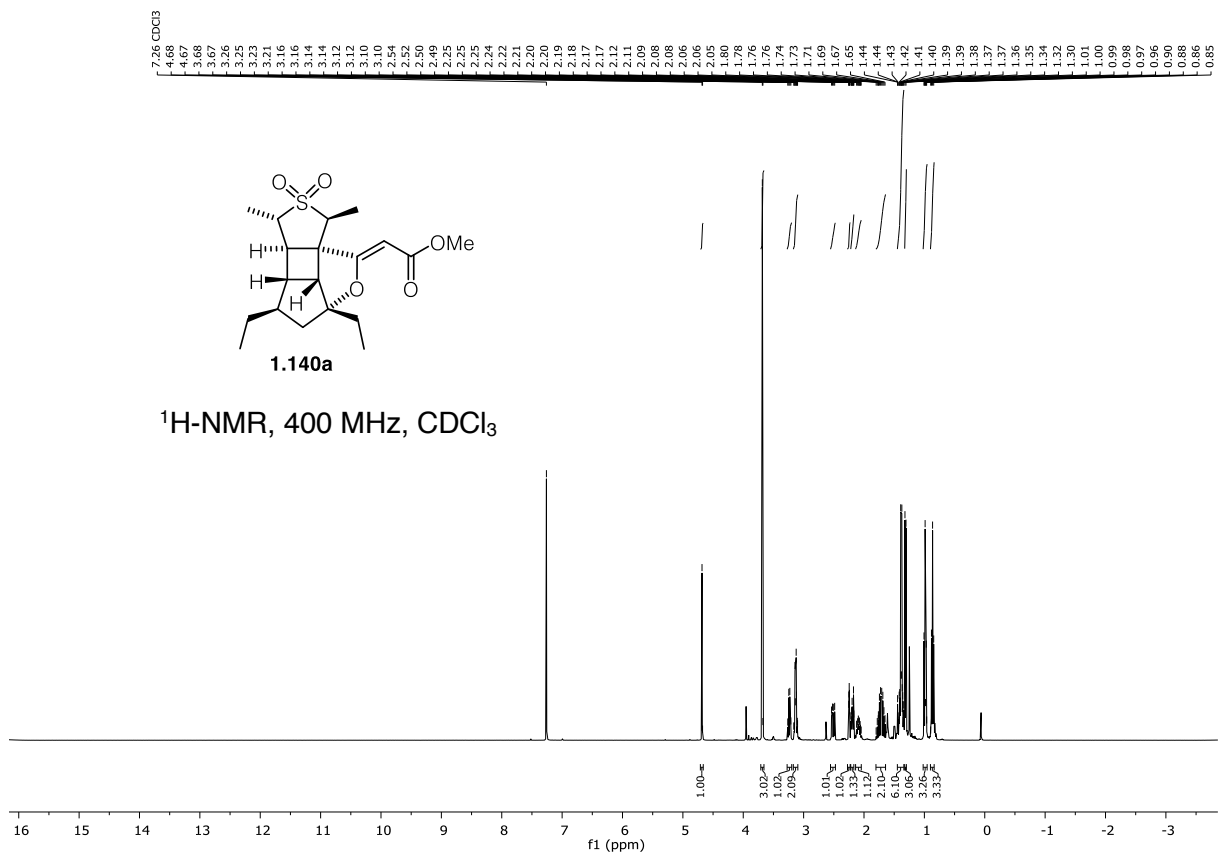


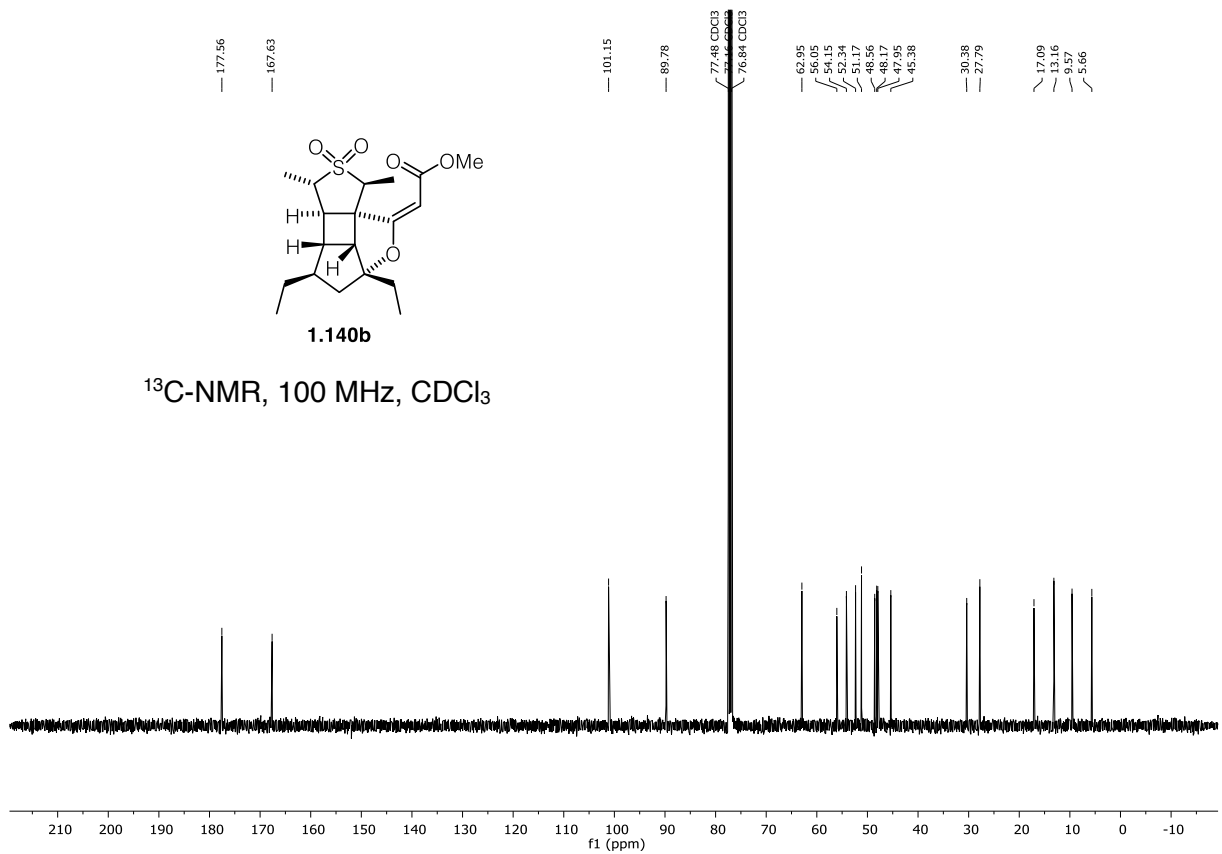
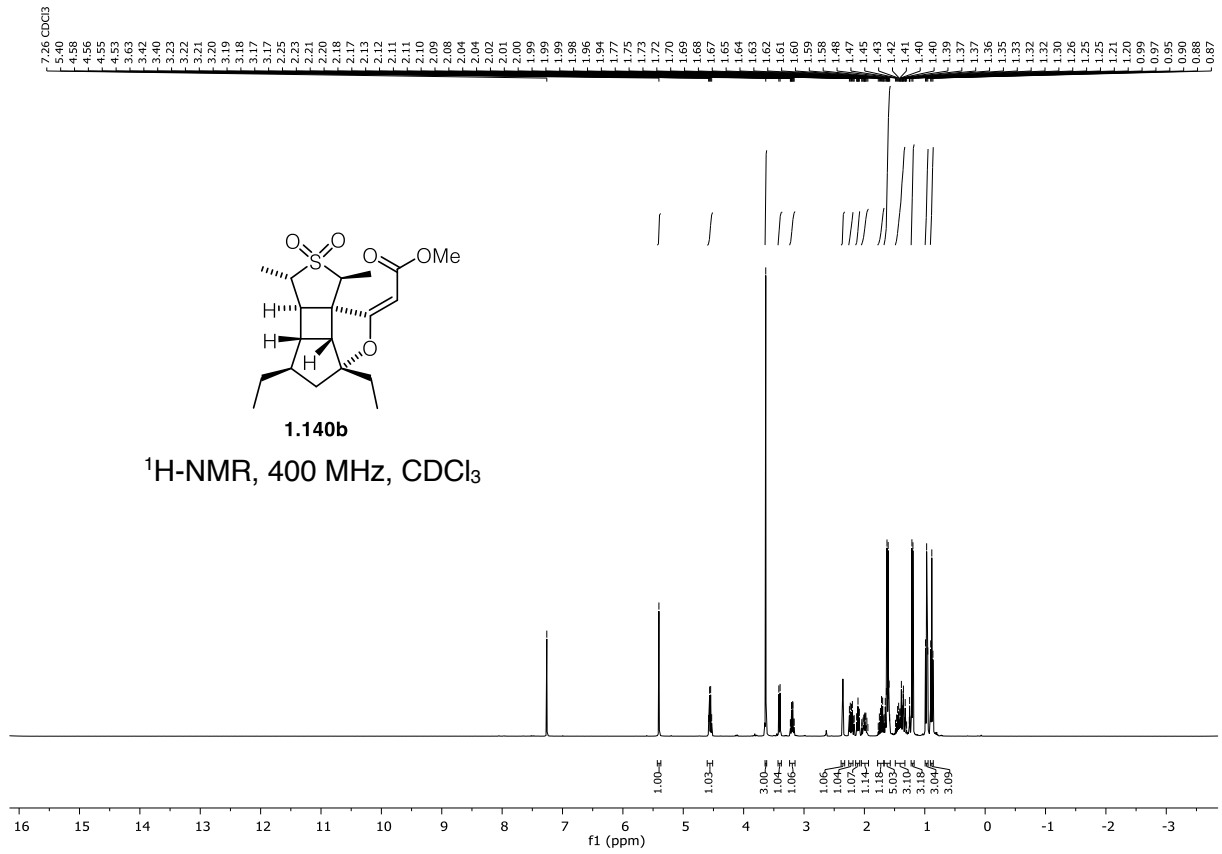


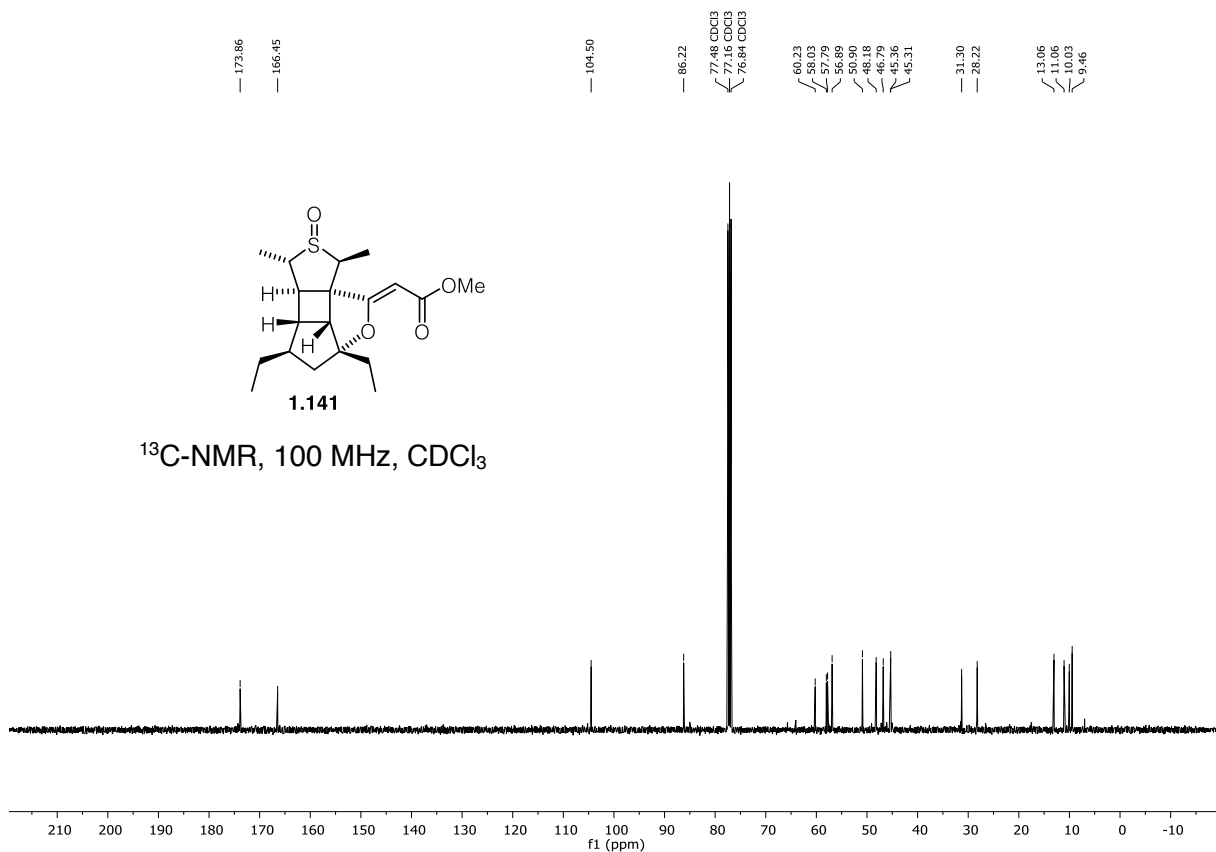
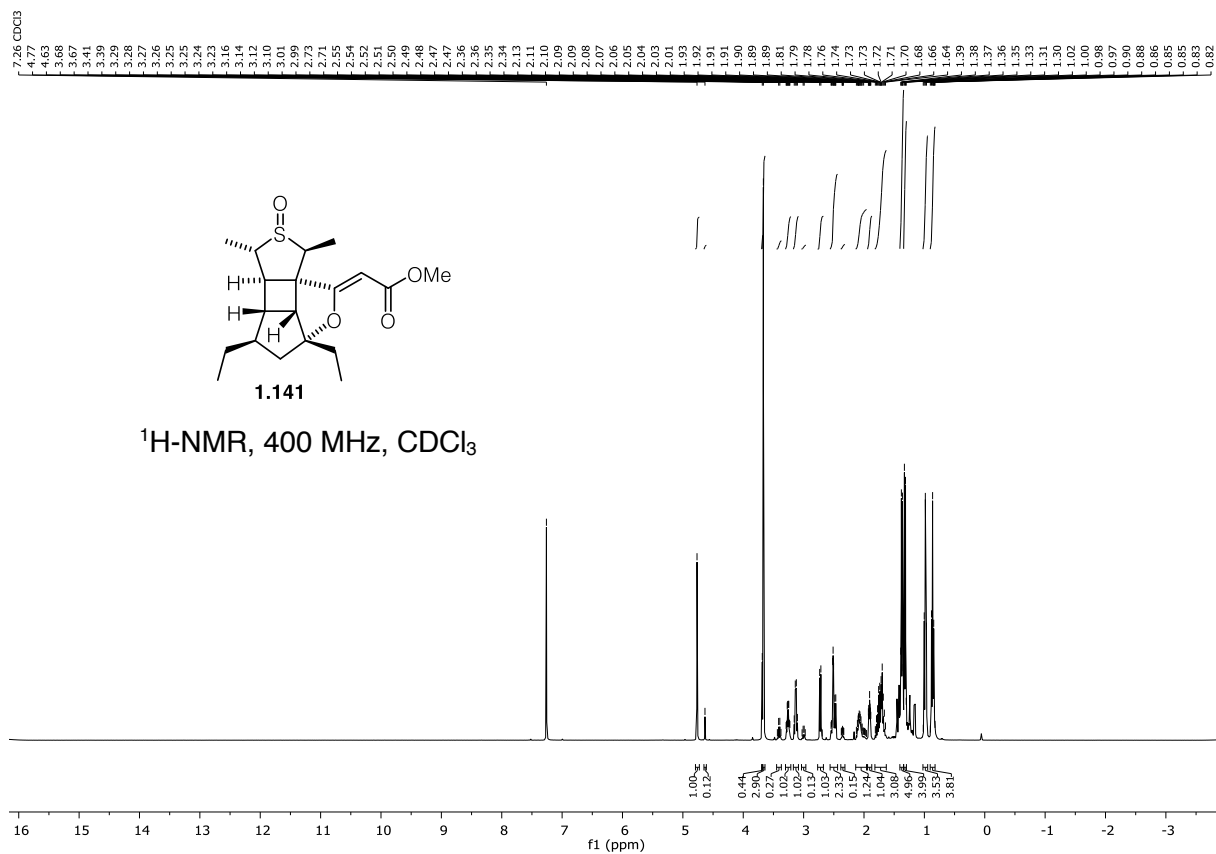


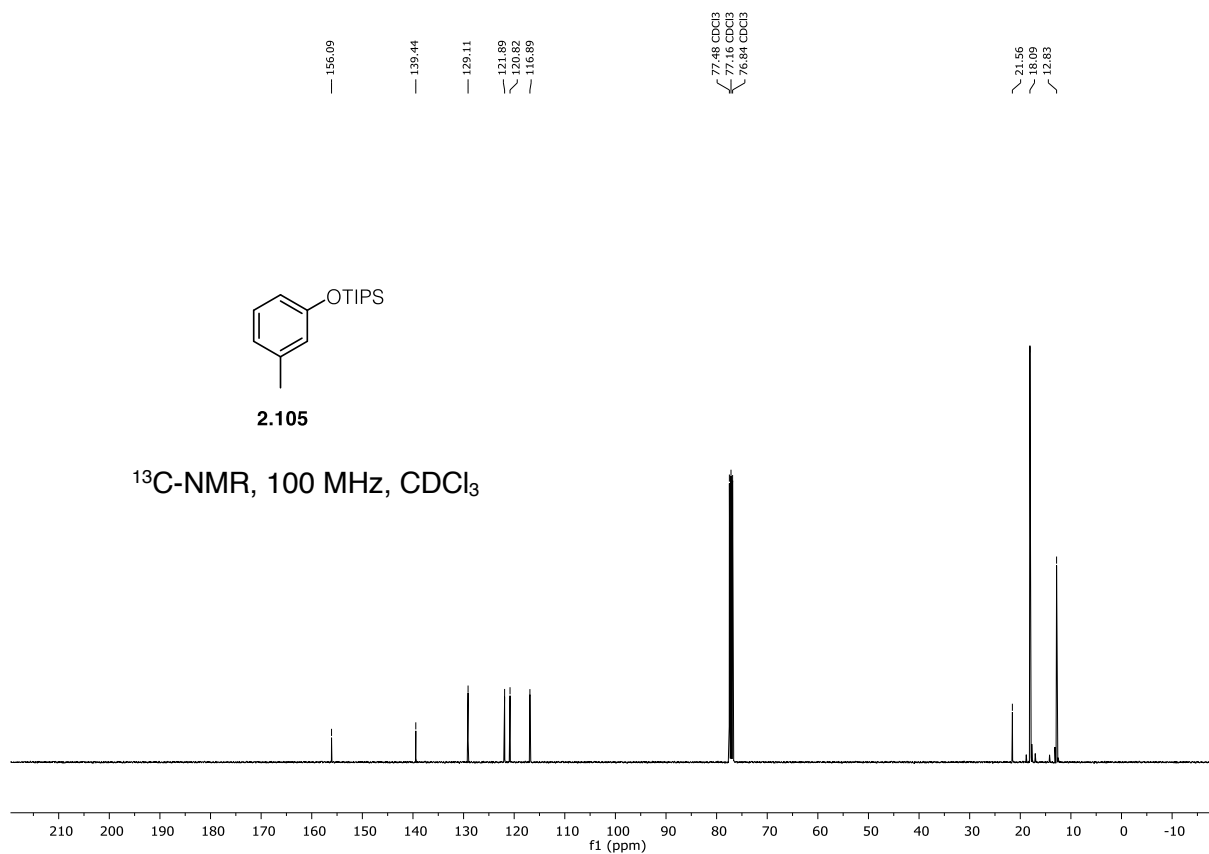
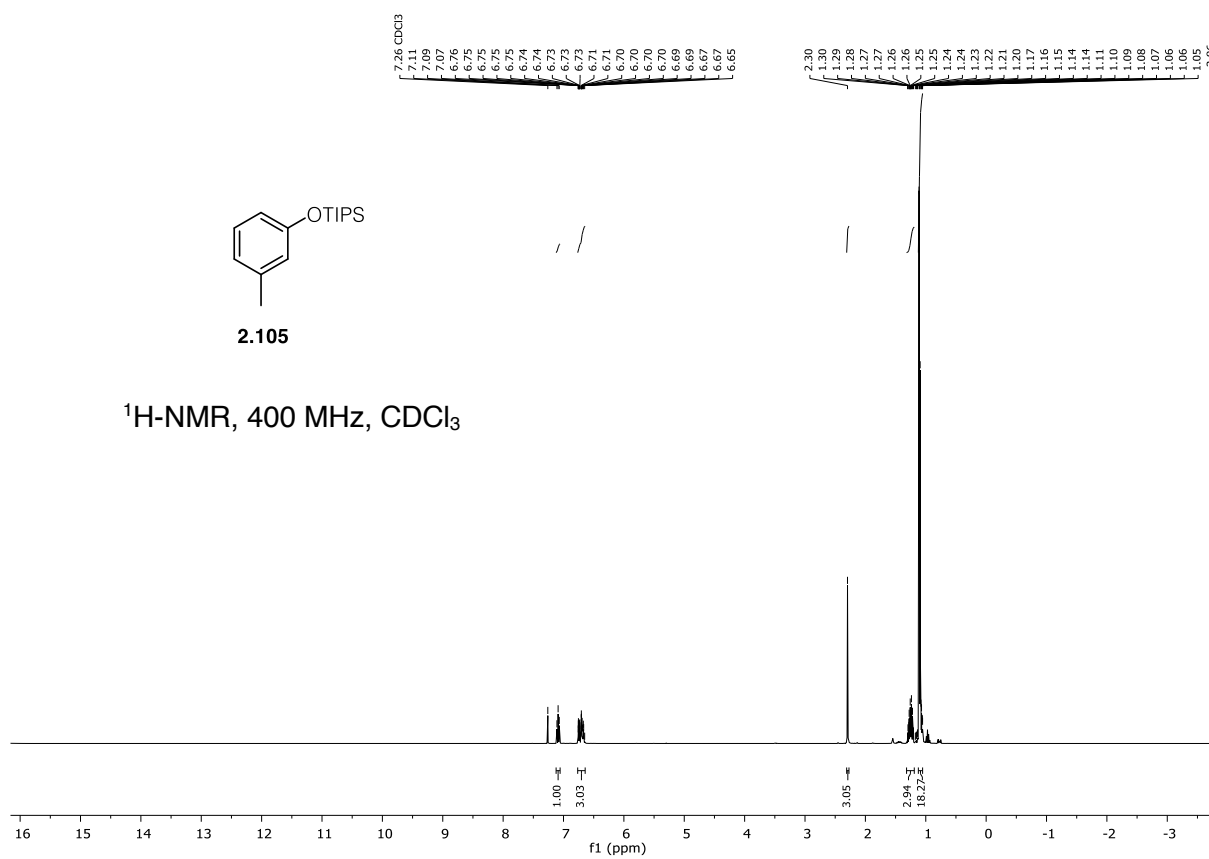


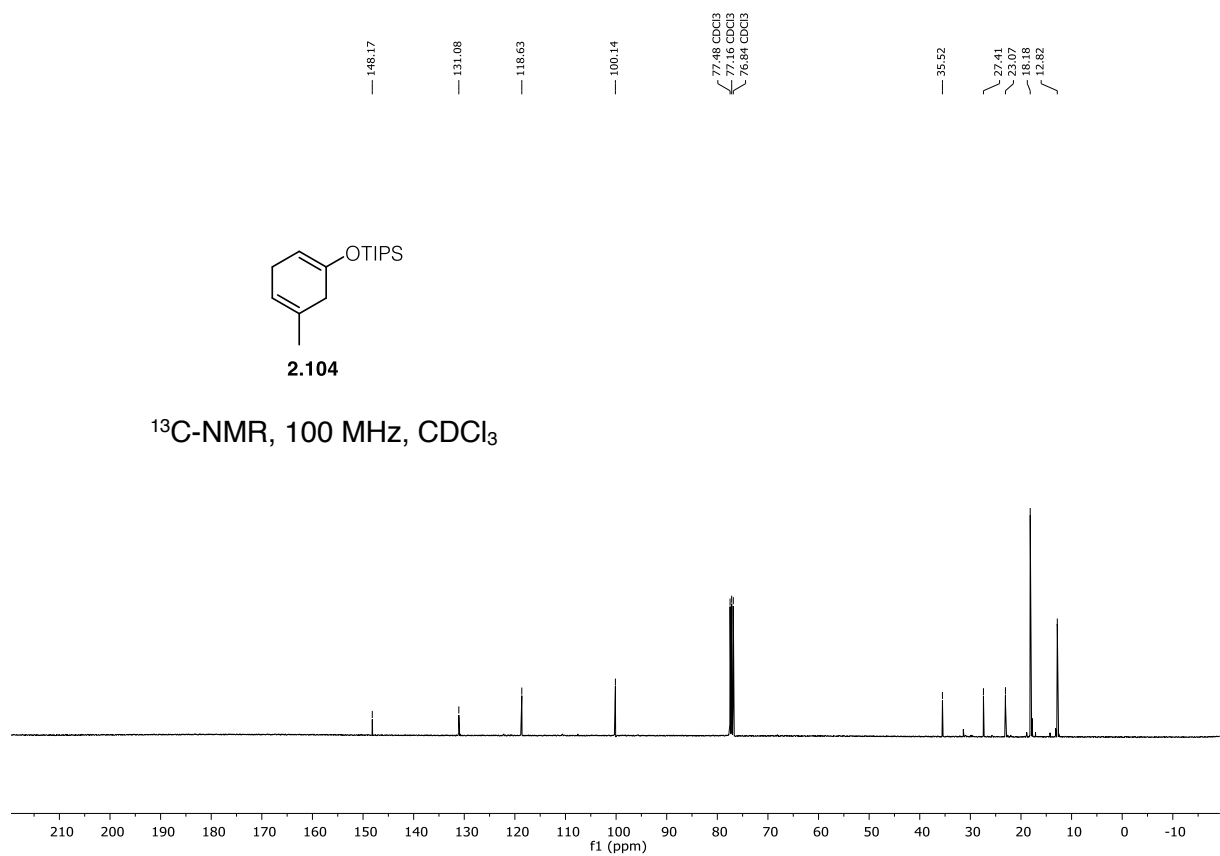
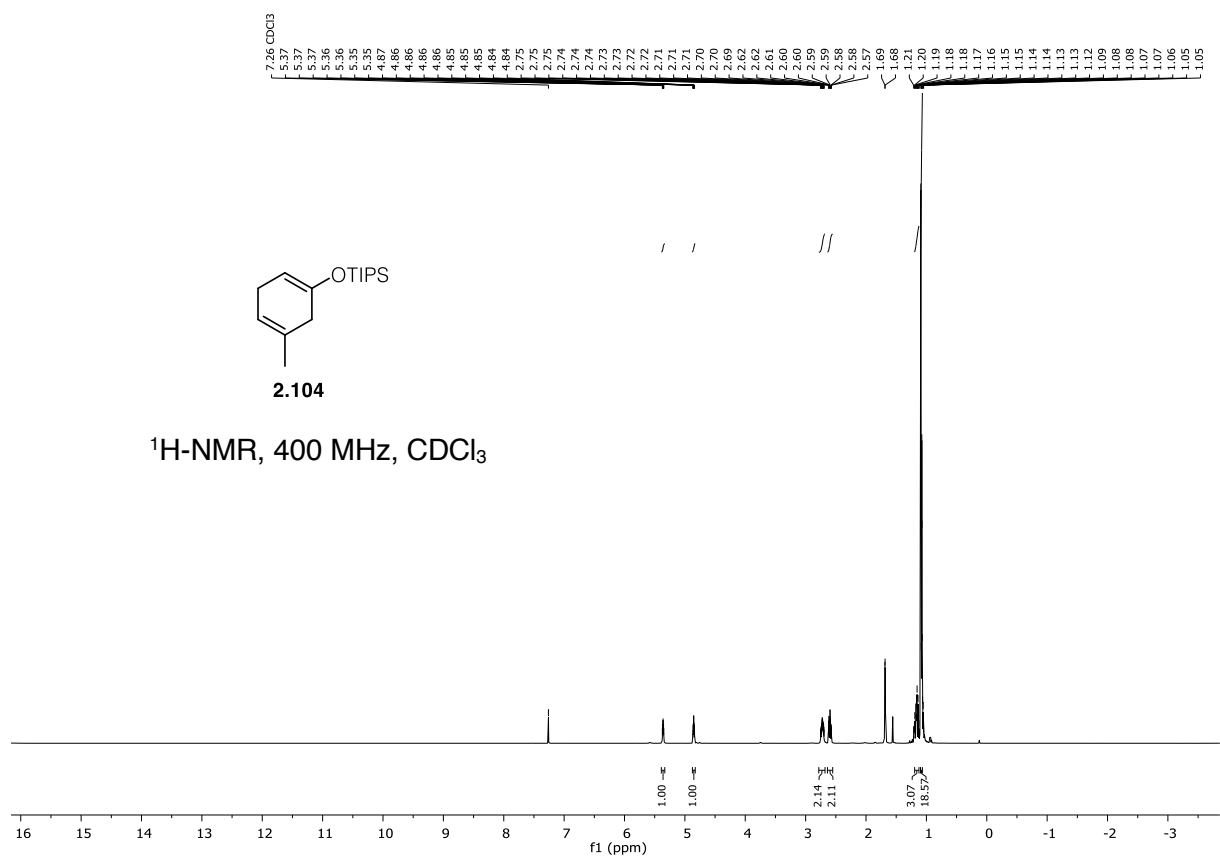


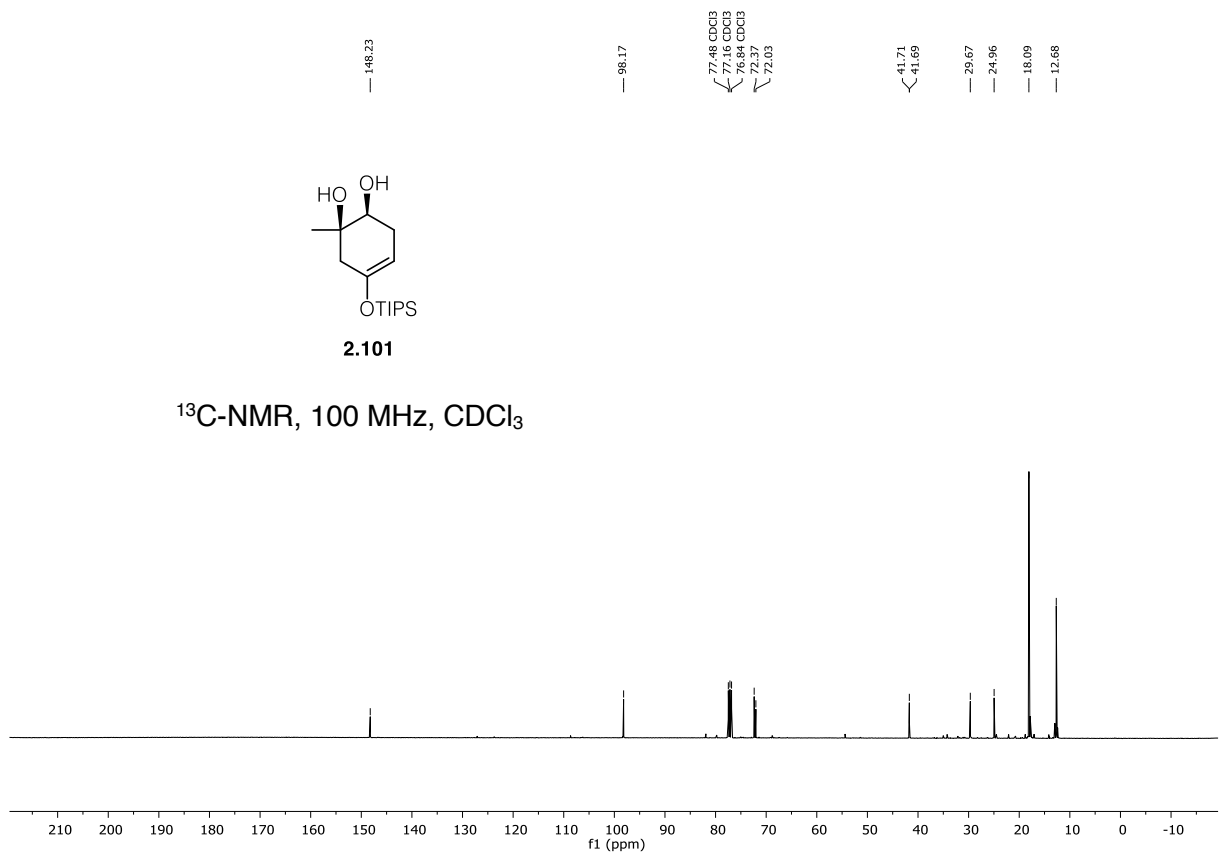
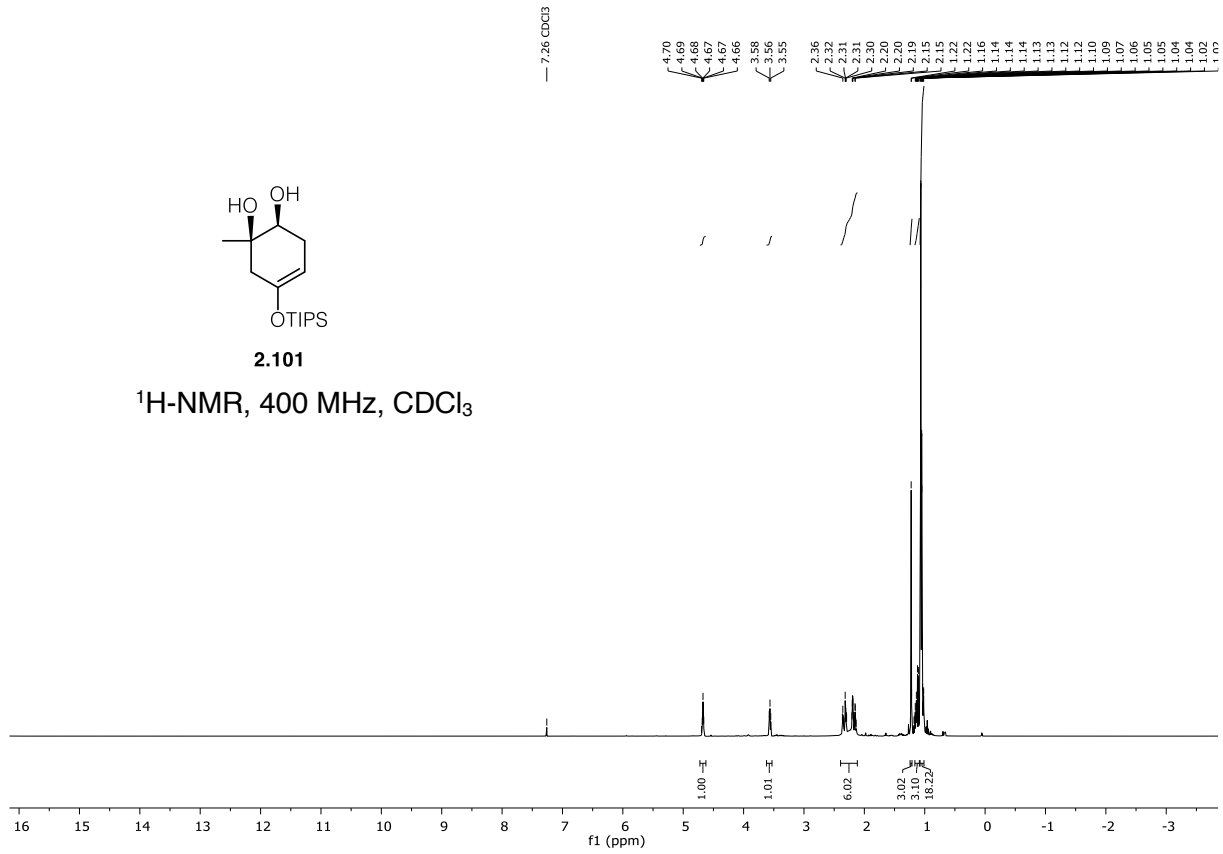


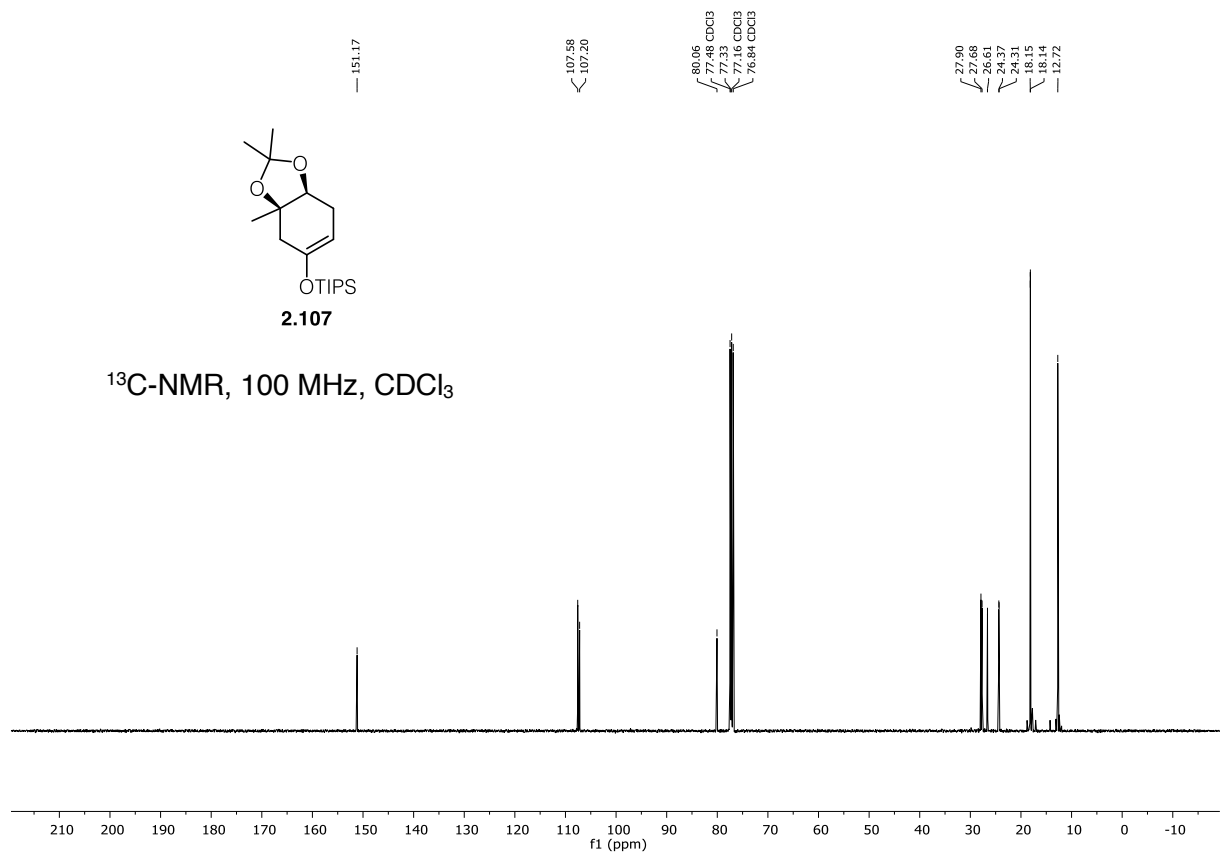
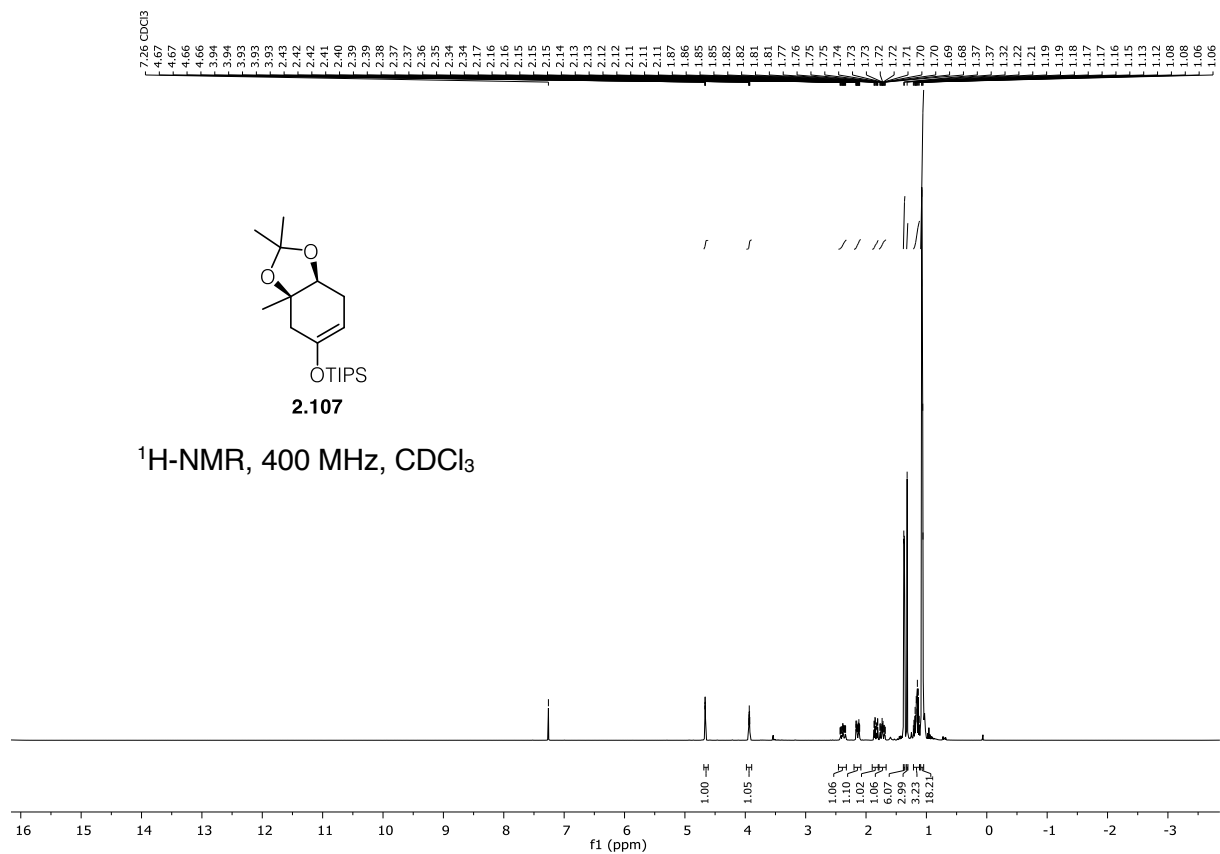


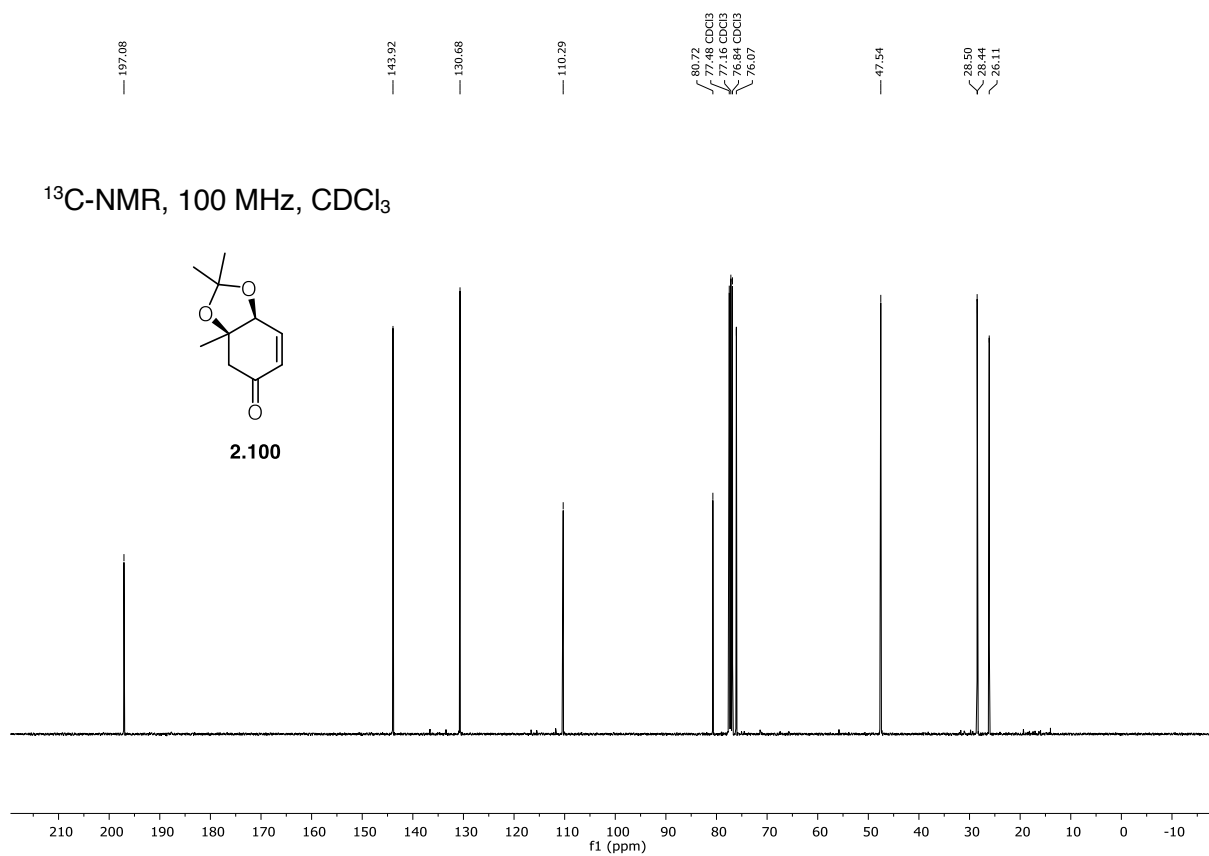
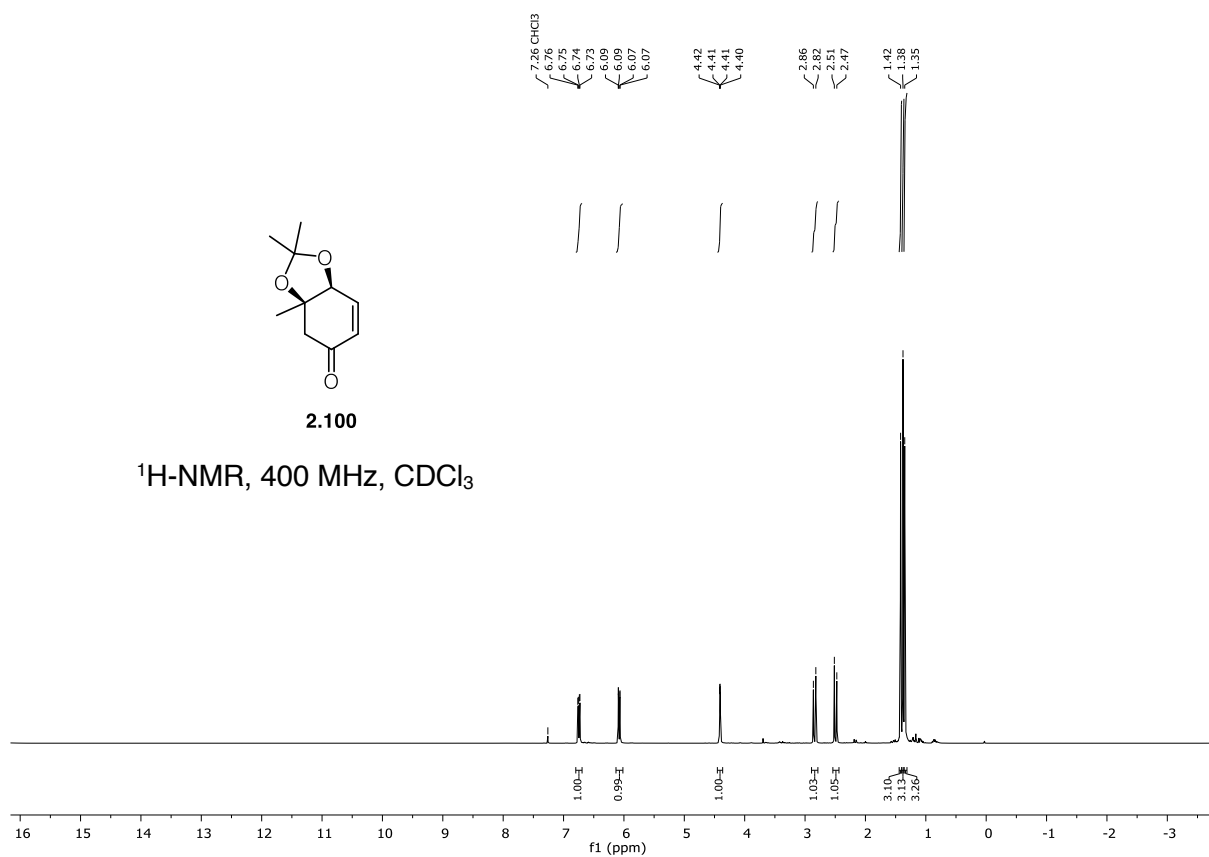


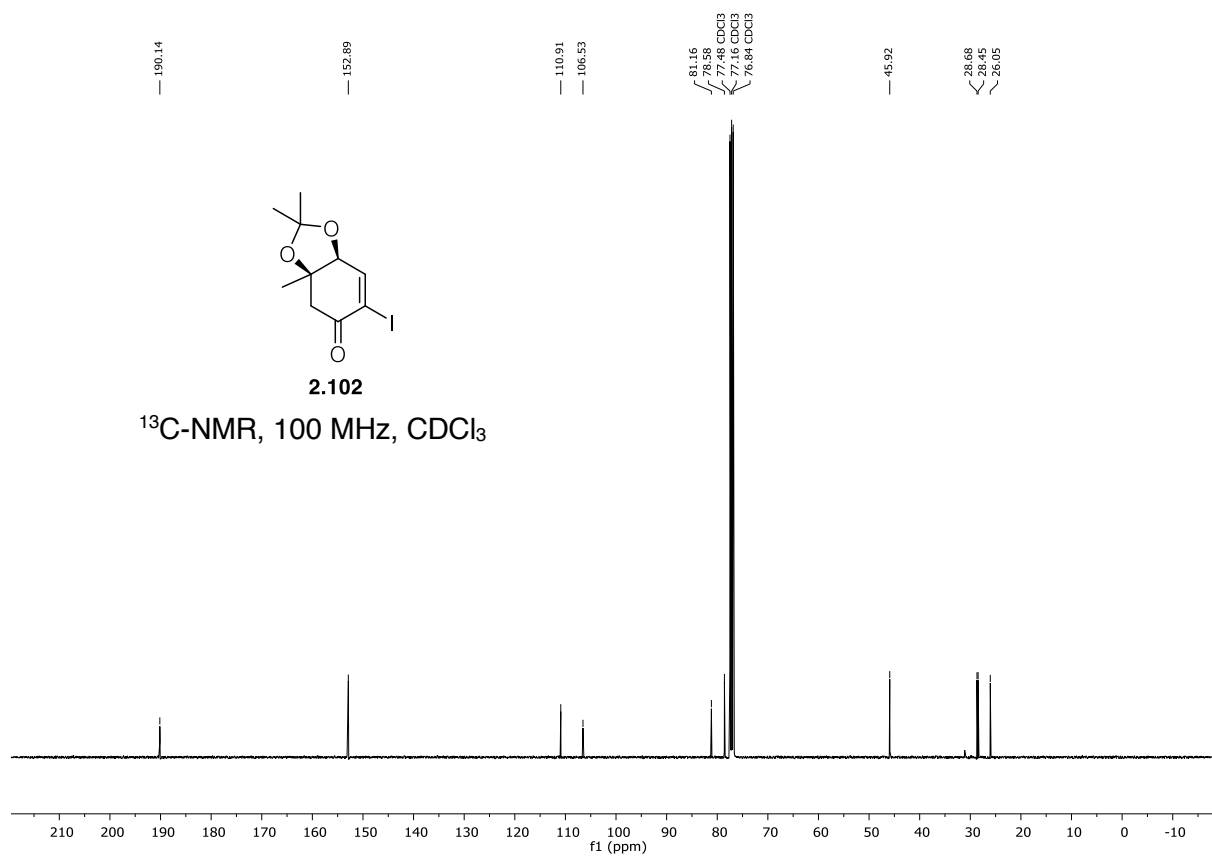
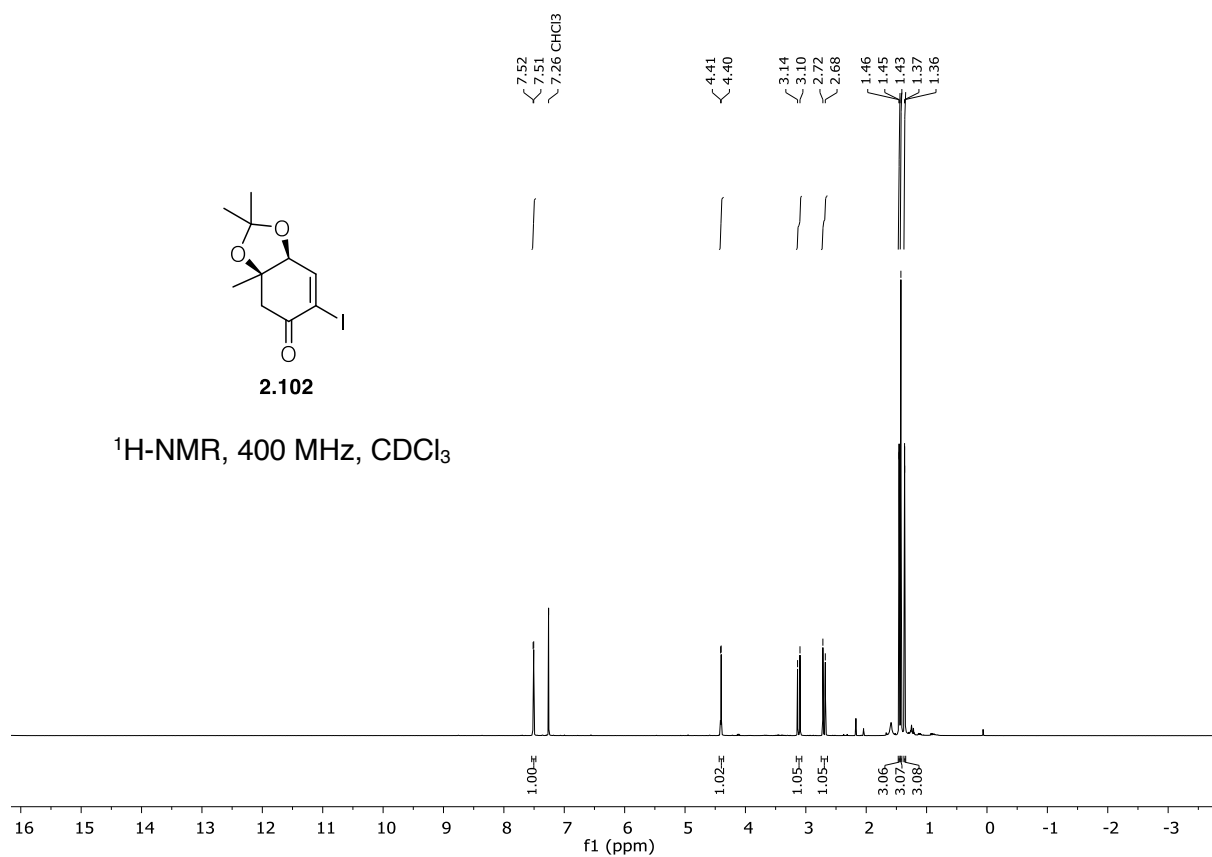
7.2.2 ^1H and ^{13}C NMR spectra of Chapter II

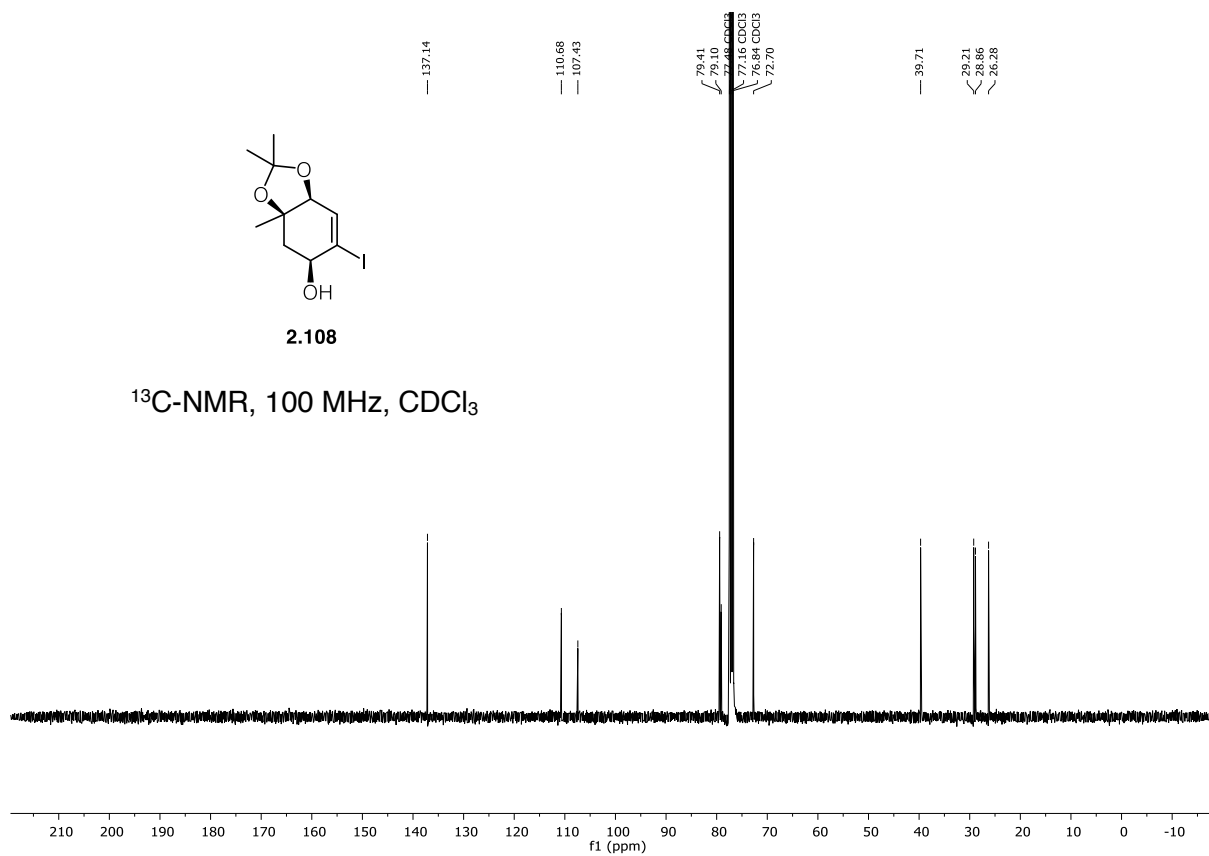
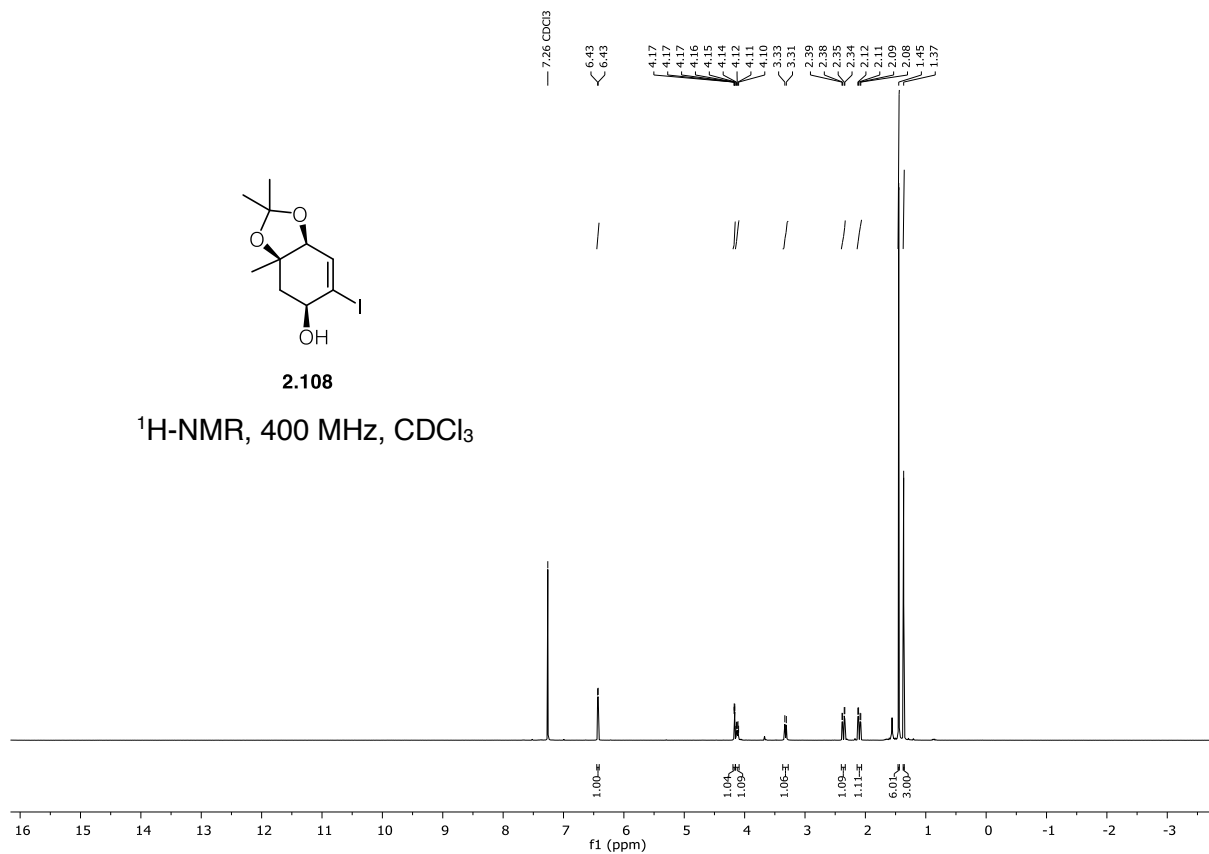


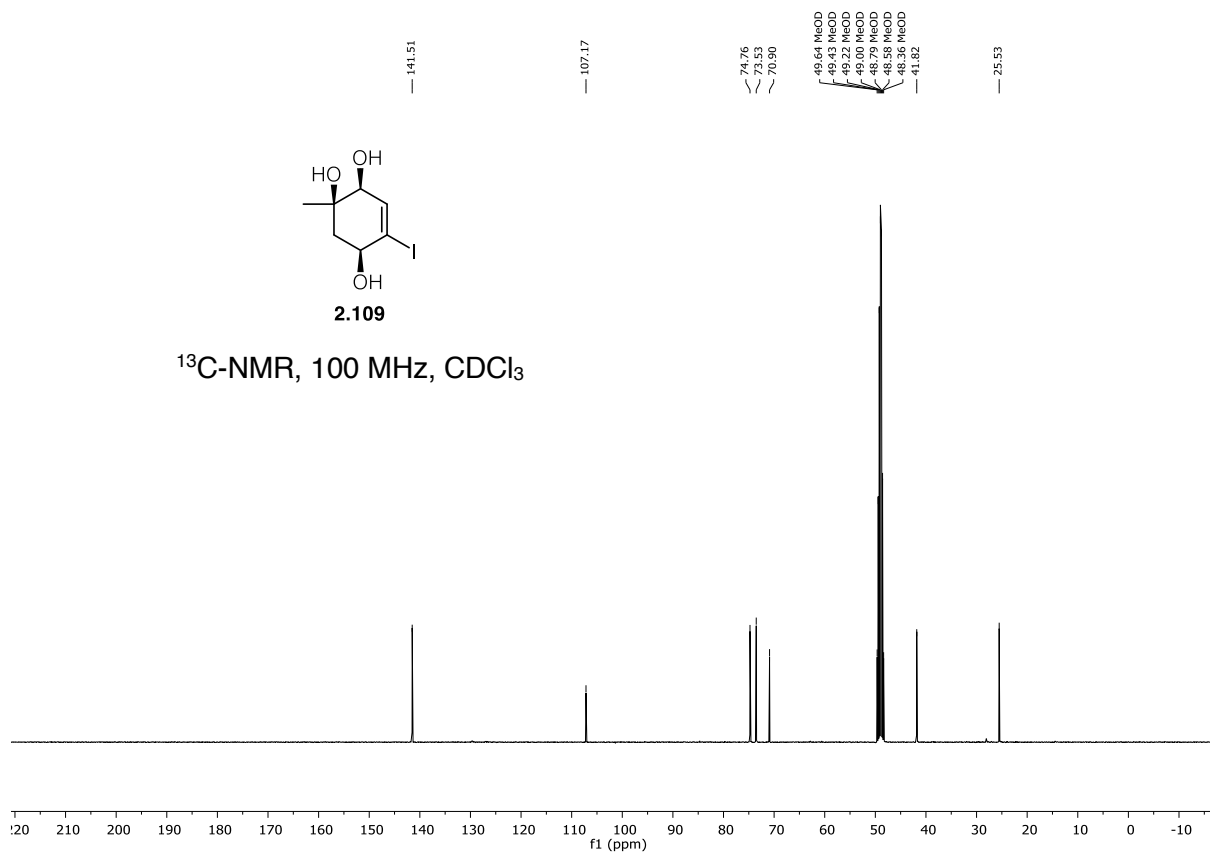
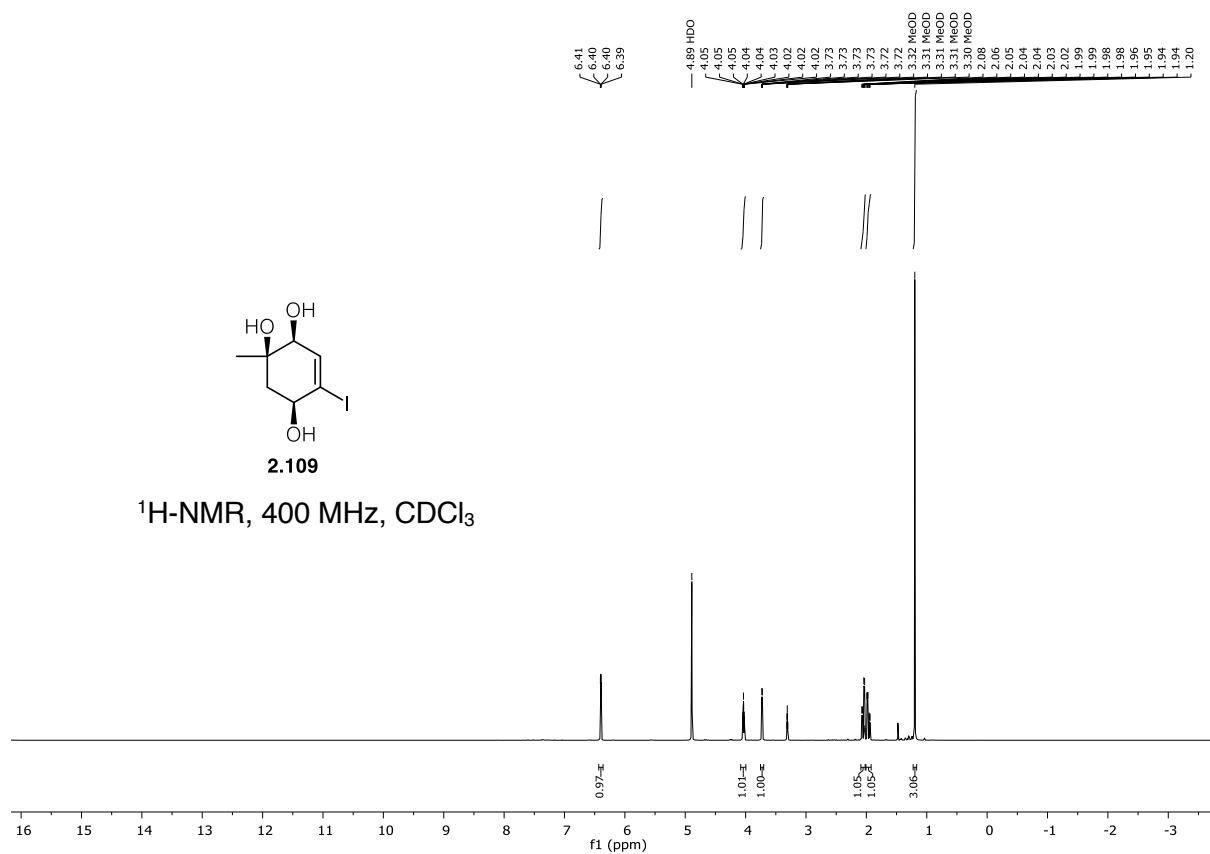


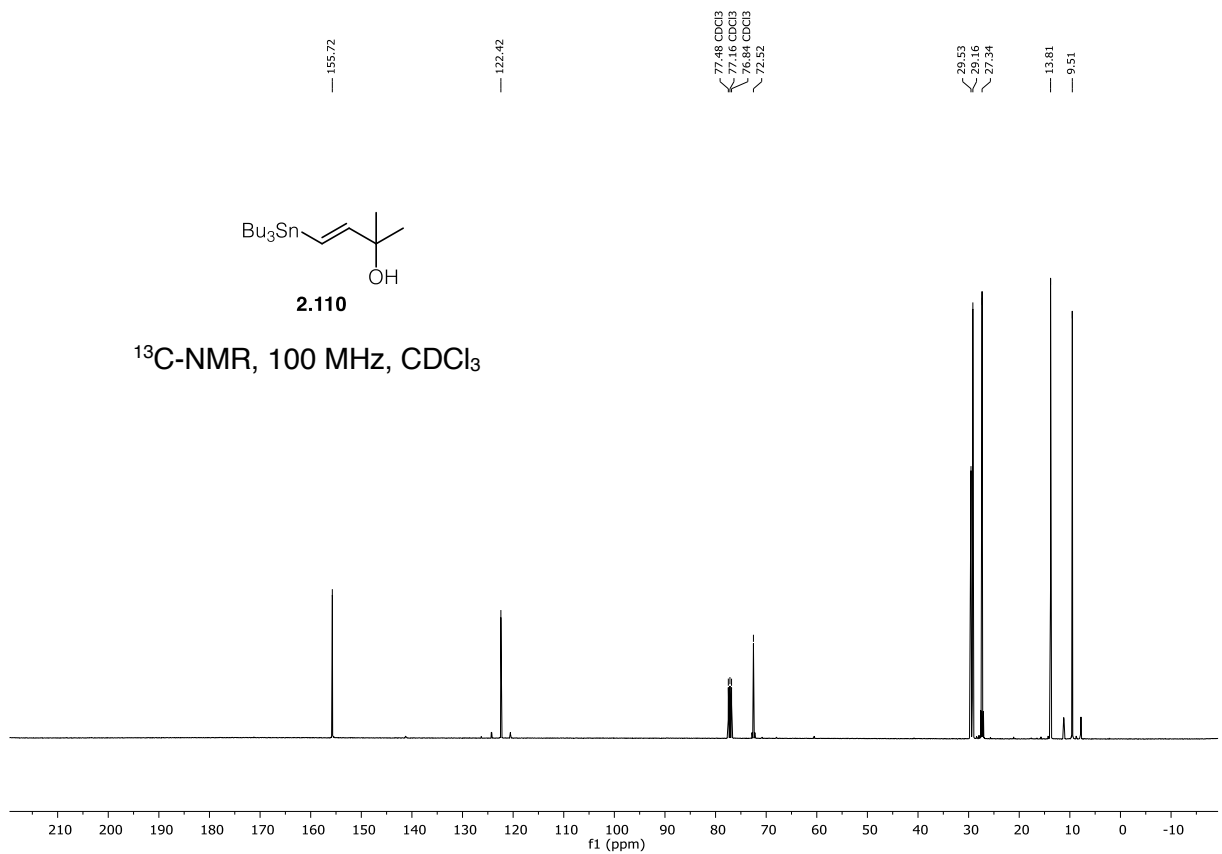
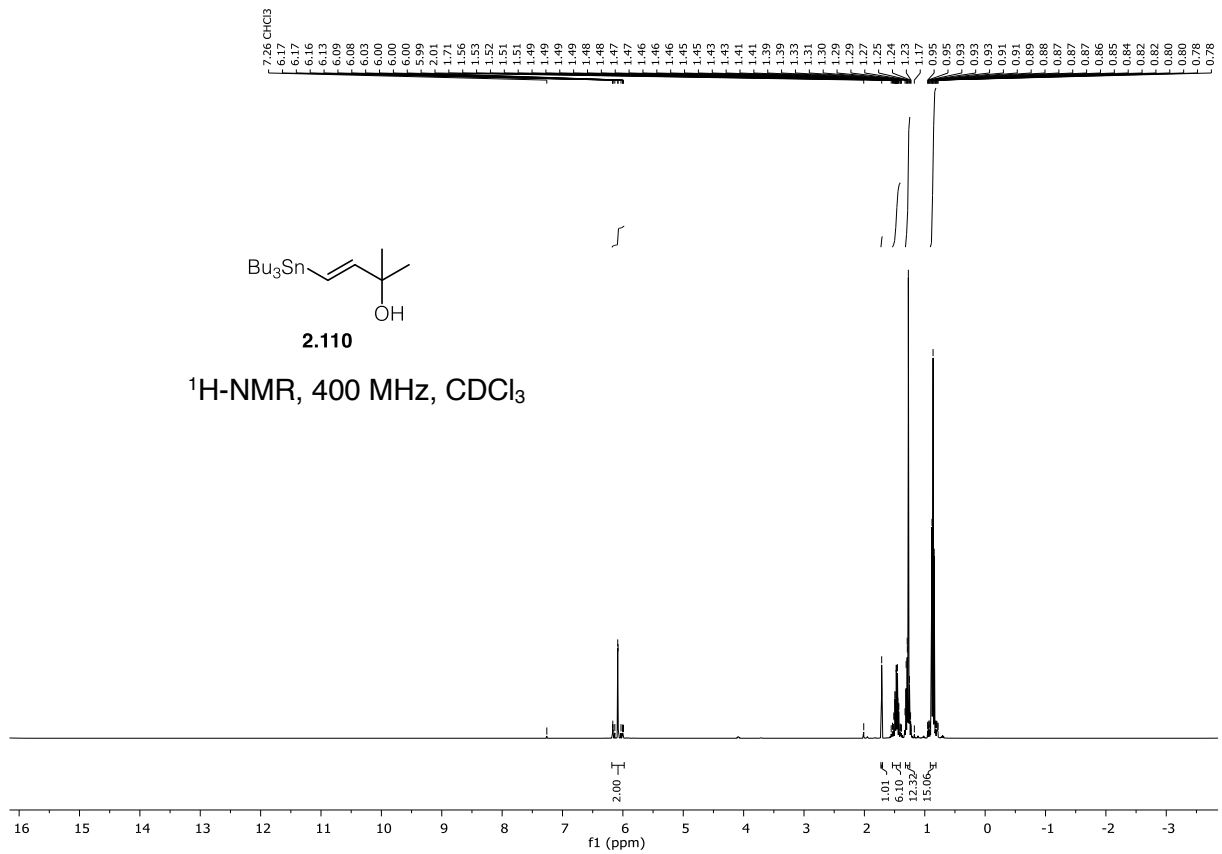


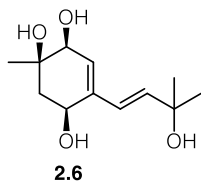




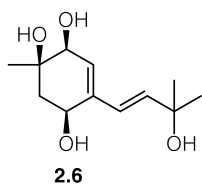
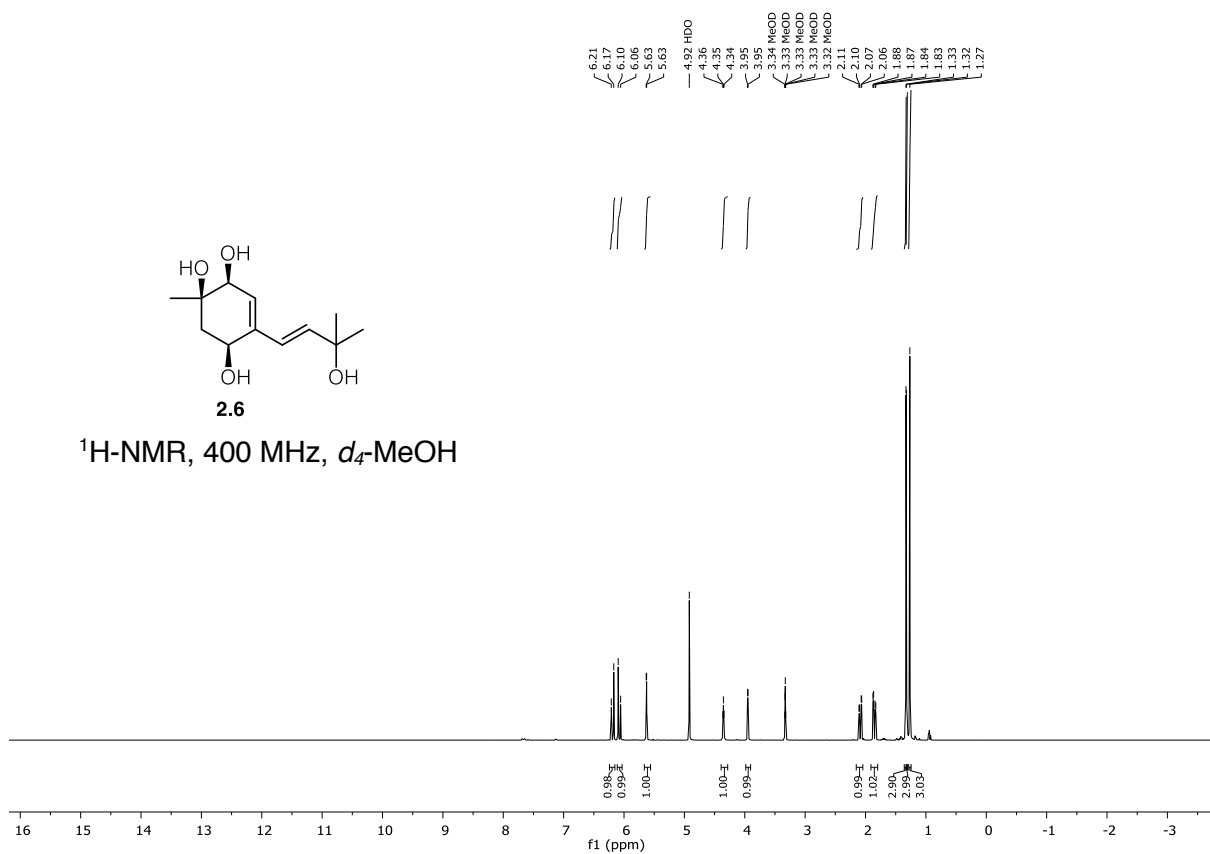




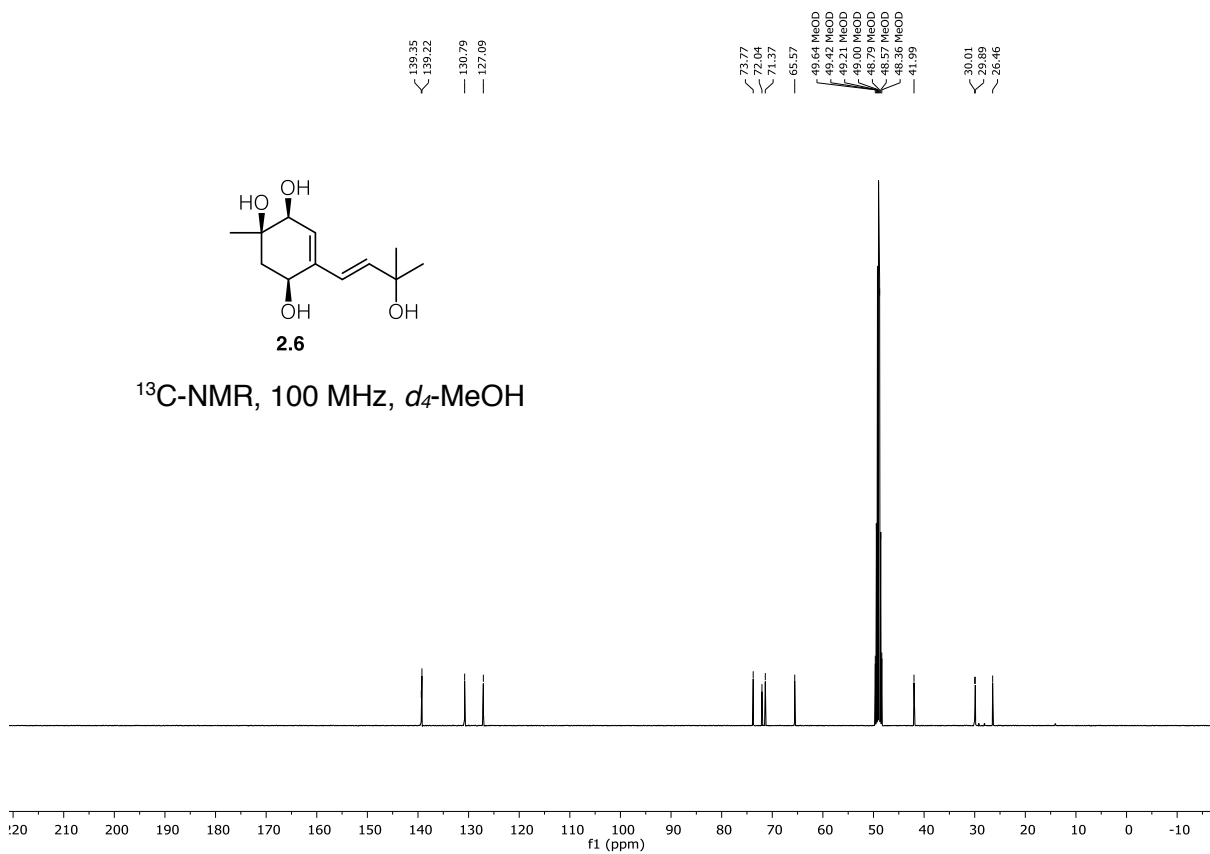


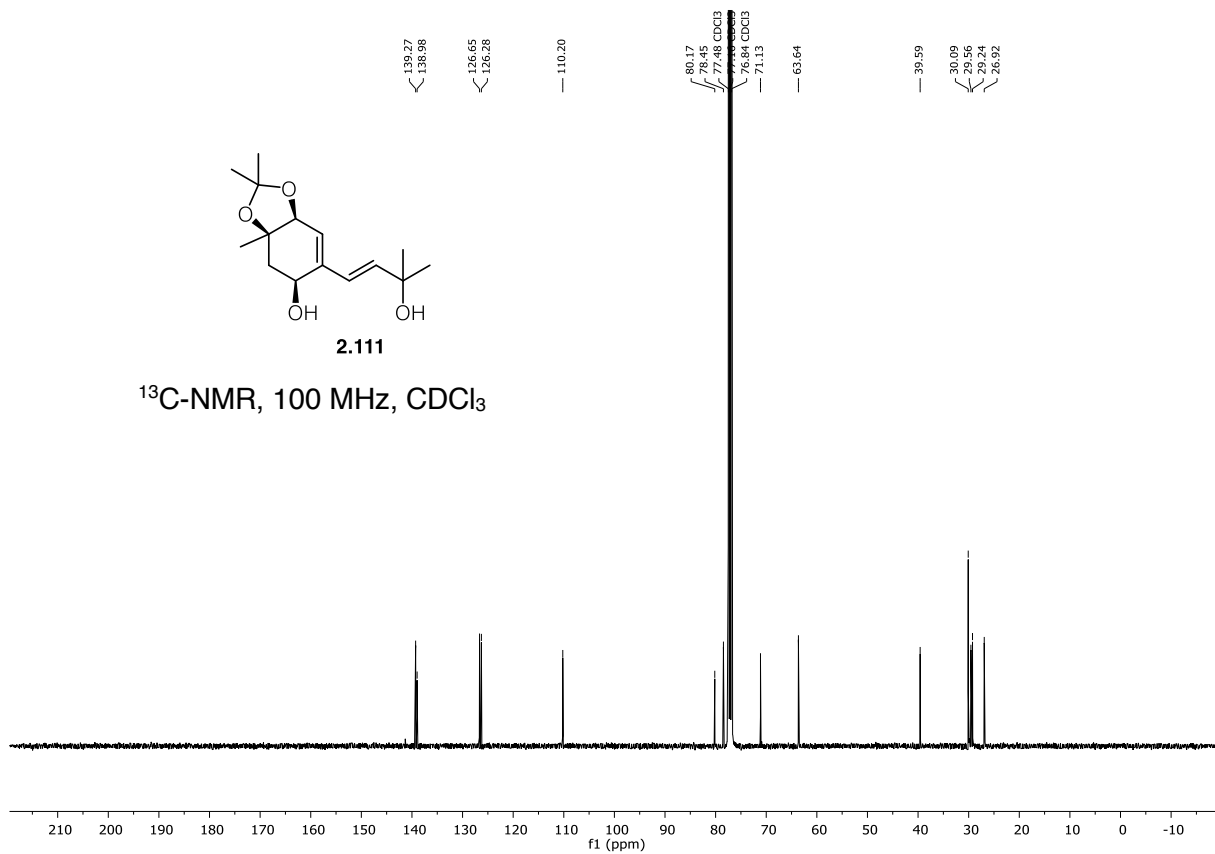
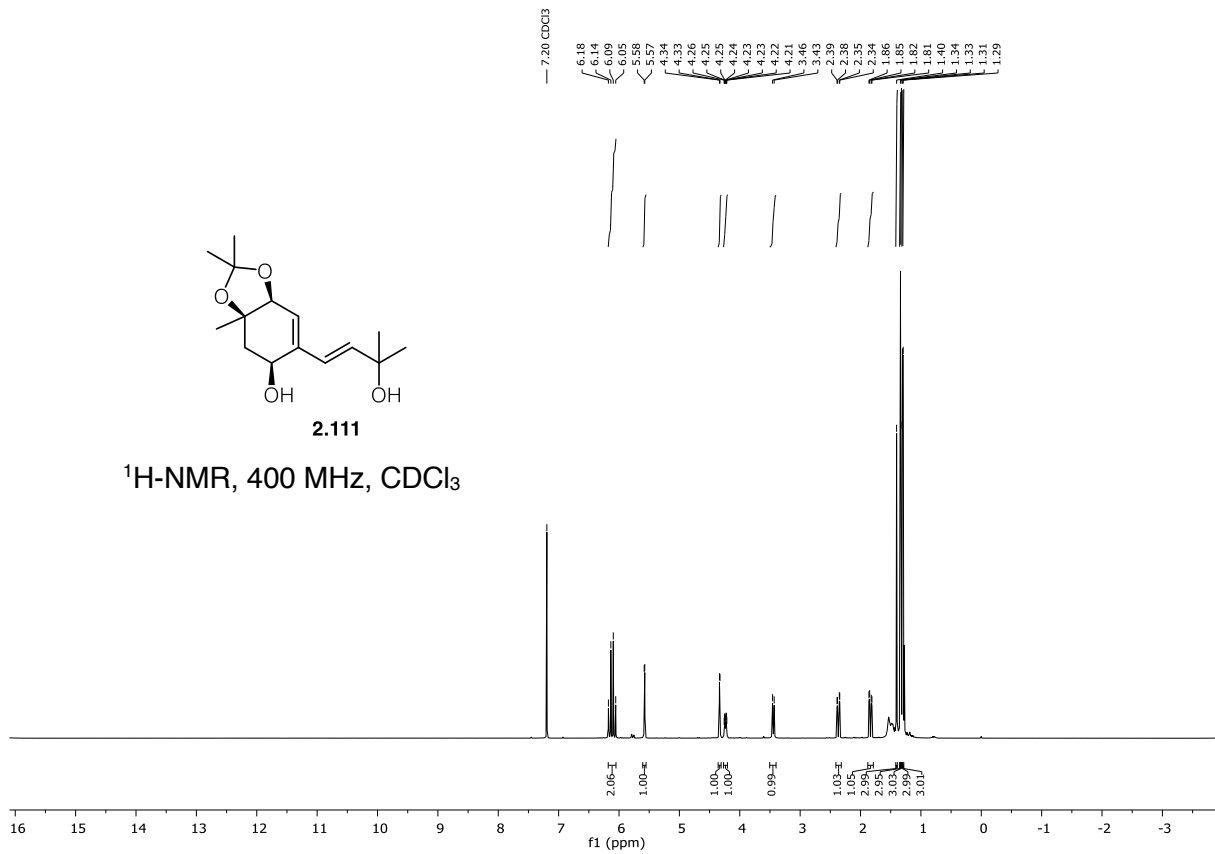


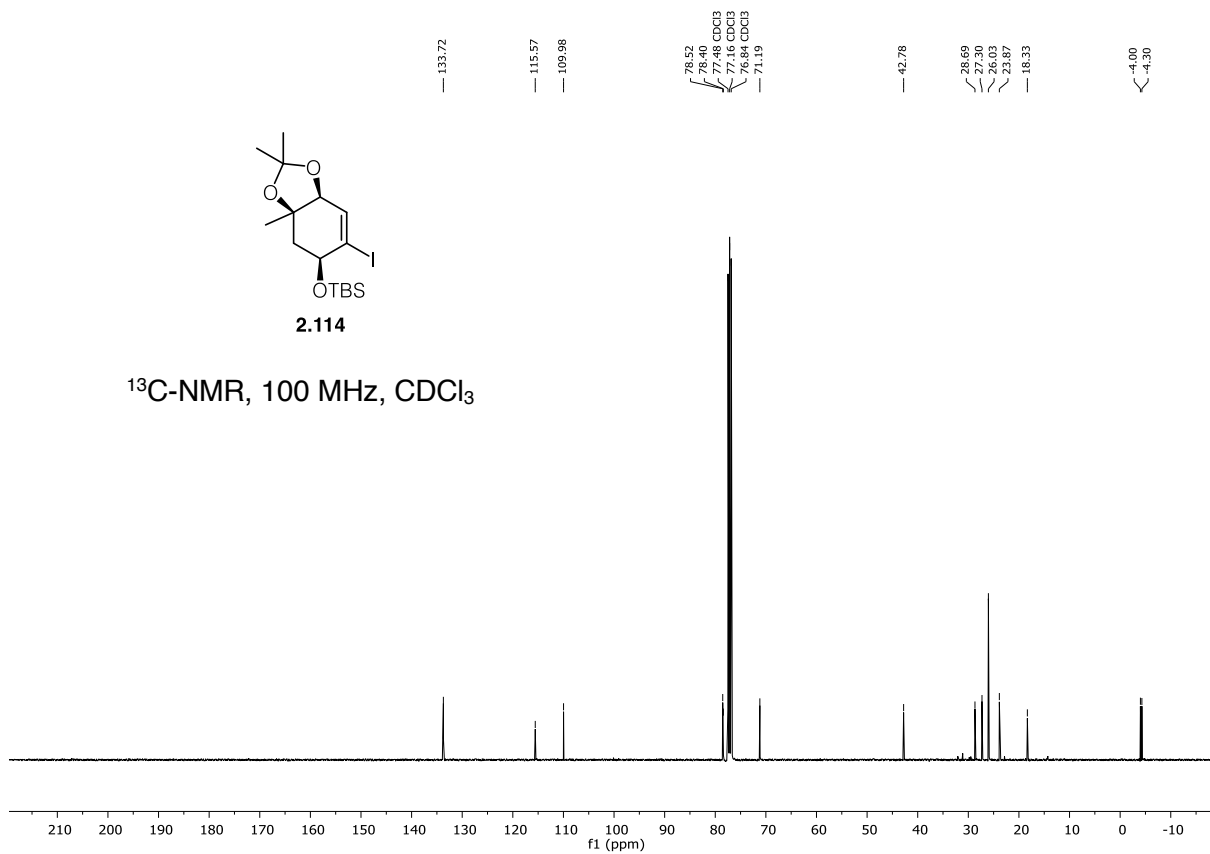
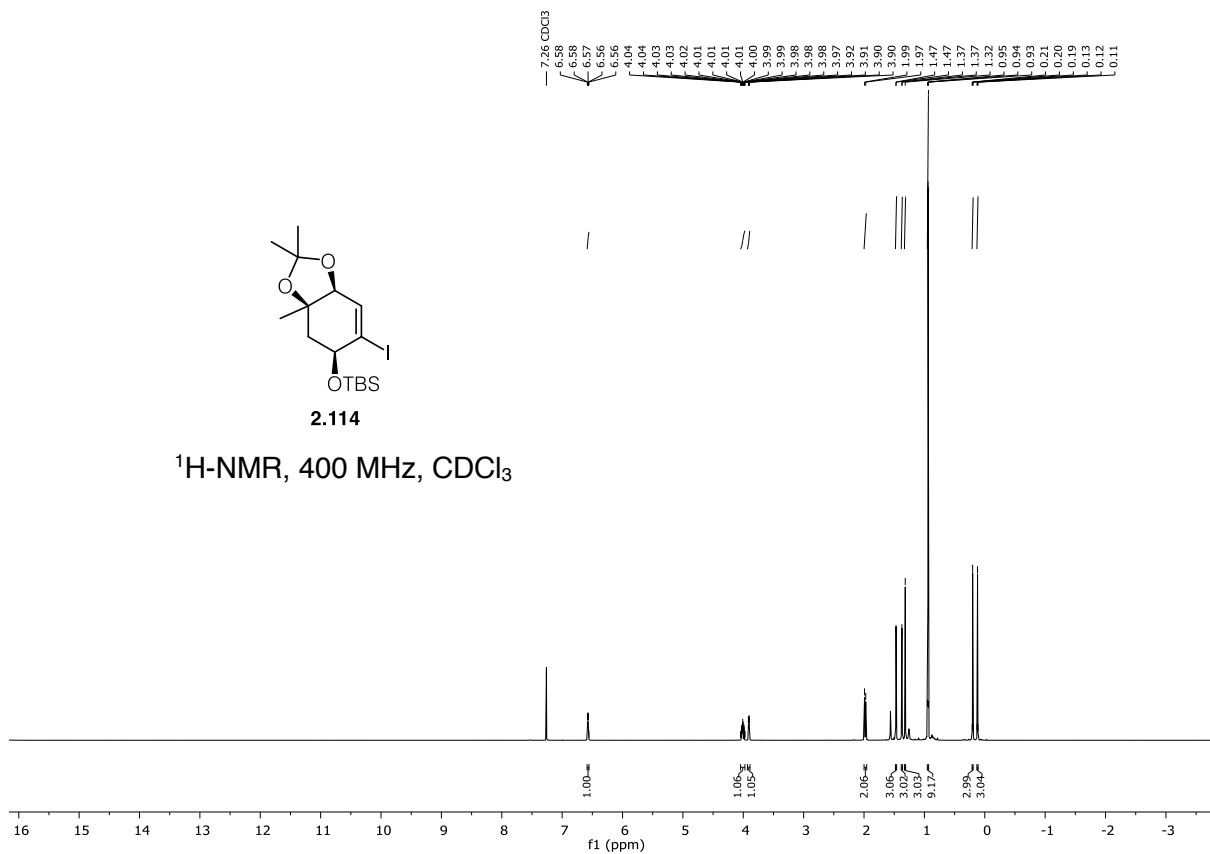
$^1\text{H-NMR}$, 400 MHz, $d_4\text{-MeOH}$

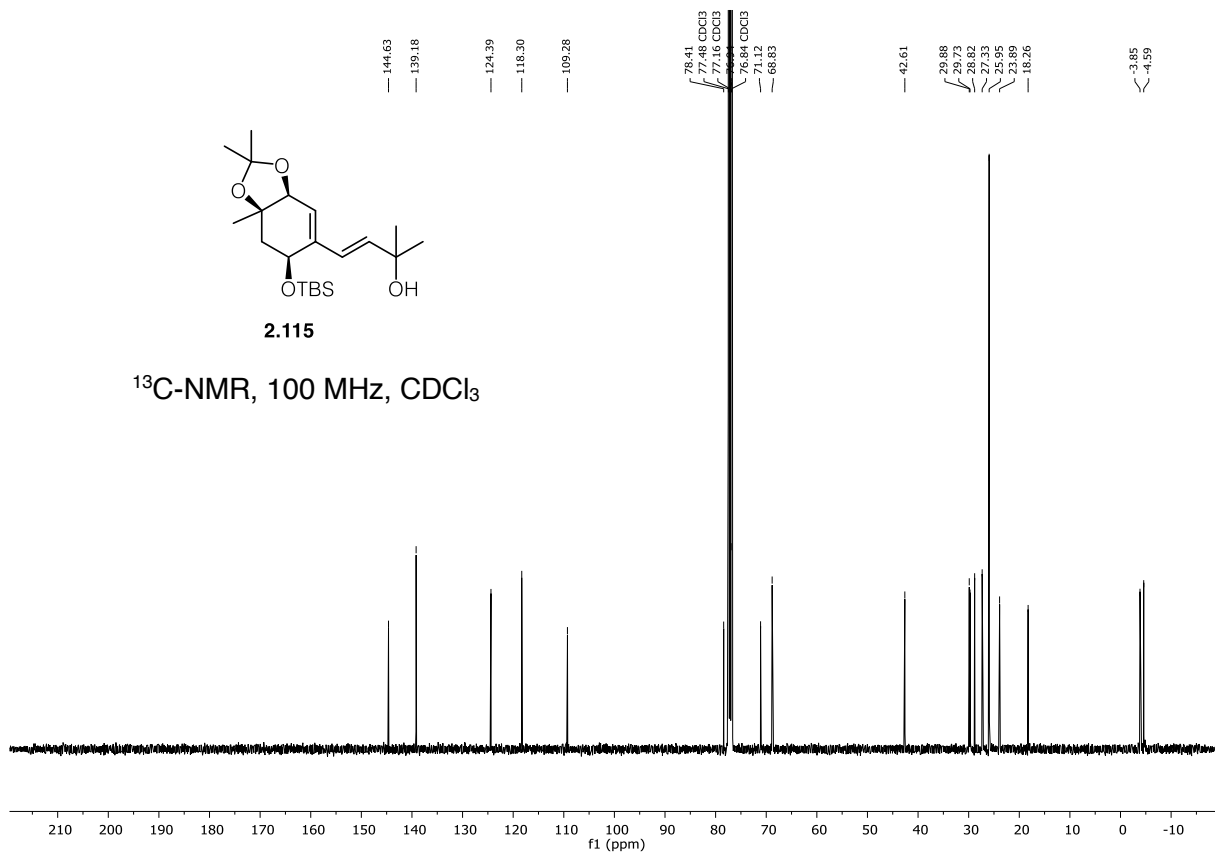
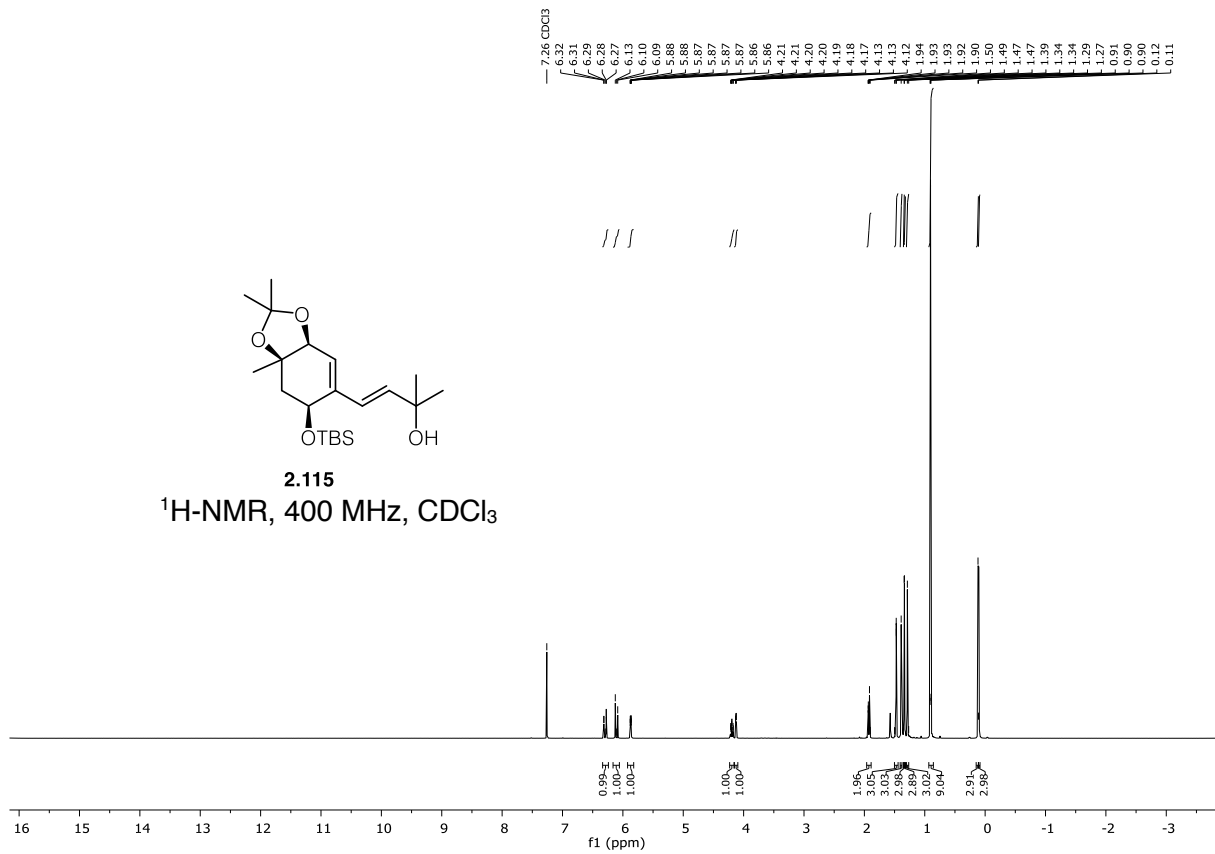


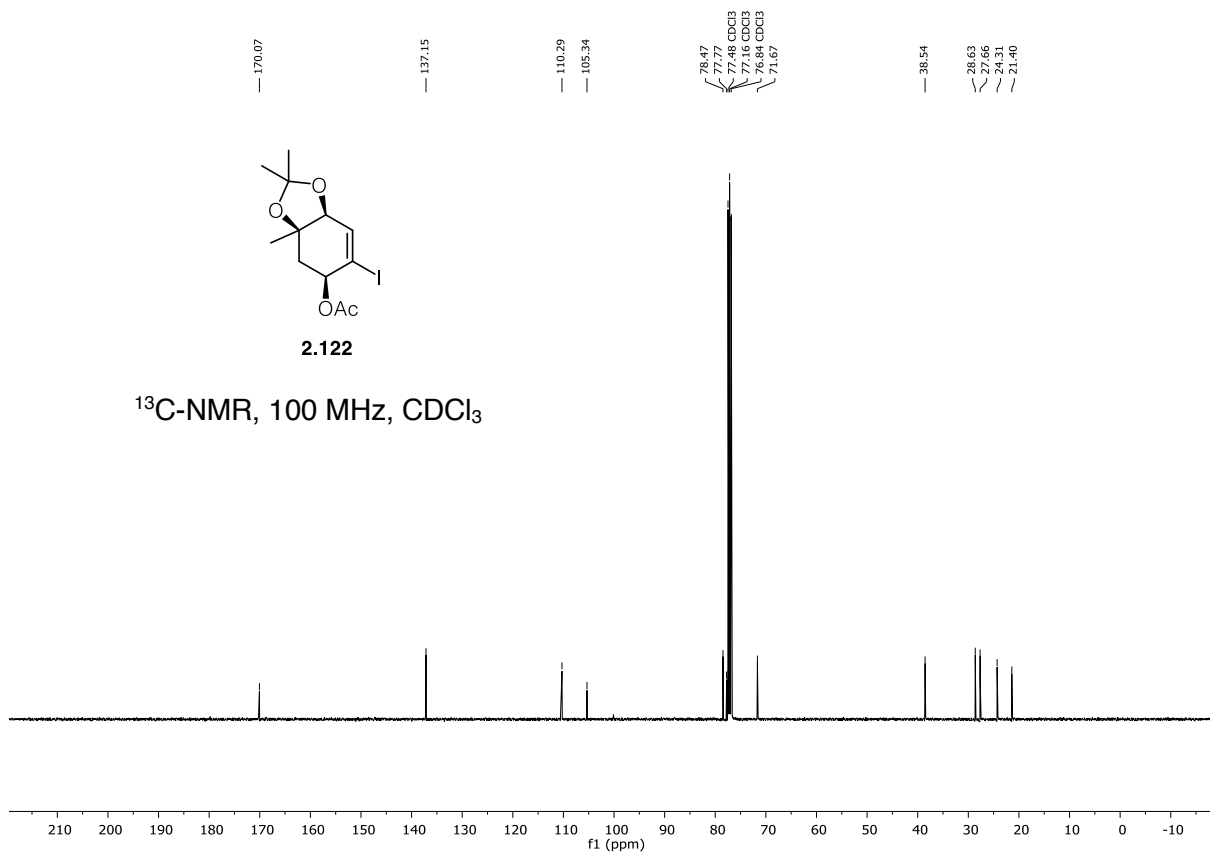
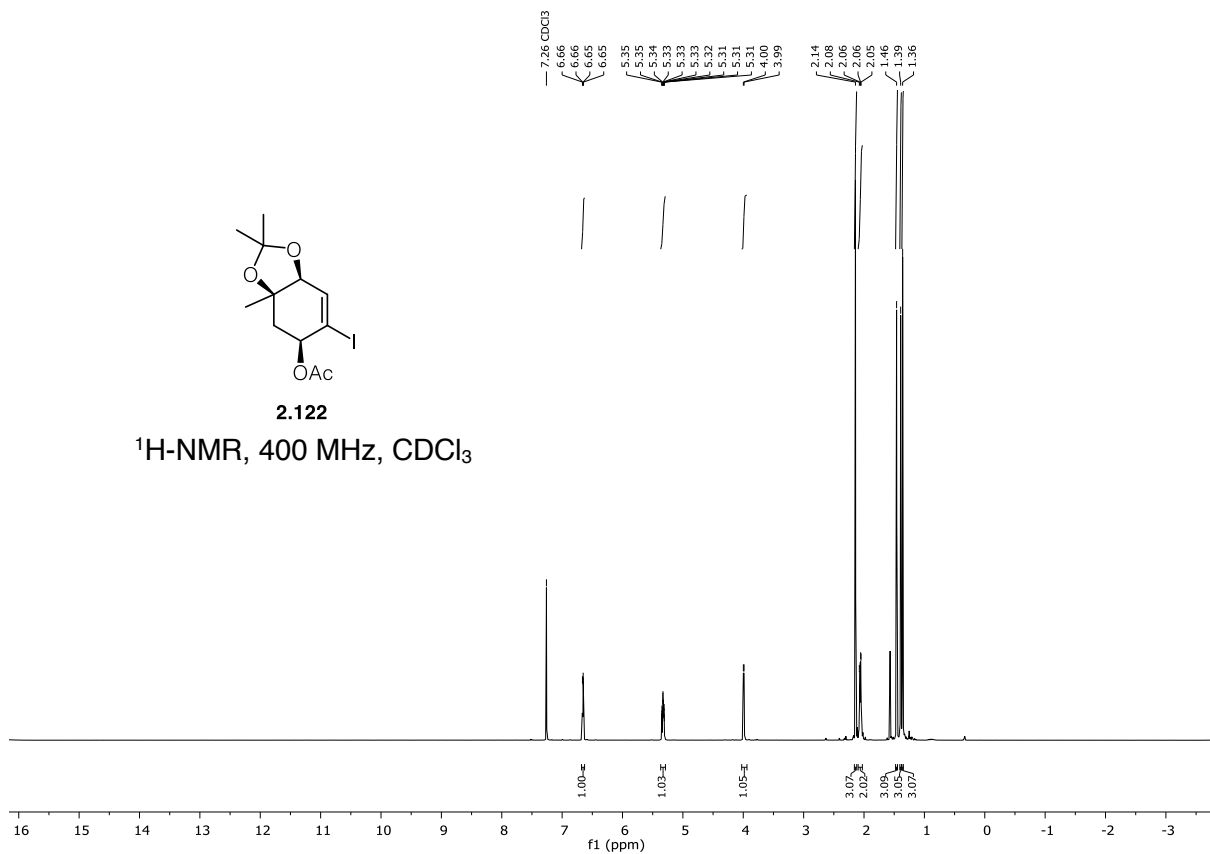
$^{13}\text{C-NMR}$, 100 MHz, $d_4\text{-MeOH}$

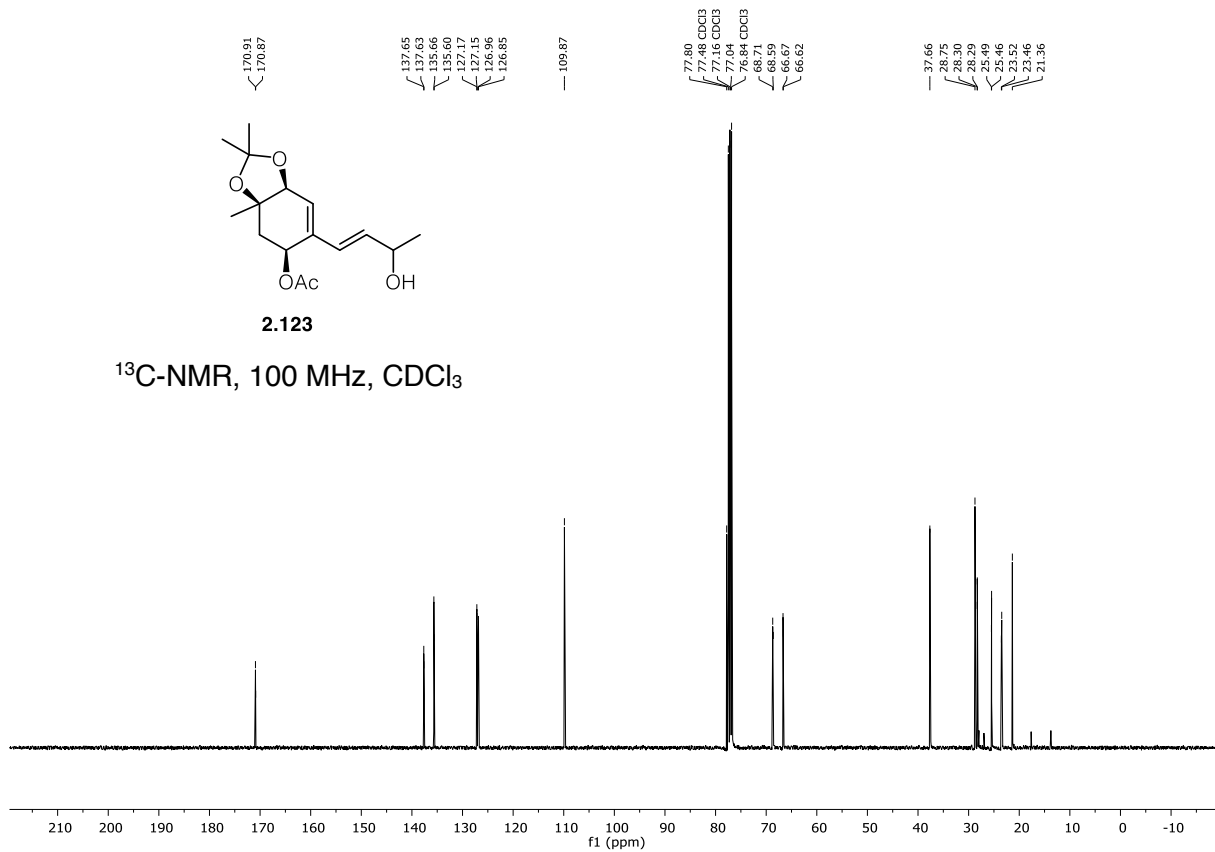
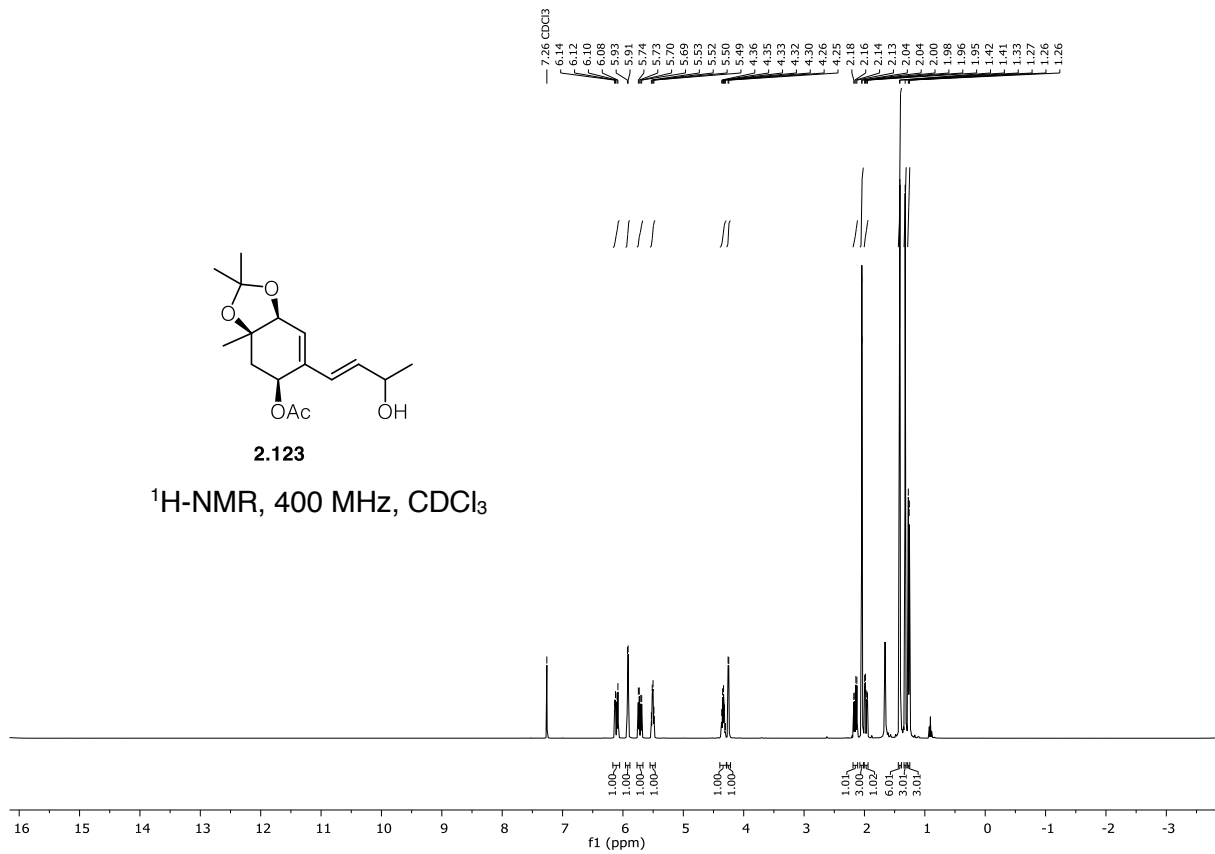


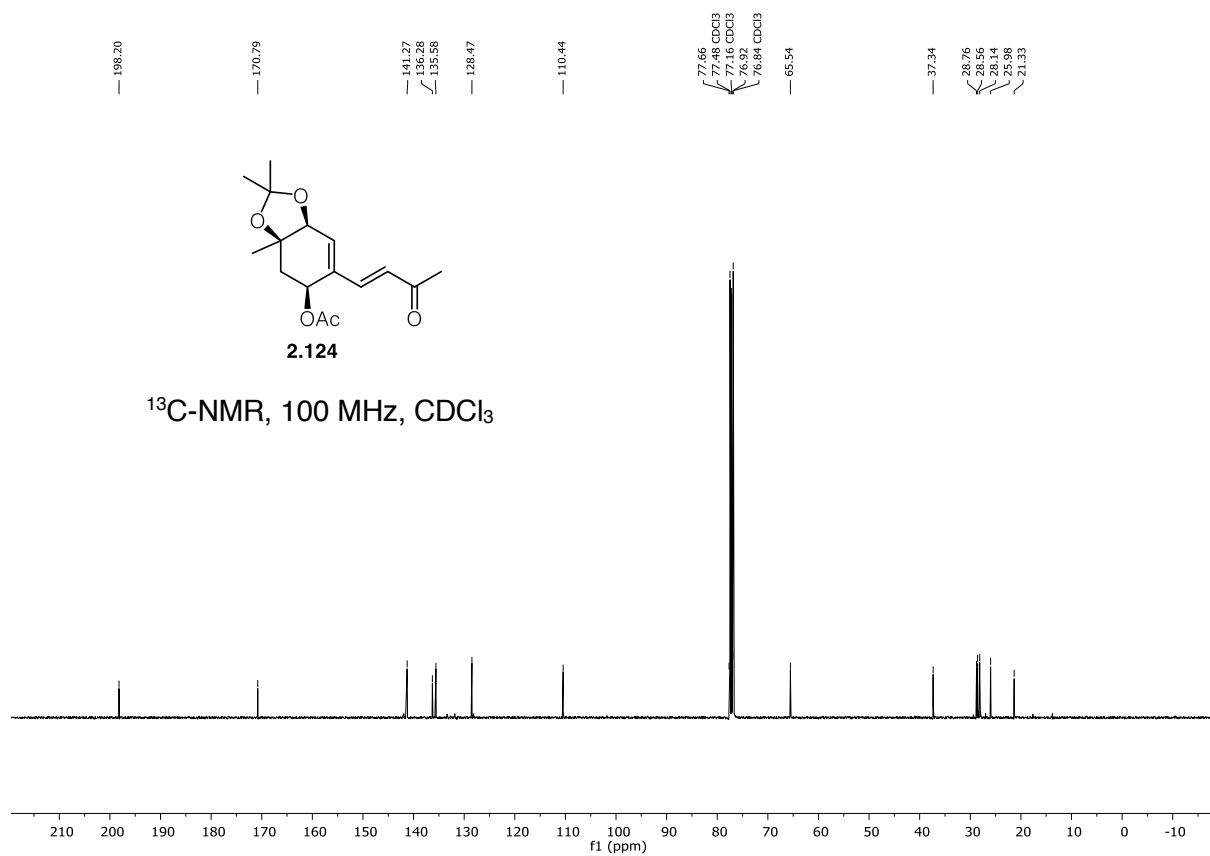
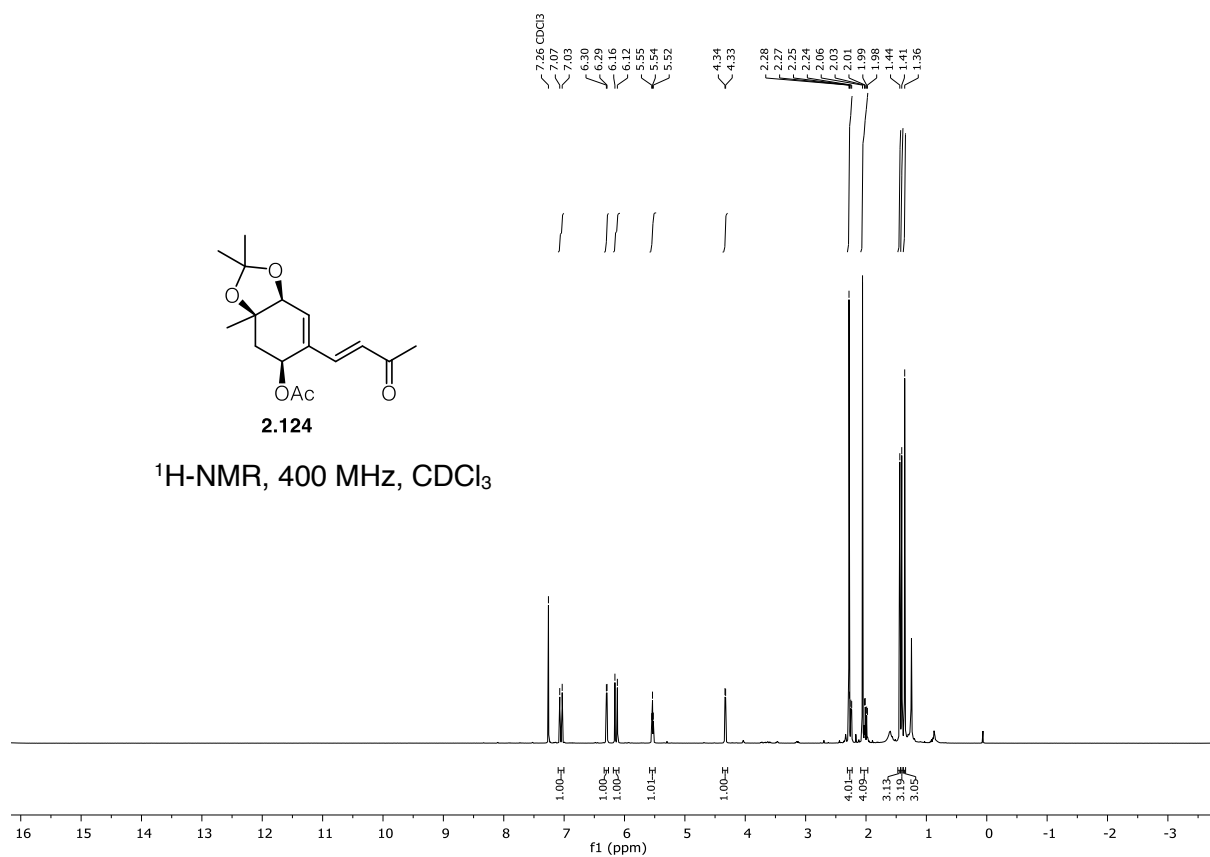


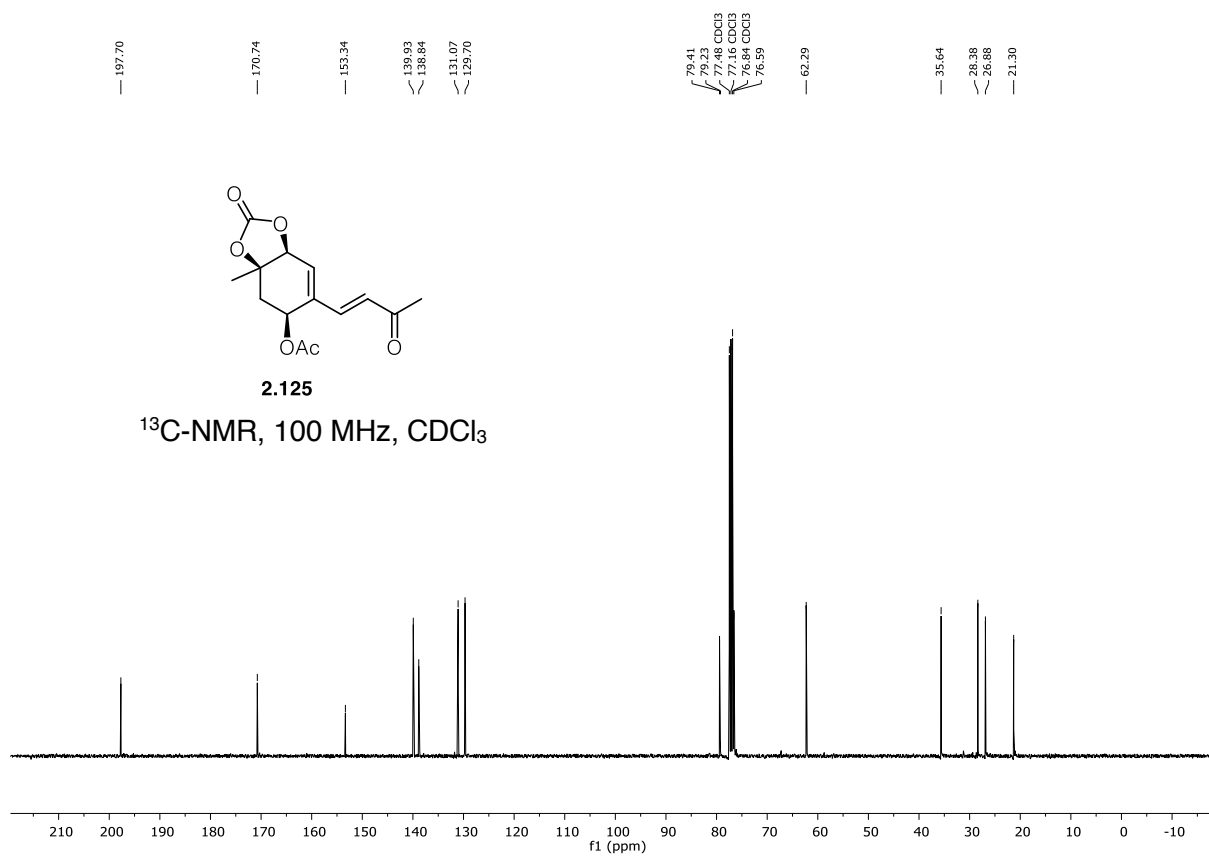
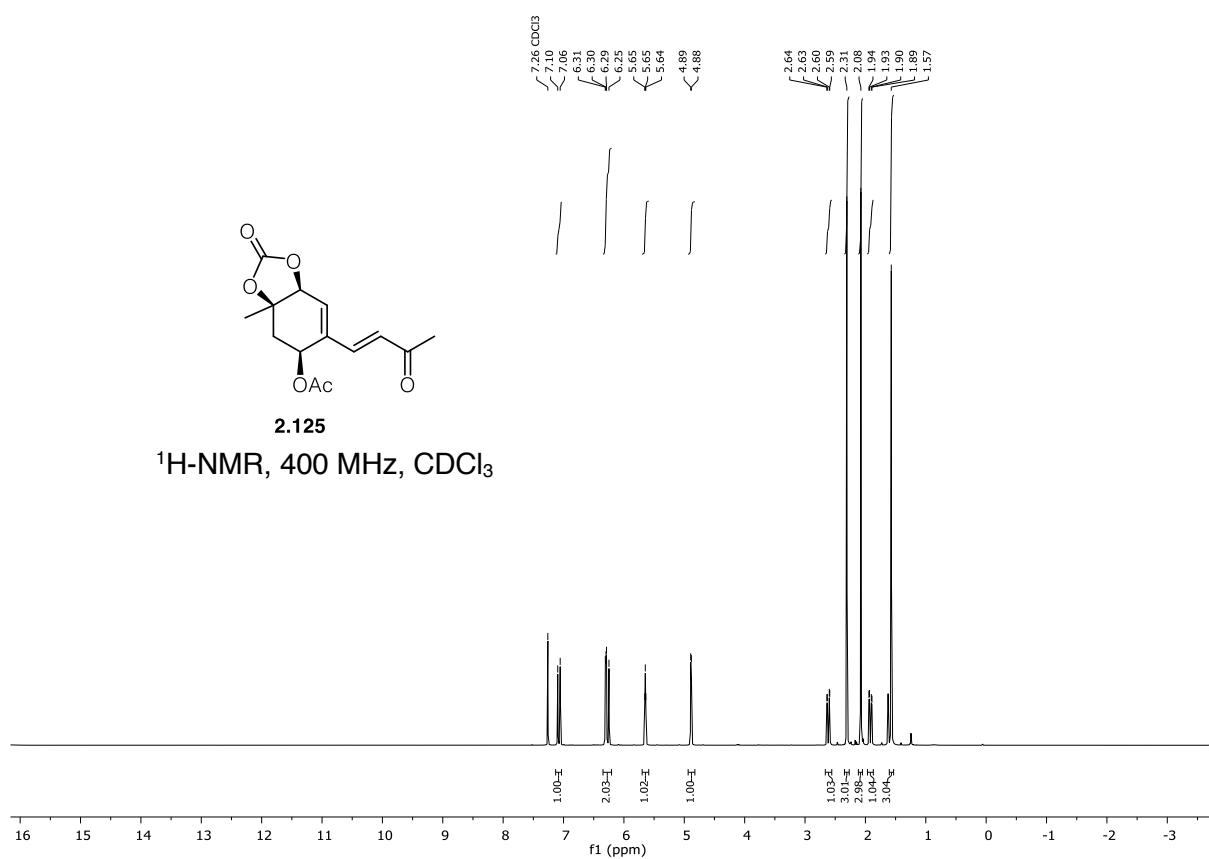


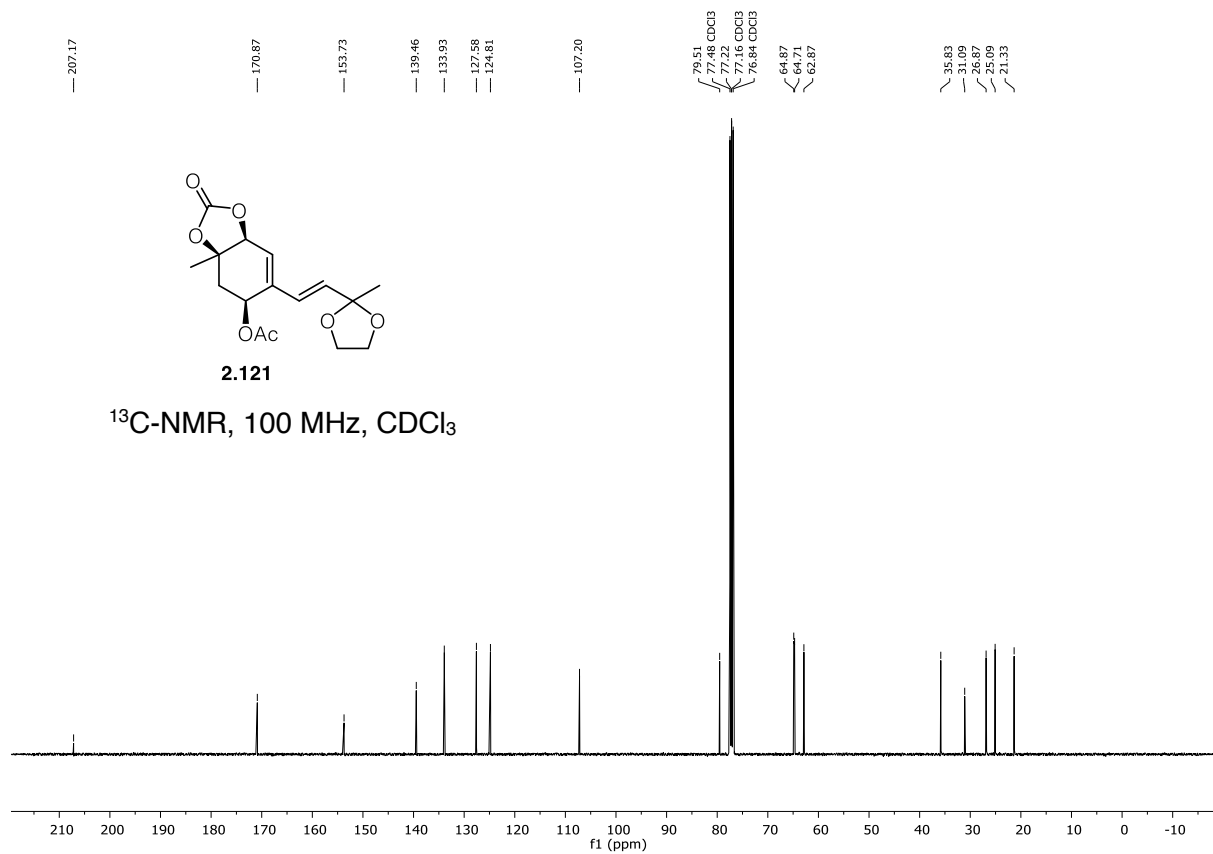
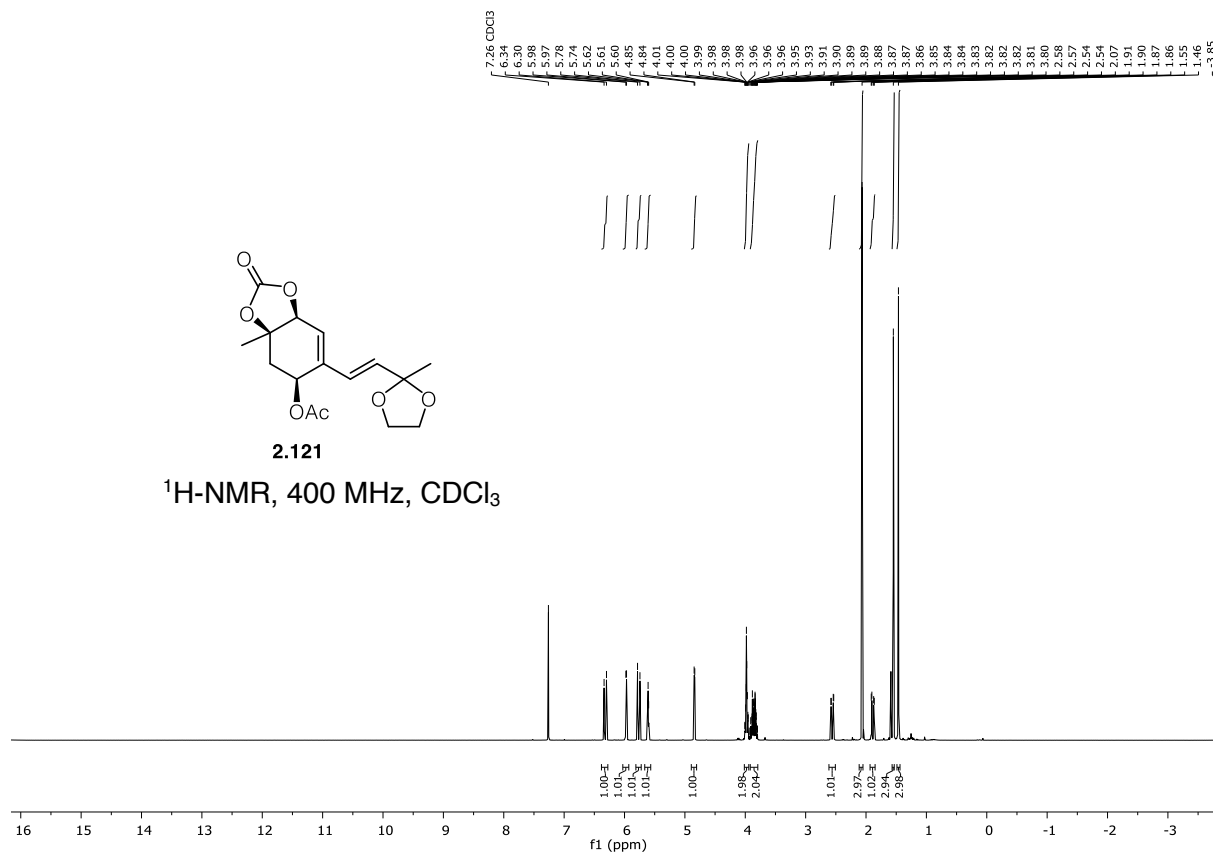


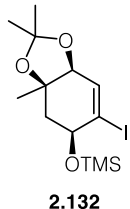




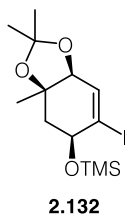
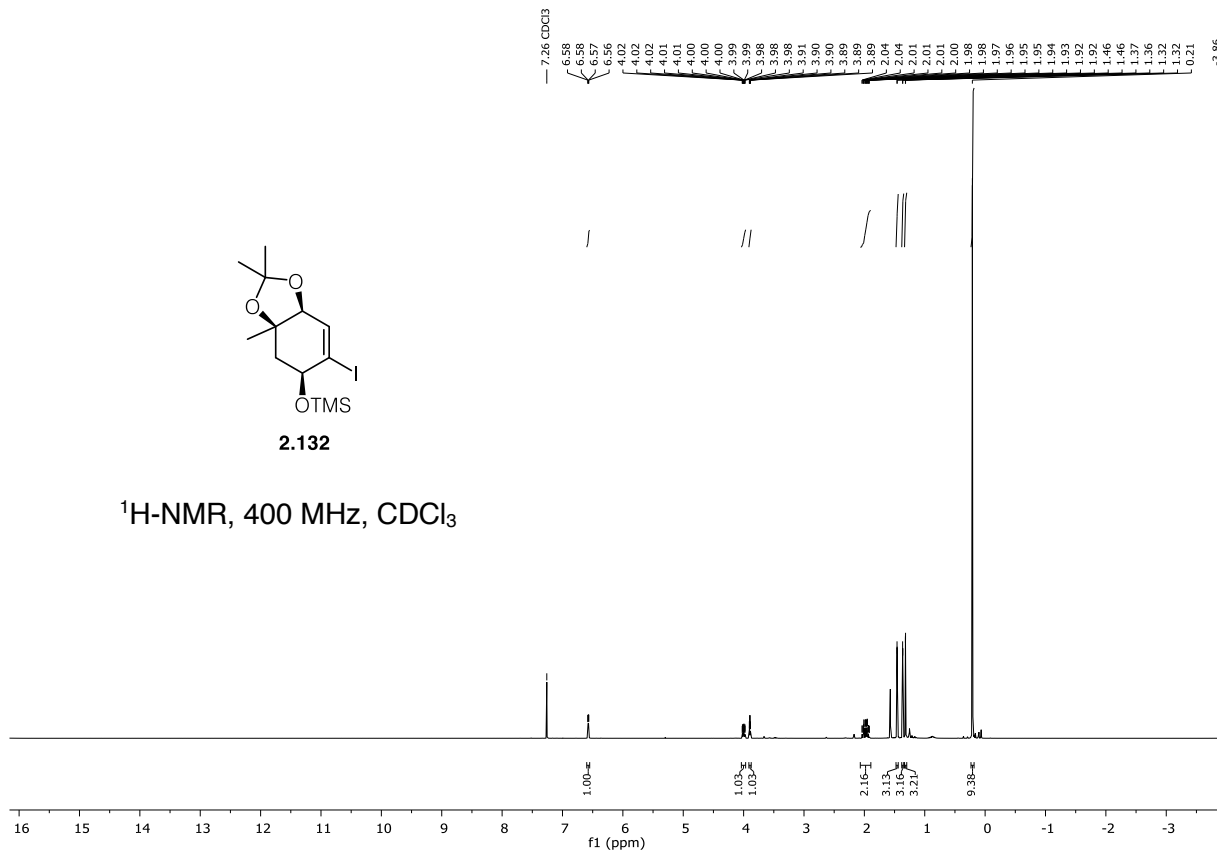




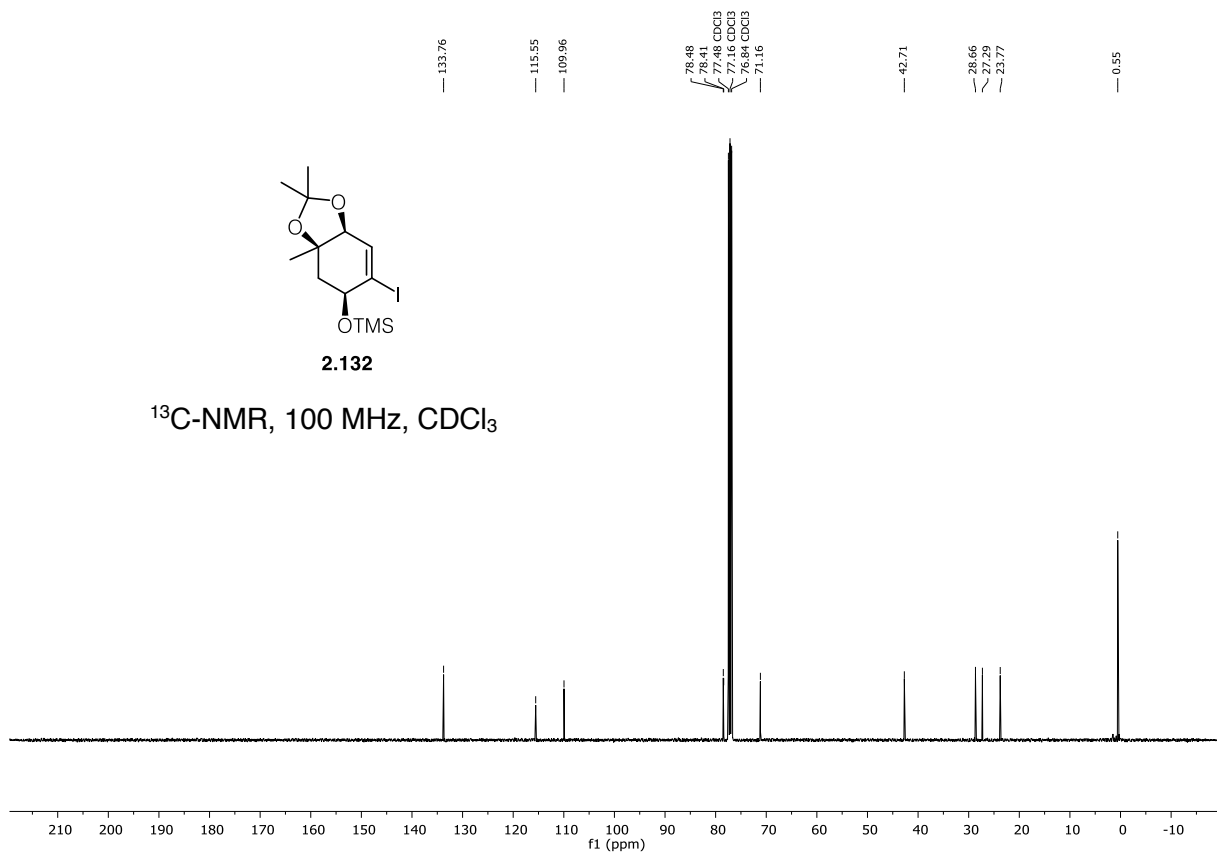


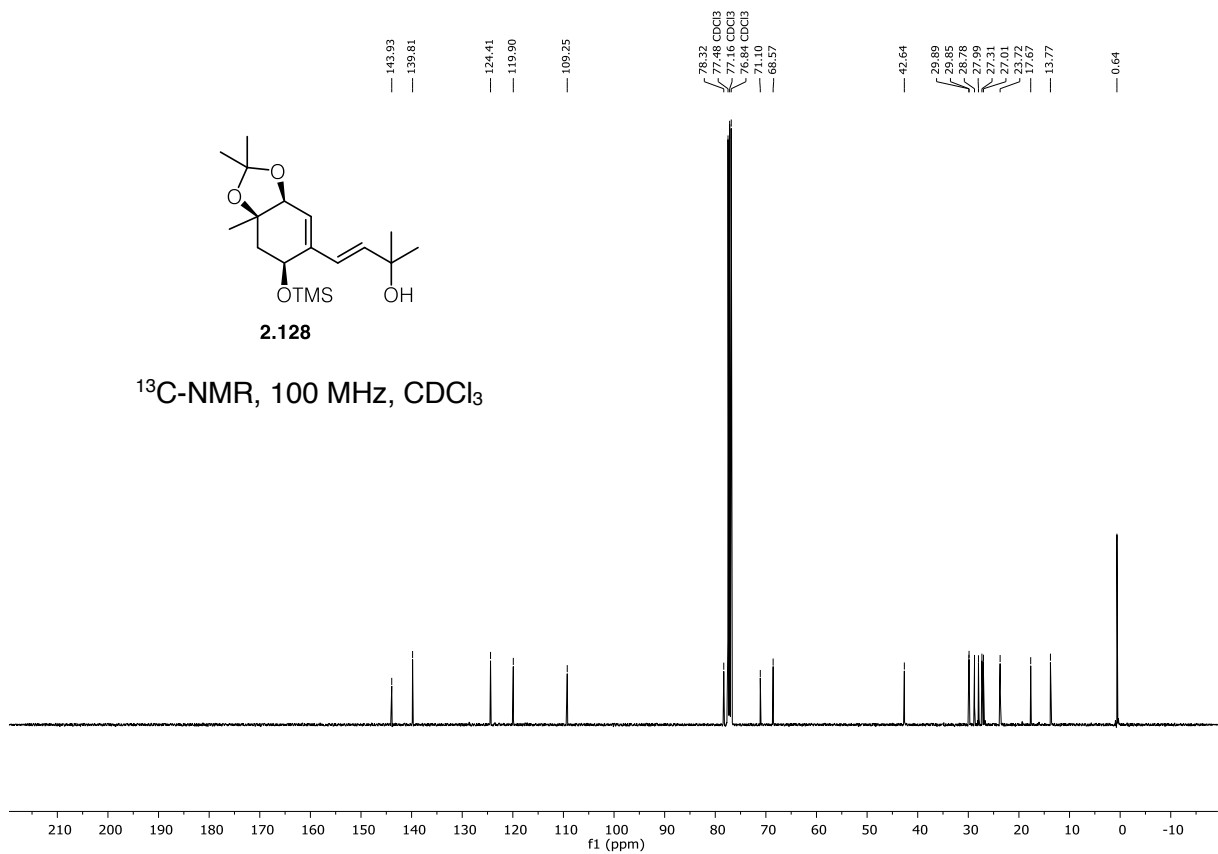
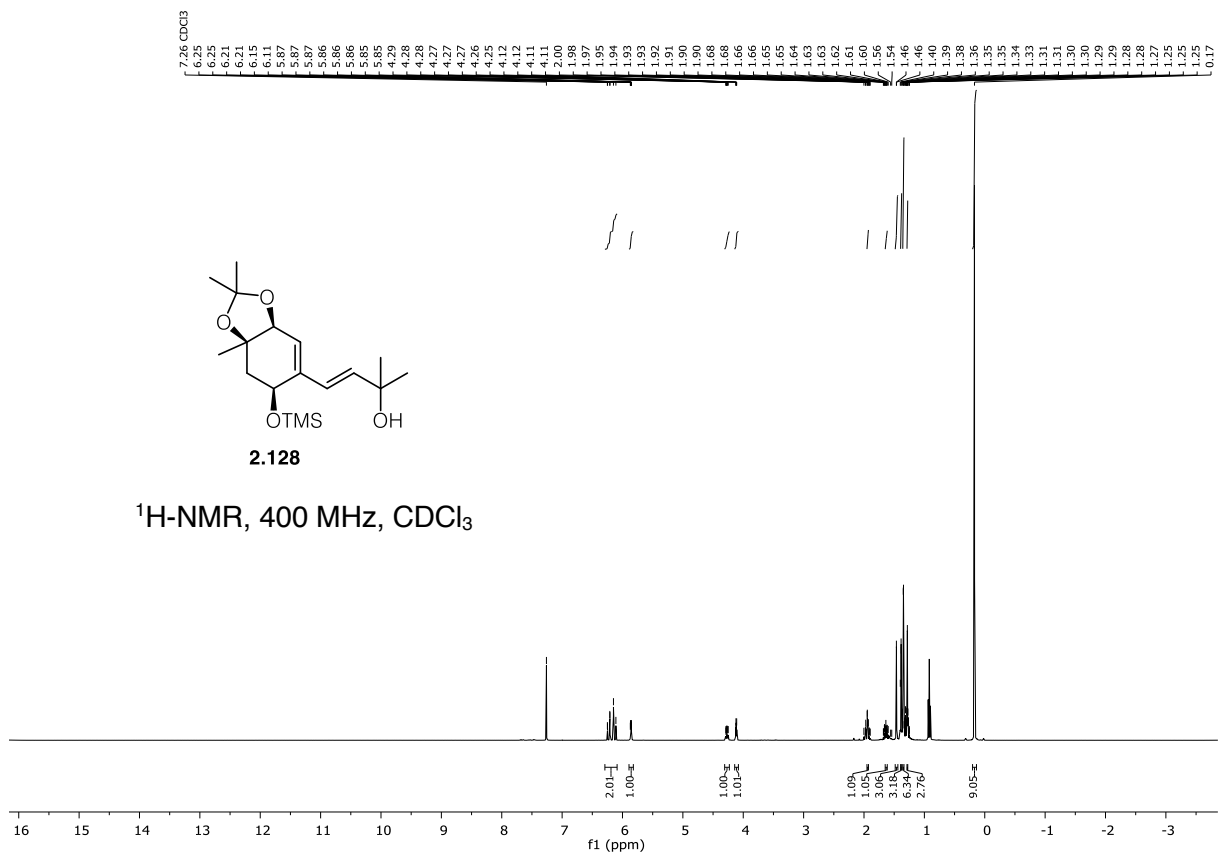


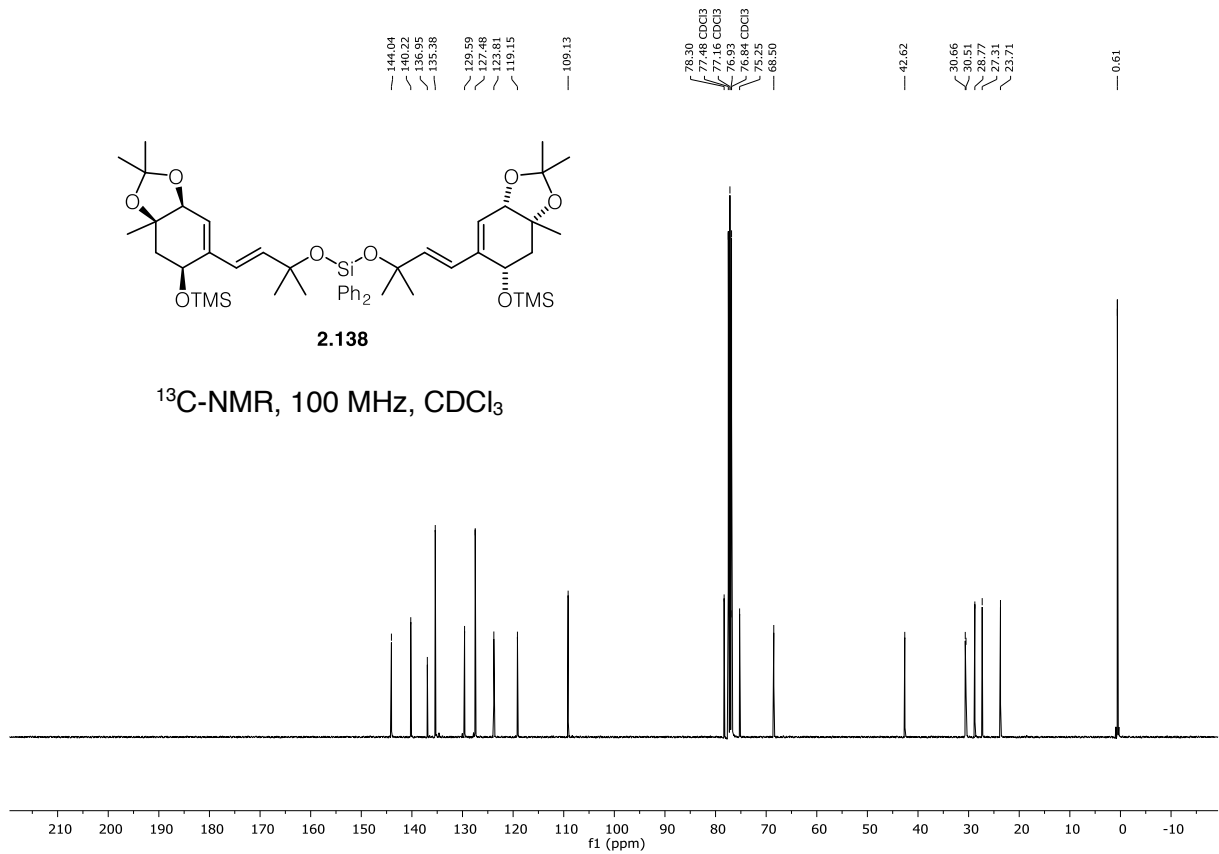
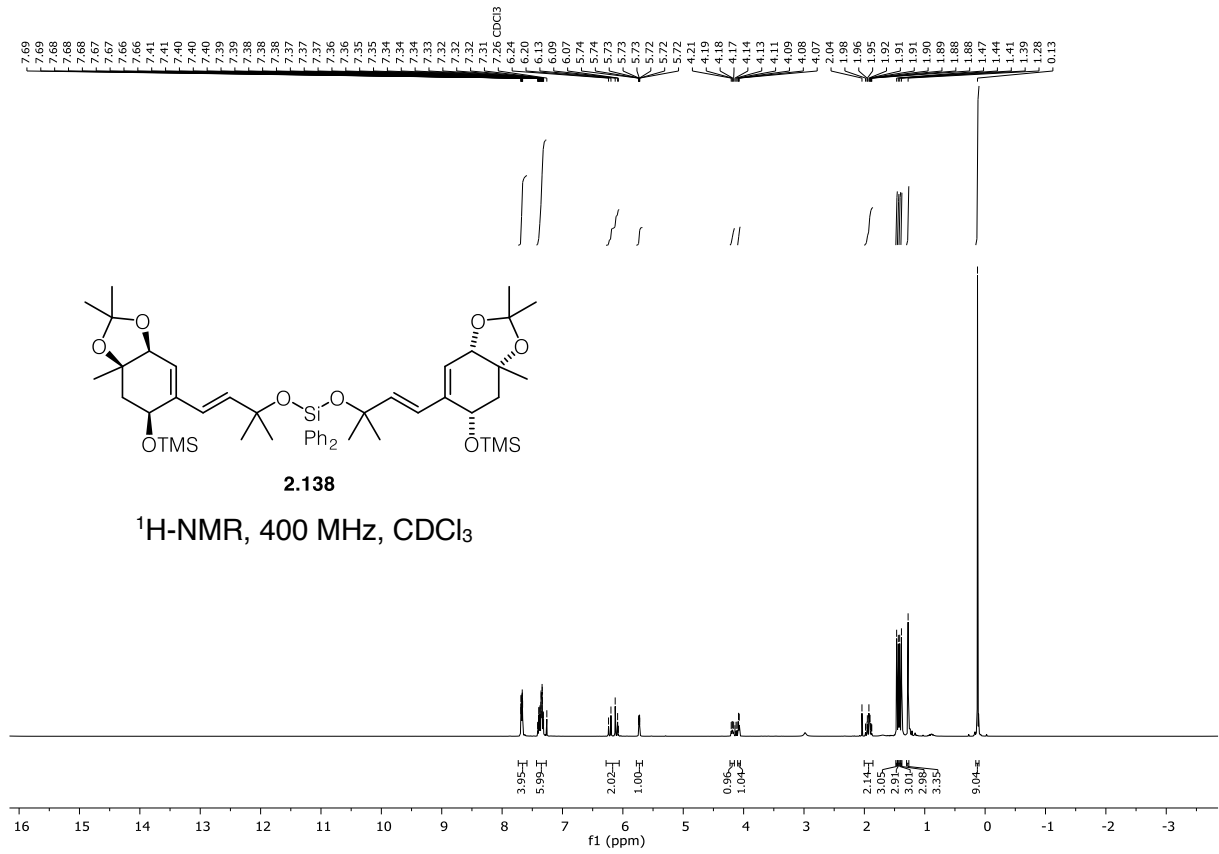
¹H-NMR, 400 MHz, CDCl₃

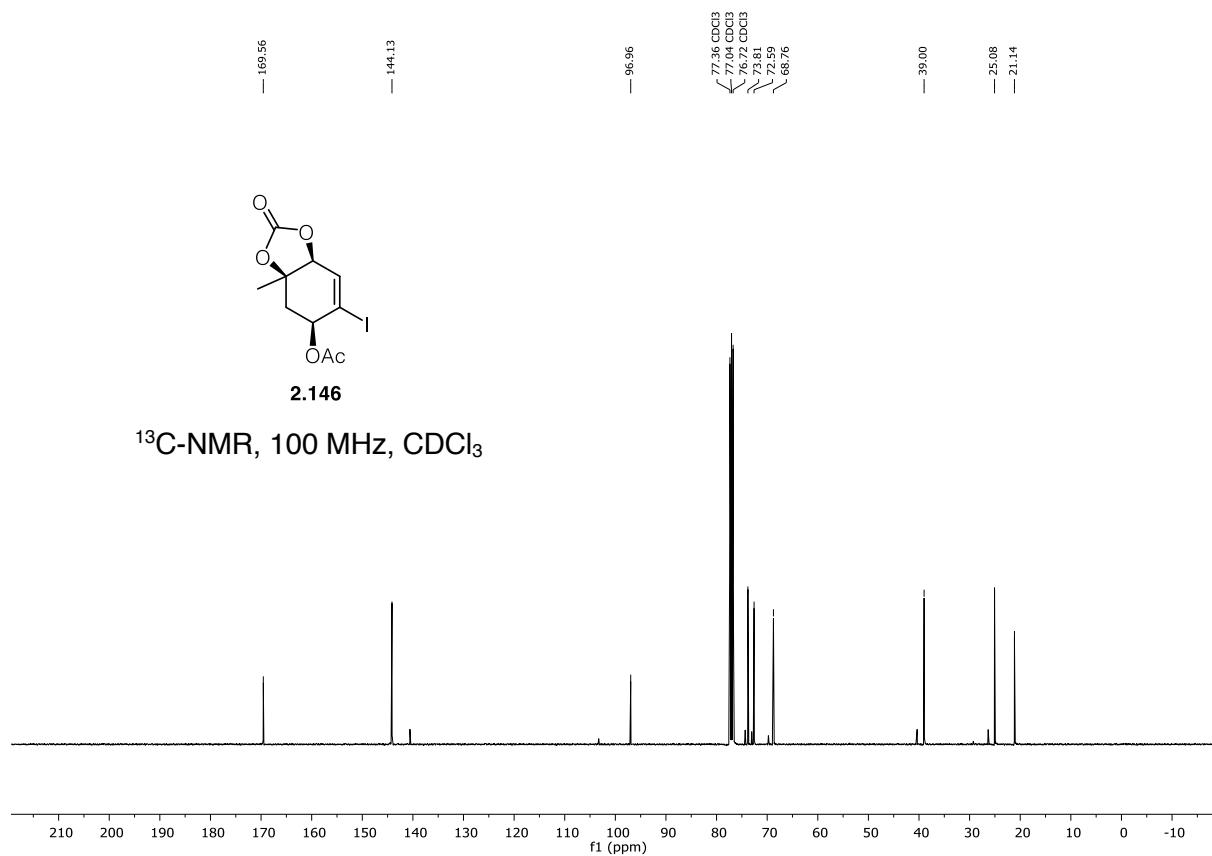
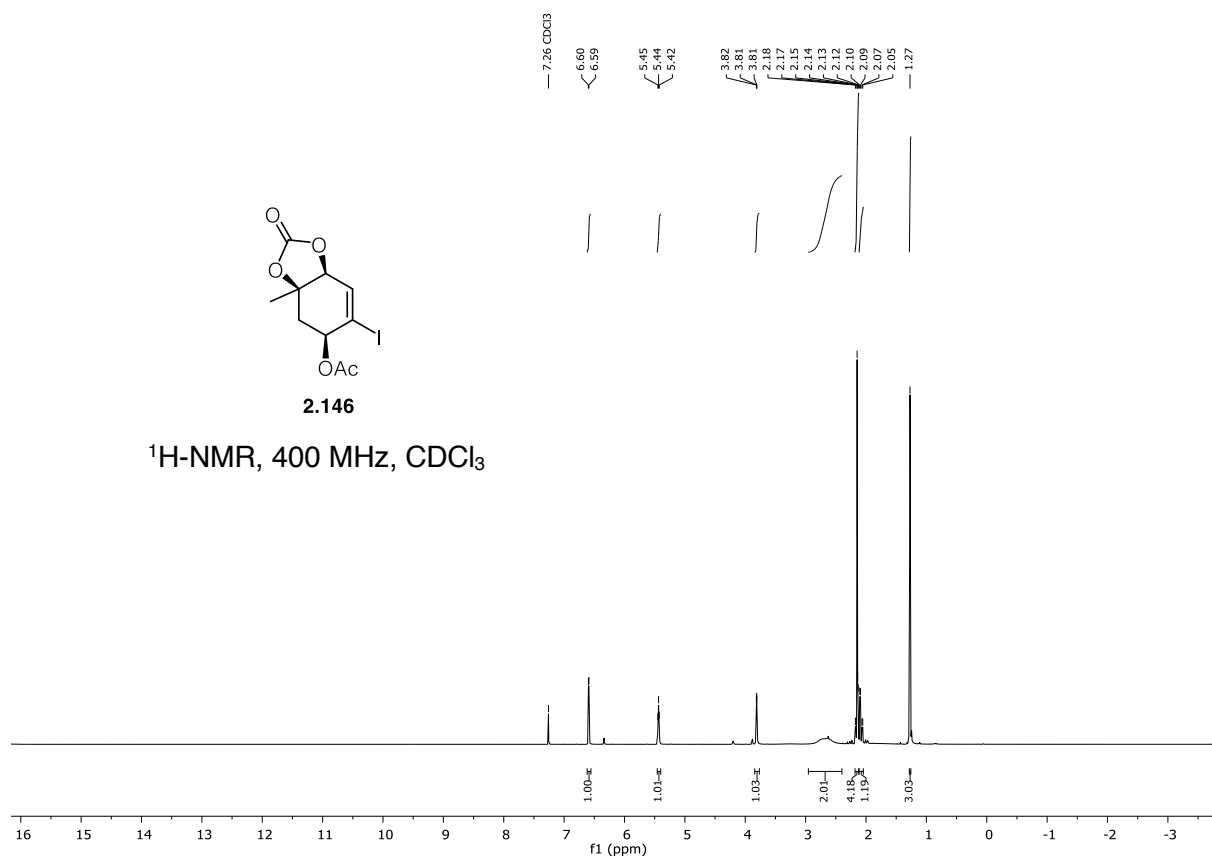


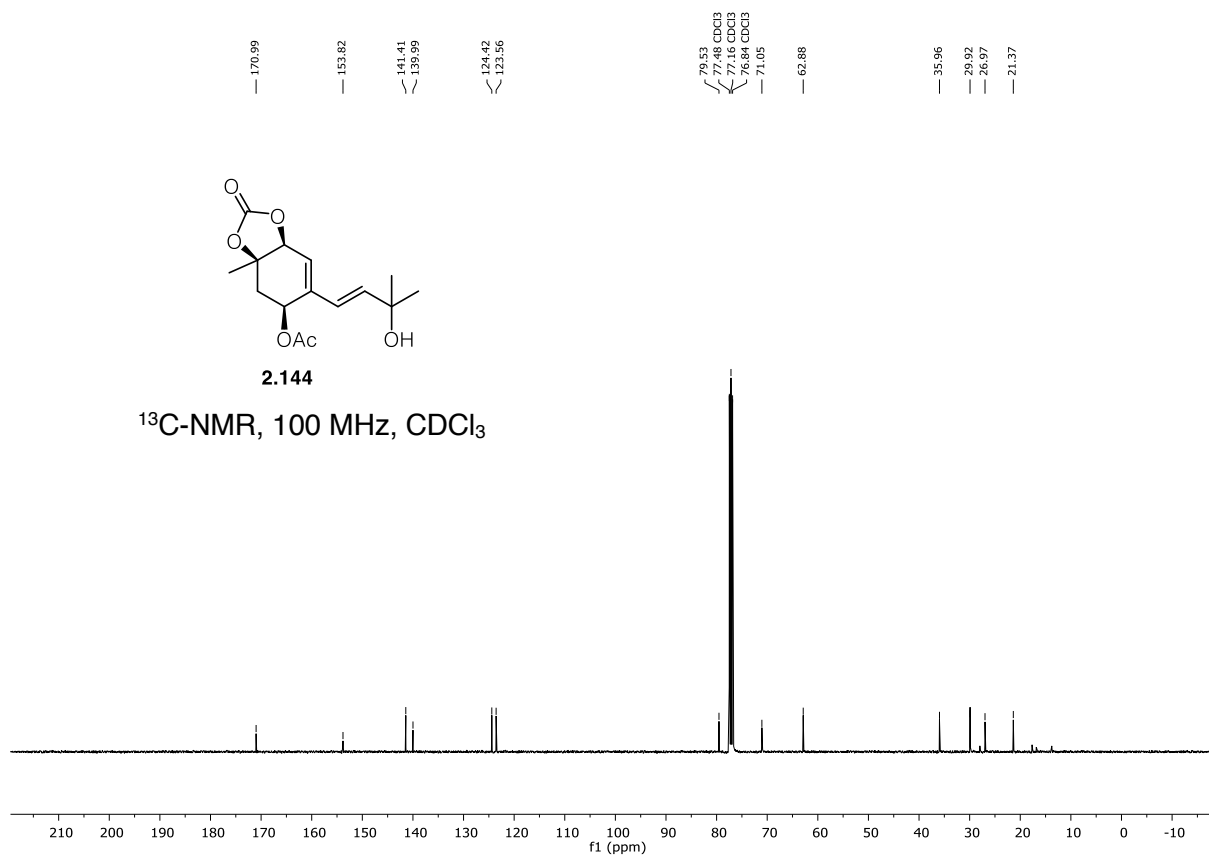
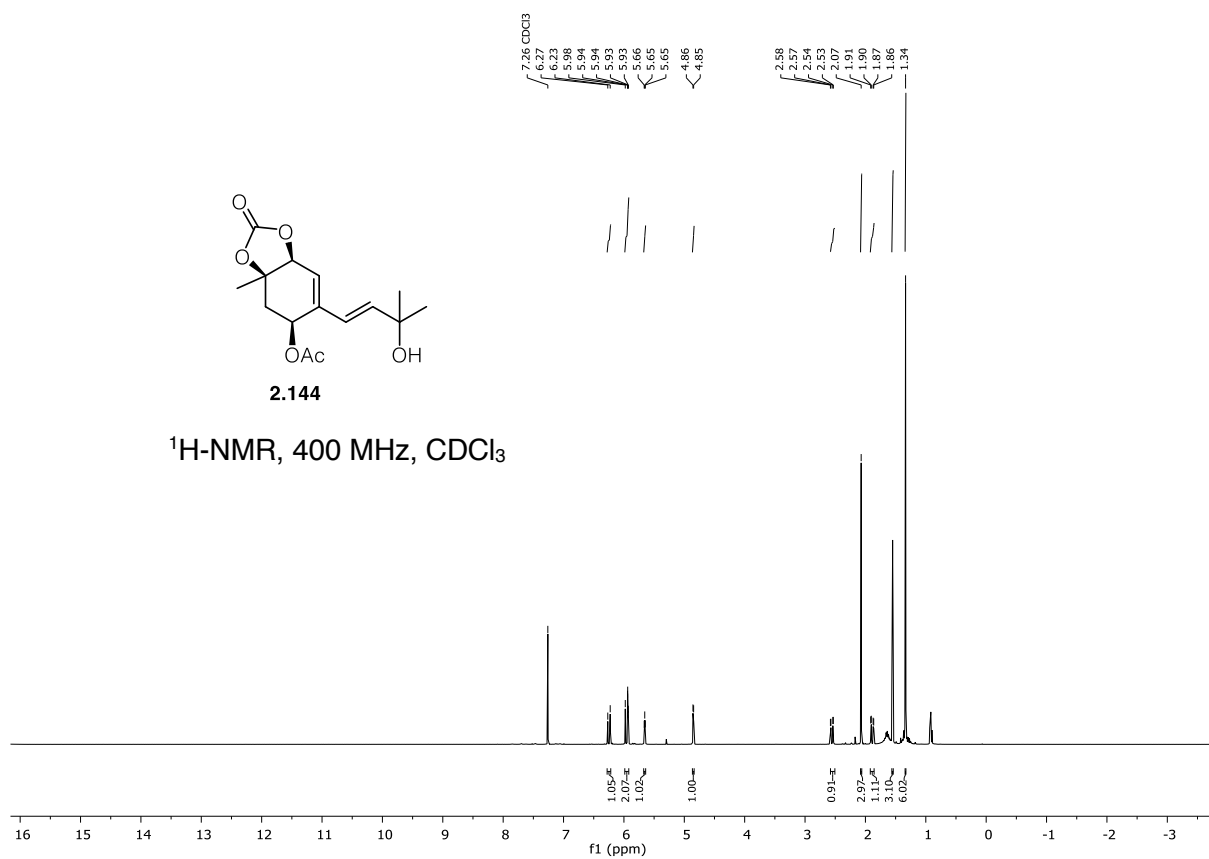
¹³C-NMR, 100 MHz, CDCl₃

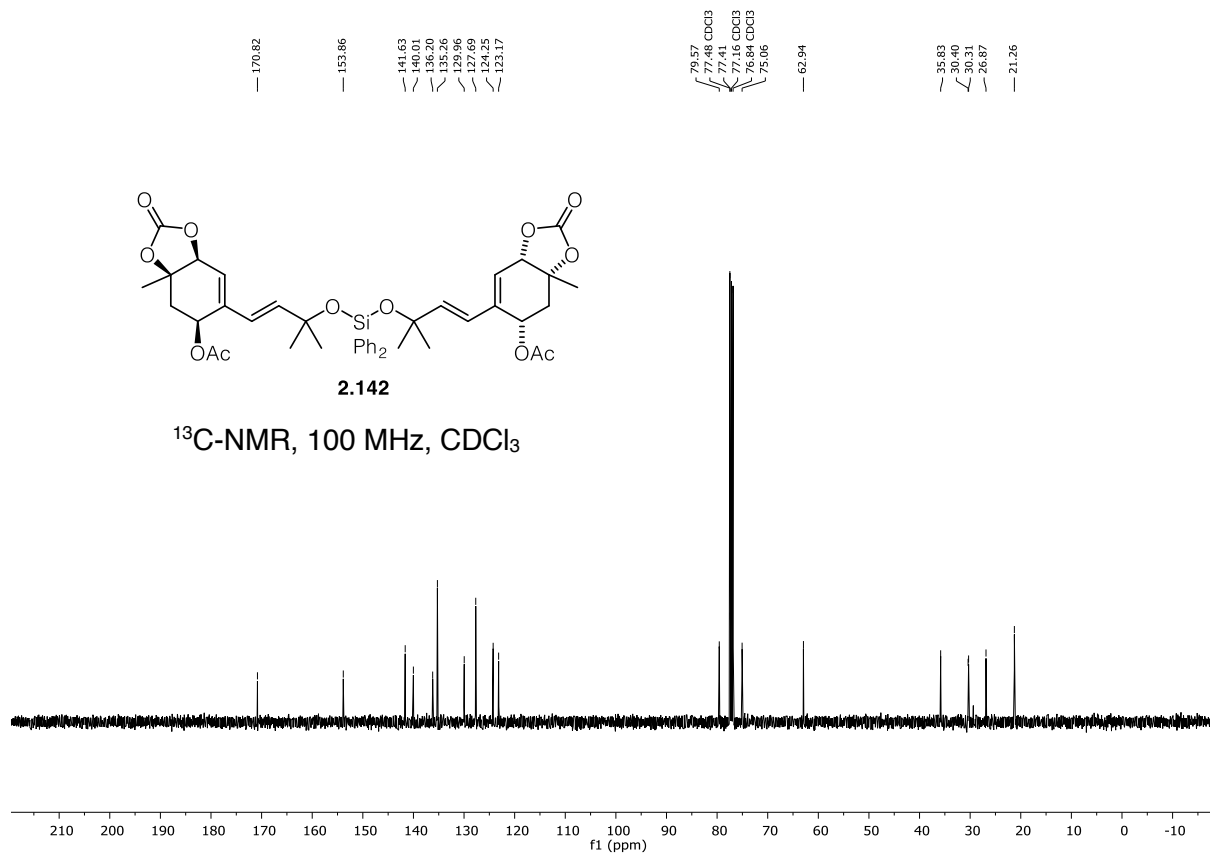
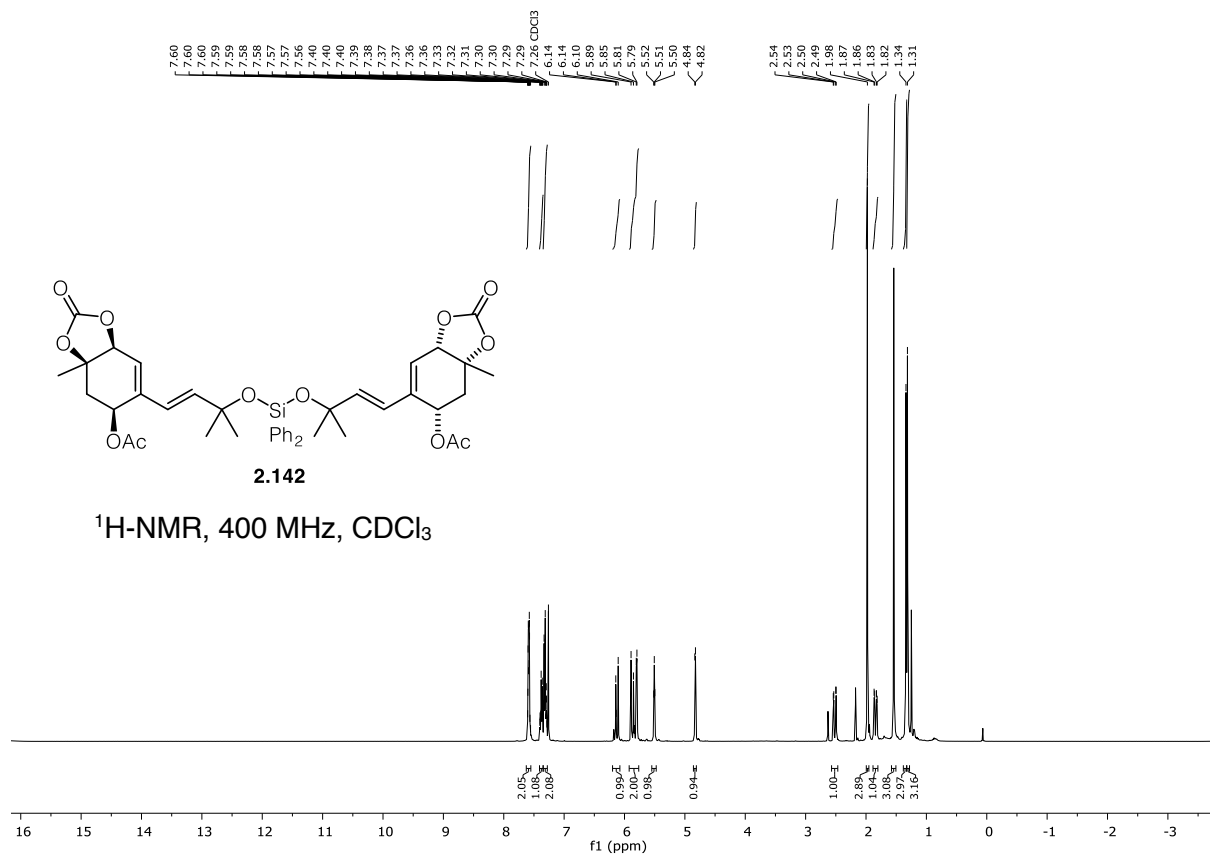


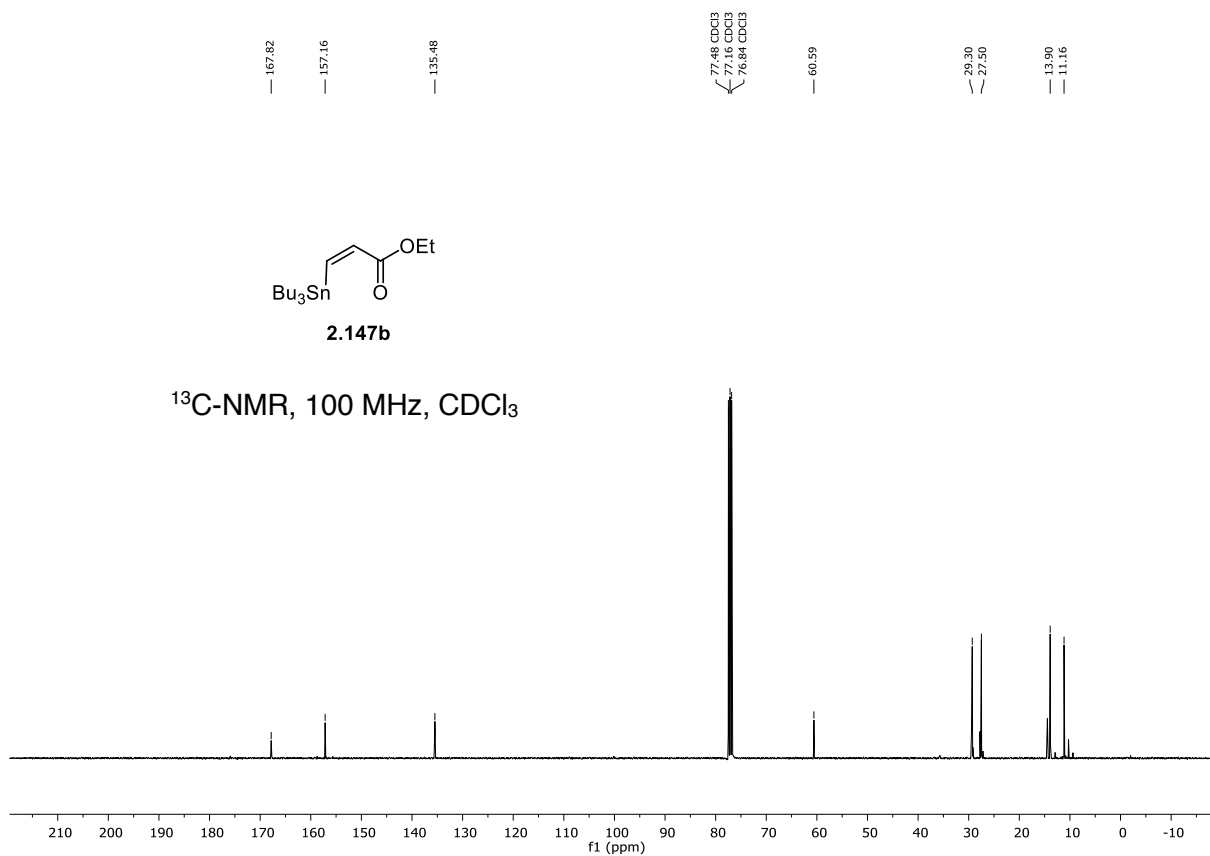
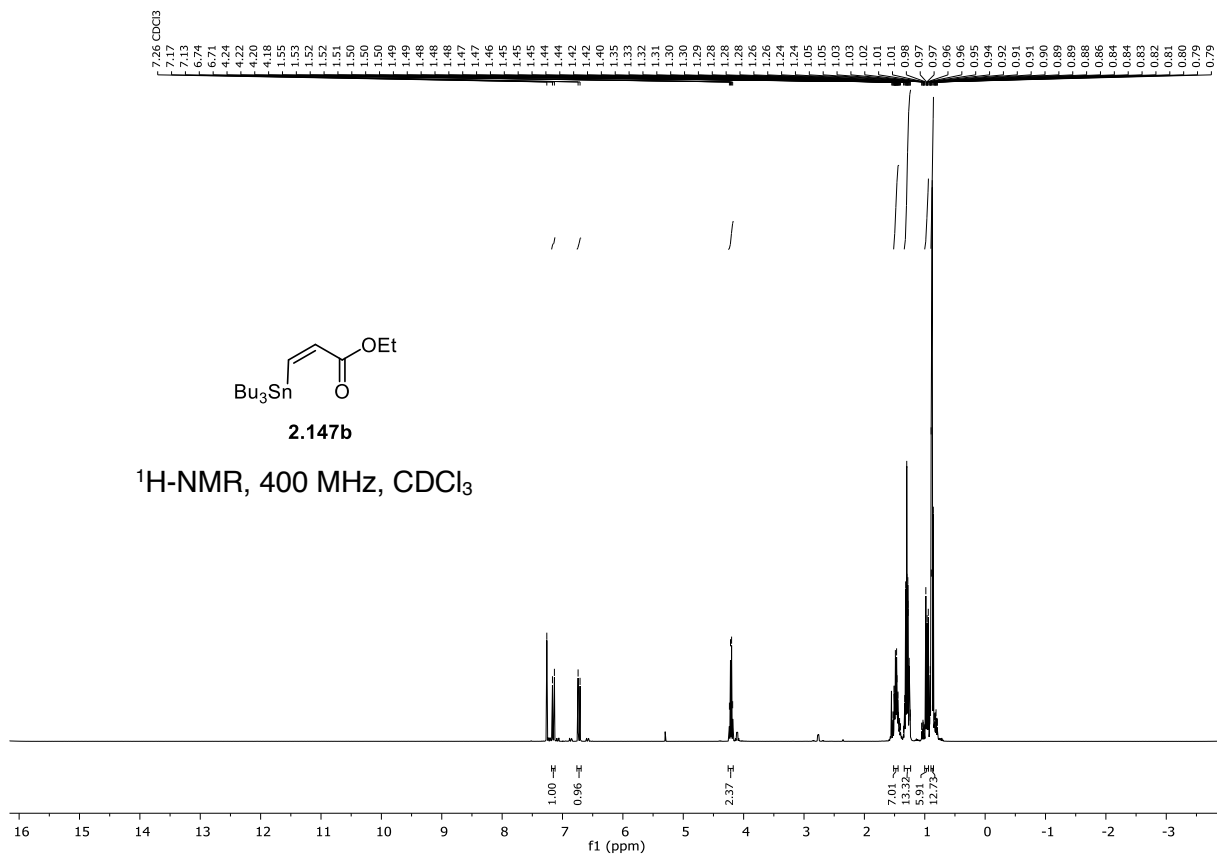


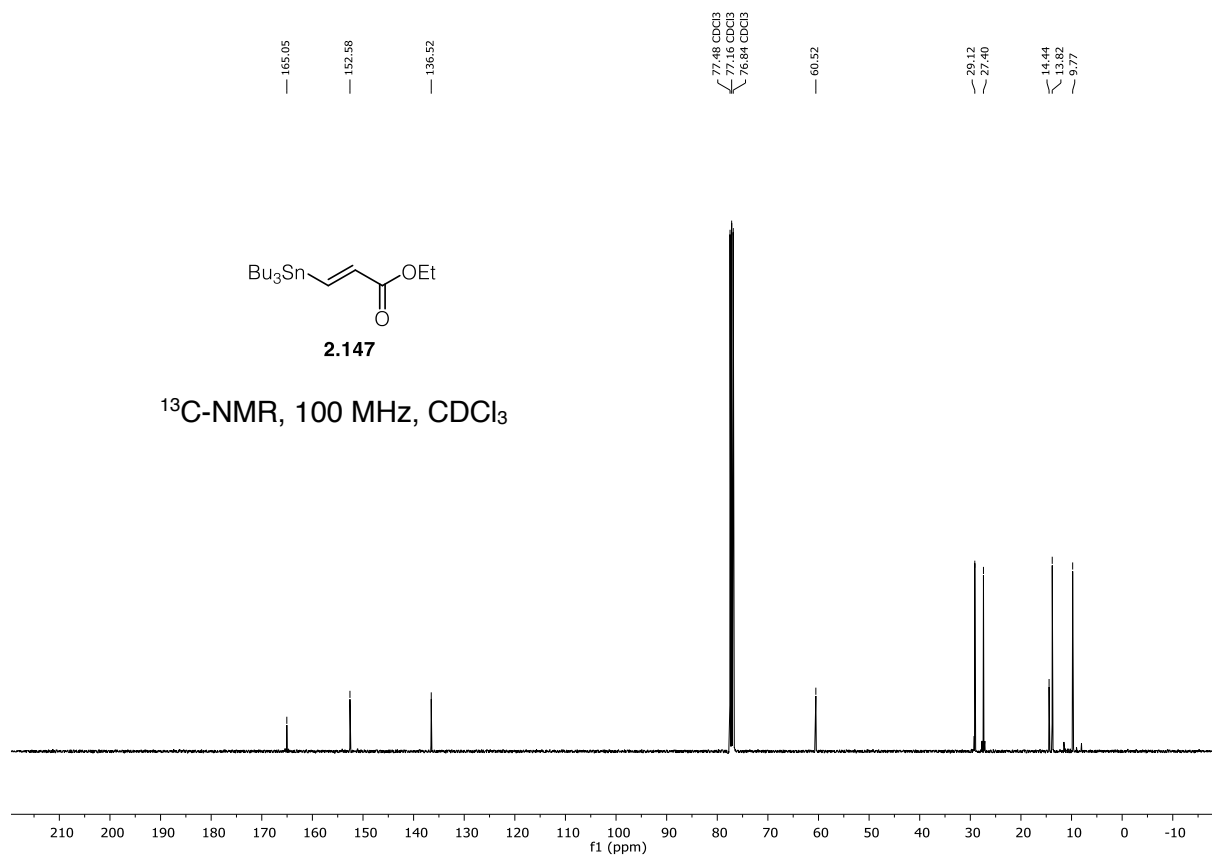
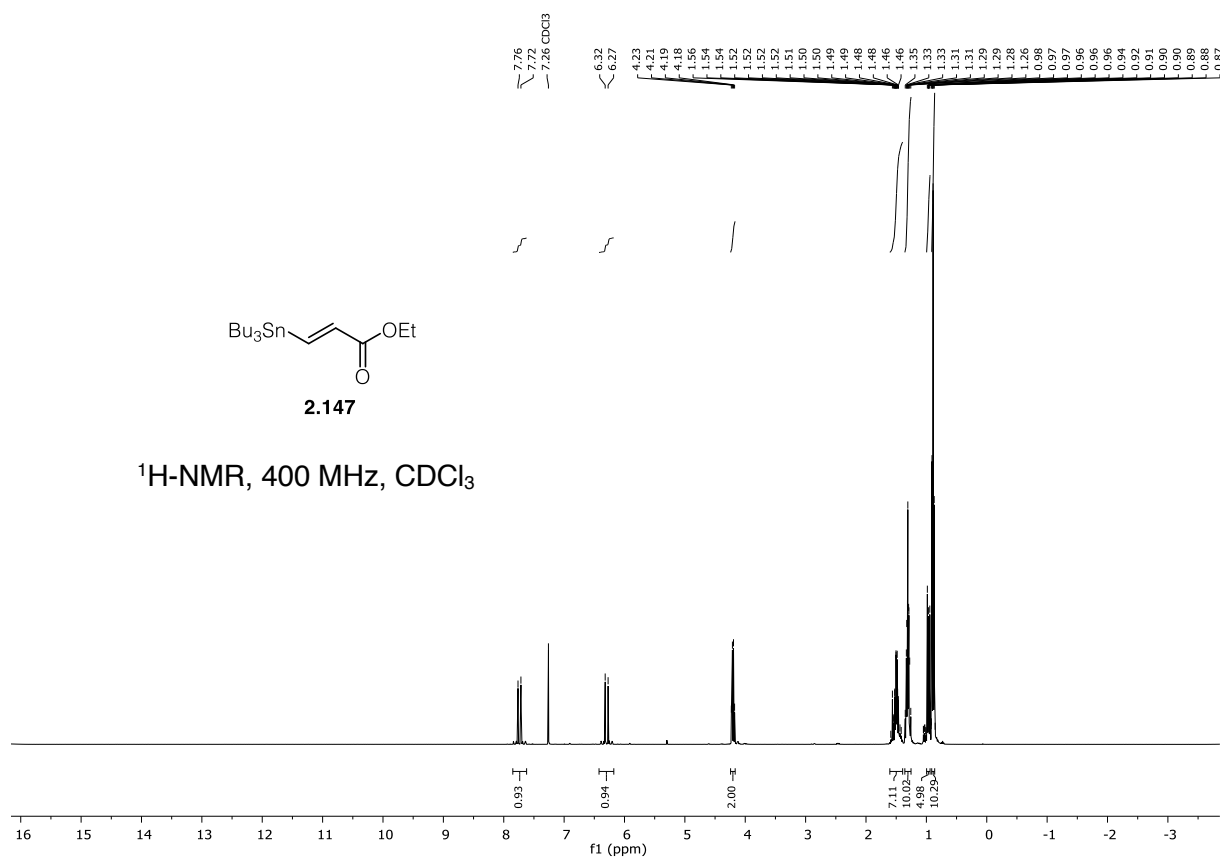


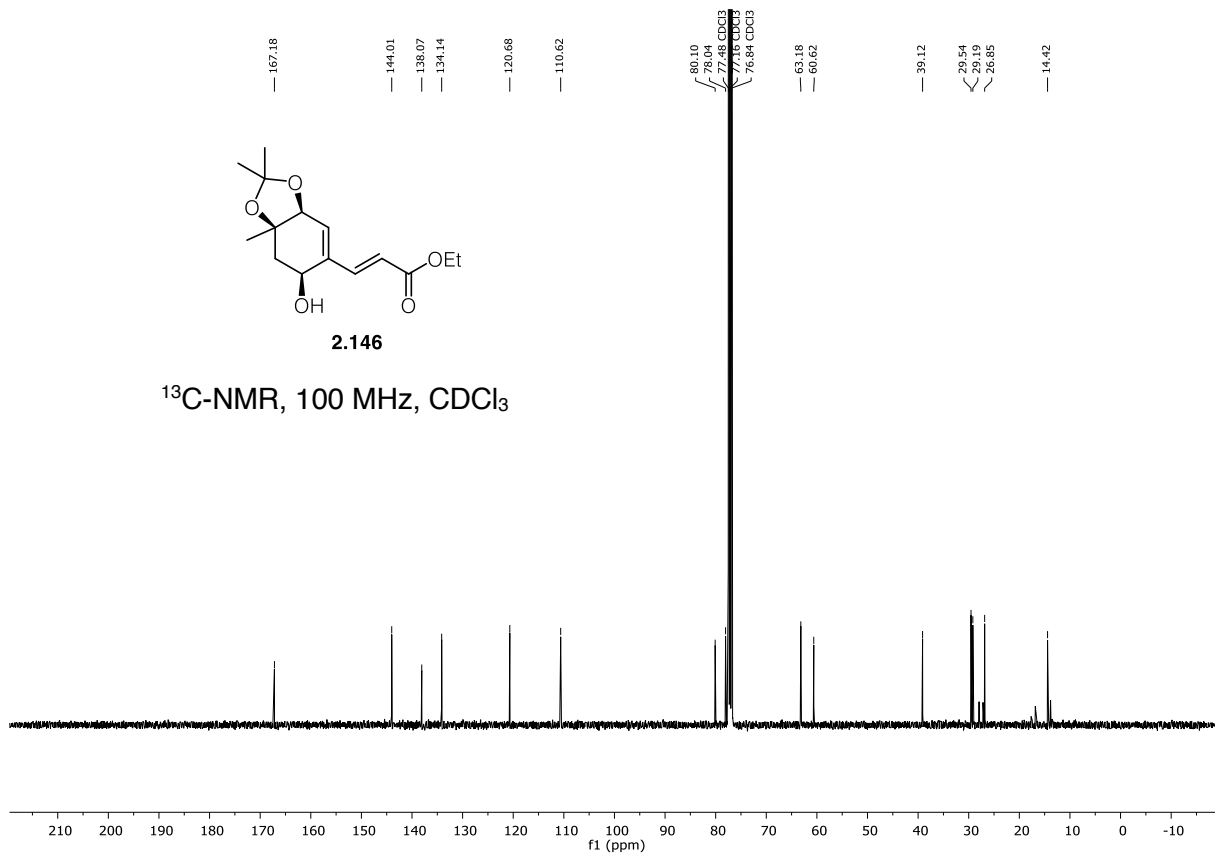
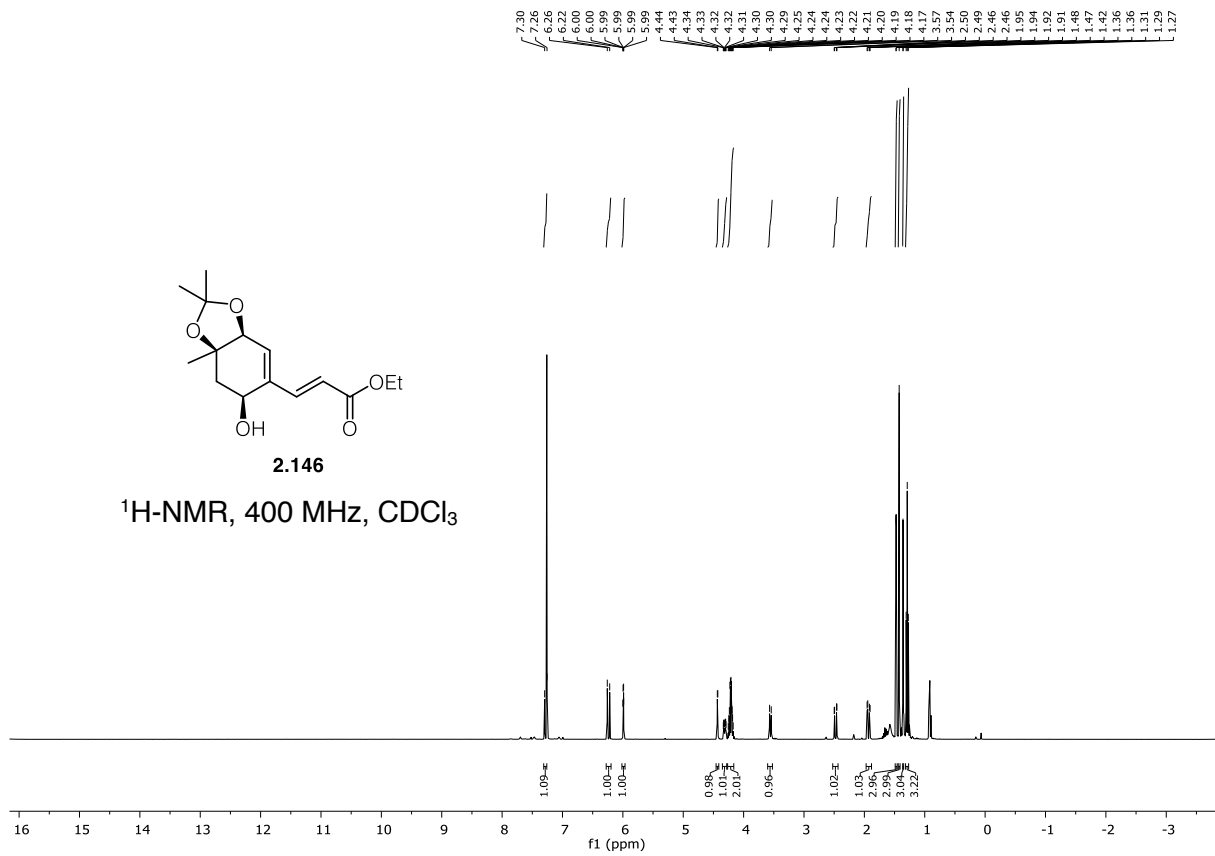


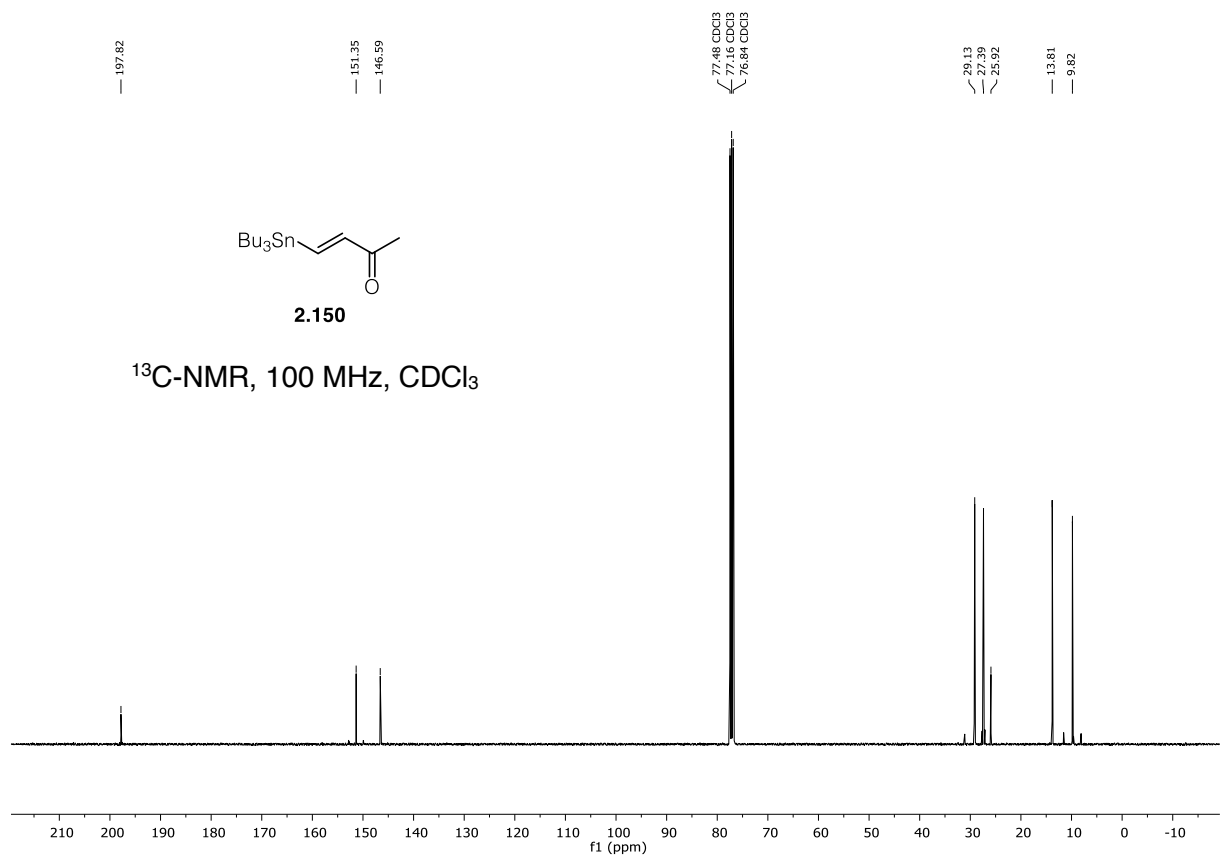
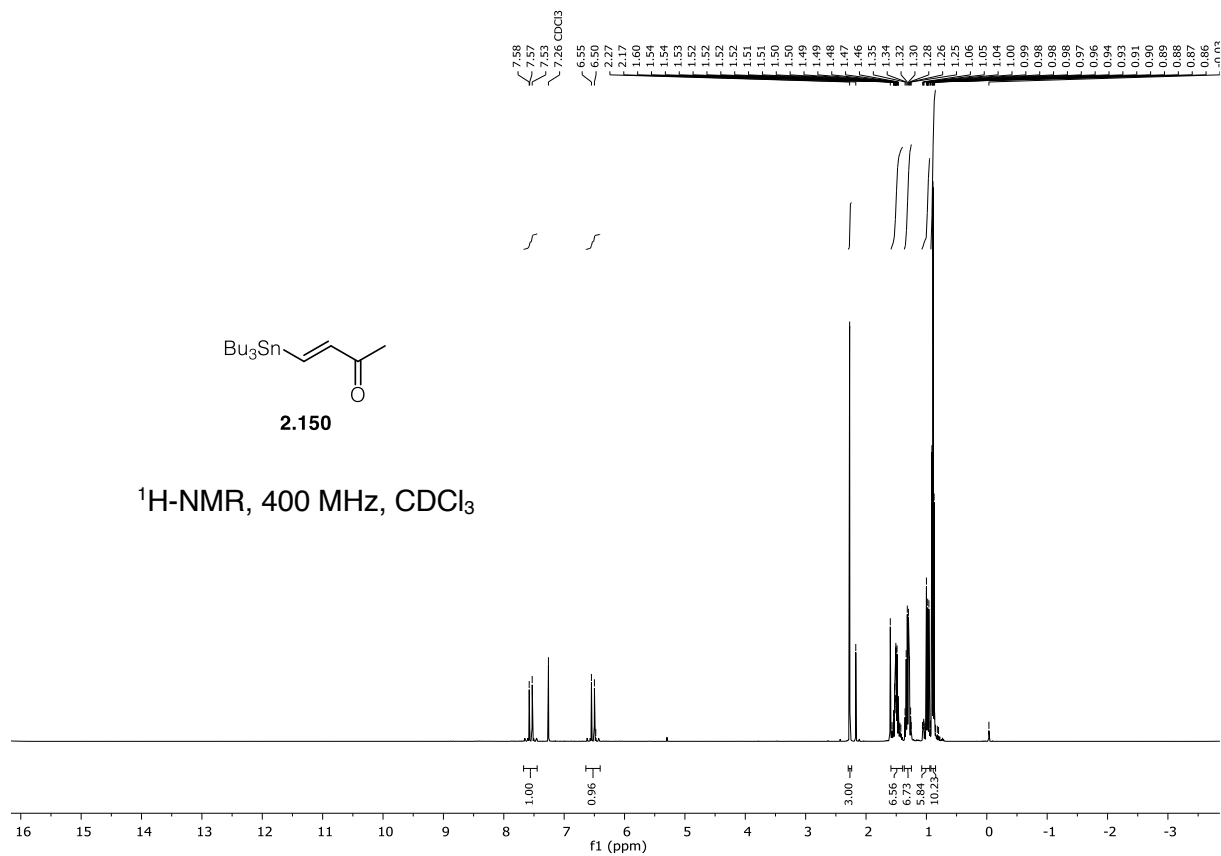


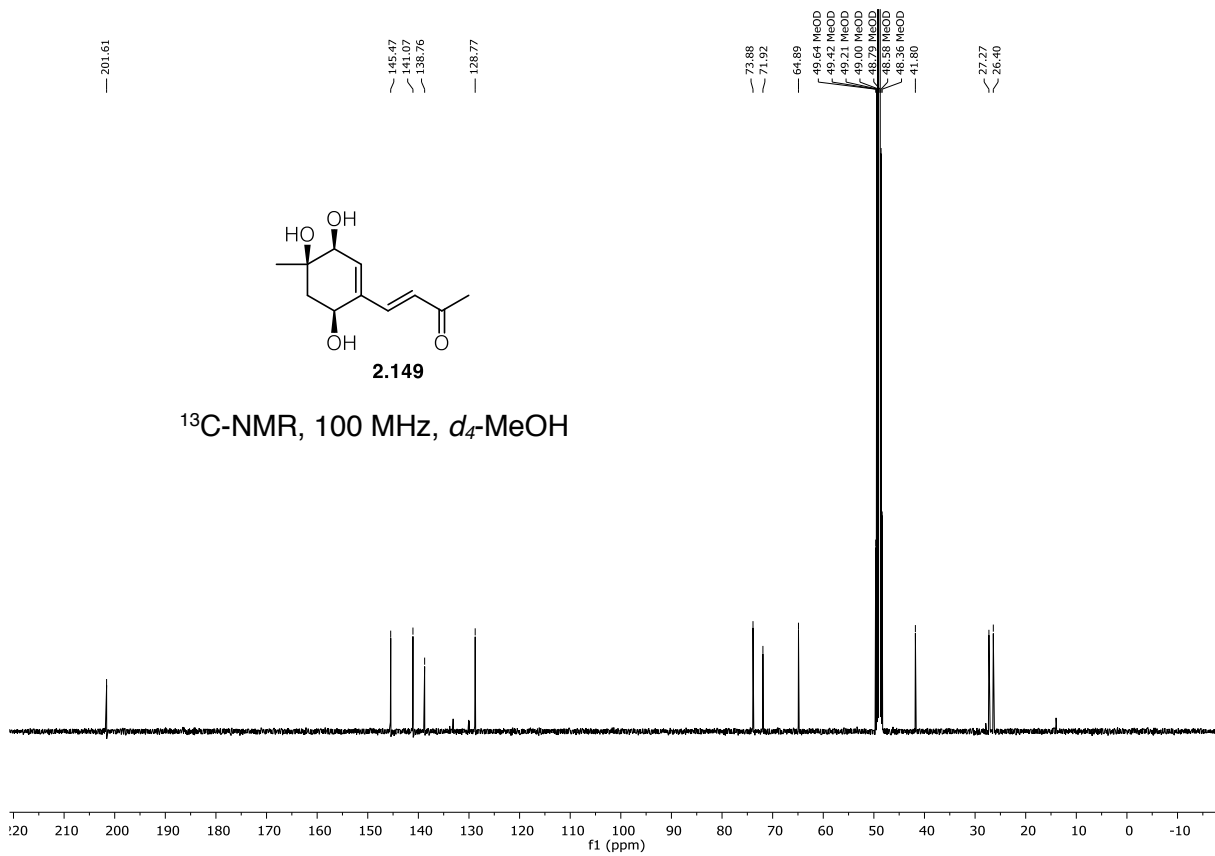
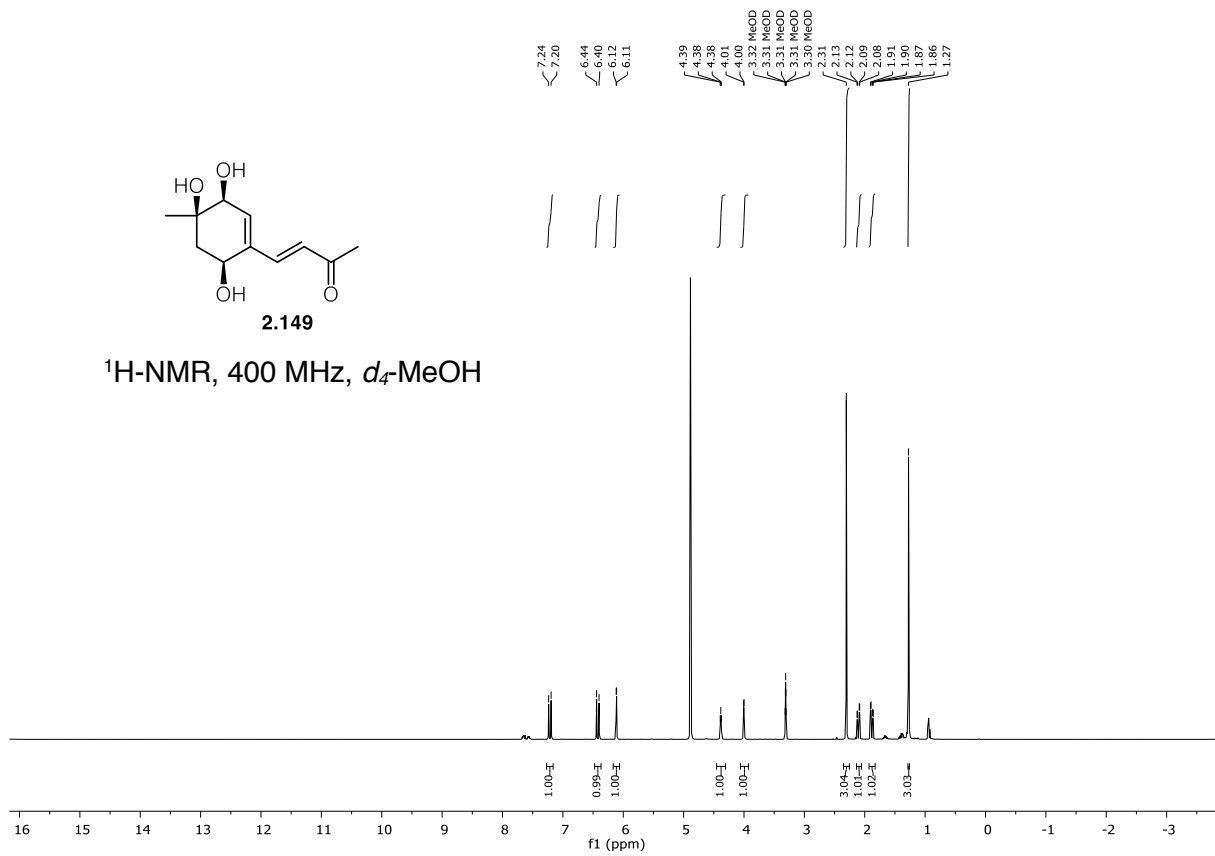


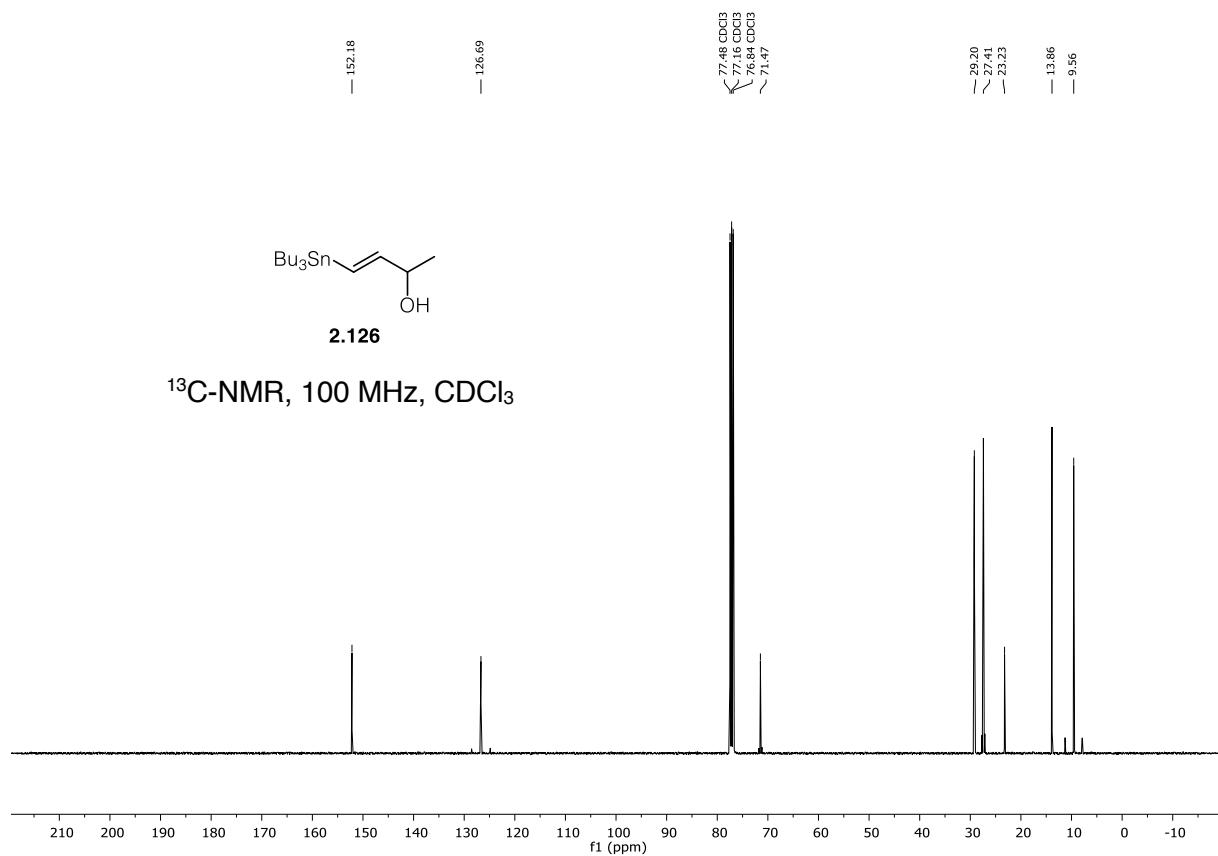
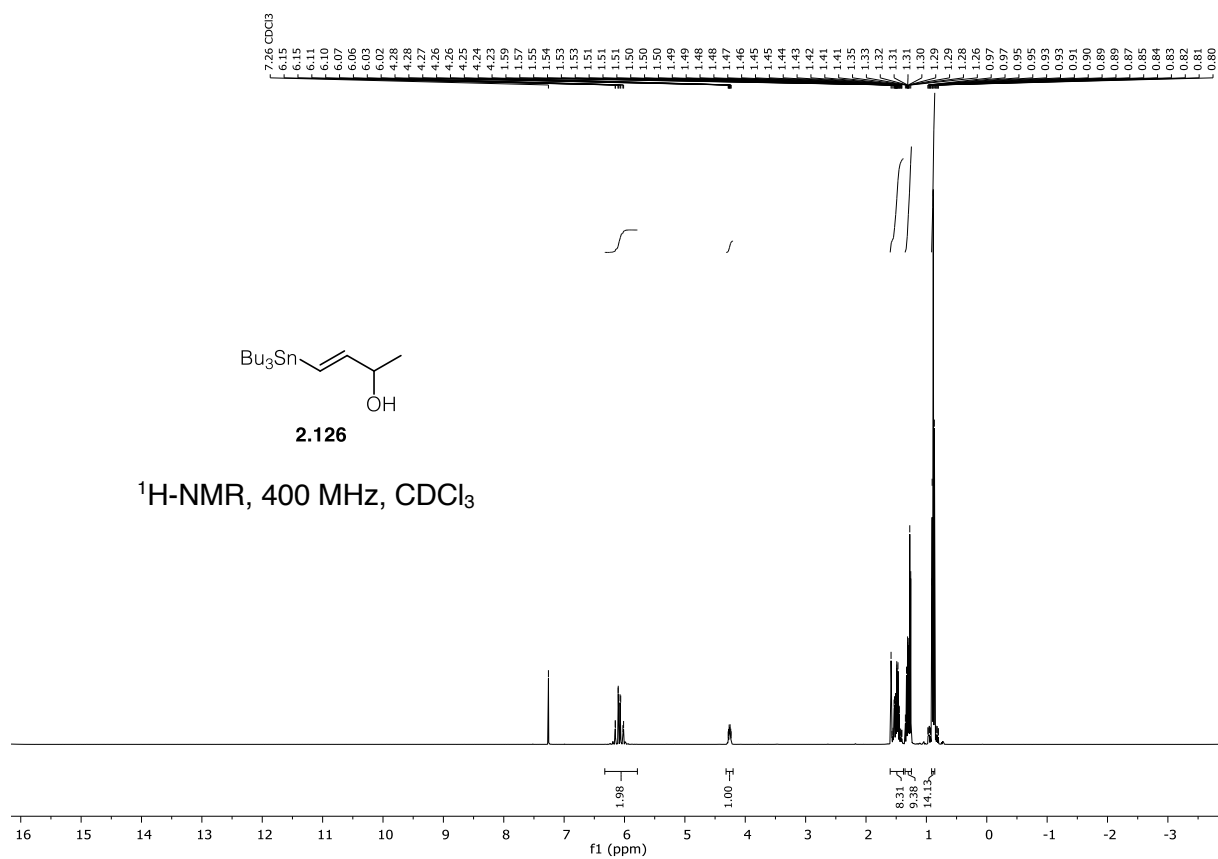


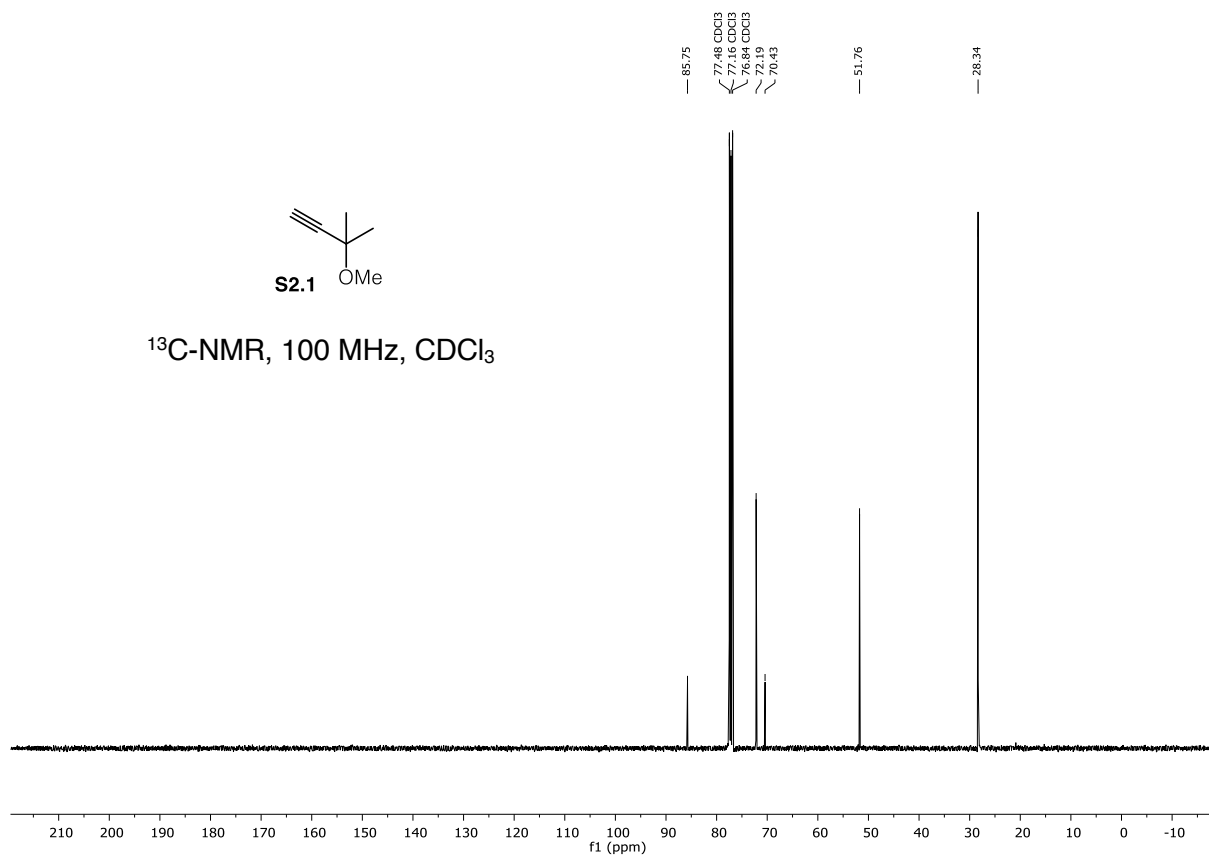
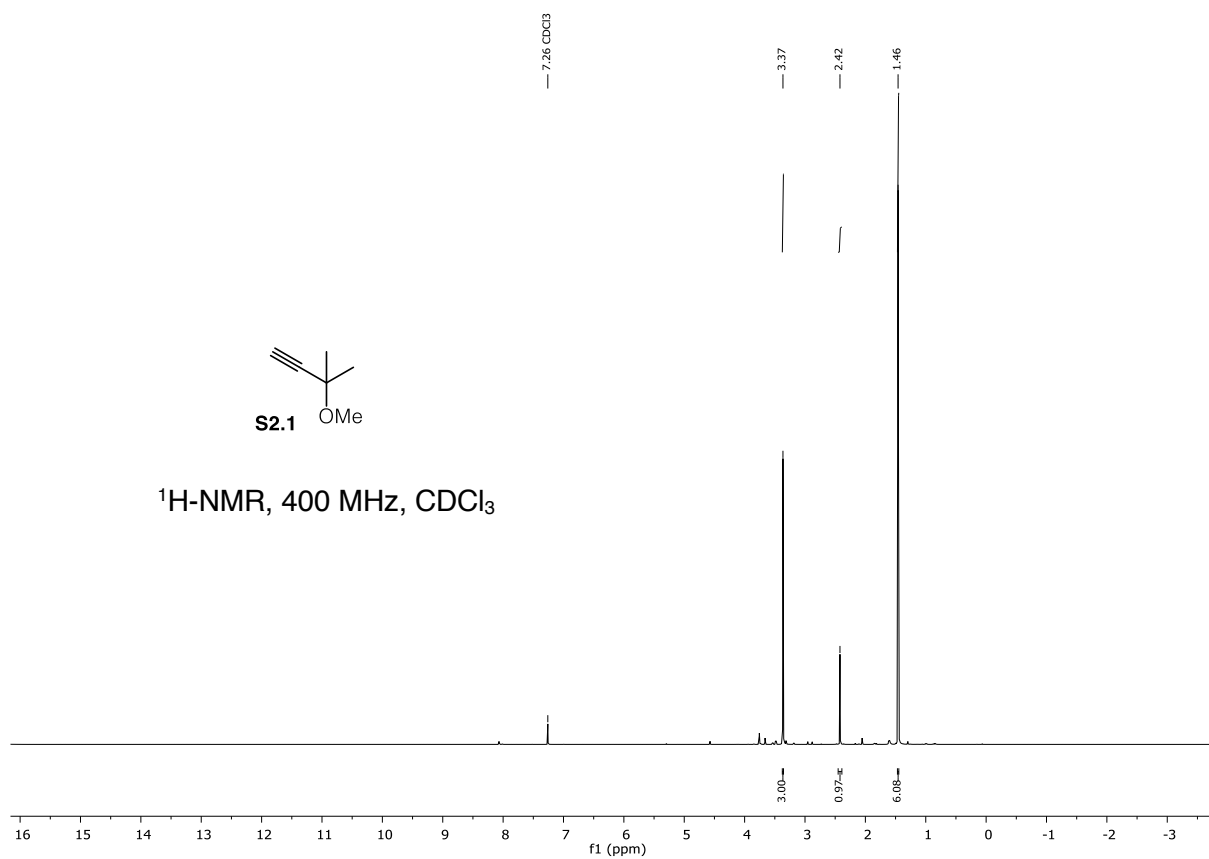


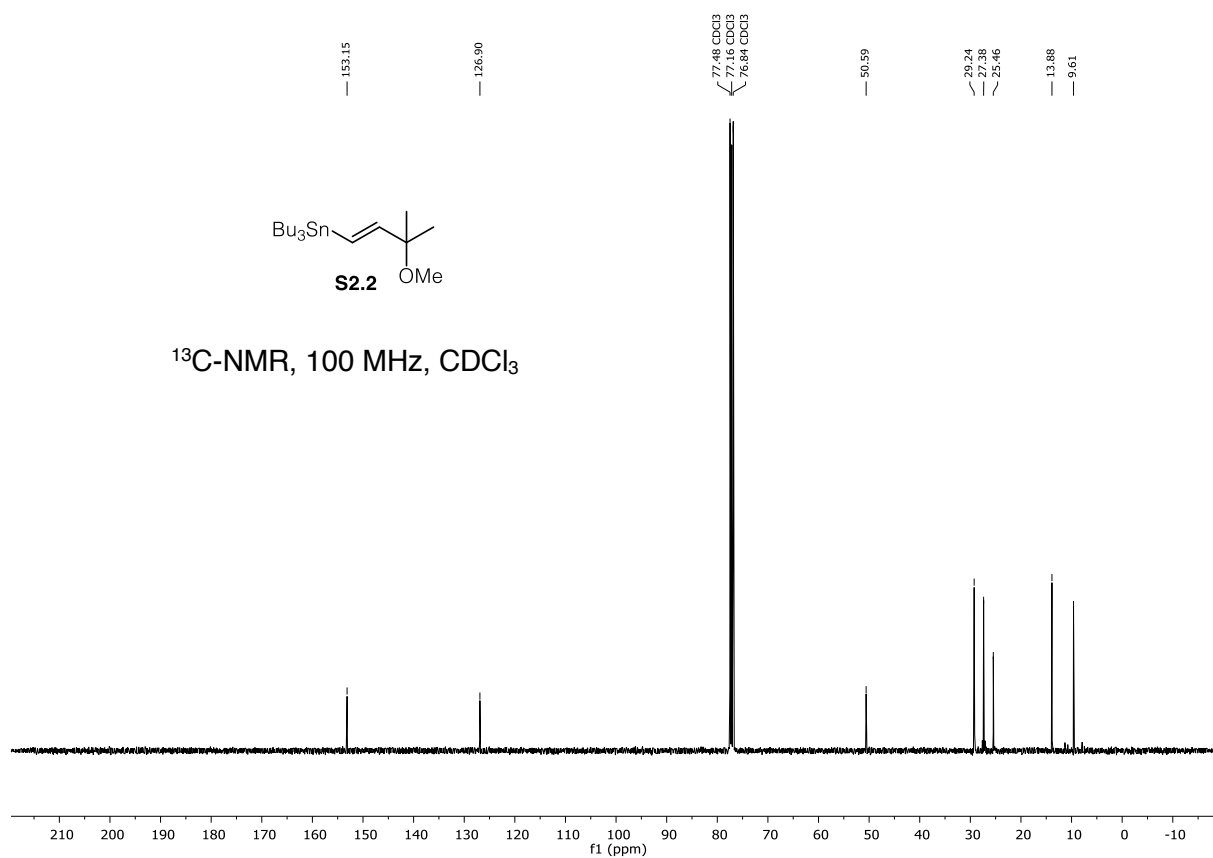
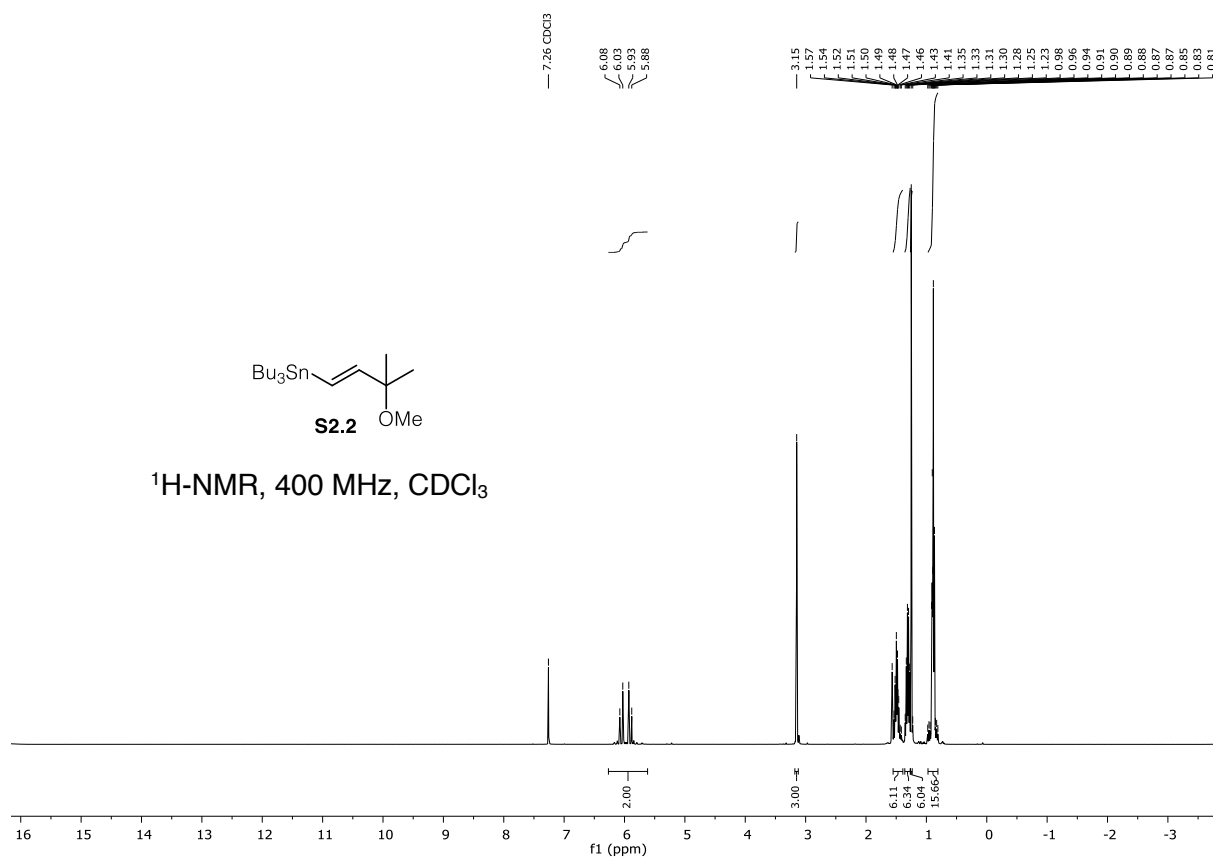


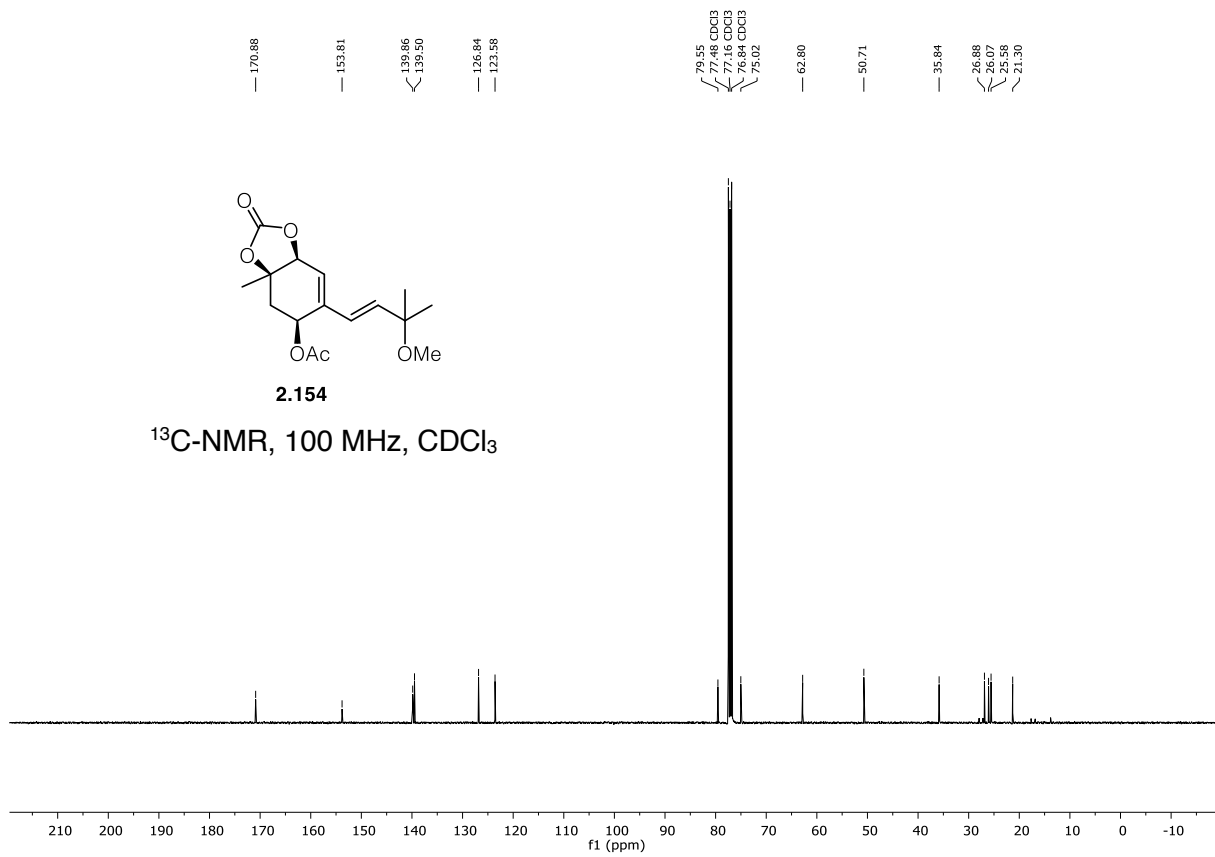
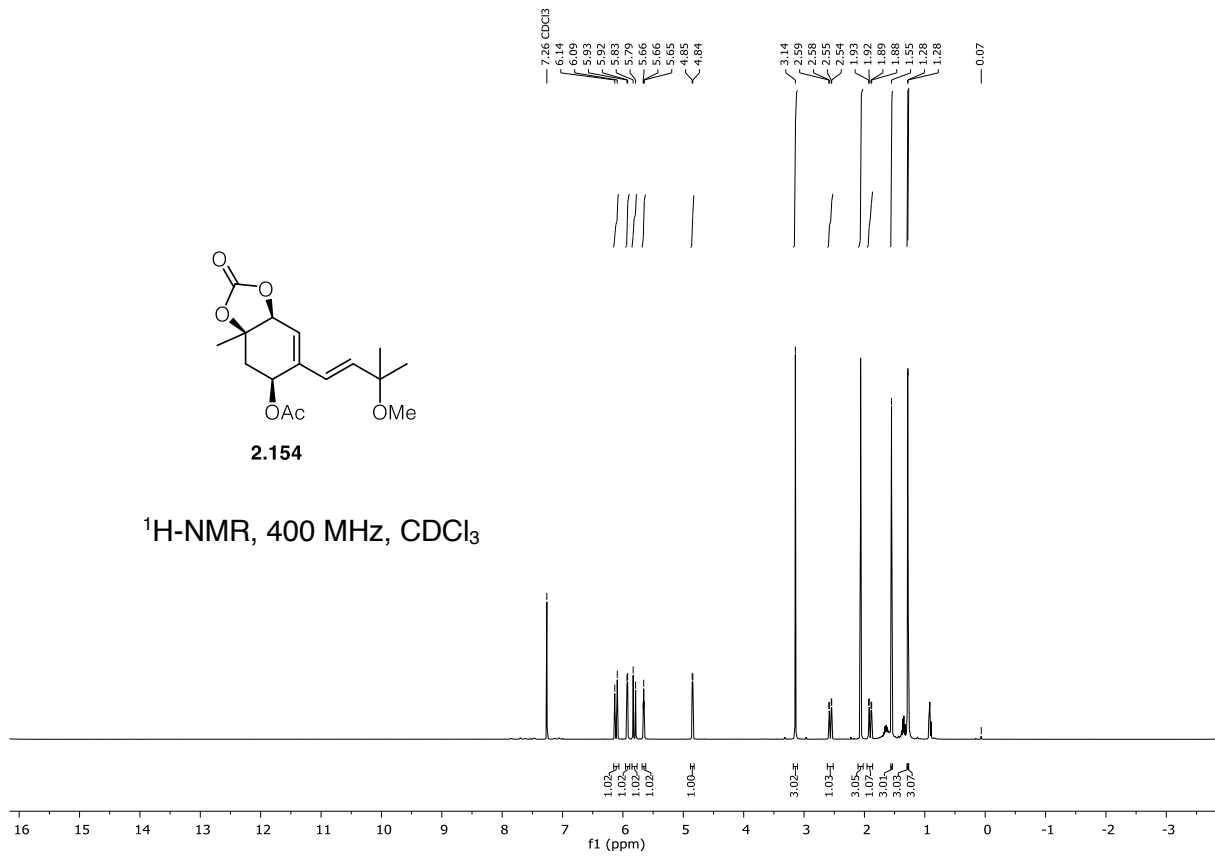


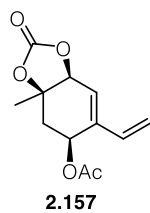




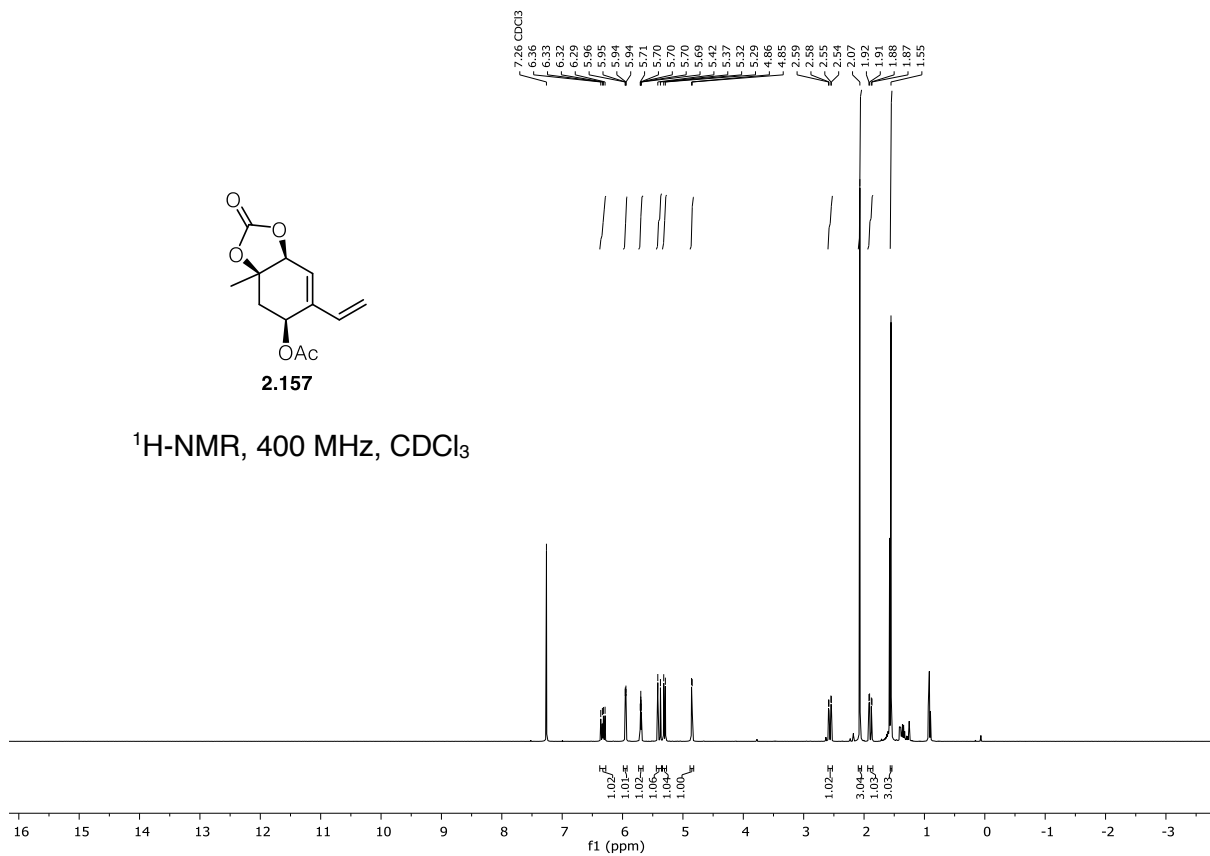








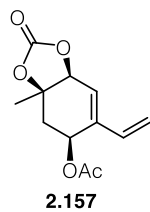
$^1\text{H-NMR}$, 400 MHz, CDCl_3



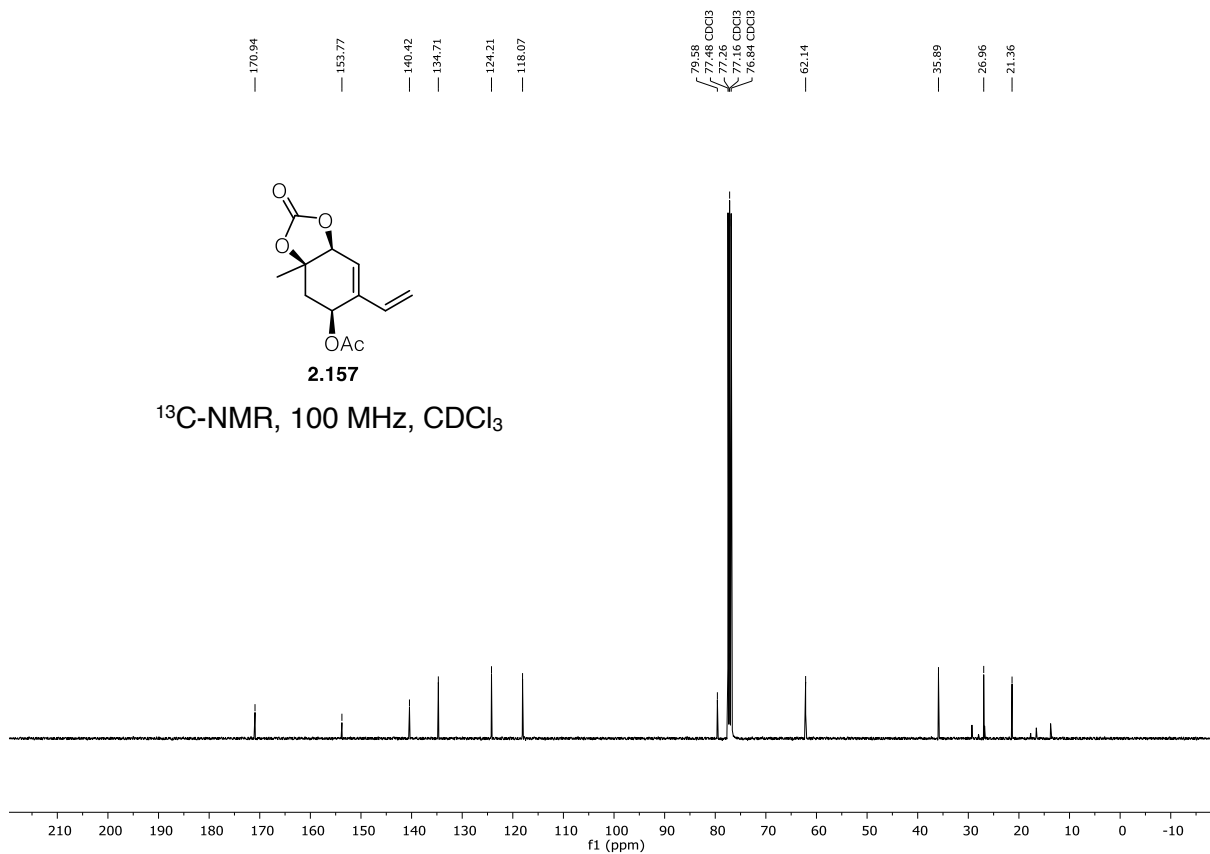
Chemical structure of **2.157** is shown above the spectrum.

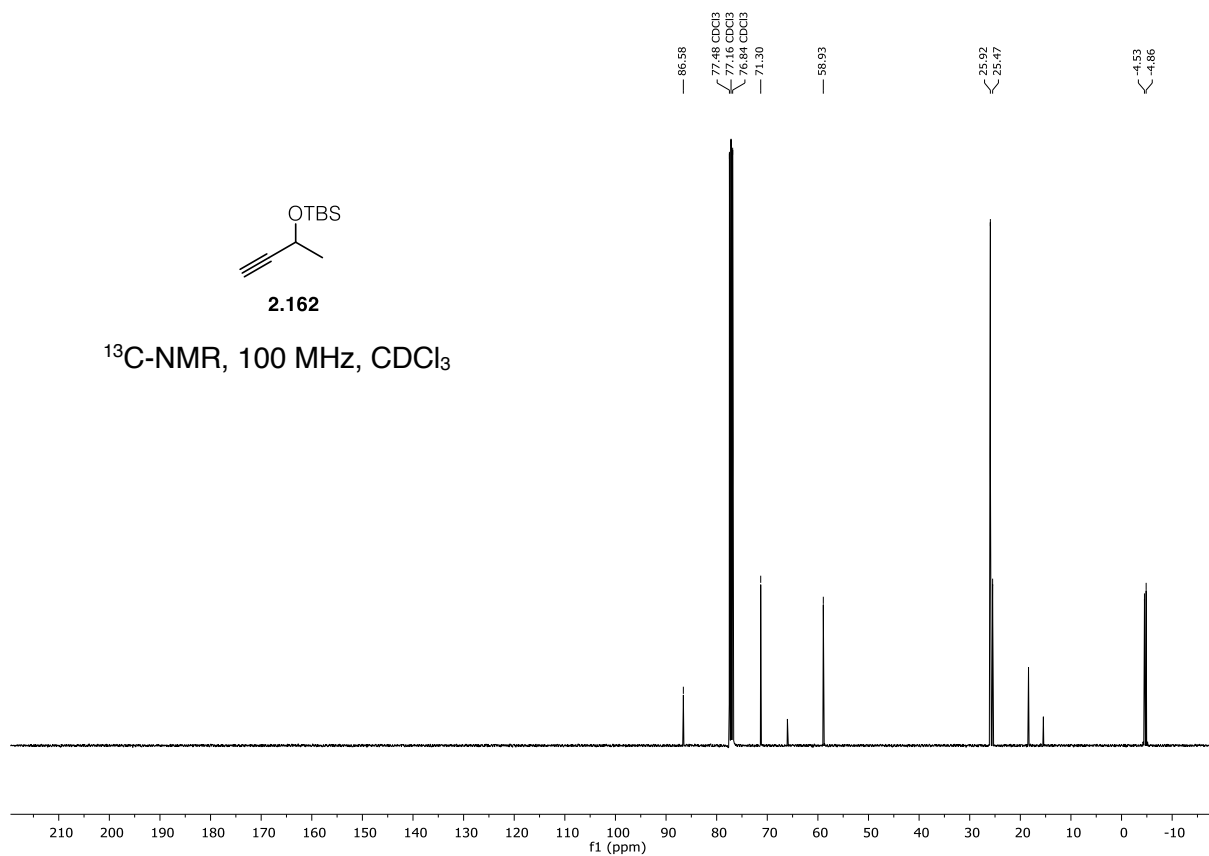
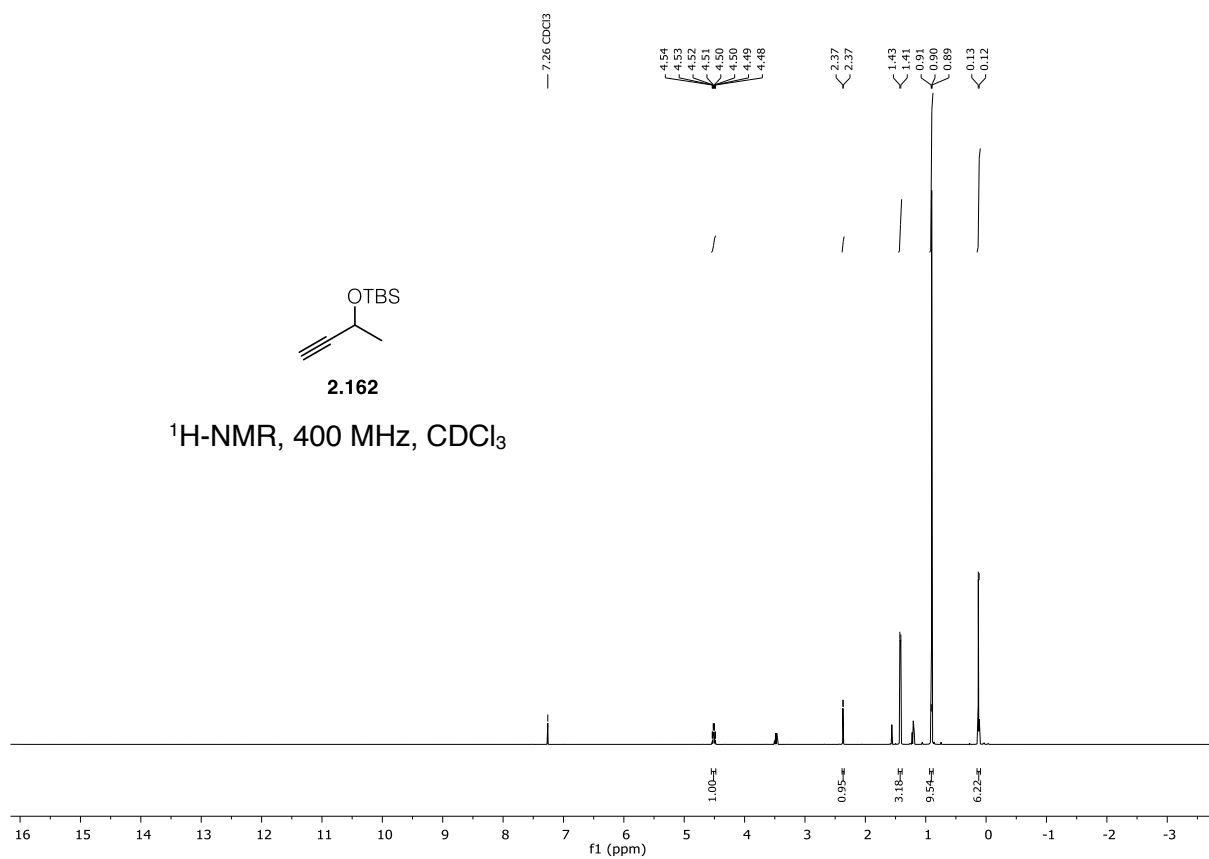
$^{13}\text{C-NMR}$ spectrum (100 MHz, CDCl_3) showing peaks (ppm):

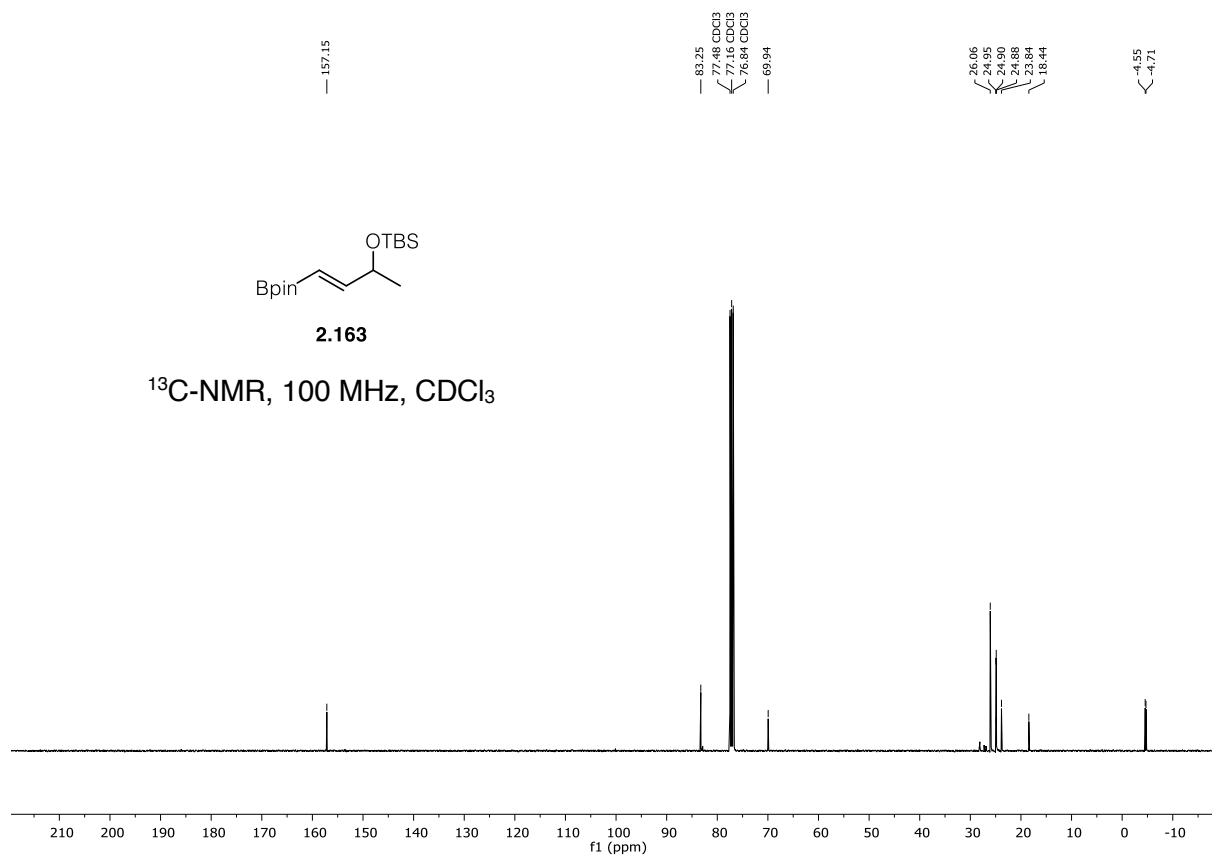
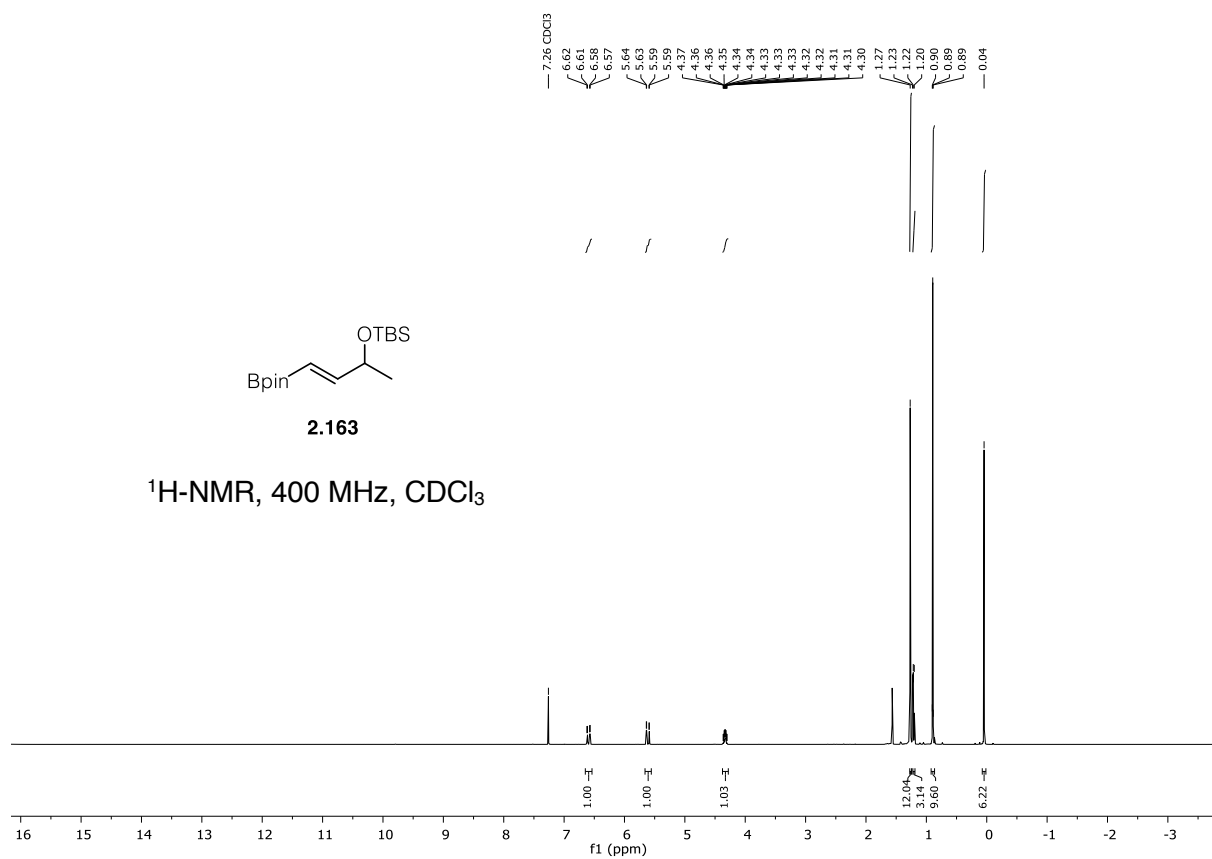
170.94
153.77
140.42
134.71
124.21
118.07
79.58
77.48
77.26
77.16
76.84
62.14
35.89
26.96
21.36

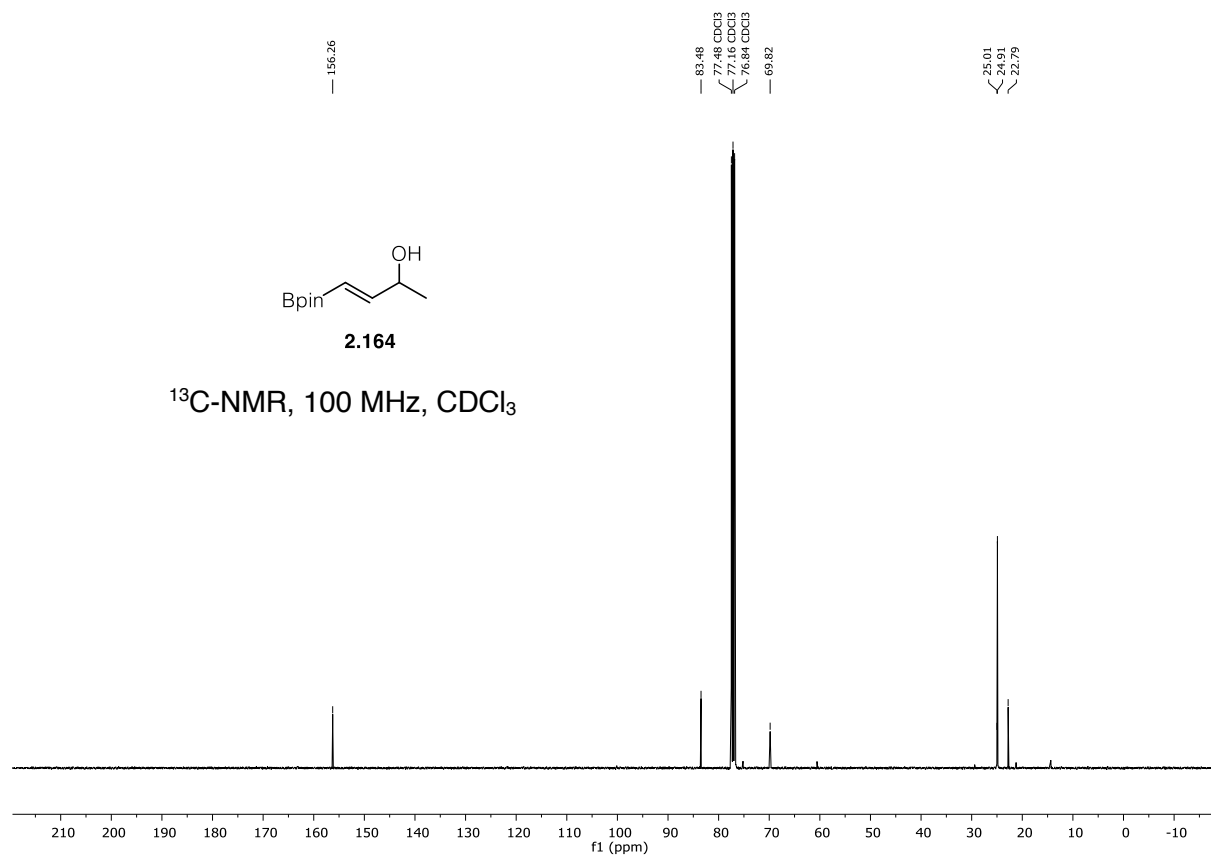
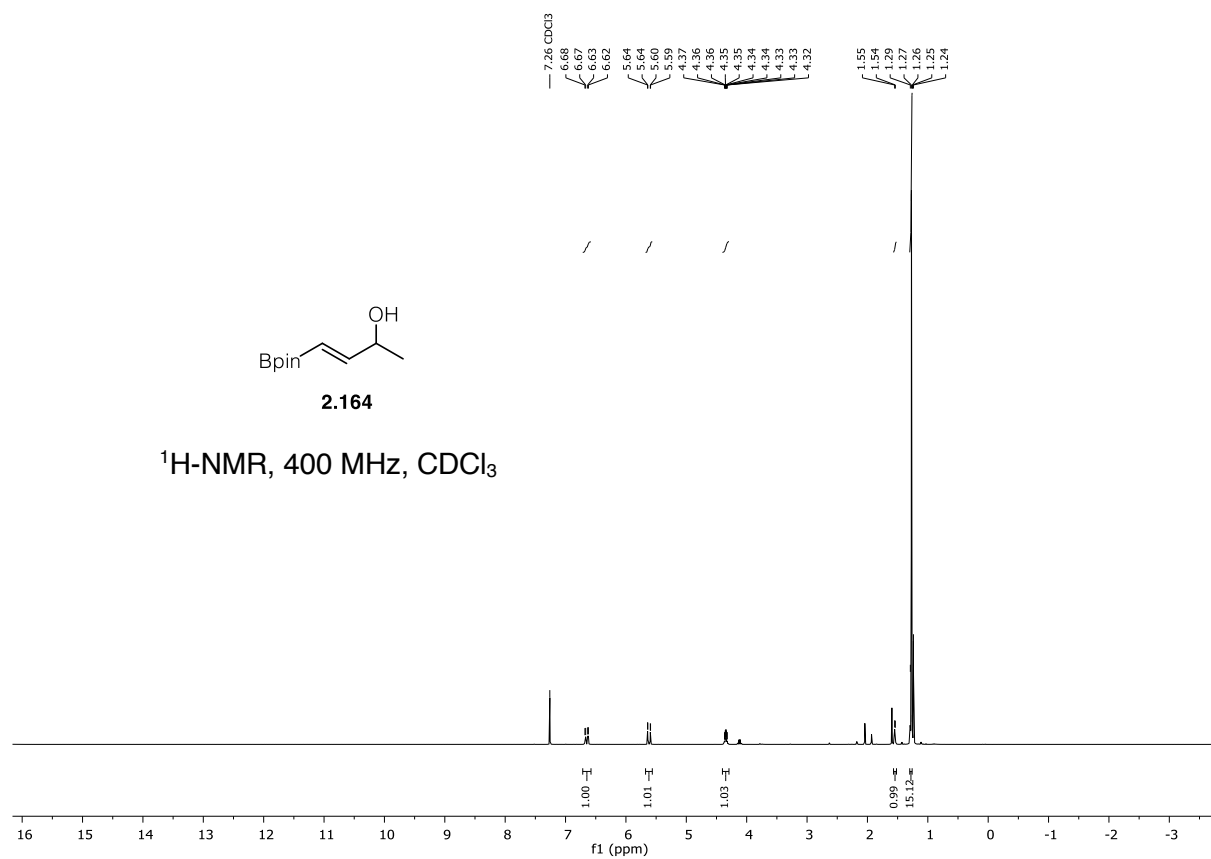


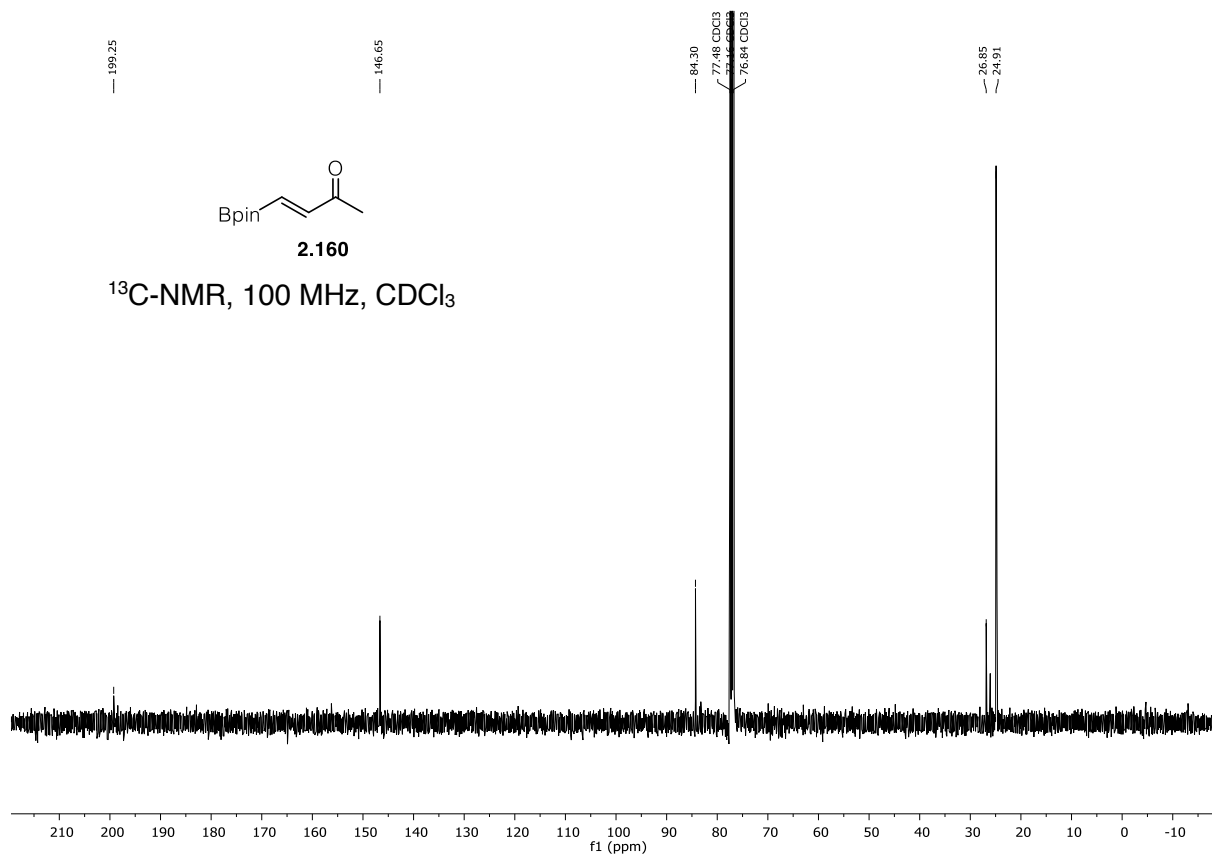
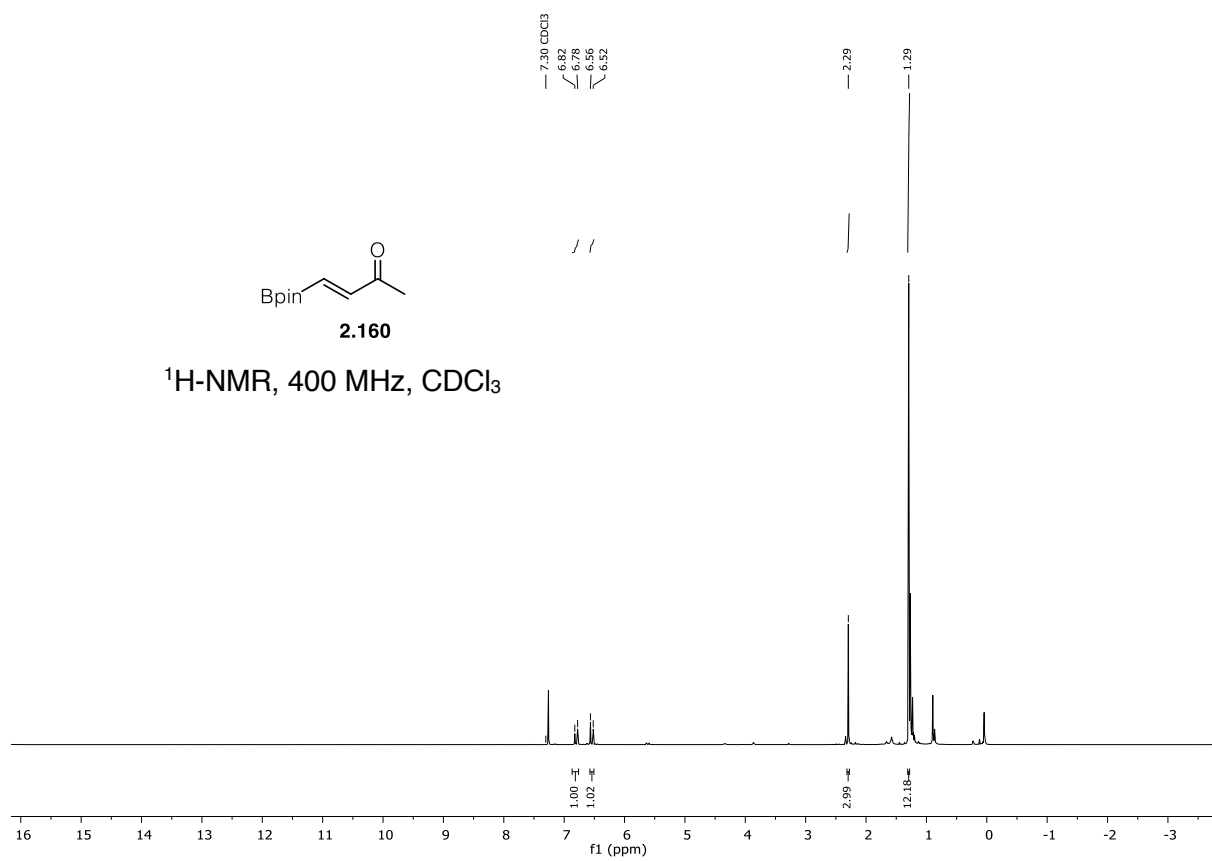
$^{13}\text{C-NMR}$, 100 MHz, CDCl_3

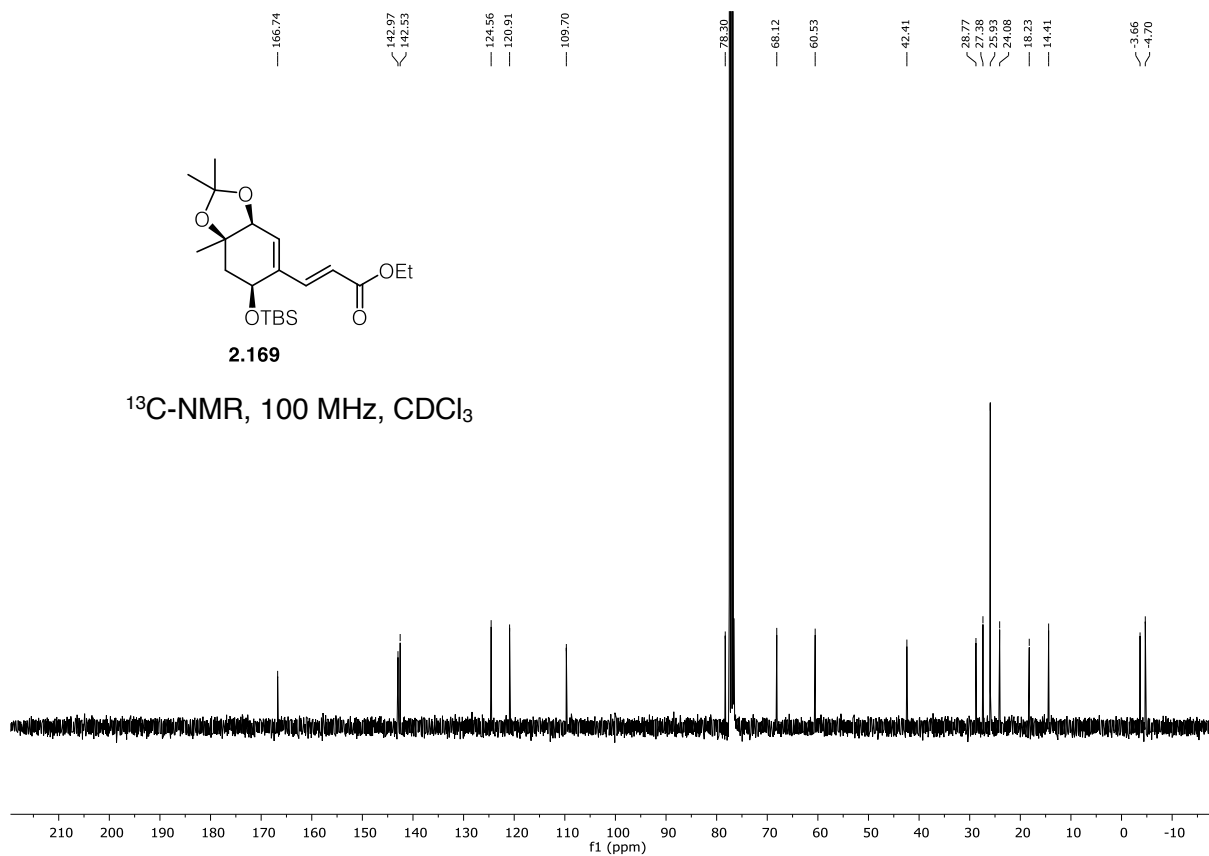
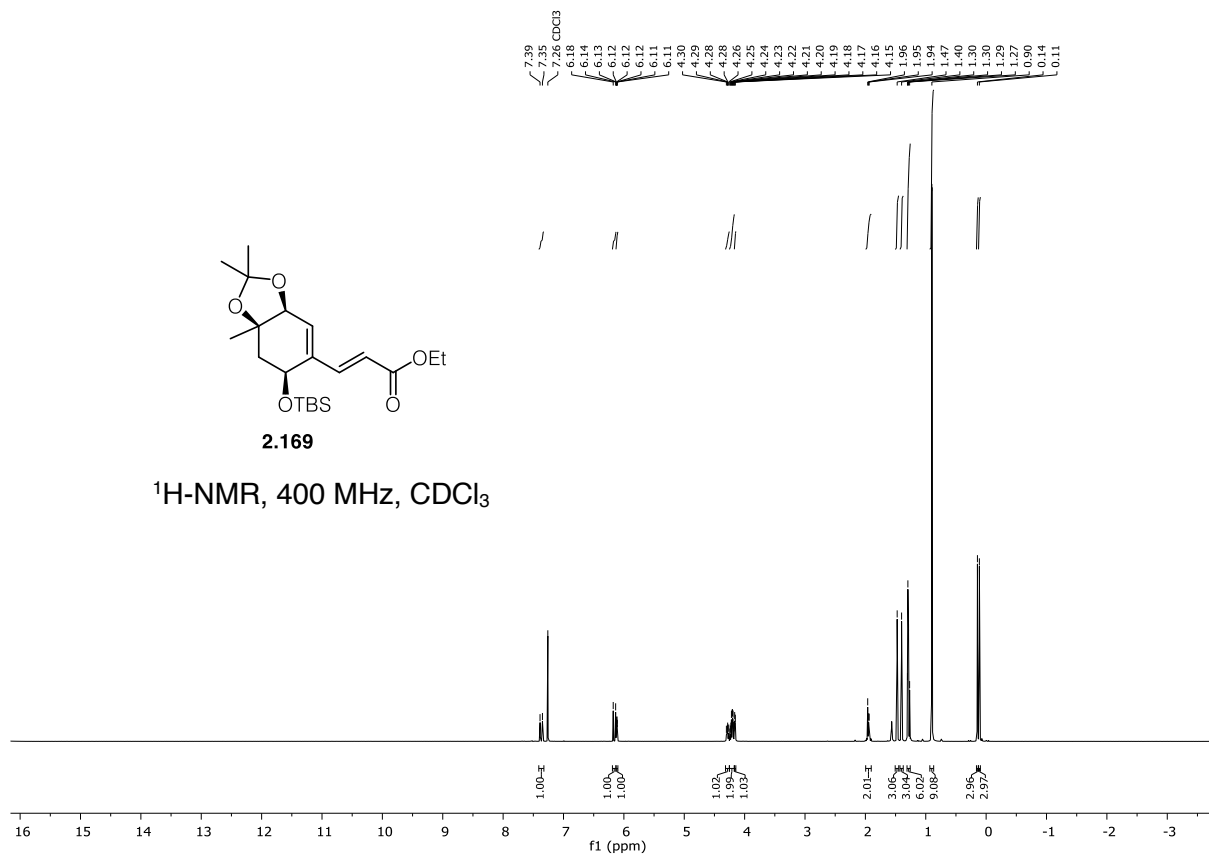


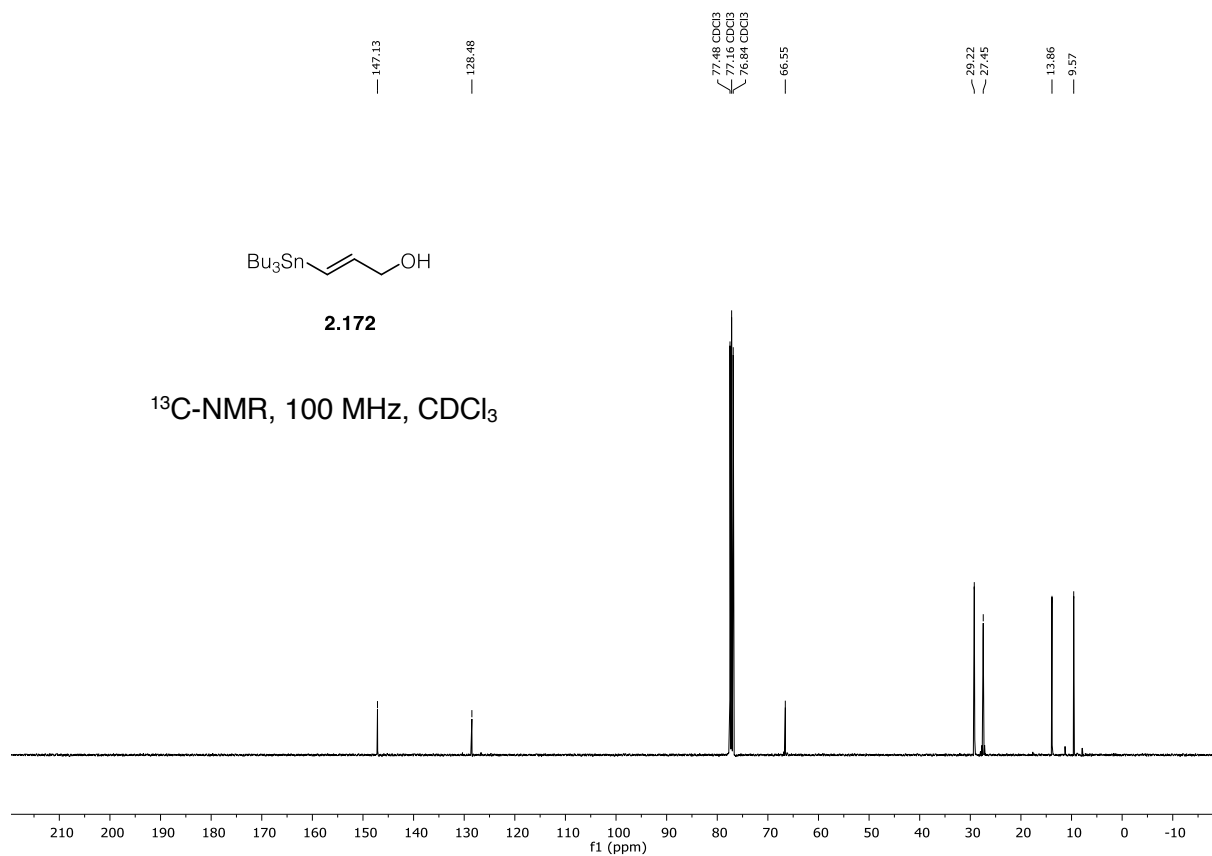
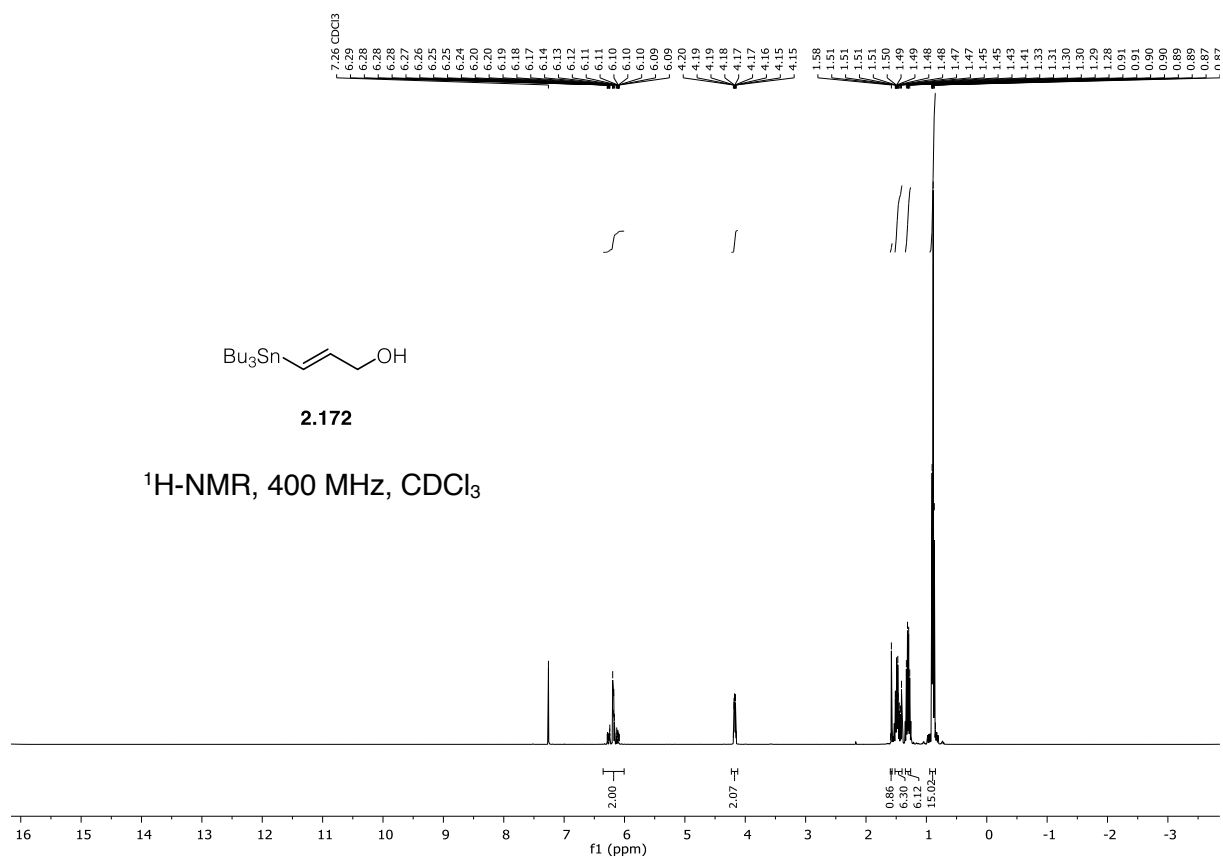


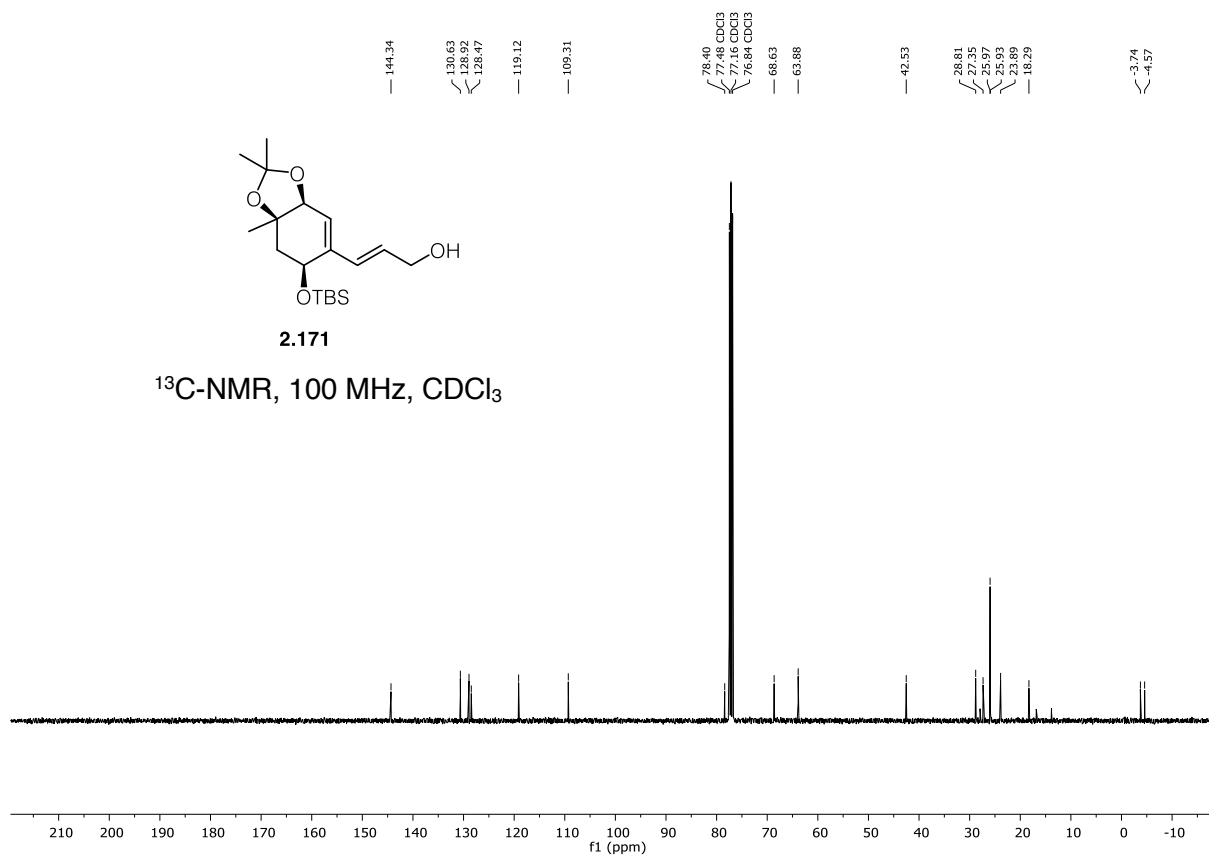
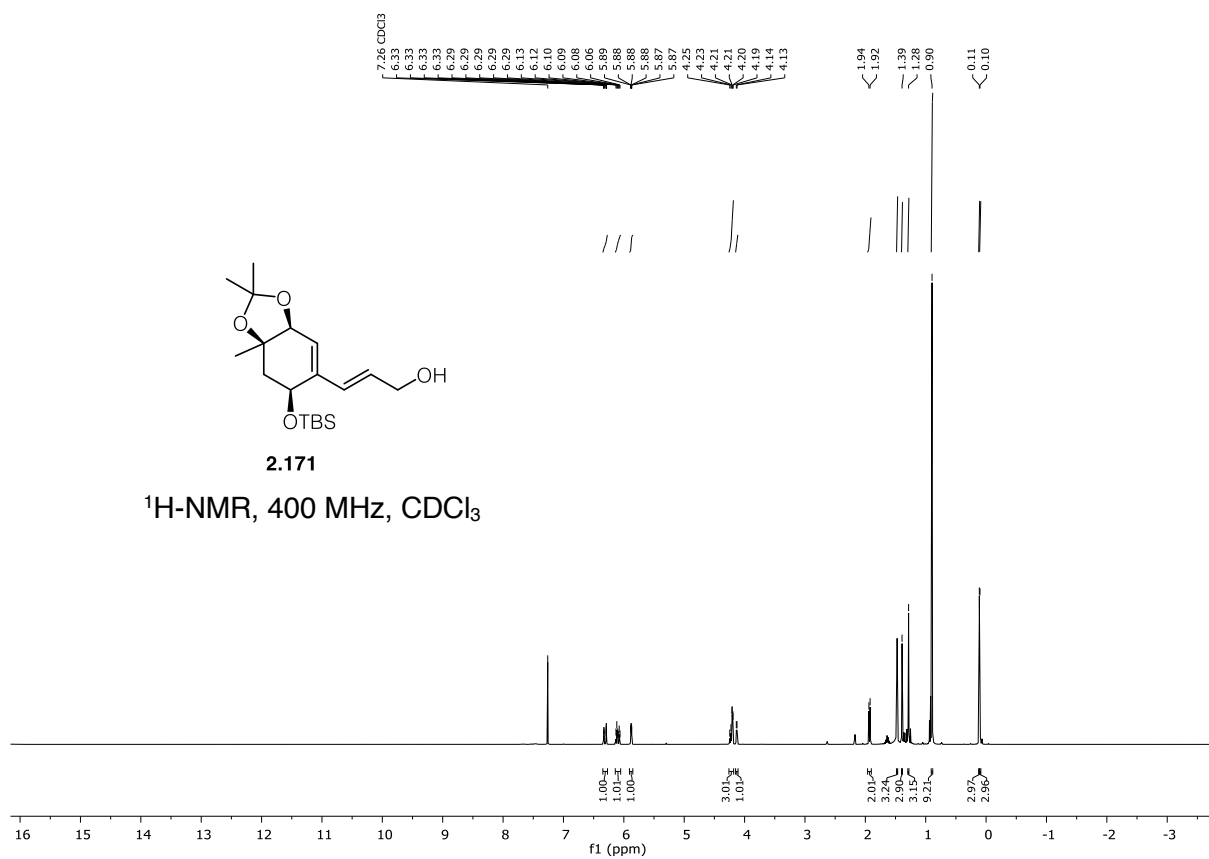


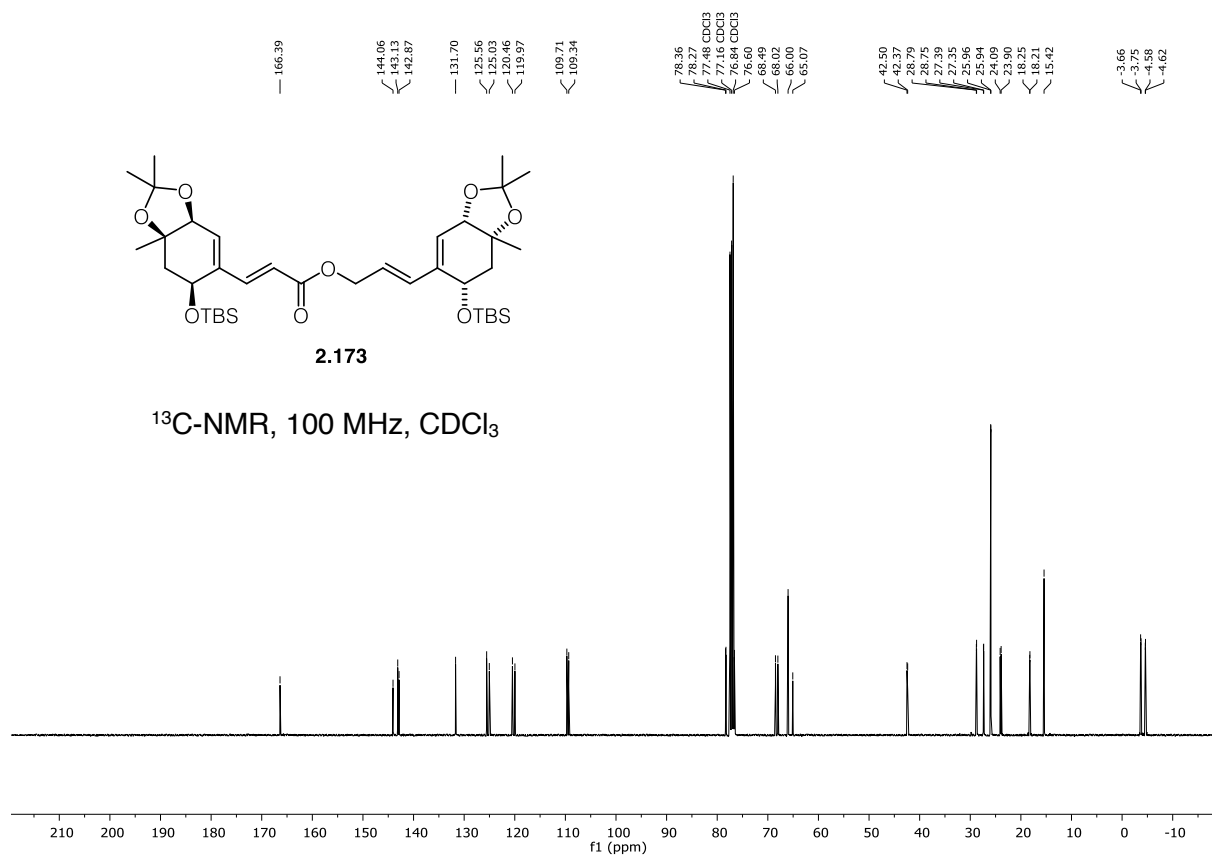
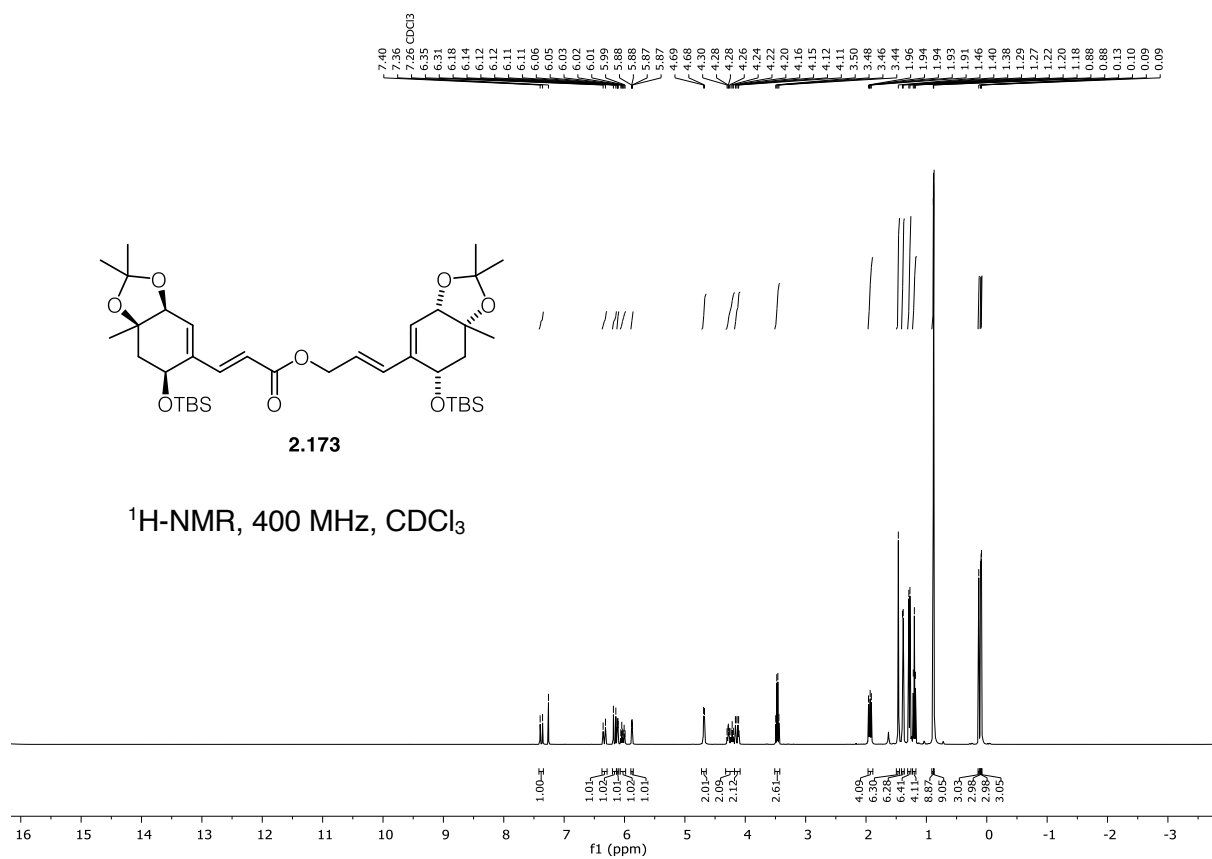


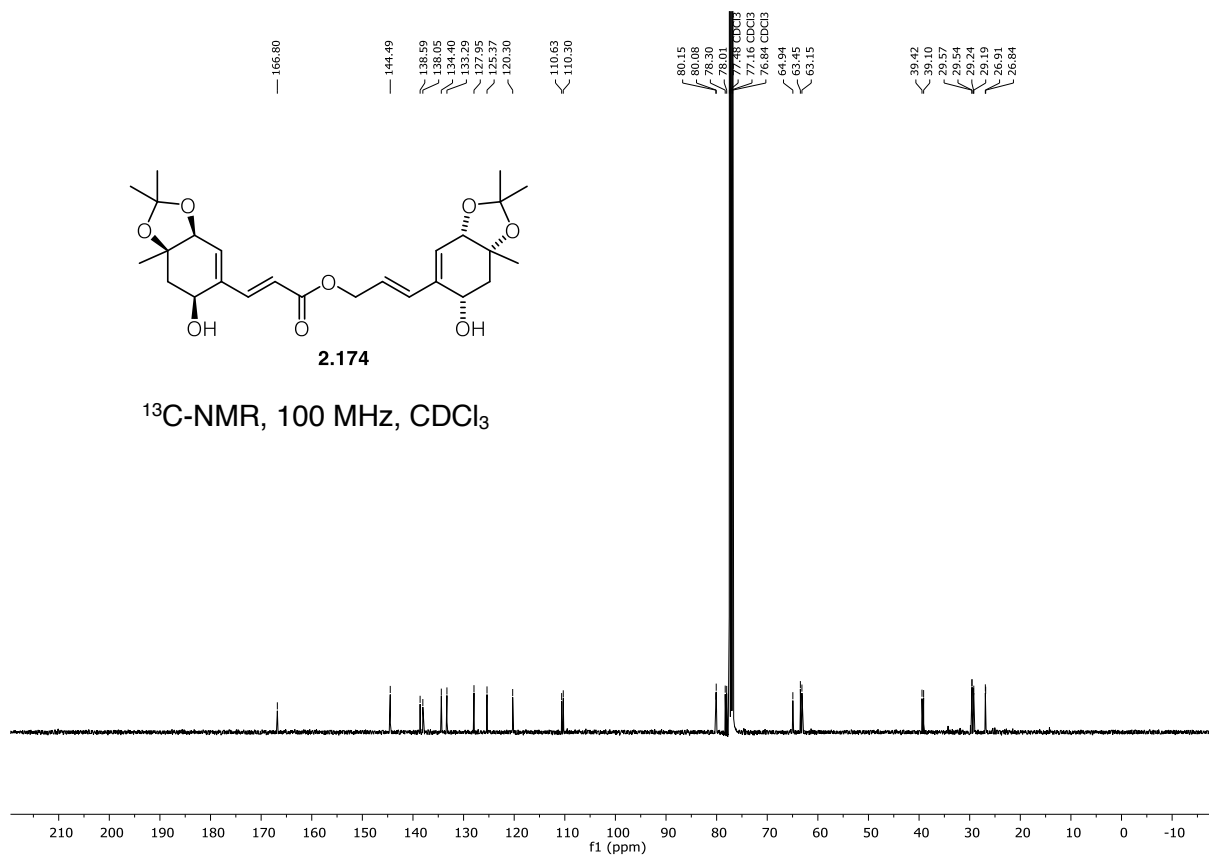
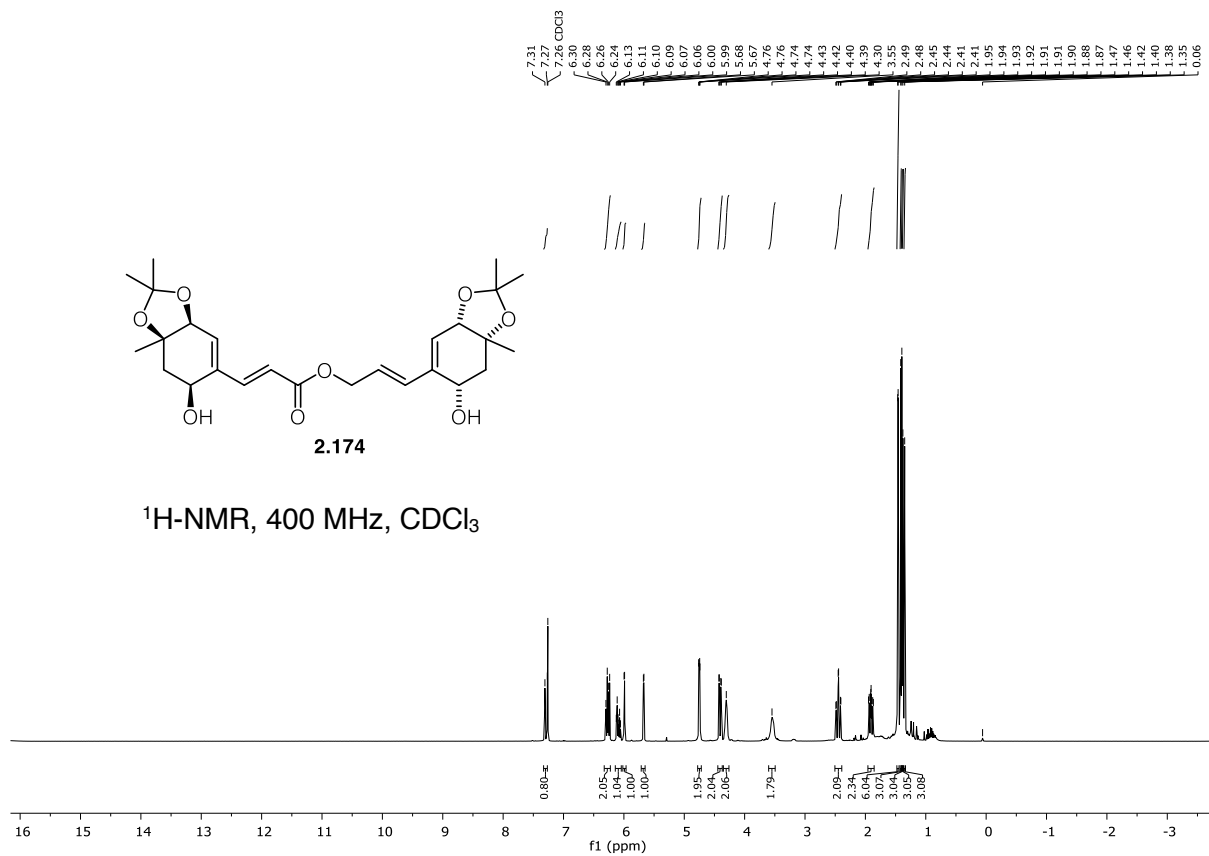


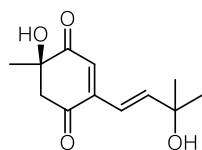




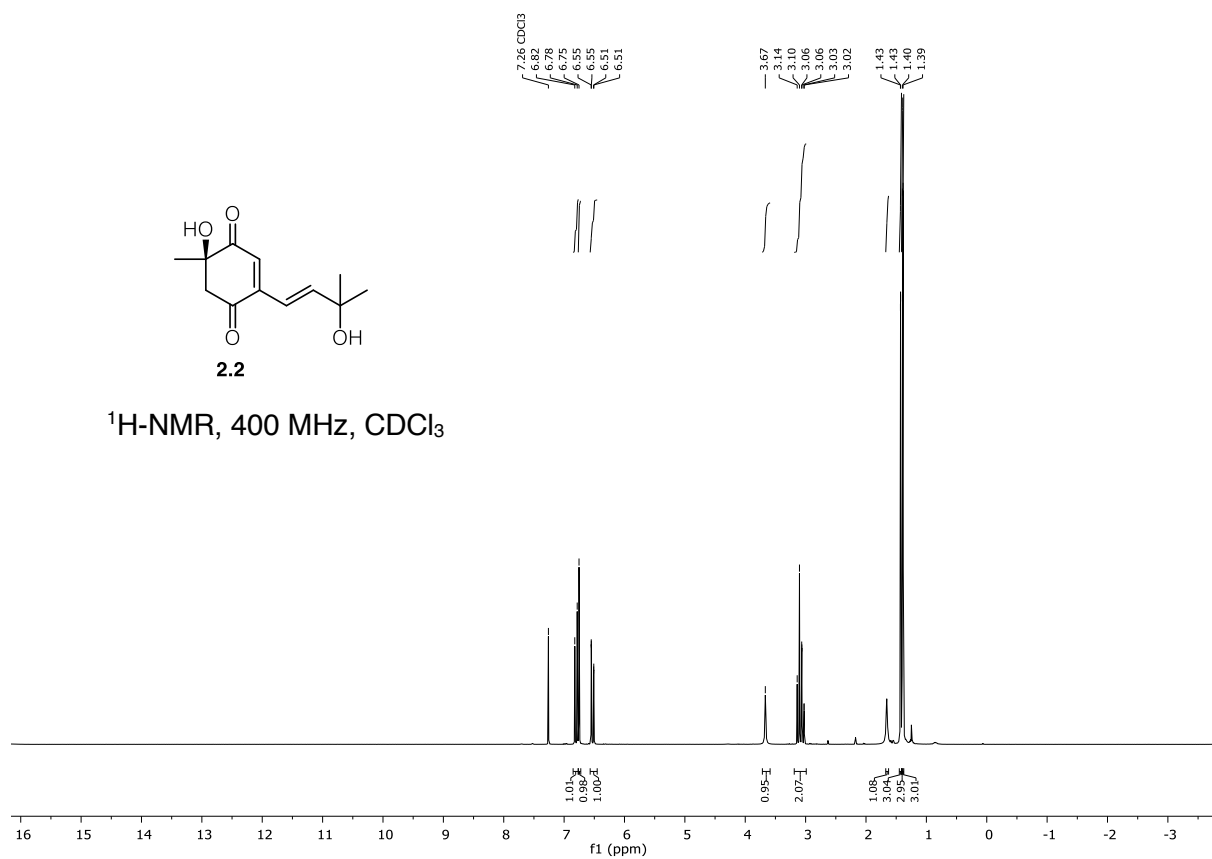








2.2

¹H-NMR, 400 MHz, CDCl₃

201.84

195.58

149.54

147.90

130.00

118.45

77.48 CDCl₃77.16 CDCl₃76.84 CDCl₃

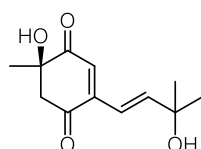
75.28

71.59

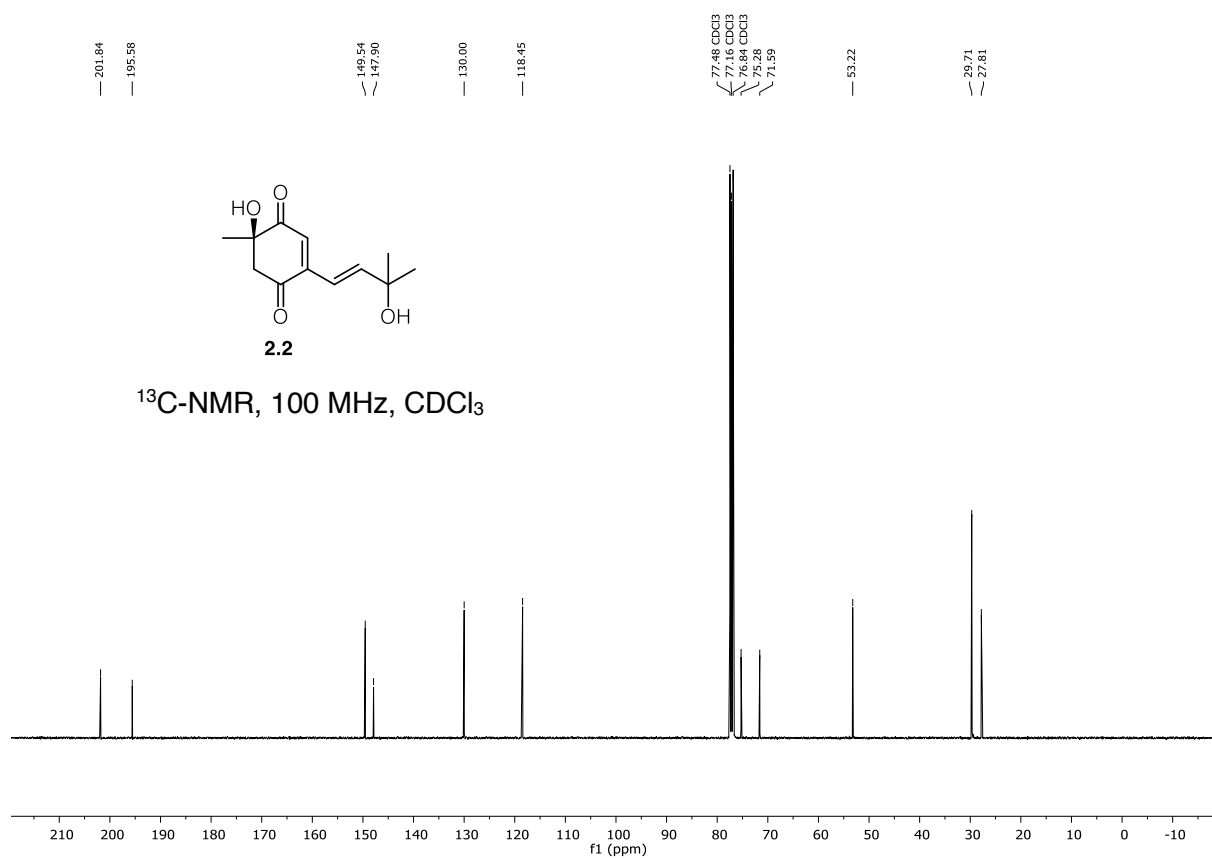
53.22

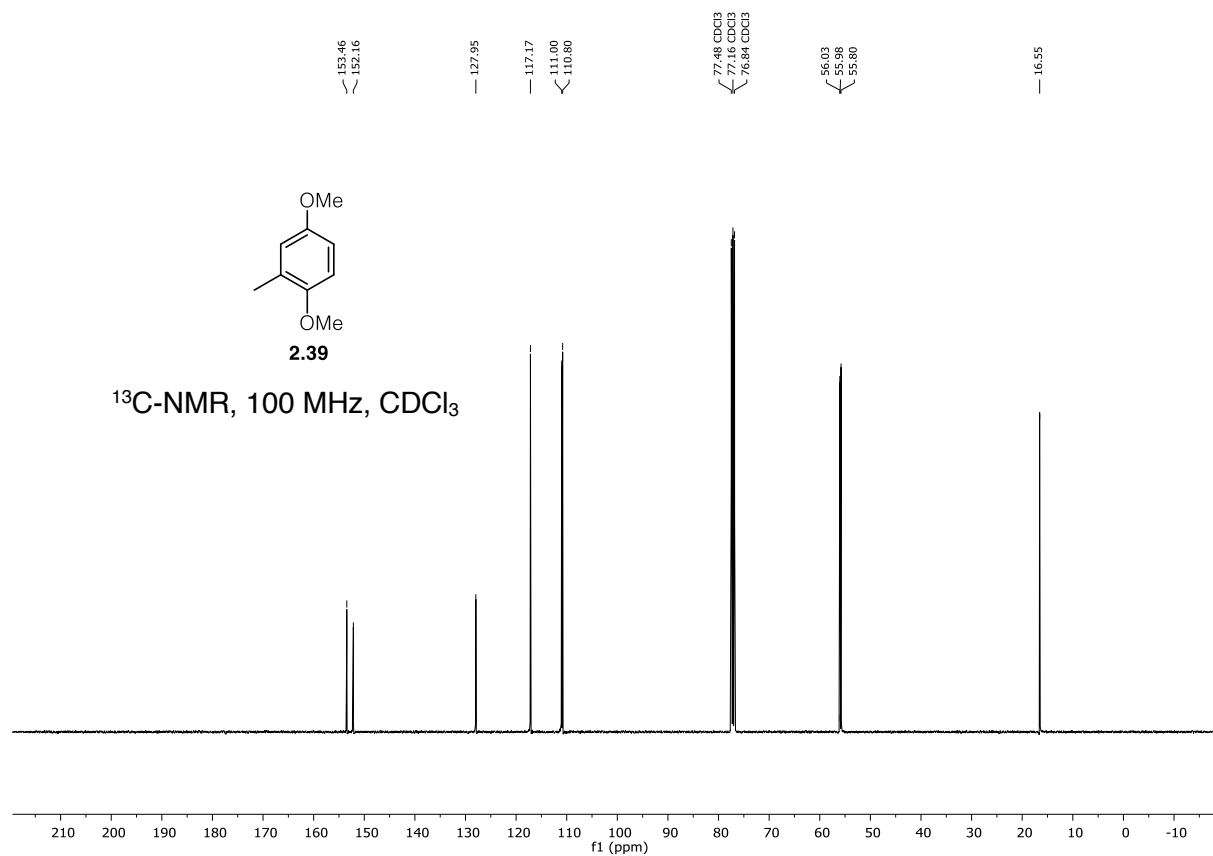
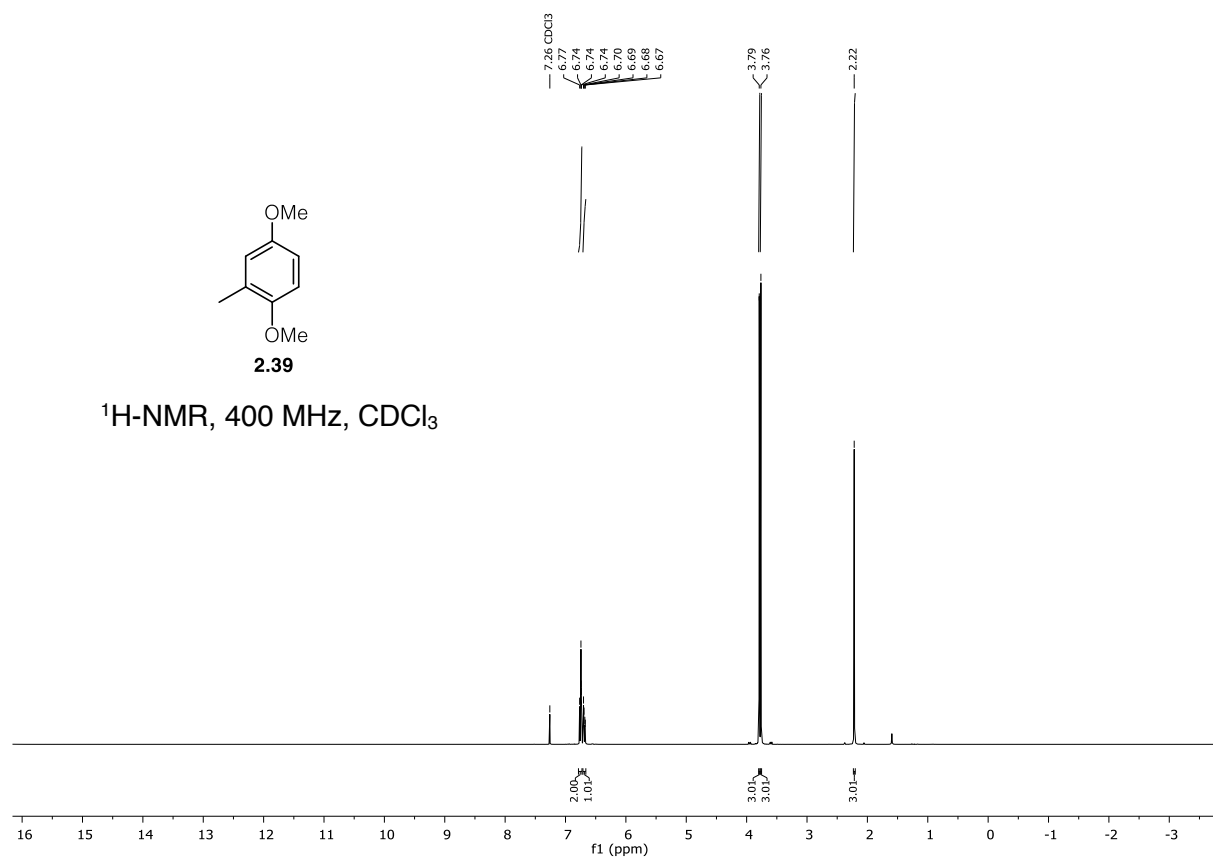
39.71

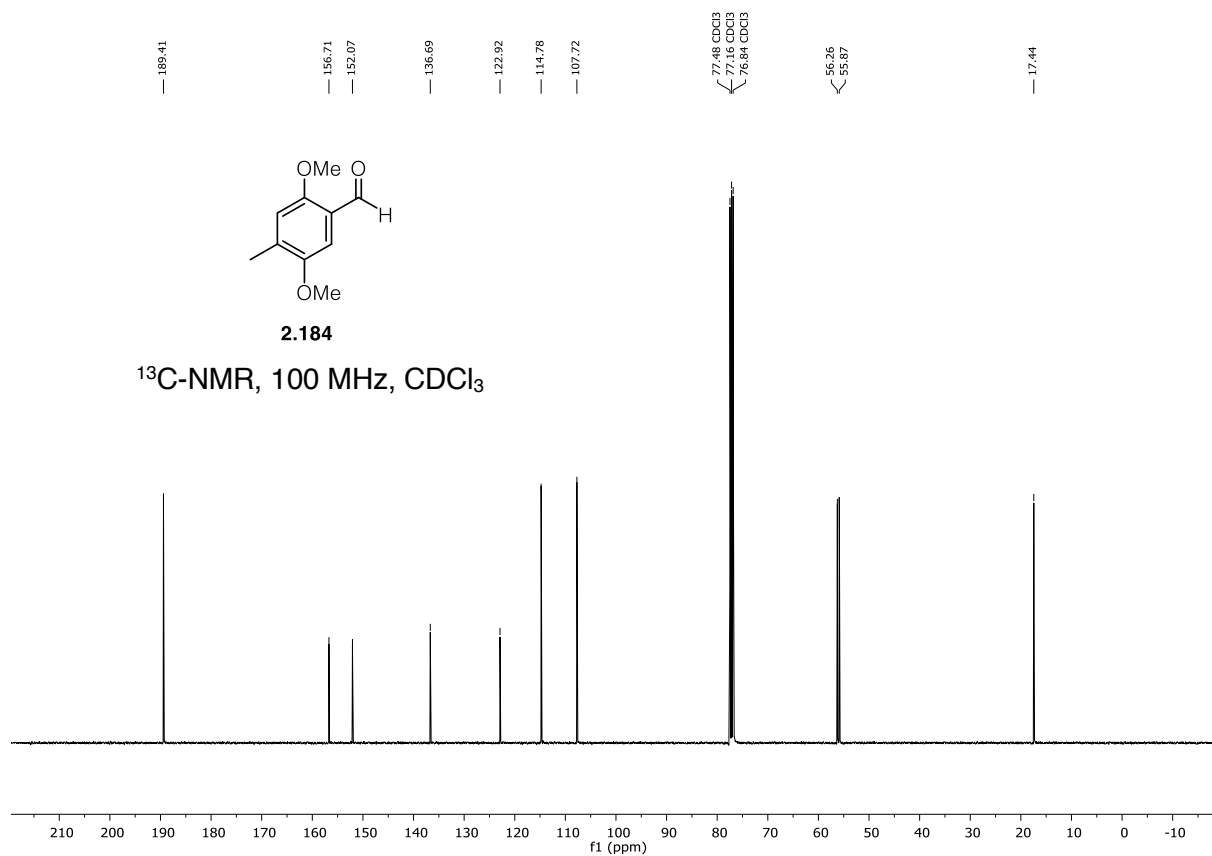
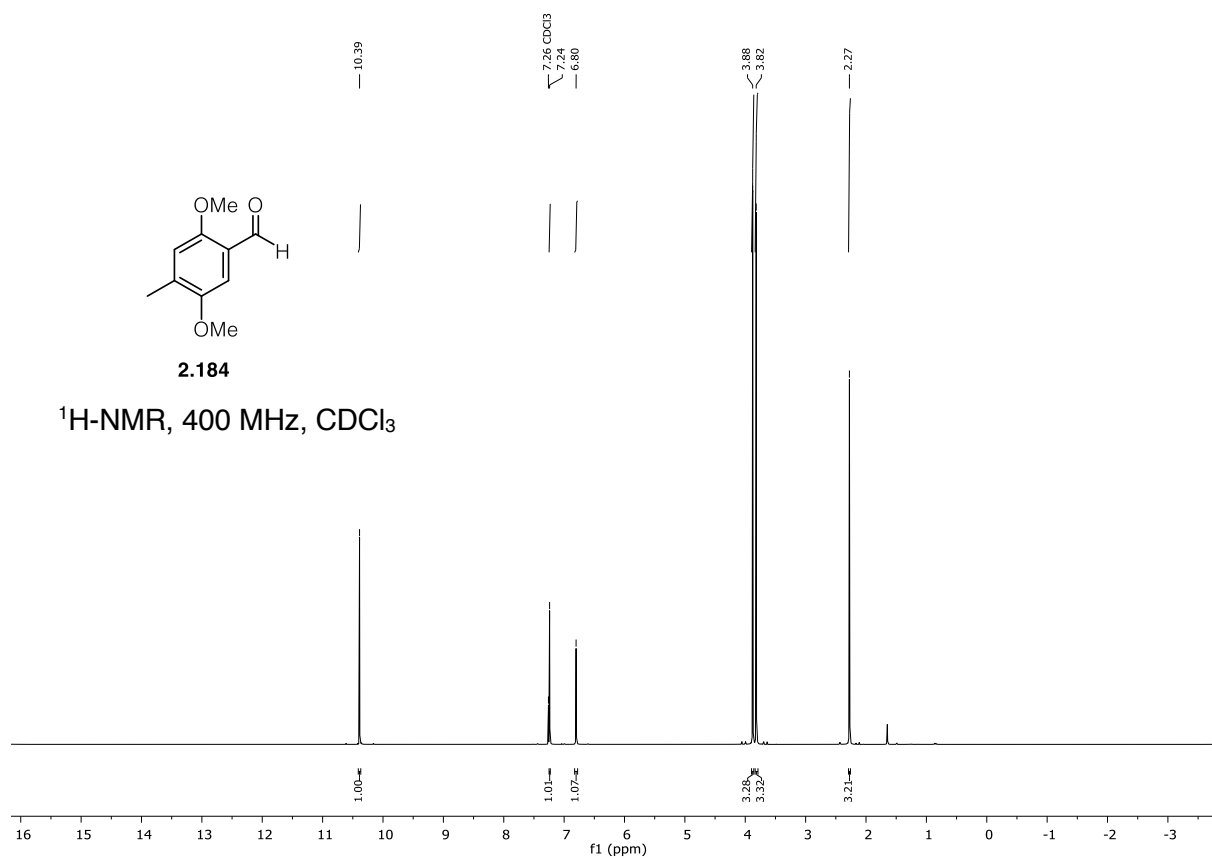
37.81

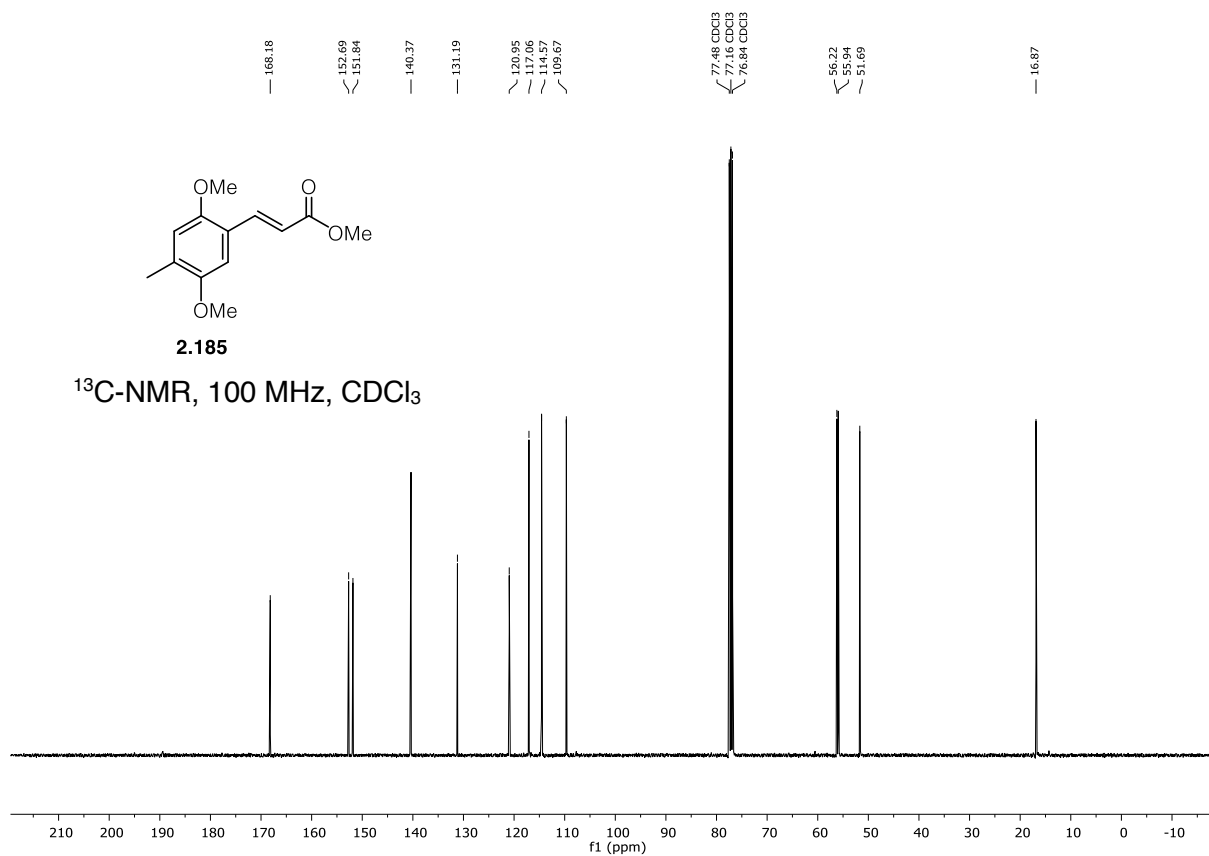
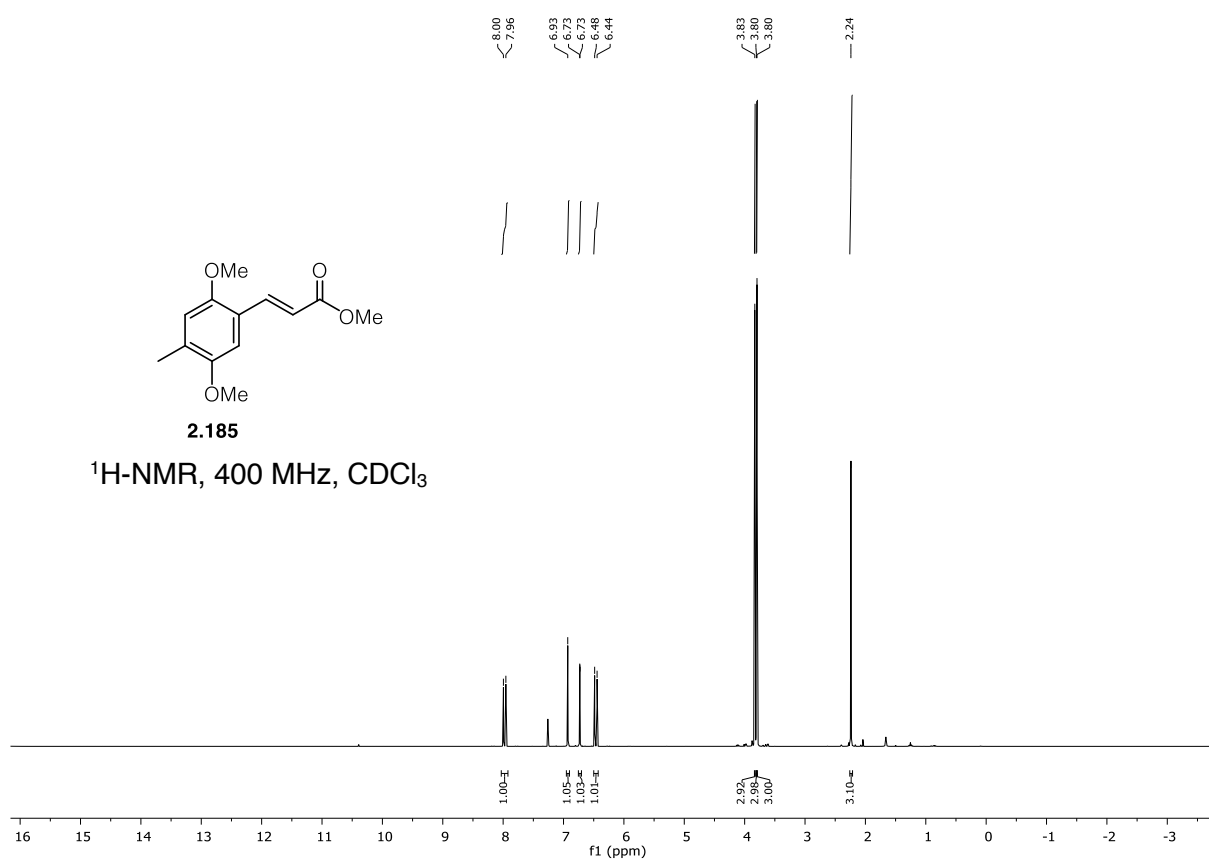


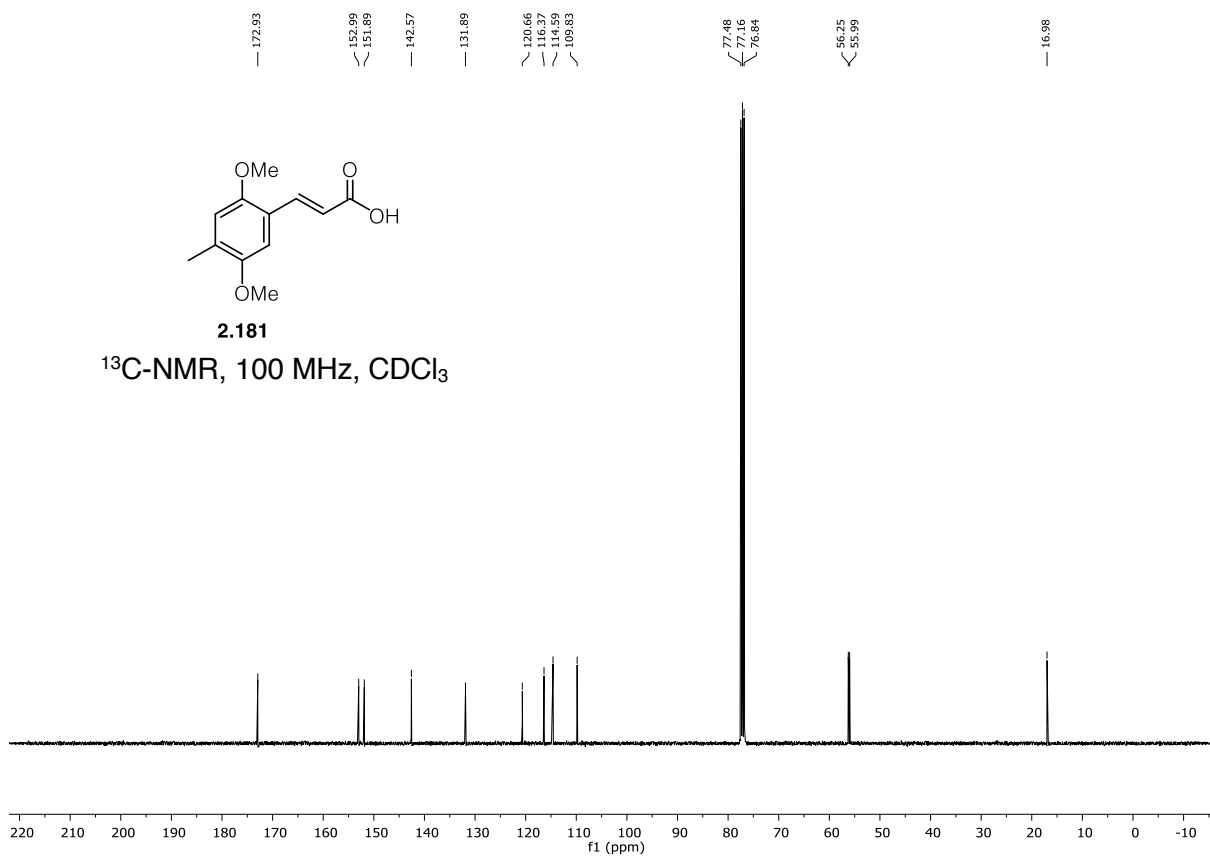
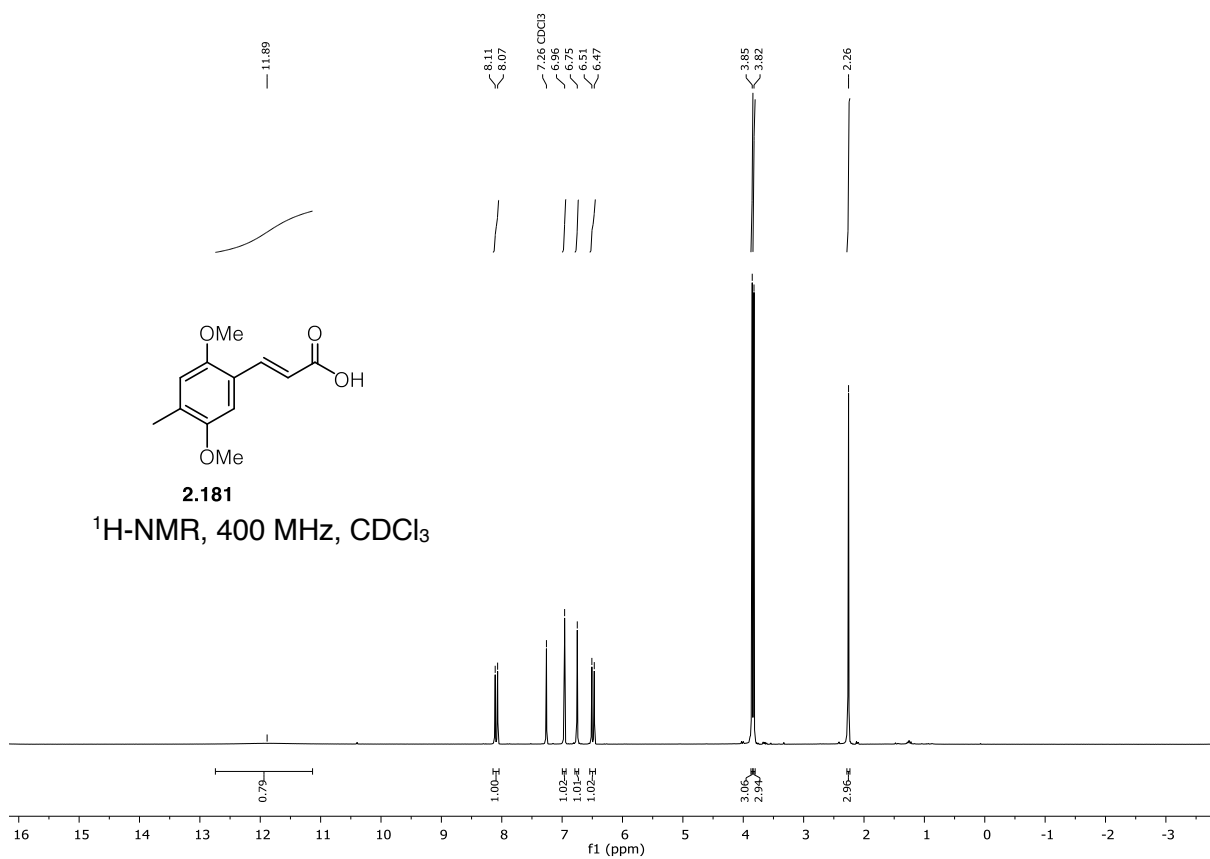
2.2

¹³C-NMR, 100 MHz, CDCl₃

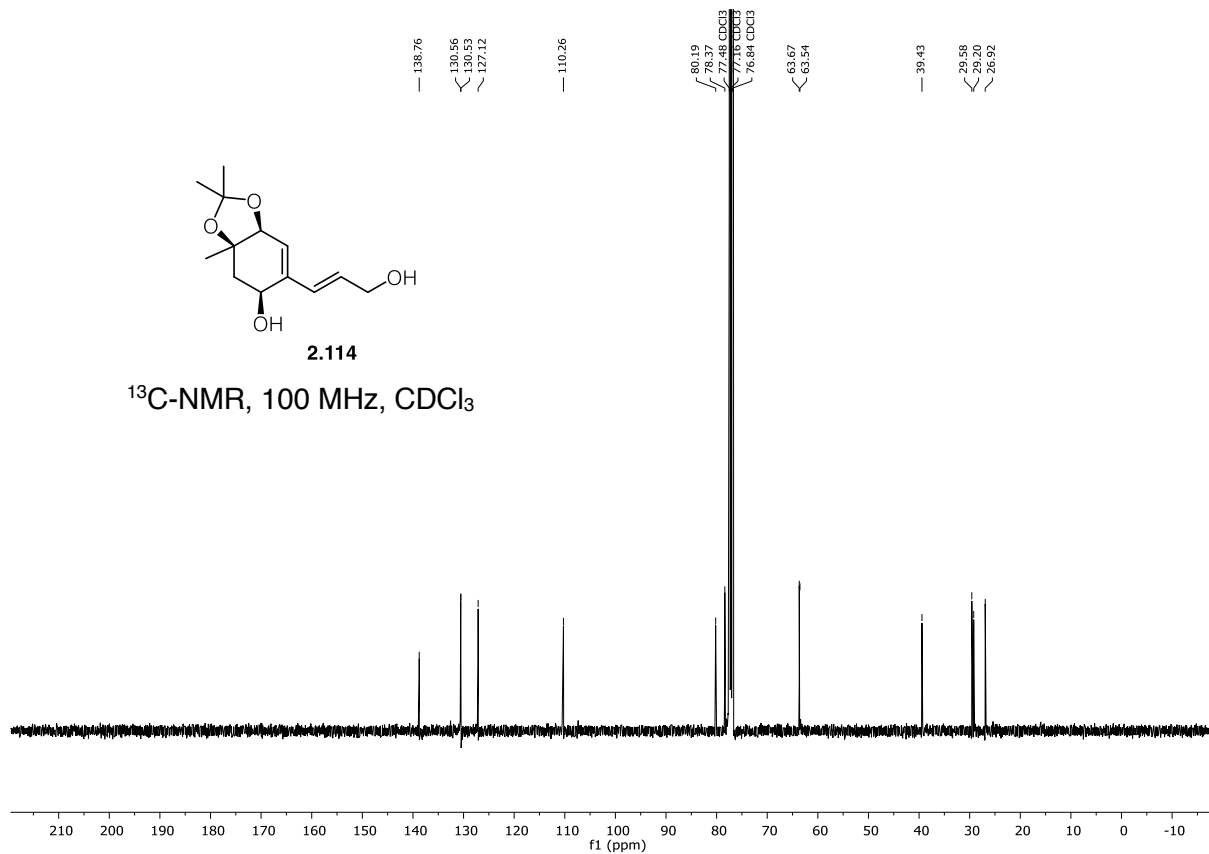
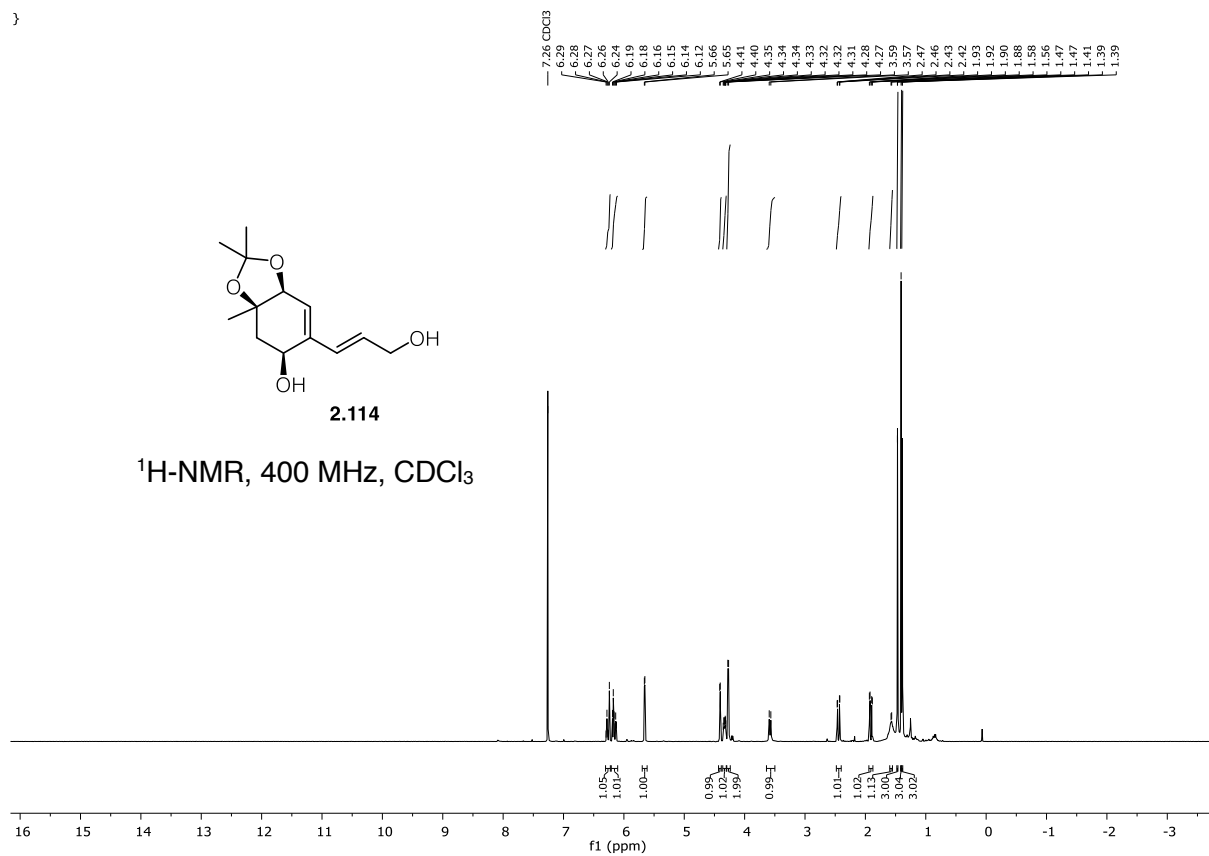


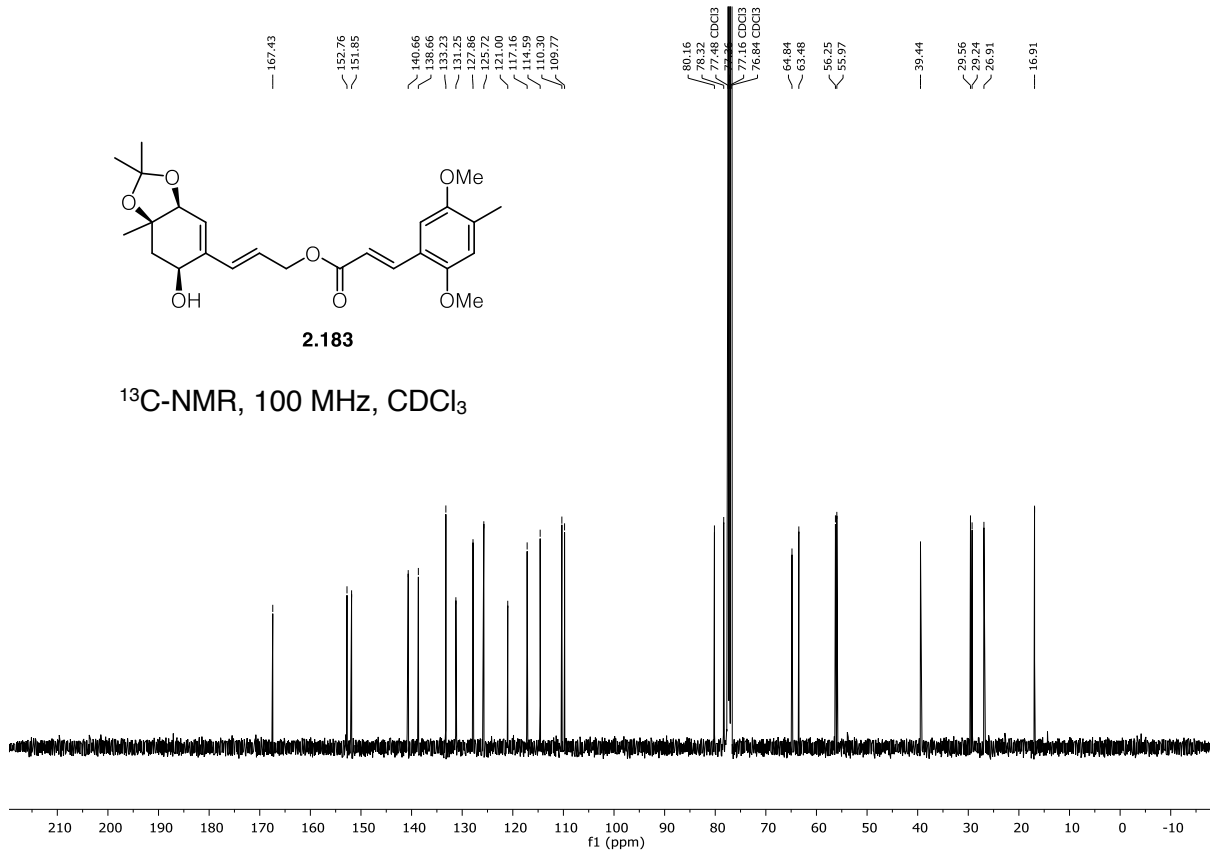
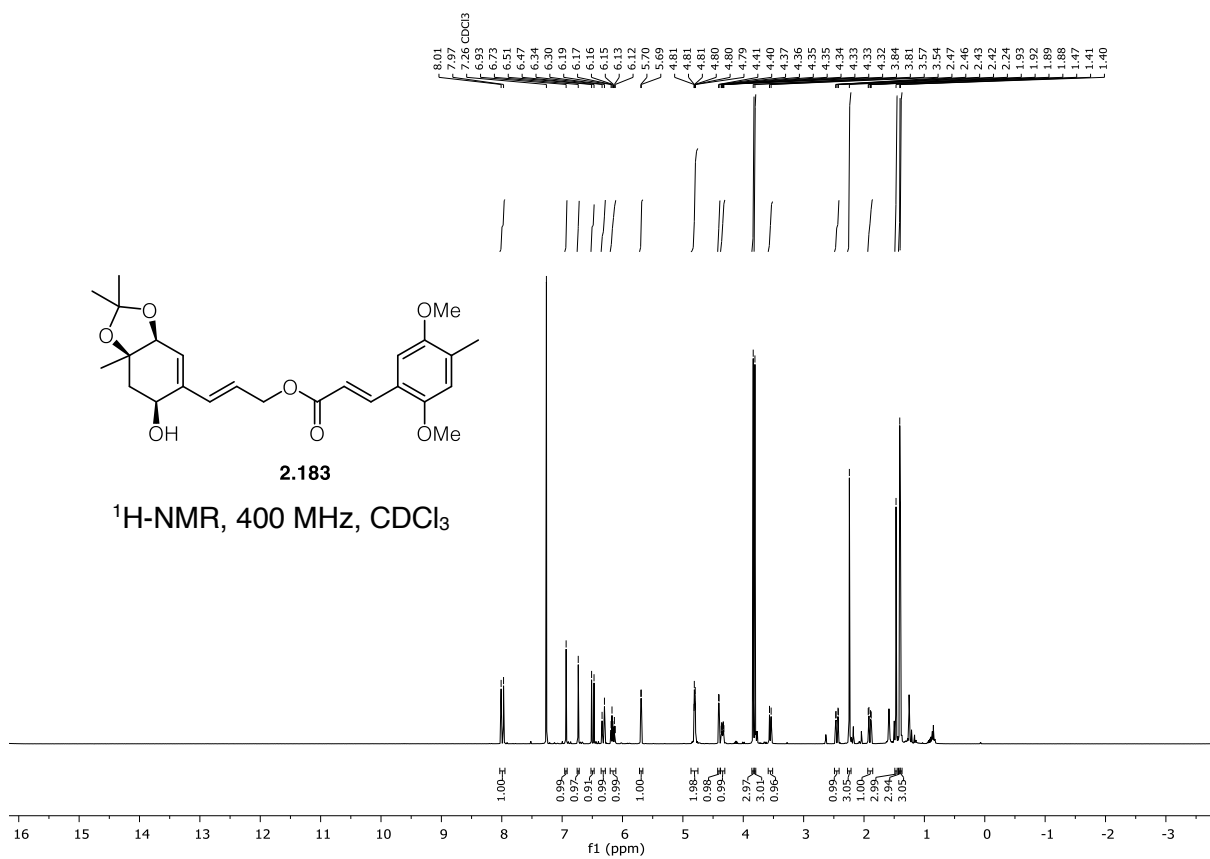


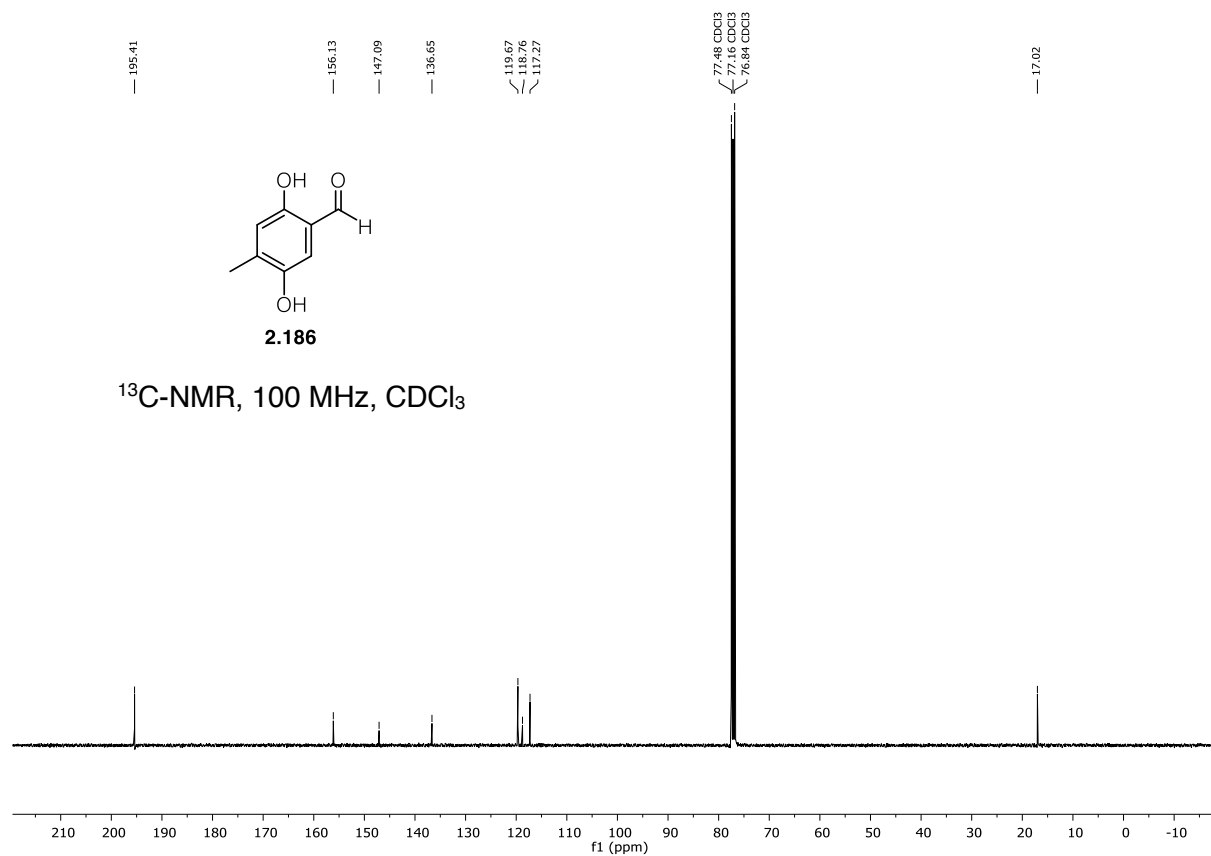
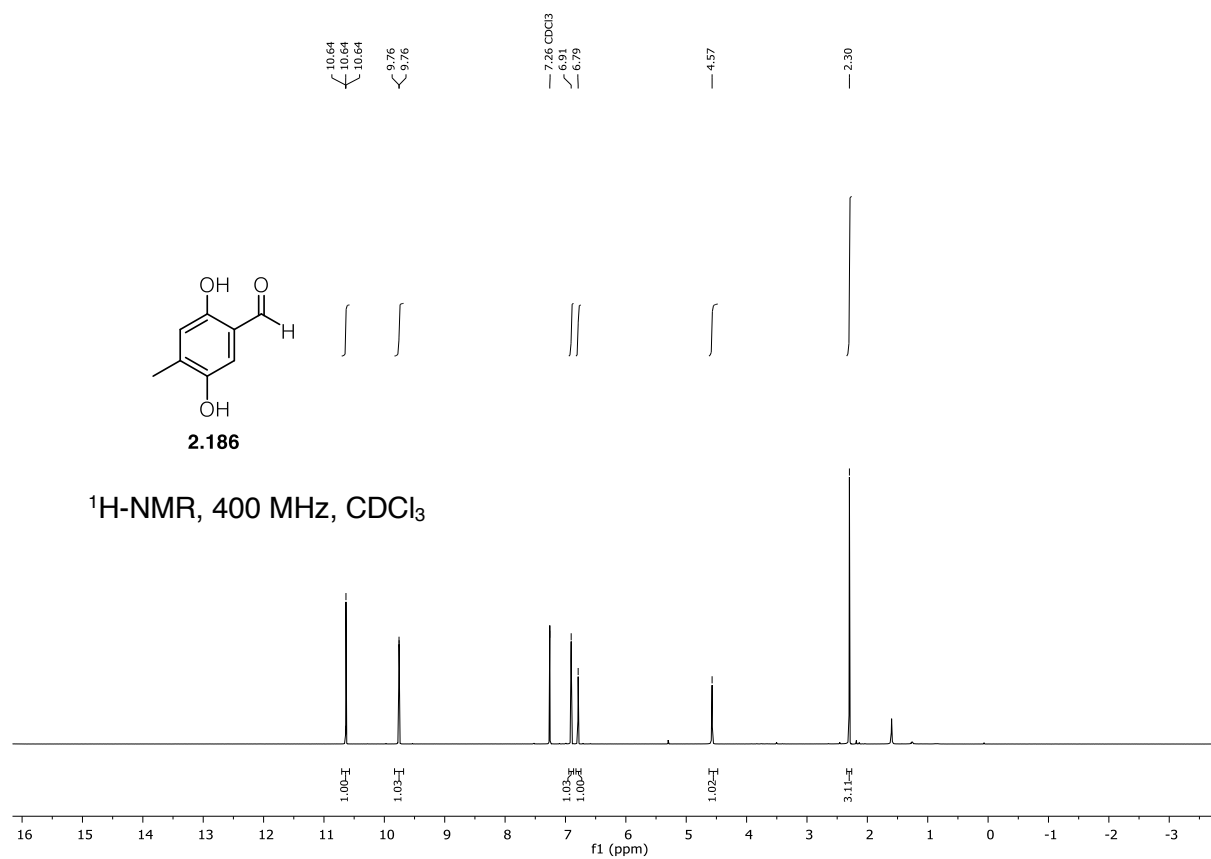


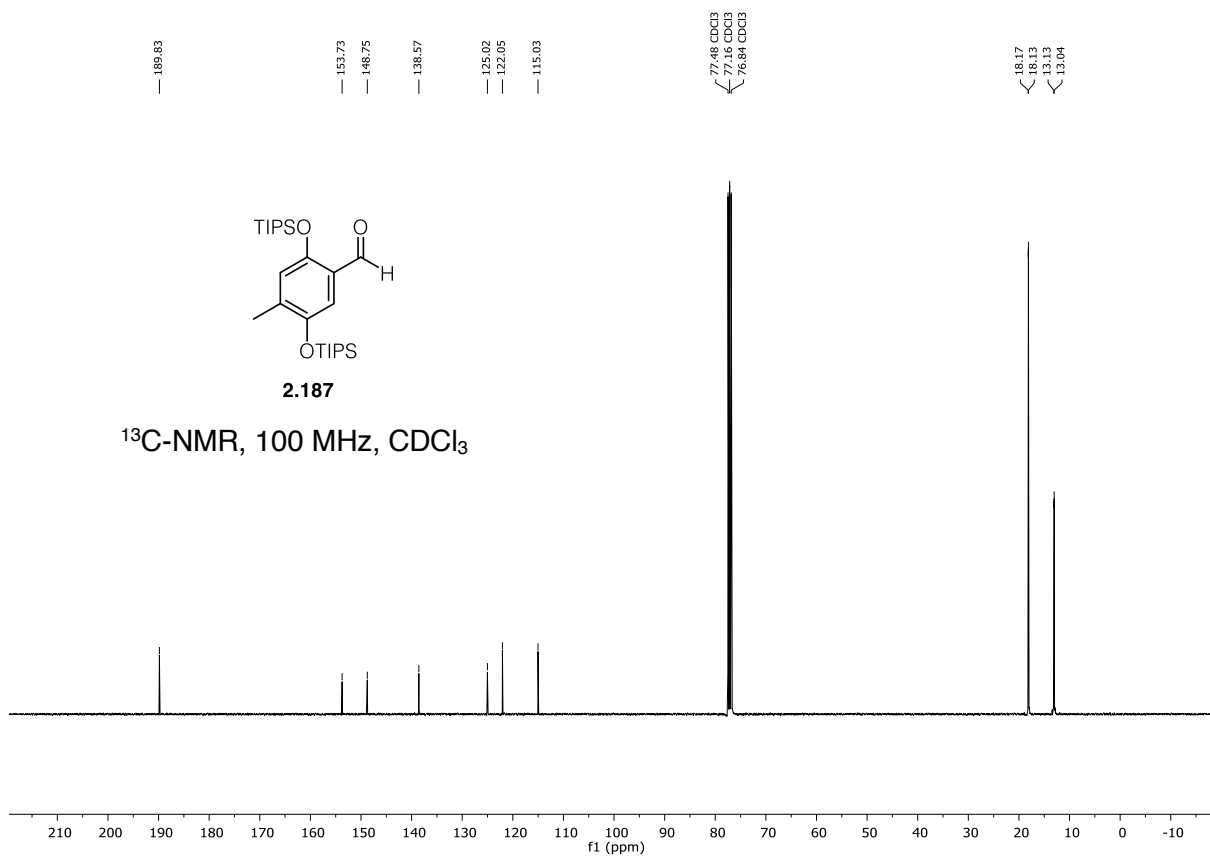
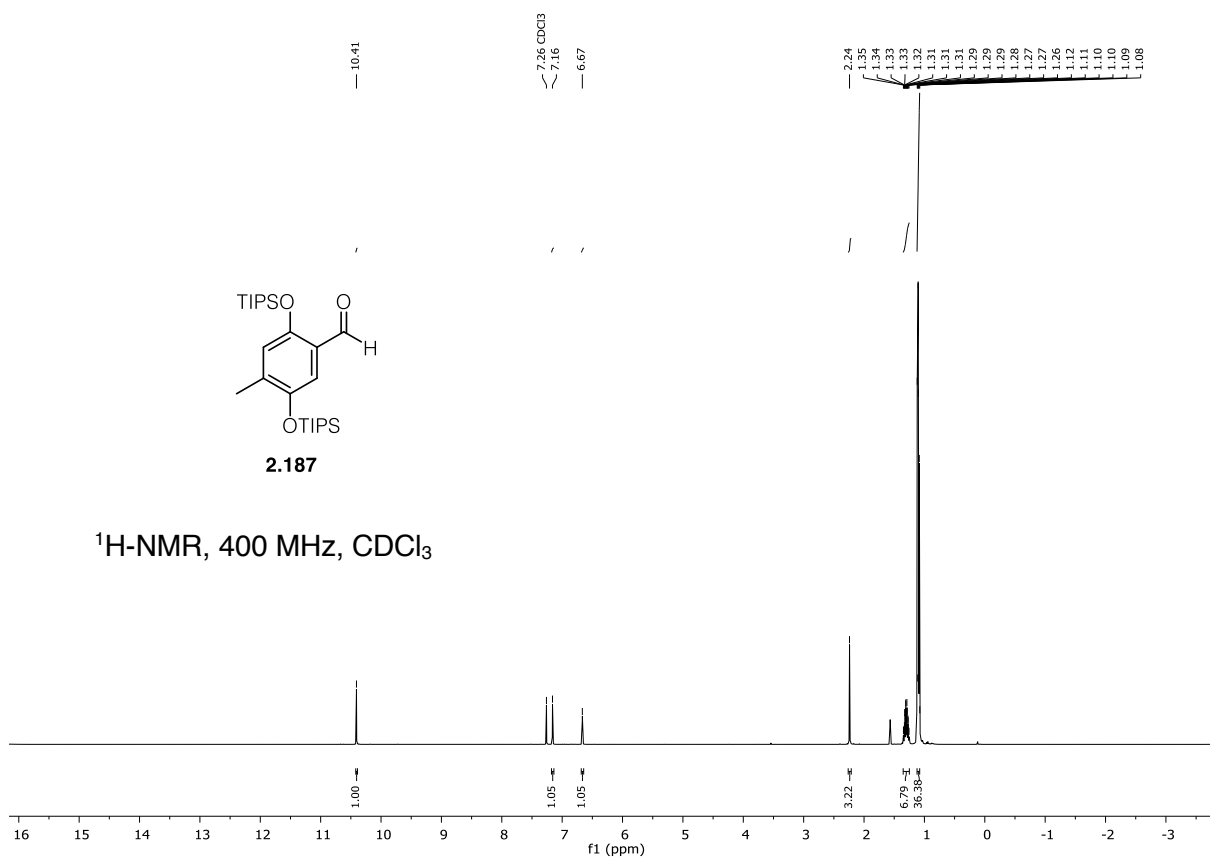


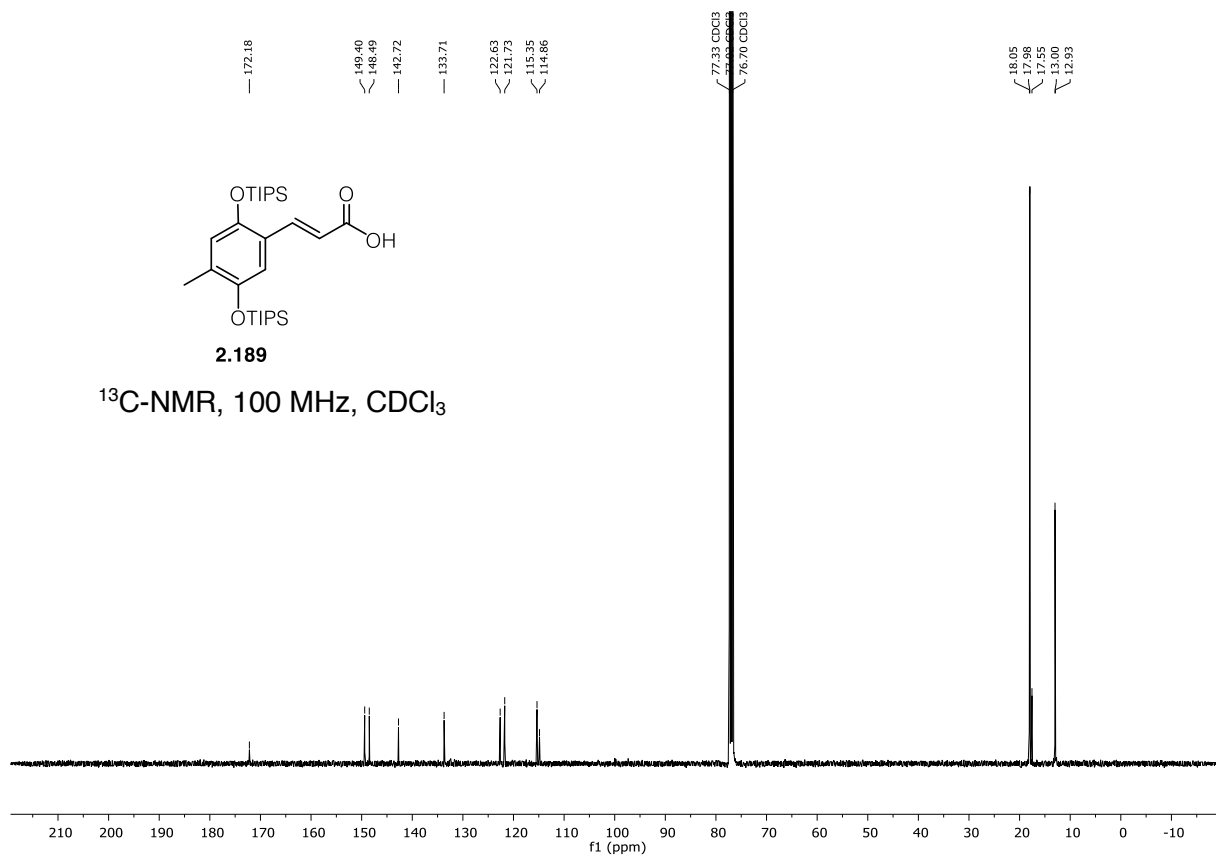
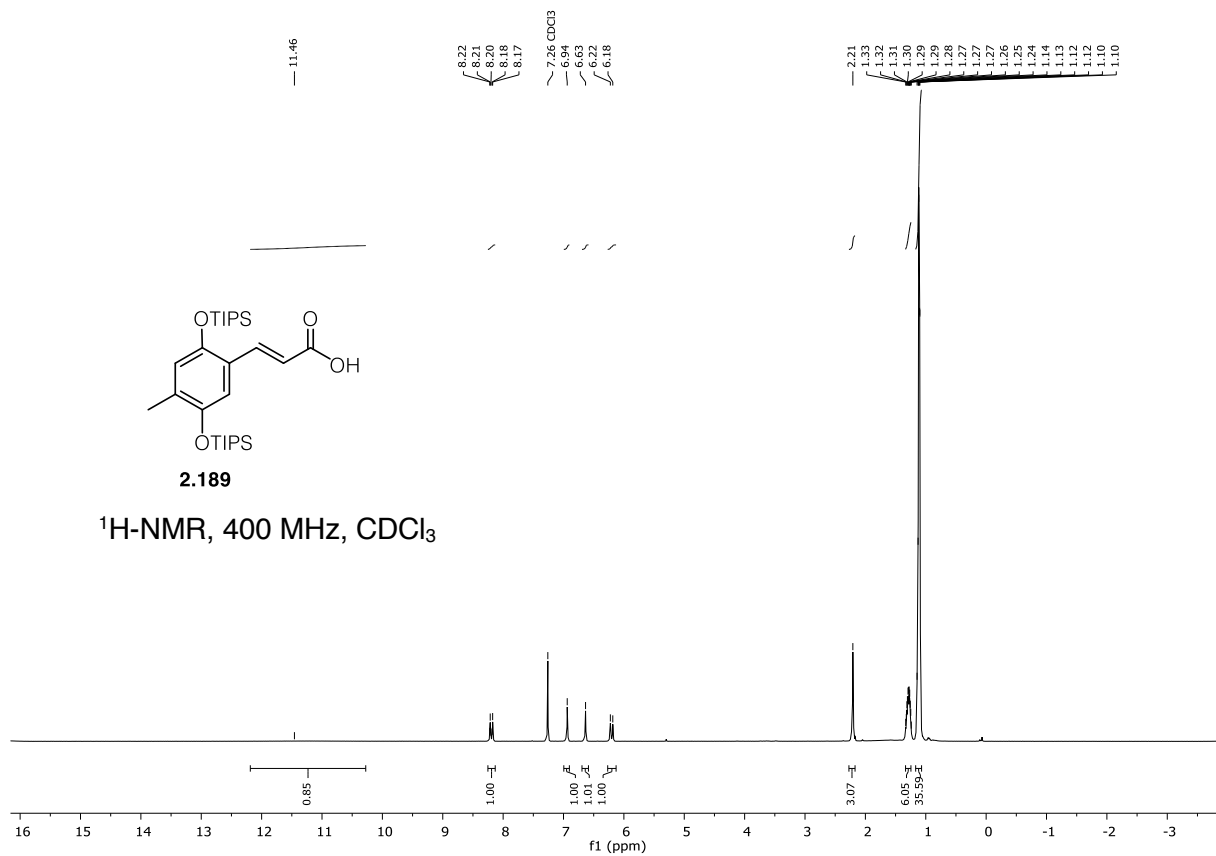
}

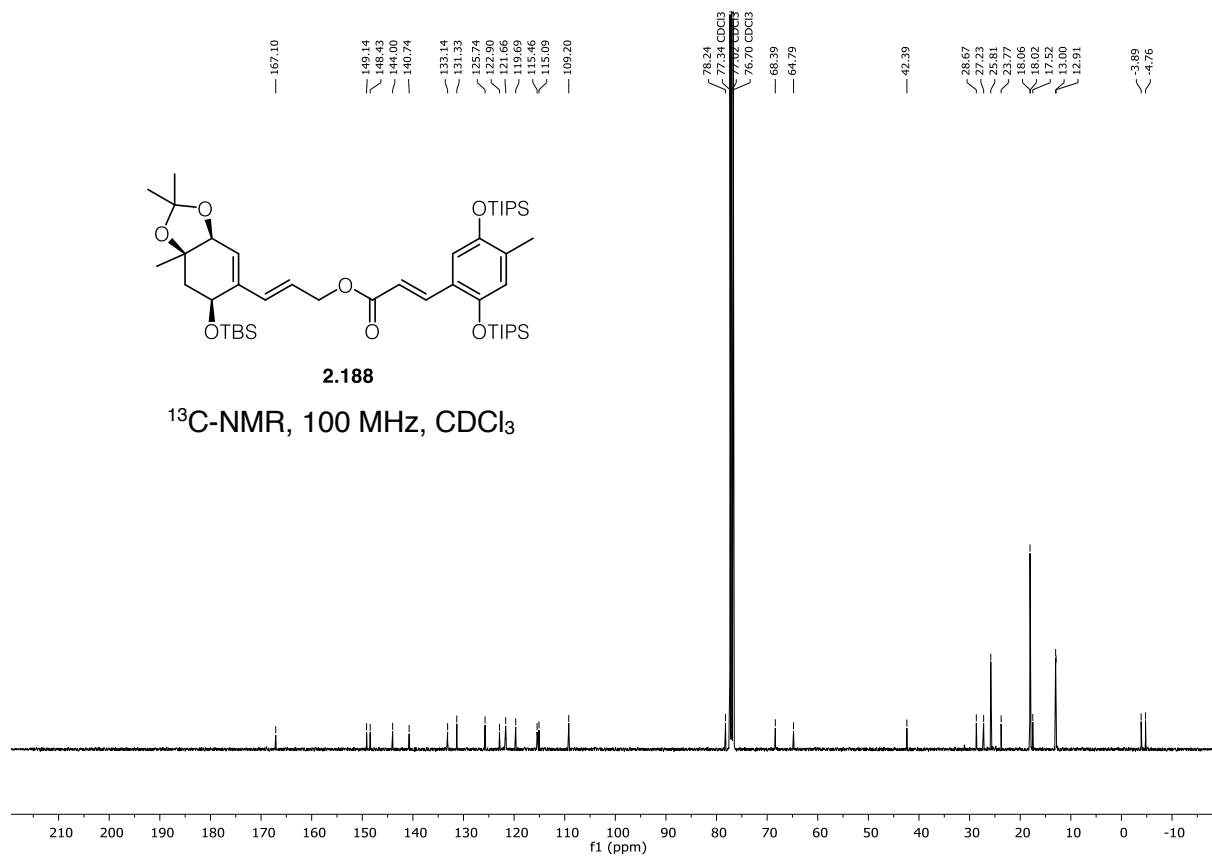
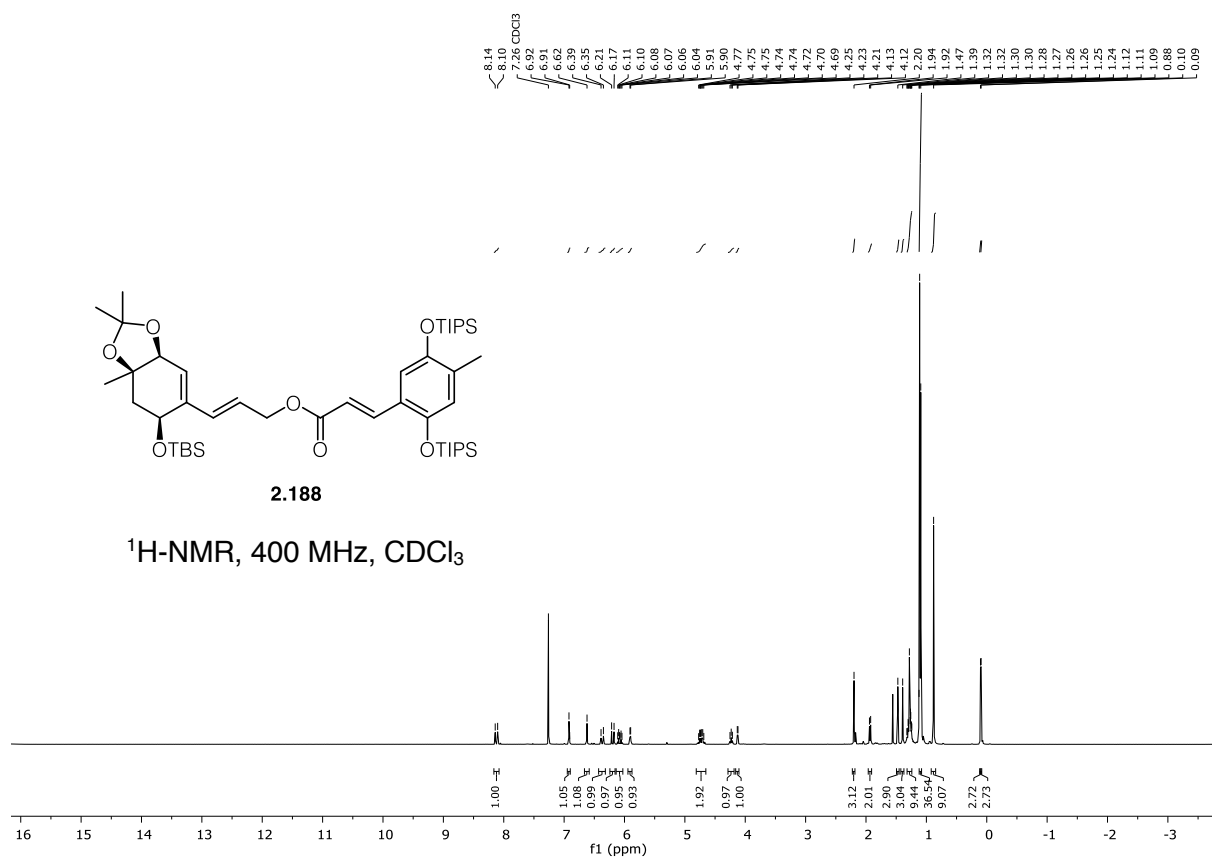


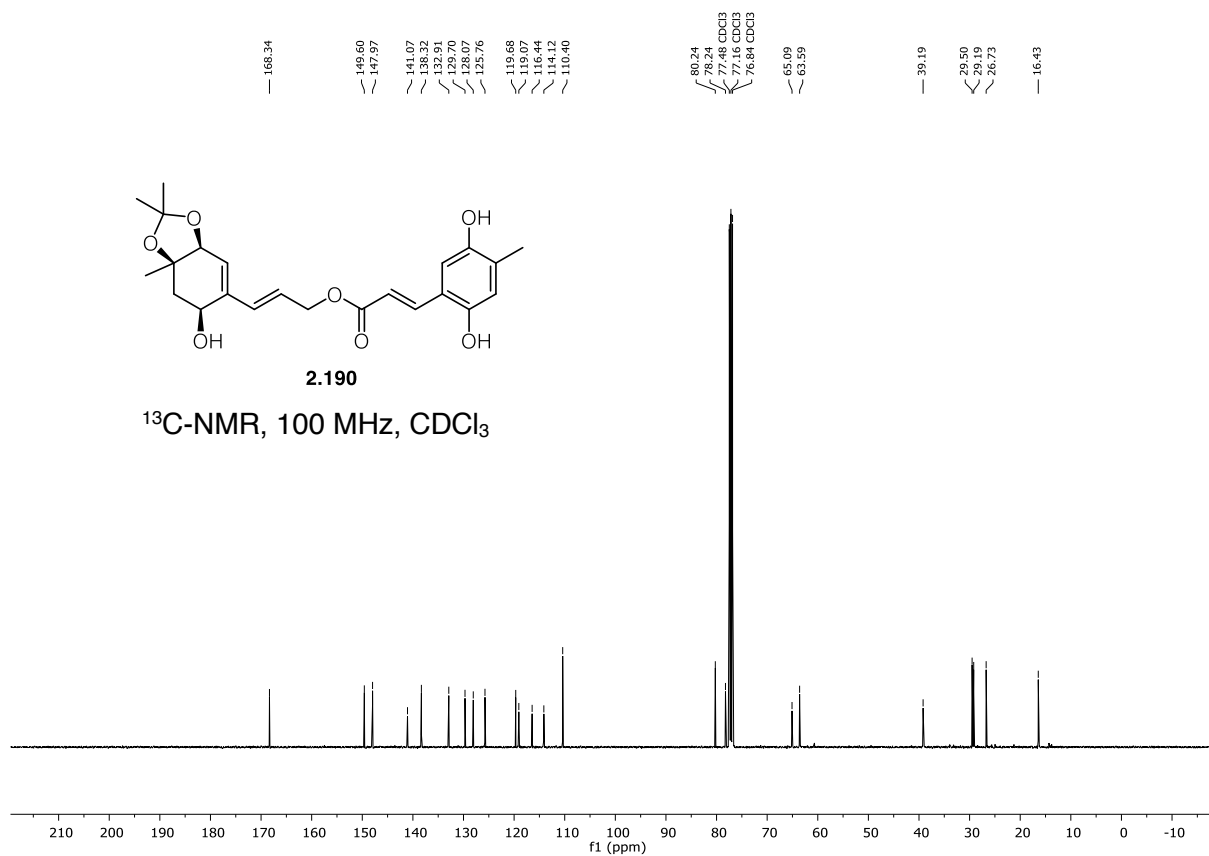
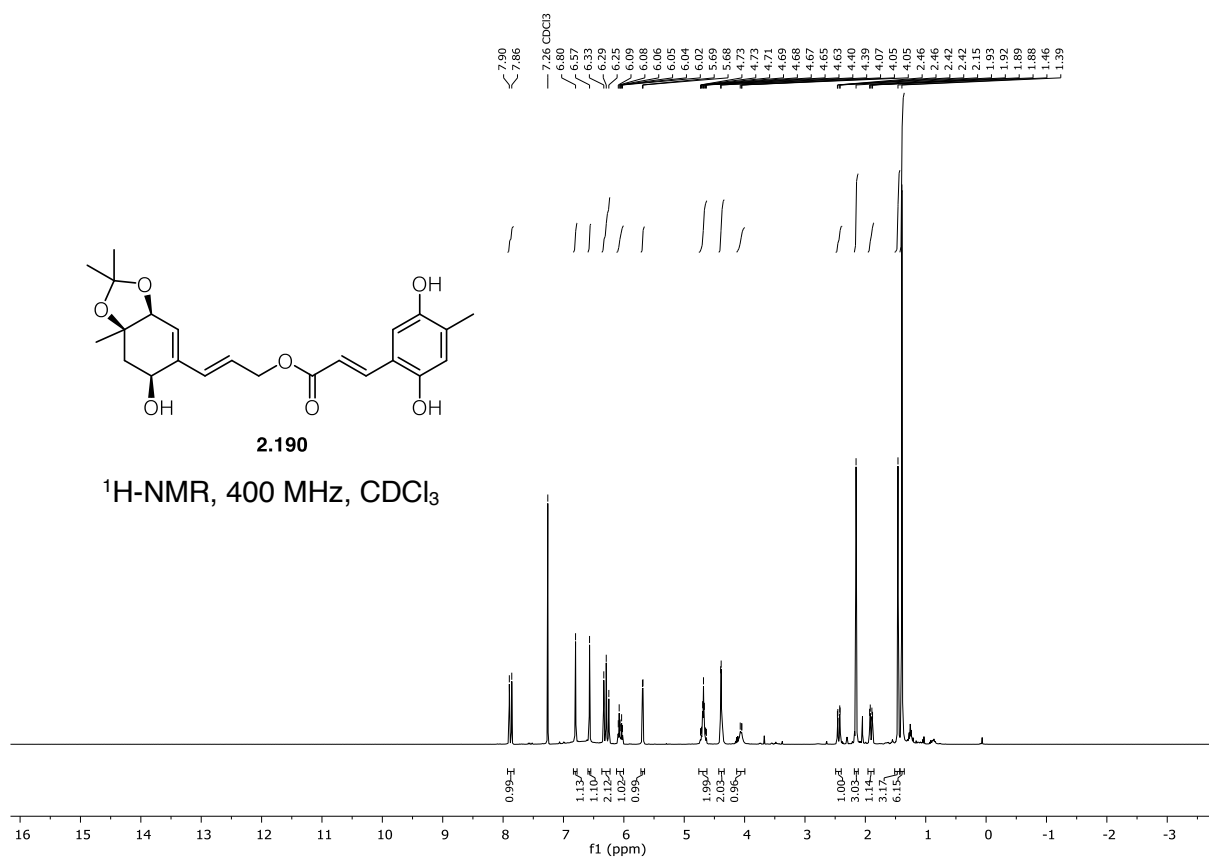


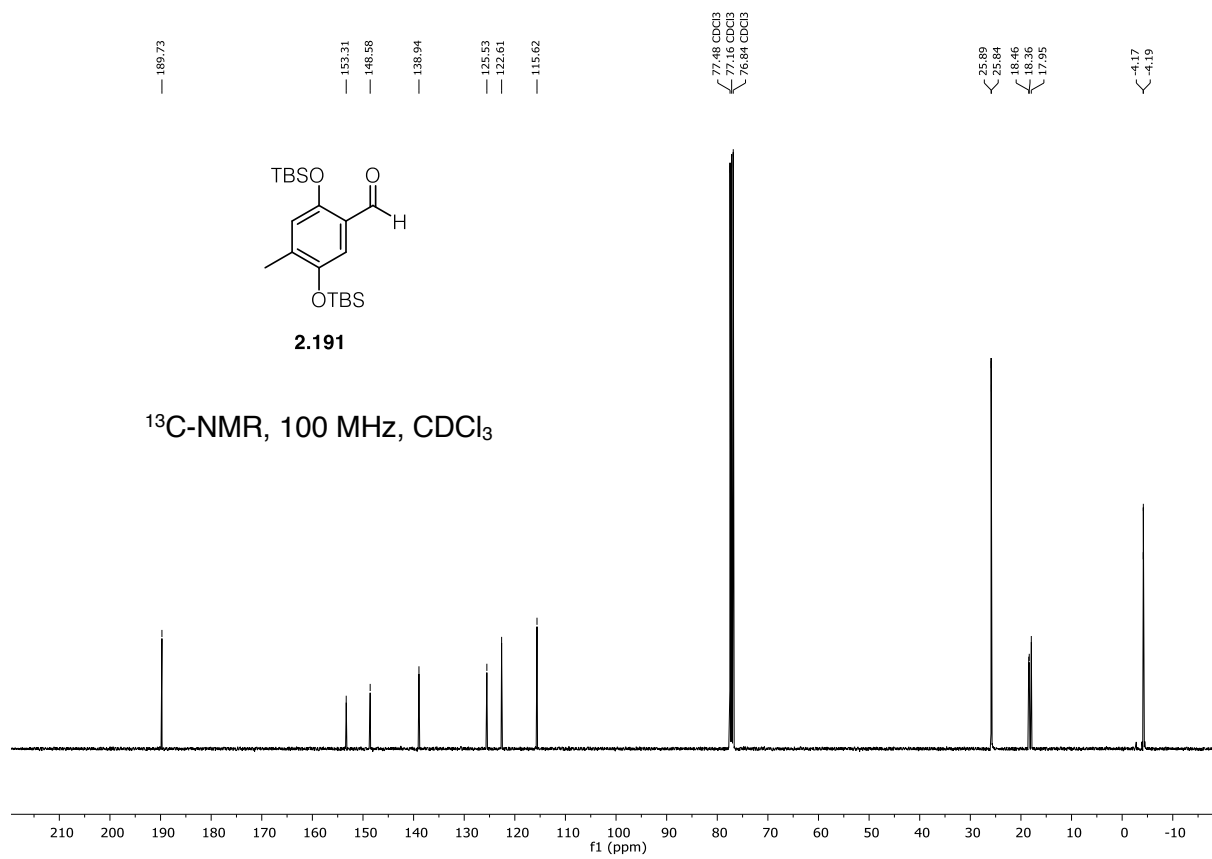
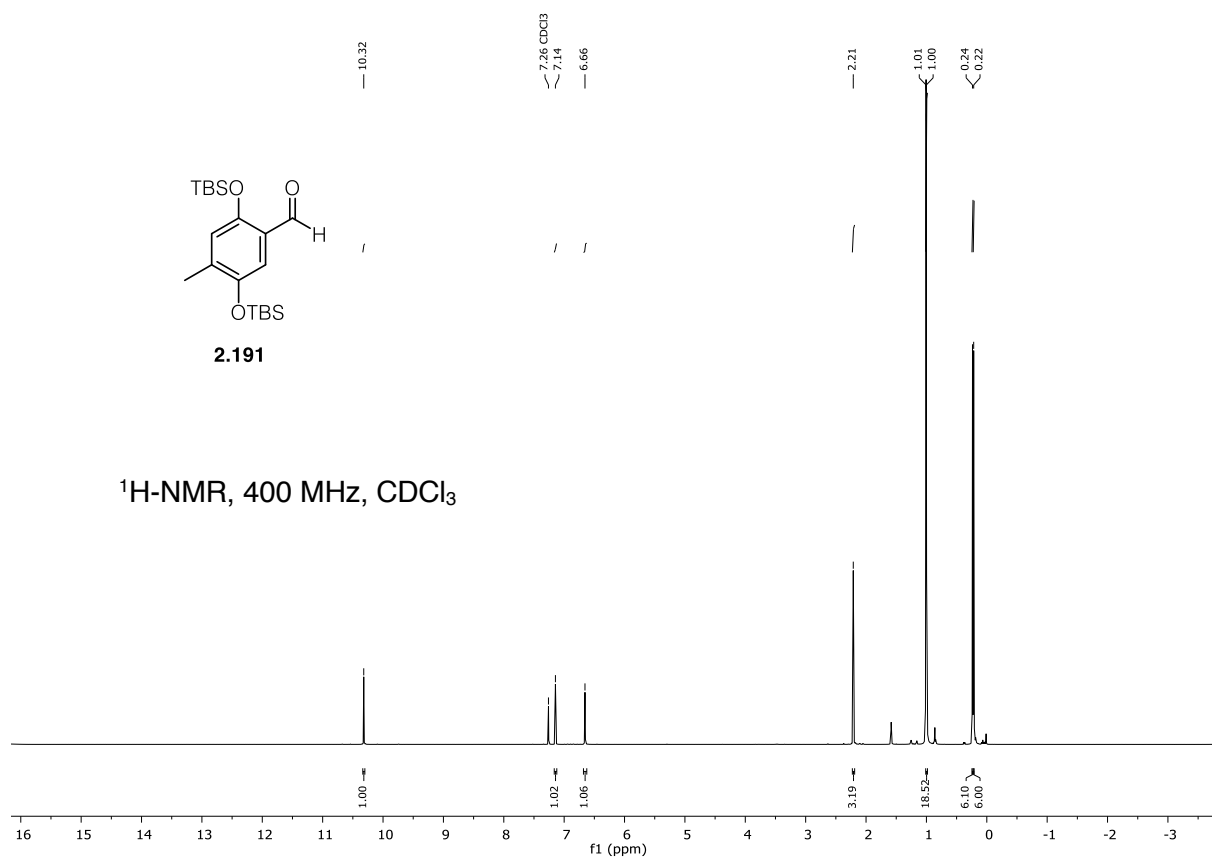


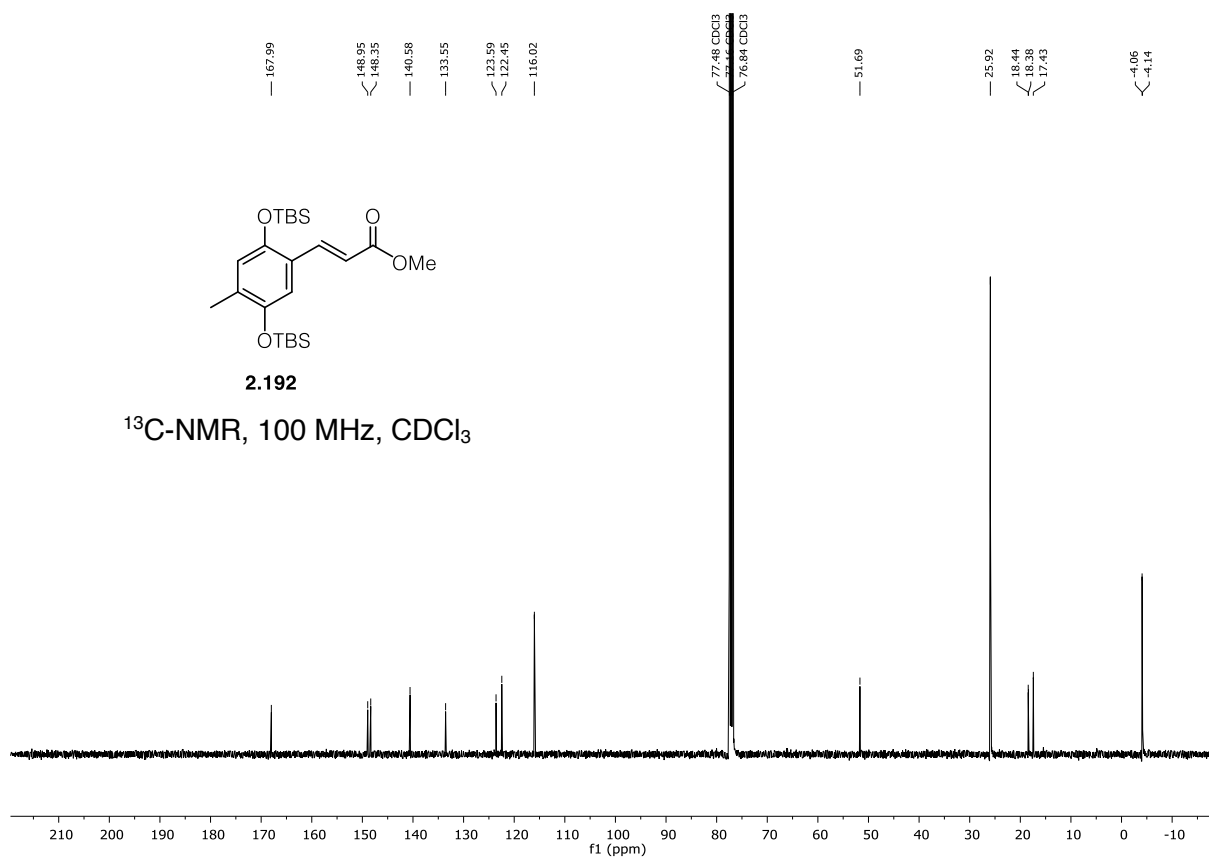
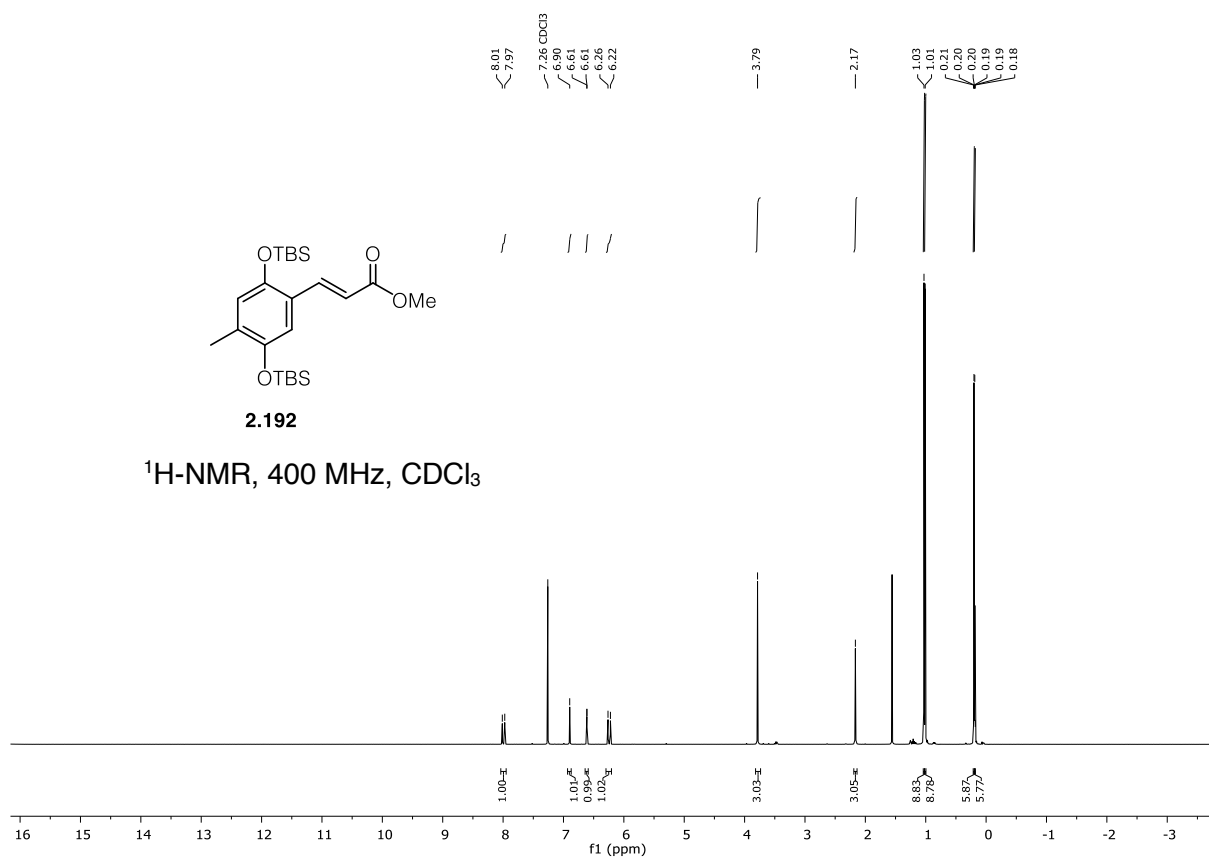


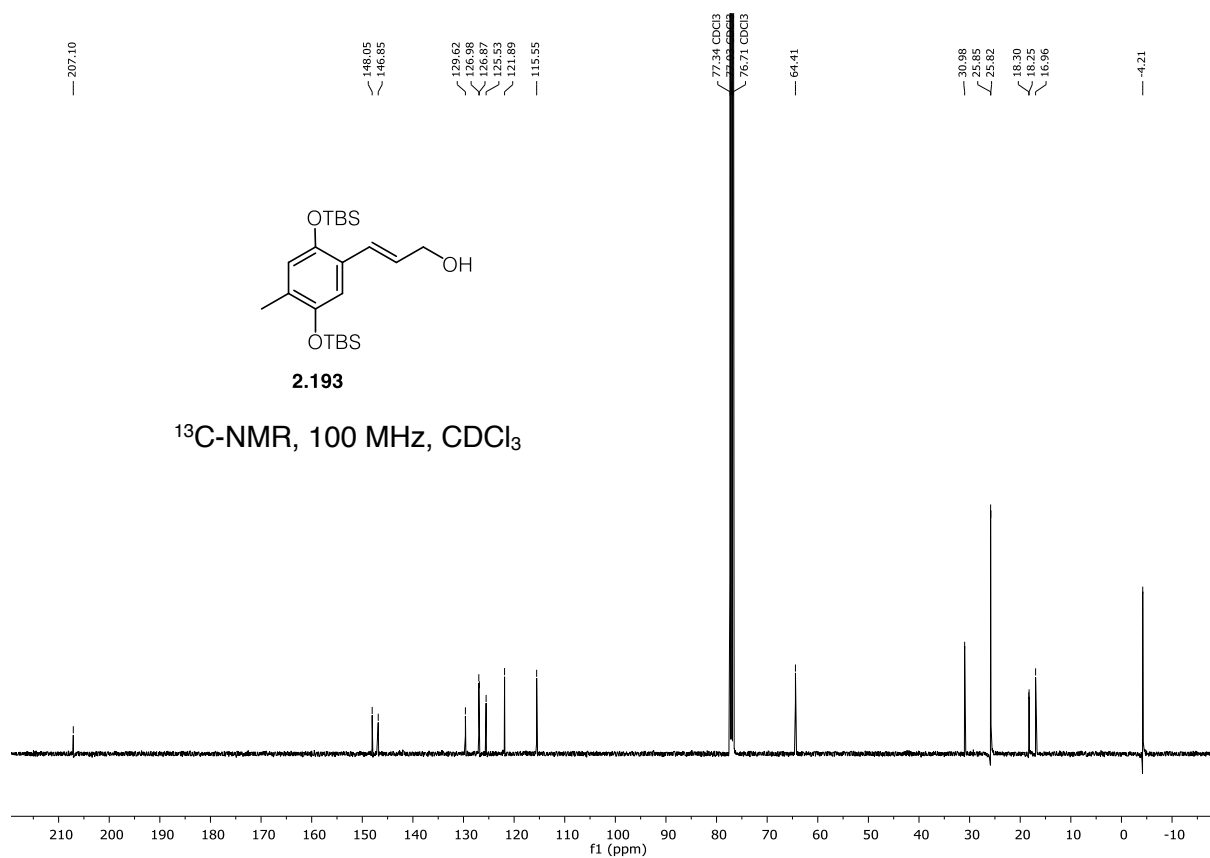
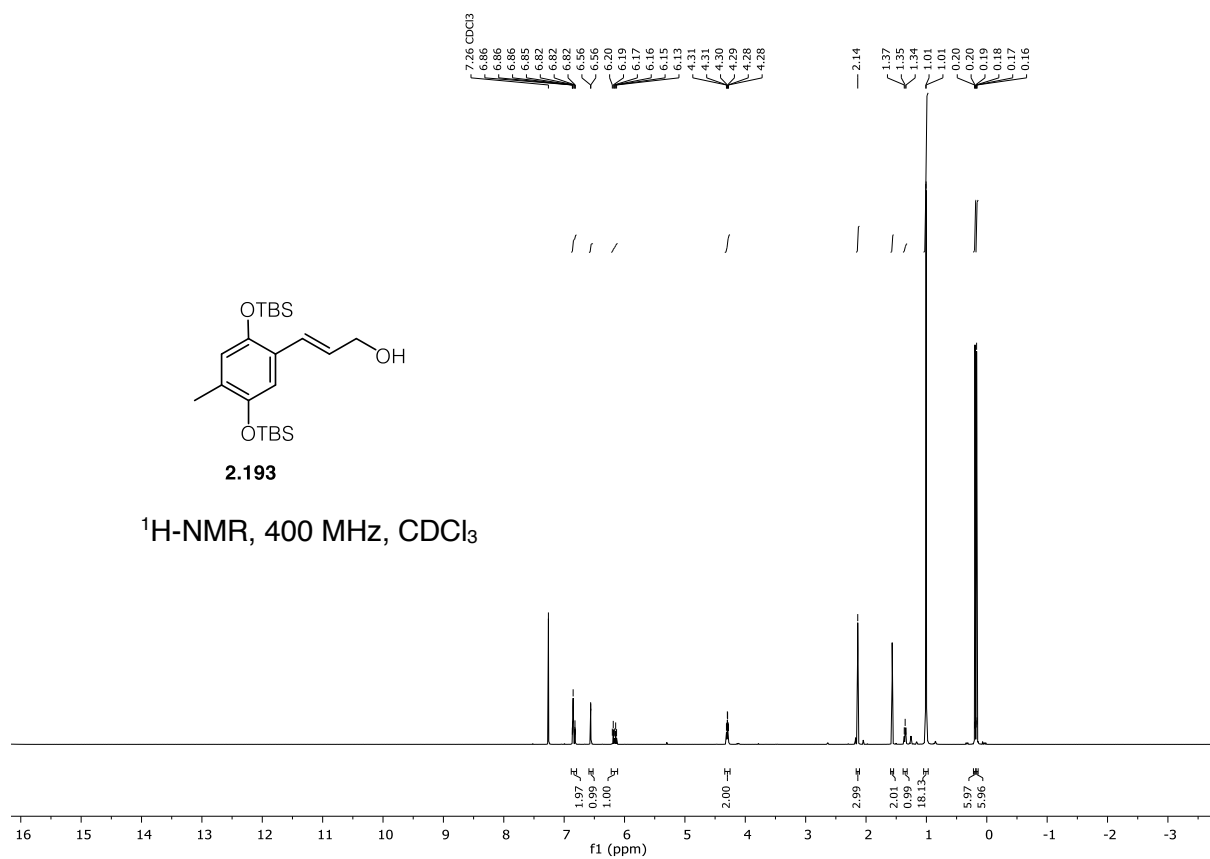


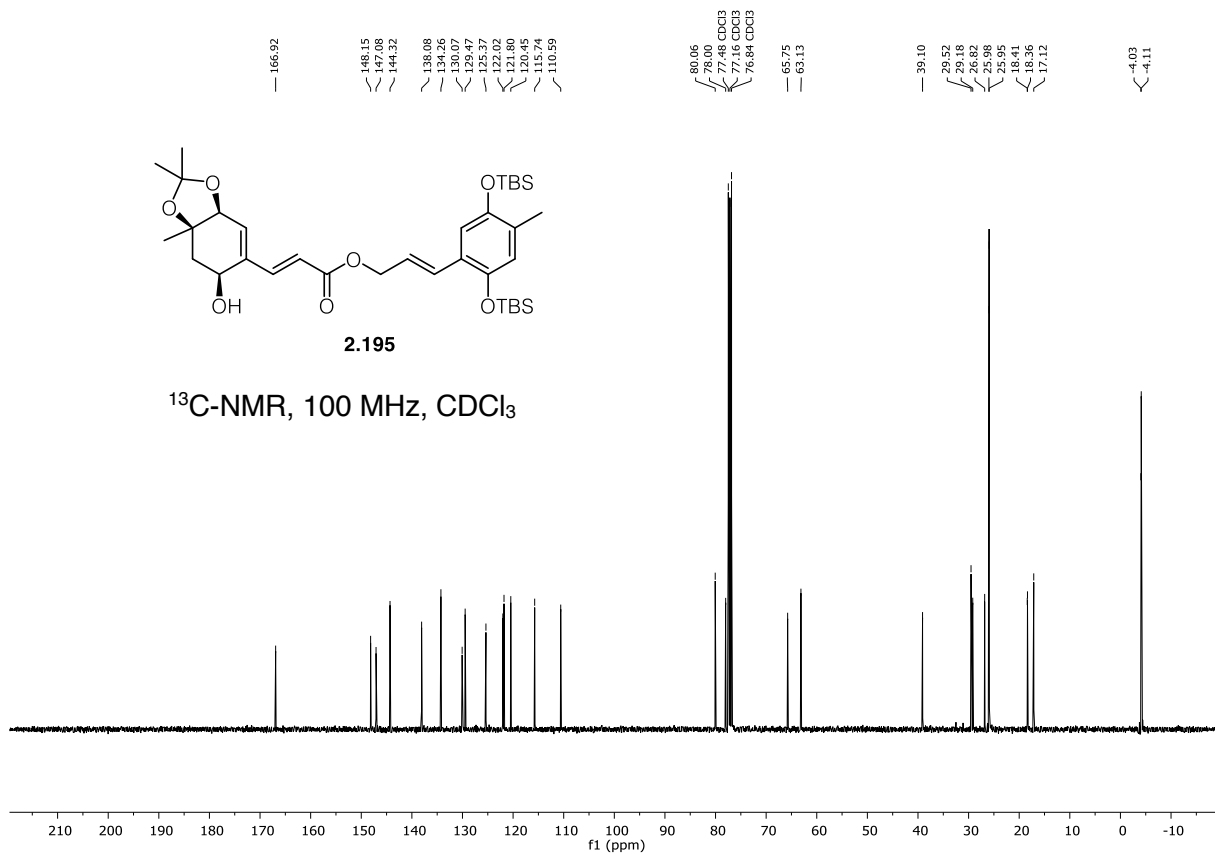
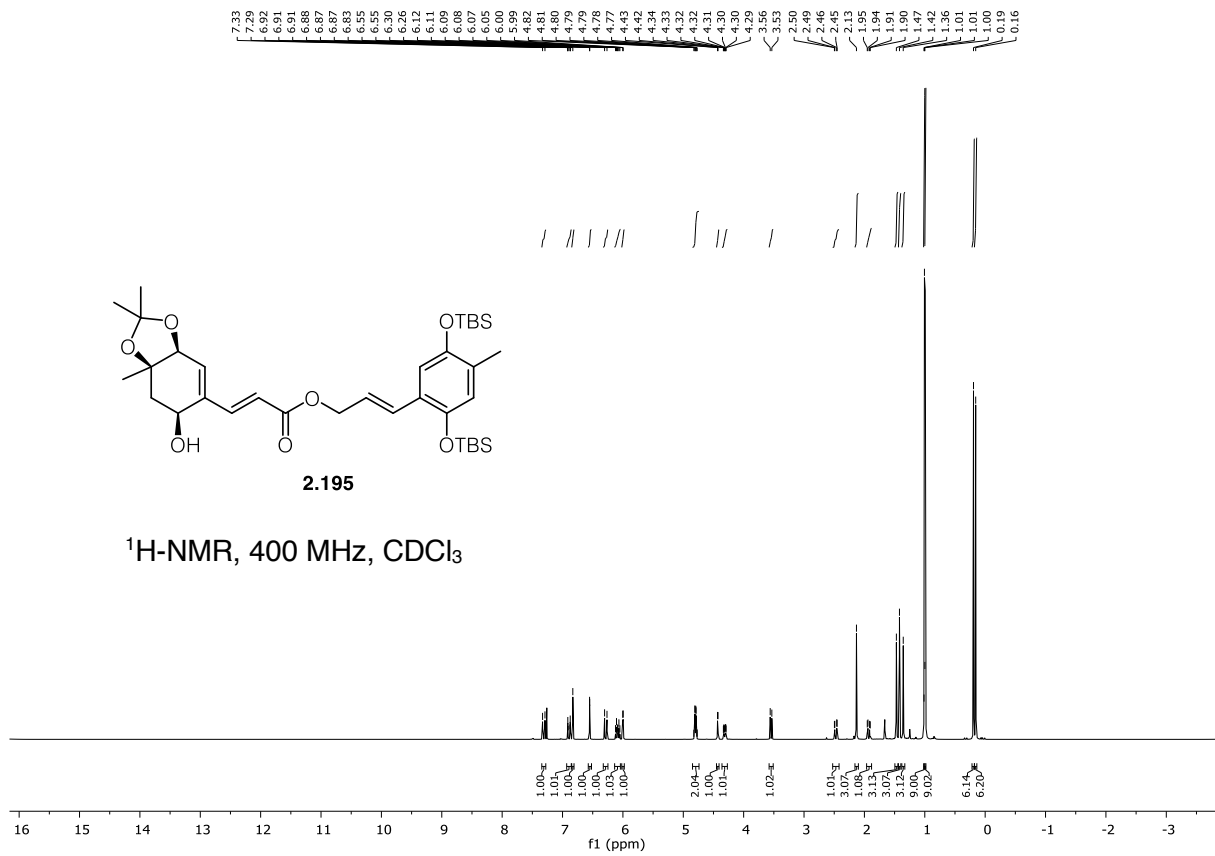


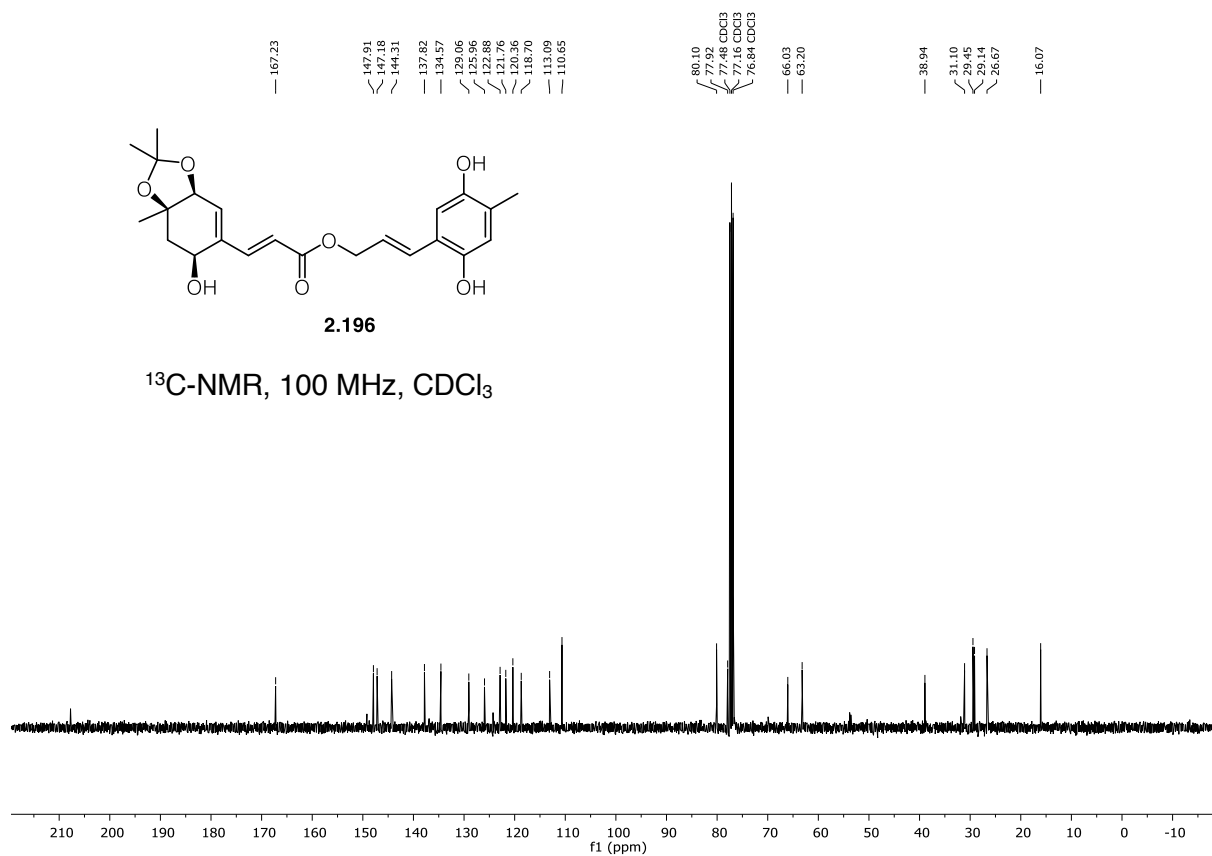
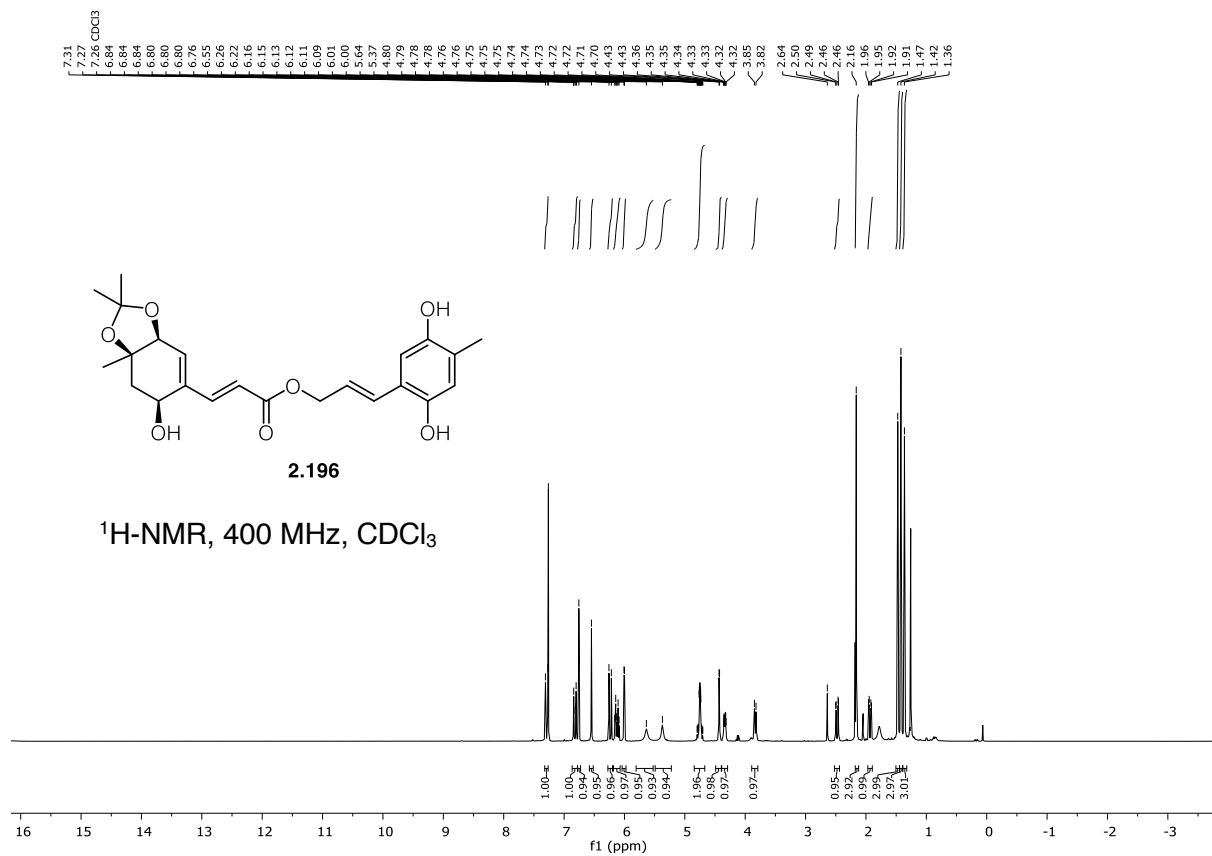


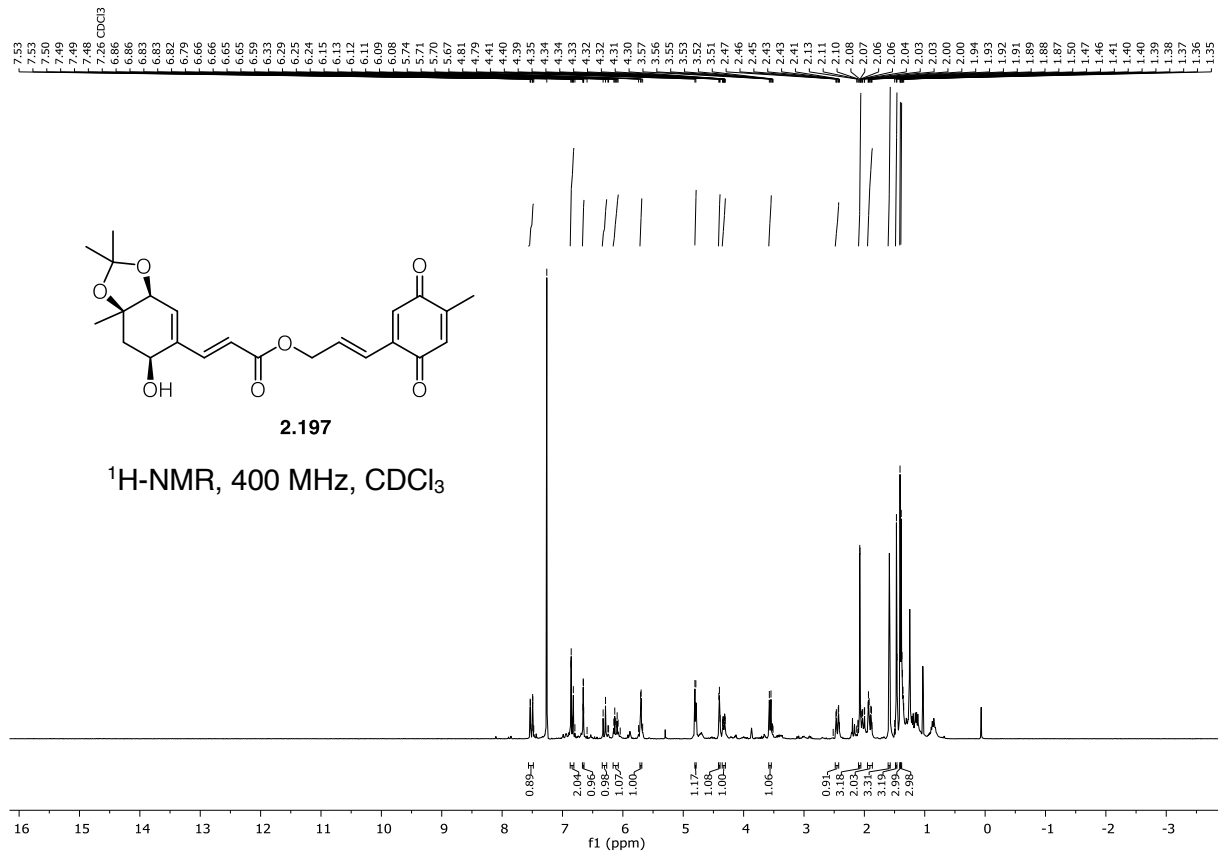
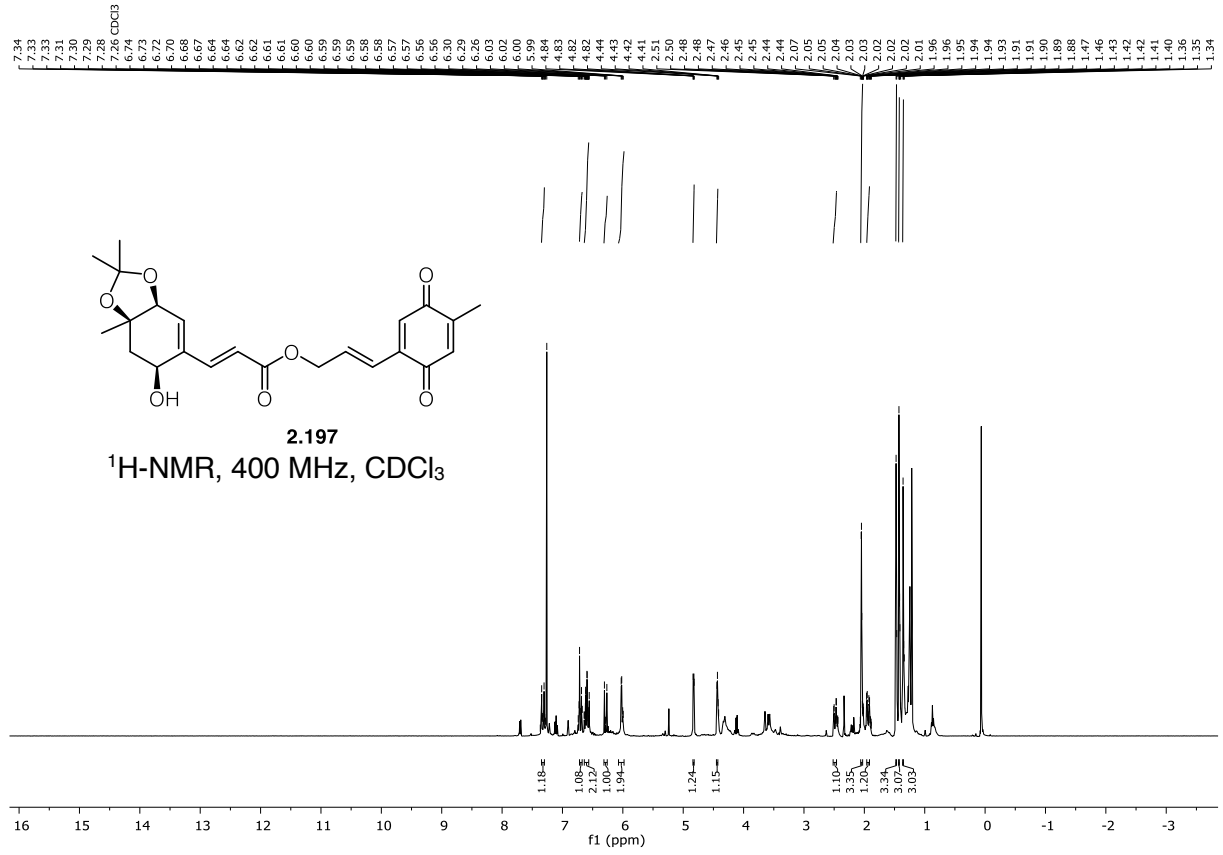


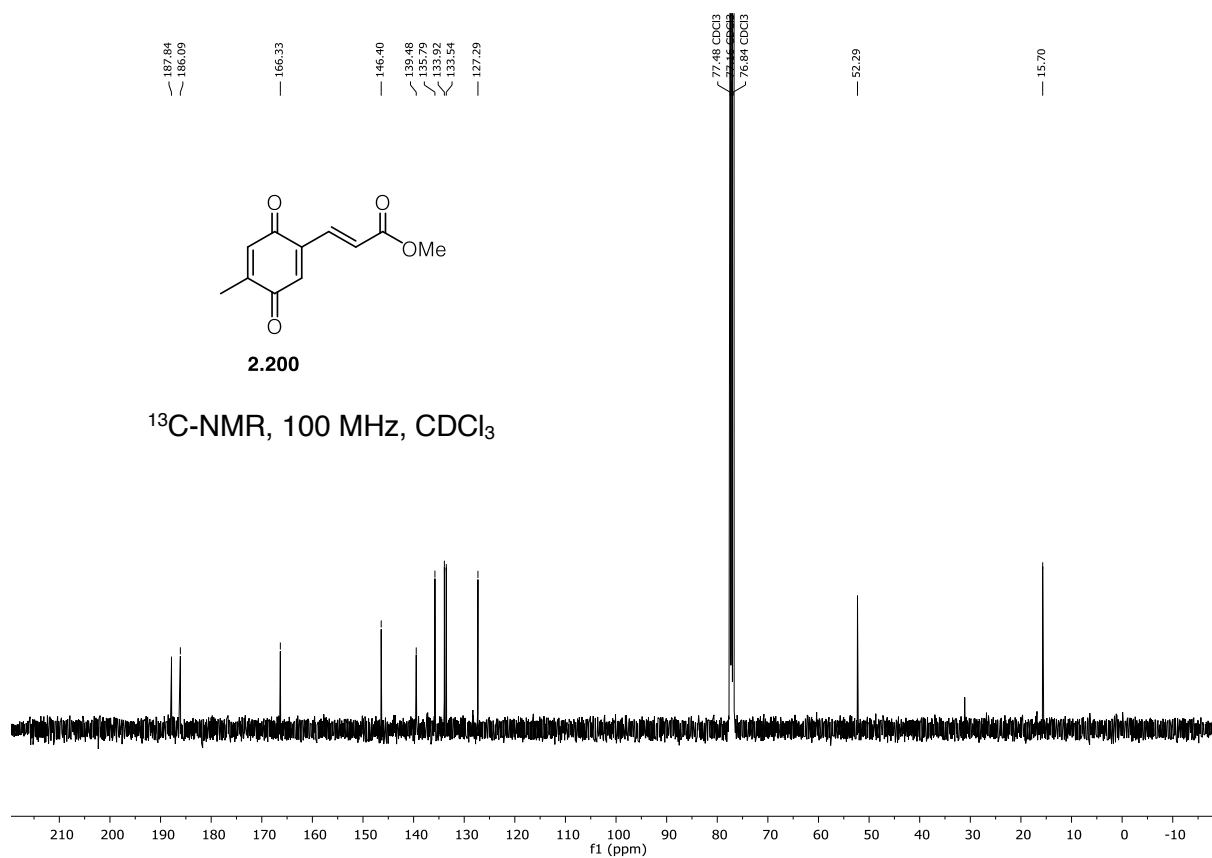
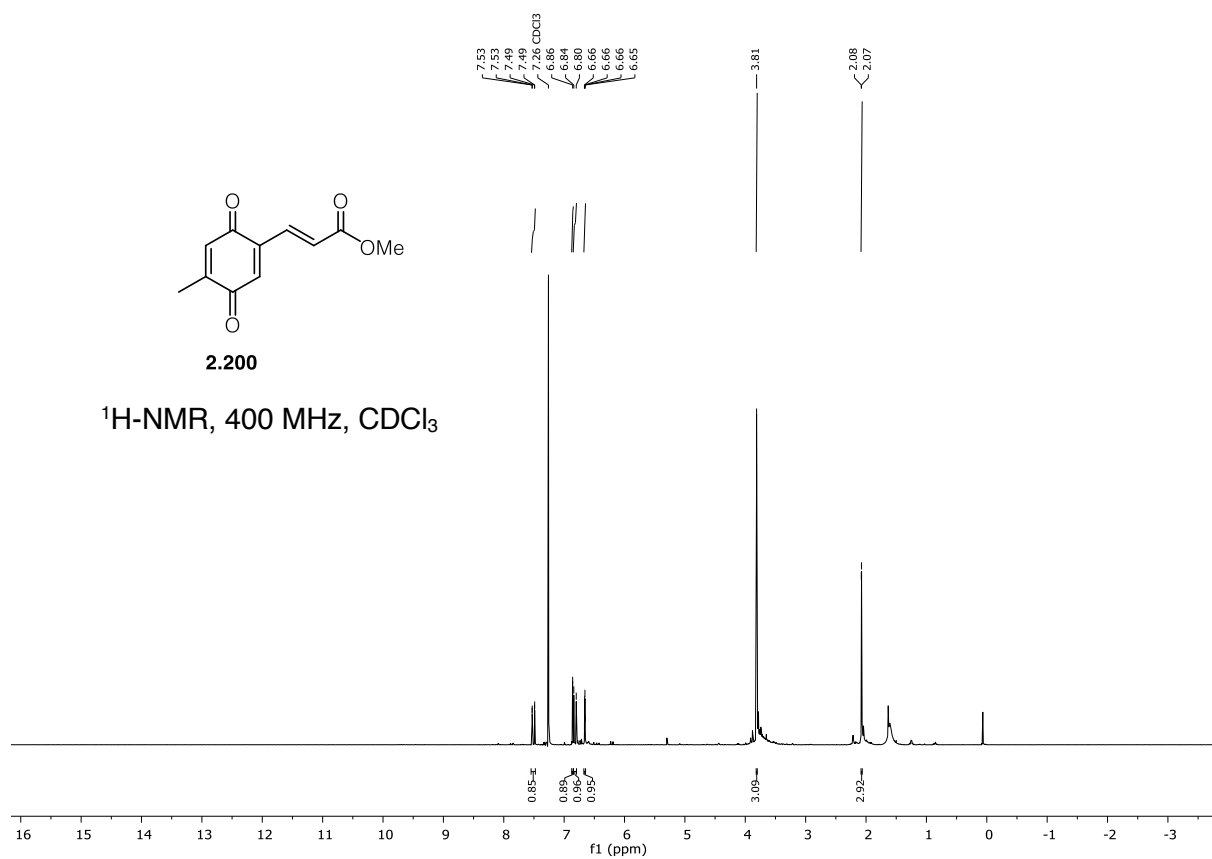


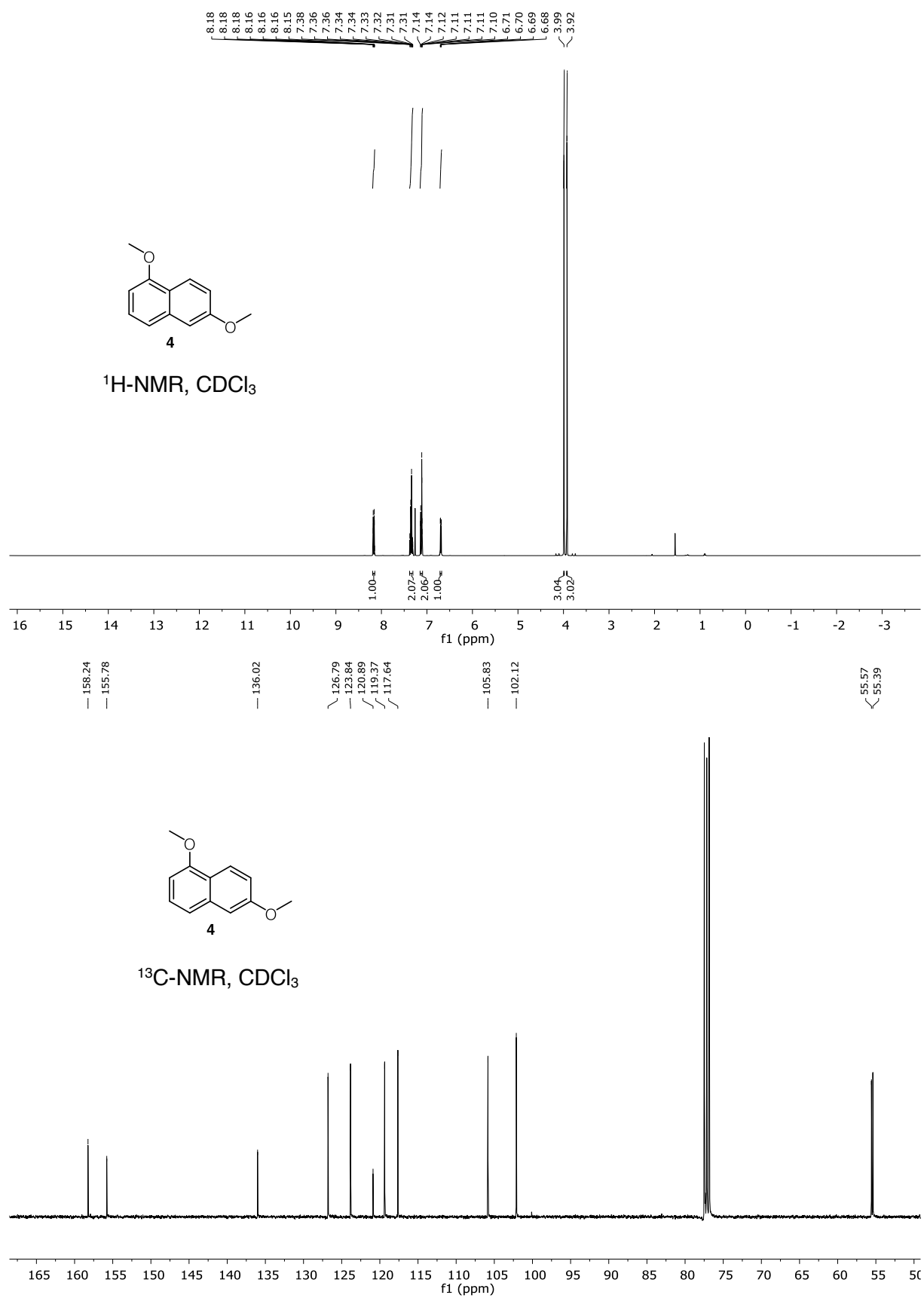


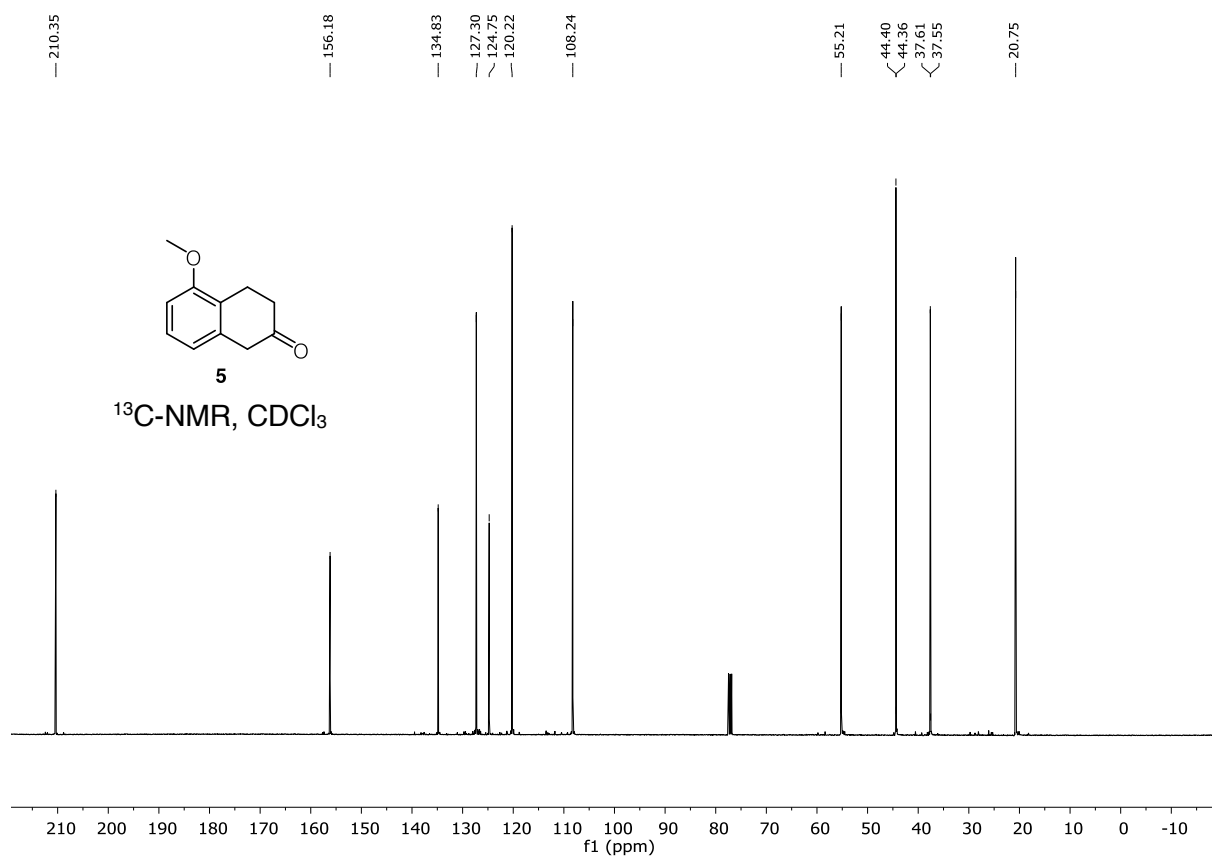
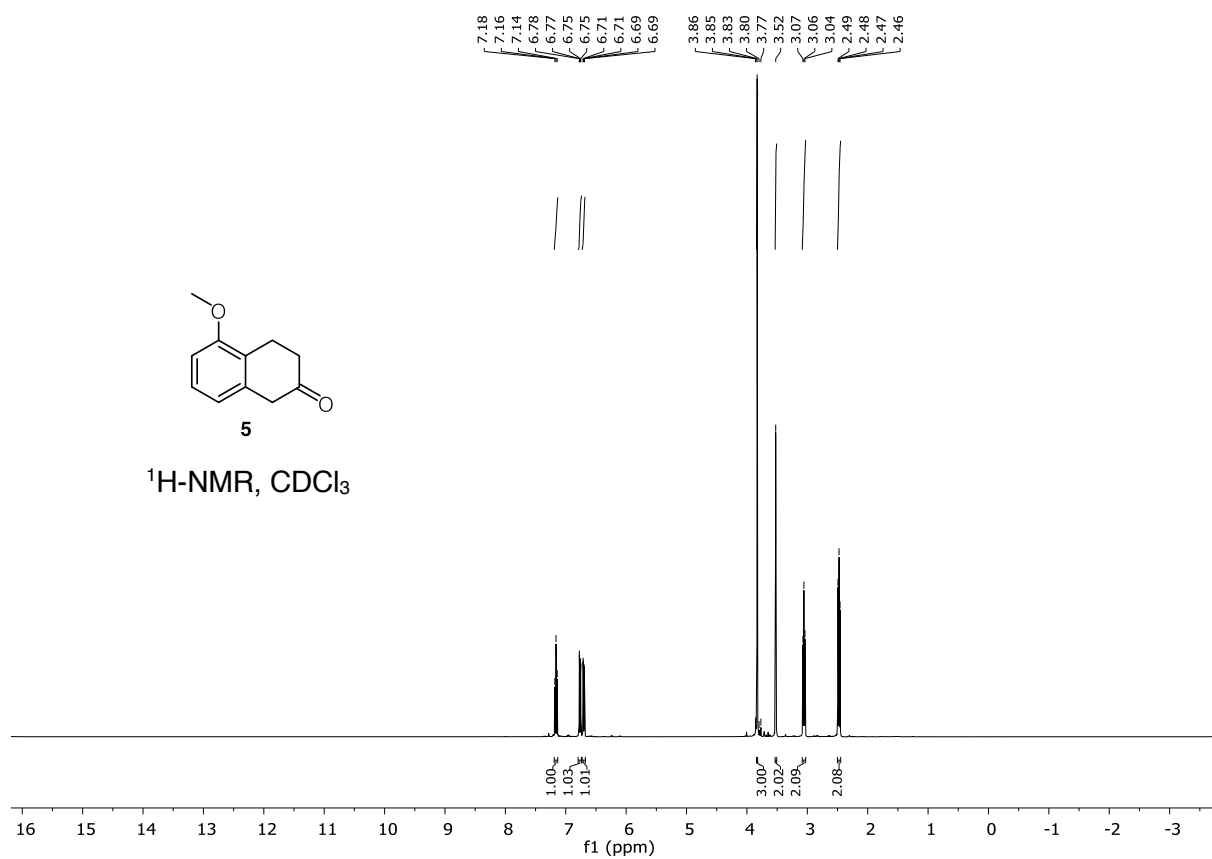


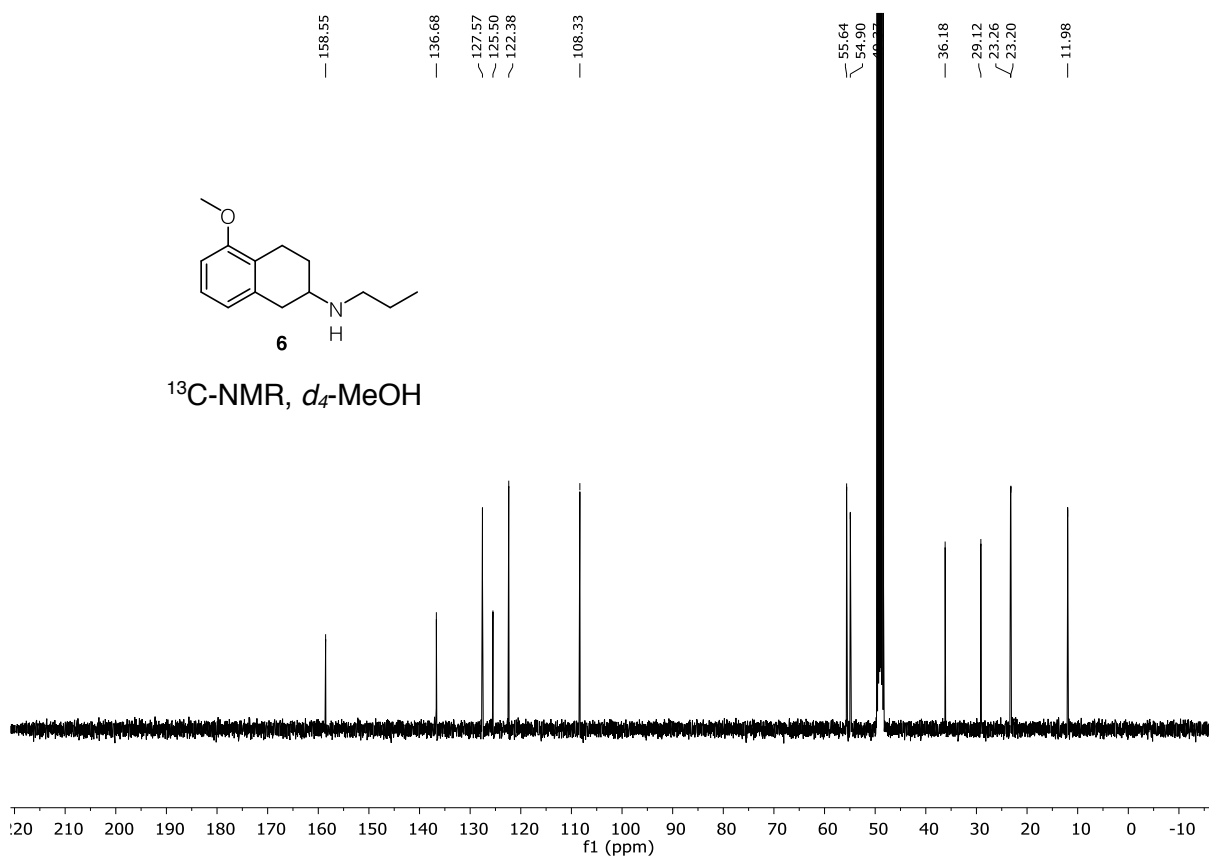
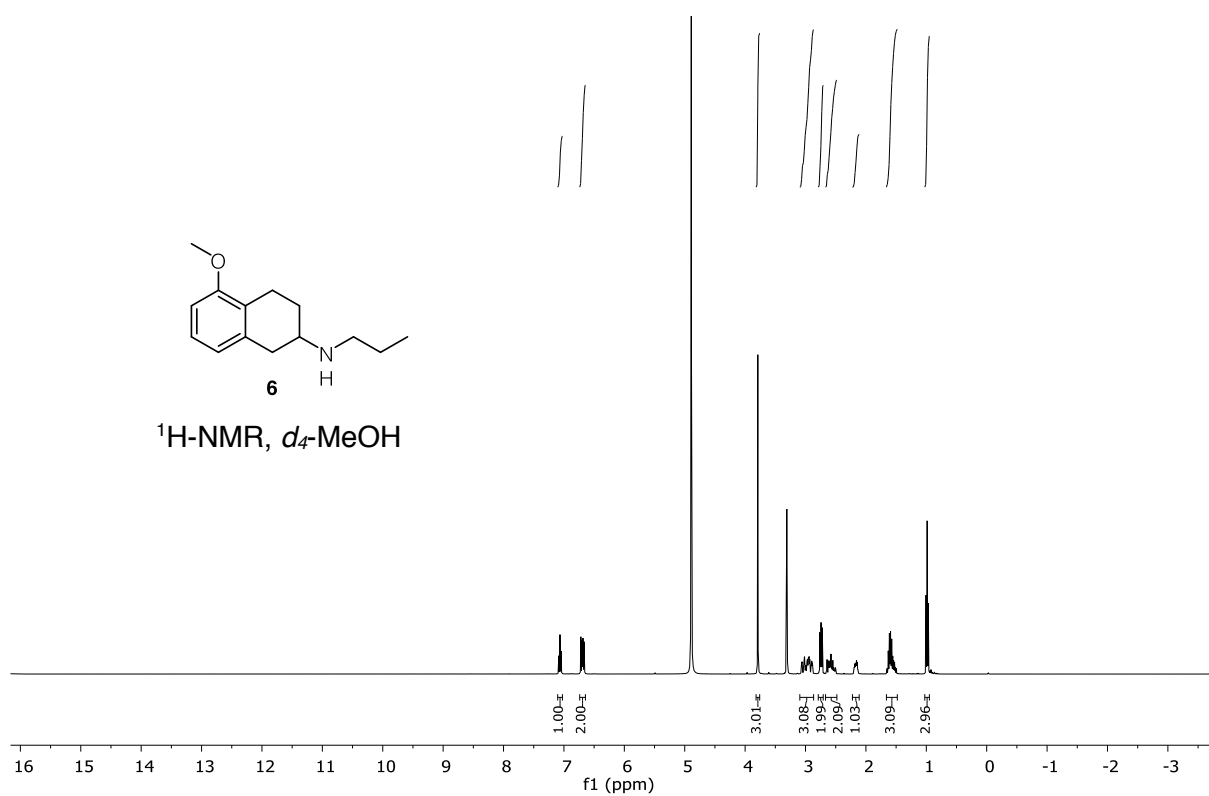


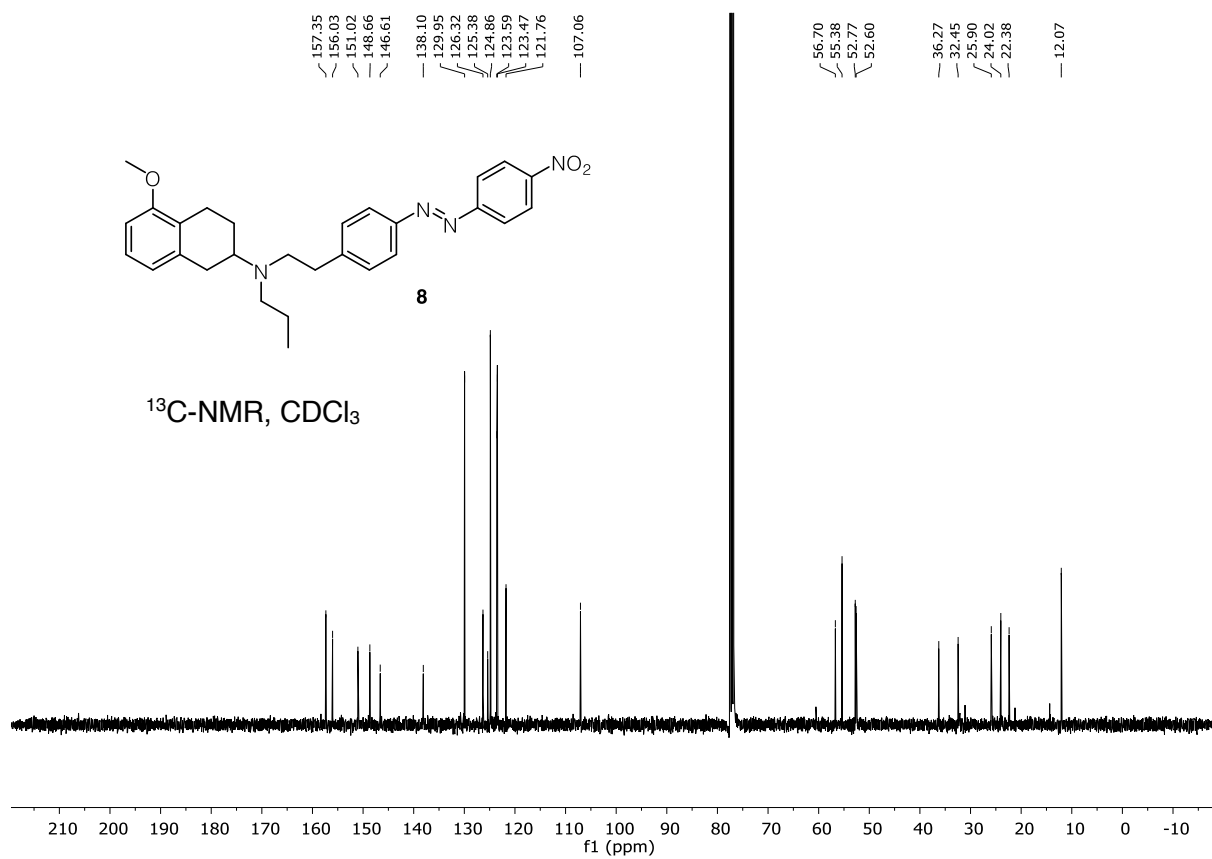
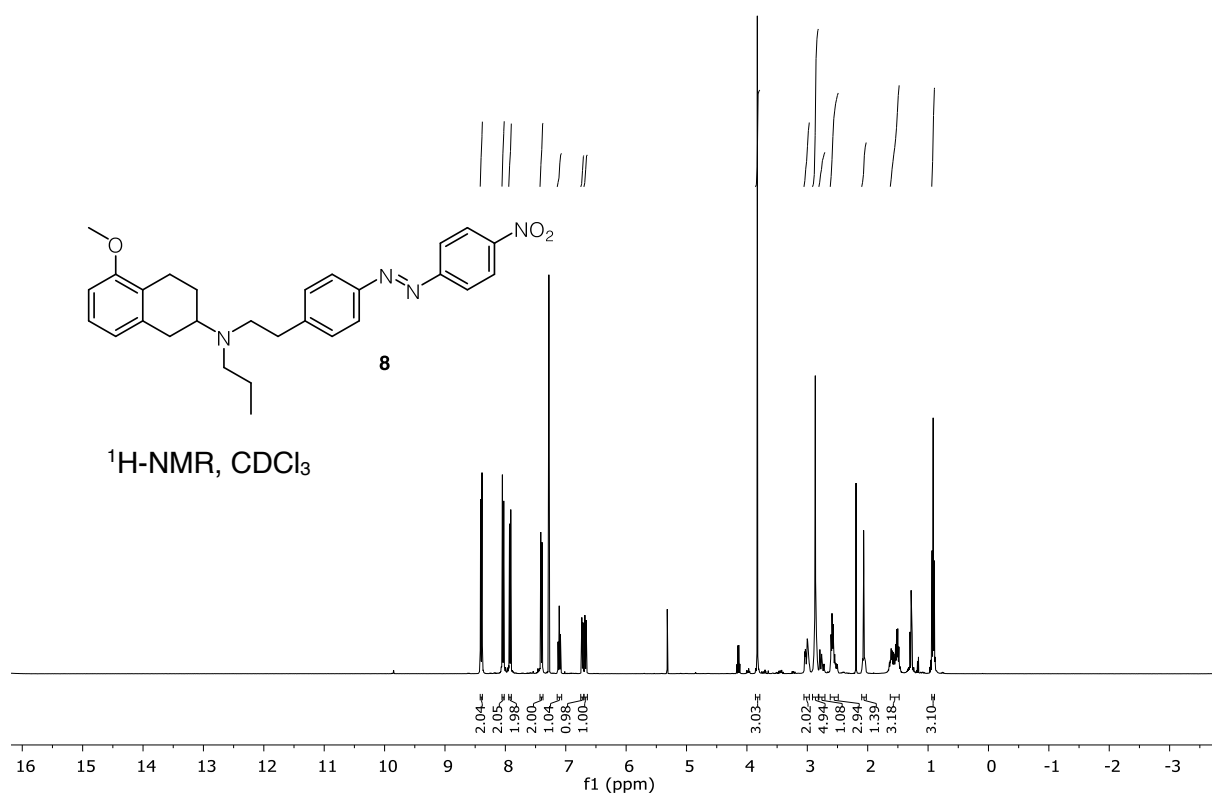


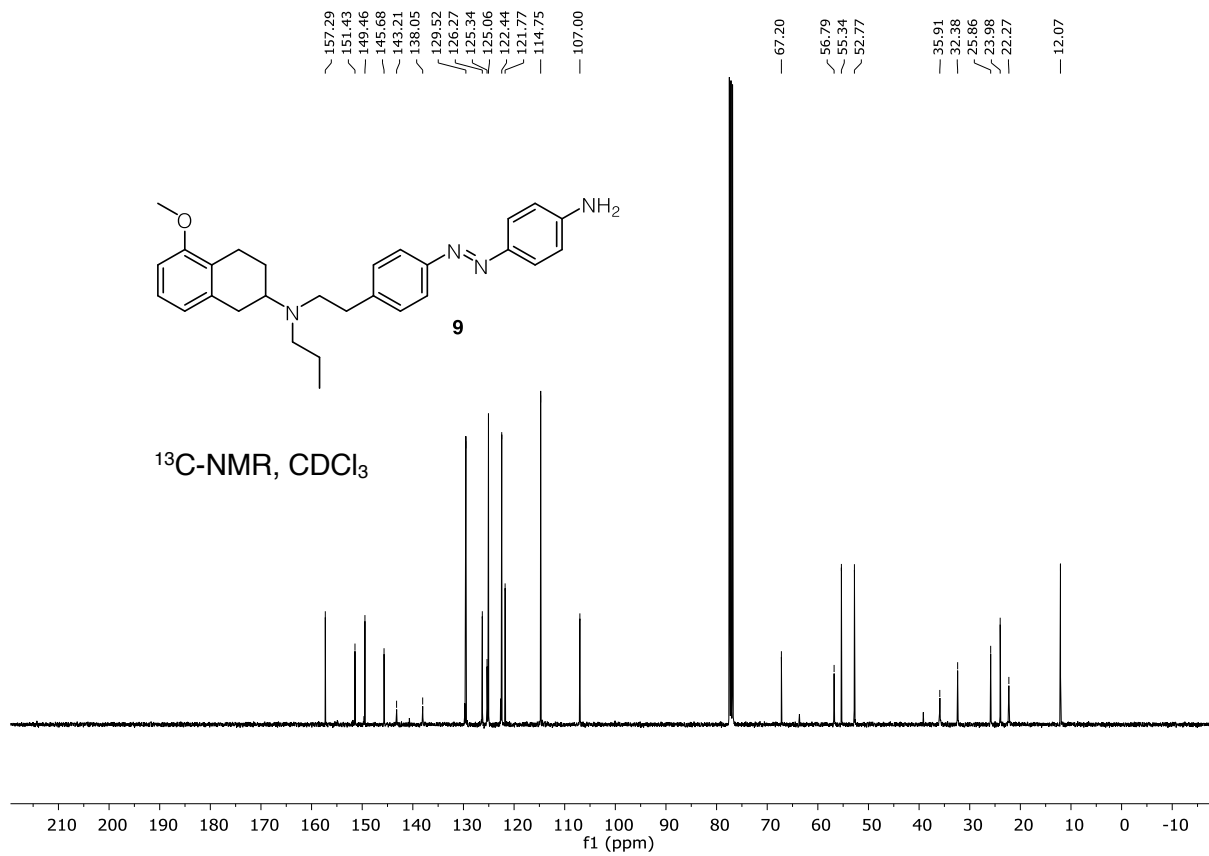
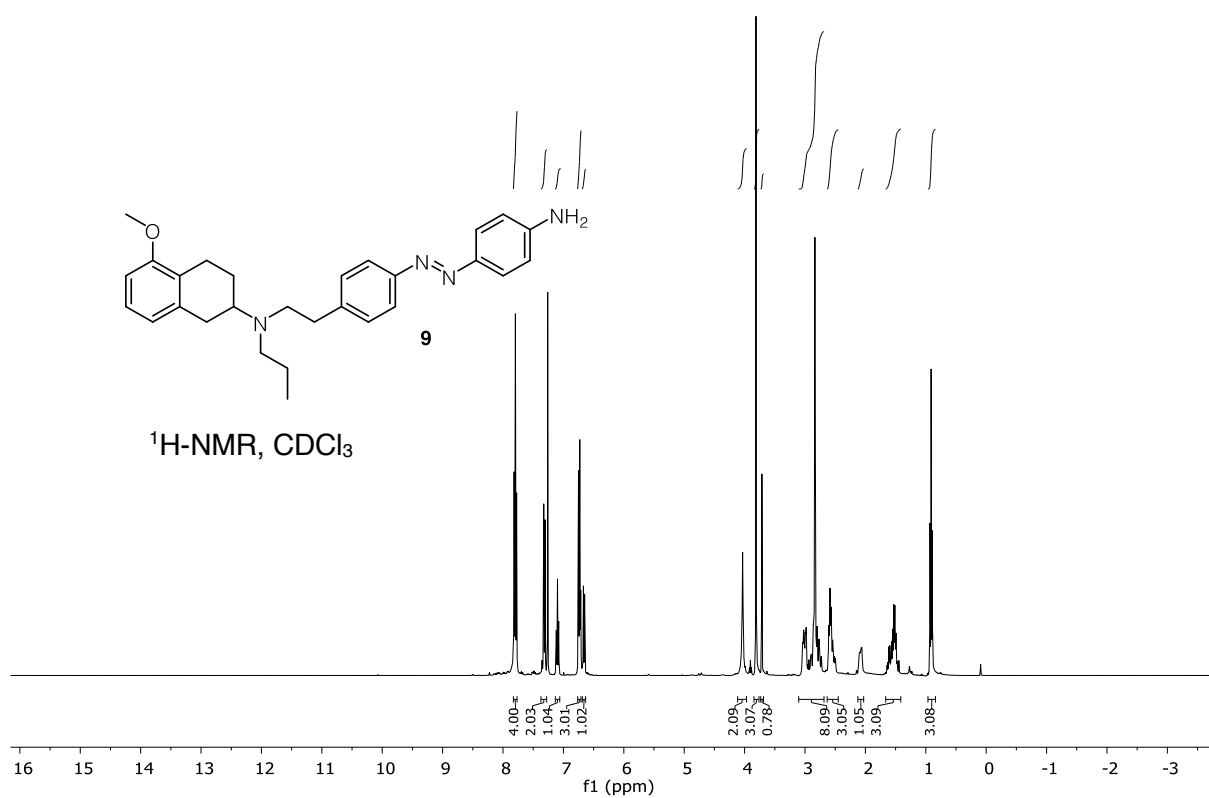


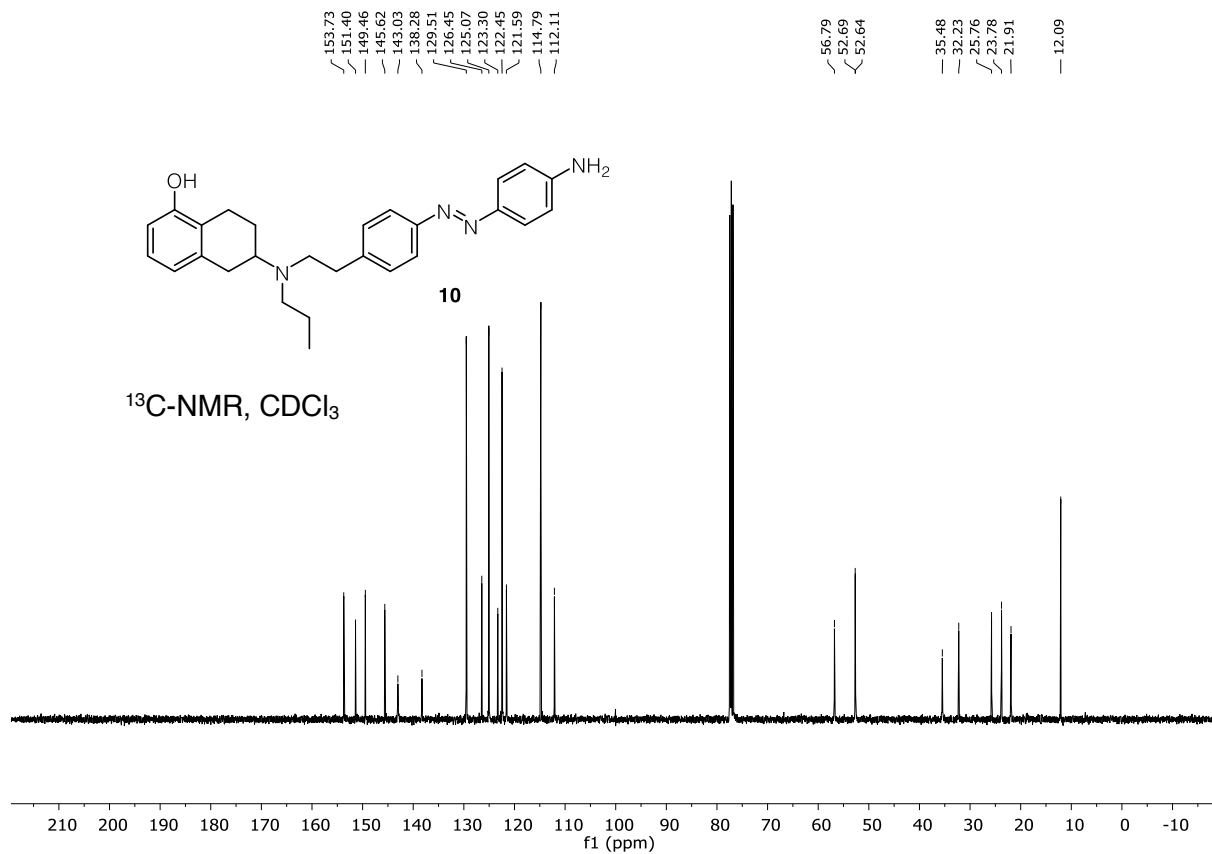
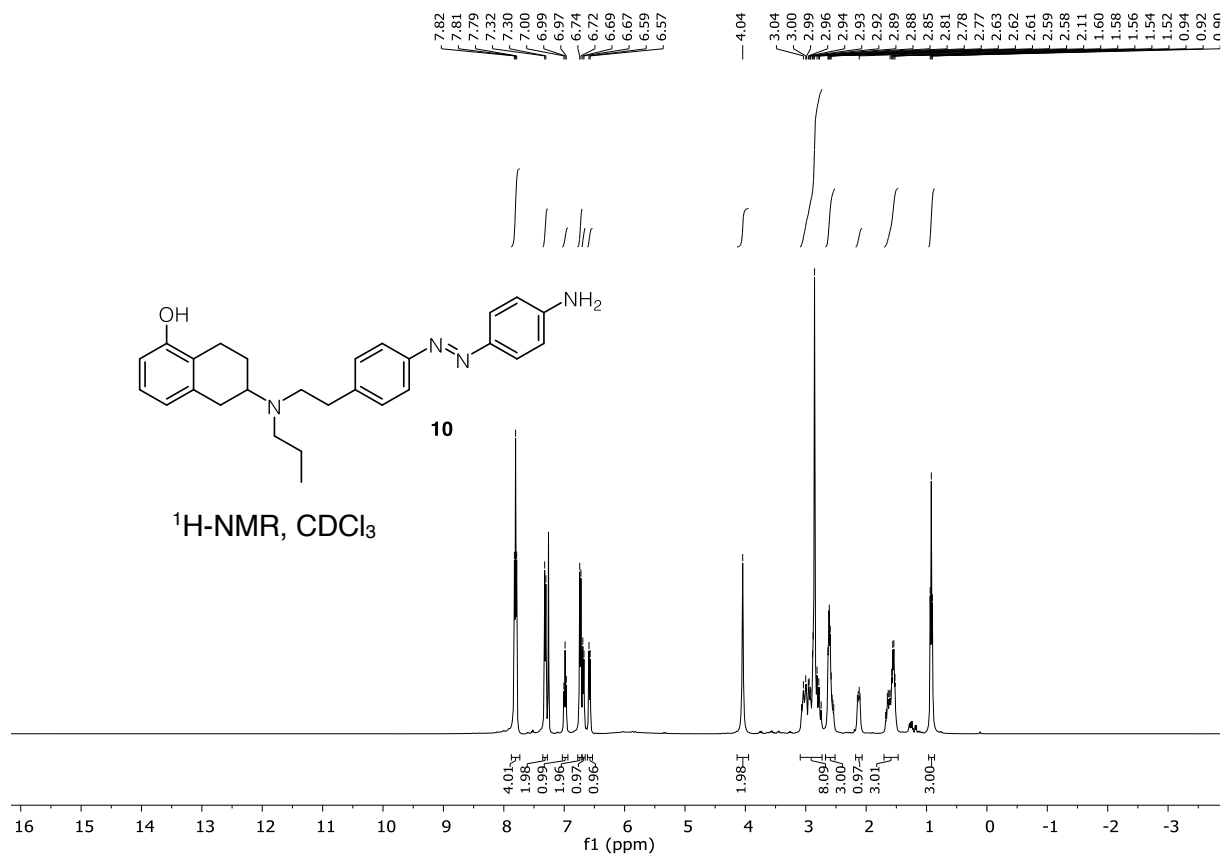
7.2.3 ^1H and ^{13}C NMR spectra of Chapter III

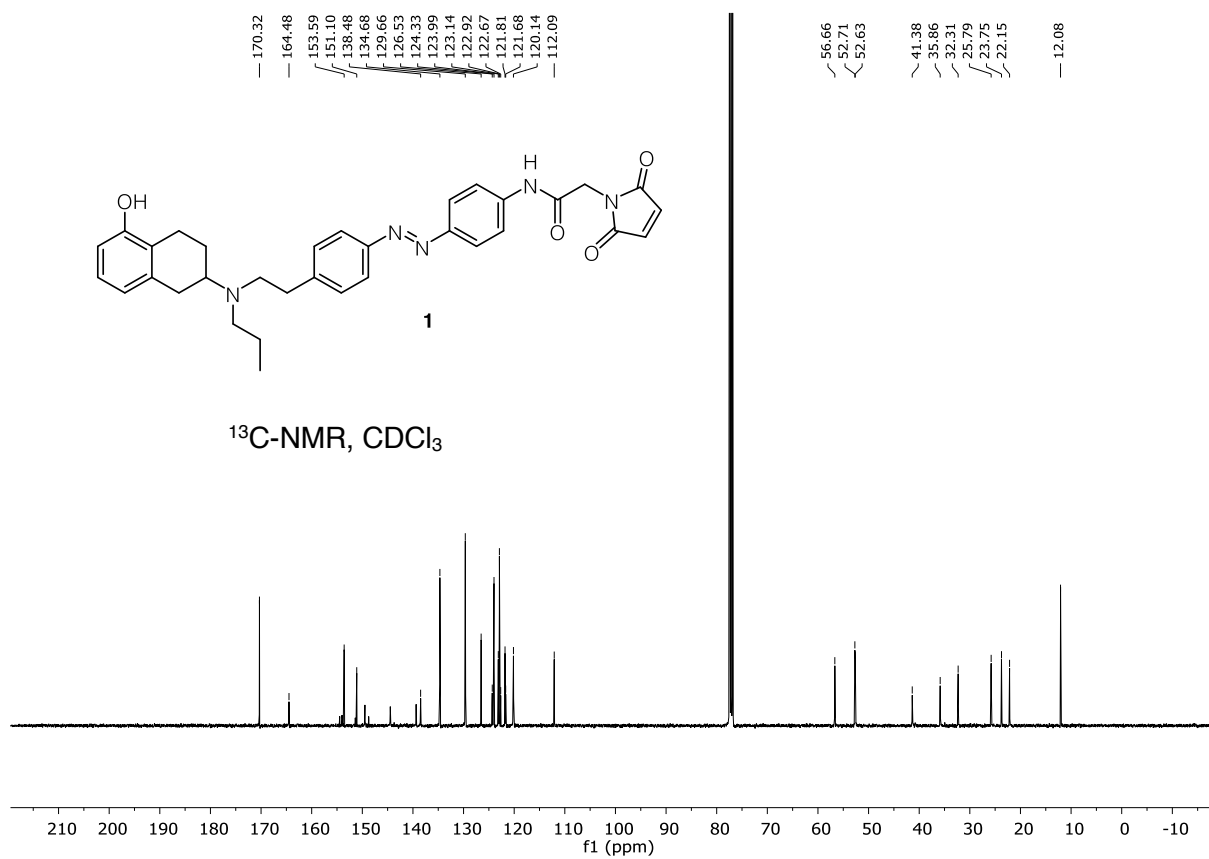
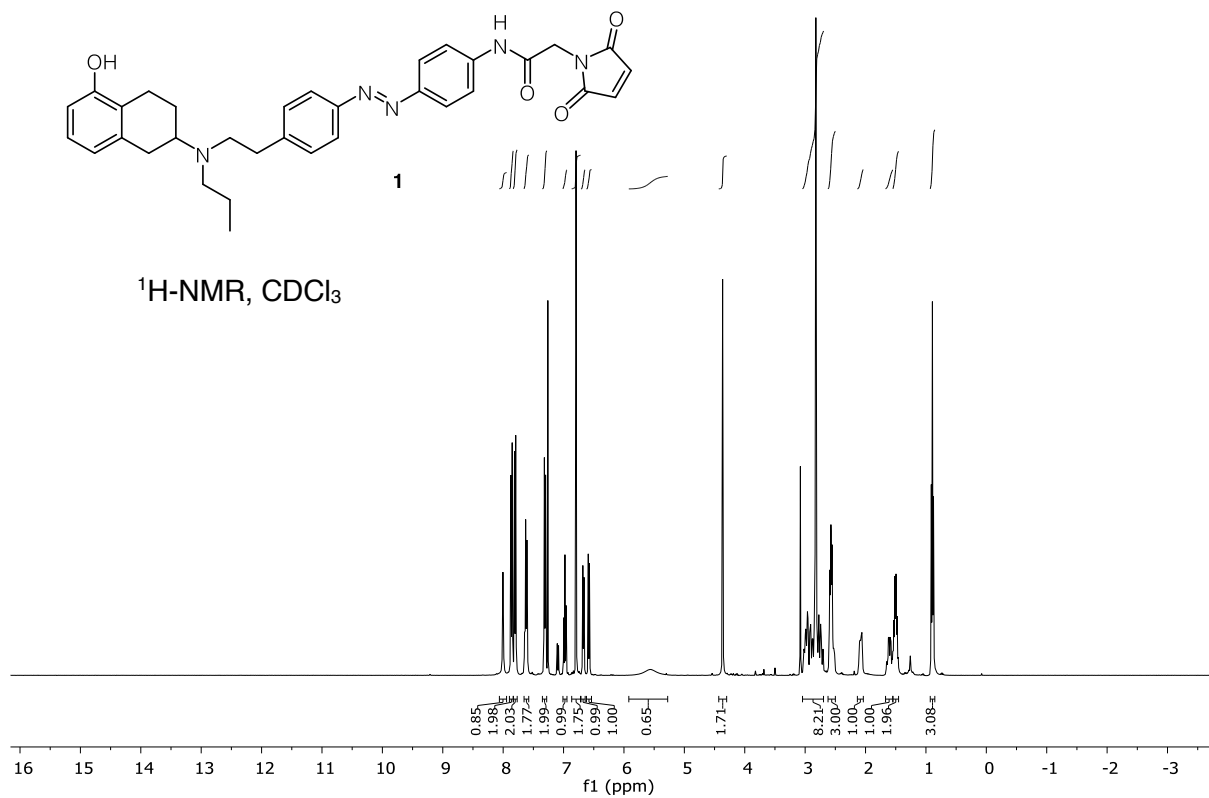


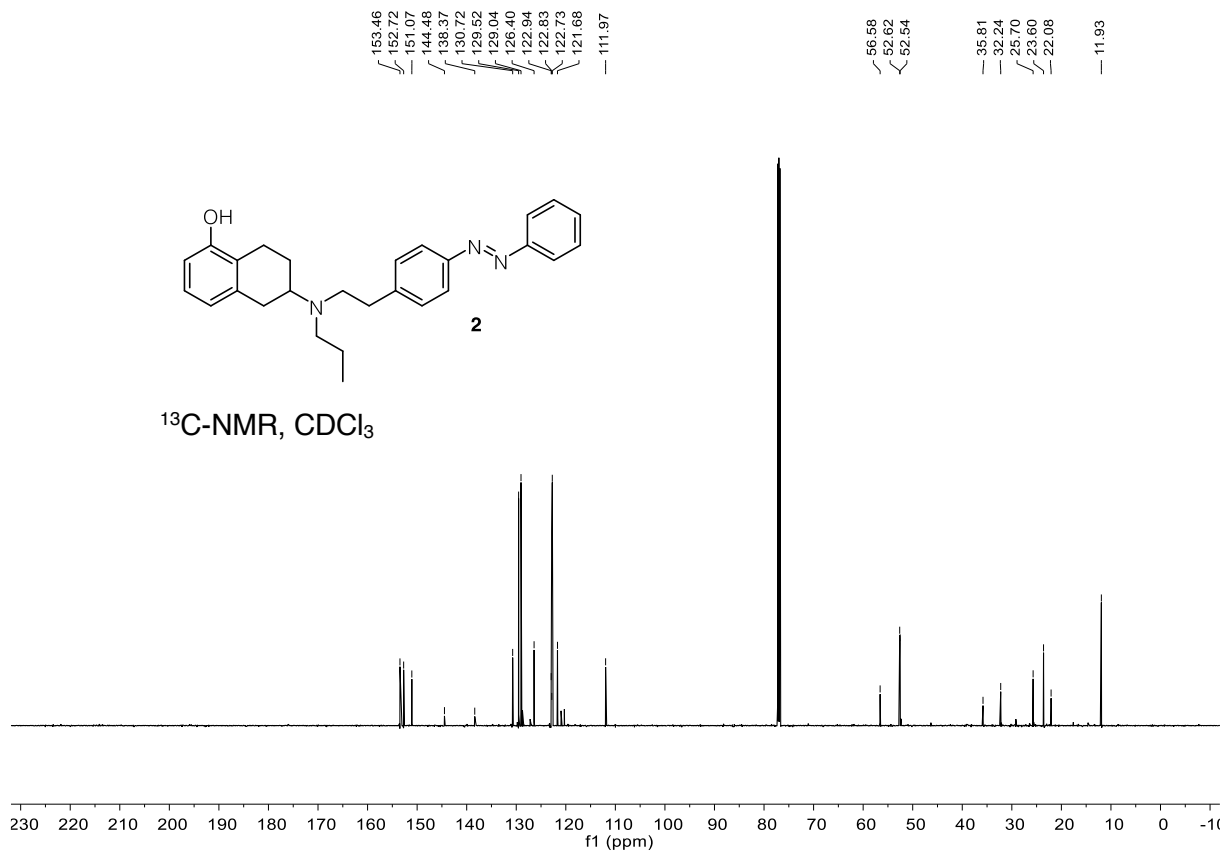
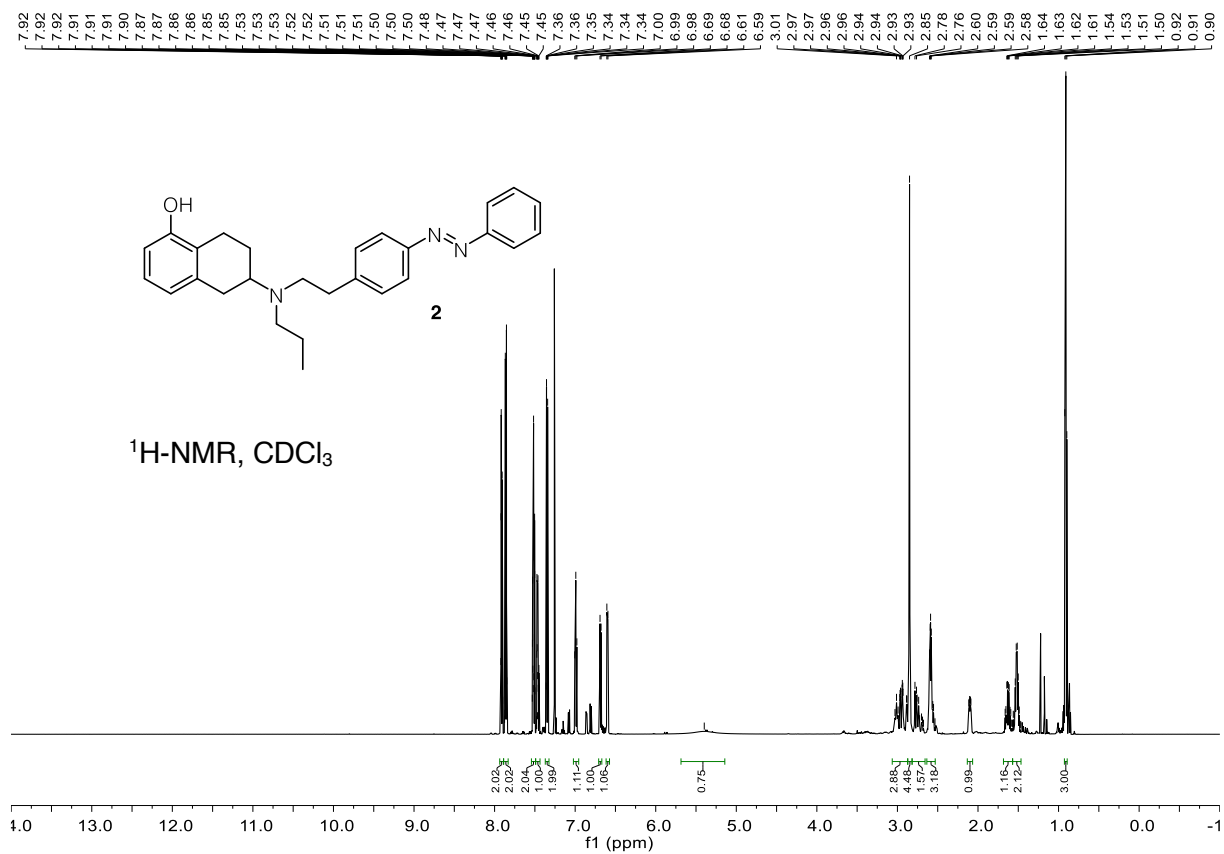


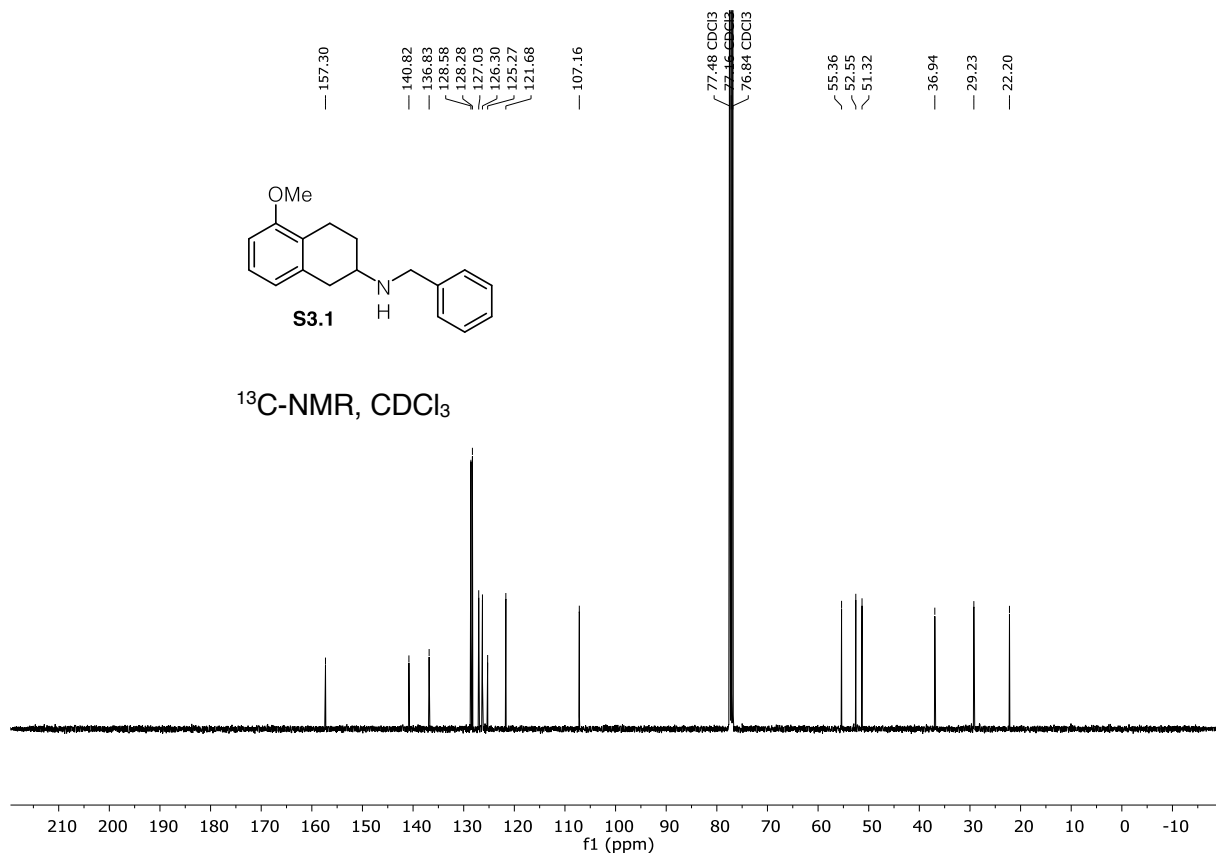
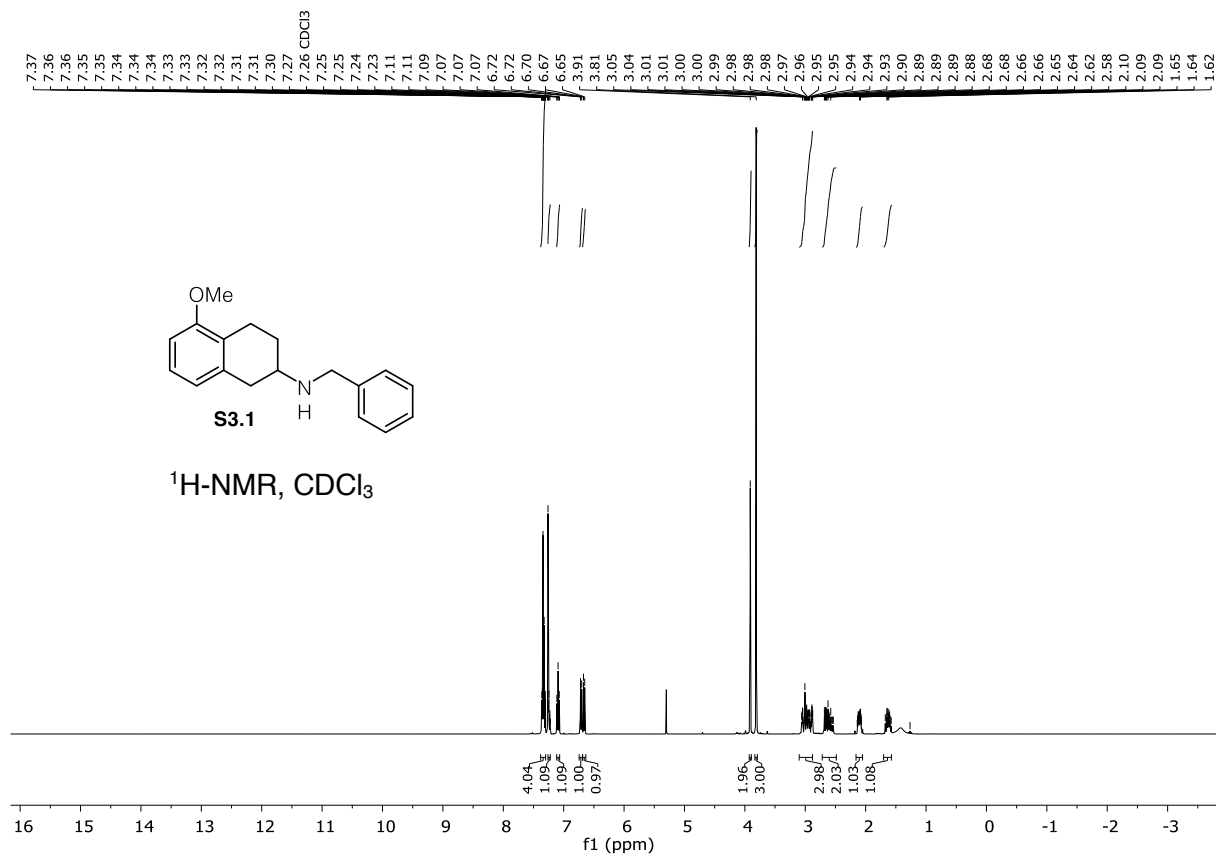


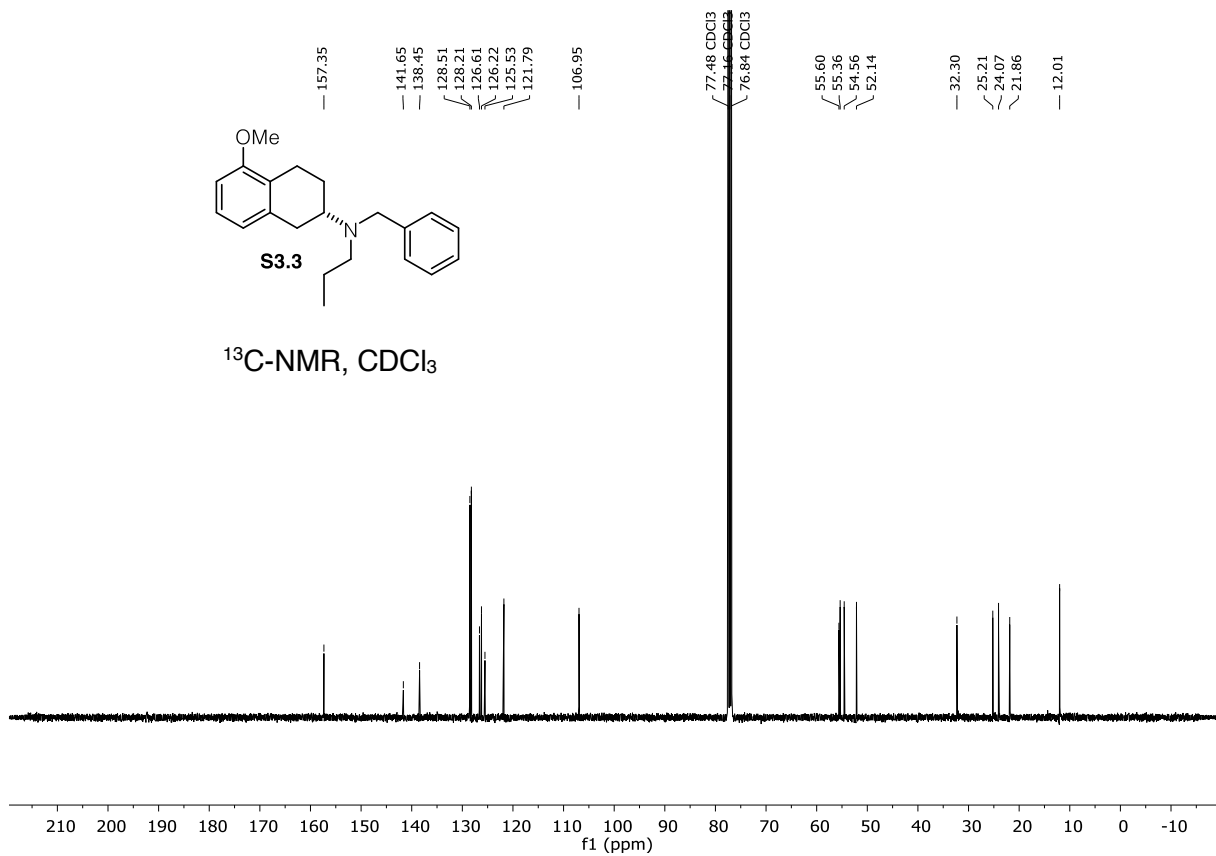
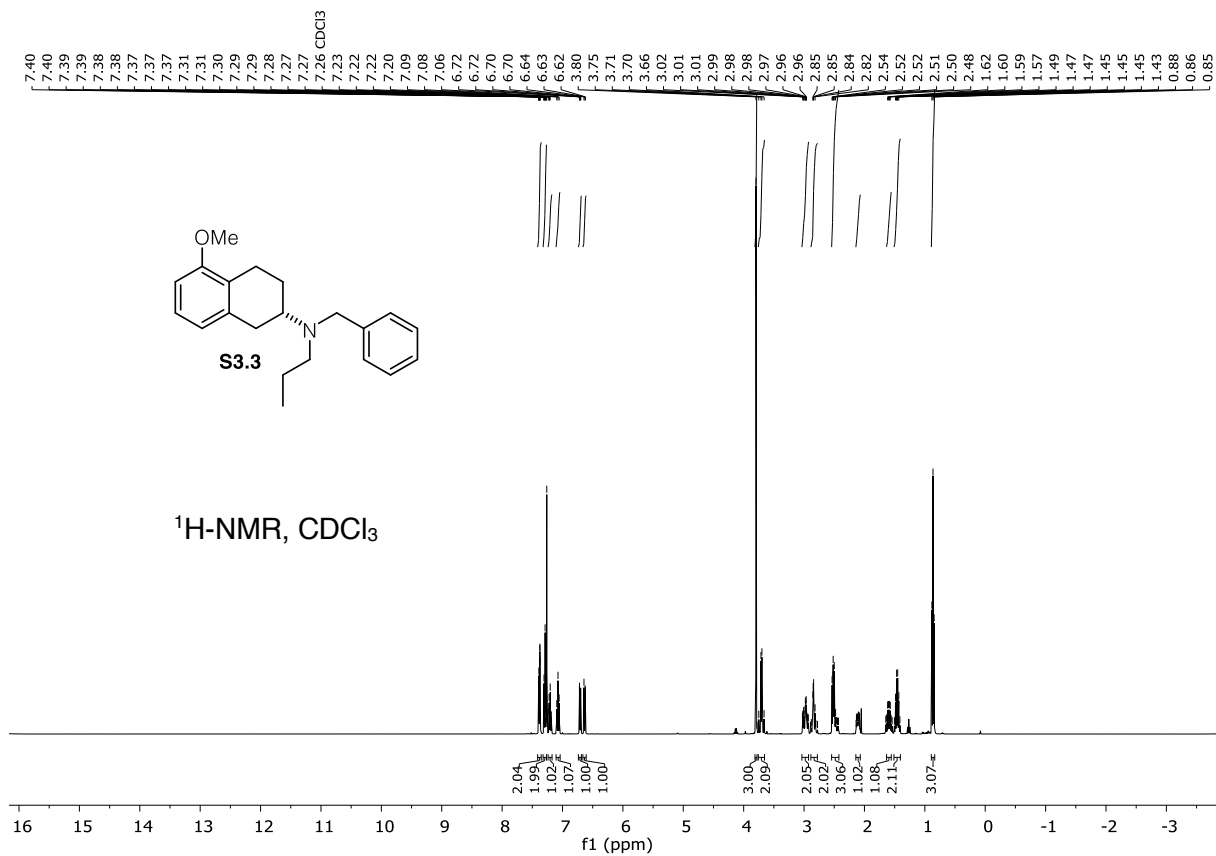


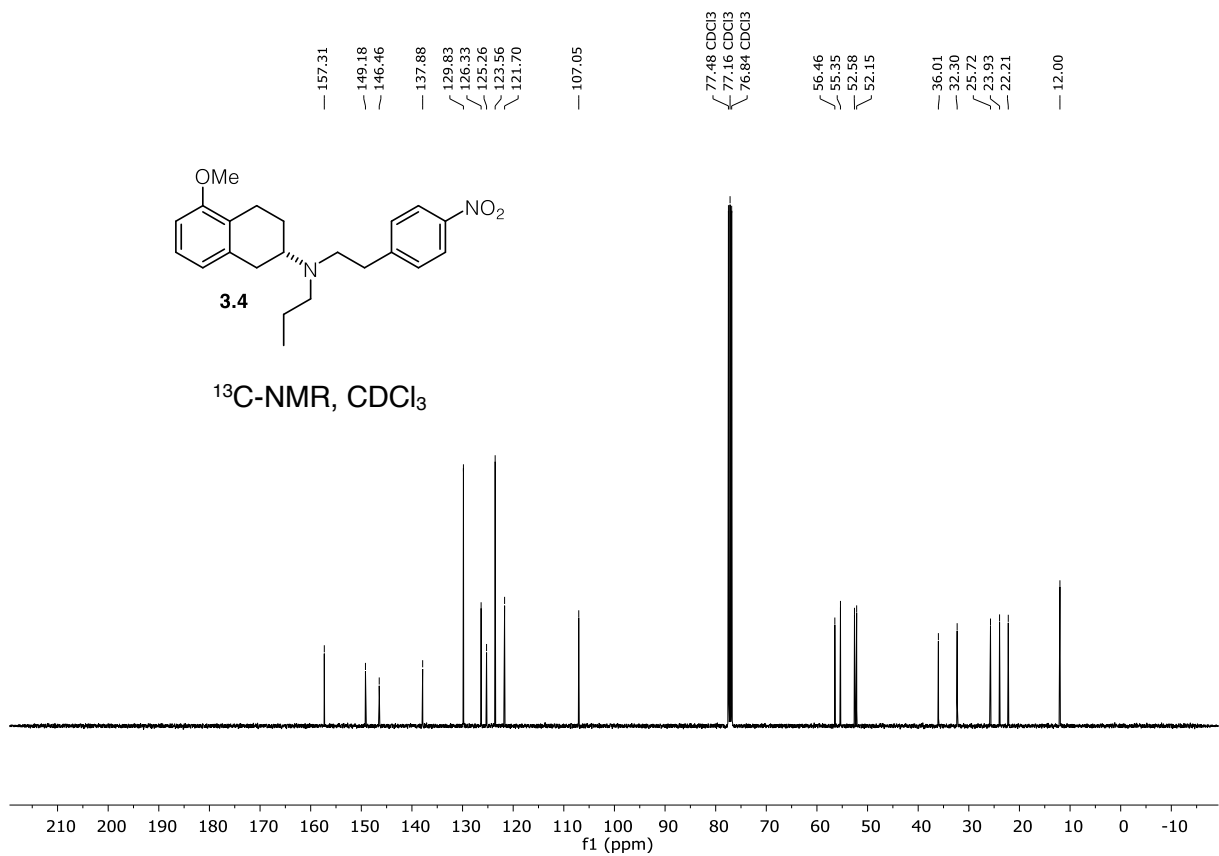
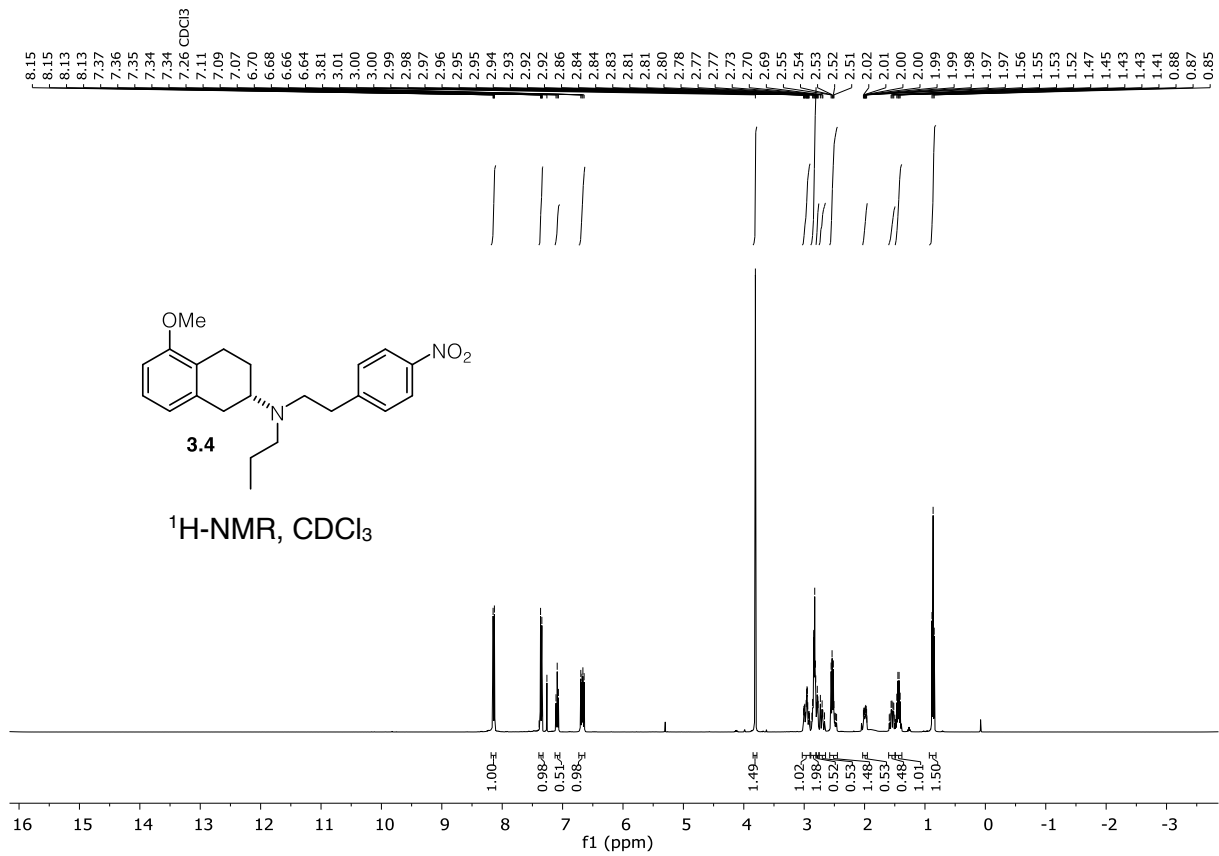


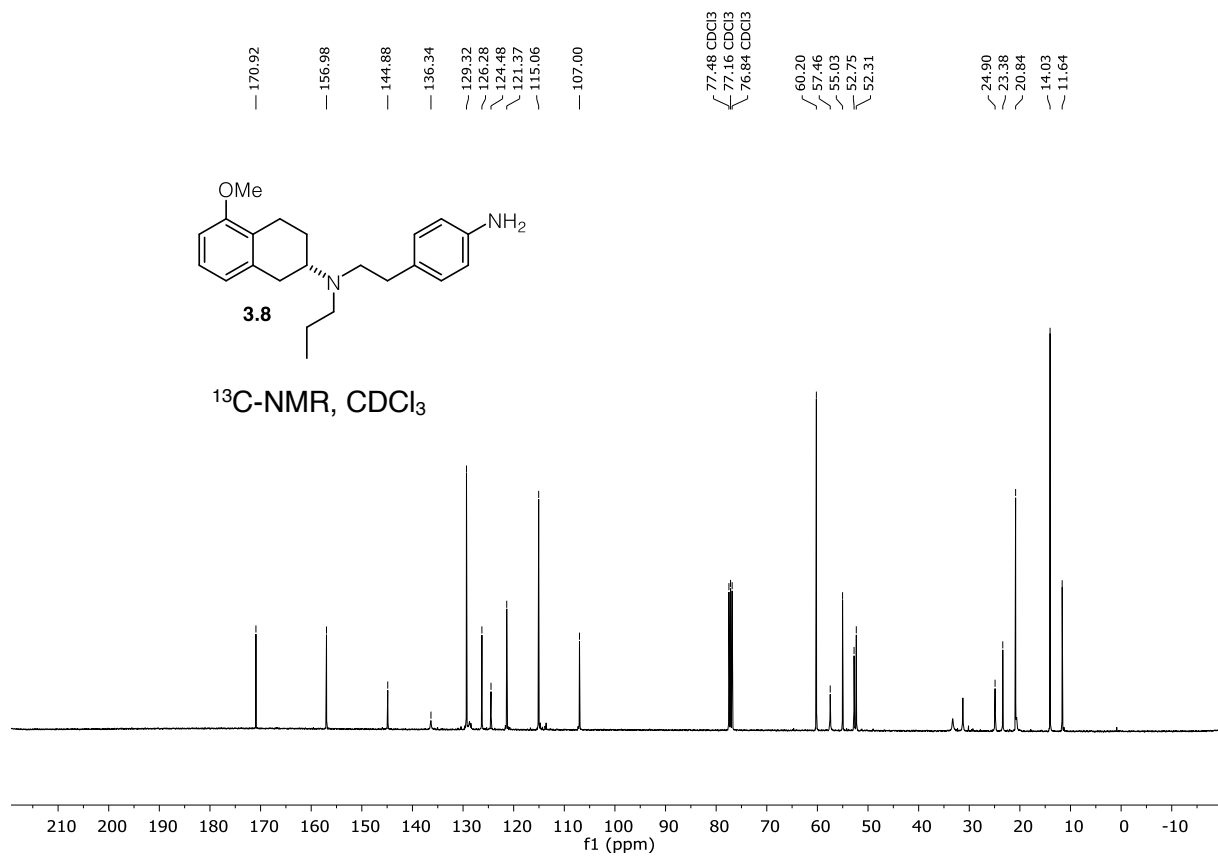
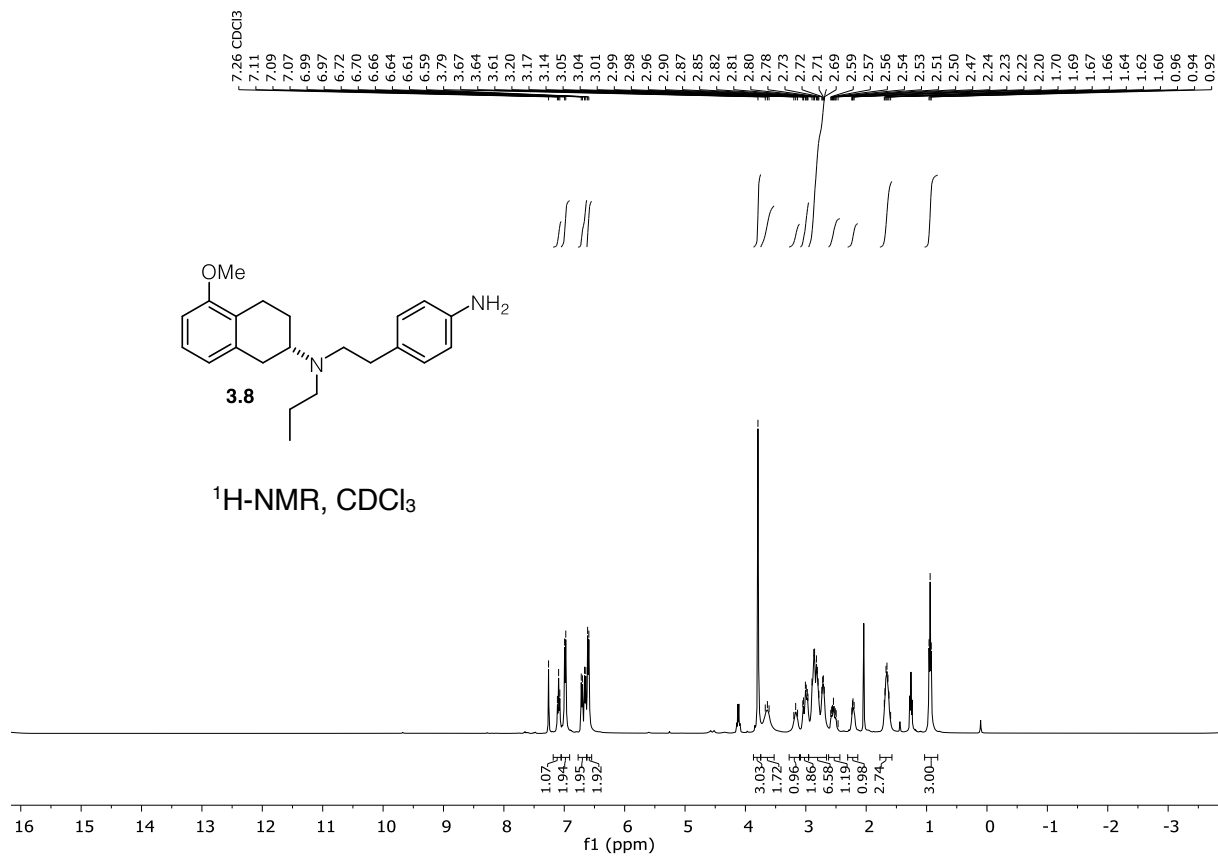


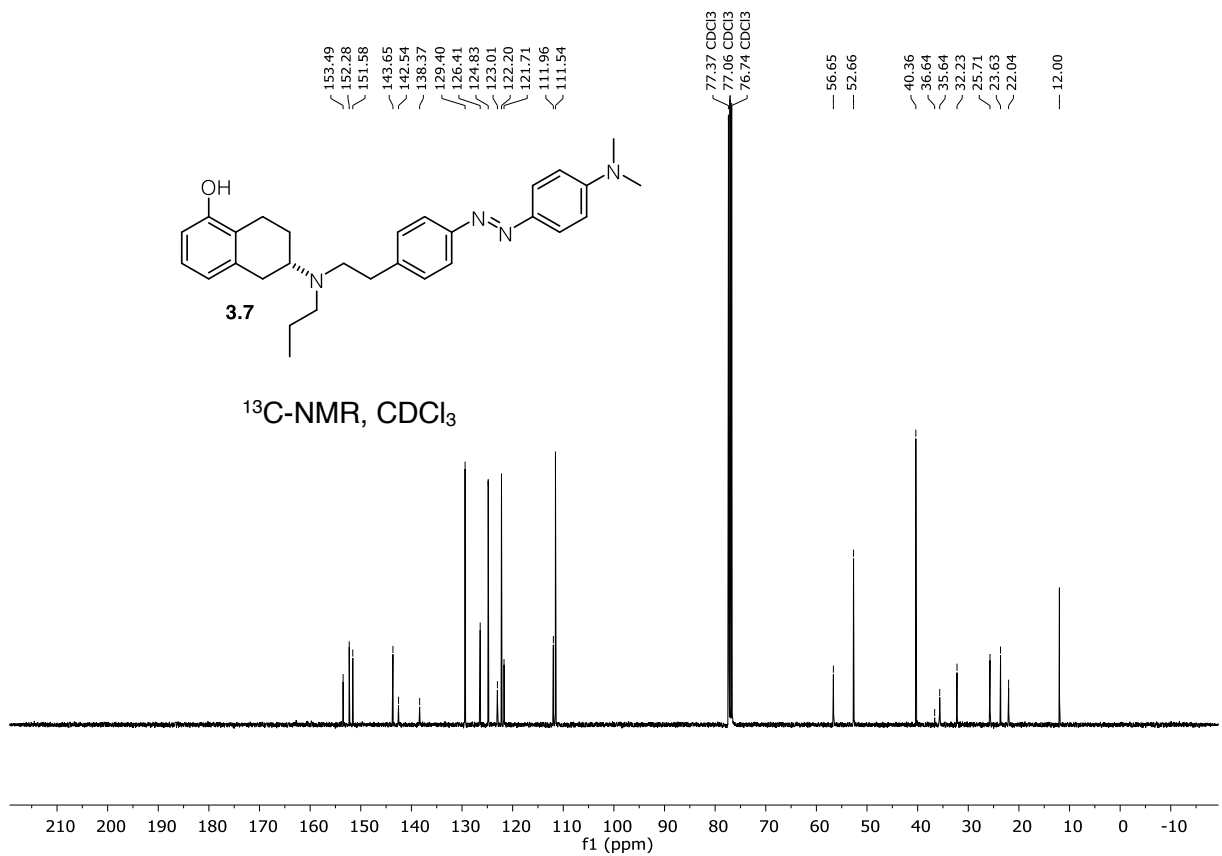
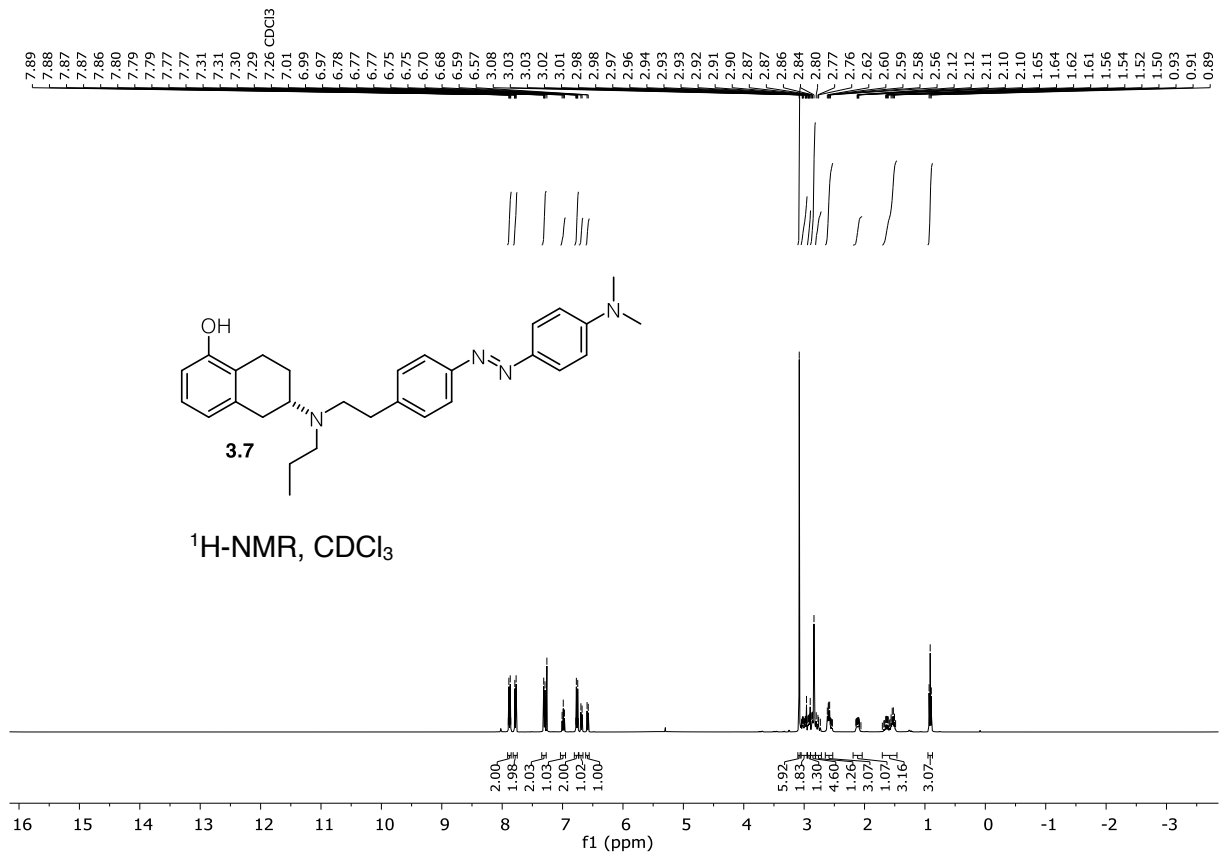


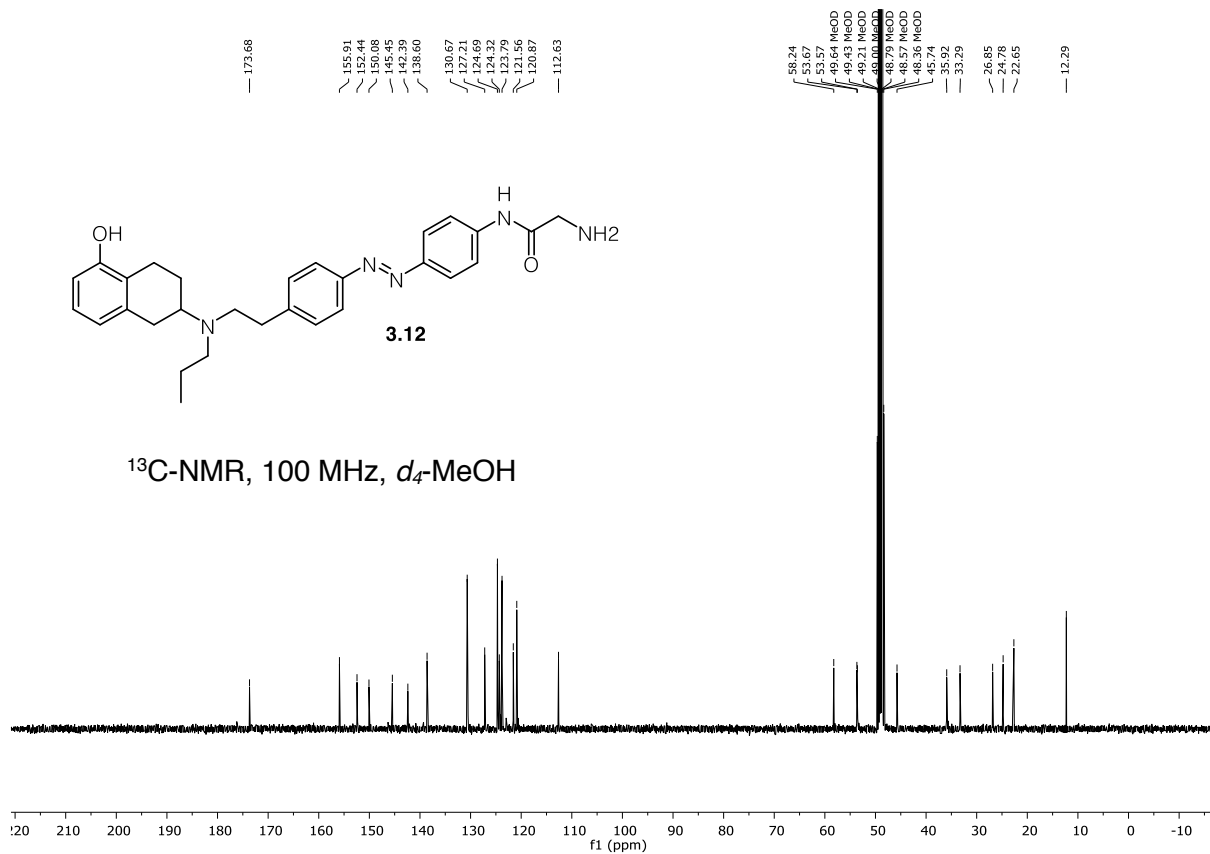
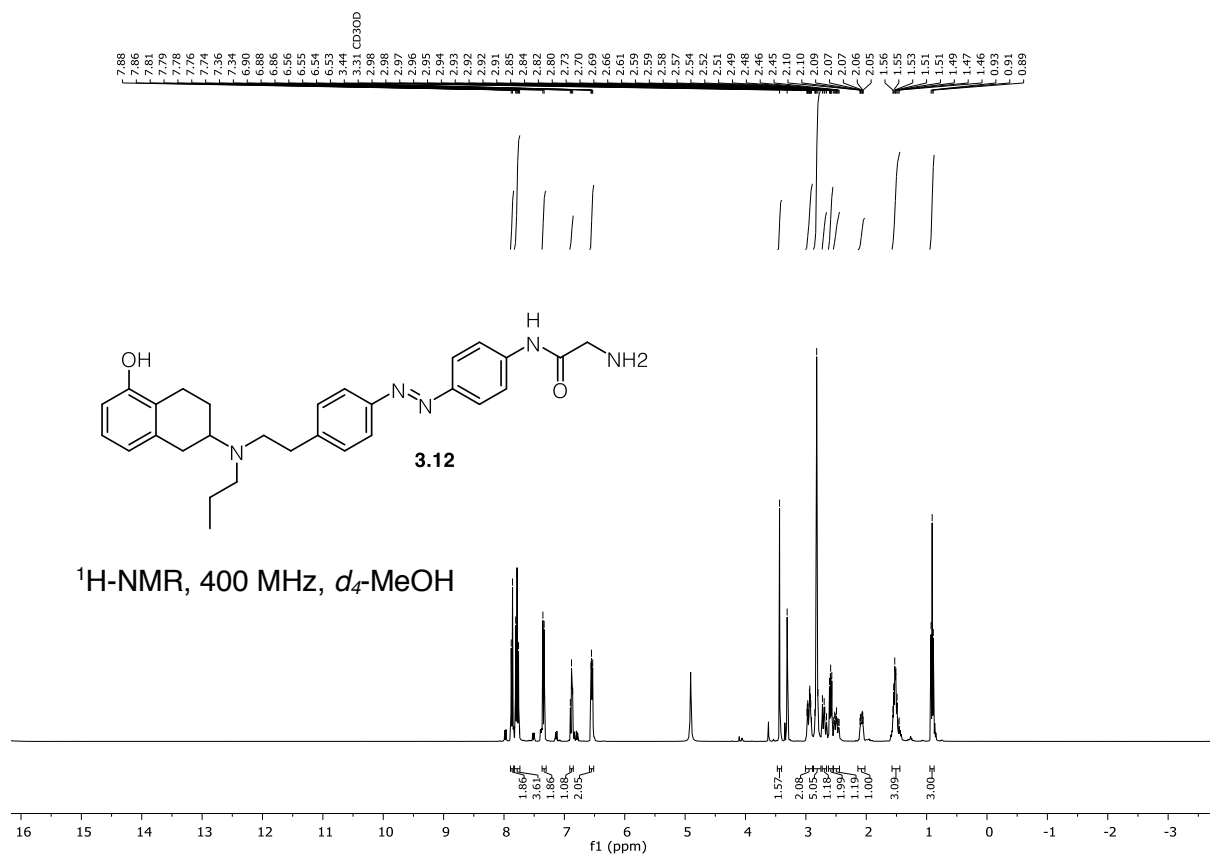


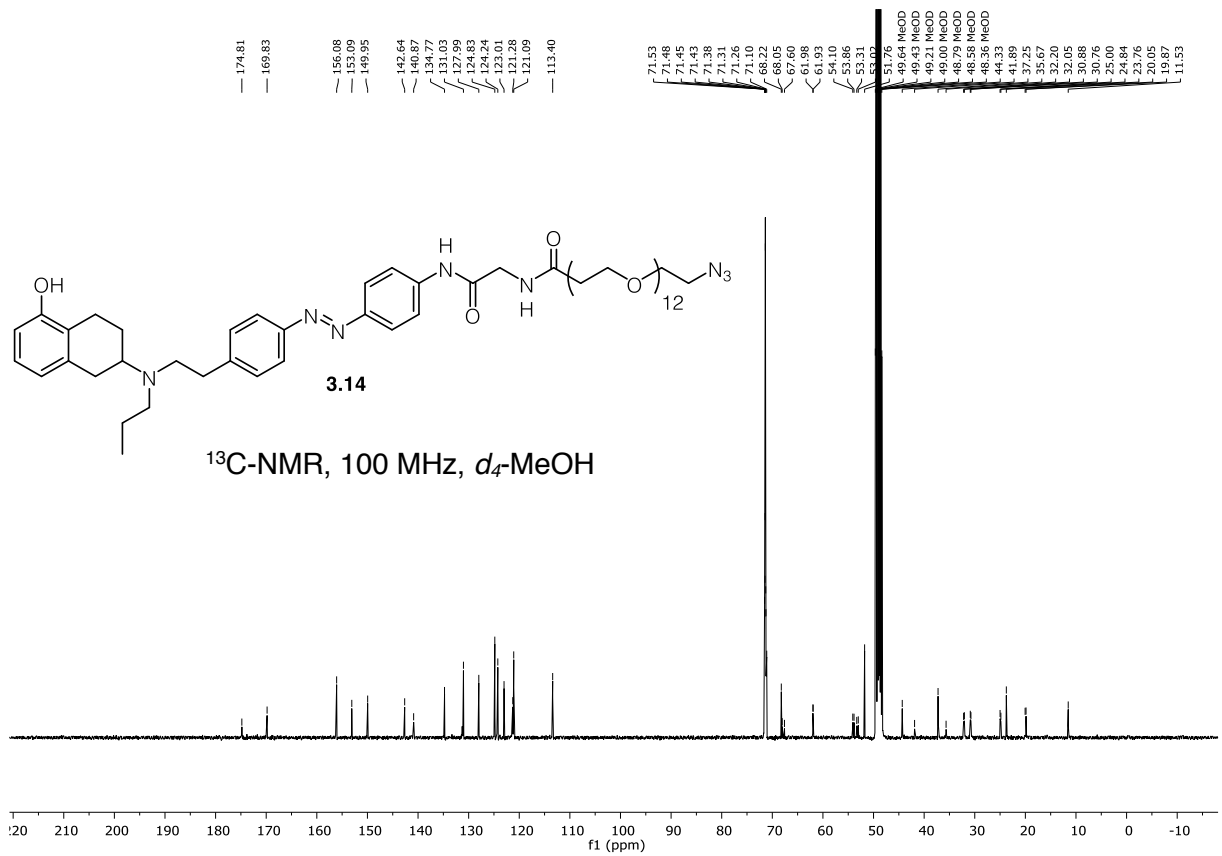
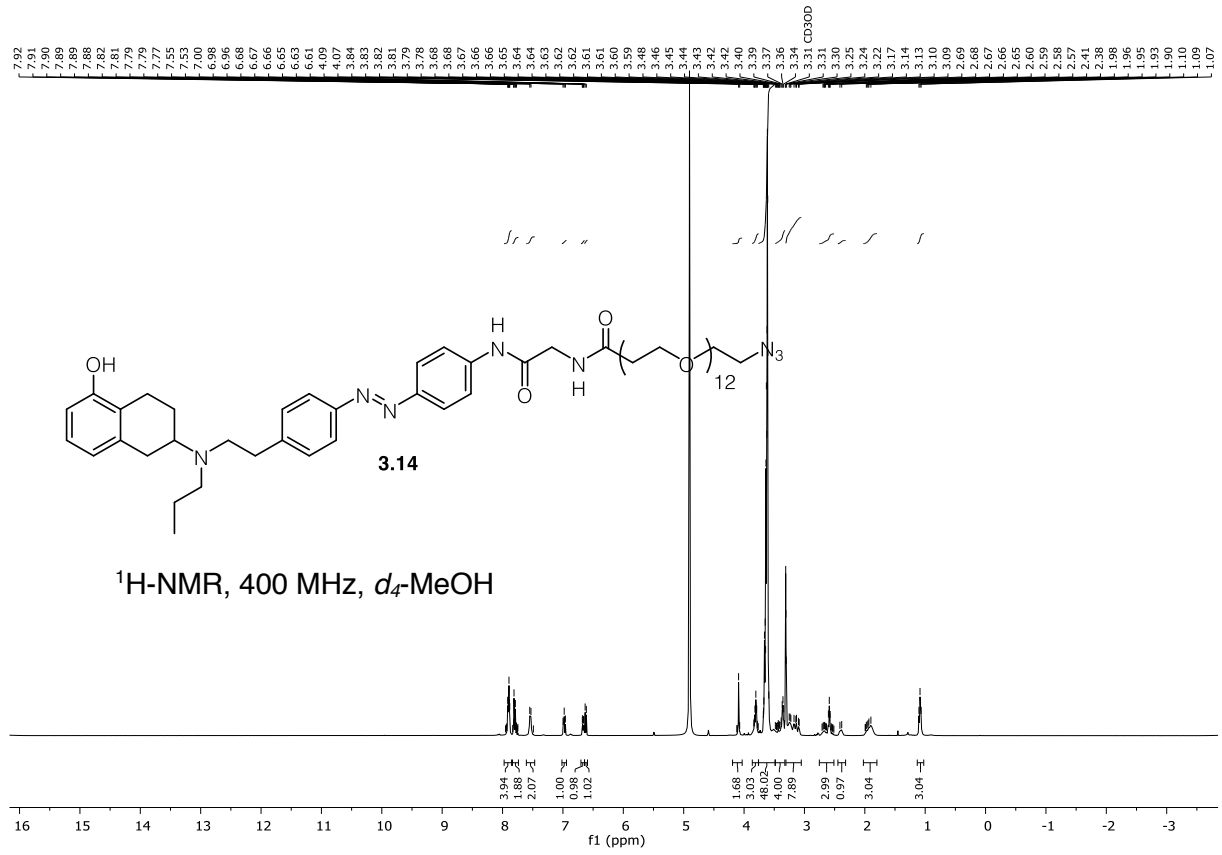


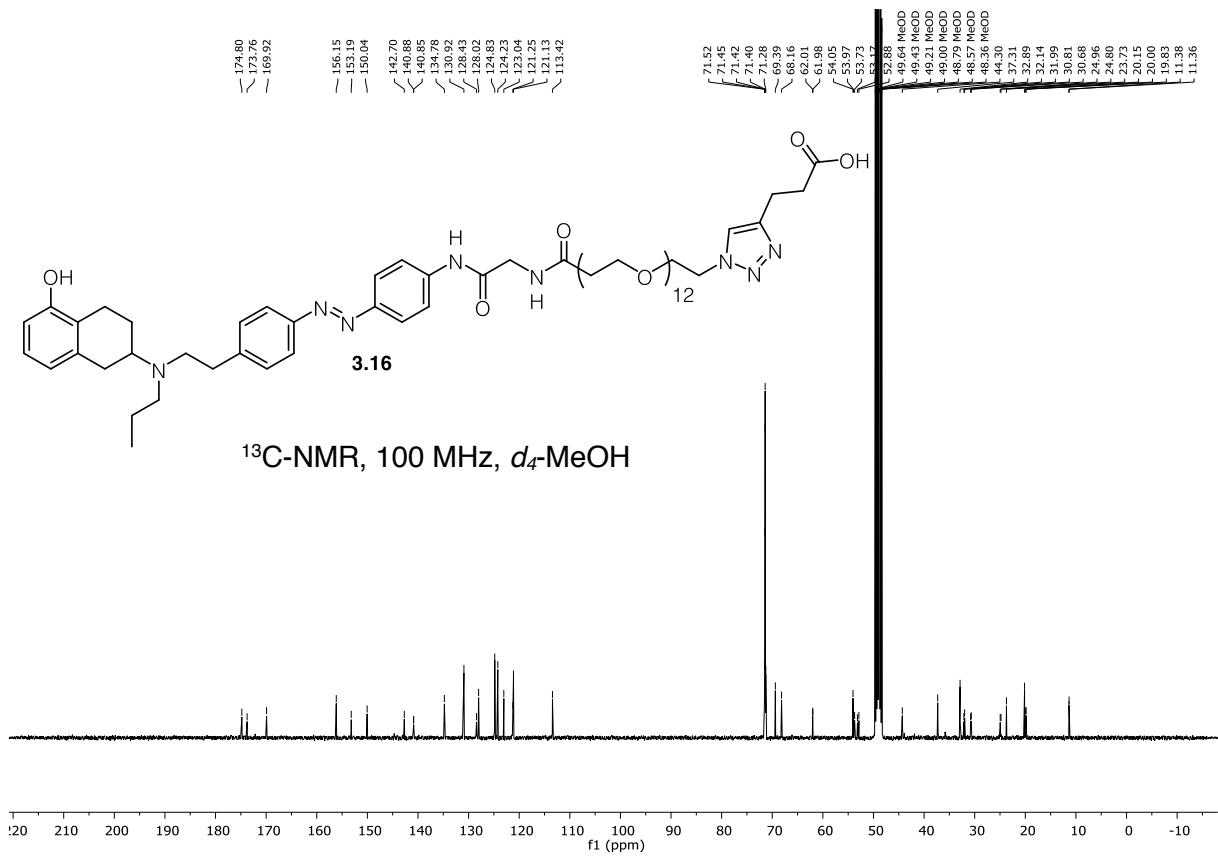
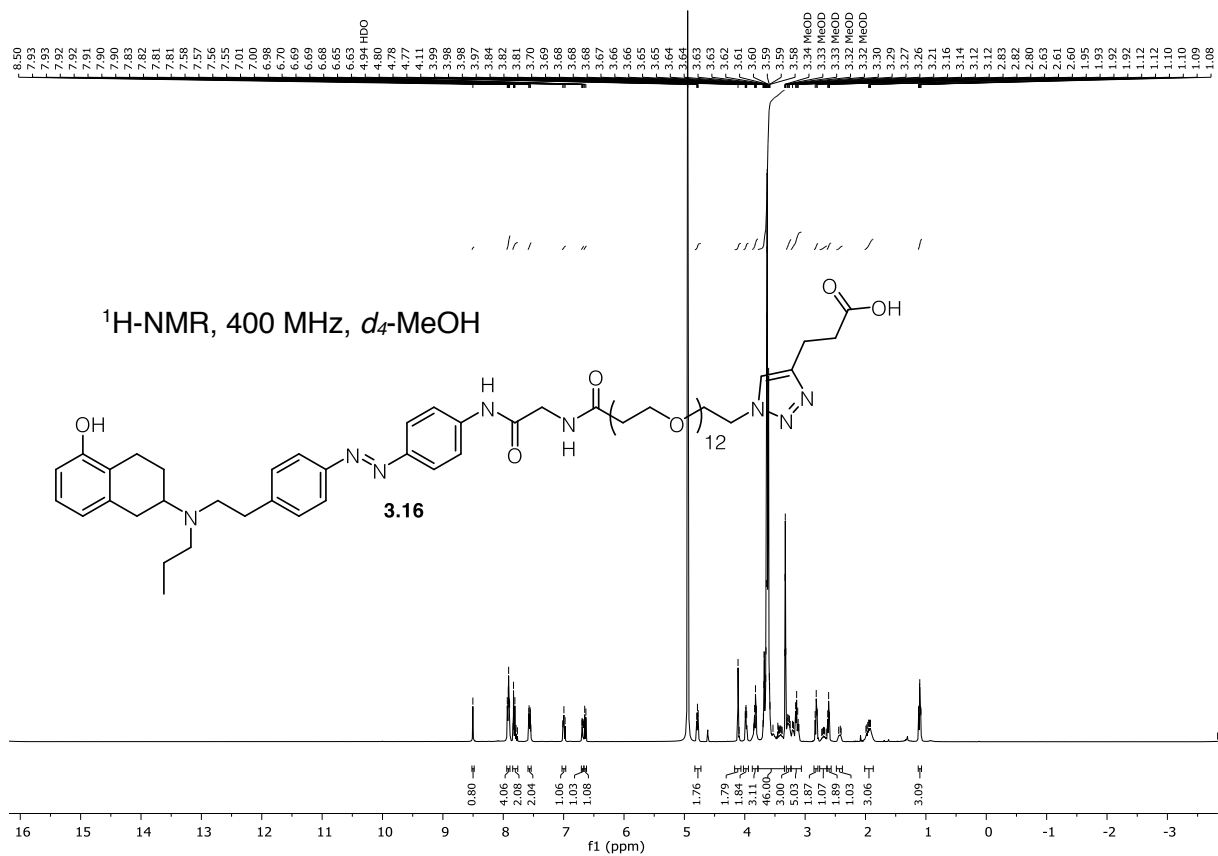


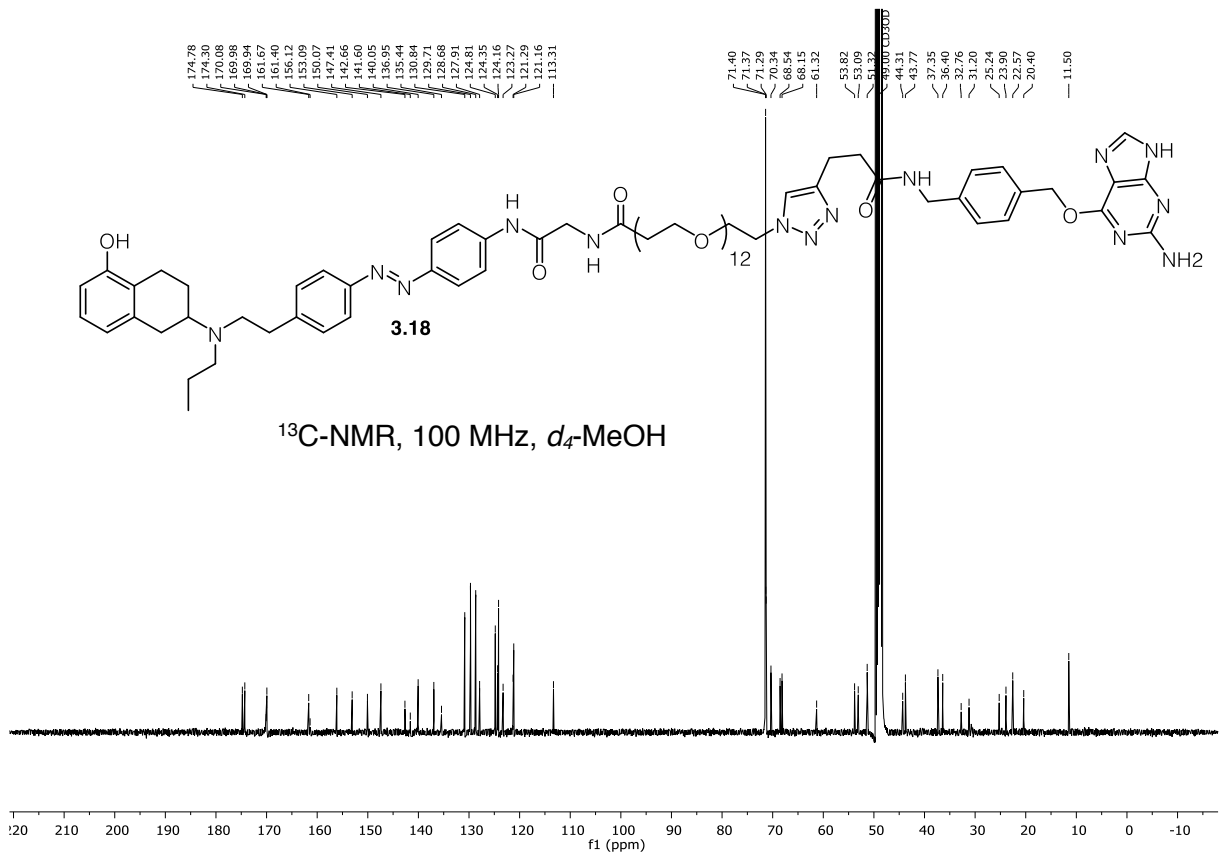


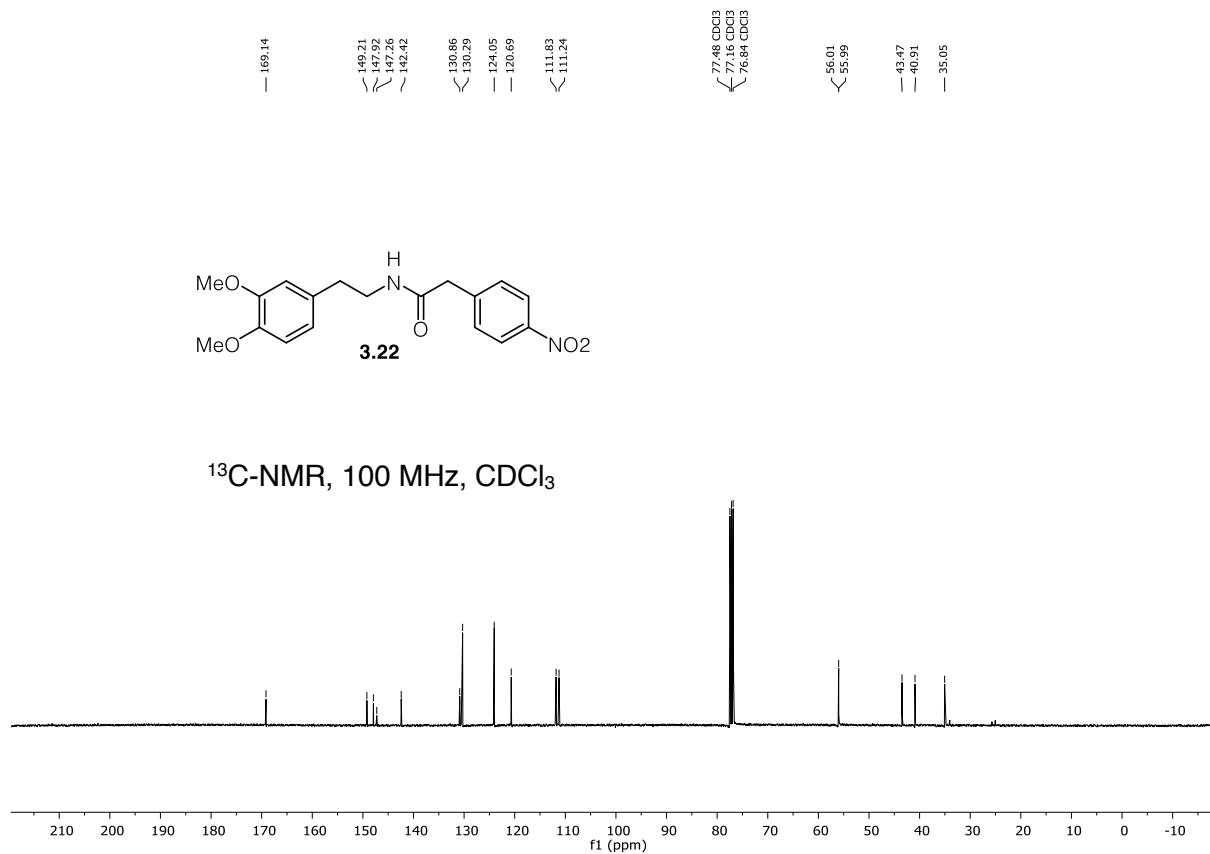
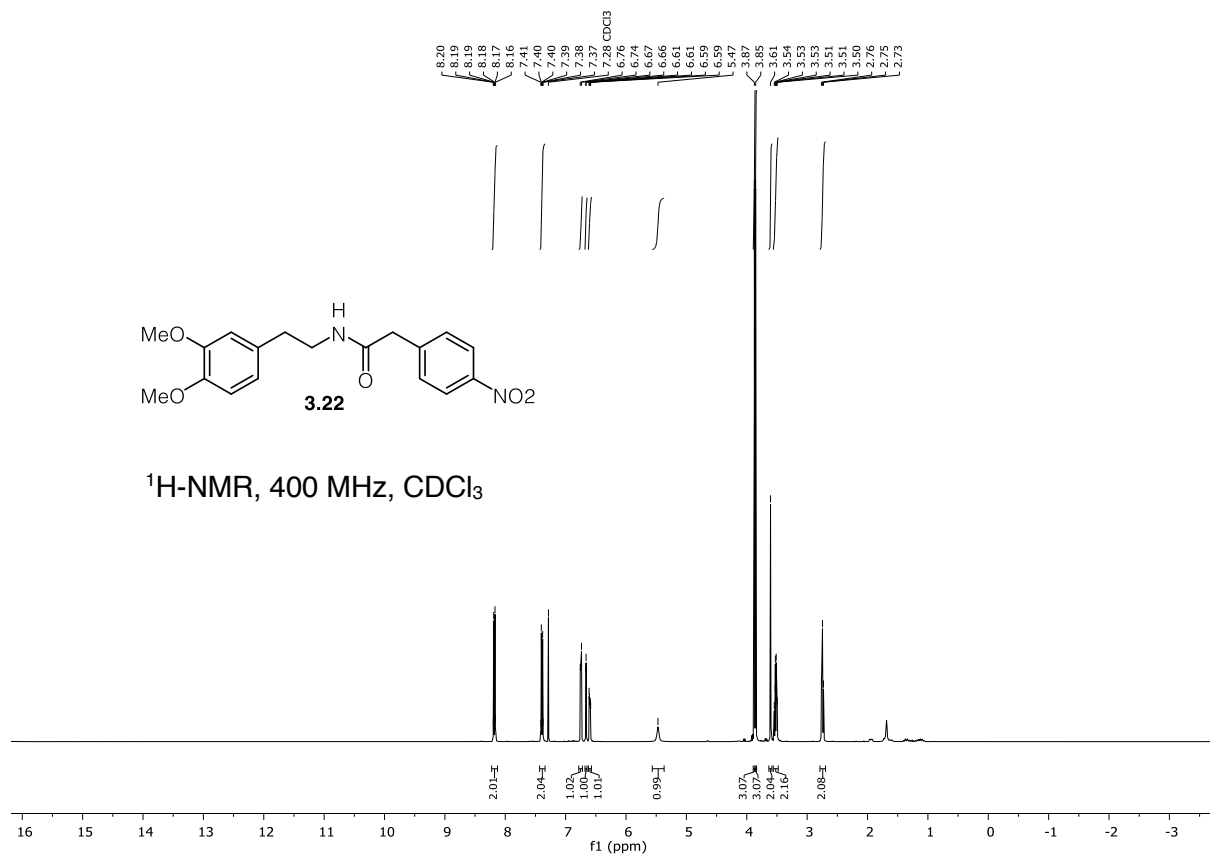


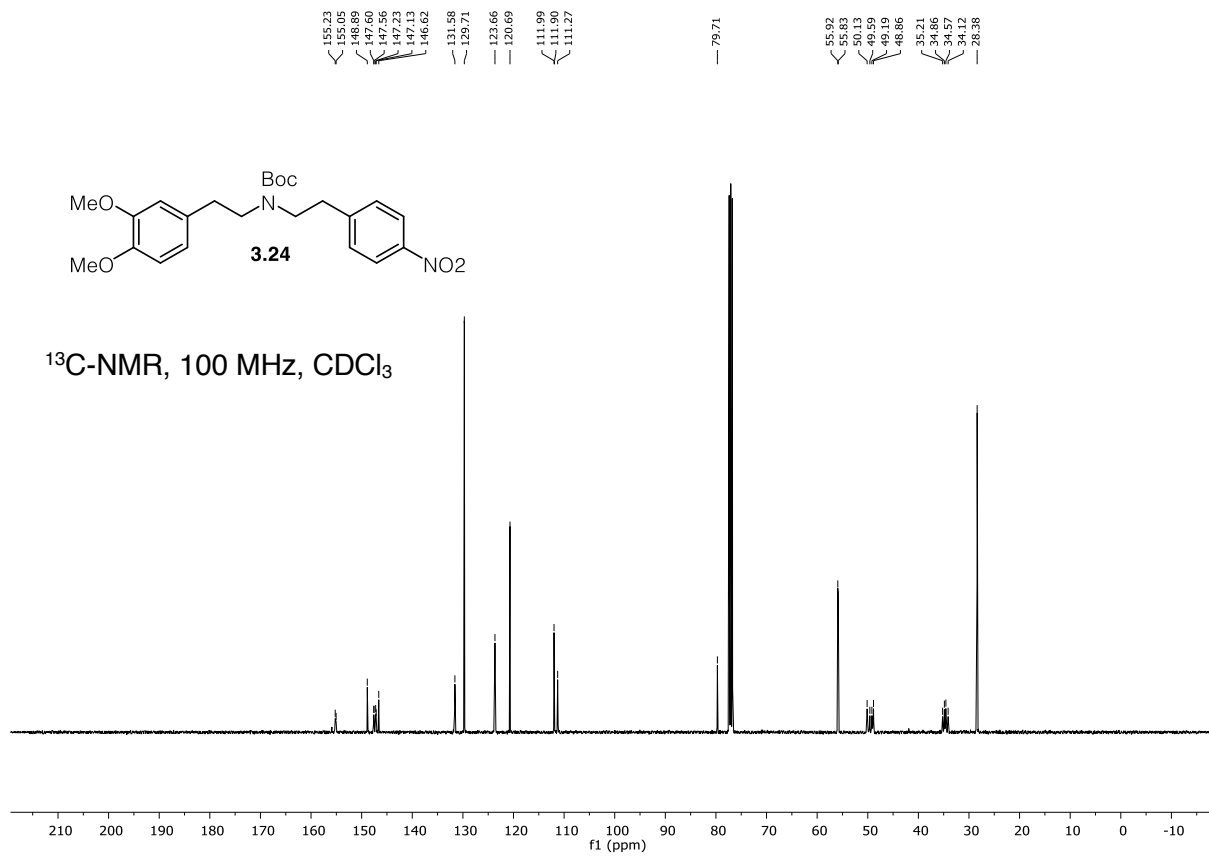
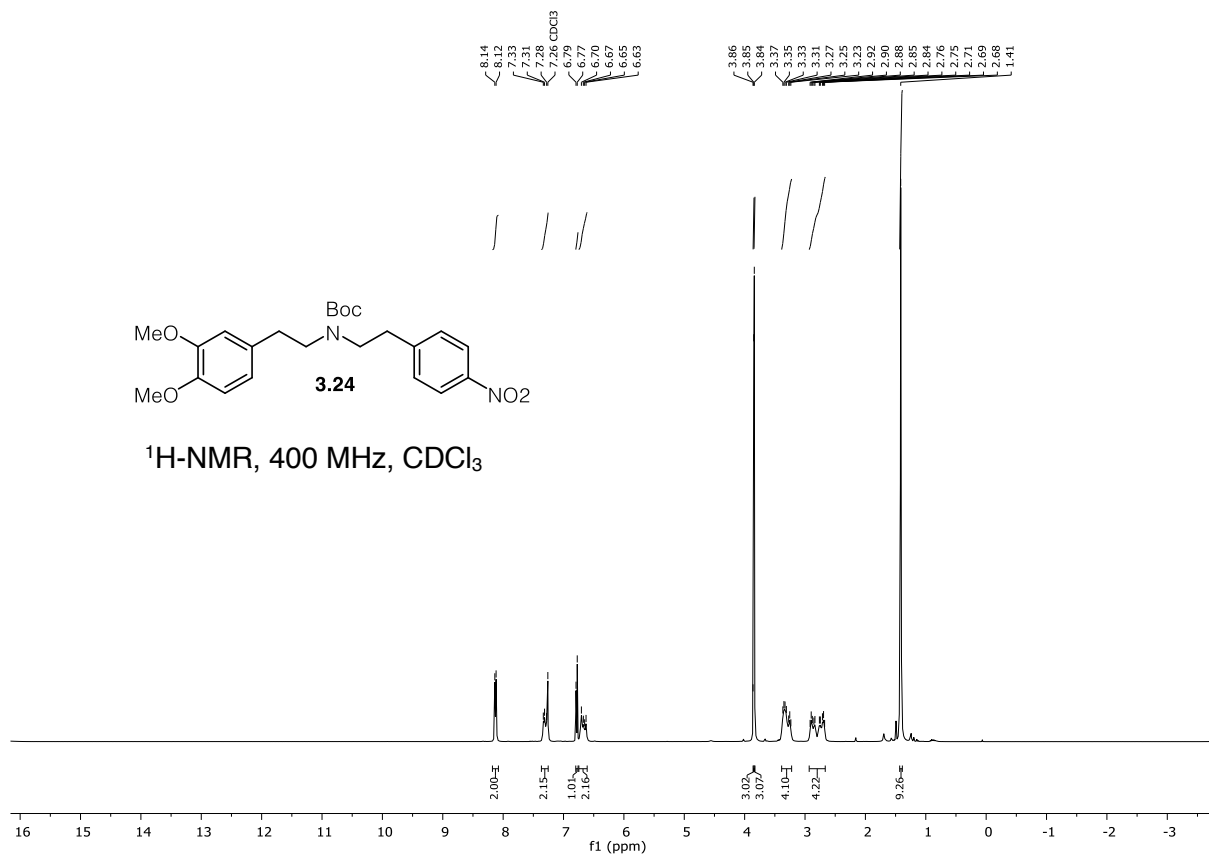


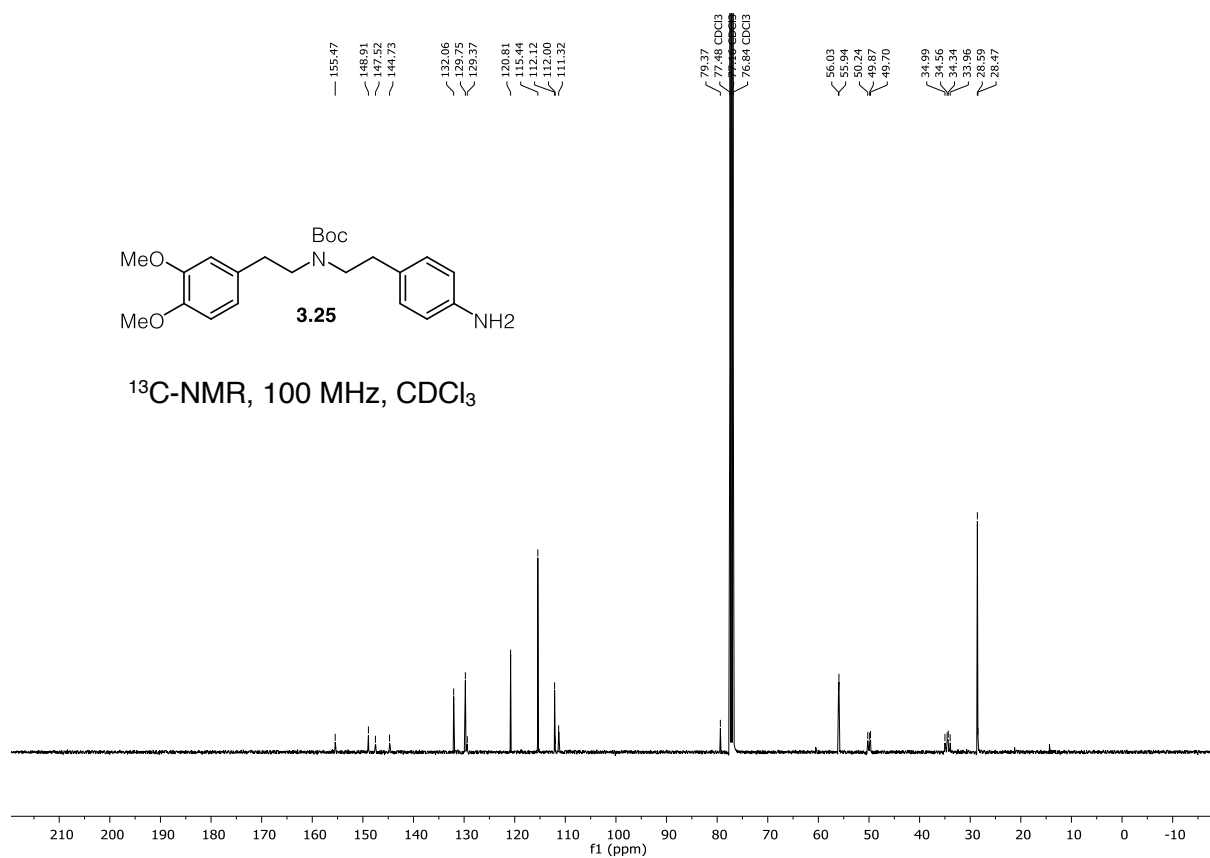
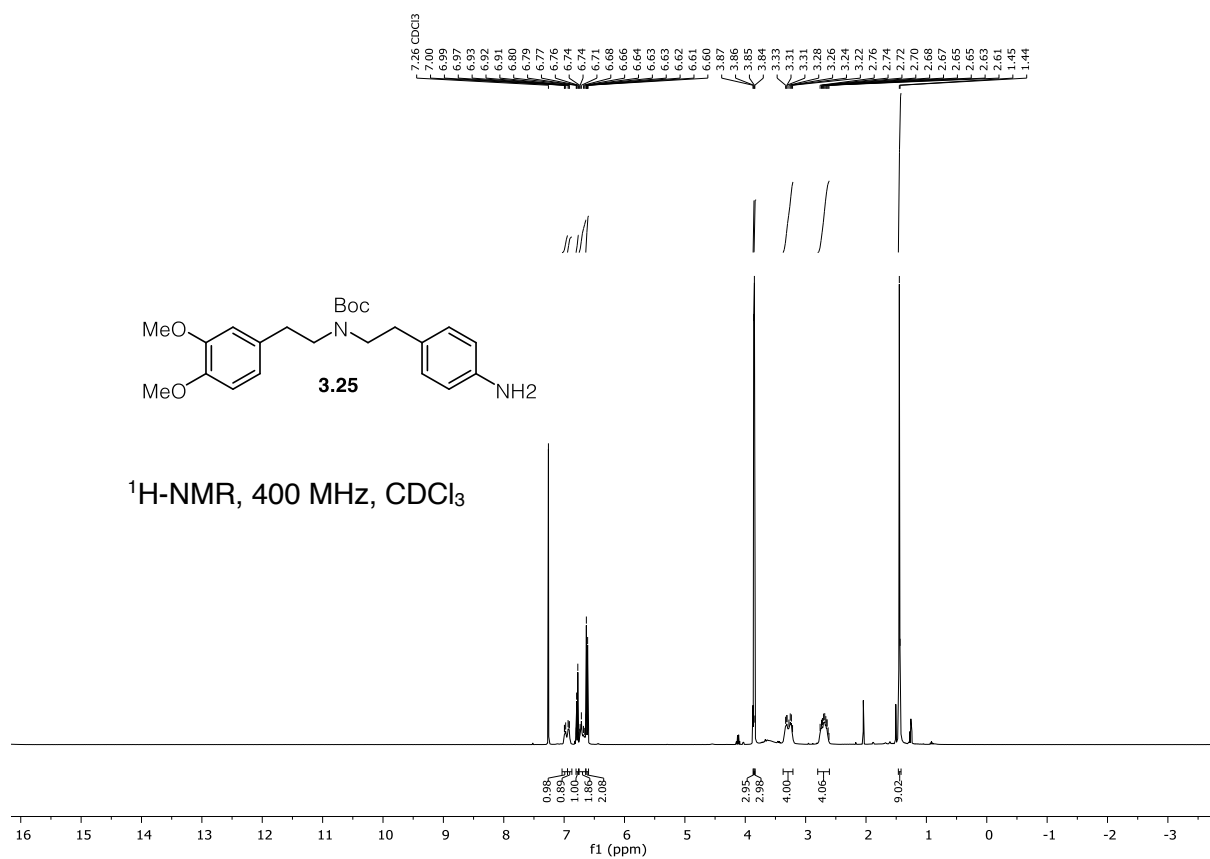


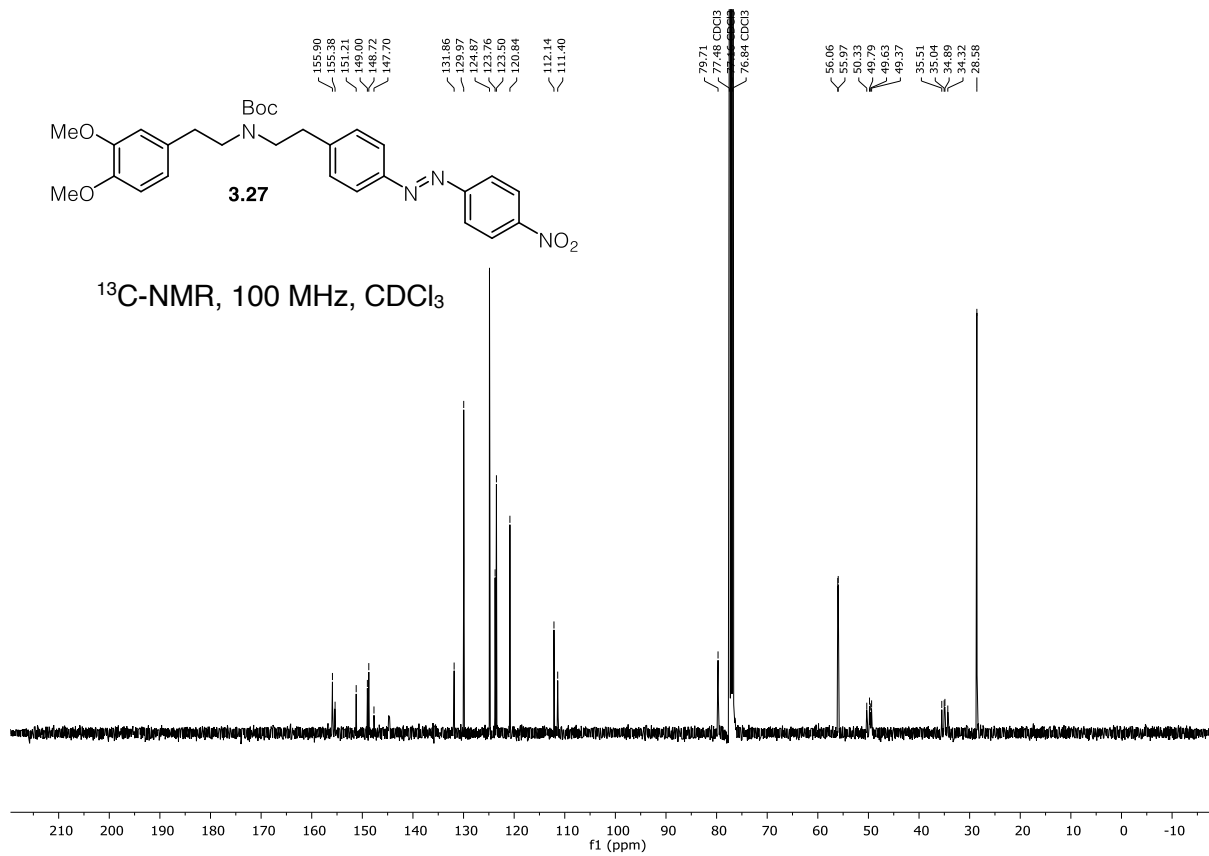
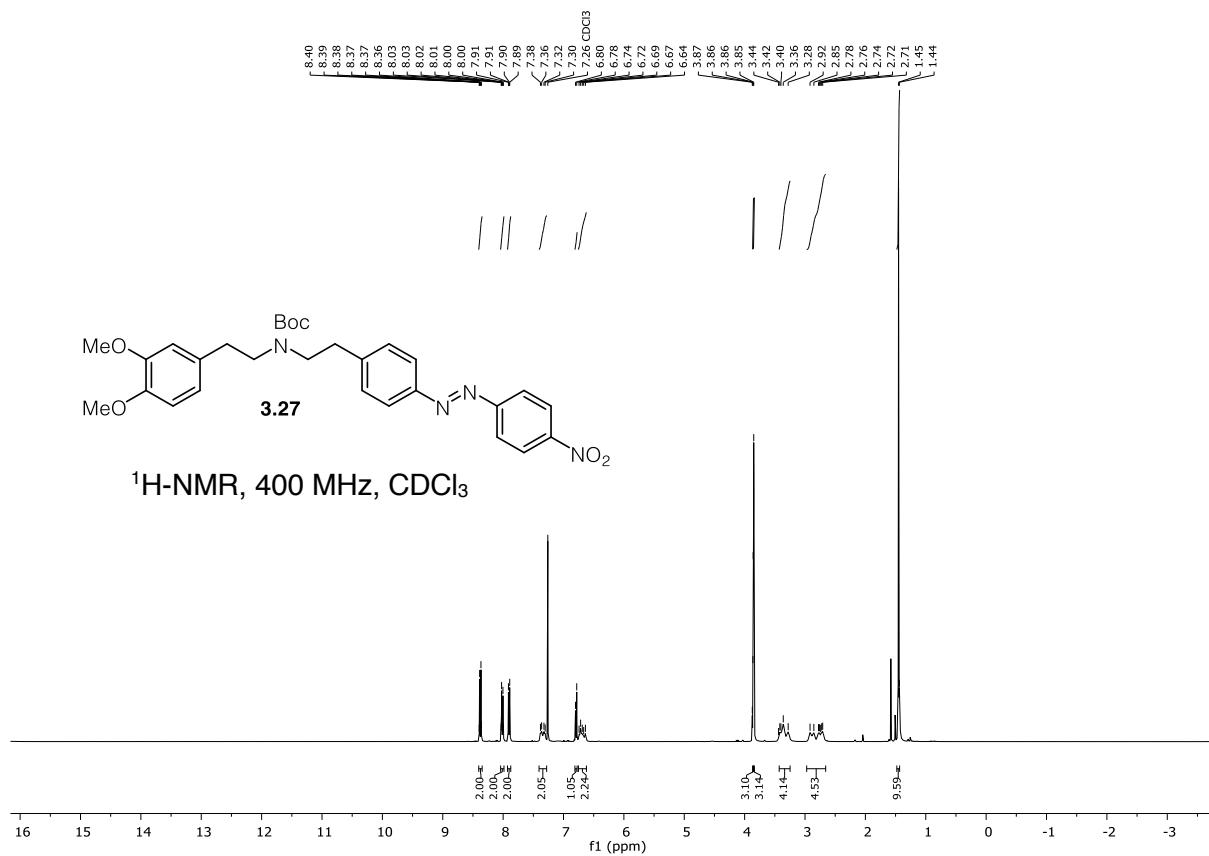


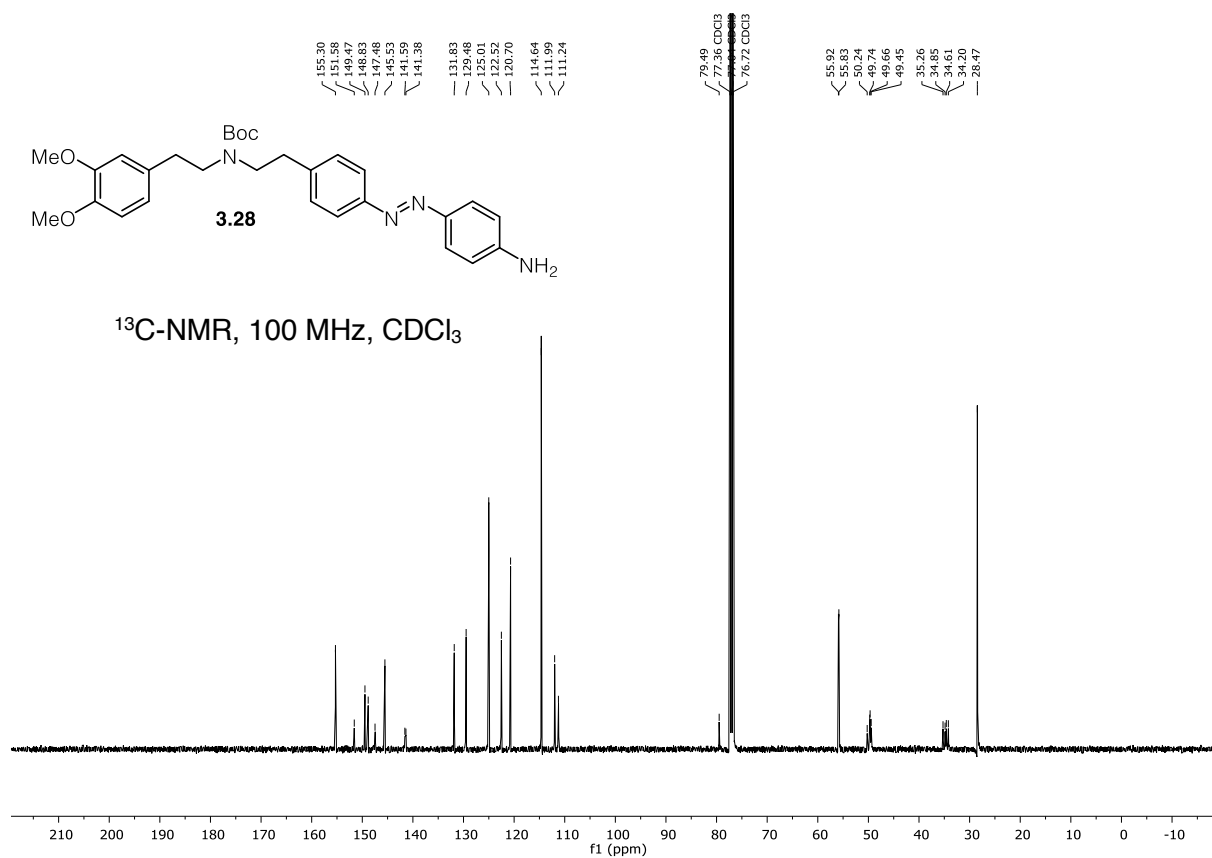
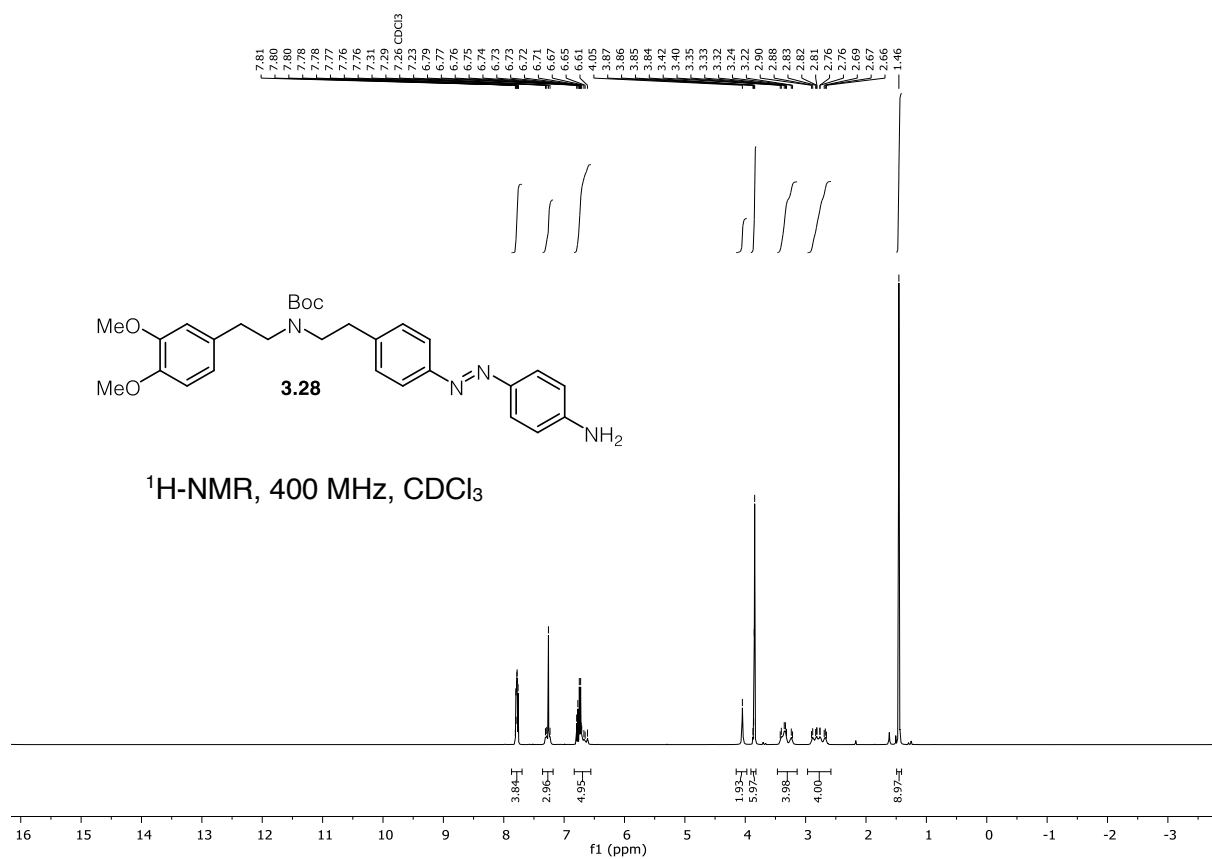


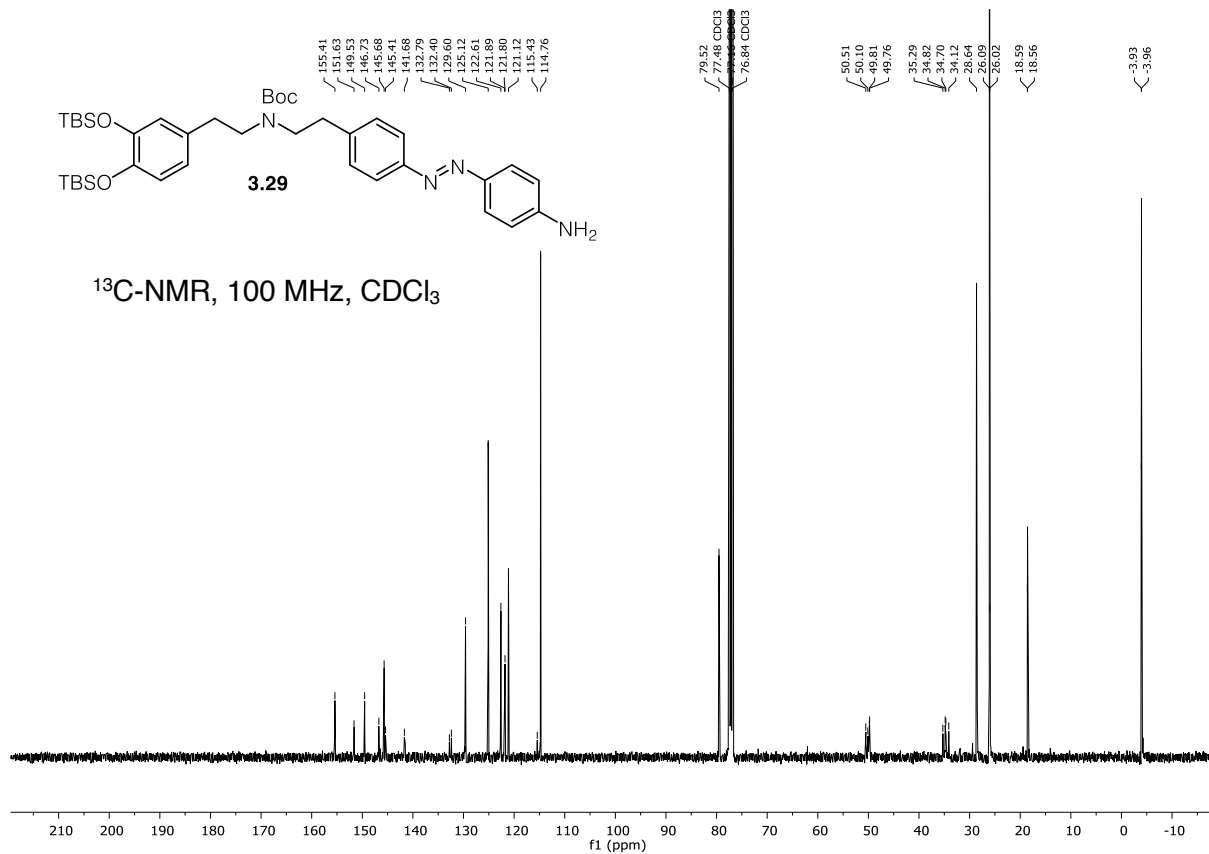
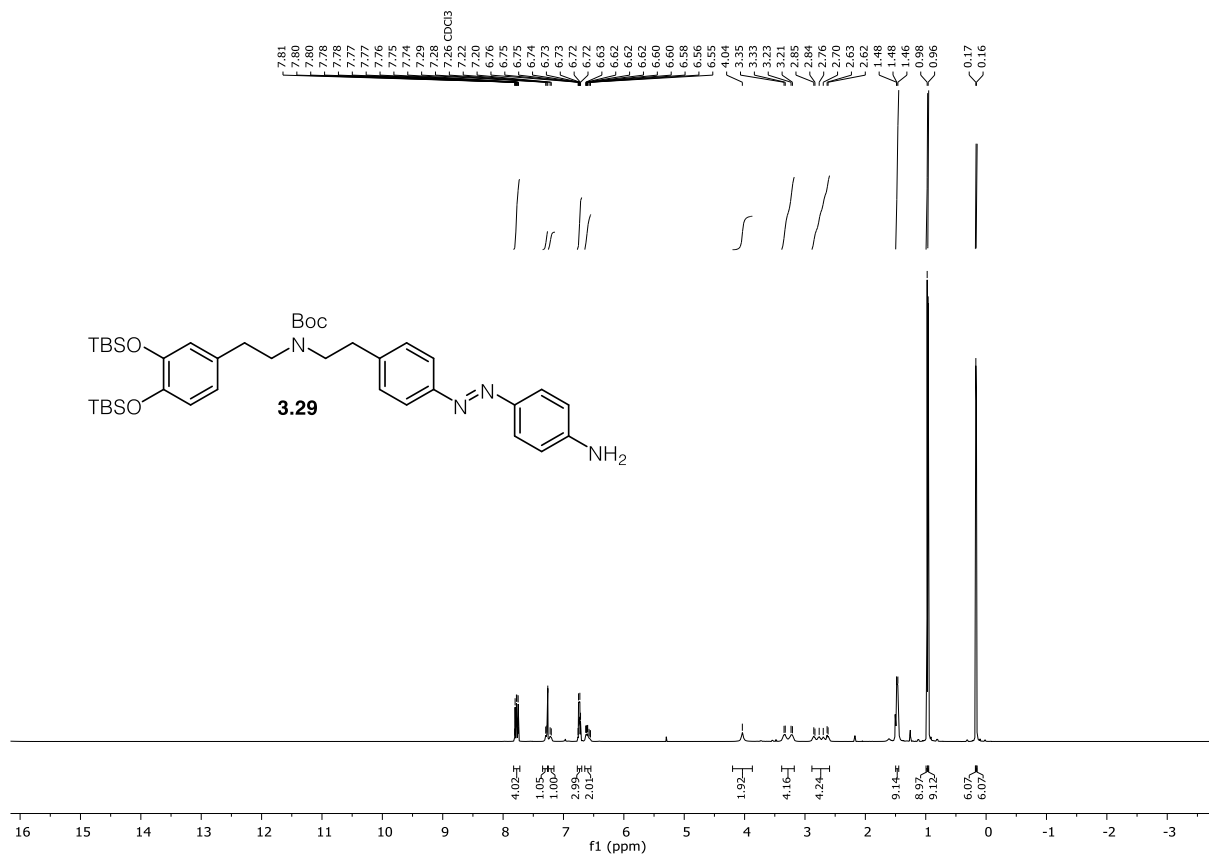


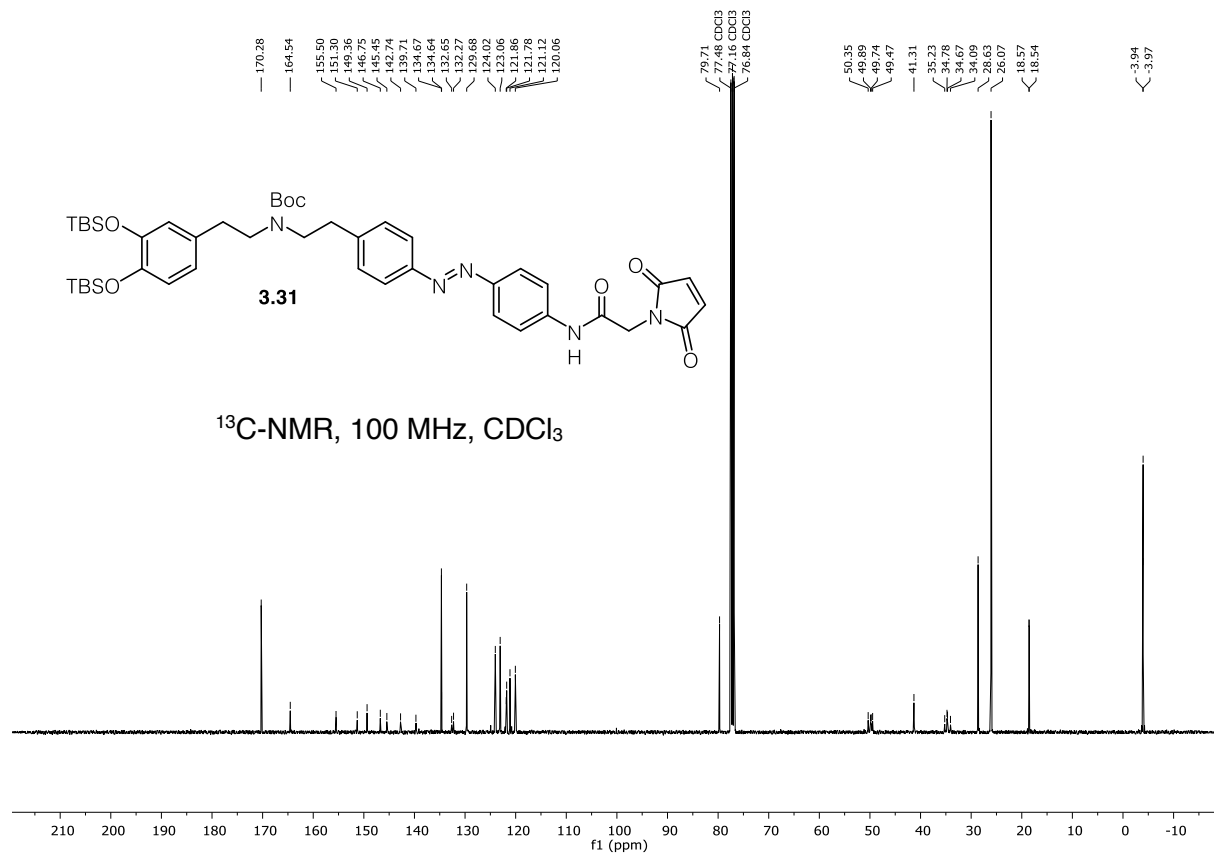
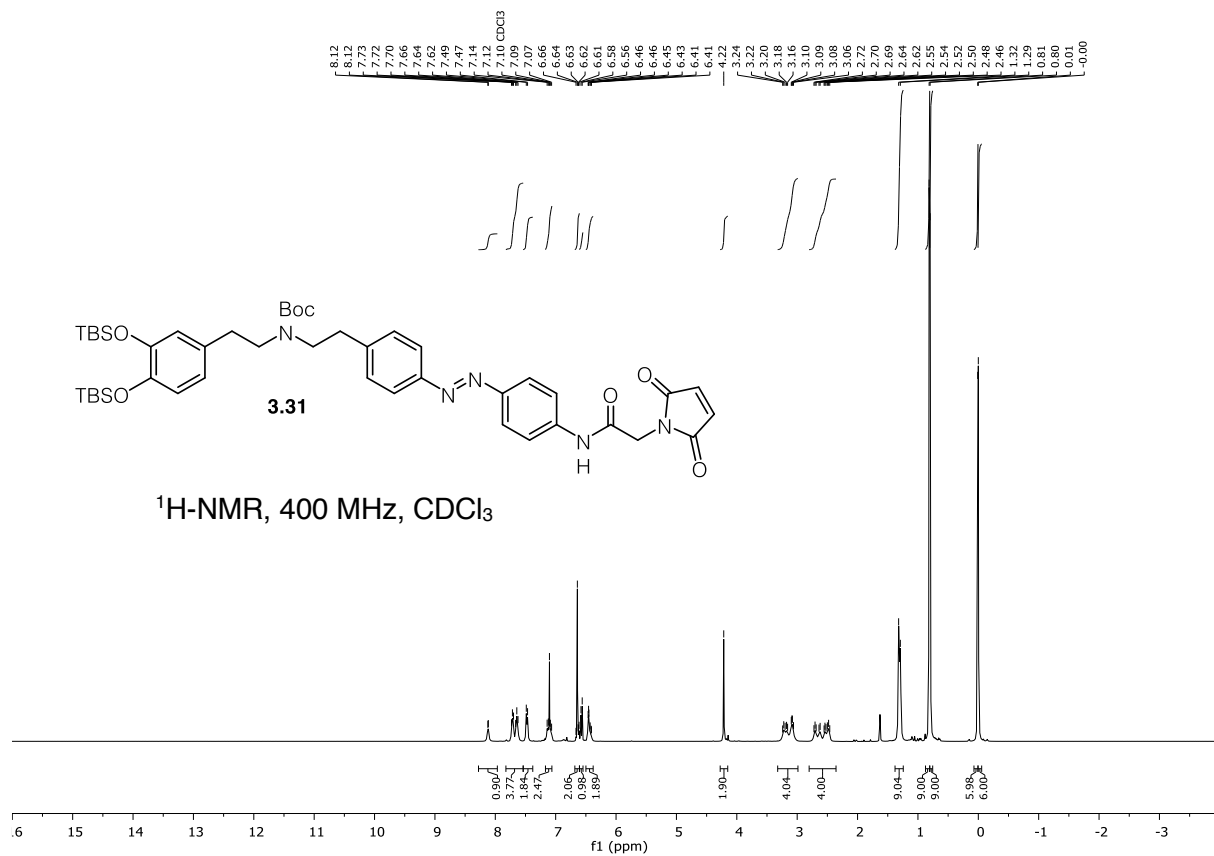


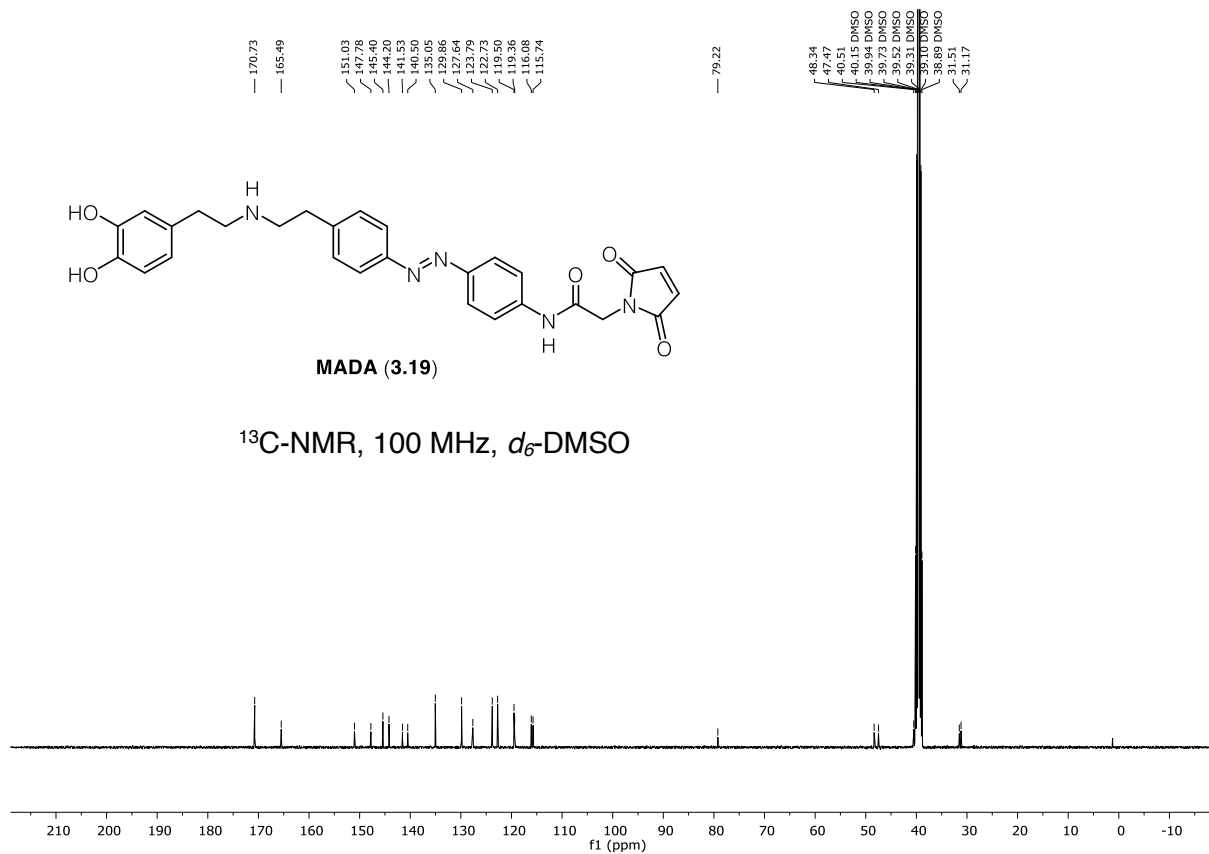
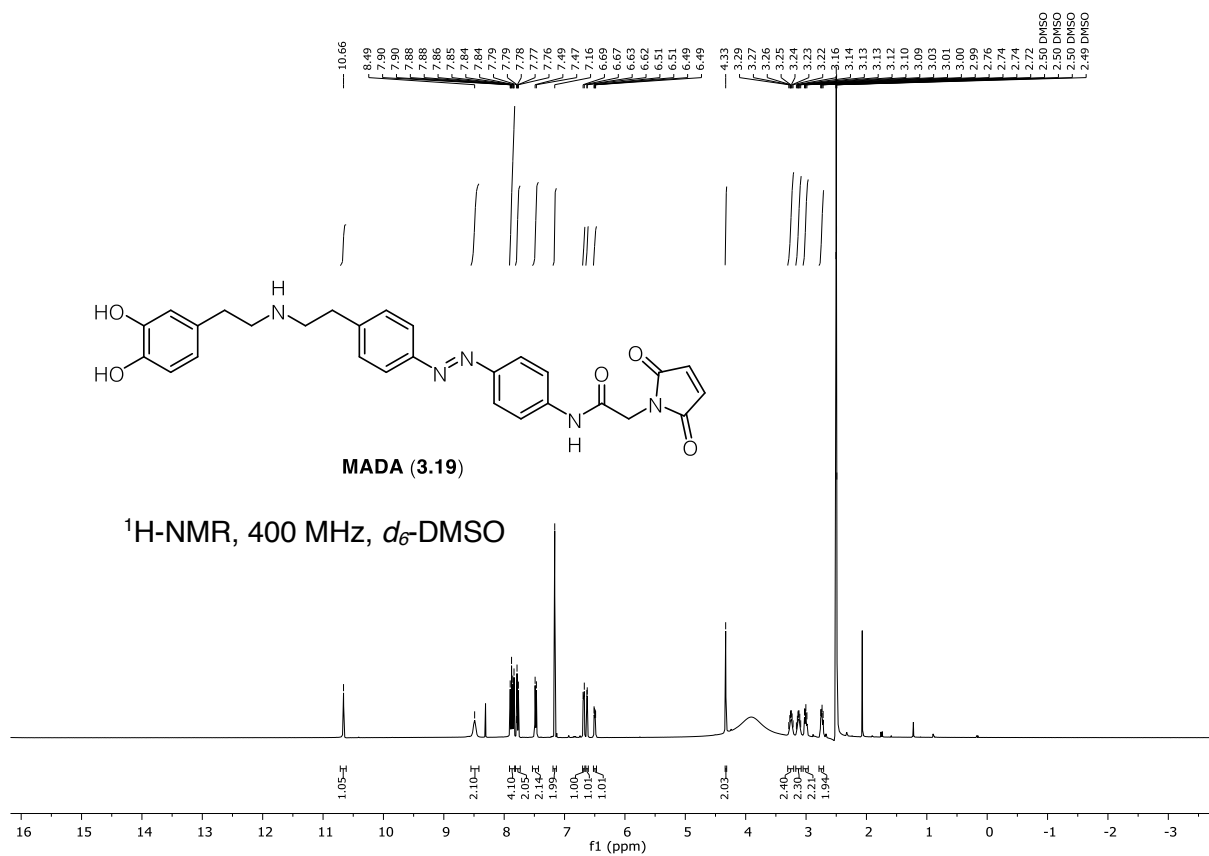


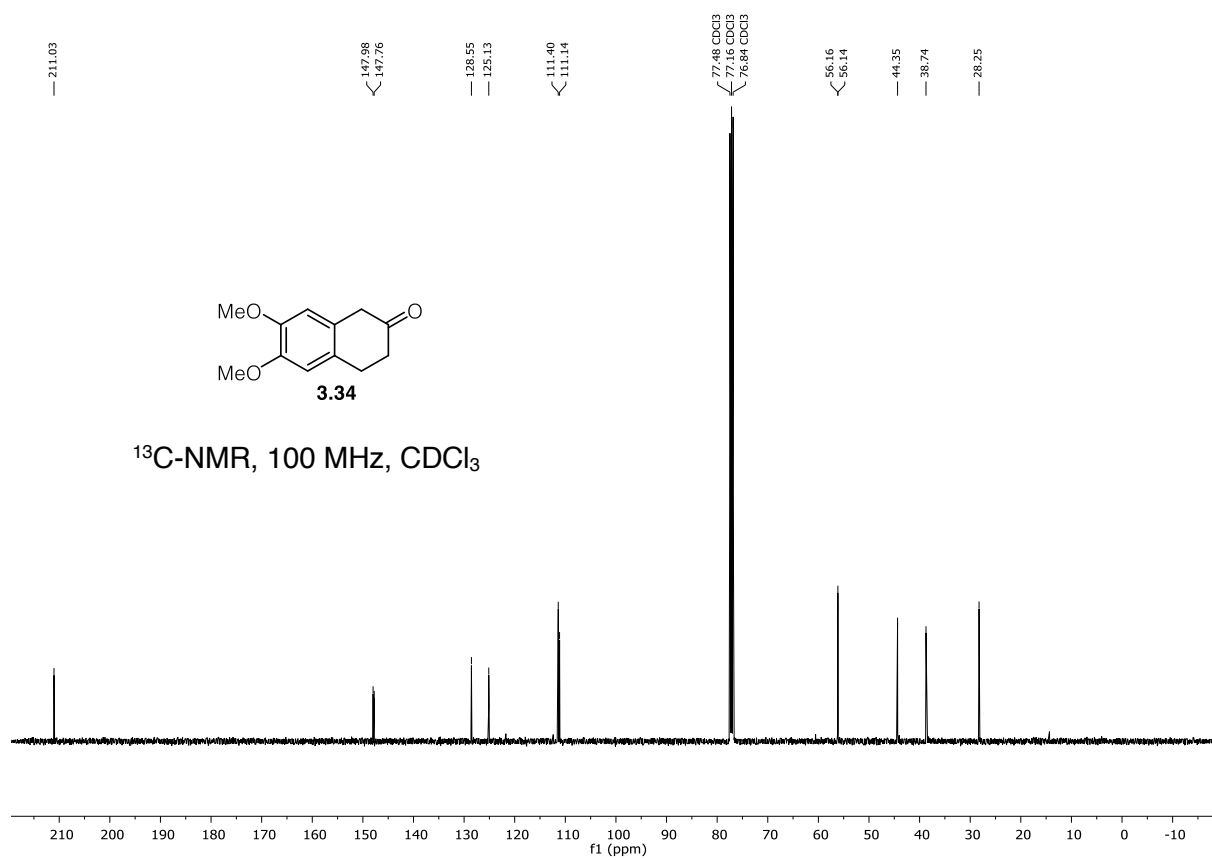
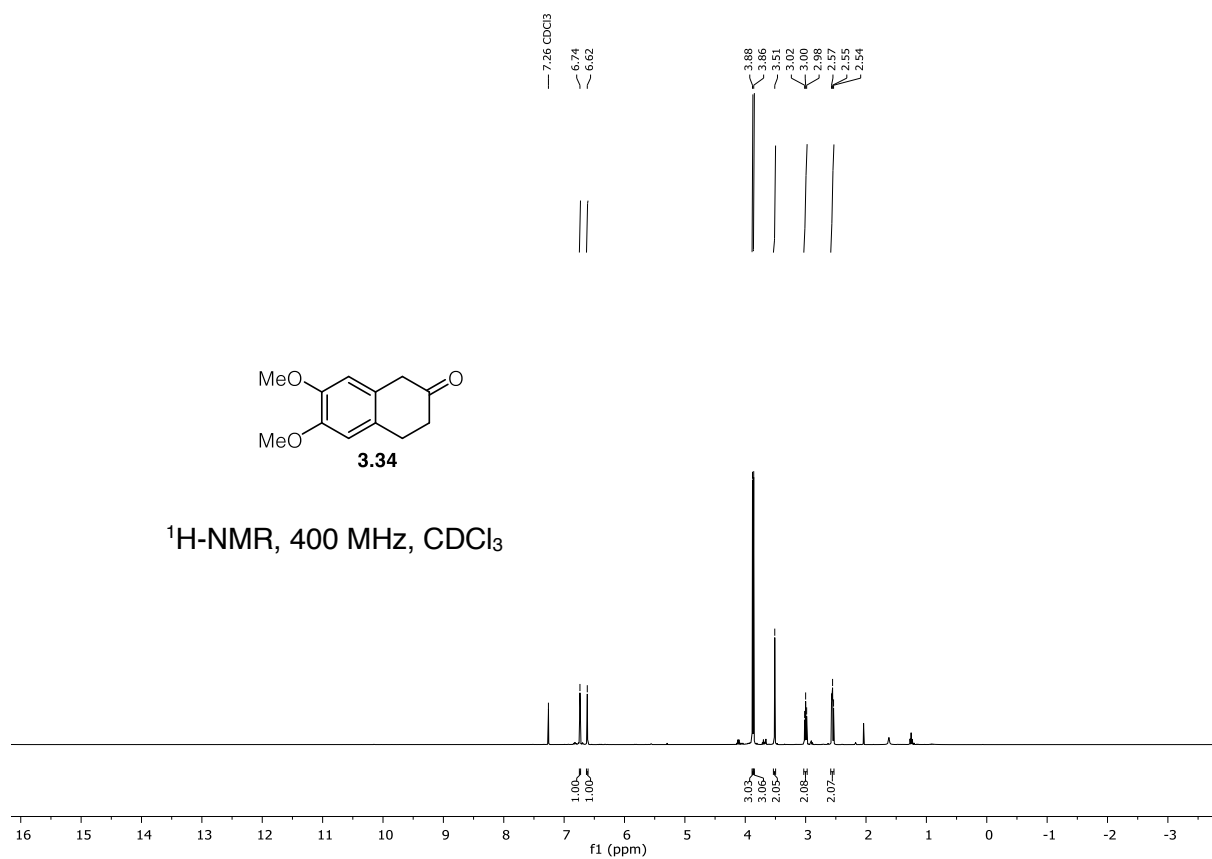


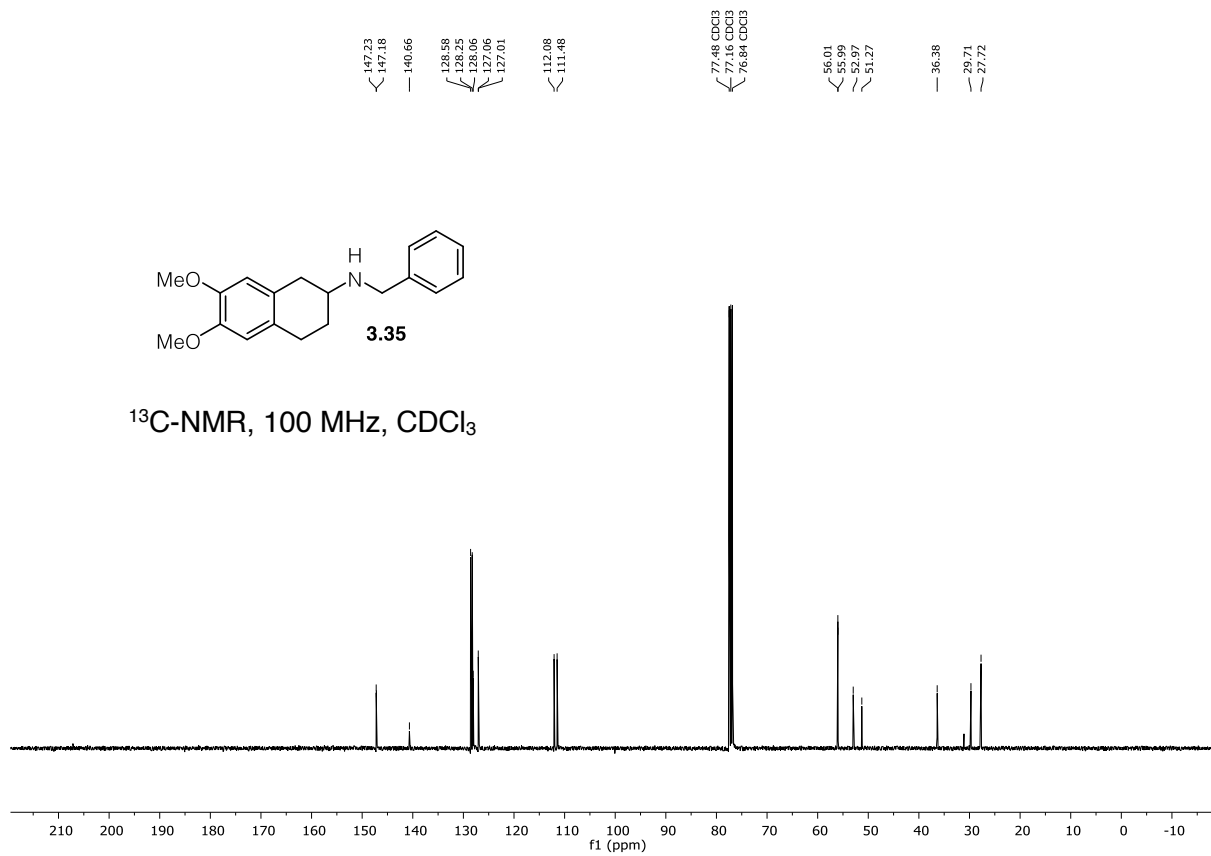
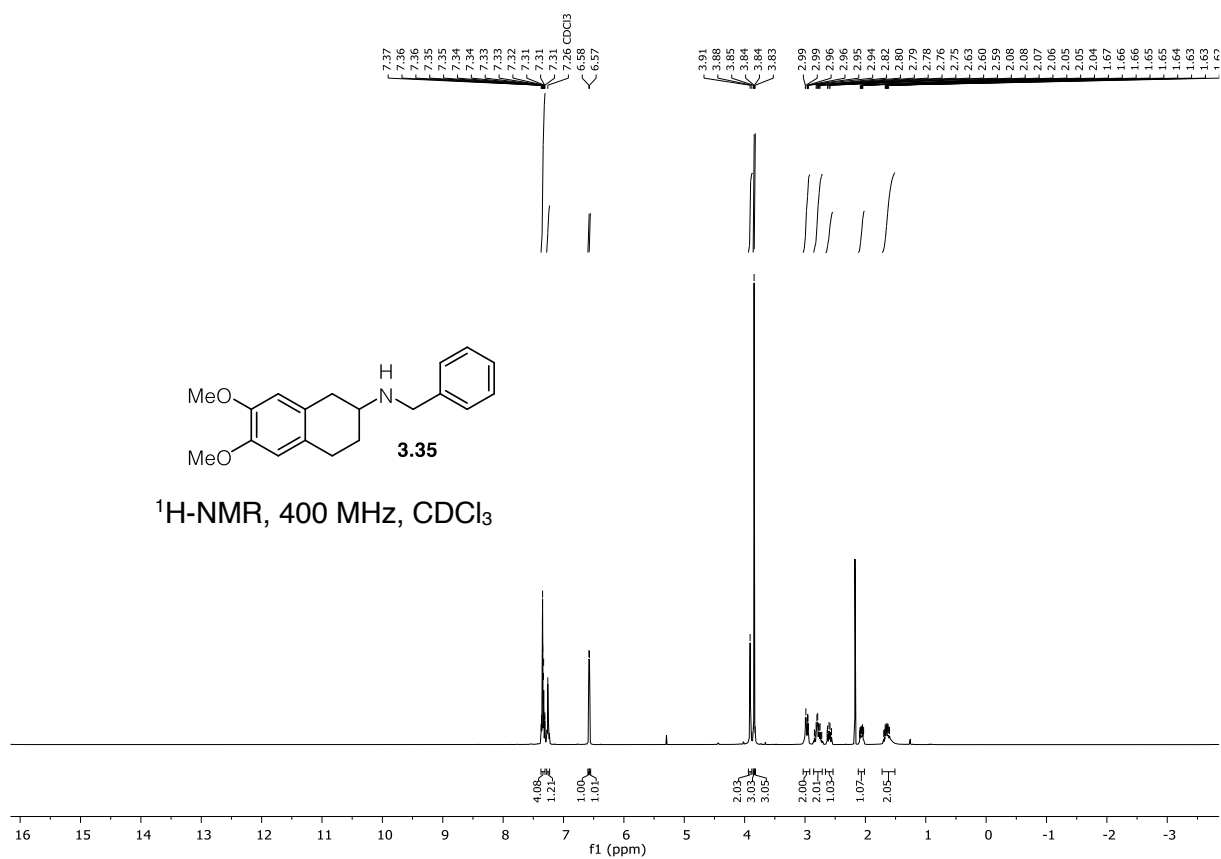


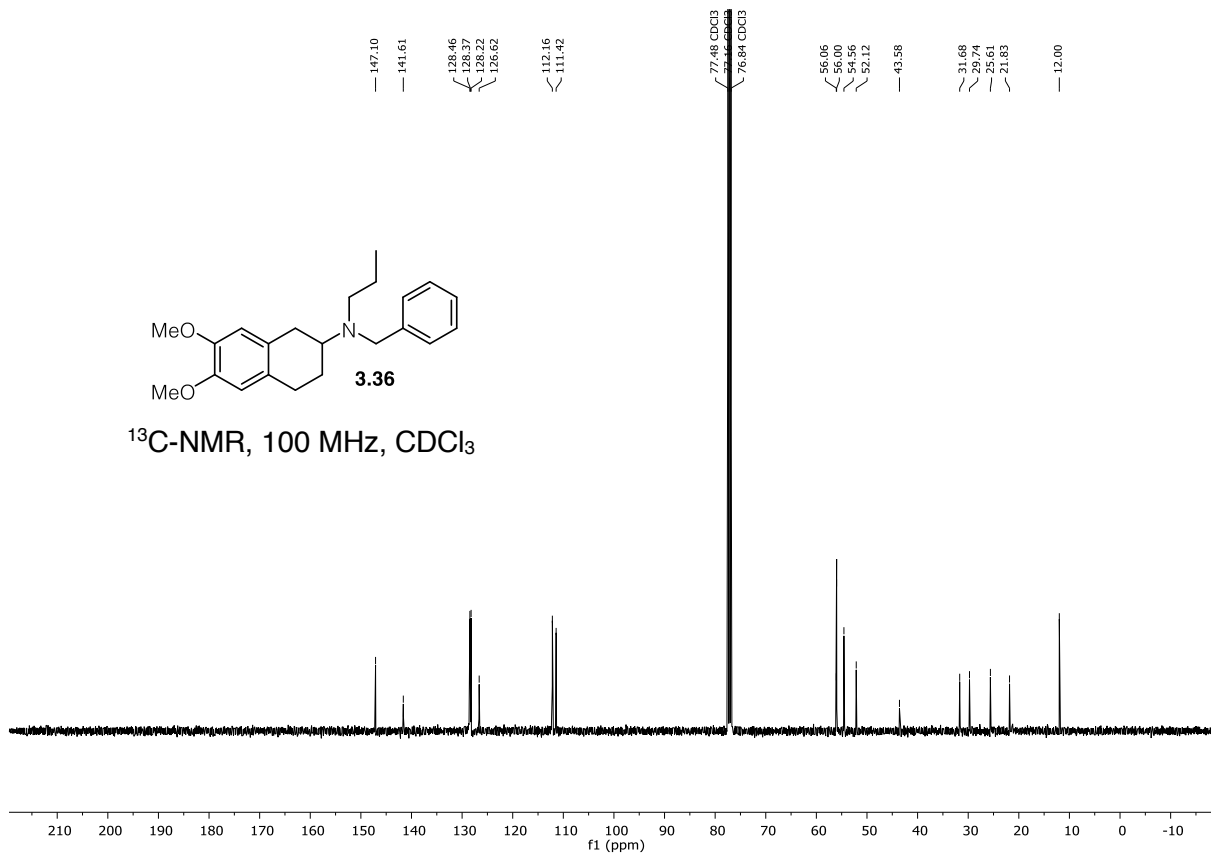
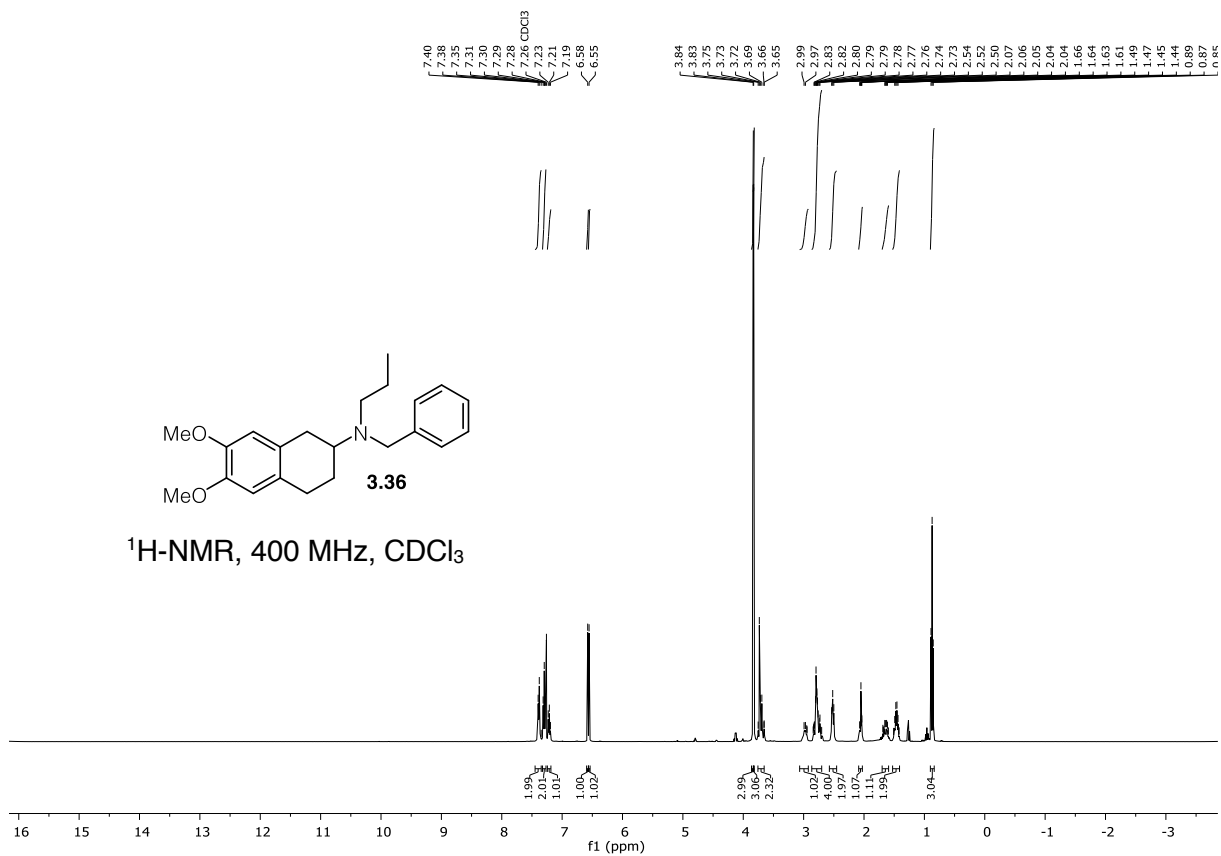


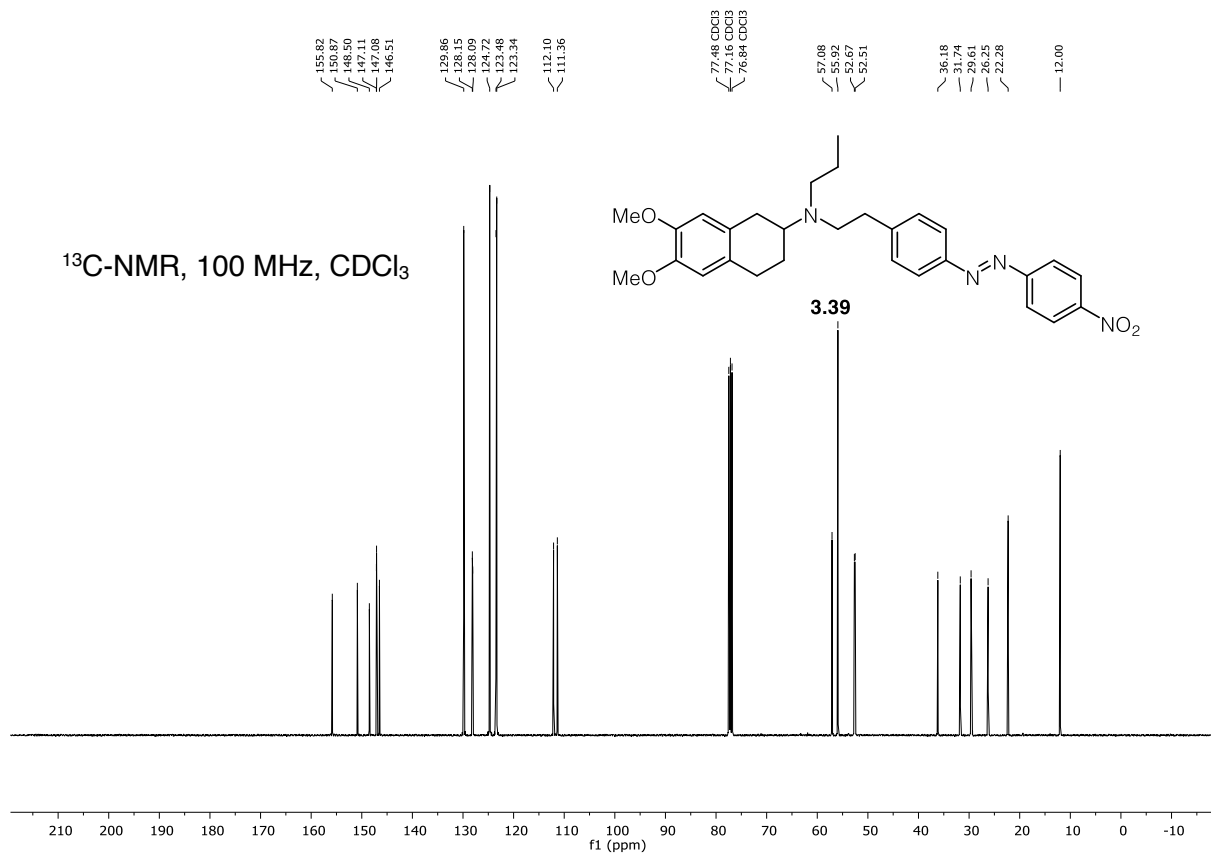
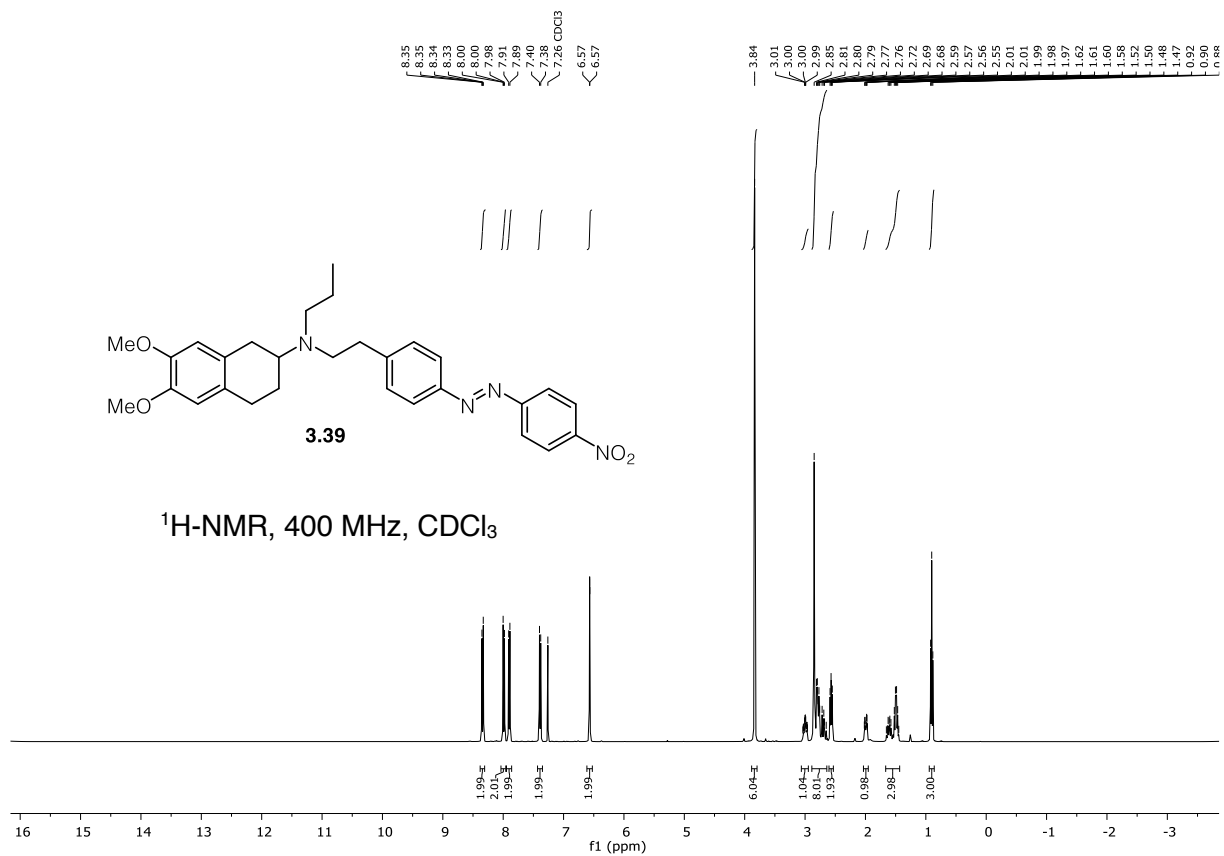


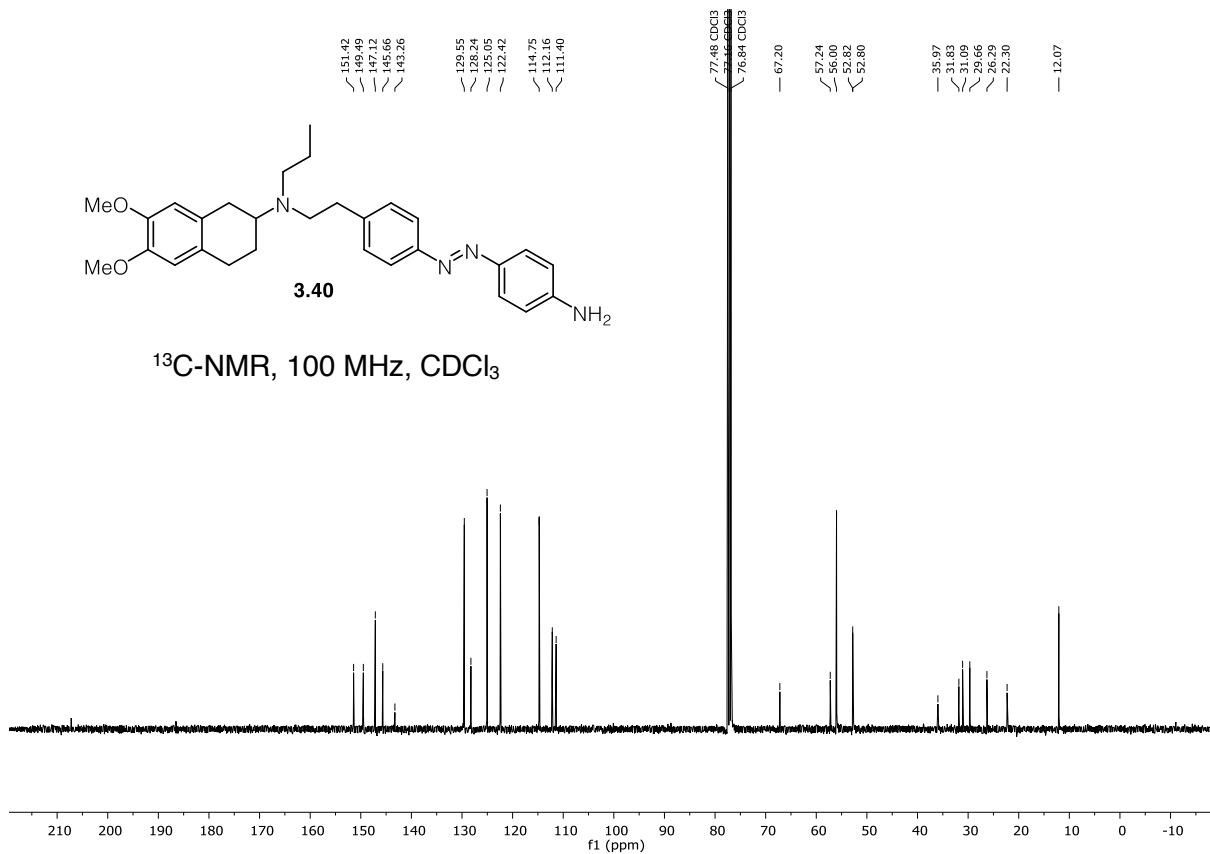
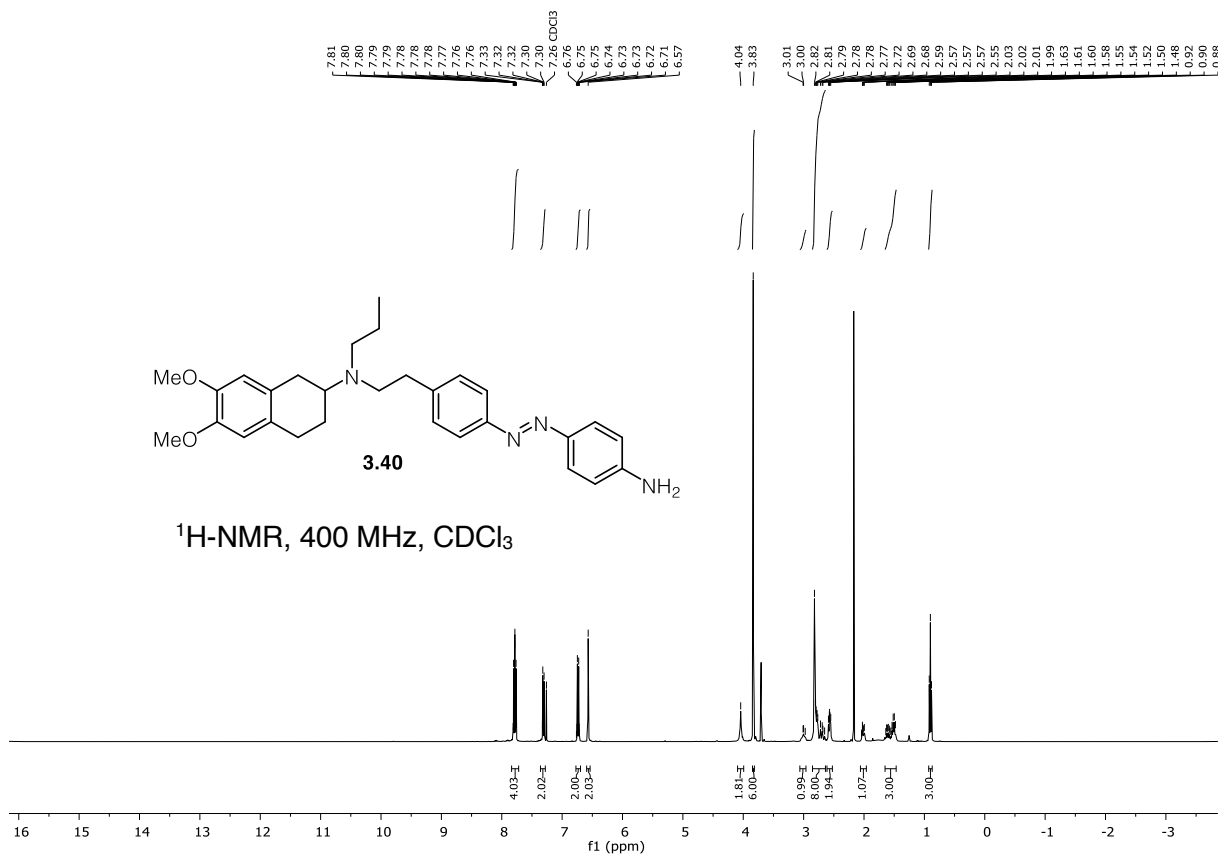


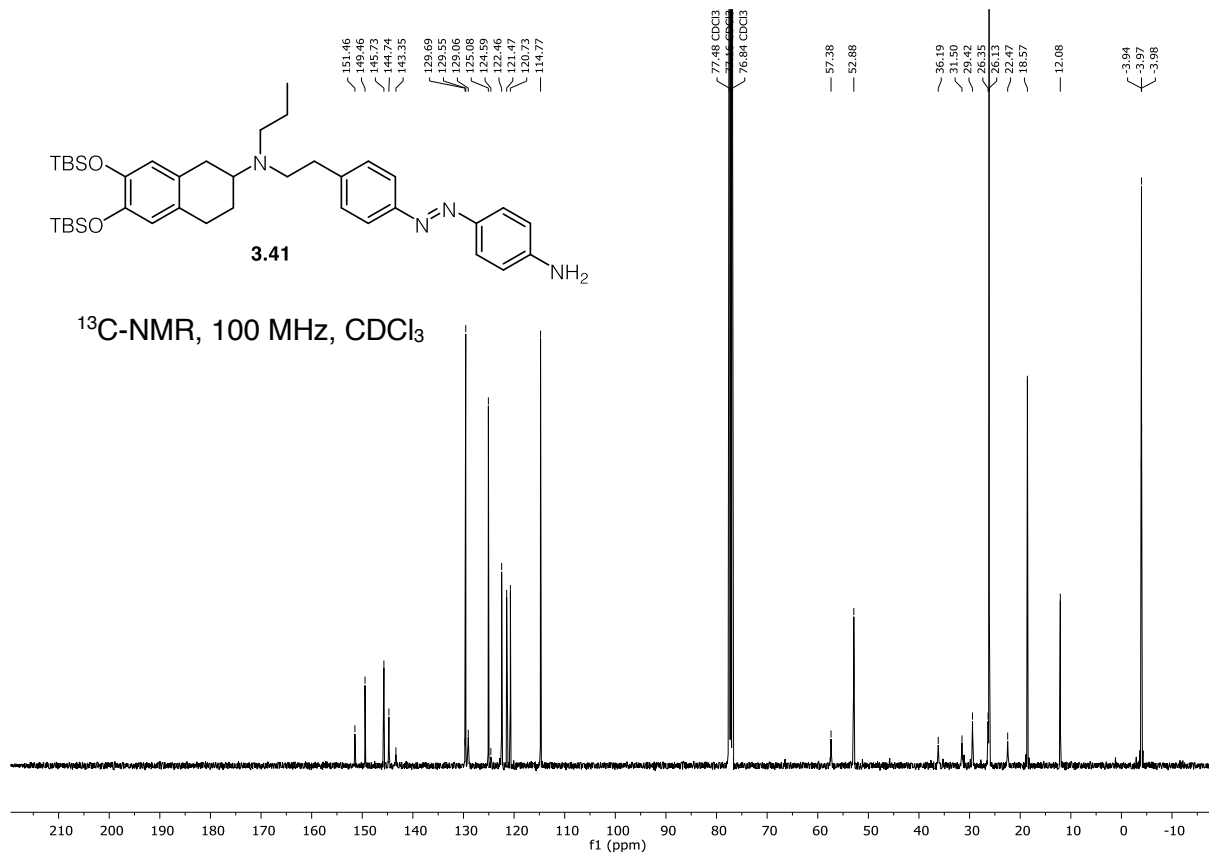
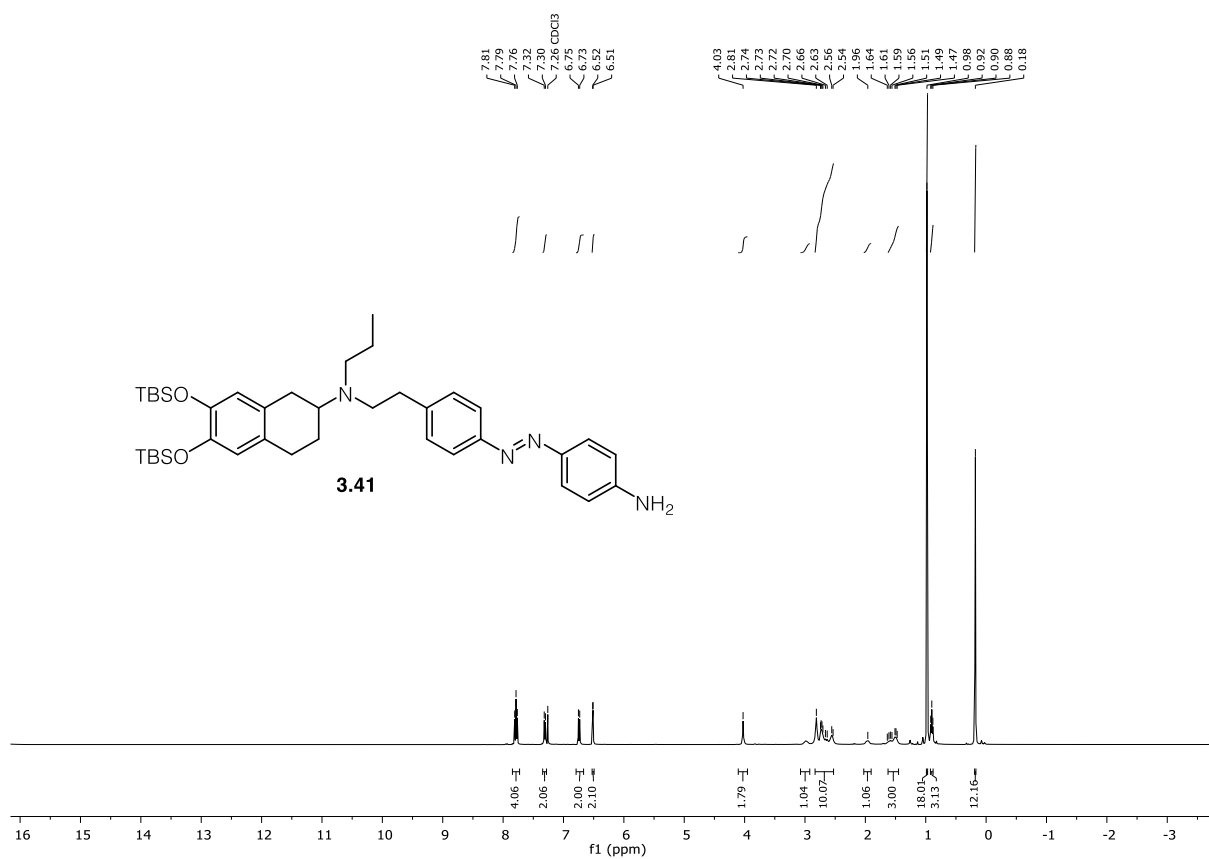


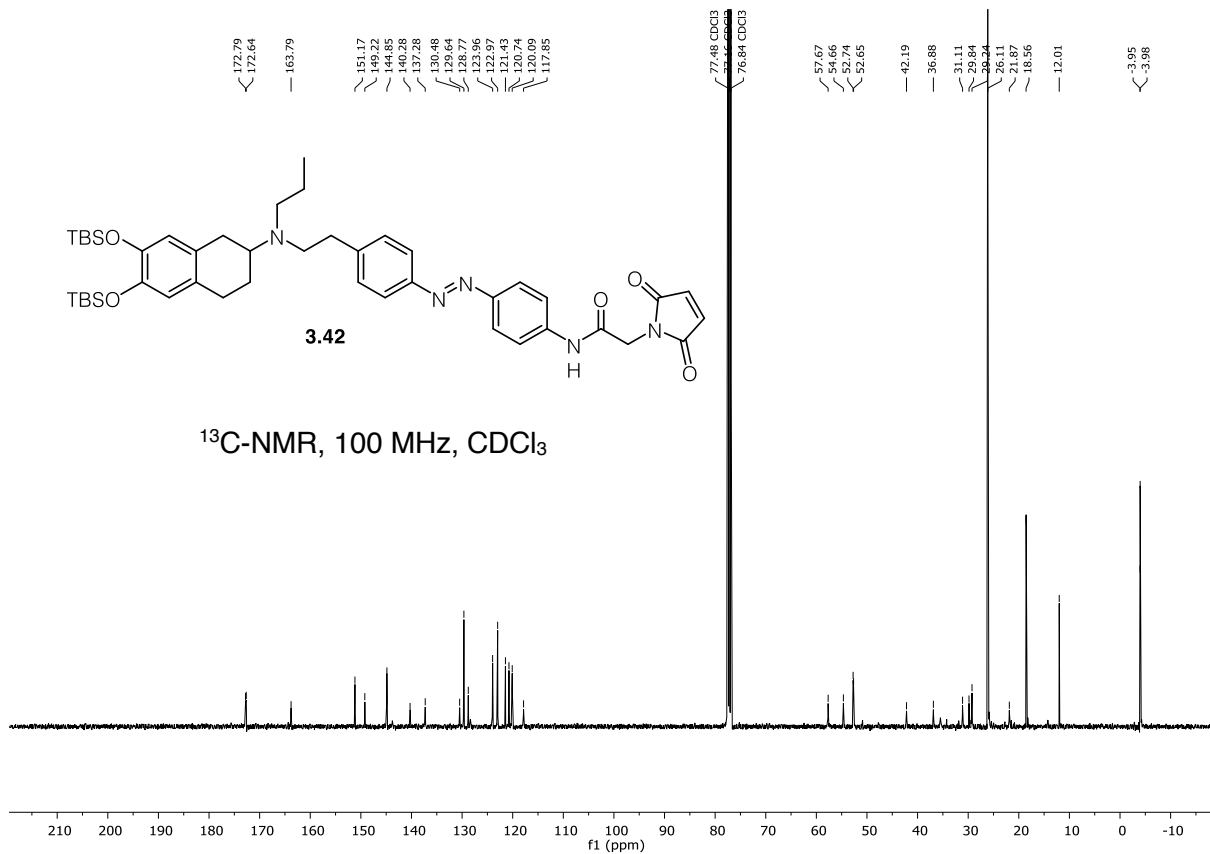
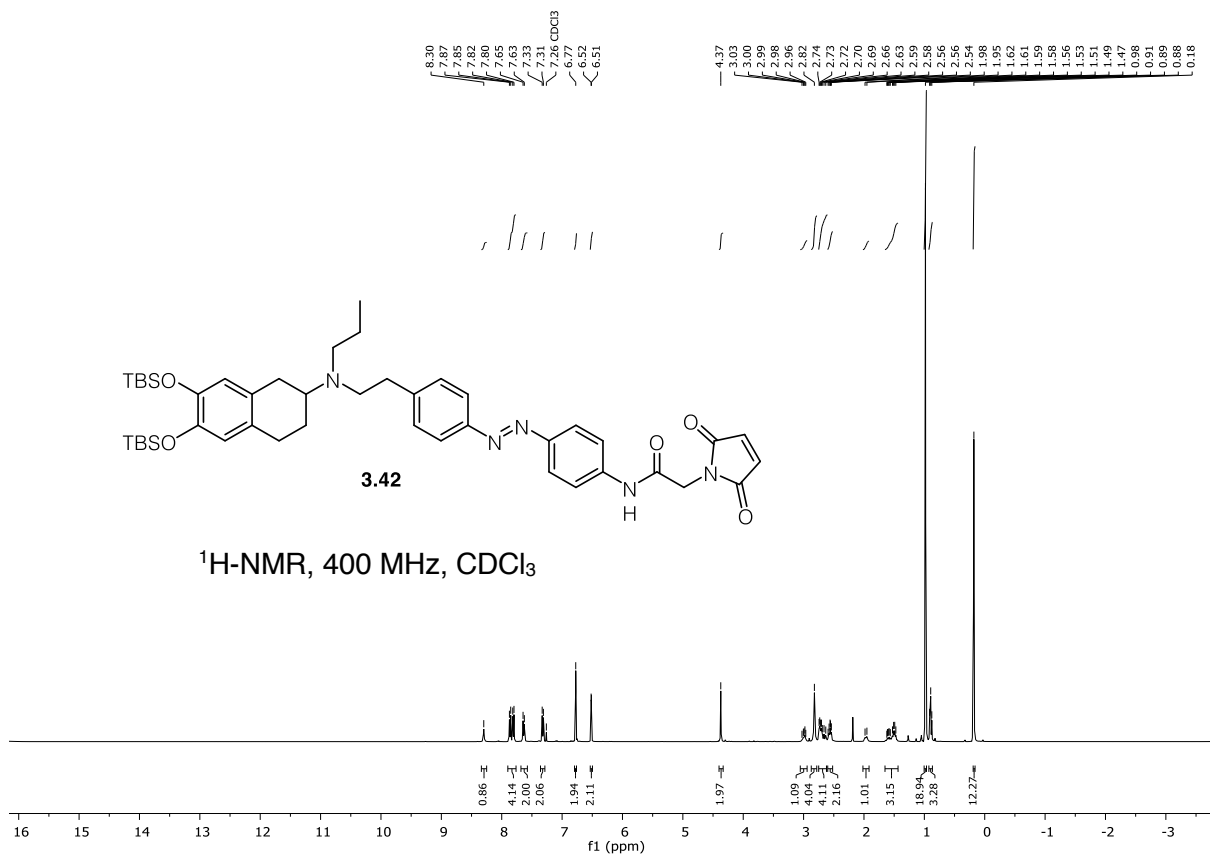


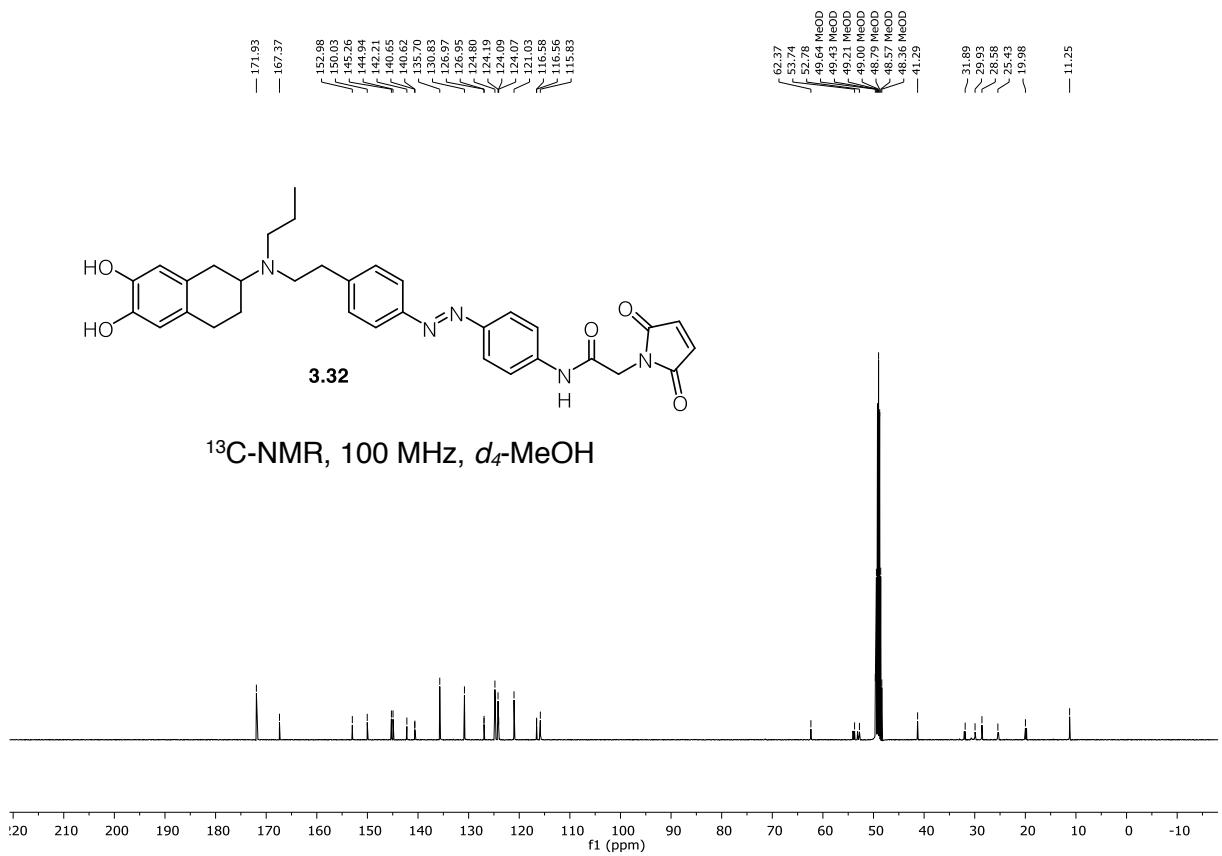
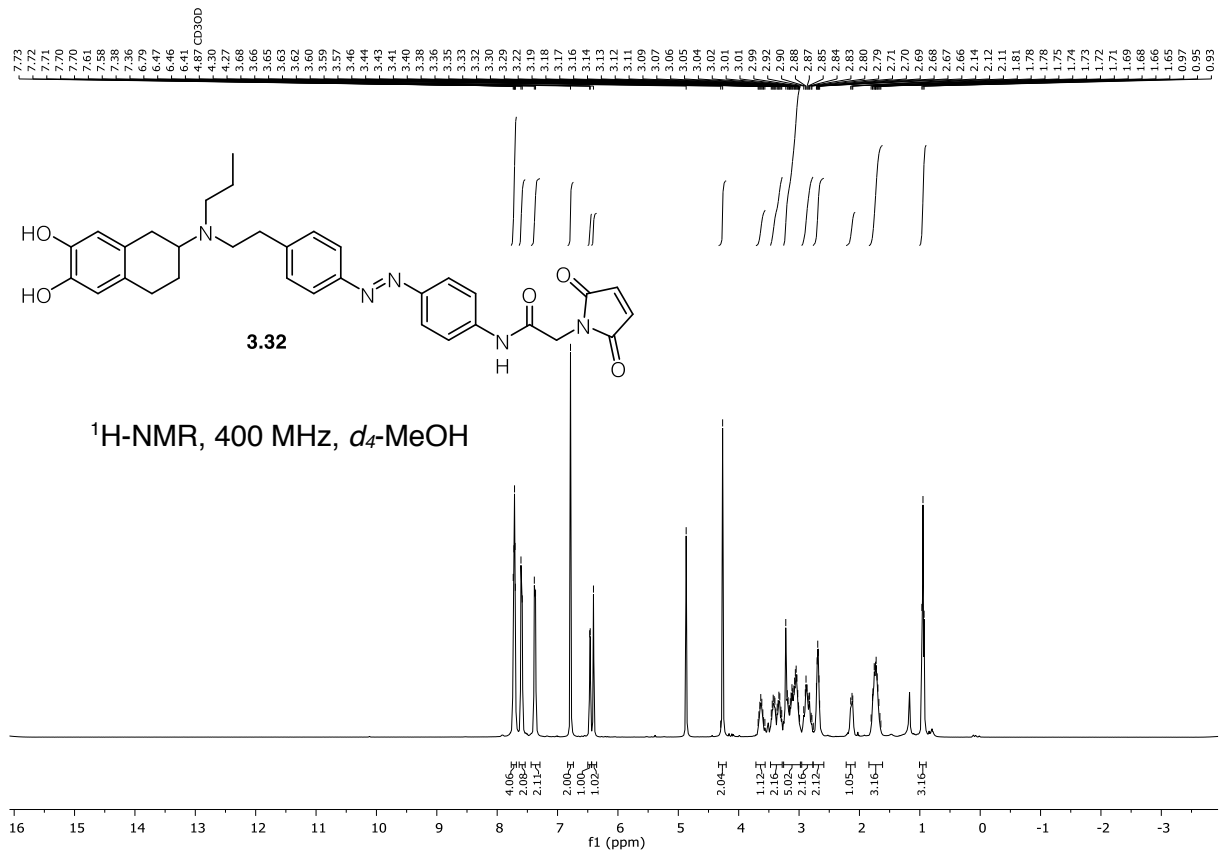


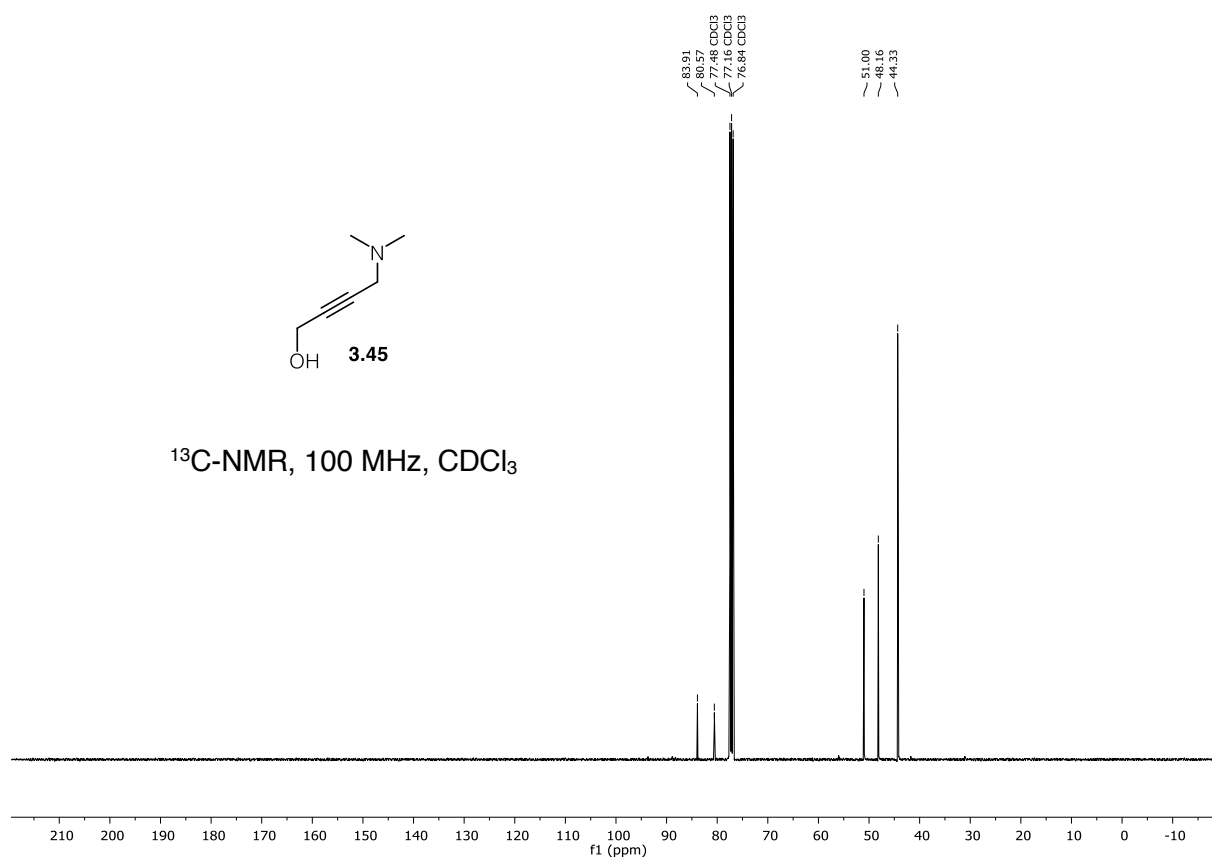
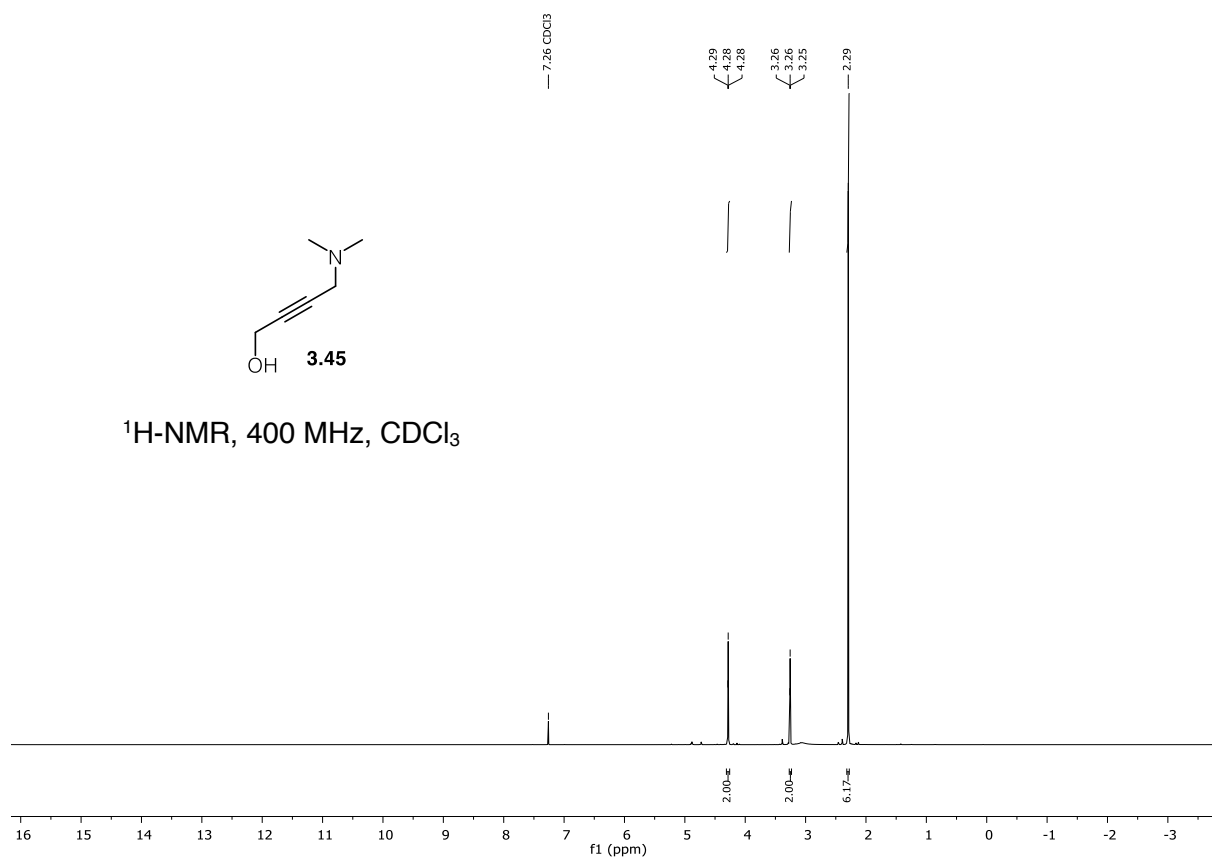


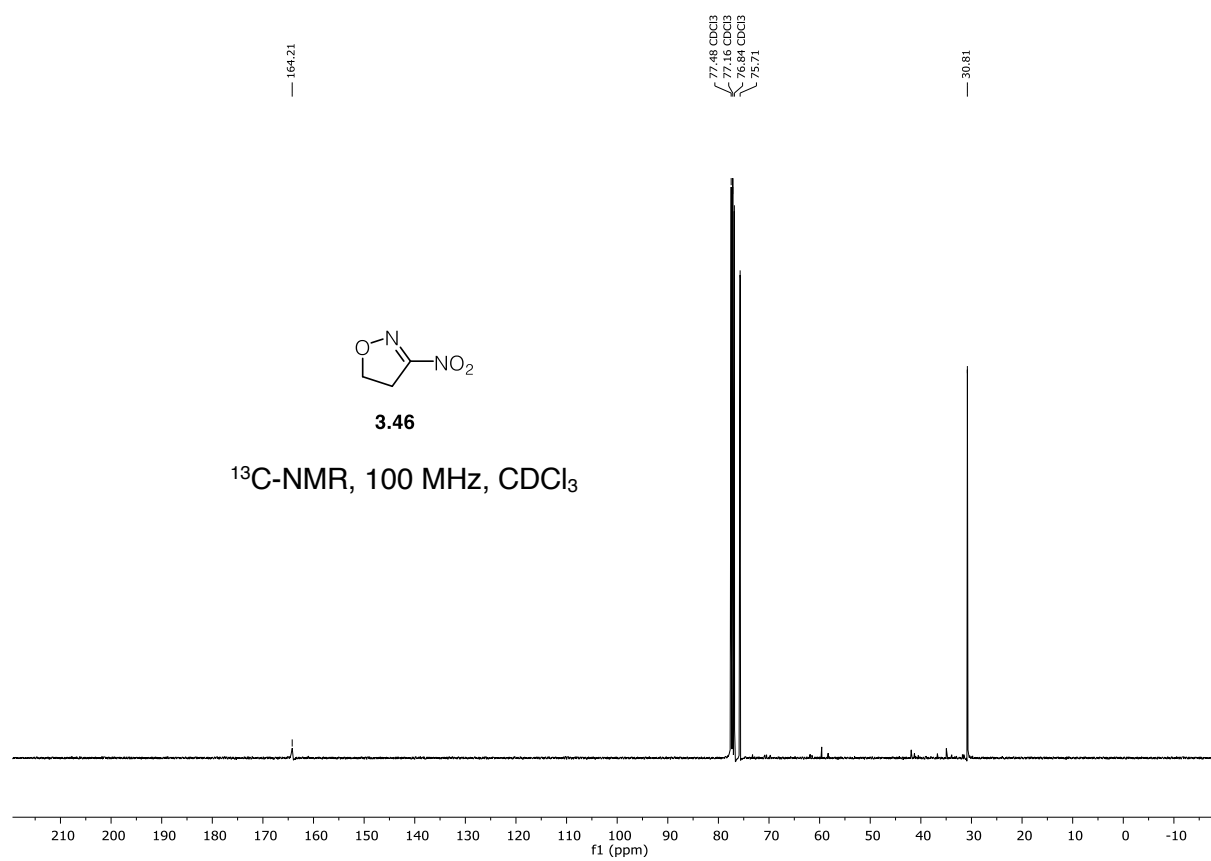
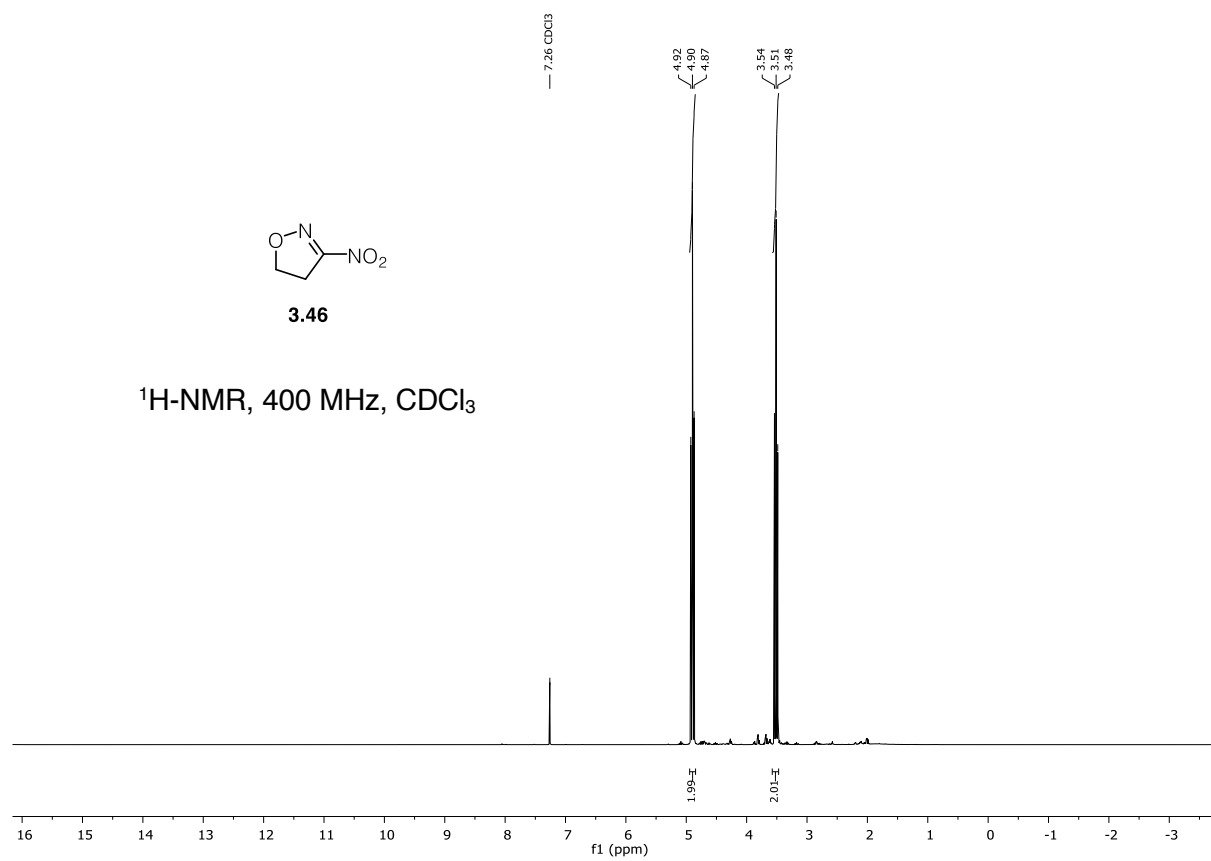


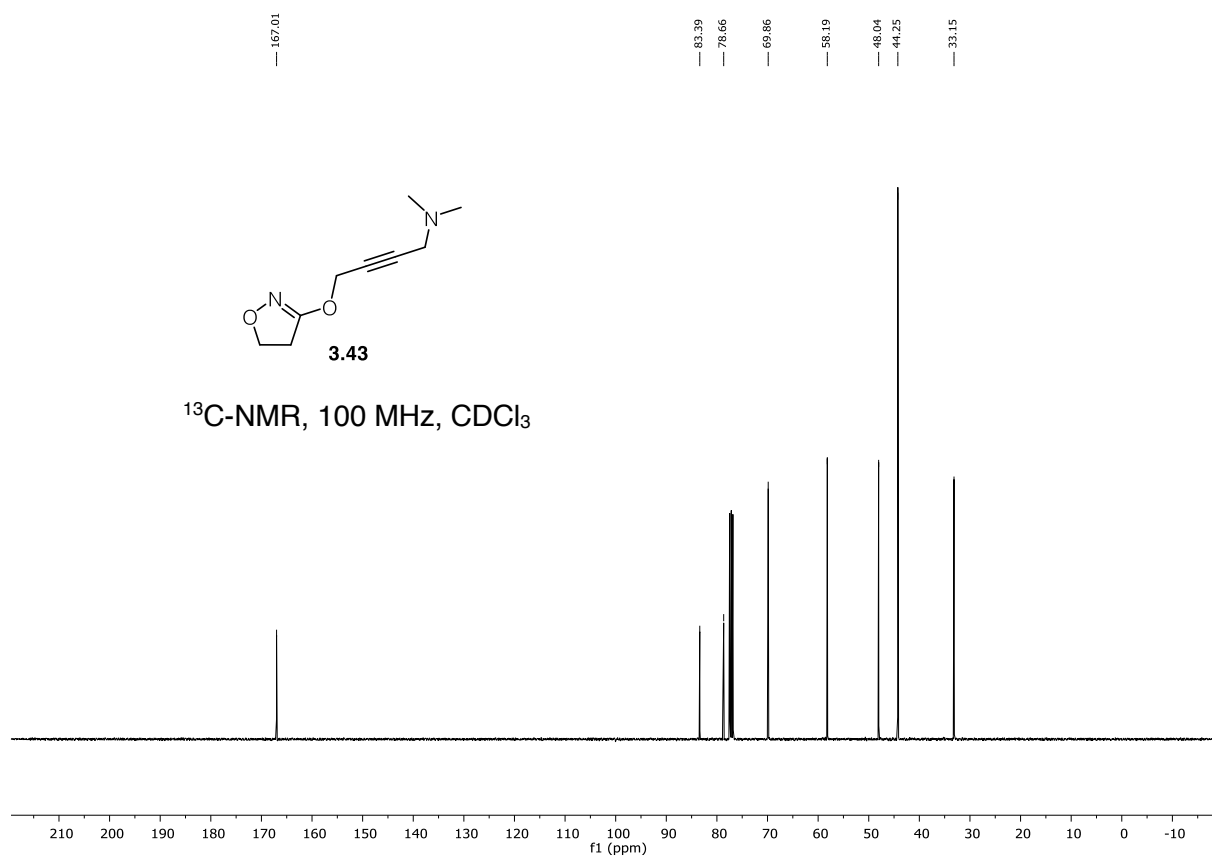
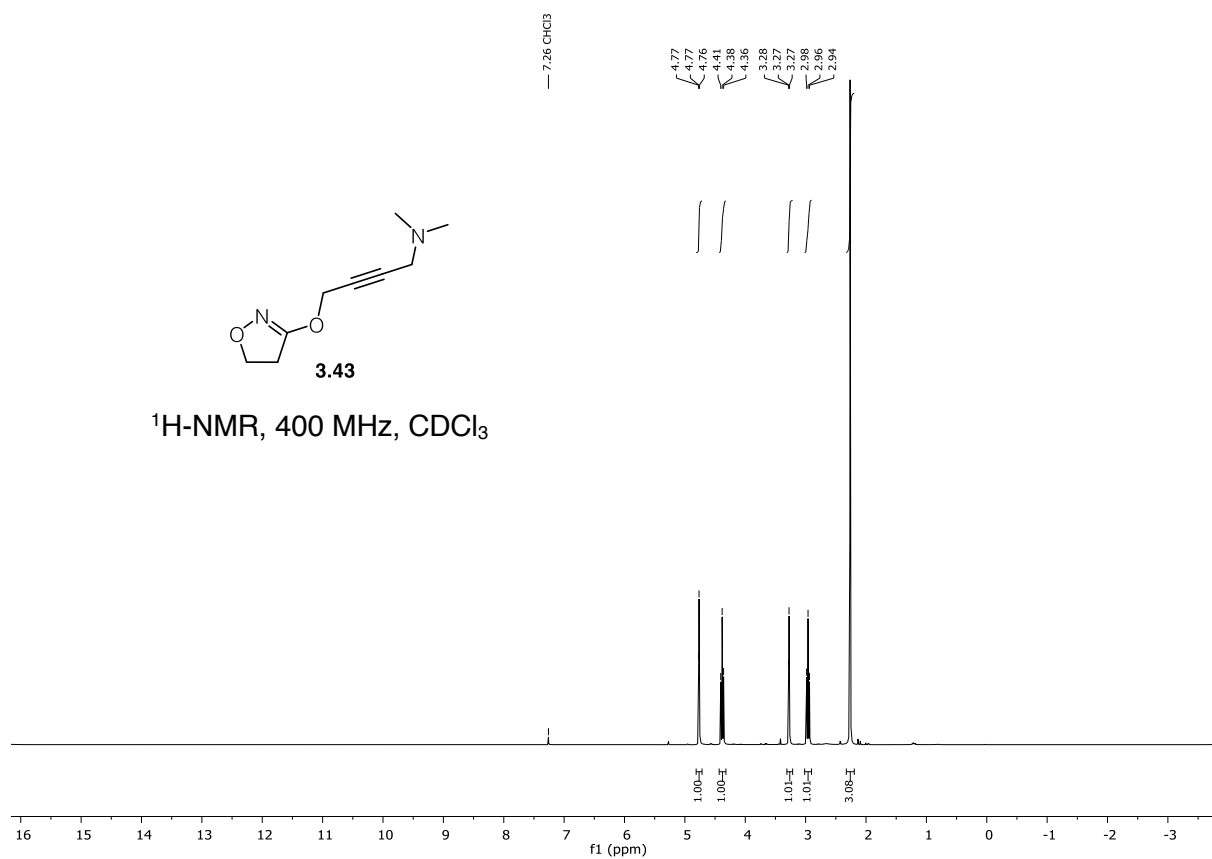


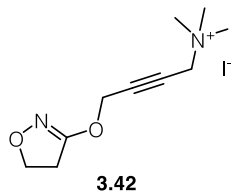




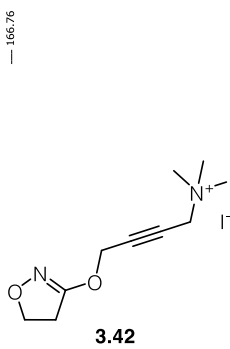
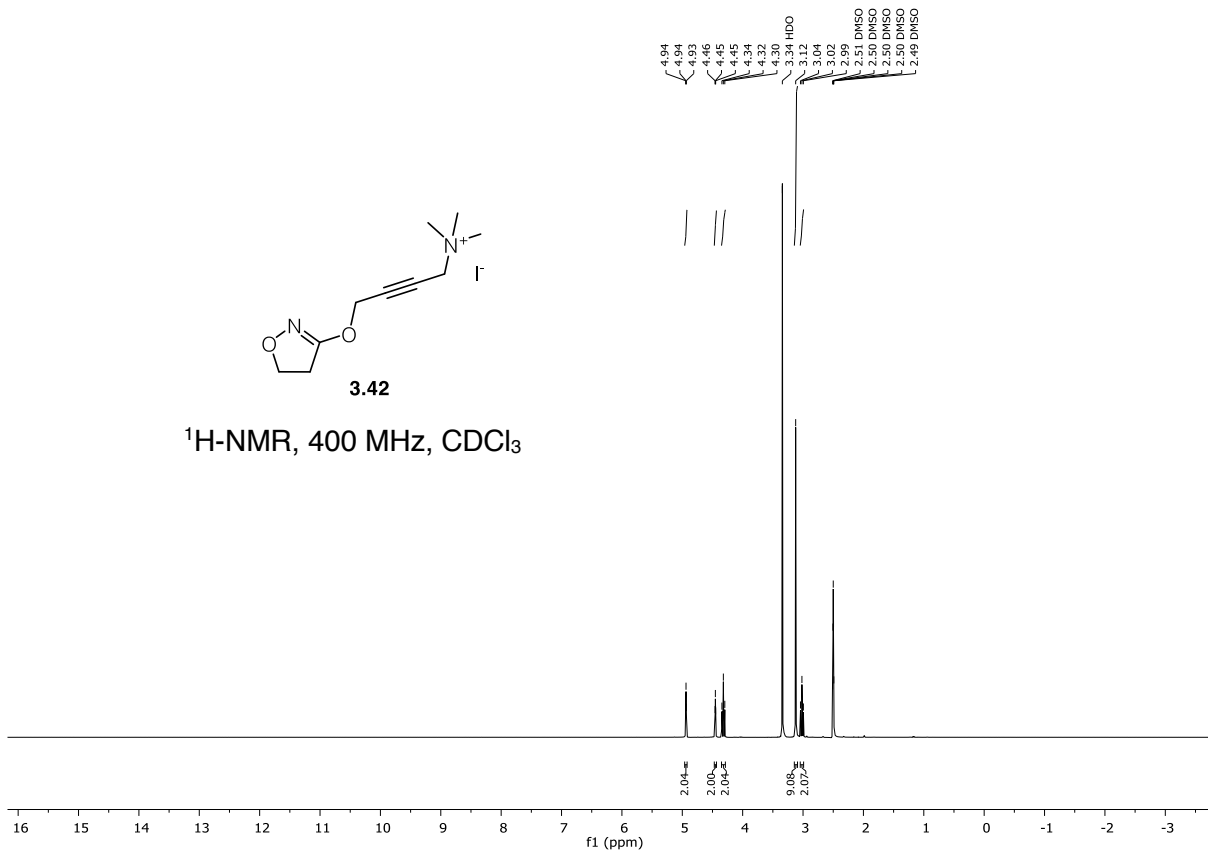




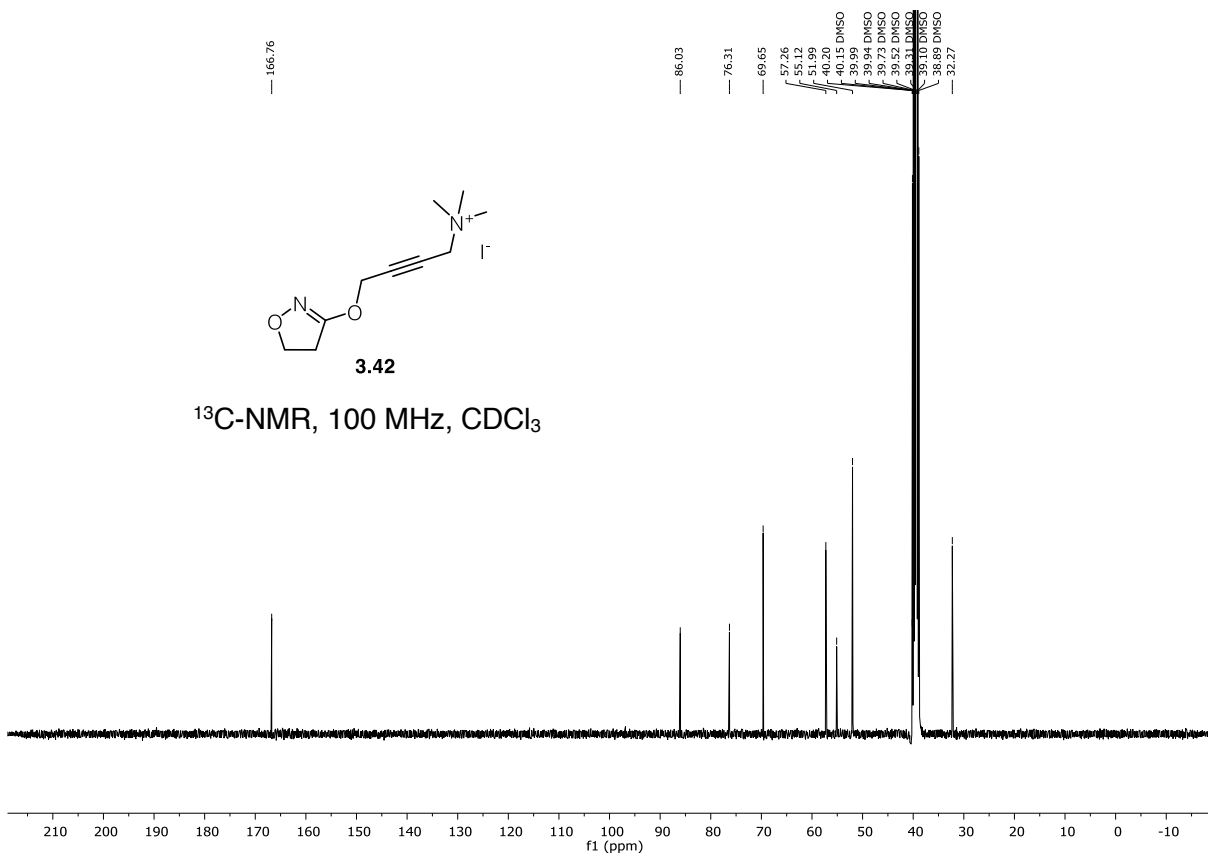


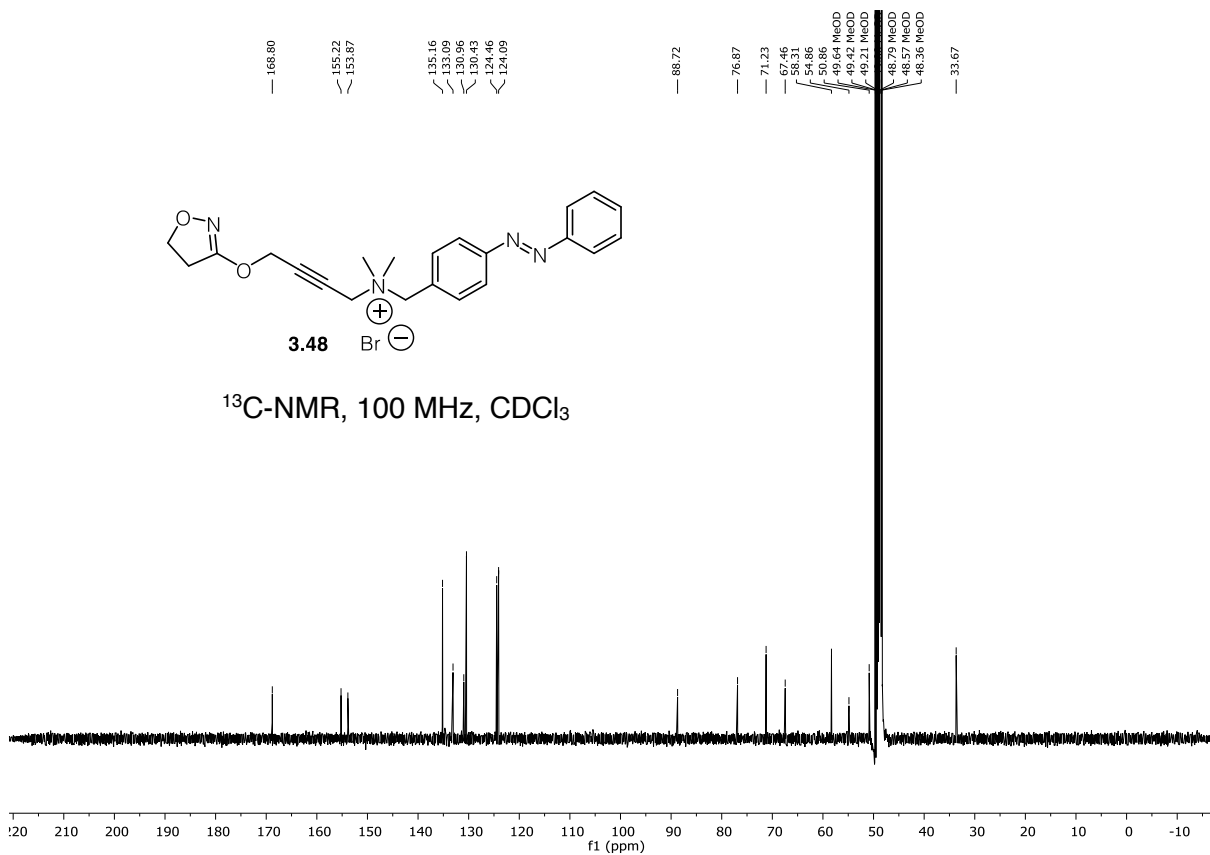
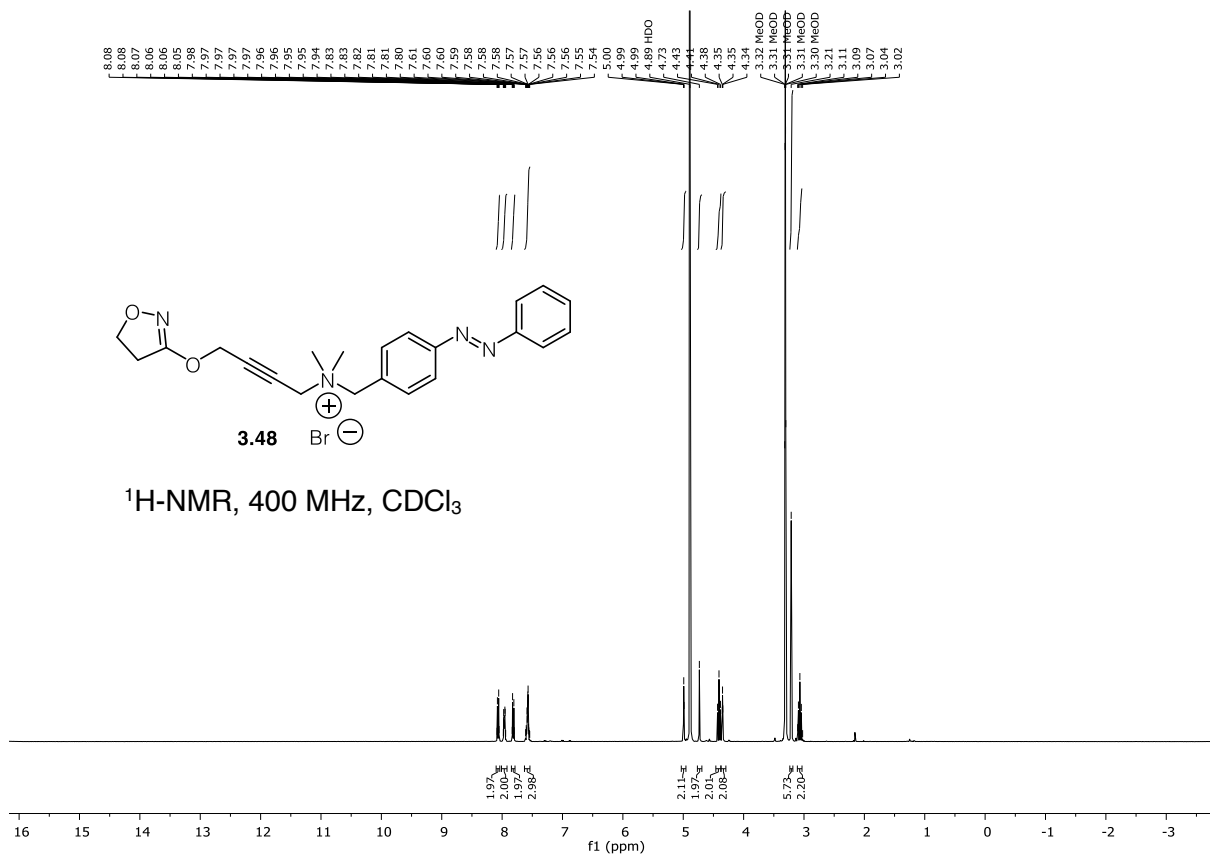


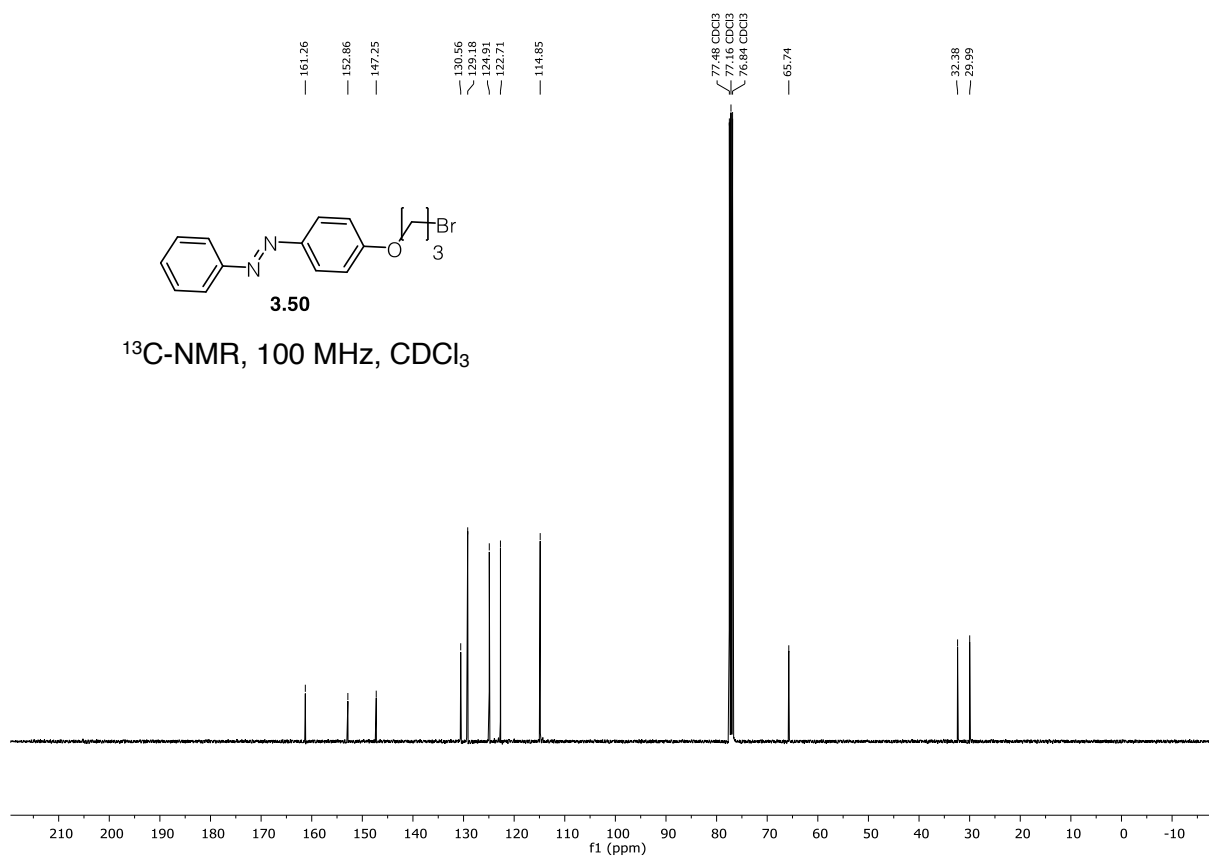
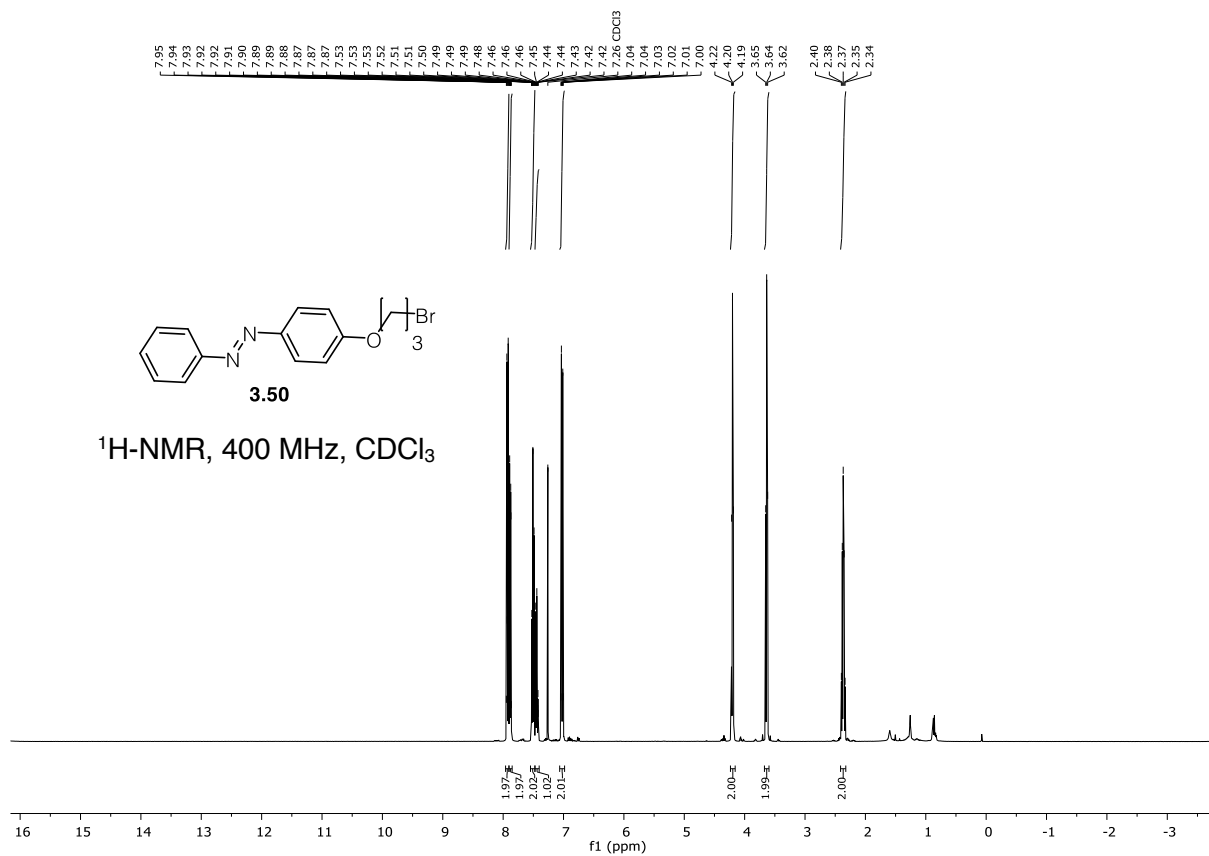
¹H-NMR, 400 MHz, CDCl₃

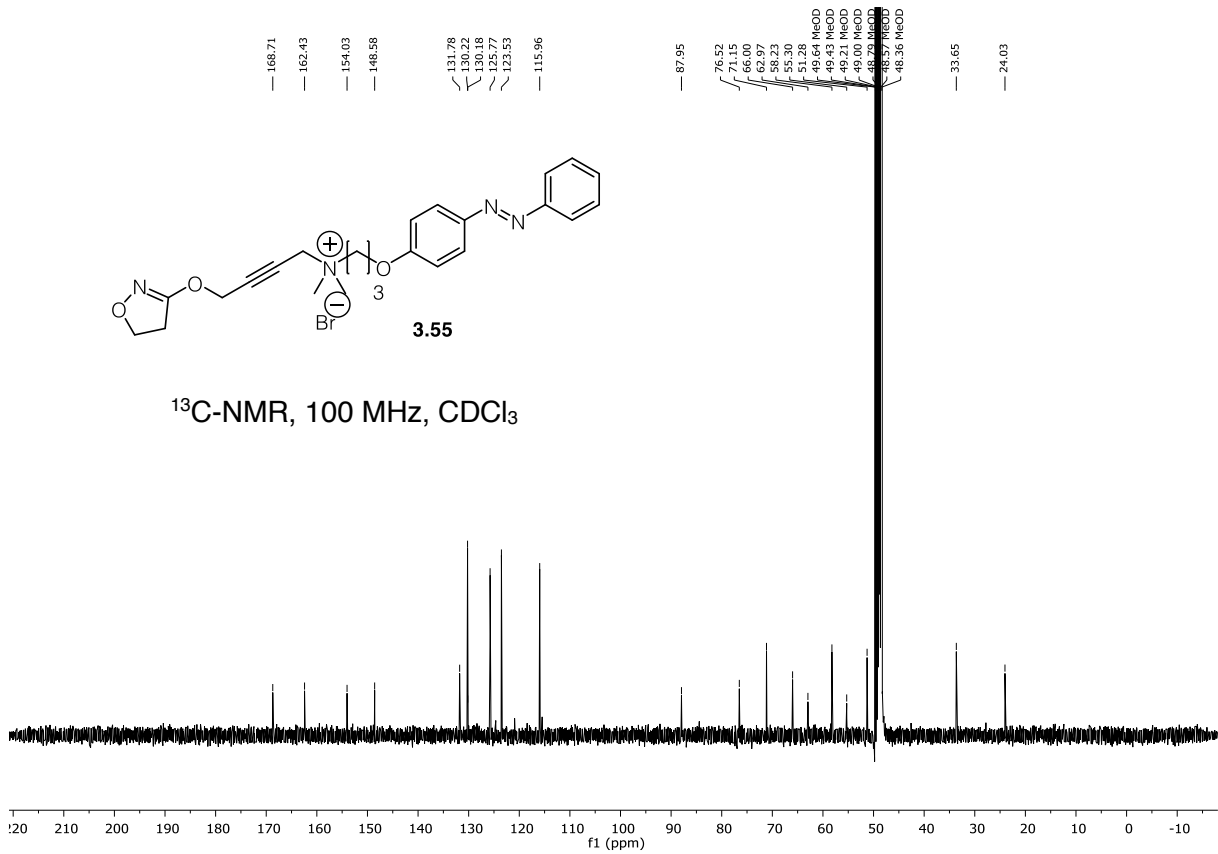
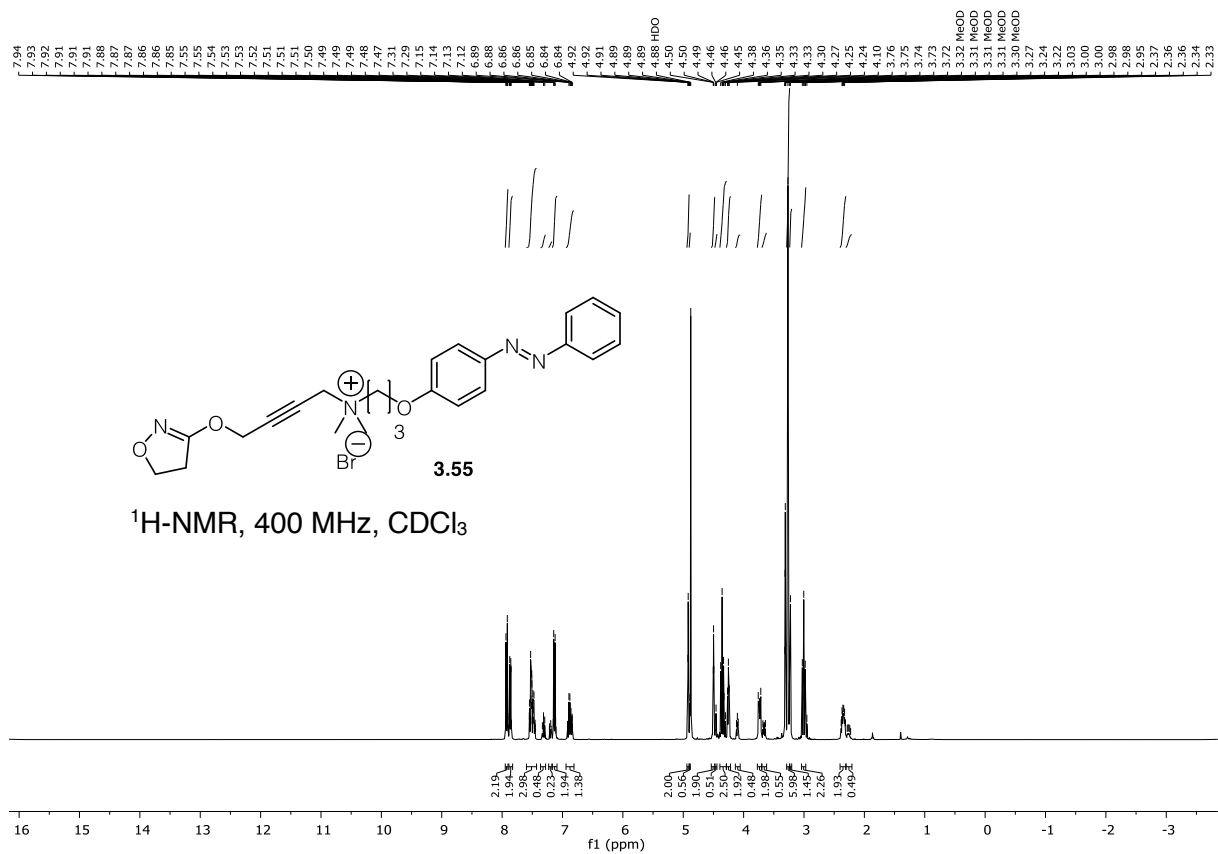


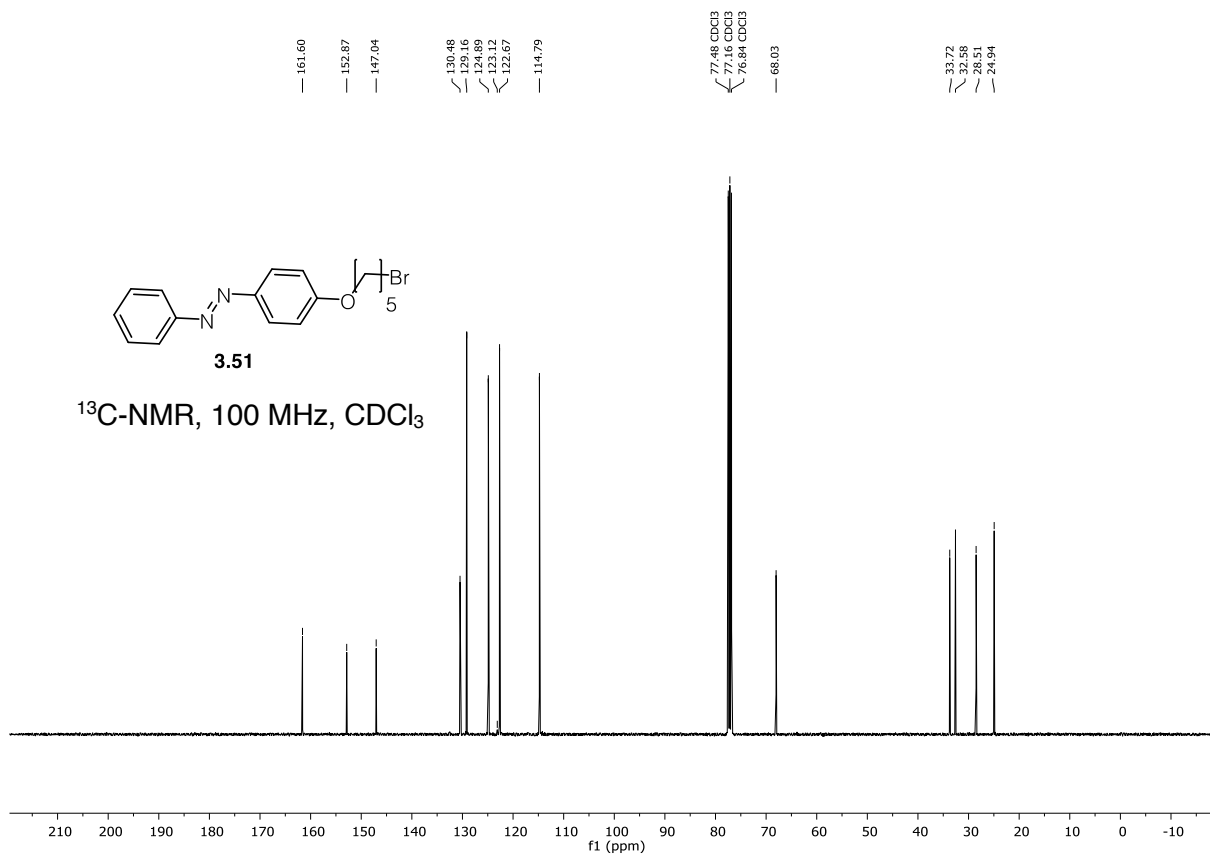
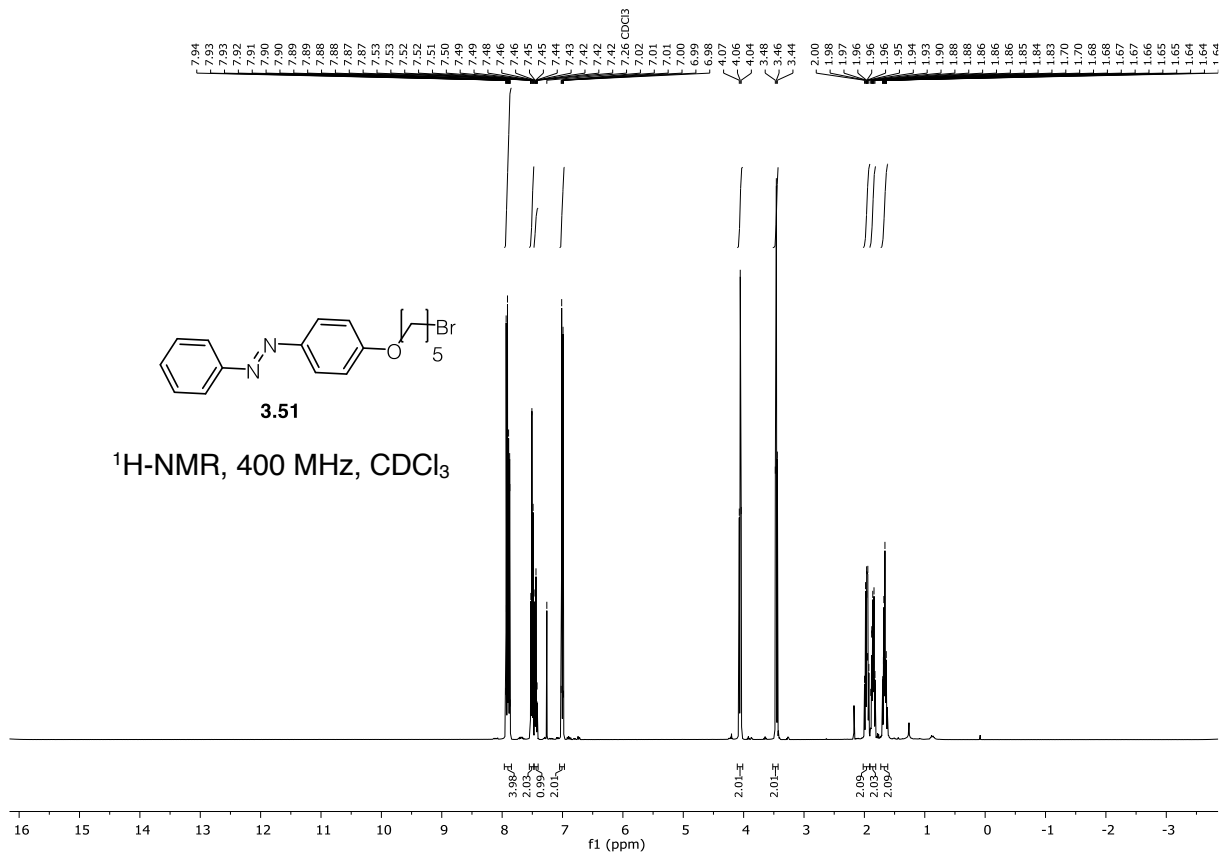
¹³C-NMR, 100 MHz, CDCl₃

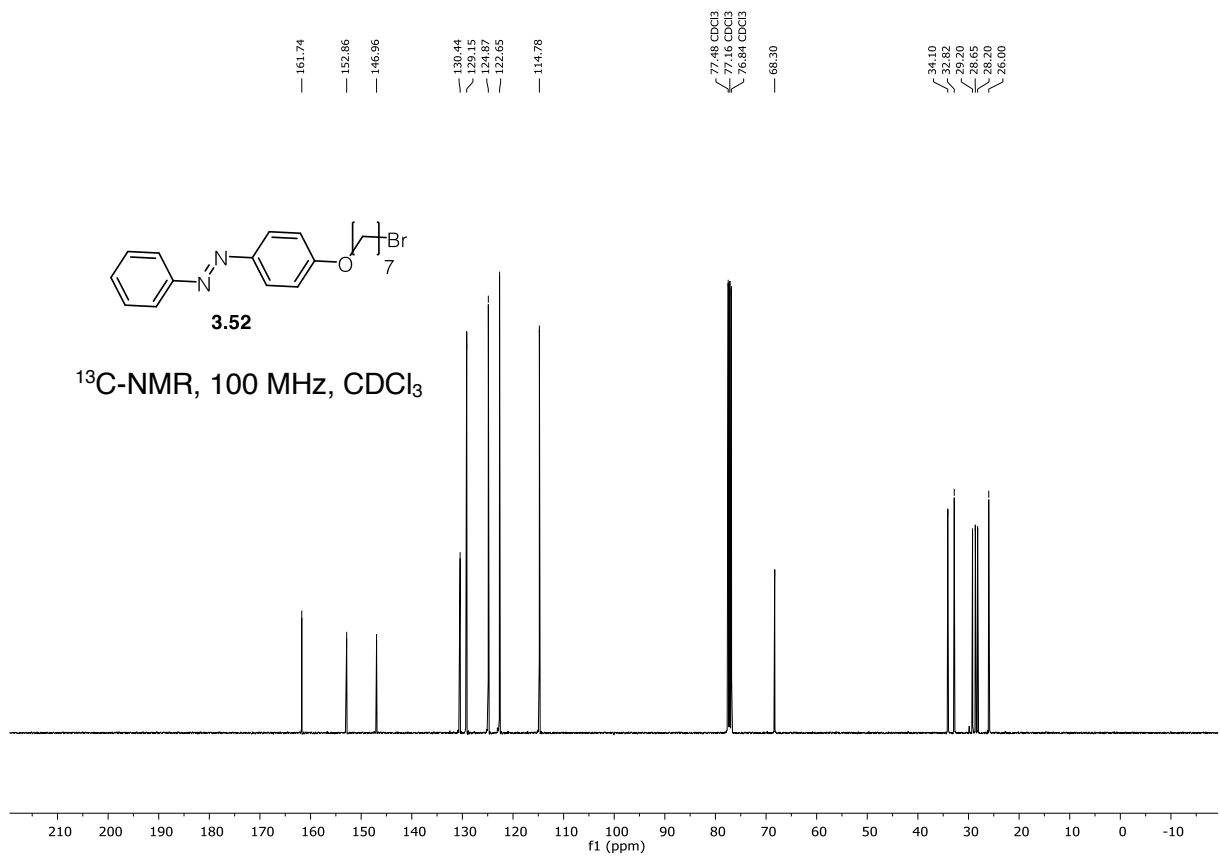
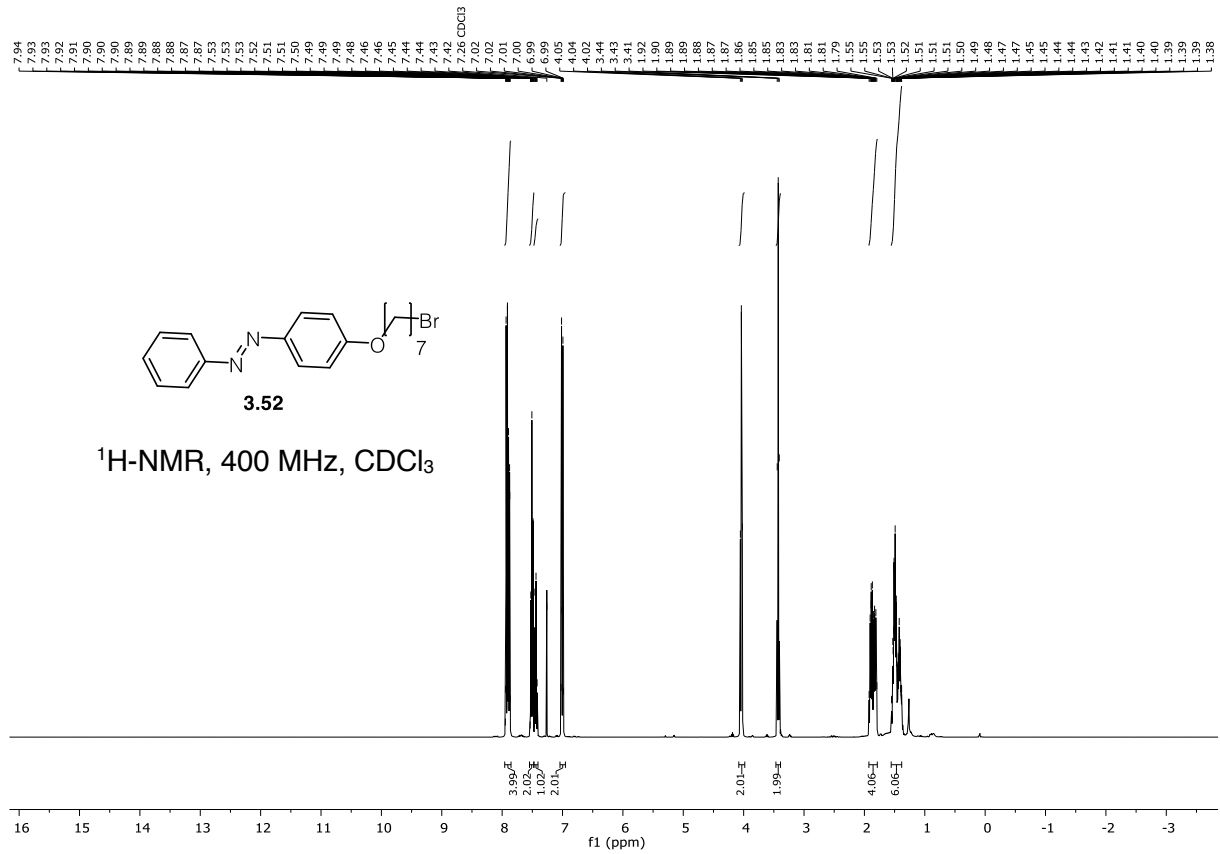


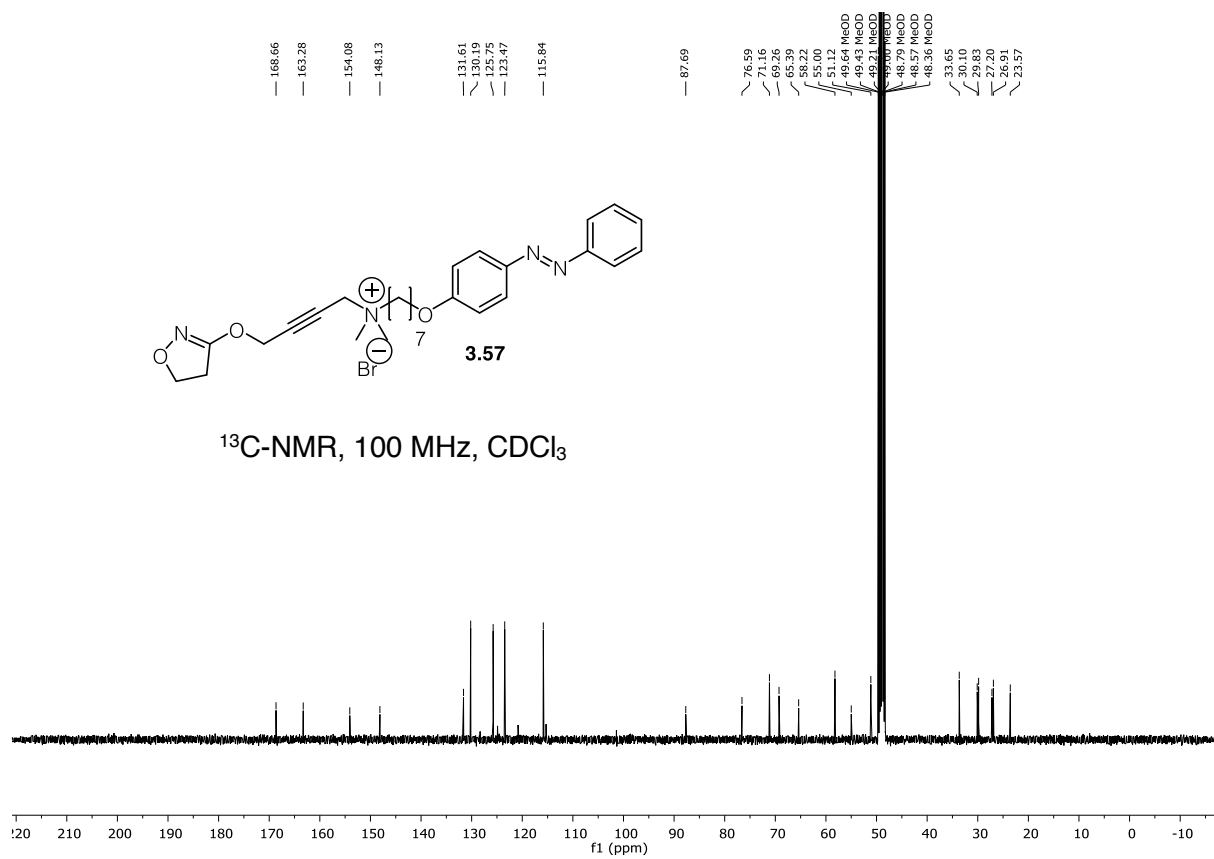
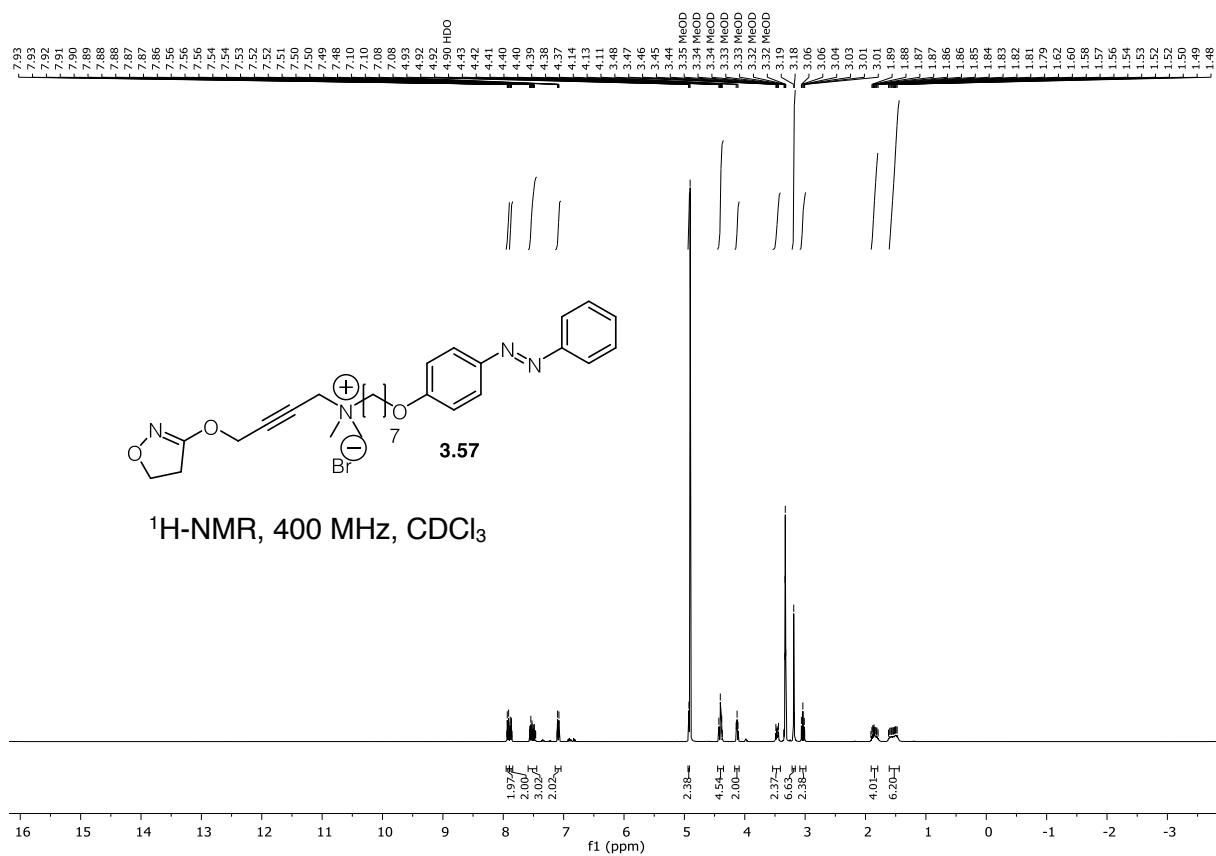


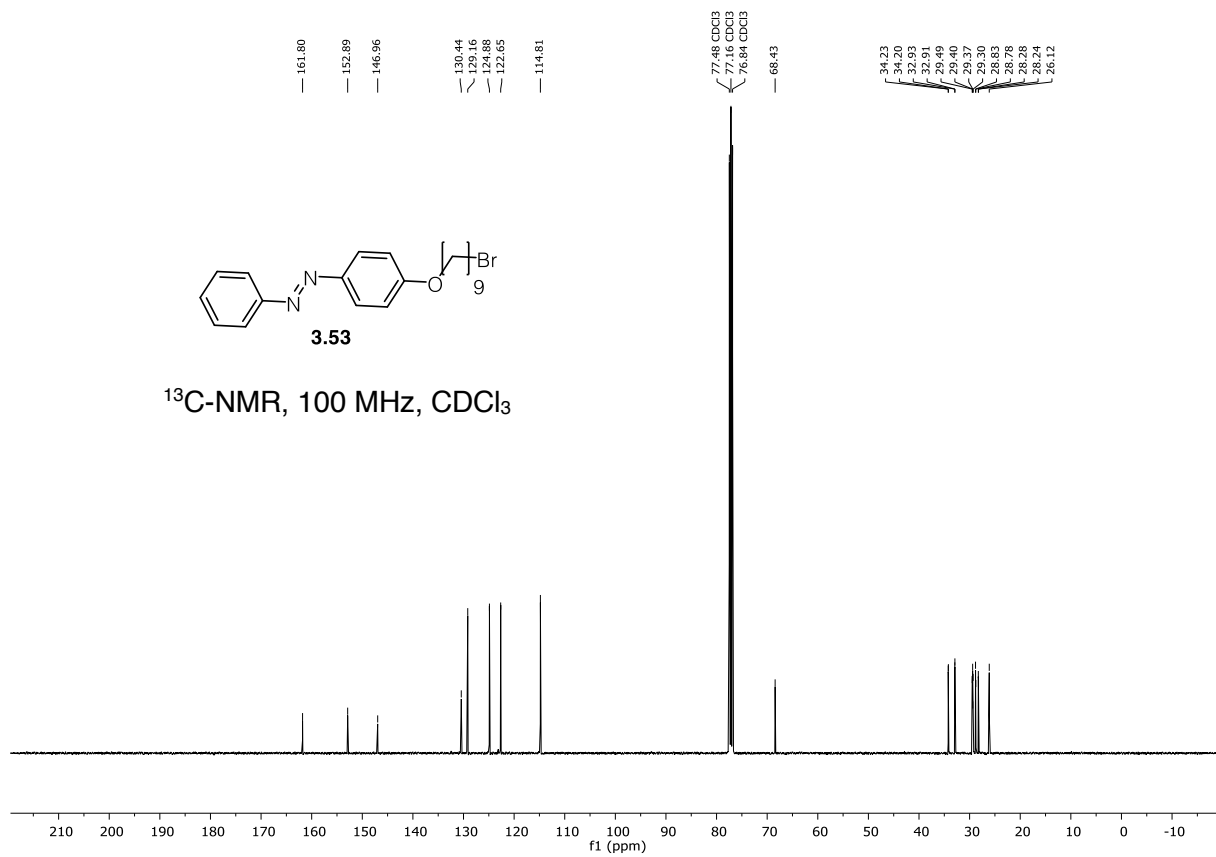
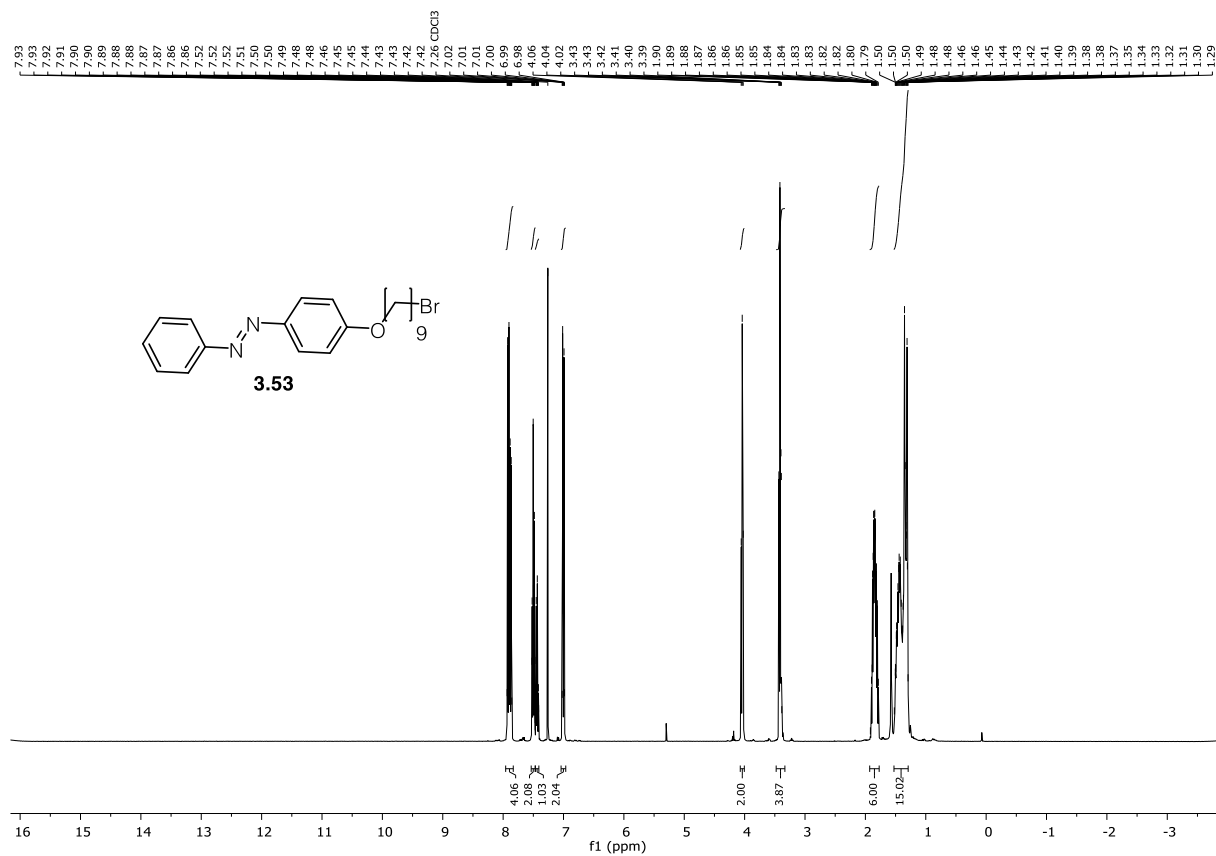


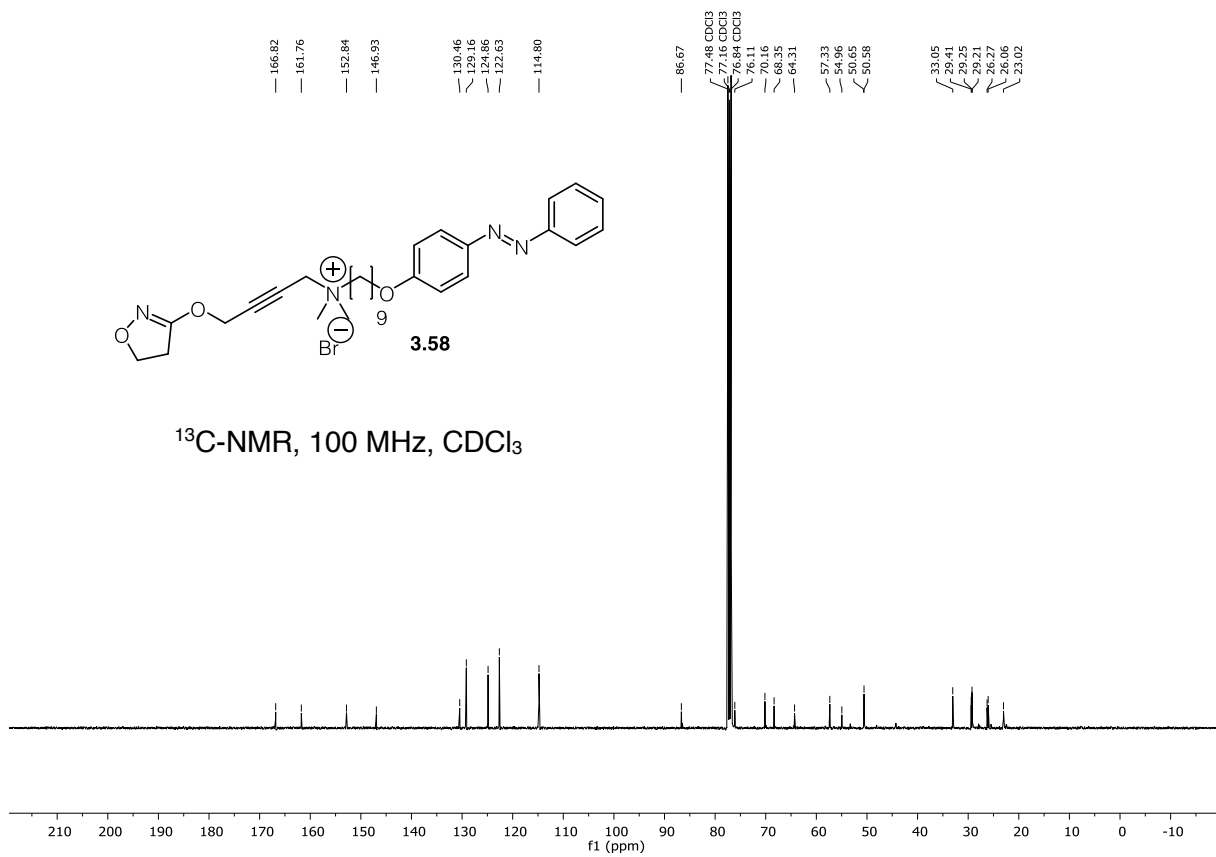
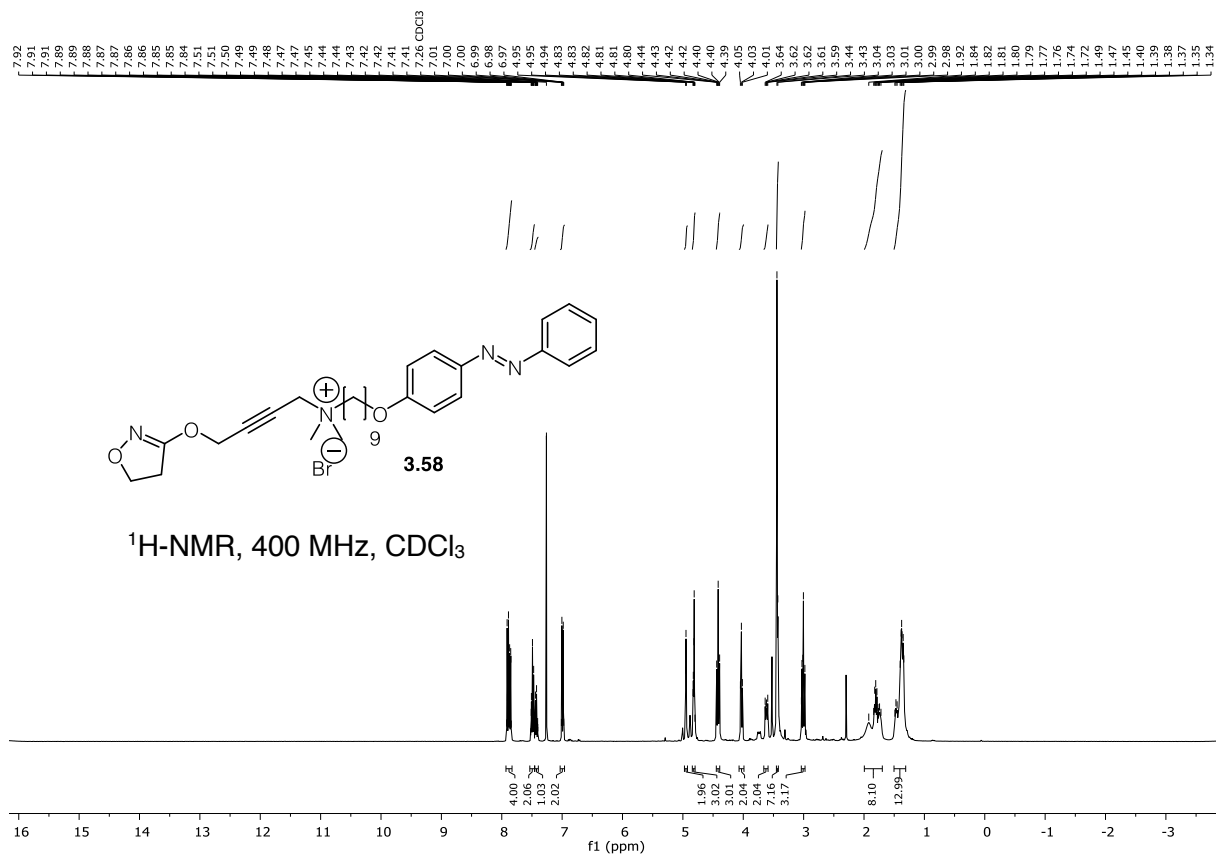


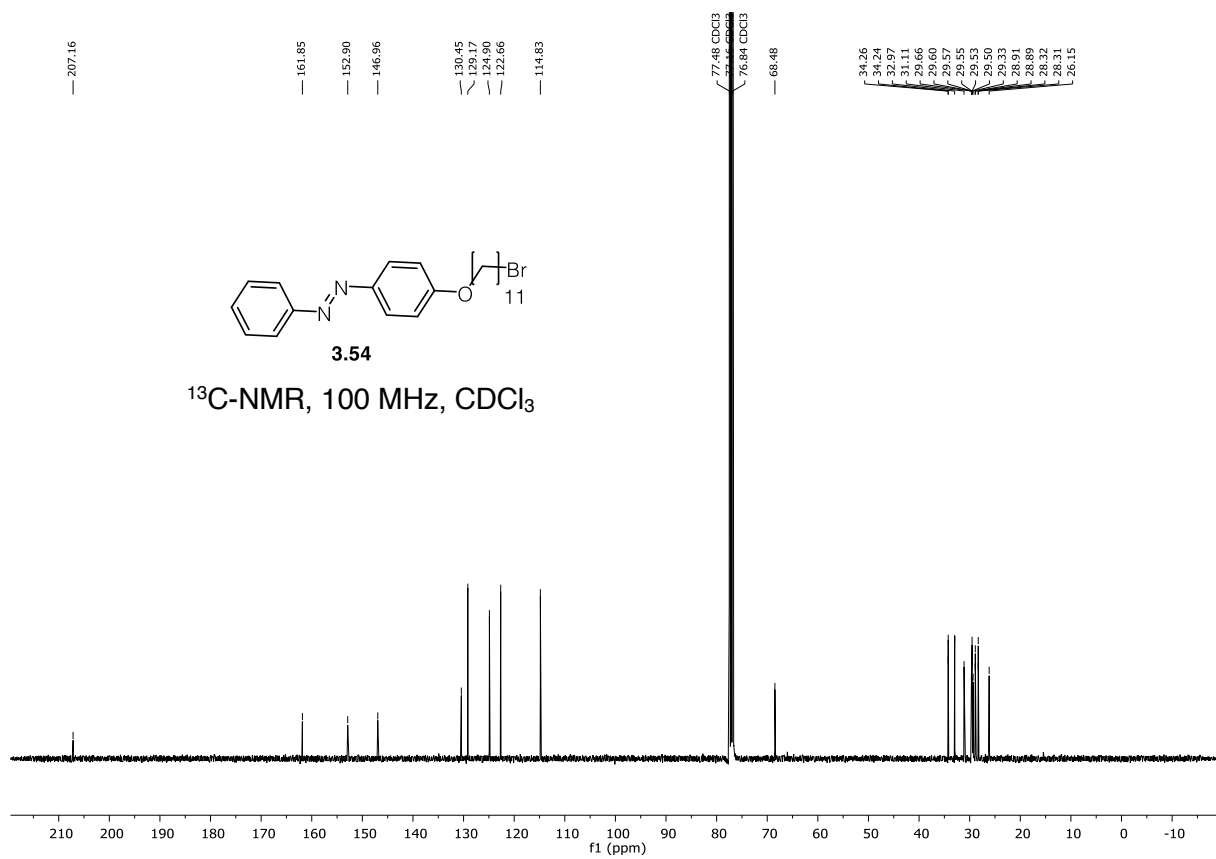
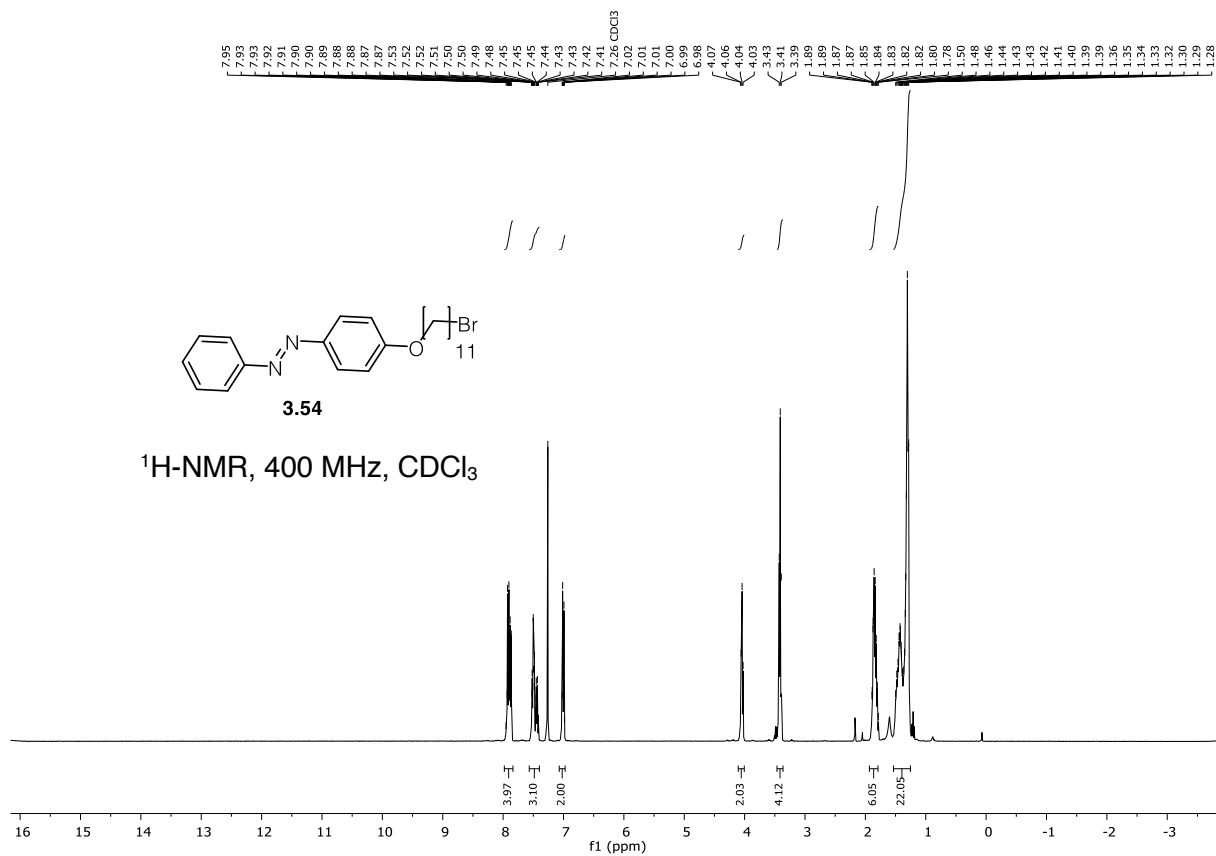


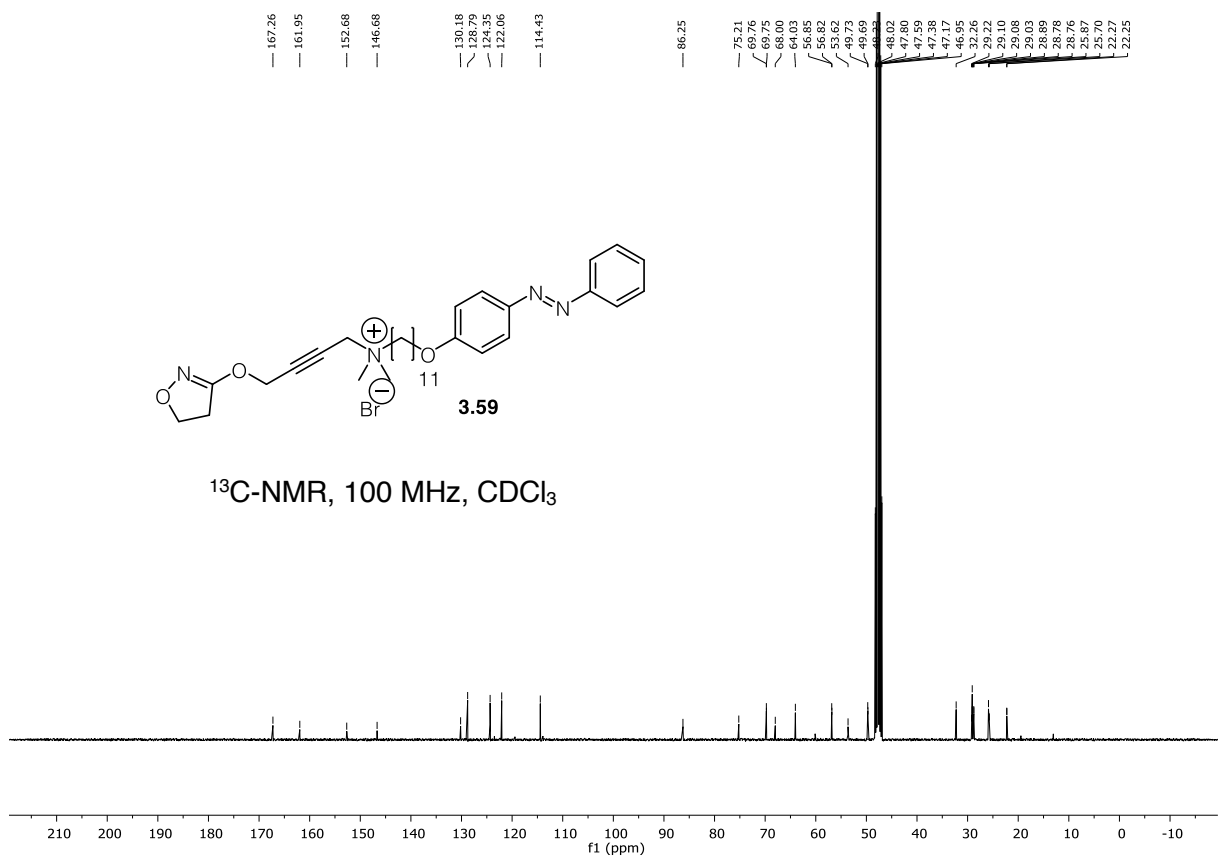
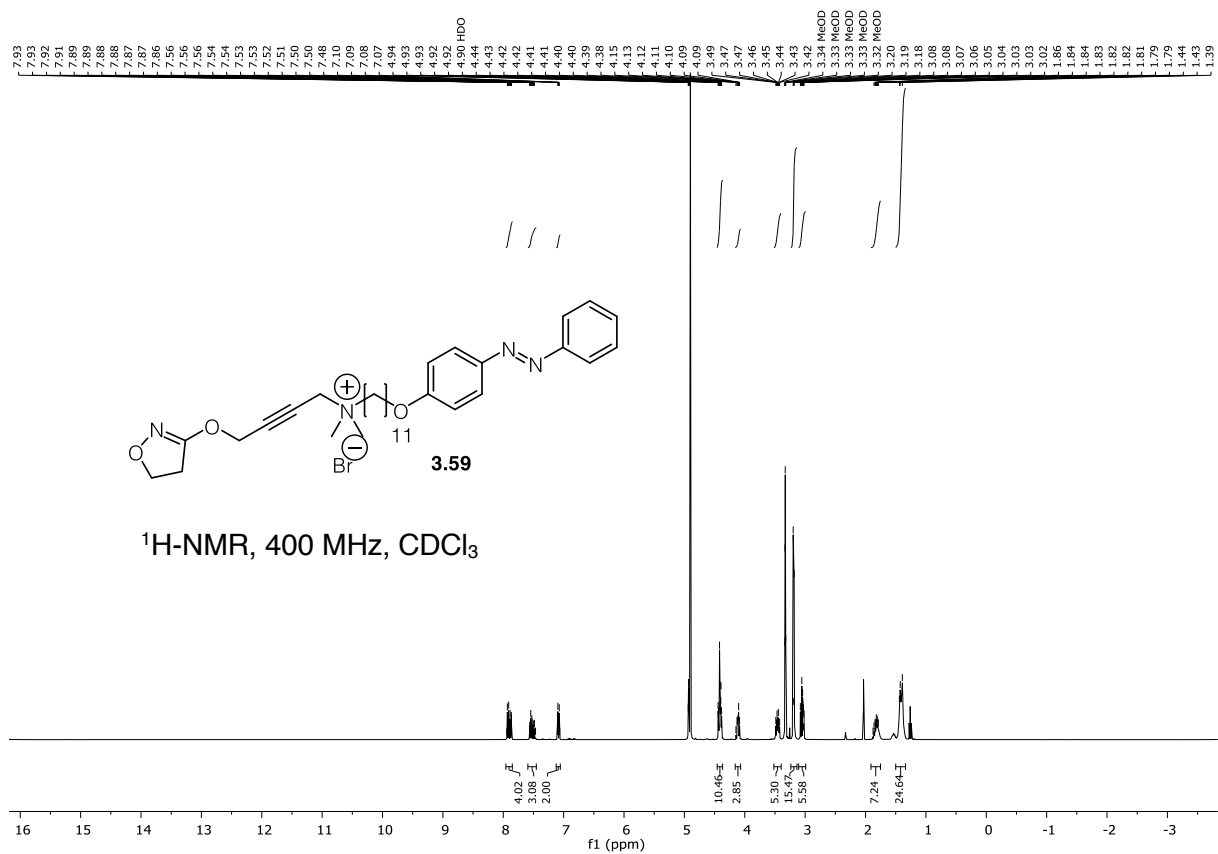


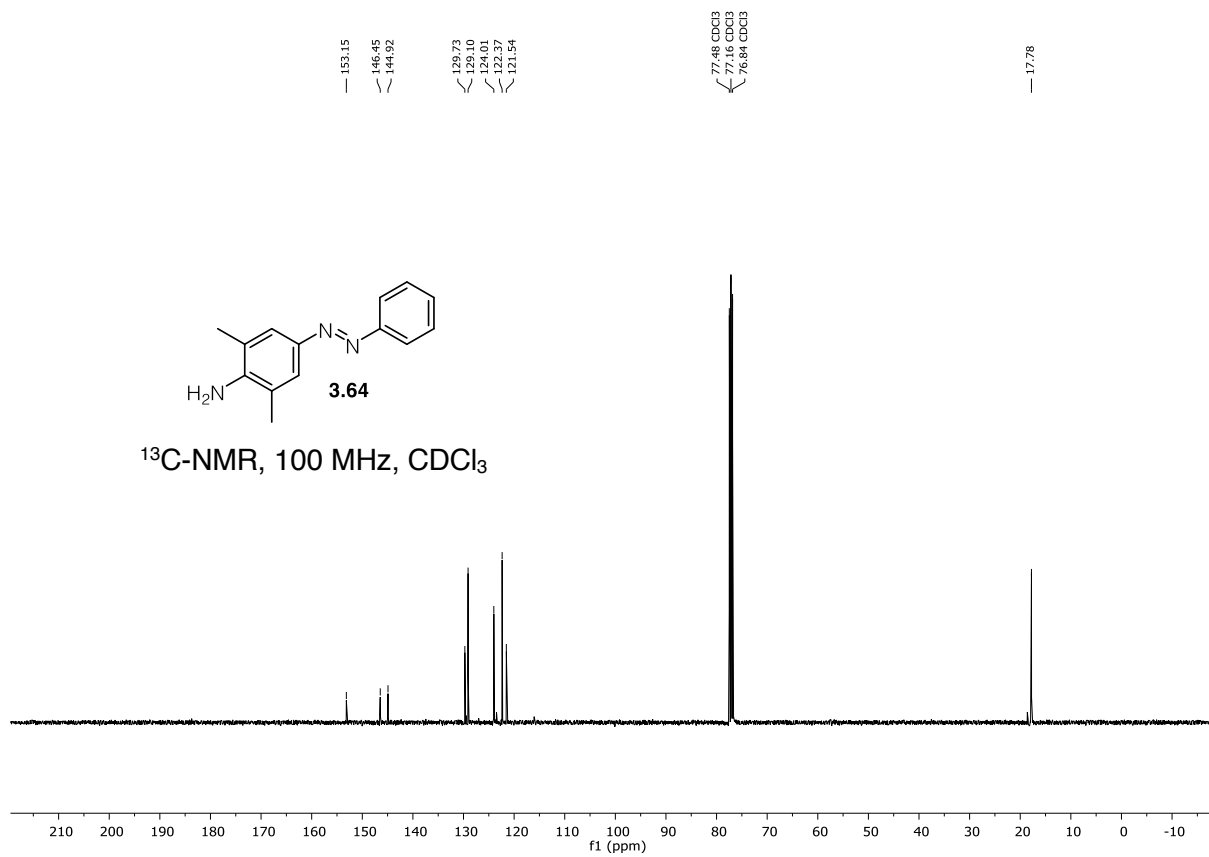
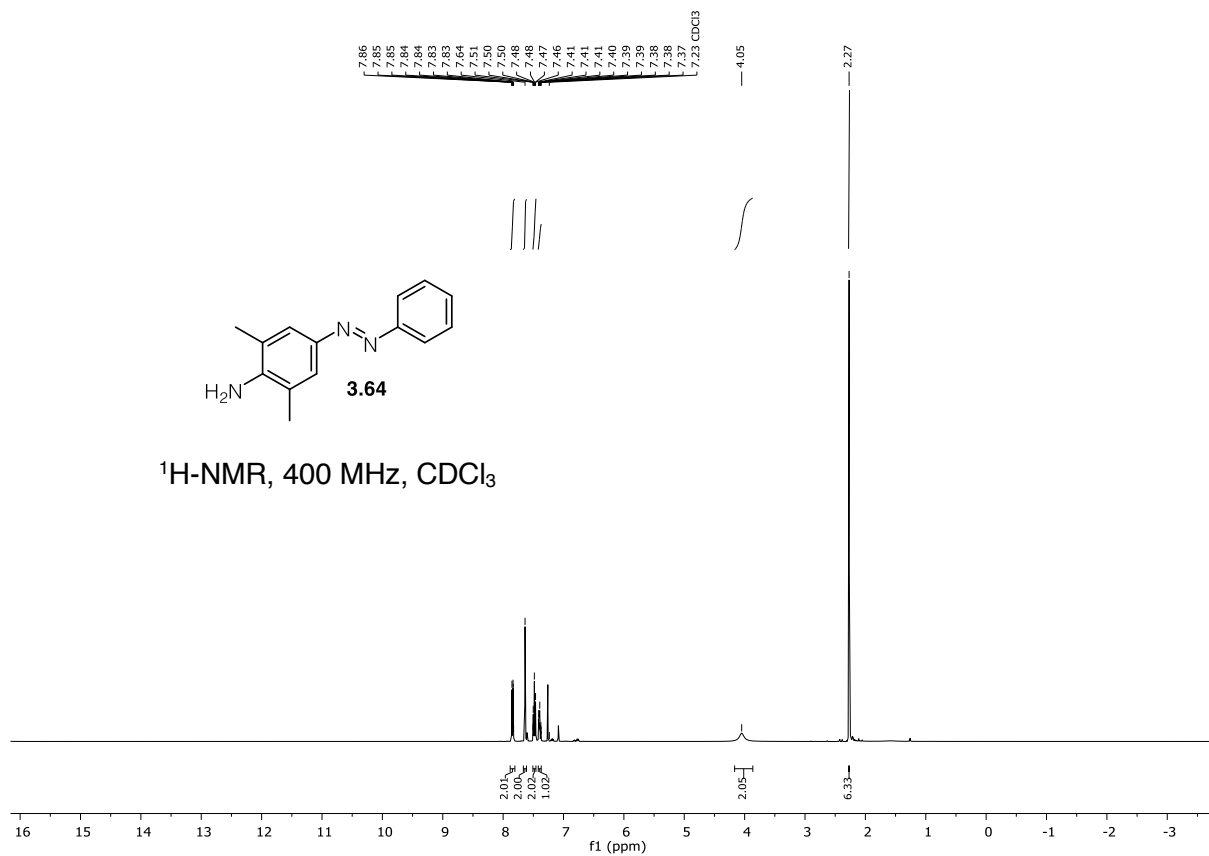


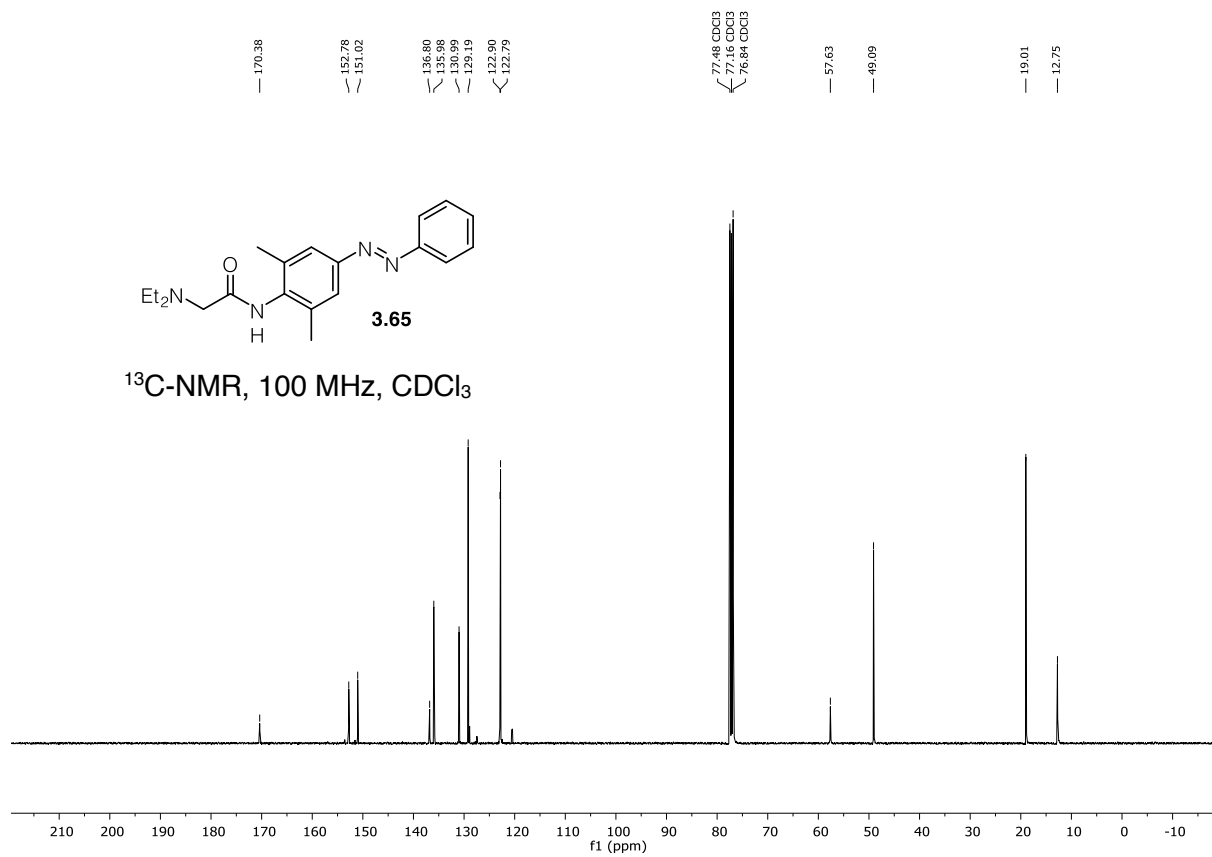
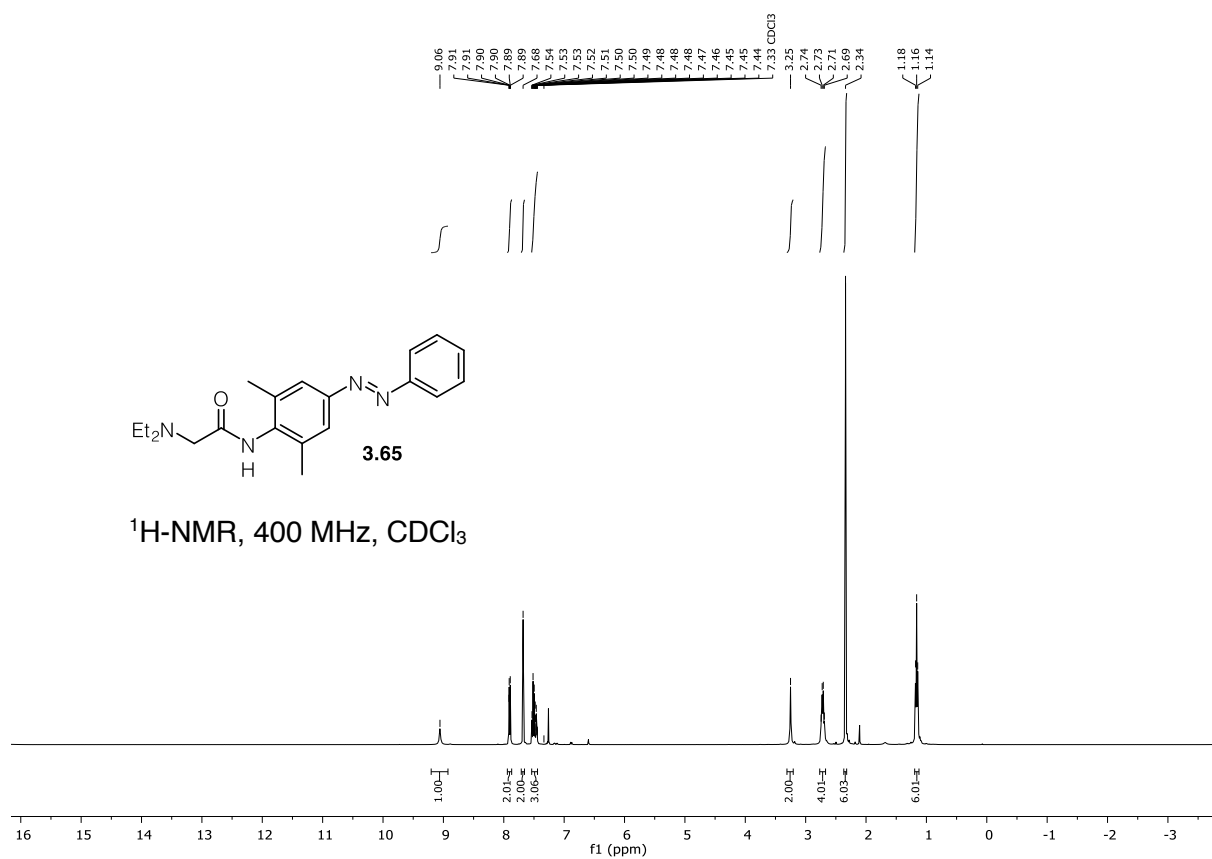


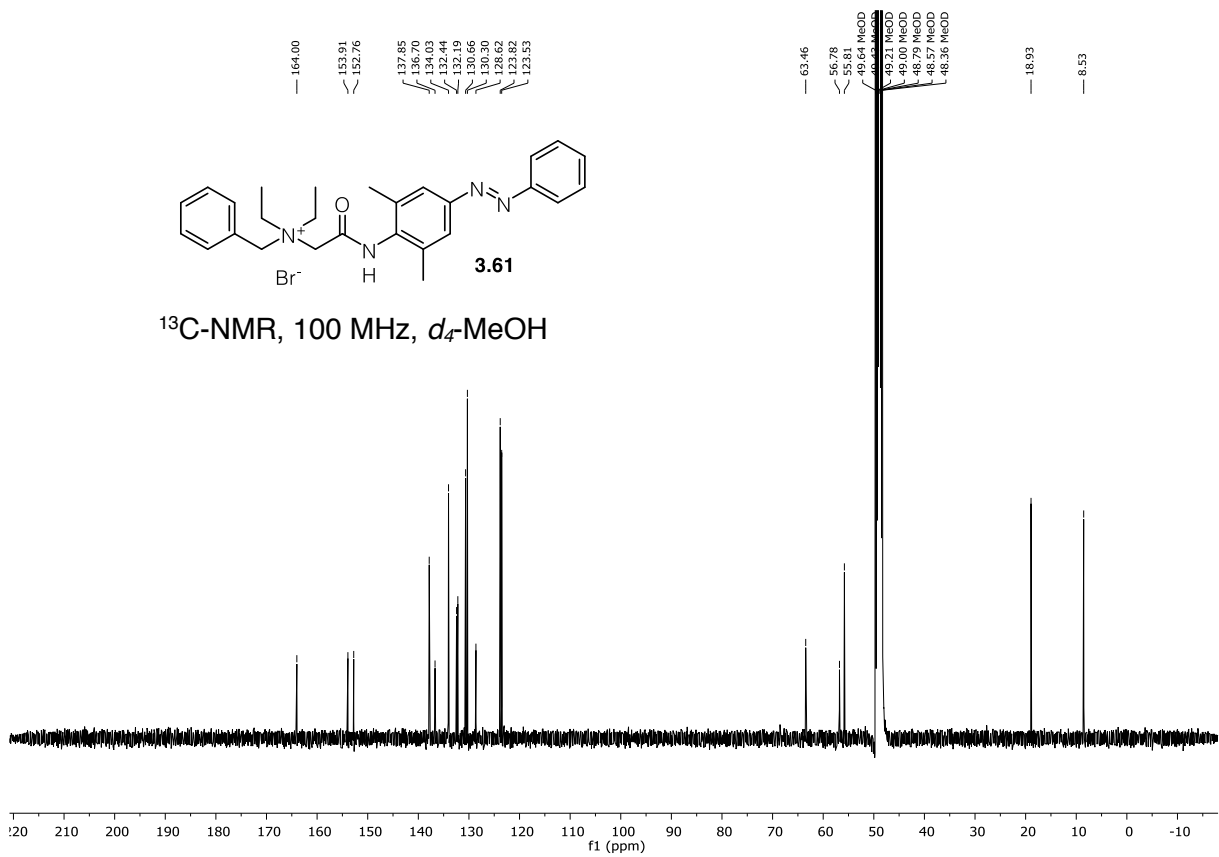
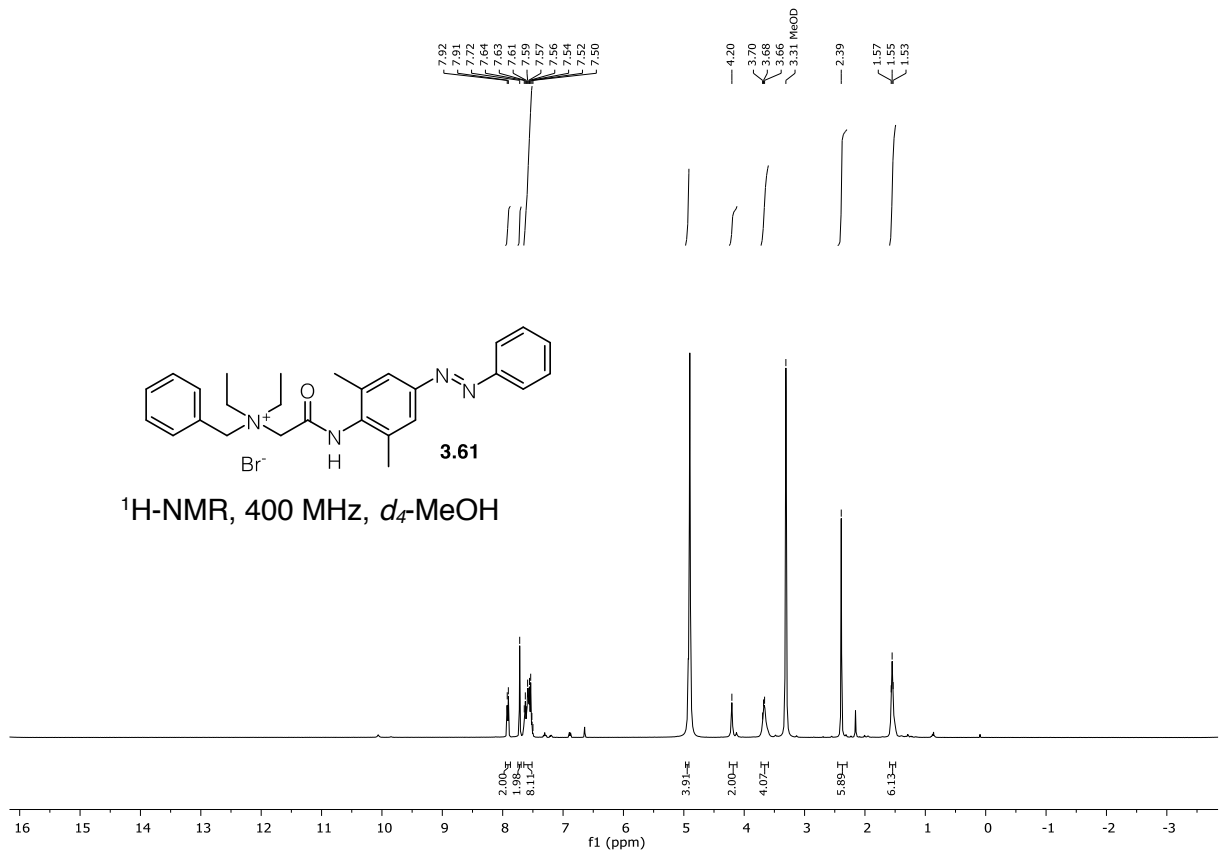


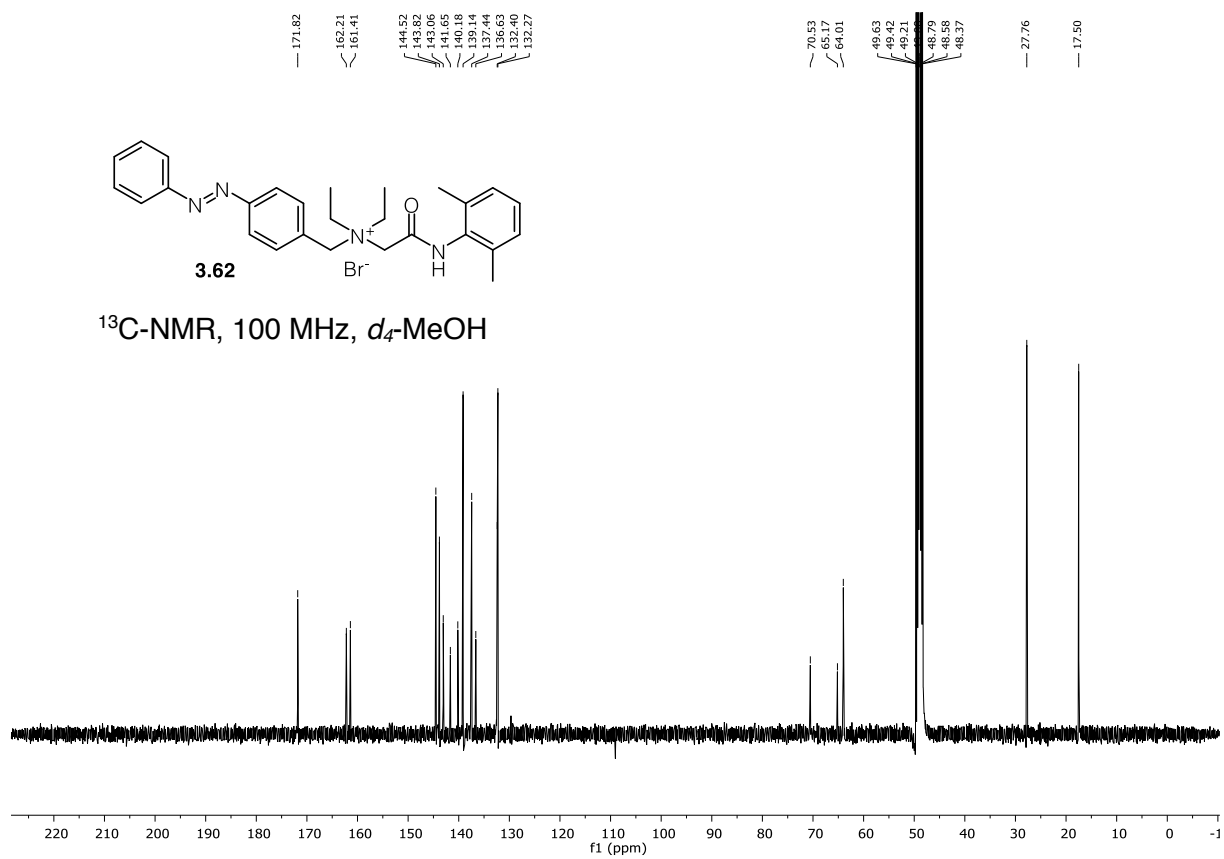
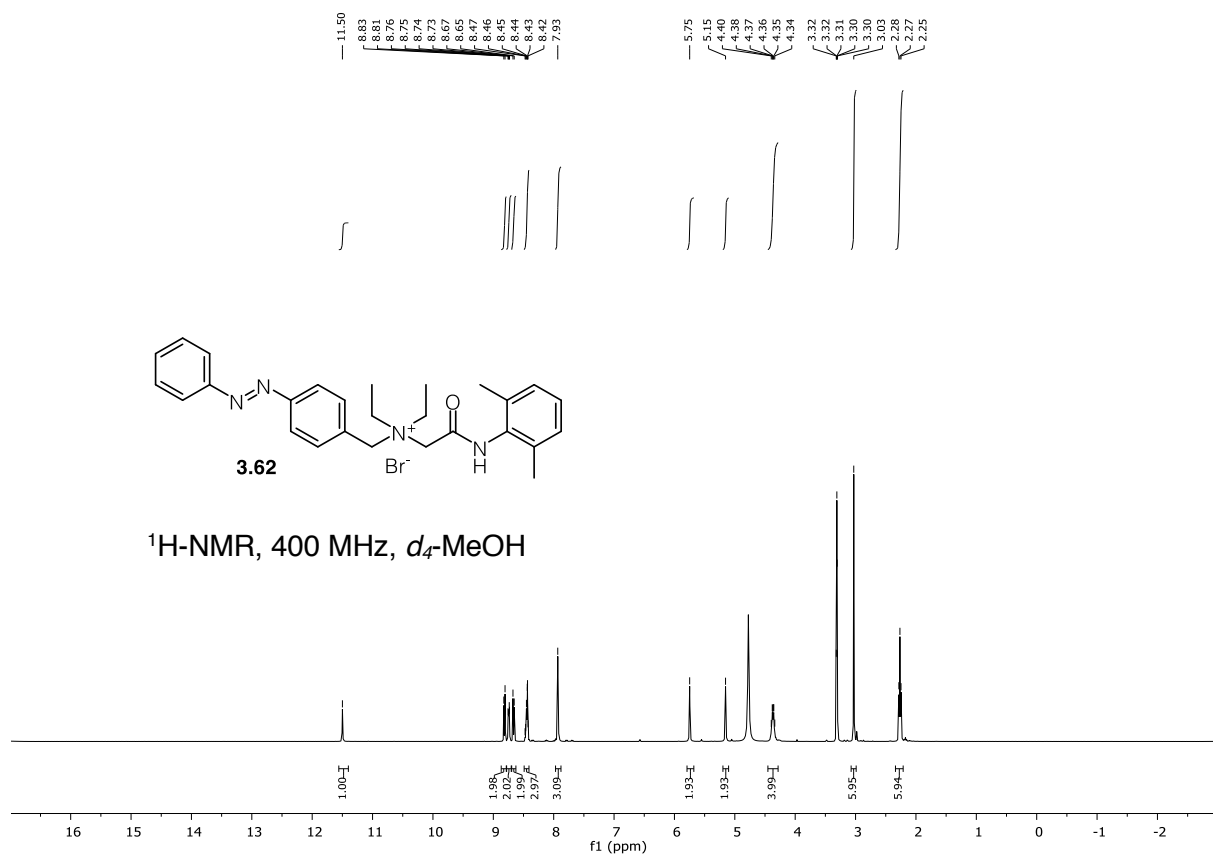


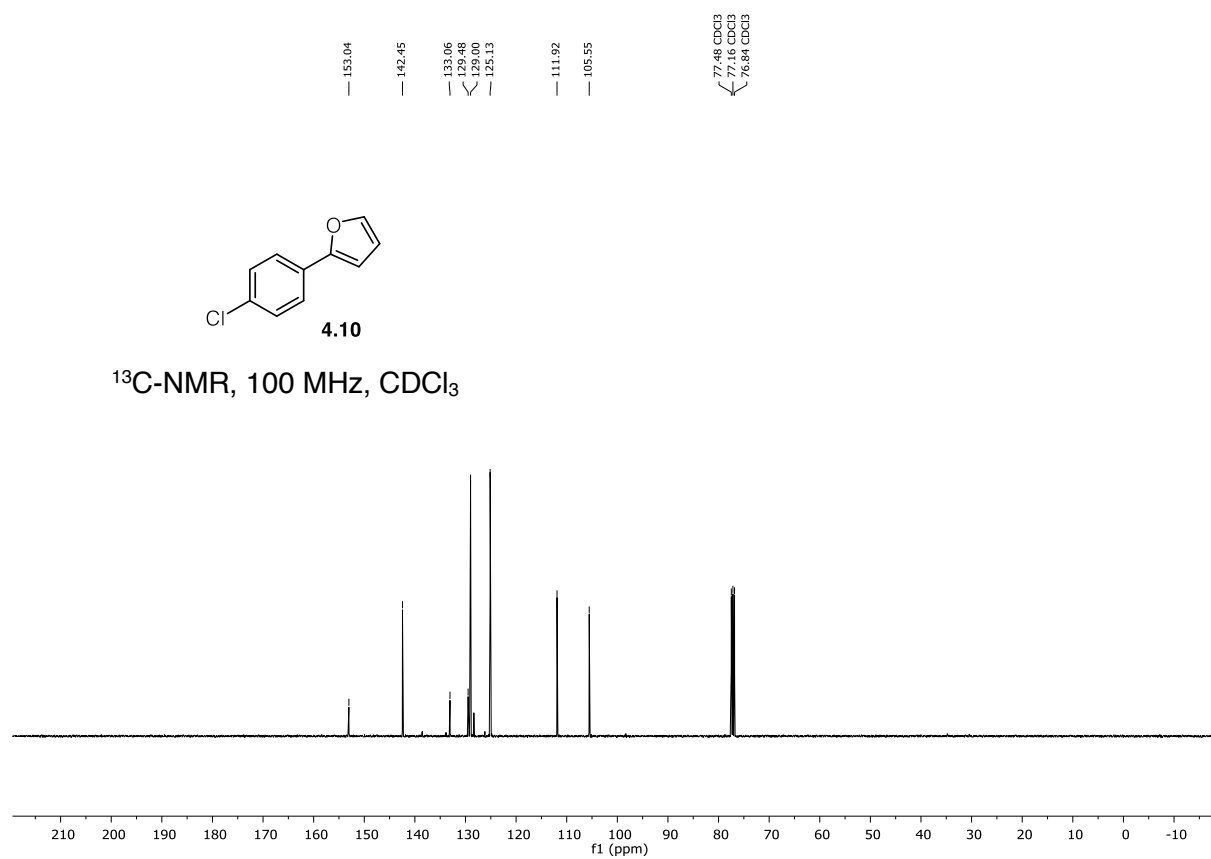
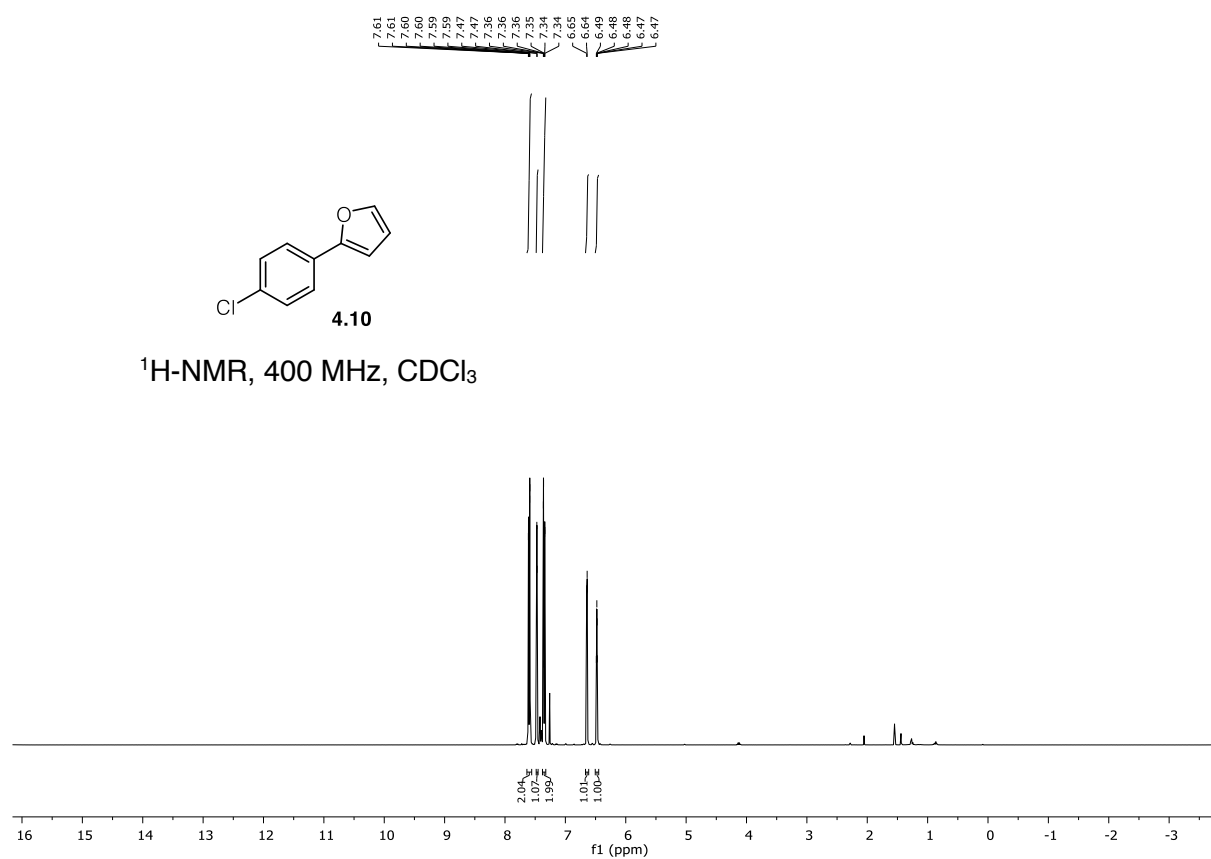


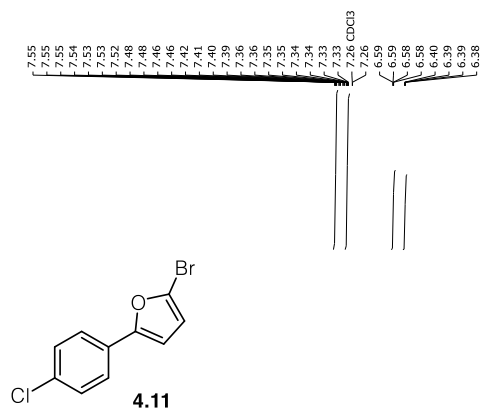




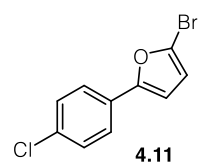
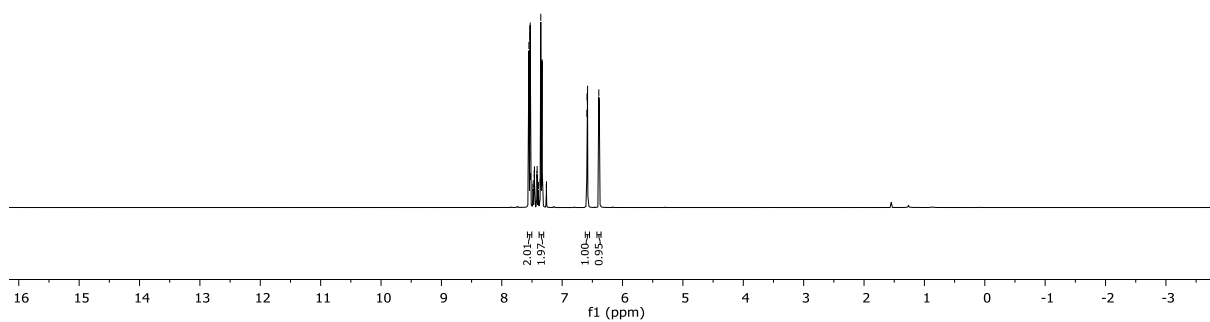




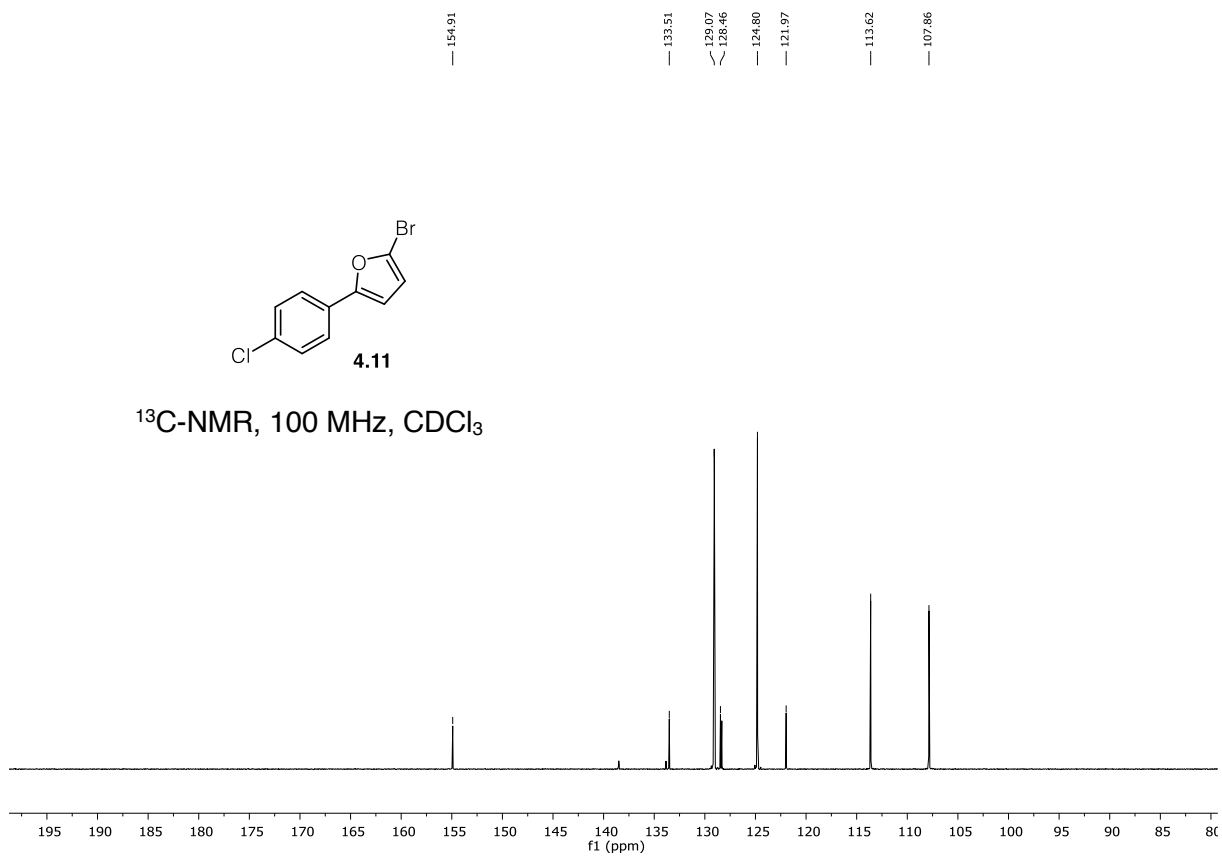
7.2.4 ^1H and ^{13}C NMR spectra of Chapter IV

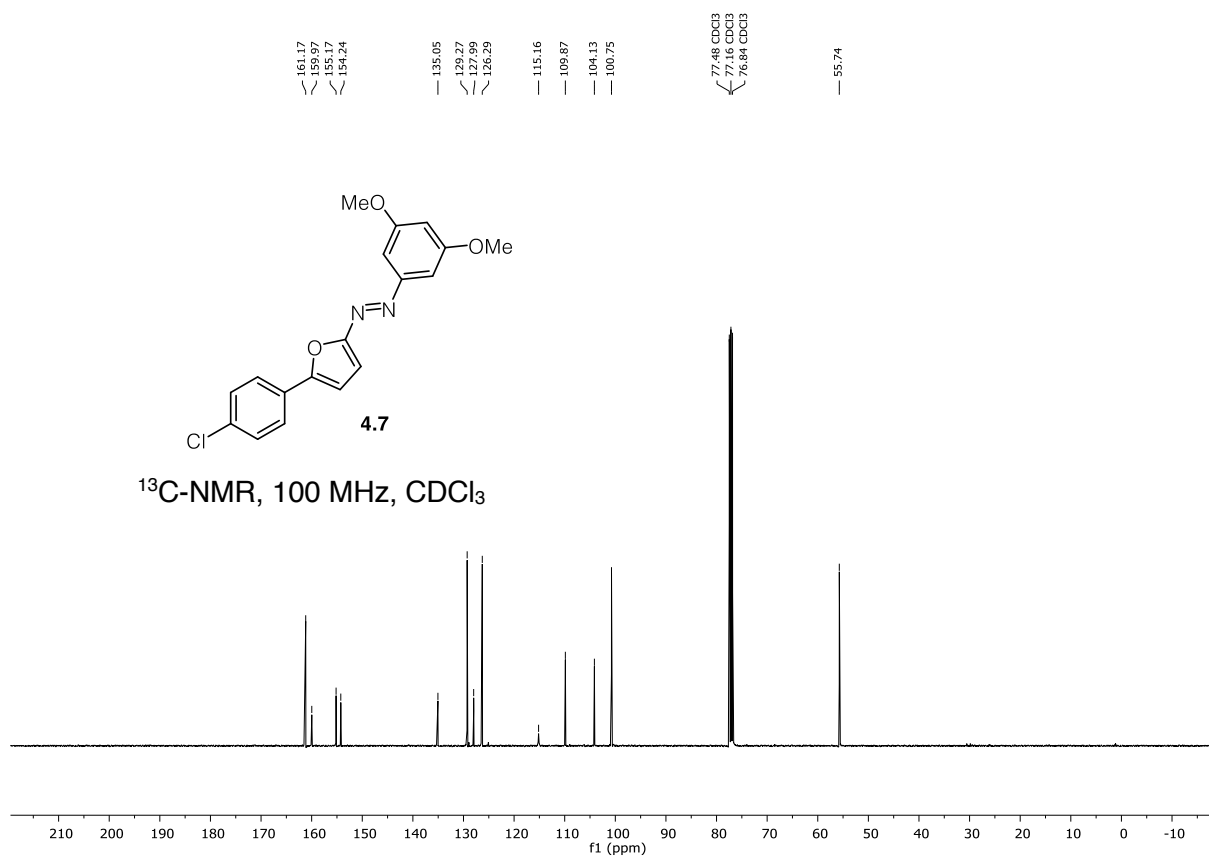
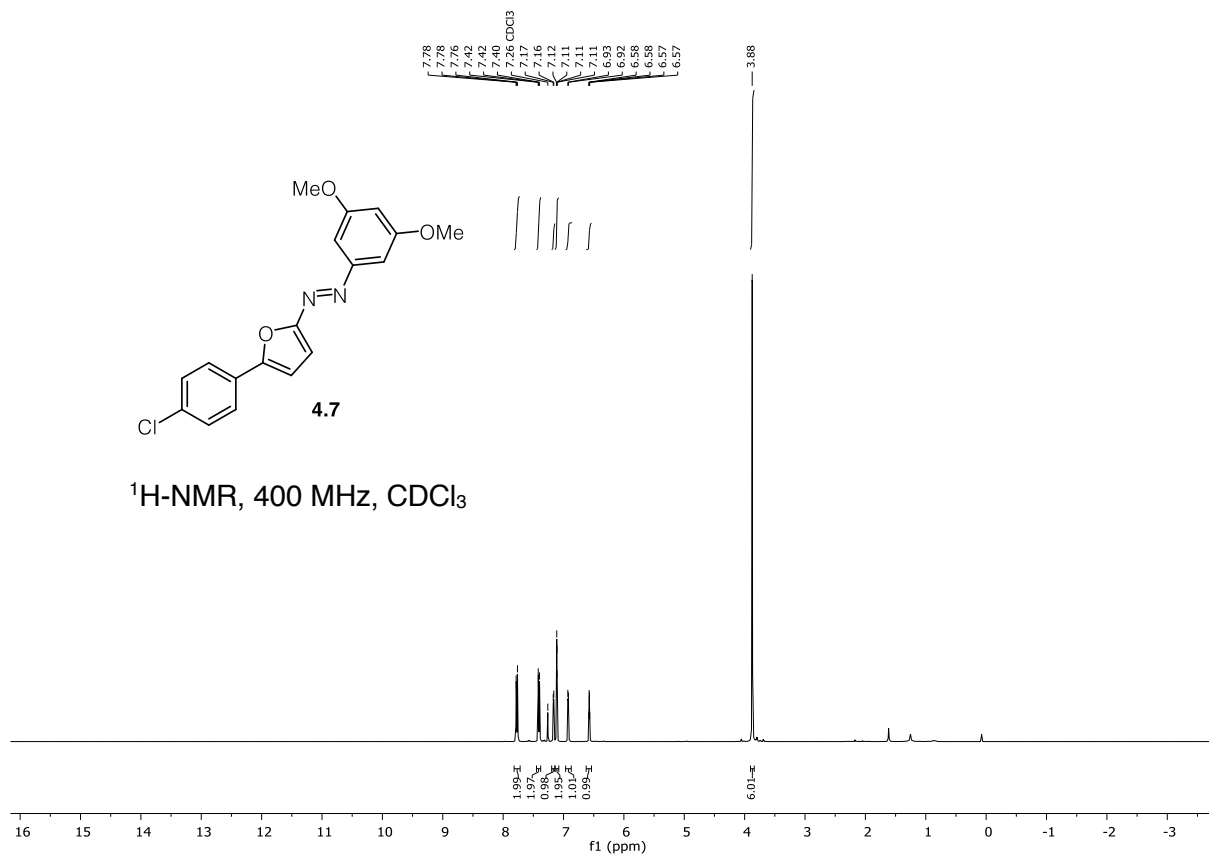


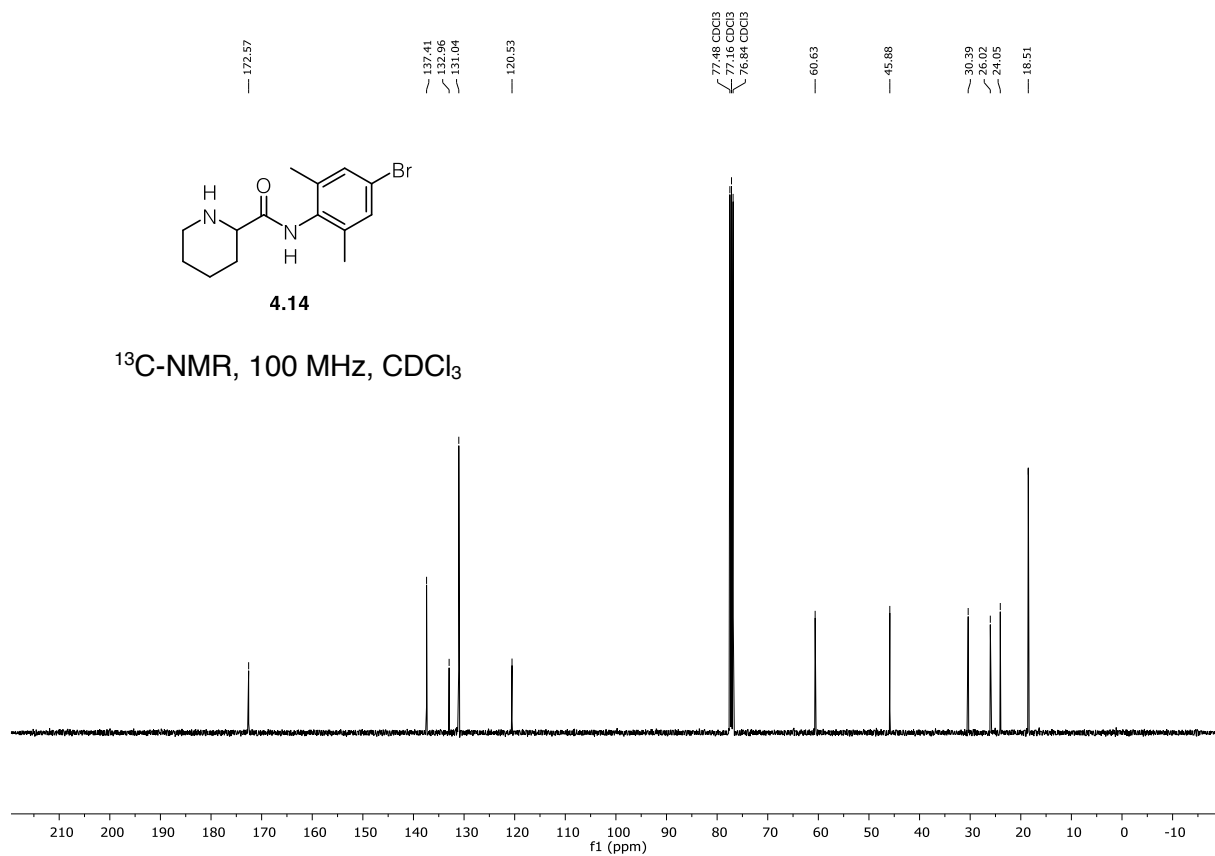
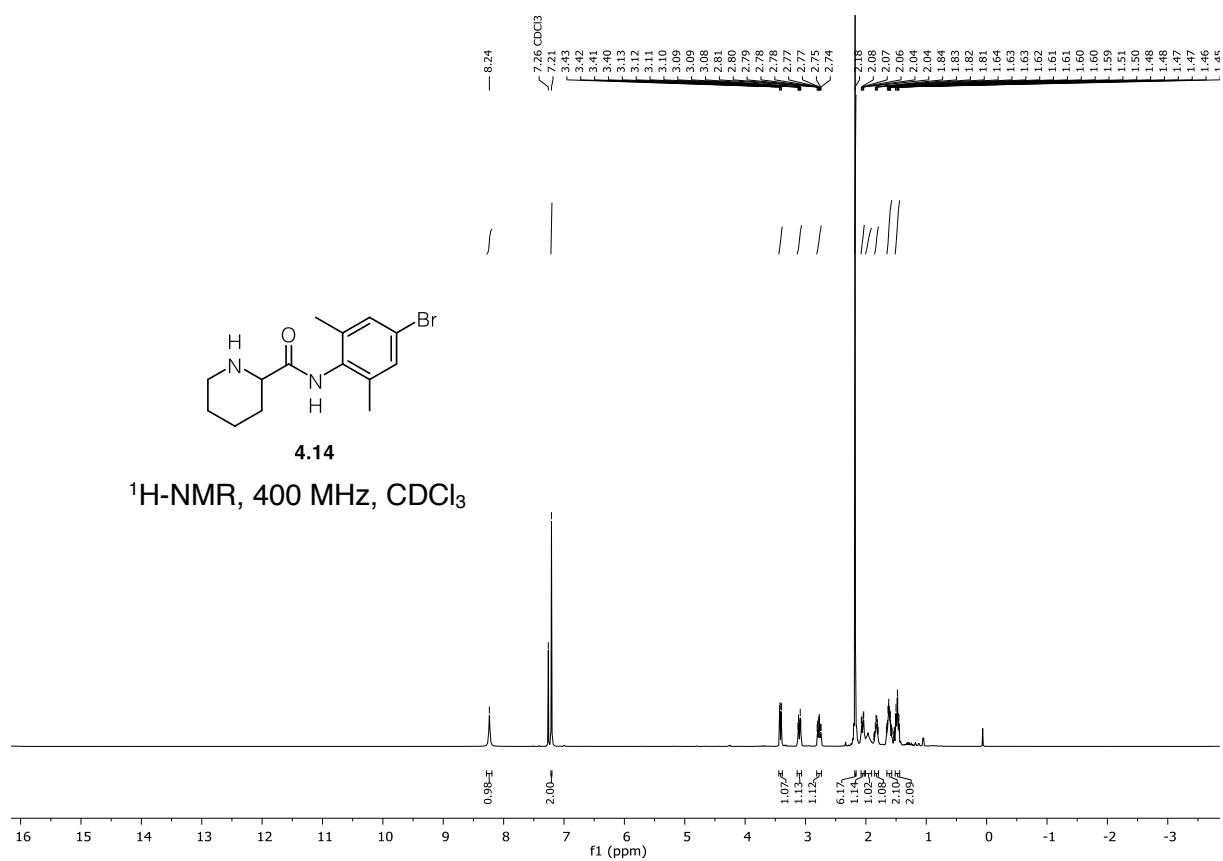
¹H-NMR, 400 MHz, CDCl₃

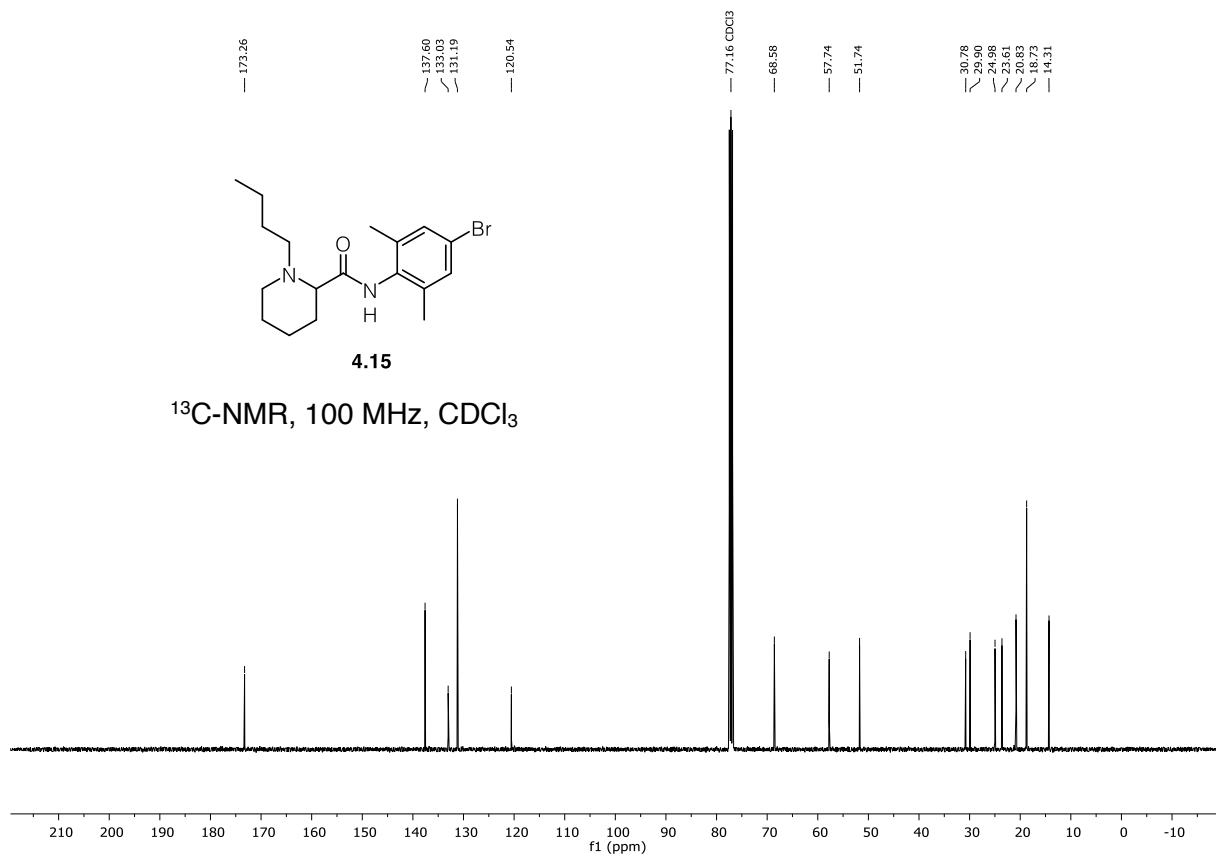
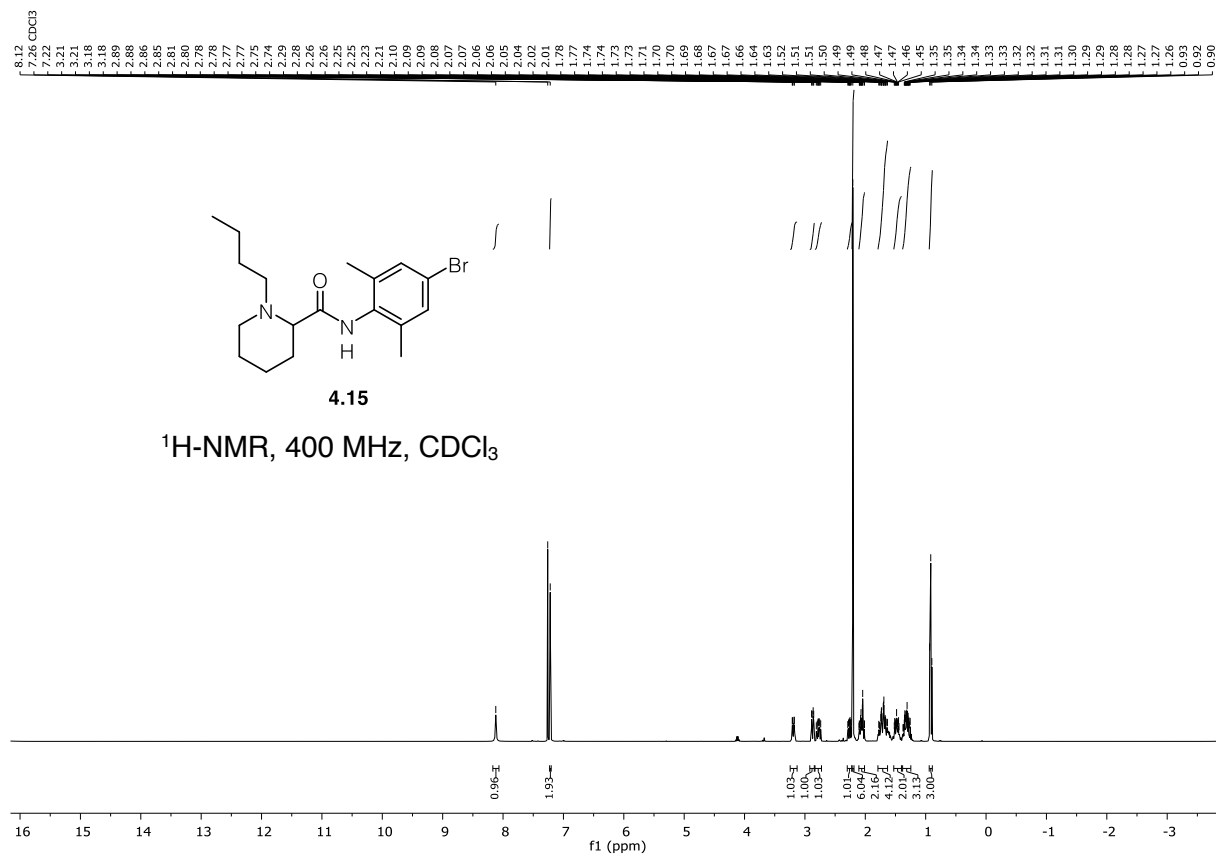


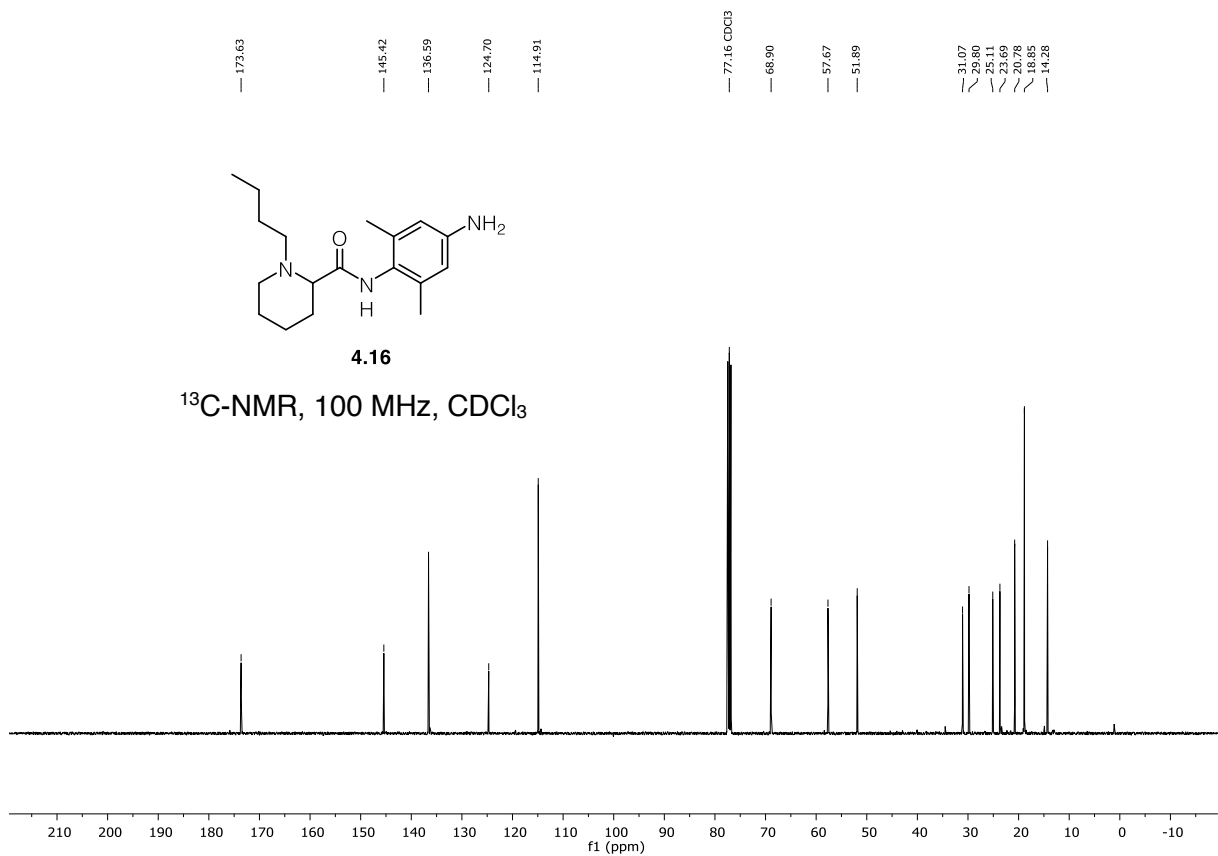
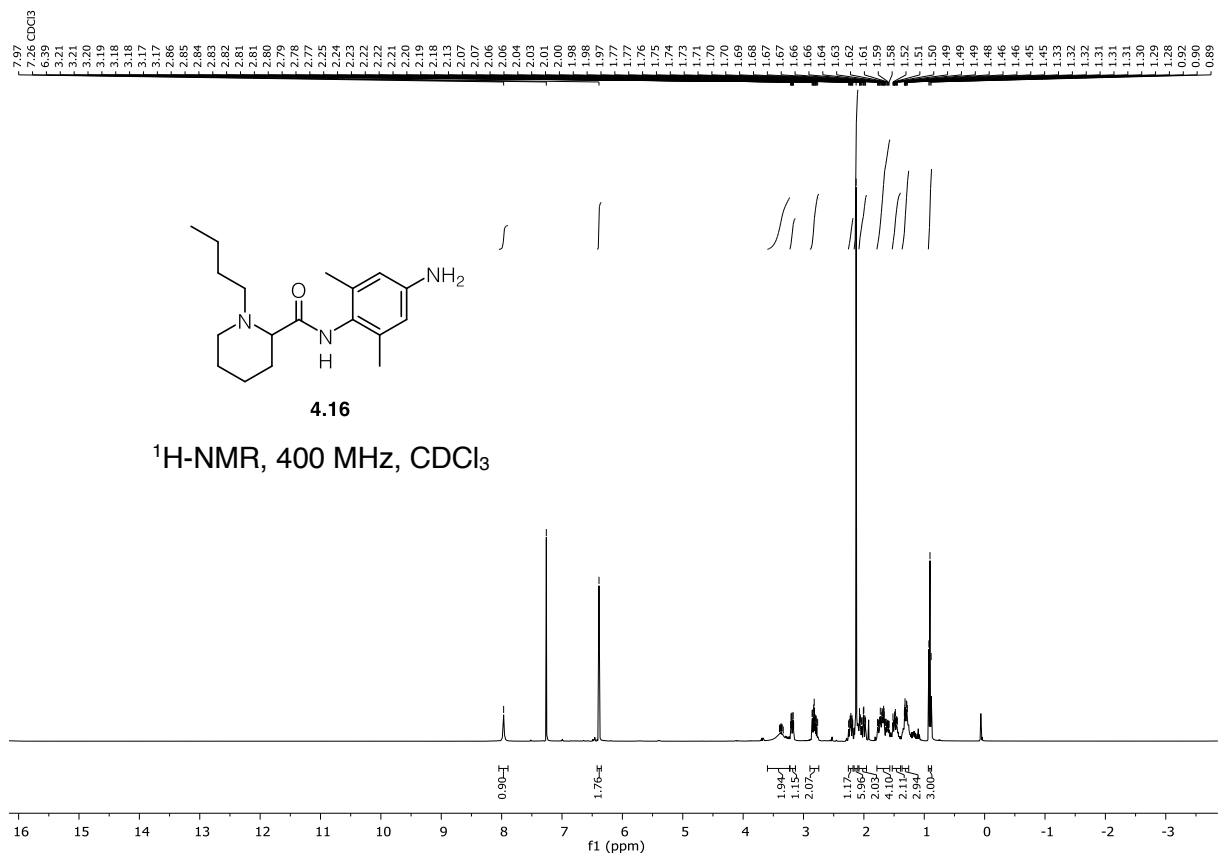
¹³C-NMR, 100 MHz, CDCl₃

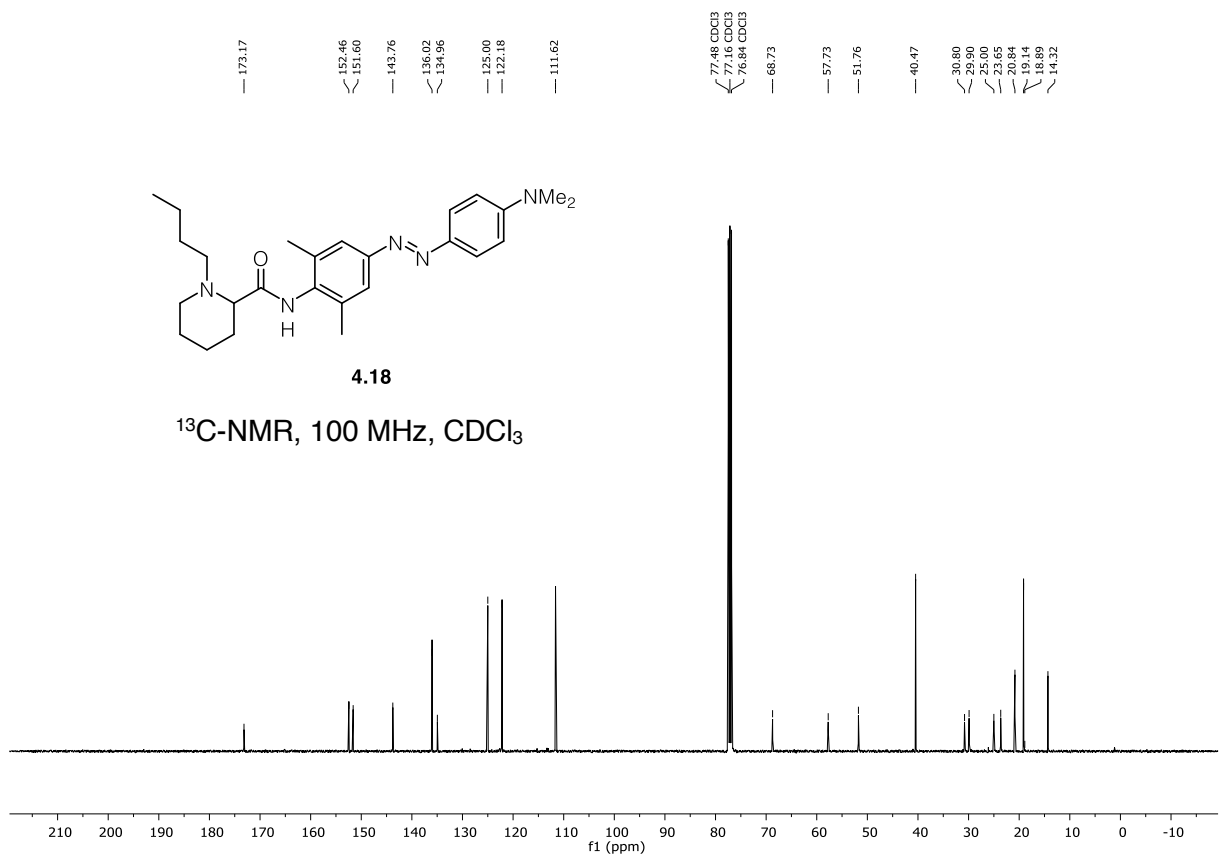
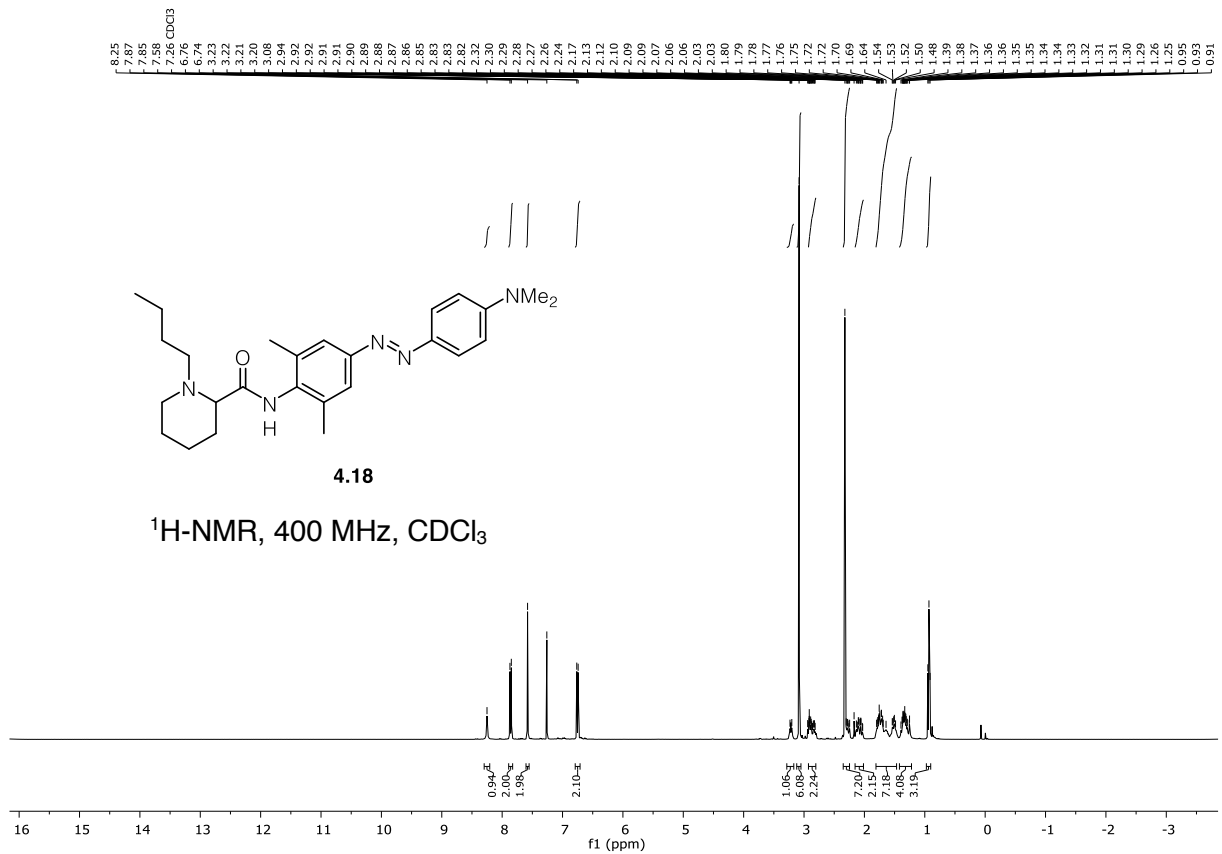


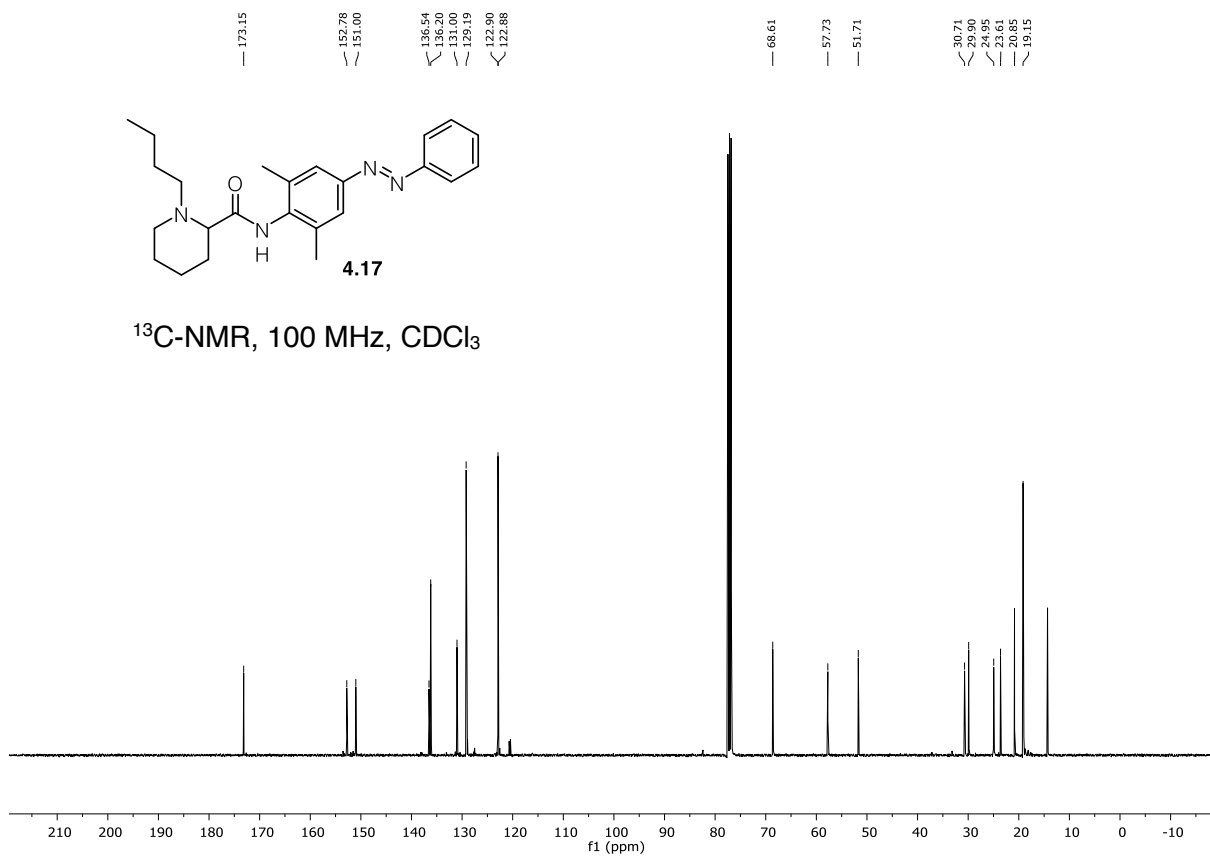
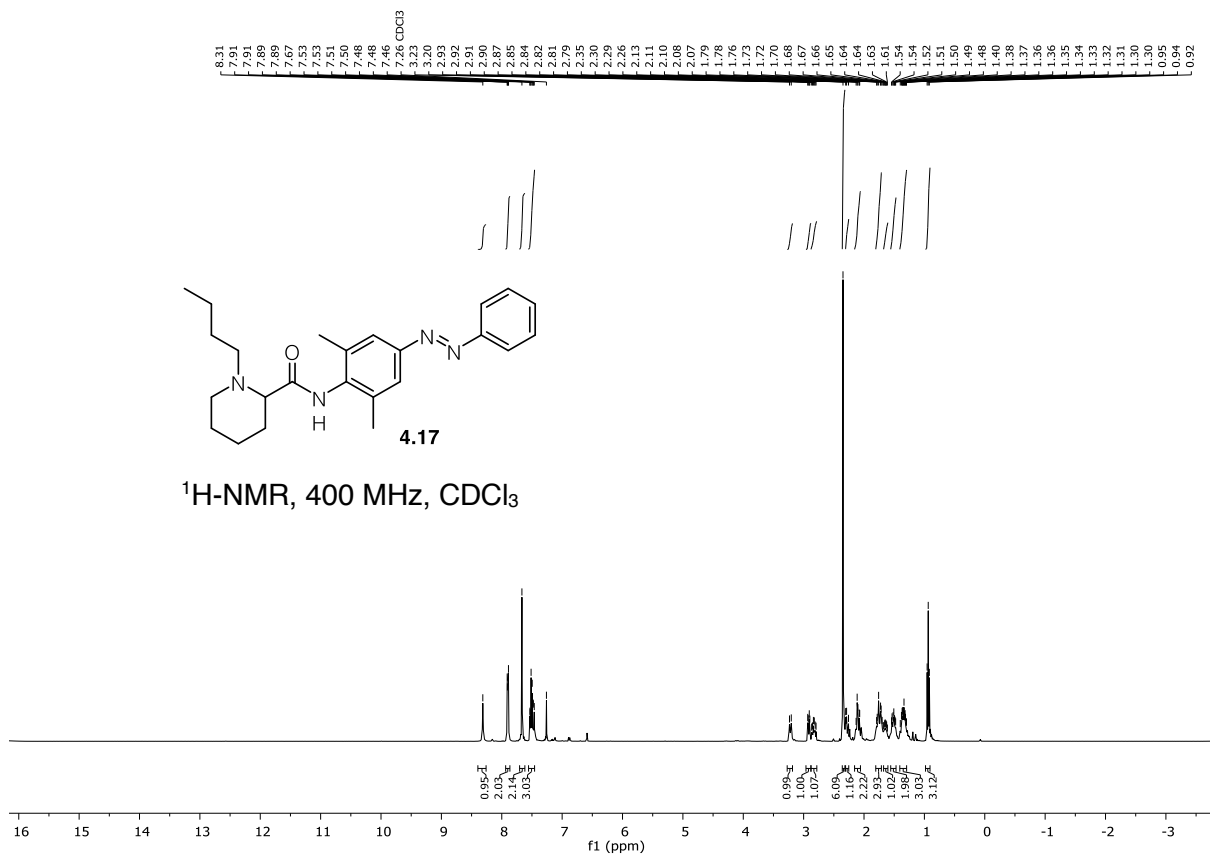


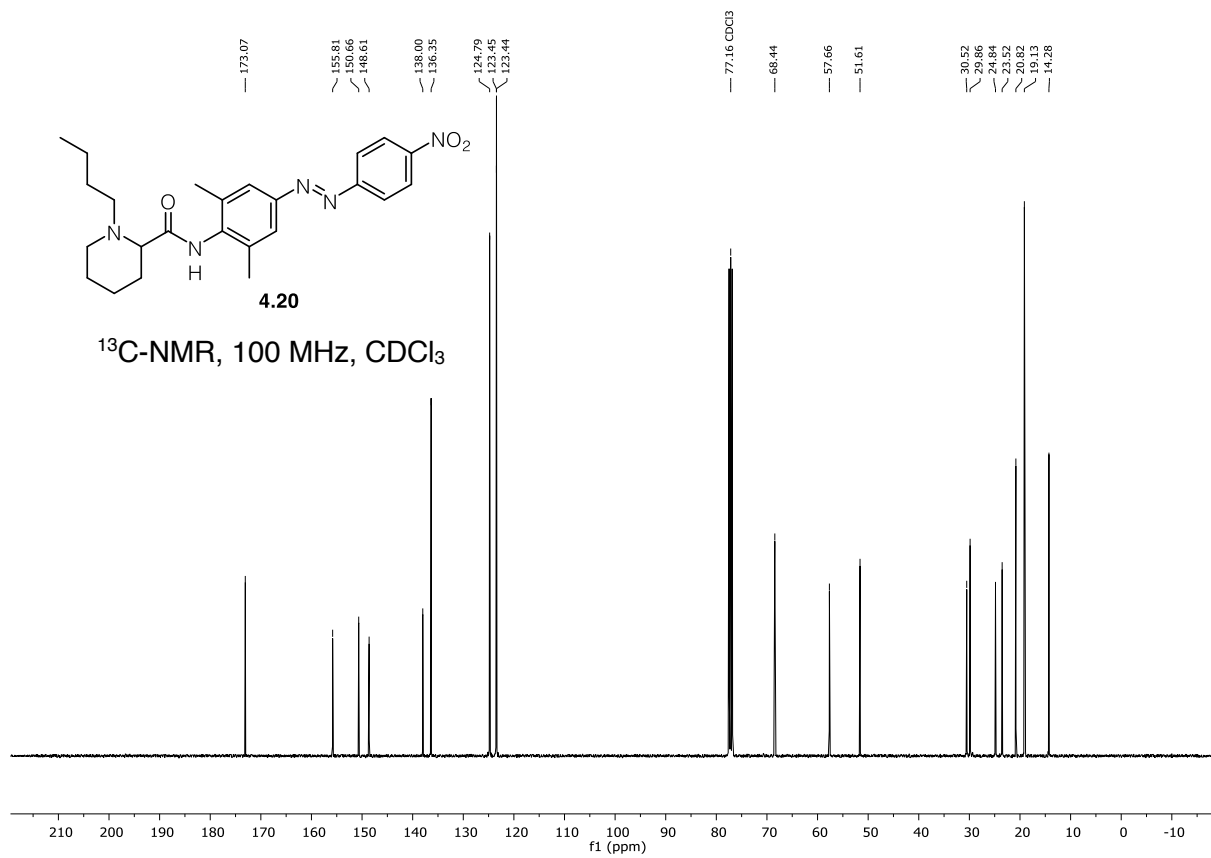
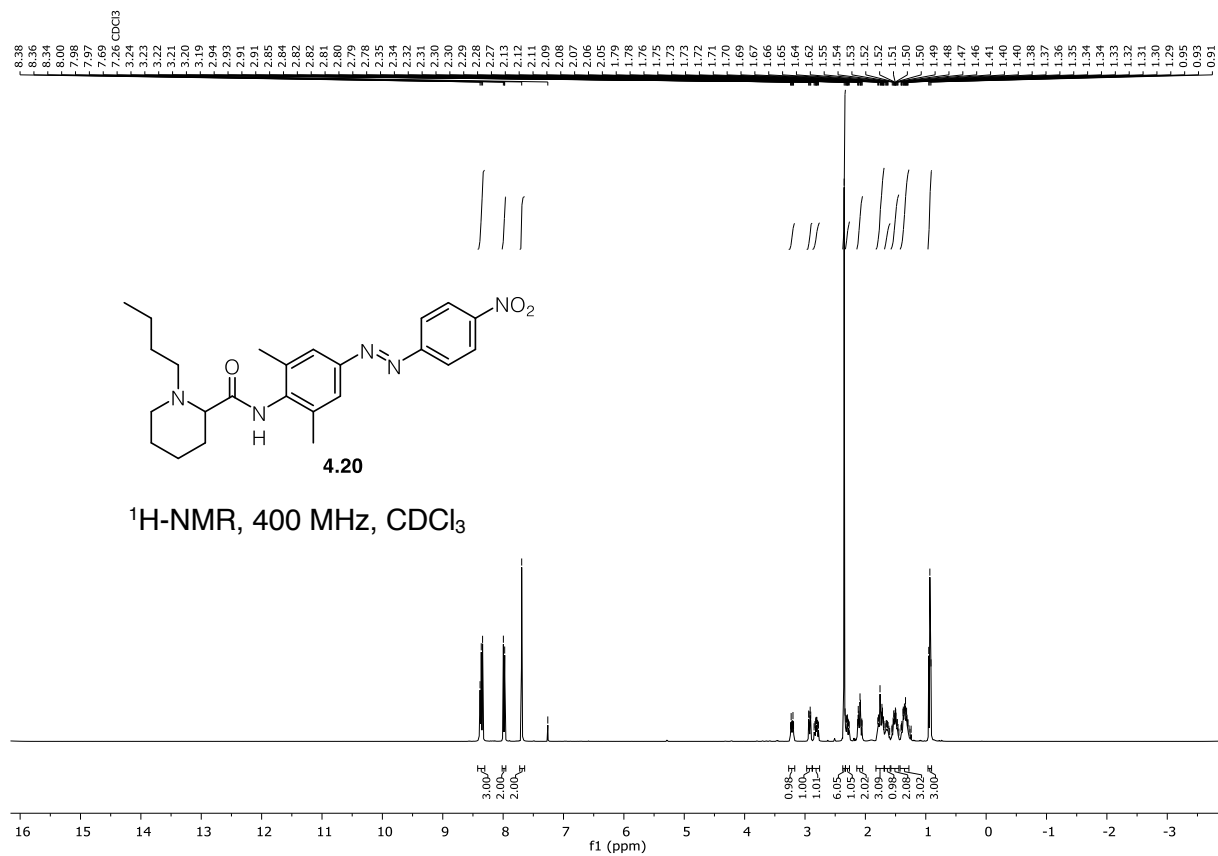


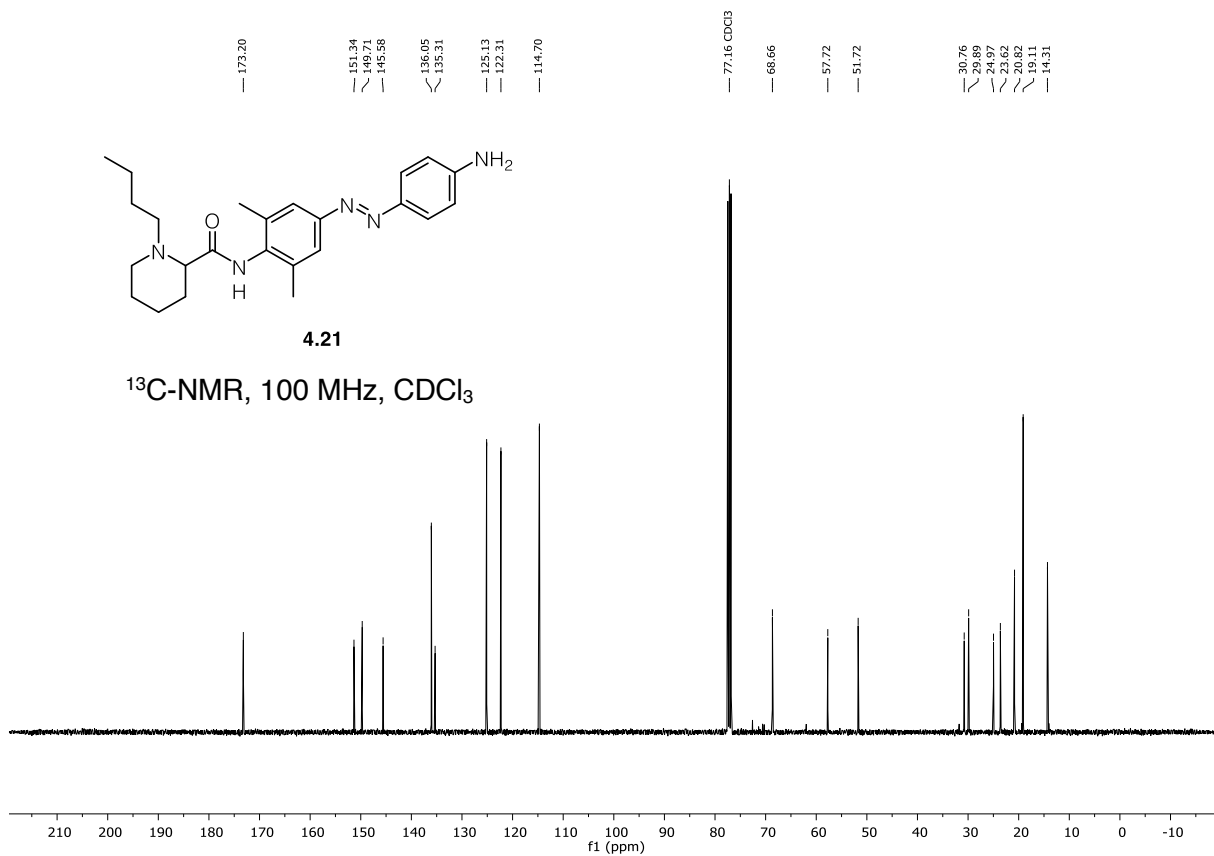
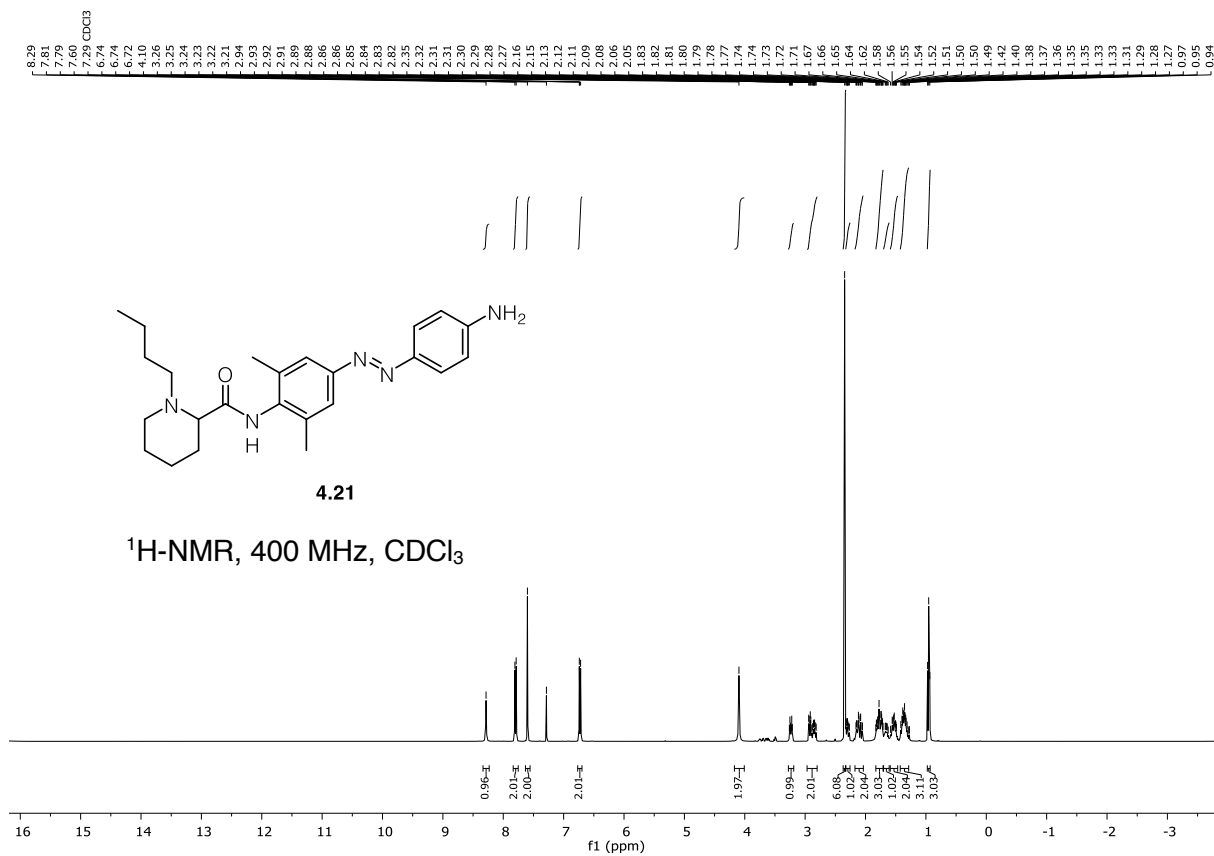


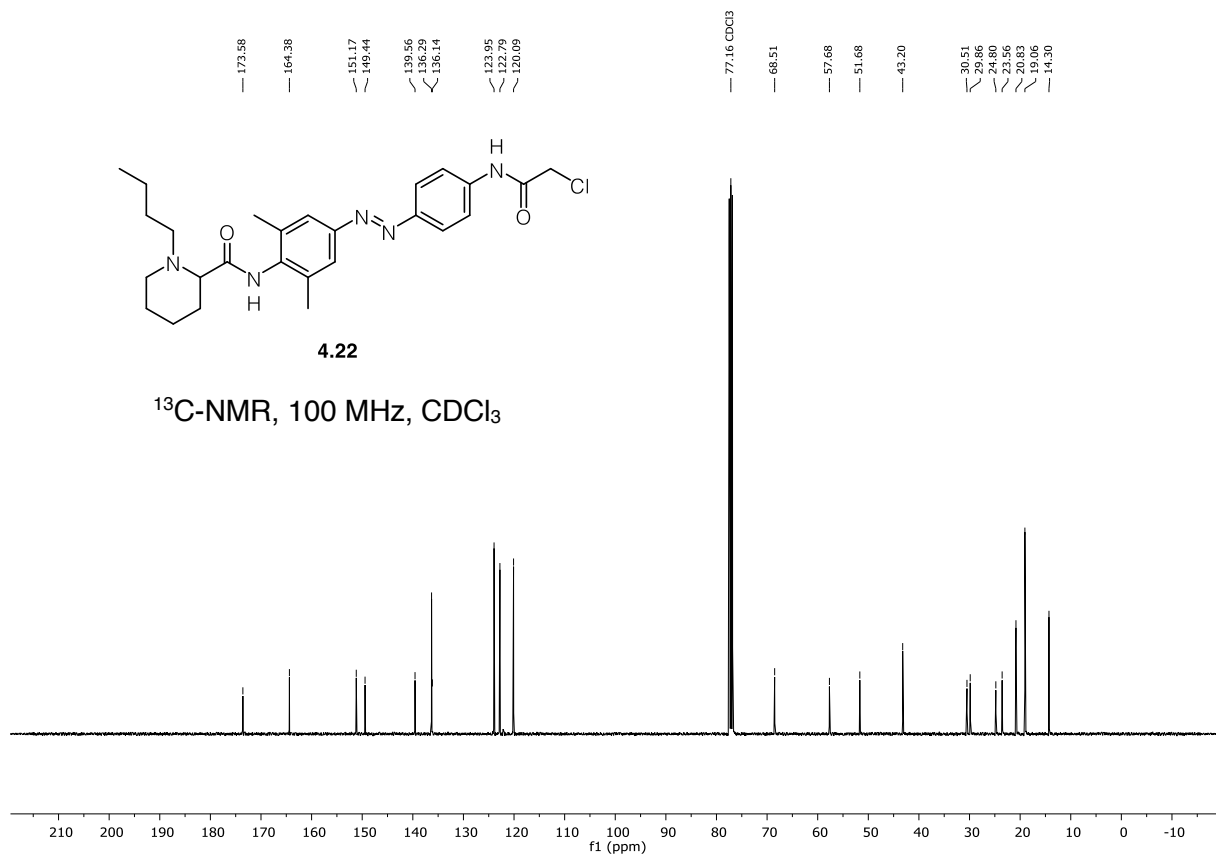
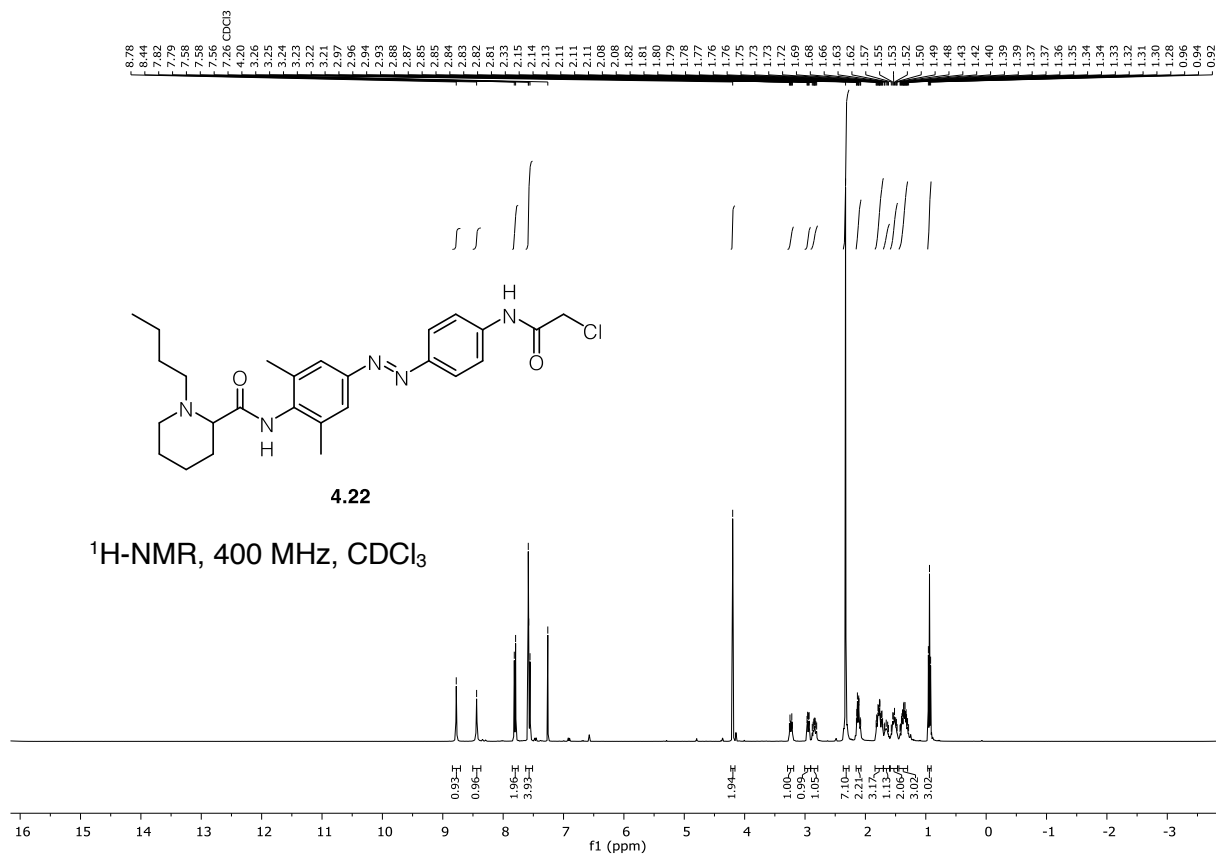


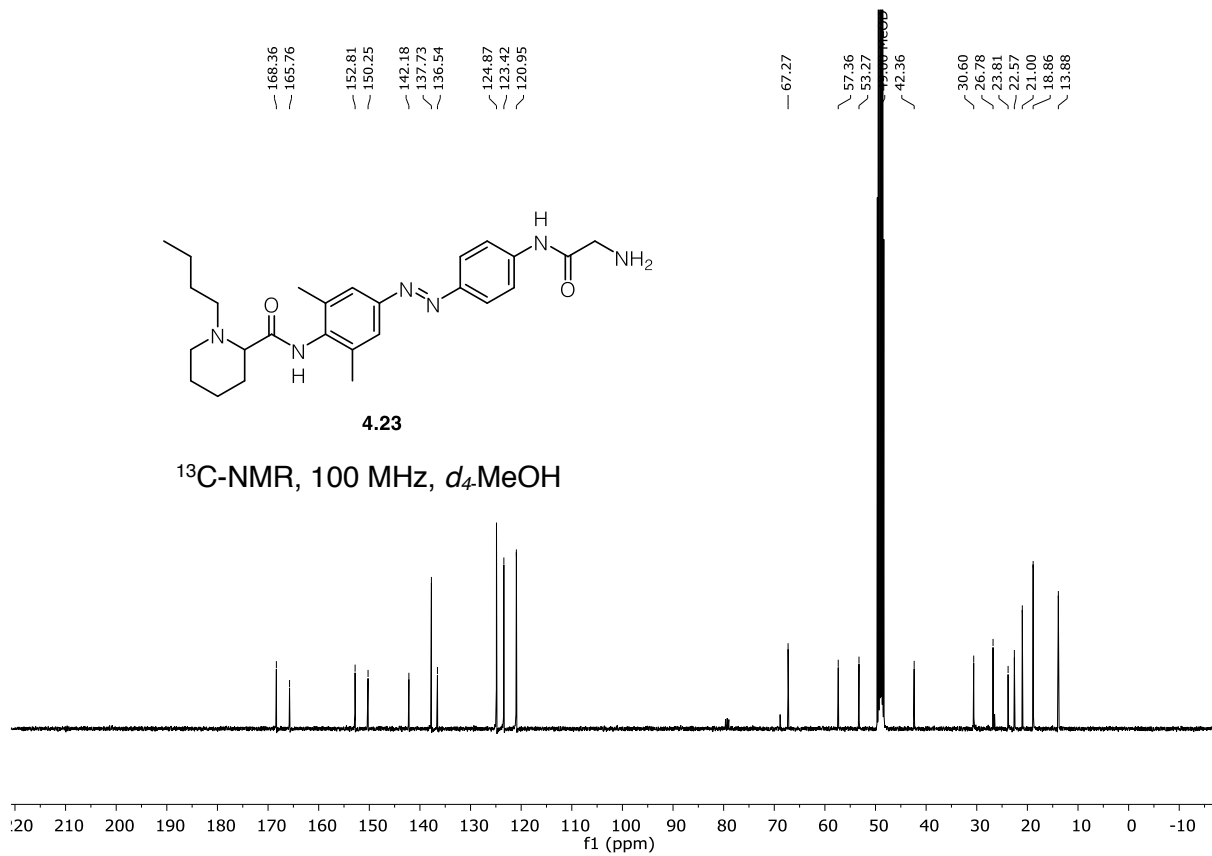
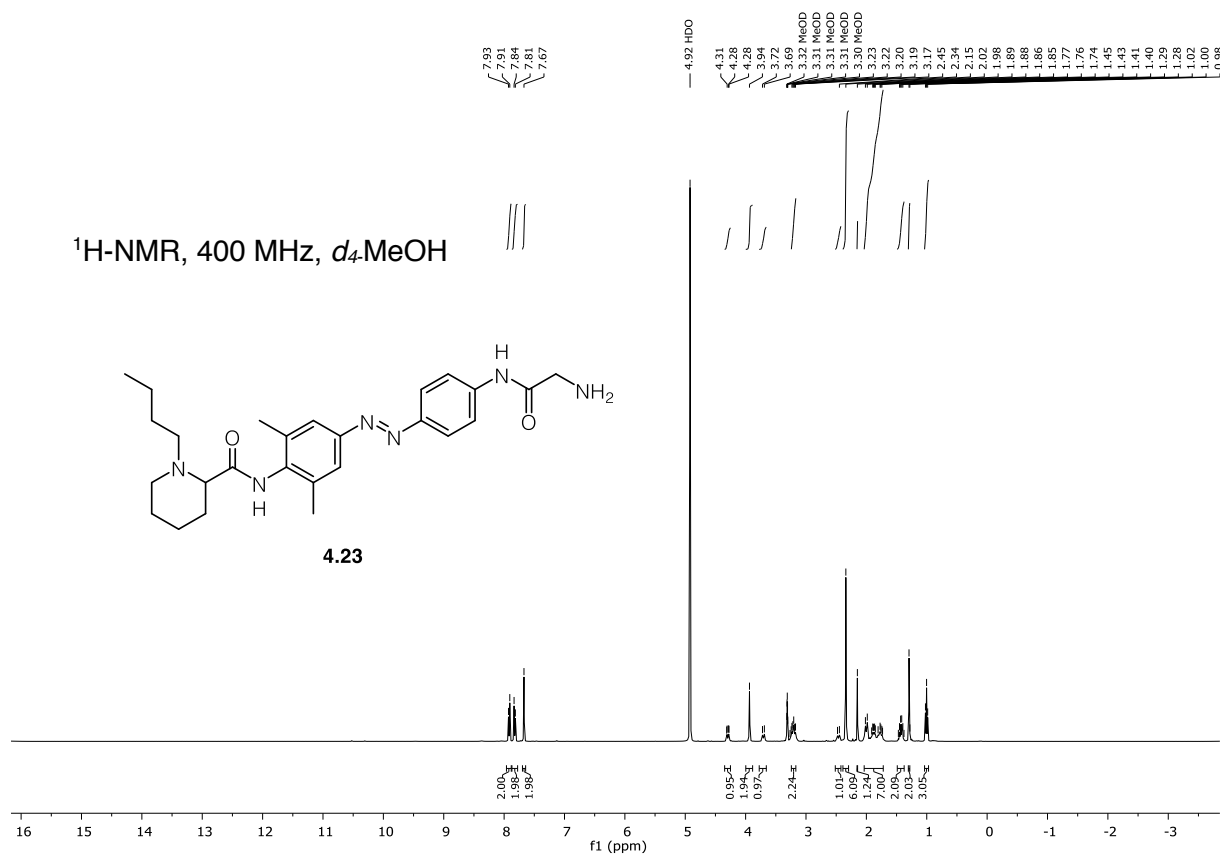


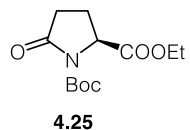




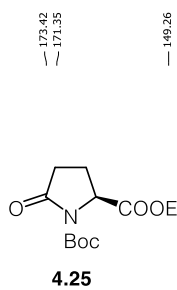
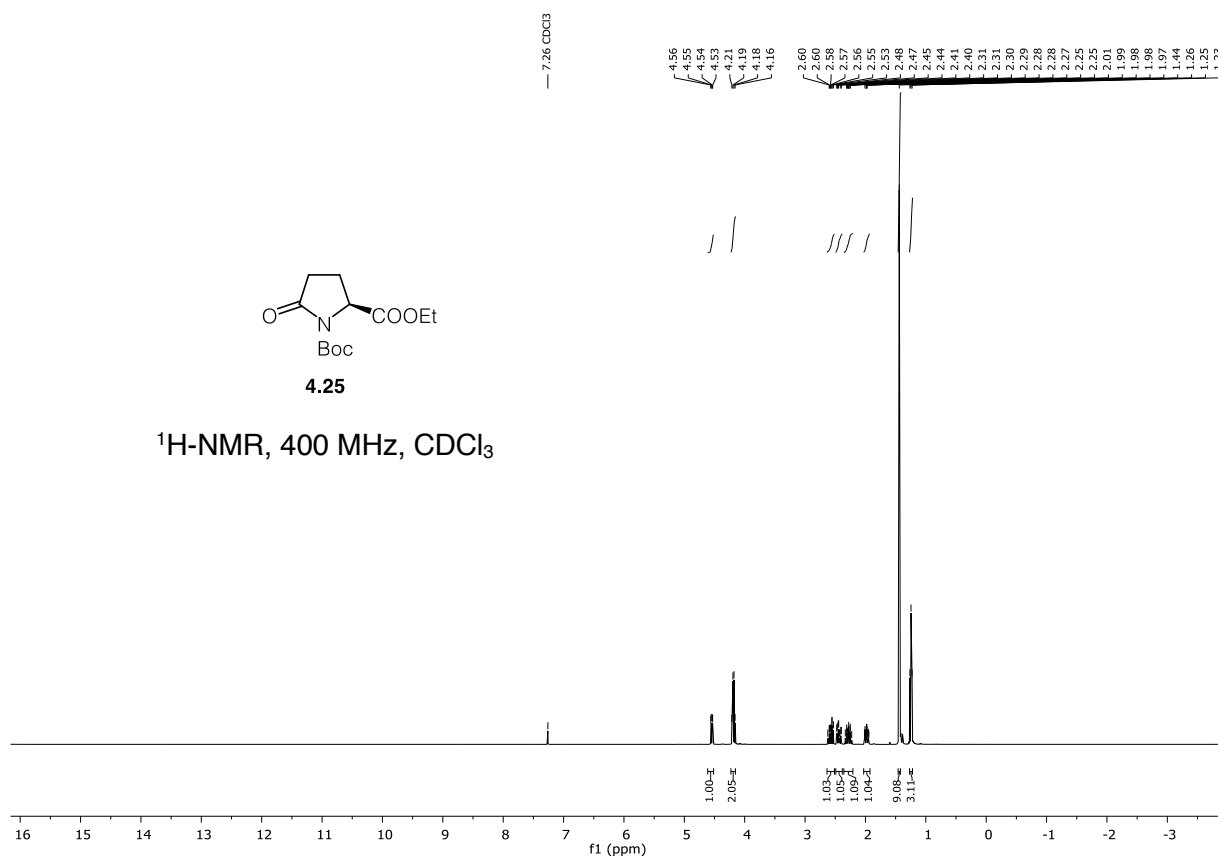




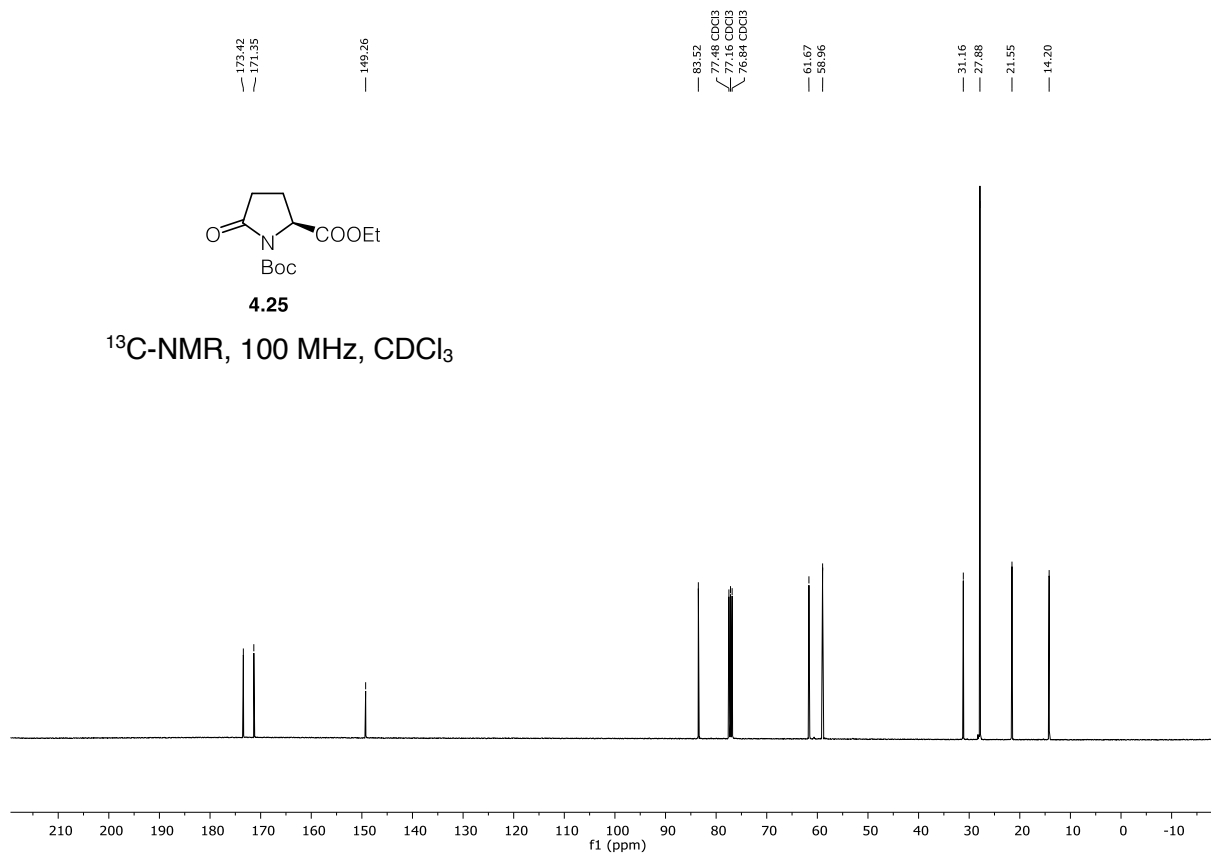


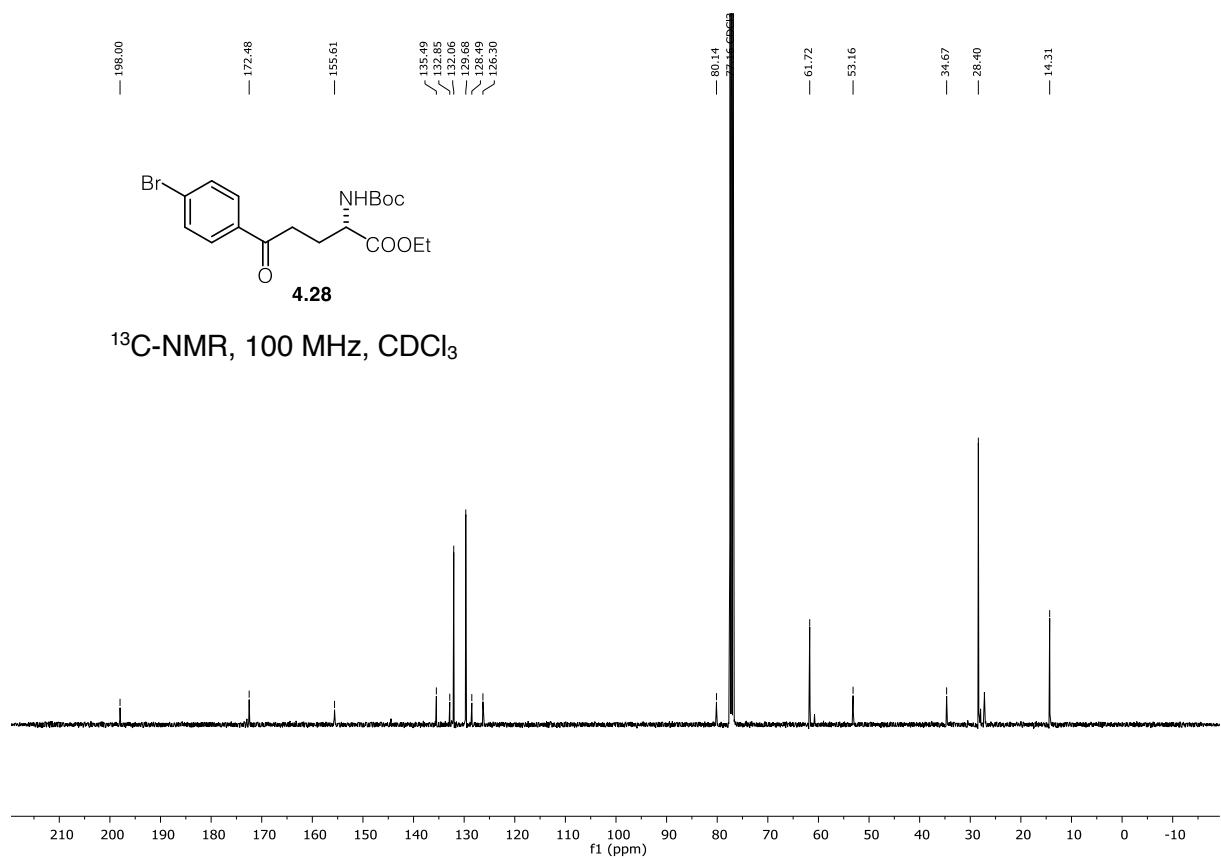
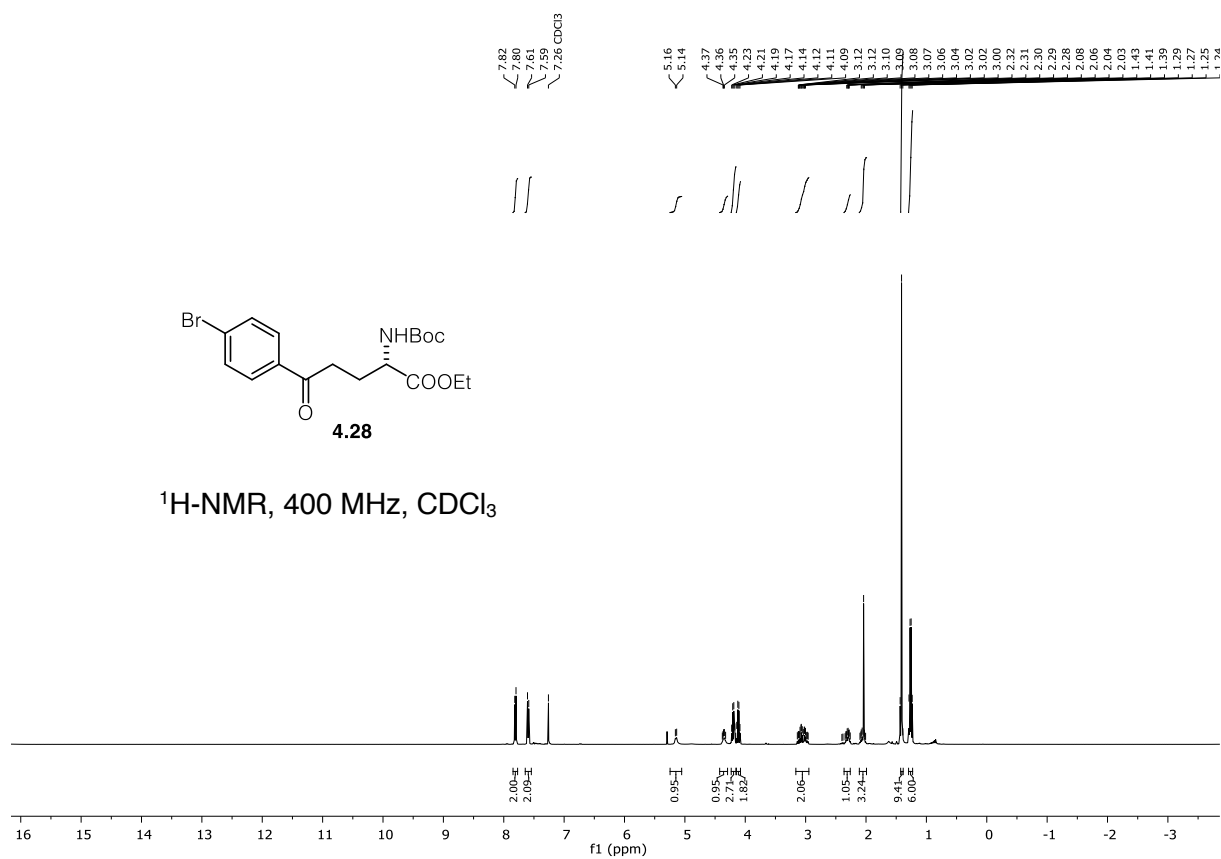


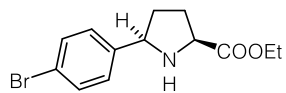
$^1\text{H-NMR}$, 400 MHz, CDCl_3



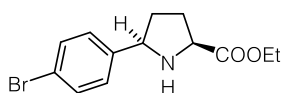
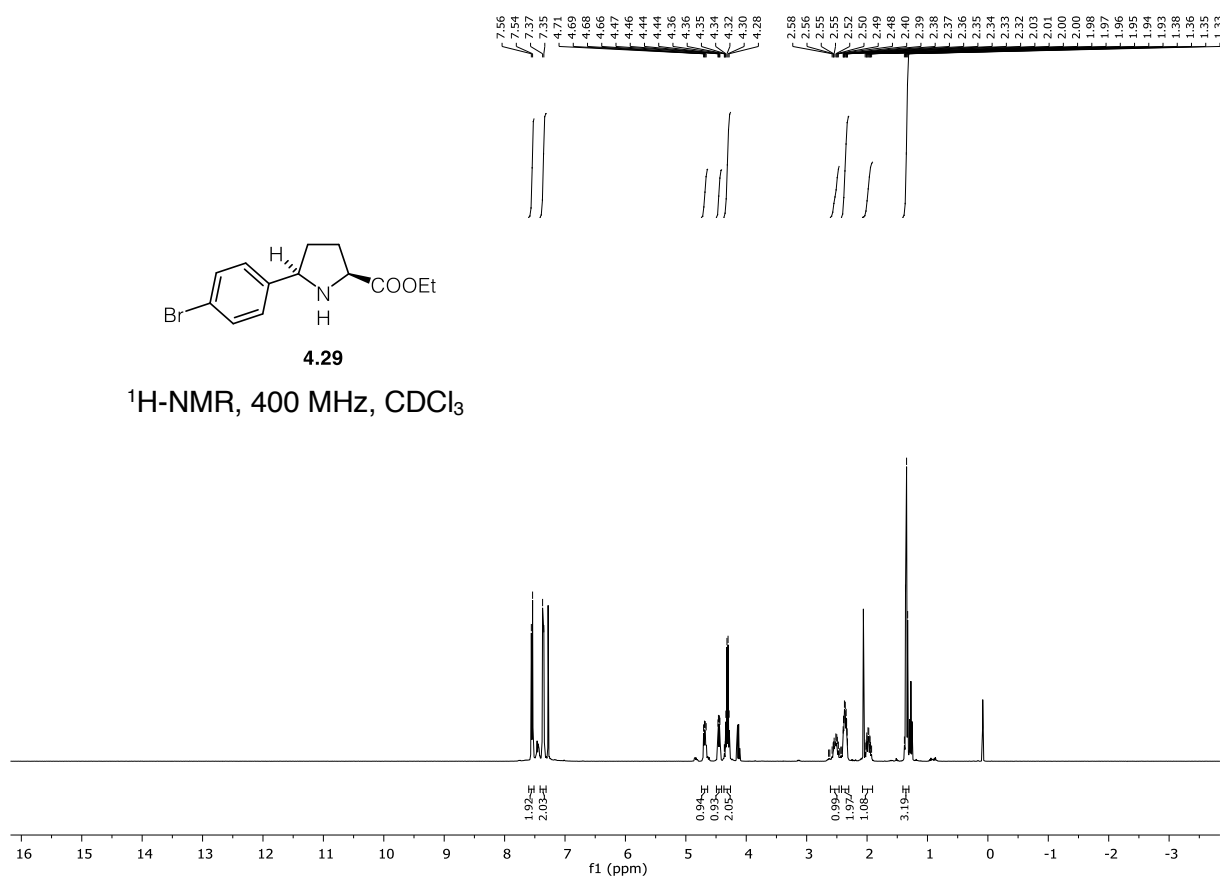
$^{13}\text{C-NMR}$, 100 MHz, CDCl_3



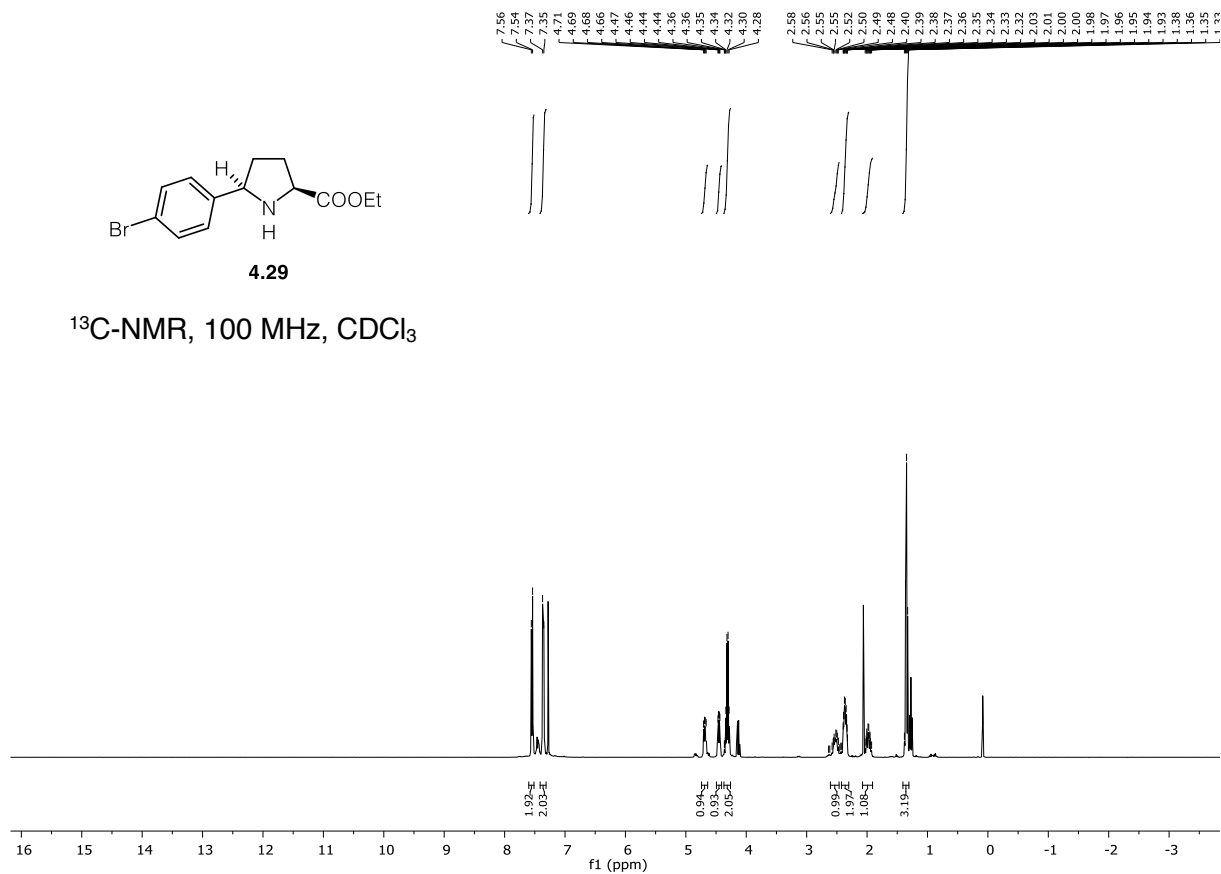


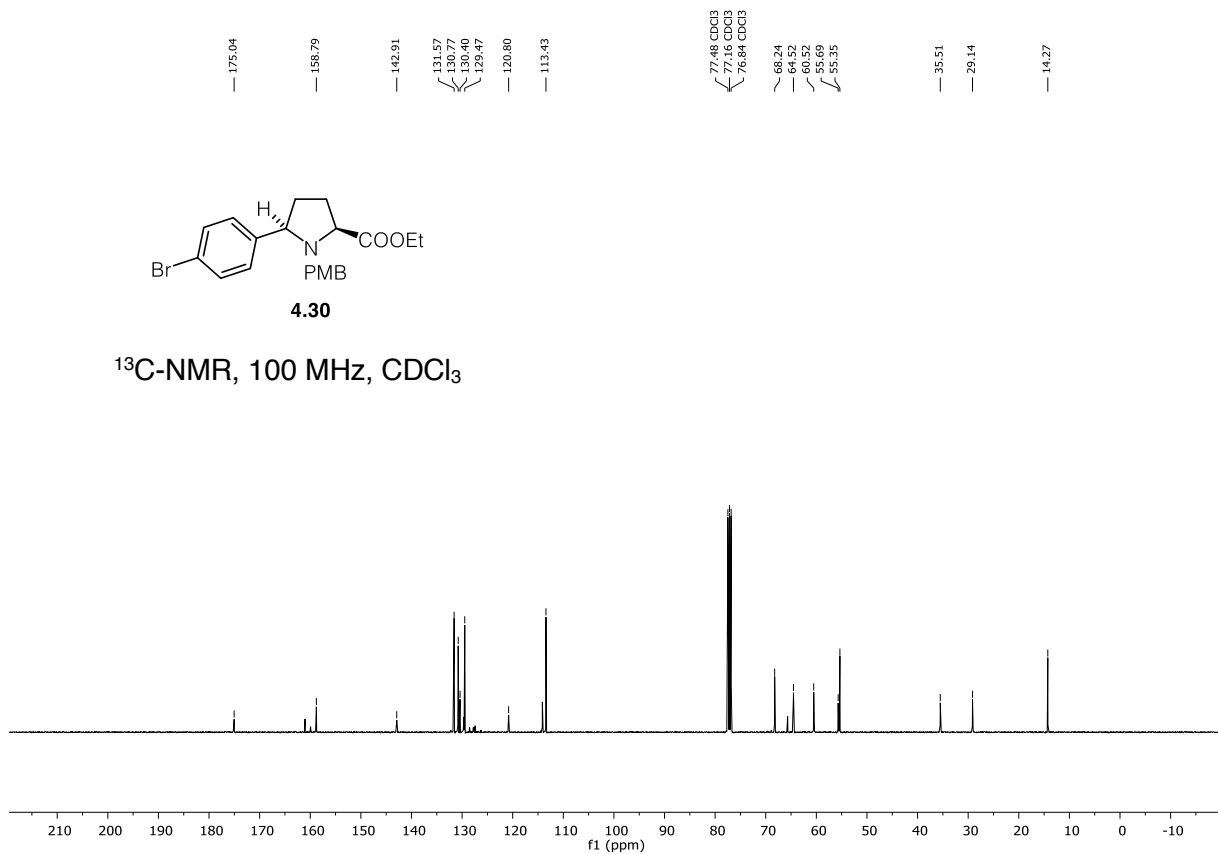
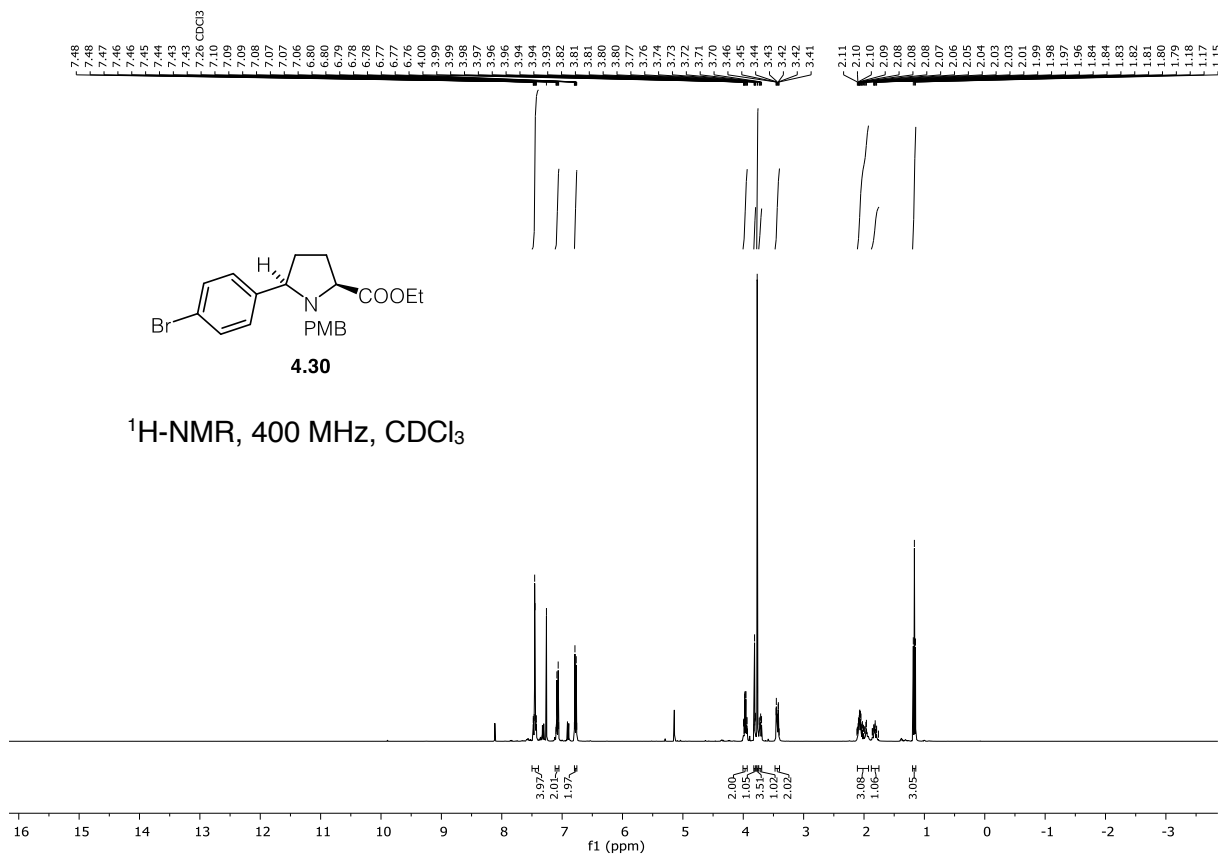


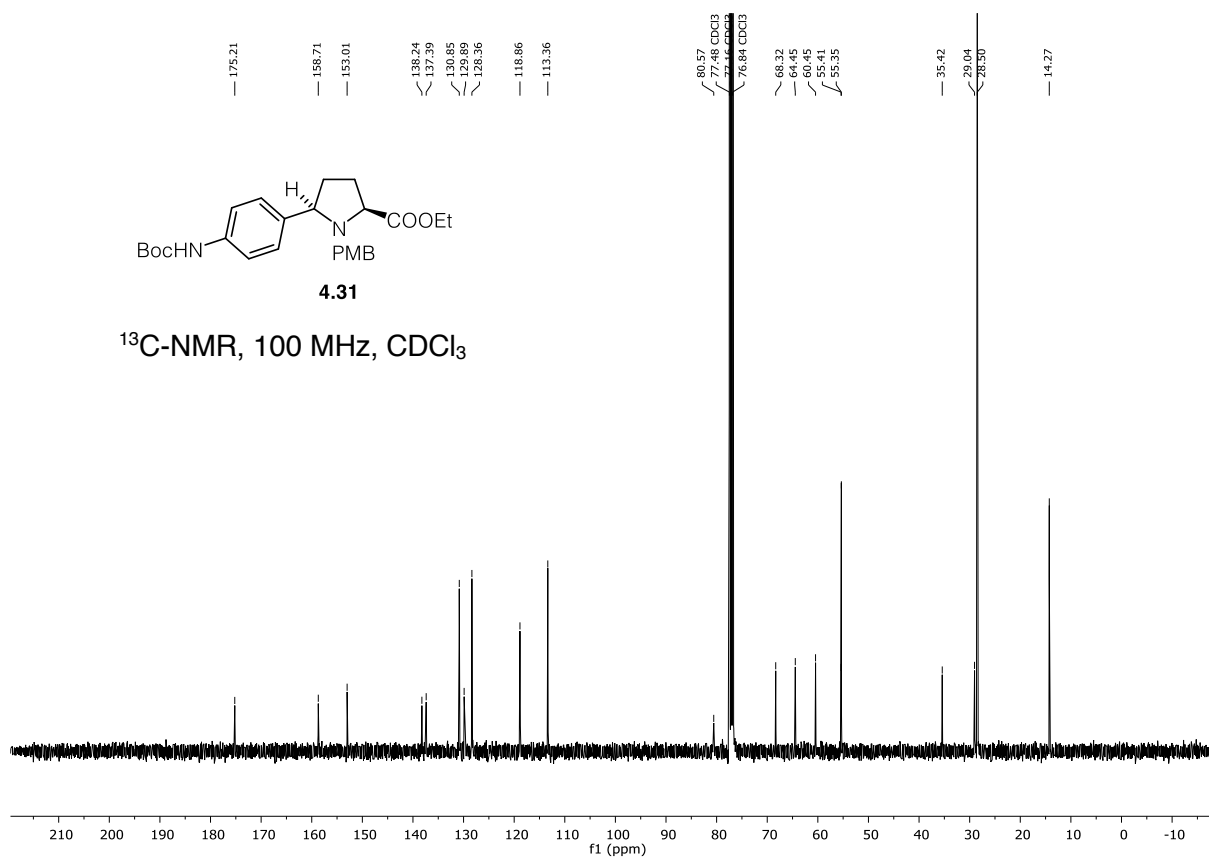
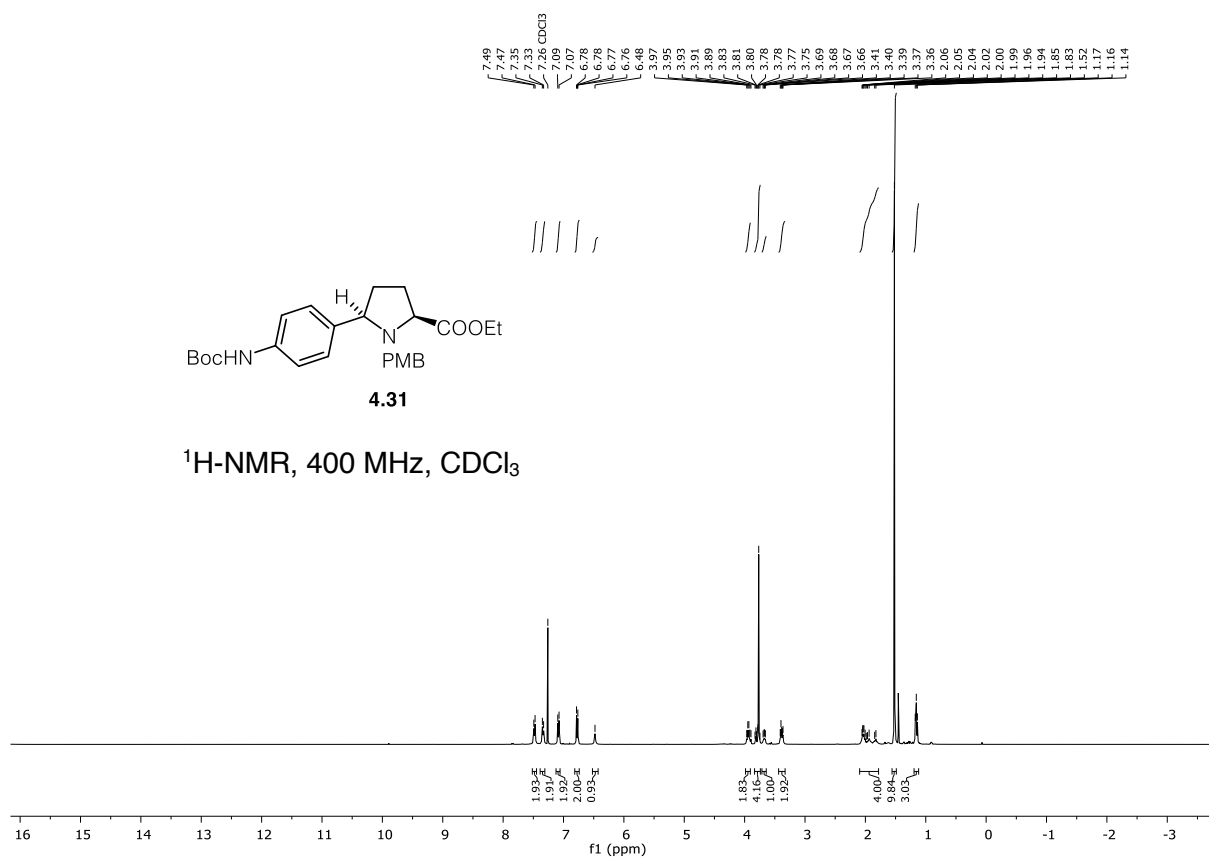
4.29

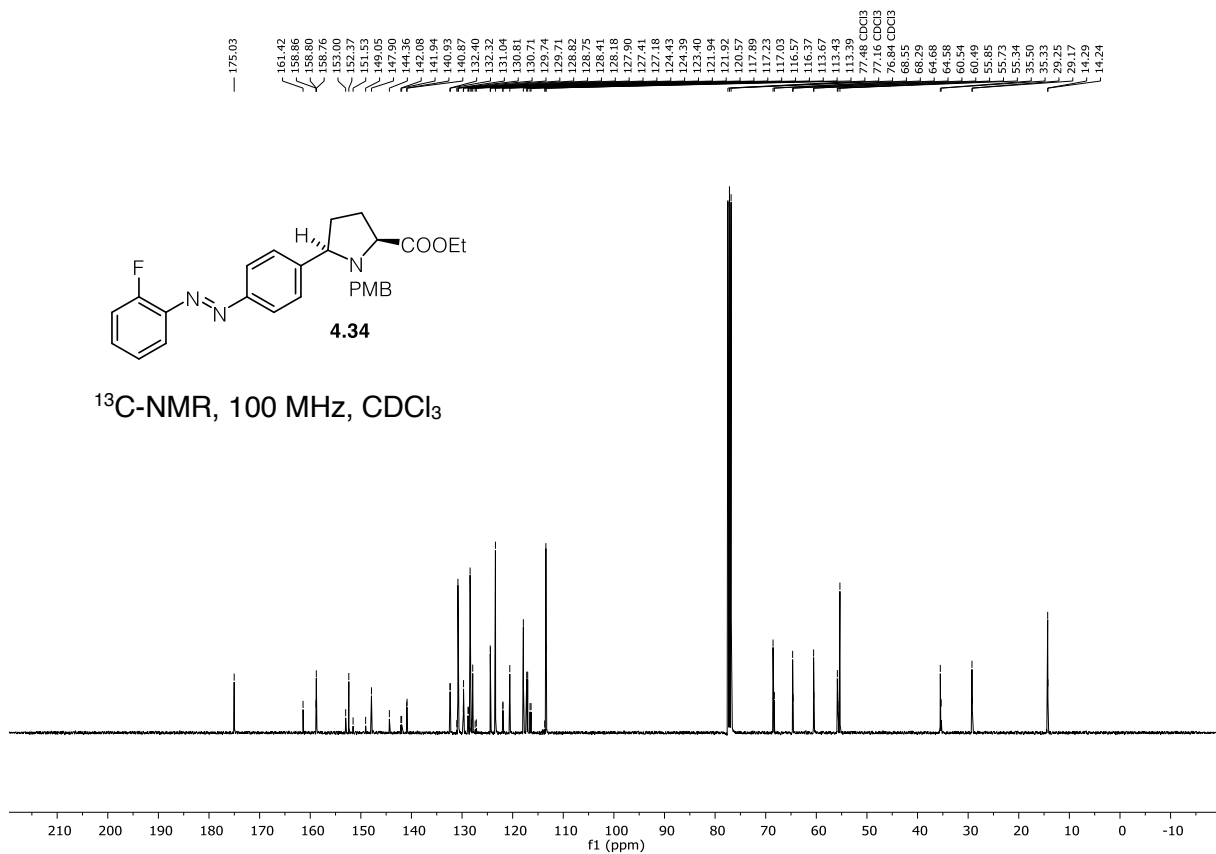
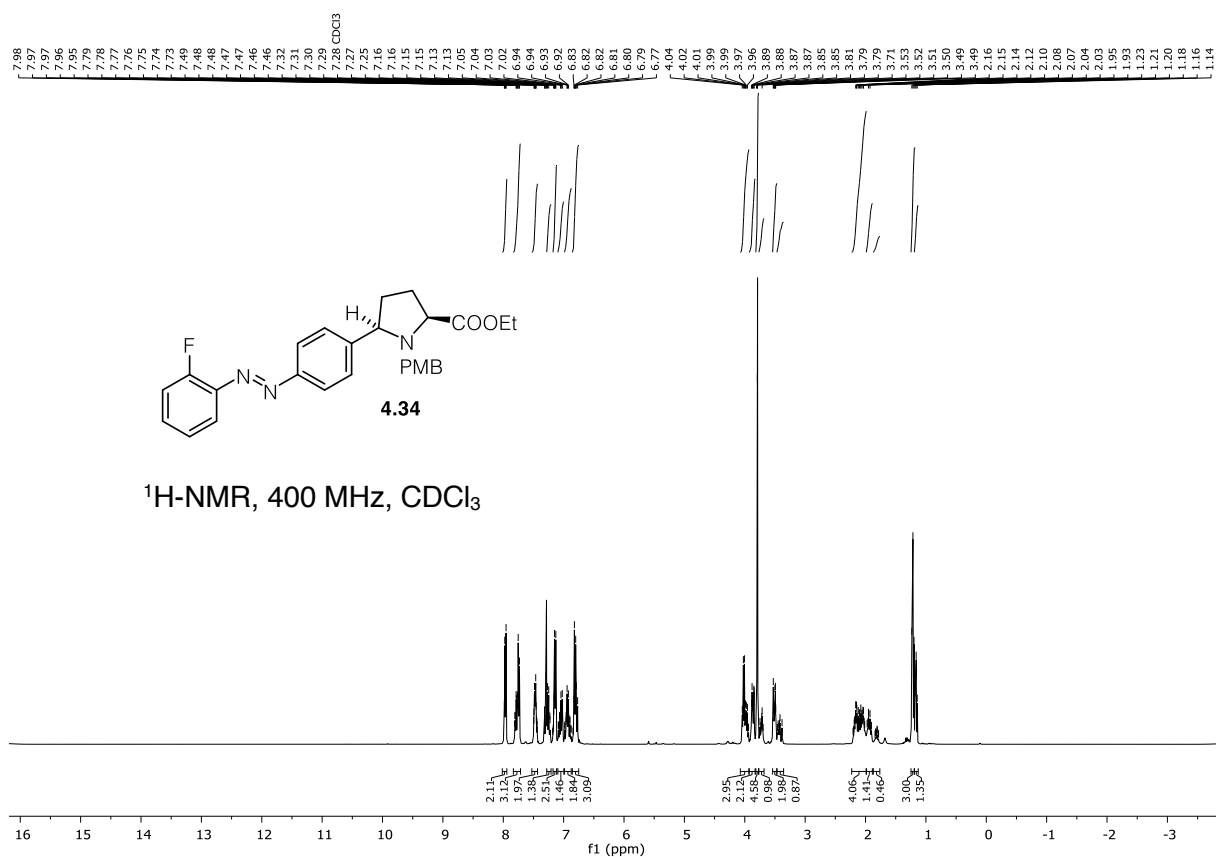
 $^1\text{H-NMR}$, 400 MHz, CDCl_3 

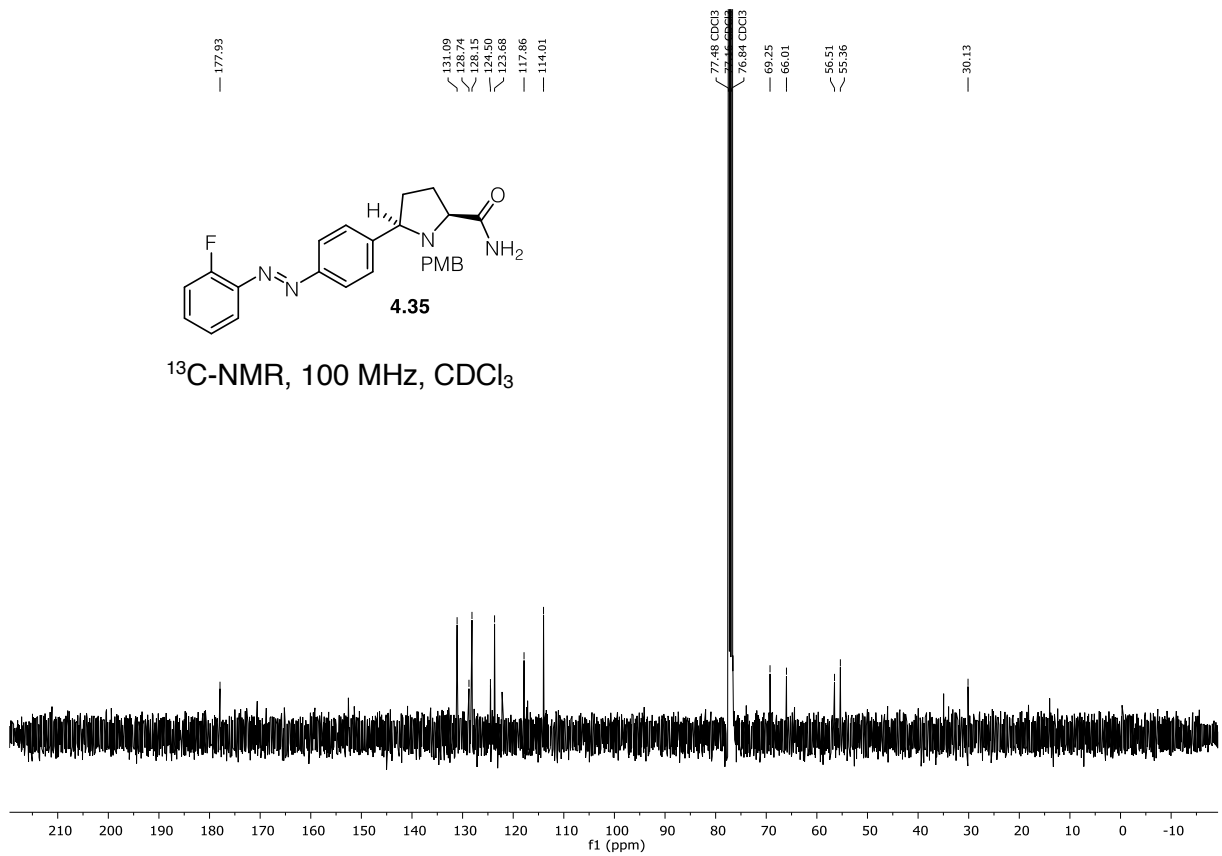
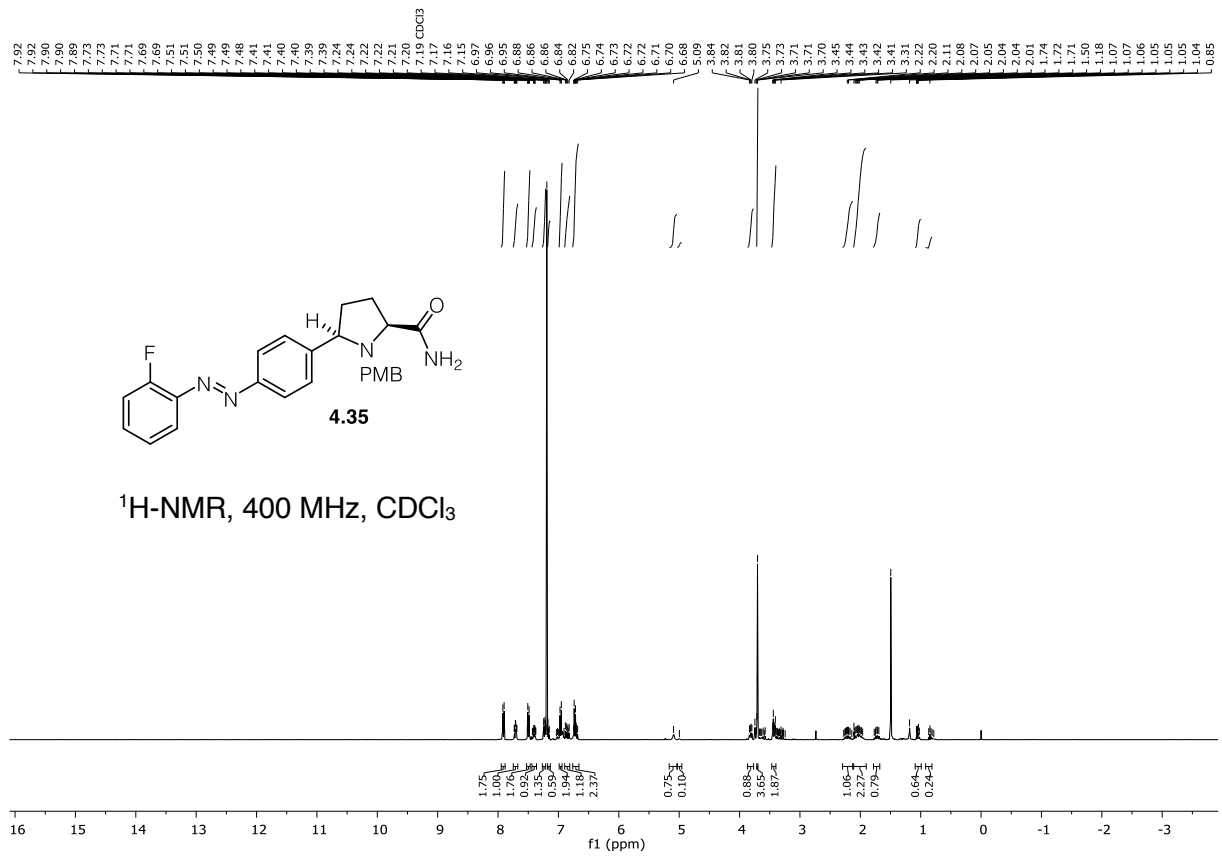
4.29

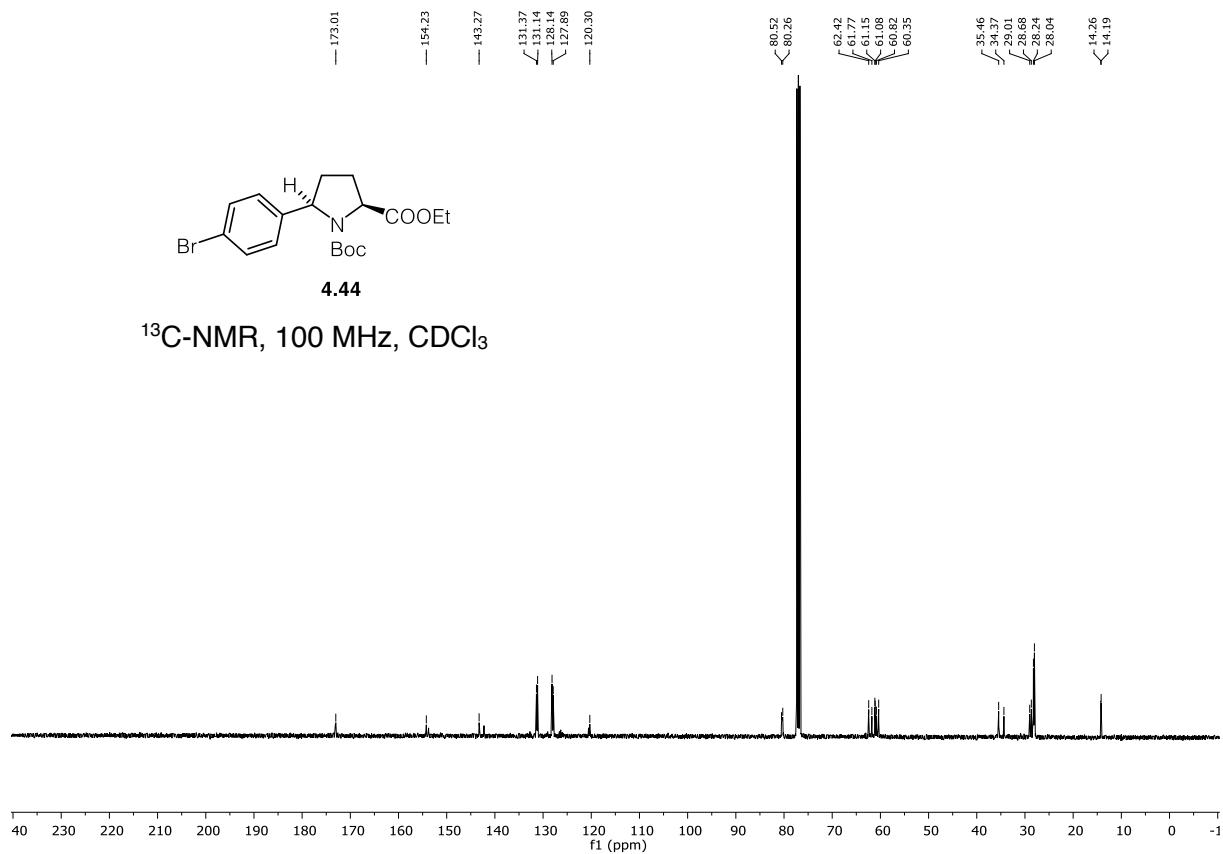
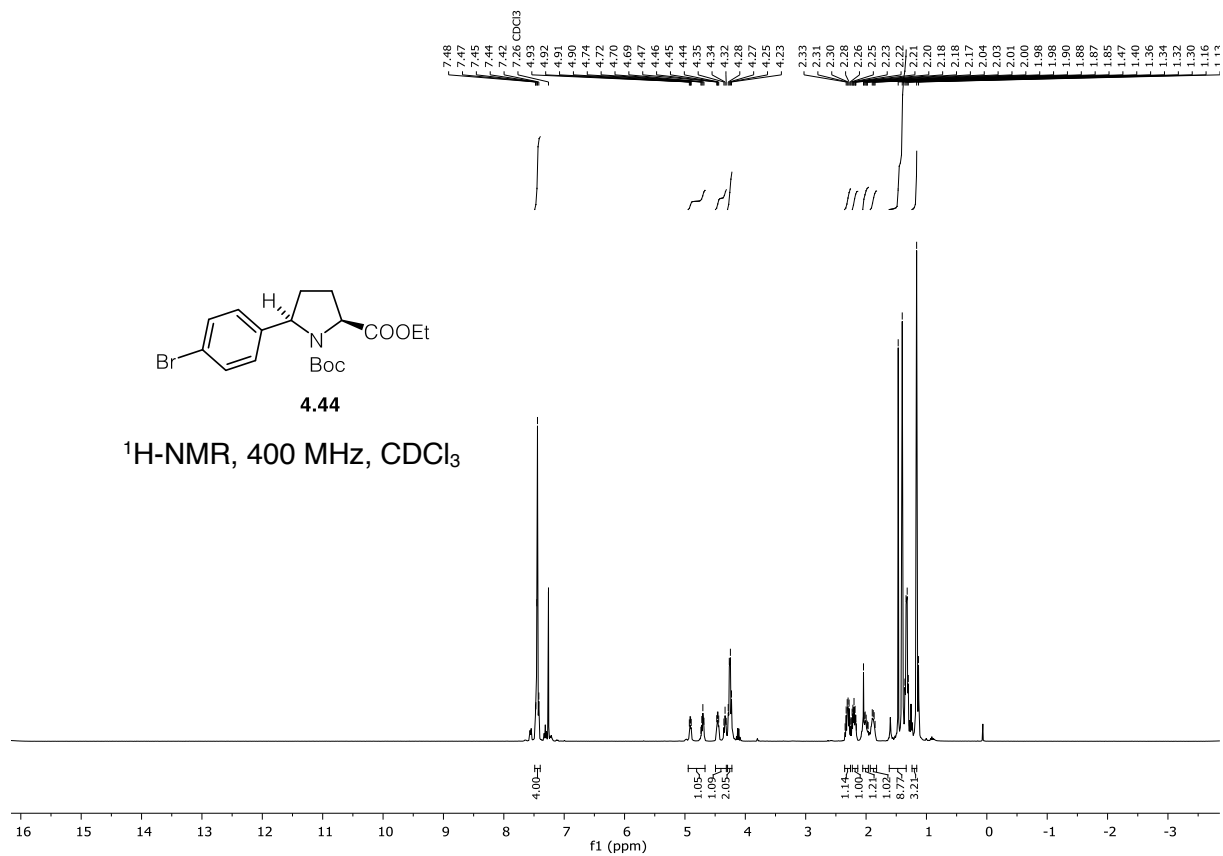
 $^{13}\text{C-NMR}$, 100 MHz, CDCl_3 

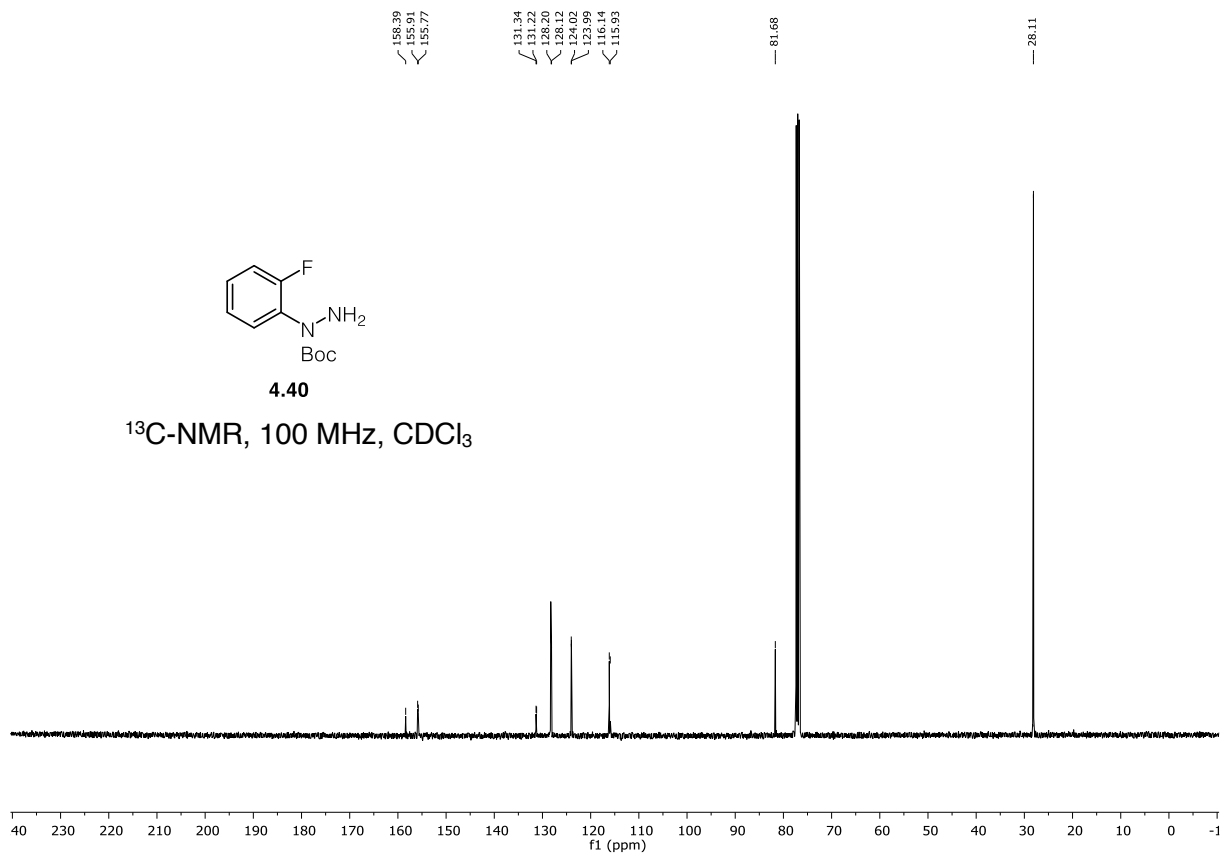
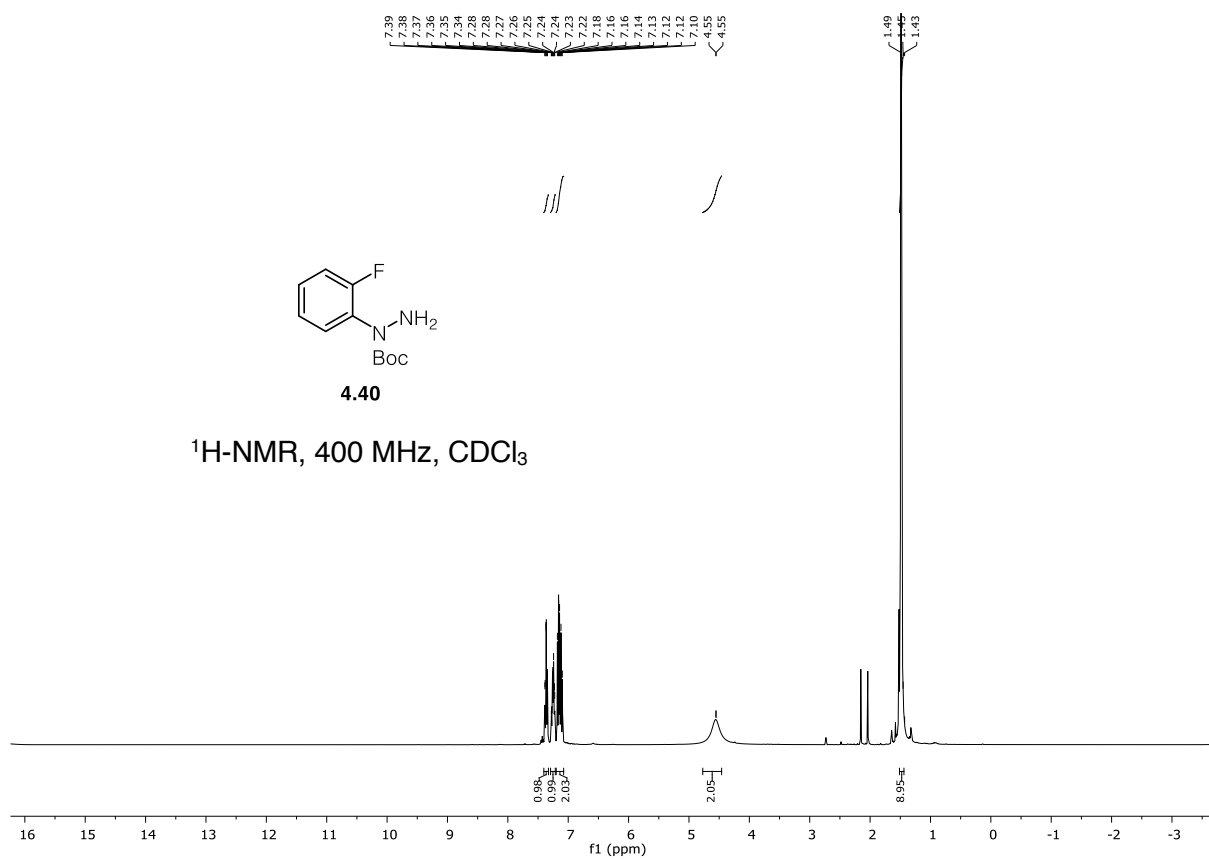


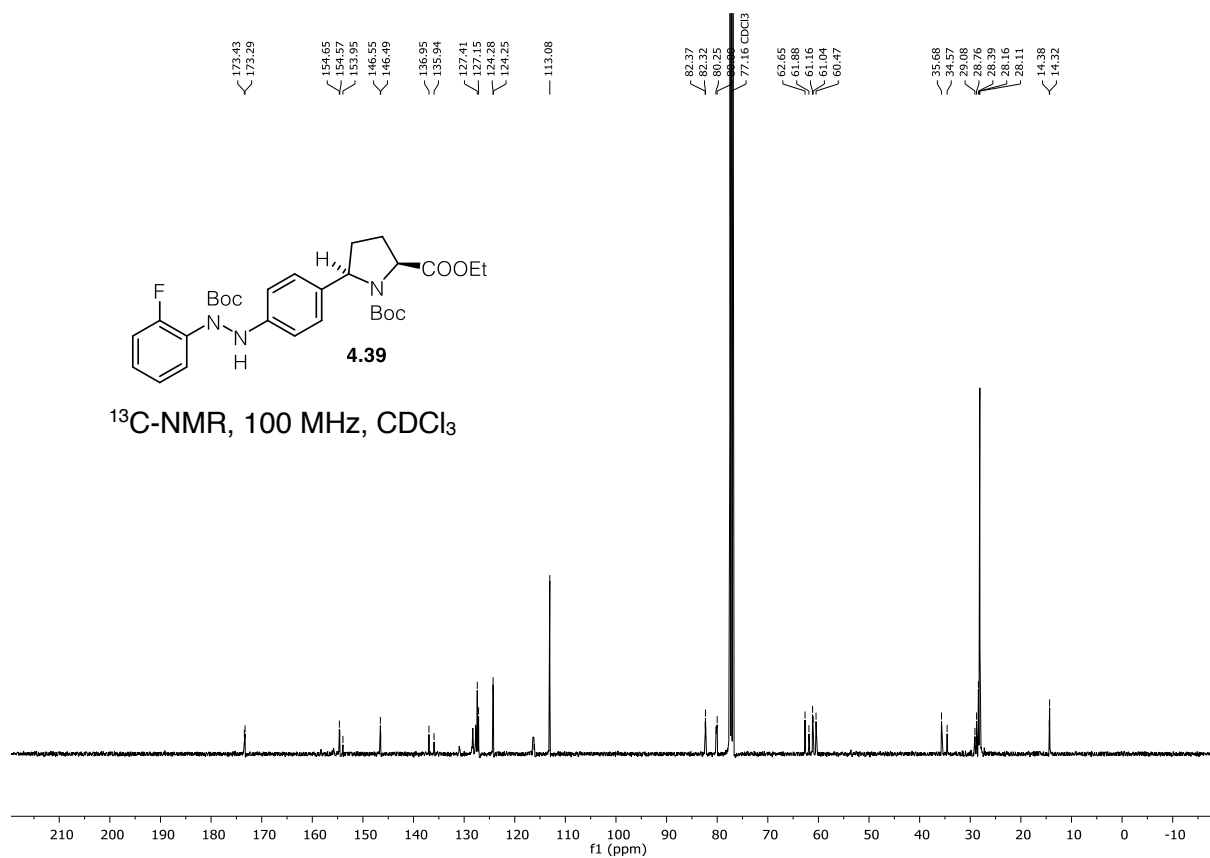
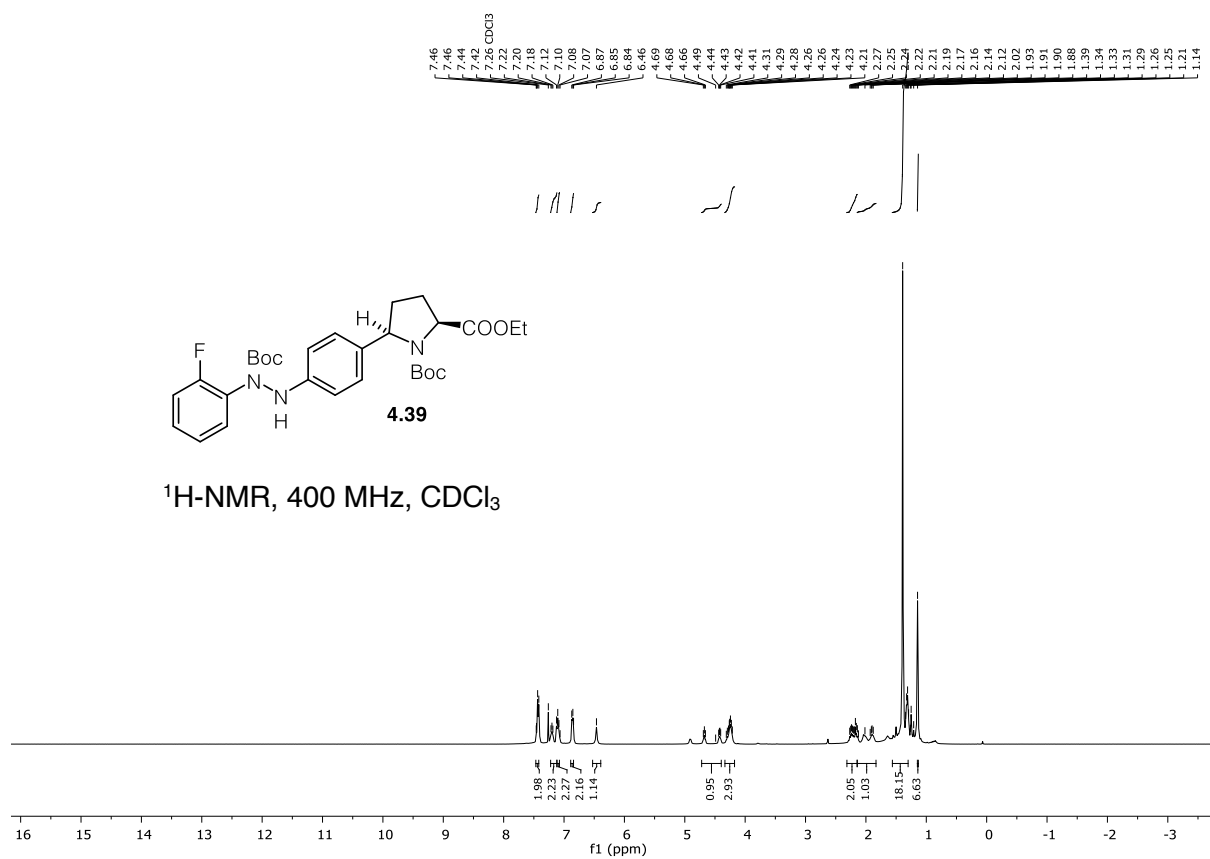


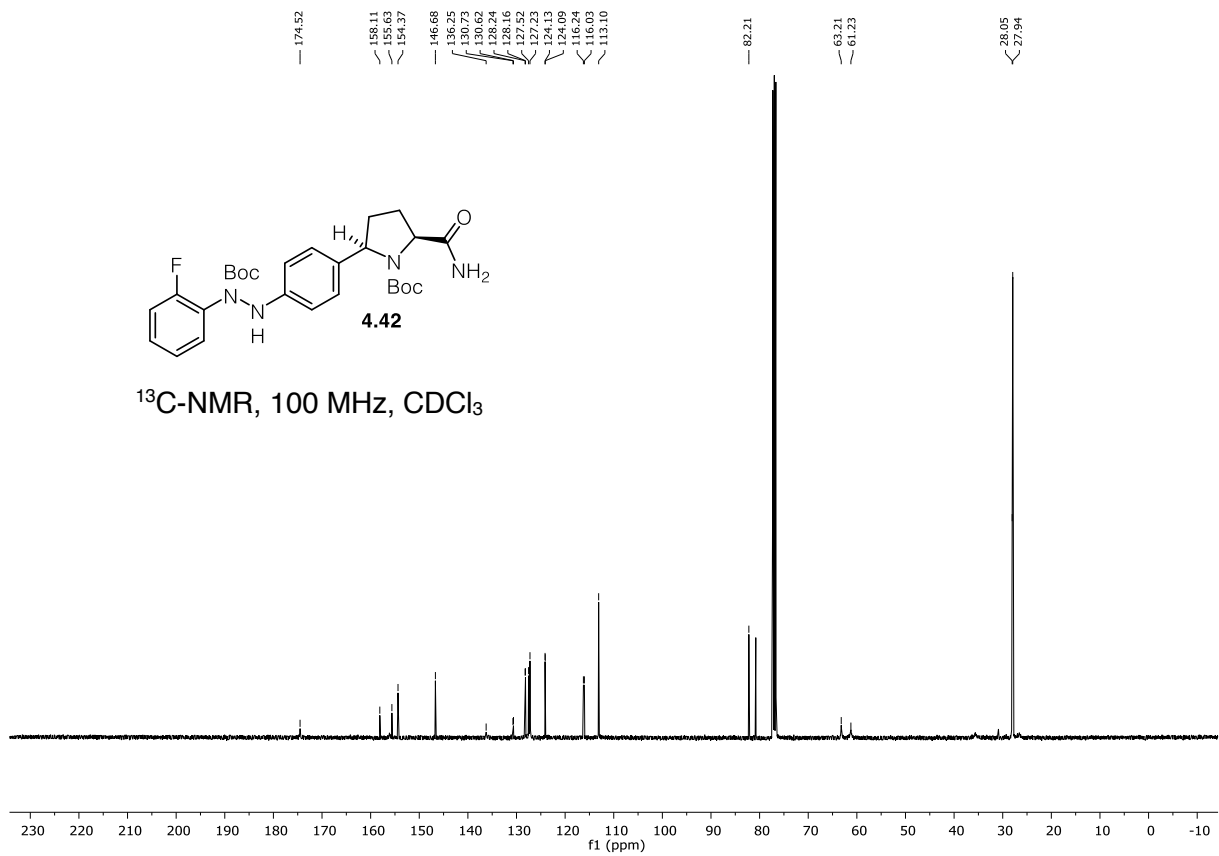
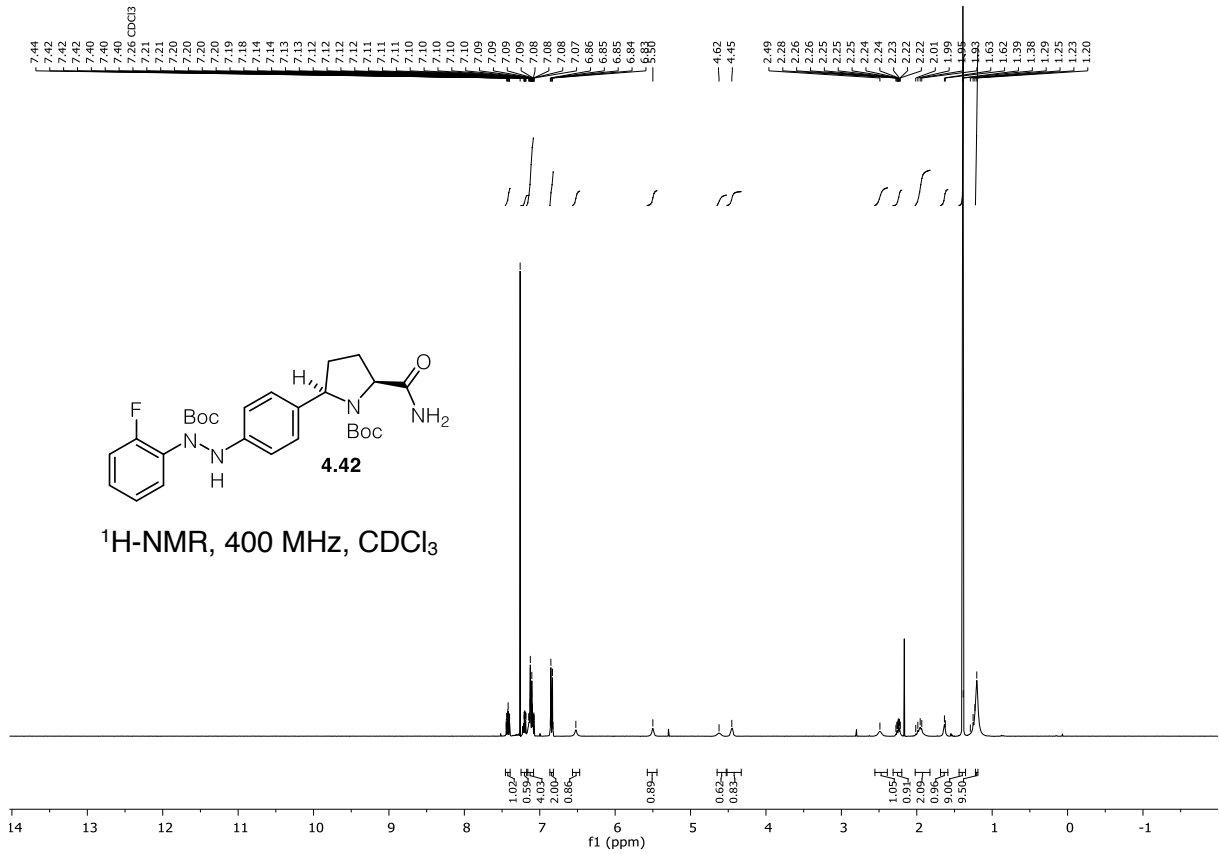


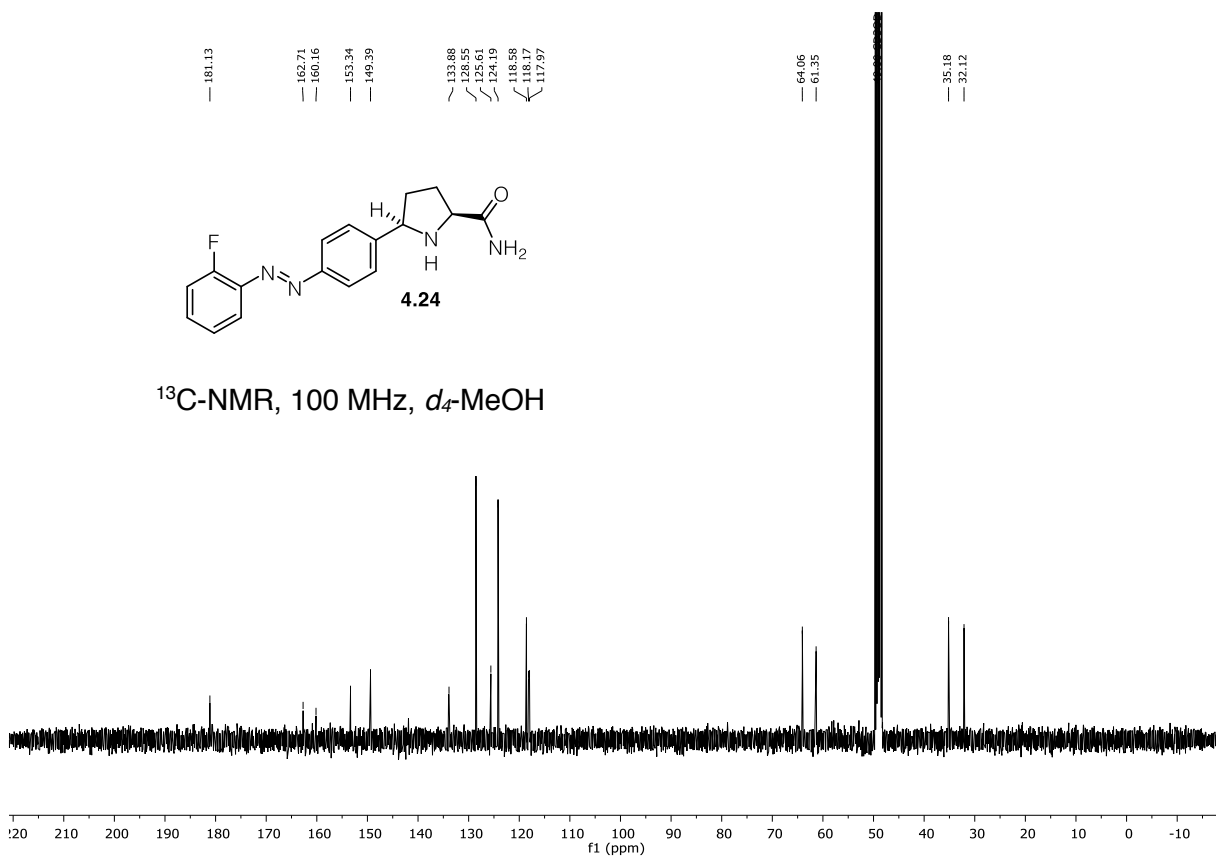
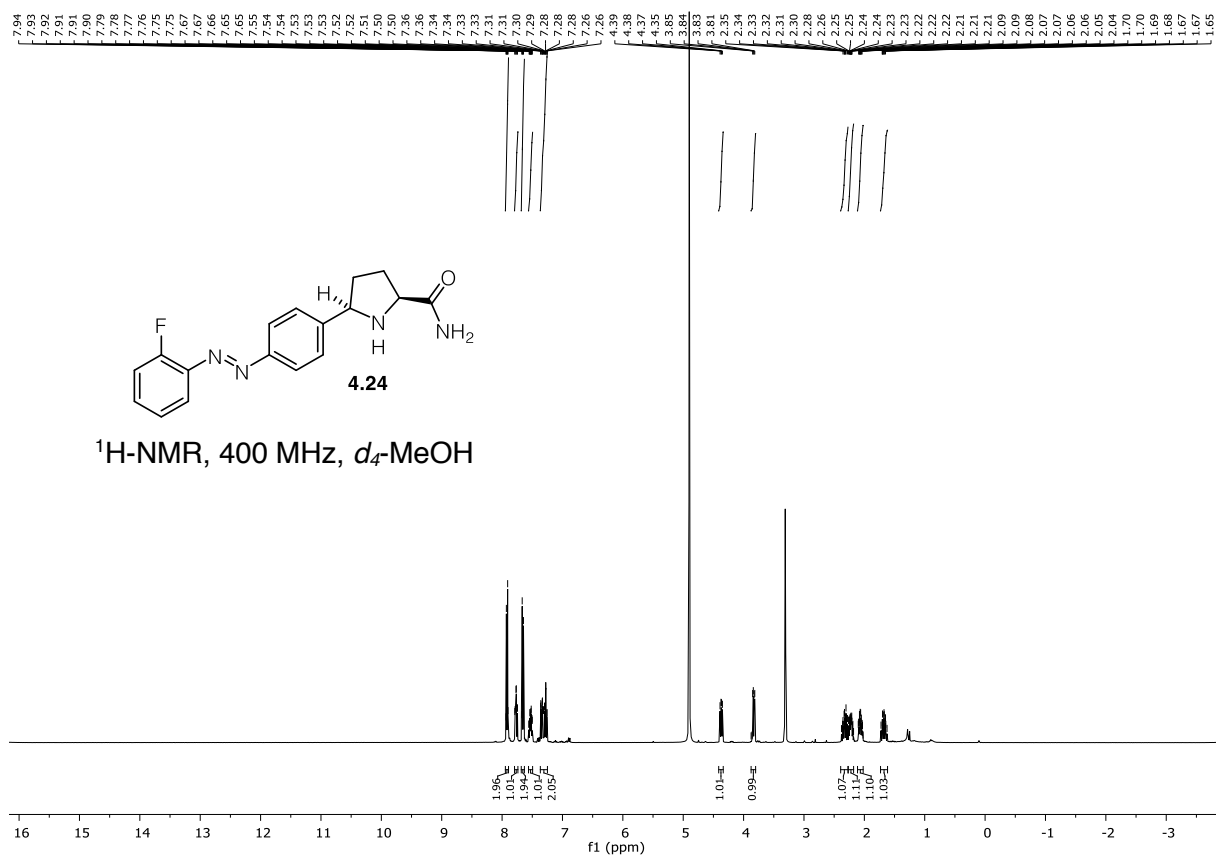


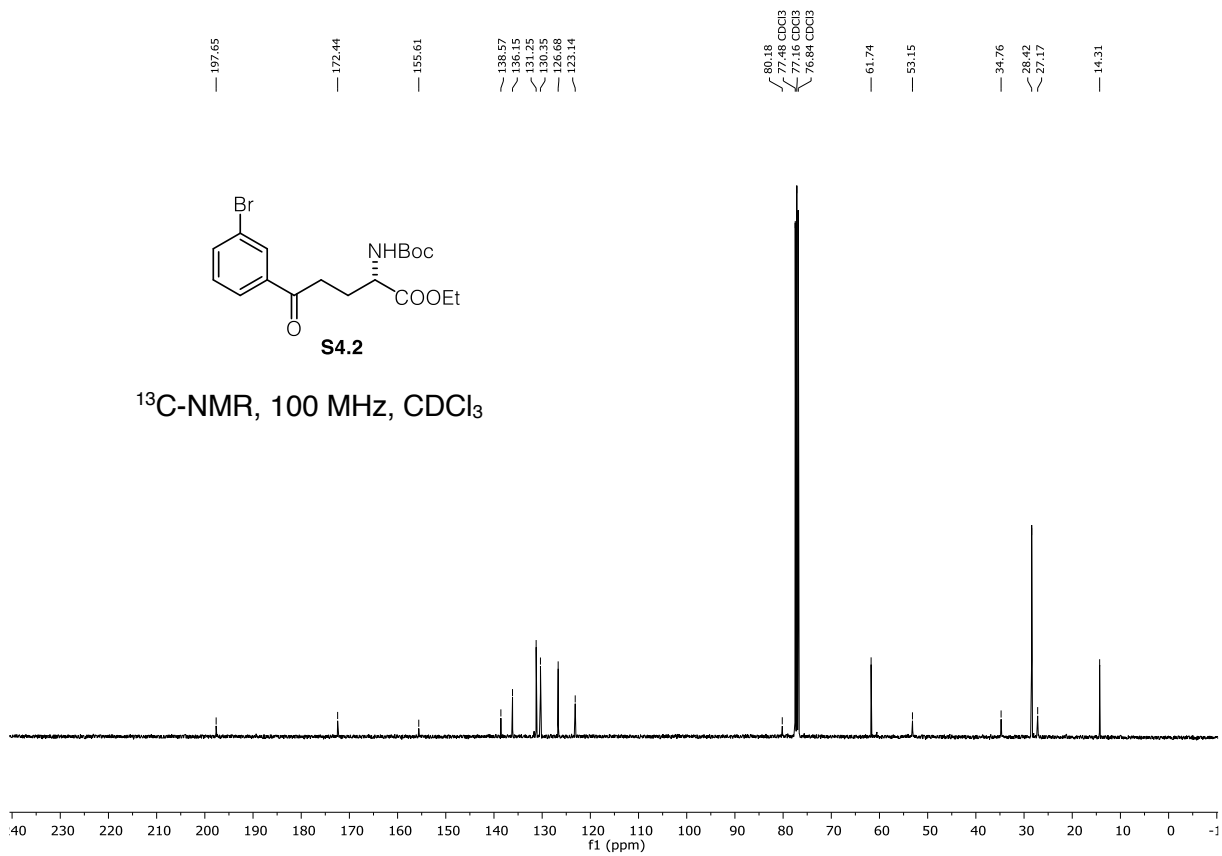
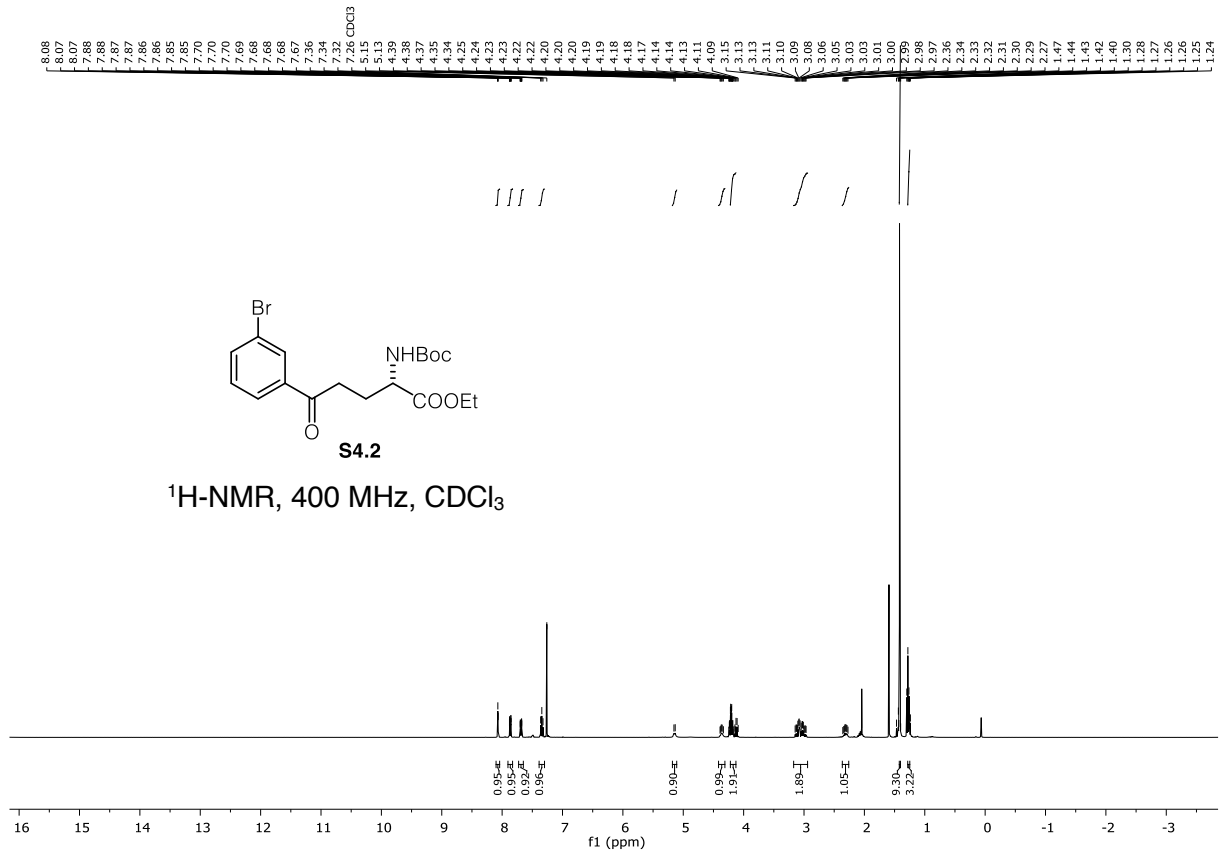


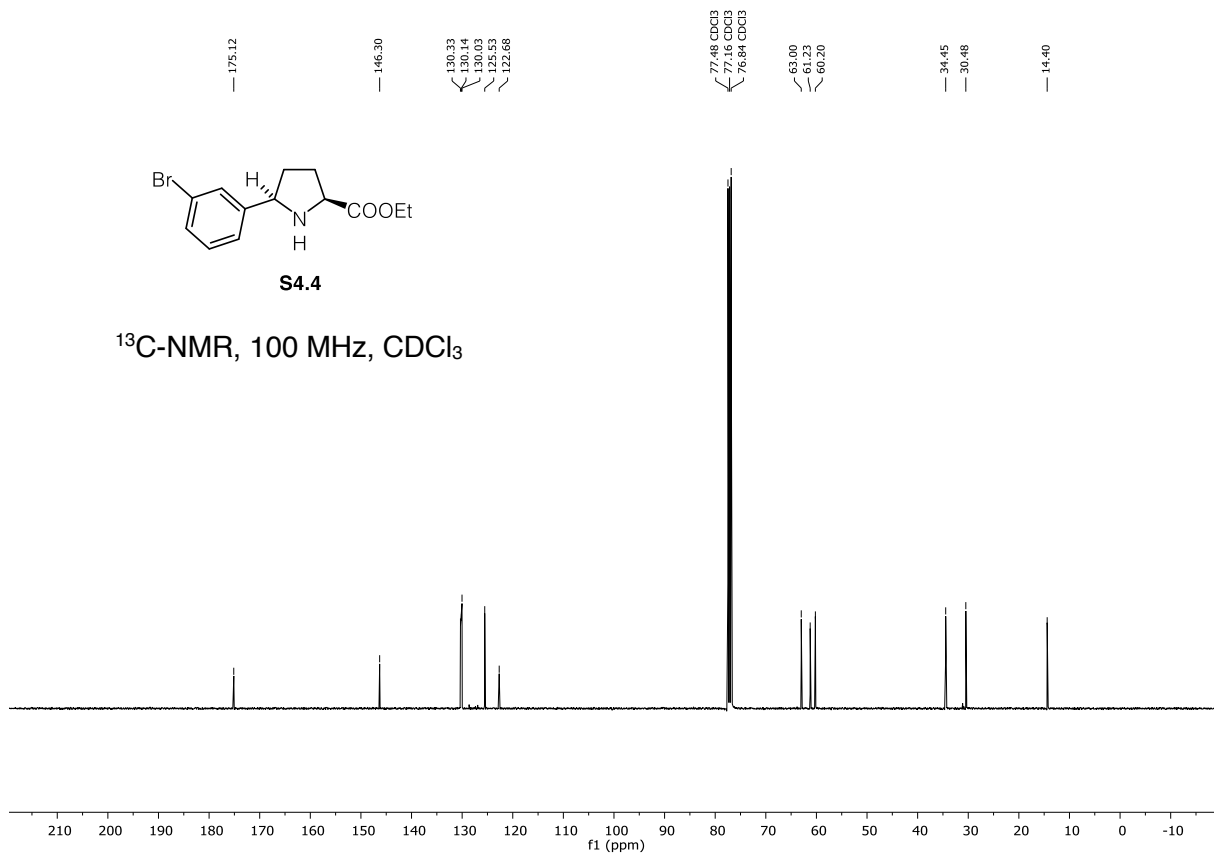
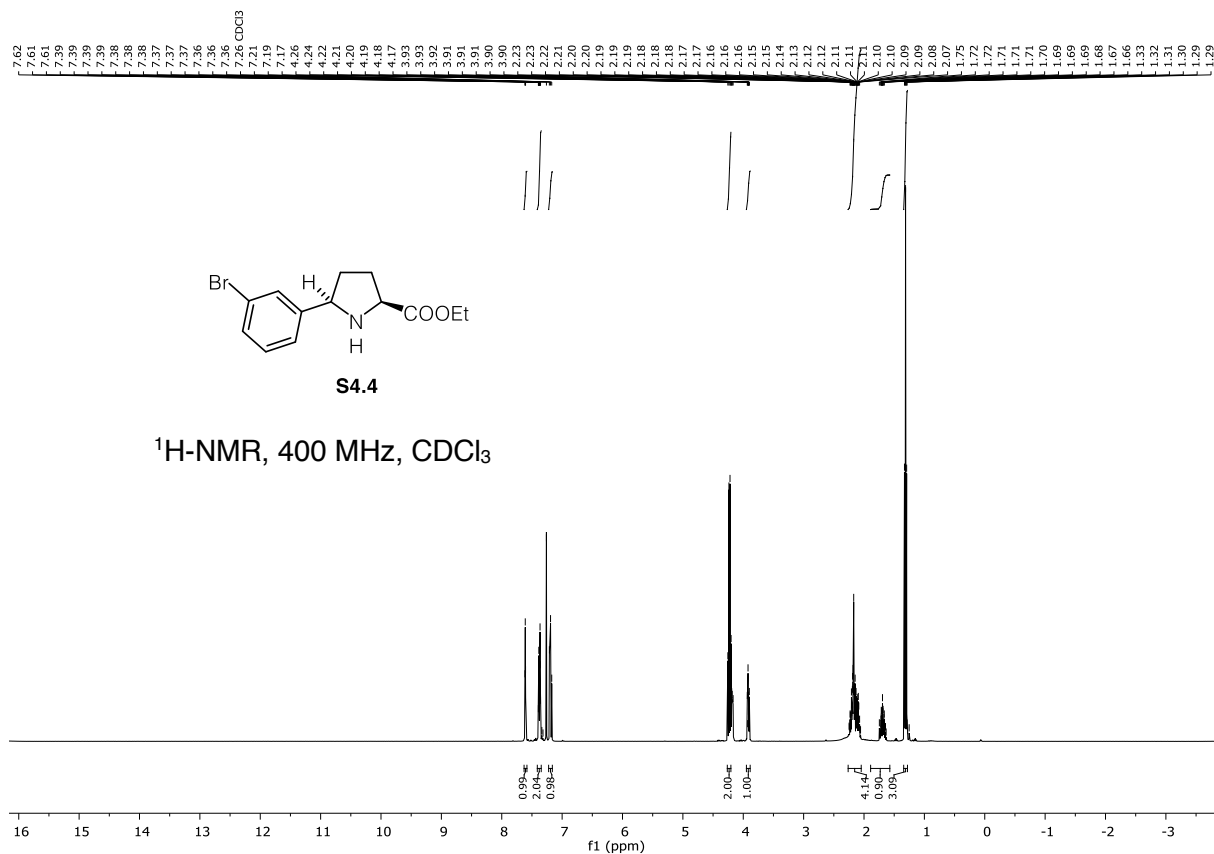


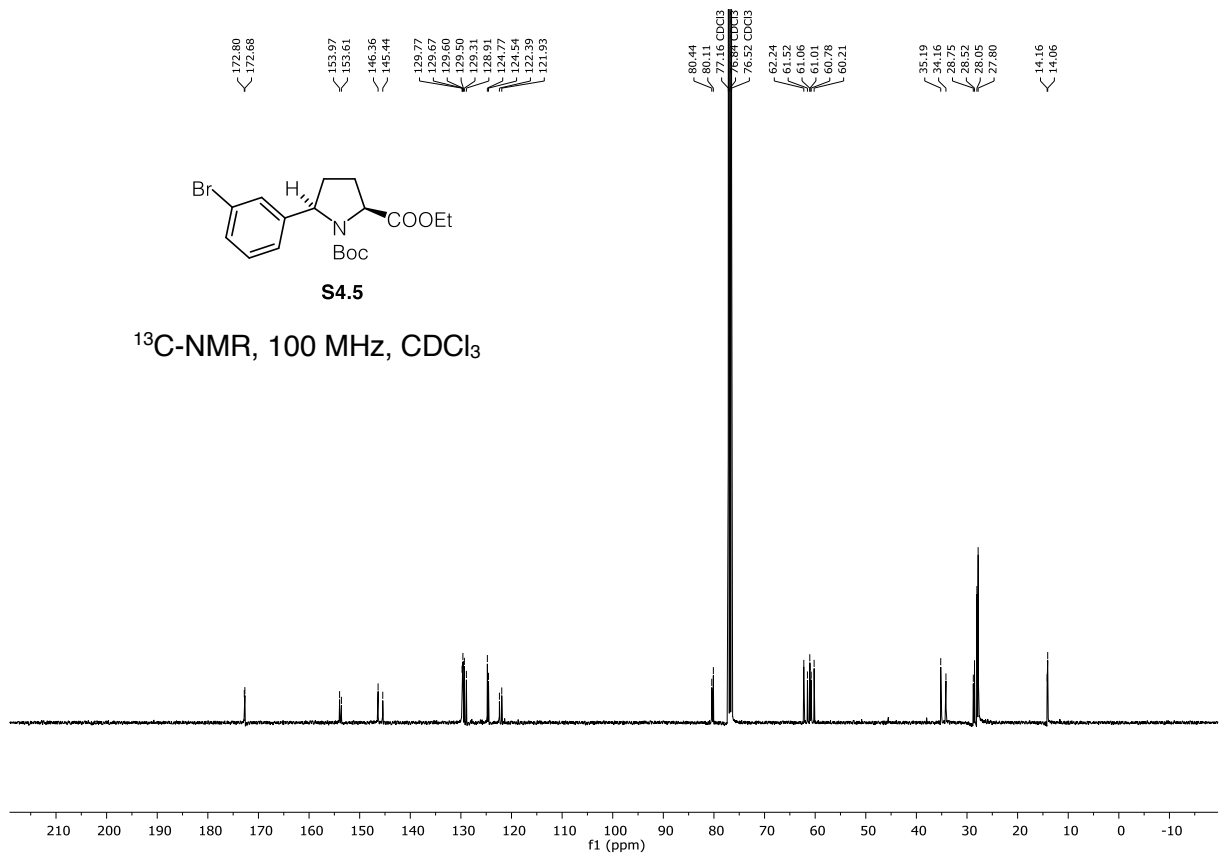
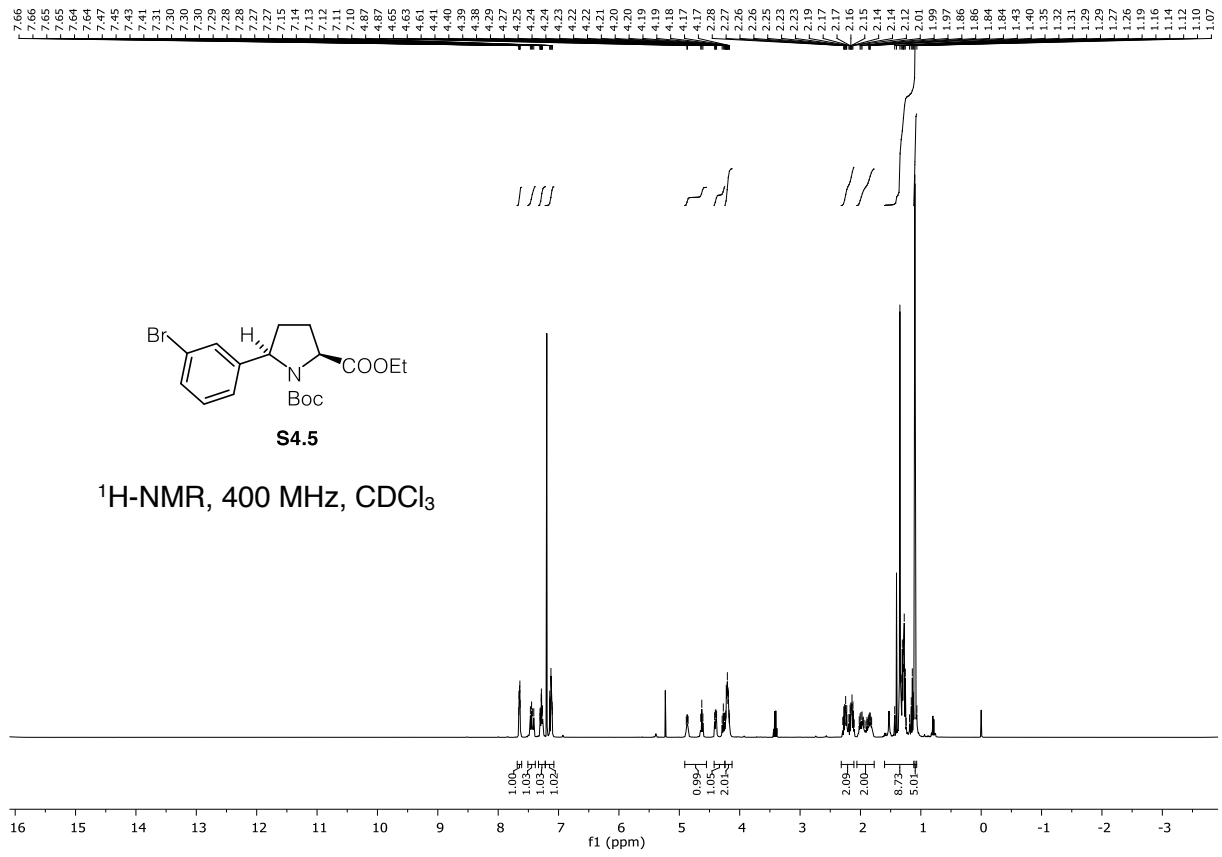


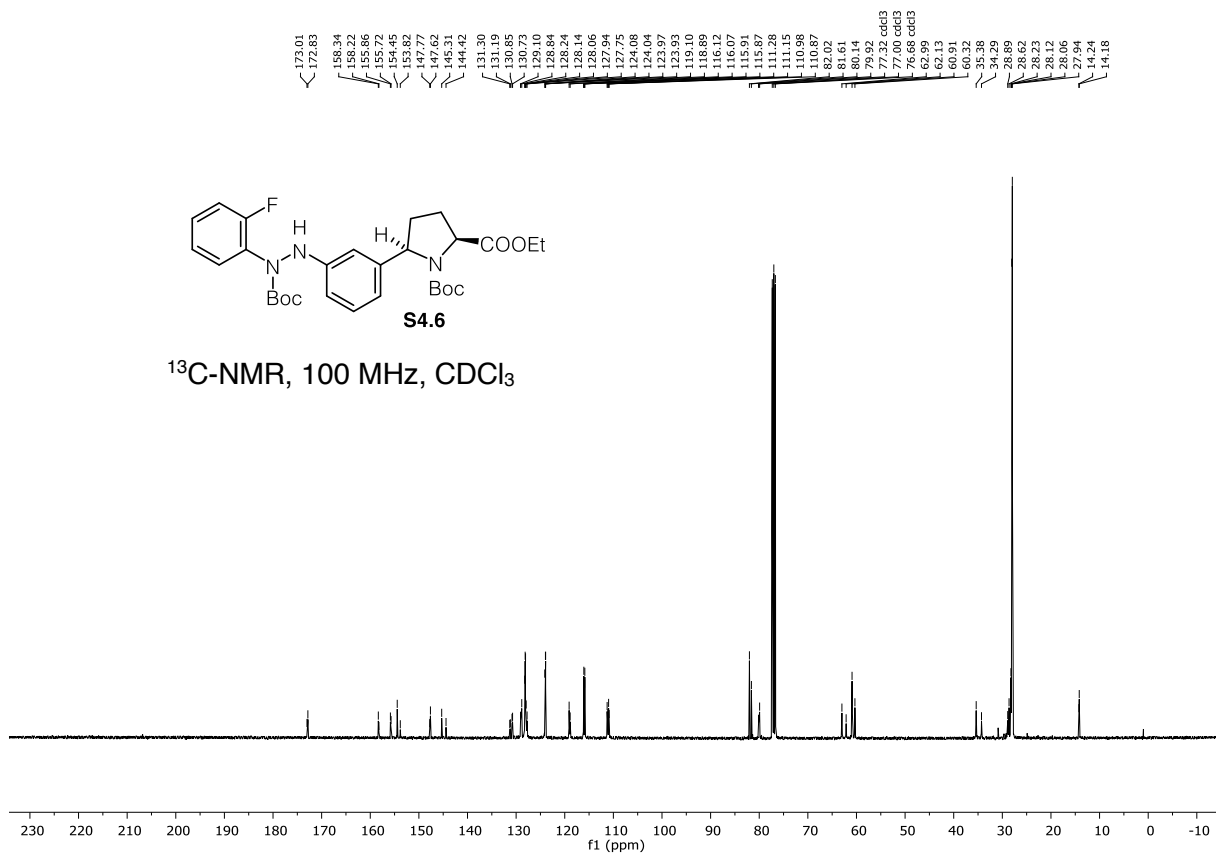
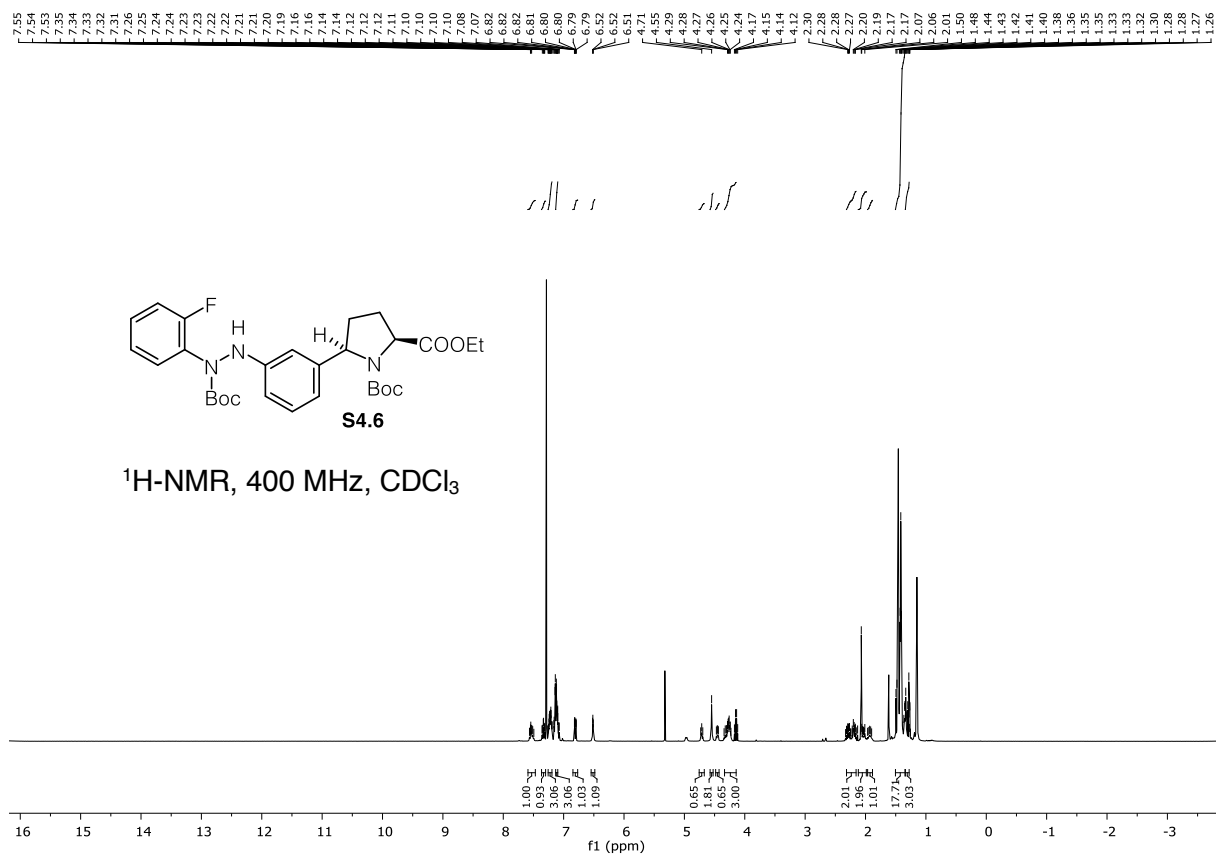


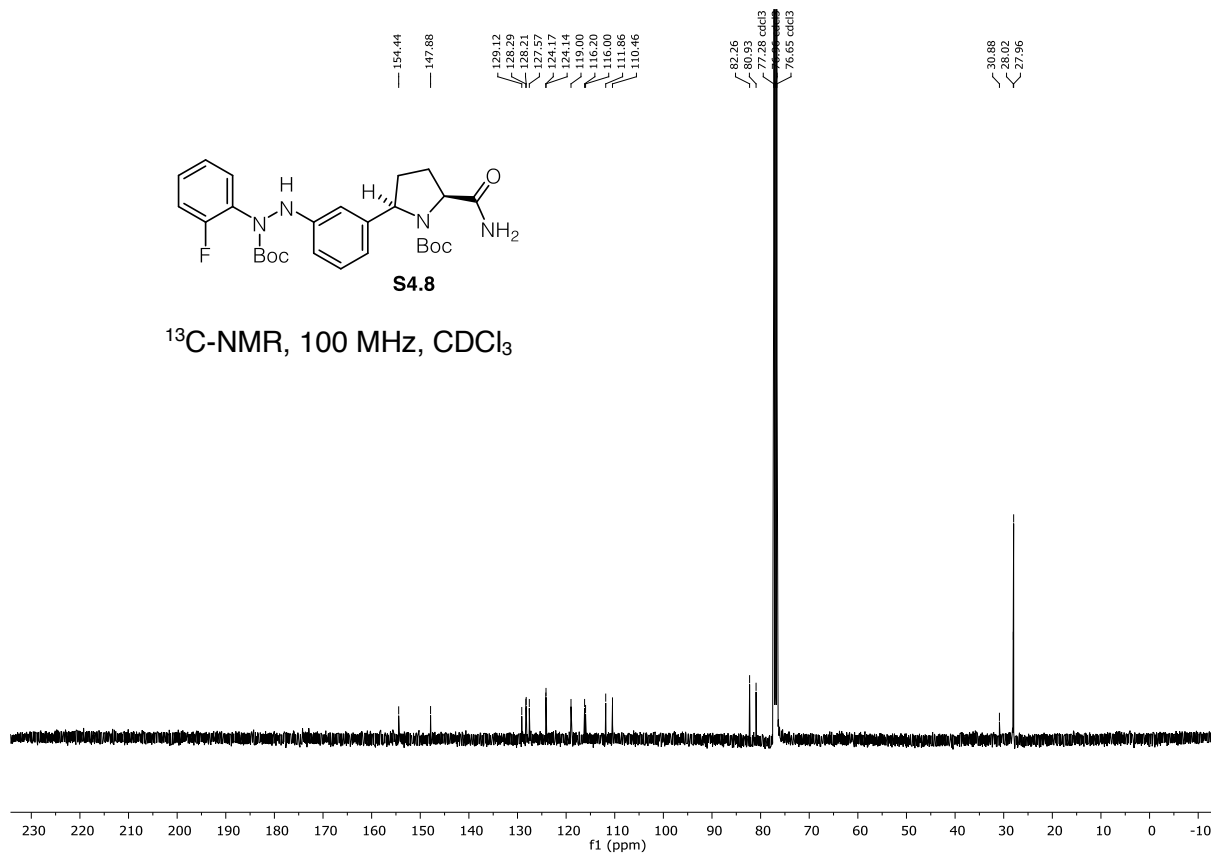
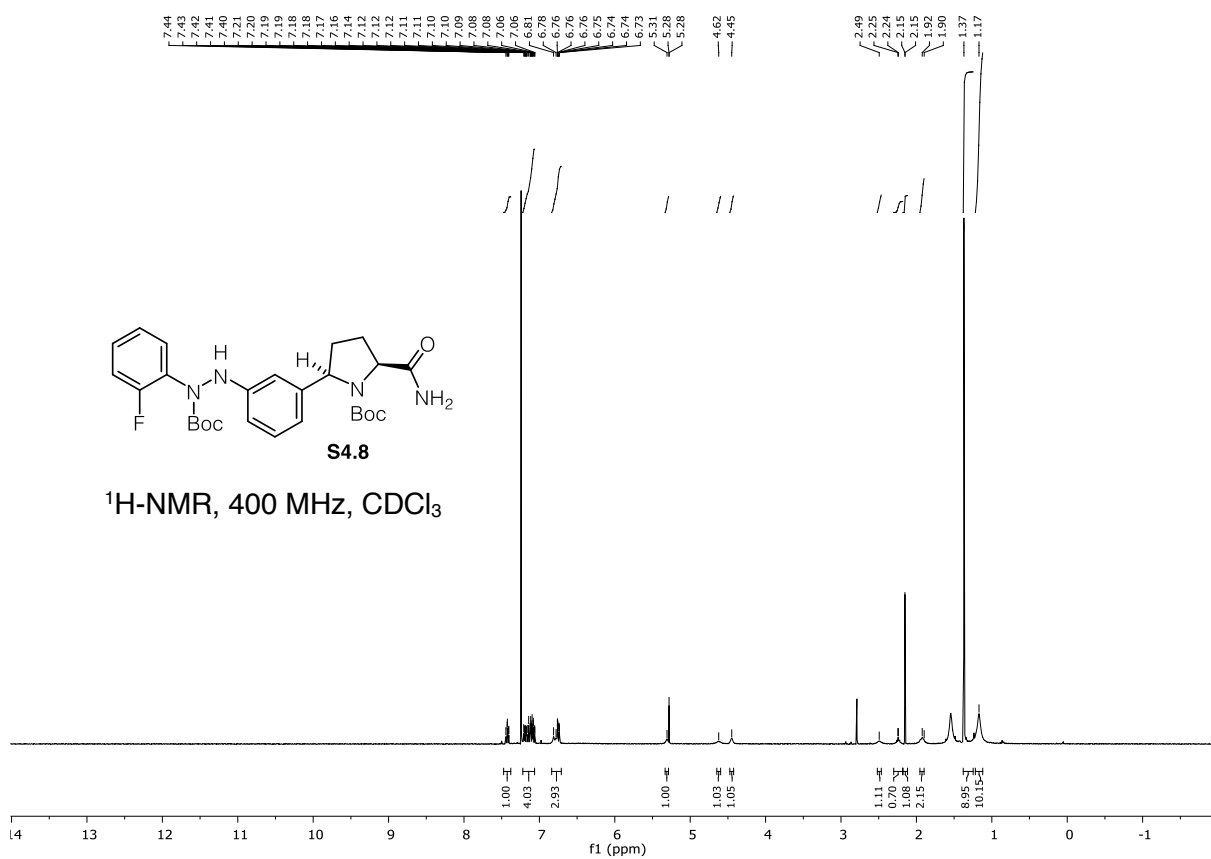


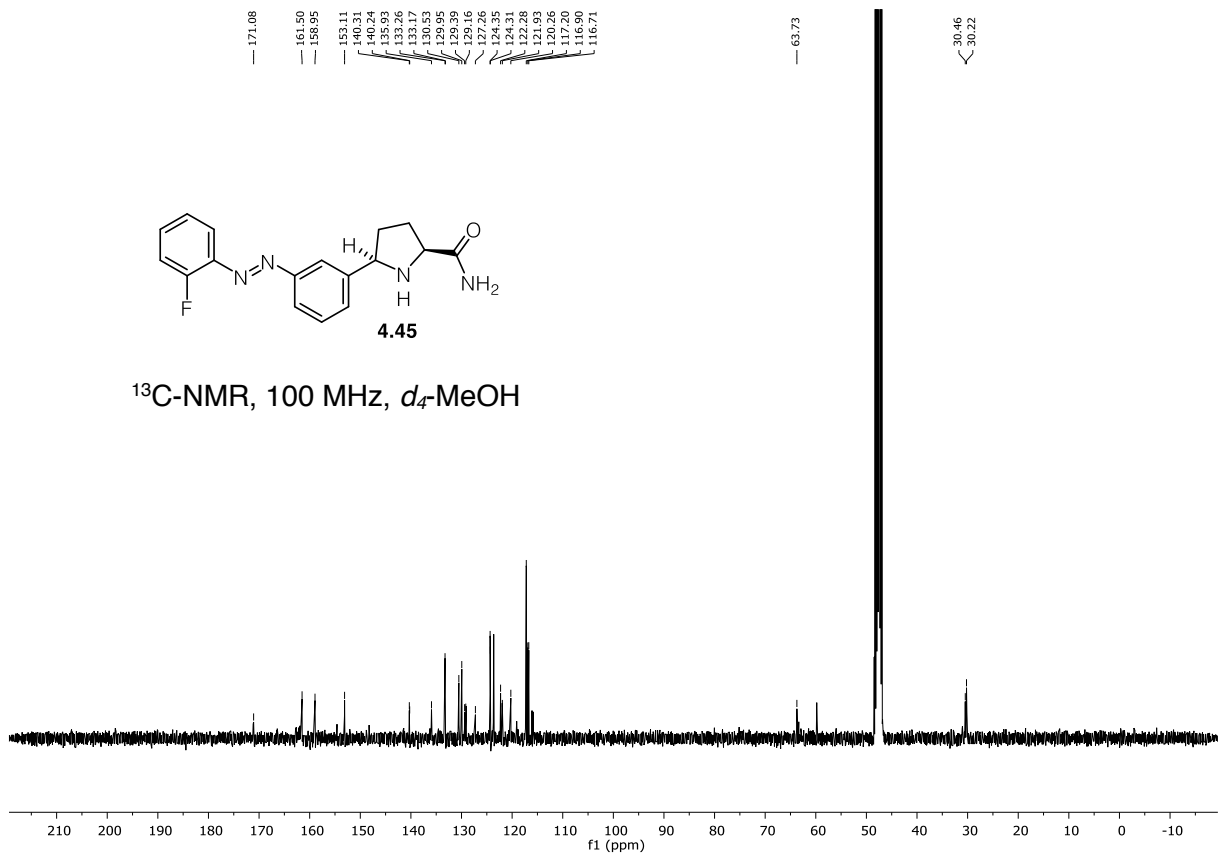
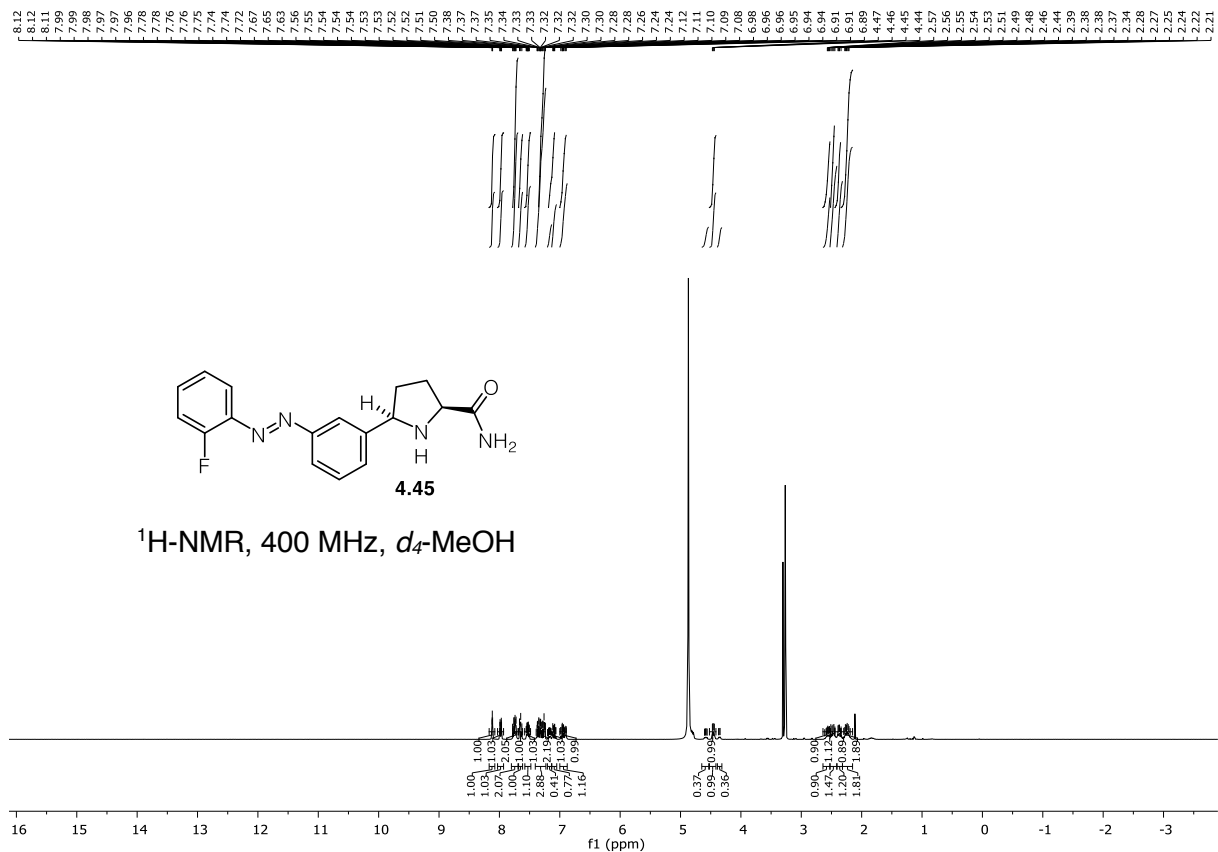


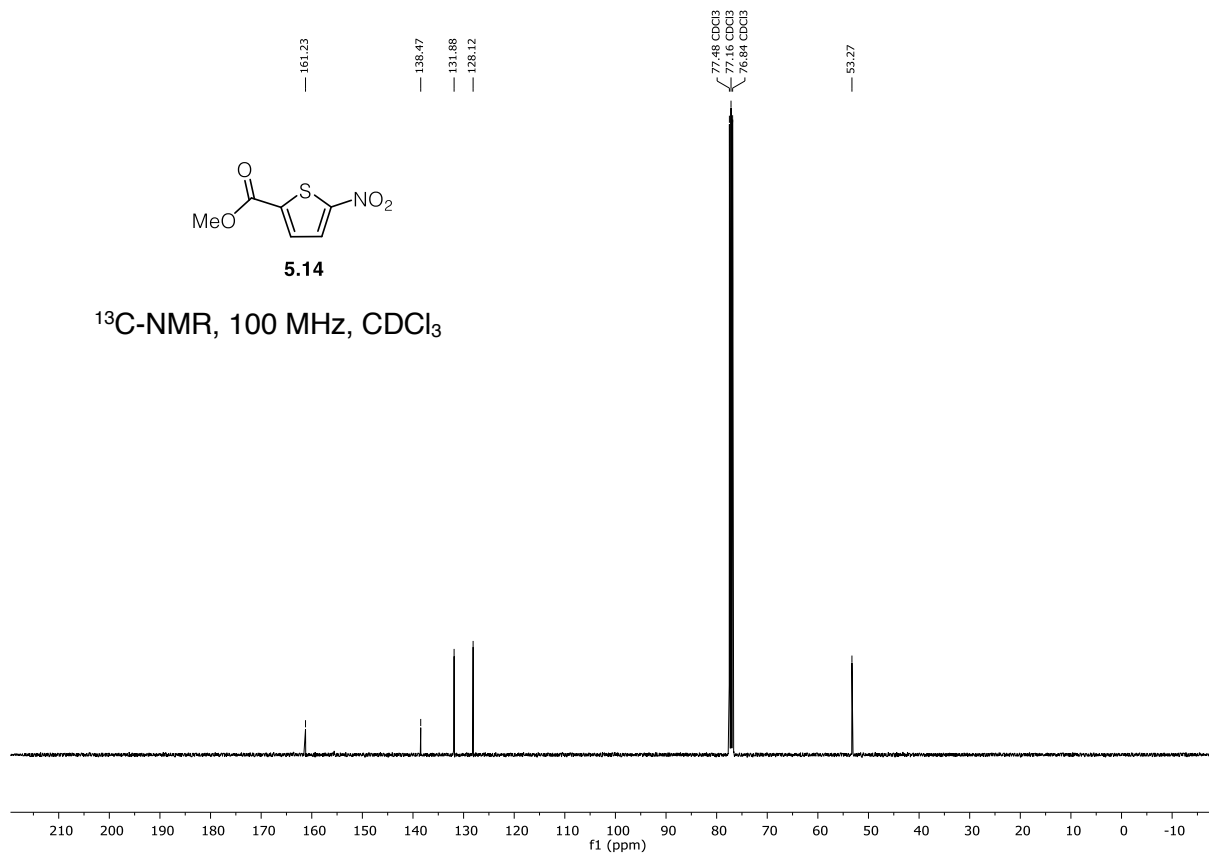
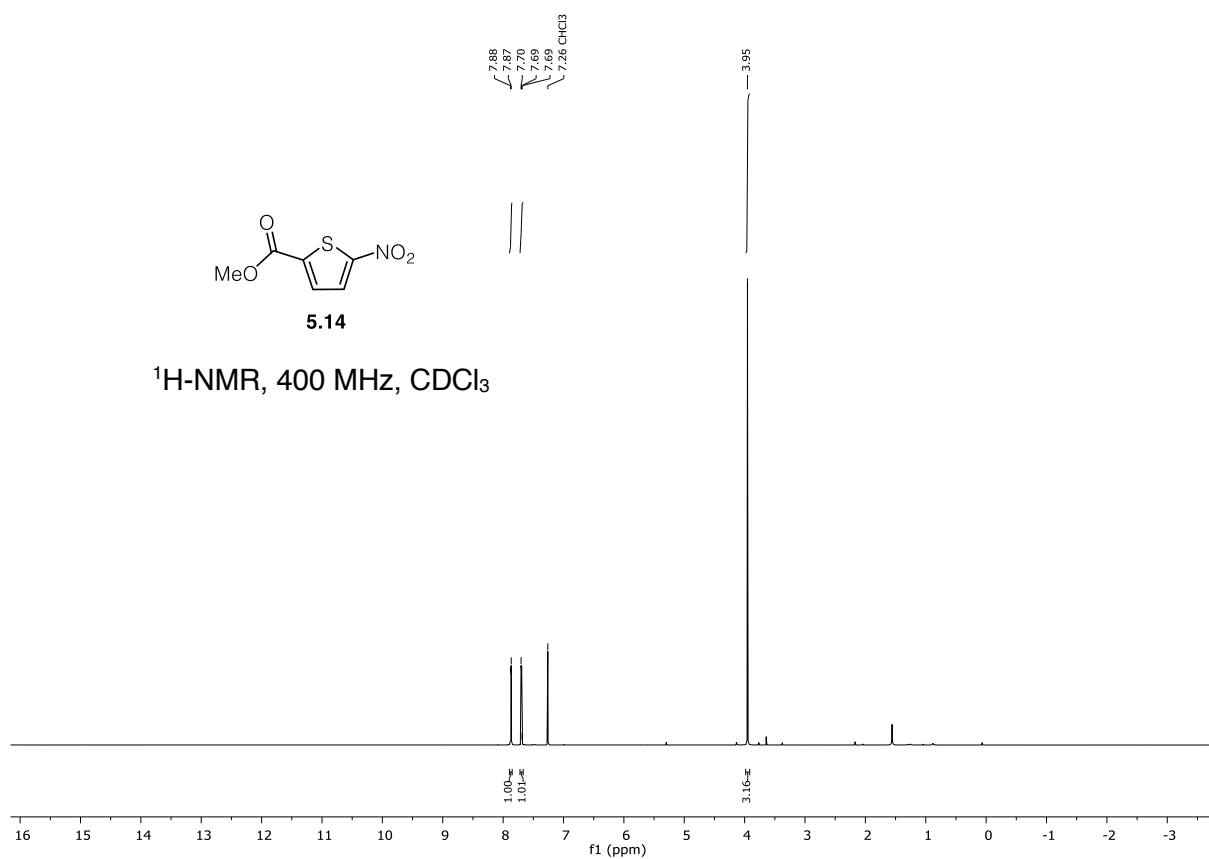


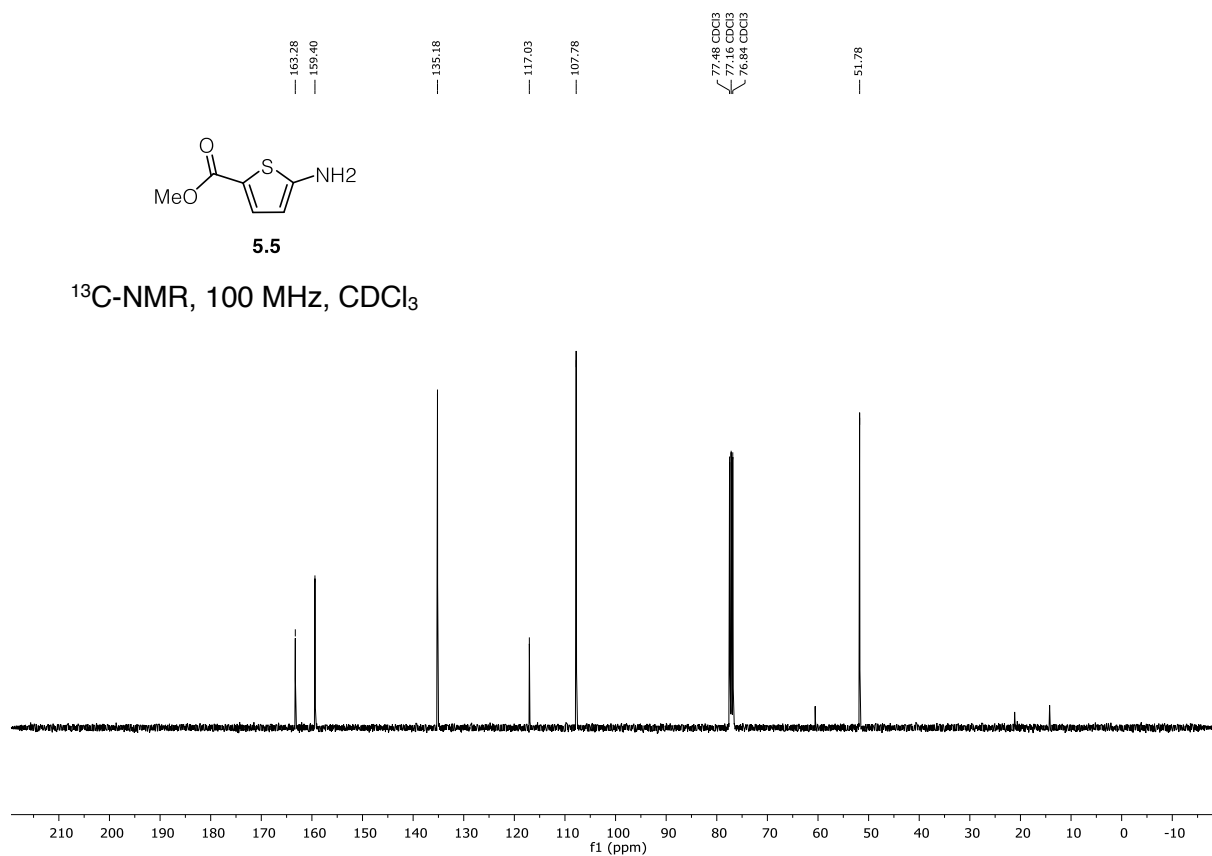
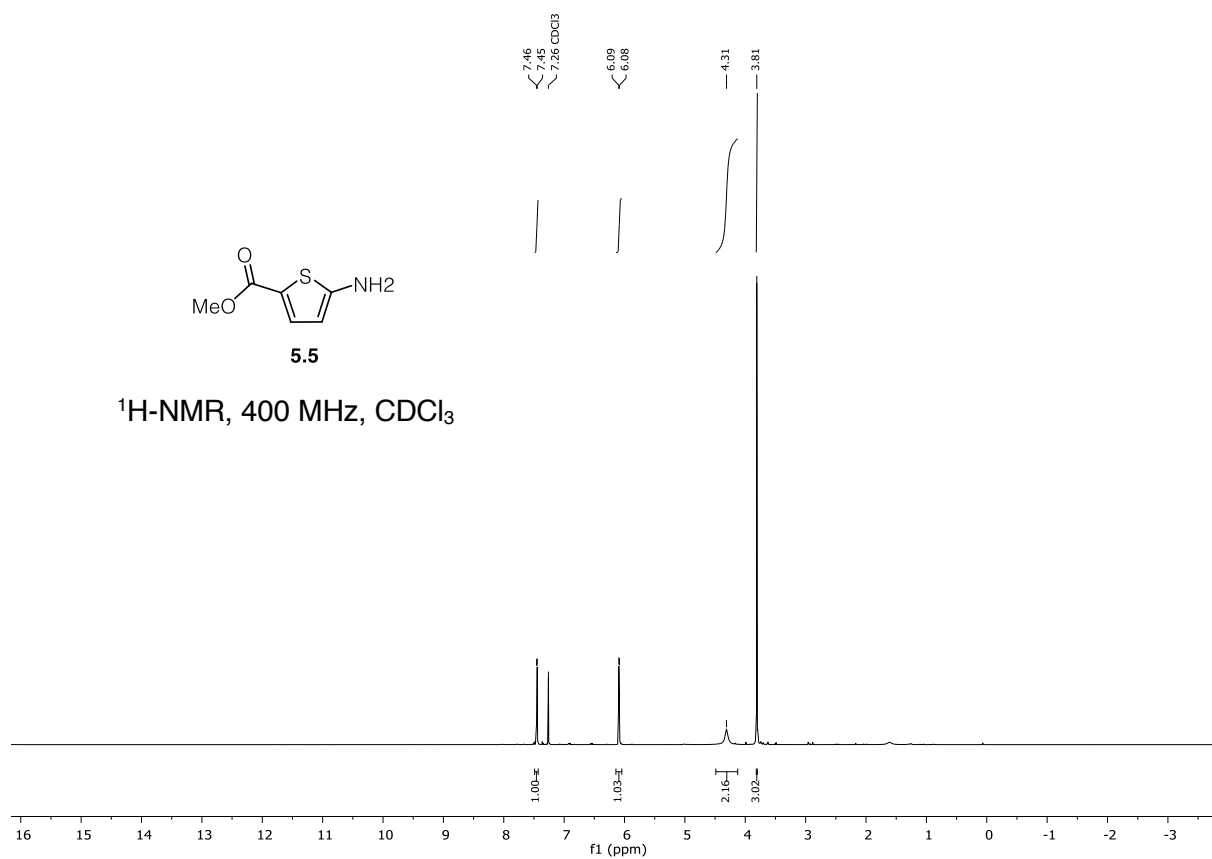


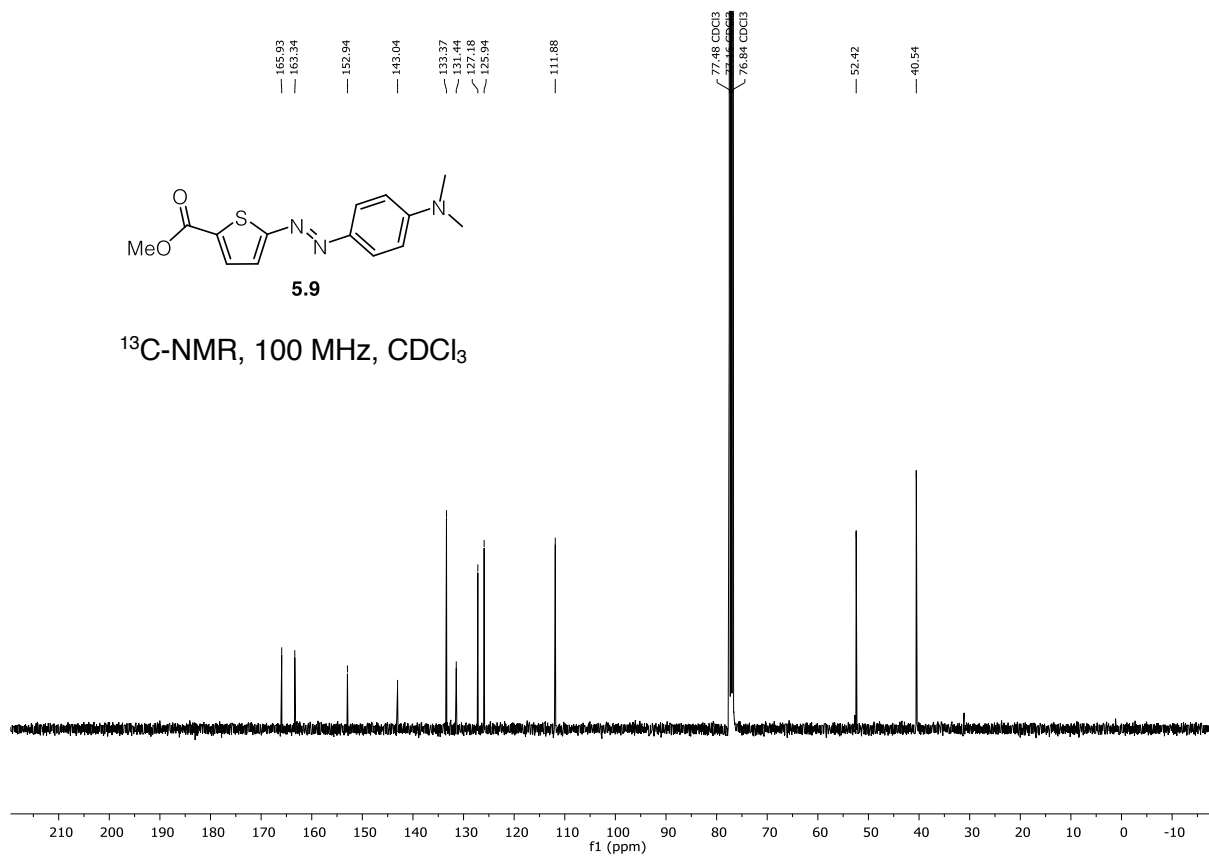
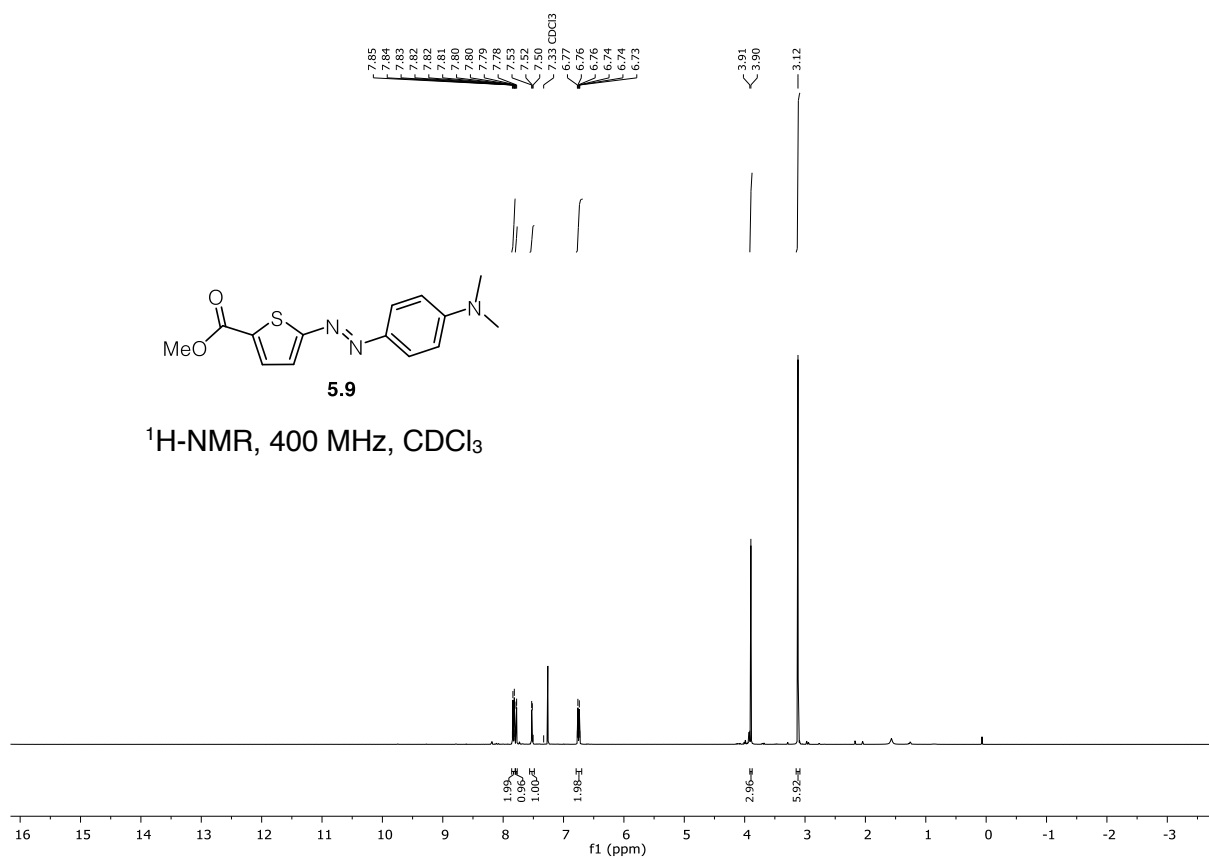


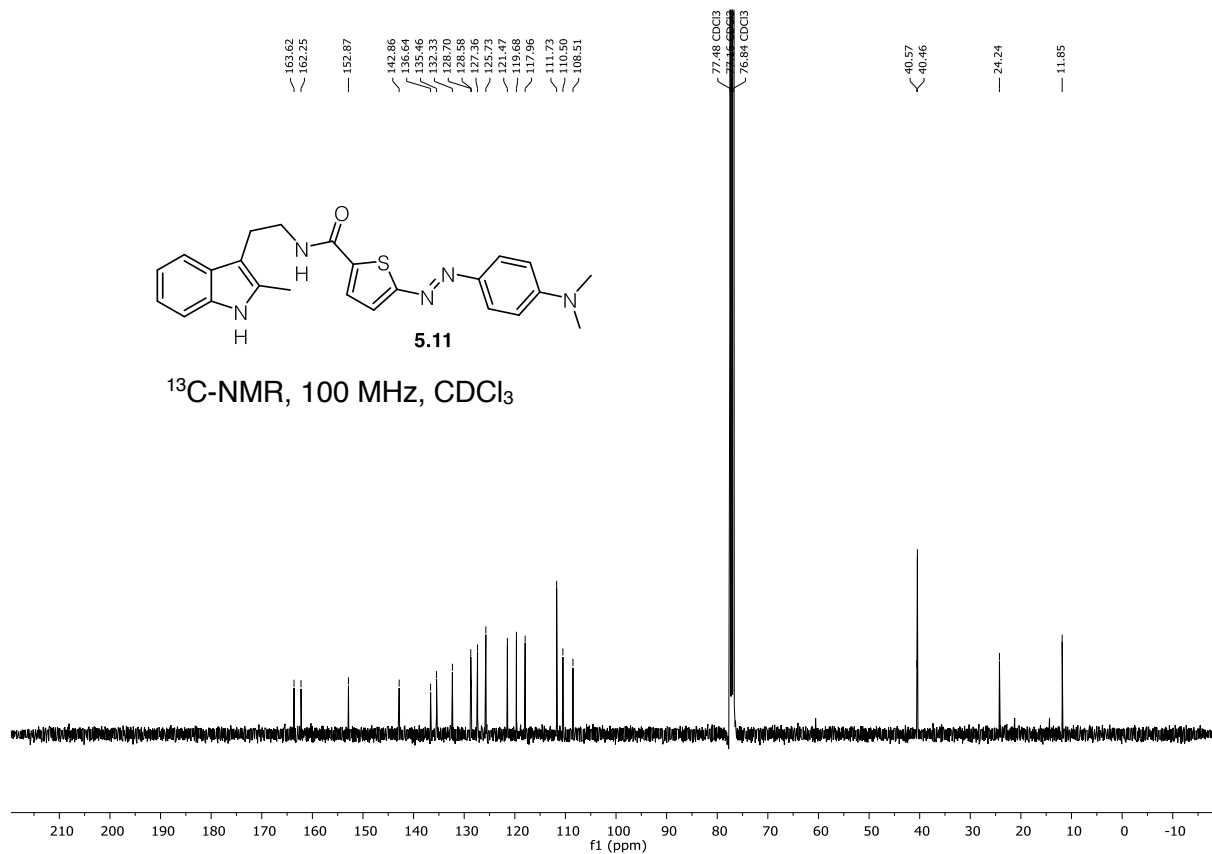
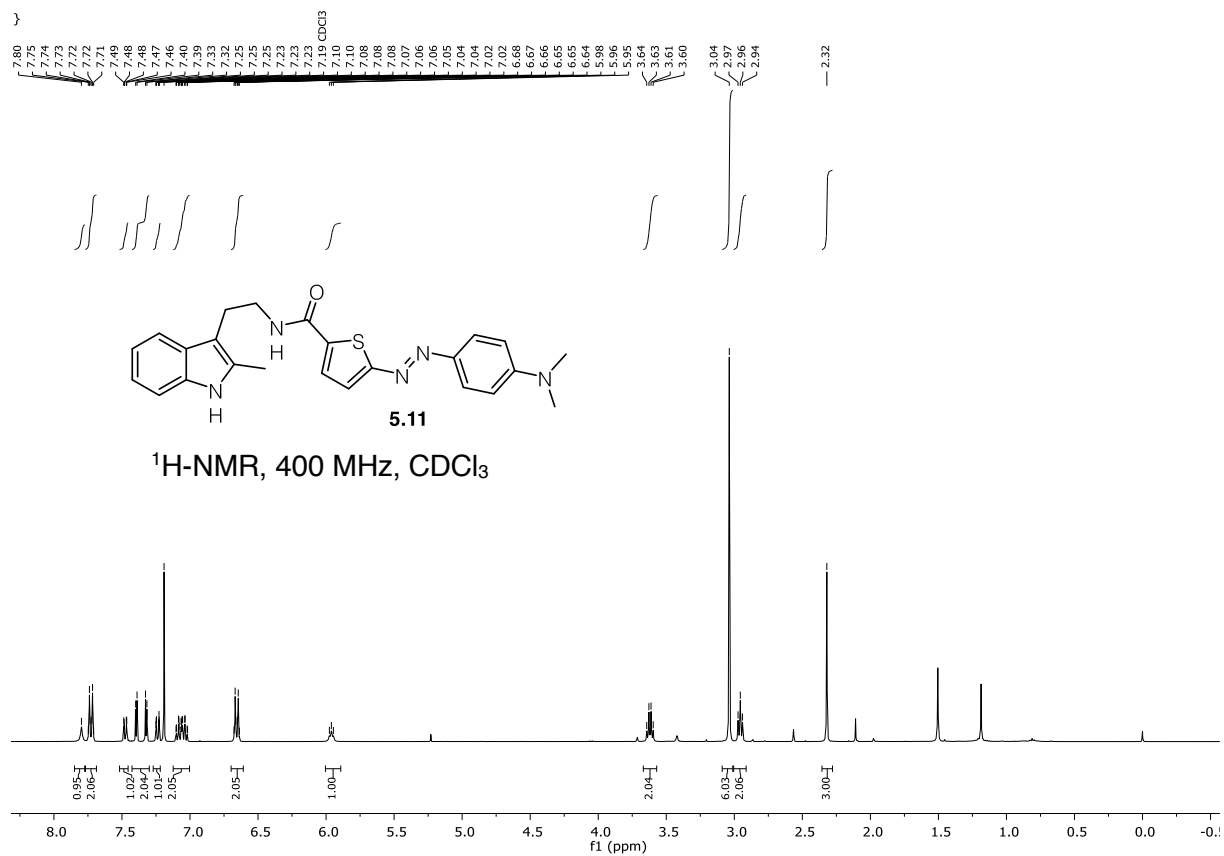


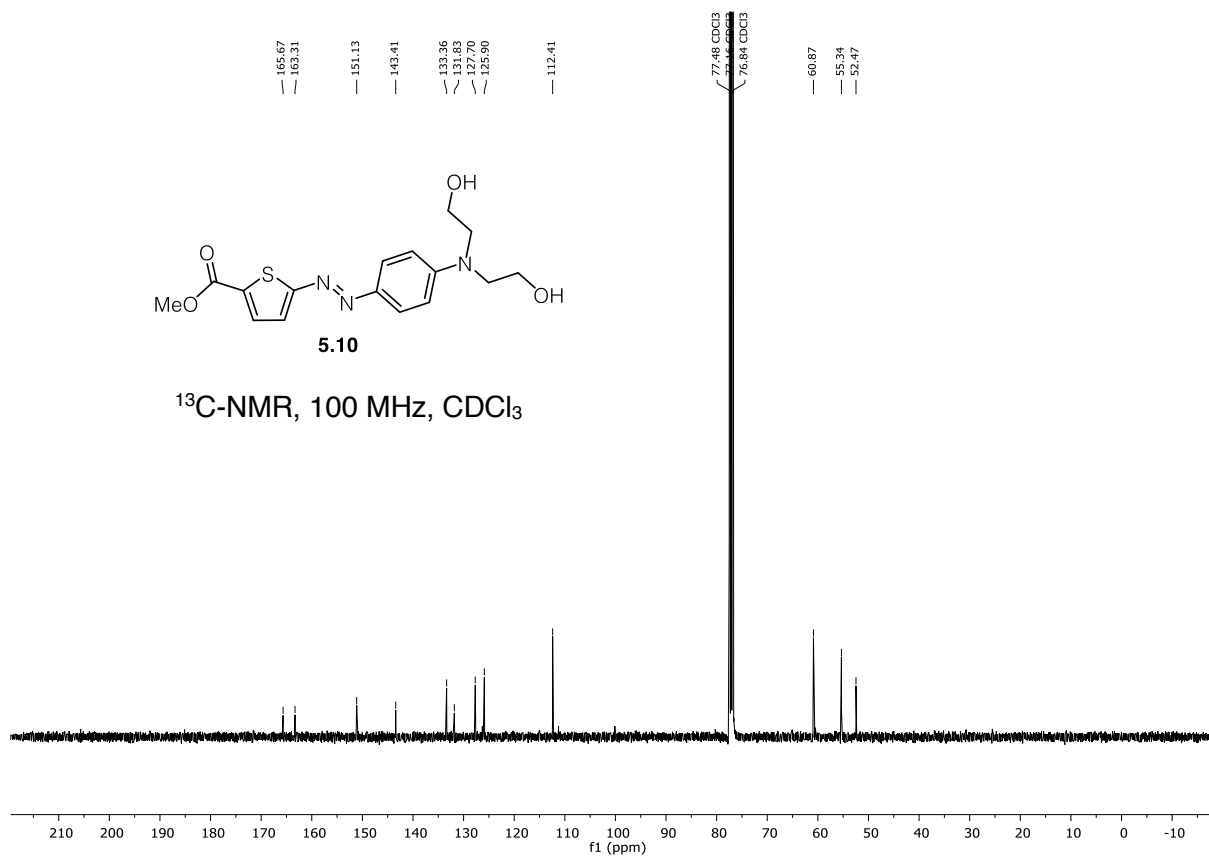
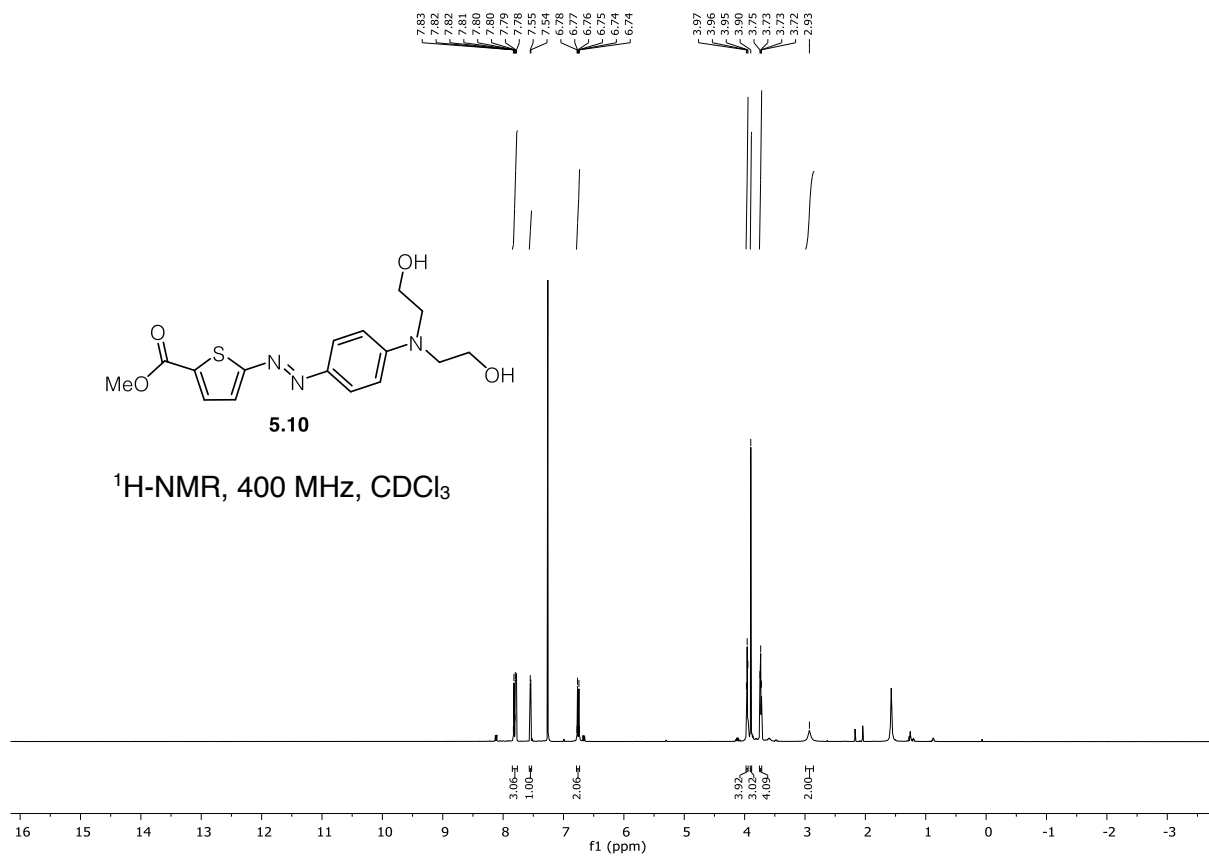


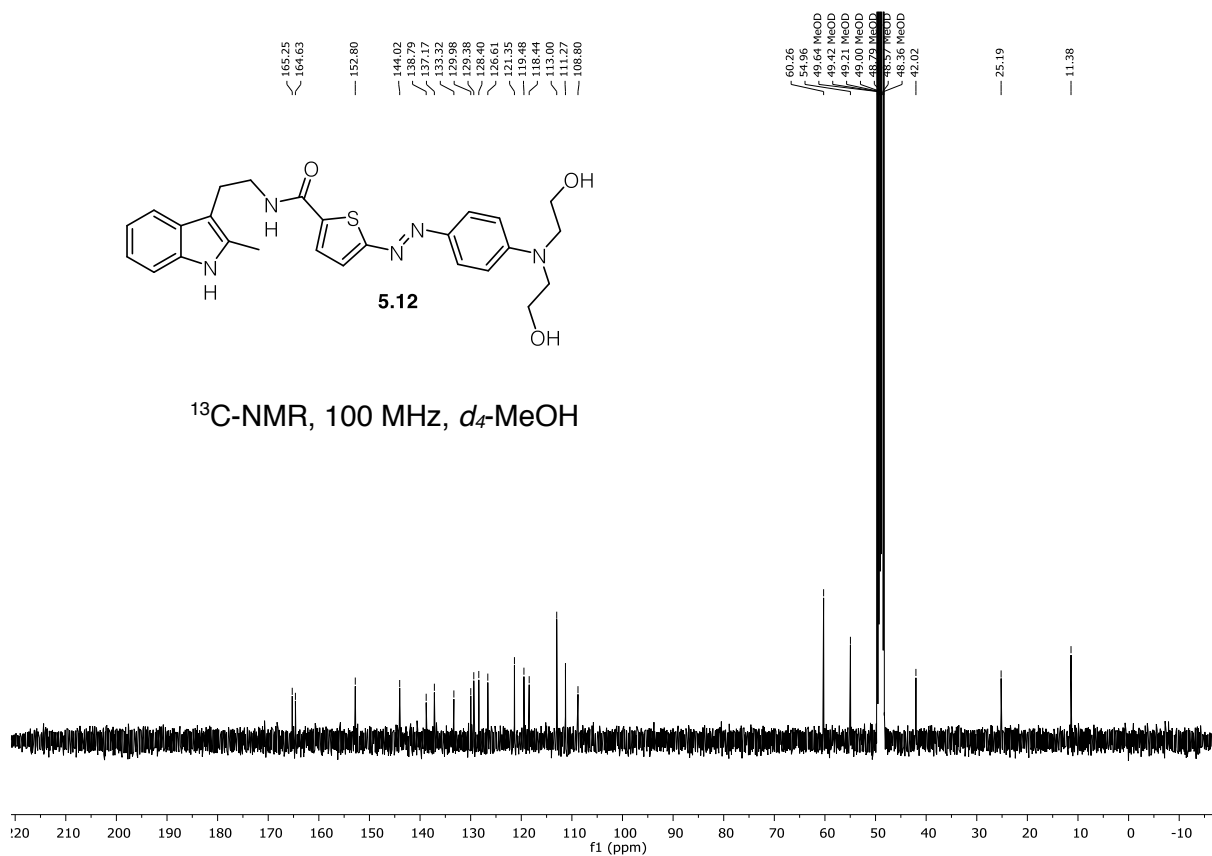
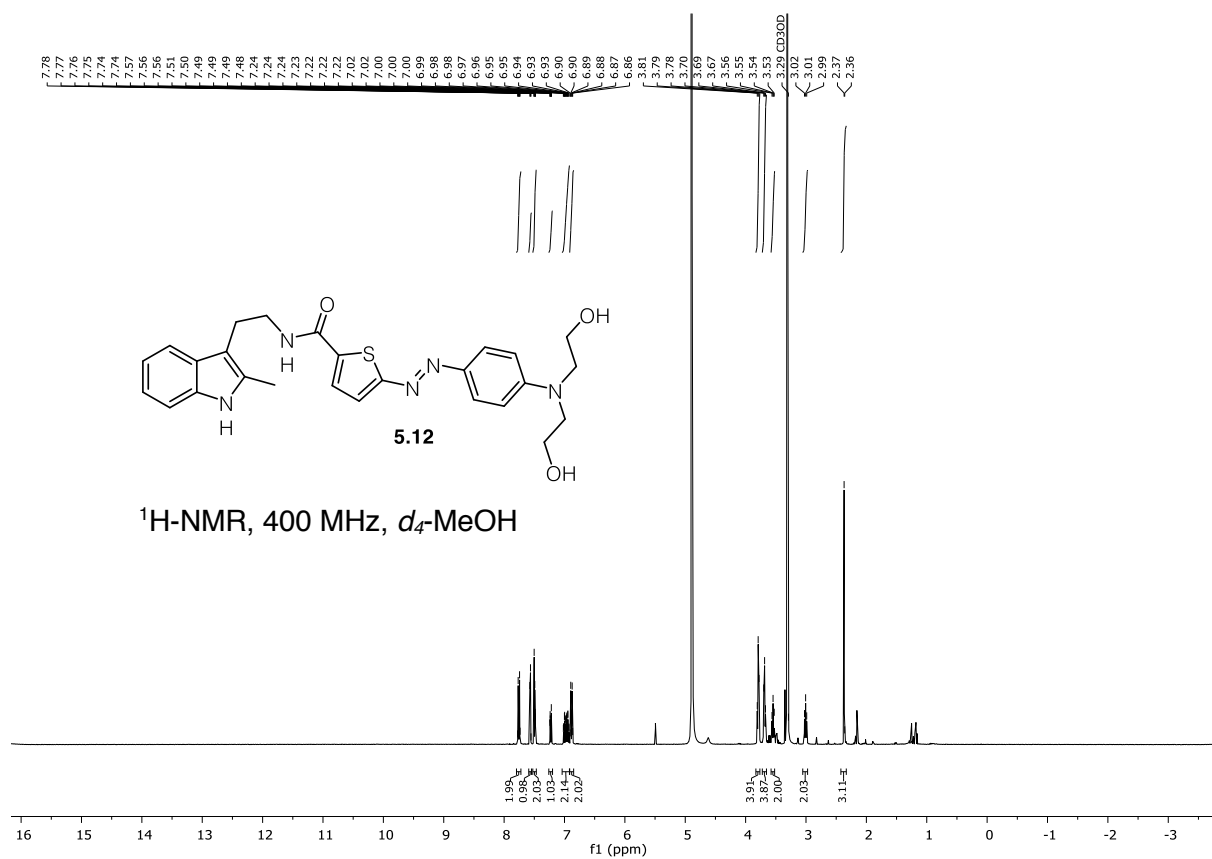
7.2.5 ^1H and ^{13}C NMR spectra of Chapter V

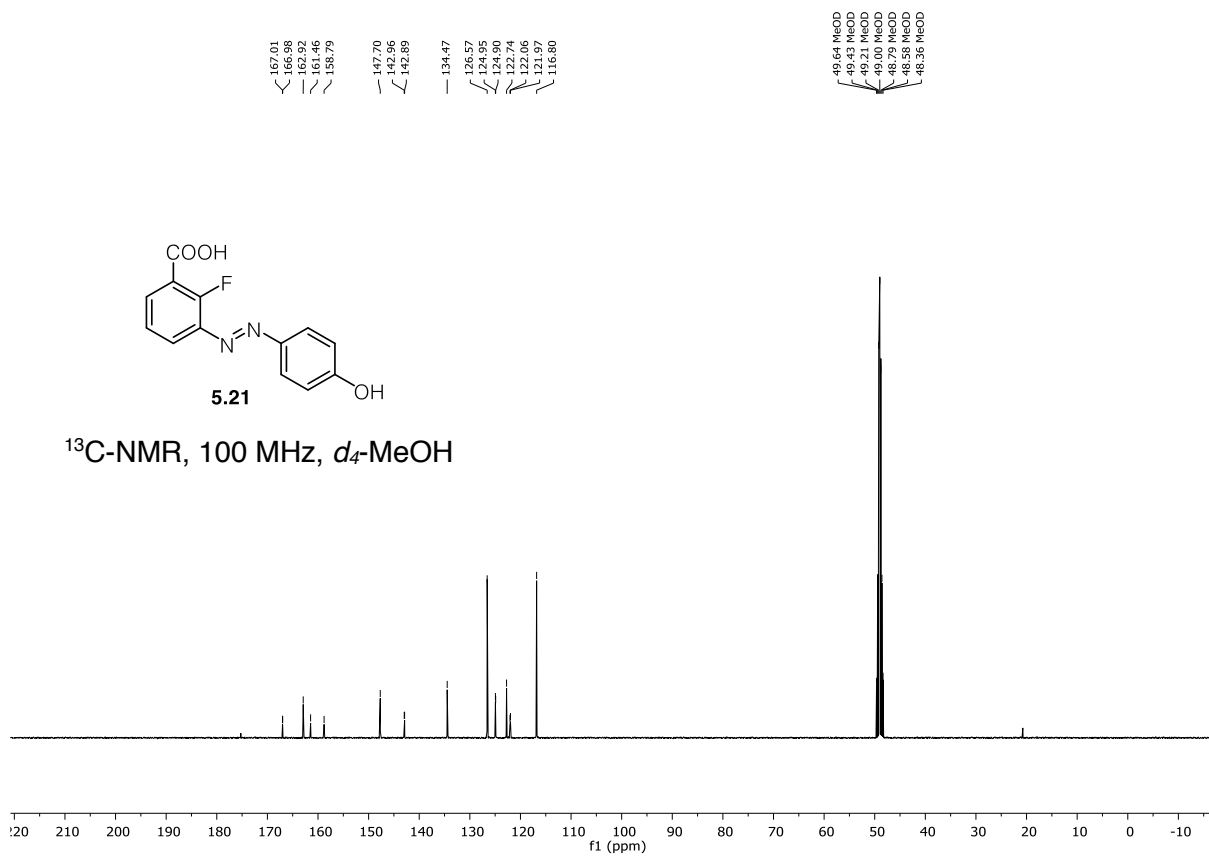
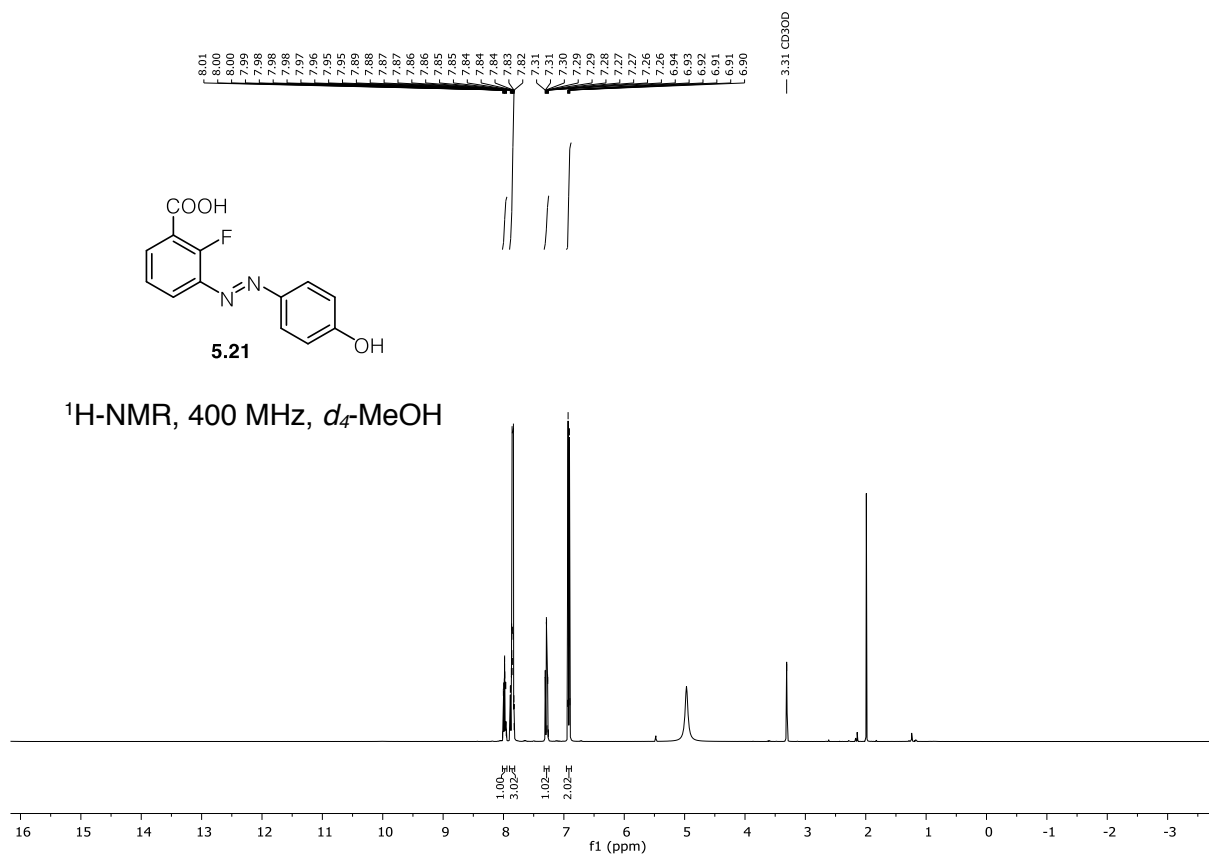


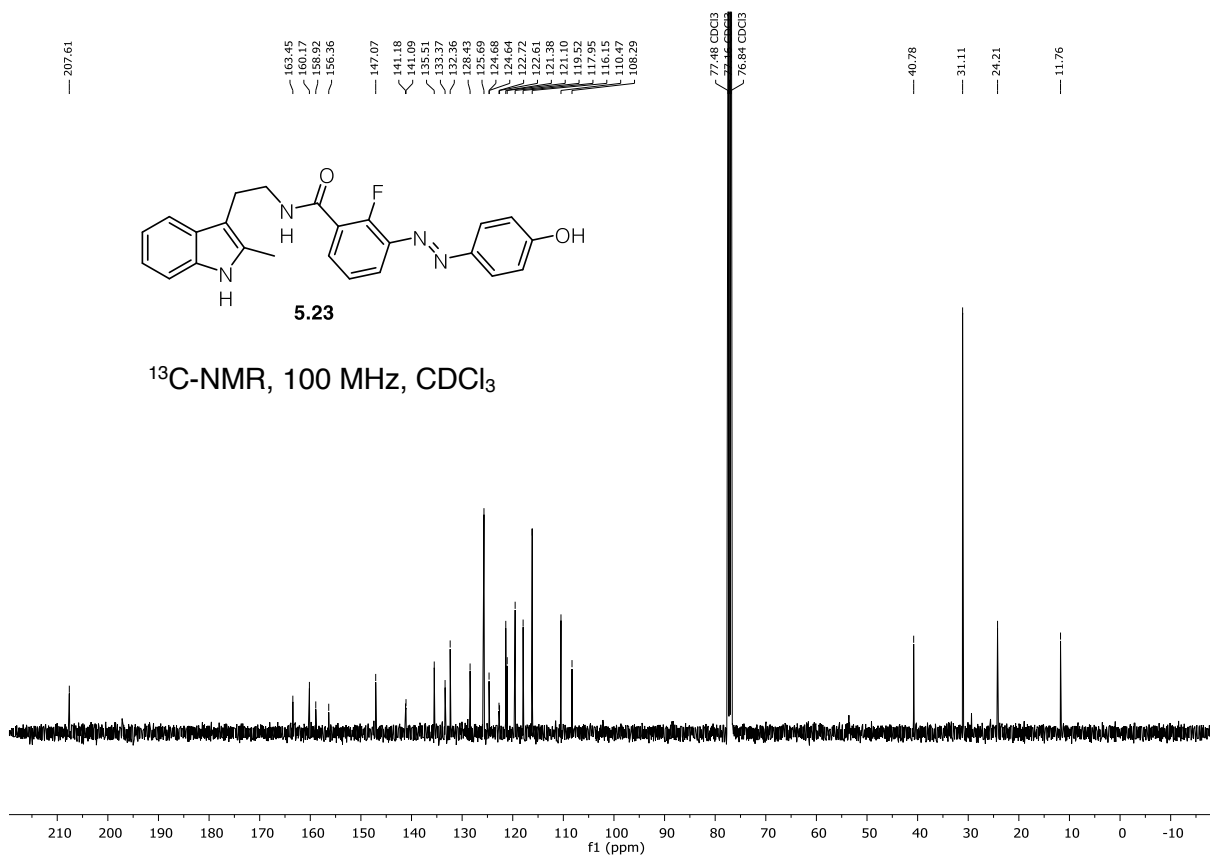
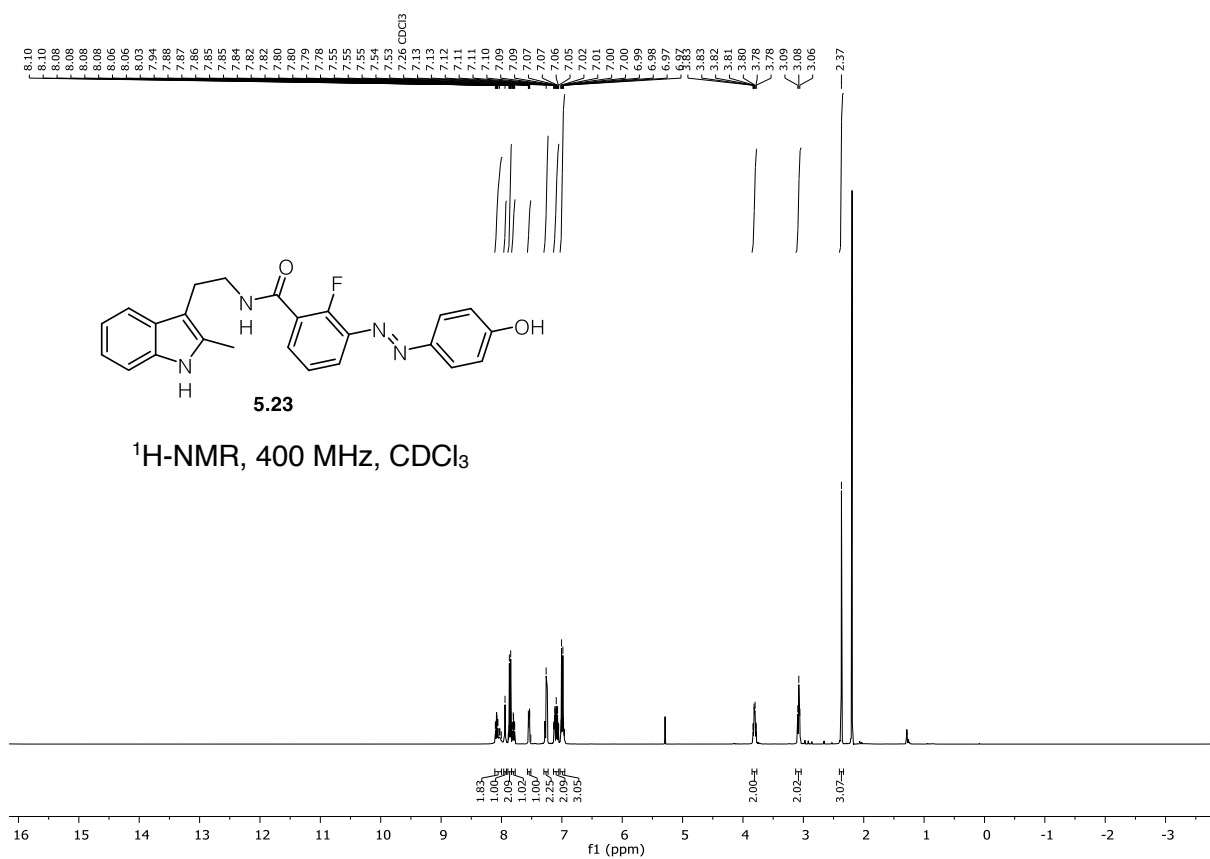


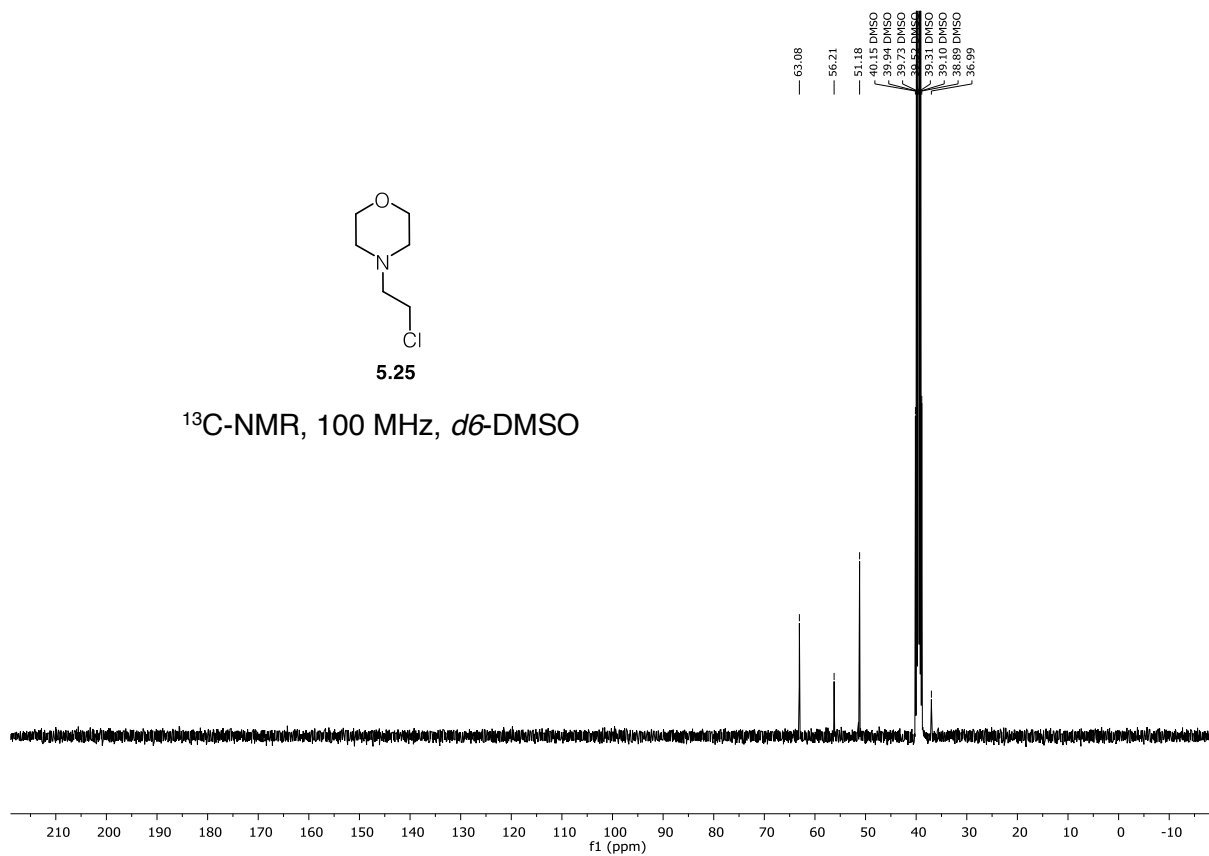
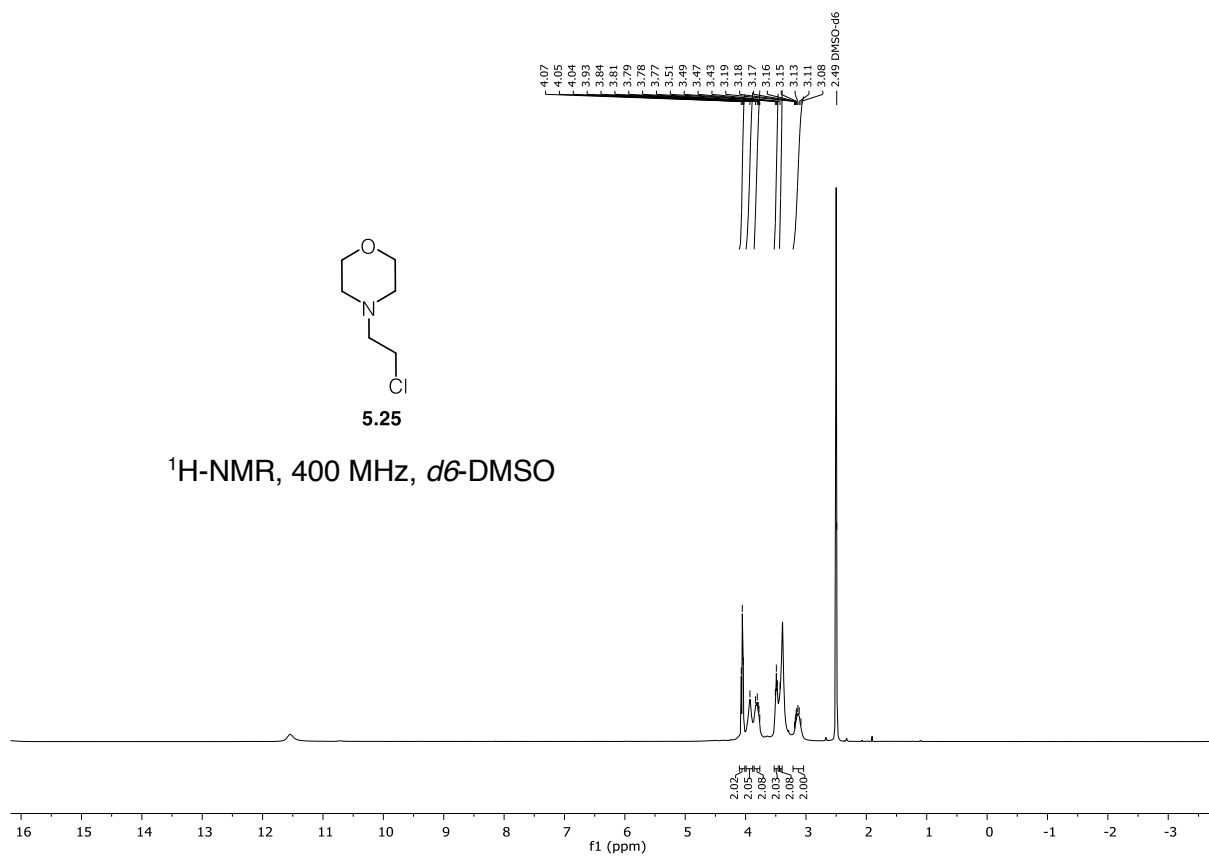


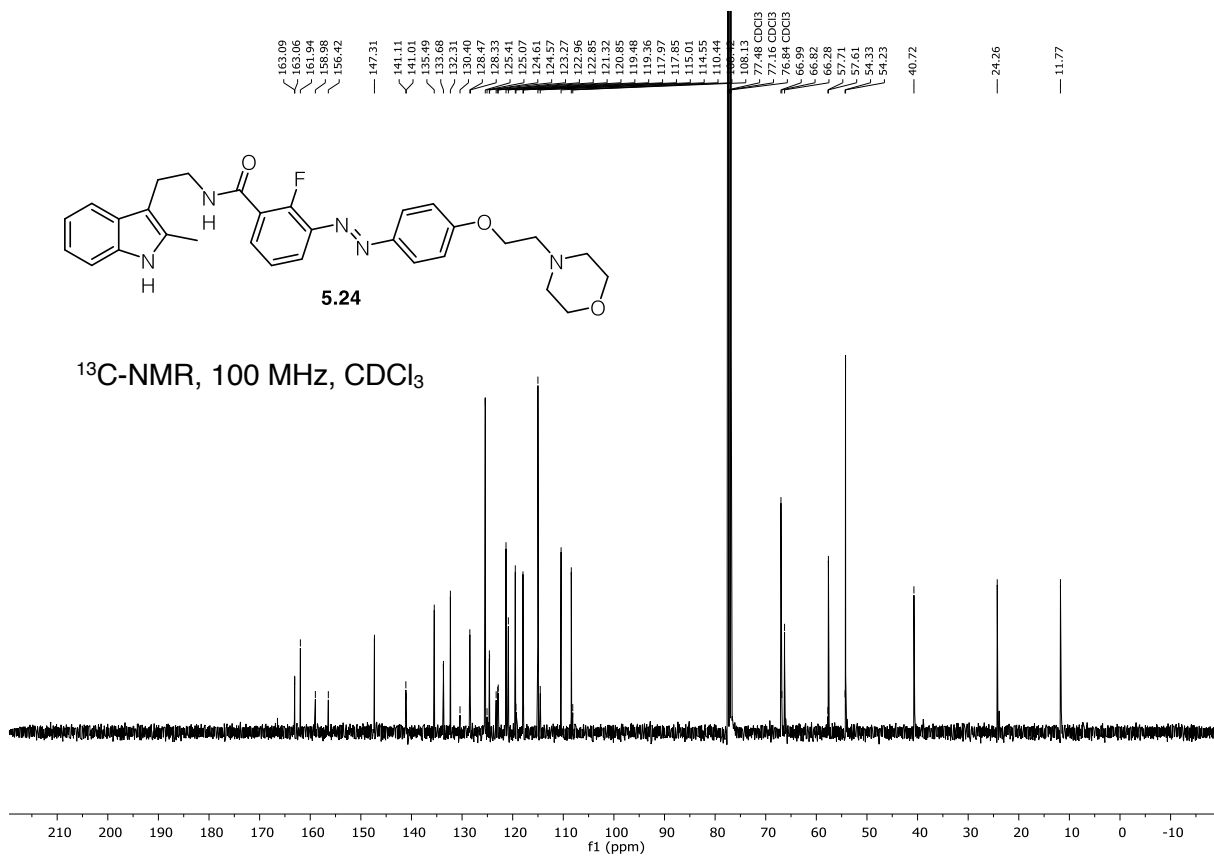
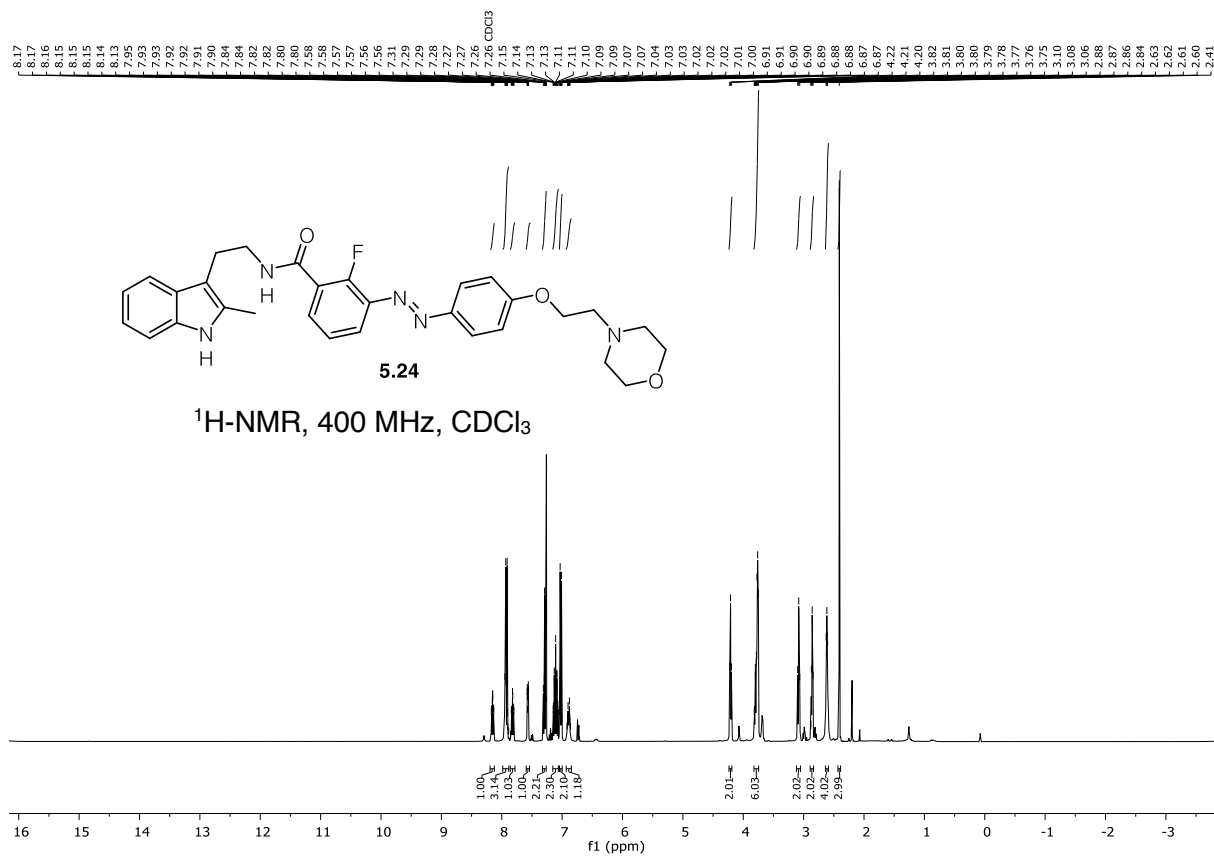


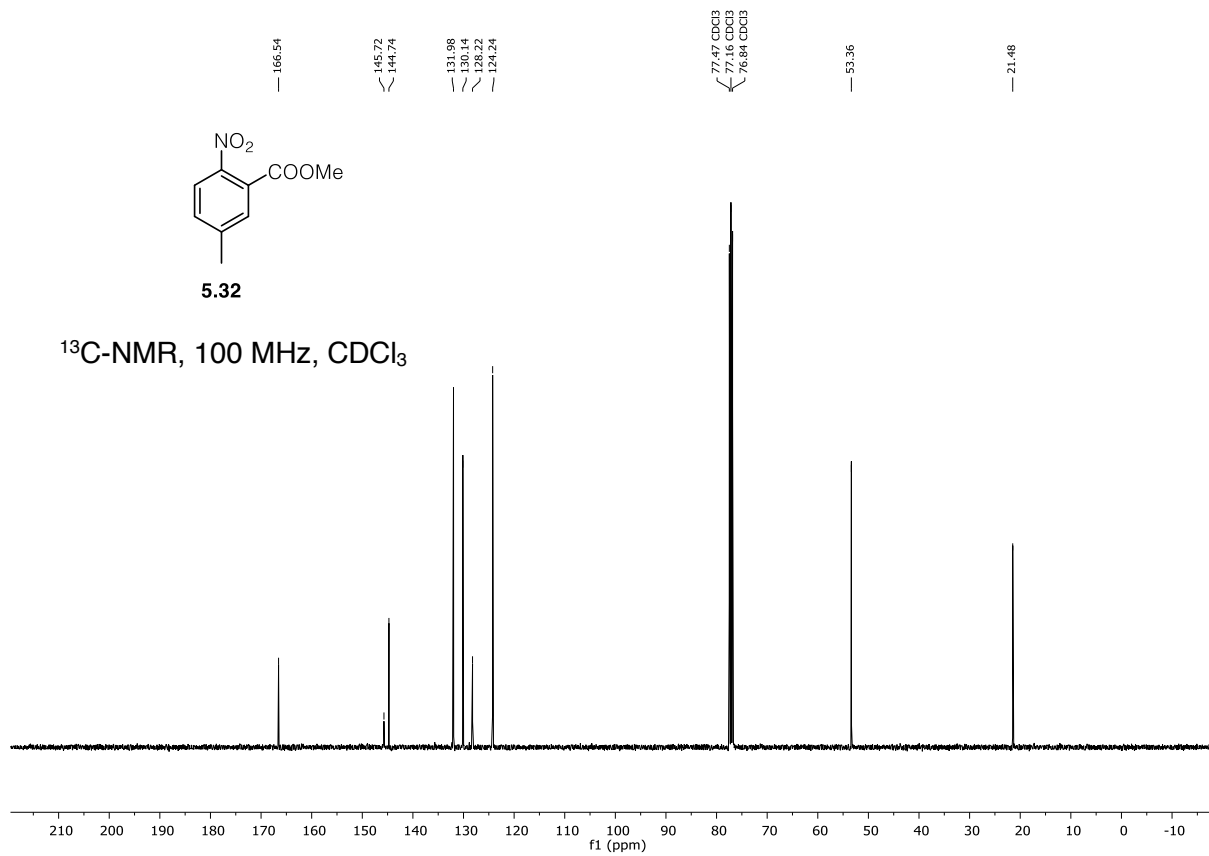
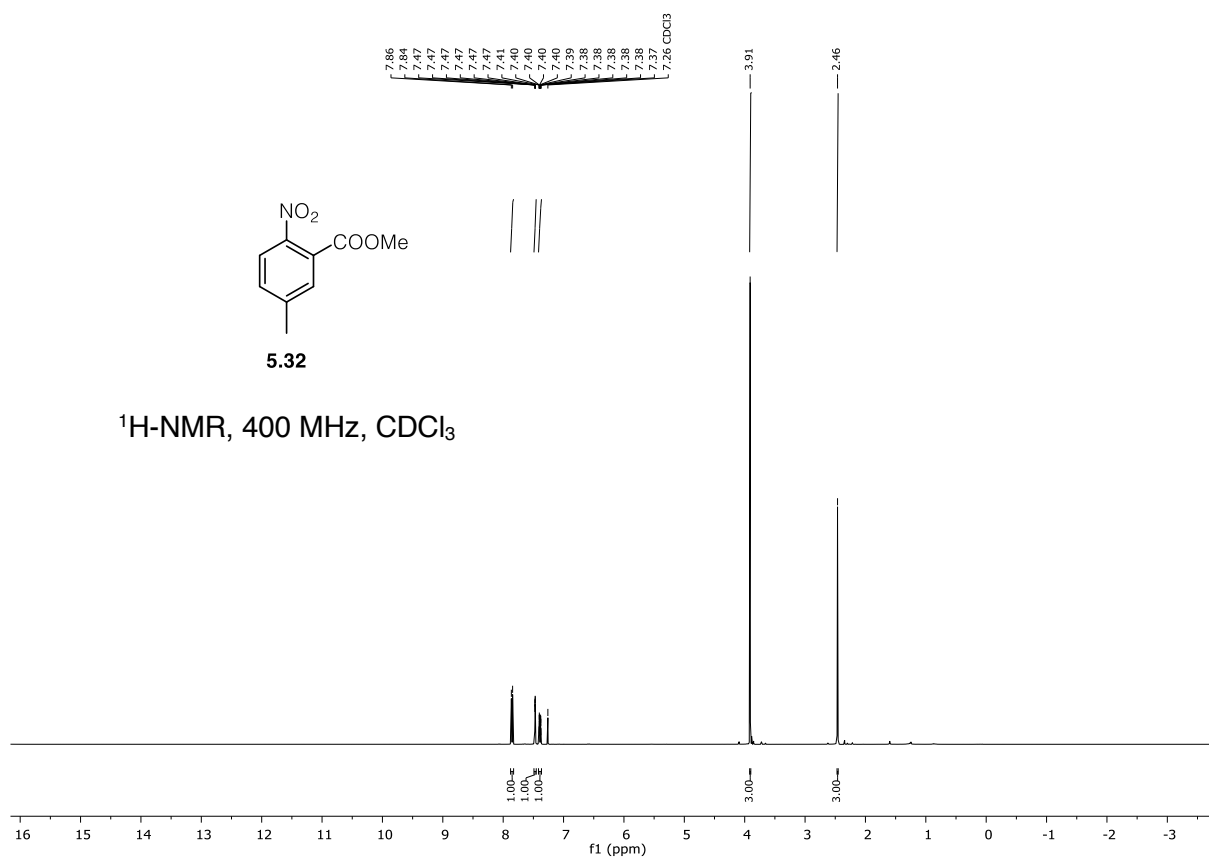


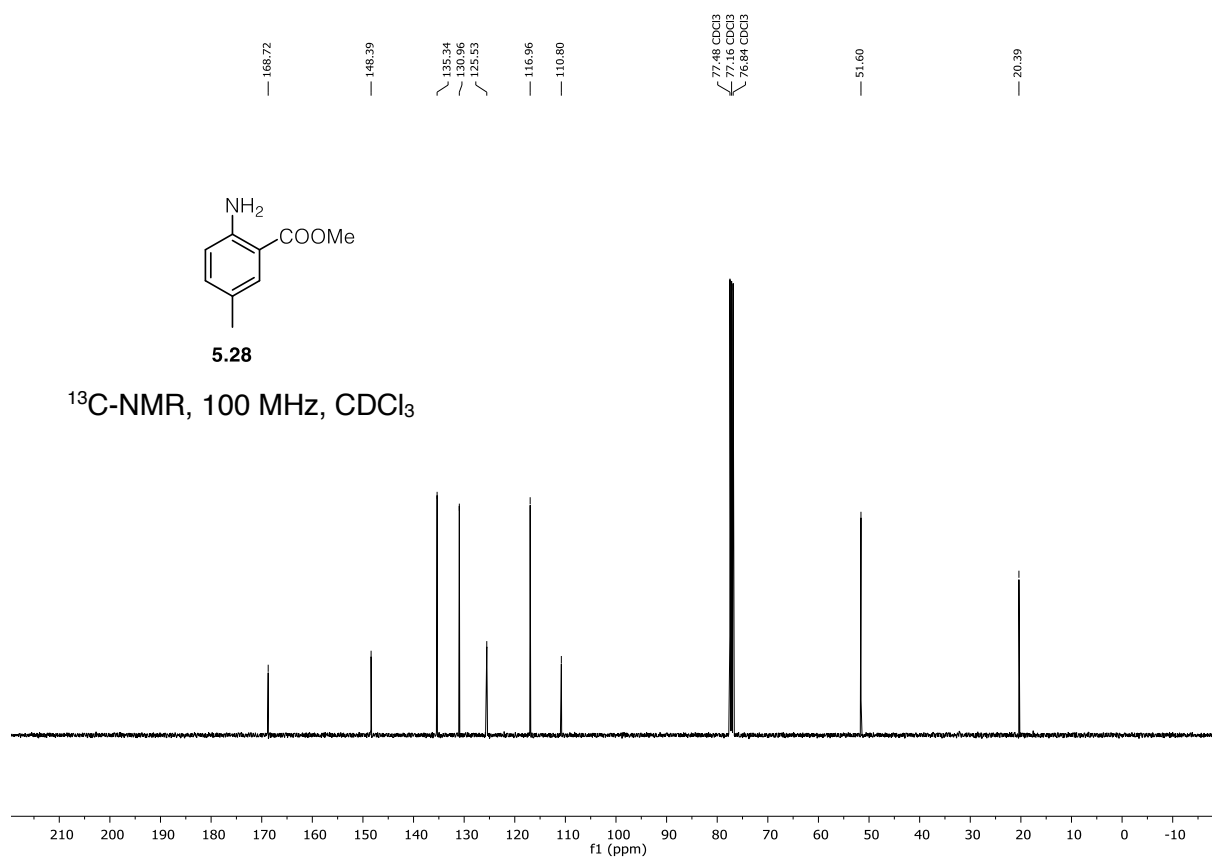
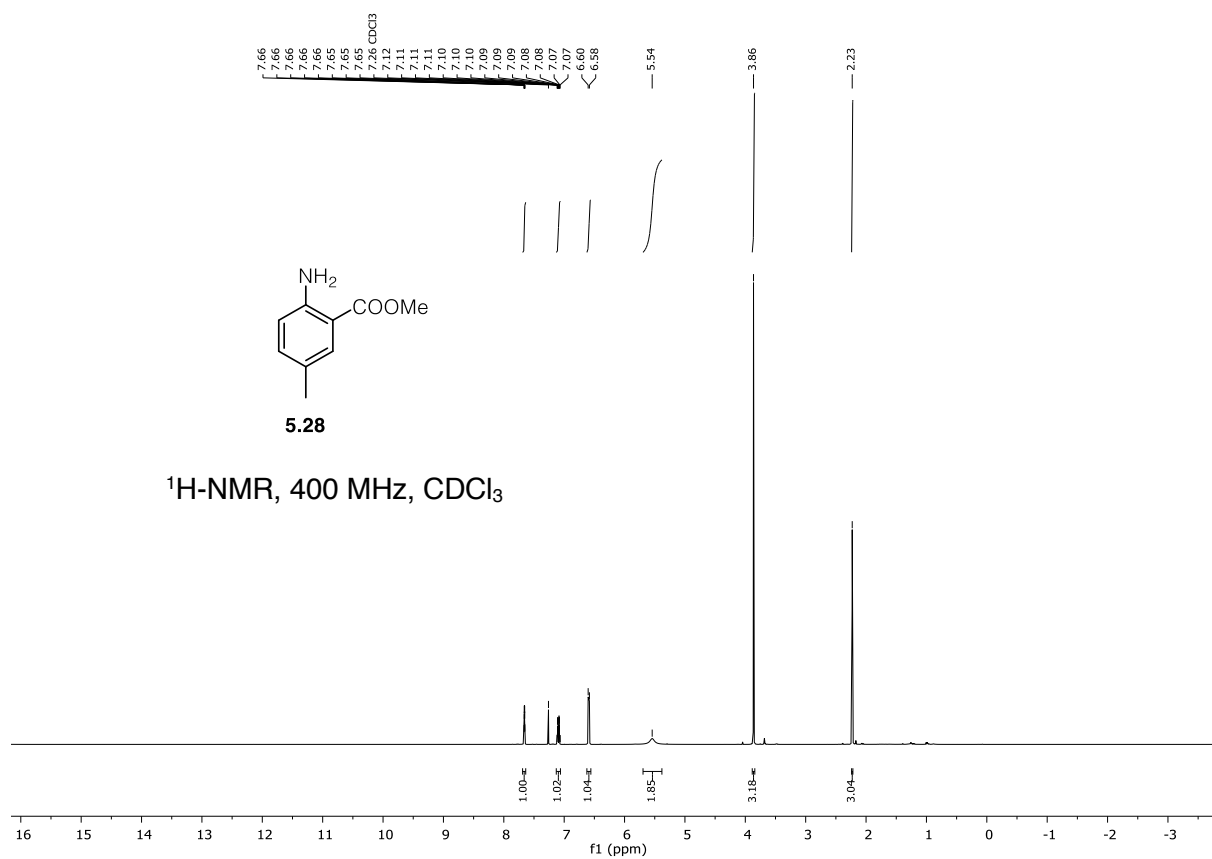


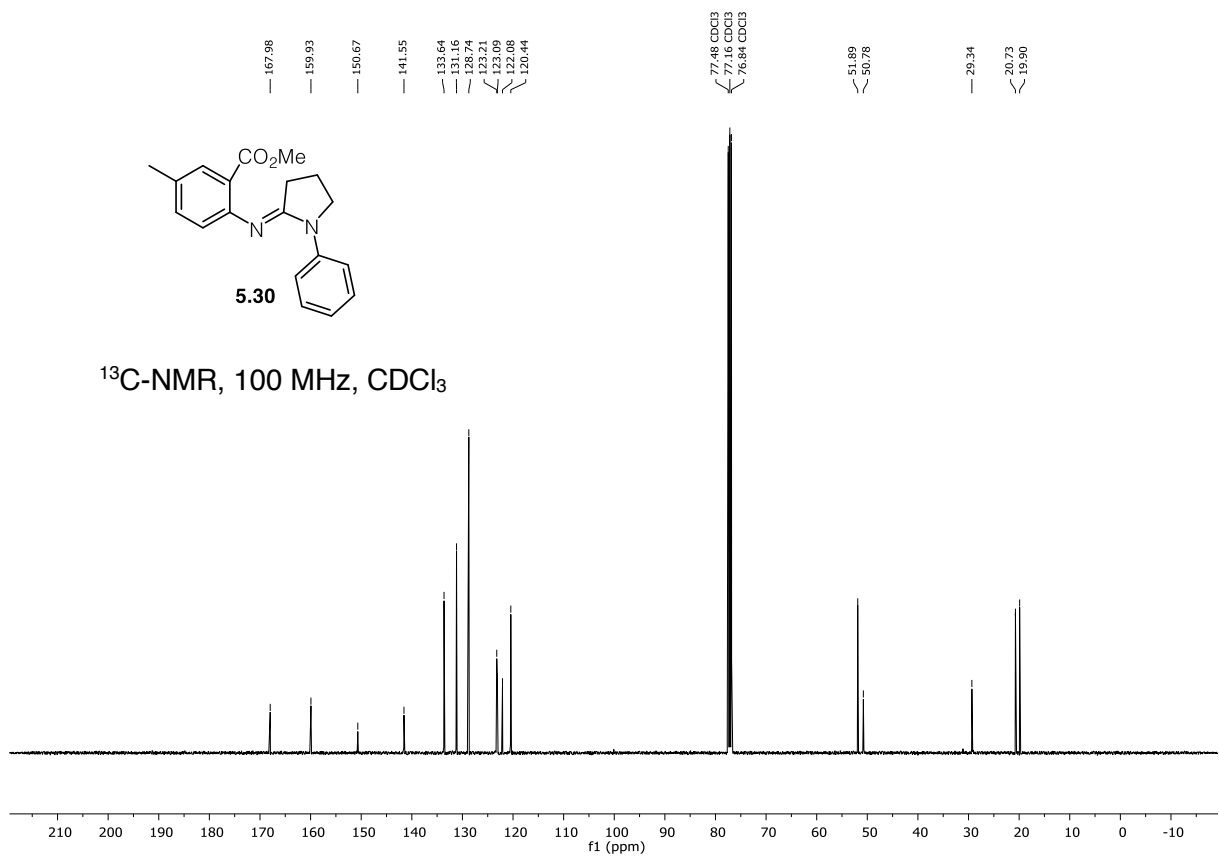
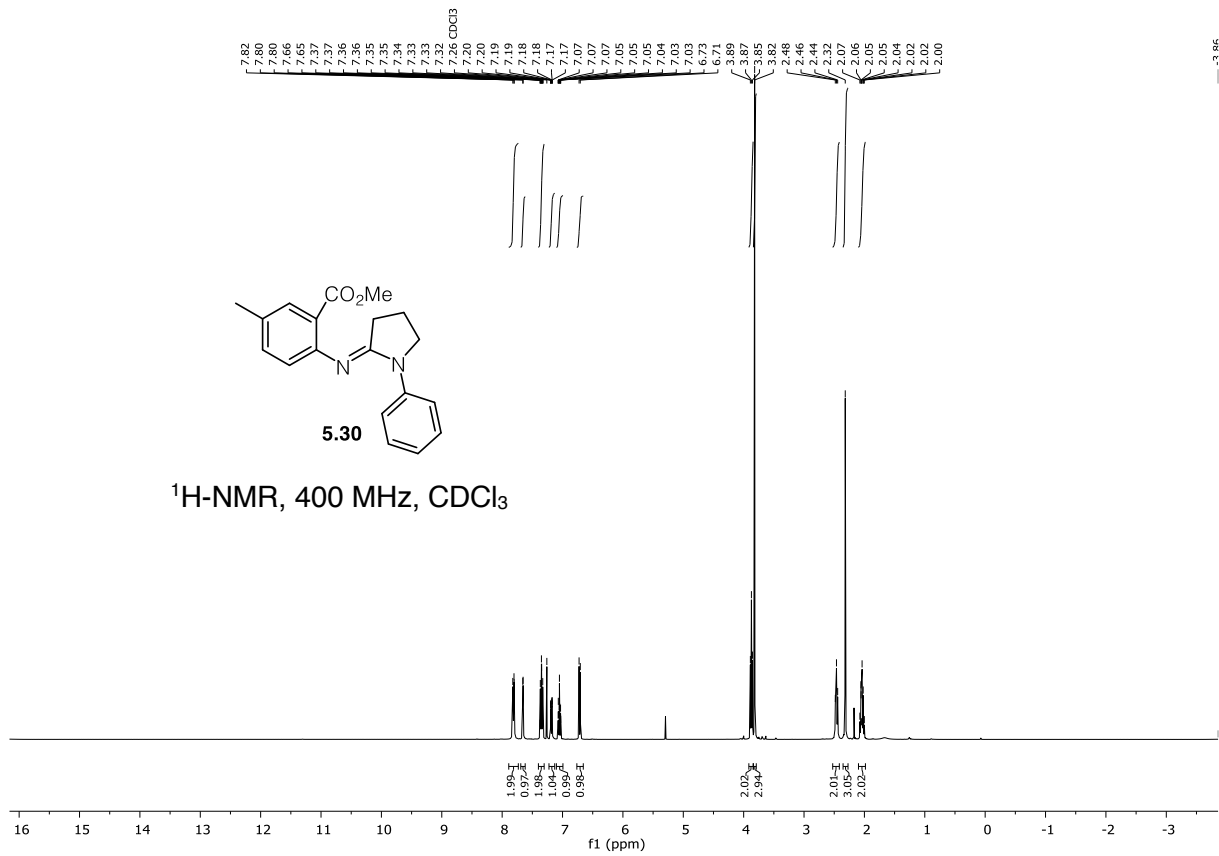


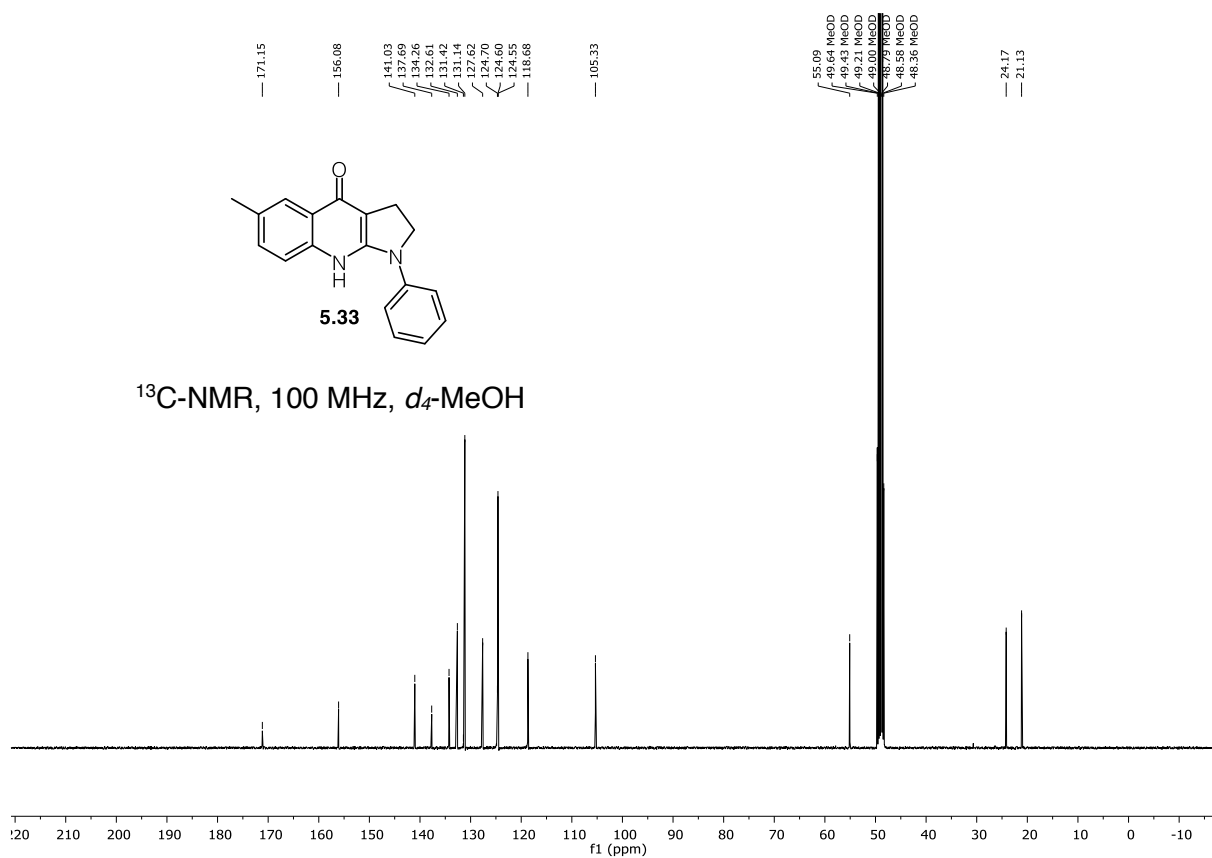
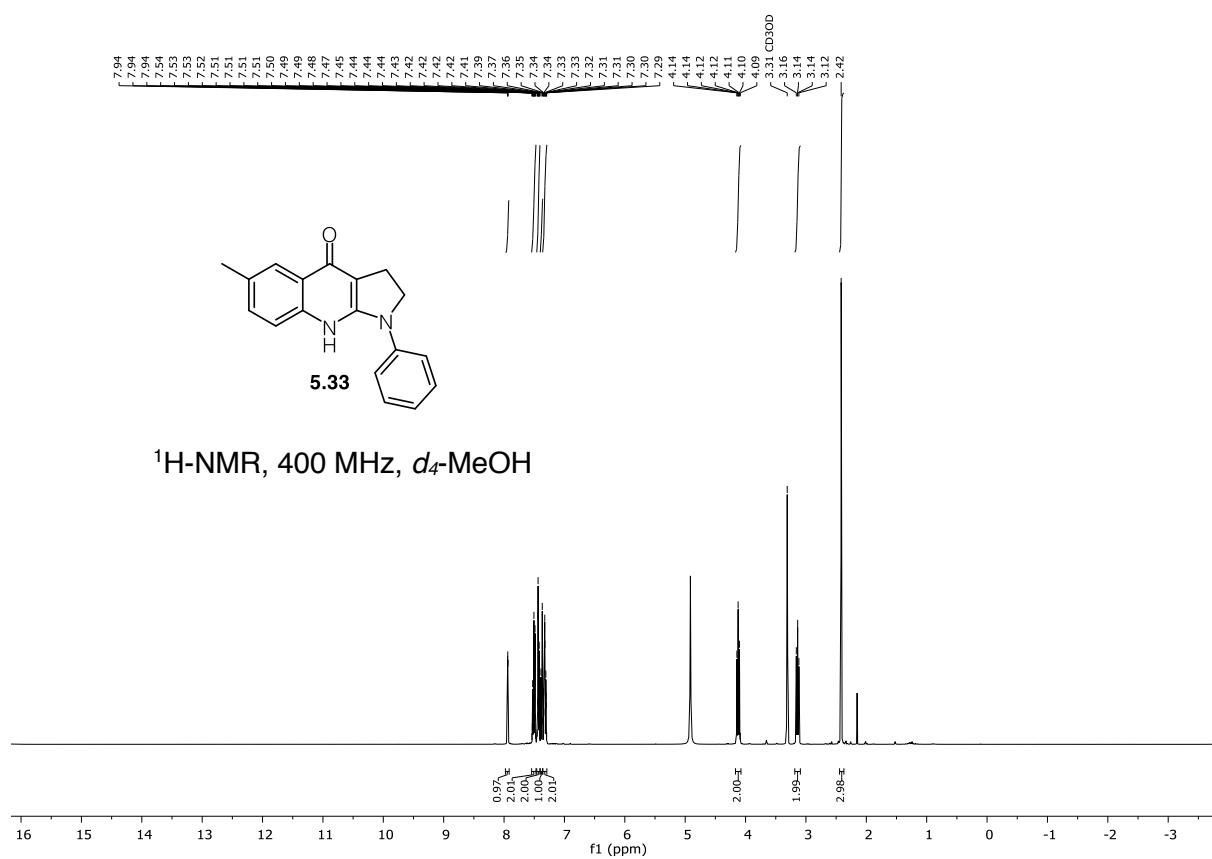


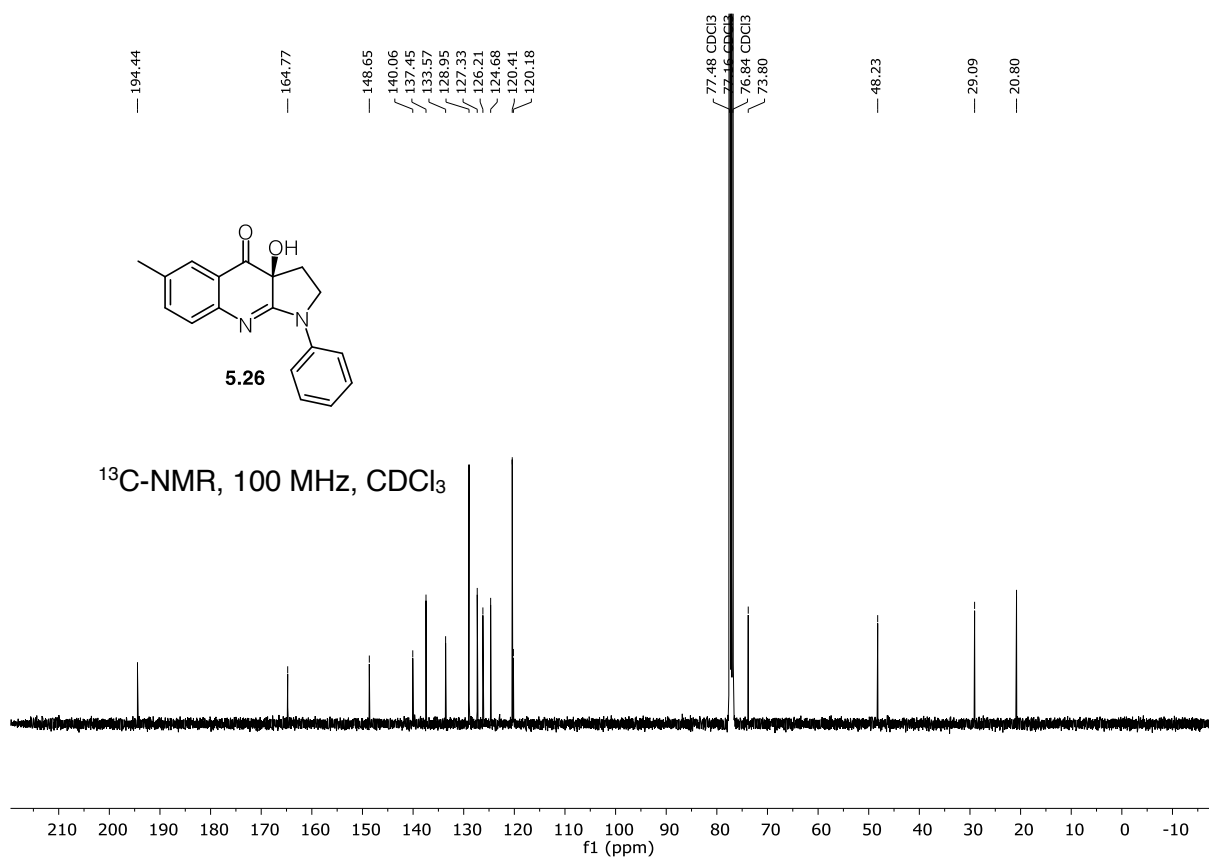
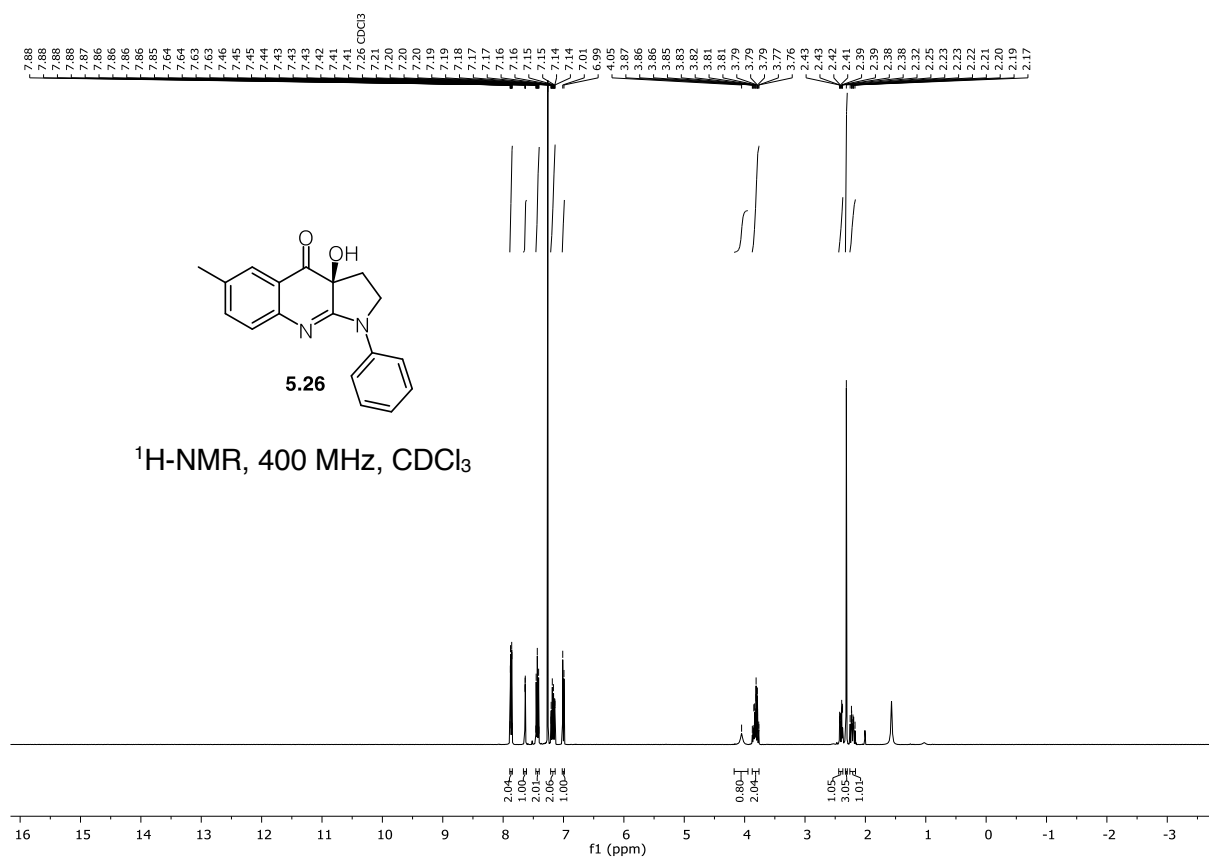


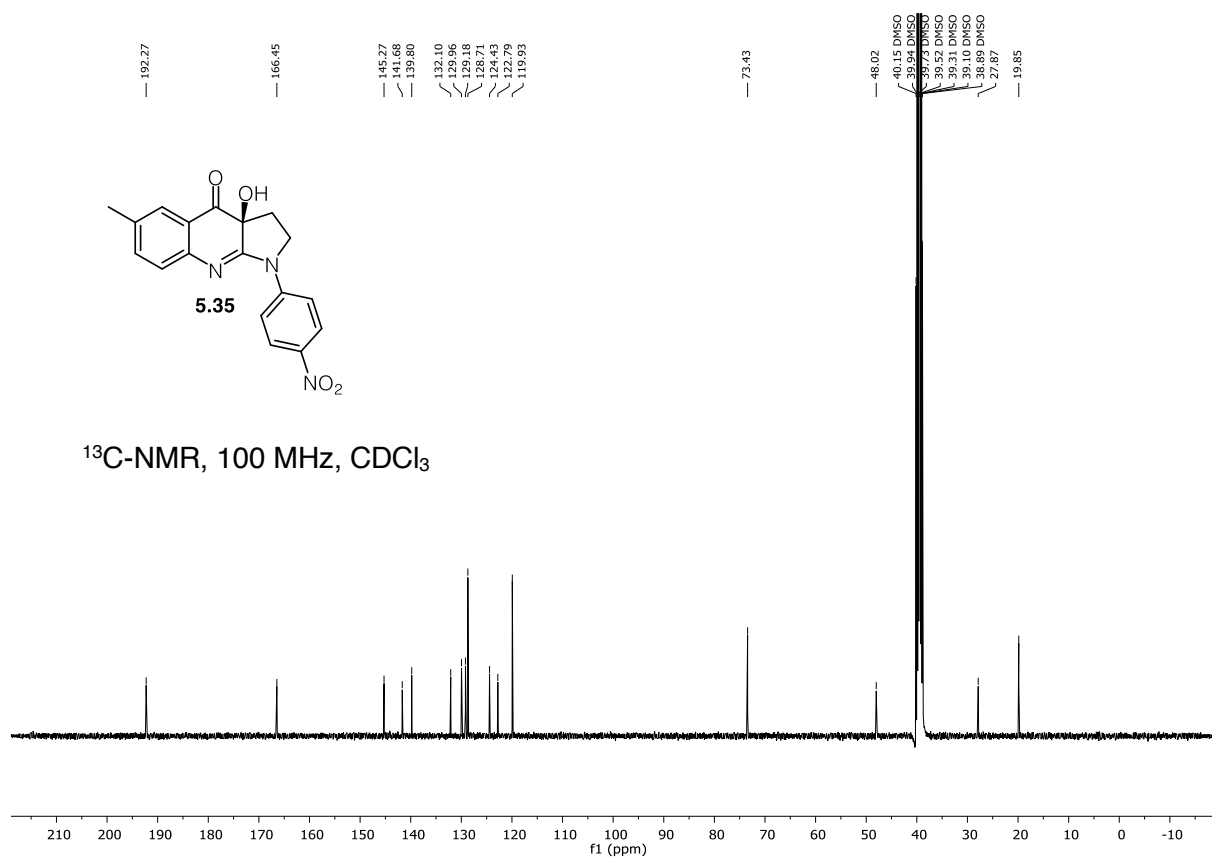
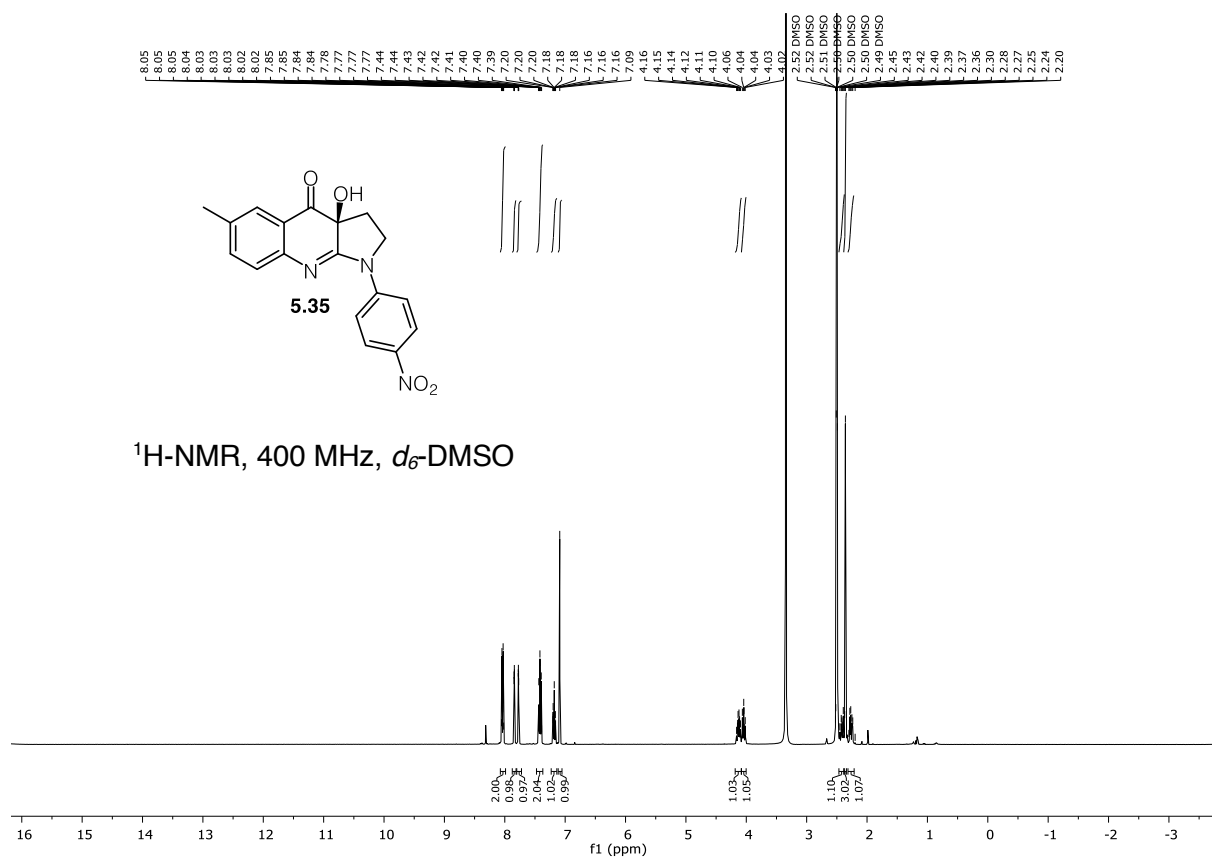


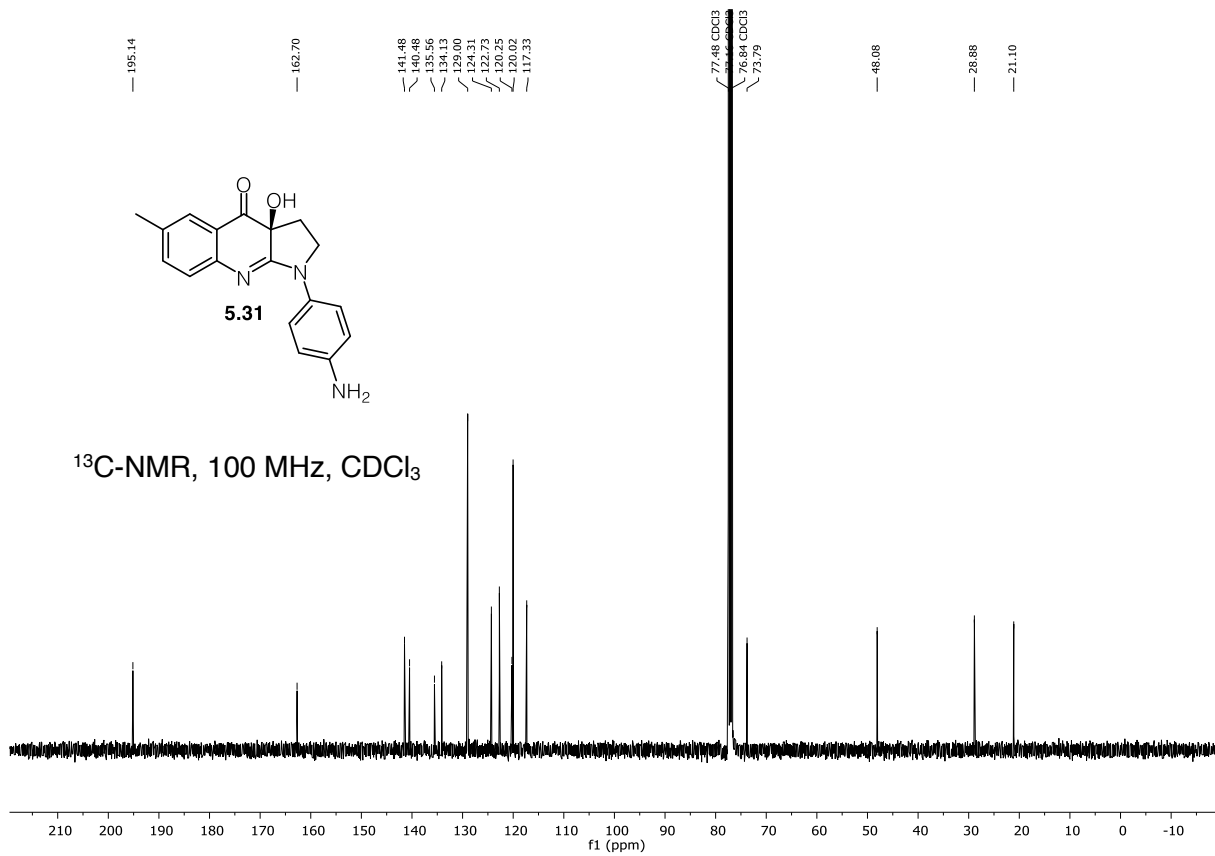
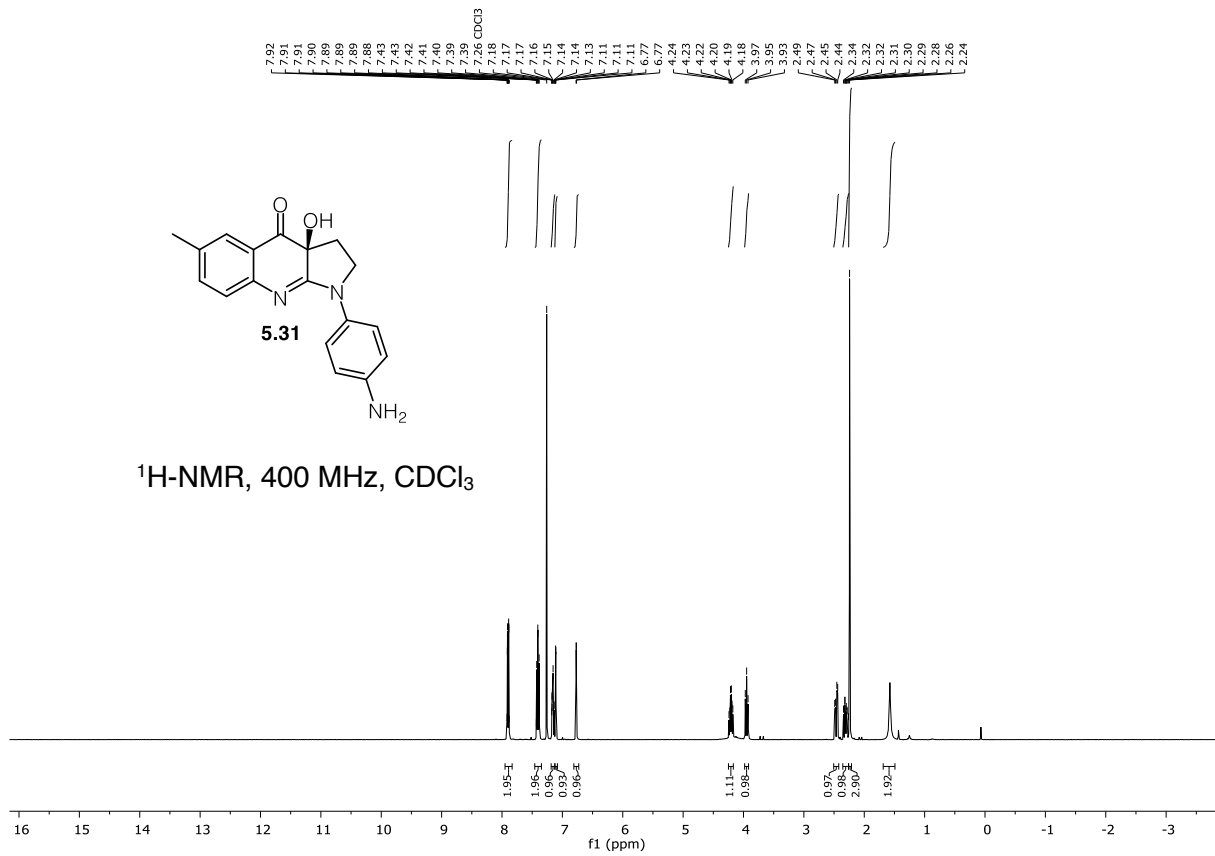


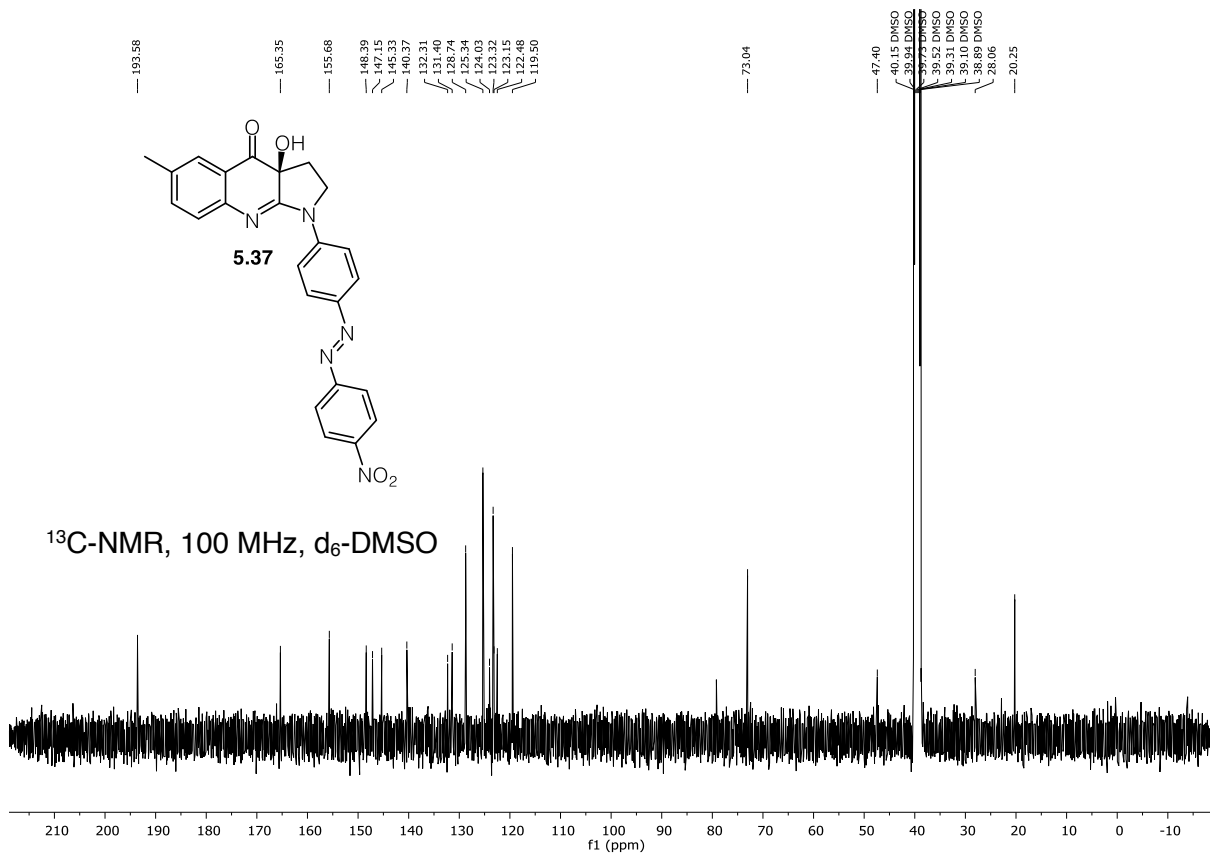
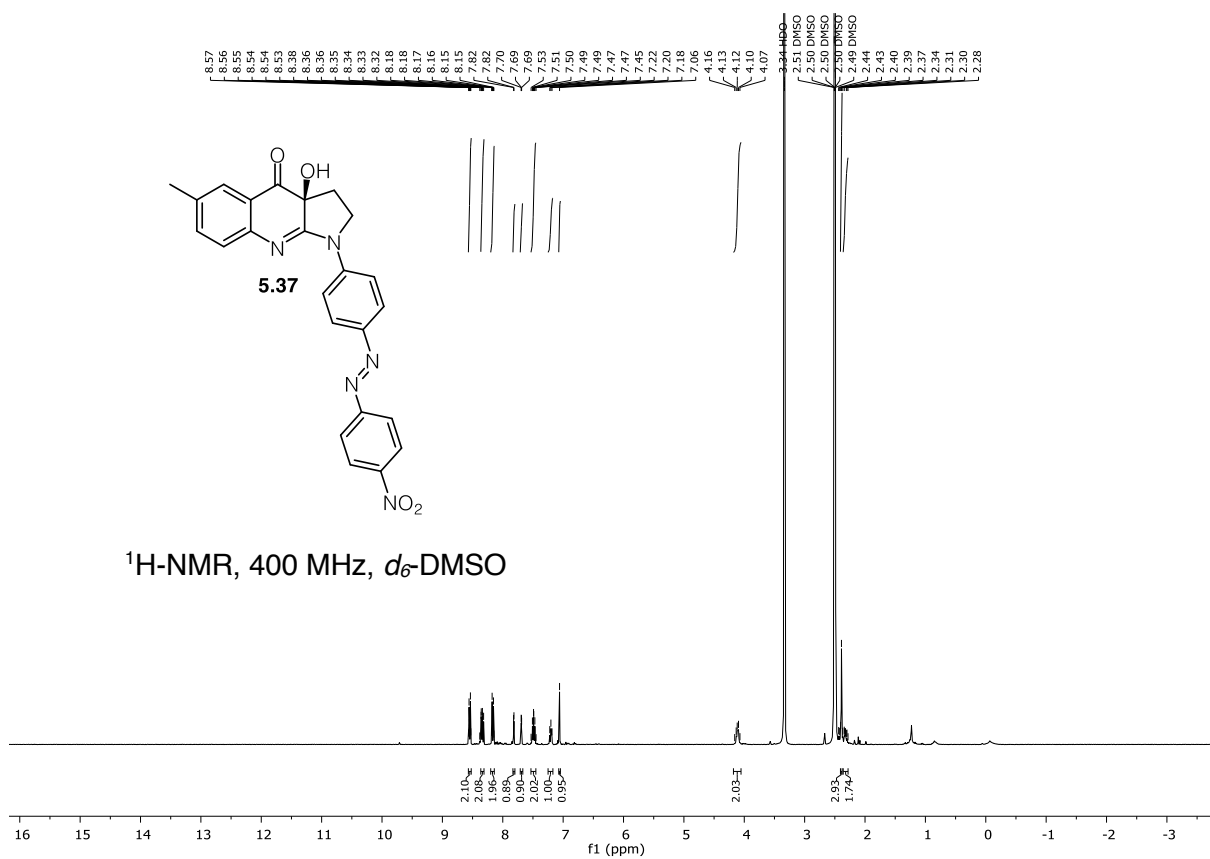


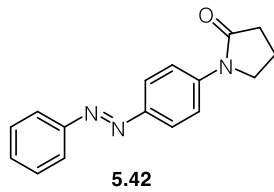




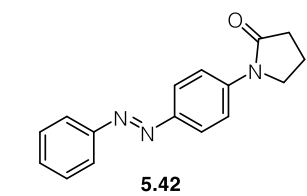
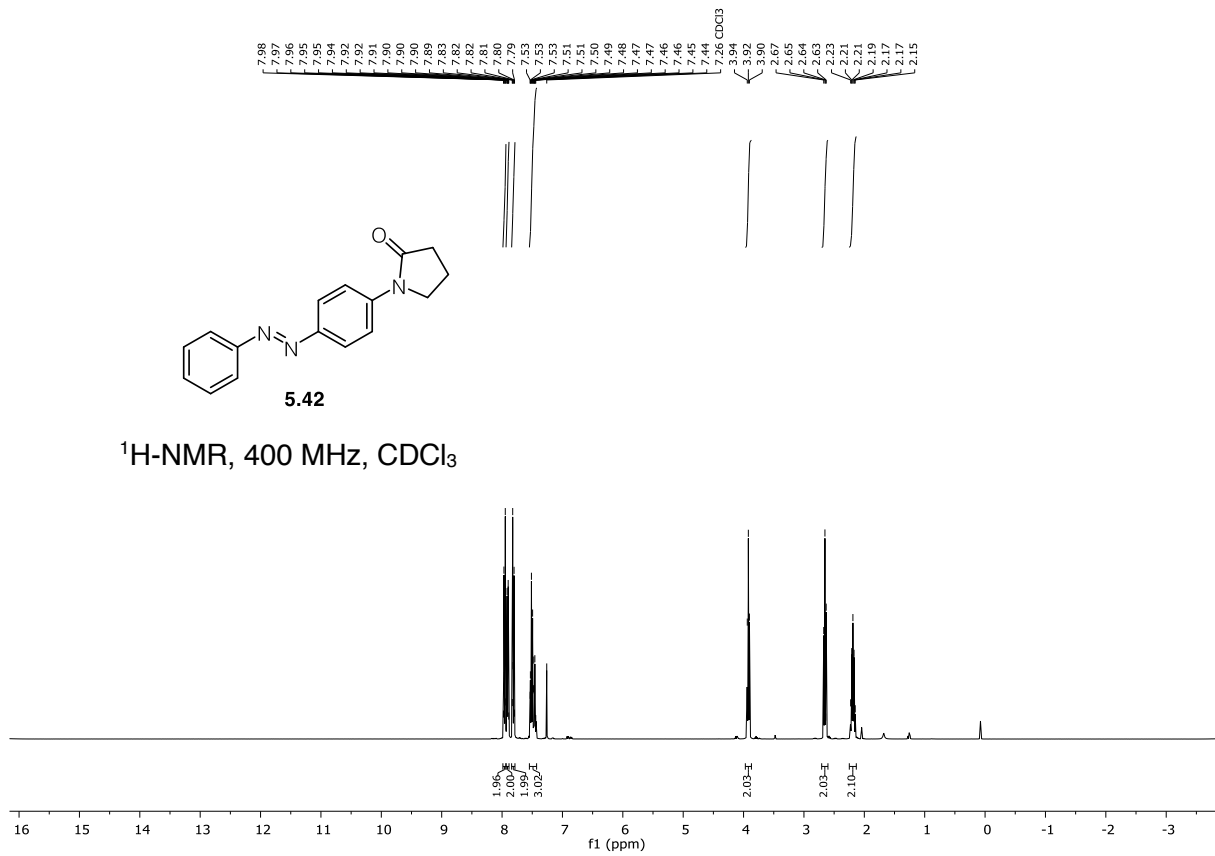




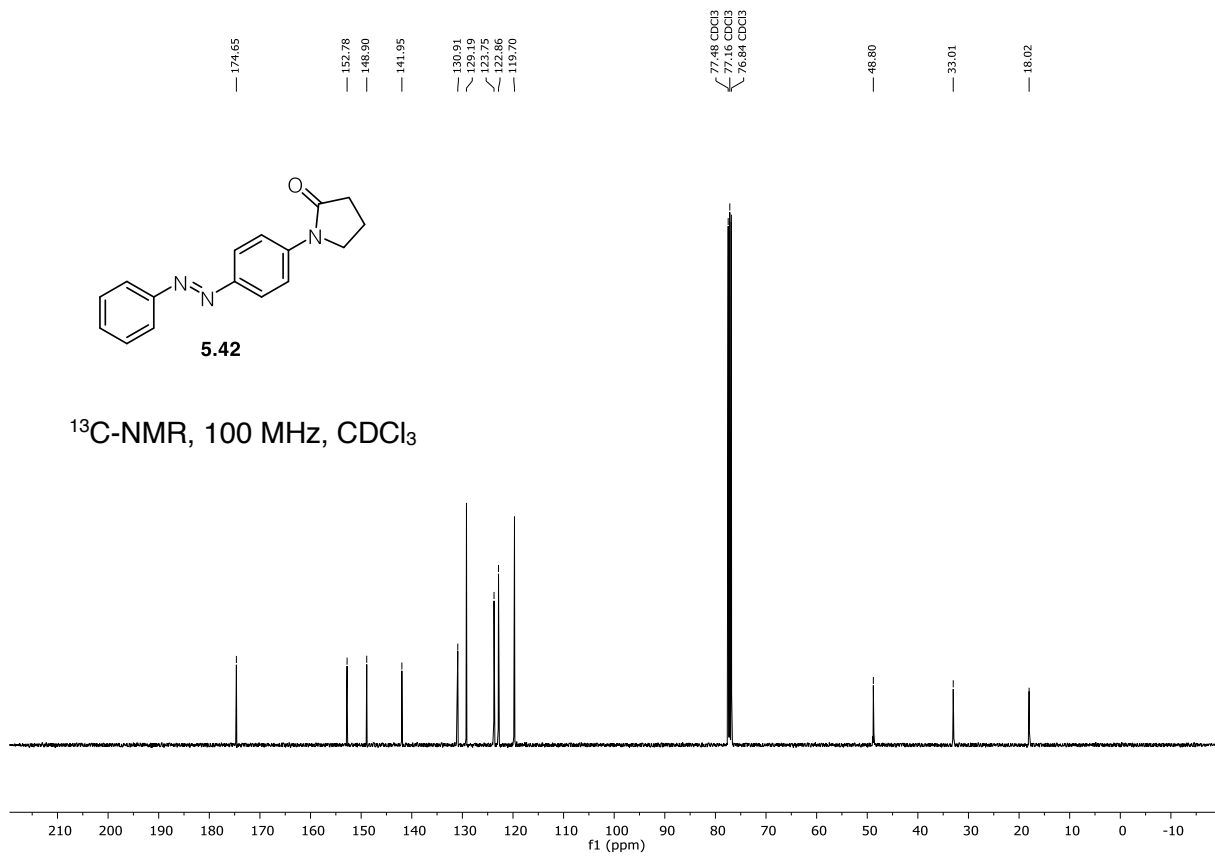


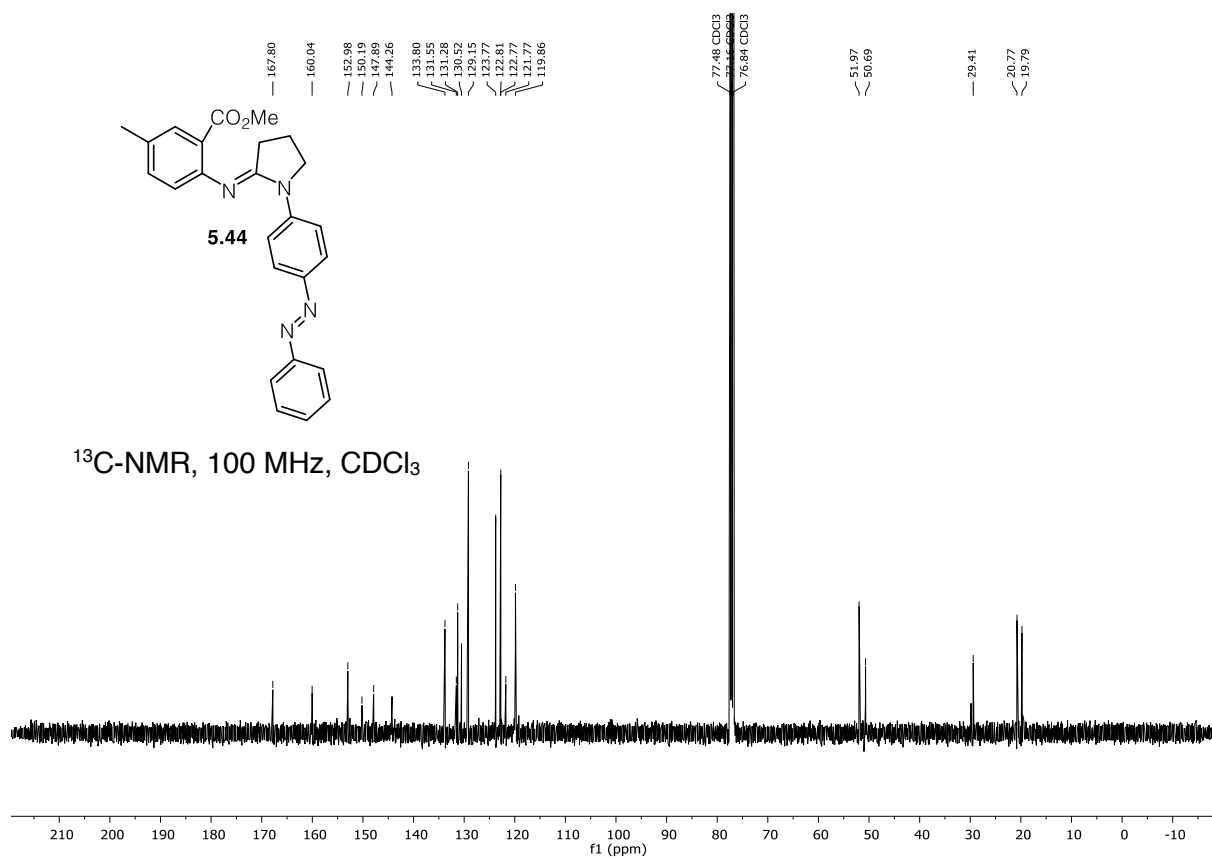
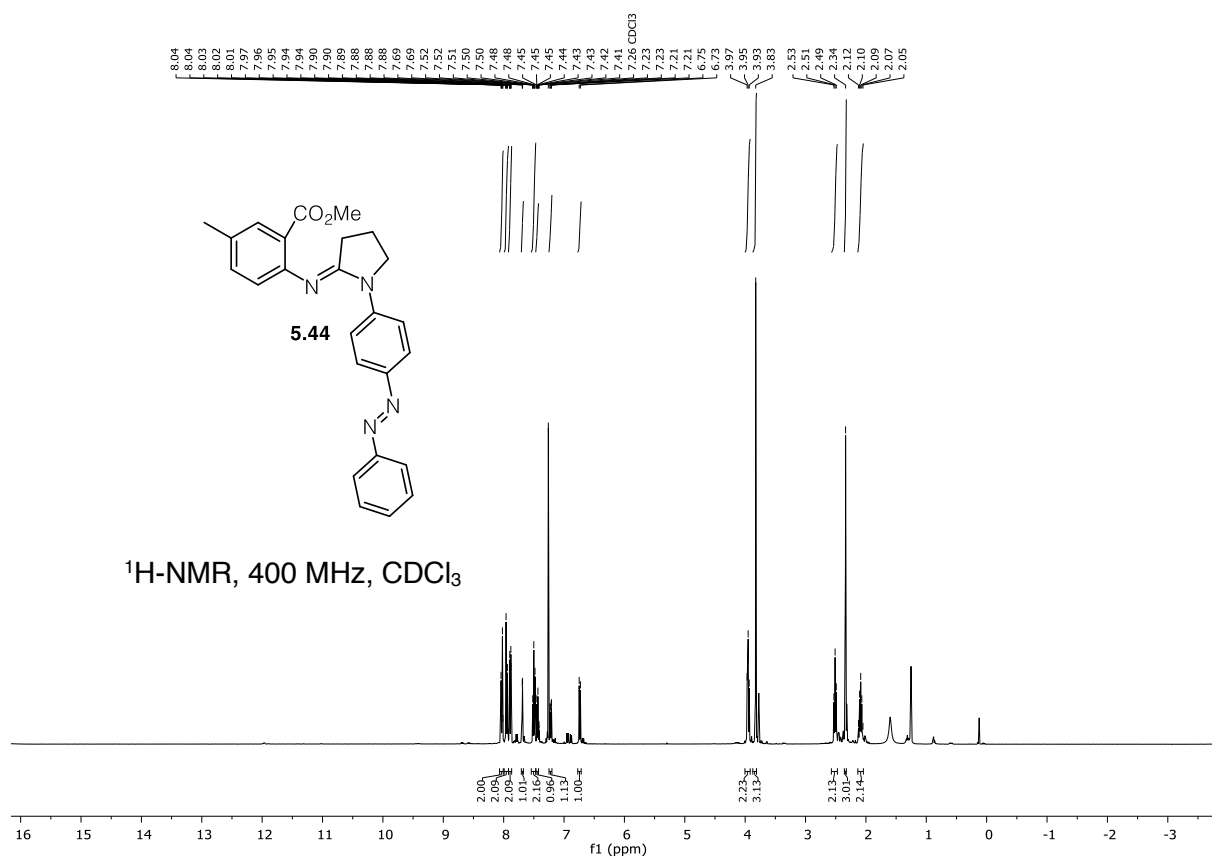


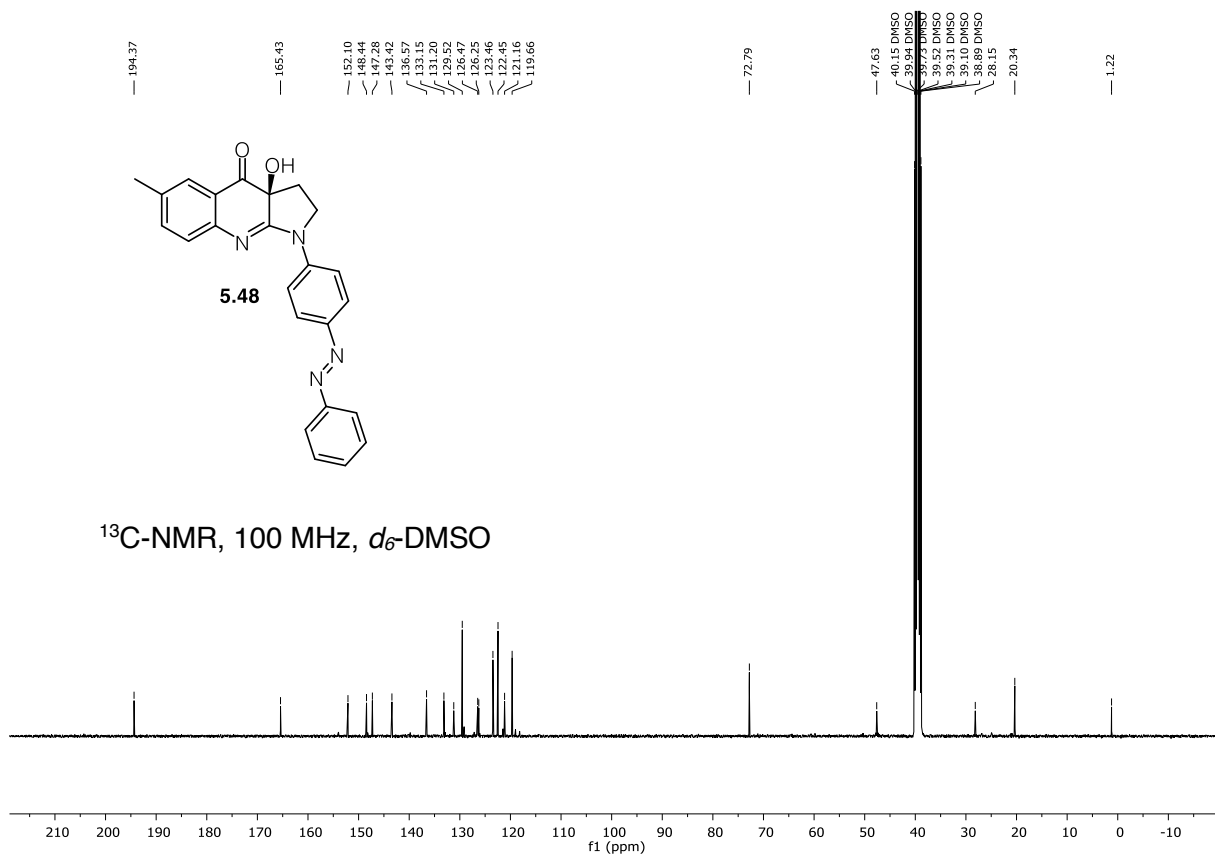
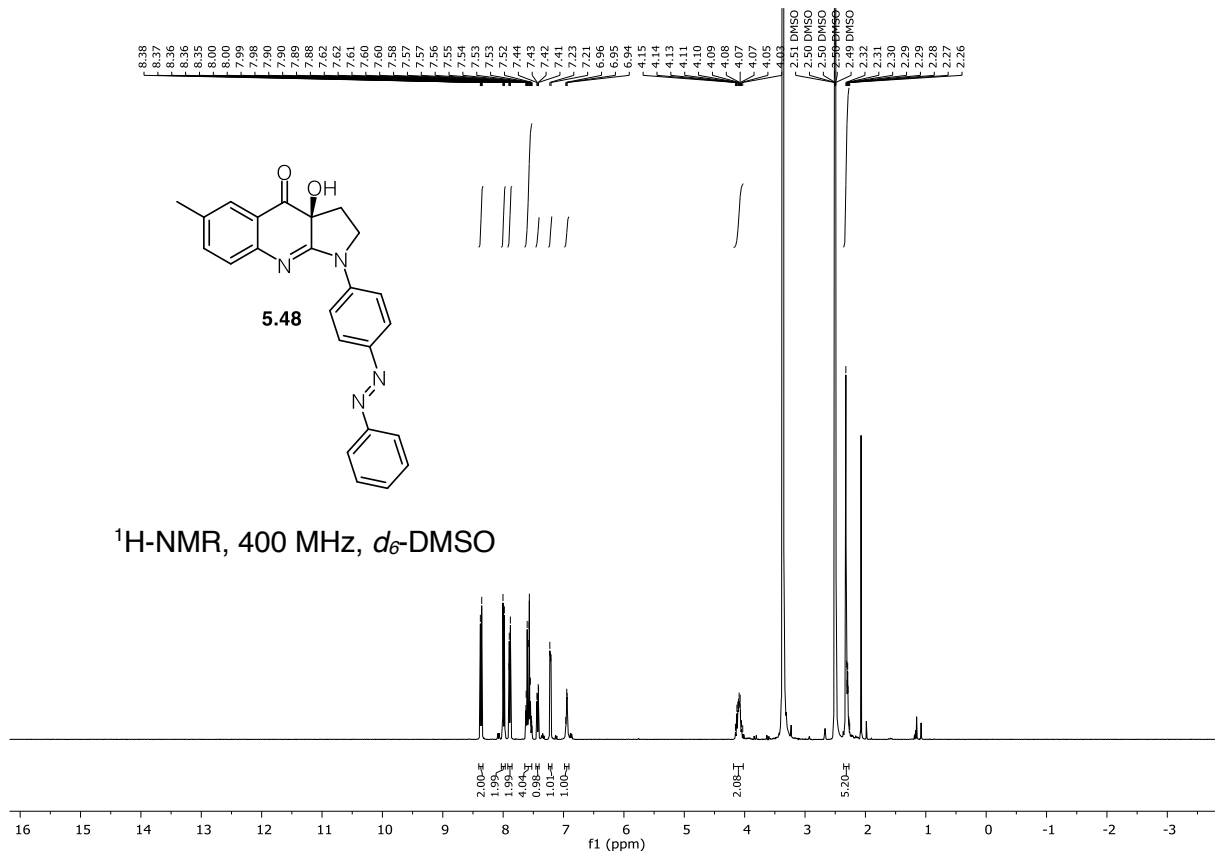
$^1\text{H-NMR}$, 400 MHz, CDCl_3

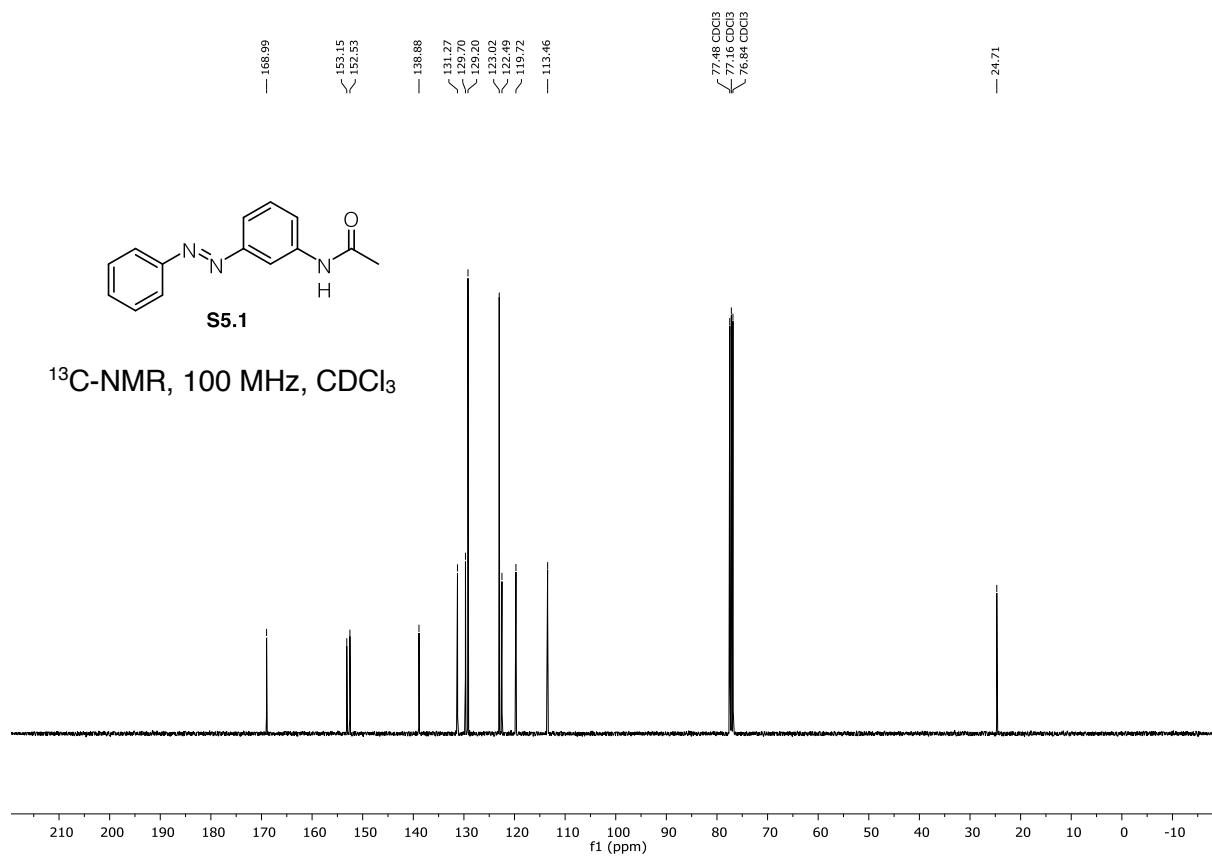
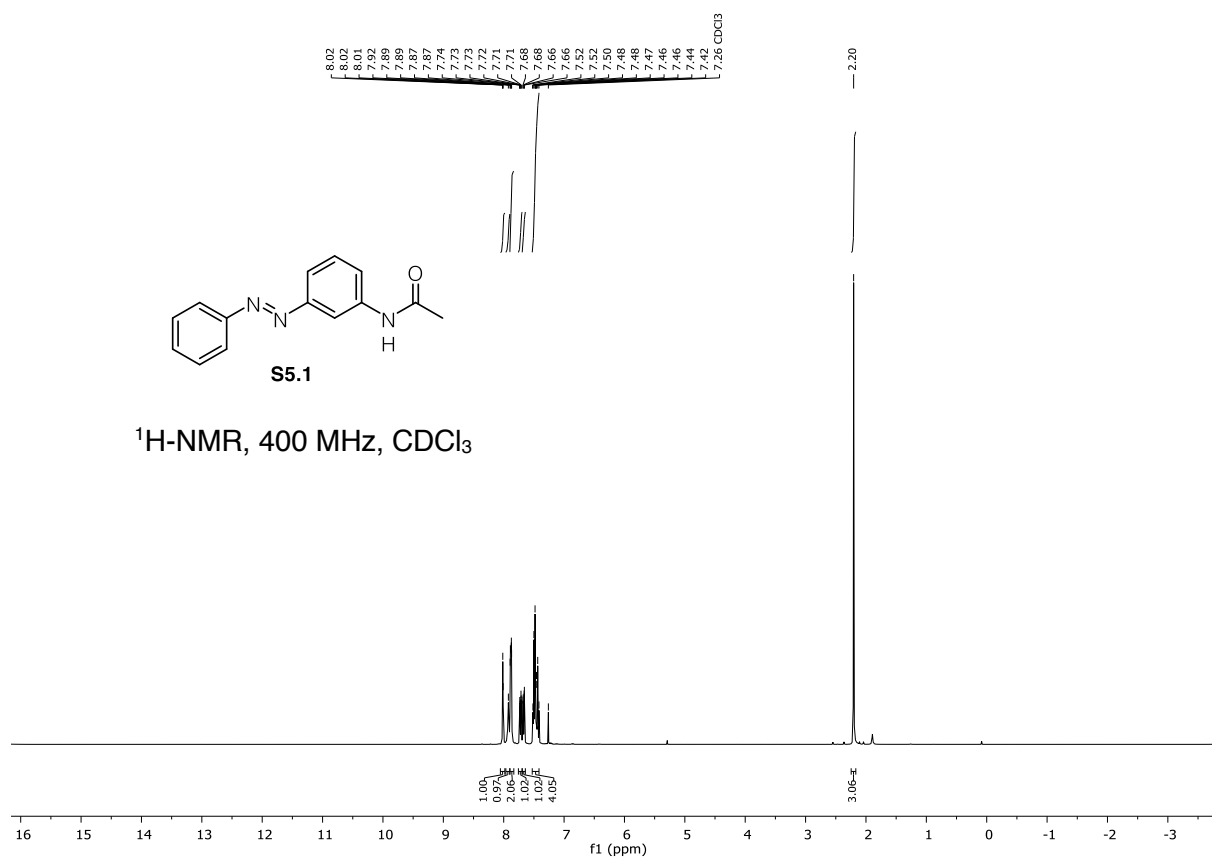


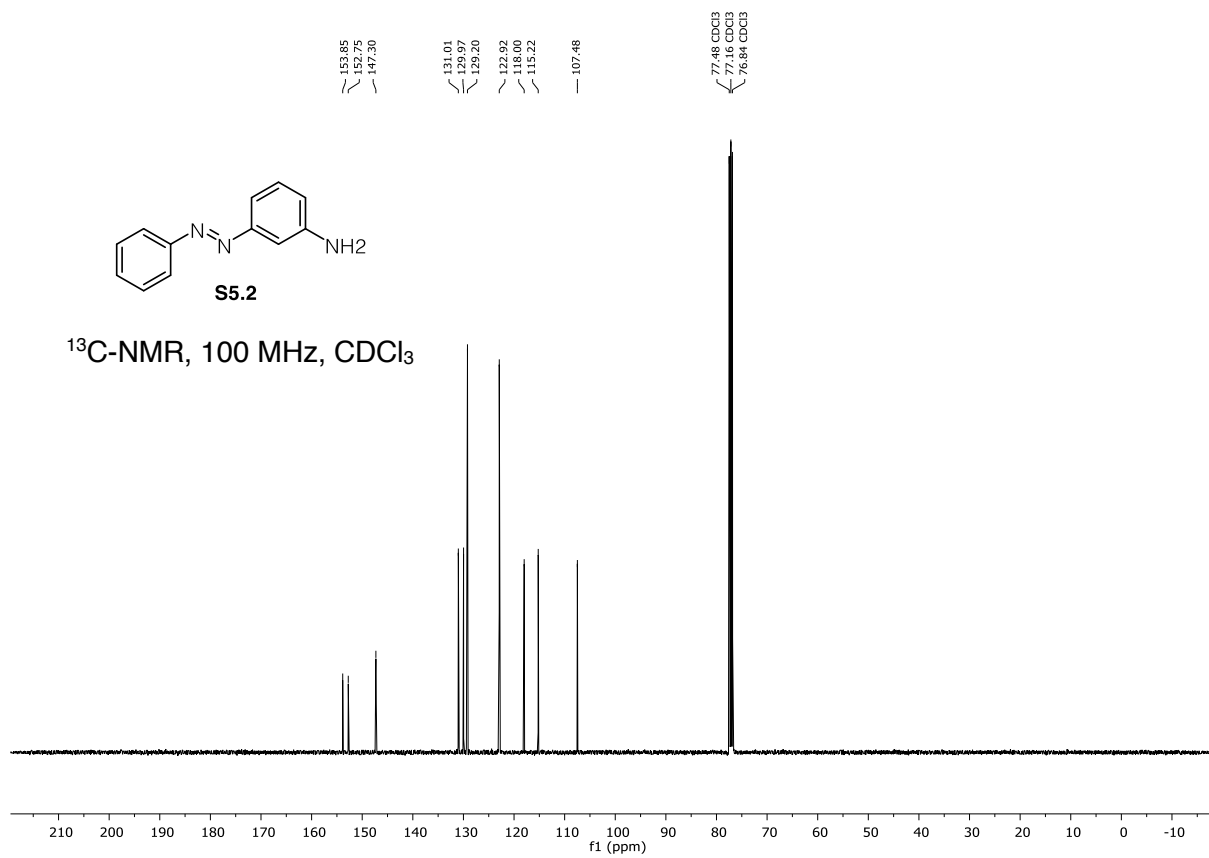
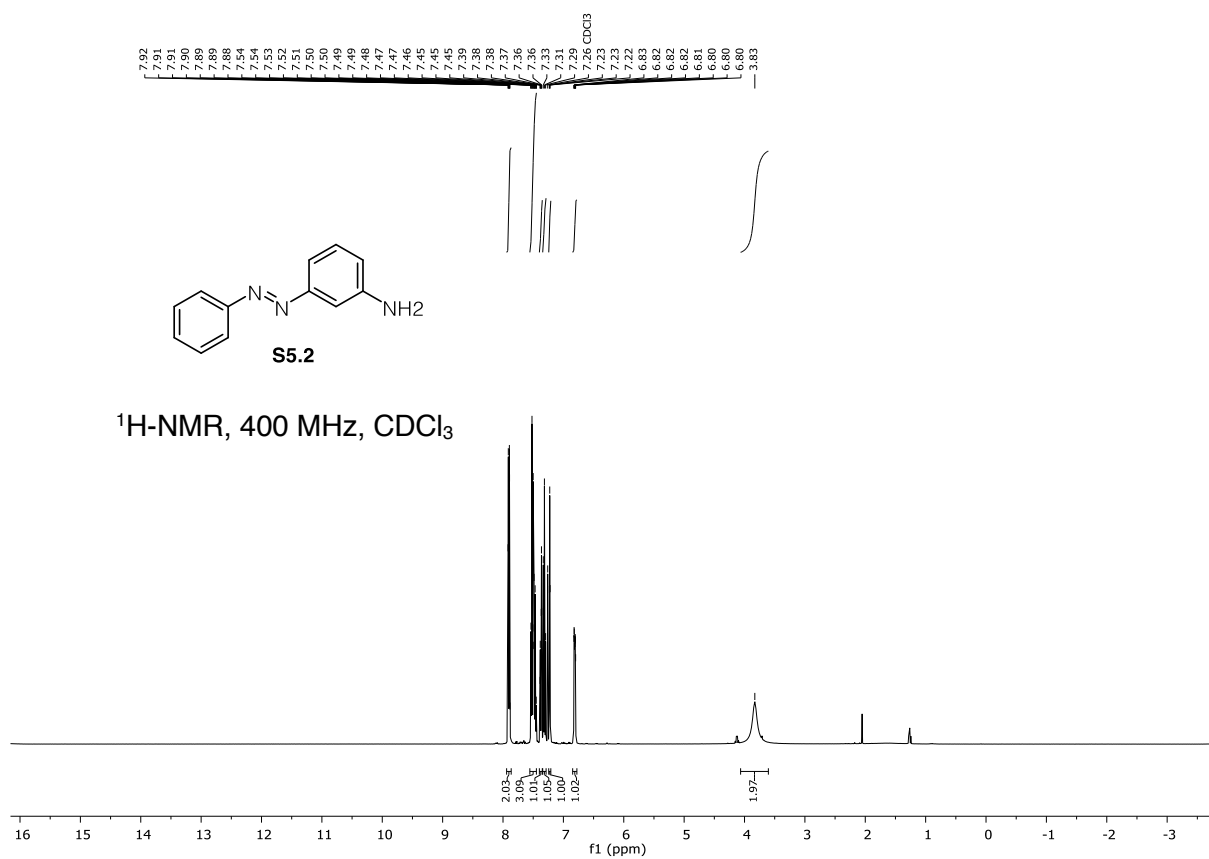
$^{13}\text{C-NMR}$, 100 MHz, CDCl_3

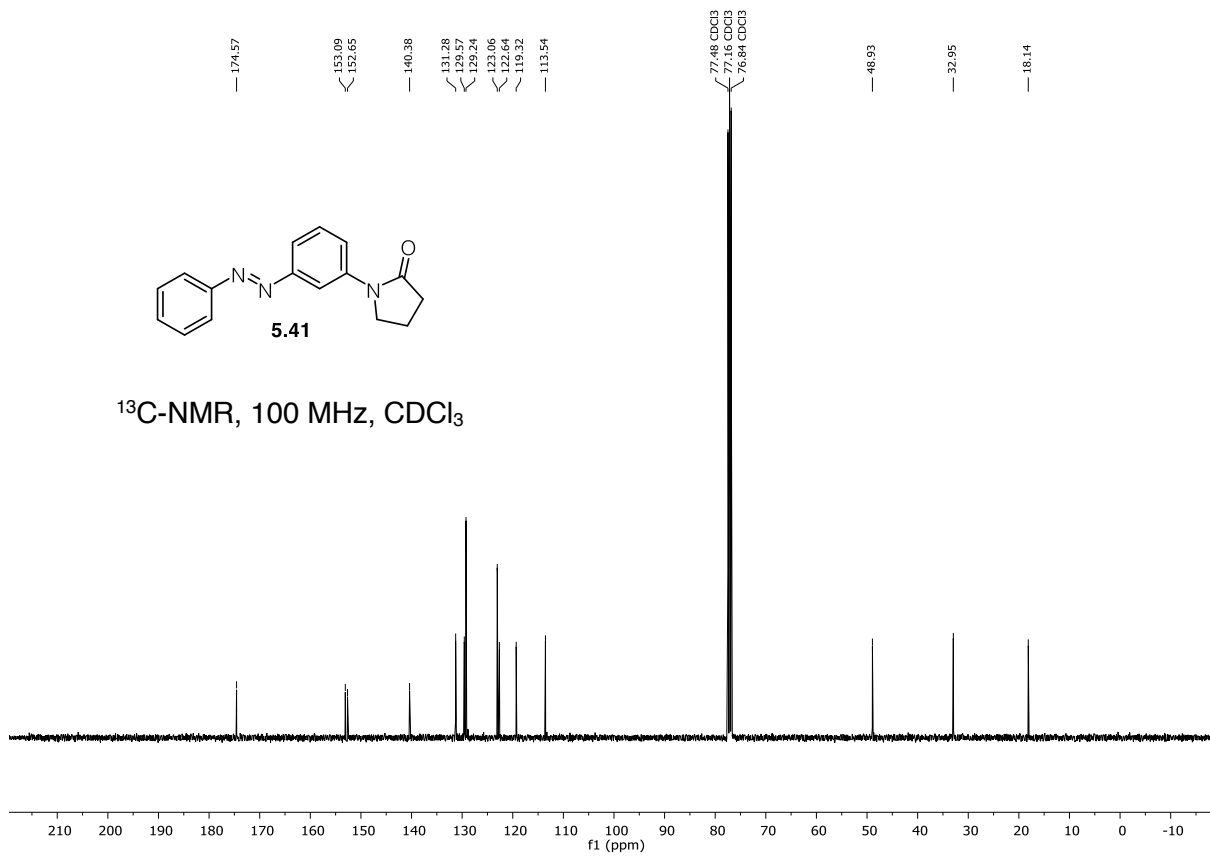
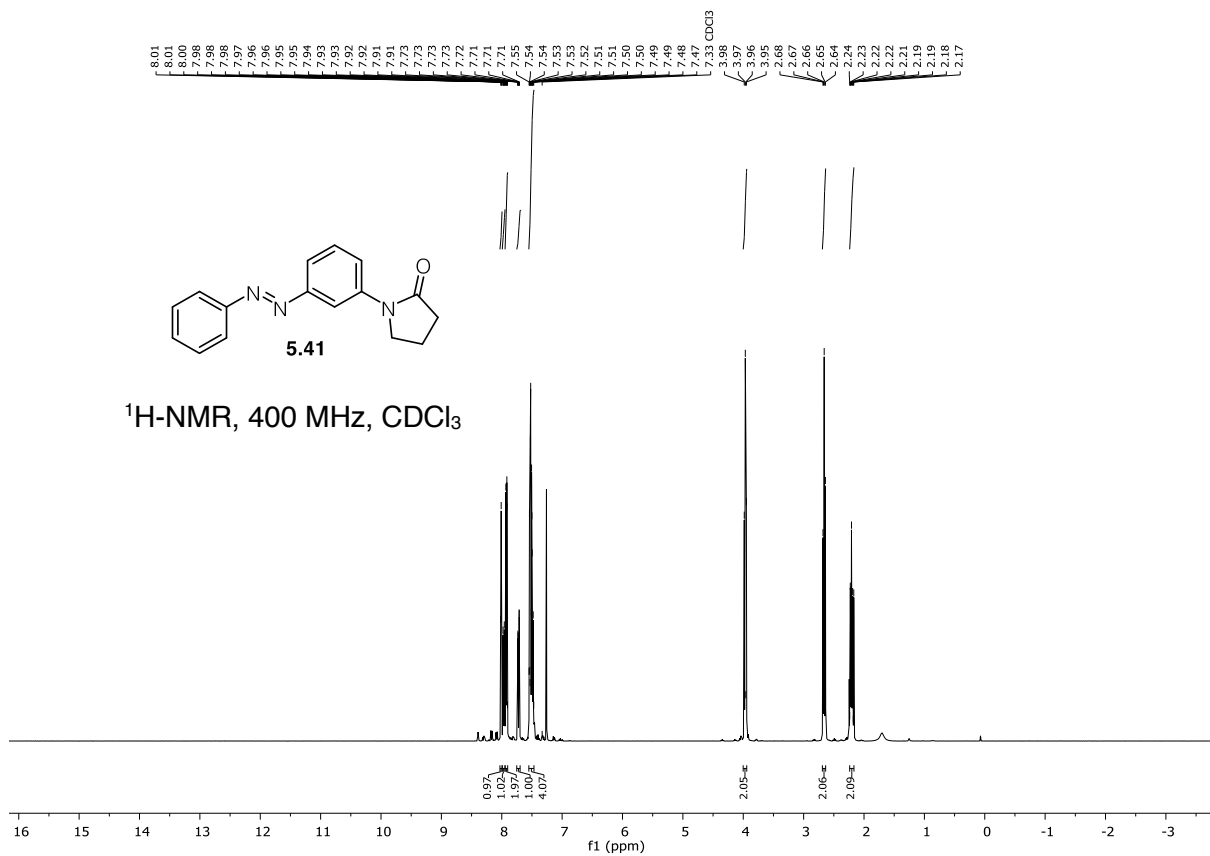


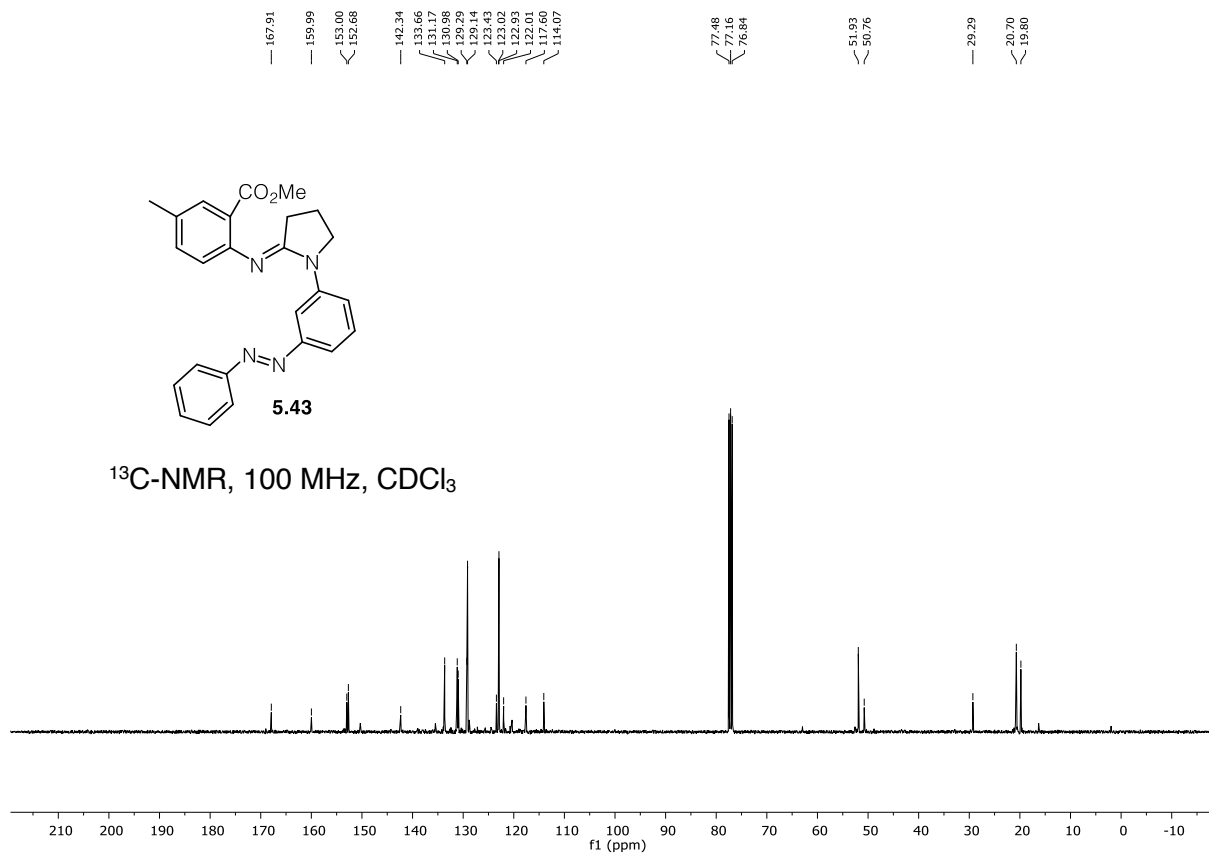
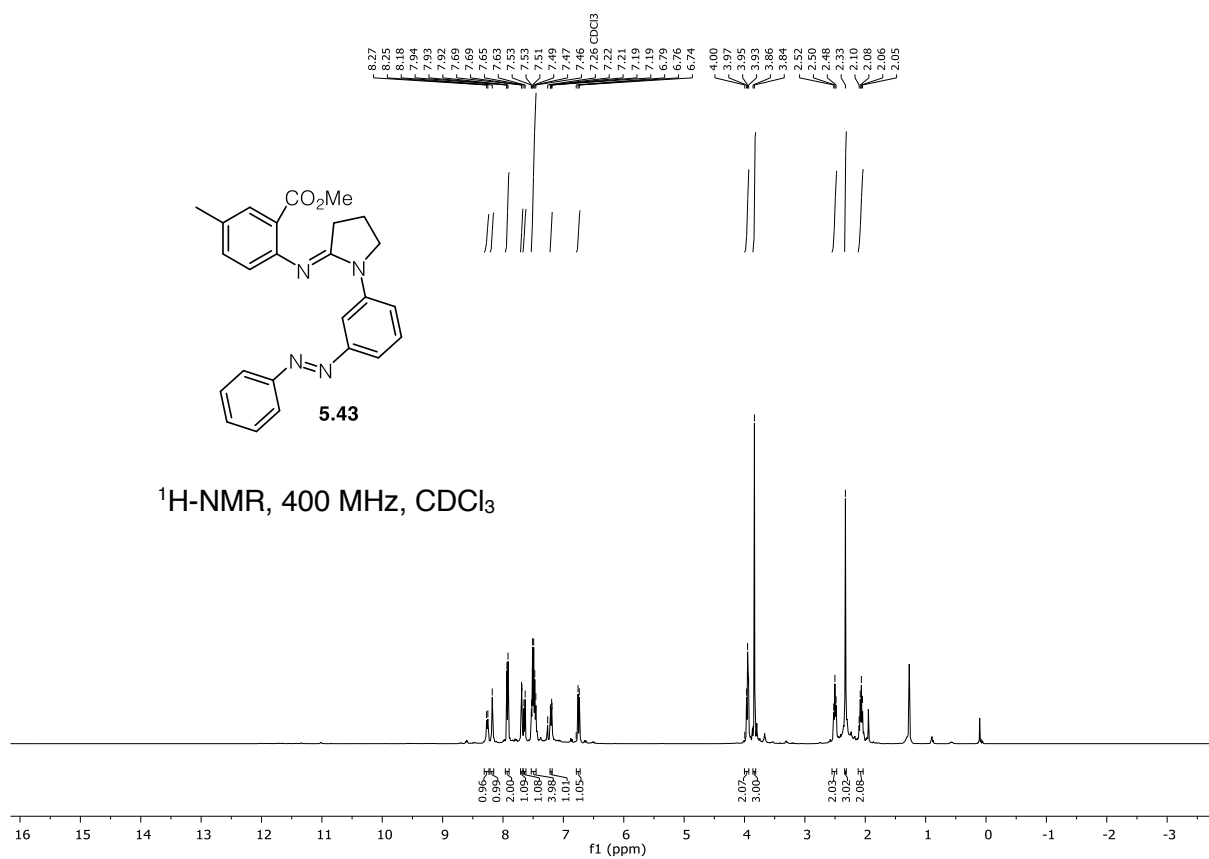


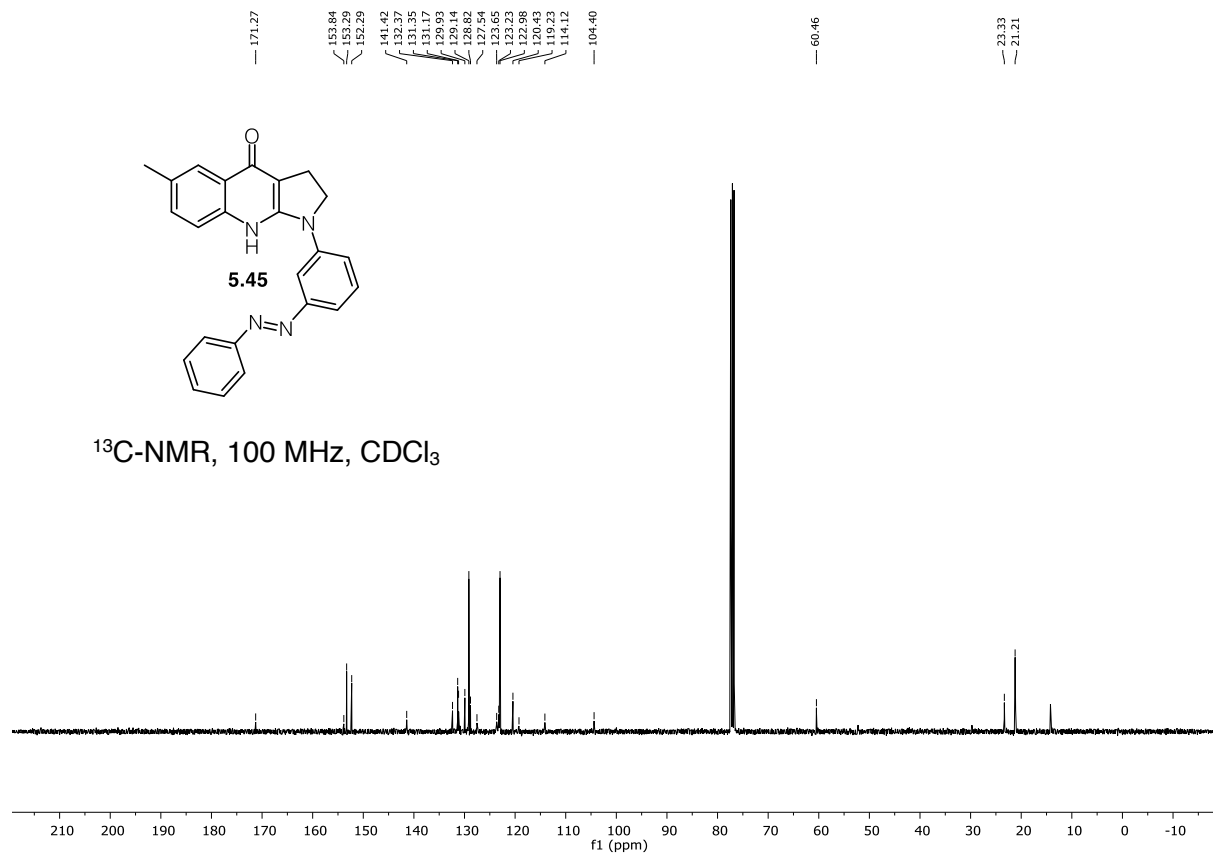
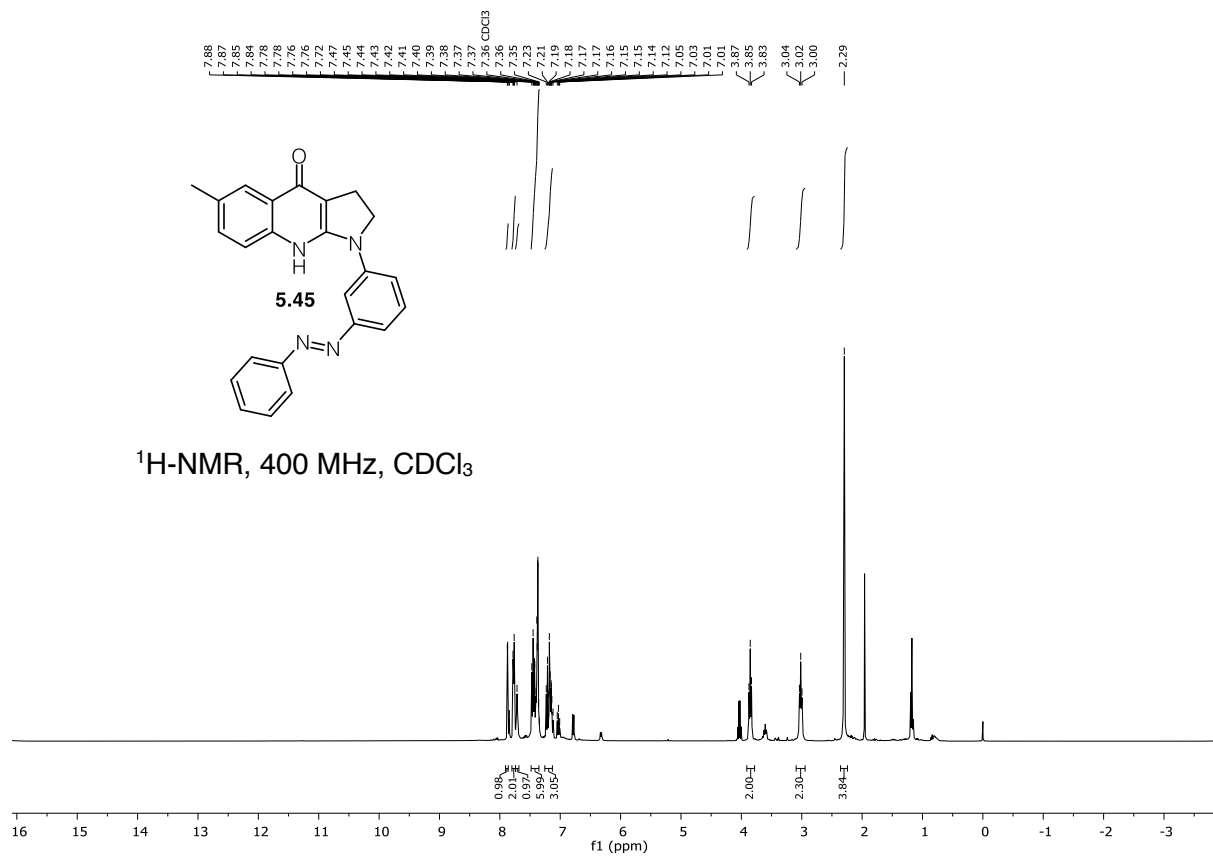


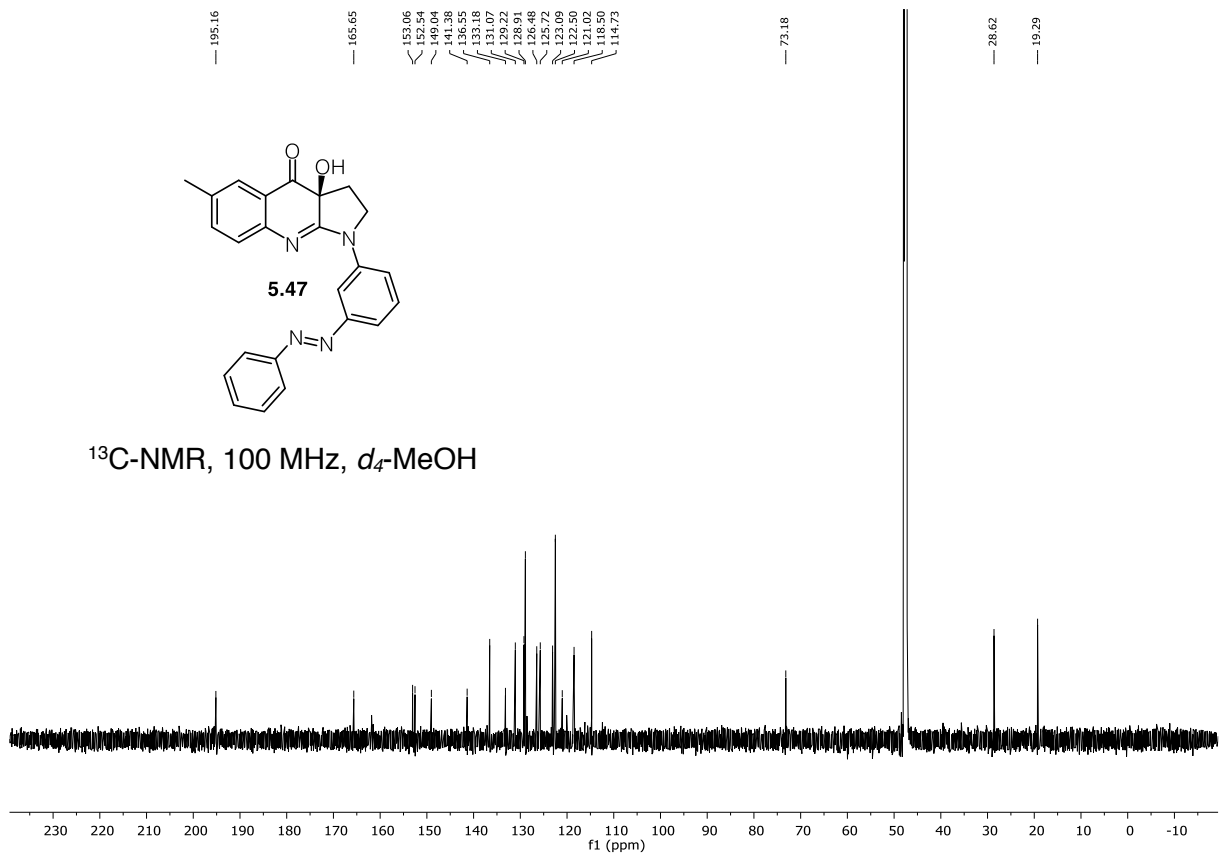
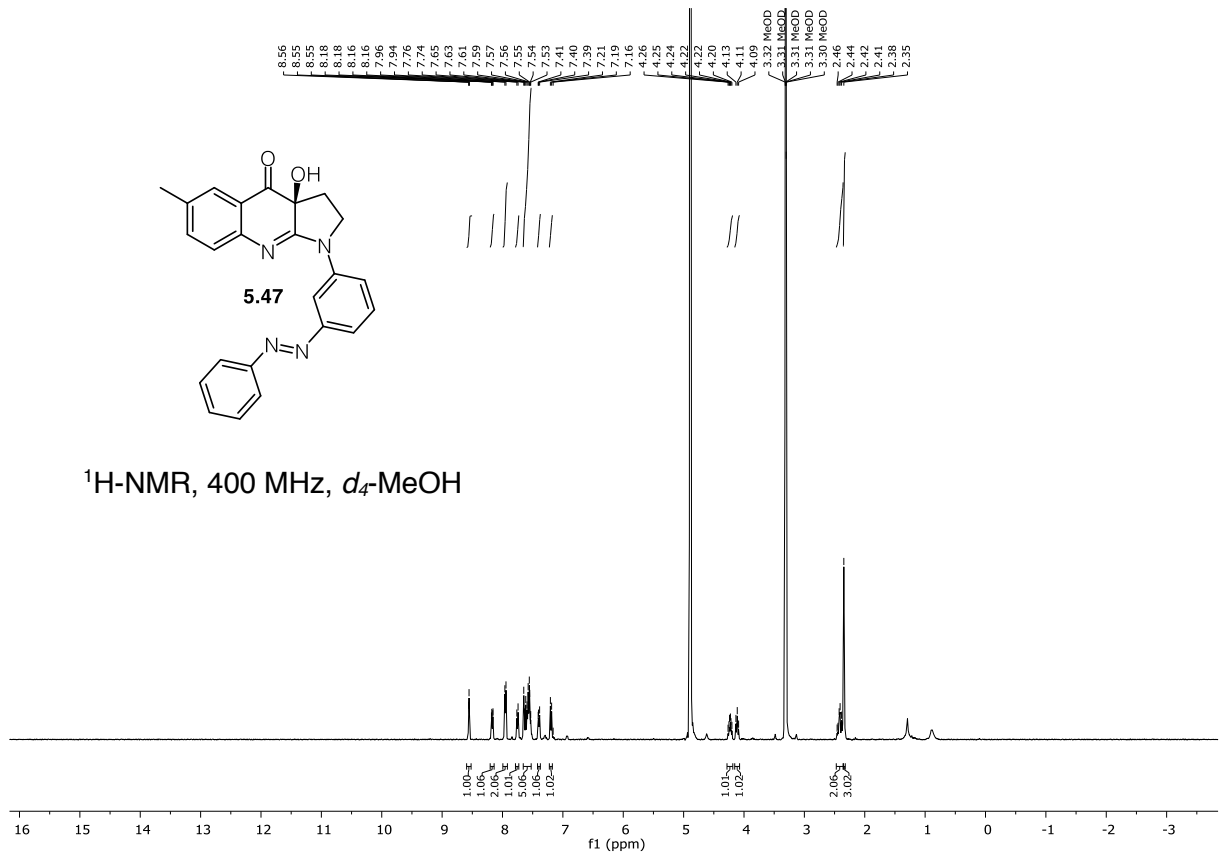












7.3 Literature

1. Kobayashi, M.; Kondo, K.; Kitagawa, I., Antifungal peroxyketal acids from an okinawan marine sponge of plakortis sp. *Chem. Pharm. Bull.* **1993**, *41* (7), 1324-1326.
2. Davidson, B. S., Cytotoxic five-membered cyclic peroxides from a Plakortis sponge. *The Journal of Organic Chemistry* **1991**, *56* (23), 6722-6724.
3. Rahm, F.; Harges, P. Y.; Kitching, W., Metabolites from marine Sponges of the genus plakortis. *Heterocycles* **2004**, *64*, 523-575.
4. Piao, S. J.; Song, Y. L.; Jiao, W. H.; Yang, F.; Liu, X. F.; Chen, W. S.; Han, B. N.; Lin, H. W., Hippolachnin A, a new antifungal polyketide from the South China Sea sponge *Hippospongia lachne*. *Org Lett* **2013**, *15* (14), 3526-9.
5. Wilson, D., Endophyte. *Oikos* **1995**, *73* (2), 274-276.
6. Arnone, A.; Nasini, G.; Panzeri, W.; de Pava, O. V.; Malpezzi, L., Acremine G, dimeric metabolite from cultures of *Acremonium byssoides* A20. *J Nat Prod* **2008**, *71* (1), 146-9.
7. Wu, P.; Xue, J.; Yao, L.; Xu, L.; Li, H.; Wei, X., Bisacremine E-G, Three Polycyclic Dimeric Acremines Produced by *Acremonium persicinum* SC0105. *Org Lett* **2015**, *17* (19), 4922-5.
8. Higgs, M. D.; Faulkner, D. J., Plakortin, an antibiotic from *Plakortis halichondrioides*. *The Journal of Organic Chemistry* **1978**, *43* (18), 3454-3457.
9. Cafieri, F.; Fattorusso, E.; Tagliatela-Scafati, O.; Ianaro, A., Metabolites from the sponge *Plakortis simplex*. Determination of absolute stereochemistry of plakortin. Isolation and stereostructure of three plakortin related compounds. *Tetrahedron* **1999**, *55* (22), 7045-7056.
10. Campagnuolo, C.; Fattorusso, E.; Romano, A.; Tagliatela-Scafati, O.; Basilico, N.; Parapini, S.; Taramelli, D., Antimalarial Polyketide Cycloperoxides from the Marine Sponge *Plakortis simplex*. *European Journal of Organic Chemistry* **2005**, *2005* (23), 5077-5083.
11. Patil, A. D.; Freyer, A. J.; Bean, M. F.; Carte, B. K.; Westley, J. W.; Johnson, R. K.; Lahouratate, P., The plakortones, novel bicyclic lactones from the sponge *Plakortis halichondrioides*: Activators of cardiac SR-Ca²⁺-pumping ATPase. *Tetrahedron* **1996**, *52* (2), 377-394.
12. Ueoka, R.; Nakao, Y.; Kawatsu, S.; Yaegashi, J.; Matsumoto, Y.; Matsunaga, S.; Furihata, K.; van Soest, R. W.; Fusetani, N., Gracilioethers A-C, antimalarial metabolites from the marine sponge *Agelas gracilis*. *J Org Chem* **2009**, *74* (11), 4203-7.
13. Festa, C.; De Marino, S.; D'Auria, M. V.; Deharo, E.; Gonzalez, G.; Deysard, C.; Petek, S.; Bifulco, G.; Zampella, A., Gracilioethers E-J, new oxygenated polyketides

from the marine sponge *Plakinastrella mamillaris*. *Tetrahedron* **2012**, *68* (49), 10157-10163.

14. Festa, C.; D'Amore, C.; Renga, B.; Lauro, G.; De Marino, S.; D'Auria, M. V.; Bifulco, G.; Zampella, A.; Fiorucci, S., Oxygenated polyketides from *Plakinastrella mamillaris* as a new chemotype of PXR agonists. *Mar Drugs* **2013**, *11* (7), 2314-27.

15. Rasik, C. M.; Brown, M. K., Total synthesis of gracilioether F: development and application of lewis Acid promoted ketene-alkene [2+2] cycloadditions and late-stage C-H oxidation. *Angew Chem Int Ed Engl* **2014**, *53* (52), 14522-6.

16. Norris, M. D.; Perkins, M. V.; Sorensen, E. J., Biomimetic total synthesis of gracilioethers B and C. *Org Lett* **2015**, *17* (3), 668-71.

17. Ruider, S. A.; Carreira, E. M., A Unified Strategy to Plakortin Pentalenes: Total Syntheses of (+/-)-Gracilioethers E and F. *Org Lett* **2016**, *18* (2), 220-3.

18. Shen, X. Y.; Peng, X. S.; Wong, H. N., Total Synthesis of (+/-)-Gracilioether F. *Org Lett* **2016**, *18* (5), 1032-5.

19. Xu, Z. J.; Wu, Y., Efficient Synthetic Routes to (+/-)-Hippolachnin A, (+/-)-Gracilioethers E and F and the Alleged Structure of (+/-)-Gracilioether I. *Chemistry* **2017**, *23* (9), 2026-2030.

20. Ruider, S. A.; Sandmeier, T.; Carreira, E. M., Total synthesis of (+/-)-hippolachnin A. *Angew Chem Int Ed Engl* **2015**, *54* (8), 2378-82.

21. Festa, C.; Lauro, G.; De Marino, S.; D'Auria, M. V.; Monti, M. C.; Casapullo, A.; D'Amore, C.; Renga, B.; Mencarelli, A.; Petek, S.; Bifulco, G.; Fiorucci, S.; Zampella, A., Plakilactones from the marine sponge *Plakinastrella mamillaris*. Discovery of a new class of marine ligands of peroxisome proliferator-activated receptor gamma. *J Med Chem* **2012**, *55* (19), 8303-17.

22. Kubanek, J.; Andersen, R. J., Evidence for the Incorporation of Intact Butyrate Units in the Biosynthesis of Triophamine. *Tetrahedron Letters* **1997**, *38* (36), 6327-6330.

23. Stierle, D. B.; Faulkner, D. J., Metabolites of three marine sponges of the genus *Plakortis*. *The Journal of Organic Chemistry* **1980**, *45* (17), 3396-3401.

24. Akiyama, M.; Isoda, Y.; Nishimoto, M.; Kobayashi, A.; Togawa, D.; Hirao, N.; Kuboki, A.; Ohira, S., Stereocontrolled synthesis of (\pm)-methyl 3,6-epoxy-4,6,8-triethyl-2,4,9-dodecatrienoate, a major metabolite of Caribbean sponge, *Plakortis halichondrioides*, using reactions of alkylidenecarbenes in one pot. *Tetrahedron Letters* **2005**, *46* (44), 7483-7485.

25. Datta, R.; Dixon, R. J.; Ghosh, S., A convenient access to the tricyclic core structure of hippolachnin A. *Tetrahedron Letters* **2016**, *57* (1), 29-31.

26. McCallum, M. E.; Rasik, C. M.; Wood, J. L.; Brown, M. K., Collaborative Total Synthesis: Routes to (+/-)-Hippolachnin A Enabled by Quadricyclane Cycloaddition and Late-Stage C-H Oxidation. *J Am Chem Soc* **2016**, *138* (7), 2437-42.
27. Govender, N. P.; Patel, J.; van Wyk, M.; Chiller, T. M.; Lockhart, S. R.; Group for Enteric, R.; Meningeal Disease Surveillance in South, A., Trends in antifungal drug susceptibility of *Cryptococcus neoformans* isolates obtained through population-based surveillance in South Africa in 2002-2003 and 2007-2008. *Antimicrob Agents Chemother* **2011**, *55* (6), 2606-11.
28. Loyse, A.; Thangaraj, H.; Easterbrook, P.; Ford, N.; Roy, M.; Chiller, T.; Govender, N.; Harrison, T. S.; Bicanic, T., Cryptococcal meningitis: improving access to essential antifungal medicines in resource-poor countries. *The Lancet Infectious Diseases* **2013**, *13* (7), 629-637.
29. Sabiiti, W.; Robertson, E.; Beale, M. A.; Johnston, S. A.; Brouwer, A. E.; Loyse, A.; Jarvis, J. N.; Gilbert, A. S.; Fisher, M. C.; Harrison, T. S.; May, R. C.; Bicanic, T., Efficient phagocytosis and laccase activity affect the outcome of HIV-associated cryptococcosis. *J Clin Invest* **2014**, *124* (5), 2000-8.
30. Li, S. S.; Mody, C. H., *Cryptococcus*. *Proc Am Thorac Soc* **2010**, *7* (3), 186-96.
31. Reetz, M. T.; Chatziiosifidis, I.; Schwellnus, K., A General Procedure for Intramolecular α -tert-Alkylation of Carbonyl Compounds. *Angewandte Chemie International Edition in English* **1981**, *20* (8), 687-689.
32. Dauben, W. G.; Koch, K.; Smith, S. L.; Chapman, O. L., Photoisomerizations in the α -Tropolone Series: The Mechanistic Path of the α -Tropolone Methyl Ether to Methyl 4-Oxo-2-cyclopentenylacetate Conversion. *Journal of the American Chemical Society* **1963**, *85* (17), 2616-2621.
33. Zweifel, G.; Steele, R. B., A new and convenient method for the preparation of isomerically pure α,β -unsaturated derivatives via hydroalumination of alkynes. *Journal of the American Chemical Society* **1967**, *89* (11), 2754-2755.
34. Zhu, J.; Yang, J. Y.; Klunder, A. J. H.; Liu, Z. Y.; Zwanenburg, B., ChemInform Abstract: A Stereo- and Enantioselective Approach to Clavulones from Tricyclodecadienone Using Flash Vacuum Thermolysis. *ChemInform* **2010**, *26* (37), no-no.
35. Demuyne, A. L. W.; Levecque, P.; Kidane, A.; Gammon, D. W.; Sickel, E.; Jacobs, P. A.; De Vos, D. E.; Sels, B. F., Retro-Diels-Alder Reactions of Masked Cyclopentadienones Catalyzed by Heterogeneous Brønsted Acids. *Advanced Synthesis & Catalysis* **2010**, *352* (18), 3419-3430.

36. Krasovskiy, A.; Kopp, F.; Knochel, P., Soluble lanthanide salts (LnCl₃.2LiCl) for the improved addition of organomagnesium reagents to carbonyl compounds. *Angew Chem Int Ed Engl* **2006**, *45* (3), 497-500.
37. Zhou, T.; Peters, B.; Maldonado, M. F.; Govender, T.; Andersson, P. G., Enantioselective synthesis of chiral sulfones by Ir-catalyzed asymmetric hydrogenation: a facile approach to the preparation of chiral allylic and homoallylic compounds. *J Am Chem Soc* **2012**, *134* (33), 13592-5.
38. Winter, N.; Trauner, D., Thiocarbonyl Ylide Chemistry Enables a Concise Synthesis of (+/-)-Hippolachnin A. *J Am Chem Soc* **2017**, *139* (34), 11706-11709.
39. Arnone, A.; Assante, G.; Bava, A.; Dallavalle, S.; Nasini, G., Acremines H–N, novel prenylated polyketide metabolites produced by a strain of *Acremonium byssoides*. *Tetrahedron* **2009**, *65* (4), 786-791.
40. Assante, G.; Dallavalle, S.; Malpezzi, L.; Nasini, G.; Burruano, S.; Torta, L., Acremines A–F, novel secondary metabolites produced by a strain of an endophytic *Acremonium*, isolated from sporangiophores of *Plasmopara viticola* in grapevine leaves. *Tetrahedron* **2005**, *61* (32), 7686-7692.
41. Suciati; Fraser, J. A.; Lambert, L. K.; Pierens, G. K.; Bernhardt, P. V.; Garson, M. J., Secondary metabolites of the sponge-derived fungus *Acremonium persicinum*. *J Nat Prod* **2013**, *76* (8), 1432-40.
42. Garson, M. J.; Hehre, W.; Pierens, G. K.; Suciati, Revision of the Structure of Acremine P from a Marine-Derived Strain of *Acremonium persicinum*. *Molecules* **2017**, *22* (4).
43. Yurchenko, A. N.; Smetanina, O. F.; Kalinovskiy, A. I.; Pushilin, M. A.; Glazunov, V. P.; Khudyakova, Y. V.; Kirichuk, N. N.; Ermakova, S. P.; Dyshlovoy, S. A.; Yurchenko, E. A.; Afiyatullo, S., Oxirapentyns F-K from the marine-sediment-derived fungus *Isaria felina* KMM 4639. *J Nat Prod* **2014**, *77* (6), 1321-8.
44. Wu, P.; Yao, L.; Xu, L.; Xue, J.; Wei, X., Bisacremines A-D, Dimeric Acremines Produced by a Soil-Derived *Acremonium persicinum* Strain. *J Nat Prod* **2015**, *78* (9), 2161-6.
45. Mehta, G.; Sunil Kumar, Y. C.; Khan, T. B., Total syntheses of the fungal metabolites (±)-acremine A, B and I. *Tetrahedron Letters* **2010**, *51* (39), 5112-5115.
46. Arkoudis, E.; Lykakis, I. N.; Gryparis, C.; Stratakis, M., Biomimetic synthesis of dimeric metabolite acremine G via a highly regioselective and stereoselective Diels-Alder reaction. *Org Lett* **2009**, *11* (14), 2988-91.
47. Mehta, G.; Khan, T. B.; Sunil Kumar, Y. C., Total synthesis of the fungal metabolite (±)-acremine G: acceleration of a biomimetic Diels–Alder reaction on silica gel. *Tetrahedron Letters* **2010**, *51* (39), 5116-5119.

48. Lei, X.; Johnson, R. P.; Porco, J. A., Jr., Total synthesis of the ubiquitin-activating enzyme inhibitor (+)-panepophenanthrin. *Angew Chem Int Ed Engl* **2003**, *42* (33), 3913-7.
49. Magnuson, S. R.; Sepp-Lorenzino, L.; Rosen, N.; Danishefsky, S. J., A Concise Total Synthesis of Dysidiolide through Application of a Dioxolenium-Mediated Diels–Alder Reaction. *Journal of the American Chemical Society* **1998**, *120* (7), 1615-1616.
50. Irgartinger, H.; Stadler, B., Synthesis, Structures and Topochemistry of 2-Monovinyl-Substituted 1,4-Benzoquinones. *European Journal of Organic Chemistry* **1998**, *1998* (4), 605-626.
51. Noland, W. E.; Kedrowski, B. L., Synthesis of Angular Quinoid Heterocycles from 2-(2-Nitrovinyl)-1,4-benzoquinone. *The Journal of Organic Chemistry* **1999**, *64* (2), 596-603.
52. Kienzler, M. A.; Suseno, S.; Trauner, D., Vinyl quinones as Diels-Alder dienes: concise synthesis of (-)-halenaquinone. *J Am Chem Soc* **2008**, *130* (27), 8604-5.
53. Lobermann, F.; Mayer, P.; Trauner, D., Biomimetic synthesis of (-)-pyncnanthuquinone C through the Diels-Alder reaction of a vinyl quinone. *Angew Chem Int Ed Engl* **2010**, *49* (35), 6199-202.
54. Zhang, Z.; Chen, J.; Yang, Z.; Tang, Y., Rapid biomimetic total synthesis of (+/-)-rossinone B. *Org Lett* **2010**, *12* (23), 5554-7.
55. Lobermann, F.; Weisheit, L.; Trauner, D., Intramolecular vinyl quinone Diels-Alder reactions: asymmetric entry to the cordiachrome core and synthesis of (-)-isoglaziovianol. *Org Lett* **2013**, *15* (17), 4324-6.
56. Woo, C. M.; Lu, L.; Gholap, S. L.; Smith, D. R.; Herzon, S. B., Development of a Convergent Entry to the Diazofluorene Antitumor Antibiotics: Enantioselective Synthesis of Kinamycin F. *Journal of the American Chemical Society* **2010**, *132* (8), 2540-2541.
57. Gassman, P. G.; Singleton, D. A.; Wilwerding, J. J.; Chavan, S. P., Acrolein acetals as allyl cation precursors in the ionic Diels-Alder reaction. *Journal of the American Chemical Society* **1987**, *109* (7), 2182-2184.
58. Gassman, P. G.; Lottes, A. C., Cyclobutane formation in the $2\pi + 2\pi$ cycloaddition of allyl and related cations to unactivated olefins. Evidence for the second step in the proposed mechanism of the ionic diels-alder reaction. *Tetrahedron Letters* **1992**, *33* (2), 157-160.
59. Sammakia, T.; Berliner, M. A., Asymmetric Diels-Alder Reactions with .alpha.,.beta.-Unsaturated Acetals. *The Journal of Organic Chemistry* **1994**, *59* (23), 6890-6891.

60. Pabon, R. A.; Bellville, D. J.; Bauld, N. L., Cation radical Diels-Alder reactions of electron-rich dienophiles. *Journal of the American Chemical Society* **1983**, *105* (15), 5158-5159.
61. Mlcoch, J.; Steckhan, E., Photochemically Initiated, Electron-Transfer-Catalyzed Diels-Alder Reactions of Electron-Rich Dienophiles. *Angewandte Chemie International Edition in English* **1985**, *24* (5), 412-414.
62. Nicewicz, D. A.; Nguyen, T. M., Recent Applications of Organic Dyes as Photoredox Catalysts in Organic Synthesis. *ACS Catalysis* **2013**, *4* (1), 355-360.
63. Bellville, D. J.; Bauld, N. L.; Pabon, R.; Gardner, S. A., Theoretical analysis of selectivity in the cation radical Diels-Alder. *Journal of the American Chemical Society* **1983**, *105* (11), 3584-3588.
64. Drew, S. L.; Lawrence, A. L.; Sherburn, M. S., Total synthesis of kingianins A, D, and F. *Angew Chem Int Ed Engl* **2013**, *52* (15), 4221-4.
65. Grée, R.; Laabassi, M.; Mosset, P.; Carrié, R., Stereo- and enantioselective synthesis of some e,z dienols and ethers. *Tetrahedron Letters* **1985**, *26* (19), 2317-2318.
66. Wender, P. A.; Correia, C. R. D., Intramolecular photoinduced diene-diene cycloadditions: a selective method for the synthesis of complex eight-membered rings and polyquinanes. *Journal of the American Chemical Society* **1987**, *109* (8), 2523-2525.
67. Hammond, G. S.; Turro, N. J.; Liu, R. S. H., Mechanisms of Photochemical Reactions in Solution. XVI.1 Photosensitized Dimerization of Conjugated Dienes. *The Journal of Organic Chemistry* **1963**, *28* (12), 3297-3303.
68. Trecker, D. J.; Henry, J. P., Cumulative Effects in Small Ring Cleavage Reactions. A Novel Cyclobutane Rearrangement. *Journal of the American Chemical Society* **1964**, *86* (5), 902-905.
69. Hammond, G. S.; DeBoer, C. D., Multiplicity of Mechanisms in the Cope Rearrangement. *Journal of the American Chemical Society* **1964**, *86* (5), 899-902.
70. Fleming, S. A.; Parent, A. A.; Parent, E. E.; Pincock, J. A.; Renault, L., Mechanistic analysis of the photocycloaddition of silyl-tethered alkenes. *J Org Chem* **2007**, *72* (25), 9464-70.
71. Ward, S. C.; Fleming, S. A., [2 + 2] Photocycloaddition of Cinnamyloxy Silanes. *The Journal of Organic Chemistry* **1994**, *59* (21), 6476-6479.
72. Fleming, S. A.; Ward, S. C., Stereocontrolled photochemical [2 + 2] cycloaddition. *Tetrahedron Letters* **1992**, *33* (8), 1013-1016.
73. Nicolaou, K. C.; Snyder, S. A.; Montagnon, T.; Vassilikogiannakis, G., The Diels-Alder Reaction in Total Synthesis. *Angewandte Chemie International Edition* **2002**, *41* (10), 1668-1698.

74. Barcellos, T.; Tauber, K.; Kroutil, W.; Andrade, L. H., Stereocomplementary asymmetric bioreduction of boron-containing ketones mediated by alcohol dehydrogenases. *Tetrahedron: Asymmetry* **2011**, *22* (18-19), 1772-1777.
75. Palczewski K, k. T., hori T, behnke CA, motoshima H, fox BA, trong IL, teller DC, okada T, stenkamp RE, yamamoto M, miyano M. , Crystal structure of rhodopsin: a G protein-coupled receptor. . *American journal of ophthalmology* **2000**, *130* (6), 865.
76. Wettschureck, N.; Offermanns, S., Mammalian G proteins and their cell type specific functions. *Physiol Rev* **2005**, *85* (4), 1159-204.
77. Philip, F.; Sengupta, P.; Scarlata, S., Signaling through a G Protein-coupled receptor and its corresponding G protein follows a stoichiometrically limited model. *J Biol Chem* **2007**, *282* (26), 19203-16.
78. Foord, S. M.; Bonner, T. I.; Neubig, R. R.; Rosser, E. M.; Pin, J. P.; Davenport, A. P.; Spedding, M.; Harmar, A. J., International Union of Pharmacology. XLVI. G protein-coupled receptor list. *Pharmacol Rev* **2005**, *57* (2), 279-88.
79. Cherezov, V.; Rosenbaum, D. M.; Hanson, M. A.; Rasmussen, S. G.; Thian, F. S.; Kobilka, T. S.; Choi, H. J.; Kuhn, P.; Weis, W. I.; Kobilka, B. K.; Stevens, R. C., High-resolution crystal structure of an engineered human beta2-adrenergic G protein-coupled receptor. *Science* **2007**, *318* (5854), 1258-65.
80. Jiang, M.; Bajpayee, N. S., Molecular mechanisms of go signaling. *Neurosignals* **2009**, *17* (1), 23-41.
81. Beaulieu, J. M.; Gainetdinov, R. R., The physiology, signaling, and pharmacology of dopamine receptors. *Pharmacol Rev* **2011**, *63* (1), 182-217.
82. Missale, C.; Nash, S. R.; Robinson, S. W.; Jaber, M.; Caron, M. G., Dopamine receptors: from structure to function. *Physiol Rev* **1998**, *78* (1), 189-225.
83. Beaulieu, J. M.; Espinoza, S.; Gainetdinov, R. R., Dopamine receptors - IUPHAR Review 13. *Br J Pharmacol* **2015**, *172* (1), 1-23.
84. Rask-Andersen, M.; Almen, M. S.; Schioth, H. B., Trends in the exploitation of novel drug targets. *Nat Rev Drug Discov* **2011**, *10* (8), 579-90.
85. Chien, E. Y.; Liu, W.; Zhao, Q.; Katritch, V.; Han, G. W.; Hanson, M. A.; Shi, L.; Newman, A. H.; Javitch, J. A.; Cherezov, V.; Stevens, R. C., Structure of the human dopamine D3 receptor in complex with a D2/D3 selective antagonist. *Science* **2010**, *330* (6007), 1091-5.
86. Perreault, M. L.; Hasbi, A.; O'Dowd, B. F.; George, S. R., Heteromeric dopamine receptor signaling complexes: emerging neurobiology and disease relevance. *Neuropsychopharmacology* **2014**, *39* (1), 156-68.

87. Cannon, J. G., Structure-activity relationships of dopamine agonists. *Annu Rev Pharmacol Toxicol* **1983**, *23*, 103-29.
88. Seiler, M. P.; Stoll, A. P.; Closse, A.; Frick, W.; Jatou, A.; Vigouret, J. M., Structure-activity relationships of dopaminergic 5-hydroxy-2-aminotetralin derivatives with functionalized N-alkyl substituents. *Journal of Medicinal Chemistry* **1986**, *29* (6), 912-917.
89. van Vliet, L. A.; Tepper, P. G.; Dijkstra, D.; Damsma, G.; Wikstrom, H.; Pugsley, T. A.; Akunne, H. C.; Heffner, T. G.; Glase, S. A.; Wise, L. D., Affinity for dopamine D2, D3, and D4 receptors of 2-aminotetralins. Relevance of D2 agonist binding for determination of receptor subtype selectivity. *J Med Chem* **1996**, *39* (21), 4233-7.
90. Biswas, S.; Zhang, S.; Fernandez, F.; Ghosh, B.; Zhen, J.; Kuzhikandathil, E.; Reith, M. E.; Dutta, A. K., Further structure-activity relationships study of hybrid 7-[[2-(4-phenylpiperazin-1-yl)ethyl]propylamino]-5,6,7,8-tetrahydronaphthalen-2-ol analogues: identification of a high-affinity D3-preferring agonist with potent in vivo activity with long duration of action. *J Med Chem* **2008**, *51* (1), 101-17.
91. Donthamsetti, P. C.; Winter, N.; Schonberger, M.; Levitz, J.; Stanley, C.; Javitch, J. A.; Isacoff, E. Y.; Trauner, D., Optical Control of Dopamine Receptors Using a Photoswitchable Tethered Inverse Agonist. *J Am Chem Soc* **2017**, *139* (51), 18522-18535.
92. Chan, T. R.; Hilgraf, R.; Sharpless, K. B.; Fokin, V. V., Polytriazoles as copper(I)-stabilizing ligands in catalysis. *Org Lett* **2004**, *6* (17), 2853-5.
93. Zheng, J.; Li, Y.; Sun, Y.; Yang, Y.; Ding, Y.; Lin, Y.; Yang, W., A generic magnetic microsphere platform with "clickable" ligands for purification and immobilization of targeted proteins. *ACS Appl Mater Interfaces* **2015**, *7* (13), 7241-50.
94. Kassianidis, E.; Pearson, R. J.; Philp, D., Probing structural effects on replication efficiency through comparative analyses of families of potential self-replicators. *Chemistry* **2006**, *12* (34), 8798-812.
95. Charlton, J. L.; Koh, K.; Plourde, G. L., An asymmetric synthesis of 2-amino-6,7-dihydroxy-1,2,3,4-tetrahydronaphthalene (ADTN). *Canadian Journal of Chemistry* **1990**, *68* (11), 2028-2032.
96. Horn, A. S.; Grol, C. J.; Dijkstra, D.; Mulder, A. H., Facile syntheses of potent dopaminergic agonists and their effect on neurotransmitter release. *J Med Chem* **1978**, *21* (8), 825-8.
97. Langmead, C. J.; Watson, J.; Reavill, C., Muscarinic acetylcholine receptors as CNS drug targets. *Pharmacol Ther* **2008**, *117* (2), 232-43.
98. P., C. M.; Birdsall, N. J., International Union of Pharmacology. XVII. Classification of Muscarinic Acetylcholine Receptors. *Pharmacological Reviews* **1998**, *50* (2), 279-290.

99. Smith, R. S.; Araneda, R. C., Cholinergic modulation of neuronal excitability in the accessory olfactory bulb. *J Neurophysiol* **2010**, *104* (6), 2963-74.
100. Ishii, M.; Kurachi, Y., Muscarinic Acetylcholine Receptors. *Current Pharmaceutical Design* **2006**, *12*, 3573-3581.
101. Krejci, A.; Michal, P.; Jakubik, J.; Riczny, J.; Dolezal, V., Regulation of signal transduction at M2 muscarinic receptor. *Physiological research* **2004**, *53 Suppl 1*, S131-40.
102. Simon, M. I.; Strathmann, M. P.; Gautam, N., Diversity of G proteins in signal transduction. *Science* **1991**, *252* (5007), 802-808.
103. Dell'Acquat, M. L.; Carroll, R. C.; Peralta, E. G., Transfected m2 Muscarinic Acetylcholine Receptors Couple to G_i1 and G_i3 in CHinese Hamster Ovary Cells. *The Journal of Biological Chemistry* **1993**, *268* (8), 5676-5685.
104. Haga, K.; Kruse, A. C.; Asada, H.; Yurugi-Kobayashi, T.; Shiroishi, M.; Zhang, C.; Weis, W. I.; Okada, T.; Kobilka, B. K.; Haga, T.; Kobayashi, T., Structure of the human M2 muscarinic acetylcholine receptor bound to an antagonist. *Nature* **2012**, *482* (7386), 547-51.
105. Kruse, A. C.; Hu, J.; Pan, A. C.; Arlow, D. H.; Rosenbaum, D. M.; Rosemond, E.; Green, H. F.; Liu, T.; Chae, P. S.; Dror, R. O.; Shaw, D. E.; Weis, W. I.; Wess, J.; Kobilka, B. K., Structure and dynamics of the M3 muscarinic acetylcholine receptor. *Nature* **2012**, *482* (7386), 552-6.
106. Thal, D. M.; Sun, B.; Feng, D.; Nawaratne, V.; Leach, K.; Felder, C. C.; Bures, M. G.; Evans, D. A.; Weis, W. I.; Bachhawat, P.; Kobilka, T. S.; Sexton, P. M.; Kobilka, B. K.; Christopoulos, A., Crystal structures of the M1 and M4 muscarinic acetylcholine receptors. *Nature* **2016**, *531* (7594), 335-40.
107. Comings, D. E.; Wu, S.; Rostamkhani, M.; McGue, M.; Lacono, W. G.; Cheng, L. S.; MacMurray, J. P., Role of the cholinergic muscarinic 2 receptor (CHRM2) gene in cognition. *Mol Psychiatry* **2003**, *8* (1), 10-1.
108. Dallanoce, C.; Conti, P.; De Amici, M.; De Micheli, C.; Barocelli, E.; Chiavarini, M.; Ballabeni, V.; Bertoni, S.; Impicciatore, M., Synthesis and functional characterization of novel derivatives related to oxotremorine and oxotremorine-M. *Bioorganic & Medicinal Chemistry* **1999**, *7* (8), 1539-1547.
109. Langmead, C. J.; Christopoulos, A., Supra-physiological efficacy at GPCRs: superstition or super agonists? *Br J Pharmacol* **2013**, *169* (2), 353-6.
110. Antony, J.; Kellershohn, K.; Mohr-Andra, M.; Kebig, A.; Prilla, S.; Muth, M.; Heller, E.; Disingrini, T.; Dallanoce, C.; Bertoni, S.; Schrobang, J.; Trankle, C.; Kostenis, E.; Christopoulos, A.; Holtje, H. D.; Barocelli, E.; De Amici, M.; Holzgrabe, U.; Mohr, K.,

Dualsteric GPCR targeting: a novel route to binding and signaling pathway selectivity. *FASEB J* **2009**, *23* (2), 442-50.

111. Mohr, K.; Trankle, C.; Kostenis, E.; Barocelli, E.; De Amici, M.; Holzgrabe, U., Rational design of dualsteric GPCR ligands: quests and promise. *Br J Pharmacol* **2010**, *159* (5), 997-1008.

112. Disingrini, T.; Muth, M.; Dallanoce, C.; Barocelli, E.; Bertoni, S.; Kellershohn, K.; Mohr, K.; De Amici, M.; Holzgrabe, U., Design, synthesis, and action of oxotremorine-related hybrid-type allosteric modulators of muscarinic acetylcholine receptors. *J Med Chem* **2006**, *49* (1), 366-72.

113. Kloeckner, J.; Schmitz, J.; Holzgrabe, U., Convergent, short synthesis of the muscarinic superagonist iperoxo. *Tetrahedron Letters* **2010**, *51* (27), 3470-3472.

114. Chandrashekar, J.; Mueller, K. L.; Hoon, M. A.; Adler, E.; Feng, L.; Guo, W.; Zuker, C. S.; Ryba, N. J. P., T2Rs Function as Bitter Taste Receptors. *Cell* **2000**, *100* (6), 703-711.

115. Galindo, M. M.; Voigt, N.; Stein, J.; van Lengerich, J.; Raguse, J. D.; Hofmann, T.; Meyerhof, W.; Behrens, M., G protein-coupled receptors in human fat taste perception. *Chem Senses* **2012**, *37* (2), 123-39.

116. Meyerhof, W.; Batram, C.; Kuhn, C.; Brockhoff, A.; Chudoba, E.; Bufe, B.; Appendino, G.; Behrens, M., The molecular receptive ranges of human TAS2R bitter taste receptors. *Chem Senses* **2010**, *35* (2), 157-70.

117. Margolskee, R. F., Molecular mechanisms of bitter and sweet taste transduction. *J Biol Chem* **2002**, *277* (1), 1-4.

118. Deckmann, K.; Filipinski, K.; Krasteva-Christ, G.; Fronius, M.; Althaus, M.; Rafiq, A.; Papadakis, T.; Renno, L.; Jurastow, I.; Wessels, L.; Wolff, M.; Schutz, B.; Weihe, E.; Chubanov, V.; Gudermann, T.; Klein, J.; Bschleipfer, T.; Kummer, W., Bitter triggers acetylcholine release from polymodal urethral chemosensory cells and bladder reflexes. *Proc Natl Acad Sci U S A* **2014**, *111* (22), 8287-92.

119. Zheng, K.; Lu, P.; Delpapa, E.; Bellve, K.; Deng, R.; Condon, J. C.; Fogarty, K.; Lifshitz, L. M.; Simas, T. A. M.; Shi, F.; ZhuGe, R., Bitter taste receptors as targets for tocolytics in preterm labor therapy. *FASEB J* **2017**, *31* (9), 4037-4052.

120. Waxman, S. G.; Dib-Hajj, S.; Cummins, T. R.; Black, J. A., Sodium channels and pain. *Proceedings of the National Academy of Sciences* **1999**, *96* (14), 7635-7639.

121. Waxman, S. G.; Zamponi, G. W., Regulating excitability of peripheral afferents: emerging ion channel targets. *Nat Neurosci* **2014**, *17* (2), 153-63.

122. Lai, H. C.; Jan, L. Y., The distribution and targeting of neuronal voltage-gated ion channels. *Nat Rev Neurosci* **2006**, *7* (7), 548-62.

123. Catterall, W. A., From ionic currents to molecular mechanisms: the structure and function of voltage-gated sodium channels. *Neuron* **2000**, *26* (1), 13-25.
124. Long, S. B.; Tao, X.; Campbell, E. B.; MacKinnon, R., Atomic structure of a voltage-dependent K⁺ channel in a lipid membrane-like environment. *Nature* **2007**, *450* (7168), 376-82.
125. Catterall, W. A.; Goldin, A. L.; Waxman, S. G., International Union of Pharmacology. XLVII. Nomenclature and structure-function relationships of voltage-gated sodium channels. *Pharmacol Rev* **2005**, *57* (4), 397-409.
126. Payandeh, J.; Gamal El-Din, T. M.; Scheuer, T.; Zheng, N.; Catterall, W. A., Crystal structure of a voltage-gated sodium channel in two potentially inactivated states. *Nature* **2012**, *486* (7401), 135-9.
127. Payandeh, J.; Scheuer, T.; Zheng, N.; Catterall, W. A., The crystal structure of a voltage-gated sodium channel. *Nature* **2011**, *475* (7356), 353-8.
128. Armstrong, C. M., Sodium channels and gating currents. *Physiol Rev* **1981**, *61* (3), 644-83.
129. Kaczmarek, L. K., Non-conducting functions of voltage-gated ion channels. *Nat Rev Neurosci* **2006**, *7* (10), 761-71.
130. Dib-Hajj, S. D.; Yang, Y.; Black, J. A.; Waxman, S. G., The Na(V)1.7 sodium channel: from molecule to man. *Nat Rev Neurosci* **2013**, *14* (1), 49-62.
131. Browne, L. E.; Blaney, F. E.; Yusaf, S. P.; Clare, J. J.; Wray, D., Structural determinants of drugs acting on the Nav1.8 channel. *J Biol Chem* **2009**, *284* (16), 10523-36.
132. Zimmermann, K.; Leffler, A.; Babes, A.; Cendan, C. M.; Carr, R. W.; Kobayashi, J.; Nau, C.; Wood, J. N.; Reeh, P. W., Sensory neuron sodium channel Nav1.8 is essential for pain at low temperatures. *Nature* **2007**, *447* (7146), 855-8.
133. Jarvis, M. F.; Honore, P.; Shieh, C. C.; Chapman, M.; Joshi, S.; Zhang, X. F.; Kort, M.; Carroll, W.; Marron, B.; Atkinson, R.; Thomas, J.; Liu, D.; Krambis, M.; Liu, Y.; McGaraughty, S.; Chu, K.; Roeloffs, R.; Zhong, C.; Mikusa, J. P.; Hernandez, G.; Gauvin, D.; Wade, C.; Zhu, C.; Pai, M.; Scanio, M.; Shi, L.; Drizin, I.; Gregg, R.; Matulenko, M.; Hakeem, A.; Gross, M.; Johnson, M.; Marsh, K.; Wagoner, P. K.; Sullivan, J. P.; Faltynek, C. R.; Krafte, D. S., A-803467, a potent and selective Nav1.8 sodium channel blocker, attenuates neuropathic and inflammatory pain in the rat. *Proc Natl Acad Sci U S A* **2007**, *104* (20), 8520-5.
134. Giannerini, M.; Fananas-Mastral, M.; Feringa, B. L., Direct catalytic cross-coupling of organolithium compounds. *Nat Chem* **2013**, *5* (8), 667-72.

135. Ruetsch, Y.; Boni, T.; Borgeat, A., From Cocaine to Ropivacaine: The History of Local Anesthetic Drugs. *Current Topics in Medicinal Chemistry* **2001**, *1* (3), 175-182.
136. Solth, A.; Siebrands, C. C.; Friederich, P., Inhibition of Kv4.3/KChIP2.2 channels by bupivacaine and its modulation by the pore mutation Kv4.3V401I. *Anesthesiology* **2005**, *103* (4), 796-804.
137. Punke, M. A.; Licher, T.; Pongs, O.; Friederich, P., Inhibition of human TREK-1 channels by bupivacaine. *Anesthesia and analgesia* **2003**, *96* (6), 1665-73, table of contents.
138. González, T.; Longobardo, M.; Caballero, R.; Delpón, E.; Tamargo, J.; Valenzuela, C., Effects of Bupivacaine and a Novel Local Anesthetic, IQB-9302, on Human Cardiac K⁺ Channels. *Journal of Pharmacology and Experimental Therapeutics* **2001**, *296* (2), 573-583.
139. Nilsson, J.; Madeja, M.; Arhem, P., Local anesthetic block of Kv channels: role of the S6 helix and the S5-S6 linker for bupivacaine action. *Molecular pharmacology* **2003**, *63* (6), 1417-29.
140. Bagal, S. K.; Chapman, M. L.; Marron, B. E.; Prime, R.; Storer, R. I.; Swain, N. A., Recent progress in sodium channel modulators for pain. *Bioorg Med Chem Lett* **2014**, *24* (16), 3690-9.
141. Large, C. H.; Bison, S.; Sartori, I.; Read, K. D.; Gozzi, A.; Quarta, D.; Antolini, M.; Hollands, E.; Gill, C. H.; Gunthorpe, M. J.; Idris, N.; Neill, J. C.; Alvaro, G. S., The efficacy of sodium channel blockers to prevent phencyclidine-induced cognitive dysfunction in the rat: potential for novel treatments for schizophrenia. *J Pharmacol Exp Ther* **2011**, *338* (1), 100-13.
142. Keppel Hesselink, J. M., Moving targets in sodium channel blocker development: the case of raxatrigine: from a central NaV1.3 blocker via a peripheral NaV1.7 blocker to a less selective sodium channel blocker. *Journal of Medicine and Therapeutics* **2017**, *1* (1).
143. King, G. F.; Vetter, I., No gain, no pain: NaV1.7 as an analgesic target. *ACS Chem Neurosci* **2014**, *5* (9), 749-51.
144. Fletcher, D. A.; Mullins, R. D., Cell mechanics and the cytoskeleton. *Nature* **2010**, *463* (7280), 485-92.
145. Dominguez, R.; Holmes, K. C., Actin structure and function. *Annu Rev Biophys* **2011**, *40*, 169-86.
146. Otterbein, L. R.; Graceffa, P.; Dominguez, R., The crystal structure of uncomplexed actin in the ADP state. *Science* **2001**, *293* (5530), 708-11.

147. Blanchoin, L.; Boujemaa-Paterski, R.; Sykes, C.; Plastino, J., Actin dynamics, architecture, and mechanics in cell motility. *Physiol Rev* **2014**, *94* (1), 235-63.
148. Goley, E. D.; Welch, M. D., The ARP2/3 complex: an actin nucleator comes of age. *Nat Rev Mol Cell Biol* **2006**, *7* (10), 713-26.
149. Borths, E. L.; Welch, M. D., Turning on the Arp2/3 Complex at Atomic Resolution. *Structure (London, England : 1993)* **2002**, *10* (2), 131-135.
150. Pollard, T. D., Regulation of actin filament assembly by Arp2/3 complex and formins. *Annu Rev Biophys Biomol Struct* **2007**, *36*, 451-77.
151. Beach, J. R.; Bruun, K. S.; Shao, L.; Li, D.; Swider, Z.; Remmert, K.; Zhang, Y.; Conti, M. A.; Adelstein, R. S.; Rusan, N. M.; Betzig, E.; Hammer, J. A., Actin dynamics and competition for myosin monomer govern the sequential amplification of myosin filaments. *Nat Cell Biol* **2017**, *19* (2), 85-93.
152. Robinson, R. C.; Turbedsky, K.; Kaiser, D. A.; Marchand, J. B.; Higgs, H. N.; Choe, S.; Pollard, T. D., Crystal structure of Arp2/3 complex. *Science* **2001**, *294* (5547), 1679-84.
153. Nolen, B. J.; Tomasevic, N.; Russell, A.; Pierce, D. W.; Jia, Z.; McCormick, C. D.; Hartman, J.; Sakowicz, R.; Pollard, T. D., Characterization of two classes of small molecule inhibitors of Arp2/3 complex. *Nature* **2009**, *460* (7258), 1031-4.
154. Baggett, A. W.; Cournia, Z.; Han, M. S.; Patargias, G.; Glass, A. C.; Liu, S. Y.; Nolen, B. J., Structural characterization and computer-aided optimization of a small-molecule inhibitor of the Arp2/3 complex, a key regulator of the actin cytoskeleton. *ChemMedChem* **2012**, *7* (7), 1286-94.
155. Hetrick, B.; Han, M. S.; Helgeson, L. A.; Nolen, B. J., Small molecules CK-666 and CK-869 inhibit actin-related protein 2/3 complex by blocking an activating conformational change. *Chem Biol* **2013**, *20* (5), 701-12.
156. Shutova, M.; Yang, C.; Vasiliev, J. M.; Svitkina, T., Functions of nonmuscle myosin II in assembly of the cellular contractile system. *PLoS One* **2012**, *7* (7), e40814.
157. Hartman, M. A.; Spudich, J. A., The myosin superfamily at a glance. *J Cell Sci* **2012**, *125* (Pt 7), 1627-32.
158. Geeves, M. A., Review: The ATPase mechanism of myosin and actomyosin. *Biopolymers* **2016**, *105* (8), 483-91.
159. O'Connell, C. B.; Tyska, M. J.; Mooseker, M. S., Myosin at work: motor adaptations for a variety of cellular functions. *Biochim Biophys Acta* **2007**, *1773* (5), 615-30.
160. Conti, M. A.; Adelstein, R. S., Nonmuscle myosin II moves in new directions. *J Cell Sci* **2008**, *121* (Pt 1), 11-8.

161. Straight, A. F.; Cheung, A.; Limouze, J.; Chen, I.; Westwood, N. J.; Sellers, J. R.; Mitchison, T. J., Dissecting temporal and spatial control of cytokinesis with a myosin II Inhibitor. *Science* **2003**, *299* (5613), 1743-7.
162. Varkuti, B. H.; Kepiro, M.; Horvath, I. A.; Vegner, L.; Rati, S.; Zsigmond, A.; Hegyi, G.; Lenkei, Z.; Varga, M.; Malnasi-Csizmadia, A., A highly soluble, non-phototoxic, non-fluorescent blebbistatin derivative. *Sci Rep* **2016**, *6*, 26141.
163. Kovacs, M.; Toth, J.; Hetenyi, C.; Malnasi-Csizmadia, A.; Sellers, J. R., Mechanism of blebbistatin inhibition of myosin II. *J Biol Chem* **2004**, *279* (34), 35557-63.
164. Shu, S.; Liu, X.; Korn, E. D., Blebbistatin and blebbistatin-inactivated myosin II inhibit myosin II-independent processes in Dictyostelium. *Proc Natl Acad Sci U S A* **2005**, *102* (5), 1472-7.
165. Ramamurthy, B.; Yengo, C. M.; Straight, A. F.; Mitchison, T. J.; Sweeney, H. L., Kinetic mechanism of blebbistatin inhibition of nonmuscle myosin IIb. *Biochemistry* **2004**, *43* (46), 14832-9.
166. Allingham, J. S.; Smith, R.; Rayment, I., The structural basis of blebbistatin inhibition and specificity for myosin II. *Nat Struct Mol Biol* **2005**, *12* (4), 378-9.
167. Lucas-Lopez, C.; Allingham, J. S.; Lebl, T.; Lawson, C. P.; Brenk, R.; Sellers, J. R.; Rayment, I.; Westwood, N. J., The small molecule tool (S)-(-)-blebbistatin: novel insights of relevance to myosin inhibitor design. *Org Biomol Chem* **2008**, *6* (12), 2076-84.
168. Kolega, J., Phototoxicity and photoinactivation of blebbistatin in UV and visible light. *Biochem Biophys Res Commun* **2004**, *320* (3), 1020-5.
169. Mikulich, A.; Kavaliauskiene, S.; Juzenas, P., Blebbistatin, a myosin inhibitor, is phototoxic to human cancer cells under exposure to blue light. *Biochim Biophys Acta* **2012**, *1820* (7), 870-7.
170. Kepiro, M.; Varkuti, B. H.; Vegner, L.; Voros, G.; Hegyi, G.; Varga, M.; Malnasi-Csizmadia, A., para-Nitroblebbistatin, the non-cytotoxic and photostable myosin II inhibitor. *Angew Chem Int Ed Engl* **2014**, *53* (31), 8211-5.
171. Kepiro, M.; Varkuti, B. H.; Bodor, A.; Hegyi, G.; Drahos, L.; Kovacs, M.; Malnasi-Csizmadia, A., Azidoblebbistatin, a photoreactive myosin inhibitor. *Proc Natl Acad Sci U S A* **2012**, *109* (24), 9402-7.
172. Bass, R. J.; Gordon, D. W., A Convenient Route to Tropolone Ethers. *Synthetic Communications* **2006**, *15* (3), 225-228.